

BIRLA CENTRAL LIBRARY

PILANI [ RAJASTHAN ]

Class No. 537.33

Book No. C36W

Accession No- 49103







MASSACHUSETTS INSTITUTE OF TECHNOLOGY  
RADIATION LABORATORY SERIES

LOUIS N. RIDENOUR, *Editor-in-Chief*

---

**WAVEFORMS**

MASSACHUSETTS INSTITUTE OF TECHNOLOGY  
RADIATION LABORATORY SERIES

Board of Editors

LOUIS N. RIDENOUR, *Editor-in-Chief*

GEORGE B. COLLINS, *Deputy Editor-in-Chief*

BRITTON CHANCE, S. A. GOUDSMIT, R. G. HERB, HUBERT M. JAMES, JULIAN K. KNIPP,  
JAMES L. LAWSON, LEON B. LINFORD, CAROL G. MONTGOMERY, C. NEWTON, ALBERT  
M. STONE, LOUIS A. TURNER, GEORGE E. VALLEY, JR., HERBERT H. WHEATON

---

1. RADAR ~~SYSTEM~~ ENGINEERING—*Ridenour*
2. RADAR AIDS TO NAVIGATION—*Hall*
3. RADAR BEACONS—*Roberts*
4. LORAN—*Pierce, McKenzie, and Woodward*
5. PULSE GENERATORS—*Glasoe and Lebacqz*
6. MICROWAVE MAGNETRONS—*Collins*
7. KLYSTRONS AND MICROWAVE TRIODES—*Hamilton, Knipp, and Kuper*
8. PRINCIPLES OF MICROWAVE CIRCUITS—*Montgomery, Dicke, and Purcell*
9. MICROWAVE TRANSMISSION CIRCUITS—*Ragan*
10. WAVEGUIDE HANDBOOK—*Marcwitz*
11. TECHNIQUE OF MICROWAVE MEASUREMENTS—*Montgomery*
12. MICROWAVE ANTENNA THEORY AND DESIGN—*Silver*
13. PROPAGATION OF SHORT RADIO WAVES—*Kerr*
14. MICROWAVE DUPLEXERS—*Smullin and Montgomery*
15. CRYSTAL RECTIFIERS—*Torrey and Whitmer*
16. MICROWAVE MIXERS—*Pound*
17. COMPONENTS HANDBOOK—*Blackburn*
18. VACUUM TUBE AMPLIFIERS—*Valley and Wallman*
19. WAVEFORMS—*Chance, Hughes, MacNichol, Sayre, and Williams*
20. ELECTRONIC TIME MEASUREMENTS—*Chance, Hulsizer, MacNichol, and Williams*
21. ELECTRONIC INSTRUMENTS—*Greenwood, Holdam, and MacRae*
22. CATHODE RAY TUBE DISPLAYS—*Soller, Starr, and Valley*
23. MICROWAVE RECEIVERS—*Van Voorhis*
24. THRESHOLD SIGNALS—*Lawson and Uhlenbeck*
25. THEORY OF SERVOMECHANISMS—*James, Nichols, and Phillips*
26. RADAR SCANNERS AND RADOMES—*Cady, Karelitz, and Turner*
27. COMPUTING MECHANISMS AND LINKAGES—*Svoboda*
28. INDEX—*Henney*

# WAVEFORMS

*Edited by*

**BRITTON CHANCE**

ASSISTANT PROFESSOR OF BIOPHYSICS, UNIVERSITY OF PENNSYLVANIA

**VERNON HUGHES**

DEPARTMENT OF PHYSICS, COLUMBIA UNIVERSITY

**EDWARD F. MacNICHOL**

DEPARTMENT OF BIOPHYSICS, UNIVERSITY OF PENNSYLVANIA

**DAVID SAYRE**

DEPARTMENT OF PHYSICS, ALABAMA POLYTECHNIC INSTITUTE

**FREDERIC C. WILLIAMS**

PROFESSOR OF ELECTRO-TECHNICS, MANCHESTER UNIVERSITY

OFFICE OF SCIENTIFIC RESEARCH AND DEVELOPMENT  
NATIONAL DEFENSE RESEARCH COMMITTEE



NEW YORK · TORONTO · LONDON  
McGRAW-HILL BOOK COMPANY, INC.

1949

# WAVEFORMS

COPYRIGHT, 1949, BY THE  
MCGRAW-HILL BOOK COMPANY, INC.  
PRINTED IN THE UNITED STATES OF AMERICA

*All rights reserved. This book, or  
parts thereof, may not be reproduced  
in any form without permission of  
the publishers.*

VIII

THE MAPLE PRESS COMPANY, YORK, PA.

## *WAVEFORMS*

### *EDITORIAL STAFF*

BRITTON CHANCE	EDITOR
V. W. HUGHES	VOLUME EDITOR
E. F. MACNICHOL, JR.	VOLUME EDITOR
DAVID SAYRE	VOLUME EDITOR
F. C. WILLIAMS	VOLUME EDITOR

### *CONTRIBUTING AUTHORS*

P. R. BELL  
F. B. BERGER  
A. S. BISHOP  
BRITTON CHANCE  
G. D. FORBES  
A. H. FREDERICK  
G. R. GAMERTSFELDER  
JOHN W. GRAY  
EVERETT B. HALES  
J. V. HOLDAM, JR.  
V. W. HUGHES  
ROBERT C. KELNER  
E. F. MACNICHOL, JR.  
DUNCAN MACRAE, JR.  
DAVID SAYRE  
ROBERT M. WALKER  
F. C. WILLIAMS  
ROGER B. WOODBURY



## *Foreword*

---

THE tremendous research and development effort that went into the development of radar and related techniques during World War II resulted not only in hundreds of radar sets for military (and some for possible peacetime) use but also in a great body of information and new techniques in the electronics and high-frequency fields. Because this basic material may be of great value to science and engineering, it seemed most important to publish it as soon as security permitted.

The Radiation Laboratory of MIT, which operated under the supervision of the National Defense Research Committee, undertook the great task of preparing these volumes. The work described herein, however, is the collective result of work done at many laboratories, Army, Navy, university, and industrial, both in this country and in England, Canada, and other Dominions.

The Radiation Laboratory, once its proposals were approved and finances provided by the Office of Scientific Research and Development, chose Louis N. Ridenour as Editor-in-Chief to lead and direct the entire project. An editorial staff was then selected of those best qualified for this type of task. Finally the authors for the various volumes or chapters or sections were chosen from among those experts who were intimately familiar with the various fields, and who were able and willing to write the summaries of them. This entire staff agreed to remain at work at MIT for six months or more after the work of the Radiation Laboratory was complete. These volumes stand as a monument to this group.

These volumes serve as a memorial to the unnamed hundreds and thousands of other scientists, engineers, and others who actually carried on the research, development, and engineering work the results of which are herein described. There were so many involved in this work and they worked so closely together even though often in widely separated laboratories that it is impossible to name or even to know those who contributed to a particular idea or development. Only certain ones who wrote reports or articles have even been mentioned. But to all those who contributed in any way to this great cooperative development enterprise, both in this country and in England, these volumes are dedicated.

L. A. DuBRIDGE.





## *Preface*

---

THE need for a means of preserving the value of the technical developments in the field of radar was foreseen as early as the summer of 1944, and, at the suggestion of I. I. Rabi and L. A. DuBridge, a committee consisting of L. J. Haworth, G. E. Valley, and the editor considered the form of the books on circuits and laid plans for Vols. 17 to 23. The termination of hostilities in August 1945, permitted the initiation of intensive activity under the direction of L. N. Ridenour and resulted in the completion of manuscript for these volumes by June 30, 1946. The amount of circuit material was so large that writing was attempted on a mass scale, and an unusually large number of authors have contributed to this volume. In spite of the very short time permitted, an attempt has been made to give a comprehensive survey of basic circuit techniques used in the generation and manipulation of voltage and currents by linear and nonlinear circuit elements. This book includes, therefore, a large number of basic circuit operations. Since radar circuit techniques have greatly expanded the methods and scope of this subject, considerable revision and extension of terminology have been required. An attempt has been made to classify logically the nonlinear circuit elements and the separate and combined functions that are obtained from the use of both linear and nonlinear circuit elements. The classification is not exhaustive, but it is believed to cover all practical cases of the radar circuit technique. The subject of amplification is treated in Vol. 18, and the more complex functions derived from those basic processes are time measurement, computation, and cathode-ray-tube display; these are discussed in Vols. 20, 21, and 22.

Much important material in this field is already available in standard texts on communications and electronics, and some of this background material has been omitted. The method of approach to the subject matter of this book probably differs from that of standard text books; the authors of this volume are experimentalists, none are teachers. The experimental point of view has, therefore, been definitely emphasized, and many important details on the physical realizability of electronic circuits are included. Mathematical representation of most of these circuits is difficult because they depend upon nonlinearities, and the avail-

able mathematics on this subject has not yet proved to be of great value in the analysis and design of practical circuits.

The approach to the writing of this book differs in a second way from that of other books. Much of the information presented here has not yet appeared in journal articles or comprehensive reports. Therefore, much of the original material has not yet stood the test of wide circulation and discussion. It has been extremely difficult to establish the proper perspective with regard to much of the material, and some distortions in the value of subject matter, remaining from the influence of the war effort, may still be evident.

The foreword has already indicated the difficulty of giving proper credit to all those who have contributed to the writing or to the experimental developments that have made the work possible. Many of the circuits described here originated in other laboratories in this country or in the United Kingdom, and much credit is due these workers. However, references in the text have been limited to (1) journal papers written by personnel of radar laboratories and (2) declassified reports on radar. Much of the success of this particular volume is due to the perseverance, self-sacrifice, and loyalty of those members of the former Precision Group of the Radiation Laboratory who have continued with this project to its successful termination.

It is a special pleasure to acknowledge the generous support and encouragement of this project by the British Laboratories—brought about largely through the efforts of Sir Robert Watson-Watt and Dr. B. V. Bowden. Through their generosity and that of F. S. Barton of BAC and W. B. Lewis of TRE, several experts have visited with the Radiation Laboratory Office of Publications for a month at a time in order to exchange information, and credit is due N. F. Moody of TRE, who contributed data on British circuits. We are extremely fortunate in having one member of TRE (F. C. Williams) as a major contributor and volume editor.

A number of Staff Members have contributed valuable background material that has been extremely useful in preparing the final manuscript: E. B. Hales, J. Irving, C. Sherwin, L. Pourciau, and R. B. Woodbury.

Of the many waveform photographs used to illustrate this volume, nearly all were taken by C. M. Connelly, the associated photographic work having been carried out by P. D. Bales. Credit for this work is gratefully acknowledged.

Much credit is due those who have assisted in the mechanical task of preparing manuscript. The work of Nora Van der Groen and Joan Leamy was outstanding. The assistance of the following is also gratefully acknowledged: Alyce Rueckert, Helene Benvie, Joan Brown, Teresa Sheehan, Barbara Davidson, and Hannah Paul.

The production and drafting problems could never have been solved without the able support of the typing pool and drafting room under C. Newton, M. Dolbeare, M. Phillips, and V. Josephson. In addition, the careful supervision of English and style under the guidance of L. B. Linford has been most helpful.

The publishers have agreed that ten years after the date on which each volume in this series is issued, the copyright thereon shall be relinquished, and the work shall become part of the public domain.

THE AUTHORS.

CAMBRIDGE, MASS.,  
*October, 1948.*



# Contents

---

FOREWORD . . . . .	vii
PREFACE. . . . .	ix
CHAP. 1. INTRODUCTION . . . . .	1
SCOPE AND VIEWPOINT. . . . .	1
1-1. Viewpoint . . . . .	1
1-2. Relation to Preceding Books. . . . .	3
1-3. Content of This Volume . . . . .	4
1-4. Relation to the Succeeding Volumes . . . . .	5
1-5. Method of Treatment . . . . .	6
1-6. Uses of Waveforms. . . . .	7
BASIC CONCEPTS AND THE METHOD OF APPROACH. . . . .	8
1-7. Basic Concepts . . . . .	8
1-8. Method of Approach. . . . .	15
CHAP. 2. OPERATIONS ON WAVEFORMS WITH LINEAR CIRCUIT ELEMENTS . . . . .	17
2-1. Linear Circuit Elements. . . . .	17
2-2. Potential Division and Addition. . . . .	18
2-3. Waveform Shaping by Passive Elements . . . . .	19
2-4. Linear Amplifiers Using Negative Feedback. . . . .	24
2-5. Plate-to-grid Feedback Amplifiers . . . . .	27
2-6. Linear Shaping Amplifiers, Capacitance Feedback . . . . .	31
2-7. The Use of Operational Notation. . . . .	37
CHAP. 3. OPERATIONS WITH NONLINEAR CIRCUIT ELEMENTS . . . . .	40
INTRODUCTION . . . . .	40
3-1. Ideal Elements. . . . .	41
3-2. Basic Operations. . . . .	42
OPERATIONS WITH NONLINEAR CIRCUIT ELEMENTS. . . . .	43
3-3. Initiation of Waveforms . . . . .	43
3-4. Amplitude Selection . . . . .	44

3-5. Amplitude Comparison . . . . .	45
3-6. Time Selection . . . . .	47
3-7. Amplitude Modulation . . . . .	49
3-8. Time Modulation . . . . .	52
3-9. Phase Modulation . . . . .	53
3-10. Amplitude Demodulation . . . . .	53
3-11. Level-setting . . . . .	54
3-12. Time Demodulation . . . . .	55
3-13. Amplitude Discrimination . . . . .	57
CHARACTERISTICS OF NONLINEAR CIRCUIT ELEMENTS. . . . .	58
3-14. High-vacuum Diode . . . . .	58
3-15. <del>Contact</del> Rectifiers . . . . .	68
3-16. Photocells . . . . .	72
3-17. Cutoff in Grid Tubes . . . . .	73
3-18. Plate-voltage vs. Plate-current Nonlinearities . . . . .	77
3-19. Grid-current Nonlinearities . . . . .	80
3-20. Composite Characteristics . . . . .	81
3-21. Gas-filled Tubes . . . . .	82
3-22. Feedback Circuits . . . . .	85
3-23. Multiple Circuits . . . . .	86
3-24. Multivariable Elements . . . . .	87
3-25. Curved Characteristics . . . . .	91
3-26. Displacement Elements . . . . .	92
3-27. More Complete Descriptions of Physical Elements . . . . .	92
CHAP. 4. SINUSOIDAL WAVEFORM GENERATORS . . . . .	101
CONTINUOUS WAVES. . . . .	101
4-1. General Properties . . . . .	101
4-2. Resonant-circuit Oscillators . . . . .	104
4-3. Crystal Oscillators . . . . .	106
4-4. Phase-shift Oscillators . . . . .	110
4-5. Bridge Oscillators . . . . .	115
4-6. Negative-resistance Oscillators . . . . .	123
4-7. Beat-frequency Oscillators . . . . .	124
4-8. Electromechanical Sine-wave Generators . . . . .	125
STABILIZATION OF OSCILLATORS . . . . .	126
4-9. Amplitude Stabilization . . . . .	126
4-10. Frequency Stabilization . . . . .	128
POLYPHASE SINUSOIDS. . . . .	131
4-11. Generation of Circular Sweep for Cathode-ray Tube . . . . .	132
4-12. Resistance-reactance Phase Shifters . . . . .	136
PULSED OSCILLATIONS. . . . .	140
4-13. Ringing Circuit . . . . .	141
4-14. Pulsed Hartley Oscillator . . . . .	142
4-15. Pulsed Crystal Oscillators . . . . .	145

PULSED POLYPHASE SINUSOIDS . . . . .	148
4-16. RC-Feedback Circuit. . . . .	150
4-17. Phase-splitting Amplifier . . . . .	154
4-18. Pulsed Oscillations for Use with Synchros. . . . .	156
CHAP. 5. GENERATION OF FAST WAVEFORMS. . . . .	159
INTRODUCTION . . . . .	159
5-1. Methods and Principles in the Generation of Fast Waveforms. . . . .	159
5-2. Applications. . . . .	161
5-3. Other Practical Design Considerations . . . . .	162
MULTIVIBRATORS . . . . .	163
5-4. Bistable Multivibrators. . . . .	164
5-5. Monostable Multivibrators . . . . .	166
5-6. Astable Multivibrators . . . . .	171
5-7. Analysis of the Transition between States. . . . .	174
5-8. Analysis of the Timing Process . . . . .	177
5-9. Obtaining Fast Transition. . . . .	179
5-10. Monostable Circuits for Very Short Pulses . . . . .	179
5-11. Obtaining Fast Recovery—Highly Unsymmetrical Astable Multi- vibrators . . . . .	183
5-12. Triggering and Synchronization . . . . .	187
5-13. Stabilizing the Duration of a Quasi-stable State . . . . .	190
5-14. Varying the Duration of a Quasi-stable State . . . . .	194
PHANTASTRON-TYPE CIRCUITS. . . . .	195
5-15. Introduction: Miller Sweep Generation. . . . .	195
5-16. The Screen-coupled Phantatron. . . . .	197
5-17. The Sanatron and Sanaphant . . . . .	200
5-18. The Cathode-coupled Phantatron. . . . .	203
CHAP. 6. BLOCKING OSCILLATORS AND DELAY-LINE PULSE GEN- ERATORS. . . . .	205
6-1. Blocking Oscillators . . . . .	205
PULSE WAVEFORMS . . . . .	211
6-2. The Transformer. . . . .	211
6-3. The Tube. . . . .	213
TRIGGERING METHODS. . . . .	218
6-4. Introduction. . . . .	218
RECOVERY TIME . . . . .	223
6-5. General Considerations. . . . .	223
6-6. Frequency Division . . . . .	225
6-7. Random Variations in PRF. . . . .	225



PRACTICAL CIRCUITS. . . . .	226
6-8. General Considerations. . . . .	226
6-9. Plate-to-grid Feedback . . . . .	226
6-10. Some Applications of Blocking Oscillators. . . . .	233
6-11. Delay-line Pulse Generators. . . . .	238
6-12. Use of a Delay Line in Terminating a Step Function. . . . .	238
6-13. Feedback Networks . . . . .	242
6-14. Delay Line Used to Terminate Regenerative Action . . . . .	245
6-15. Duplication of Pulses by Means of Delay Lines . . . . .	247
CHAP. 7. GENERATION OF TRIANGULAR WAVEFORMS . . . . .	254
GENERAL CONSIDERATIONS. . . . .	254
7-1. Definition and Types. . . . .	254
7-2. Characteristics of Triangular Waveforms . . . . .	255
7-3. Uses of Triangular Waveforms. . . . .	257
7-4. Methods of Generating Triangular Waveforms. . . . .	257
DETAILED DISCUSSIONS OF METHODS OF GENERATION . . . . .	259
7-5. Condenser Charging through Resistor. . . . .	259
<i>Use of High Variational Impedance. . . . .</i>	261
7-6. Inductance in Series with Resistor . . . . .	261
7-7. Vacuum-tube Variational Impedances . . . . .	264
<i>Circuits Involving Positive and Negative Feedback. . . . .</i>	266
7-8. Use of the Cathode Follower . . . . .	267
7-9. A Cathode-follower Circuit with a Compensating Network . . . . .	274
<i>Circuits Involving Negative Feedback. . . . .</i>	278
7-10. General Theory and Classification . . . . .	278
7-11. Single-stage Amplifier Circuits, Externally Gated. . . . .	280
7-12. Multistage Amplifier Circuits, Externally Gated. . . . .	284
7-13. Internally Gated Circuits. . . . .	285
CHAP. 8. GENERATION OF SPECIAL WAVEFORMS . . . . .	289
8-1. Introduction. . . . .	289
8-2. Special Triangles and Rectangles. . . . .	290
8-3. Trapezoids . . . . .	297
8-4. Exponentials . . . . .	297
8-5. Hyperbolas . . . . .	301
8-6. Hyperbolic Waveforms by Algebraic Operations; by Charge Compensation. . . . .	302
8-7. Hyperbolic Waveforms by Summing Exponentials . . . . .	304
8-8. Parabolas. . . . .	305
8-9. Higher Powers and Series Approximations. . . . .	312
8-10. The Sums of Sinusoids . . . . .	318
8-11. Pulse Shaping. . . . .	318
8-12. Approximation of Curves by Segments . . . . .	318

SPECIAL CURRENT WAVEFORMS . . . . .	317
<i>Introduction</i> . . . . .	317
8-13. Derivation of a Current Waveform from a Voltage Waveform. . .	317
8-14. Current-waveform Generators. . . . .	318
8-15. Level-setting of Current Waveforms . . . . .	321
CHAP. 9. AMPLITUDE, SELECTION, COMPARISON AND DISCRIMI- NATION. . . . .	325
9-1. Introduction. . . . .	325
9-2. Amplitude Selection . . . . .	325
9-3. Diode Selectors . . . . .	328
9-4. Germanium-crystal Selectors . . . . .	331
9-5. Triode and Pentode Selectors . . . . .	331
9-6. Compensation of Cathode Drifts. . . . .	333
9-7. Quasi Selectors. . . . .	334
9-8. Amplitude Comparison. . . . .	335
9-9. Amplifiers for Comparators . . . . .	335
9-10. Simple Diode Comparator. . . . .	338
9-11. Grid-controlled Comparators . . . . .	339
9-12. Multivibrator Comparators . . . . .	341
9-13. Blocking-oscillator Comparator . . . . .	342
9-14. The Multiar. . . . .	343
9-15. Other Forms of the Multiar. . . . .	344
9-16. Two-way Comparators . . . . .	348
9-17. Sine-wave Comparators . . . . .	348
9-18. Sine-wave Peak Comparison. . . . .	350
9-19. Sine-wave Zero Comparison. . . . .	352
9-20. Sine-wave-comparator Amplifiers. . . . .	355
9-21. Amplitude Discrimination. . . . .	357
9-22. Direct-coupled Discriminators. . . . .	358
9-23. Modulated-carrier-amplitude Discriminators. . . . .	362
CHAP. 10. TIME SELECTION . . . . .	364
10-1. Introduction. . . . .	364
10-2. Amplitude Selectors . . . . .	365
10-3. Switch Circuits . . . . .	370
10-4. Multiple-coincidence Circuits . . . . .	381
10-5. Adjacent Time Selectors . . . . .	384
10-6. Cathode-ray-tube Displays . . . . .	387
CHAP. 11. ELECTRICAL AMPLITUDE MODULATION . . . . .	389
11-1. Introduction. . . . .	389
11-2. Signal-controlled Amplitude Selectors. . . . .	390
11-3. Carrier-controlled Switches . . . . .	396
11-4. Balanced Triodes, Tetrodes, and Multigrid Tubes . . . . .	413
11-5. Variable-capacitance Modulators. . . . .	418
11-6. Negative-feedback Diode Modulator . . . . .	420
11-7. Modulation with Nonlinear Magnetic Circuits. . . . .	421
11-8. Summary. . . . .	425

CHAP. 12. ELECTROMECHANICAL MODULATORS . . . . .	427
12-1. Introduction . . . . .	427
POTENTIOMETERS . . . . .	428
12-2. Fundamental Characteristics . . . . .	428
12-3. Linear Potentiometers . . . . .	431
12-4. Sinusoidal Potentiometers . . . . .	434
12-5. Nonlinear Potentiometers . . . . .	436
12-6. Synchros . . . . .	439
12-7. Use with Sinusoidal Carriers . . . . .	444
12-8. Complex-voltage-waveform Modulation—The Problem . . . . .	447
12-9. Complex-current-waveform Modulation . . . . .	450
12-10. Variable Condensers . . . . .	455
12-11. Use with Sinusoidal Carrier . . . . .	457
12-12. Complex-waveform Modulation . . . . .	461
12-13. Variacs . . . . .	463
12-14. Photomechanical Modulators . . . . .	463
CHAP. 13. TIME MODULATION . . . . .	466
13-1. Introductory Remarks . . . . .	466
GENERAL PROPERTIES OF T-M WAVEFORMS . . . . .	466
13-2. Examples of T-m Waveforms . . . . .	466
13-3. Fundamental T-m Methods . . . . .	467
13-4. Applications . . . . .	469
13-5. Transfer Functions—Linear and Nonlinear . . . . .	470
13-6. Control Signals . . . . .	471
13-7. Errors—General Accuracy Considerations . . . . .	472
VOLTAGE SAWTOOTH METHOD . . . . .	477
13-8. Introduction . . . . .	477
13-9. Representative Circuit. Switching and Comparison Methods . . . . .	477
13-10. Problems with Miller Negative-going Sweeps . . . . .	483
13-11. Slow and Nonlinear Sweeps—Regenerative Pickoffs . . . . .	485
13-12. Internally Gated Circuits . . . . .	486
PHASE-MODULATION METHOD . . . . .	490
13-13. Introduction . . . . .	490
13-14. Phase-modulating Potentiometer . . . . .	491
13-15. Phase-shifting Condensers . . . . .	492
13-16. Synchro Phase-modulators . . . . .	497
STORAGE TUBE METHOD . . . . .	499
13-17. Storage Tubes . . . . .	499
CHAP. 14. AMPLITUDE AND TIME DEMODULATION . . . . .	501
14-1. Introduction . . . . .	501
14-2. Types of Amplitude Demodulation . . . . .	502
14-3. Amplitude Selectors . . . . .	503

14-4.	Phase-sensitive Detectors. . . . .	511
14-5.	Demodulators Employing Switching . . . . .	513
14-6.	Difference Detectors with Constant Output. . . . .	524
14-7.	General Considerations in Time Demodulation. . . . .	532
14-8.	Simplified Negative-feedback Time Demodulator. . . . .	537
14-9.	Mechanical Demodulation by Cathode-ray-tube Display . . . .	539
14-10.	Amplitude Demodulation by Electronic Servomechanisms. . . .	543
CHAP. 15. SINUSOIDAL FREQUENCY MULTIPLIERS AND DIVIDERS		545
SINUSOIDAL FREQUENCY MULTIPLIERS. . . . .		545
15-1.	Introduction. . . . .	545
15-2.	Harmonic Generation. . . . .	546
15-3.	Frequency-selecting Filters . . . . .	548
<i>Frequency Multipliers</i> . . . . .		551
15-4.	Practical Multiplier Circuits. . . . .	551
SINUSOIDAL FREQUENCY DIVIDERS. . . . .		556
15-5.	Introduction. . . . .	556
15-6.	Dividers Using a Time Base. . . . .	559
15-7.	Regenerative Dividers . . . . .	560
15-8.	Dividers with Regeneration and Modulation. . . . .	562
CHAP. 16. PULSE-RECURRENCE-FREQUENCY DIVISION. . . . .		567
GENERAL CONSIDERATIONS. . . . .		567
16-1.	Definition. . . . .	567
16-2.	Characteristics of Pulse-recurrence-frequency Dividers . . . .	567
16-3.	Uses of Pulse-recurrence-frequency Dividers. . . . .	568
16-4.	Methods for Accomplishing Continuous Pulse-recurrence-frequency Division. . . . .	569
SOME FUNDAMENTAL CIRCUITS AS CONTINUOUS FREQUENCY DIVIDERS . . .		572
16-5.	Monostable Multivibrators . . . . .	572
16-6.	Astable Multivibrator Dividers . . . . .	575
16-7.	Phantastron-type Dividers . . . . .	577
16-8.	Blocking Oscillator Dividers. . . . .	582
16-9.	Blocking Oscillators in Divider Chains . . . . .	588
16-10.	Gas-tube Dividers . . . . .	591
MORE ELABORATE DIVIDER SCHEMES, AND INTERMITTENT-FREQUENCY DIVISION . . . . .		592
16-11.	Pulse-selection PRF Dividers . . . . .	592
16-12.	Frequency Division Using Resonant Stabilization . . . . .	595
16-13.	Divider Chains with Feedback. . . . .	599
16-14.	Intermittent Pulse-recurrence-frequency Division . . . . .	600
CHAP. 17. COUNTING. . . . .		602
INTRODUCTION . . . . .		602
17-1.	The Problem . . . . .	602
17-2.	General Method. . . . .	602

SEQUENCE CIRCUITS. . . . .	604
17-3. Scale-of-two. . . . .	604
17-4. Thyatron Ring Counters. . . . .	612
ENERGY STORAGE COUNTERS . . . . .	614
17-5. General Considerations. . . . .	614
17-6. Storage Circuits . . . . .	615
17-7. Energy-storage Counter Circuits. . . . .	619
17-8. Combination of Counters . . . . .	624
CHAP. 18. MATHEMATICAL OPERATIONS ON WAVEFORMS—I. . . .	629
ADDITION AND SUBTRACTION OF VOLTAGES AND CURRENTS . . . . .	629
18-1. General Considerations. . . . .	629
18-2. Linear Passive Networks . . . . .	632
18-3. Addition and Subtraction by Means of Vacuum Tubes . . . . .	640
18-4. Summary. . . . .	647
DIFFERENTIATION AND INTEGRATION. . . . .	648
18-5. Methods of Differentiation and Integration . . . . .	608
18-6. Theoretical Approaches. . . . .	654
18-7. Practical Circuits . . . . .	658
CHAP. 19. MATHEMATICAL OPERATIONS ON WAVEFORMS—II . . .	667
19-1. Introduction. . . . .	667
MULTIPLICATION AND DIVISION. . . . .	668
19-2. Relation of Multiplication to Other Operations . . . . .	668
19-3. Multipliers Using Tube Characteristics. . . . .	669
19-4. Logarithmic Devices . . . . .	670
19-5. Multiplying Devices Using Carrier Waveforms. . . . .	674
SQUARES AND SQUARE ROOTS. . . . .	678
19-6. Circuits for Producing Squares and Square Roots . . . . .	678
19-7. Squaring Circuits . . . . .	679
19-8. Square-root-extracting Circuits . . . . .	686
19-9. Other Quadratic Elements. . . . .	691
19-10. Testing of Circuits Producing Squares and Square Roots . . . . .	693
CHAP. 20. OSCILLOSCOPIC TECHNIQUES IN WAVEFORM MEASURE- MENT . . . . .	694
20-1. Introduction. . . . .	694
20-2. Oscilloscopes and Meters . . . . .	694
20-3. Amplitude Measurements. . . . .	695
20-4. Time Measurements . . . . .	697
20-5. Waveform Measurements. . . . .	699
20-6. Frequency Measurements. . . . .	702
20-7. Phase Measurements. . . . .	705

20-8. Impedance Measurements. . . . .	706
20-9. Harmonic Distortion in Pulsed Sinusoids . . . . .	706
CHAP. 21. STORAGE TUBES. . . . .	707
INTRODUCTION . . . . .	707
21-1. General Definition of a Storage Tube. . . . .	707
21-2. General Methods, Applications . . . . .	707
21-3. Theory of Storage Action. . . . .	708
21-4. Deflection Modulation . . . . .	713
21-5. Signal-plate Modulation . . . . .	714
21-6. Focus Modulation . . . . .	716
21-7. Frequency-modulated Carrier with Intensity Modulation . . . . .	716
DESCRIPTION OF APPARATUS USED IN STORAGE-TUBE EXPERIMENTS . . . . .	717
21-8. Intensity Modulation Tests. . . . .	717
21-9. Deflection Modulation Tests. . . . .	722
21-10. Storage-tube Synchronizing Devices . . . . .	727
21-11. Storage-tube Time Demodulator . . . . .	728
CHAP. 22. ELECTRICAL DELAY LINES . . . . .	730
22-1. Introduction. . . . .	730
THEORY OF ELECTRICAL DELAY LINES. . . . .	731
22-2. Propagation Function and Characteristic-impedance Function. . . . .	731
<i>Response of Networks with Particular <math>\gamma</math> and <math>Z_0</math> Functions</i> . . . . .	732
22-3. Ideal Transmission Network and Distortion. . . . .	732
22-4. Amplitude Distortion. . . . .	733
22-5. Phase Distortion. . . . .	735
22-6. Amplitude and Phase Distortion. . . . .	739
22-7. Reflection. . . . .	742
TYPES OF DELAY LINES . . . . .	742
22-8. Lumped-constant Lines. . . . .	743
22-9. Distributed-constant Lines . . . . .	745
22-10. Correction Methods . . . . .	746
USES OF DELAY LINES. . . . .	747
22-11. Synchronization and Generation of Waveforms . . . . .	747
22-12. High-impedance Cable . . . . .	748
MEASUREMENT OF PROPERTIES OF DELAY LINES . . . . .	749
22-13. Attenuation Function $\gamma_1$ . . . . .	749
22-14. Phase Function $\gamma_2$ . . . . .	749
22-15. Characteristic Impedance. . . . .	750
CHAP. 23. SUPERSONIC DELAY DEVICE . . . . .	751
23-1. Introduction. . . . .	751

THEORY OF SUPERSONIC DELAY DEVICE . . . . .	752
23-2. The Quartz Crystal as an Electromechanical Transducer . . . . .	752
23-3. Acoustical Media . . . . .	755
23-4. Radiation and Propagation . . . . .	757
23-5. Some Special Cases of Transducer Equivalent Circuits and Associated Electrical Circuits . . . . .	759
SOME EXAMPLES OF DELAY LINES. . . . .	752
23-6. "Trigger" Delays . . . . .	762
23-7. Delay Lines Providing Faithful Reproduction . . . . .	763
BIBLIOGRAPHY . . . . .	764
APPENDIX A: Negative-capacity Amplifier . . . . .	767
APPENDIX B: Cathode-compensated Amplifier. . . . .	771
GLOSSARY . . . . .	775
INDEX . . . . .	777

## CHAPTER 1

### INTRODUCTION

BY BRITTON CHANCE AND F. C. WILLIAMS

#### SCOPE AND VIEWPOINT

BY BRITTON CHANCE

This book deals with the applications of circuit techniques to the generation of waveforms, both sinusoidal and otherwise, and to the manipulation of waveforms to meet specific needs. The title, *Waveforms*, refers to currents or voltages considered as functions of time in a rectangular coordinate system. This book includes a discussion of those waveforms having durations as short as  $0.01 \mu\text{sec}$ .

**1.1. Viewpoint.**—One object of this book is obvious: it is to make available to those in industrial and academic laboratories techniques of established value that have been developed for radar timing and indicating applications, and it is intended to survey not only developments made at the Radiation Laboratory but also developments made at other laboratories in this country and in the United Kingdom. In this respect we are particularly fortunate in having had the closest cooperation with these laboratories.

This book is written for the circuit designer in government, industrial, or academic research laboratories who chooses to carry out a timing, computation, or measurement operation by means of electrical circuits. The material of the book has therefore been classified according to circuit functions, in order that the circuit designer may immediately find a compilation of useful circuits for accomplishing a particular function and select the one best suited to his needs.

In this respect the classification of material differs somewhat from that of earlier books concerned with electronic circuits where classification according to circuit type or tube type was often employed. Considerable difficulty was experienced in attempting to use such a classification because of the versatile nature of electrical circuits. For example, electronic switches may be used to carry out many entirely different functions in which the design considerations of the associated circuits are quite dissimilar, although the actual switching elements are identical. A similar difficulty arises in discussing a circuit like the multivibrator; it too may



be used for a variety of purposes. Yet the design considerations differ markedly depending upon whether it is used, for example, for pulse generation or for frequency division.

The material of this book begins with a survey of the properties of linear and nonlinear circuit elements which are applicable to all the circuit functions of the book. From that point on the discussion proceeds according to function—first the generation of simple waveforms, next the processes of amplitude and time analysis, modulation, demodulation, and frequency multiplication and division. Mathematical operations and the properties of special components constitute the closing chapters. This classification permits easy comparative evaluation of the various methods for accomplishing a given function and a reasonably complete summary of the useful methods. The discussion is continued on the functional viewpoint to the more complex systems for time measurement, data transmission, computation, and display, which are the subjects of Vols. 20, 21, and 22 of the Series.

In connection with these circuit developments there has been an even more active development in a highly descriptive circuit jargon in the various laboratories. This jargon is word-saving and often presents a vivid picture of the physical operations of the particular circuit—for example, “flip-flop” or “flopover,” referring to different types of multivibrator circuits. Considerable difficulty has been encountered in adhering to the colloquial jargon throughout this book since many of these names refer to a specific circuit but connote an action obtainable from many circuits. For example, a thyratron pulse generator can be made to carry out all the functions of a “flip-flop” but rarely bears this name. It has, therefore, been necessary to define new terms which may have a greater generality of application. In choosing these terms, an attempt has been made to define only the basic processes and circuit functions and to maintain the “given” name for the various circuits—for example, multivibrator, phantatron, sanatron, blocking oscillator, etc. A glossary of terms starts on page 775, and it is intended that this be the connecting link between the terminology in this book and that used in various laboratories.

Finally, we have attempted to indicate some directions in which future developments can proceed. Nearly always limits to the performance have been set by the characteristics of circuit components, such as vacuum tubes, resistors, capacitors, transformers, etc. Much progress has been made in the standardization and in the improvement of the quality of circuit components during the war, but there yet remain many basic factors that limit the rapidity or the stability of action of these circuits. Whenever possible, the limitations imposed by available components have been pointed out, and in many cases a comparison of com-

ponents is made. It is our hope that the discussions are presented in such a manner as to stimulate original thought and circuit development by the reader.

**1-2. Relation to Preceding Books.**—Volumes 17 to 22 of this series include the important phases of the work of the Receiver Components Division of the Radiation Laboratory, and hence much of the material in these volumes is closely related. Some of the material of these volumes has applications in other volumes of this series, in particular that concerned with Pulse Generators (Vol. 5) and those concerned with Systems (Vols. 1 to 3). Since much of this work concerns properties of circuit components themselves, the first volume of the group, Vol. 17, is called *Components Handbook* and includes available information on fixed components, resistors, capacitors, and inductors, and much information about the characteristics of precision potentiometers, variable capacitors, and synchros. In addition, the characteristics of vacuum and gas-filled tubes are presented. This material is of particular interest for circuit designs that require operation with a high degree of precision over a wide range of temperatures. Much of this material is essential to the satisfactory construction of the circuits described in this volume, and, unless the reader has similar information already available, he is referred to Vol. 17 before embarking upon the construction of any of the precision circuits of this book and of Vols. 20 and 21.

Volume 18, *Vacuum-tube Amplifiers*, is of some interest to the readers of this book because of the extensive discussion of linear analysis and transient response and the transfer characteristics of linear circuit elements. In addition, wide-band amplifiers are discussed in detail. Although the requirements for these amplifiers are not usually identical with those used in waveform generation, many important data on the operation of wideband amplifiers with and without feedback for waveform amplification are presented and are extremely valuable to the reader of this book. The discussion of direct-coupled amplifiers, low-frequency high-precision amplifiers, and frequency-selective amplifiers is also useful.

Many of the circuits described in the present volume have been presented in earlier works, but the application of these circuits to radar has resulted in basic improvements and in the extension of the operating range of the circuits. The circuit technique previous to the war is well represented in a number of textbooks to which the reader may refer.<sup>1</sup>

<sup>1</sup> H. J. Reich, *Theory and Applications of Electron Tubes*, McGraw-Hill, New York, 1944; F. E. Terman, *Radio Engineers' Handbook*, McGraw-Hill, New York, 1943; F. E. Terman, *Radio Engineering*, 2nd ed., McGraw-Hill, New York, 1937; M.I.T. E. E. Staff, *Applied Electronics*, Wiley, New York, 1943; J. G. Brainerd *et al.*, *Ultra-high-frequency Techniques*, Van Nostrand, New York, 1942; O. S. Puckle, *Time Bases*,

**1-3. Content of This Volume.**—This book covers several definite aspects of circuit techniques involving precisely controlled voltages and currents of various waveforms. There are two introductory chapters (2 and 3) dealing with operations on waveforms with linear and nonlinear circuit elements. The application of these basic elements to the generation of waveforms is the subject of the next chapters (4, 5, 6, 7, and 8). Sinusoids, pulses, rectangles, triangles, trapezoids, hyperbolas, parabolas, and exponential waves of both voltage and current are considered in detail with special regard to methods which ensure their rapid initiation and the accurate control of their shape. The next two chapters of the book (9 and 10) are devoted to a discussion of the methods for analyzing a waveform with respect to amplitude or time, and include the various methods of selecting a portion of a given wave. Special emphasis is placed upon the important process of marking the instant of equality of two waves, which is basic in precision timing techniques.

Variation of the parameters of amplitude- or time-analysis methods also leads to important modulation and demodulation processes, and the next chapters (11, 12, 13, and 14) treat those methods of modulation and demodulation which have been found to be of most use in precision circuits. At this point the scope of the book is expanded to include operations with slowly varying voltages or mechanical signals, since many important circuit operations depend upon modulation in accordance with controllable shaft rotation. The complementary demodulation processes are presented, and special emphasis is given to those circuits that are suitable for operating with intermittent waveforms.

The important process of linearly modulating the time interval between two portions of a waveform (linear time modulation) is discussed in some detail since this is a basic process in accurate time measurement, and a summary of methods is included. It is unfortunate that time did not permit a presentation of the methods of frequency modulation and frequency selection. Much of this material has been covered in standard texts and, in addition, some twin-T selective circuits are given in Vol. 18, Chap. 10.

The next three chapters—15, 16, and 17—treat the basic aspects of the synchronization of waveform generators to accomplish frequency multiplication and division of sinusoids or pulses. Many of these processes depend upon aperiodic counting circuits, and a chapter is devoted to their characteristics.

The precision of the basic processes described in the earlier chapters is sufficient to permit a number of basic mathematical operations to be carried out with reasonable accuracy. For example, a hyperbolic wave

may be used to solve a right triangle, or a parabolic wave may be generated to obtain the square of a quantity. Methods of addition, subtraction, differentiation, integration, multiplication, division, squaring, and square-root extraction are given in Chaps. 18 and 19.

Chapter 20 treats the techniques used in the measurements of waveforms which can be carried out with a simple oscilloscope. This chapter does not, however, treat oscilloscope-design principles.

The last chapters treat delay devices which are a specialized but extremely important class of components in which an input wave is reproduced at the output after a fixed delay. The cathode-ray-tube storage device is the most recent and certainly the most versatile of these, and the available data are summarized. In addition, a treatment of the properties of electrical delay lines and supersonic devices is given in the closing chapters.

**1-4. Relation to the Succeeding Volumes.**—The application of the basic circuits of the present volume to the problems of radar range measurement, precision data transmission, and computation is the content of the next two books, Vols. 20 and 21. In addition, the application of the various timing waves to cathode-ray-tube display systems is the subject of Vol. 22. Lastly, some of the timing and synchronizing circuits are used in microwave receivers, the subject of Vol. 23. The interdependence of this book and Vol. 20, *Electronic Time Measurements*, is, however, the greatest, and much of the material of that book represents a natural continuation from the material on time modulation and frequency multiplication and division to the problem of synchronization and precision time measurement in radar systems. For example, Chap. 4 of Vol. 20, "Fixed-time Markers," is a natural extension of the basic circuits for frequency multiplication and division. Similarly the details of construction and performance of precision time modulators useful in radar systems are given in Chaps. 5 and 6 of Vol. 20. Chapters 7, 8, and 9 of Vol. 20 give examples of manual and automatic time-measuring systems. Chapters 10 and 11 continue the application of pulse-timing techniques to precision data transmission, and Chap. 12 gives the detailed considerations involved in the cancellation of waveforms through the use of supersonic delay devices.

The material of Vol. 21 dealing with automatic computation and electronic-instrument servomechanisms depends to a certain extent on the material of this volume. The portions of that book devoted to voltage and current regulators and to design and construction practice are of considerable importance for those interested in building a complete apparatus that will perform satisfactorily under adverse conditions. In addition, a portion of Vol. 21 is devoted to the characteristics of test equipment for timing and computation devices.

**1-5. Method of Treatment.**—The method of approach to the content of this book is discussed in considerable detail later, but it is suitable to state here that the main emphasis is upon what the circuit does, how it does it, and what difficulties the circuit designer would have to avoid in order to duplicate the results quoted. Wherever possible, a diagram of a well-engineered circuit and the characteristics of precision components are given.

A number of waveform photographs have been taken at various points in these circuits and are believed to illustrate their operation better than an equal amount of print.

The approach to the circuit technique described in this volume has not been strictly mathematical but as much mathematics as has been found useful has been included, and quantitative relationships are given wherever possible. Some of the nonlinear circuits discussed—notably the blocking oscillator and to a lesser extent the multivibrator—pose very difficult and as yet unsolved mathematical problems, and no rigorous mathematical design procedures are yet available which apply in general to these circuits. A satisfactory approach to circuit-design problems is described in the next section and includes a subdivision of the operation of the nonlinear circuit into several stages, in each of which the operation is approximately linear. In addition, an extremely useful table for the shaping properties of various linear networks and a simplified operator technique greatly implement the problems of circuit design. Unfortunately, many of the circuit designs of this volume were carried out without the benefit of these useful tools.

Of particular importance are the improvements in the precision, reliability, and producibility of the circuits described here since vast numbers of similar equipments have been called upon to operate under singularly adverse conditions and have been required to give visual or other indications to a high degree of precision. It is possible that the enduring value of this work will lie more in the basic approaches to the question of precision than in the specific circuits that have been developed under the urgent stress of war conditions.

In approaching the problems of precision, reliability, and producibility, the circuit engineer has summarized these requirements by a single requirement—"designability"—that is, the development of circuits whose operation can be predicted accurately. If component tolerances and the conditions of service (temperature range, humidity, etc.) have been taken into account and a single experimental model has been built, it is to be expected that a "designable" circuit can be reproduced in quantity with no further difficulty. Although this circuit design often leads to the use of more components than the minimum necessary, these extra components are usually paid for in terms of increased reliability, producibility, and

precision. In addition, the servicing problem should be more simple, since the operation of the circuit can be precisely specified, and consequently the location of a fault can be easily determined. The design principle has, of course, wide acceptance in most branches of engineering, but because of the difficulties in specifying all the properties of the components used in circuit design, the specialized nature of the design work, and, on the other hand, the extreme ease of assembly and modification of experimental electrical equipment, this principle has not found universal acceptance. This is especially true in the case of extremely complex circuit configurations, components for which complete specifications are not available, or circuits involving excessive nonlinearities. The approach to the circuit technique presented in the next section, however, gives general principles whereby the principle of "designability" may be applied to most of the circuits of this volume.

Definite exceptions to the principle of designability may be made in experimental equipment where production is not required and where the useful life of the apparatus may be considerably less than that of the components. Such equipment is often used in physical experiments and usually operates as closely as possible to the fundamental limitations of the components in order that the maximum sensitivity and accuracy may be obtained.

**1-6. Uses of Waveforms.**—The principal uses of waveforms are indicated by the content of the other volumes associated with this book, and the discussion already given in Sec. 1.4 indicates such applications. These and other important applications are enumerated as follows:

1. Timing waveforms for cathode-ray-tube displays.
2. Fixed electronic timing indices.
3. Movable electronic timing indices.
4. Synchronization of timing circuits including frequency multiplication and division.
5. Synchronization in angle for cathode-ray-tube or other display.
6. Precise communication of audible or positional information by pulse timing methods.
7. Application to high-resolution television.
8. Applications of precise timing techniques to electrophysiology.
9. Application of precise measurement techniques in physics, chemistry, and biology.
10. Applications of precise time-measurement techniques to nuclear physics.

There are, in addition, two important applications which present important possibilities but about which very little has been done as yet. The first is the use of waveforms in computation. The simple mathe-

mathematical operations, especially integration, have been carried out with reasonable accuracy and appropriate methods are described in this volume. But the more promising use of these pulse techniques appears to be in the sequential or digital computers.<sup>1</sup> These computers permit extreme flexibility and rapidity in the mathematical solution of complex problems, and a pulse representation of mathematical quantities is of great use in these projects, as are the methods of storing and counting information.

Amplitude or time-modulated pulse trains present interesting possibilities for multichannel communication, since the mutual interference-rejection property of simple time selectors is excellent compared with that of more complicated frequency selectors.

Lastly, many applications of this precision circuit technique to industrial measurement and process control are possible, and it is believed that the basic material of this book combined with the practical examples of time measurement and computation in Vols. 20 and 21 will suggest to the reader a large number of new practical applications.

## BASIC CONCEPTS AND THE METHOD OF APPROACH

BY F. C. WILLIAMS

Previous treatment of waveforms has been directed mainly to sinusoids and the various manipulations that can be performed on them, such as addition (and subtraction), amplification, modulation and demodulation in amplitude, frequency, and phase. Some attention has been given to the effect of nonlinearities, but this effect has most often been treated in terms of the harmonic distortion introduced. This distortion has usually been reduced by avoiding nonlinearities. In modulation and demodulation, however, nonlinear elements have been widely employed, but even here, Fourier analysis, in terms of harmonic components, is often used as an analytical weapon. It has also been the practice to break up complex waveforms into their sinusoidal components to render them suitable for formal mathematical attack.

In approaching the subject matter of this book it is preferable to make a clean break with the traditional approach. It is the object of this chapter to indicate why this is so, to outline the new approach, and to illustrate briefly by example the new processes and concepts that are to be discussed in detail in later chapters.

**1-7. Basic Concepts.** *Linear Elements.*—The waveforms that will be considered are not sine waves, but square waves, pulses, and even more complicated shapes (see Fig. 1-1). When two waves are added, the result is far less similar to the originals than is the case with sine waves, and

<sup>1</sup> "Eniac," Moore School of Electrical Engineering, U. of Pennsylvania.

the concepts of amplitude change and phase shift are of little use; they are largely replaced by new concepts of shape, duration, and time of occurrence. Again, complex networks that merely shift the phase and modify the amplitude of a sine wave completely transform the shape of

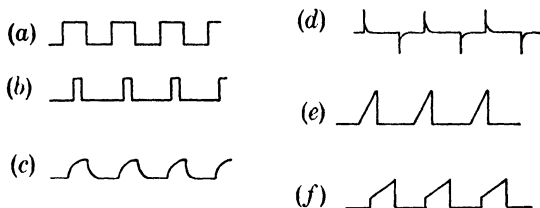


FIG. 1.1.—Examples of waveforms. (a) Symmetrical rectangular wave (square wave). (b) Pulses. (c) Result of quasi integration of (a). (d) Result of quasi differentiation of (a). (e) Triangular wave. (f) Trapezoidal wave.

the nonsinusoidal input. The effect is illustrated in Fig. 1.2, which shows the effect of applying a sine wave and square wave to two  $RC$ -networks. The general process of changing wave shape by impedance relations, of which the above is an example, is termed “linear shaping.”

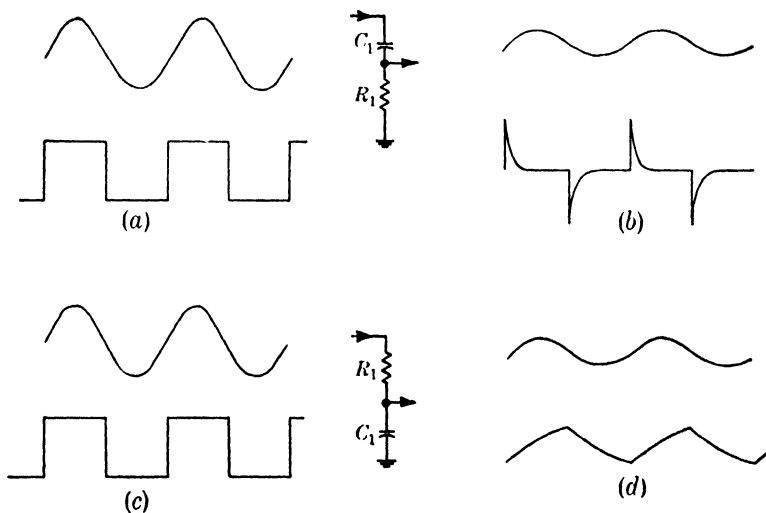


FIG. 1.2.—The effect of applying a sine wave and a square wave to two  $RC$ -networks. In (b) the sinusoid is attenuated by the ratio of the resistance to the total impedance. The square wave is, however, quasi-differentiated; only the high-frequency components are passed. In (d) the sinusoid is attenuated by the ratio of the reactance to the total impedance. The square wave is quasi-integrated; only the low frequency components are passed.

For reasons that will become apparent later the amplifier is rarely used in its normal role, but even when it is, the conditions of operation are somewhat different since now the highly critical eye, or the even more critical electrical instrument, replaces the rather indiscriminating ear, and higher fidelity is demanded. In this connection, negative-feedback



amplifiers have proved invaluable. Another very important use of negative feedback in amplifiers is the control it gives over input- and output-impedance characteristics. Many waveforms appear initially across unsuitably high impedances, and the amplifier may be used not to increase the size of the waveform but to make it available with low source impedance. The well-known cathode follower is a typical example. The process of linear shaping is often carried out in amplifiers, particularly in the negative feedback type; such amplifiers are called "linear shaping amplifiers."

*Use of Nonlinear Elements.*—Another method of changing wave shape is by overloading an amplifier. Here deliberate use is made of the nonlinearities at the extremities of thermionic-tube characteristics. These nonlinearities were previously regarded as a nuisance, but in this field

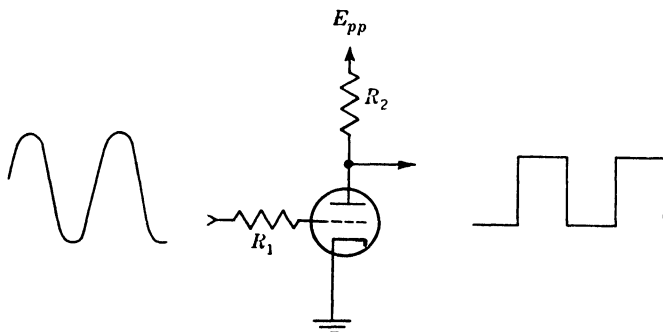


FIG. 1·3.—Conversion of a sinusoid to a square wave by an overloaded amplifier. The output is that which would be attained from a tube with zero grid base; actually the sides of the output waveform will not be vertical.

they are often of prime importance, the nuisance role being allotted often to the short, sensibly linear part which joins the nonlinearities. For example, in generating a square wave from a sinusoid, the circuit of Fig. 1·3 may be used. Here the grid is swung rapidly from cutoff to zero bias by a large sinusoidal input. The tube is either "turned on" or "turned off" for the bulk of the cycle, and the sensibly linear transition of anode current between these conditions is undesirable since it causes the sides of the output wave to be sloping instead of vertical. The shorter the linear part, in terms of grid voltage, the steeper the sides will be; the ideal would be to reduce it to zero.

In this example the nonlinear characteristic is regarded as having abrupt transitions between separate linear states rather than as a continuous nonlinear curve; the precise curvature of the characteristic is rendered unimportant by the use of a large input waveform. This is typical of the major use of nonlinear elements and will be discussed in more detail later (Sec. 1·8).

There are, of course, circumstances in which the circuit elements are required that have a continuous nonlinear law of specified shape, such as a parabolic or exponential curve. Typical uses of nonlinear operation of this type are in multiplication and division of the instantaneous values of two waveforms and in instantaneous squaring and extraction of square roots. Instances of this kind are, however, comparatively rare due in no small measure to the difficulty of obtaining in quantity elements that obey the required law with sufficient accuracy.

*Operations in the Amplitude Axis.*—Very often the precise position of a voltage waveform in the voltage axis (d-c level) is of considerable importance; it may be specified in two ways. First the mean level of the wave may be held at a particular voltage. This is the well-known process of

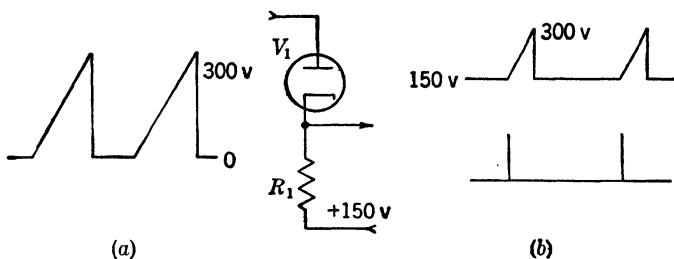


FIG. 1-4.—Amplitude selection and comparison. As the cathode of the diode  $V_1$  is biased at +150 volts, only that part of the triangular waveform exceeding +150 volts appears in the output as indicated at (b). The lower line of (b) indicates a pair of pulses derived by amplification and shaping. This combination of selection, amplification and shaping is termed “amplitude comparison.”

“biasing.” Second, a certain part of a waveform may be held at a certain voltage level. This is often called “d-c restoration.” Both are processes of “level setting.” The first involves linear and the second nonlinear elements.

When the general level of the wave has been fixed, it may be required to reproduce only that part of the wave that exceeds a certain level. This process is called “amplitude selection” and is illustrated in Fig. 1-4. Here a sawtooth waveform starting from zero volts is applied to the plate of a diode whose cathode is connected to 150 volts through the resistance  $R_1$ . The diode will not conduct until the input waveform exceeds 150 volts; thereafter conduction will cause the output to follow the input until the waveform once more falls below 150 volts and thus gives the output shown. The circuit in this way “selects” that part of the waveform that exceeds 150 volts.

The instants at which the input waveform has the value 150 volts are indicated by abrupt discontinuities in the slope of the output waveform. Since the sharpness of these discontinuities can be increased considerably by subsequent amplification, so an extremely abrupt dis-

continuity is obtained which can be used to mark precisely the instant of equality of the input wave and the fixed potential. The amplifier often includes shaping processes which produce a marker pulse, as shown on the lower line of Fig. 1-4b. In the interests of economy regenerative amplifiers are preferred to linear amplifiers for this purpose and will be discussed later. The general process of thus marking the instant of equality of two waveform amplitudes is called "amplitude comparison" and forms the basis of nearly all methods of precise range measurements.

Another important use of amplitude comparison is revealed if the 150-volt supply to which  $R_1$  is returned is replaced by a potential that varies relative to 150 volts in accordance with an input signal. The time elapsing between the start of the linear rise in  $a$  and the occurrence of the pulse in  $b$  will be modulated in accordance with the signal intelligence. This is an example of the important process of "time modulation." The inverse process, that of recovering the intelligence from a time-modulated waveform, is called "time demodulation."

Another useful process, somewhat similar to amplitude selection, is that of "amplitude discrimination." Here the objective is to determine whether one waveform is of greater or less amplitude than another; the magnitude of the difference is also indicated approximately, but the emphasis is on the sense of the difference. The process may be either continuous, as in the case of equating two continuous quantities, or discontinuous as in the equating of an amplitude-modulated sinusoid to a d-c reference level—for example, in automatic-gain-control circuits.

*Operations in the Time Axis.*—Corresponding to those processes in the amplitude axis there are similar processes in the time axis. These are known as "time selection," "time discrimination," and "time comparison." Here there is no fixed reference as there was in the amplitude axis, and its place must be taken by repeated reference points synchronous with the waveform. In many cases the reference point will be a portion of the waveform itself; in others it will exist separately as a pulse train.

In this connection it is of great value to consider only one complete cycle of the waveform and to treat the beginning of this waveform as a single reference point in the time axis. This is the picture that results from displaying the waveform on a cathode-ray tube with a linear sweep of duration equal to the waveform duration and triggered by the reference pulse or by the chosen reference point of the waveform. In this way, the complexities of multiple time references are avoided, and the discussion of operations in the time axis is simplified.

Time selection is the process of separating one event from other events by virtue of the time, relative to the reference instant, at which that event occurs. A crude example is the well-known phase-sensitive rectifier, where the circuit responds only to alternate half cycles. More refined

examples often occur in pulse-radar practice—for instance, where it is required to separate the echo of a particular object from other echoes, which may be similar except for the time delay with respect to the transmitted pulse. The selector will pass only that echo which arrives in an interval having a certain time delay. The system will, of course, provide no selection against echoes with equal or nearly equal time delays. Figure 1-5 shows a train of typical echoes *a*, together with a locally generated selector pulse *b*. This selector pulse is arranged to embrace the wanted echo. It is used to operate some form of switch circuit that will pass a signal occurring during the pulse and reject anything occurring before or after the pulse. The output waveform of the time selector is shown at *c*.

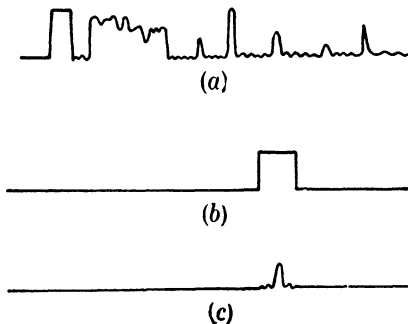


FIG. 1-5.—Time selection. A train of typical radar echoes is shown in (a). A locally generated selector pulse is indicated in (b), and the selected echo in (c).

If the train of echoes of Fig. 1-5*a* is displayed on a cathode-ray tube by means of the triangular timing wave of Fig. 1-4, an alternative method of time selection is available. A mechanical aperture may be used to block off all but the wanted pulse. For visual use this aperture, which might be movable, would perform the selection function. For nonvisual use, where an electrical signal is wanted, a photocell pickoff can be used. For this purpose an intensity-modulated display is preferable to the amplitude-modulated display shown.

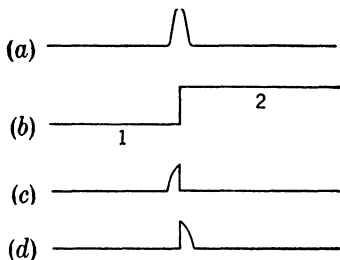


FIG. 1-6.—Time selection and discrimination. The portions of the pulse displayed in (a) overlapping Portion 1 and Portion 2 of selector pulse (b) are rectified and subtracted; the difference gives an indication of the relative times of occurrence of the signal and the step. The portions of the signal (a) occurring before and after selector pulse (b) are indicated as (c) and (d) respectively.

*b*, that portion of *a* occurring before the step can be compared with that portion occurring after the step, by rectifying the two portions separately and comparing the rectified output voltages. The portion selected for the first rectifier circuit *c* is obtained from a time selector operated by a selector pulse consisting of Portion 1 of pulse *b*, and that

Time selection with abrupt apertures as indicated in Fig. 1-5 can be made extremely sensitive to small variations of the relative times of occurrence of signal and selector pulse. An amplified view of a signal *a* and one edge of pulse *b* is indicated in Fig. 1-6. If it is required to know whether the center of the pulse shown in *a* occurs before or after the step shown in

for the second detector circuit  $d$  is obtained from a time selector operated by Portion 2 of pulse  $b$ . If the rectified outputs are balanced against each other, the difference measures, over a limited range, the extent to

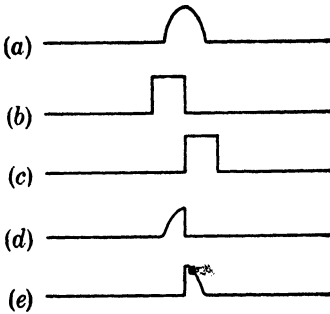


FIG. 1-7.—Time discrimination by a pair of time selectors. The input signal is indicated as (a) and the adjacent selector pulses as (b) and (c). The overlapping portions of the signal and selector pulses are indicated as (d) and (e). Rectification and subtraction of (d) and (e) give a signal which is extremely sensitive to the time of occurrence of (a) relative to (b) and (c).

Time discriminators very often employ two adjacent short-period time selectors, each followed by a rectifier (see Fig. 1-7). The first rectifier measures the amount of the pulse contained in the first selector interval  $b$ , and the second one, the amount contained in the second selector interval  $c$ . If the two outputs are opposed, zero output is obtained when the pulse is centered on the junction of the two selectors; when the pulse is misaligned the sense of the output depends on the sense of the misalignment. If the misalignment is too great, with the result that the pulse does not lie in either selector interval, the output is again zero. The circuit thus performs the function of selection as well as that of discrimination.

By analogy with amplitude comparison, time comparison may be defined as “the process of determining the amplitude of a waveform at a given instant”; but it is a special case of time selection in which the selected interval is made very

which the center of the pulse occurs before or after the step. This is the process of time discrimination, and although an approximate measure of the magnitude of the time difference is given, the sense of the difference is the major feature. If the time variation of the signal is in accordance with intelligence, a time discriminator demodulates this intelligence and converts it into a signal useful for visible or audible indication or for control purposes.

As in time selection, the step may be replaced by a mechanical aperture on an intensity-modulated CRT display. Here the step would be replaced by a partition having a photocell on each side. The outputs of the photocells are directly comparable to the rectifier outputs considered above.

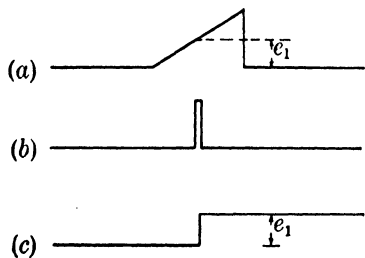


FIG. 1-8.—Time comparison. Time selection of a portion of wave (a) by a narrow selector pulse (b) gives a pulse of amplitude  $e_1$  which, during the first cycle of detection is used to obtain waveform (c). The amplitude of (c) is a measure of the time delay of (b) with respect to (a) and is therefore used for time demodulation.

narrow in order to give the instantaneous amplitude. For the purposes of waveform analysis, where it is required to determine amplitude as a function of time, amplitude comparison, which finds time as a function of amplitude, is the preferred method. On the other hand, time comparison is extremely useful for obtaining an output voltage that varies depending upon the relative time of occurrence of the selector pulse and the waveform. If, for example, a triangular timing waveform is used as indicated in Fig. 1-8, the output from a detector following the time selector will give a voltage linearly related to the delay of the selector pulse with respect to the time of initiation of the triangular wave. This is a useful method of time demodulation.

**1-8. Method of Approach.**—Enough has now been said to indicate the nature of the problem to be discussed. The sinusoidal approach involving Fourier analysis and linear circuits will clearly be of little help. What approach can be substituted for it? Unfortunately, there is no simple answer to this question. There is no continuous mathematical approach that can handle the nonlinearities; and mathematical approaches are constantly hampered by the need to change parameters and even whole equations when a nonlinearity is encountered. Consequently, a great deal of physical argument is needed to reestablish the mathematics in terms of new conditions. These arguments are greatly simplified by considering the circuit diagram in conjunction with a set of waveform diagrams which illustrate the cyclic variations of potential or current, as a function of time, at selected points in the circuit. In this connection it is useful to draw the diagrams in a column, to a common time scale, and arrange them in cause-effect order. Thus the diagrams of Fig. 1-4 would appear as in Fig. 1-9.

In the application of the method to this simple case, the top waveform  $e_1 = kt$  would be drawn. Then, at the beginning of the waveform, the equation for  $e_2$  is  $e_2 = E$  volts since the diode is nonconducting. During the rise of potential, this equation holds until  $e_1 = E$ , when the diode conducts. A new equation,  $e_2 = E + (e_1 - E) \left( \frac{R}{R_d + R} \right)$ , then holds, where  $R_d$  is the resistance of the diode. This equation holds until  $e_1$  again falls below  $E$ . Thereafter the first equation is again relevant. It is not always possible to draw the whole of the top waveform immediately. Sometimes this can be drawn only up to the first nonlinearity on account of some loading or feedback introduced by the nonlinearity. In such cases progressive development of the whole column of waveforms from some assumed starting condition is the usual procedure. The cycle is complete when all the initial conditions are reinstated. If the initial conditions are not reinstated, either the assumed conditions were unsuitable, or the system is incapable of repetitive operation.

The process just described illustrates a basic principle in the technique of waveform generation. This is concerned with the method of use of nonlinear components. If the calculation process given is to be valid, it is essential that the nonlinear component should comprise separate linear states and not exhibit continuous nonlinearity over any considerable range of operation. Thus the diode has been treated as having infinite resistance when the plate is negative relative to the cathode, and as having a fixed resistance  $R_d$  when the plate is positive. These two states are inevitably joined by a period of transition where  $R_d$  is variable. It is a major principle of circuit design to choose the waveform amplitudes and nonlinear elements in such a way that this transition is of negligible duration. For this reason high waveform amplitudes are used in conjunc-

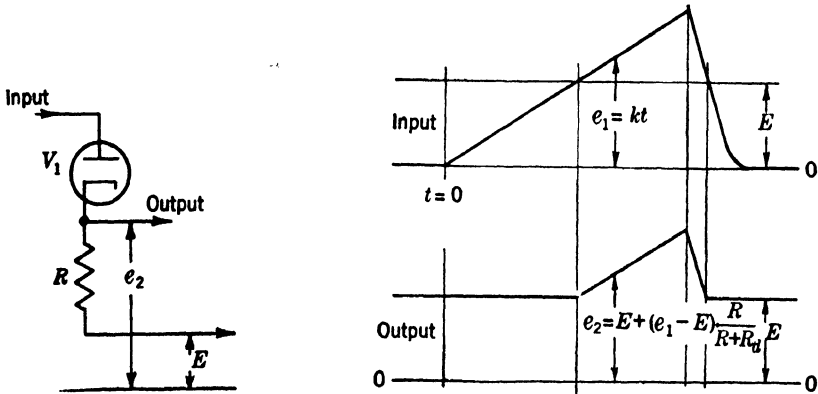


FIG. 1-9.—Illustration of circuit diagram and set of waveforms.

tion with nonlinear elements in which marked curvature of the characteristic is limited to a small range of applied voltage. Furthermore, when the major variations of  $R_d$  have been passed,  $R_d$  still exhibits some small variations with operating conditions. It is a further principle of design to choose components and conditions such that these variations are also negligible. For example, in Fig. 1-9, if a precise output waveform were wanted,  $R$  would be made much greater than  $R_d$ ; consequently variations of  $R_d$  would be incapable of influencing the output appreciably. A further reason for adopting this policy of rendering negligible the effects of transition curvature and  $R_d$  variation lies in the fact that two samples of a given nonlinear element are unlikely to be precisely equivalent, and circuits that depend on precisely known nonlinear characteristics are troublesome in production and use for this reason.

Applications of these and other principles to the design of these circuits are developed in Chap. 2.

## CHAPTER 2

### OPERATIONS ON WAVEFORMS WITH LINEAR CIRCUIT ELEMENTS

BY F. C. WILLIAMS

**2.1. Linear Circuit Elements.**—These comprise the components, resistance, capacitance, and inductance, and also linear amplifiers. With regard to the components, the major consideration is stability of value with time and temperature. This is difficult to achieve in higher values of resistance, and large variations may be observed with resistances in excess of 5 megohms. The higher values of capacitance, where paper dielectric is used, are also subject to variations and have leakage associated with them which is very dependent on temperature. It is also worth noting that inductance always has resistance associated with it

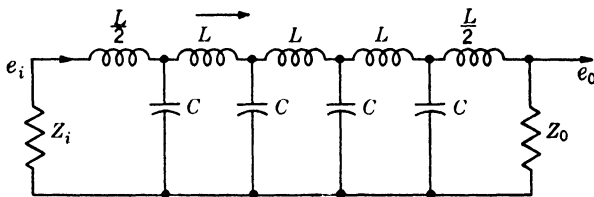


FIG. 2-1.—A delay line made up of lumped inductance and capacity. The delay for each section is approximately  $\sqrt{LC}$ . (This neglects mutual coupling between the inductances, so usually a larger delay is obtained.) Cutoff frequency equals approximately  $1/\pi \sqrt{LC}$ , characteristic impedance =  $\sqrt{L/C}$ .

because of copper losses, dielectric losses, and, in the case of iron-cored structures, iron losses. These points are dealt with at length in Vol. 17.

Another useful circuit element is the delay line, which may be either continuously wound, or made up of lumped inductance and capacitance as shown in Fig. 2-1. One function of this device is to delay a waveform for a period equal to the transmission time of the line with a minimum change of shape; for this use it should be terminated by its characteristic impedance. If it is not so terminated, reflection will occur and the wave shape will be modified. This has been found a very useful method of linear shaping. For instance, it can be used to convert a step function into a pulse whose duration is defined by the transmission time of the delay line.

Delay lines can be made to give only relatively short delays, of the order of 10  $\mu\text{sec}$  or less; with longer delays the shape of the waveform is



not preserved. When longer delays are needed, more complex arrangements are used, such as supersonic delay tanks and storage tubes (see Chaps. 23 and 21).

Transformers of two classes are finding increasing use. In the first type (Fig. 2-2a), the waveform is passed without appreciable change of shape, and the transformer is used to transform the impedance level, to shift the waveform in the voltage axis, or to produce it across a winding that is free at both ends and that can therefore be connected in series with other waveform sources. These are usually called "pulse-passing" transformers. In the second type, considerable shaping of the wave is introduced by choosing the primary inductance such that a short time constant is formed with the resistive load (see Fig. 2-2b). The second type is referred to as "differentiating" transformers.

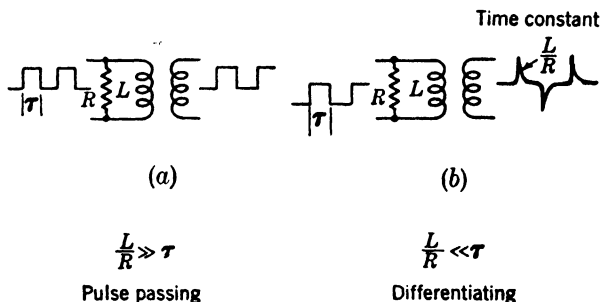


FIG. 2-2.—Two types of pulse transformers useful in waveform shaping. For a current waveform, in (a) the input is reproduced in the output, and in (b) the input is approximately differentiated.

Amplifiers of normal design are occasionally used, but negative feedback is very widely employed for a variety of uses. Its use for impedance conversion is typified by the simple case of the cathode follower. Negative feedback also provides stability of gain and some very flexible methods of linear shaping of waveforms, as will be explained later.

It should be noted that where circuits are composed entirely of linear elements, the final result is independent of the order in which they operate upon the waveform, and, in parallel networks, may be obtained by simple addition of the component outputs. Similarly, a complex waveform may be broken into its component parts, and the responses to the components may be determined separately and added to give the total output. Any circuit nonlinearity invalidates these methods of analysis.

**2-2. Potential Division and Addition.**—Circuits suitable for potential division and addition are shown in Fig. 2-3.<sup>1</sup> The solutions in the right-

<sup>1</sup> So long as elements of one type only are employed, such as resistance, the use of nonsinusoidal waveforms does not greatly affect the uses or mathematical approach for circuit calculations. This is also true of networks made up of mixed components

hand column can be obtained by using Thévenin's theorem in its inverted form—that is, “the potential difference between any two points in a linear network is the current flowing in a short circuit connecting those two points multiplied by the impedance of the network measured between those points, when the short circuit is removed.” In each of these formulas the net impedance from *A* to ground enters into the solution; this has not been evaluated in terms of the input impedances because it is often necessary to connect a small impedance from *A* to ground to reduce

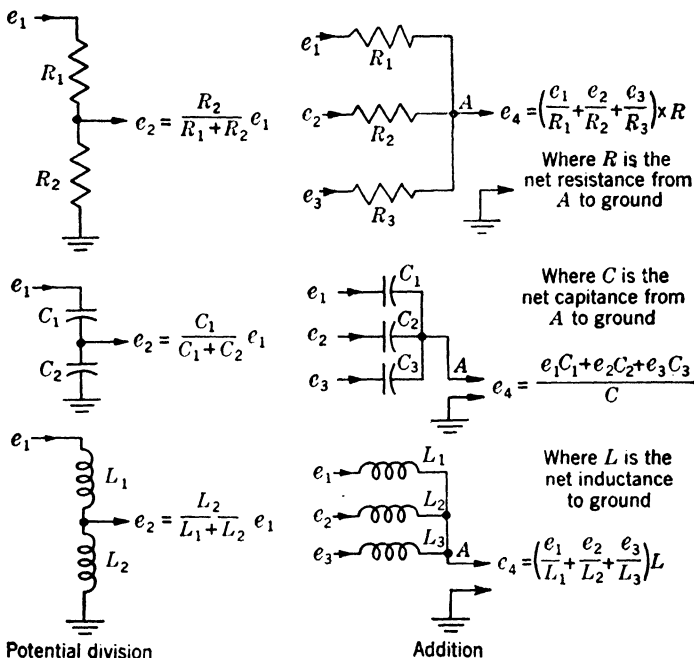


FIG. 2-3.—Some examples of the use of passive circuit elements for potential division and for addition.

mutual coupling between the input voltages; when this is done this impedance may be the controlling factor in the value of the impedance *A* to ground.

**2.3. Waveform Shaping by Passive Elements.**—When the components in the various arms of a network are dissimilar, some departure from standard analytical processes becomes necessary, for now the statement that the impedance of  $R$  and  $L$  in series is  $R + j\omega L$  will apply only to the sinusoidal component of the waveform of frequency  $\omega/2\pi$ . Hence the operational notation  $R + pL$  will be used, where  $p$  represents  $d/dt$ . The

provided every arm is similar—that is, in the case of arms comprising  $R$  and  $C$  in parallel, each arm must have the same time constant. The same is true if the arms comprise  $R$  and  $C$  in series, but series and parallel arms must not be mixed.

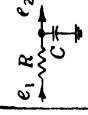
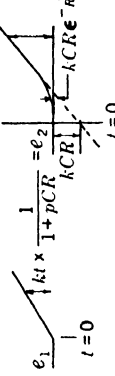
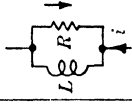
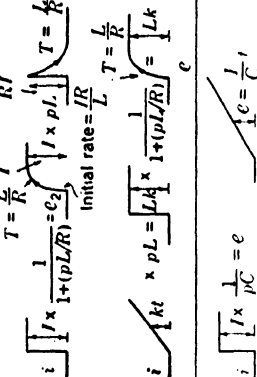

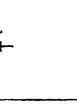
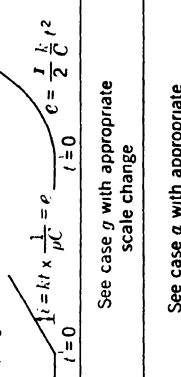
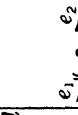
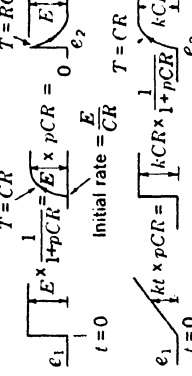
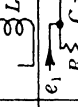
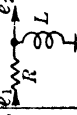
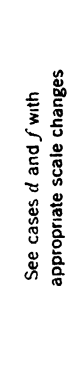
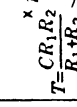
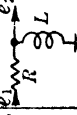
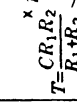
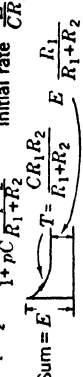
justification for this representation and for the operations to be performed with functions of  $p$  will be considered below (Sec. 2-7). For convenience the name "impedance" will still be applied to quantities such as  $R + pL$ . The main use of the notation will be not as a shorthand approach to formulation of the differential equation of the complete circuit but rather as a way of writing down an immediately recognizable transformation of wave shape. The most commonly used combinations of  $L$ ,  $R$ , and  $C$  have associated with them an operationally stated transfer function and also a known "waveform conversion" effect. Figure 2-4 indicates the operators of the more useful networks, together with the responses to step functions of amplitude and slope. Of the networks shown, the only one for which a mathematical solution need be sought is  $a$ ; the remainder become obvious by inspection if the operator is broken into its component parts and applied step by step in the appropriate order. It is essential to memorize this first case, not only because it occurs very frequently, but also because so many others rest on it, as may be seen from the figure. The properties of  $a$  may be summarized by the statement that when it is disturbed by a discontinuity in the input, it will approach a steady state exponentially with the time constant,  $T = CR$ . This steady state is usually obvious from physical reasoning. This response is described in the figures by the arrow and the notation " $T = CR$ " and by the additional symbols which indicate the steady state.

In  $a$  and  $b$  the transfer function is of the form  $1/(1 + pT)$ , and the resulting waveform conversions for step functions of voltage are shown.

The function shown in  $c$  is  $R/(1 + pT)$  and has the dimensions of impedance since it converts a current waveform to a voltage waveform. Its effect is broken up into two steps,  $\times R$ , and  $\times 1/(1 + pT)$ . The second factor rests on the solution for case  $a$ .

This process of breaking the operator up into recognizable conversions is continued in  $d$ ,  $e_2 = e_1 pCR/(1 + pCR) = e_1 \times pCR \times 1/(1 + pCR)$ , and the sketches show how, by choosing the appropriate order of use of the component operators, recognition can be eased. Thus  $pCR = \left( CR \frac{d}{dt} \right)$  is simply  $CR \times$  the slope of the input curve; this is easy to apply when the step function is in slope but difficult when it is in amplitude. Therefore,  $1/(1 + pCR)$  is taken first when the step function is in amplitude, and only finite rates of change remain on which  $pCR$  operates. Other examples of operator breakup are given in the next two cases ( $e$  and  $f$ ).

Case  $g$  is a most important one, since it forms the basis of nearly all triangular waveform generators; it is the process of supplying a constant current to a condenser. The condenser voltage, which is  $(1/C) \int_0^t Idt$ , is a linear rise of voltage with time. The less important case of a step func-

<p>a</p> 	$\frac{e_2}{e_1} = \frac{1}{1 + pCR}$	$E - e_2 = E e^{-\frac{t}{RC}}$ $e_1 \times \frac{1}{1 + pCR} = e_2$ $t = 0 \quad \text{Initial rate} = \frac{E}{CR}$ 		$\frac{e_2}{e_1} = \frac{pL}{1 + (pL/R)}$	$T = \frac{L}{R}$ $i \times \frac{1}{1 + (pL/R)} = e_2$ $\text{Initial rate} = \frac{RI}{L}$ $T = \frac{L}{R}$ 
<p>b</p> 	$\frac{e_2}{e_1} = \frac{1}{1 + pL/R}$	<p>See case a with appropriate scale change</p>		$\frac{e_2}{e_1} = \frac{1}{pC}$	$i \times \frac{1}{pC} = e$ $t = 0$ $c = \frac{1}{C}$ 
<p>c</p> 	$\frac{e_2}{e_1} = \frac{R}{1 + pCR}$	$T = CR$ $i \times R \times \frac{1}{1 + pCR} = e$ $t = 0$ $T = CR$ 		$\frac{e_2}{e_1} = \frac{1}{Lp}$	<p>See case g with appropriate scale change</p>
<p>d</p> 	$\frac{e_2}{e_1} = \frac{pL/R}{1 + pCR}$	$T = CR$ $E \times \frac{1}{1 + pCR} = e_2$ $t = 0$ $\text{Initial rate} = \frac{E}{CR}$ $T = CR$ 		$\frac{e_2}{e_1} = \frac{1}{1 + pL/R}$	<p>See case a with appropriate scale change</p>
<p>e</p> 	$\frac{e_2}{e_1} = \frac{pL/R}{1 + pL/R}$	<p>See cases d and f with appropriate scale changes</p>		$\frac{e_2}{e_1} = \frac{R_1}{R_1 + R_2}$	$T = \frac{R_1}{R_1 + R_2}$ $E \times \frac{1}{1 + pC \frac{R_1 R_2}{R_1 + R_2}} = e_2$ $\text{Initial rate} = \frac{E}{CR_1 R_2}$ $\text{Sum} = E$ $T = \frac{R_1 R_2}{R_1 + R_2}$ 

tion of voltage applied to an inductance is shown in case *h*. Case *j* is included to illustrate the procedure in more complicated cases. The two terms in the numerator are taken separately and the component waveforms added to give the final result.

Examples of this sort can be continued indefinitely, but perhaps enough has been said to indicate the method of approach. The value of this method lies in the fact that very many of the waveforms of value are made up of step functions of amplitude or slope, either added or occurring one after another. Since the circuits are linear, the principles of superposition hold and allow considerable extension of these basic transformations. For example, a square pulse (see Fig. 2-5*a*) simply comprises

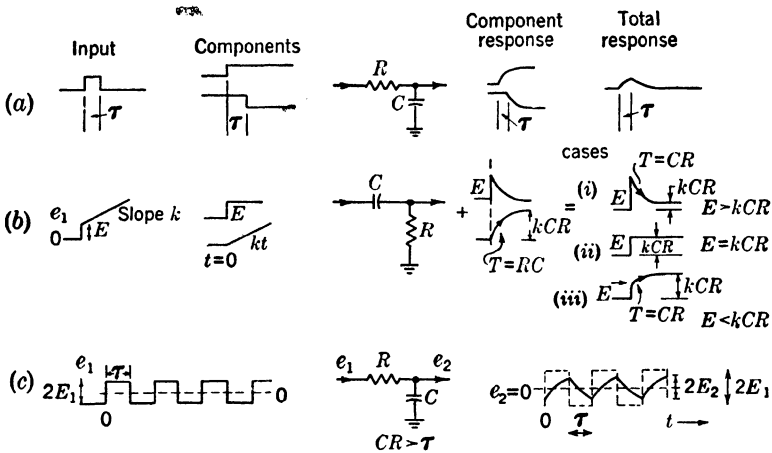


FIG. 2-5.—The response of passive networks to waveforms made up of combinations of step functions of amplitude or rate of change of amplitude (slope). In (a) the input has two component step functions; in (b) a step function of amplitude and of rate of change; and in (c) a repetitive step function of amplitude.

two equal and opposite step functions displaced from each other in time by the pulse width. The response of any of the above circuits to such a pulse can be found by adding the known responses to these two step functions. Similarly the parts of the waveform shown in Fig. 2-5*b* may be applied separately, and the responses to the component step functions can be assessed and added. These methods are useful so long as the waveform is not repeated at a rate high compared with the settling time of the circuit, for if such is the case it may be necessary to add many waveforms covering many complete cycles of the input wave before a steady state is reached.

At first sight this would appear to exclude from the method all circuits containing integrators, since these have an infinite settling time. Fortunately, this difficulty is nearly always removed by the use of some non-linear element which resets the integrator to a fixed starting level once

per cycle. In the few cases where this is not done, the solution can often be found by physical argument, as in Fig. 2-5c. Clearly the output wave must be symmetrical about 0, and each section of it must be a part of an exponential approach to either  $+E_1$  or  $-E_1$ ; thence, if the output amplitude is  $2E_2$  as indicated,

$$E_1 - E_2 = (E_1 + E_2)e^{-\frac{\tau}{RC}} \quad (1)$$

or,

$$E_2 = \frac{E_1(1 - e^{-\frac{\tau}{RC}})}{(1 + e^{-\frac{\tau}{RC}})}, \quad (2)$$

and the waveform is specified in amplitude and shape. More generally, the steady-state response for any such repetitive input may be calculated by imposing a boundary condition of continuity at each input step.

Another use of the general method lies in the synthesis of networks to compensate for some unwanted but inevitable feature of another network. A case in point is that in which it is required to generate a linear rise of current in an inductor in response to a step function of voltage. Here Case *h* of Fig. 2-4 might be used if it could exist, giving the operator  $1/Lp$ . In fact, case *i* is all that can be had, and its operator can be reexpressed as

$$\frac{1}{Lp} \times \frac{1}{1 + r/Lp}.$$

Evidently to obtain the desired result the step function should first be passed through a network defined by the operator  $(1 + 1/pT)$ , where  $T = L/r$ . Figure 2-6 shows such a network, the step function being one of current. The output voltage is as shown, and when applied to the inductor—through a cathode follower, for example, to avoid loading the network—the current in the inductor is

$$I \times \frac{R}{Lp} \left(1 + \frac{1}{RCp}\right) \left(\frac{1}{1 + \frac{r}{Lp}}\right) \quad (3)$$

$$= \frac{RI}{Lp} \quad \text{or} \quad \frac{I}{rCp} \quad \text{if } RC = \frac{L}{r}. \quad (4)$$

This represents a linear rise of current at the rate  $I/rC$  amp/sec, which is the required result.

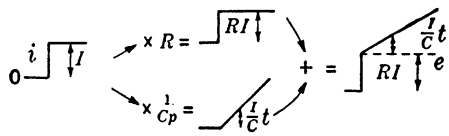
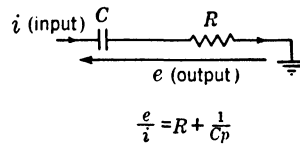


FIG. 2-6.—Response of  $RC$ -network to step function of current.

**2-4. Linear Amplifiers Using Negative Feedback.**—In normal amplifier usage the output amplitude exceeds the input amplitude. In many of the applications considered here this will not be true since it is sound practice to maintain waveforms throughout the system, from generation to final use, at the highest possible amplitude level. The reason for this is, as has been explained, that variations in the properties of nonlinear elements are thereby rendered less important. The major uses of amplifiers are for impedance changing and inversion. Negative feedback is extensively used to give good linearity and flexible impedance control particularly since the reduction of gain due to feedback is not a disadvantage in this field.

The simplest case of the use of negative-feedback amplifiers for impedance changing is that where a waveform is developed across a high impedance and it is required to supply the waveform to a load. Here cathode

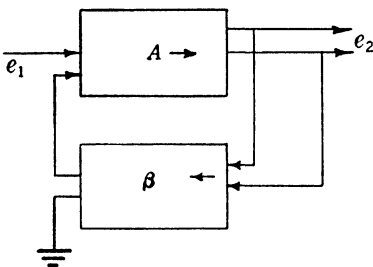


FIG. 2-7.—Block diagram of negative-feedback amplifier.

followers are commonly used. They represent the simplest possible use of negative feedback and yield high linearity and low output impedance. Where cathode followers do not suffice, either because some gain is needed or because even lower output impedance is called for, a multistage negative-feedback amplifier employing voltage feedback would be used. These have been discussed at some length in Vol. 18, Chap. 9 of this series, with particular attention to the problem of stability, and only their salient properties need be noted here.

*Amplifiers with Voltage Feedback.*—Referring to Fig. 2-7, which is the conventional figure for voltage feedback, the gain is

$$G = \frac{e_2}{e_1} = \frac{A}{1 + A\beta}, \quad (5)$$

where  $A$  is the gain without feedback and  $\beta$  is the fraction of the output that is *subtracted* from the input voltage. The value of  $A$  may be either positive or negative, depending on the method of applying the feedback, but  $A\beta$  is always positive in negative feedback amplifiers. Provided  $A\beta$  is much greater than unity, Eq. (5) reduces to

$$G = \frac{e_2}{e_1} \approx \frac{1}{\beta}, \quad (6)$$

and the gain depends mainly on the passive elements which determine  $\beta$ .

*Stability of Gain.*—The dependence of the gain  $G$  with feedback on the gain  $A$  of the amplifier without feedback can be assessed as follows.

From Eq. (5)

$$\mathfrak{G} = \frac{A}{1 + A\beta}.$$

Therefore,

$$\frac{d\mathfrak{G}}{dA} = \frac{1}{(1 + A\beta)^2},$$

so that

$$\frac{d\mathfrak{G}}{\mathfrak{G}} = \frac{1}{1 + A\beta} \frac{dA}{A}. \quad (7)$$

If  $A$ ,  $\beta$ , and  $\mathfrak{G}$  are all real at the frequency of interest, this equation indicates that  $\mathfrak{G}$  varies only  $1/(1 + A\beta)$  per cent per one per cent change of  $A$ .

**Output Impedance.**—If the amplifier of gain  $A$  has output impedance  $Z$  it will deliver  $A/Z$  amps per input volt into a short circuit across its output terminals. The factor  $A/Z$  may be defined as the “transfer admittance” of the amplifier. In single-stage amplifiers this factor is the negative of the mutual conductance as usually defined,  $g_m$  being treated as positive when  $A$  is negative. To distinguish the difference,  $A/Z$  will be denoted by  $g_T$ ; but it should be remembered that although in multistage amplifiers  $A/Z$  may be complex, in single stage amplifiers it is equal to  $-g_m$ .

If unit change of voltage is impressed on the output terminals of the feedback amplifier by an external source, the current drawn from that source will be  $(1/Z + \beta g_T) = (1/Z + \beta A/Z)$ , and the effective output impedance is therefore  $Z/(1 + A\beta)$ . This can be interpreted in two ways: first as a reduction of the impedance without feedback ( $Z$ ) in the ratio  $1/(1 + A\beta)$ , or second (and this is more useful) as a paralleling of  $Z$  and

$$(1/\beta)(Z/A) = (1/\beta g_T).$$

The equivalent output circuit is shown in Fig. 2-8 together with a load  $Z_L$ . Since  $A\beta$  is nearly always large, the shunt  $Z$  has very little effect and the output impedance is very nearly

$$Z_0 = \frac{1}{\beta g_T}. \quad (8)$$

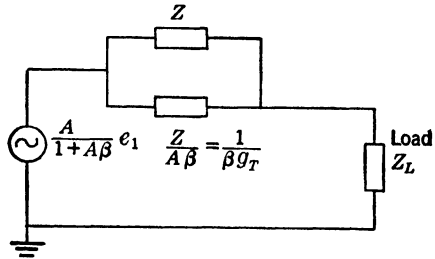


FIG. 2-8.—Equivalent output circuit of feedback amplifier. The output impedance ( $Z$ ) of the amplifier without feedback  $Z$ , is shunted by  $\frac{Z}{A\beta}$ .



This impedance can be made extremely low by using high  $g_r$ , and the output voltage is then sensibly independent of the load  $Z_L$ .

**Input Impedance.**—Feedback also influences the effective input impedance, but here the effect is very dependent on the method of applying the feedback, and a general result cannot be quoted. If the feedback is applied to the cathode of the first stage of the amplifier the potential

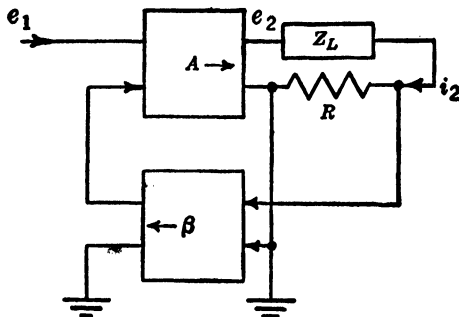


FIG. 2-9.—Block diagram indicating the use of current feedback.

difference between grid and cathode of this tube is

$$e_1 - \beta e_2,$$

and the current flowing in the grid-cathode impedance,  $Z_i$ , is

$$\frac{e_1 - \beta e_2}{Z_i}.$$

Hence the load seen by  $e_1$  is

$$(Z_i)_{\text{eff}} = \frac{e_1 Z_i}{e_1 - \beta e_2} = (1 + A\beta) Z_i$$

from Eq. (5).

In this configuration both  $A$  and  $\beta$  are positive. If  $A$  is negative (phase inverting amplifier), feedback is usually obtained by means of an adding network in the grid circuit (see Fig. 2-10) and the result does not apply. Such amplifiers are discussed in Sec. 2-5.

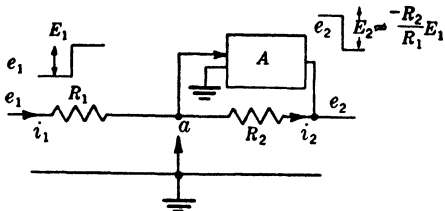


FIG. 2-10.—Block diagram of plate-to-grid-feedback amplifier. The gain is  $e_2/e_1 \approx -R_2/R_1$ .

wanted in the load. Here current feedback is used (see Fig. 2-9). The previous formulas apply if  $(R/Z_L)\beta$  is written for  $\beta$ , provided  $R \ll Z_L$  at

**Amplifiers with Current Feedback.**—Corresponding results can be obtained for the case where accurate output currents are

all the frequencies of interest. Hence,

$$e_2 = \frac{A}{1 + A\beta \frac{R}{Z_L}} e_1 \approx \frac{Z_L}{R\beta} e_1 \quad \text{if } A\beta \frac{R}{Z_L} \gg 1 \quad (9)$$

and

$$i_2 \approx \frac{e_2}{Z_L} \approx \frac{e_1}{\beta R} \quad (10)$$

and in this case the output *current* is defined by passive components and is sensibly independent of  $Z_L$ . This lack of dependence on load is not so easily illustrated by an equivalent circuit here as it was with voltage feedback, and since this circuit is much less frequently used it is sufficient to note that the output circuit of the amplifier appears as an effective high voltage in series with a very high internal resistance. It is worth noting as a design point that it is advantageous to use pentode output stages since these tend to deliver current proportional to input voltage and so assist the action.

**2.5. Plate-to-grid Feedback Amplifiers.**—A particular form of feedback which finds many applications is shown in Fig. 2.10. In this circuit,  $A$  must be negative for negative feedback. The gain  $\mathcal{G}$  is easily derived from Eq. (5) by noting that the effective input voltage is  $e_1 \frac{R_2}{R_1 + R_2}$

and that  $\beta = -\frac{R_1}{R_1 + R_2}$ ; therefore,

$$\frac{e_2}{e_1} = \mathcal{G} = \frac{A}{1 - A \frac{R_1}{R_1 + R_2}} \cdot \frac{R_2}{R_1 + R_2}, \quad (11)$$

and if  $-A \frac{R_1}{R_1 + R_2} \gg 1$ , then

$$\frac{e_2}{e_1} \approx -\frac{R_2}{R_1}. \quad (12)$$

This purely mathematical approach does not give any inkling of the physical mechanism by which the result is achieved, and it is worth while to arrive at the same result by a physical argument to see what it really means. Referring then to Fig. 2.10, let  $e_1 = 0$  and let the amplifier be adjusted so that  $e_2$  is also zero. Point  $a$  will also be at zero and  $i_1 = i_2 = 0$ . Now let  $e_1$  be discontinuously raised to  $E_1$ —that is, a “step function” of height  $E_1$  is applied. As soon as this happens, and before the potential at  $a$  has had time to change (in view of the fact that there is some capacitance to ground at this point) a current  $i_1 = E_1/R_1$  will flow, and will tend to raise the potential of  $a$ . But if  $a$  rises,  $e_2$  falls, since  $A$  is negative,

and a current  $i_2 = -e_2/R_2$  flows and tends to bleed off the input current  $i_1$  which was causing  $a$  to rise. If the input resistance of the amplifier is sensibly infinite, as is usual, point  $a$  will continue to rise until the whole of  $i_1$  is bled off through  $R_2$  by  $i_2$ , and then  $i_1 = i_2$ . The time taken to achieve this result will depend on the speed of response of the amplifier, but often it will be so rapid that it can be treated as instantaneous. The result now is that the input current flows on past  $a$  and traverses  $R_2$ , generating across it a potential difference,  $-R_2 i_1$ , and if  $a$  has departed but little from zero, the output voltage will be very nearly

$$E_2 = -R_2 i_1 = -\left(\frac{R_2}{R_1}\right) E_1.$$

The extent of the final departure of  $a$  from zero will depend on  $A$  and will be  $E_2/A$ , which can be neglected if  $A$  is sufficiently large.

Viewed in this way, the function of the amplifier is to prevent appreciable potential changes at  $a$  by bleeding off through  $R_2$  the input current  $i_1$  which would cause these changes. This it does by appropriate adjustment of  $e_2$ . In fact, it generates a virtual ground at  $a$  which draws no current, and  $i_1$  flows on through  $R_2$  to generate  $e_2$ . This action is summarized in Fig. 2-10, where the grounded arrow indicates that  $a$  is held sensibly at ground potential.

Although the operation has been described in terms of step-function input, it is clear that the mechanism holds for any input waveform provided only that the speed of response of the amplifier is appropriate to the degree of time resolution demanded in the output.

It follows from Eq. (8) and the associated discussion that the output impedance of this circuit is very nearly  $-(R_1 + R_2)/R_1 \cdot (1/g_T)$ , where  $g_T$  is necessarily negative. Since  $R_1$  and  $R_2$  are usually approximately equal (input and output waveforms being of comparable magnitude) this will be only a few hundred ohms even if the amplifier has but one stage ( $-1/g_T = 1/g_m = 150$  ohms). In this respect it is similar to the cathode follower and is often referred to as a "plate follower," although its phase-reversing properties are more properly conveyed by another common name, the "see-saw" circuit. The origin of this name is that  $R_1$  and  $R_2$  can be regarded as a "see-saw" plank pivoted at  $a$  so that when  $e_1$  goes down  $e_2$  goes up by  $R_2/R_1$  times as much. The circuit is widely used for generating paraphase waveforms in time-base circuits; in such cases  $R_1 = R_2$ .

*Addition in Feedback Amplifiers.*—Referring to Fig. 2-10, if a second input voltage  $e_3$  is connected through a resistance  $R_3$  to the input terminal of the amplifier  $a$ , an additional current  $e_3 = e_3/R_3$  will flow to  $a$  and, by the argument of the previous section, must also flow in  $R_2$ ; this produces an additional output voltage closely equal to  $-(e_3/R_3)R_2$ . The total

output voltage is thus

$$e_2 = -\frac{R_2}{R_1} e_1 - \frac{R_2}{R_3} e_3.$$

The circuit therefore performs the function of addition. Some mutual coupling exists between the two input voltages since the potential of  $a$  will change slightly in response to each input voltage. This effect is very small if  $A$  is large. It can best be evaluated by reference to the effective input impedance seen at  $a$ , which is discussed below. Further quantities may be added, to any desired scale, through additional input resistors.

*Effective Input Impedance at  $a$ .*—A knowledge of the effective input impedance seen at  $a$  is of considerable value in making second-order calculations when the approximations given above do not suffice. This may be calculated as follows: if a change  $e_o$  is impressed on  $a$ , the other end of  $R_2$  will move through  $Ae_o$  so that the voltage across  $R_2$  is  $(1 - A)e_o$ , and the current drawn by  $R_2$  is  $[(1 - A)/R_2]e_o$ ; hence the effective input resistance is  $R_2/(1 - A)$ , which tends to zero as the numerical value of  $A$  is increased.<sup>1</sup>

Figure 2-11 shows the equivalent input and output circuits of the amplifier feeding a load  $Z_L$ . This diagram permits accurate detailed analysis where the approximations are inadequate. The dotted resistance  $R_3$  represents other input resistors used for addition. Mutual interaction between added quantities is proportional to  $R_2/(1 - A)$  and can be made small by increasing  $A$ .

*Practical Examples.*—Two practical examples of plate-to-grid negative-feedback amplifiers are shown in Fig. 2-12. Figure 2-12a indicates a single-stage feedback amplifier using a high  $-g_m$  pentode such as type 6AC7. The cathode is held at about +2.5 volts to prevent grid current and the screen potential is adjusted so that  $e_2 = 0$  when  $e_1 = 0$ . The output voltage  $e_2$  is in accordance with the relations expressed above and

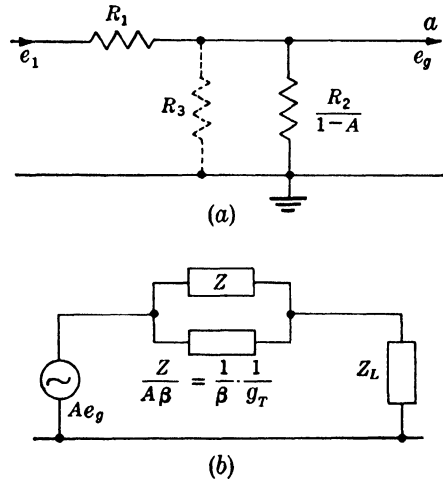


FIG. 2-11.—Equivalent circuit showing effective impedances of the plate-to-grid feedback amplifier. (a) is the equivalent input circuit and (b) is the equivalent output circuit.  $Z_L$  is the load supplied. Note that for the single-stage amplifier of Fig. 2-12b,  $-g_T = g_m$ ,  $-1/\beta = 1 + [R_2(R_1 + R_3)/R_1R_3]$ , and  $Z \approx R_p$ .

<sup>1</sup> It is important to remember here that  $A$  is essentially negative.

a swing of  $\pm 70$  volts with respect to ground is easily obtainable. An alternative form suitable for positive outputs only is indicated in Fig. 2-12b. The cathode is again biased to  $+2.5$  volts and the screen voltage is adjusted to make  $e_g = 0$  when  $e_1 = 0$ . If  $R_3 = R_2$ , the anode potential will then be  $+150$  volts (by feedback action in  $R_2$  and  $R_3$ ). Departures of  $e_2$  from  $150$  volts will be related to  $e_1$  in the ratio  $(-R_2/R_1)$ .

*Advantages of Negative Feedback.*—The equivalent circuit (Fig. 2-11) resembles that of a triode amplifier and it is interesting to examine the reasons for using feedback; in the triode cases, Fig. 2-11a would, of course, consist entirely of real resistors. Triodes with amplification factors approaching  $100$  ( $A$ ), combined with an internal resistance of about  $450\Omega$  ( $3/g_m$  for  $R_1 = R_2 = R_3$ ), are unobtainable, and with a practical triode it would be necessary to sacrifice either the low output impedance, which confers the benefit of output voltage sensibly independent of  $Z_L$ , or the low input impedance  $R_2/(1 - A)$ , which confers the benefit of small mutual interaction between added input voltages. Even if such a triode were available its characteristics would be both curved and indefinite and the compensation of variation of  $A$ , achieved by appropriate variations of  $R_2/(1 - A)$  in the feedback case, would be lost. Linearity and constancy of gain would therefore be sacrificed. In cases where direct

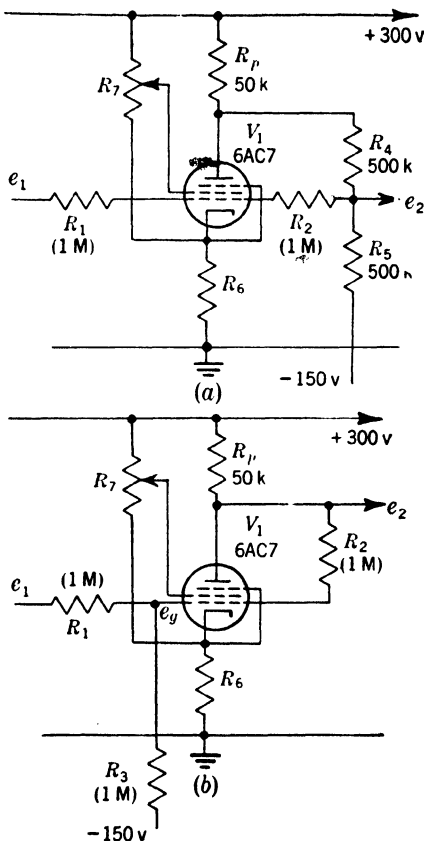


FIG. 2-12.—Practical forms of single-stage plate-to-grid feedback amplifiers. (a) is suitable for outputs of both polarities, while (b) is suitable for positive outputs only. With the values shown the gain is very near unity in both cases.

coupling is used the d-c level of the output of the nonfeedback amplifier would be vastly more dependent on supply voltage changes than is the case with feedback (this is particularly true of the circuit of Fig. 2-12a, in which none of the supply voltages has any first order effect on the d-c level of the output voltage). It should be noted,

however, that feedback does not diminish the effect of any variations of supply voltage or tube characteristics which directly or indirectly influence the grid-cathode voltage required to produce a given output voltage. Contact potential and screen potential are typical examples; their effective value at the grid is part of the input voltage and feedback cannot eliminate the effects of their variation.

**2-6. Linear Shaping Amplifiers, Capacitance Feedback.**—A further major use of feedback is made evident if  $R_2$  in Fig. 2-10 is replaced by a condenser  $C_2$  (see Fig. 2-13). Once again the amplifier must strive to hold  $a$  near ground by changing  $e_g$ , thus drawing off  $i_1$  through  $C_2$ . But when current flows into a condenser, the potential across it,  $e_2$ , is

$$-\frac{1}{C_2} \int i_1 dt + B;$$

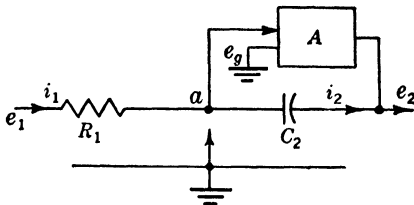


FIG. 2-13.—Amplifier with capacitance feedback.

and since  $i_1 = e_1/R_1$ ,  $e_2 = -(1/C_2 R_1) \int e_1 dt + B$ . Such a circuit therefore performs the function of integration. In particular, if  $e_1$  is a step function of amplitude  $E_1$  starting from zero and if  $e_2$  also starts from zero, then

$$e_2 = -\frac{E_1}{C_2 R_1} \int_0^t dt = -\frac{E_1 t}{C_2 R_1}, \quad (13)$$

and the input step function is modified by the circuit into a linearly descending voltage. This then is the second principal function of feedback—that of providing linear shaping circuits whose operation is defined

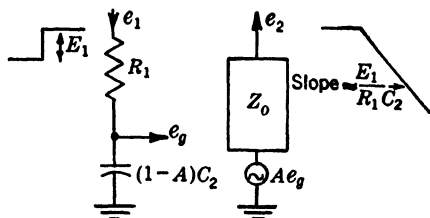


FIG. 2-14.—Equivalent circuit of capacitance-feedback amplifier of Fig. 2-13.

by passive elements in spite of the incorporation of thermionic tubes. Since this circuit is of prime importance, it is worth studying from an alternative viewpoint—that is, in terms of the effective input impedance at  $a$ . By the same process as was used for resistive feedback the input impedance can be shown to be that of a condenser  $(1 - A)C_2$ , assuming that  $A$  is not complex.<sup>1</sup> The equivalent circuit is then as in Fig. 2-14, in which  $Z_0$  is the effective output impedance, equal to  $Z/(1 + A\beta)$ , where

<sup>1</sup> This is the well-known "Miller Effect." See J. M. Miller, "Dependence of the Input Impedance of a Three Element Vacuum Tube upon the Load in the Plate Circuit," *Nat. Bur. Standards Sci. Paper* 351.

$Z$  is the output impedance of the amplifier of gain  $A$  and  $\beta$  is complex. The circuit is instructive in that it shows that  $e_o$  is a segment of an exponential rise toward  $E_1$  with time constant  $(1 - A)R_1C_2$ , and that the open-circuit output voltage  $Ae_o$  is a segment of an exponential of time constant  $(1 - A)R_1C_2$  approaching a voltage  $AE_1$ . Following the policy of using large waveforms,  $E_1$  will be made roughly equal to the supply voltage, so that  $e_2 (= Ae_o)$  will traverse only about  $1/A$  of the whole exponential before the amplifier overloads; the sweep of output voltage will therefore be very nearly linear (see Fig. 2-15), even if only one pentode stage is used ( $A \approx -100$ ).

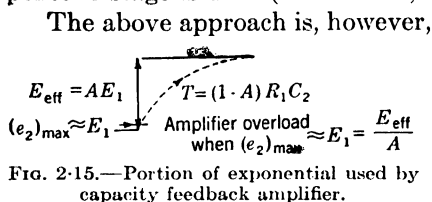


FIG. 2-15.—Portion of exponential used by capacity feedback amplifier.

The above approach is, however, not suitable for detailed calculations of circuit performance since  $Z$  is complex and  $A$  will not be constant but will vary on account of curvature of tube characteristics. The preferred approach for detailed work is by successive approximation, using the fact that whatever current flows in  $R_1$  must flow into  $C_2$ . The first step is to assume perfect operation (that is,  $a$  at constant potential) and so find a first approximation to  $e_2$ . Knowing this,  $e_o (= e_2/A)$  can be estimated, if necessary by reference to tube characteristics. A more accurate assessment of current in  $R_1$  is then possible, leading to a new assessment of the potential across  $C_2$ ;  $e_2$  can then be found by subtracting  $e_o$  from the potential across  $C_2$ . The process is graphical and somewhat lengthy. It is rarely necessary since knowledge of the physical principles involved will usually permit choice of conditions such that the errors in the first approximation are negligible. The same approach is useful in assessing the effect of loading the output. If the load is linear, it can, of course, be included in  $A$ ; but if it is nonlinear, particularly if it is in the form of a load that is suddenly picked up during the sweep (for example, by conduction in a diode performing amplitude selection; see Fig. 1-9), the current that must be supplied at any instant is known and the necessary rise in grid voltage to supply it is easily found and its probable effect assessed.

*The General Case.*—The general case of linear shaping in feedback amplifiers is shown in Fig. 2-16, where  $Z_1$  and  $Z_2$  replace  $R_1$  and  $R_2$ . The diagram has been simplified by omitting the amplifier, whose only function is to hold  $a$  near ground potential, as indicated by the grounded arrow, and to provide a sink for  $i$ .

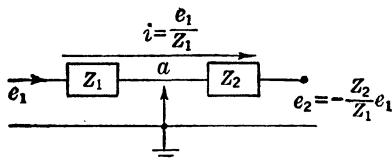


FIG. 2-16.—Simplified block diagram of negative-feedback amplifier used in shaping processes.





It is obvious from this figure that

$$\frac{e_2}{e_1} \approx -\frac{Z_2}{Z_1}$$

Figure 2-17 shows the shaping effects that can be obtained with common forms of  $Z_1$  and  $Z_2$ . The notation and method of derivation are the same as in Fig. 2-4. The extension beyond Fig. 2-4 lies in the fact that now the relation  $e_2 = -\frac{Z_2}{Z_1} e_1$  allows us to introduce configurations that could not otherwise be treated simply.

In Cases 1 and 6, the input and feedback impedances are similar and there is no change of shape. This is true of any case in which  $Z_1$

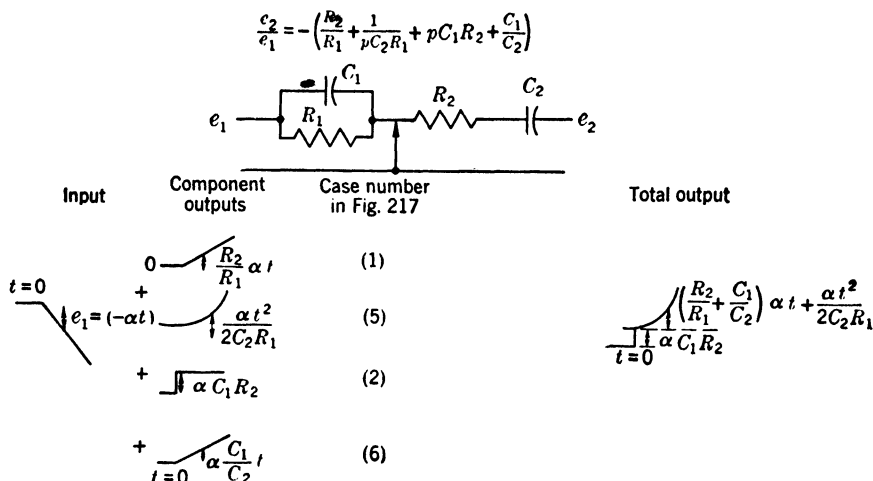


FIG. 2-18.—Illustration of the process of calculation in circuits with shunt input components and series output components.

and  $Z_2$  are similar—for example, in Cases 11 and 16 with  $R_1C_1 = R_2C_2$  there is no change of shape. When  $C$  is included in the output network, without resistive shunt, a constant of integration is introduced, whereas if  $C$  is included in the input network without resistive shunt, any constant in the input will be lost. In practice the constants of integration are usually eliminated on the output side by some form of resetting action. Cases having parallel input components or series output components can be calculated by addition of results for simpler cases, since shunt components in the input circuit give additive components of  $i$ , and series components in the output circuit give additive components of  $e_2$ . For instance, consider Fig. 2-18, which is Case 12 of Fig. 2-17. In this figure

$$\frac{e_2}{e_1} = -\left(\frac{1}{R_1} + pC_1\right) \times \left(R_2 + \frac{1}{pC_2}\right) \quad (14)$$

$$= - \left( \frac{R_2}{R_1} + \frac{1}{pC_2R_1} + pC_1R_2 + \frac{C_1}{C_2} \right), \quad (15)$$

which is an addition of the component responses given by Cases 1, 5, 2, and 6 of Fig. 2-17. The figure demonstrates the addition of component responses to form the total response.

Inductance has not been included in these figures since very little use has been found for it in this type of circuit. Also a range of inductors is not available as a standard component.

Where the solution cannot be found by inspection, the formulas obtained by the method can be solved as differential equations, remembering that  $p$  represents  $d/dt$ .

So far  $Z_1$  and  $Z_2$  have been treated as simple two-terminal networks in which no components are grounded. If they are replaced by three-terminal networks, the third terminal being grounded, the means by which the equation  $e_2/e_1 \approx -Z_2/Z_1$  was deduced indicates that this solution still holds, provided  $Z_1$  is defined as the transfer impedance from  $e_1$  to  $a$ —that is,  $Z_1 = e_1/i_1$  (see Fig. 2-19)—and provided  $Z_2$  is similarly defined as  $e_2/i_2$ .

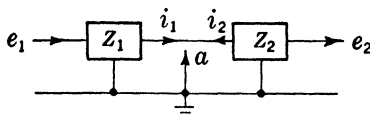


FIG. 2-19.—Block diagram of negative-feedback with three-terminal networks.

Since a given network may be used for either input or feedback purposes the more useful networks are shown in Fig. 2-20 together with their transfer impedances. When the networks are used as feedback networks the operator is used as it stands; when used as input networks the inverse of the operator is used. This figure largely supersedes Fig. 2-17 for design purposes. The problem of stability will not be considered here, since it is dealt with in full elsewhere (Vol. 18, Chap. 9); the problem is no different from that arising with other types of feedback, and is important only when both input and feedback networks are complicated structures. All the configurations shown in Fig. 2-17 are stable for single-stage amplifiers.

*The Bootstrap Circuit.*—It is interesting to note that the choice of ground point in Fig. 2-13 is quite arbitrary; the circuit operation described is quite independent of whether the circuit is grounded or not. The circuit can therefore be redrawn as in Fig. 2-21,  $e_1$  being still the input voltage to the amplifier, but now  $e_3$  is the voltage from  $a$  to ground and  $e_2$  is measured in the reverse sense, so that  $A$  is positive. The potential across  $C_2$  in response to step function input of amplitude  $E_1$  will not be changed by the change of ground point, but now, since  $b$  is grounded, this potential will appear at  $a$ , relative to ground, and will be positive-going instead of negative-going.

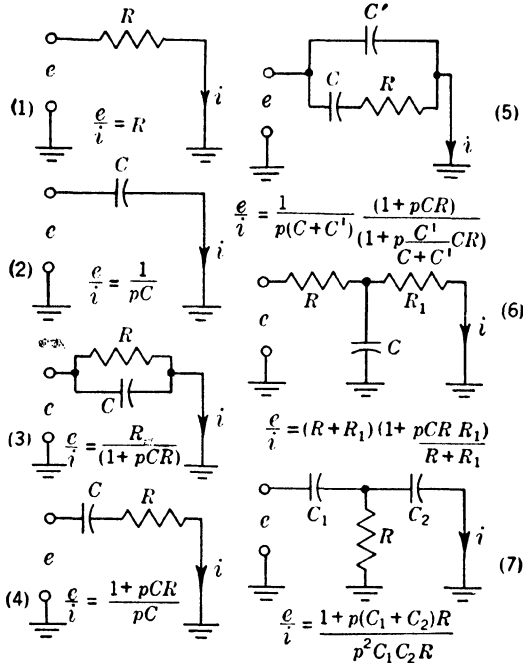


FIG. 2-20.—Common input and feedback networks and their associated transfer impedances. The ground connection into which  $i$  flows is the virtual ground at  $a$  in Fig. 2-19.

The mechanism here is as follows. Starting with the condition  $e_1 = e_2 = e_o = e_3 = 0$ , when a step function of height  $E_1$  is introduced,

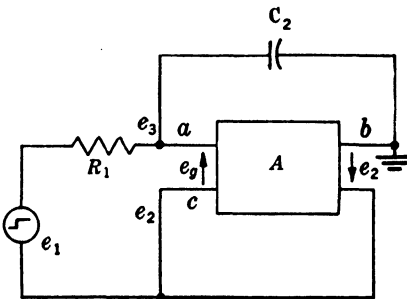


FIG. 2-21.—Block diagram of "bootstrap circuit." This is Fig. 2-13 with the ground connection moved to the amplifier output lead.

because, as the input generator  $e_1$  charges  $C_2$ , its potential, relative to ground, is raised, as it were "by its own bootstrap."

$C_2$  begins to charge at the rate  $E_1/R_1C_2$  volts/sec, and the potential of  $a$  begins to depart from that of  $c$ , producing input to the amplifier  $e_o = e_3 - e_2$ . But  $e_o = e_2/A$ ; therefore  $e_3 = e_2(1 + 1/A)$ . Hence as  $e_3$  rises,  $e_2$  follows it very closely, provided  $A$  is large. It follows that the potential across  $R_1$  is maintained as  $C_2$  charges, and a sensibly constant current flows into  $C_2$ , giving a linear rise of voltage at  $a$  and  $c$  relative to ground. This circuit is called the "bootstrap circuit"

A practical form of the circuit with a single stage amplifier is shown in Fig. 2-22a. The switch  $S_1$  serves to introduce the effective unit function input by holding the circuit in the starting condition when it is closed.

Figure 2-22b shows the Miller Integrator with single-stage amplifier for comparison. Apart from the change of earth point and the precise position of the  $E_{pp}$  supply and  $S_1$ , the circuits are identical. The Miller circuit has the advantage that both its supplies,  $E_1$  and  $E_{pp}$ , and the amplifier cathode are taken with respect to ground so that high gain pentodes can easily be used. The need for a floating  $E_1$  supply in the bootstrap circuit is its major disadvantage; a variety of substitutes for the floating supply have been devised. The advantages of bootstrap connection lie mainly in the easier arrangement of the switch  $S_1$  and in easier compensation of drifts due to heater voltage variation; these matters are discussed in later chapters.

Development in the United States was mainly in terms of the bootstrap circuit; in England the Miller Integrator was preferred. The resulting circuits were superficially very different, but once the equivalence of the two is realized it is easy to interchange developments between the techniques with considerable advantage to both. This "duality" was not realized until recently and it is interesting to note, in retrospect, that the major differences in the range-measuring techniques developed on opposite shores of the Atlantic arose fundamentally from the simple fact that whereas in America the plate was *grounded*, in England the cathode was *earthed*.

**2.7. The Use of Operational Notation.**<sup>1</sup>—In the preceding sections the effect of a network on an input waveform has been described by a fraction

<sup>1</sup> By D. M. MacRae, Jr.

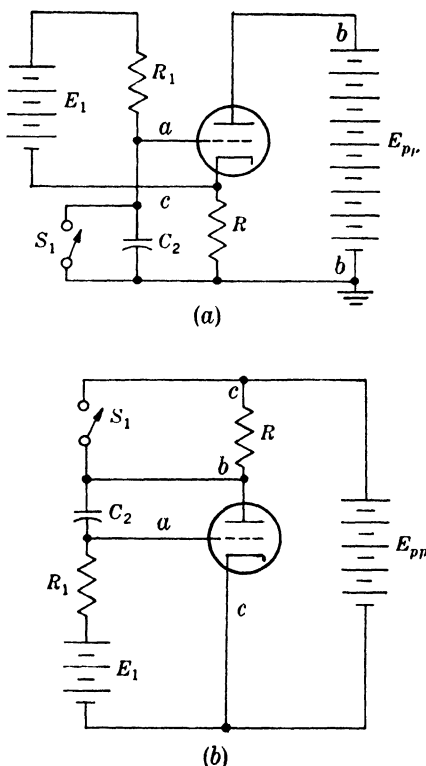


FIG. 2-22.—Comparison of bootstrap (a) and Miller Integrator (b) linear sweep generators with single-stage amplifiers. The circuits are fundamentally the same, differing only in ground connection, power supply, and switching arrangements.

(a “transfer function”) having polynomials in  $p$  as numerator and denominator. It is of interest to examine the operations performed on these “functions of  $p$ ” and the conditions of their validity.<sup>1</sup> There are several ways in which these operations may be regarded.

The simplest interpretation of the operational expression of the transfer function of a network is to consider the symbol  $p$  as a shorthand for  $d/dt$  in the differential equations of the network. If  $d/dt$  is substituted for  $p$  in the transfer function

$$\frac{e_2}{e_1} = \frac{pCR}{1 + pCR},$$

for example, the result is

$$\frac{e_2}{e_1} = \frac{CR \frac{d}{dt}}{1 + CR \frac{d}{dt}}.$$

The correct interpretation is that the operational equation is simply a convenient shorthand for the differential equation of the circuit

$$e_2 + CR \frac{de_2}{dt} = CR \frac{de_1}{dt}.$$

The indicated addition  $\left(1 + CR \frac{d}{dt}\right)$  here corresponds to the addition of the two waveforms  $e_2$  and  $CR \frac{de_2}{dt}$ ; the indicated “division” corresponds to the fact that the denominator of the transfer function operates on  $e_2$ .

Another relatively simple outlook on the operational notation, which justifies the use of algebraic operations but is limited in validity, is the assumption that input and output voltages have the form  $Ae^{pt}$ , where  $p$  is a complex exponent. Substitution of this function in the differential equation<sup>2</sup> yields an algebraic equation in which  $p$  takes the place of  $d/dt$ . A corresponding transfer ratio may be expressed and has the same form as the operational transfer function written as a shorthand for the differential equation. For any given exponent  $p$ , this measures a complex numerical ratio of the output amplitude to the input amplitude.<sup>3</sup> The special case when  $p$  is purely imaginary ( $p = j\omega$ ) corresponds to the usual complex sine-wave analysis, and by extension to the Fourier integral may be used to express the response of networks to waveforms for which the Fourier integral converges.

<sup>1</sup> For a detailed treatment of this subject, see Vol. 18, Chap. 1.

<sup>2</sup> If the behavior of the network is originally expressed by an integrodifferential equation, it is assumed here that a corresponding differential equation has been obtained by repeated differentiation.

<sup>3</sup> This approach is discussed in detail in H. W. Bode, *Network Analysis and Feedback Amplifier Design*, Chap. II, Van Nostrand, New York, 1945.

A more general justification for the treatment of  $p$  as an algebraic quantity may be arrived at by use of the Laplace transform.<sup>1</sup> This transformation converts the differential equation of a network into an algebraic equation, but does not depend for its validity on the assumption of any particular form of input waveform. The Laplace transform  $F(p)$  of a function  $f(t)$  is defined by the equation

$$F(p) = \mathcal{L}f(t) = \int_0^{\infty} f(t)e^{-pt} dt,$$

where  $p$  is a complex quantity. If this transformation is performed on both sides of the differential equation of a linear network, the result is an algebraic equation relating the transform of the input waveform,  $\mathcal{L}(e_i)$ , to the transform of the output waveform,  $\mathcal{L}(e_o)$ . The ratio  $\mathcal{L}(e_o)/\mathcal{L}(e_i)$  assumes exactly the same form of the "transfer function" defined by either of the two preceding methods; in this case, however, the operations indicated are genuine algebraic operations and the expression is valid for any waveform for which the integral converges.<sup>2</sup>

The output waveform is then one which has the transform

$$\mathcal{L}(e_i) \cdot (\text{transfer function}) = \mathcal{L}(e_o).$$

The output waveform may be found, if its transform is known, either by an inverse transformation involving an integral similar to that for the direct transformation, or from a knowledge of the transforms of commonly occurring waveforms.

For the applications of this chapter, neither the transform nor its inverse need be computed by integration. The transfer function is arrived at by the conventional impedance analysis. The transform of  $e_i$  is not used explicitly, but considerations are based on a step-function input; the waveforms  $e_i$  and  $e_o$ , rather than their transforms, are associated with one another. The value of considering the Laplace transform for these relatively simple cases, therefore, is that it affords an algebraic interpretation of the transfer function and justifies in a sense the indication of algebraic operations. For more complicated networks and waveforms, the Laplace-transform approach is often the most convenient method of solving the differential equations; the expansion of a transform in partial fractions is then justified, and the actual computation of the integral for the direct and inverse transforms may be done.

<sup>1</sup> See, for example, M. F. Gardner and J. L. Barnes, *Transients in Linear Systems*, Wiley, New York, 1942; H. S. Carslaw and J. C. Jaeger, *Operational Methods in Applied Mathematics*, The Clarendon Press, Oxford, 1941.

<sup>2</sup> If  $j\omega$  is substituted for  $p$  in the above integral, the result is the Fourier transform of  $f(t)$ . Formally the two transformations are the same, except for a differing range of validity. If in the Laplace transform the quantity  $p$  has a positive real part, the integral converges for some functions (e.g., a positive step function) for which the corresponding Fourier integral does not converge.

## CHAPTER 3

### OPERATIONS WITH NONLINEAR CIRCUIT ELEMENTS

By R. KELNER, J. W. GRAY, AND BRITTON CHANCE

#### INTRODUCTION

The idealized *linear* circuit element is the resistor, inductor, or capacitor that relates two measurable quantities, a voltage and a current, by a constant of proportionality between the quantities or between one quantity and the time derivative of the other. The operations of the preceding chapter are all performed by combinations of such linear passive elements with the addition of linear amplifiers in some cases. However, the virtue of the ideal linear element—proportionality for all values of applied voltage—is also a limitation. Thus, an applied sinusoid can produce only other sinusoidal waveforms in a network of linear elements. Likewise an oscillator or generator composed of linear elements can produce only sinusoids.

*Nonlinear* elements provide a means for generating other waveforms. The nonlinear two-variable element may relate its variables according to a curved or discontinuous function or may provide entirely different relationships for different ranges of the variables (a diode, for example). Particularly useful is the *multivariable* nonlinear element that relates three or more variables. The multigrid vacuum tube and some simple circuits are often used as multivariable elements.

The number of variables in an element may be taken as the number of useful quantities. According to this convention, a triode voltage amplifier is a two-variable element relating input voltage and output voltage. Alternatively the triode may be regarded as a three-variable element in which the plate-voltage vs. plate-current relation is controlled by the grid bias. Only in *nonlinear* three-variable elements can the third variable “control” a two-variable function. Multivariable elements are required for such operations as multiplication (three variables) or selection between two bounds (four variables).

This chapter describes the most important operations that are performed with nonlinear elements. Some common nonlinear characteristics are included together with stability data that are not widely available. This information is essential for the design of precise waveform generators.

**3.1. Ideal Elements.**—Among the nonlinear characteristics, several useful classes may be distinguished. For two-variable elements or multi-variable elements for which all variables except two are held constant, the ideal characteristics are illustrated in Fig. 3-1. The *linear* element is familiar. The *curved* characteristic is continuous and has a continuous first derivative. In a *broken-line* characteristic, two or more linear or curved segments are separated by a *break* or discontinuity of slope. A *discontinuous* characteristic possesses a jump discontinuity. A *hysteresis*

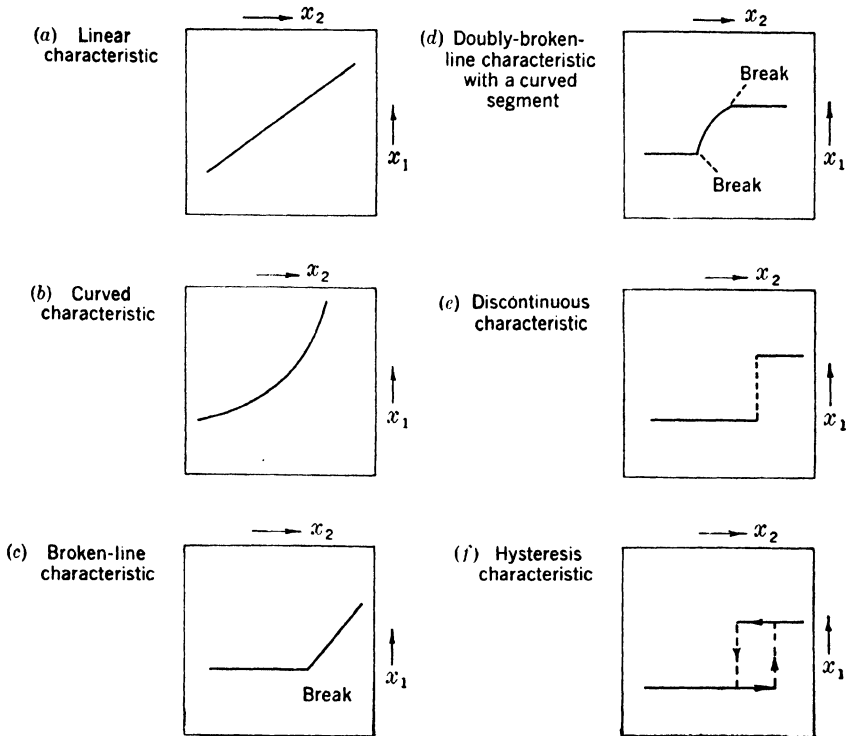


FIG. 3-1.—Ideal two-variable characteristics. The variables  $x_1$  and  $x_2$  may be any useful quantities.

characteristic relates the two variables according to their *present and past* values. Useful hysteresis characteristics must be cyclic (repeatable) yielding a double-valued function, depending upon direction.

A multivariable element may exhibit any of the above characteristics if all variables but two are held constant. A set of two-variable curves corresponding to a set of discrete values of a third variable is called a “nonconstant characteristic.” The third variable may be called a “parametric variable,” but the distinction is dependent only upon the data presentation or the usage of the element and not upon a property



of the characteristic. A two-dimensional parametric representation of a three-variable characteristic is illustrated in Fig. 3-2. This type of graph is familiar in the form of vacuum-tube characteristics.

Although these terms are useful for circuit analysis by physical argument, no symbols for the "broken-line element," etc., are in common use. It may be desirable to introduce such symbols at some future time.

**3-2. Basic Operations.**<sup>1</sup>—These sections will indicate the application of the ideal nonlinear circuit elements to the basic operations usually employed in circuit technique. The basic linear operations are addition, subtraction, and linear shaping; corresponding with these there are three additional operations. The first of these is the selection process, most

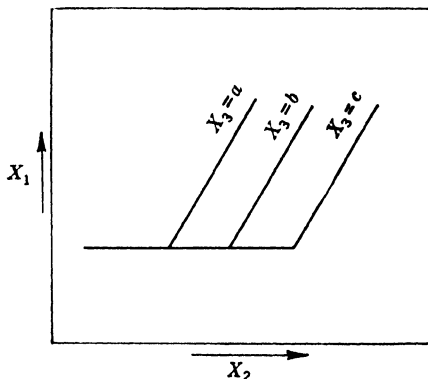


FIG. 3-2.—Ideal three-variable nonlinear characteristics.

commonly used in radio receivers as frequency selection and, in that case, dependent upon linear circuit elements. It is often found desirable to select a portion of a waveform with respect to amplitude, phase, or time, and in these operations nonlinear circuit elements are commonly employed.

The second process is that of discrimination, and a well-known example is frequency discrimination, commonly used in automatic-frequency-control circuits for indicating the equality of two frequencies or the sense and approximate magnitude of the difference between them. But this process is also commonly carried out in terms of amplitude, time, or phase. Each discriminator circuit has inputs in terms of amplitude, frequency, time, or phase, but gives as an output a voltage indicating the equality or the sense and magnitude of the inequality.

The third process is a newer one and has no well-known analogies in radio-receiver practice; it is the indication of the instant of equality of two voltages in amplitude, frequency, or phase. This process has been extensively used in radar timing equipment where the moment of equality of the amplitude of a sinusoidal or triangular wave to a parametric voltage is required. The process has not yet been extensively used in terms of phase and frequency. The comparison process has an inverse aspect; one may wish to know the amplitude, phase, or frequency corresponding to a

<sup>1</sup> Sections 3-2 to 3-4 by Britton Chance.

given time. This is essentially a sampling process and one of the important methods for demodulation.

The processes of selection and comparison depend for their operation upon nonlinearities or nonconstancies in the amplitude, frequency, phase, or time characteristic of a circuit. Although nonlinear responses in frequency and phase (with respect to a reference phase) are readily obtained with linear circuit elements, nonlinear amplitude characteristics are not; the nonlinear properties of vacuum tubes are therefore of considerable interest. The following discussion defines in detail processes of selection, comparison, and discrimination which have been useful in the generation and manipulation of waveforms. The detailed description and practical circuits are presented in the appropriate chapters of this volume.

### OPERATIONS WITH NONLINEAR CIRCUIT ELEMENTS

**3.3. Initiation of Waveforms.**—The initiation of waveforms is one of the most frequent uses of nonlinear and nonconstant circuit elements and

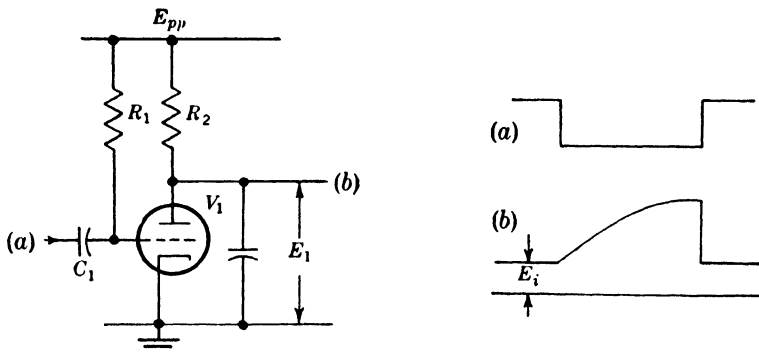


FIG. 3-3.—The initiation of an exponential waveform by a triode switch—a negative rectangular wave is applied to the grid of a nonconstant circuit element.

needs no detailed definition. The process of waveform generation is illustrated in Fig. 3-3. A large switching wave is applied to the broken-line characteristic of a vacuum tube—for example, a triode. Constant grid current supplied through  $R_1$  maintains the triode on the upper flat portion of the broken-line characteristic. The negative switching wave, which is large compared with the grid base of the tube, will initiate an exponential waveform at the plate of the triode. The grid base should be short in order that the switching wave may give rapid initiation of the exponential wave. Quick recovery time requires a large current for the conducting portion of the broken-line characteristic.

Another important function of the conducting portion of the characteristic is the establishment of the initial potential of the exponential

wave denoted by  $E_i$  in Fig. 3-3. Whereas this initial level may not be of great importance for crude measurements made by cathode-ray-tube displays, it is of utmost importance in precision operations, where a slight variation of  $E_i$  would cause serious errors in precision-timing operations depending upon amplitude comparison (see Sec. 3-5). Reasonable stability is obtainable in this circuit since the plate current is relatively independent of small variations of grid current. Often the initial level of a wave is set equal to an arbitrary value or to its peak value by "d-c restoration." Since this may depend upon the more complicated processes of time selection and demodulation, it is discussed in Secs. 3-6 and 3-12.

**3-4. Amplitude Selection.**—Amplitude selection is defined as the process of selecting a portion of a waveform lying above or below a

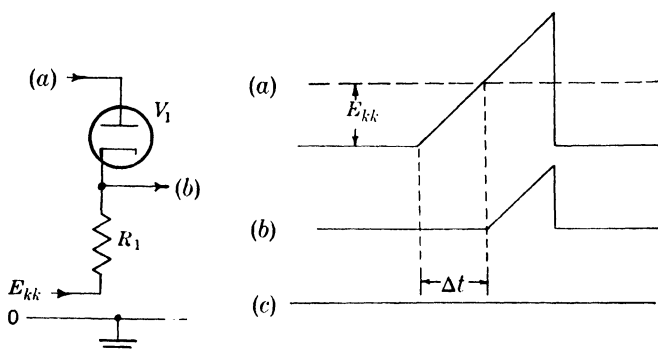


FIG. 3-4.—Amplitude selection by means of the broken-line characteristic of diode  $V_1$ . The portion  $b$  of wave  $a$ , which exceeds the cathode potential of  $V_1$ , is selected and has a time delay  $\Delta t$ .

boundary or within two bounds. The selected portion of the input wave is undistorted. Perfect amplitude selection requires the ideal broken-line characteristic, but a satisfactory approximation to this is obtained by using the broken-line characteristic of diodes or germanium crystals at large input amplitudes. Figure 3-4 is a typical example of the selection of a triangular wave  $a$  lying above the cathode potential  $E_{kk}$  of  $V_1$ , and waveform  $b$  is obtained. The potential  $E_{kk}$ , at which the amplitude selector operates, is often termed "the reference potential."

A practical use of amplitude selection is indicated in Fig. 3-5, where the top of portions of a pulse train obtained on differentiation of a square wave is selected. This results in elimination of the negative excursions of the pulse train and the slower parts of the positive excursions. These pulses are then suitable for display on a cathode-ray tube as time markers.

One may also select portions of a wave below a limit, giving the familiar operation of clipping or limiting as indicated in Fig. 3-6, where

the lower half of a sinusoidal wave is selected. A more useful method for obtaining square waves from sinusoids is that of amplitude selection between limits indicated in Fig. 3·7. This method depends upon the doubly broken-line characteristic obtained from two diodes (*A*). In this case the positive limit is set by  $E_1$ , the negative limit by  $E_2$ , and the

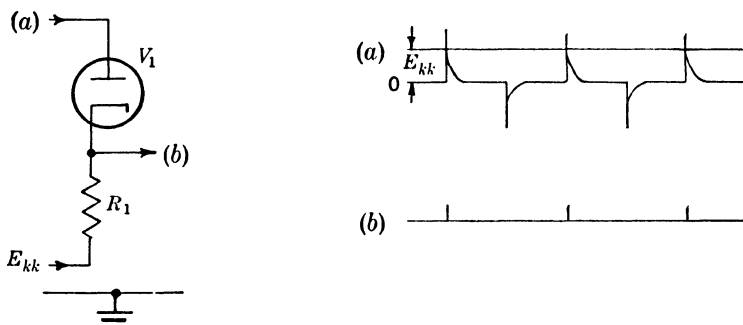


FIG. 3·5.—Waveform-shaping by amplitude selection. The negative pulses and the broad bases of the positive pulses are eliminated by diode amplitude selector  $V_1$ . These pulses are suitable for timing indices.

square waves of *b* are obtained. For this particular purpose, amplitude selection may also depend upon the broken-line characteristic obtained at the grid of a pentode (*B*) where the positive limit is set by bottoming of the pentode and the negative limit set by cutoff.

For the selection of rapidly varying waveforms, small values of  $R_1$  are required in Figs. 3·4, 3·6, and 3·7, and the broken-line characteristic should be abrupt and have a minimum resistance.

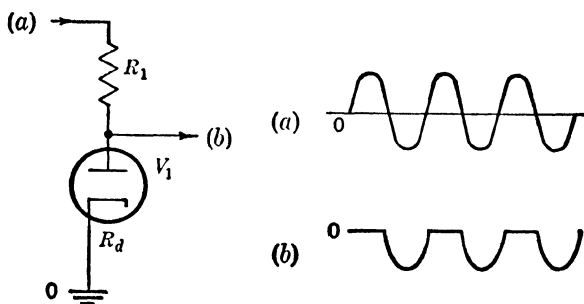


FIG. 3·6.—Amplitude selection of the negative half cycles of a sinusoidal wave.

**3·5. Amplitude Comparison.**—If in Fig. 3·4 it is desired to determine the exact moment of equality of the triangular wave and the cathode potential of the diode, wideband amplification and differentiation give a sharp pulse *c*, which precisely marks the time of equality of the triangular wave and the fixed voltage. This is the process of amplitude comparison

and may be defined in mathematical terms as the process of determining the abscissa of a waveform given its ordinate, or, in physical terms, the indication of the instant of equality of the amplitudes of two waveforms.

In the interests of economy, linear amplification of an amplitude-selected wave is rarely used since regenerative devices having the backlash or hysteresis characteristic are preferred. Their operation is, however, nearly always initiated by amplitude selection—for example, by the electron current initiating ionization in a gas-discharge tube or by the selection of a small voltage initiating regeneration in a positive-feedback circuit. It is, however, best practice to employ a diode amplitude selector

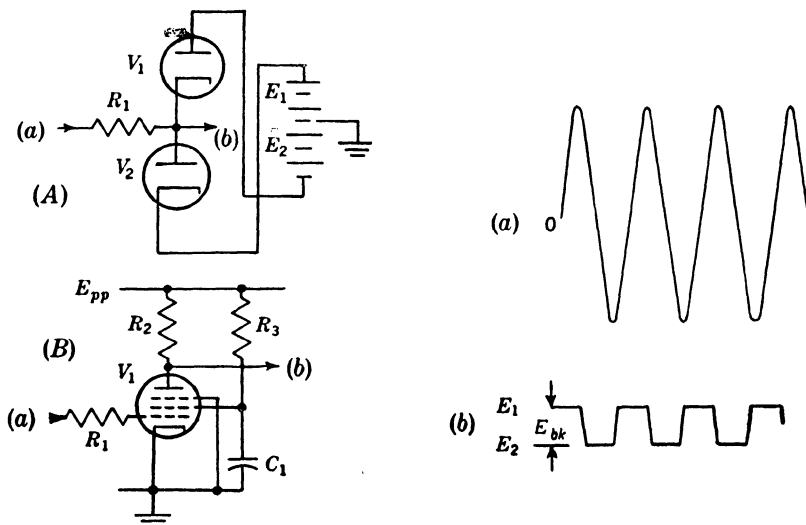


FIG. 3-7.—Amplitude selection between limits  $E_1$  and  $E_2$  by the two broken-line characteristics (A). Sinusoidal wave  $a$  is converted into the rectangular wave  $b$ . The non-linear characteristic of the pentode circuit (B) is also useful for this purpose.

at the input of any of these devices in order to obtain a stable voltage at which amplitude selection occurs. The detailed design considerations that permit a diode amplitude selector to determine the operating point of a device having a hysteresis or backlash characteristic are discussed in Chap. 9.

An example of a simple amplitude comparator is indicated in Fig. 3-8. A triangular wave is connected to the grid of a thyatron—for example, type 2051 by resistance-capacitance network  $R_1C_1$  and d-c restorer  $V_2$  (see Sec. 3-11). The level of the waveform is therefore adjustable by means of a potentiometer  $R_3$  and, if set, for example, to a negative value, the moment at which the firing potential of  $V_1$  is exceeded is indicated by a sharp spike shown in waveform diagram  $b$ .

In a number of important applications the amplitude comparator

and the timing-waveform generator are interconnected in such a way that the amplitude comparator resets the waveform generator, with the result that repetitive or relaxation oscillations are sustained. The hysteresis or backlash characteristic at the plate of the hot-cathode gas

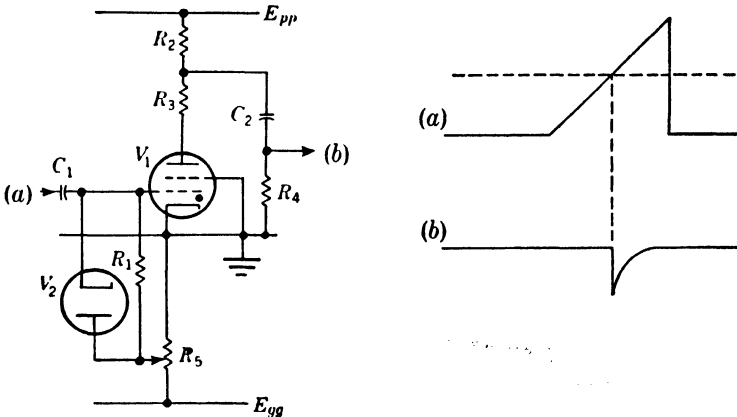


FIG. 3-8.—Amplitude comparison indicating the use of the discontinuous characteristic. The moment of equality of the triangular wave *a* to the firing potential of  $V_1$  is indicated by the sharp spike *b*.

diode gives a good illustration of this as is indicated in Fig. 3-9. If the gas diode is nonconducting, a positive exponential wave is generated at *a*. At the instant the plate potential equals the striking potential for the arc, an abrupt transition is observed, a large current flows, and the plate potential of the gas diode falls below the extinction potential. In this way the waveform generator is reset and then a new exponential is generated. The circuit operation, therefore, includes the distinct processes of waveform initiation (Fig. 3-3) and amplitude comparison (Fig. 3-8) that are basic in the operation of relaxation oscillators and rectangular waveform generators (see Chaps. 5 and 6).

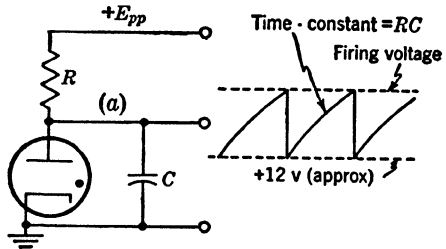


FIG. 3-9.—Gas-diode relaxation oscillator. This circuit combines waveform generation and amplitude comparison by means of the discontinuous characteristic of the gas diode to terminate the waveform and give recycling operation or relaxation oscillations.

**3-6. Time Selection.**—Time selection is similar to amplitude selection except that the operation is performed on the abscissa (time axis) of the waveform. A time selector may select a waveform occurring within a given interval or a portion of a waveform occurring before or after a given time. The selected portion should be undistorted. The simplest

method of time selection is that illustrated in Fig. 3-10 where a rectangular selecting pulse  $b$  is added to waveform  $a$ , giving  $c$ . Amplitude selection of  $c$  gives selected wave  $d$ . In all cases the amplitude of the selector pulse must exceed that of unwanted pulses. Also the bias  $E_{kk}$  of the amplitude

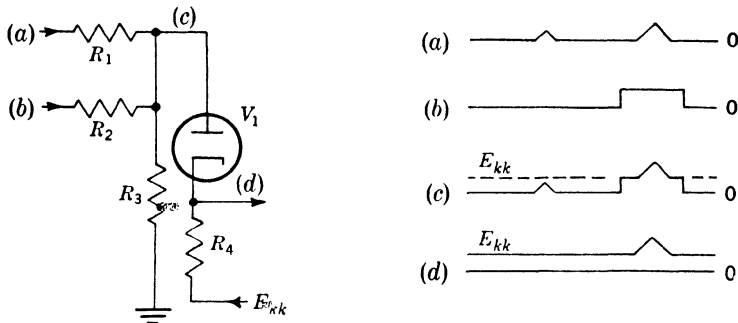


FIG. 3-10.—Time selection. Waves  $a$  and  $b$  added in  $c$  are connected to amplitude selector  $c$  giving time selection in  $d$ .

selector and the amplitude of the selector pulse must be critically adjusted lest some portions of the signal be lost or portions of the selector pulse appear in the output. The latter effect is termed “pedestal” and is usually undesirable.

Operation independent of the amplitude of the selector pulse is readily obtainable by using the multivariable characteristics exhibited by the pentode. As shown in Fig. 3-11, the selector pulse is applied to the suppressor grid and the input signal to the control grid of normally nonconducting pentode  $V_1$ . The operation is substantially independent of the amplitude of the selector pulse which exceeds the upper limit of the broken-line characteristic of the suppressor grid. In most time selectors, however, a faithful reproduction of the input signal is required, and therefore negative feedback is desirable in order

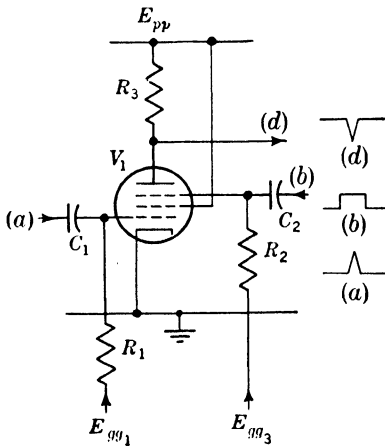


FIG. 3-11.—Time selection by means of the multivariable characteristic of pentode  $V_1$ .

to minimize distortion due to the curvature of the pentode characteristic.

The coincidence of a large number of inputs may be indicated by connecting a number of simple time selectors in series or by taking advantage of other control electrodes—for example, the screen potential of the pentode. These combinations are discussed in Chap. 10.

The time selectors discussed above respond only to signals of one polarity (unidirectional switches) and often equal response to signals of both polarities is required. This is readily achieved by using two broken-line characteristics. A true equivalent to the single-pole single-throw switch is obtained and is often termed a "bidirectional switch." In these circuits the selector pulse is coupled to the circuit elements by condensers or transformers, often depending upon whether normally conducting or normally nonconducting operation is desired, as indicated respectively by Figs. 3·12*a* and *b*. In Fig. 3·12*a* the input is short-circuited in the absence of negative selector pulse applied to the plate of  $V_1$  and positive selector pulse applied to the cathode of  $V_2$ . On the other hand, switch

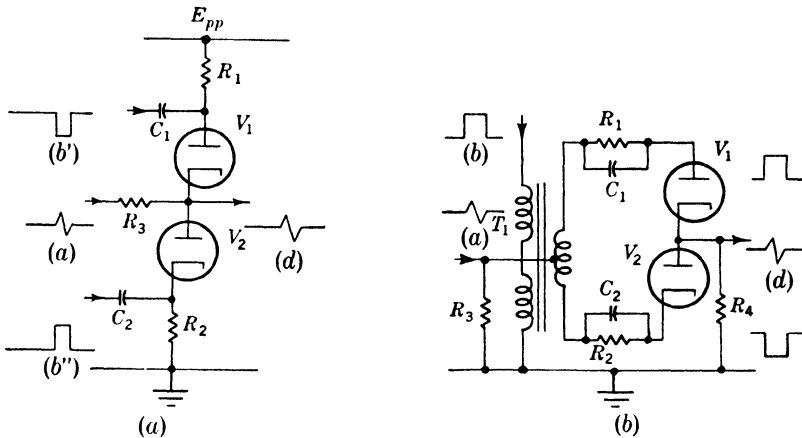


FIG. 3-12.—Time selection by means of two broken-line characteristics, in (a) obtained from normally conducting diodes and in (b) obtained from normally nonconducting diodes. These time selectors are suitable for signals of both polarities.

circuit *b* is normally opened and is closed only by a positive selector pulse applied to the plate of  $V_1$  and a negative selector pulse applied to the plate of  $V_2$ . The switch is maintained open by the voltages accumulated across  $R_1C_1$  and  $R_2C_2$ .

Many other types of switch circuits specialized for various types of time selection are described in detail in Chap. 10.

**3·7. Amplitude Modulation.**—A number of important modulation processes depend upon variation of the reference potential of an amplitude selector. Amplitude modulation, which is defined as modulation in which the amplitude of the waveform is the main characteristic that is varied, is illustrated in the simple example of Fig. 3·13. Here the variation of the reference potential of a diode amplitude selector is in accordance with the signal waveform *b* and results in amplitude modulation of the pulse train *c*. For large values of the input waveform *a*, this process is linear because of the relatively abrupt broken-line characteristic of the diode.



Another method employs two broken-line characteristics—for example, that of the diode switch circuits of Fig. 3·12. In Fig. 3·14, the signal is short-circuited through  $V_1$  and  $V_2$  in the absence of the carrier

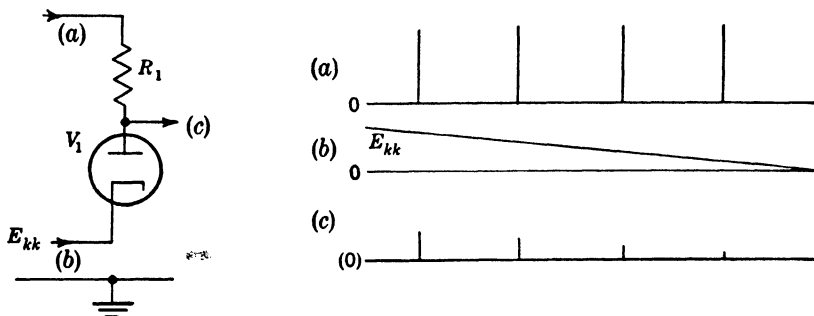


FIG. 3·13.—Electrical amplitude modulation. Amplitude selection of pulse train  $a$  in response to variation of  $E_{kk}$  of amplitude selector  $V_1$  gives amplitude-modulated pulse train  $c$ .

pulse, but the short circuit is released for the duration of the carrier pulses as shown at  $d$  of Fig. 3·14. In the circuit of Fig. 3·12b the carrier-controlled switch,  $V_1$  and  $V_2$ , is interposed between input  $a$  and output  $d$

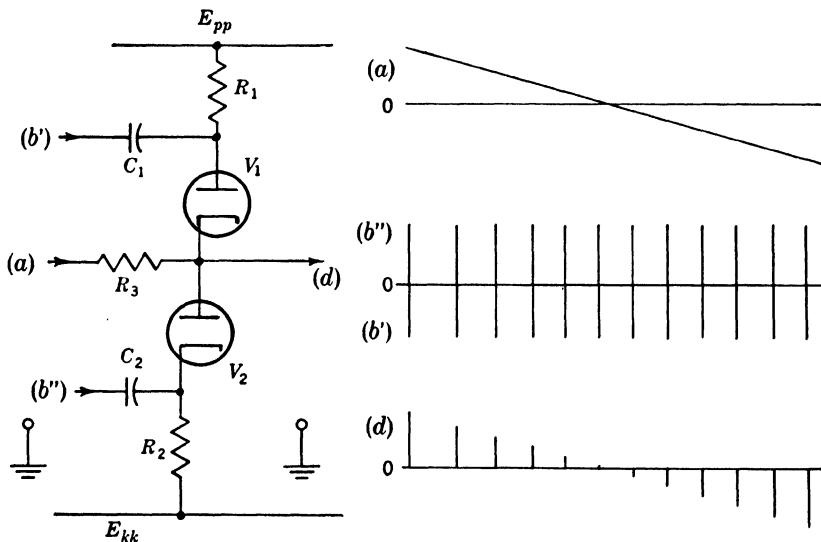


FIG. 3·14.—Phase-sensitive amplitude modulation by means of a bidirectional switch. Signal  $a$  is connected to the output terminal by carrier pulses  $b'$  and  $b''$ , giving amplitude-modulated pulse train  $d$ . The polarity of the modulated output reverses with a reversal of the sign of the input.  $E_{pp} = -E_{kk}$ ,  $R_1 = R_2$ .

and interrupts the signal. Carrier pulses of the appropriate polarity applied to the plate of  $V_1$  and the cathode of  $V_2$  close the switch and connect the signal to the output terminal  $d$ .

Other types of nonlinearity have been used in amplitude modulation. The carrier-controlled mechanical switch is an excellent example; it has the most stable nonlinear characteristic. The above discussion has been limited to variation of a resistance by the carrier frequency, but often inductance or capacitance is varied (see Chap. 11).

An important feature of the modulator circuits based upon the bidirectional switch circuits is that the polarity or phase of the output is identical with that of the input, giving what is called "bidirectional modulation" as indicated by the waveform diagram *d* of Fig. 3-14.

An important error in the amplitude modulation of slowly varying signals may be the variation in contact potential of the modulating

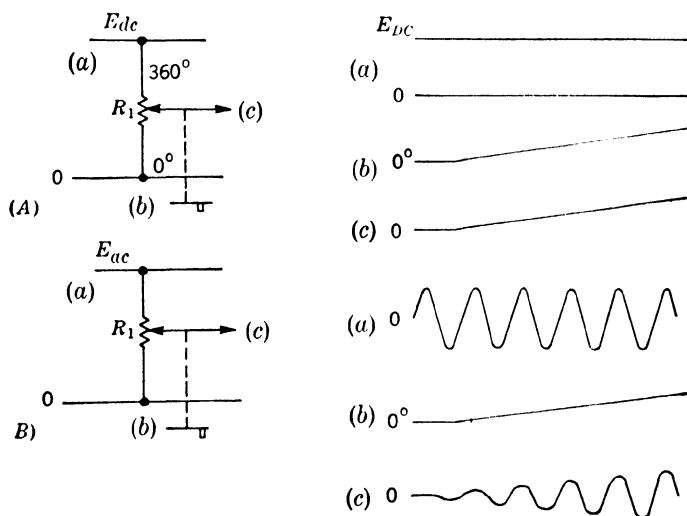


FIG. 3-15.—Electromechanical amplitude modulation. (A) indicates the modulation of a d-c (zero frequency) carrier, (B) the modulation of an alternating carrier.

element with variations of heater voltage. This difficulty is reduced by employing a pair of diodes, since the variation of one may balance the other. The effect of heater voltage is eliminated by the use of germanium crystals, but the greatest stability is obtained by employing a mechanical switch.

Often amplitude modulation is required in response to mechanical input signals, and resistors, inductors, and capacitors are commonly varied and give amplitude modulation of a steady voltage as shown in Fig. 3-15a or of an alternating carrier as shown in Fig. 3-15b. An interesting feature of Fig. 3-15b is that the phase of the output wave may be made reversible with respect to a center tap on the potentiometer. Thus the amplitude of the a-c wave indicates the magnitude of the displace-

ment, and the phase of the a-c wave indicates the sign of the displacement with respect to the center tap, thus giving bidirectional modulation.

**3-8. Time Modulation.**—Amplitude selection of a portion of sinusoidal, triangular, or other time-variable waveforms gives a modulation that is called “time modulation” and is defined as modulation of the time of appearance of a portion of a waveform with respect to a reference time, which may be defined by the waveform itself.

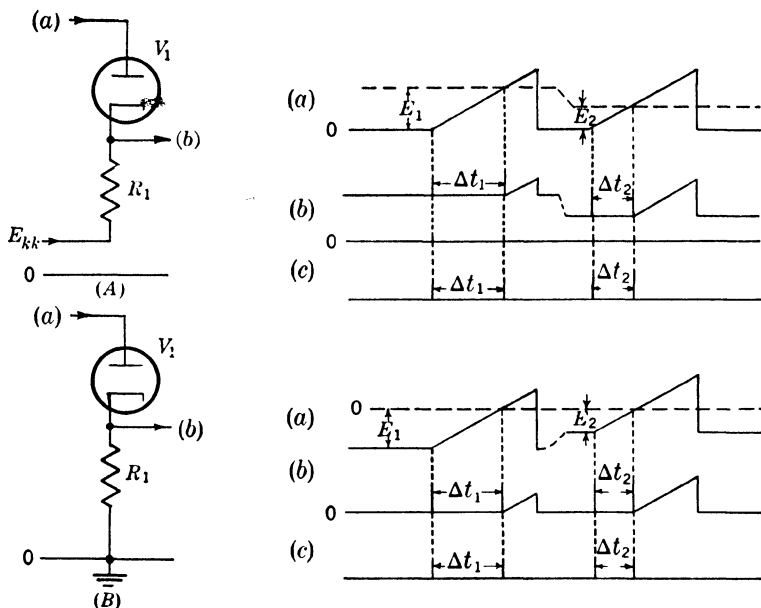


FIG. 3-16.—Time modulation by amplitude selection. In (a) the cathode potential  $E_{kk}$  of  $V_1$  is varied, and the level of the waveform is maintained constant. In (b) the cathode potential of the amplitude selector is maintained constant and the level of the waveform is varied. Time modulation of the interval between the initiation of the triangular waveform and the selection of portion  $b$  is obtained. Amplification and differentiation may be used to obtain pulse  $c$ .

Figure 3-16a indicates that variation of the reference potential of amplitude selector  $V_1$  between the values  $E_1$  and  $E_2$  gives amplitude selection of portions of the input wave  $a$  at times  $\Delta t_1$  and  $\Delta t_2$ . For a triangular waveform,  $\Delta t$  is linearly related to  $E_{kk}$ . Amplification and shaping of the output of the selector gives accurate time indices indicated in  $c$ . The whole process may be represented as that of amplitude comparison with a variable reference potential.

The reference voltage of the amplitude comparator need not be variable in order to produce time modulation. For example, the level at which the triangular waveform of Fig. 3-16b is generated might be

varied, giving a similar variation of the interval between the initiation of the wave and the generation of the index.

**3-9. Phase Modulation.**—A fundamentally different method of obtaining time modulation by amplitude comparison at a fixed reference voltage depends upon phase modulation of a timing wave. For example, in Fig. 3-17 the phase of a sinusoidal wave is shifted from that of  $a$  to that of  $b$  giving a corresponding shift in the time at which the wave passes through zero in the positive direction. Continuous inductance and capacitance phase shifters (Fig. 3-17) have made this a very convenient method for modulation in response to mechanical input signals. There are as yet no highly precise phase modulators responding to electrical signals.

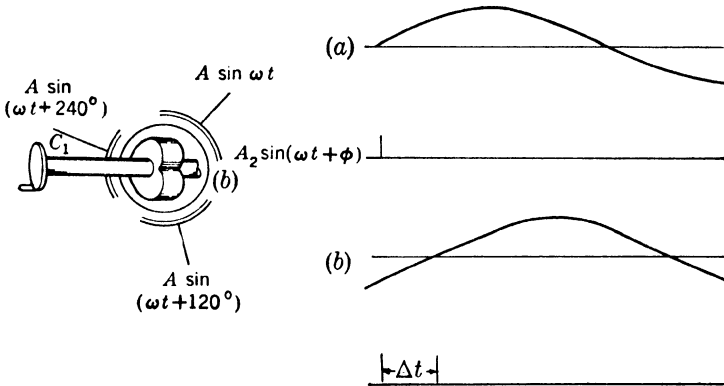


FIG. 3-17.—Electromechanical phase modulation. Three-phase sinusoids applied to variable condenser  $C_1$  give modulation of the phase of the output in response to a mechanical signal. The diagrams indicate the time modulation of a pulse obtained by amplitude comparison.

Phase modulation may be defined similarly to the other forms of modulation: it is a process of modulation in which the phase of a waveform is varied with respect to a reference phase.

**3-10. Amplitude Demodulation.**—Amplitude demodulation may be defined as the process by which information is obtained from an amplitude-modulated waveform about the signal imparted to the waveform in modulation. Many methods of detection depend upon the broken-line characteristic used for the amplitude selection of values of the modulated wave which exceed a potential accumulated upon a storage or memory circuit. An example of this is indicated in Fig. 3-18 where the resistance-capacitance combination  $R_1 C_1$  is charged to the peak value of the positive excursions of the modulated carrier  $a$ , giving the demodulated or detected output shown in  $b$ . The resistance is necessary to provide decay of the potential of  $b$  at a rate sufficient to give response to decreasing values of the modulated input.

A much more efficient detector circuit uses a bidirectional switch that is operated for a predetermined interval at the carrier frequency to connect the modulated input to a storage condenser as indicated in Fig. 3-19. The outstanding property of this detector circuit is that no shunt resistor is needed in order to secure an output response to decreases

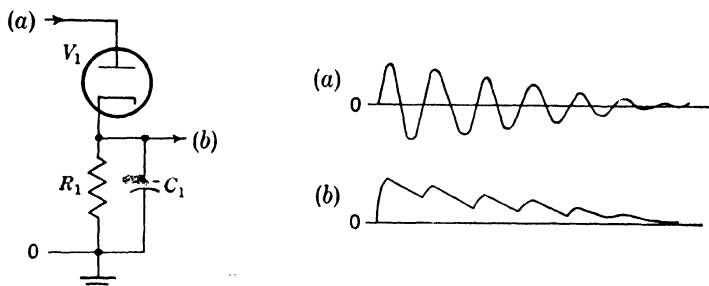


FIG. 3-18.—Peak detection by means of a diode amplitude selector. Exponential decay of the output is obtained by  $R_1$ .

of the input signal as was the case in Fig. 3-18. As indicated by waveform diagram *c*, the output therefore proceeds in a series of steps each equal to the peak amplitude of the last signal pulse. This results in a considerable reduction of carrier content for a given speed of response. In addition, a detector circuit of the switch type has the advantage of

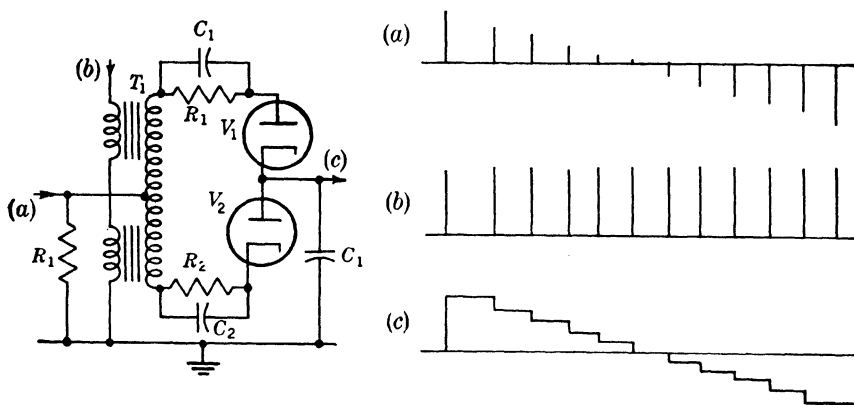


FIG. 3-19.—Phase-sensitive detection with constant output obtained with a bidirectional switch. The bidirectional property of the switch circuit permits constant output between carrier pulses and gives reversal of the polarity of the output in response to phase reversal of the modulated wave.

time selectivity, and interfering waveforms not coincident with the switching pulse will not affect the output. The detailed properties of this important circuit are discussed in Chap. 14.

**3-11. Level-setting.**—The output of the detector of the type illustrated in Figs. 3-18 and 3-19 may be used to establish at an arbitrary

potential the level of a wave at the instant of its peak value or, in the case of the switch detector, at any chosen instant. These circuits, sometimes called "d-c restorers," do not necessarily restore the original level of a wave, but rather hold a particular part of the input wave at an entirely new level. This is indicated in Fig. 3-20*a*, where the level of the wave is established by the potential accumulated across  $C_1$ , which with an appropriate choice of circuit constants is equal to the negative peak value of the applied triangular waveform. In this particular case, the peak

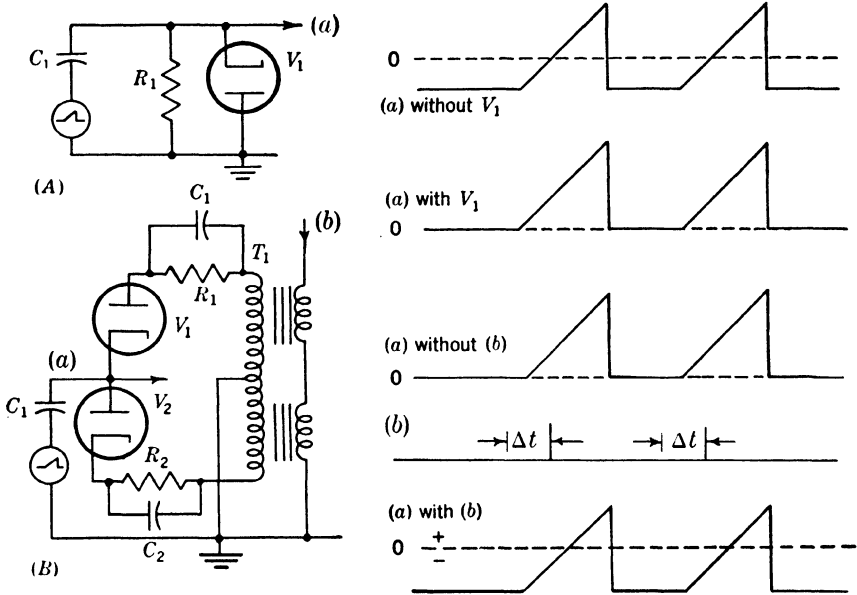


FIG. 3-20.—Level-setting (d-c restoration) by means of two types of detector circuits (A) indicates the use of a peak detector to maintain the maximum excursions of wave *a* at ground potential. (B) employs a switch detector to set the level of waveform *a* at its value at the time of occurrence of switching pulse *b*.

value of the triangular waveform does not fall below ground potential except for the small voltage required to maintain the charge upon  $C_1$ . Figure 3-20*b* illustrates the establishment of the level of a waveform at an arbitrary time  $\Delta t$  with respect to its initiation. Other applications of these techniques of level setting are described later in this volume and in Vols. 20 and 22.

**3-12. Time Demodulation.**—A simple method of time demodulation is indicated in Fig. 3-21, where the time of occurrence of a rectangular pulse is modulated in accordance with signal information. Time selection of a portion of this modulated wave with respect to the recurrent selector pulse *b* gives a rectangular wave of variable duration as indicated in *c*. The area of this wave may be detected by a circuit similar to that of

Fig. 3-18 by inserting resistance in series with the diode to avoid detection of the peak value of the wave. Alternatively, the rectangular wave  $c$  may be converted into a triangular wave of variable amplitude by means of the circuit of Fig. 3-3. The output of this circuit is then peak-detected by the circuit of Fig. 3-18. This represents the process of time demodulation, which may be defined as the process by which information is recovered from a time-modulated waveform about the signal imparted to the waveform in time modulation.

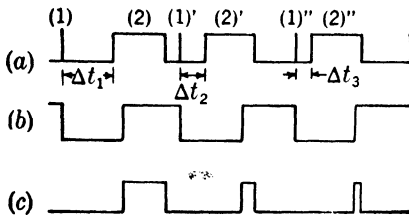


FIG. 3-21.—Conversion of a time-modulated wave into a duration-modulated wave for the purposes of time demodulation. The rectangles 2, 2', and 2'' are time-modulated with reference to the pulses 1, 1', and 1'' and are converted into duration-modulated pulses in  $c$  by time selection with  $b$ . The duration-modulated waves in  $c$  are then to be average-detected or converted into a triangular wave and then peak-detected.

the time of occurrence of pulse  $b$  as indicated in Fig. 3-22.

This extremely efficient and simple time demodulator has, however, the disadvantage that it is sensitive to interfering pulses occurring at any time during waveform  $a$ . Time-demodulation circuits used in radar range measurements employ a negative-feedback system for time demodulation, which has great time selectivity and accuracy and consists of a time-discriminating element and a time-modulating element. The time-discrimination element usually consists of a pair of time selectors, composed, for example, of two elements of the circuit of Fig. 3-11, where time-modulated pulses  $a$  of Fig. 3-23 are connected to the parallel-connected control grids, and selector pulses  $b$  and  $c$  are connected to the suppressor grids. The output  $d$  of the first time selector represents the overlap of  $a$  and  $b$ , and the output  $e$  of the second time selector, the overlap of  $a$  and  $c$ . Detection and subtraction of the areas of pulses  $d$  and  $e$  are carried out by circuits called "difference detectors" (see Chap. 14). This circuit gives zero output if outputs

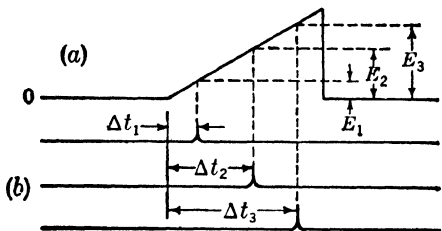


FIG. 3-22.—Time demodulation by time comparison. A switch circuit of Fig. 3-19, operating at times  $\Delta t_1$ , etc., connects timing wave  $a$  to the output circuit giving potentials  $E_1$ , etc.

$d$  and  $e$  are of equal areas; and, if  $d$  and  $e$  are of unequal areas because of time modulation of the input pulses, the circuit gives a demodulated output. This combination of circuit elements is termed a "time discriminator," and its function may be defined as that of indicating by zero output equality of the times of occurrence of the input pulse and the selector pulses and inequality by the sense and approximate magnitude of the output.

The demodulated output of the time discriminator is not, however, used to represent directly the modulating signal. The output is connected to an electrically controlled time modulator in a negative-feedback system and thereby furnishes merely a control voltage to the time modulator, which, in turn, generates the selector pulses. In this way the selector pulses are constrained to follow the modulation of the input signal. The linearity of the operation, therefore, depends upon that of the time modulator and not upon that of the time discriminator, and consequently extremely high accuracies are obtained (see Vol. 20, Chaps. 8 and 9).

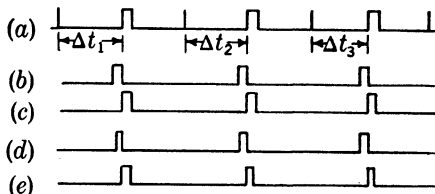


FIG. 3-23.—The use of time selection in time discrimination. The time of occurrence of the modulated pulses in  $a$  with respect to selector pulses  $b$  and  $c$  is compared in a pair of time selectors giving pulses  $d$  and  $e$ . These pulses are detected, and their areas are subtracted in a difference detector. The whole process represents time discrimination.

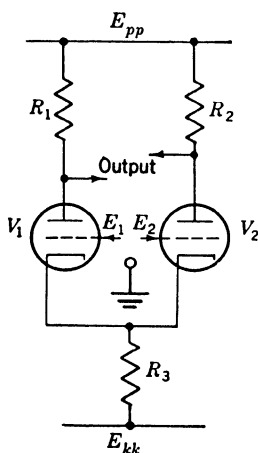


FIG. 3-24.—Amplitude discriminator. The plate potentials are equal for equal grid voltages and are unequal in the sense and approximate magnitude of unequal grid voltages. In addition, a common-mode signal, the sum or average value of the two input signals, is rejected providing  $R_3 \geq (R_1 + R_2)/2$ , where  $E_{pp}$  and  $E_{kk}$  are fixed.

**3-13. Amplitude Discrimination.**—Just as a time discriminator indicates the time inequality of two events, an amplitude discriminator is a means for indicating the equality or inequality of two voltages. Similarly, the sense and approximate magnitude of differences are indicated. Amplitude discrimination may depend upon linear circuit elements and may be accomplished by the subtraction of two voltages  $E_1$  and  $E_2$ . The subtraction may be carried out by inversion and addition, or it may be carried out by a differential or balanced amplifier circuit, as shown in Fig. 3-24. Equality of grid voltages gives equality of plate voltages for balanced circuit

components, and inequalities of grid voltages give corresponding inequalities of plate voltages.



An important aspect of this process is the necessity for the rejection of common potential variations of the input signal—for example, a signal applied in series with the ground return of both grids of Fig. 3-24. For balanced components this signal does not affect the differential mode of operation of the amplifier, since it occurs in the common mode of operation of the inputs. Such a signal is therefore called a “common mode” signal. These common-mode signals are rejected only as long as the circuit components of the differential amplifier are balanced and, hence, operating linearly.

Amplitude discrimination may depend upon phase-sensitive modulation and demodulation systems, and in these devices the rejection of common-mode effects is generally complete.

Amplitude discriminators are used extensively as an element in negative-feedback systems—for example, in amplifiers and servomechanisms.

Usually the voltage inputs to an amplitude discriminator are both varying slowly with time, but in certain cases it may be desired to equate the peak value of a wave to a steady voltage.

#### CHARACTERISTICS OF NONLINEAR CIRCUIT ELEMENTS<sup>1</sup>

Although the important properties of an element are summarized in its ideal characteristic, every physical unit exhibits departures from this ideal. In most cases, the major task of a circuit designer is to determine the size and effectiveness of these sources of error. The data of this type that are given here cannot be exhaustive, but only exemplify the information that the designer of precision circuits must obtain by measurements on many units under various conditions.

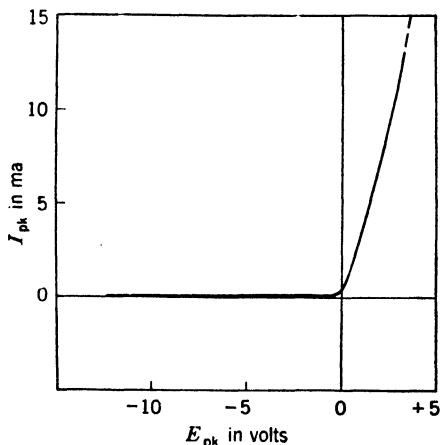


FIG. 3-25.—Typical average broken-line diode plate characteristic (6AL5).

For applied voltages, more negative than a few tenths of a volt, the current is negligible ( $10^{-8}$  amp in most diodes and  $10^{-16}$  amp for special tubes); for applied voltages positive with respect to the “break,” the current increases rapidly with increasing voltage. The break in the characteristic is not perfect since

<sup>1</sup> Sections 3-14 to 3-27 by R. Kelner and J. W. Gray.

#### 3-14. High-vacuum Diode.—

A diode provides a broken-line relationship between voltage and current. The average characteristic of a representative diode is shown in Fig. 3-25. For applied

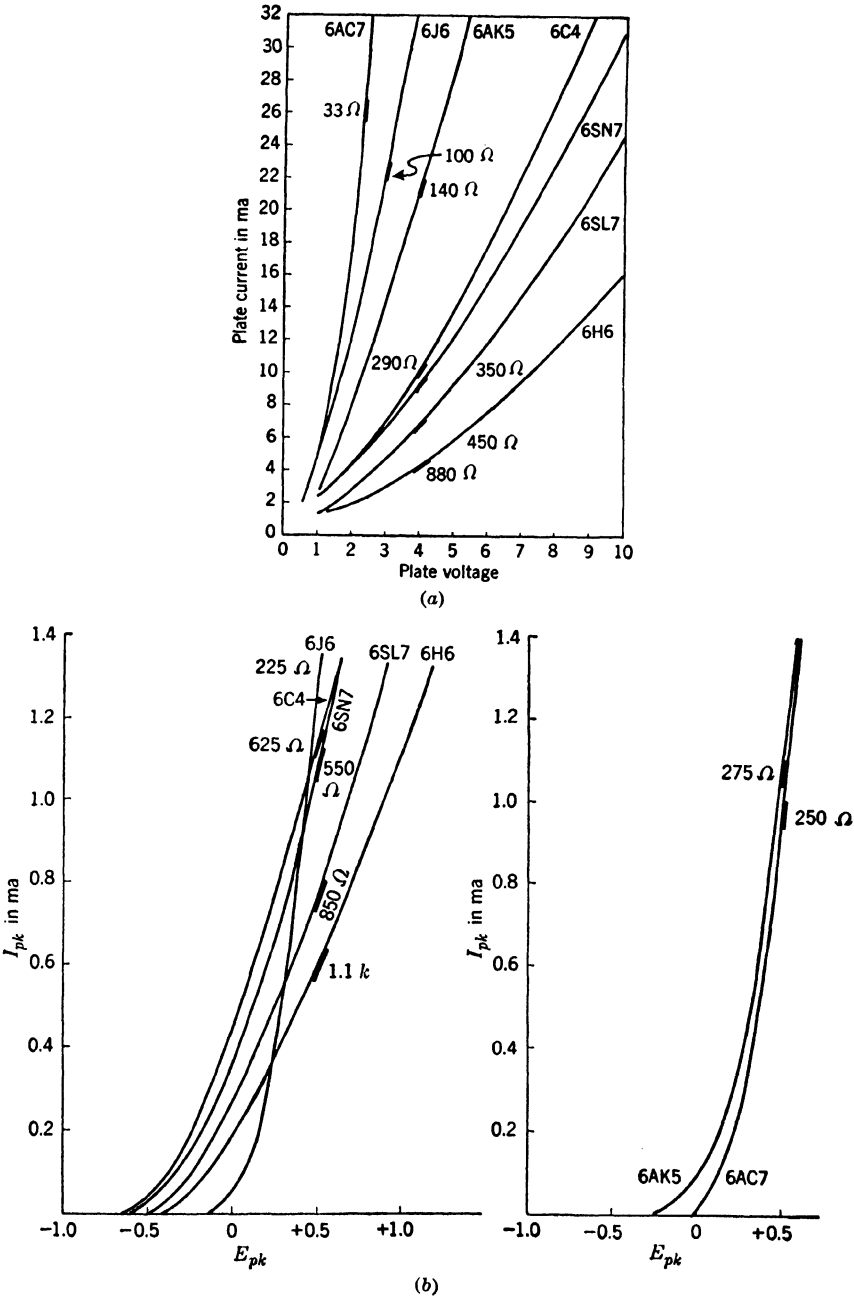


FIG. 3-26.—Average conduction characteristic for several diodes,  $E_{ff} = 6.3$  volts. (a) High voltages ( $E_{pk}$ , 1 volt to 10 volts). (b) Low voltages ( $E_{pk} < 1$  volt).

there is no discontinuity in slope but only an exponentially shaped transition region. The conducting segment of the characteristic is shaped according to a power law. These two regions may be seen on the curves of Fig. 3-26. The diode has the great advantage of approximating an open switch for one segment of its characteristic.

The most common means for utilizing the diode characteristic is a series circuit with a resistor. The characteristic relating the voltage across the combination and the voltage across the resistor is shown in Fig. 3-27. The extent in voltage of the conducting segment is greatly increased and the segment is linear. The increase in the range of the

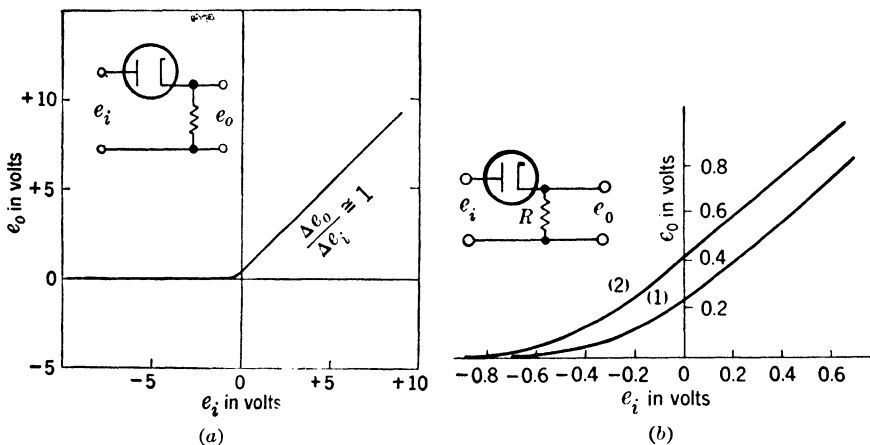


FIG. 3-27.—Diode-resistor circuit characteristic (6AL5)  $E_{ff} = 6.3$ , average tube. (a) Broken-line characteristic with linear conduction segment. (b) Expansion of break. The size of resistance affects the effective break voltage slightly but not the shape (sharpness) of break. (1)  $R = 10k$ , (2)  $R = 100k$ .

voltages (for allowable currents) is very effective in stabilizing the element against cathode drifts. The exponential decrease of current extends over a small percentage of the voltage range and is therefore very nearly the ideal break. The curvature may be troublesome if very accurate selection is necessary. The exact voltage of the “break” is defined only to the extent that subsequent circuits define the output voltage level at which a response is observable: the higher the subsequent amplification, the earlier will apparent conduction occur.

Since the break is of primary interest for most applications of the diode, a discussion of the nature of its exponentiality is appropriate. The diode consists of a two-electrode element in which electrons are emitted from the hot surface of the cathode and are repelled or attracted by the potential of the plate with respect to the cathode. Because of initial electron velocities, a small amount of current flows despite small negative plate voltages. The distribution of the normal components of velocities

of the electrons emitted from a hot surface explains the exponential decrease of current as the plate voltage becomes more negative. (Note the linear semilogarithmic curves of Fig. 3-28.)

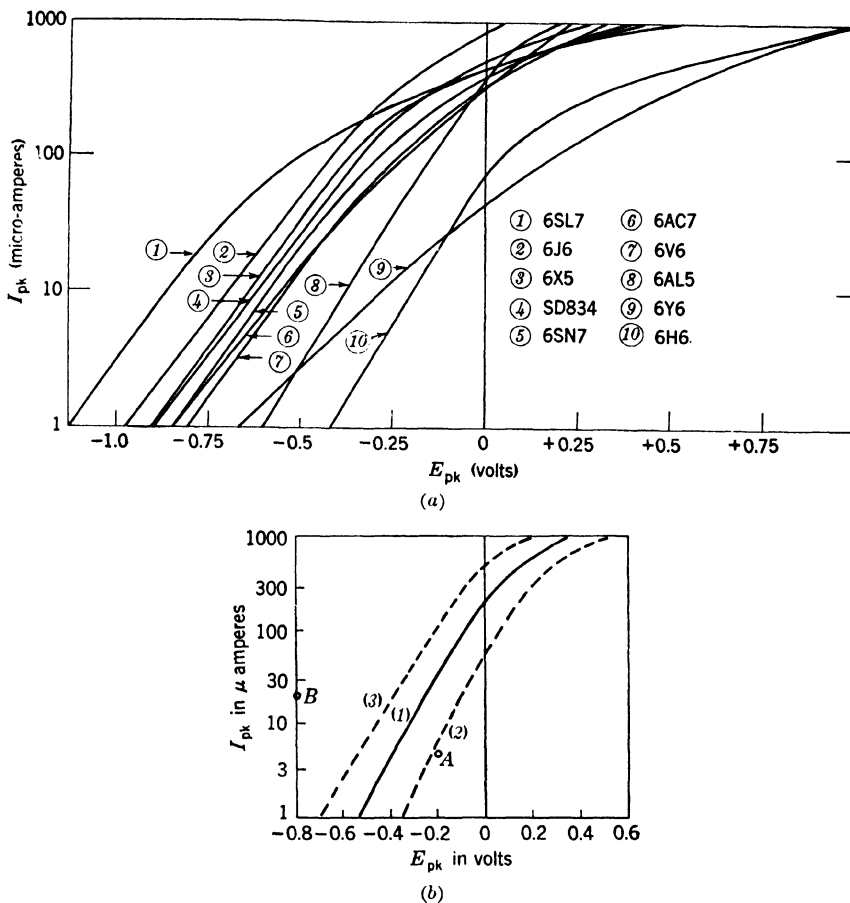


FIG. 3-28.—Expanded plate characteristics near break. The grid tubes are diode-connected. (a) Average characteristic for several tube types. (b) Effect of heater-voltage variation upon an average 6AL5 characteristic: (1) normal heater voltage, 6.3 volts; (2) 85 per cent; (3) 115 per cent. A similar parallel shift occurs between units of the same type of tube at normal heater voltage. The JAN specifications require that all JAN tubes have a characteristic passing between points A and B.

Of the total number of electrons emitted in a given time, the portion having sufficient energy to reach a surface of potential  $E$  volts below that of the cathode is  $e^{-\frac{11,600}{T}E}$ , where  $T$  is temperature in degrees Kelvin. Thus, the total plate current is proportional to this expression if  $-E$  is the minimum potential to be found between plate and cathode of a diode

having plane parallel electrodes. For ordinary currents this potential is determined by the space charge, and is far below the plate potential; but if the plate voltage and current are rather low, this is no longer the case. The minimum potential becomes practically identical with the sum of plate potential and contact potential. The latter is a constant voltage, depending only on electrode materials. Thus, for small currents the plate current is approximately

$$i_p \approx I e^{\frac{11,600}{T}(e_p + E_w)}, \quad (1)$$

where  $e_p$  is plate-to-cathode voltage,  $E_w$  is contact potential, and  $I$  is total emission current. Both  $I$  and  $E_w$  may be omitted by introducing  $i_o$  as the plate current at zero plate voltage (assuming the relation to hold at this point):

$$i_p \approx i_o e^{\frac{11,600}{T}e_p}. \quad (2)$$

An oxide-coated cathode is operated normally between 1000° and 1100°K; hence Eq. (2) in this case is approximately

$$i_p \approx i_o e^{e_p/0.09}. \quad (3)$$

If the current is expressed logarithmically,

$$\ln i_p \approx \frac{e_p}{0.09} + \ln i_o, \quad (4)$$

$$\log_{10} i_p \approx \frac{e_p}{0.21} + \log_{10} i_o. \quad (5)$$

The current thus increases geometrically with respect to plate voltage, increasing tenfold for each 0.21-volt increment of voltage. The measured characteristics of Fig. 3-28 follow the predicted relationship [Eq. (5)] closely except for small variations in slope.

The above applies to concentric cylindrical electrodes as well as to plane-parallel configuration.<sup>1</sup> The end effects of other tube geometries seem to result in a larger figure than the 0.21 volt quoted above. The increase never is more than about 50 per cent, however, and the value is quite constant for a given tube (filamentary cathodes are not considered here).

The value of plate current below which the logarithmic relationship is fairly linear depends on cathode area and interelectrode spacing, and ranges from 50 to 300  $\mu$ a for receiving tubes, whether they are diodes or diode-connected triodes, etc. Figure 3-28b shows the curve for a 6AL5 diode. This has cylindrical electrodes with very little end effect, and the semilogarithmic curve is linear up to 100  $\mu$ a.

<sup>1</sup> J. Millman and S. Seely, *Electronics*, McGraw-Hill, New York, 1941.

**Cathode Temperature.**—Cathode temperature (heater voltage) affects the total electron emission, and the most noticeable effect of temperature variation is a shifting of the curve with respect to plate voltage. That is, a given change in temperature may be offset by a certain change of plate voltage, which is largely independent of the value of the current. The temperature change, as shown by Eq. (2), affects the slope of the logarithmic curve, so that the effect on plate voltage at a given current is slightly greater at lower currents. The relative insignificance of the latter effect is shown by the dashed curves in Fig. 3-28b, which were obtained with higher and lower heater voltages applied.

Lowering the heater voltage shifts the curve to the right; the steepening effect is small in comparison.

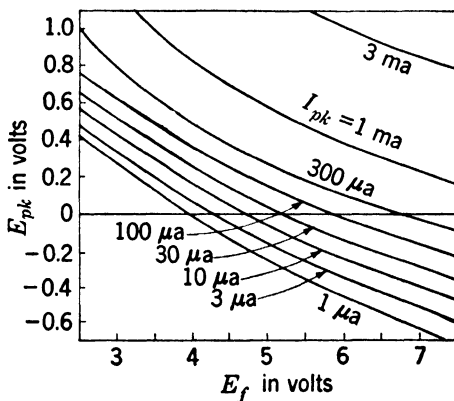


FIG. 3-29.—Voltage shift at constant diode (6-L5) current caused by heater-voltage change.

The effect of heater voltage is shown more completely in Fig. 3-29 where the plate voltage required for various constant values of current is plotted against heater voltage. It is seen that, in the neighborhood of normal heater voltage, the plate voltage for any given current must increase by about 0.1 volt for a 10 per cent decrease of heater voltage. This figure seems to apply, as an approximation, to all tubes with oxide-coated cathodes. There is some variation from it, perhaps 20 per cent in either direction, with respect both to tube types and to tubes of the same type. This variation from tube to tube is an important consideration in the design of circuits wherein an attempt is made to eliminate the effect of heater-voltage variation by balancing the shift in one tube against that in another. More will be said of this method of cancellation in Sec. 9-6. A more complete discussion of the whole subject appears in Chap. 11, Vol. 18 of the Series. Pentode drifts are largely canceled by those of a compensating diode in one of the methods discussed there.

*Drift.*—Drift of the characteristics as the tube ages can cause appreciable shift in the operating voltage. This drift is due mainly to change of the cathode affecting the total emission, and has the same general effect as heater-voltage variation, shifting the curve of Fig. 3-28a to the right or left without appreciably affecting its shape. As a tube ages, the general trend is toward the right. The drift may be quite large and erratic in a new tube, but after a few hundred hours with heater voltage applied, drift decreases to a fairly small average rate, such as 10 or 20 mv per week. The short-term drift over a few hours is more erratic but may be as small as  $4 \mu\text{v}/\text{min}$ .

A lateral drift of the curve of Fig. 3-28a, whether the result of heater-voltage change or change of the cathode with time, produces an equal lateral drift in Fig. 3-27b, so that a drift of the characteristics of a certain number of millivolts results in that many millivolts change of the operating point of a comparator diode, regardless of the resistance employed.

*Factors Affecting Slope of Characteristic.*—The lack of definition due to the curvature of Fig. 3-27b would be lessened by a steepening of the logarithmic curve of Fig. 3-28a. As already pointed out, this is accomplished to a small degree by lowering the heater voltage. The slope of the logarithmic curve is inversely proportional to cathode temperature, but a very large decrease of this will reduce the emission to zero. Reducing the heater voltage to half of normal decreases the temperature and increases the slope of the curve by about 20 per cent, without reducing the emission enough to affect the operation of most circuits employing broken-line characteristics. This may be permissible and advisable if the maximum current drawn in operation is considerably less than the emission so that the cathode surface is not endangered. A given percentage heater-voltage variation has slightly less effect upon diode voltage at a constant current if the absolute value of heater voltage is low. Rate of drift may also be decreased by the reduced temperature.<sup>1</sup>

The best cathode material is that which will give satisfactory emission at the lowest temperature since the constant of Eq. (2) is not a function of material. Thus, thoriated tungsten would have a characteristic much less steep than that of Fig. 3-28a, as it is operative at above  $2000^\circ\text{K}$ .

As has been stated, tubes with electrodes neither plane-parallel nor cylindrical produce characteristics somewhat less steep than that of Fig. 3-28a, but nevertheless linear. The 6J6 has a plane cathode, but the

<sup>1</sup> If a fixed resistor is employed to drop the heater voltage from normal to half of normal, the change of heater resistance caused by deterioration of the heater will have no effect on the heater power and therefore none on the cathode temperature, thus affecting a further decrease of the drift. The effect of variation of heater-supply voltage, however, is increased by about thirty per cent by the series resistor because of the change of heater resistance with temperature.

end effects are large. As revealed by the slopes of the diode characteristics plotted logarithmically in Fig. 3-30a with grid tied to plate, the slope at normal temperature is one decade in plate current per 0.3 volt. The dashed curves show the effect of operating with grid connected to cathode. These curves are slightly steeper, though still not so steep as in Fig. 3-28a, until the current becomes large, when the resistance becomes much greater than with the usual diode connection. There is little effect on the shift with heater voltage at the low currents.

Figure 3-30b, for a diode-connected 6SH7, shows that the suppressor grid connected to the cathode has no apparent effect.

A filamentary cathode is quite unsatisfactory for most applications to waveform generation and analysis. Aside from the need for a separate filament supply, and the large amount of hum (if alternating current is used), the nonuniform cathode potential results in a much more curved characteristic.

Some low-current d-c amplifier tubes<sup>1</sup> utilize a filamentary cathode, and may be used advantageously if stability rather than sharpness of break is important since the 10-ma filament current may be regulated electronically, and this source of drift is thereby eliminated. The diode, type V-21, has a rated inverse peak voltage of 3500 volts and an approximate leakage resistance of  $10^{16}$  ohms. The plate current is  $250\text{ }\mu\text{a}$  at 5 volts  $E_{pk}$ .

In general, the best diode has a cylindrical oxide-coated unipotential cathode and a cylindrical plate, and is operated at a subnormal heater voltage. The types 6AL5 and VR-91 (British) have a cylindrical structure. For most applications, where the current is rather low, the size, power rating, and nominal conductance are immaterial. Employing two diodes in parallel is of no advantage, since the combined logarithmic characteristic has then the same slope.

*Tolerance of Characteristics.*—There is considerable shift to the right and left of the curve of Fig. 3-28b between different samples of the same tube type, although the slope of the curve is quite independent of this. For example, the 6AL5 JAN specifications require that each diode will cause between 5 and  $20\text{ }\mu\text{a}$  to flow in a 40-k resistor from cathode to plate. This allows the curve (at  $E_f = 6.3$  volts) to be anywhere between points A and B in Fig. 3-28b. The shift of the curve which may occur translates directly into a change of the operating voltage of the device, and must be taken into account in some way with a “zero” adjustment.

In many amplitude selectors in which a diode is employed, its shift with respect to heater voltage is balanced against that in another diode by causing either the reference input voltage or the wave itself to be shifted. This is accomplished in a more satisfactory way if the two diodes

<sup>1</sup> Victoreen Instrument Co.



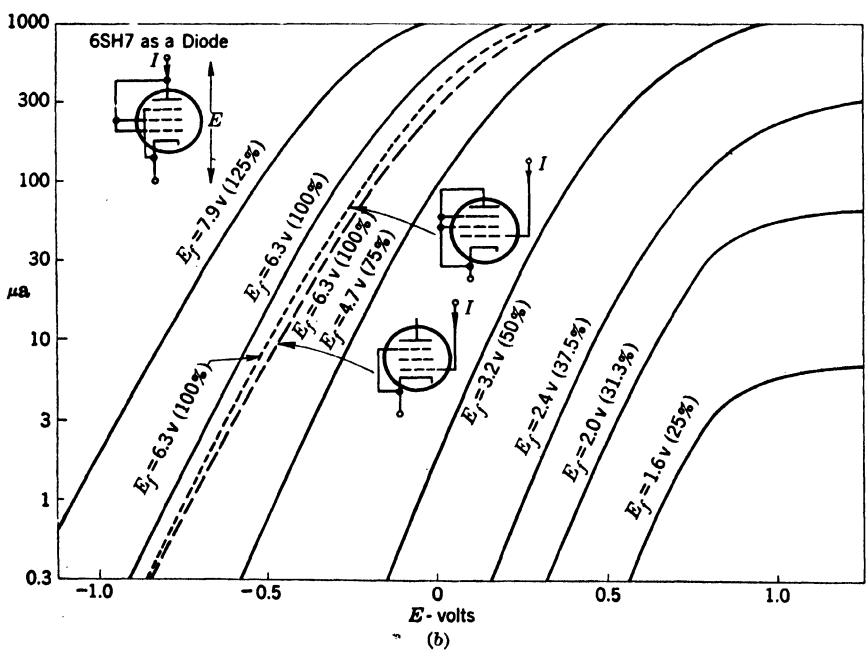
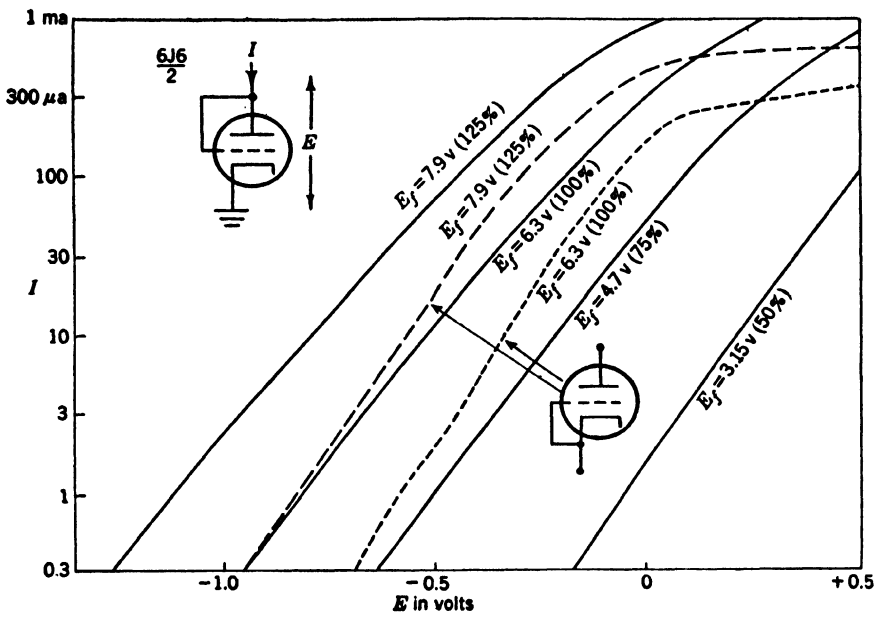


FIG. 3-30.—Characteristics of grid tubes, diode-connected. (a) Characteristics of 6J6, diode-connected. (b) Characteristics of 6SH7, diode-connected

are the sections of a double-diode tube since the characteristics thereof are most likely to be similar. The zero adjustment required is also somewhat reduced, for the same reason. The JAN specifications for the 6AL5 permit a difference of only  $5 \mu\text{a}$  between the values of current that each of the diodes in a given tube passes through a 40-k resistor, while, as stated above, it may vary by  $15 \mu\text{a}$  from tube to tube. The result of this specification is that there should be no more than 0.25 volt, laterally, between the curves for a pair of diodes. The curves for a 6SU7 double triode, diode-connected (grid to plate), should be within 0.1 volt of each other, by extrapolation from one of the JAN specifications pertaining to triode operation.

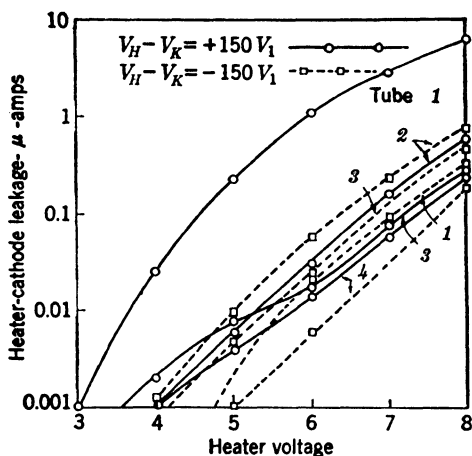


FIG. 3-31.—Effect of cathode temperature on heater-cathode leakage of diodes. One section of each of four 6H6's.

*Leakage.*—At ordinary inverse voltages the reverse current in a good diode is in most applications negligible. In diode-connected grid tubes, however, it may become appreciable, sometimes rising to over  $0.01 \mu\text{a}$  at  $-100$  volts. Since reverse current is mainly the result of ionization, it is nonlinear with respect to inverse voltage and increases more rapidly at higher voltages. It is not very greatly affected by cathode temperature. Surface leakage may also be present, both inside and outside the tube. If special precautions are taken, the base leakage resistance between any two pins may be held above a thousand megohms, even at high temperatures and humidities.

Leakage takes place between the cathode and heater, and may be several microamperes for some tube constructions. It is therefore desirable to design the circuits so that the cathode-to-ground resistance is low, or to provide a separate “floating” heater supply for the diode.

Reduced heater voltage may reduce the leakage considerably. For a

number of triodes (6SN7) operated as diodes, with the cathode 150 volts negative with respect to the heaters, the average leakage has been observed to change from  $\frac{3}{10} \mu\text{a}$  at 6.0 heater volts to  $\frac{1}{20} \mu\text{a}$  at 4.5 heater volts. The results of a test on the 6H6 diode are shown in Fig. 3-31. A majority of

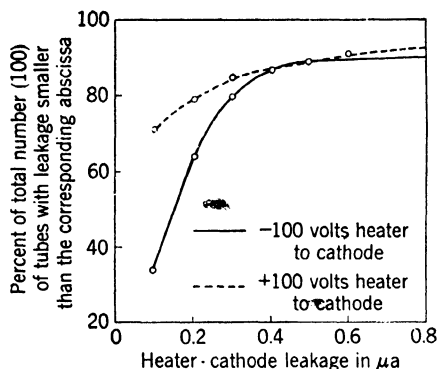


FIG. 3-32.—Heater-cathode leakage for 100 tubes (Sylvania 6SN7 GT triodes).  $E_{ff} = 6.3$  volts,  $E_{pk} = +250$  volts,  $E_{a1} = -8$  volts.

the tubes have leakage currents less than  $\frac{1}{10} \mu\text{a}$  at 6.3 heater volts. The leakages of one hundred triodes (6SN7) operated at ordinary cathode temperatures are indicated in Fig. 3-32. Over half the units have leakage currents less than  $\frac{1}{20} \mu\text{a}$ . In another test at a few milliamperes of plate current it was found that the life of the tube was not lessened by operation at  $E_f = 4.8$  volts.

Capacitive current will flow through the tube in either direction at high frequencies. Ordinary analytical methods may be

applied in the calculation of this current from the known interelectrode and the measured wiring capacitances. For most diodes, a few micromicrofarads are present.

**3-15. Contact Rectifiers.**—Crystal rectifiers were formerly used in communications receivers and have been recently applied as detectors

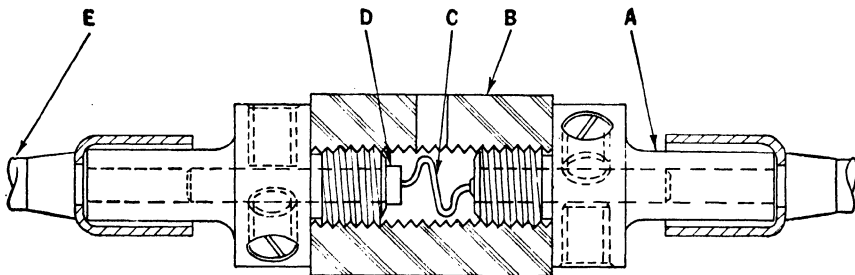


FIG. 3-33.—Germanium-crystal rectifier cross section. (From J. H. Scaff and H. C. Theurer, "Preparation of High Back Voltage Germanium Rectifiers," NDRC 14-555, p. 28.) A—Metal end piece. B—Ceramic insulator. C—Point contact. D—Germanium wafer. E—Pigtail connector.

and converters of uhf signals. Their characteristic resembles the diode characteristic, but the effects of electron transit time, interelectrode capacitance, "contact potential," drift, and curved break in the characteristic are smaller than for the diode. These contact rectifiers are simply made; a pointed wire of a conducting material such as tungsten is

placed in contact with a crystal of silicon, germanium, or some other semiconductor. A germanium crystal is shown in Fig. 3-33. The contact rectifier requires no filament supply and, in general, is smaller and has a longer operating life than the diode.

The surface contact rectifier is familiar as a converter of a-c power to d-c, and is particularly useful for large current loads at low voltages and small current loads at high voltages.<sup>1</sup> The characteristic of a selenium surface is shown in Fig. 3-34. Copper oxide or selenium rectifiers are often used for a-c meters that are to be accurate to 1 or 2 per cent.<sup>1</sup>

The applications of these devices to waveform-shaping have not been important. This is due chiefly to the excessive reverse current at low reverse voltages, the negative-resistance characteristic that is entered at higher reverse and forward voltages, variations from unit to unit, and a

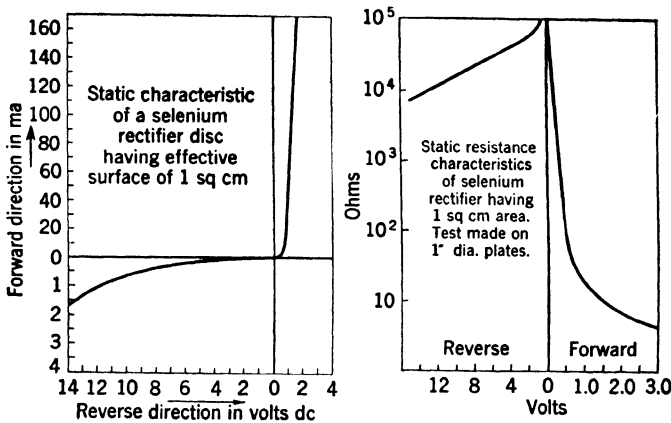


FIG. 3-34.—D-c characteristics of the selenium rectifier.

severe temperature sensitivity. Hysteresis, drift, spontaneous and vibration noise and aging effects have been observed.

These sources of error have been investigated and reduced greatly in the past few years, since the uhf crystal detectors are extensively used in radar (see Vol. 15 of the Series). Among the crystal materials that have been investigated, germanium is outstanding for high back resistance at comparatively high voltages. The germanium crystal has been studied considerably with a view toward waveform-shaping applications. In some instances (in addition to those of the first paragraph of this section), the crystal may be substituted for the high-vacuum diode.<sup>2</sup> The negative-resistance characteristic may occasionally be of some use.

<sup>1</sup> See "Selenium Rectifiers," *Engineering Manual and Standard Element Specifications*, Bulletin RDP-107, Fansteel Metallurgical Corporation, North Chicago, Ill.

<sup>2</sup> See E. C. Cornelius, "Germanium Crystal Diodes," *Electronics*, **19**, 118 (February 1946).

*Germanium Crystals.*—A typical germanium-crystal characteristic is shown in Fig. 3-35. The back-voltage characteristic is sufficiently good that such a unit could be used in place of a diode for many waveform

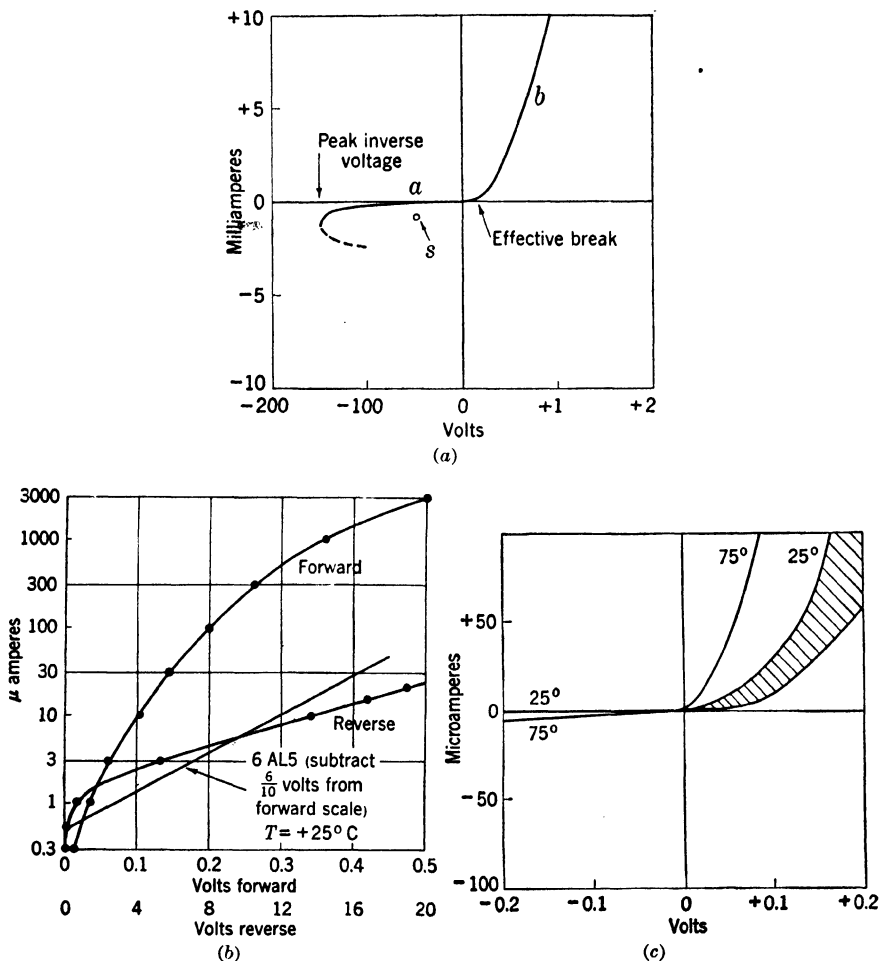


FIG. 3-35.—Typical germanium-crystal characteristics (d-c). (a) Complete characteristic. Forward and back voltage scales are different. A resistance of 100,000 ohms may be realized at *a* and of 200 ohms at *b*. Point *s* represents the maximum reverse current permitted by the specification for the WE D-172925 d-c restorer crystal (0.85 ma at -50 volts). (b) Expanded characteristic. (c) Variations in the expanded characteristic. The shaded area indicates the variation from one unit to the next at 25°C.

operations. Unfortunately, the closest specification for the WE D-172925 d-c restorer crystal permits larger back currents, as is shown in the figure by the point *s*, defining maximum back current.

The variation of characteristic in manufactured units is great as Fig. 3-36 indicates.<sup>1</sup> The best method for preparing the materials, assembling the units, and stabilizing the characteristics (by heat and voltage cycles) resulted in the distributions shown. If inferior methods are used, a much smaller percentage of crystals suitable for waveform operations at high voltages is found.

The temperature dependence of the characteristic is larger for high-back-resistance units than for low-back-resistance units. A complete characteristic is shown for several different temperatures in Fig. 3-37.

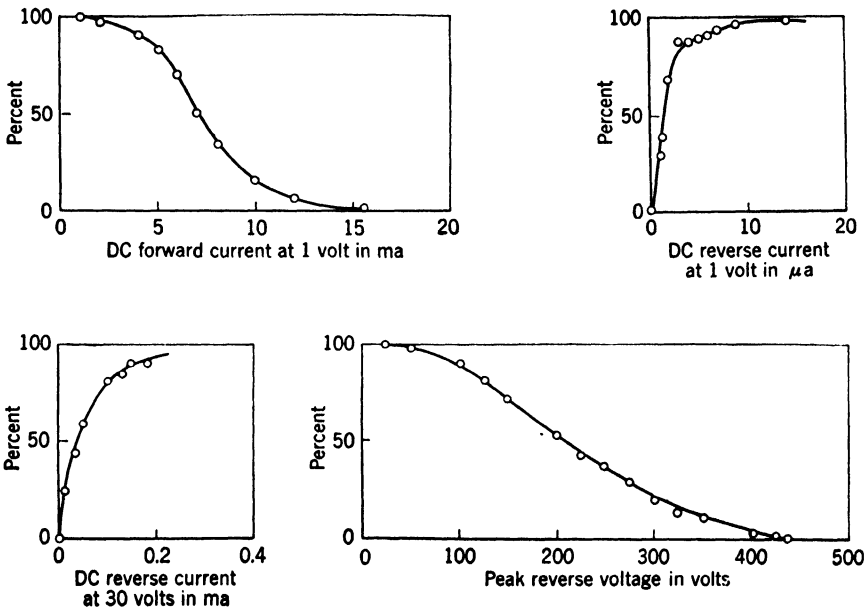


FIG. 3-36.—Variations in germanium-crystal units at 25°C. (From J. H. Scaff, NDRC 14-555.) The ordinate is the percentage of manufactured units having the characteristic (at worst) specified by the corresponding abscissa.

The comparative insensitivity to temperature at large forward and back voltages suggests that the crystals are suitable for operations utilizing these portions of the characteristics if temperature variations are expected. For high-voltage waveform operations for which low back current and stability of break are important, temperature control is necessary.

An advantage of the crystal is that zero current corresponds to zero applied voltage since no power can be supplied by the element. In order to take advantage of this stability, the effective break should be placed at as low a current as possible. The current at the effective break is defined by the neighboring circuits for any application of the crystal. For various

<sup>1</sup> J. H. Scaff and H. C. Theuerer, "Final Report on Preparation of High Back Voltage Germanium Rectifiers," NDRC 14-555, Bell Telephone Laboratories.

units supposedly prepared in an identical manner, the effective break voltage may vary by one or two tenths of a volt if it is defined at too high a current value. A few hundred microvolts of noise are generated in the germanium-crystal rectifier, though some crystals have been observed that generate as little as  $10\mu\text{v}$  of noise.

The shunt capacitance of the point contact rectifier may be from  $\frac{1}{10}$  to  $\frac{5}{10}\mu\text{f}$ . This is a factor of 10 lower than diode capacitance. At ultra-high frequencies this property is important.

The shape of the break is shown in Fig. 3-35b. The theory of the crystal rectifier is not yet complete, but the rise of current is roughly

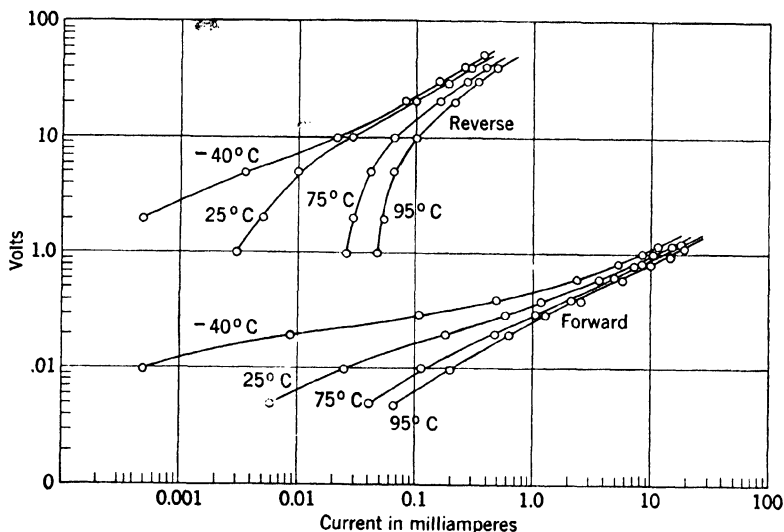


FIG. 3-37.—Effect of temperature upon the d-c characteristics of a typical germanium rectifier. (From J. H. Scaff, NDRC 14-555.)

represented by a positive exponential rising from a negative current value and passing through the origin. Deviations from an exponential characteristic are always present and may be represented by a small resistance in series with the truly exponential element. At room temperatures the crystal-rectifier logarithmic slope may theoretically be five times that of the ideal thermionic diode with its cathode at  $1000^\circ\text{K}$ . Actually the average crystal characteristic does rise more rapidly than the diode at low currents. The two characteristics may be compared in Fig. 3-35b. This slope for the crystal characteristic may vary by a factor of 2 or 3 from unit to unit and with large temperature changes (see Figs. 3-35c and 3-37).

**3-16. Photocells.**—The characteristic of a high-vacuum photocell (two metallic unheated electrodes) is given in Fig. 3-38 for two values of incident light intensity. The voltage-current curve<sup>1</sup> exhibits two breaks.

<sup>1</sup> See M.I.T. E. E. Staff, *Applied Electronics*, Wiley, New York, 1943, p. 105.

At the origin the potential difference between electrodes reverses direction, and the electrons emitted by the surface exposed to light are drawn back to the emitting surface. The distribution of initial electron velocities determines the shape of cutoff characteristic.

As the plate or collector electrode is made positive with respect to the cathode, a larger and larger percentage of the emitted electrons are collected. The flat portion of the characteristic corresponds to the collection of all emitted electrons. The addition of gas to the photocell introduces ionization effects. The current does not become independent of the applied voltage in this case.

The photocell is also an example of a multivariable element, relating a current, a voltage, and a light intensity. The common applications of the photocell require a resistance in series with the element. The  $IR$ -drop across the resistor is the useful output and the light intensity is the useful input.

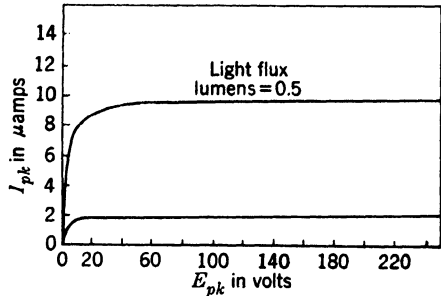


FIG. 3-38.—High-vacuum photocell 919 (average plate characteristics).

**3-17. Cutoff in Grid Tubes.**—The addition of one or more grids between a thermionic cathode and a plate electrode results in the familiar current “valve.” The plate-cathode current  $I_{pk}$  is considered, at least for amplifier usage, to be controlled by the grid-cathode voltage  $E_{gk}$  as well as by the plate-cathode voltage  $E_{pk}$ . More generally, the element relates these three variables in the manner described in Sec. 3-27. This is a multivariable element and provides a variety of multivariable characteristics and nonlinear two-variable characteristics.

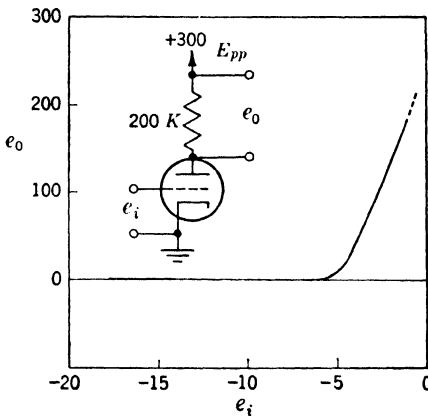


FIG. 3-39.—Broken-line cutoff characteristic (6SL7). The value of  $e_i$  at which the break occurs is a function of  $E_{pk}$ .

$E_{gk}$  to  $E_{pk}$  relation (with  $\Delta E_{pk}$  proportional to  $-\Delta I_{pk}$ ) is the most descriptive characteristic. The relationship may be nearly linear over large portions of the characteristic as may be seen in Sec. 3-27. As the grid is made more negative, however, the tube “cuts off.” The characteristic

If the triode is connected as for ordinary amplifier applications, the



shows a break at the cutoff bias. The sector of grid control is called the "grid base." For the cutoff tube, the characteristic is flat—the output does not vary as the input is varied. Such a curve is shown for the 6SL7 in Fig. 3-39.

This is a very useful broken-line characteristic. The same triode element may perform a nonlinear operation and amplification. The impedance of the grid circuit may be very high on both sides of the break (on the grid base and "beyond" or "below" cutoff). The diode circuits, on the other hand, exhibit different impedances on the two sides of the break, an inherent property of the direct nonlinearity.

The sharpness of the break may be shown by plotting  $I_{pk}-E_{gk}$  curves for various fixed values of  $E_{pk}$  (for a triode) or  $E_{g_2k}$  (for a pentode). The curve is logarithmic in the low-current region but is considerably less sharp than the diode cutoff curve. Any potential between the control grid and the next electrode (plate or screen) causes the slope of the logarithmic characteristic to be less than for the diode. For the best definition of the break, the plate or screen voltage should be as low as possible. The grid base is also shortened for these low plate or screen potentials.

Figure 3-40 shows the effect of the plate-to-grid potential on the slope of the logarithmic relationship of current to voltage in the low-current region. The plate-to-grid potential rather than plate-to-cathode potential was held constant in each curve, so that the diode characteristic ( $e_{pg} = 0$ ) could be included for comparison. Total cathode current is the ordinate for the same reason; but for all values of  $e_{gk}$  below about  $-0.8$  to  $-1.0$  volt this is almost entirely plate current.

In triode operation the slope of the logarithmic characteristic is evidently constant up to as high a current as in diode operation, but with diminishing slope for greater plate potentials. All tubes give about the same slope for the diode curve, but there is much variation between tube types in the rate of decrease of slope with respect to plate potential. In general, well-constructed high- $\mu$  tubes are less affected by plate voltage than are low- $\mu$  tubes.

In so far as the curves of Fig. 3-40 are straight, the transconductance is proportional to the current. If the slope of a curve is

$$\frac{d \log_{10} i}{de_{gk}} = \frac{1}{E_0}, \quad (6)$$

$E_0$  being the increment of  $e_{gk}$  producing a tenfold increase of current, then

$$\frac{di}{de_{gk}} = \frac{2.3i}{E_0}, \quad (7)$$

where  $i$  is the plate current wherever  $e_{gk}$  is below about  $-1$  volt. [The fact that  $e_{pg}$  is fixed for each curve, rather than  $e_{pk}$ , only means that the

transconductance is  $\mu/(\mu + 1)$  of the expression of Eq. (7).] Thus, a high- $\mu$  triode, at a given plate voltage and current will have a higher transconductance in the low-current region than will a low- $\mu$  tube, regardless of rating or nominal transconductance. At a plate voltage of 90 volts and a plate current of 0.1 ma, the transconductance of the 6SL7 is 400, while that of the 6SN7 is only 140  $\mu$ mho. Another conclusion to be

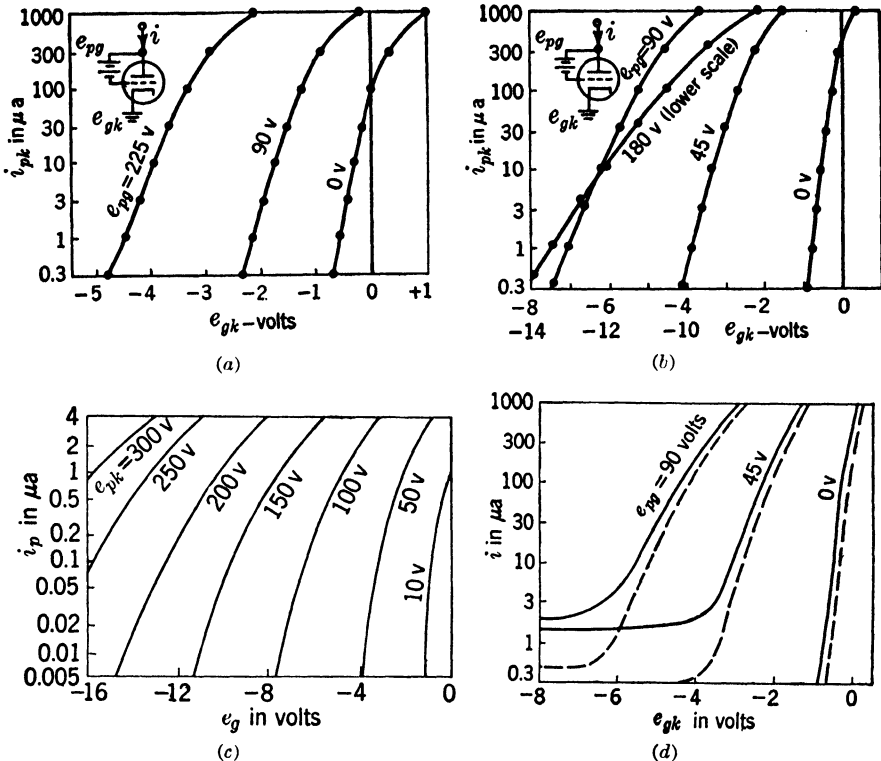


FIG. 3-40.—Logarithmic cutoff characteristics of triodes. (a) 6SL7; (b) 6SN7; (c) 6SN7; (d) 6J6. Figures (a), (b), and (d) have  $E_{pg}$  as parameter, (c)  $E_{pk}$ . Figure 3-71 is the 6SL7 characteristic with  $E_{pk}$  as parameter. The 6J6 characteristic shows incomplete cutoff, such as is observed in many 6J6 tubes. In (d),  $E_{ff} = 85$  per cent normal for the dashed curves (see Fig. 11-2, Vol. 18 of this series for other low-current triode characteristics).

drawn from Eq. (7) is that in the low-current region no increase of transconductance may be obtained by employing tubes in parallel since the current, and therefore the transconductance, of each tube is lessened. It will be remembered that this conclusion applies also to the variational resistance of diodes.

In many tubes the cutoff is incomplete, so that a measurable plate current will flow regardless of grid bias. This is subject to large variations from tube to tube. It is always greater at higher plate potentials, and is

usually decreased with a decrease of heater voltage. Figure 3-40*d* reveals the effect in the case of one 6J6 triode.

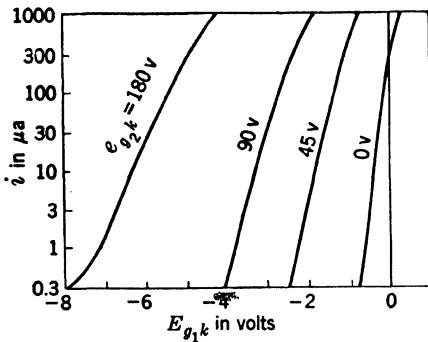


FIG. 3-41.—Logarithmic cutoff characteristics of pentode (6SH7).  $E_{g2k}$  as parameter.

shown in Fig. 3-42. The plate-to-cathode voltages are used rather than plate-to-grid voltages.

Biases on other grids may cut off plate current if made sufficiently negative. The slope of the logarithmic curve is usually smaller than for

Curves similar to those of Fig. 3-40 are given for a pentode in Fig. 3-41. In this case the different curves are for different screen potentials, the plate potential being held fixed at 90 volts. The effect of the latter on total current was found to be very slight although it does affect the ratio of screen to plate current.

The cutoff characteristics of several triodes and pentodes are

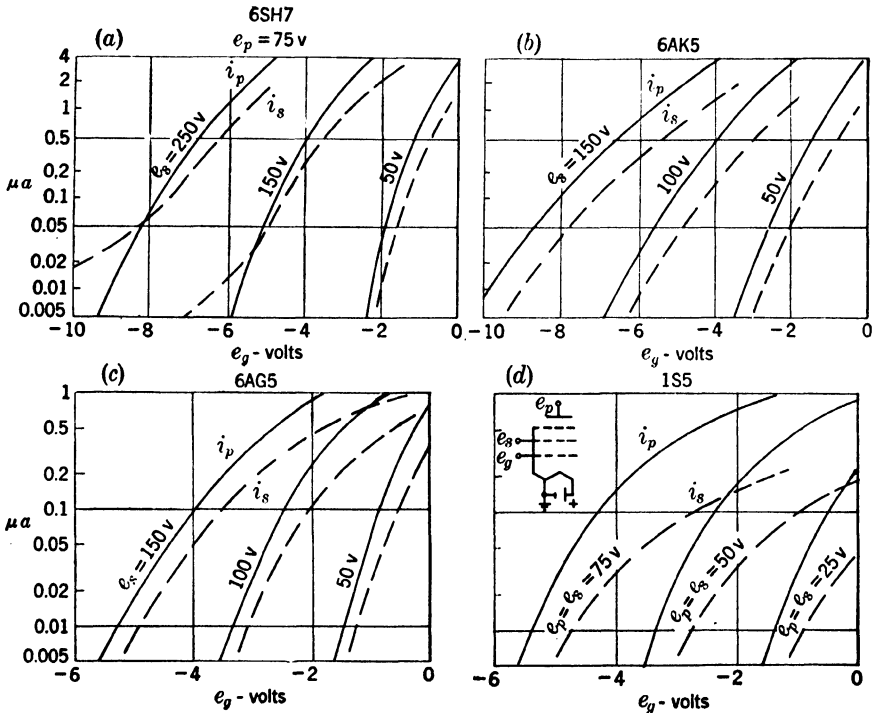


FIG. 3-42.—Logarithmic cutoff characteristics of several pentodes.  $E_{g2k}$  as parameter.

the curve corresponding to first control-grid cutoff. The multivariable nonlinearities are often useful, however, and Sec. 3-24 is devoted to the elements possessing them.

In comparing the pentode and the triode as nonlinear elements, an important consideration is the isolation of the screen voltage from the output signal in the case of the pentode. In order to provide a large output signal, the supply voltage must be large for a triode. This, however, implies that the grid base is comparatively large. For the pentode, however, a short grid base and a large output may be obtained together. The screen voltage may have a lower bound imposed by its effect on control-grid current.

The most important distinction between the diode and the triode (cutoff) nonlinear elements is that the diode break is considerably more stable with respect to tube change. If this factor and the sensitivity to triode plate potential are considered, the diode is clearly preferable for most precision operations.

**3-18. Plate-voltage vs. Plate-current Nonlinearities.**—In the last section a two-variable characteristic—the broken-line transfer characteristic of a vacuum-tube amplifier—was discussed. The important variables for that nonlinear relation are input voltage and output voltage.

If the relationship of  $E_{pk}$  to  $I_{pk}$  were examined for the circuits of the last section, it would be convenient to consider them as nonconstant with respect to  $E_{pk}$ . The relationship between  $E_{pk}$  and  $I_{pk}$  also has two nonlinearities. The first may be called “bottoming” and, for the pentode, occurs below the “knee” in the plate characteristic. The transition from the usual plate impedance of several hundred kilohms to this low value is the break in the characteristic. The impedance at the plate-cathode terminals is 1 or 2k for many pentodes (that of the 6AG5 is larger). The break is not sharp compared with a diode break but is often useful for comparatively nonprecise operations. An example of this break is shown in Fig. 3-43 for a constant grid bias of  $-1$  volt on the 6SH7 tube.

The same curve shows the second break, the cutoff of plate current for negative  $E_{pk}$ . This effect is sharper than the knee and may equal the sharpness of diode cutoff for small values of  $E_{pk}$ . The stability of this break is generally worse than for the diode, but the sensitivity to cathode temperature is approximately the same.

For switch-tube applications, the same curve for a constant value of

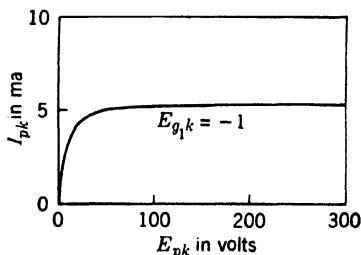


FIG. 3-43.—The “knee” and “bottoming effects.” A broken-line characteristic for a pentode (6SH7).  $E_{ff} = 6.3$  volts,  $E_{g2k} = 100$  volts.

grid current rather than grid bias may be desired. Such a curve is shown in Fig. 3-44 for the 6AG7 pentode. This too, is a doubly broken-line characteristic. The beam-power tetrode has a plate characteristic

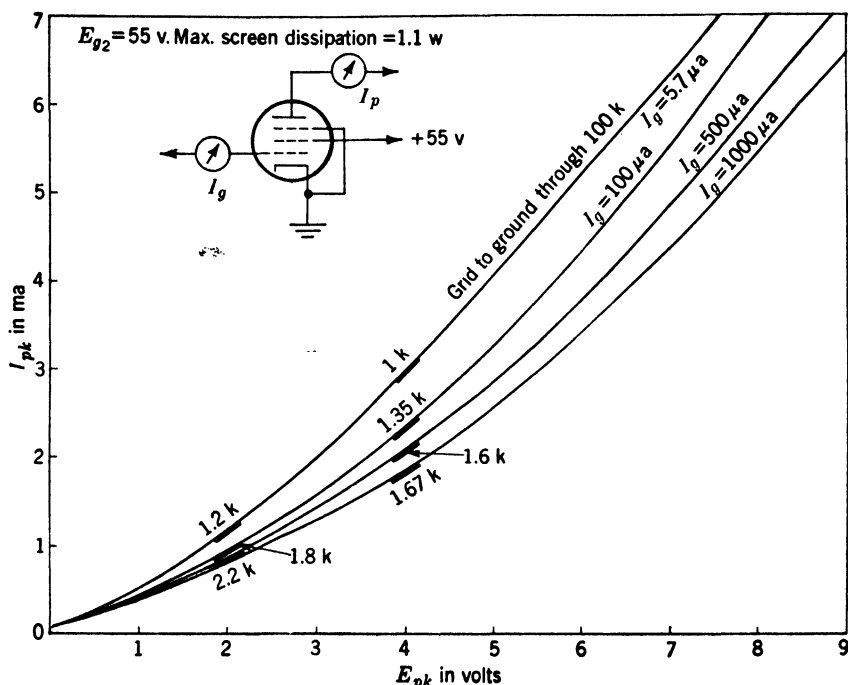


FIG. 3-44.—Pentode characteristic in low-plate-resistance region (6AG7).  $E_{g2k} = 55$  volts. Maximum screen dissipation = 1.1 watts.

that is similar to that of the pentode but less sharp for either constant control-grid voltage or current. See Fig. 3-45.

For the triode connection of a pentode, the “bottoming” or “knee” break disappears for the negative grid biases. The cutoff break remains, and the variational plate impedance of a triode is low so that the triode may be said to retain the two left-hand segments of Fig. 3-43. Thus the “bottoming” operation that is often useful in setting the lower bound of a plate waveform may be performed with triodes. Part of the cutoff break is shown for a pentode, pentode- and triode-connected in Fig. 3-46. The complete triode characteristic is

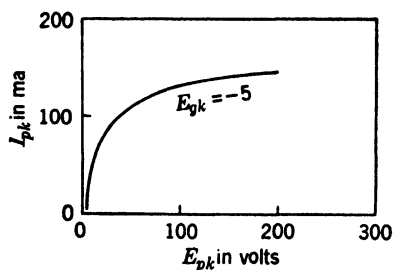


FIG. 3-45.—Broken-line characteristic for a beam tetrode (6Y6-G).  $E_{gk} = -5$  volts,  $E_{g2k} = 135$  volts.

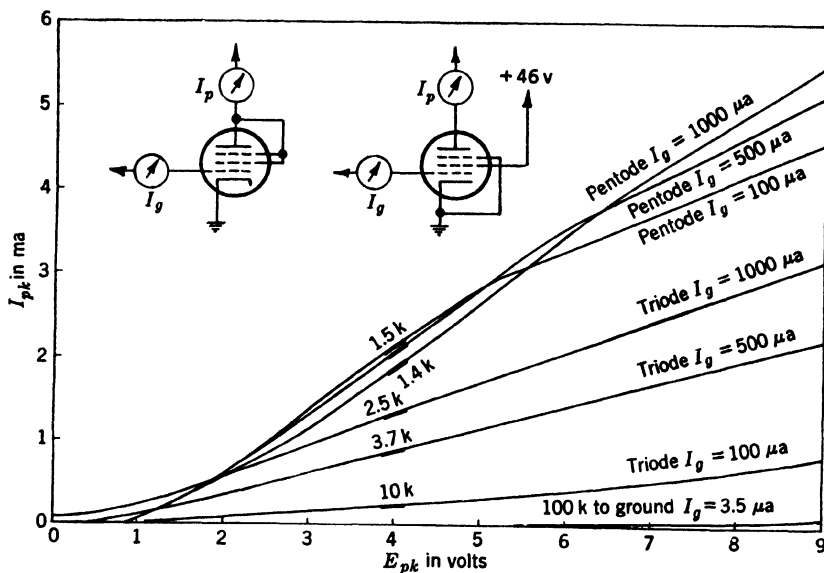


FIG. 3-46.—Triode and pentode connections, low-plate-voltage region (6AK5).  $E_{v2k} = 46$  volts. Maximum screen dissipation = 0.3 watt.

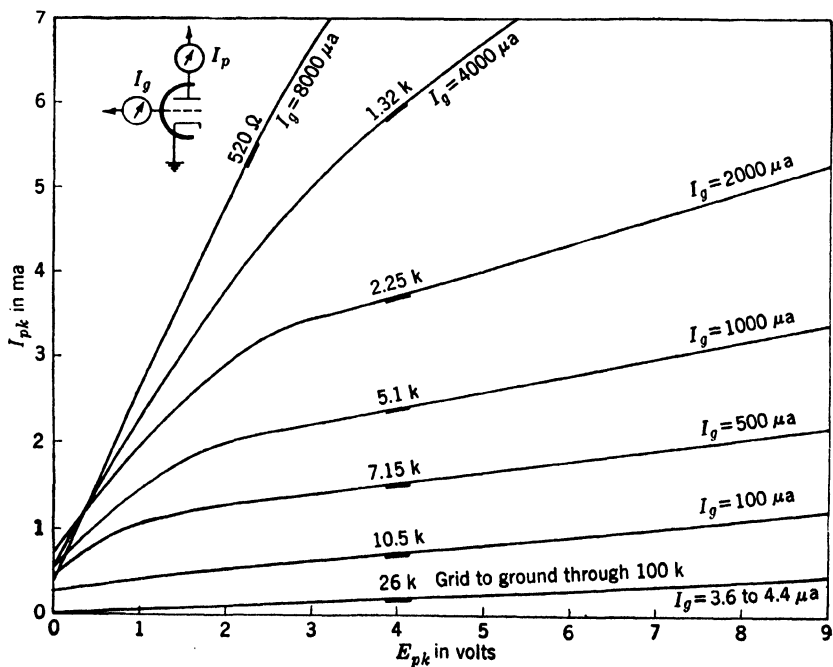


FIG. 3-47.—Triode in low-plate-voltage region (6SN7). For large grid-current values, a "knee" is present.

acteristic is doubly broken. A doubly broken triode characteristic can be obtained at a constant positive control-grid bias.

The upper segment of two-triode  $E_{pk}$ - $I_{pk}$  characteristics for constant values of grid current are shown in Fig. 3-47. The lower portions of the break are exponential, and like the pentode may be nearly as sharp as but not so stable as the diode cutoff. (This part of the characteristic is not well known. From Fig. 3-69 it would appear that the corresponding curves for constant values of  $E_{gk}$  would be similar in shape. An upper bound can be placed on the plate current for  $E_{pk} = E_{gk}$ . The characteristic of the diode-connected tube provides the sum of plate and grid currents in this case.)

### 3-19. Grid-current Nonlinearities.—

The flow of electrons to the first control grid of a vacuum tube is very small if  $-E_{gk}$  is negative and larger than about one volt, provided the next electrode is at a comparatively high potential so as to maintain the electron velocities through the grid openings. The grid current is desired to be negligible for most amplifier applications but may provide two useful nonlinear characteristics.

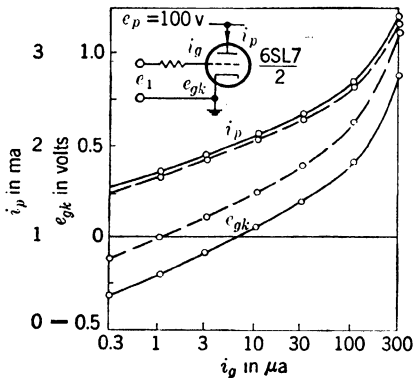


FIG. 3-48.—Grid-current characteristic of a triode with fixed  $E_{pk}$  (6SL7). (Dashed curves,  $E_{gk} = 85$  per cent of normal.)

The first is the direct nonlinearity in the grid-voltage vs. grid-current curve. This effect is similar to the diode broken-line effect and may be explained in the

same way. The break is an exponential curve as may be seen in Fig. 3-48. The slope of the logarithmic curve is approximately the same as for the diode.

The characteristic is taken with a large series grid resistor (the voltage across the resistor provides a measure of the grid current). Such a resistor or its equivalent—the internal impedance of a waveform generator—is necessary in order to limit the grid current if the applied wave-form  $e_1$  assumes positive values. The series resistor and the grid-to-cathode circuit provide a characteristic corresponding to the resistor-diode circuit of Sec. 3-4.

The second nonlinearity is produced by the same circuit as the first. The mutual characteristic between  $e_1$  and  $i_p$  (or  $i_p R_L$ , for an amplifier circuit) possesses a sharp break. Just as cutoff bounds the grid base at a low value, so the flow of grid current provides an upper and sharper

boundary. Cathode temperature variation shifts the grid voltage at any given grid current, just as for a diode, resulting in very little change of plate current. The stability of the upper bound of the mutual characteristic permits this break to be used in precision circuits.

The lines of constant grid current on a plate characteristic follow the lines of constant grid bias very closely. The grid and plate currents have a fixed ratio. This fact may be observed for the 6SL7 tube in Fig. 3-69. Another grid-current characteristic for this tube is shown in Fig. 3-70. The cutoff of grid current at negative values of  $E_{gk}$  is not complete. The JAN specification for the 6SL7 at  $E_{gk} = -2$  and  $E_{pk} = +250$  allows a maximum current flow to the grid of  $1 \mu\text{a}$ . The 6SU7 (selected 6SL7) has a much smaller value of maximum current for a similar operating condition ( $0.01 \mu\text{a}$ ). Other standard receiving tubes (except the 6AK5 pentode) are permitted a larger flow of grid current under similar (Class A amplifier) operating conditions (1 or  $2 \mu\text{a}$ ).

Pulses of grid current may assume large values if the average power is held rather low ( $\frac{1}{2}$  watt for the 6SN7 tube). Blocking oscillators make use of this region of triode characteristics. Such tube characteristics are described in Chap. 6. The plate-cathode characteristic of a triode with a very positive grid appears on the basis of a few tests to be that of a low impedance diode without filament-voltage drift effects.

**Suppressor Grid.**—Unlike the control-grid characteristic, with its high  $\frac{\partial i_{pk}}{\partial e_{gk}}$  value for positive  $E_{gk}$ , the suppressor grid tends to lose control of plate current for positive biases. The combination of this effect and of the grid current to the suppressor grid at positive biases results in a sharp break in the  $E_{gk} - I_{pk}$  characteristic. Such a characteristic is shown in Fig. 3-49. For low values of plate voltage a similar effect may be observed with the first control grid of a 6AC7. The resultant waveform in a pulse amplifier may be observed in Fig. 9-40.

**3-20. Composite Characteristics.**—The cutoff and grid-current breaks for a triode provide a doubly broken mutual characteristic. The effects that cause the breaks have been described in the last three sections and will not be discussed further here.

Figure 3-50 shows the mutual characteristic for a triode-amplifier circuit, with two different values of  $E_{pp}$  and of load resistance. The effect of

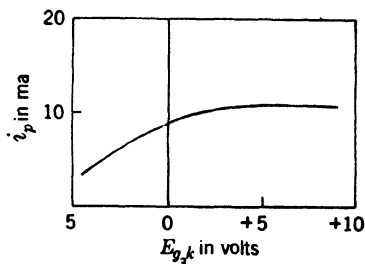


FIG. 3-49.—Suppressor-grid-characteristic break at  $E_{g3k} = 0$  volt.  $E_{ff} = 6.3$  volts,  $E_{pk} = 120$  volts,  $E_{g2k} = 120$  volts,  $E_{g1k} = -1$  volt (6AS6).



variation of the series grid resistor is also illustrated. In the cases where  $R = 0$ , the upper break is caused by plate-bottoming. The size of grid base is directly proportional to  $E_{pp}$ .

The doubly broken-line characteristic at the pentode plate is shown in Fig. 3-51. The two breaks correspond to the knee in the plate characteristic and to the cutoff of plate current by plate voltage.

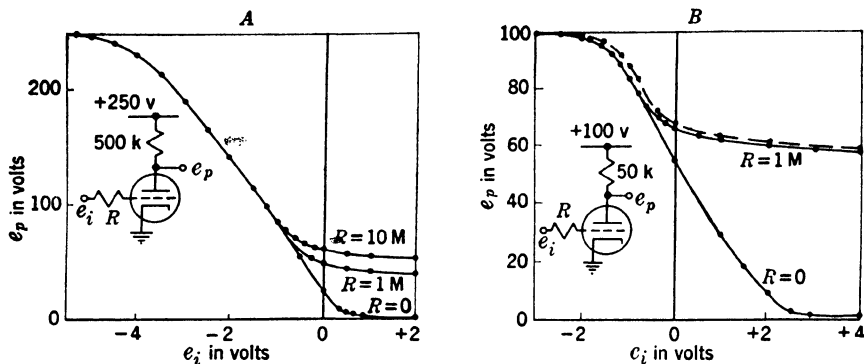


FIG. 3-50.—Doubly broken amplifier characteristics.

A complete suppressor-grid characteristic is shown in Fig. 3-52. The sharpness of second-control-grid breaks are in general inferior to those of the first control grid.

**3-21. Gas-filled Tubes.**—Conduction through a gaseous atmosphere between two electrodes is characterized by a distinctly nonlinear voltage-

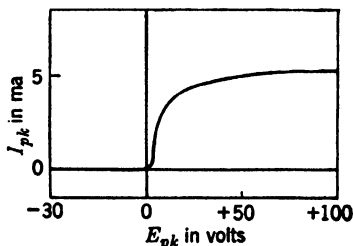


FIG. 3-51.—Doubly broken plate characteristic (6SH7).  $E_{ff} = 6.3$  volts,  $E_{g2k} = 100$  volts,  $E_{g1k} = -1$  volt.

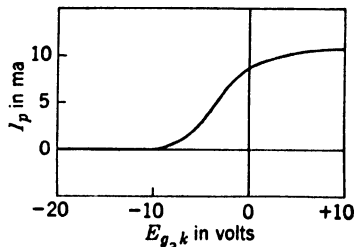


FIG. 3-52.—Doubly broken suppressor characteristic (6AS6).  $E_{ff} = 6.3$  volts,  $E_{pk} = 120$  volts,  $E_{g2k} = 120$  volts,  $E_{g1k} = -1$  volt.

current curve.<sup>1</sup> Several different regions are defined by different effects, but the most valuable nonlinearities are provided by the ionization of the gas. Additional freeing of electrons and nullification of space charge by the ionized particles make large currents available. The current flow

<sup>1</sup> M.I.T. E. E. Staff, *Applied Electronics*, Wiley, New York, 1943, p. 198, Figs. 13 and 14.

may increase spontaneously after ionization has progressed sufficiently and must, therefore, be limited by an external resistance in order to prevent injury to the electrodes. The voltage drop across the tube may be constant over a wide range of currents.

The regenerative nature of the breakdown or rise of current is an important property of gas tubes. Such effects are observed in regenerative vacuum-tube circuits.

With two unheated electrodes in a gas tube (the commercial voltage-regulator tube—for example, the VR-105), the constant voltage after breakdown (60 to 150 volts) is the property of greatest interest. The applied voltage for breakdown is somewhat above this constant voltage and is subject to considerable variation with time, temperature, tube unit, and incident light. For this reason, the discontinuity in the cold-cathode gas-diode characteristic is not much used for amplitude comparison. The

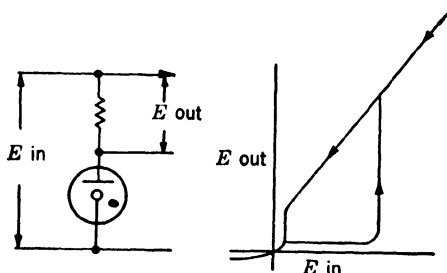


FIG. 3-53.—Characteristic discontinuities for a cold-cathode gas-diode circuit. The characteristic has both discontinuities and hysteresis properties.

characteristic of a gas-diode and series resistor circuit is shown in Fig. 3-53.

With a thermionic cathode the characteristic is similar to that of the high-vacuum thermionic diode for voltages less than the ionization potential (not the breakdown potential of the element) of the gas. As the plate-to-cathode voltage is increased, breakdown occurs as for the cold-cathode diode, but current prior to breakdown is considerably higher. The break in the high-vacuum diode characteristic is present as well as the ideal break at the breakdown potential. The latter point on the characteristic is subject to the same variability as the corresponding point for the cold-cathode tube and to cathode drifts in addition.

For many purposes it is desirable to control the start of the regenerative increase of current in a gas tube by means other than the acceleration of electrons by diode plate bias.<sup>1</sup> In particular, a grid structure around a thermionic cathode permits the firing to be controlled by the grid-cathode bias. The bias at which regeneration is self-sustaining is approximately

<sup>1</sup> *Ibid.*, p. 244.

as constant as is the high-vacuum triode bias for a specified current. The discontinuous characteristic that is provided by some grid-controlled gas-filled tubes with negligible grid current before firing is shown in Fig. 3-54.

The grid current that flows before and after firing may affect the applied waveform. A series resistance to limit the grid current after firing is often necessary. The conducting gas-filled tube has "noise" of much greater amplitude than that of a vacuum tube; under suitable conditions

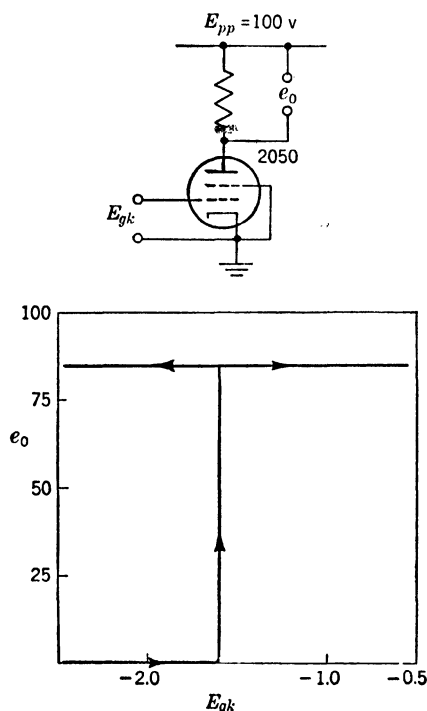


FIG. 3-54.—Grid-controlled hot-cathode gas-tube circuits. Voltage-transfer characteristic. The firing may not be turned off by the grid potential but only by an auxiliary means of lowering the plate current.  $E_{gk}$  at firing is a function of  $E_{pp}$ .

current in a high-vacuum triode. The breakdown potential is therefore subject to the same sort of drifts due to aging and change of heater voltage and to others due to the variation in gas composition and density. Figure 3-55 shows the effect of heater voltage on the critical potential in a 2050 thyratron. The curves have much the same slope as for a hard-vacuum tube, and a fair degree of compensation for heater-voltage variation may be achieved by balancing the effect with a diode or triode.

A fundamental difficulty in the application of ionization processes to

this may be as much as several volts.

During conduction, the plate current is determined by the supply voltage and the series impedance, the plate-to-cathode voltage (generally between 5 and 20 volts) being almost entirely independent of plate current. When the plate current is flowing the grid has little control, and means must be provided to extinguish the current by dropping the plate-to-cathode voltage to some low or negative value. The current flow must be reduced to a value of 0.5 to 5 ma.

Before initiation of plate current, the negative potential of the grid acts to keep electrons from the cathode from reaching the high gradient produced by the plate potential, where they would acquire sufficient velocity to ionize the gas. The grid potential at which enough electrons get through to cause breakdown thus depends on the initial velocities at the cathode, just as does the voltage that is required to obtain a certain current

fast waveform control is the relative slowness of ion movement. The breakdown may be delayed by a microsecond or more from the time at which the critical voltage condition is attained. This delay may vary from one repetition of a waveform to the next. The time required for deionization is considerably greater and is dependent upon the degree of ionization and the voltages available to remove ions. This recovery time may be from 15 to 200  $\mu$ sec for various tubes and operating conditions.

**3-22. Feedback Circuits.**—The regenerative nature of the firing of a gas-filled tube is described in Sec. 3-21. The characteristic of that element possesses a discontinuous segment and a hysteresis property that describes the irreversible nature of the firing. Such properties can also be found in regenerative vacuum-tube amplifiers.

The doubly broken-line characteristic of Sec. 3-20 may have a large slope on the central segment. This corresponds to a high-gain element. If the signal levels at which saturation of the amplifier occurs are held fixed and the gain is increased, as, for example, by additional stages, the result is as shown in Figs. 3-56*a*, *b*, and *c*. The entire range of output

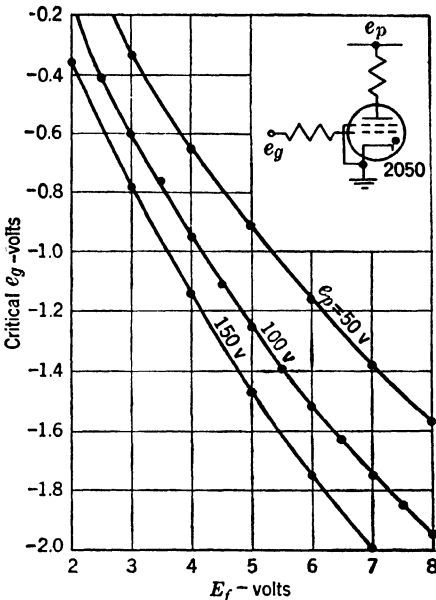


Fig. 3-55.—Effect of cathode temperature on thyatron firing potential.

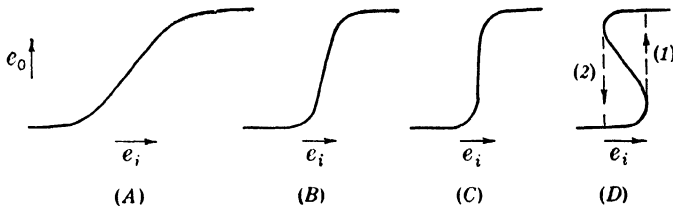


Fig. 3-56.—Effect of conductive regeneration on amplifier characteristics.

variable is traversed for a smaller and smaller increment at the input. The characteristic approaches a true discontinuity.

Regeneration is employed to provide very high gain in a single element. The effect of d-c-coupled regeneration is shown in Fig. 3-56, including Fig. 3-56*d*. These characteristics provide even more variety

than that produced by the increase of gain with additional stages. As d-c regeneration is increased, the element may pass through the condition for a simple discontinuity and exhibit hysteresis properties (see Fig. 3-56*d*). Adjustment  $c$  is often called the "infinite-gain amplifier" since the output signal is produced by an infinitesimal input increment. This characteristic would be suitable for many applications where a discontinuity is desired at the same value of a variable regardless of the direction of approach if the element gain and gain variation were stable. The vacuum-tube gain varies considerably, of course, and the voltage value

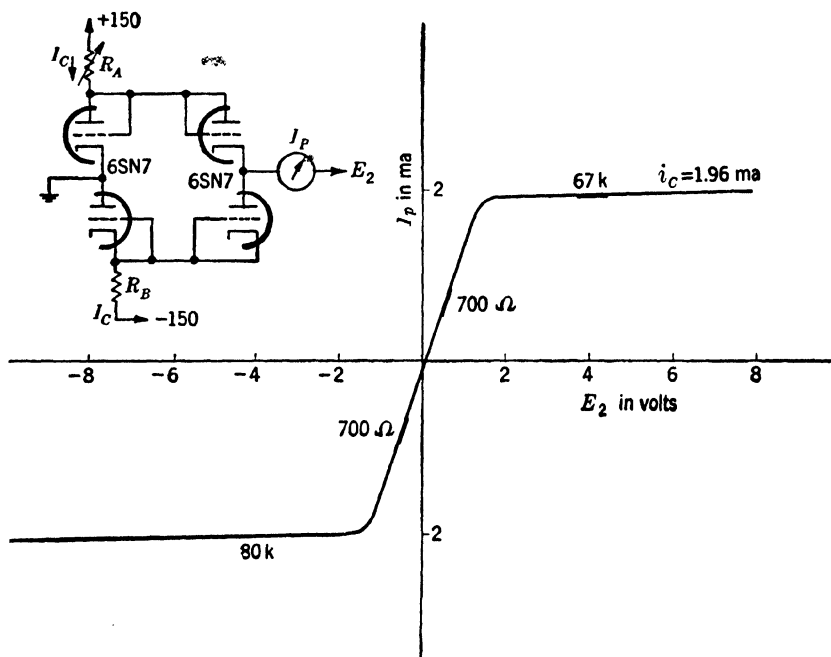


FIG. 3-57.—Four-diode element giving a doubly broken characteristic symmetrical about the origin. Two 6SN7's are used, diode-connected.

for regeneration also varies. Balanced circuits may be used to compensate systematic cathode drifts. The time scale of operation is limited by the stray reactances. Two circuits and their characteristics for various amounts of feedback are given in Sec. 9-16. These examples are not designed for rapid operation, and the point of regeneration is very unstable in each case.

**3-23. Multiple Circuits.**—By the combination of several diodes and resistances, simple circuits can be formed that have doubly broken-line characteristics of various kinds. Two examples appear in Figs. 3-57 and 3-58 for the 6H6 and 6SN7 (diode-connected). For identical resistors

and tubes with identical characteristics, the curves are symmetrical about the origin. The bidirectional conduction of these circuits may be necessary for some operations.

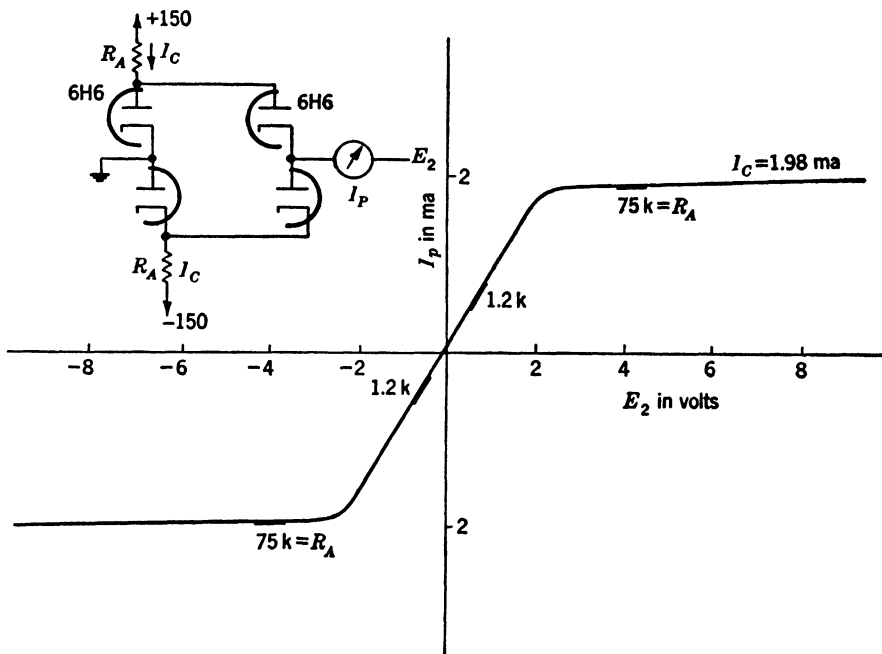


FIG. 3-58.—Four-diode element using 6H6's.

For many purposes, however, two-diode sections provide a suitable doubly broken-line characteristic (see Chap. 9:3). A representative circuit is shown in Fig. 3-59. A two-crystal characteristic is shown in Fig. 3-60. This circuit, used as an amplitude comparator, is discussed in Chap. 9.

**3-24. Multivariable Elements.**—The multigrid vacuum tube is an example of a multivariable element that relates several electrode potentials to the plate-cathode current and to grid currents. Other multivariable elements are constructed as circuits of two-variable elements.

The pentode has been shown to possess several two-variable nonlinear characteristics. For some of these, all variables except two are held constant; for others, the attention is focused on two variables, such as input voltage and output voltage, despite the variation of others. The current variables are ignored if voltage relationships are

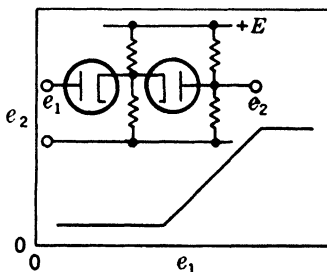


FIG. 3-59.—Two-diode element giving a nonsymmetrical doubly broken characteristic.

important, except during the calculation of the transfer characteristic of the element.

If three variables are in use, their relationship may be represented by a simple equation or by a set of graphs. The nonlinear functions are of the greatest interest, since linear multivariable elements are equivalent to circuits of linear two-variable elements.

The major portions of the 6AS6 pentode characteristic are shown in Fig. 3-61. The breaks in the several two-variable characteristics are not given in detail, but they are similar to the breaks that are previously

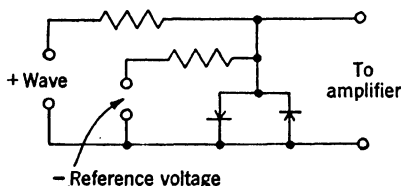
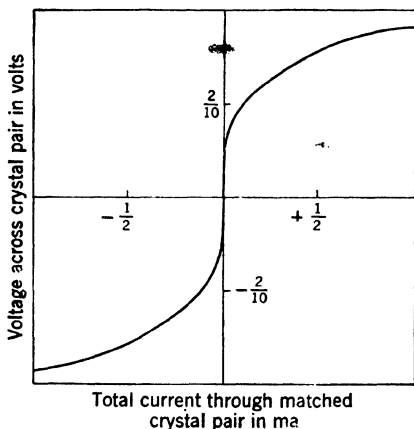


FIG. 3-60.—Two-crystal characteristic.

6SA7 is less sharp than that of the 6AS6, and the tube is also less suitable as a multiplier. The switching of an amplifier on and off is a comparatively nonprecise application for which the 6SA7 characteristic is suitable.

The VR-116 (British pentode) suppressor-cutoff characteristic is shown in Fig. 3-63. This tube has been much used where two-control grids are required.

A triode is a three-variable element, but the effect of plate voltage upon plate current is often an undesired effect. If this relation is used in a circuit operation, the triode may be considered a two-control electrode element. The 6K6 triode may pass a plate current proportional to the

described for pentodes, except for the suppressor-cutoff break. The 6AS6 is designed with a comparatively sharp suppressor-cutoff characteristic so that this tube is often called a "two-control-grid tube." The screen grid bias exercises less effective control over the plate current but may be a useful variable.

One important property of the 6AS6 is the dependence of the variation in plate current upon the product of  $\Delta E_{v,k}$  and  $\Delta(E_{v,k} - E_{v_1,k})$ . This property is utilized for a multiplying circuit in Chap. 19.

A second control grid (Grid No. 3) in a pentagrid converter tube (6SA7) provides the characteristics shown in Fig. 3-62. The second control grid is placed between two screen grids, and a suppressor shields the plate from the outer screen. The cutoff break of the

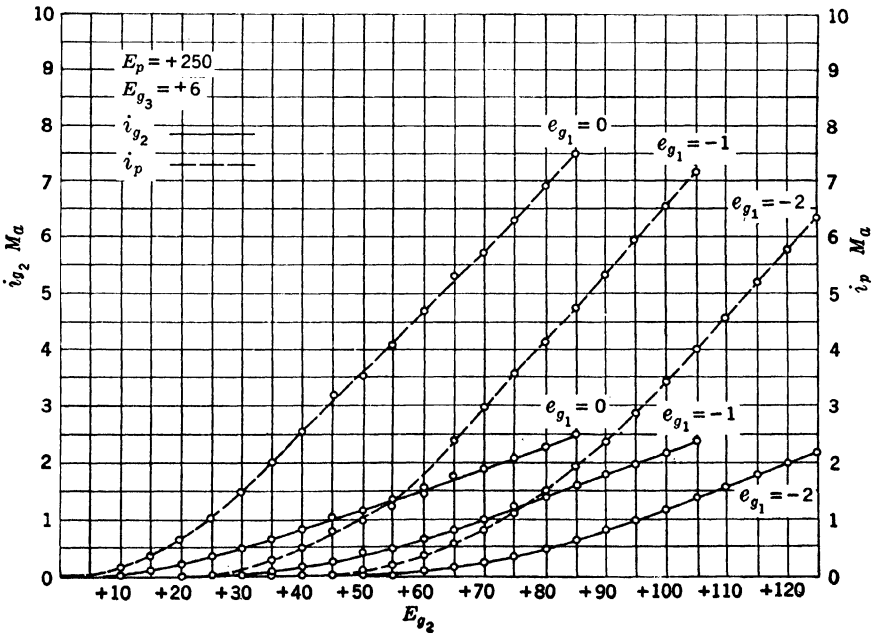
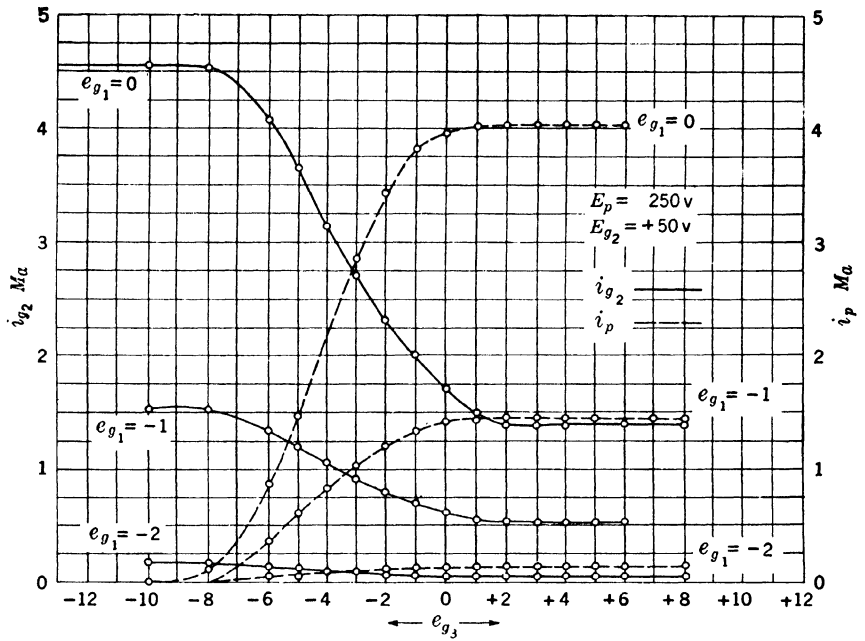


FIG. 3-61.—Three-control-grid characteristic of 6AS6. The first grid curve is not given. Above, suppressor characteristic. Below, screen characteristic.



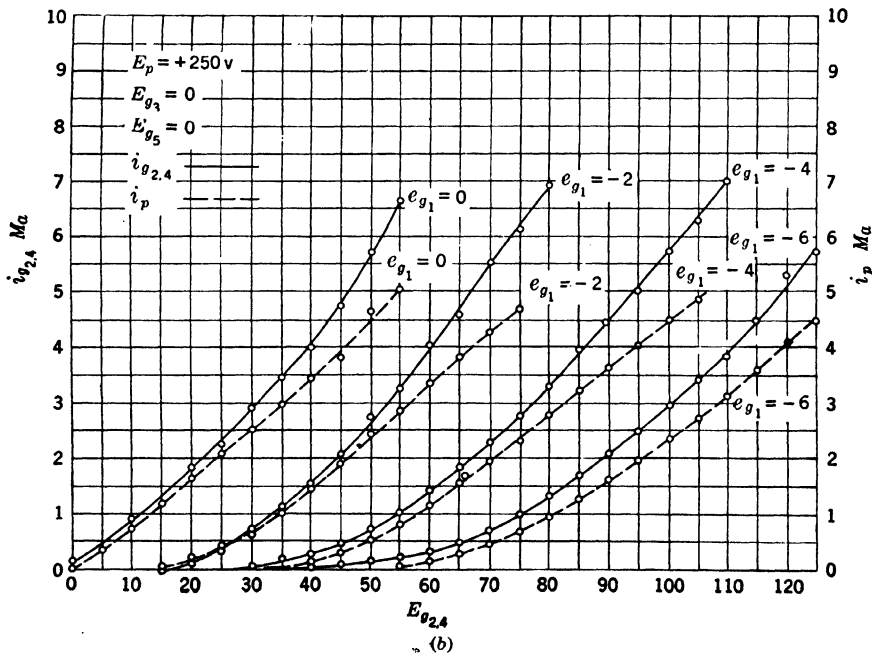
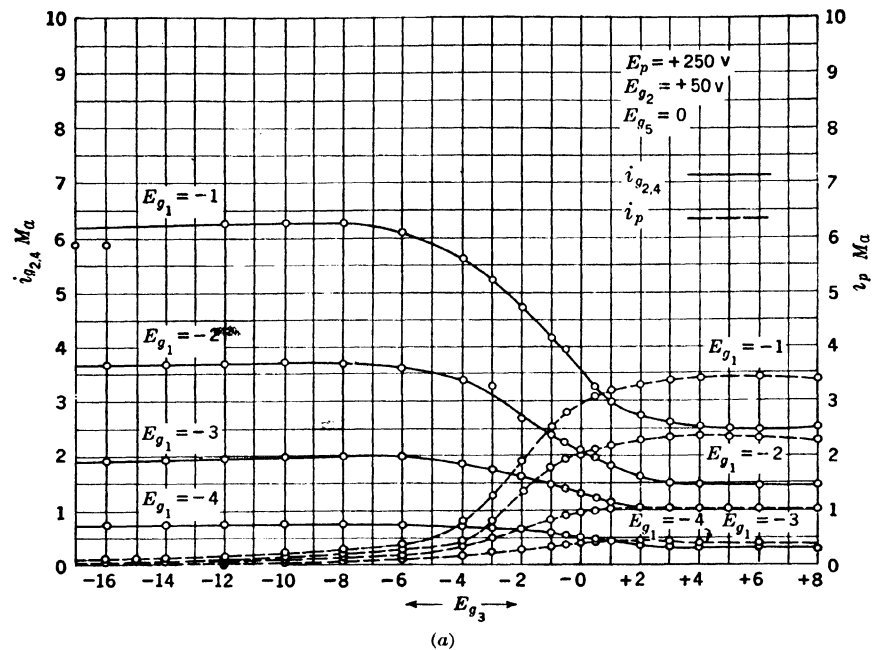


FIG. 3-62.—Three-control-grid characteristic of 6SA7. The first grid curve is not given.  
(a)  $E_{a-k}$  characteristic. (b) Screen characteristic.

product of the incremental plate and grid signals in some operating regions (see Chap. 19).

A pair of triodes may be connected in many different combinations to give a three-variable relationship. An unusual example is shown in Fig. 3-64. The approximately identical response to positive or negative values of  $E_2$  may be desirable in some instances. If two triodes are connected in parallel with a common plate resistor or in series with one tube serving as plate resistor for the other, many of the functions of a two-control-grid amplifier can be performed.

**3-25. Curved Characteristics.**—This characteristic is used for special applications such as the generation of curved waveforms, the synthesis of curved functions in computers, or modulation by curvature. The curved characteristics that are at present available are neither as stable nor as faithful to the desired curve as are linear elements.

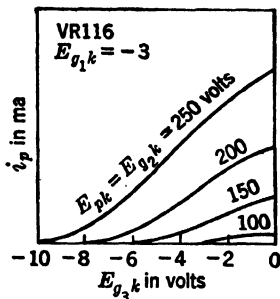


FIG. 3-63.—VR-116 suppressor characteristic.

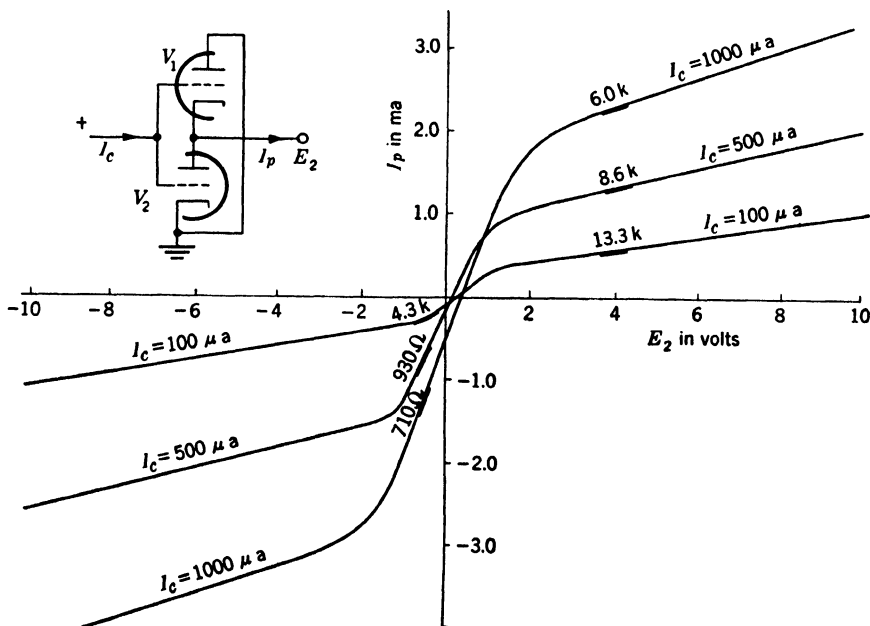


FIG. 3-64.—A multivariable characteristic from a two-triode circuit.

In Sec. 3-14, the curvature of the thermionic-diode characteristic is described. For high currents, a power law is obeyed; for low currents, an

exponential. An exponential grid characteristic for a triode is given in Sec. 3-19. These curvatures find use in some automatic logarithm computers. (The exponential waveform may be simply generated by linear networks.) Thus, the grid current for a triode is obtained from a photoelectric cell, in a photographic densitometer, so that the plate current of the triode is a measure of the logarithm of the illumination of the cell.

The curvature for many elements obeys a square law. Such characteristics are described in detail in Chap. 19. The stability of shape (fidelity) of a vacuum-tube plate characteristic is better than its stability of absolute values.

The variable- $\mu$  pentode has a curved transfer characteristic that is used for AGC. This characteristic is achieved by varying the spacing between grid wires, and some variation in the type of curvature is possible.

**3-26. Displacement Elements.**—The concept of waveform may be profitably extended to include nonelectrical physical systems. The preoccupation of this volume with electrical systems does not exclude some systems such as meter and cathode-ray-tube indicators. There are a number of nonlinear characteristics available with such elements.

The use of a mask with a visual presentation of any variable by displacement provides a broken-line characteristic. The connection between the observer and the data is completely severed for a range of values of the variable. This may be said to correspond to an ideal diode characteristic. Nonlinear scales are a flexible and often-used device for focusing attention upon a particular region of the variable.

The meter is restricted to the presentation of slowly varying quantities. Special galvanometers may provide fast response, and the cathode-ray oscilloscope, even faster response; the latter is limited only by transit-time effects. The oscilloscope is often used for a displacement presentation, and masking is perfectly possible in this case.

Automatic control of electric circuits by a photocell, perhaps on a cathode-ray-tube face, or by electrical contacts to which the electron beam can be switched by deflection, provides a set of valuable nonlinear relations. The latter device has been developed for a special waveform—coding operation.

**3-27. More Complete Descriptions of Physical Elements.**—The “element” of the preceding sections may be described symbolically by

$$F_1(X_1, X_2, X_3, \dots) = 0, \quad (8)$$

where  $F_1$  represents a set of graphs, a set of equations, or some tables of data. The variables  $X_1, X_2, X_3, \dots$  are those inputs and outputs that are useful to the circuit designer. Among them he may designate inde-

pendent variables, dependent variables, or parametric variables. These names are often helpful in analyzing a circuit by physical reasoning.

*Reactive Effects.*—If inductances or capacitances are present within the element,  $F_1$  must be equivalent to equations containing derivatives with respect to time. Such elements are said to have reactive characteristics. In order to simplify the descriptions of such elements, all distributed reactances are lumped and all elements are broken down into simple elements until the lumped reactances can be placed across the external terminals of the element.<sup>1</sup> The element may then be considered to be resistive, and the reactive effects are computed by a circuit analysis. The resistive characteristic must often be represented by linear segments for such calculations. This may not lead to excessive errors if the reactive effects are comparatively small. Throughout the remainder of this volume nonlinear elements are treated in this way. Nonlinear reactances have only a few special applications in waveform-shaping. "Nonlinear characteristic" will be taken to imply the resistive component of a nonlinear characteristic unless "nonlinear reactance" is specified. Therefore  $F_1$  contains no derivatives with respect to time,<sup>2</sup> although other derivatives represented by the hysteresis characteristics may be present.

*Complete Characteristic Sources of Error.*—The functional relationship of  $F_1$  is incomplete; for a careful circuit design, the sources of error that cause deviations from the normal or average must be known as well. The

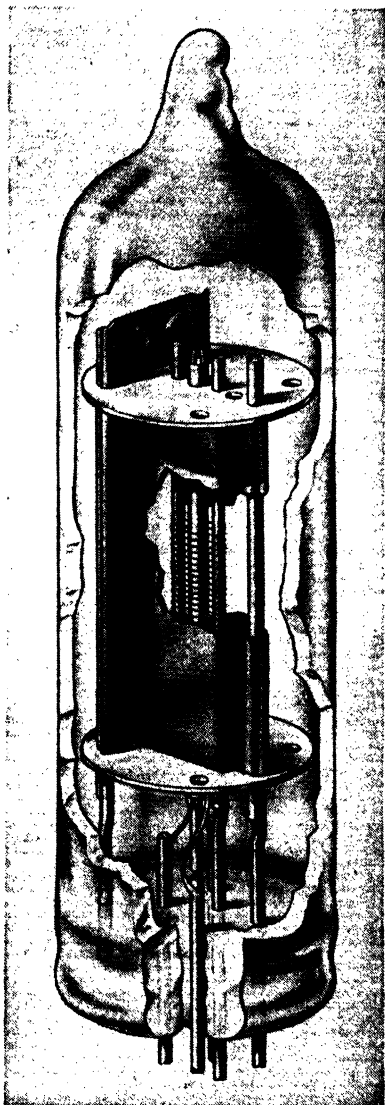


FIG. 3-65.—Subminiature high- $\mu$  triode (SD-917).

<sup>1</sup> See M.I.T. E. E. Staff, *Electric Circuits*, Wiley, New York, 1943, Chap. 1.

<sup>2</sup> Unless time is a useful variable.

*sources of error* cannot be distinguished from the *useful variables* until a particular use for the element is prescribed. For elements used in a familiar way, however, the distinction between useful variables (or, simply, variables)  $X_1, X_2, X_3, \dots$  and sources of error  $\alpha, \beta, \gamma, \dots$  is clear. The complete (resistive) characteristic becomes

$$F_2(X_1, X_2, X_3, \dots; \alpha, \beta, \gamma, \dots) = 0. \quad (9)$$

The sources of error may include temperature, age, usage, incident light, atmosphere in the tube, the geometry of the electrode structure. Sources

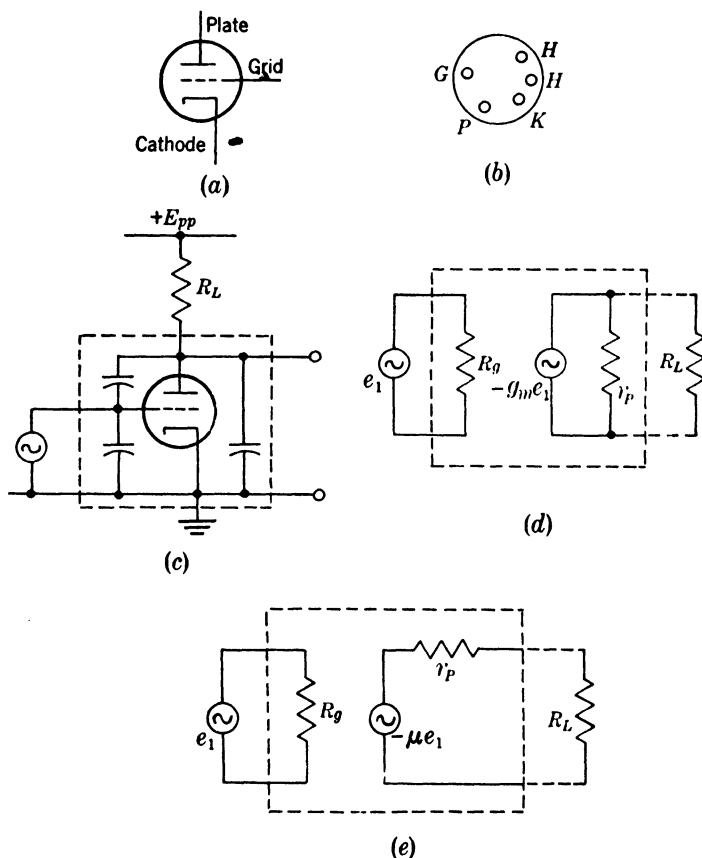


FIG. 3-66.—Triode symbols.

of error in one application may be useful variables in another. The screen-cathode voltage of a pentode is a familiar example.

The means for representing these undesired effects are graphs, or data, showing the departure of a characteristic from a standard or average value for an incremental change in the source of error. The analytical

equivalent is a knowledge of the partial derivatives or differences of the useful variables with respect to the sources of error, for some regions of the ideal characteristic. The relationship  $F_2$  is never represented completely.

The data of this chapter consist, in part, of important deviations from the average characteristics. The manufacturer's handbook data and the textbook descriptions of elements seldom include this information, even though it is required for accurate circuit design. The remaining data included in this chapter are made up of unfamiliar portions of common characteristics. In particular, the exact shape of the characteristics near cutoff of current is of interest. When new applications of elements are made, or greater predictability is desired, the designer is usually forced to take extensive new data.

In order to clarify the relation of ordinary vacuum-tube characteristics to a more complete description, the high- $\mu$  triode is discussed here. The construction of such an element is shown in Fig. 3-65 with the filament wires, cathode, grid, and plate visible as concentric structures. The common symbols for this element are shown in Fig. 3-66.

In the manufacturer's published tube data, the following information may be found:

1. Rated heater voltage and current.
2. Interelectrode capacitance values.
3. Maximum average tube dimensions, base type, and base connections.
4. A set of  $E_{pk}$ ,  $E_{gk}$ , maximum plate-power dissipation, amplification factor,  $\frac{\partial e_{pk}}{\partial e_{gk}}$ , transconductance,  $\frac{\partial i_{pk}}{\partial e_{gk}}$ , plate current, and plate resistance,  $\frac{\partial e_p}{\partial i_p}$ , recommended for Class A-1 a-c amplifier usage with an average tube.
5. A plate characteristic such as is shown in Fig. 3-67.

This information is sometimes all that is necessary to design an amplifier for which extreme economy, linearity, and stability are not important. The manufacturers may supply, in addition, curves of transconductance or plate resistance vs plate current for several values of plate voltage, or plate current vs. grid voltage for several values of plate voltage (a

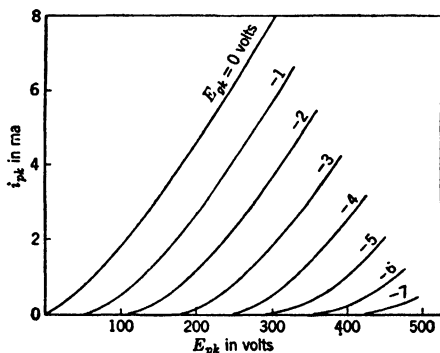


FIG. 3-67.—Average plate characteristics for high- $\mu$  triode (6SL7).  $E_{ff} = 6.3$  volts.

transfer characteristic). A third representation of this three-variable characteristic would designate plate current as a parameter.<sup>1</sup>

For amplifier operation with all signals sufficiently small so that the element may be considered linear, the triode may be represented by an equivalent generator and resistance. The constant-voltage and constant-current generator circuits of Fig. 3-66 are used when the load resistance is high or low respectively compared with the plate resistance of the tube. The two simple familiar analytical expressions corresponding to these circuits are derived from the equations

$$\Delta i_{pk} = g_m \Delta e_{gk} + \frac{1}{r_p} \Delta e_{pk} \quad (10)$$

and

$$\Delta e_{pk} = -R_L \Delta i_{pk}. \quad (11)$$

These expressions are

$$\begin{aligned} \Delta e_{pk} &= -\frac{\mu R_L}{R_L + r_p} \Delta e_{gk} \\ &\cong -\mu \Delta e_{gk} \quad \text{if } R_L \gg r_p \end{aligned} \quad (12)$$

and

$$\begin{aligned} \Delta e_{pk} &= -g_m \Delta e_{gk} \frac{R_L r_p}{R_L + r_p} \\ &\cong -g_m \Delta e_{gk} R_L \quad \text{if } R_L \ll r_p. \end{aligned} \quad (13)$$

This analytical approximation is widely used despite the fact that  $g_m$ ,  $r_p$ , and, to a lesser extent,  $\mu$  are not constant throughout the triode characteristic. For larger signals in high plate-current regions, a three-halves-power law approximates a plate curve at constant grid voltage. An exponential law is suitable for expressing the low-current control by grid voltage. These more exact expressions may be necessary for some applications of the tube. The variation in tube characteristics from various sources of error is so large that the exact analysis is usually not profitable.<sup>2</sup>

The two less familiar representations are shown in Figs. 3-68a and 3-68b. The complete three-variable characteristic could be represented by a three-dimensional model as in Fig. 3-68c. The two-dimensional graphs are projections onto coordinate planes of sections of the characteristic surface. All of these provide the same information, the characteristic of an average tube at 6.3 filament volts. They all assume that there are only three useful variables for this high- $\mu$  triode—plate current, grid voltage, and plate voltage. For some tubes the plate characteristic and

<sup>1</sup> See E. L. Chaffee, *Theory of Thermionic Vacuum Tubes*, McGraw-Hill, New York, 1933.

<sup>2</sup> An exception is nonlinear modulators. See M.I.T. E. E. Staff, *Applied Electronics*, Wiley, New York, 1943, Chap. 12.

grid current are given for the positive grid region in addition to the above data.

For a particular high- $\mu$  triode unit in operation, the characteristic may vary widely from the average because of sources of error. The size of

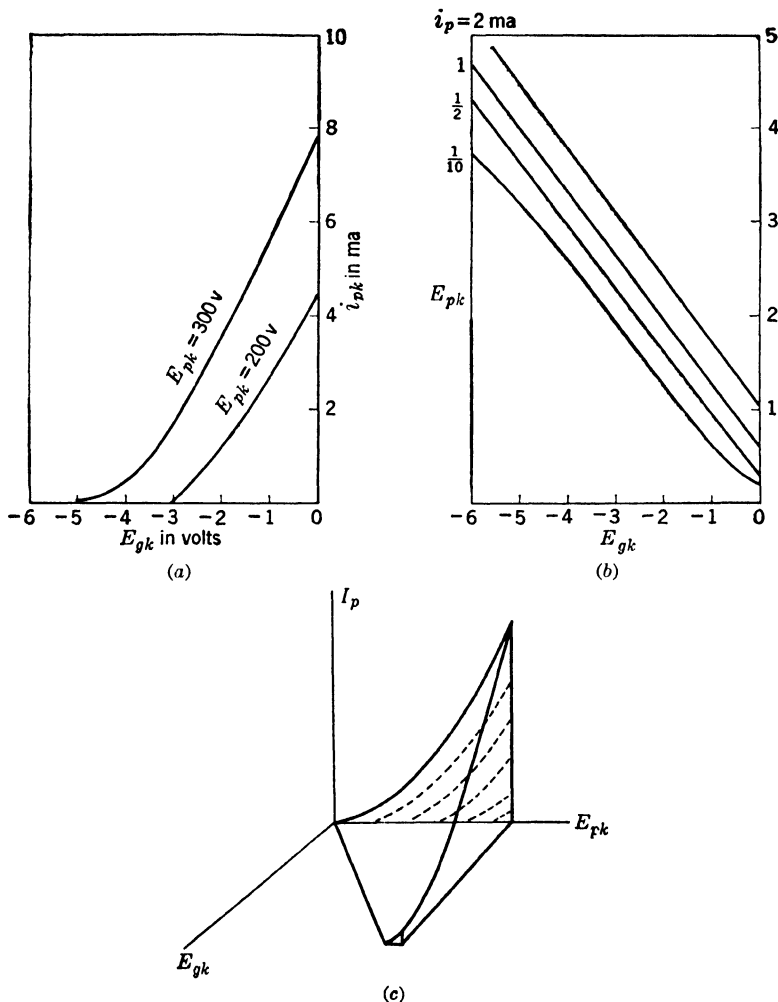


FIG. 3-68.—Other average characteristics ( $E_{ff} = 6.3$ ). (a) Transfer characteristic, voltage to current (6SL7). (b) Transfer characteristic, voltage to voltage (6SL7). (c) Three-dimensional 6SL7 characteristic.

such effects as these is not often specified. For precision equipment the size of these effects was excessive, and selection of the tubes near the average has been practiced during the war. This process has been standardized in the *Joint-Army-Navy Specification for Radio Electron*



*Tubes.* Some excerpts from the specification for a high- $\mu$  triode, the 6SL7 (one section), follows in order to illustrate the important sources of error.

*Excerpts from the JAN specification for a hi- $\mu$  triode (6SL7).*

Ratings (as in manufacturers' data).

$$E_f = 6.3 + 10\% \text{ volts absolute maximum}$$

$$E_{pk} = +275 \text{ volts absolute maximum}$$

$$P_p = 1.1 \text{ watts absolute maximum}$$

$$E_{hk} = 100 \text{ volts absolute maximum}$$

*Test Conditions.*

$$E_f = 6.3 \text{ volts}$$

$$E_{pk} = +250 \text{ volts}$$

$$E_{ok} = -2 \text{ volts}$$

*Vibration Test.* The tube is connected under the test conditions (4000-ohm load resistor) and vibrated with a simple harmonic motion of 0.04-in. amplitude at frequencies from 12 to 25 cps. The resultant alternating current appearing across the load resistor must not exceed 400 mv rms.

*Heater Current.* With  $E_f = 6.3$  volts, the heater current may vary from 275 to 325 ma.

*Heater Insulation.* With the heater voltage applied, 100 volts is applied between the heater and the cathode. The current flow between the two elements must not exceed 20  $\mu$ a for either polarity of applied voltage.

*Grid Current.* Under test conditions the current flowing to the grid (positive ion and secondary emission current) shall not exceed 1  $\mu$ a.

*Plate Current.* Under test conditions the plate current shall be within the range of 1.4 to 3.2 ma. With  $E_{ok}$  reduced to  $-5.5$  volts, the plate current must not exceed 25  $\mu$ a.

*Transconductance.* Under test conditions, the transconductance shall be within the range of 1200 to 2000  $\mu$ mhos.

*Amplification Factor.* Under test conditions the amplification factor shall be within the range of 55 to 85.

Other tests are specified for a-c amplification, life test (500 hr before transconductance falls below its limit), noise, emission, the physical dimensions of the tube.

From the tolerance of the specification, the large variations that are common in unselected tubes may be inferred. The plate characteristic for  $E_{ok} = -2$ , even of a selected tube at 6.3 filament volts, can only be predicted to lie within a region such as that shown as a shaded area in

Fig. 3-69. The actual characteristic for a given unit is usually, but not always, parallel to the average characteristic. The effect of varying the filament voltage for an average tube is shown for one grid bias,  $E_g = -4$  on the same graph. These effects are additive and are smaller than would be observed on unselected tubes. (These sources of error affect all constant-grid-voltage curves similarly.) A tube life of 500 hr means that the characteristic drifts out of the specified region in 500 hr.

The JAN specification represents an enormous improvement in the predictability of vacuum-tube characteristics. This standardization is essential for accurate circuits and for maximum reliability. The development of tubes that will satisfy more stringent stability requirements seems desirable in view of applications in computers and laboratory instruments. However, it is not expected that it will be economically feasible to select all commercial vacuum tubes even to the JAN specification.

Even the JAN specification is aimed at only a few of the possible applications of the high- $\mu$  triode. For some purposes a knowledge of the average grid-current characteristic (see Fig. 3-70) is desirable. Another use

of the circuit may require a more exact knowledge of the transfer characteristic near cutoff. Such a curve is shown in Fig. 3-71. The effect of various sources of error on these curves is not shown, although it is often of interest.

An illustration of the inherent similarity of all the variables—useful, parametric, or sources of error—may be noticed in the triode. Grid current is a source of error in an amplifier that is ideally linear. It is a useful variable if a resistance is placed in series with the grid signal, for a useful nonlinear characteristic is provided. The plate-voltage vs. plate-current curve for a fixed value of grid current is shown in Fig. 3-69. The grid current is shown as a parametric variable in the double-triode circuit of Fig. 3-64.

For linear amplifier service the  $E_{pk}$  voltage is an independent variable; it changes continuously. If the plate and cathode terminals of the tube are to provide a resistance, variable in steps, the  $E_{pk}$  voltage is a controlling parametric variable. Similarly, if the plate-cathode impedance

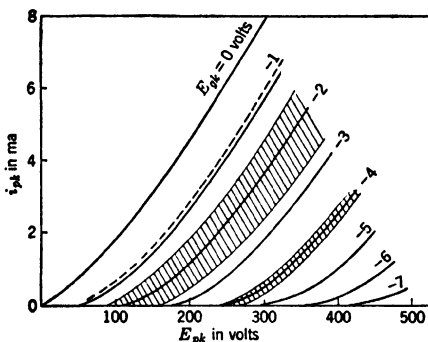


Fig. 3-69.—Deviations from average plate characteristics. The effects of JAN prescribed unit-to-unit variation and of a  $\pm 10$  per cent variation in  $E_{ff}$  are shown. The plate current and plate voltage for which 1  $\mu$ a of  $G_1$  current flows is shown (dashed) to be parallel to a constant grid-bias curve. All curves are affected similarly to those shown with tube and  $E_{ff}$  variations.

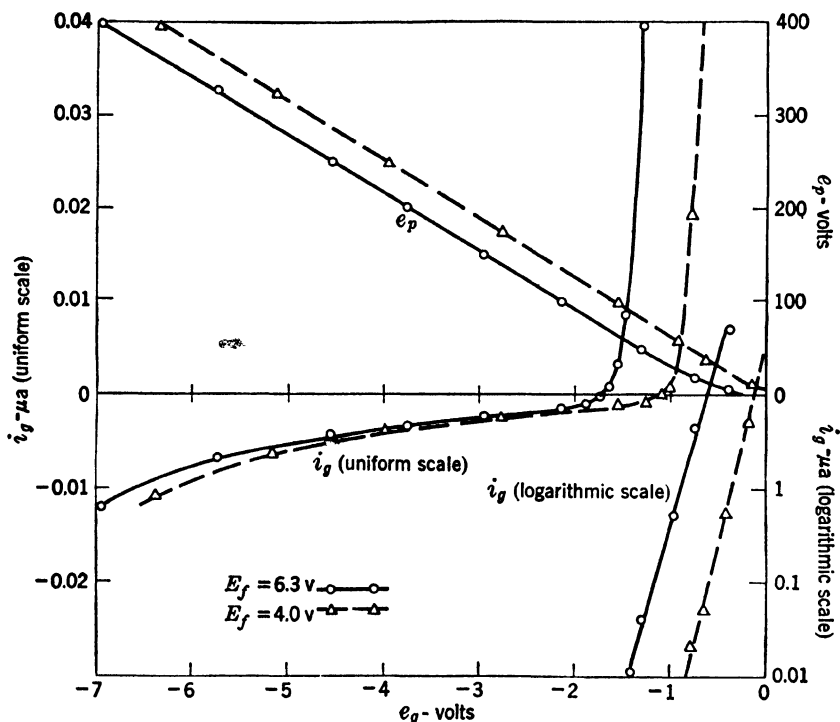


FIG. 3-70.—Negative and positive grid current in a triode operated with constant plate current (6SL7),  $i_p = 0.1$  ma.

is to be low or infinite (a switch), the  $E_{ok}$  must assume two distinct and fixed values.

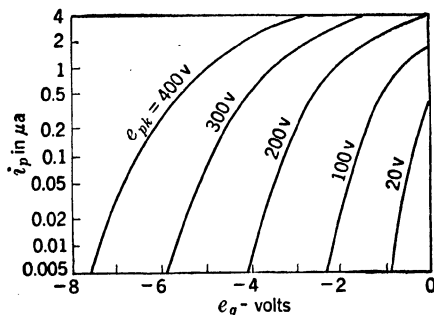


FIG. 3-71.—Expanded cutoff characteristic (6SL7 triode).

There is a useful distinction between mutual and direct electrical characteristics. A *direct* characteristic relates current and voltage at a single pair of terminals. A *mutual* characteristic relates variables at two different pairs of terminals, which may share a terminal. The mutual characteristic often provides isolation between one variable and another or, in other words, be-

tween the waveform generator and a circuit operating on the waveform. Thus, an “electron-coupled” device is described by a mutual characteristic. In such circuits, the choice of independent variable and dependent variable is prescribed by the unidirectional isolation.

## CHAPTER 4

### SINUSOIDAL WAVEFORM GENERATORS

BY G. R. GAMERTSFELDER AND J. V. HOLDAM

#### CONTINUOUS WAVES

Classical electrical circuit theory has been concerned largely with circuits in which the variations of current, voltage, and charge are sinusoidal functions of time. The emphasis is entirely understandable since sinusoidal variations occur so frequently in the solution to network problems. Indeed the sine function, along with the exponential function, may be considered one of the “natural” modes of an electrical circuit. In the introduction to this volume it has been emphasized that the point of view would be essentially different from the classical, and that attention would be focused on methods of generating nonsinusoidal waveforms for particular applications. On this basis, it might seem that a chapter on the sinusoidal waveform is out of place. However, in the development of the art, new uses have been found for the sinusoidal waveform, often in conjunction with other less standard waveforms, and for this reason the present chapter is included. Emphasis will be placed on the generation of sinusoidal waveforms having frequency stability, amplitude stability, and freedom from harmonics.

**4-1. General Properties.**—The sinusoid is unique among waveforms in that its shape is unaffected by any linear network. Because of this property it is, in principle, one of the easiest of waveforms to generate. Suppose that a sinusoidal voltage is applied to a linear amplifier. The output of the amplifier will have the same shape as the input and will differ from it only in amplitude and phase. If the output is passed through a suitable linear network, the amplitude and phase can be so altered that the voltage is an exact replica of the input voltage. If the original voltage source is removed and the output of the linear network is connected to the amplifier input, the circuit continues to operate in exactly the same manner, and the result is a sinusoidal oscillator. Ordinarily the characteristics of the amplifier and feedback network are such that the output and input are in phase at only one frequency, and thus the frequency of oscillation is determined by the phase-shift properties of the amplifier and feedback network. Such a generalized feedback oscillator is illustrated in Fig. 4-1. If the gain of the amplifier is  $A$  and the

transfer function of the feedback network is  $\beta$ , both being complex numbers and functions of frequency, the required condition for sustained oscillations may be written

$$A\beta = 1 \quad (1)$$

Since both  $A$  and  $\beta$  are complex quantities their product is also a complex quantity. Both  $A$  and  $\beta$  are functions of frequency and, in any practical system, functions of amplitude. In any system that can sustain continuous oscillation, the frequency and the amplitude adjust themselves

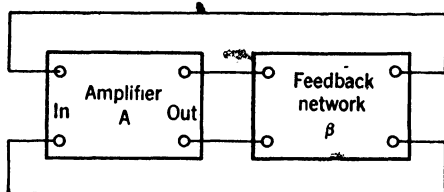


FIG. 4-1.—Generalized feedback oscillator.

so that Eq. (1) is fulfilled. The problem of design is to make  $A$  and  $\beta$  the proper functions of frequency and amplitude so that the desired frequency is generated and the desired amplitude is obtained.

The production of continuous oscillations can be looked upon from another standpoint—that of negative resistance. Consider, for example, a simple resonant circuit composed of an inductance  $L$  and capacitance  $C$  in series as shown in Fig. 4-2. The a-c resistance of the circuit, which can never be completely eliminated, is represented by  $R$ . A solution of the differential equation for the circuit indicates that, if by some means a current is started, the natural behavior of the circuit is oscillatory, the amplitude of the oscillations decreasing exponentially with time. The oscillations are associated with the interchange of energy between the inductance and capacitance. However, the resistance  $R$  is constantly dissipating energy, and therefore the amplitude must continually decrease. If energy is supplied to the circuit at the same rate as that at which the resistance  $R$  dissipates it, there is no decrease of amplitude. From the circuit standpoint a negative resistance equal in magnitude to  $R$  and connected in parallel with  $R$  makes the effective resistance infinite, preventing any net flow of current in this branch and hence preventing the dissipation of energy. Such a negative resistance is equivalent to a source of energy. The production of negative resistances will be discussed later; for the present it is intended only to point out that such a device is capable of maintaining the natural oscillations of a resonant circuit at constant amplitude.

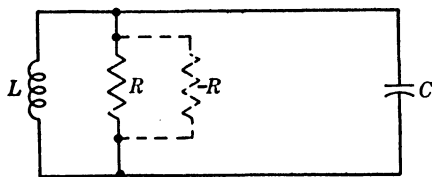


FIG. 4-2.—Generalized negative-resistance oscillator.

In any practical circuit the amount of negative resistance depends upon the amplitude of oscillation and balances the dissipation for one

amplitude only. Also, circuits that can be used as negative-resistance elements usually contain reactive components that influence the resonant frequency. Just as in the case of feedback amplifiers, the frequency and amplitude establish themselves at levels where the negative resistance exactly cancels the dissipative resistance in the circuit.

These two ways of looking at an oscillating circuit are not meant to imply a rigid classification of oscillator types. Frequently a given oscillator circuit can be analyzed equally well from either point of view. Usually, however, the circuit configuration makes one or the other of the two viewpoints more natural, and hence the oscillator circuits discussed in this chapter are divided according to this rather arbitrary criterion.

*Amplitude Stability and Wave Shape.*—It has been pointed out that both  $A$  and  $\beta$  are functions of the amplitude of oscillation, and that as a result the amplitude adjusts itself so that Eq. (1) holds true. For the amplitude of oscillation to be held constant, either  $A$  and  $\beta$  must be held constant, or their variations with variable external conditions must have compensating amplitude characteristics.

In general, both  $A$  and  $\beta$  depend on time (age), temperature, and supply voltage. Consequently, it is generally necessary to use regulated voltage supplies and components with low temperature coefficients. Furthermore, it is generally necessary to include in  $\beta$  elements that compensate for the change in  $A$  with time and temperature.

Automatic-gain-control circuits, composed of active elements, can be designed to stabilize the amplitude to about 0.1 per cent. Passive nonlinear elements, that is, thermistors, etc., in either the positive- or negative-feedback loops are more efficient than AGC circuits, but are not as effective for stabilization. Stabilization employing these methods is discussed more fully in Sec. 4-9.

In order to preserve good wave shape it is necessary that the nonlinear elements employed in the stabilization circuit have time responses that are long compared with the period of the oscillation. This assures that the stabilizing element is linear for the oscillatory AC, a necessary condition for a sinusoidal waveform to be unaffected by the element.

*Frequency Stability.*—The frequency dependence of  $A$  and  $\beta$  is usually determined by a circuit having a transfer function in which the phase angle changes rapidly with frequency near the oscillation frequency. Consequently, the frequency stability can usually be tied down to a few components in the circuit. In most circuits the frequency is also somewhat dependent on the characteristic of the active element in the circuit, particularly on the plate resistance of the oscillator tube.

In Sec. 4-10, the most common methods of making the frequency independent of temperature and aging are discussed. The principal methods employed are plate loading of the oscillator tube so that changes

in the plate resistance are negligible compared to the total resistance, and temperature compensation of the resonant element, particularly the condensers. Circuits that employ crystals for the frequency-determining element are made stable in frequency by thermostatically controlling the crystal temperature or by employing a crystal cut that has a low temperature coefficient. In practical circuits, crystal oscillators can be made to be stable within a few tenths of a part per million per degree centigrade, whereas *LC*-oscillators can be made stable to a few parts per million per degree centigrade.

**4-2. Resonant-circuit Oscillators.**—Oscillators in which one or more resonant circuits are used to determine the frequency of oscillation are probably more widely used than any other type—particularly for radio frequencies. Crystal oscillators are included in this category because a crystal is equivalent to a resonant circuit; but since their properties are somewhat different they are considered in a separate section. The principal advantages of this type of circuit are simplicity, high efficiency, and the fact that the resonant circuit discriminates strongly against harmonics of the oscillation frequency. The use of oscillators for delivering large amounts of a-c power is not treated here; frequency stability, amplitude stability, and good waveform are the matters of primary concern.

The *LC*-oscillator circuits most commonly used are the Hartley, Colpitts, tuned-plate, tuned-grid, and tuned-plate tuned-grid. These circuits are discussed in all standard references such as Terman,<sup>1</sup> and satisfactory operating conditions have been established for each circuit. The theoretical treatment of these circuits is also complete. Williams derives the conditions for oscillation by negative resistance methods, and Reich and Chaffee establish these conditions by feedback methods.<sup>2</sup>

It is generally necessary to verify experimentally the operating conditions and stability of any *LC*-oscillator circuit. The theoretical treatment of such circuits generally assumes that  $\mu$  and  $R_p$  are constant—that is, the tube characteristics can be properly represented by equally spaced straight lines. These assumptions are justified only for Class *A* operation and when negligible grid current is allowed to flow. For Class *C* operation there may be considerable error.

It is also generally assumed that the losses in the inductance can be represented by a series resistance. This assumption is not justified if detailed performance characteristics are desired from the theoretical

<sup>1</sup> F. E. Terman, *Radio Engineers' Handbook*, McGraw-Hill, New York, 1943, Sec. 6.

<sup>2</sup> N. H. Williams, *Electron Tubes*, Edwards Brothers, Ann Arbor, 1937; H. J. Reich, *Theory and Application of Electron Tubes*, McGraw-Hill, New York, 1939, Chap. 10; Chaffee, *Theory of Thermionic Vacuum Tubes*, McGraw-Hill, New York, 1933, Chap. 13.

treatment. For example, an isolated inductor—one that is not magnetically coupled to another circuit—may be represented either as a series or parallel combination of inductance and resistance for any single frequency. Because the inductor is completely characterized at a given frequency by a single quantity, namely its impedance, the impedance can be synthesized in any way whatsoever as long as it has the correct magnitude and angle. The theoretical conditions for oscillation and frequency of oscillation depend upon the model chosen to represent the inductor. For example, in the case of a tuned-plate oscillator, where the inductor is characterized by a series inductance and resistance, the conditions for oscillation are

$$M = \frac{CrR_p + L}{\mu} \quad (2)$$

and

$$\omega^2 = \frac{1}{L_c} \left( 1 + \frac{r}{R_p} \right). \quad (3)$$

The frequency-determining elements are  $L$  and  $C$ ;  $r$  is the series resistance;  $R_p$  is the plate resistance of the oscillator tube;  $\mu$  is the amplification factor of the oscillator tube, and  $M$  is the mutual inductance between the resonant circuit and the secondary winding of the inductor.

If the inductor is synthesized as a parallel combination of inductance and resistance, the conditions for oscillation are

$$M = \frac{L}{\mu} \left( 1 + \frac{R_p}{R} \right) \quad (4)$$

and

$$\omega^2 = \frac{1}{LC}, \quad (5)$$

where  $R$  is the resistance in parallel with  $L$ . The correct representation is even more complicated than a combination of series and parallel resistance, since it is also necessary to take into account the distributed capacity of the inductor winding. As a result, it is rarely worth while to make an elaborate theoretical examination, taking into account all of the possible variables; the direct approach of laboratory experimentation generally yields satisfactory results more quickly.

Figure 4·3 shows a modified Hartley oscillator designed to operate on approximately 20 kc/sec. The amplitude and frequency stability of this circuit are discussed in Secs. 4·9 and 4·10.

When an output of large amplitude is desired and extremely good wave shape, frequency stability, and amplitude stability are not required, oscillators are usually operated Class C. The grid bias is so adjusted that the tube conducts for only a fraction of a cycle, with the result that





and spring factors which determine the mechanical resonance of the crystal, and  $r$  corresponds to the frictional damping of the mechanical oscillations. Ordinarily the damping is very small and as a result the  $Q$  of the circuit is very high and may range from 2000 to 500,000, depending upon the manner in which the plate is cut and the method of mounting.

The capacitance  $C'$  is usually much larger than  $C$ . At frequencies such that the reactances of  $L$  and  $C$  are nearly equal, the impedance of the  $LrC$  branch is so small that the effect of  $C'$  can be neglected, and the crystal behaves as a series-resonant circuit. At some slightly higher frequency the impedance of the  $LrC$  branch is principally an inductive reactance equal to the reactance of  $C'$ . In this region the crystal behaves as a parallel-resonant circuit. The difference between the series-resonant and parallel-resonant frequencies depends upon the ratio of  $C'$  to  $C$ . If  $\omega_s$  is the series-resonant frequency,  $\omega_p$  is the parallel-resonant frequency, and  $k$  is the ratio of  $C'$  to  $C$

$$\frac{\omega_p}{\omega_s} = \sqrt{1 + \frac{1}{k}} \quad (6)$$

At frequencies remote from either  $\omega_p$  or  $\omega_s$  the crystal appears simply as a capacitance  $C'$ .

Since a crystal has the properties of a resonant circuit, it can be used in a feedback oscillator to determine the frequency of oscillation. Crystals are very stable and are affected to only a slight degree by temperature and hence are ideally suited to this application.<sup>1</sup>

Figure 4-5 shows an example of a crystal oscillator using the parallel resonance of the crystal as the frequency-determining characteristic. The plate circuit is tuned to a frequency somewhat higher than the parallel-resonant frequency of the crystal so that at the oscillation frequency the plate circuit has an inductive component of impedance. The coupling to the grid circuit is through the grid-plate capacitance of the tube.

In the Pierce oscillator, Fig. 4-6, the crystal is connected directly between plate and grid. Since the crystal has a low impedance near its series-resonant frequency, there is sufficient feedback at this frequency to maintain oscillation. The capacitance from grid to ground is used to control the grid excitation. Since the grid circuit is capacitive, the crystal must appear inductive to give the proper phase shift between plate and grid. At most, this phase shift is less than  $180^\circ$ , and for that reason the additional phase shift must be achieved by loading the plate circuit of the tube capacitively—by use of a detuned resonant circuit

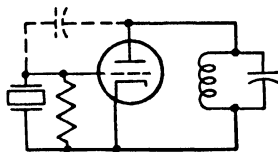


FIG. 4-5.—Crystal oscillator equivalent to the tuned-grid circuit.

<sup>1</sup> Vol. 17 gives the physical characteristics of the principal types of crystals used in radar timing systems.

whose resonant frequency is less than the crystal frequency. In some cases a resistor or an untuned choke can be used for the plate load if there is sufficient stray capacitance from plate to ground.

A widely used variation of the tuned-plate tuned-grid crystal oscillator is the Tritet shown in Fig. 4-7. A tetrode or pentode is used and the screen grid is connected as an anode for a series-fed tuned-plate tuned-grid oscillator. The parallel-

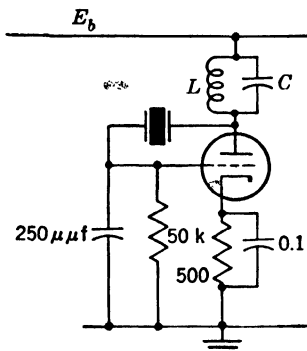


FIG. 4-6.—Pierce crystal oscillator.

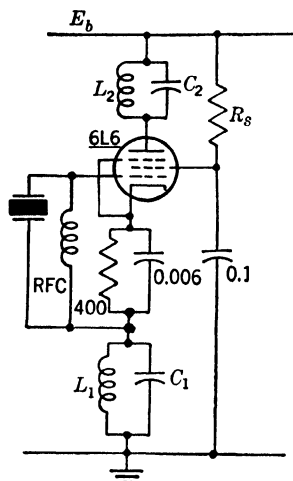


FIG. 4-7.—Tritet oscillator.

resonant plate circuit may be tuned to the crystal frequency or it may be tuned to a harmonic of the crystal frequency. Electron coupling reduces the usual reaction of the load on the oscillator and hence increases the frequency stability.

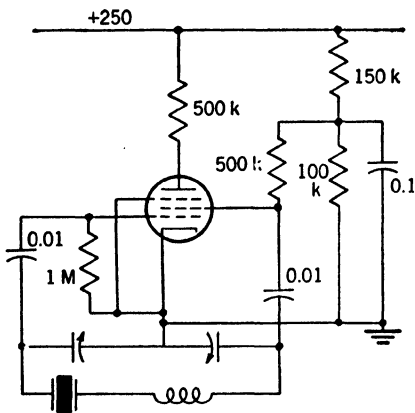


FIG. 4-8.—Standard frequency oscillator.

The circuit shown in Fig. 4-8 is often used as a frequency standard at about 100 kc/sec. Here the crystal acts as a filter in series with the inductance of an electron-coupled Colpitts oscillator. When the circuit is tuned approximately to the crystal frequency, it oscillates at the frequency for which the crystal has its lowest impedance, that is, its series-resonant frequency. The frequency can be varied over a range of about 0.01 per cent by the tuning condensers.

The circuit shown in Fig. 4-9 is used in the CPN-11 and CPN-12 to control accurately the recurrence frequency in the AT Loran equipment. For master-station operation the resistor  $R_1$  in series with the crystal is bypassed by a small condenser and no correction voltage is applied to  $R_1$ .

The circuit is equivalent to a tuned plate-tuned-grid oscillator, and the proper feedback phase is realized when the plate circuit has a natural resonance at 115 kc/sec. Since the oscillator is a pentode, it is necessary to use an external capacitance between the plate and grid circuit ( $C_2$  in the figure) to supply regeneration. The crystal has a low temperature coefficient, and the stability is further improved by thermostatically controlling the temperature of the crystal mount. Capacitances  $C_1$  and  $C_2$  are selected with the proper temperature coefficient to improve the stability even further. The short-time stability of this circuit is at least as good as 2 parts per million per hour; the long-time stability is much better.

For slave-station operation  $R_1$  is the cathode load of a cathode follower whose grid input is the fundamental frequency. The phase and amplitude of the grid input to the cathode follower are automatically controlled

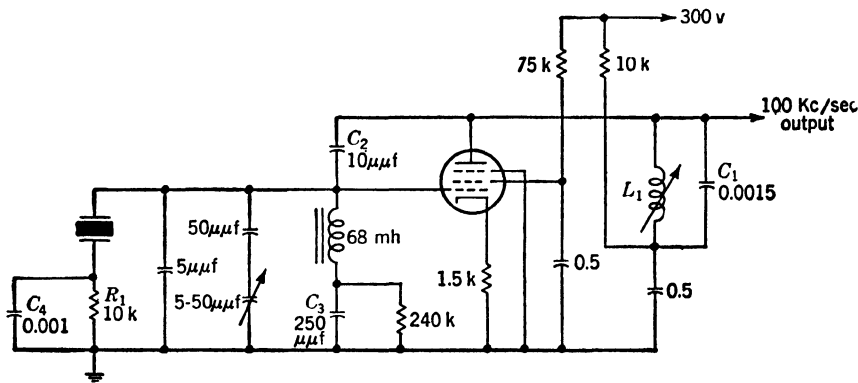


FIG. 4-9.—100 kc/sec crystal oscillator, AN/CPN-11,12.

so that the slave station's oscillator maintains exact synchronization with the master station.

Oscillators employing low-frequency crystals as the frequency-determining element have a somewhat different design than the crystal oscillators discussed in the preceding paragraphs. Figure 4-10 shows the construction of a low-frequency crystal and Fig. 4-11 shows a circuit employing such a unit. The crystal is wire-supported and vibrates in either a longitudinal or a face flexure mode, depending on the cut. The division of the electrode surfaces makes the unit a four-terminal network. The two pairs of electrodes are coupled primarily by the mechanical vibration of the crystal; hence, in an oscillator, direct feedback through the shunt capacity is avoided.

In Fig. 4-11 the crystal is shown with four electrodes, two of which are connected to ground. Resistors  $R_1$  and  $R_2$  may be made adjustable in order to control the amplitude of AC on the plate of  $V_1$  and the ampli-

tude of the crystal excitation. With the exception of the crystal connections, the circuit is standard. Tube  $V_2$  is an amplitude-limiting diode for the purpose of delayed AGC (see Sec. 4-9). The plate load is not tuned because, for the use to which this circuit was put, a sinusoidal waveform was not essential. In this circuit the purest sinusoidal waveform is found at the grid of  $V_1$ .

**4-4. Phase-shift Oscillators.**—A phase-shift oscillator consists of a simple amplifier, usually a single tube, whose output is fed back to the input through a phase-shifting network composed of reactive and resistive elements. In a sense, the classification is artificial since the above description applies to any of the feedback oscillators discussed in this chapter. The circuits to be considered here differ in that the amplitude of the feedback voltage does not have a maximum at the oscillation frequency.

A typical phase-shift oscillator, shown in Fig. 4-12, consists of a triode amplifier that drives a phase-shifting network composed of three resistance-capacitance sections, the output of which is fed back to the grid. The plate load of the amplifier is a resistance that is low compared with the impedance of the phase-shifting network at the frequency of oscillation, with the result that the voltage at the plate is roughly  $180^\circ$  out of phase with the grid voltage. At the frequency of oscillation the phase-shifting network produces an additional  $180^\circ$  phase shift. If the attenuation in the phase-shifting network ( $1/\beta$ ) at this frequency is equal to the gain of the amplifier, the condition  $A\beta = 1$  is satisfied.

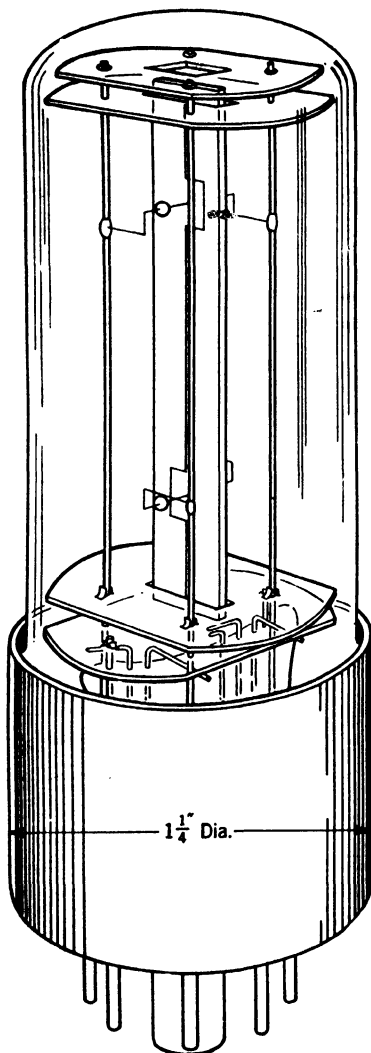


FIG. 4-10.—Low-frequency crystal.  
(Bell Telephone Labs.)

There are four kinds of phase-shifting networks, illustrated in Fig. 4-13, that can be used in this type of oscillator, some of them having advantages over the others for particular applications. For analysis, it



of  $\omega_1$  for the four networks is given in Table 4-1. If  $T_1$  is the value of  $T$  at the frequency of oscillation, Eq. (8) becomes

$$T_i = \frac{1}{1 + 5k_1^2} \tag{11}$$

Substituting the value of  $k_1$  from Eq. (10) gives

$$T_1 = -\frac{1}{29} \tag{12}$$

In the simple one-tube phase-shift oscillator considered here, the transfer function is identically  $\beta$  and the gain of the amplifier stage is identically

$A$ . Hence  $\beta_1 = T_1 = -\frac{1}{29}$  and in order to satisfy the requirement  $A\beta = 1$ , the gain  $G$  of the amplifier must be  $-29$ . Since the gain is a function of the signal amplitude, the amplitude of oscillations will be

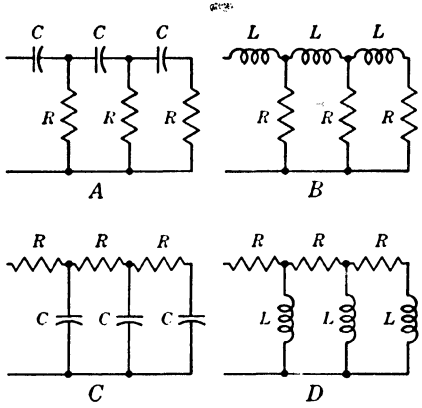


FIG. 4-13.—Phase-shifting networks suitable for phase-shift oscillators.

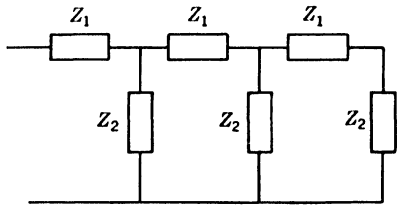


FIG. 4-14.—Generalized phase-shifting network for phase-shift oscillators.

stabilized at that value which makes the gain  $-29$ . The negative signs for  $A$  and  $\beta$  denote a  $180^\circ$  phase shift in both the amplifier and the filter.

TABLE 4-1.—VALUES OF CONSTANTS FOR FOUR TYPES OF PHASE-SHIFTING NETWORKS SHOWN IN FIG. 4-13

	A	B	C	D
$Z_1$	$\frac{1}{j\omega C}$	$j\omega L$	$R$	$R$
$Z_2$	$R$	$R$	$\frac{1}{j\omega C}$	$j\omega L$
$k$	$\frac{1}{j\omega RC}$	$\frac{j\omega L}{R}$	$j\omega RC$	$\frac{R}{j\omega L}$
$\omega_1$	$\frac{1}{RC \sqrt{6}}$	$\frac{R \sqrt{6}}{L}$	$\frac{\sqrt{6}}{RC}$	$\frac{R}{L \sqrt{6}}$
$k_n$	$\frac{k_1}{n}$	$nk_1$	$nk_1$	$\frac{k_1}{n}$
$ H_2 $	0.368	1.18	1.18	0.368
$ K_2 $	1.25	0.23	0.23	1.25

The curvature of the amplifier characteristics which gives rise to this amplitude stability also introduces harmonics into the output. However, harmonic distortion so introduced is multiplied by a factor  $H$  where

$$H = \frac{1}{1 - A\beta}, \quad (13)$$

because these distortion voltages are also fed back to the amplifier input.

Let  $H_n$ ,  $k_n$ , and  $\beta_n$  respectively be the value of  $H$ ,  $k$ , and  $\beta$  for the  $n$ th harmonic of the oscillation frequency. For oscillators employing networks  $A$  or  $D$  of Fig. 4-13, the value of  $k_n$  is equal to  $k_1/n$ ; whereas for oscillators employing networks  $B$  or  $C$  in Fig. 4-13,  $k_n$  is equal to  $nk_1$ . For  $A$  and  $D$ ,

$$\beta_n = \frac{1}{1 + \frac{6k_1}{n} + \frac{5k_1^2}{n^2} + \frac{k_1^3}{n^3}}$$

or

$$\beta_n = \frac{1}{1 - j \frac{6\sqrt{6}}{n} - \frac{30}{n^2} + j \frac{6\sqrt{6}}{n^3}};$$

hence,

$$1 - A\beta_n = 1 + \frac{29}{1 - \frac{30}{n^2} - j \frac{6\sqrt{6}}{n} \left( \frac{1}{n} - \frac{1}{n^3} \right)},$$

or

$$H_n = \frac{1}{1 - A\beta_n} = \frac{\frac{n^2 - 30}{n^2 - 1} - j \frac{6\sqrt{6}}{n}}{30 - j \frac{6\sqrt{6}}{n}}. \quad (14)$$

For  $B$  and  $C$  it is only necessary to replace  $n$  by  $1/n$  and  $j$  by  $-j$ , giving

$$H_n = \frac{\frac{1 - 30n^2}{1 - n^2} + j \frac{6\sqrt{6}}{n}}{30 + j \frac{6\sqrt{6}}{n}}. \quad (15)$$

The absolute value of  $H_n$  is of principal interest and the value of  $|H_2|$ , that is, the reduction in second harmonic, is included in Table 4-1. Note that for  $B$  and  $C$  this quantity is greater than 1, indicating that the distortion is enhanced rather than reduced by the feedback. For networks  $B$  and  $C$ , the limiting value of  $|H_n|$ , as the order of the harmonic  $n$  approaches infinity, is 1. For  $A$  and  $D$ , however, the factor  $|H_n|$  decreases with increasing  $n$ , having  $\frac{1}{30}$  as a limiting value.

The above remarks apply if the output is taken from the plate. If the output is taken from the grid,  $n^{\text{th}}$  harmonic distortion introduced



by the tube is multiplied by a factor  $K_n$ , where

$$\begin{aligned} K_n &= \frac{\beta_n}{\beta_1} H_n \\ &= \frac{\beta_n}{\beta_1(1 - A\beta_n)} \\ &= \frac{1}{\frac{\beta_1}{\beta_n} - A\beta_1} \\ K_n &= \frac{1}{\frac{\beta_1}{\beta_n} - 1} \end{aligned}$$

For  $A$  and  $D$

$$K_n = \frac{-29}{\left(1 - \frac{1}{n^2}\right) \left(30 - j \frac{6\sqrt{6}}{n}\right)}$$

and for  $B$  and  $C$

$$K_n = \frac{-29}{(1 - n^2)(30 - jn6\sqrt{6})}$$

Values of  $|K_n|$  are also given in Table 4-1. It is apparent that for  $A$  and  $D$  the purest waveform is obtained at the plate, for  $B$  and  $C$  at the grid.

Phase-shift oscillators are particularly adapted for fixed audio frequencies. Variable-frequency operation is possible but is not as easily achieved as in some other types. It is necessary to vary three elements simultaneously in order to keep the value of  $\beta$  at the oscillation frequency equal to  $-\frac{1}{29}$ .

The input impedance  $Z_i$  of the phase-shifting network is

$$Z_i = Z_2 \left( \frac{1 + 6k + 5k^2 + k^3}{3 + 4k + k^2} \right). \quad (16)$$

At the frequency of oscillation Eq. (16) becomes

$$Z_i = \frac{-29Z_2}{-3 \pm 4j\sqrt{6}}. \quad (17)$$

If variable-frequency operation of the oscillator is desired, it is important that the impedance presented to the plate circuit of the amplifier be constant to prevent change of amplitude with frequency. Equation (17) shows that the impedance of the network at the oscillation frequency is proportional to  $Z_2$ , and since at this frequency  $Z_1 = kZ_2$  and one of these elements is a resistance, the impedance is in every case proportional to  $R$ . Hence, tuning should be done by a simultaneous variation of the three reactive elements. Because variable inductances

are inconvenient, networks *A* and *C* are more easily adapted to variable-frequency than networks *B* and *D*. Network *C* has an advantage in that the three capacitances have a common terminal that is at ground potential, making it possible to use an ordinary 3-gang variable condenser. However, the waveform produced is not as pure as that given by *A*, in which the capacitances do not have a common terminal. It is possible to vary the frequency by tuning only one of the reactance elements, but the frequency range is limited and an automatic gain control is necessary to keep the amplitude constant.

A phase-shifting network having much less attenuation than those illustrated in Fig. 4-13 can be built by making the impedance of the second section high compared with the first, and the third high compared with the second.<sup>1</sup> In the limiting design of such a network, the phase shift per section is exactly  $60^\circ$  and the attenuation per section  $\frac{1}{3}$ , giving a total attenuation of  $\frac{1}{27}$ , and hence requiring an amplifier with a gain of 27.

The reduction in harmonic distortion is also slightly greater than given in Table 4-1. The network is not, however, suited to variable-frequency operation because of the difficulty of varying three unequal elements and keeping their ratios constant. Figure 4-15 shows a network that resembles this type, designed for fixed-frequency operation. This circuit employs a network of type *A* and hence has a good output waveform. Bias is obtained from the cathode resistor, which is bypassed with a large condenser to prevent a-c degeneration.

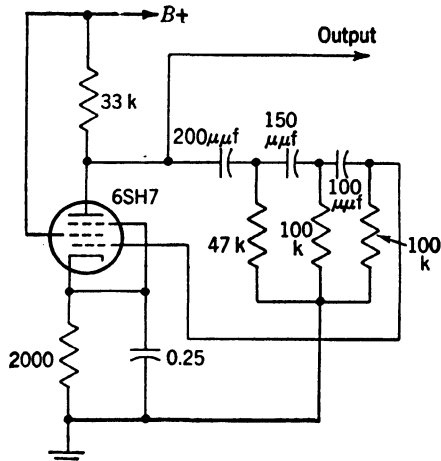


FIG. 4-15.—5090-cycle phase-shift oscillator (AN/ART-18).

employs a network of type *A* and hence has a good output waveform. Bias is obtained from the cathode resistor, which is bypassed with a large condenser to prevent a-c degeneration.

It is also possible to reduce the attenuation by using four sections in the phase-shifting network instead of three; however, this method also complicates the problem of achieving variable-frequency operation.

**4-5. Bridge Oscillators.**—A high degree of frequency stability and excellent waveform can be achieved in an oscillator combining positive and negative feedback. The two feedback paths can conveniently be realized by the use of a bridge circuit as shown in the generalized bridge oscillator in Fig. 4-16. A bridge oscillator is an amplifier having a differential input with the output fed back to the input through a bridge circuit or equivalent. The function of the bridge circuit is to allow

<sup>1</sup> R. W. Johnson, *Proc. I.R.E.*, **33**, 597 (September 1945).

regeneration at only one frequency, all other frequencies being degenerated. The so-called null networks have amplitude and phase

responses which make them ideally suited to application in the bridge circuit of oscillators of this type.

The most common null networks<sup>1</sup> are the twin-T, the bridged-T, and the Wien bridge illustrated in Fig. 4-17. By proper choice of the parameters  $k$  and  $b$ , the transfer function  $T'$  for these null networks can be represented by

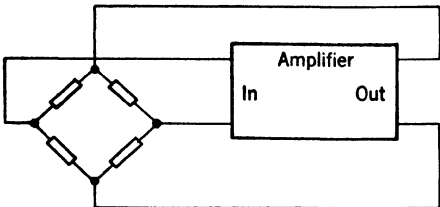


FIG. 4-16.—Generalized bridge oscillator.

the transfer function  $T'$  for these null networks can be represented by

Network	Circuit	Condition for null	k	b
Twin T		$\omega_0 = \frac{n^{1/2}}{RC}$	1	$= 2(n^{1/2} + \frac{1}{n^{1/2}})$ $= 4$ for $n = 1$
Bridged T		$\omega_0^2 LC = 1$ $R = \frac{Q\omega_0 L}{4}$	1	$\frac{2}{Q}$
Wien bridge		$\omega_0 = \frac{1}{RC}$ $\frac{R_2}{R_1 + R_2} = \frac{1}{3}$	$\frac{1}{3}$	3

FIG. 4-17.—Characteristics of null networks.

<sup>1</sup> The transfer functions for various null networks are derived in Vol. 18, Chap. 10.

$$T = \frac{E_0}{E_i} = \frac{k}{1 - j \frac{b}{\left(\frac{\omega}{\omega_0} - \frac{\omega_0}{\omega}\right)}}, \quad (18)$$

where  $\omega$  is the angular frequency and  $\omega_0$  is the null angular frequency, and the values for  $k$  and  $b$  are given in Fig. 4-17. Figure 4-18 shows how the phase and amplitude of the transfer function vary with frequency.

The amplitude and phase angle of the transfer functions for the twin-T and Wien bridge and for a bridged-T in which the inductance has a  $Q$  of 10 are plotted on a logarithmic frequency scale in Fig. 4-19.

Since the twin-T and the bridged-T are three-terminal networks, they can be used in the same way to form a bridge oscillator. The remainder of the bridge consists of a resistance voltage divider as shown in Fig. 4-20. The output  $E_0$  is  $A$  times the difference between the input voltages,  $E_1 - E_2$ , and is assumed to be real. If the resistance voltage divider  $R_1 R_2$  is so arranged that  $E_1 = E_0/A$ , then for the null frequency of the bridged-T network  $E_2$  is zero, the feedback factor  $\beta$  is just  $1/A$ , and the condition  $A\beta = 1$  is satisfied, and oscillations can occur. At all other frequencies, the voltage  $E_2$  is not zero and the feedback factor  $\beta$  is  $1/A - T$ .

The amplifier output  $E_0$  is  $A$  times the difference between the input voltages and is assumed to be real and not a function of frequency. If

$$\frac{R_2}{R_1 + R_2} = \frac{1}{A}, \quad (19)$$

the feedback factor  $\beta$  is given by

$$\beta = \frac{1}{A} - T \quad (20)$$

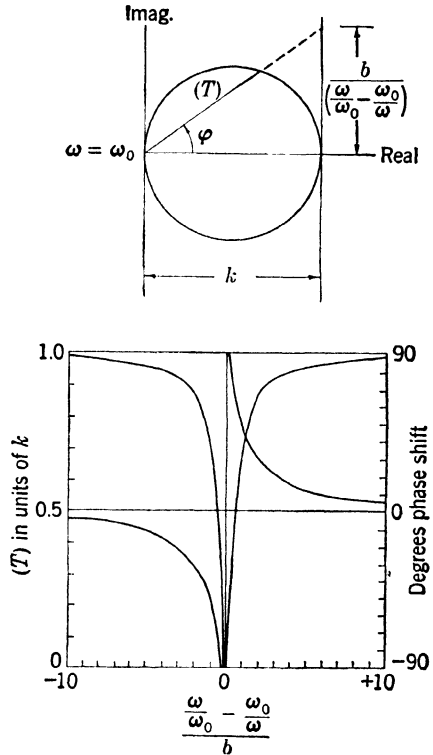


FIG. 4-18.—Generalized transfer function for null networks.

and at the null frequency  $T$  is zero and the condition for oscillation is satisfied. Regeneration occurs at all frequencies through the resistors

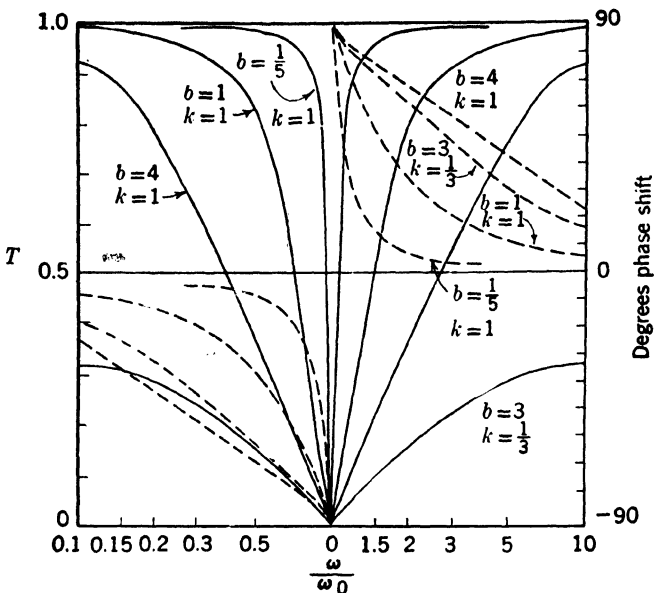


FIG. 4·19. —Transfer functions for null networks.

$R_1R_2$  but it is counteracted by the null network at all frequencies except the null frequency.

Because the Wien bridge is a four-terminal network, it cannot be

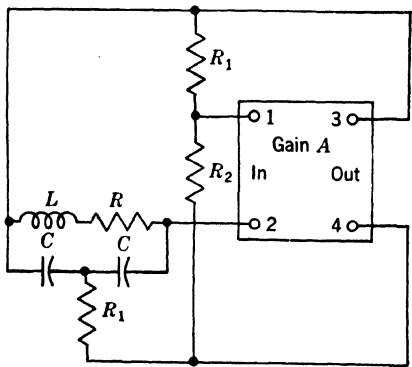


FIG. 4·20.—Bridged-T oscillator.

used in the same fashion as the twin-T and bridged-T networks. However, a feedback factor  $\beta$  of the form of Eq. (20) can be obtained in a simple way. Since this circuit is already a bridge circuit no additional feedback path is needed: the amplifier inputs are connected to points  $c$  and  $d$  of Fig. 4·17c. The transfer function of a balanced Wien bridge can be written as

$$T = \frac{R_2}{R_1 + R_2} - F = \frac{1}{3} - F, \quad (21)$$

where  $F$  is the transfer function of the three-terminal reactive half of the bridge. The transfer function  $F$  is given by

$$F = \frac{1}{3 + j\left(\frac{\omega}{\omega_0} - \frac{\omega_0}{\omega}\right)}, \quad (22)$$

which has a maximum amplitude of  $\frac{1}{3}$  at  $\omega = \omega_0$ .

If the bridge is unbalanced by changing  $R_1$  and  $R_2$  to  $R'_1$  and  $R'_2$ , and the points  $c$  and  $d$  are connected to the amplifier input in the proper phase, the feedback factor can be written

$$\beta = F - \frac{R'_2}{R'_1 + R'_2}. \quad (23)$$

Substituting the value of  $F$  from Eq. (21),

$$\beta = \frac{1}{3} - \frac{R'_2}{R'_1 + R'_2} - T.$$

If  $R'_1$  and  $R'_2$  are made to satisfy the equation

$$\frac{R'_2}{R'_1 + R'_2} = \frac{1}{3} - \frac{1}{A},$$

then

$$\beta = \frac{1}{A} - T \quad (24)$$

which is identical to Eq. (20).

It should be noted here that for the Wien bridge oscillator positive feedback is applied through the network containing reactive elements and negative feedback through pure resistances; whereas with the twin-T and bridged-T the network containing reactive elements is in the negative feedback loop and the resistances in the positive feedback loop. The form of the net feedback is the same, however, for all cases.

Because the net feedback is negative at harmonics of the oscillation, frequency distortion produced in the amplifier will be reduced. Specifically, the harmonic distortion is multiplied by a factor

$$H = \frac{1}{|1 - A\beta|}.$$

From Eqs. (20) or (24)

$$H = \frac{1}{A|T|}. \quad (25)$$

High gain is therefore desirable, provided the gain is not accompanied by excessive distortion. For fixed amplifier gain the best waveform is obtained when  $|T|$  is large at the harmonic frequencies. The rate at which  $|T|$  increases as the frequency deviates from the null frequency is determined by the factors  $b$  and  $k$  in Eq. (18).

The relative merits of the three oscillators from the standpoint of good waveform can be seen from Fig. 4-19. The value of  $|T|$  for the Wien bridge at  $\omega = 2\omega_0$  is about 0.15. For the twin-T, the maximum value of  $b$ , obtained for  $n = 1$ , makes the value of  $|T|$  at  $\omega = 2\omega_0$  about 0.34. For a bridged-T in which the inductance has a  $Q$  of 10,  $|T|$  is nearly equal to its maximum value of unity at  $\omega = 2\omega_0$ . Therefore the bridged-T oscillator is inherently capable of producing the most nearly pure sinewave.

For optimum frequency stability the phase angle of  $\beta$  should change as rapidly as possible with frequency. The bridged-T is superior in this respect also and the phase changes most rapidly with frequency when the  $Q$  is high. However, it must be remembered that inductors, particularly at audio frequencies, are less stable than resistors or condensers. They are susceptible to pick-up from power lines or stray fields. These facts may more than offset the advantage of the steep phase-frequency characteristic.

Of the three oscillators discussed, the Wien bridge oscillator is best adapted to variable-frequency operation. Simultaneous variation of the two capacitances  $C$ , or the two resistors  $R$ , will provide a convenient frequency control and does not require any alteration in the values of  $R_2$  and  $R_1$ . A 2-gang variable condenser with a ratio of 10 between maximum and minimum capacitance will produce a 10 to 1 change in frequency. By combining such a condenser with a switch to change the values of  $R$  in steps, a total range of 10,000 to 1 in frequency has been achieved in a production instrument.

The twin-T oscillator is not as well suited to variable frequency operation. An examination of the conditions for a null in Fig. 4-17 shows the nature of the difficulty. For the twin-T, the oscillation frequency  $\omega_0$  can be changed by a variation in  $R$ ,  $C$ , or  $n$ . If  $R$  is varied, a 3-gang variable resistance can be used as a control. If such a resistance is used, and if  $n$  has its optimum value of unity, one of the variable resistors must be equal to half the value of the other two. If  $n$  is made equal to  $\frac{1}{2}$ , all three resistors will be equal. If  $n$  is made equal to 2, the three capacitances will be equal and a 3-gang variable condenser can be used as a control. The frequency can be changed by a variation of only two elements, namely the shunt resistance and shunt capacitance, but this involves a peculiar relation between the values of the two elements and the frequency. Moreover the value of  $n$  (and  $b$ ) changes with frequency and therefore the shape of the transfer function depends on the oscillation frequency.

Tuning of the bridged-T oscillator requires a simultaneous variation of at least two elements, one of which is a resistance and the other an inductance or capacity. Such a variation, maintaining the required relation between these elements, is very difficult in practice.





voltage from  $V_4$  is fed back to the grid of  $V_1$  to form the positive loop. The amplitude of the oscillation is measured by  $V_3$  and controls the gain of  $V_4$  to correct the amount of positive feedback. By thus varying the amount of positive feedback the amplitude of oscillation is stabilized.

The circuit shown in Fig. 4-23 is designed for variable frequency operation with stable output. The elements  $R_1$  and  $C_1$  form the reactive network in the positive feedback loop and  $R_2$  and  $R_3$ , being connected to the cathode of  $V_1$ , provide the negative feedback. The thermally nonlinear resistance  $R_3$  operates to maintain constant amplitude independent of frequency.

*Crystal-bridge Oscillator.*—It was pointed out in the discussion of the bridged-T oscillator that the purity of the output is closely related to

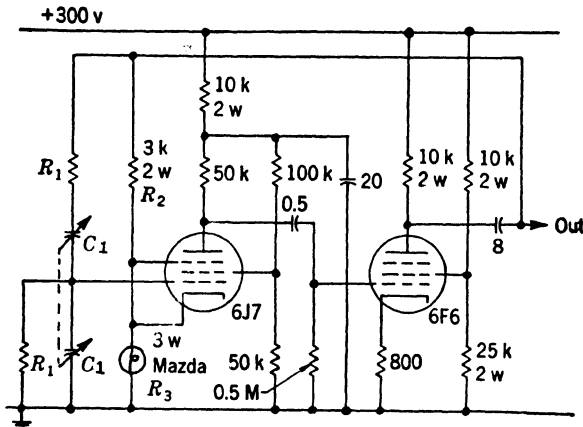


FIG. 4-23.—Wien-bridge oscillator.

the  $Q$  of the circuit. If a high- $Q$  crystal is used as the reactive “network,” the stability is very good. With reasonable care the frequency stability can be held to one part in  $10^8$  or  $10^9$ , being limited only by the frequency stability of the crystal. Figure 4-24 shows an oscillator<sup>1</sup> that employs a crystal as the reactive arm of a bridge. The crystal is operated at its series resonance to minimize the effect of stray shunt capacity and, together with the fixed resistor  $R_3$ , it forms the negative-feedback arm of the bridge. Resistors  $R_2$  and  $R_1$  form the positive-feedback arm of the bridge and  $R_1$  is a tungsten-filament lamp, which exhibits thermal nonlinearity. The bridge is operated slightly unbalanced—otherwise there would be no signal or the grid of  $V_1$ —but the unbalance becomes very large and degenerative if the feedback frequency is not exactly at the crystal resonance. Resistor  $R_1$  increases in resistance with dissipation.

<sup>1</sup> See L. A. Meacham, “The Bridge-stabilized Oscillator,” *Proc. I.R.E.*, **26**, 1278 (October 1938).

pated power and thus operates to maintain a constant output. Over large ranges of plate and heater voltages, the frequency stability is limited only by the crystal. If the crystal is operated in a thermostatically controlled oven, a stability as good as 1 part in  $10^9$  can be achieved.

*Summary.*—Of the various bridge-oscillator circuits discussed in this section, the crystal-bridge oscillator has by far the greatest amplitude stability and frequency stability. Following the crystal-bridge oscillator are the bridged-T, the twin-T, and the Wien bridge in that order. Frequency and amplitude stabilization depend on the constancy of the components and on the use of a stabilizing nonlinear element. As far as

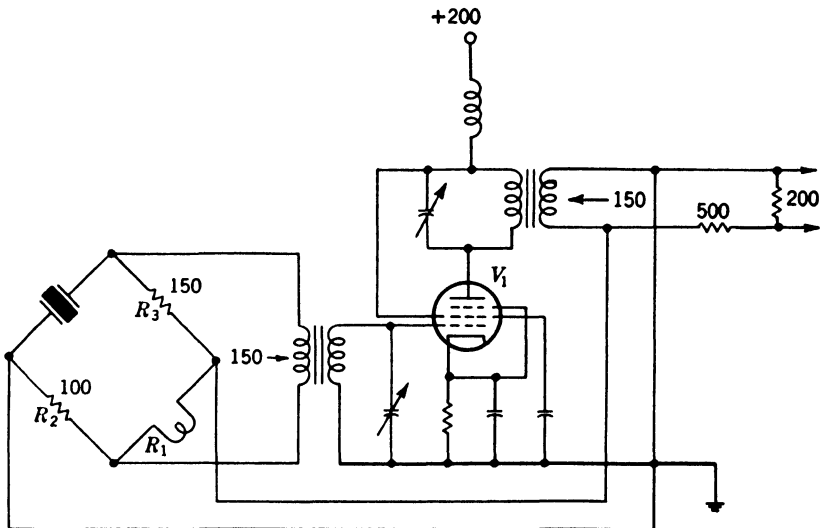


FIG. 4-24.—Crystal-bridge oscillator.

waveform is concerned, there is little difference between the crystal-bridge and the bridged-T oscillator with a  $Q$  as great as 10. Since the maximum value of  $T$  is 1, maximum harmonic rejection is obtained if the  $Q$  is as large as 10.

**4-6. Negative-resistance Oscillators.**—In the introduction to this chapter it was shown that a parallel-resonant circuit shunted by a suitable negative resistance is capable of sustained oscillations. Devices that exhibit negative resistance can be constructed in several ways. One of the simplest and best known methods makes use of the secondary emission from the plate of a vacuum tube. An oscillator employing this type of negative resistance is called a “dynatron oscillator.” Most modern tubes are treated to reduce secondary emission but some older tubes exhibit this phenomenon very markedly. Since secondary emis-

sion characteristics change with age and use, the dynatron is unsuited to use as a precision oscillator.

A more satisfactory method of obtaining a negative resistance is based upon the fact that in a pentode in which the suppressor grid is at negative potential, an increase in suppressor voltage causes a decrease in screen current, even though the screen voltage increases by the same amount as the suppressor. If the screen is capacitively coupled to the suppressor, an increase in screen voltage is accompanied by a decrease in screen current; the tube then has a negative resistance between screen and cathode. A tuned circuit between screen and cathode may be capable of sustained oscillations. An oscillator of this type, called a

transitron, is illustrated in Fig. 4·25. The negative resistance obtained in this way is much more stable than the dynatron negative resistance since it does not depend upon the surface characteristics of the tube elements.

The transitron oscillator shown in Fig. 4·25 has component values for satisfactory oscillation at about 1 Mc/sec. The exact frequency is determined by  $L_1C_1$  in the usual way and the principal component that has to be changed for different frequency operation is  $C_1$ . The advantages of the circuit as an oscillator are that  $L_1C_1$  is a two-terminal network and the plate circuit is electron coupled to the oscillatory circuit. These advantages

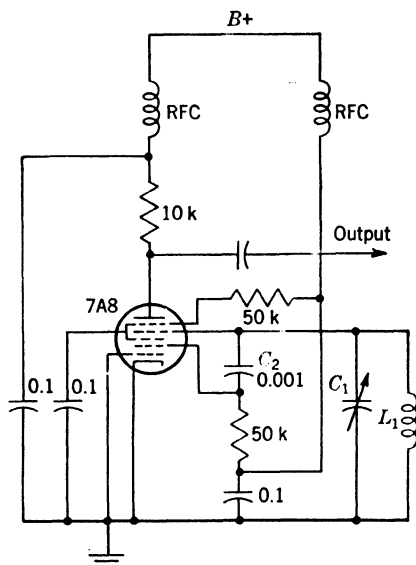


FIG. 4·25.—Transitron oscillator.

make the circuit very stable—the frequency stability being limited primarily by the temperature coefficients of  $L_1$  and  $C_1$ , and the amplitude stability being limited by regulation of the supply voltage. The control grid can be used in an AGC circuit to stabilize the amplitude.

A negative resistance can be obtained by the use of positive feedback from the output to the input of a noninverting amplifier. Oscillators using this type of negative resistance, however, are usually treated as feedback oscillators.

**4·7. Beat-frequency Oscillators.**—If two sinusoidal currents differing slightly in frequency are added together and passed through a nonlinear element, the output will contain not only the original frequencies, but also frequencies equal to the sum and difference of the original frequencies.

A low-pass filter can then be used to eliminate all but the difference frequency. Devices of this sort are called "beat-frequency oscillators." Strictly speaking, they are not oscillators but generate the desired sinusoidal waveform by means of a heterodyne action. They have the advantage that a small percentage change in the frequency of one oscillator causes a large percentage change in the difference frequency, with the result that a large range of output frequencies can be covered with a single tuning control. This same property may be considered a disadvantage from the standpoint of frequency stability and can be very troublesome at low beat frequencies.

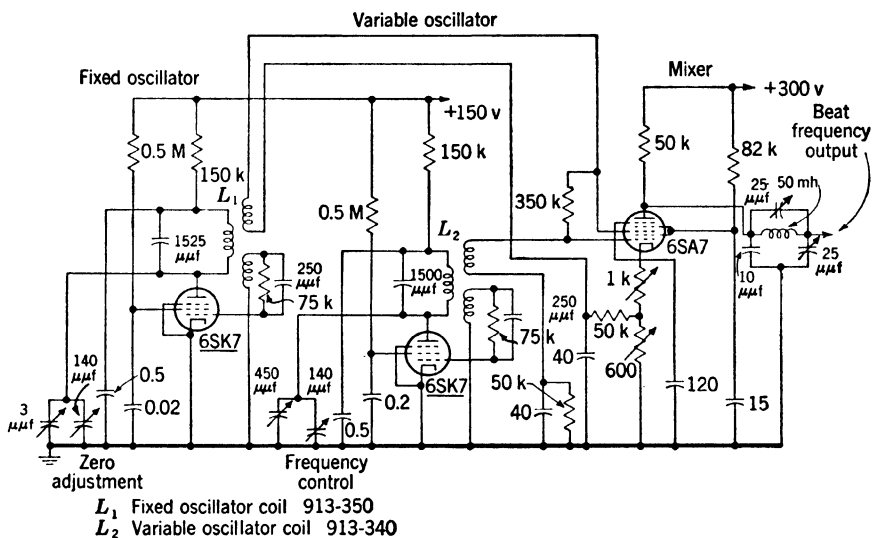


FIG. 4-26.—Beat-frequency oscillator. (General Radio.)

A diagram of a beat-frequency oscillator is shown in Fig. 4-26. Outputs from the two high-frequency oscillators are taken from tertiary windings on the transformers and are applied to the multigrid-tube modulator. The filter on the output selects only the beat frequency.

In designing a beat-frequency oscillator the following precautions should be taken: (1) The two high-frequency oscillators should be made as nearly alike as possible so that frequency variations due to temperature or voltage changes will be about the same for both. (2) They should be well shielded and decoupled from each other to minimize any tendency to synchronize. (3) In order to have the beat frequency free of harmonics, the high-frequency oscillators should have no distortion.

**4-8. Electromechanical Sine-wave Generators.**—Frequently it is desirable to produce sinusoidal waveforms with frequencies as low as a fraction of a cycle per second. Such waveforms are useful, for example,

in the testing of the response of servomechanisms. Ordinary oscillator circuits can not be used conveniently for frequencies as low as this, and it is generally necessary to resort to some sort of electromechanical device.

The electromechanical devices that lend themselves to this application are potentiometers, variable condensers, synchros, and cam-interrupted light beams. These methods are discussed in Chap. 12, in Vol. 17 and Vol. 22. Potentiometers, variable condensers, and cam-interrupted light beams are admirably suited to the generation of waveforms of arbitrary shape, whereas synchros are carefully designed to make the output-vs.-shaft rotation a true sinusoid.

Since this chapter deals exclusively with sinusoidal waveforms, only the synchro is discussed, since synchros are engineered to give exact sinusoidal output with mechanical rotation.

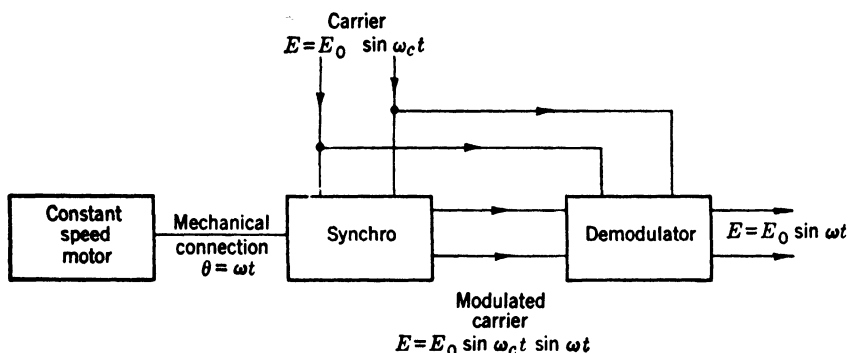


FIG. 4-27.—Electromechanical oscillator.

Figure 4-27 is a schema of a mechanical assembly using a synchro to generate a low-frequency sinusoidal waveform. The synchro rotor is mechanically connected to a constant-speed motor (or a variable-speed motor if variable frequency is desired) through sufficient gear reducers to cause the synchro rotor to turn at the same angular rate as the desired sinusoidal output. Most synchros are designed either for 60-cps or for 400-cps carrier operation. Assuming a 10 to 1 ratio between carrier and modulation frequencies (for good carrier rejection), the maximum frequency output is 6 or 40 cps. The principal use of such systems, however, is the generation of sinusoidal waveforms at lower frequencies. There is no lower limit since the circuits are carrier operated and give output for zero mechanical rate.

## STABILIZATION OF OSCILLATORS

**4-9. Amplitude Stabilization.**—The qualities most often required of an oscillator are the following: (1) the waveform must be pure, that is, free of harmonics, (2) the amplitude must be constant, and (3) the frequency

must be constant. It is the purpose of this section to consider how these requirements can be met.

In many respects purity of waveform and amplitude stability are mutually exclusive, at least in a simple circuit. Waveform purity depends on the linearity of the characteristics of the oscillator tube, whereas amplitude stability depends on the nonlinearity of characteristics with signal amplitude to maintain  $A\beta = 1$  during component aging and supply-voltage variations. Methods of stabilization include grid-leak biasing, grid limiting, variation of grid bias produced by rectified output, and control of feedback factor either by a thermosensitive element or by a variable-gain feedback amplifier controlled by the rectified output. For applications that require good amplitude stabilization and purity of waveform, the latter is by far the best approach. This principle of amplitude stabilization by thermosensitive elements without waveform distortion is employed in the bridge oscillators shown in Figs. 4-22, 4-23, and 4-24. In all three circuits the amplitude is controlled by automatically varying the amount of feedback. Waveform distortion is kept to a minimum by operating all tubes in class A and by degenerating harmonics in the feedback loop. Vol. 21, Sec. 14-5 contains other examples of stabilized oscillators employing nonlinear resistance elements.

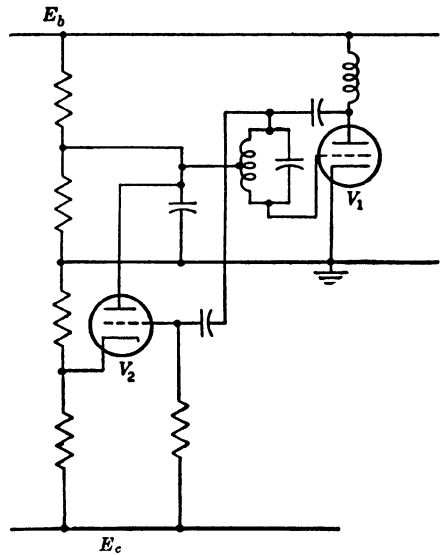


FIG. 4-28.—Delayed AGC for amplitude stabilization.

Variable regeneration is not practical for  $LC$ -oscillators such as are discussed in Sec. 4-2. Regeneration in these oscillators is usually the result of mutual inductance or capacitance—that is, quantities that are not easily varied. Consequently, for such circuits, the output is stabilized either by grid current in the oscillator or by a separate AGC circuit. Since grid current, no matter how small, introduces some distortion into the output waveform, AGC circuits are required when purity of waveform as well as amplitude stability is a specification.

Terman<sup>1</sup> describes a simple arrangement for stabilizing amplitude without distorting the waveform. A biased diode is connected to the

<sup>1</sup> F. E. Terman, *Radio Engineers' Handbook*, McGraw-Hill, New York, 1943, Sec. 6.

oscillator tank circuit to absorb energy when the amplitude of oscillation is greater than the bias. Such a system can be made to introduce less than 0.01 per cent distortion.

Figure 4-28 is a schema of a Hartley oscillator with delayed AGC. The cathode of  $V_2$  is biased positive by an amount equal to the desired amplitude of the a-c oscillator output. If the output of  $V_1$  is greater than the positive bias of the cathode of  $V_2$ , the amplified difference between the a-c amplitude and the bias voltage is plate-detected in  $V_2$  and used to reduce the gain of  $V_1$ . The positive supply voltage that is first applied to the grid of  $V_1$  assures that oscillations start and build up rapidly.

The grid of  $V_2$  presents very little loading to the plate of  $V_1$  since it need not draw grid current, but probably introduces some harmonic distortion. If  $V_1$  were an electron-coupled oscillator, the plate loading would have much less effect on the frequency and the harmonic distortion would be very small. The accuracy of this method of amplitude stabilization is limited by the drift of the reference voltage at the cathode of  $V_2$  and by the drift in grid-cathode cutoff characteristic of  $V_2$ .

**4-10. Frequency Stabilization.**—The frequency of an oscillator is determined by the fact that the condition for oscillation given in Eq. (1) is ordinarily satisfied at only one frequency. Anything that varies the phase angle of either  $A$  or  $\beta$  changes the frequency of oscillation.

Frequency stability is greatest if somewhere in the circuit there is an element or network of elements whose phase angle changes very rapidly with frequency. A very slight change in frequency will then cause a sufficient change in the phase angle to compensate any spurious shift. An example of such an element is a resonant circuit. At the resonant frequency the phase angle is zero but a slight shift in frequency causes a large change in phase angle. Since the rate of change of phase angle with frequency increases with the  $Q$  of the resonant circuit, high- $Q$  circuits are desirable for good frequency stability. A quartz crystal is equivalent to a resonant circuit with an exceedingly high  $Q$  and is therefore almost invariably used when frequency stability is important. The  $Q$  of crystals is so high that in a crystal oscillator the frequency is almost independent of the values of the other circuit components.

The most obvious cause of frequency variation is a change in the values of the circuit components due to either temperature effects or mechanical deformation. The latter can be avoided by proper design and good construction practice.

The effects of temperature are of two kinds: those due to local heating either by vacuum-tube filaments or by power dissipated in circuit elements, and those due to changes in ambient temperature. The only remedies for the former are to choose overrated components and mount

them in well ventilated regions so that the temperature rise is reduced (see Chap. 17, Vol. 21) and to allow the circuit to warm up for a period sufficiently long to establish temperature equilibrium. Frequency variation due to changes in ambient temperature can be reduced by temperature compensation, provided the temperature change is slow enough for all the critical components to be equally affected. Temperature compensation is a process of choosing components with proper regard to their temperature coefficients so that the net effect of a temperature change is zero. The process is usually based upon the assumption that the value of a component varies linearly with temperature, that is, that an equation of the form

$$A = A_0[1 + k(T - T_0)] \quad (26)$$

can be written where  $A$  is the value at a temperature  $T$ ,  $A_0$  is the value at a temperature  $T_0$ , and  $k$  is the temperature coefficient. This assumption is valid if the temperature change is not too great. As an example of the process of temperature compensation, suppose that a resonant circuit oscillator is built and that experiment shows that the frequency  $\omega$  increases with temperature. In order to compensate for this change some circuit component, whose effect on frequency is known, is made to vary with temperature in such a way as to make the change in frequency zero. For a resonant circuit oscillator the frequency is given approximately by

$$\omega = \frac{1}{\sqrt{LC}}, \quad (27)$$

and for that reason  $C$  is a convenient element to use for the compensation. It is necessary first to determine quantitatively the effects of changing the temperature of all components except  $C$ . The most satisfactory way of finding these effects is to use for  $C$  a condenser whose temperature coefficient  $k_1$  is known. Then if the oscillator circuit is subjected to a known change in temperature  $\Delta T$ , and a frequency change  $\Delta\omega$  is observed, the proper temperature coefficient  $k_2$  of  $C$  is:

$$k_2 = k_1 + \frac{2}{\omega} \frac{\Delta\omega}{\Delta T}. \quad (28)$$

A similar analysis for an oscillator with  $RC$  tuning where the frequency is specified by

$$\omega = \frac{1}{RC} \quad (29)$$

yields for the desired temperature coefficient of the condenser,

$$k_2 = k_1 + \frac{1}{\omega} \frac{\Delta\omega}{\Delta T}. \quad (30)$$



In some instances it is possible to choose resistors with compensating characteristics, and an analysis similar to the above can be made assuming the condenser is fixed and selecting the temperature coefficient of the resistor to provide temperature compensation. When either method is used, it is generally advisable to choose the fixed component with a low temperature coefficient.

Suppose there is available an assortment of condensers with coefficient  $k_a$  greater than  $k_2$  and an assortment with coefficients  $k_b$  less than  $k_2$ . The values of two condensers,  $C_a$  and  $C_b$ , that have these coefficients and will give a total capacitance  $C_0$  with coefficient  $k_2$  can then be determined from the following equations:

$$C_{a_0} = \frac{C_0(k_2 - k_b)}{k_a - k_b} \quad (31)$$

and

$$C_{b_0} = \frac{C_0(k_2 - k_a)}{k_b - k_a}. \quad (32)$$

If condensers are not available in the exact sizes specified by Eqs. (31) and (32) it is necessary to add a small trimming condenser to set the frequency to the required value. This trimmer will usually be so small a part of the total tuning capacity, however, that its variation with temperature will be unimportant.

The frequency of an oscillator will usually be found to change with variations in heater current and plate supply voltage. This change can often be traced to a change in the plate resistance of the tube. For example, Eq. (3) shows how the frequency of a tuned-plate oscillator depends on the plate resistance of the tube. In order to minimize the effects of these variations, the effective plate resistance may be increased by the addition in the plate circuit of any external resistance that is large compared with the actual plate resistance. Thus a change in the actual plate resistance becomes only a small change in the total or effective plate resistance and hence causes much less change in frequency. For maximum frequency stability, the stabilizing resistance should be 2 to 5 times the tube plate resistance, and a low- $\mu$  tube should be used for the oscillator if the resistor is in the plate circuit.

Figure 4-3 shows a modified Hartley oscillator with resistance stabilization. A 12,500-ohm resistor,  $R_1$ , is in the cathode circuit but performs the function of plate resistance stabilization. Being in the cathode circuit it is equivalent to  $12,500 \times (\mu + 1)$  ohms in the plate circuit. This constitutes a nearly constant plate resistance since  $\mu$  is constant and  $12,500 \times (\mu + 1)$  is large compared with  $r_p$ .

Llewellyn has shown that for resonant circuit oscillators it is possible to minimize the effect of changes in supply voltages by inserting suitable

reactances in the plate and grid leads.<sup>1</sup> These series reactances can conveniently be the grid and plate blocking condensers.

The interelectrode capacitances of the tube frequently affect the frequency of oscillation. Since these capacitances are not constant, the circuit should be so designed that they are small compared with other frequency-determining capacitances. In the case of a resonant circuit oscillator, such a design entails the use of a low  $L$  to  $C$  ratio in the tuned circuit. A low  $L$  to  $C$  ratio is also desirable since it increases the effective  $Q$  of the tuned circuit. Many authors<sup>2</sup> have treated the effects on frequency of variations in tube characteristics. For most oscillators employing high- $Q$  circuits it is possible to minimize the effects of tube variations and to make the frequency essentially independent of them.

The effect of a load on an oscillator is to introduce phase shifts because of the impedance coupled into the resonant circuit. The coupled impedance also serves to reduce the circuit  $Q$  and thus reduce frequency stability. To achieve maximum stability the load should not be coupled directly to the oscillator but should be isolated from it by a buffer amplifier. Electron-coupling allows the functions of oscillator and buffer to be combined in a single tube.

### POLYPHASE SINUSOIDS

Phase modulators (see Chap. 13) require two or more sinusoidal wave trains of the same frequency that have a definite phase relationship. For example, a phase-shifting condenser used to produce a continuously variable phase shift requires three sinusoidal voltages differing in phase by  $120^\circ$ ; also the production of a circular sweep on a cathode-ray tube requires two sinusoidal voltages whose phases differ by  $90^\circ$ . Usually there is also a requirement for the relative amplitudes of the voltages.

There are two approaches to the problem of producing polyphase sinusoidal waveforms. A polyphase oscillator<sup>3</sup> or generator can be devised; or the output of a single-phase oscillator or generator can be split into several channels, each of which shifts phase by an appropriate amount to achieve the desired output phase relations. Devices of the first kind are apt to be more complex and to involve considerable interdependence of the phase and amplitude controls. They have not been used to any great extent and will not be considered here.

<sup>1</sup> F. B. Llewellyn, "Constant Frequency Oscillators," *Proc. I.R.E.*, **19**, 2063 (December 1931).

<sup>2</sup> See, for instance, F. E. Terman, *Radio Engineers' Handbook*, McGraw-Hill, New York, 1943, Sec. 6, Fig. 5.

<sup>3</sup> Rene Mesny, "Generation of Polyphase Oscillations by Means of Electron Tubes," *Proc. I.R.E.*, **15**, p. 471 (August 1925); I. Takas, "Fundamental Considerations on Four-phase Oscillator Circuits," *Electro. Tech. J.*, **3**, p. 75 (April 1939).

Because of rather large tolerances on values of components, and because tube capacitances and stray wiring capacitances are not precisely predictable, it is necessary that any device for producing polyphase waveforms involve some adjustable components in order to achieve the exact phase and amplitude relations desired. An  $n$ -phase device will require  $n - 1$  adjustments for phase and  $n - 1$  adjustments for amplitude. For convenience these adjustments should be independent—that is, the setting of one phase should not affect the other phases or any of the amplitudes. Complete independence of the controls is never achieved, and it is necessary to make repeated settings until all phase and amplitude conditions are simultaneously satisfied.

#### 4-11. Generation of Circular Sweep for Cathode-ray Tube.—An

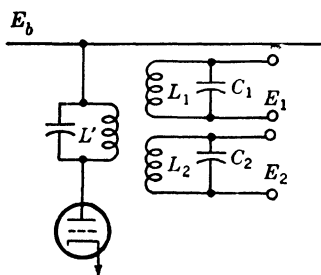


FIG. 4-29.—Circuit for making circular sweep.

exceedingly simple and accurate time base can be achieved by causing the electron beam in a cathode-ray tube to follow a circular path with constant angular velocity. This results in a circular trace on the face of the tube upon which timing pulses can be superimposed by means of a radial deflecting electrode, or by intensity modulation of the electron beam. The use of these circular sweeps is discussed in Vol. 20, Sec. 8-7 and in Vol. 22, Chap. 7 of this series.

The motion of a point on a circle with constant angular velocity can be resolved into two component sinusoidal motions of equal amplitude along two axes in the plane of the circle, the relative phases being equal to the angle between these axes. To achieve a circular motion of the electron beam in a cathode-ray tube requires two sinusoidal voltages differing in phase by the angle between the two pairs of deflecting plates, and having amplitudes inversely proportional to the deflection sensitivities of the plates. The following analysis will be simplified by assuming that the deflection sensitivities are equal and that the two pairs of plates are mutually perpendicular. The required voltages will then be of equal amplitude and  $90^\circ$  apart in phase. In practice the phase and amplitude controls are adjusted by observing the trace and making it circular, so this assumption does not restrict the validity of the discussion.

The method most commonly used for producing the required voltages is illustrated in Fig. 4-29. The tuned primary  $L'$  of the transformer is in the plate circuit of an oscillator or amplifier. Two secondaries  $L_1$  and  $L_2$ , tuned by condensers  $C_1$  and  $C_2$ , are loosely coupled to the primary and are connected to the two pairs of deflecting plates of the cathode-ray tube. If there is no coupling between  $L_1$  and  $L_2$  and the mutual inductances between the primary and the two secondaries are the same, the

voltages induced in  $L_1$  and  $L_2$  are the same.<sup>1</sup> Let this voltage be  $V$ . The equivalent circuit of Fig. 4-30 represents either secondary, the only difference in the two being the value of  $C$ . When it becomes necessary to distinguish between the two secondaries the subscripts 1 and 2 will be used, otherwise they will be omitted. The resistance  $r$  represents the a-c losses in the circuit and the ratio of the reactance of  $L$  to  $r$  will be represented by  $Q$ .

$L_1$  and  $L_2$  are tuned so that the vector impedances  $Z_1$  and  $Z_2$  have angles of approximately  $+45^\circ$  and  $-45^\circ$  as shown in Fig. 4-31. This

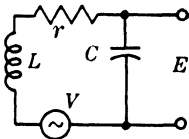


FIG. 4-30.—Equivalent circuit for either secondary of Fig. 4-29.

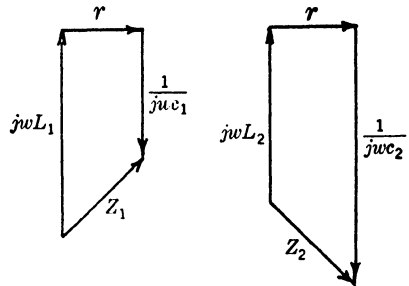


FIG. 4-31.—Vector-impedance diagrams for circuit of Fig. 4-30.

relation is not exact since, if the angles were exactly  $+45^\circ$  and  $-45^\circ$ , the magnitudes of the two impedances  $Z_1$  and  $Z_2$  would be equal and the magnitudes of the currents would be the same; however, since the capacitive reactances in the two circuits are not equal, the output voltages which are the products of the currents and the capacitive reactances would not be equal in magnitude. The required relation between the voltages  $E_1$  and  $E_2$  is

$$E_2 = jE_1. \quad (33)$$

$E$  is given by

$$E = \frac{V}{Z} \frac{1}{j\omega C}, \quad (34)$$

or

$$E = \frac{V}{\left[ r + j \left( \omega L - \frac{1}{\omega C} \right) \right] j\omega C}, \quad (35)$$

or

$$E = \frac{V}{1 - \omega^2 LC + j\omega r C}. \quad (36)$$

Substitution in Eq. (33) gives

$$1 - \omega^2 LC_1 + j\omega r C_1 = j - j\omega^2 LC_2 - \omega r C_2, \quad (37)$$

<sup>1</sup> The F. W. Sickles Co. has built most of the coil assemblies used in this application. The Sickles number for the 82-kc/sec coil is RE 10001; 163-kc/sec, 13386; 820-kc/sec, 12907.

and equating real and imaginary parts

$$\left. \begin{aligned} \omega^2 LC_1 - \omega r C_2 &= 1 \\ \omega r C_1 + \omega^2 LC_2 &= 1 \end{aligned} \right\} \quad (38)$$

Solving the simultaneous equations of Eq. (38) for  $C_1$  and  $C_2$ ,

$$C_1 = \frac{\omega L + r}{\omega(\omega^2 L^2 + r^2)} \quad (39)$$

and

$$C_2 = \frac{\omega L - r}{\omega(\omega^2 L^2 + r^2)} \quad (40)$$

Setting

$$\frac{\omega L}{r} = Q$$

Eqs. (39) and (40) may be rewritten

$$C_1 = \frac{1}{\omega^2 L} \frac{Q(Q+1)}{Q^2+1} \quad (41)$$

$$C_2 = \frac{1}{\omega^2 L} \frac{Q(Q-1)}{Q^2+1} \quad (42)$$

Both of these expressions can be expanded in powers of  $1/Q$ . Taking the first two terms of the expansions gives a very close approximation if  $Q$  is reasonably large, say 10 or more, so

$$C_1 \cong \frac{1}{\omega^2 L} \left(1 + \frac{1}{Q}\right) \quad (43)$$

and

$$C_2 \cong \frac{1}{\omega^2 L} \left(1 - \frac{1}{Q}\right) \quad (44)$$

Note that  $1/\omega^2 L$  is the value of capacitance necessary to tune either secondary to resonance. Equation (36) can be written<sup>1</sup>

$$E = \frac{V}{[(1 - \omega^2 LC)^2 + \omega^2 r^2 C^2]^{1/2}} e^{-j \tan^{-1} \frac{\omega r C}{1 - \omega^2 LC}} \quad (45)$$

<sup>1</sup> Substituting Eqs. (41) and (42) in Eq. (45) and letting  $\omega L/r = Q$  gives

$$E_1 = V \left(\frac{Q^2+1}{2}\right)^{1/2} e^{j \tan^{-1} \frac{Q+1}{Q-1}}, \quad (46)$$

$$E_2 = V \left(\frac{Q^2+1}{2}\right)^{1/2} e^{-j \tan^{-1} \frac{Q-1}{Q+1}}, \quad (47)$$

and shows that the analysis is correct since the requirement expressed in Eq. (33) is fulfilled.

It is of interest to see how the values of  $E_1$  and  $E_2$  are affected by small changes in  $C_1$  and  $C_2$ . Writing Eq. (45) in the form

$$E = |E|e^{i\theta}, \quad (48)$$

$$\frac{dE}{E} = \frac{d|E|}{|E|} + jd\theta. \quad (49)$$

But from Eq. (36)

$$\frac{dE}{E} = \frac{\omega^2 LC(1 - \omega^2 LC) - \omega^2 r^2 C^2 - j\omega r C}{(1 - \omega^2 LC)^2 + \omega^2 r^2 C^2} \frac{dC}{C}. \quad (50)$$

Equating real and imaginary parts of Eqs. (49) and (50)

$$\frac{d|E|}{|E|} = \frac{\omega^2 LC(1 - \omega^2 LC) - \omega^2 r^2 C^2}{(1 - \omega^2 LC)^2 + \omega^2 r^2 C^2} \frac{dC}{C} \quad (51)$$

and

$$d\theta = \frac{-\omega r C}{(1 - \omega^2 LC)^2 + \omega^2 r^2 C^2} \frac{dC}{C}. \quad (52)$$

Again substituting from Eqs. (41) and (42) and letting  $\omega L/R = Q$  these may be written

$$\frac{d|E_1|}{|E_1|} = -\frac{Q+1}{2} \frac{dC_1}{C_1}, \quad (53)$$

$$\frac{d|E_2|}{|E_2|} = \frac{Q-1}{2} \frac{dC_2}{C_2}, \quad (54)$$

$$d\theta_1 = -\frac{Q+1}{2} \frac{dC_1}{C_1}, \quad (55)$$

and

$$d\theta_2 = -\frac{Q-1}{2} \frac{dC_2}{C_2}. \quad (56)$$

If the percentage changes in  $C_1$  and  $C_2$  are the same (the usual behavior if the changes are caused by variations in ambient temperature), the changes in the phase angles are very nearly equal with the consequence that the relative phase of  $E_1$  and  $E_2$  is not appreciably affected. However, there is considerable change in the absolute phase resulting in a shift in the zero point of the time scale. The changes in amplitude are in opposite directions with the result that the pattern on the cathode-ray tube becomes elliptical. The effect of ellipticity on the accuracy of the time scale is discussed in Vol. 22, Chap. 7 of this series.

The variations in output voltage caused by changes in tuning capacitance are proportional to the  $Q$  of the secondary windings, as indicated in Eqs. (53), (54), (55), and (56). It would be advantageous from this standpoint to use low  $Q$  windings. However, the amplitude of the output voltage is also proportional to  $Q$  as shown by Eqs. (46) and (47) and the discrimination against harmonics is proportional to  $Q$ . For these

reasons a high  $Q$  circuit is desirable. Obviously a compromise must be made. It has been found in practice that with a  $Q$  of 35 a sufficient degree of temperature compensation can be achieved so that, under laboratory conditions, the pattern will remain circular for many hours. For any application in which a wide range of temperatures is encountered, it would probably be necessary to use a lower  $Q$ .

Although the phase and amplitude controls are in no sense independent, it is quite easy to make the adjustments by watching the trace on the tube and tuning the two secondaries alternately for minimum eccentricity of the ellipse.

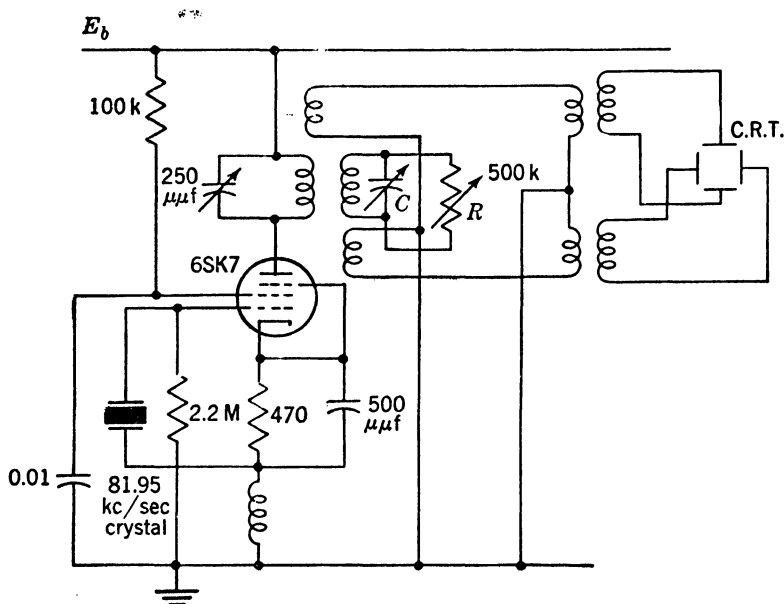


FIG. 4-32.—SCR-584 circular-sweep circuit.

Another method of generating a circular sweep makes use of the  $90^\circ$  difference in phase between the voltages in two loosely coupled resonant circuits. This method, illustrated in Fig. 4-32, was used in the SCR 584 radar. Link coupling between the resonant circuits and the deflecting plates is used in order to reduce the effects of stray capacitances. In use, the primary is tuned for maximum amplitude, after which the secondary amplitude and phase are adjusted by means of the condenser  $C$  and the loading resistor  $R$ . These adjustments are made by visual observations of the trace on the CRT.

**4-12. Resistance-reactance Phase Shifters.**—A series combination of a resistance and a reactance can be used to shift the phase of a sinusoidal waveform. If an alternating voltage is applied across the combination,

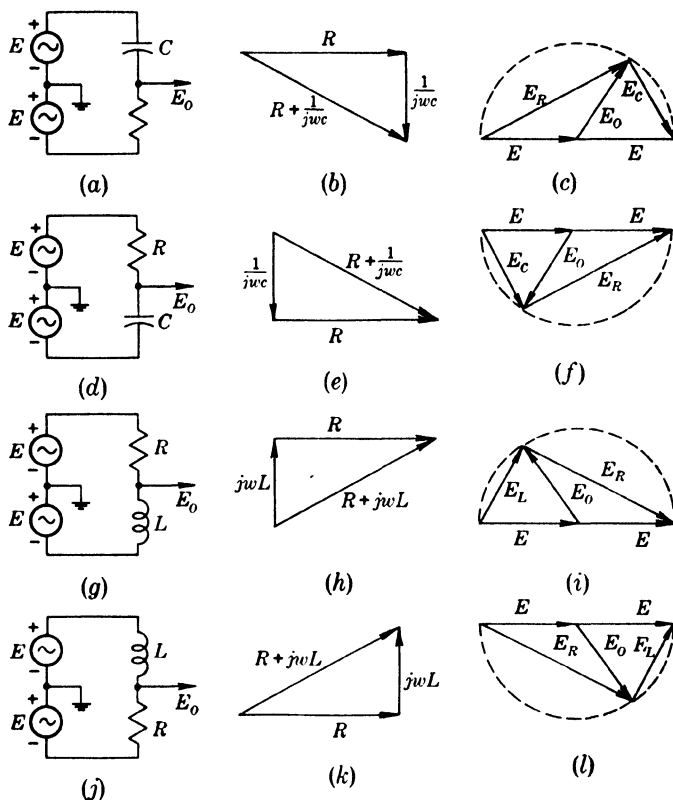


FIG. 4-33.—Resistance-reactance phase-shifting circuits.

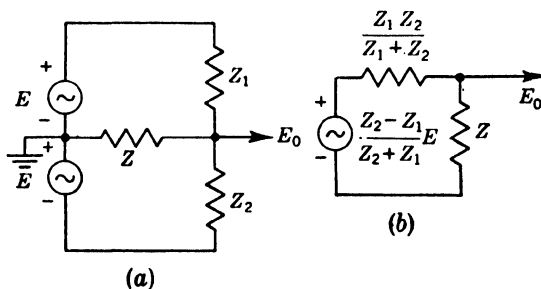


FIG. 4-34.—Equivalent circuit for determining effect of load impedance on resistance-reactance phase shifter.

the voltage across either element differs in phase from that across the other by  $90^\circ$  and differs in phase from the applied voltage by an amount that depends upon the ratio of the reactance to the resistance. In the arrangements illustrated in Fig. 4-33 the resistance-reactance combination is connected across a balanced or push-pull voltage source, which may be a



center-tapped transformer or a phase-inverting amplifier. The output voltage is then taken between ground and the junction of the resistance and reactance. Since the voltages across the two elements are  $90^\circ$  out of phase and since their sum must equal the applied voltage  $2E$ , the locus of a graph of the output voltage is a semicircle with  $2E$  as a diameter as shown in the vector diagrams in Fig. 4-33. The phases of the output voltage with respect to the voltage  $E$  for the four cases shown are:

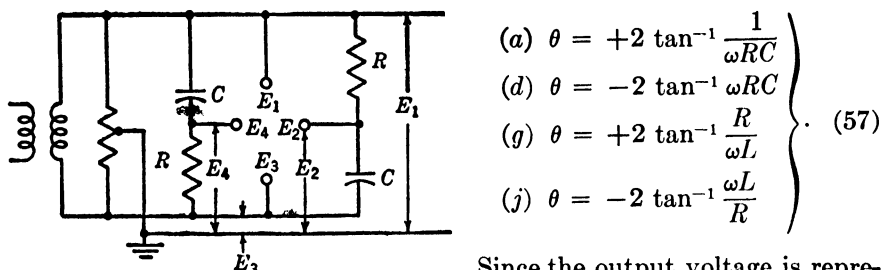


FIG. 4-35.—Four-phase voltage system.

Since the output voltage is represented as a radius of the semicircle, its magnitude is always equal to the magnitude of  $E$ .

The above relations are true only if no current is drawn from the output terminal. The effect of an impedance  $Z$  connected between the output terminal and ground can be found in the following way. Let the phase-shifting elements be generalized as  $Z_1$  and  $Z_2$ . Then in the circuit of Fig. 4-34a, the voltage  $E_0$  can be shown to be

$$E_0 = \frac{Z_2 - Z_1}{Z_2 + Z_1} E \frac{Z}{\frac{Z_1 Z_2}{Z_1 + Z_2} + Z} \quad (58)$$

and hence the circuit can be represented by the equivalent circuit of Fig. 4-34b, in which a generator having an open circuit voltage equal to  $\frac{Z_2 - Z_1}{Z_2 + Z_1} E$  and an internal impedance  $\frac{Z_1 Z_2}{Z_1 + Z_2}$  is connected across the load impedance  $Z$ . It can be easily shown that the equivalent generator voltage is equal to the voltage output expected with infinite load impedance, that is, the amplitude is equal to the amplitude of  $E$  and the phase given by the appropriate expression in Eq. (57). From this equivalent circuit the output to be expected for any  $Z$  can readily be calculated.

In Fig. 4-35 the circuits of Figs. 4-33a and 4-33d have been combined to provide a four-phase voltage system suitable for the operation of a phase-shifting condenser. For this application the voltages should be

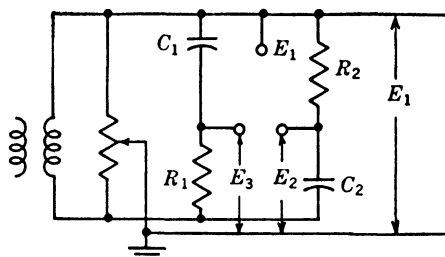


FIG. 4-36.—Three-phase voltage system.

$90^\circ$  apart in phase and, hence,  $R$  should be made equal to  $1/\omega C$ . A variable resistance across the transformer is used instead of a center tap on the transformer, since a more accurate voltage balance can be obtained in this way. It is sometimes necessary also to connect a capacitance from one end of the transformer secondary to ground to make the voltages at the two ends of the transformer  $180^\circ$  apart in phase. A similar arrangement shown in Fig. 4-36 can be used for a 3-terminal phase-shifting condenser. The phases in this case must differ by  $120^\circ$ , therefore the relations between the components must be,

$$\frac{1}{\omega C_1} = R_1 \tan 60^\circ = \sqrt{3} R_1 \quad (59)$$

$$\frac{1}{\omega C_2} = \frac{R_2}{\tan 60^\circ} = \frac{R_2}{\sqrt{3}} \quad (60)$$

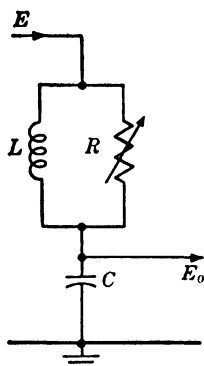


FIG. 4-37.—Phase-shifting circuit.

Another method of obtaining a phase-shift variable between  $0$  and  $180^\circ$  is shown in Fig. 4-37. Since the input and output have a common terminal, neither a transformer nor a phase inverter is required.

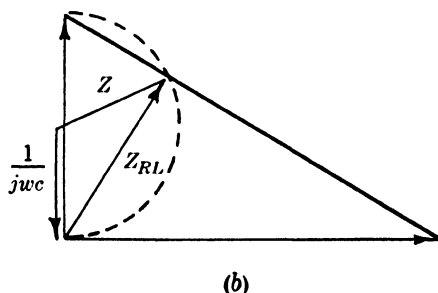
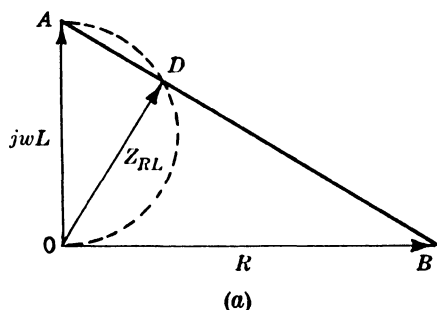


FIG. 4-38.—Impedance-vector diagrams for circuit of Fig. 4-37.

Figure 4-38a is an impedance diagram for the part of the circuit composed of the resistance  $R$  and the inductance  $L$  in parallel. If  $OA$  represents the reactance of  $L$ , and  $OB$  the resistance  $R$ , then  $OD$ , drawn perpendicular to  $AB$ , represents both in amplitude and angle the impedance of the parallel combination.<sup>1</sup> Since angle  $ODA$  is  $90^\circ$ , a plot of the locus of  $D$  as  $R$  is varied from  $0$  to  $\infty$  is a semicircle with  $OA$  as diameter. Figure 4-38b is the impedance diagram for the complete circuit. The reactance of the capacitance  $C$  is made equal to one half the reactance of  $L$  and, therefore, the sum of the impedances  $Z_{RL}$  and  $1/j\omega C$  will always be a radius of

the semicircle. Thus the total impedance of the circuit  $Z$  is of constant magnitude.   
<sup>1</sup>This is a general theorem applicable to any two parallel impedances having angles that differ by  $90^\circ$ .

stant magnitude equal to  $1/\omega C$  and has a phase angle that varies from  $-90^\circ$  through 0 to  $+90^\circ$  as  $R$  ranges from zero to infinity. The voltage  $E_0$  across  $C$  will then be equal in magnitude to the applied voltage  $E$  and will lag it in phase by an angle  $2 \tan^{-1} R/\omega L$  which may be varied from 0 through  $90^\circ$  to  $180^\circ$ .

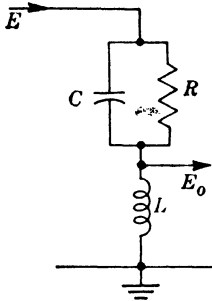


FIG. 4-39.—Phase-shifting circuit.

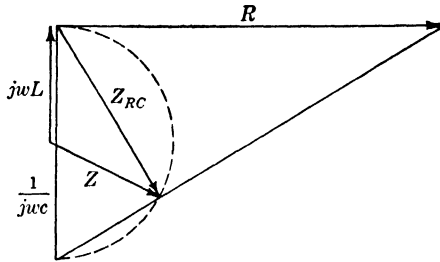


FIG. 4-40.—Impedance-vector diagram for circuit of Fig. 4-39.

To obtain a voltage which leads the input by an angle variable from  $0^\circ$  to  $180^\circ$ , the circuit of Fig. 4-39 may be used. Here  $1/\omega C$  is made equal to  $2\omega L$  as shown in the vector diagram of Fig. 4-40. The angle of lead is  $2 \tan^{-1} \omega RC$ .

### PULSED OSCILLATIONS

The importance of sinusoidal waveforms in time measurement has been discussed in the introduction to this chapter. In general, the use of a continuous sine wave for measuring the time interval between two recurrent events requires that the earlier event be synchronized with the sine wave. In many instances, however, the events are not periodic and the starting time of the interval is not predictable. It then becomes necessary to achieve synchronization by allowing the

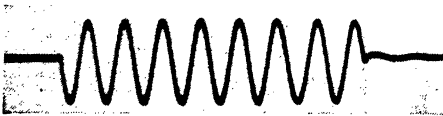


FIG. 4-41.—Pulsed sinusoidal oscillation.

earlier event to initiate the timing waveform. The required waveform is one that is zero until the beginning of the interval, becomes sinusoidal for a time greater than the interval, and then returns to zero and remains there until the start of the next timing interval. It is necessary that the oscillations always start in the same phase, and it is desirable that the starting transient be of as short a duration as possible. In addition, it should be possible to stop the oscillations quickly in order that the circuit may be ready for another timing cycle. This type of waveform, illustrated in Fig. 4-41, is known as a pulsed sinusoidal oscillation.

In order to start an oscillation with no transient, all voltages and

currents in the quiescent state must have values that they will have simultaneously at some instant in the steady state. To achieve this in a simple manner, one chooses an oscillating circuit that involves the fewest components. Phase-shift oscillators or bridge oscillators are obviously unsuited to this application. Resonant circuit oscillators, in particular the Hartley circuit, are better adapted to this type of operation, provided certain precautions are taken in regard to time constants involved in the biasing circuits.

**4-13. Ringing Circuit.**—The circuit shown in Fig. 4-42, a parallel resonant circuit connected to a constant voltage  $E$  through a current limiting resistor  $R$ , is a logical introduction to the discussion of a pulsed Hartley oscillator. The a-c losses in the resonant circuit are represented by a shunt resistor  $r$  rather than by a resistance in series with  $L$ . This gives a more accurate representation of the starting conditions since the d-c resistance of  $L$  is usually small compared with the a-c resistance and  $L$  short circuits  $r$  for direct current.

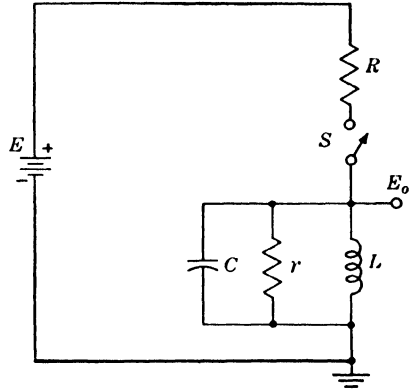


FIG. 4-42.—Circuit for producing damped sinusoidal oscillations.

Initially the switch  $S$  is closed and a steady current equal to  $E/R$  flows through the inductance. At time  $t = 0$  the switch is opened and the subsequent behavior of the circuit is determined by the differential equation

$$LrC \frac{d^2i}{dt^2} + L \frac{di}{dt} + ri = 0 \quad (61)$$

where  $i$  is the current through the inductance.

The solution is

$$i = Ae^{-\frac{t}{2rC}} \cos(\omega t + \phi) \quad (62)$$

where

$$\omega = \sqrt{\frac{1}{LC} - \frac{1}{4r^2C^2}}. \quad (63)$$

The arbitrary constants  $A$  and  $\phi$ , evaluated by noting that when  $t = 0$ ,  $i = E/R$  and  $di/dt = 0$ , are

$$\tan \phi = \frac{-1}{2rC\omega} \quad (64)$$

and

$$A = \frac{E}{R} \sqrt{1 + \frac{1}{4r^2C^2\omega^2}}. \quad (65)$$

The voltage  $E_0$  is then given by

$$E_0 = L \frac{di}{dt} = -\frac{E}{R} \left( 1 + \frac{1}{4r^2 C^2 \omega^2} \right) \omega L e^{-\frac{t}{2rC}} \sin \omega t. \quad (66)$$

The quantity  $rC\omega$  is just the  $Q$  of the resonant circuit. Neglecting  $1/4Q^2$  in comparison with 1, Eq. (66) can be rewritten

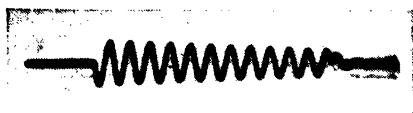


FIG. 4-43.—Damped oscillation produced by circuit in Fig. 4-44.

$$E_0 = -\frac{E}{R} \omega L e^{-\frac{\omega t}{2Q}} \sin \omega t. \quad (67)$$

Equation (67) indicates that the voltage  $E_0$  is a damped sinusoidal oscillation, the rate of damping being such that the amplitude is reduced to  $1/e$  of its initial value in  $Q/\pi$  cycles.

Figure 4-43 is a photograph of a waveform of this type produced by the circuit of Fig. 4-44. It is identical with the circuit of Fig. 4-42 except that the oscillations are initiated by a triode that is made non-conducting by a negative gate applied to its grid. This gate must be so large that the tube is completely cut off for all subsequent values of the cathode voltage, that is, it must be greater than the cutoff voltage plus the initial amplitude of the oscillations.

The waveform of Fig. 4-43 is not the desired waveform and has been discussed principally as an introduction to the material to follow. However, in some applications, time markers are generated by connecting the damped sinusoid to an amplitude comparator (see Chap. 9). If the point of amplitude selection is not exactly zero, there will be some error in the generated time markers, although the zeros of the sinusoidal waveform are equally spaced.

#### 4-14. Pulsed Hartley Oscillator.—

In order to prevent the decay of the oscillations in the ringing circuit, it is necessary to replace the energy dissipated in the resistance  $r$ . This can be done by means of the circuit of Fig. 4-45 which will be recognized as that of a Hartley oscillator. As in the previous case the oscillations are initiated by a negative gate applied to the grid of  $V_1$ . The voltage from point  $b$  of the resonant circuit is applied to the grid of a second vacuum tube  $V_2$  connected as a cathode follower, the cathode being returned through a resistance  $R_1$  to the center tap  $a$  of the inductance. Assuming perfect coupling between the two halves of the inductance, the impedance looking into

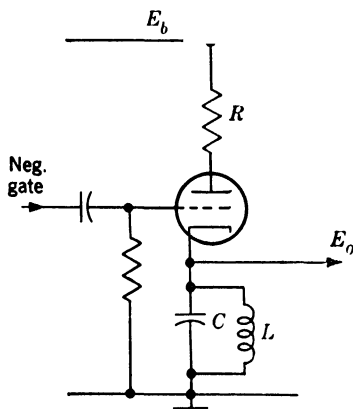


FIG. 4-44.—Ringing circuit.

the center tap is  $Q\omega L/4$  and is resistive. Hence if  $R_1$  is equal to  $Q\omega L/4$ , the voltage fed back to the center tap will be one half the voltage at  $b$ . Because of the auto-transformer action of  $L$ , the net feedback voltage at the grid of  $V_2$  is just twice the voltage at  $a$ , or is just equal to the voltage at  $b$ . Assuming  $V_2$  to have unity gain, it is apparent that the condition  $A\beta = 1$  is satisfied and that oscillations of constant amplitude will occur. In practice, the gain of  $V_2$  is always slightly less than unity, and the coupling between the two halves of  $L$  is not perfect. The effect of these factors is to reduce the amount of feedback; this can be compensated for by a reduction in  $R_1$ . Usually  $R_1$  is a variable resistor and is adjusted to give oscillations of constant amplitude.

At the end of the negative gate,  $V_1$  again becomes conducting so that the oscillations are rapidly damped to zero amplitude, usually within 2 or 3 cycles, by the low-cathode impedance of  $V_1$ .

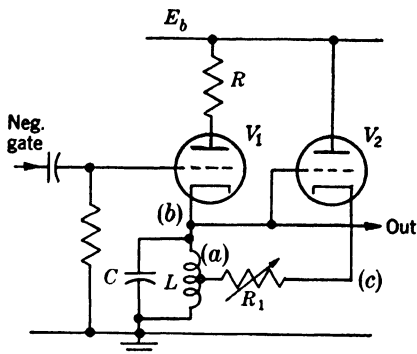


FIG. 4-45.—Pulsed Hartley oscillator.

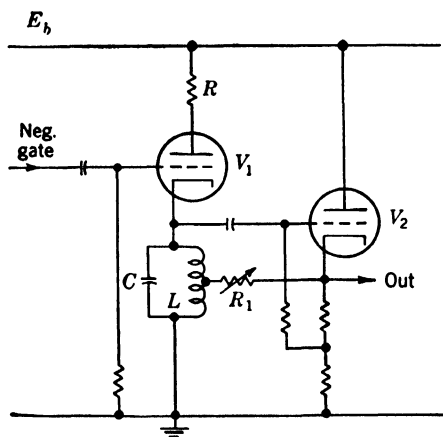


FIG. 4-46.—Pulsed Hartley oscillator with low-impedance output.

with respect to ground as shown in Fig. 4-46.

The frequency stability of this oscillator is very good, since the oscillator tube  $V_2$  is operated in a linear region and no grid current flows. In a carefully designed oscillator at 160 kc/sec, the frequency changed by less than 10 parts per million with a change in supply voltage from

Because of the distortion in  $V_2$ , the waveform at  $b$  is more pure than that at  $c$ . However, the impedance at  $c$  is much the lower, and for any load other than the grid of a vacuum tube the output is taken from  $c$ . In some cases, it may even be necessary to add a buffer amplifier to reduce the reaction of the load on the oscillator. The waveform at  $c$  is particularly bad for large amplitudes of oscillation because of the tendency of  $V_2$  to cut off on the negative grid-voltage swings. This fault can be eliminated by biasing the grid of  $V_2$  positive

100 to 400 volts, by less than 1 part per million with a change in filament voltage from 4.5 to 8 volts, and by 5 parts per million per degree centigrade. The operation of the circuit here is quite different from that in the conventional r-f oscillator in which the tube operates in class C. As a result, there is little or no amplitude stability in the ordinary sense. That is, if the clamp tube  $V_1$  remains nonconducting for a sufficiently long time, the oscillations eventually either decay to zero amplitude or build up until grid current limits the amplitude. For most uses this lack of amplitude stability is not to be considered as a defect, since the circuit is allowed to oscillate for so short a time that no appreciable change in amplitude occurs.

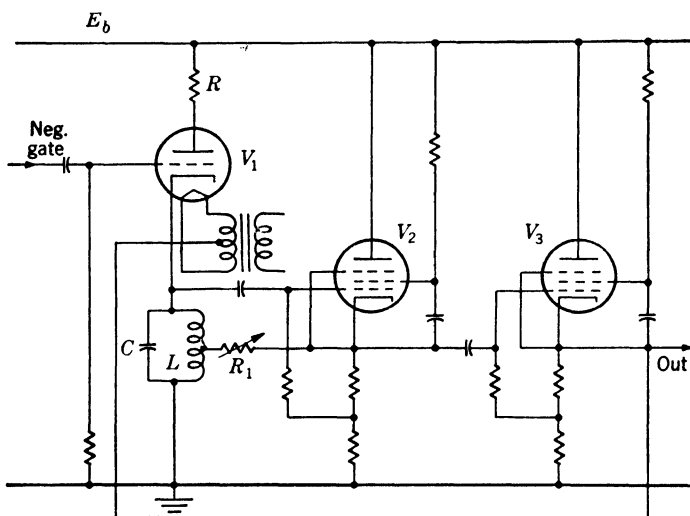


FIG. 4-47.—Pulsed Hartley oscillator to minimize effect of tube change on frequency.

It will be noted that the input capacitance of  $V_2$  and the cathode-heater capacitance of  $V_1$  form a part of the tuning capacitance of the resonant circuit. As long as the same tubes are used these external capacitances cause no trouble, but if it becomes necessary to change these tubes, a change in frequency may be observed. In cases where it is not feasible to reset the oscillator frequency after changing a tube, the circuit of Fig. 4-47 will minimize this effect. The heater of  $V_1$  is energized from a transformer separate from the normal filament supply. The secondary winding of this transformer is maintained at the same, or very nearly the same, r-f potential as the cathode of  $V_1$  by connecting either the center tap or one side to a buffer cathode follower  $V_3$  driven from the oscillator. If the ratio of the a-c voltage at the cathode of  $V_3$  to the a-c voltage of the cathode of  $V_1$  is  $B$ , the apparent capacitance from the cathode of  $V_1$  to ground due to the heater-cathode capacitance

is  $(1 - B)$  times the heater-cathode capacitance. Thus  $B$  will be the product of the gains of  $V_2$  and  $V_3$  and will be slightly less than unity. Hence the quantity  $(1 - B)$  is very small, and changes in heater cathode capacitance have much less effect on the frequency. The input capacitance of  $V_2$  can be minimized by using a pentode with the screen grid bypassed to the cathode. Use of a pentode also increases the gain of  $V_2$  and makes the quantity  $B$  approach one more closely.

An alternative form of the pulsed Hartley oscillator has the resonant circuit in the plate circuit of the switch tube, as shown in Fig. 4-48. Here the plate supply voltage for the switch tube is taken from a voltage divider on the power supply. The circuit has several disadvantages. The voltage divider must be bypassed to ground so that the top end of the resonant circuit is at ground potential for a-c. Variations in duty ratio change the potential obtained from the divider and hence the amplitude of the oscillations. Furthermore, at the end of the period of oscillation the circuit is damped only by the plate resistance of  $V_1$ , which is much higher than the cathode resistance. Although this circuit has the advantage that a separate biasing circuit for the grid of  $V_2$  is not necessary to get a good waveform from the cathode of  $V_1$ , it is, on the whole, inferior to the circuit discussed previously.

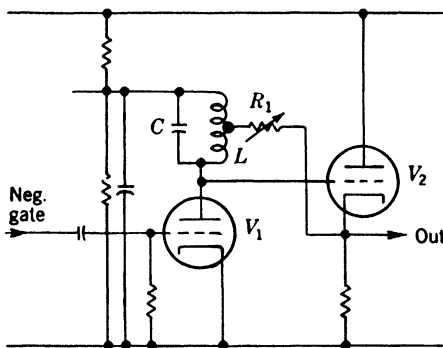


FIG. 4-48.—Pulsed Hartley oscillator with plate clamping.

**4-15. Pulsed Crystal Oscillators.**—In Sec. 4-3, Fig. 4-4 shows the equivalent circuit of a crystal—a resistance, inductance, and capacitance in series shunted by a capacitance. The equivalent  $Q$  of a crystal is so high that when oscillations are started they continue with a very small decrement, and regeneration is unnecessary. A feature of the crystal which restricts its application is that several of the connections between the impedance elements of the equivalent circuit are inaccessible. As a result, oscillations of the crystal cannot be initiated in the same manner as in the pulsed Hartley oscillator, and it is difficult to stop the oscillations at the end of the timing interval.

A complete pulsed crystal oscillator designed for operation at 82 kc/sec is shown in Fig. 4-49.<sup>1</sup> A positive gating voltage applied to the grid of  $V_1$  cuts off the current in  $V_2$  by raising the cathode voltage. The transformer differentiates the current waveform in the plate circuit of  $V_2$ , and the balanced secondary winding applies the pulse to the two input

<sup>1</sup> Another pulsed crystal oscillator is described in Vol. 21, Chap. 7.



terminals of the crystal bridge. The function of the bridge circuit is to allow the voltage pulse from the transformer secondary to excite the crystal without having the pulse appear in the bridge output. For the pulse to be completely eliminated, the bridge would have to be balanced for all the frequencies contained in the pulse, a condition that could only

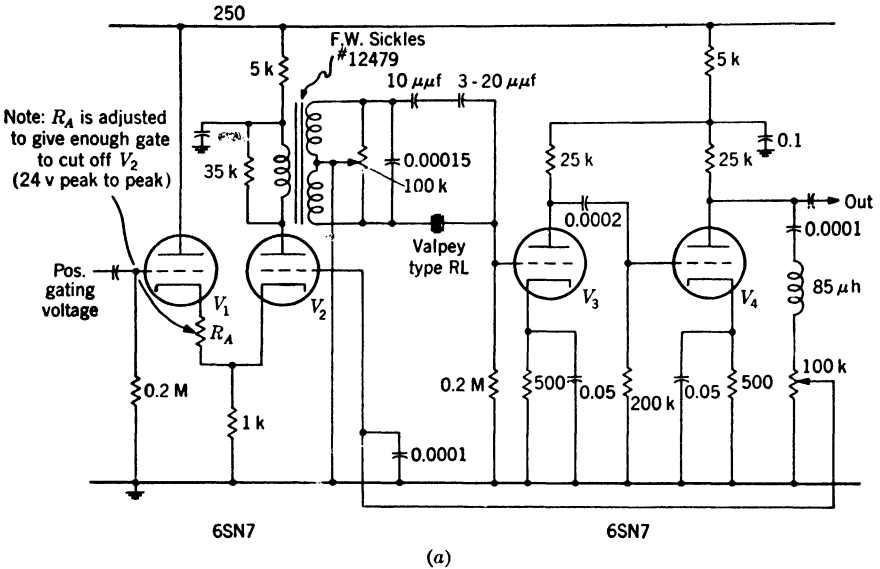


FIG. 4-49.—(a) Pulsed crystal oscillator, 82 kc/sec. (b) Output waveform from pulsed crystal oscillator, 82 kc/sec.

be achieved by using identical crystals in two branches of the bridge. This is no solution, however, for both crystals would be excited and their voltage output would cancel in exactly the same way as the pulse.

At frequencies not near the natural frequency the crystal appears as a fixed capacitance, and, therefore, the most satisfactory balance is obtained with a capacitance in the opposite branch of the bridge, as shown in the circuit. The frequencies in the pulse which are near the

crystal frequency are not balanced out and cause some distortion at the beginning of the pulsed oscillation; the duration of the distortion, however, can be restricted to about one-half a cycle. Figure 4-49b is a photograph of the output pulsed sinusoid; it shows the distortion due to the unbalanced residue of the pulse.

The output of the bridge circuit is amplified by  $V_3$  and  $V_4$ , the output being taken from the plate of  $V_4$ . At the end of the gate,  $V_2$  again becomes conducting. The grid of  $V_2$  is connected through a phase correction network to the amplifier output so that when  $V_2$  conducts, the amplified crystal voltage is applied to the crystal in opposite phase. Thus the termination of the input gate quickly damps the output voltage. Small changes in gate width or in repetition rate have no effect on amplitude provided the quiescent period corresponds to 30 to 50 times the crystal period.

The amplitude of the oscillations as a function of time is proportional to the quantity  $e^{-\frac{\omega t}{2Q}}$  where  $\omega$  is the angular frequency of the oscillations and  $Q$ , in terms of the equivalent circuit of the crystal, is  $\omega L/R$ . The relative amplitude can be expressed in terms of the number of cycles  $n$  as  $e^{-\frac{\pi n}{Q}}$ . If  $N$  is the number of cycles required for the amplitude to be reduced  $P$  per cent, it is evident that

$$e^{-\frac{N\pi}{Q}} = 1 - \frac{P}{100},$$

or

$$-\frac{N\pi}{Q} = \ln \left( 1 - \frac{P}{100} \right).$$

But, if  $P$  is small,

$$\ln \left( 1 - \frac{P}{100} \right) \cong -\frac{P}{100};$$

so

$$N = \frac{QP}{100\pi}.$$

If, for example,  $Q$  is 3000, the amplitude decreases only one per cent in 10 cycles.

It is well known that quartz crystals can oscillate in any or all of several modes, each of which has its characteristic frequency. There will, in general, be one mode that is more easily excited than any of the others. However, it is possible for a coupling between modes to exist so that excitation of one mode induces excitation of the other. This condition can be very troublesome in a pulsed crystal oscillator since it leads to an output voltage containing two or more frequencies which

are not harmonically related and which are therefore useless for time measurement. A crystal cut has been developed in which the coupling between modes has been virtually eliminated and single frequency oscillations can be obtained. This has been done for an 80-kc bar,<sup>1</sup> but it is presumed that crystals for frequencies up to several hundred kc/sec can be made in the same manner.

Chapter 21 describes a method of using a continuous crystal oscillator to obtain pulses that are synchronized with a random trigger. Such a circuit avoids the necessity of pulsing the crystal.

#### PULSED POLYPHASE SINUSOIDS

The problem of shifting the phase of a pulsed oscillation is much more difficult than that of shifting the phase of a continuous oscillation (Secs. 4-11 and 4-12). The nature of the difficulty can best be seen by considering the response of one of the circuits, described in Sec. 4-12 to a pulsed oscillation. Let a pulsed oscillation of the form

$$\begin{aligned} E &= 0 & t < 0 \\ E &= A \sin \omega t & t > 0 \end{aligned} \quad (68)$$

be applied to the circuit of Fig. 4-33a. The differential equation for the current for  $t > 0$  is

$$R \frac{di}{dt} + \frac{1}{C} i = 2A\omega \cos \omega t, \quad (69)$$

the solution of which is

$$i = \frac{2A \sin (\omega t + \theta)}{\left[ R^2 + \frac{1}{\omega^2 C^2} \right]^{1/2}} + B e^{-\frac{t}{RC}} \quad (70)$$

where

$$\theta = \tan^{-1} \frac{1}{\omega RC}. \quad (71)$$

The output voltage  $E_0$  is given by  $iR - E$  which, after some simplification, can be written

$$E_0 = A \sin (\omega t + 2\theta) + B R e^{-\frac{t}{RC}}. \quad (72)$$

The requirement that  $E_0$  be zero at  $t = 0$  determines the arbitrary constant  $B$ , giving

$$E_0 = A \sin (\omega t + 2\theta) - A \sin 2\theta e^{-\frac{t}{RC}}. \quad (73)$$

In the above expression the first term represents the desired output.

<sup>1</sup> This crystal is manufactured by the Valpey Co. and is called type RL.

The second term, required to satisfy the initial conditions, is a decaying exponential, which distorts the early part of the output voltage. Eventually, of course, the exponential term becomes so small that it may be neglected in comparison with the sinusoidal term; but, until the exponential is small, the output waveform is not useful for time measurement. Note that the initial amplitude of the transient term is proportional to the sine of the angle of phase shift and that the time constant  $RC$  is inversely proportional to the tangent of one half the angle. For small phase shift angles, the initial amplitude is small but the function decays very slowly; whereas for large angles, near  $180^\circ$ , the initial amplitude is comparable to the amplitude of the sinusoidal term and decays rapidly. Figure 4-50 is a photograph of the waveform  $E_0$  for a phase angle of  $60^\circ$ . The number of cycles elapsing before the exponential term becomes less than  $P$  times the amplitude of the sinusoidal term can be found in terms of the angle of phase shift  $2\theta$  by solving the equations.

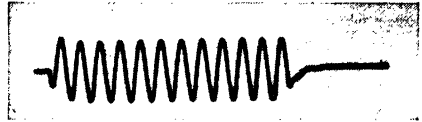


FIG. 4-50.—Pulsed oscillation shifted in phase by  $60^\circ$  by circuit of Fig. 4-33a.

$$A \sin 2\theta e^{-\frac{t}{RC}} = PA \quad (74)$$

$$\frac{\sin 2\theta}{P} e^{-\frac{t}{RC}} = 1 \quad (75)$$

$$\ln \frac{\sin 2\theta}{P} - \frac{t}{RC} = 0 \quad (76)$$

But from Equation (25)

$$\frac{1}{RC} = \omega \tan \theta \quad (77)$$

$$\frac{1}{RC} = \frac{2\pi}{T} \tan \theta \quad (78)$$

where  $T$  is the period of the oscillation.

Whence

$$\frac{t}{RC} = 2\pi \frac{t}{T} \tan \theta \quad (79)$$

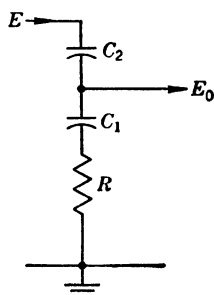
But  $t/T$  is just the number ( $n$ ) of cycles which have elapsed. Therefore,

$$n = \frac{\ln \frac{\sin 2\theta}{P}}{2\pi \tan \theta} \quad (80)$$

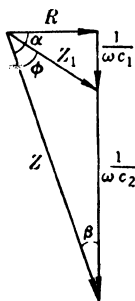
For a given application, the accuracy requirements determine how small the exponential must become in order to be negligible. At small angles the useful portion of the waveform is delayed by several cycles; whereas

for angles greater than  $90^\circ$  the delay is less than a cycle. In many instances it is required to measure very small time intervals; the allowable delay, therefore, is only a small fraction of a cycle.

**4-16. RC-feedback Circuit.**—At the sacrifice of useful output amplitude, the time constant of the exponential term can be made as small as desired. Consider the circuit of Fig. 4-51*a* and the corresponding vector impedance diagram of Fig. 4-51*b*. This circuit will shift phase by an angle between 0 and  $90^\circ$ . The capacitance  $C_1$  and the resistance  $R$  are chosen so that the phase angle of their combined impedance is approximately  $-(90^\circ - \phi)$  where  $\phi$  is the desired angle of phase shift. The value of  $C_2$  is made so small that its reactance is large compared with



(a)



(b)

FIG. 4-51.—Circuit for shifting phase of pulsed oscillation and vector-impedance diagram.

either  $R$  or the reactance of  $C_1$ ; the total impedance  $Z$ , therefore, very nearly equals the reactance of  $C_2$ . The angle between the total impedance and that fraction of it across which the output voltage is taken is  $\phi$  and consequently the output voltage leads the input voltage by  $\phi$ . The angle  $\phi$  is controlled principally by the values of  $C_1$  and  $R$ . The time constant for the exponential term in the output is, on the other hand, the product of  $R$  and the equivalent capacitance of  $C_1$  and  $C_2$  in series. Since  $C_2$  is small compared with  $C_1$ , this equivalent capacitance is very nearly equal to  $C_2$  and the time constant can be reduced without limit.

As a result of making  $C_2$  small, the ratio of the total impedance  $Z$  to the impedance of  $C_1$  and  $R$  becomes large and the output voltage becomes small. It is of interest to find the relation between the time constant and the reduction in amplitude. Let  $N$  be the ratio of input to output amplitudes, that is,  $Z$  to  $Z_1$ . The time constant  $\tau$  is given by

$$\tau = \frac{R}{\frac{1}{C_1} + \frac{1}{C_2}},$$

$$\tau = \frac{1}{\omega \frac{\frac{1}{C_1} + \frac{1}{C_2}}{R}}, \quad (81)$$

$$\tau = \frac{1}{\omega \tan \alpha}. \quad (82)$$

From Fig. 4-51b

$$\frac{Z_1}{\sin \beta} = \frac{Z}{\sin (\phi + \beta)} = \frac{NZ_1}{\sin \phi \cos \beta + \cos \phi \sin \beta}, \quad (83)$$

$$N \sin \beta = \sin \phi \cos \beta + \cos \phi \sin \beta,$$

$$\cot \beta = \frac{N - \cos \phi}{\sin \phi}. \quad (84)$$

But

$$\cot \beta = \tan \alpha,$$

so

$$\tau = \frac{\sin \phi}{\omega(N - \cos \phi)}. \quad (85)$$

By setting the derivative of  $\tau$  with respect to  $\phi$  equal to zero it can be shown that the maximum value of  $\tau$  occurs for  $\cos \phi = 1/N$ . Substituting this in Eq. (85) gives

$$\omega\tau_{\max} = \frac{1}{\sqrt{N^2 - 1}} \cong \frac{1}{N}. \quad (86)$$

Using the factor  $N$  and the desired total impedance  $Z$  as design parameters, the following equations may be derived from inspection of Fig. 4-51b:

$$R = Z \sin \beta, \quad (87)$$

$$\frac{1}{\omega C_1} = Z_1 \cos (\phi + \beta) =$$

$$\frac{Z}{N} \cos (\phi + \beta), \quad (88)$$

and

$$\frac{1}{\omega C_2} = Z \cos \beta - \frac{1}{\omega C_1}, \quad (89)$$

where  $\beta$  is given by Eq. (84).

In order to make the phase-shifted voltage equal in magnitude to the input voltage, an amplifier is required. Stabilization of the amplifier gain can

conveniently be achieved by use of negative feedback of the type described in Chap. 2, a practical example of which is shown in Fig. 4-52. The feedback components  $R'$  and  $C'$  appear at the input grid as an effective resistance  $R'/1 - A$  in series with a capacitance  $(1 - A)C'$ , where  $A$  is the amplifier gain. Since  $A$  is numerically large and is negative, these components comprise a small resistance in series with a large capacitance and correspond to the  $R$  and  $C_1$  of the preceding

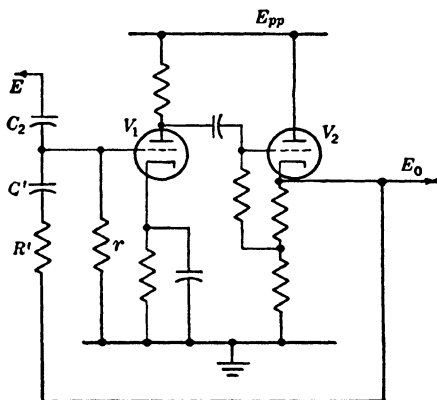


FIG. 4-52.—Stabilized amplifier for phase-shifting circuit of Fig. 4-51.

discussion. If  $R'$  and  $C'$  are so chosen that the output voltage equals the voltage applied to the input network,  $A$  and  $N$  are identical; and if  $A$  is large, the magnitude of the impedance of  $R'$  and  $C'$  will be approximately equal to the magnitude of the impedance of  $C_2$ .

The effect of a small change  $dA$  in amplifier gain can be found in the following way. Consider the generalized circuit of Fig. 4-53. The feedback factor is

$$\beta = \frac{Z'_2}{Z'_1 + Z'_2} \quad (90)$$

and in accordance with the explanation given in Chap. 2 of the behavior of feedback amplifiers, the percentage change in output voltage for a given percentage change in the value of  $A$  is given by

$$\frac{dE_o}{E_o} = \frac{\frac{dA}{A}}{1 - A\beta} \quad (91)$$

The over-all gain  $G$  is given by

$$G = \frac{E_o}{E} = \frac{\frac{Z'_1}{1 - A}}{Z'_2 + \frac{Z'_1}{1 - A}}, \quad (92)$$

since the apparent value of  $Z'_1$  is reduced by the feedback. The feedback factor  $\beta$  can be written in terms of  $G$  and  $A$  by combining Eqs. (90) and (92). Thus

$$\beta = \frac{G - A}{A(G - 1)}, \quad (93)$$

and Eq. (91) becomes

$$\frac{dE_o}{E_o} = \frac{\frac{dA}{A}}{1 - \frac{G - A}{G - 1}} = \frac{G - 1}{A - 1} \frac{dA}{A}. \quad (94)$$

In general,  $E_o$  is a complex quantity and can be written

$$E_o = |E_o|e^{j\theta}, \quad (95)$$

and

$$dE_o = d|E_o|e^{j\theta} + j|E_o|e^{j\theta}d\theta, \quad (96)$$

so that

$$\frac{dE_o}{E_o} = \frac{d|E_o|}{|E_o|} + jd\theta. \quad (97)$$

For the circuit of Fig. 4-52, the impedances  $Z'_1$  and  $Z'_2$  are so chosen that the output voltage  $E_o$  is equal in magnitude to the input voltage  $E$  and

differs in phase by an angle  $\phi + \pi$ . The term  $\pi$  in the angle occurs because of the  $180^\circ$  phase shift produced by the amplifier  $A$ . Therefore, the gain  $G$  is

$$G = e^{j(\phi+\pi)} = \cos(\phi + \pi) + j \sin(\phi + \pi). \quad (98)$$

Substituting this value of  $G$  in Eq. (94) gives

$$\frac{dE_o}{E_o} = \left[ \frac{\cos(\phi + \pi) - 1}{A - 1} + \frac{j \sin(\phi + \pi)}{A - 1} \right] dA, \quad (99)$$

and from Equation (97), equating real and imaginary parts

$$\begin{aligned} \frac{d|E_o|}{|E_o|} &= \frac{\cos(\phi + \pi) - 1}{A - 1} \frac{dA}{A} \\ \frac{d|E_o|}{|E_o|} &= \frac{1 + \cos \phi}{1 - A} \frac{dA}{A}, \end{aligned} \quad (100)$$

and

$$\begin{aligned} d\phi &= \frac{\sin(\phi + \pi)}{A - 1} \frac{dA}{A} \\ d\phi &= \frac{\sin \phi}{1 - A} \frac{dA}{A}. \end{aligned} \quad (101)$$

These equations show that if  $A$  is large, the output signal is very little affected, either in amplitude or phase, by small changes in amplifier gain.

It should be pointed out that in the amplification process the signal has been inverted, or shifted in phase by  $180^\circ$ . As a result the over-all phase shift is somewhere between  $180^\circ$  and  $270^\circ$  instead of between  $0^\circ$  and  $90^\circ$ . The signal can be reinverted by the simple expedient of inserting a resistance in the plate circuit of  $V_2$  in Fig. 4-52 equal to the resistance in the cathode circuit and taking the signal from the plate. The range of operation thus includes the first and third quadrants.

Unfortunately, an attempt to cover the two remaining quadrants by interchanging resistance and capacitance or by substituting inductance for the capacitance results in a time constant for the transient which is very long instead of very short. The second and fourth quadrants can be covered, however, by using two  $RC$ -feedback circuits in series. For example, one type of phase-shifting condenser requires three input voltages differing in phase by  $120^\circ$ . One circuit like the one in Fig. 4-52

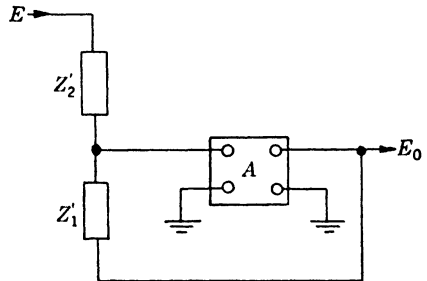


FIG. 4-53.—Generalized feedback phase-shifting circuit.



can be used to produce a leading phase of  $240^\circ$ , and a second identical circuit operated from the output of the first will give a total phase shift of  $480^\circ$  lead. These two are equivalent respectively to a  $120^\circ$  lag and a  $120^\circ$  lead.

As has been pointed out above, the limit of phase shift obtainable with this scheme is  $90^\circ$  (or  $270^\circ$ ). This limit cannot actually be achieved unless  $A$  is infinite. Since the need for phase shifts of  $90^\circ$  is frequently encountered, it is desirable to extend the limit slightly to include this angle. This can be done by replacing  $C_1$  in Fig. 4-51 by an inductance as shown in Fig. 4-54. If  $\omega L = R/N$ , where  $N$  is still the ratio of  $Z$  to  $Z_1$ , it is evident that  $Z_1$  will lead  $Z$  by  $90^\circ$ . The required value of  $C_2$  is given by

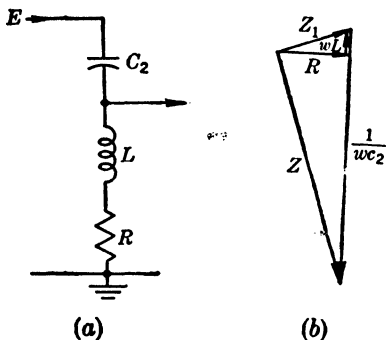


FIG. 4-54.—Circuit for shifting phase of pulsed oscillation by  $90^\circ$ .

$$\frac{1}{\omega C_2} = (N^2 + 1)\omega L. \quad (102)$$

The introduction of an inductance in this circuit makes the transient term a damped sinusoidal oscillation instead of a simple decaying exponential. A complete solution of the differential equation shows that the transient term has a frequency  $\sqrt{\frac{3N^2}{4} + 1}$  times the frequency of the applied voltage and is damped with a time constant  $2/N\omega$ . The initial amplitude of the transient is approximately  $2/\sqrt{3}$  times the steady state output amplitude if  $N$  is large. The same method of amplification can be used with this modification. Figure 4-55 is a photograph of a 16-kc/sec pulsed oscillation shifted in phase by  $90^\circ$  by this method.

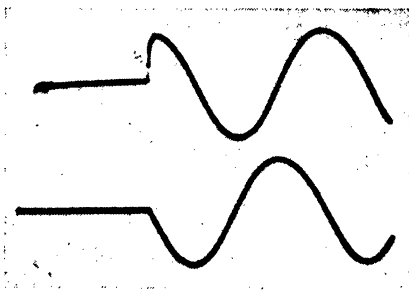


FIG. 4-55.—16-kc/sec pulsed oscillation shifted  $90^\circ$  in phase by circuit of Fig. 4-54.

It would appear that by increasing the value of  $L$ , phase shifts considerably larger than  $90^\circ$  could be obtained. It is found, however, that as the phase angle increases from  $90^\circ$  the time constant for the transient term rapidly becomes very large.

**4-17. Phase-splitting Amplifier.**—A very economical method of splitting a pulsed oscillation into two components differing in phase by  $90^\circ$  is illustrated in Fig. 4-56. Pulsed oscillations are applied to the grid of a high- $g_m$  pentode. The impedance in the cathode circuit consists of

a parallel resistance  $R_k$  and capacitance  $C$ ; the plate circuit impedance is a parallel resistance  $R_p$  and inductance  $L$ . If  $R_p$ ,  $L$ ,  $L_k$ , and  $C$  are so chosen that

$$R_k = \omega L \quad (103)$$

and

$$R_p = \frac{1}{\omega C} \quad (104)$$

the plate and cathode impedances are equal in magnitude and differ by  $90^\circ$  in phase as shown in Fig. 4-8.<sup>1</sup> Since the mutual conductance is high the voltage at the cathode reproduces very closely the input voltage, the current being whatever is required to produce this voltage. The same current flows in the plate and cathode circuits and since the impedance vectors in these two circuits are equal in magnitude and mutually perpendicular, the voltage at the plate equals the cathode voltage but is shifted in phase by  $90^\circ$ .

The only restrictions on the impedance elements are given by Eqs. (103) and (104). It would appear possible, therefore, to make  $R_k$  and

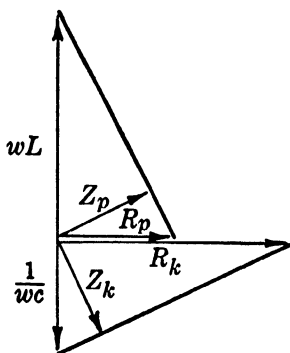


FIG. 4-57.—Vector-impedance diagram for Fig. 4-56.

the cathode may be used as a source for the feedback voltage necessary to sustain the pulsed oscillations at constant amplitude. Figure 4-58 shows a combined pulsed oscillator and phase shifter. In this figure  $R_k$  of Eq. (103) is the combination of  $R_1$  and  $R_2$  in series, paralleled by  $R_4$

<sup>1</sup> The graphical combination of parallel impedances has been explained in Sec. 4-12.

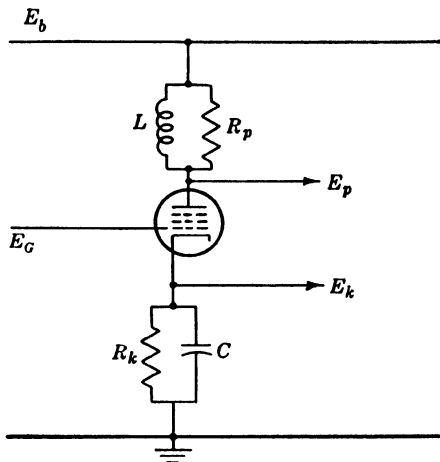


FIG. 4-56.—Method of shifting phase of pulsed oscillation by  $90^\circ$ .

or to make  $R_p$  infinite and  $C$  zero. The first possibility is ruled out, however, because it leaves no d-c path for the tube current. The second possibility is impractical because the sudden rise of current in the plate circuit excites oscillations at the antiresonant frequency of the inductance and its distributed capacitance. The best results are obtained when  $R_p$  is chosen for critical damping.

The function of phase-shifting can conveniently be combined with the production of the pulsed oscillations. Since the voltage at the cathode reproduces the grid voltage, the cathode may be used as a source for the feedback voltage necessary to sustain the pulsed oscillations at constant amplitude. Figure 4-58 shows a combined pulsed oscillator and phase shifter. In this figure  $R_k$  of Eq. (103) is the combination of  $R_1$  and  $R_2$  in series, paralleled by  $R_4$

The function of phase-shifting can conveniently be combined with the production of the pulsed oscillations. Since the voltage at the cathode reproduces the grid voltage,

and twice  $R_3$ . It is necessary to take  $2 \times R_3$  because the impedance from the center tap of the oscillator inductance to ground is equal to the feedback resistance. Figure 4-59 is a photograph of waveforms obtained at the cathode and plate of the circuit in Fig. 4-58.

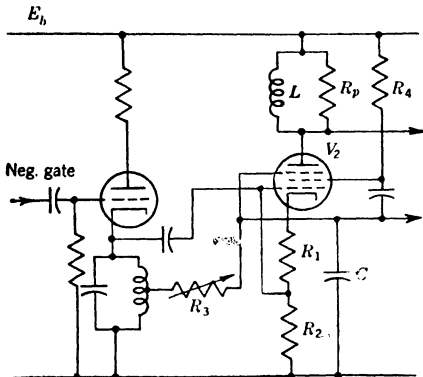


FIG. 4-58.—Combined pulsed oscillator and phase shifter.

**4-18. Pulsed Oscillations for Use with Synchros.**—In Chap. 13 of this volume the use of synchros for shifting phase continuously is discussed.

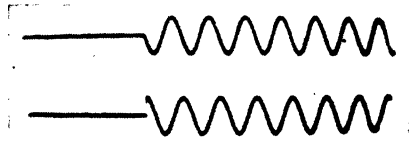


FIG. 4-59.—Waveforms obtained from circuit of Fig. 4-58.

It is shown there that the necessary input current waveforms for use with pulse oscillations are of the form

$$\left. \begin{aligned} i_1 &= K & t < 0 \\ i_1 &= A \sin \omega t + K_1 & t > 0 \\ i_2 &= K_2 & t < 0 \\ i_2 &= -A \cos \omega t + K_2 + A & t > 0 \end{aligned} \right\} \quad (105)$$

where  $A$ ,  $K_1$ , and  $K_2$  are constants.

These waveforms are illustrated in Fig. 4-60. The waveform of

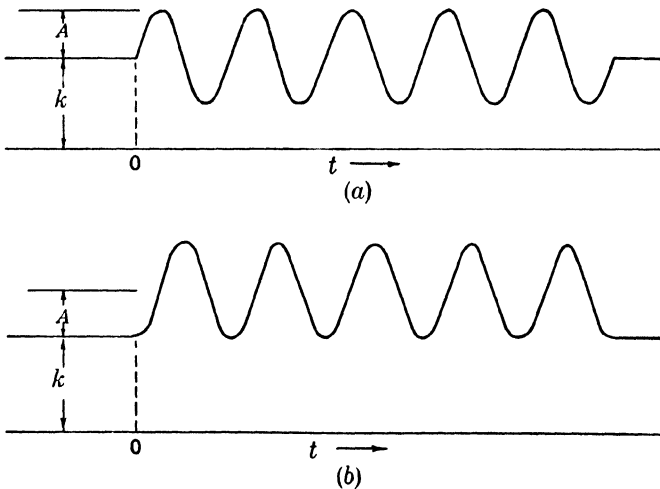


FIG. 4-60.—Current waveforms for synchro phase shifter.

Fig. 4-60*a* is (except for a change of sign) just the voltage waveform produced by a pulsed oscillator and is easily obtained. The waveform of Fig. 4-60*b* is more difficult to obtain because of the shift in average level during the interval of oscillation. Note, however, that Fig. 4-60*b* is just the current waveform in the inductance of the pulsed oscillator. If a small resistance is placed in series with the grounded end of this inductance, a waveform approximately equal to the one illustrated is obtained. The effect of this added resistance on the pulsed oscillator is to change the phase in which the oscillations start by a small amount, and to increase the amount of feedback necessary to maintain constant amplitude. The quality of the oscillations is not impaired if the added resistance is small. The voltage across this resistance will be  $90^\circ$  out of phase with the voltage across the inductance but not with the total voltage, which appears at the top of the inductance. This phase error can be compensated for by adding a small component of capacitive reactance to the resistance so that the impedance vector of this branch is at right angles to the total impedance vector  $Z$  as shown in Fig. 4-61.

Since the voltage across the resistance is small compared with the oscillator output, an amplifier is required to make the two waveforms equal in amplitude. This amplifier may be stabilized in the same way as the amplifier for the phase shifter described in Sec. 4-17, that is, by increasing the size of the resistor and by returning it not to ground but to the output of the amplifier. The value of the resistance produced in this case should be approximately equal to the reactance of the oscillator inductance.

A complete circuit is shown in Fig. 4-62. The oscillator differs from the one previously described in that the grid of the clamp tube  $V_1$  is returned to  $E_b$  instead of ground. This is necessary because the inductance in the cathode circuit is returned through the resistor  $R$  to a point that is at a positive potential with respect to ground. If the grid of  $V_1$  were at ground potential, no quiescent current would flow in the inductance and no oscillations would be produced. The resistor  $R_1$  is made variable to provide an adjustment for the amplitude of the phase-shifted output, and the phase-compensating condenser  $C$  is shunted by a variable resistance  $R_2$  to set the phase precisely. The output waveforms are applied to the grids of two pentodes whose plate circuits contain the synchro primary windings  $P_1$  and  $P_2$ . Because of the high plate resistance of the pentodes and the current feedback from the large unbypassed

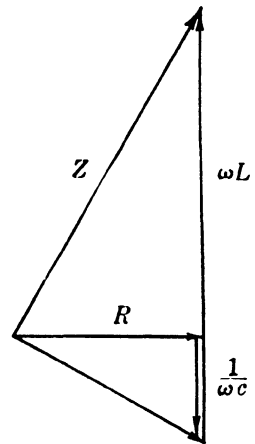


FIG. 4-61.—Vector-impedance diagram for cathode circuit of modified pulsed oscillator.



## CHAPTER 5

### GENERATION OF FAST WAVEFORMS

#### INTRODUCTION

BY DAVID SAYRE

The preceding chapter described the generation of sine waves, which may be regarded as the “smoothest” oscillations possible. There are, however, a great many uses for waveforms of precisely the opposite nature—namely, waveforms that are as *abrupt* as possible—and it is the generation of such waveforms that this chapter will treat. Such waveforms are useful primarily in *timing* applications because a definite instant in time can be associated much more accurately and unequivocally with the moment of “abruptness” in such waveforms than with any portion of a “smooth” waveform. Speed, relative of course to the time scale being used, is therefore a most valuable property of such waveforms, and in general the purpose of this chapter will be to describe how to generate pulses of short total duration and rectangles with short rise and fall times. In anticipation of later discussion, it may be stated that under the best conditions the times involved can be measured in hundredths of a microsecond.

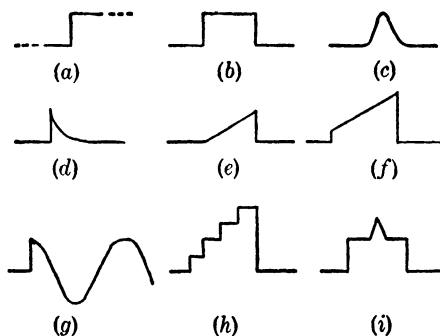


FIG. 5-1.—Examples of abrupt waveforms: (a) step function; (b) rectangle; (c) pulse; (d) fast-rising slow-falling pulse; (e) triangle; (f) trapezoid; (g) pulsed sine wave; (h) staircase; (i) triangle on a pedestal.

A large number of abrupt waveforms can be imagined, a few examples of which are given in Fig. 5-1. Of these only the simplest—pulses and rectangles—will be discussed in this chapter; the more complex waveforms involve additional processes like differentiation, integration, modulation, addition, etc., and will be discussed in other chapters.

#### 5-1. Methods and Principles in the Generation of Fast Waveforms.—

The several types of circuit that can be used to generate abrupt waveforms will be classified somewhat arbitrarily as follows for the purpose of later description:

1. Multivibrators and phantatron-type circuits.
2. Blocking oscillators.
3. Delay-line pulse generators.

Only the first of these methods will be described in this chapter; blocking oscillators and delay-line pulse generators are treated in Chap. 6; and certain pulse sharpeners and squaring circuits are described in Chap. 9.

Since these circuits generate waveforms that differ so sharply from sine waves, it is to be expected that they possess in common some property that distinguishes them from sine-wave generators. This common property is the utilization of a nonlinear element. Perfect sine waves could be generated without any such element. Abrupt waveforms, however, cannot be generated without some operation with a nonlinear element,

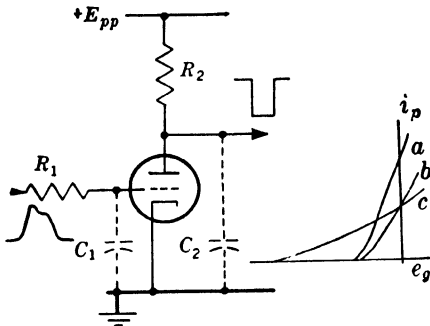


FIG. 5-2.—Limiting amplifier.

and in general, the more abrupt the nonlinearity, the more abrupt the waveform which can be generated. For this reason the analysis of any of these circuits, unlike that of a sine-wave oscillator, must take as its starting point the nonlinearities of its elements. Knowledge about the properties of these elements, their utilization in circuits, and the analysis of such circuits will therefore be of prime importance to the reader throughout this chapter, and he would do well to have the material of Chap. 3 well in mind before reading further.

It has already been stated that the most important property of abrupt waveforms is their speed at certain instants, but this is precisely the property which is most difficult to obtain. The maximum speed of the waveform at any point of a circuit is almost always limited by the ability of the circuit to deliver a large current to (or remove a large current from) that point in order to charge or discharge rapidly the capacity which loads the point. Thus, if a circuit is to generate fast waveforms, *loading capacities must be small and peak currents through them must be large.*

These principles are illustrated by the simple limiting amplifier of Fig. 5-2. In this figure tube characteristic *c* is inferior to characteristics *a* and *b* because a longer time is required to turn the tube on and off. *C*<sub>2</sub> should be kept as small as possible by using a tube with a small output capacity, designing the succeeding stage to have a small input capac-

ity, and wiring the circuit carefully.  $R_2$  should be small so that on the trailing edge of the pulse there will be a large current recharging  $C_2$ . The lower limit of  $R_2$  is determined by the required output amplitude, and for this reason tube characteristic  $a$  is superior to characteristic  $b$  since it permits a larger output pulse with an equally fast rise time, or an equal pulse with a faster rise time.  $C_1$  should be kept small, which is more difficult to do with a triode than with a pentode because of the Miller effect. Finally,  $R_1$  should be as small as is consistent with good limiting in order that large currents be available for charging and discharging  $C_1$ .

From these considerations can be gained, therefore, an accurate conception of the problems involved in the generation of fast waveforms. First, elements must be found whose nonlinearity is as abrupt as possible. Modern triodes and pentodes<sup>1</sup> exist which for ordinary plate voltages cut off with  $-4$  volts on the grid and which display a transconductance of as much as 10,000  $\mu\text{mhos}$  at zero grid voltage. As stated in Chap. 3, gas tubes and positive feedback circuits have a jump discontinuity in their characteristic and hence display a very large transconductance at one point.

Second, these elements must be capable of delivering high peak currents although the average current may often be small. The vacuum tubes just mentioned are capable of peak cathode currents of 1 amp or more,<sup>2</sup> and the same figure holds for small thyratrons. Finally, capacities to ground from critical points must be small. Many of the miniature tubes which have been developed during recent years have input and output capacities whose sum is less than 5  $\mu\text{f}$ ; regular size tubes usually show approximately double these capacities.

**5-2. Applications.**—It has already been stated that abrupt waveforms find important use as time indices, and that speed is an important property of such waveforms if the order of time resolution is to be high. Examples of such applications are: time modulation, measurement of time intervals, pulse frequency division, etc.

A related set of applications are those in which abrupt waveforms, themselves the products of nonlinear elements, are used to alter the behavior of other such elements during definite intervals of time. Such "gating" applications, as they are usually called, are exemplified by intensity gating of a cathode-ray tube, sensitivity gating of a receiver, time selection by means of a coincidence pulse, etc. In such applications a second requirement is often placed upon the shape of the gating waveform: not only must its rise and fall times be short, but also its top must

<sup>1</sup> Triodes: 7F8, 6J4. Pentodes: 6AC7, 6AG7, 6AK5.

<sup>2</sup> See R. B. Woodbury, "Pulse Characteristics of Common Receiver-type Tubes," RL Report No. 704, April 30, 1945.



be flat so that the performance of the gated element will be constant during the whole gating period—that is, rectangles, and not merely pulses, are required for such purposes.

**5-3. Other Practical Design Considerations.**—Shape of the output waveform (including speed and flatness of top), although usually the most important single consideration, is by no means the only one influencing the choice of circuit for a given application. The following list of design considerations is therefore included to provide a frame of reference by which the reader can assess the merits of a particular circuit for a particular application.

1. Shape of the waveform. The importance of speed in timing applications and of speed and flatness of top in gating applications has already been mentioned.
2. Amplitude of the waveform.
3. Load across which the output waveform is to be taken. Unless the generating circuit has a very small internal impedance, the output waveform will depend in both shape and amplitude upon the nature of the load impedance across which it is to be taken. For example, a circuit which can deliver a fast waveform across a resistance may not be able to do so across a capacity, and one which can deliver a flat-topped waveform across a resistance may not be able to do so across an inductance.
4. Polarity of the waveform.
5. Number of stable states. Fast waveform generators can be designed to have 0, 1, or 2 stable states. Typical waveforms

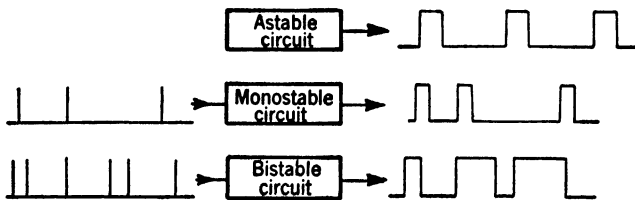


Fig. 5-3.—Action of circuits with 0, 1, and 2 stable states.

for each are shown in Fig. 5-3. A circuit with 0 stable states, called “astable” or “free-running,” generates a continuous train of waves and requires 0 triggers to execute a complete cycle; a circuit with 1 stable state, called a “monostable” or “flip-flop” circuit, requires 1 trigger for each complete cycle; and finally a circuit with two stable states, called a “bistable” or “scale of two” circuit, generates merely a step function for each trigger and therefore requires two triggers for each complete cycle. An astable circuit can sometimes be used as a quasi-monostable or

quasi-bistable circuit by triggering it at a rate high compared with its own natural frequency; likewise a monostable circuit may be used as a quasi-bistable circuit.

6. Control over frequency, pulse duration, etc. In many timing operations it is necessary to have control over the various time relationships between the fast portions of the output waveform. In pulse frequency modulation, for instance, the recurrence frequency of a train of pulses is varied, whereas in time modulation, the time interval between pulse pairs or the width of a pulse is varied (see Chap. 13). The circuit control characteristics pertaining both to accuracy and to range of control are therefore important considerations.
7. Recovery time. Rapid recovery is important in many applications where the circuit will be required to perform its cycles in rapid succession.
8. Triggering. The necessary amplitude, duration, and polarity of the trigger are sometimes important considerations. Also the effect of variations in the trigger upon circuit performance may be important.
9. Stability. Stability of the output waveform (in shape, amplitude, and all its time relationships) against changes in line voltage, tubes, etc. is often a prime necessity.
10. Economy, reliability, designability, etc.

### MULTIVIBRATORS

The discussion of multivibrators will be arranged as follows. Because the action of a multivibrator can be divided naturally into two parts—the generation of the step function and the establishment of the time interval—the first section 5-4 will describe circuits which perform only one of these actions, that is, bistable multivibrators, in which only the generation of the step function is performed, and in which there is no timing process. The following section 5-5, describing monostable multivibrators, will introduce the method whereby one of the formerly stable states is rendered only quasi-stable and its duration is established. Section 5-6 will describe the basic astable multivibrators, in which both states are only quasi-stable. In all three of these sections both plate-to-grid-coupled and cathode-coupled varieties will be presented. The succeeding two sections, 5-7 and 5-8, will discuss in greater detail the processes of step-function generation and timing, as carried out in one representative circuit. From this discussion will be obtained certain general conclusions which are of considerable design value. Finally, the later sections, 5-9 to 5-14, will discuss ways of operating or modifying the basic circuits to obtain certain desirable performance characteristics.

**5-4. Bistable Multivibrators.**—The basic plate-to-grid-coupled bistable multivibrator<sup>1</sup> is illustrated in Fig. 5-4.

The operation of this circuit depends upon the fact that a stable configuration can exist either with  $V_1$  on and  $V_2$  off, or with  $V_1$  off and  $V_2$  on, and that a rapid change from one configuration to the other can be initiated by suitably injecting a triggering pulse into the circuit. If, initially,  $V_1$  is on, its plate is at some voltage low enough to keep  $V_2$  off and the plate of  $V_2$  is in turn at a voltage high enough to keep  $V_1$  on. When a negative trigger is applied to the plate of  $V_2$  through the diode

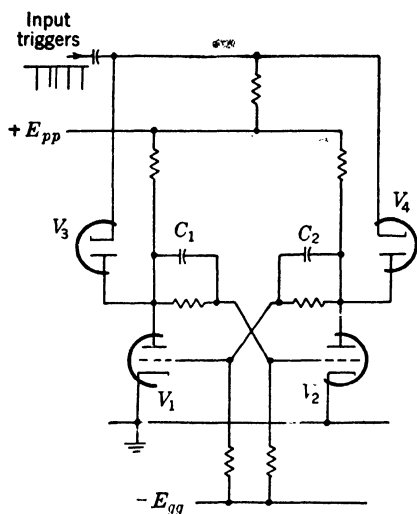


FIG. 5-4.—Basic plate-to-grid-coupled bistable multivibrator.

$V_4$ ,  $V_1$  is cut off and  $V_2$  becomes conducting. (It should be noticed that the injected trigger will go to the plate of  $V_2$  and not of  $V_1$  because the plate of the diode  $V_3$  is so much lower than its cathode that no conduction is possible even during the trigger.) Because of  $C_2$ , which like  $C_1$  is called a “speeding-up” condenser, the fast negative-going edge of the trigger is brought to the grid of  $V_1$ ;  $V_1$  is thus cut off, its plate rises and thereby raises the grid of  $V_2$ , and this rise in turn augments the action of the trigger by lowering the plate of  $V_2$  still farther.  $V_1$  is thus rapidly turned off and  $V_2$  turned on, and the net result of the trigger is

to carry the circuit from one stable configuration to the other. The waveforms of this circuit are shown in Fig. 5-5.

These waveforms have two main uses. Since the waveform at one of the plates has one-half as many rising edges as there are input triggers, the circuit can be used to divide by 2 the number of triggers coming from any source. Also, the two plate waveforms are useful for the electronic switching of waveforms, when, for instance, it is desired to display two different waveforms on alternate sweeps in a cathode-ray tube.

Since the total current drawn by the circuit is approximately the same throughout the cycle, the insertion of a moderately bypassed common cathode resistor of the proper value will provide a suitable bias and will permit the negative supply to be eliminated. Such a circuit is shown in

<sup>1</sup> Bistable circuits have also been called “scaling” circuits, “scale-of-two” circuits, and in England “lockover” circuits.

Fig. 5-6. Because the cathode bias developed will accommodate itself to the voltages and components being used, this circuit is considerably less sensitive to changes in the operating conditions than that of Fig. 5-4.

The analogous cathode-coupled bistable multivibrator is illustrated in Fig. 5-7. In this circuit, also, two stable configurations are possible: one with  $V_2$  on, in which case the cathode of  $V_1$  is high enough to cut that tube off; the other with  $V_1$  on, in which case the grid of  $V_2$  is low enough to cut that tube off. The transition from one state to the other may be initiated by injecting a trigger, or by raising or lowering the grid of  $V_1$ .

It is this latter method of control which is illustrated in the waveforms of Fig. 5-8. Here  $V_2$  is initially on and  $V_1$  is off. As the grid of  $V_1$  is raised, there comes a point where current begins to flow in  $V_1$ ; the plate of  $V_1$  and the grid of  $V_2$  drop; consequently the current through  $R_k$  decreases, the cathode of  $V_1$  drops, and thus turns  $V_1$  on more rapidly. At a definite voltage of the input waveform, therefore, the circuit flips over. Similarly, it will flop back on the trailing edge of the input, but at a lower voltage. This difference in critical voltages is a consequence of the "hysteresis effect" which is always present in relaxation oscillators, and which is discussed in Chap. 3. The output on the plate of  $V_2$  is thus a square wave whose duration is

equal to the time spent by the input between its two critical voltages. Taking the output from the plate of  $V_2$  instead of from some other point has the advantages of speed and flexibility since the stray capacity from that point to ground is small and since almost any type of load may be

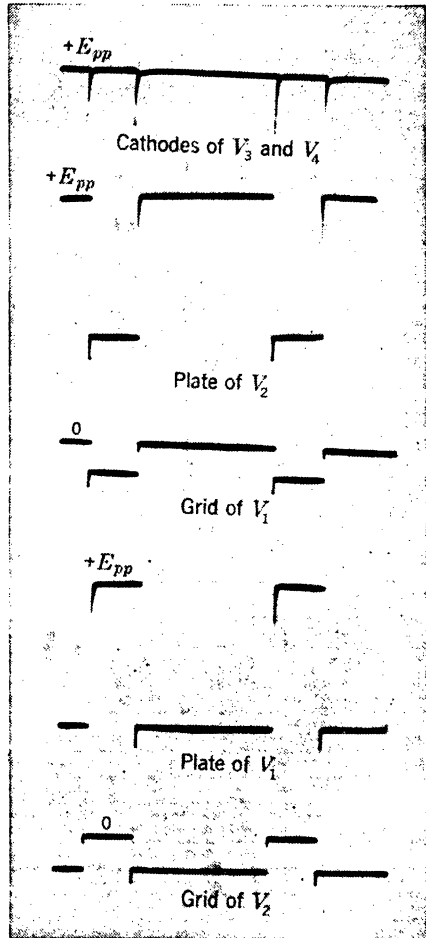


FIG. 5-5.—Waveforms of the plate-to-grid-coupled bistable multivibrator of Fig. 5-4. The trace was about 1250  $\mu$ sec long; the amplitude of the plate waveforms about 130 volts.

attached without seriously affecting the performance of the rest of the circuit. These advantages can be increased, in this and all other cathode-coupled types, by making  $V_2$  a heavy-current tube, reducing  $r_2$ , and returning the cathode of  $V_2$  to a point only part way up  $R_k$ .

The uses to which this circuit can be put are easily inferred from its waveforms. It has been used as a means of squaring an input pulse; as a regenerative amplitude comparison circuit (see Chap. 3); and as a sort of peak-reading voltmeter that indicates whether the input signal ever attains the critical voltage at which the circuit will flip over.

In this and all other cathode-coupled multivibrators greater regeneration can be obtained by also coupling the plate of  $V_2$  to the grid of  $V_1$

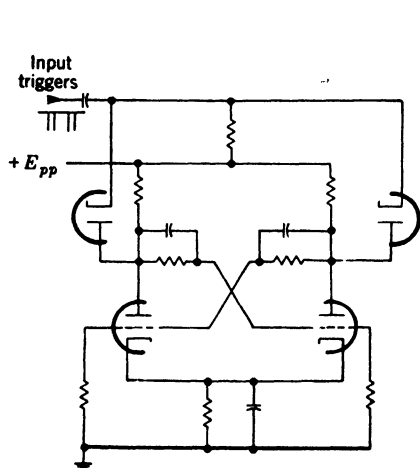


FIG. 5-6.—Plate-to-grid-coupled bistable multivibrator with cathode bias.

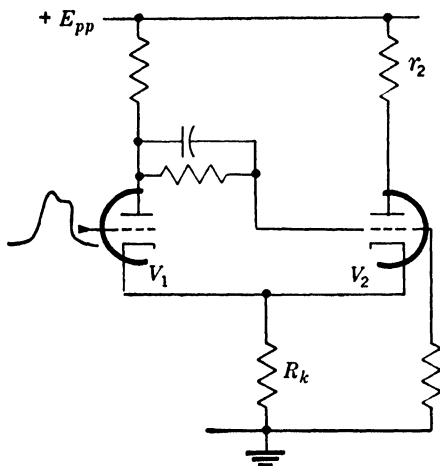


FIG. 5-7.—Basic cathode-coupled bistable multivibrator.

to obtain a circuit which is both plate-to-grid- and cathode-coupled. This usually increases somewhat the speed with which the change of state is accomplished, but does so at the expense of losing the “free” plate of  $V_2$ .

**5-5. Monostable Multivibrators.**—If in the bistable circuit of Fig. 5-4 the a-c-d-c coupling from the plate of  $V_1$  to the grid of  $V_2$  were replaced by an ordinary a-c coupling, the negative square wave on the plate of  $V_1$  would come through to the grid of  $V_2$  not as a square wave but as the exponential wave shown in Fig. 5-9. Thus  $V_2$  could not remain turned off indefinitely—that is, the state in which  $V_2$  is off and  $V_1$  is on would become a quasi-stable state, the duration of which would be determined by the time necessary for the grid of  $V_2$  to recover exponentially to a voltage where  $V_2$  can begin to draw current again and where the circuit flips back to its other (stable) state. Because of its fundamental role in establishing the duration of the quasi-stable state, the

exponential waveform is called the "timing waveform" and the coupling condenser and resistor which determine its time constant are called the "timing condenser" and "timing resistor."

From these considerations is derived the basic plate-to-grid-coupled monostable multivibrator<sup>1</sup> shown in Fig. 5-10. It should be noticed that the timing resistor  $R$  is returned not to ground but to the plate supply. This is done, when  $R$  is not too small, in order to increase the slope of the timing exponential at the moment of pickoff and thus improve the stability of duration of the generated rectangle.

Figure 5-11 illustrates the waveforms of this circuit. Initially the circuit is in its stable state, with  $V_2$  on because of  $R$ , and  $V_1$  off because of the drop in  $r_2$ . When the negative trigger is injected at the plate of  $V_1$  it is coupled by  $C$  to the grid of  $V_2$ ;  $V_2$  is cut off; the plate of  $V_2$  rises rapidly, and this rise which is coupled by  $C_1$  to the grid of  $V_1$  turns  $V_1$  on. As  $V_1$  turns on, the negative swing of the plate reinforces the effect of the trigger. Thus, after a very short time,  $V_1$  has been turned on and  $V_2$  has been turned off. This state, as pointed out above, is only quasi-stable, however, because the charge on  $C$  leaks away through  $R$  and consequently the grid of  $V_2$  rises exponentially toward  $E_{pp}$  until it reaches the critical voltage  $-E_c$ , at which  $V_2$  begins to turn on again and the circuit flops rapidly and regeneratively back to its initial state, where it remains until another trigger is injected.

A restatement of the timing mechanism might be that two processes are involved: (1) the generation of a timing waveform (the exponential on the grid of  $V_2$ ); and (2) the "picking-off" of the timing waveform at a

<sup>1</sup> Monostable multivibrators have also been called "flip-flops," "one-shot multivibrators," and "gating multivibrators."

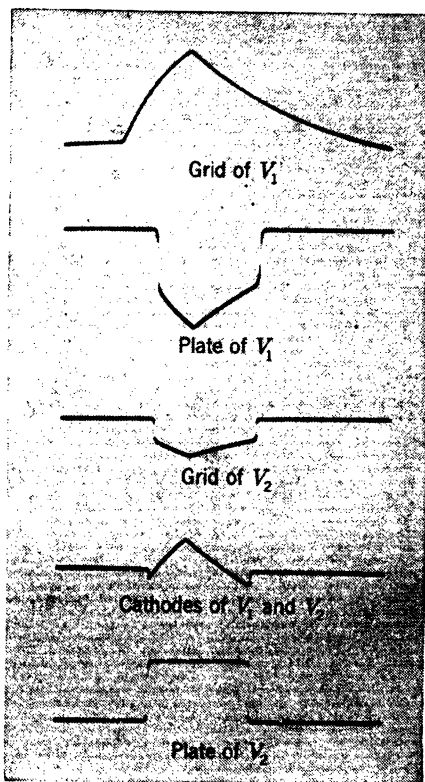


FIG. 5-8.—Waveforms of the cathode-coupled bistable multivibrator of Fig. 5-7. The trace was about 1250  $\mu\text{sec}$  long; the amplitude of the waveform at the plate of  $V_2$  about 60 volts.

definite voltage by a nonlinear element in order to provide the signal marking the end of the desired time interval. This second process is called "amplitude comparison" and is described in Chap. 3. In the circuit of Fig. 5-10  $V_2$  is the nonlinear element and  $-E_c$  is the pickoff voltage.

The origin of the overshoots in several of the waveforms is to be found at the grid of  $V_2$ . During the interval when  $V_2$  is off, the timing condenser  $C$  is being discharged. During the other portion of the cycle, therefore, it must be recharged, the electron current taking the path from the cathode to the grid of  $V_2$ , right to left through  $C$ , and up through  $r_1$ . Since the diode formed by the grid and cathode of  $V_2$  does not have zero forward resistance, this current produces on the grid a small positive signal which also appears amplified and inverted on the plate of  $V_2$  and the grid of  $V_1$ . This flow of current, which will last until  $C$  is completely recharged, is also the cause of the slow rise in the waveform at the plate of  $V_1$ . Thus the recharging of  $C$  is a bothersome problem, especially when very narrow pulses or

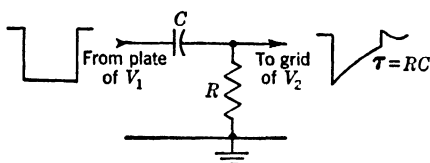


FIG. 5-9.—Method of generating the exponential timing waveform in a multivibrator.

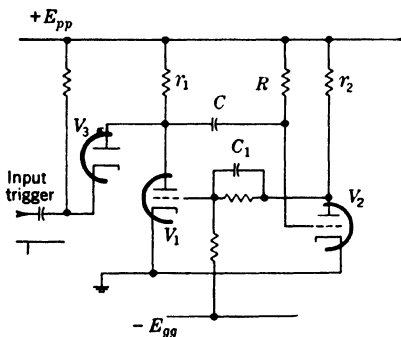


FIG. 5-10.—Basic plate-to-grid-coupled monostable multivibrator.

very rapid repetition of the cycle is desired, and special provisions must be made (see Sec. 5-11) for reducing the recharging time. A similar effect may take place at the grid of  $V_1$  when that tube is turned on if  $C_1$  is made any larger than just sufficient to match the stray capacity from the grid of  $V_1$  to ground.

The usefulness of such a circuit is obvious; it is used when rectangles of a predetermined duration are desired, one rectangle for each trigger injected.

Figure 5-12 shows the corresponding cathode-coupled monostable multivibrator, and Fig. 5-13 its waveforms.

The initial and stable state is with  $V_2$  on and  $V_1$  off. The diode  $V_4$  is used to define the initial level of the grid of  $V_2$ ; this level would otherwise vary greatly according to the electrode structure and cathode emission of  $V_2$ . When a negative trigger is injected through  $V_3$ ,  $V_2$  is turned off and the cathode of  $V_1$ , dropping to within a few volts of the grid of  $V_1$ ,

turns  $V_1$  on. A negative rectangle is thus generated at the plate of  $V_1$  and, after differentiation in the timing network  $RC$ , becomes the exponential timing waveform on the grid of  $V_2$ . After a definite time interval, therefore, the grid of  $V_2$  crosses the grid base of  $V_2$  and the circuit reverts quickly to its original state.

The circuit has two very useful properties. First, fast waveforms can be obtained in either polarity, positive from the plate of  $V_2$  and negative from the cathodes of  $V_1$  and  $V_2$ . Second, it is found that over nearly the entire operating range the duration of the rectangle generated is a linear function of the voltage impressed on the grid of  $V_1$ . Thus, by changing the setting of the potentiometer  $P$ , the duration of the rectangle can be increased steadily from almost zero to its full value, with a linearity which may be as good as 0.2 per cent of full range.<sup>1</sup> Qualitatively, the increase in rectangle duration with the grid voltage of  $V_1$  is due to (1) the increase in the amplitude of the negative rectangle at the plate of  $V_1$  with the consequent increase in the negative voltage from which the grid of  $V_2$  must recover and (2) the decrease in the amplitude of the negative rectangle at the cathodes, with the consequent increase in the voltage to which the grid of  $V_2$  must recover. These facts are illustrated by the waveforms in Fig. 5-13, where the photographs were taken for two positions of the potentiometer  $P$ .

As in the previous circuit, the recharging of  $C$  is responsible for certain overshoots and other defects of the trailing edges of the waveforms.

<sup>1</sup> The circuit of Fig. 5-12 shows poor design in one respect. The cathode of  $V_1$  should be returned to the bleeder which contains  $P$  so that variation in the bleeder resistances will tend to make the grid levels move together.

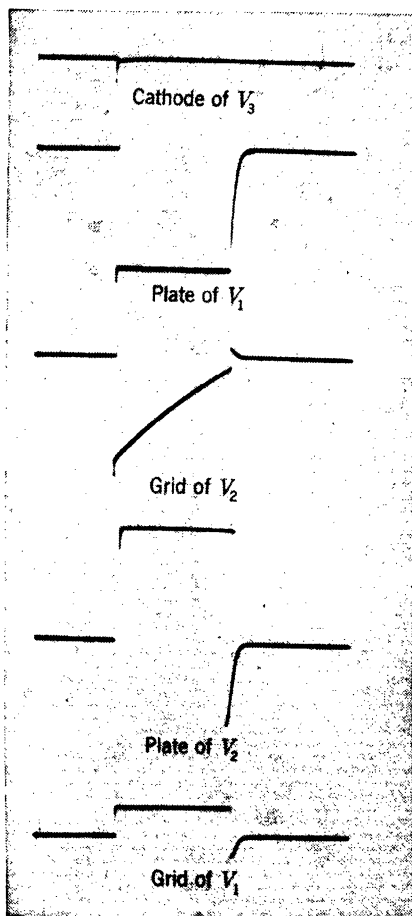


FIG. 5-11.—Waveforms of the plate-to-grid-coupled monostable multivibrator of Fig. 5-10. The trace was about 1250  $\mu\text{sec}$  long; the amplitude of the waveform at the plate of  $V_1$  about 130 volts.



It should be noticed that the bistable circuit of Fig. 5-7 has two a-c-d-c coupling paths, from the plate of  $V_1$  to the grid of  $V_2$ , and from the

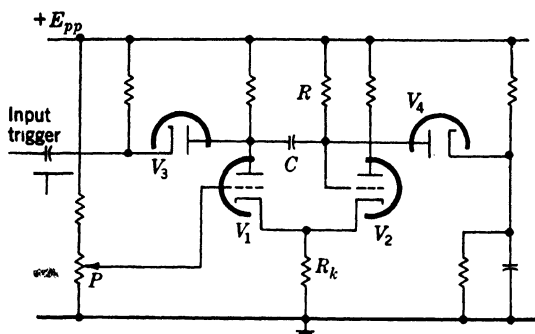


FIG. 5-12.—Basic cathode-coupled monostable multivibrator (timing network in grid circuit).

cathode of  $V_2$  back to the cathode of  $V_1$ . The monostable circuit of Fig. 5-12 was obtained by replacing the former of these a-c-d-c paths by an a-c path. As might be expected, a perfectly satisfactory circuit may be obtained by replacing the second path instead of the first. Figure 5-14 shows such a circuit, and Fig. 5-15 its waveforms.

The stable state is with  $V_1$  on and  $V_2$  off. The trigger permits the plate of  $V_1$  to rise and this rise is coupled to the grid of  $V_2$ . The cathode of  $V_2$  is thus lifted; because of  $C$  the cathode of  $V_1$  is also lifted, and  $V_1$  is turned off still further. The circuit is now in its quasi-stable state. Electron current is flowing up  $R$ , from left to right through  $C$ , and up through  $V_2$ . This current through  $C$  causes the cathode of  $V_1$  to fall exponentially toward  $-E_{kk}$  with a time constant of  $RC$  seconds, and it is this exponential which times the duration of the rectangle.

Finally, the cathode falls far enough plate of  $V_1$  falls and with it the grid of  $V_2$ ; and  $V_2$  is cut off once more. The overshoots are caused by the

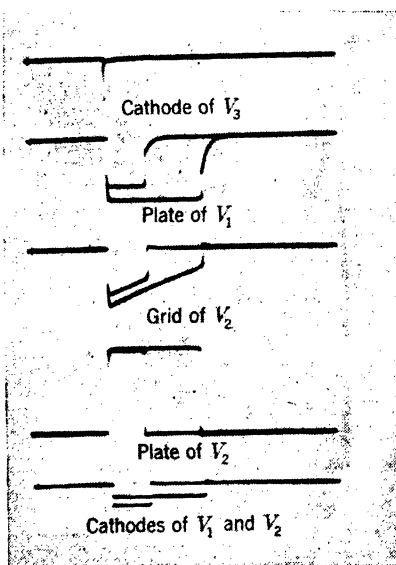


FIG. 5-13.—Waveforms of the cathode-coupled monostable multivibrator of Fig. 5-12. The trace was about 1250  $\mu\text{sec}$  long; the amplitude of the waveform at the plate of  $V_2$  about 90 volts.

to permit  $V_1$  to come on again; the plate of  $V_1$  falls and with it the grid of  $V_2$ ; and  $V_2$  is cut off once more. The overshoots are caused by the recharging of  $C$  through  $r$  and  $V_1$ .

The unusual feature of this circuit is that the timing network is in a cathode circuit and not in a grid circuit. Such an arrangement is especially valuable for the generation of very short rectangles since  $R$  can be made small. The circuit is also favorable for the generation of short rectangles because the plate of  $V_2$  is free; a fast waveform can therefore be taken from it.

#### 5-6. Astable Multivibrators.—

In Fig. 5-16 is illustrated the basic plate-to-grid-coupled astable multivibrator,<sup>1</sup> derived from the monostable form in Fig. 5-10. By the replacement of the one remaining a-c-d-c coupling with an a-c coupling both states are made quasi-stable. The waveforms are shown in Fig. 5-17.

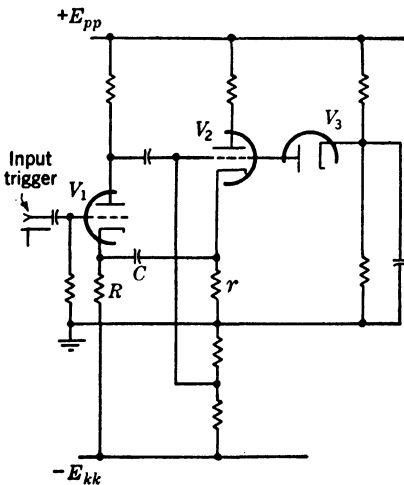


FIG. 5-14.—Another form of cathode-coupled monostable multivibrator (timing network in cathode circuit).

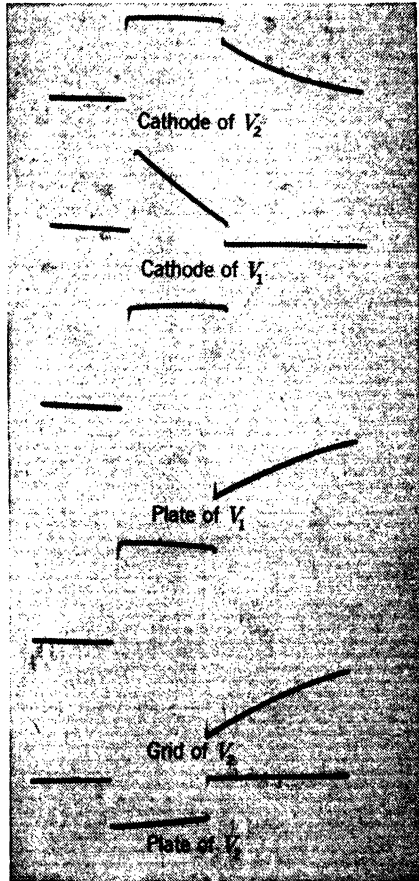


FIG. 5-15.—Waveforms of the cathode-coupled monostable multivibrator of Fig. 5-14. The trace was about 1250  $\mu$ sec long; the amplitude of the waveform at the plate of  $V_2$  about 50 volts.

A cathode-coupled astable multivibrator can be obtained by combining the two monostable forms described in the last section. Such a circuit is useful mainly as a highly unsymmetrical oscillator, with one

<sup>1</sup> Astable multivibrators have been called "free-running" or "self-running" types. In England, the word multivibrator tends to be restricted to astable circuits.

part of the cycle much shorter than the other. It will be described in Sec. 5-11, on highly unsymmetrical astable multivibrators.

A symmetrical astable multivibrator, which makes use of the same condenser for timing both halves of the cycle, is shown in Fig. 5-18 and its waveforms are illustrated in Fig. 5-19.

It should be noticed that although a-c cross-couplings are used from each plate to the opposite grid, the time constants are made very long compared with the period of the multivibrator. There is, therefore, effectively no differentiation or timing action in those networks, and the timing action is confined to the network consisting of  $C$ ,  $R_1$ , and  $R_2$ . The advantages in using a-c instead of a-c-d-c cross couplings are ease of design and freedom from the necessity of using accurate components.

Initially  $V_1$  is off and  $V_2$  is on. Electron current is flowing up through  $R_1$ , from left to right through  $C$ , and up through  $V_2$  to the plate supply. This current

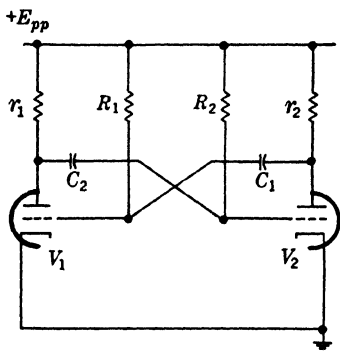


FIG. 5-16.—Basic plate-to-grid-coupled astable multivibrator.

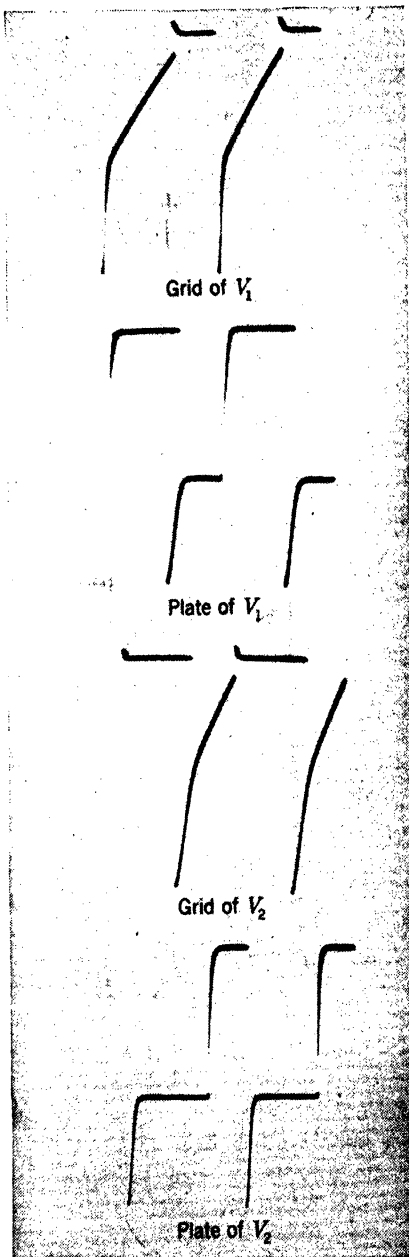


FIG. 5-17.—Waveforms of the plate-to-grid-coupled astable multivibrator of Fig. 5-16. The trace was about 1250  $\mu\text{sec}$  long; the amplitude of the plate waveforms about 180 volts.

through  $C$  is causing the cathode of  $V_1$  to fall toward ground along an exponential with a time constant  $R_1C$ . Incidentally, the plate of  $V_2$  and therefore the grid of  $V_1$  are rising because the current through  $V_2$  decreases as  $C$  charges. Thus the cathode and grid of  $V_1$  are approaching each other, and, after a definite time, current can begin to flow in  $V_1$ . A regenerative action now takes place, in which both the plate-to-grid and cathode couplings are involved. After a very short time, therefore, a new configuration is realized, in which  $V_1$  is on and  $V_2$  is off. The action now takes place exactly as before, except that the electron current flows from right to left through  $C$  and the voltage across  $C$  acts as the timing waveform for the other portion of the cycle. The

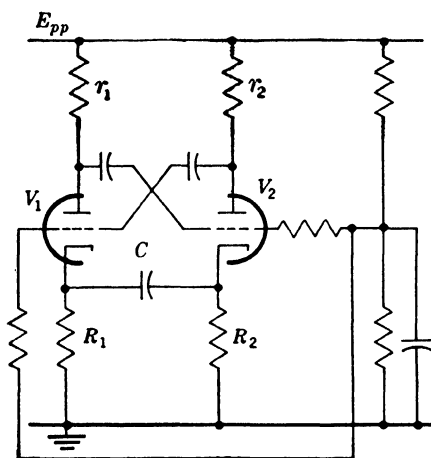


FIG. 5-18.—Symmetrical cathode-coupled astable multivibrator.

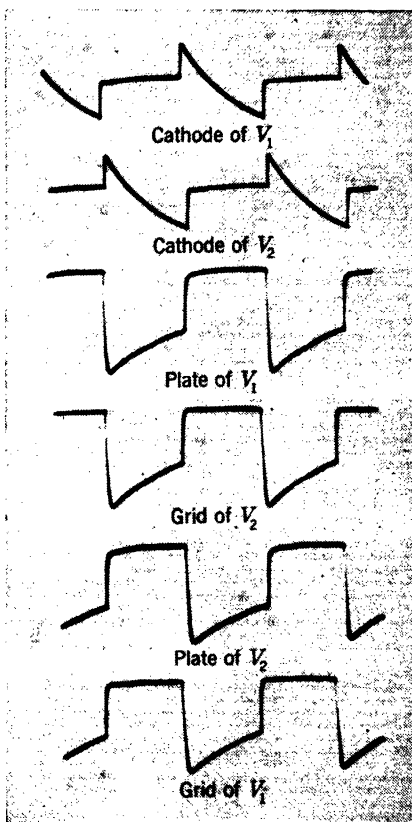


FIG. 5-19.—Waveforms of the cathode-coupled astable multivibrator of Fig. 5-18. The trace was about 125  $\mu\text{sec}$  long; the amplitude of the cathode waveforms about 80 volts peak-to-peak.

interplay between the cathodes is important and may be a little confusing; it may not at first be clear why, although at one time the cathode of  $V_1$  is capable of raising the cathode of  $V_2$ , at a later time it is incapable of preventing itself from being raised by the cathode of  $V_2$ . The explanation lies in the nature of the output impedance at the cathode of a tube; speaking roughly, it is easy to pick up the cathode but hard to keep it down.

**5-7. Analysis of the Transition between States.**—In the preceding sections the general features of operation of several basic types of multivibrators have been discussed. The two most important processes that multivibrators perform will now be analyzed in greater detail and with quantitative results. The present section will describe the transition from one state to the other; the next section will treat the timing operation.

It should be clearly understood from the start that an exact analysis of a multivibrator, especially during that instant when it is changing states, is practically impossible. So numerous are the elements involved.

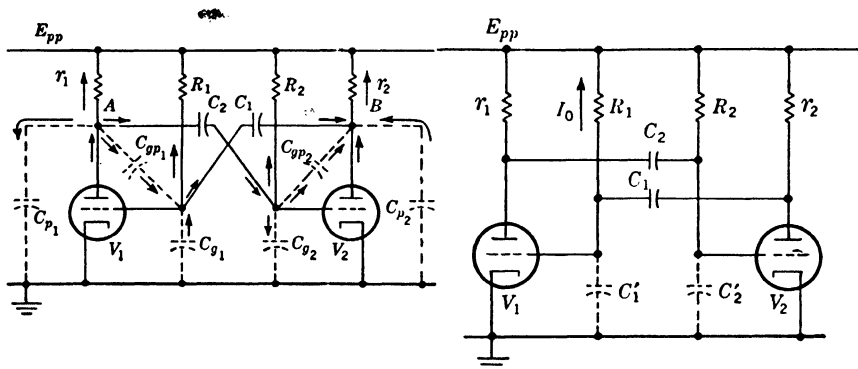


FIG. 5-20(a).—Circuit of Fig. 5-16 redrawn to show stray capacities and electron currents.  $V_1$  is coming on;  $V_2$  is being turned off.

FIG. 5-20(b).—Circuit approximately equivalent to that of Fig. 5-20(a) to be used in analysis.  $C'_1 = C_{g1} + C_{p1} + (1 + A_1)C_{gp1} + (1 + A_2)C_{gp2}$ ;  $C'_2 = C_{g2} + C_{p2} + (1 + A_1)C_{gp1} + (1 + A_2)C_{gp2}$ .

both those which are intentionally and those which are unavoidably present, and so far-reaching are the effects of the nonlinearity of the vacuum tubes, that every analysis must make several simplifying assumptions and thereby lose its exactness. This is true both of those analyses which concern themselves with the entire cycle<sup>1</sup> and those, like the ones now to be presented, which break the cycle down into two parts and treat the transition separately from the timing.

As a typical circuit for analysis the ordinary plate-to-grid-coupled astable multivibrator of Fig. 5-16 will be used. Figure 5-20a shows this circuit redrawn to include the various stray capacities which form the principal limitations on the speed with which the change of state can take place. The arrows represent the directions of electron flow during the time when  $V_1$  is coming on and  $V_2$  is being turned off.

<sup>1</sup> An excellent example of such an analysis, which uses as its basis an analytical expression approximating the tube characteristics, is the Ph. D. thesis of S. C. Snowdon, Cal. Inst. of Tech., 1945.

The circuit of Fig. 5.20a is difficult to analyze because of the presence of  $C_{op_1}$  and  $C_{op_2}$ , which prevent the circuit from being considered as two separate loops. Figure 5.20b represents an approximately equivalent circuit, in which those capacities, together with  $C_{p_1}$  and  $C_{p_2}$ , have been absorbed into  $C'_1$  and  $C'_2$ . Essentially the circuit of Fig. 5.20a may be regarded as a current source at point  $A$  (current supplied by  $V_1$ ) and a current sink at  $B$  (current taken off through  $r_2$ ) with various associated networks. The capacities which take current from  $A$  are  $C_{p_1}$ ,  $C_{op_1}$ ,  $C_2$  in series with  $C_{a_2}$ , and  $C_2$  in series with  $C_{op_2}$ ; those which give current to  $B$  are  $C_{p_2}$ ,  $C_{op_2}$ ,  $C_1$  in series with  $C_{a_1}$ , and  $C_1$  in series with  $C_{op_1}$ . Now if it is assumed that  $C_1$  and  $C_2$  are large compared with the other capacities, and if it is remembered that  $C_{op_1}$  and  $C_{op_2}$  act effectively like capacities of value  $(1 + A_1)C_{op_1}$  and  $(1 + A_2)C_{op_2}$ , where  $A_1$  is the ratio of the speeds with which the plate and grid of  $V_1$  are moving and  $A_2$  is the same for  $V_2$ , then the capacitive load on  $A$  can be represented, as in Fig. 9.20b, as  $C'_2 = C_{a_1} + C_{p_1} + (1 + A_1)C_{op_1} + (1 + A_2)C_{op_2}$ , and the capacitive source for  $B$  can be represented as

$$C'_1 = C_{a_1} + C_{p_2} + (1 + A_1)C_{op_1} + (1 + A_2)C_{op_2}.$$

In order to simplify the analysis it is assumed that  $A_1$  and  $A_2$ , and therefore  $C'_1$  and  $C'_2$ , are constant. However, it should be understood that this is not strictly true and constitutes another departure from exactness. It should also be noted that the above definitions of  $A_1$  and  $A_2$  imply  $A_1 = 1/A_2$ .

On the basis of the equivalent circuit, Fig. 5.20b, the analysis can proceed. The waveform at the grid of  $V_1$  for the period after  $V_1$  has begun to come on is assumed to be some function, given as a power series with undetermined coefficients, of the time  $t$  that has elapsed since the grid passed the grid base at  $-E_c$  volts. Both  $V_1$  and  $V_2$  are assumed to have the perfect broken-line characteristic shown in Fig. 5.21 with a slope of  $g_m$  amps/volt and a grid base of  $E_c$  volts. By means of this characteristic the waveform at the grid of  $V_1$  is translated into the current through  $V_1$  as a function of time. This current is integrated in  $C'_2$  (it is assumed that  $r_1$  draws negligible current) to give the corresponding waveform at the grid of  $V_2$ . Use of the tube characteristic of  $V_2$  gives the current through  $V_2$  as a function of time. If it is assumed that the current through  $r_2$  does not change appreciably during the change of state, then the current available for  $C'_1$  is the amount by which the current

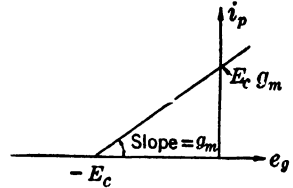


FIG. 5.21.—Ideal broken-line characteristic assumed for  $V_1$  and  $V_2$ .

through  $V_2$  has decreased plus the current  $I_0$  flowing through  $R_1$ . This sum is integrated in  $C'_1$  to yield the original waveform in a new power series containing not only the undetermined coefficients but also  $I_0$ ,  $g_m$ ,  $C'_1$ , and  $C'_2$ . This power series and the original one are set equal term by term<sup>1</sup> and the coefficients are easily found in terms of the four parameters just listed. The voltage  $v_1$  at the grid of  $V_1$  is then found to be

$$v_1 = -E_c + \frac{I_0}{C'_1} \left[ t + \frac{1}{3!} \frac{g_m^2}{C'_1 C'_2} t^3 + \frac{1}{5!} \left( \frac{g_m^2}{C'_1 C'_2} \right)^2 t^5 + \dots \right]$$

and the voltage  $v_2$  at the grid of  $V_2$  is

$$v_2 = -\frac{I_0 g_m}{C'_1 C'_2} \left[ \frac{1}{2!} t^2 + \frac{1}{4!} \frac{g_m^2}{C'_1 C'_2} t^4 + \frac{1}{6!} \left( \frac{g_m^2}{C'_1 C'_2} \right)^2 t^6 + \dots \right].$$

<sup>1</sup> If it is assumed that  $v_1 = -E_c + bt + ct^2 + dt^3 + \dots$ , then  $i_1$ , the current through  $V_1$ , is

$$i_1 = bg_m t + cg_m t^2 + dg_m t^3 + \dots$$

If all of  $i_1$  passes through  $C'_2$ , then the voltage  $v_2$  at the grid of  $V_2$  is specified by

$$v_2 = - \left( \frac{bg_m}{C'_2} t + \frac{cg_m}{C'_2} t^2 + \frac{dg_m}{C'_2} t^3 + \dots \right).$$

Integrating:

$$v_2 = - \left( \frac{1}{2} \frac{bg_m}{C'_2} t^2 + \frac{1}{3} \frac{cg_m}{C'_2} t^3 + \frac{1}{4} \frac{dg_m}{C'_2} t^4 + \dots \right).$$

The current available for charging  $C'_1$  is

$$I_0 + \frac{1}{2} \frac{bg_m^2}{C'_2} t^2 + \frac{1}{3} \frac{cg_m^2}{C'_2} t^3 + \frac{1}{4} \frac{dg_m^2}{C'_2} t^4 + \dots$$

Dividing by  $C'_1$  and integrating:

$$v_1 = -E_c + \frac{I_0}{C'_1} t + \frac{1}{6} \frac{bg_m^2}{C'_1 C'_2} t^3 + \frac{1}{12} \frac{cg_m^2}{C'_1 C'_2} t^4 + \frac{1}{20} \frac{dg_m^2}{C'_1 C'_2} t^5 + \dots$$

Equating the two expressions for  $v_1$  term by term:

$$\begin{aligned} b &= \frac{I_0}{C'_1} \\ c &= 0 \\ d &= \frac{1}{6} \frac{bg_m^2}{C'_1 C'_2} = \frac{1}{6} \frac{I_0 g_m^2}{C'_1{}^2 C'_2} \\ e &= 0 \\ f &= \frac{1}{20} \frac{dg_m^2}{C'_1 C'_2} = \frac{1}{120} \frac{I_0 g_m^4}{C'_1{}^3 C'_2}, \text{ etc.} \end{aligned}$$

From these coefficients come the expressions in the text for  $v_1$  and  $v_2$ .

$$\text{For } I_0 = 3 \times 10^{-4}, \quad g_m = 10^{-3}, \quad C'_1 = C'_2 = 6 \times 10^{-11},$$

$t$  in microseconds,

$$\begin{aligned} v_1 &= 5.6t + 258t^3 + 3580t^5 + \dots \\ v_2 &= 46.3t^2 + 1075t^4 + 9950t^6 + \dots \end{aligned}$$

In order to illustrate the waveforms represented by these solutions, it is necessary to assume a set of representative values for  $I_0$ ,  $g_m$ ,  $C'_1$ , and  $C'_2$ . Such a set might be:  $I_0 = \frac{1}{3}$  ma;  $g_m = 1000$   $\mu$ mhos;  $C'_1 = C'_2 = 60$   $\mu$ f; and  $E_c = 15$  volts. These might, for instance, be a fair set of values for a multivibrator made of the two sections of a 6SN7, with  $R_1 = 1M$ , with each grid-to-ground and plate-to-ground capacity = 15  $\mu$ f, each grid-to-plate capacity = 6  $\mu$ f, and  $A_1 + A_2 = 3$ . Under these conditions the waveforms at the two grids are calculated to be as shown in Fig. 5-22. In calculating these waveforms it was necessary to include the first seven terms of each series. Experimental rise times agree very well with these calculated ones.

It may be worth while to point out very briefly those respects in which this analysis would have to be improved before it could be considered accurate. Probably the most important improvement would be to use the actual grid-to-plate characteristic for the tubes instead of the highly idealized one of Fig. 5-21. Second, the variation of  $A_1$  and  $A_2$  during the action should not be ignored. Third, the currents through  $r_1$  and  $R_2$  should be considered, as well as the change of currents through  $R_1$  and  $r_2$ . The effect of having  $C_1$  and  $C_2$  finite should be considered. The exact circuit of Fig. 5-20a should be used instead of the approximately equivalent circuit of Fig. 5-20b. Account should be taken of the fact that during the very early part of the action the larger part of  $I_0$  is flowing not through  $C_2$ , but through  $C_1$ . Finally, the effect of the grid current in  $V_1$  upon the end of the action should be included.

The importance of this analysis is that it provides a figure of merit,  $g_m^2/C'_1C'_2$ , for tubes to be used in multivibrator circuits and therefore emphasizes, perhaps in a more quantitative manner than previously, the necessity of keeping stray capacities small and of using tubes with high transconductance.

**5-8. Analysis of the Timing Process.**—The purpose of this section is to derive some results which will be useful in Sec. 5-13 on stabilization of time intervals, and to make it possible to calculate in advance the time intervals which will be established by a multivibrator.

For the purposes of analysis the plate-to-grid-coupled astable multivibrator of Fig. 5-16 will be considered with the voltage  $v_1$  on the grid of  $V_1$  as is shown in Fig. 5-23. The initial voltage from which the grid must recover is  $-E_i$ ,  $E_u$  is the voltage to which  $R_1$  is returned ( $E_u = E_{pp}$  in

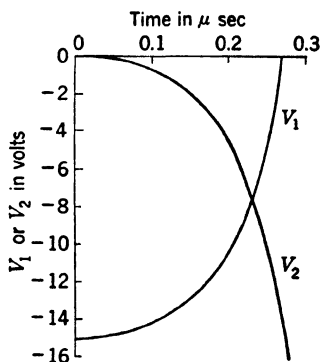


FIG. 5-22.—Calculated waveforms for the grids of a typical multivibrator.



Fig. 5-16), and  $-E_c$  is the cutoff voltage of  $V_1$  (that is, approximately the voltage at which the transition of state occurs).

Then

$$v_1 = E_u - (E_u + E_i)e^{-\frac{t}{R_1C_1}}. \quad (1)$$

To find  $T_1$ , the duration of the quasi-stable state during which  $V_1$  is off,  $v_1$  is set equal to  $-E_c$  and Eq. (1) is solved for  $t$ . It will be found that

$$T_1 = R_1C_1 \ln \frac{E_u + E_i}{E_u + E_c}. \quad (2)$$

If the circuit is symmetrical and  $E_u$ ,  $E_i$ , and  $E_c$  are the same for both portions of the cycle, then the duration  $T$  of a complete cycle is given by

$$T = T_1 + T_2 = (R_1C_1 + R_2C_2) \ln \frac{E_u + E_i}{E_u + E_c}. \quad (3)$$

This expression is slightly inexact for two reasons. First, it ignores the presence of the various stray capacities shown in Fig. 5-20a. These

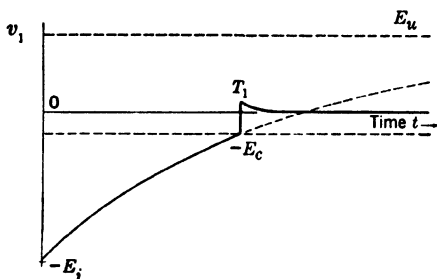


FIG. 5-23.—Multivibrator grid waveform as used in calculating the period.

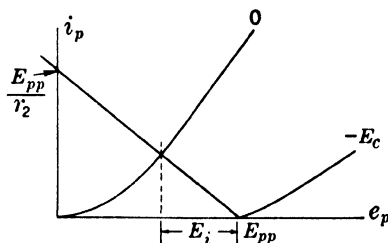


FIG. 5-24.—Graphical method for calculating  $E_i$  and  $E_c$ .

may be included by writing  $C_1 + C_{g_1} + C_{gp_1}$  for  $C_1$  and  $C_2 + C_{g_2} + C_{gp_2}$  for  $C_2$ . Second, it ignores the fact that there exists a large negative overshoot at the start of the exponential waveform (see Fig. 5-17). The effect of this overshoot will be to discharge the timing condensers somewhat, that is, to reduce the effective  $E_i$ . Therefore, if  $E_i$  is estimated by the method given below, the calculated period may be slightly too long.

In order to use Eq. (3), estimates of  $E_c$  and  $E_i$  must be made. This can be done very easily from the tube curves and with an accuracy sufficient for most purposes.  $E_c$  can be taken to be the grid base when the plate voltage is  $E_{pp}$ ;  $E_i$  is approximately the drop across the plate resistor at zero grid bias. These relations are illustrated in Fig. 5-24. For a typical triode like a 6SN7, with  $E_u = E_{pp} = 250$  v and  $r_1 = r_2 = 10$  K,  $E_i = 130$  v and  $E_c = 14$  volts, so  $\ln \frac{E_u + E_i}{E_u + E_c} = 0.36$ . If  $r_1 = r_2 = 50$  K,

the last quantity becomes 0.53. In the latter case, if the circuit is symmetrical so that  $R_1C_1 = R_2C_2 = RC$ , it will oscillate at a frequency of about  $1/RC$  cps.

**5-9. Obtaining Fast Transition.**—In Sec. 5-7 it was shown that the speed of transition depends primarily upon the quantity  $g_m^2/C_1'C_2'$ . On the basis of this fact there are listed the following practical methods by which transition times of  $0.5 \mu\text{sec}$  are easy to obtain under most circumstances and by which transition times of  $0.05 \mu\text{sec}$  are possible.

1. The stray capacities  $C_1'$  and  $C_2'$  should be kept to a minimum—that is, grid-to-ground, plate-to-ground, and grid-to-plate capacities should be kept small. Miniature tubes in general have inter-electrode capacities about one half as large as big tubes have, and pentodes have smaller grid-to-plate capacities than triodes have. The wiring should be done carefully and kept short. The ultimate in this respect can be achieved with the use of sub-miniature solder-in tubes. Any circuit attached to the multivibrator should present as low a capacity as possible. This is true of the trigger source, which should be disconnected from the multivibrator by inserting the triggers through a diode. If the output must be fed into a circuit with a large input capacity, it may first be fed into a cathode follower and from there into the desired circuit.
2. The plate resistors  $r_1$  and  $r_2$  should be kept fairly small so that the tubes will be operating at high current and therefore at high  $g_m$ . Values from 3 K to 20 K are usual. Inductive compensation may be used to increase the current available for  $C_1'$  and  $C_2'$ .
3. High- $g_m$  tubes should be used. Among triodes are: 6J4, 7F8, 6K4 (SD834), 6J6, 6SN7. Among pentodes are: 6AC7, 6AK5, 6AG7.

**5-10. Monostable Circuits for Very Short Pulses.**—The principles discussed in the last section are most important when it is necessary to use a multivibrator to generate very short pulses, whose length may be, for example, from  $0.1$  to  $2 \mu\text{sec}$ . Obviously, the generation of such pulses imposes very stringent limits on the time available for transition between states. It should be remarked, incidentally, that multivibrators are not usually the most satisfactory circuits for this purpose; blocking oscillators and gas-tube circuits are generally superior because of their ability to deliver very large peak currents during the instants when the circuit is changing states.

Figure 5-25 illustrates a plate-to-grid-coupled monostable circuit, modified from the basic circuit of Fig. 5-10 by returning  $R$  to ground instead of to the plate supply voltage in order that a small value of resistance may be used.

The major fault of this circuit is that every electrode is involved in the

action; therefore, there is no free point which can be loaded with an output circuit without slowing the action. Two general methods are available for overcoming this difficulty: use of an electron-coupled multivibrator, and use of a cathode-coupled multivibrator.

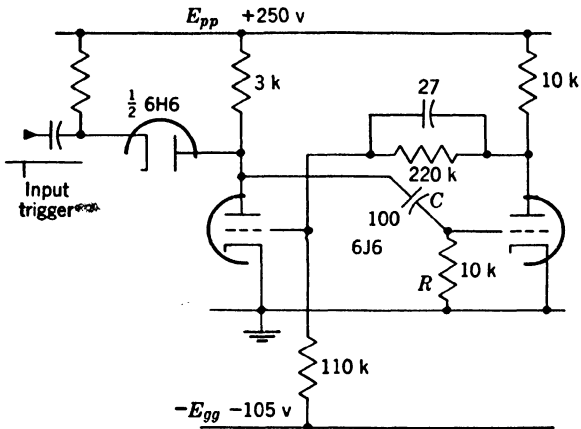


FIG. 5-25.—Plate-to-grid-coupled monostable multivibrator for generating short pulse.

Figure 5-26 illustrates an electron-coupled monostable multivibrator, in which  $V_2$  and the cathode, grid, and screen of  $V_1$  act as an ordinary circuit of the type shown in Fig. 5-25. The plate of  $V_1$  is then quite free and from it can be taken a fast negative pulse.

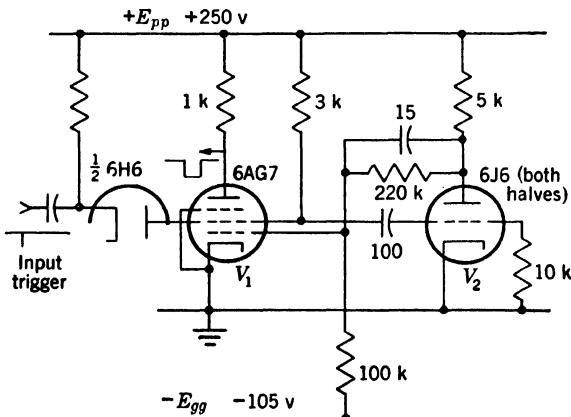


FIG. 5-26.—Electron-coupled monostable multivibrator for generating short pulse.

Among cathode-coupled types, that of Fig. 5-14 is especially useful since the timing resistor is in a cathode and can therefore be made very small. Figure 5-27 shows a circuit of this type, suitable for generating pulses of 0.5  $\mu$ sec.

There exists one more rather novel cathode-coupled type which finds use in generating pulses of stable and easily calculated duration. In

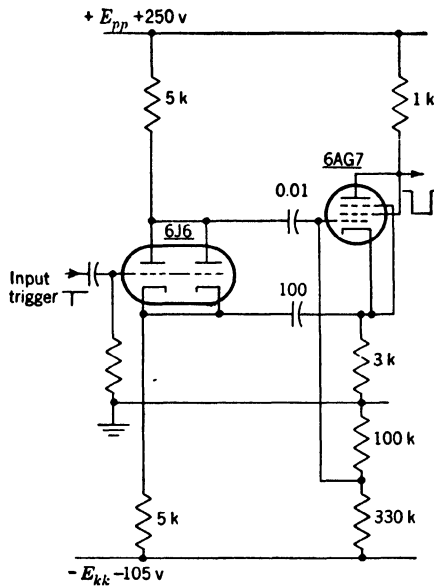


FIG. 5-27.—Cathode-coupled monostable multivibrator for generating short pulse.

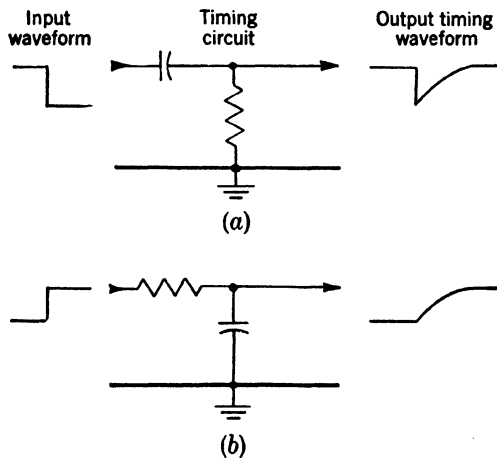


FIG. 5-28.—The generation of a timing waveform by (a) a differentiating network, and (b) an integrating network.

every one of the multivibrators thus far described the timing operation has been carried out essentially by an  $RC$  differentiating circuit, as illustrated in the upper half of Fig. 5-28. An integrating circuit might

be used equally well, however, as shown in the lower half of the figure, and the circuit to be described makes use of timing of this type.

Figure 5-29 illustrates the circuit in question and Fig. 5-30 its waveforms. Initially  $V_1$  is on, the current through  $V_1$  flowing through  $R_2$  and thus providing sufficient bias to keep  $V_2$  off. When the positive trigger is injected at the grid of  $V_2$  through the diode  $V_3$ , current flows through  $V_2$  and through  $R_2$  and  $R_1$ . The effect of this is to raise the cathode of  $V_1$  rapidly; the grid of  $V_1$  rises only slowly, however, with a speed limited by  $RC$ , and therefore  $V_1$  is turned off. Its plate rises, and this rise is coupled back to the grid of  $V_2$  by a coupling circuit whose time constant is *made* long compared with the duration of the pulse to

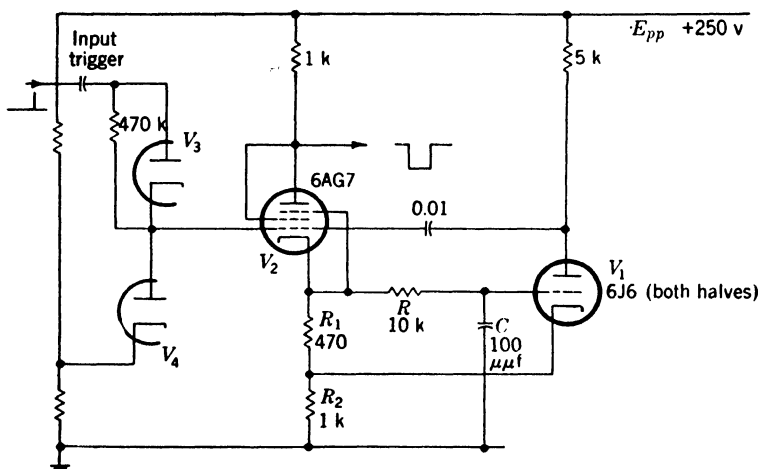


FIG. 5-29.—Cathode-coupled monostable multivibrator using an integrating network to generate the timing waveform.

be generated. The action is regenerative and after a very short time,  $V_1$  is off and  $V_2$  is on. The amplitude of the positive swing of the grid and cathode of  $V_2$  is prevented from exceeding a certain definite value by the diode  $V_4$ . Now the grid of  $V_1$  begins to rise along an exponential determined by  $R$  and  $C$ . After a definite time, it will have risen far enough to permit  $V_1$  to begin conducting again and the circuit will revert quickly to its initial state. The time  $T$ , the duration of the pulse, is given by the approximate formula

$$T = RC \ln \frac{V_2 - R_2 i_1}{\frac{R_1 V_2}{R_1 + R_2} + E_c}$$

where  $V_2$  is the voltage to which the cathode of  $V_2$  rises,  $i_1$  is the quiescent current through  $V_1$ , and  $E_c$  is the grid base of  $V_1$ .

**5-11. Obtaining Fast Recovery—Highly Unsymmetrical Astable Multivibrators.**—After every abrupt change of state in a multivibrator, some of the condensers have been “left behind,” as it were, and require a certain time to become charged to their steady voltages. Until these transients have died away the circuit has not recovered, and in general is not ready to perform another change of state, at least not in precisely the same way as it would if it were fully recovered. For instance, a bistable circuit, acting as a scale-of-two pulse counter, will not resolve two incoming pulses whose separation is much smaller than its recovery time. Thus the problem of obtaining fast recovery is often of great importance.

The speed of recovery depends inversely upon the size of the condenser to be recharged and directly upon the amount of current which is made to flow through it. In the case of bistable circuits, usually the only condensers present are the strays and the “speeding-up” condensers, which in most circuits will not exceed  $50\ \mu\text{mf}$ , with correspondingly small recovery times (for example, about  $1\ \mu\text{sec}$ ). Monostable and astable forms, however, may possess large timing condensers, the recharging of which becomes a serious problem when it is desired to make the circuit repeat a long quasi-stable state after a short time. In fact, the problem becomes most serious when it is desired to build a highly unsymmetrical astable multivibrator because then the large timing condenser, which established the long part of the cycle, must be recharged during the short part of the

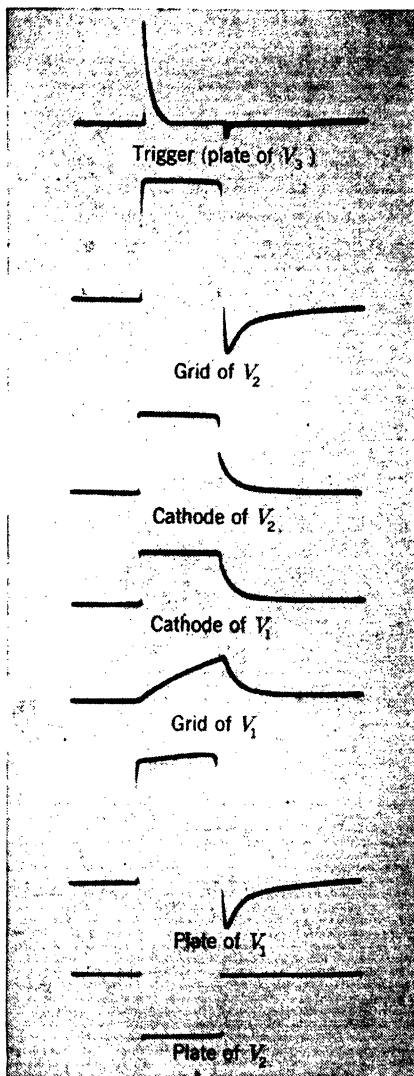


FIG. 5-30.—Waveforms of the circuit of Fig. 5-29. The trace was about  $125\ \mu\text{sec}$  long; the amplitude of the waveform at the plate of  $V_2$  about 60 volts.

cycle. Accordingly, the methods for making a multivibrator recover quickly will be illustrated in this section by several highly unsymmetrical astable circuits, from which can easily be derived monostable circuits if they are needed.

As an illustration of the problem of designing a highly unsymmetrical circuit, Fig. 5-31 shows a plate-to-grid-coupled astable circuit which might, at first glance, seem to be so arranged that the part of the cycle during which  $V_1$  is off and  $V_2$  is on would last about  $1000\ \mu\text{sec}$  (approximately  $\frac{1}{3} R_1 C_1$ ), while the other part of the cycle, since it depends only on the product  $R_2 C_2$ , could have any length down to zero. Closer examination, however, reveals that since the time needed to recharge  $C_1$

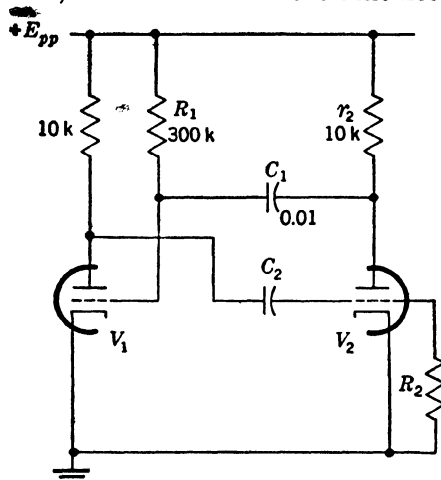


FIG. 5-31.—Incorrect highly unsymmetrical astable multivibrator.

will be several hundred microseconds for the circuit values given, there is actually a very definite lower limit to the length of the short part of the cycle.

Several methods are available for reducing the recharging time. If  $C_1$  were reduced to  $0.001\ \mu\text{f}$  and  $R_1$  increased to  $3M$ , the recharging would occupy only 30 or 40  $\mu\text{sec}$ , and reduction of  $C_1$  to  $100\ \mu\text{f}$ , with  $R_1$  equal to  $30M$ , would permit the short part of the cycle to be as little as 3 or 4  $\mu\text{sec}$ . One method, therefore, is to make the timing condenser as small, and the timing resistor as large, as other considerations will permit.

The following methods of reducing the recharging time, which are listed in the order in which they should be used, are also available:

1. The plate resistor  $r_2$  may be returned to a higher plate supply voltage, with a plate-catching diode inserted as in Fig. 5-32. The charging current is thereby increased, and only the fast initial part of the recharging is allowed to take place.

2. The plate resistor  $r_2$  may be lowered in value. In general, this will require that a heavier current tube be used for  $V_2$  since  $r_2$  was presumably already as small as the tube ratings permitted.
3. After Steps 1 and 2 are carried out the main limitation upon the charging current is the resistance of the diode formed by the grid and cathode of  $V_1$ ; a parallel diode can be added to reduce this resistance.
4. Finally, the coupling from the plate of  $V_2$  to the grid of  $V_1$  may be made through a cathode follower, in which case the current available for recharging is practically the entire current flowing through the cathode follower.

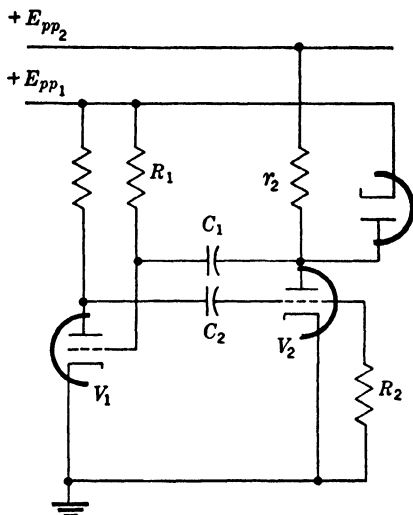


FIG. 5-32.—The use of a plate-catching diode to eliminate the slow portion of the recharging period.

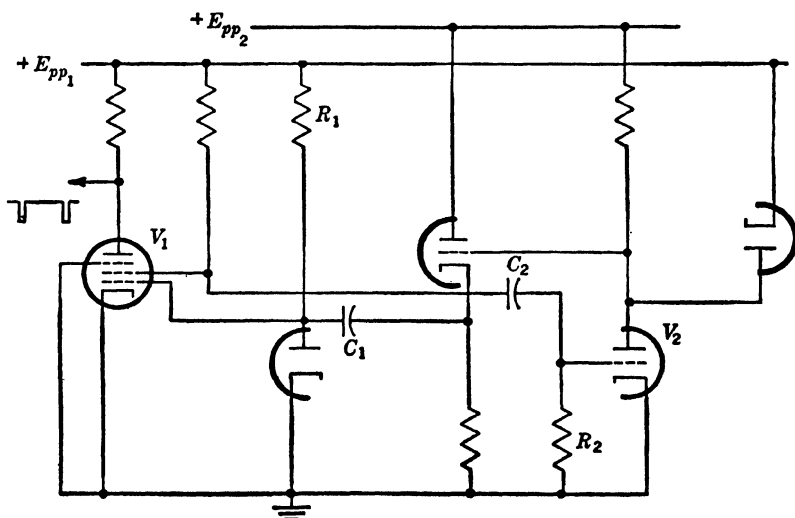


FIG. 5-33.—Highly unsymmetrical plate-to-grid-coupled astable multivibrator.

These methods are illustrated in the circuit of Fig. 5-33. The use of a pentode for  $V_1$  provides a free electrode (plate) from which a fast negative pulse of short duration can be taken. The complexity of the



circuit illustrates, in a very convincing manner, the limitations in the use of the multivibrator in highly unsymmetrical circuits.

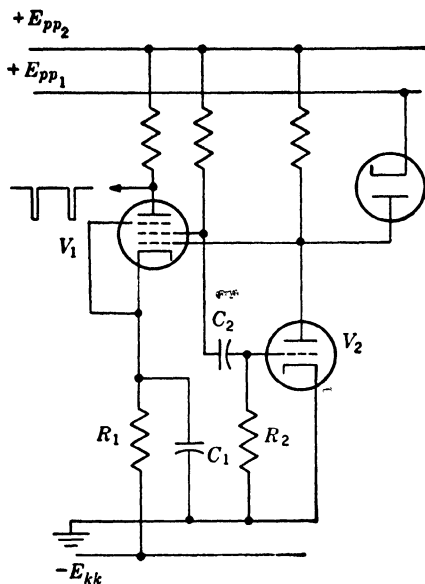


FIG. 5-34.—Another form of highly unsymmetrical plate-to-grid-coupled multivibrator.

which can be made unsymmetrical by making  $R_1$  larger than  $R_2$ . This form has the unique advantage that the timing condenser  $C$  cannot fail

A more economical way of getting  $C_1$  into the cathode circuit of a tube (where it can be rapidly recharged) is to put it directly into the cathode of  $V_1$ , as in the circuit of Fig 5-34. Here  $V_1$  is off during the long part of the cycle, its cathode dropping toward  $-E_{kk}$  with a time constant  $R_1C_1$ . After a definite time  $V_1$  comes on regeneratively, and virtually all the cathode current of  $V_1$  is used to recharge  $C_1$ . After a short time, of course,  $V_2$  comes back on and the circuit reverts to its initial state. A short, fast, negative pulse is taken from the plate of  $V_1$ .

Among cathode-coupled types, several varieties are useful. One is the symmetrical circuit of Fig. 5-18,

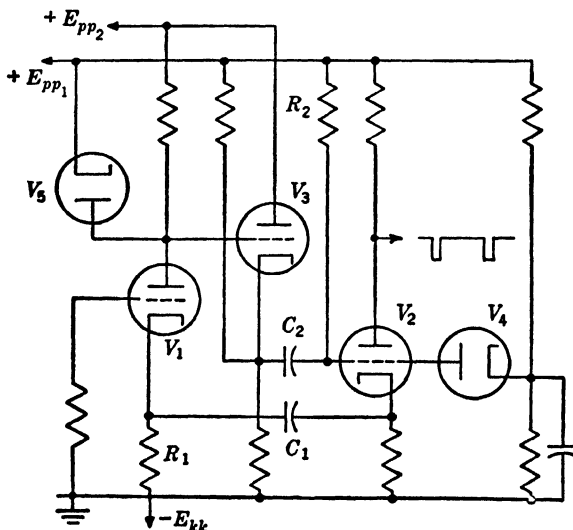


FIG. 5-35.—Highly unsymmetrical cathode-coupled astable multivibrator.

to be completely recovered since it determines not one but both portions of the cycle. Another useful circuit is that of Fig. 5-29.

The other cathode-coupled type, already mentioned in Sec. 5-6, is obtained by combining the two monostable cathode-coupled forms, one with the timing network in the grid, and the other in the cathode, both described in Sec. 5-4. This circuit is illustrated in Fig. 5-35. Here  $C_1$  and  $R_1$  time the short part of the cycle (during which  $V_1$  is off), and  $C_2$  and  $R_2$  time the long part of the cycle (when  $V_2$  is off). The condenser  $C_2$  is the difficult one to restore; hence the cathode follower  $V_3$  and the diode  $V_4$  are included to present a low-resistance path for the recharging current. The output is taken from the plate of  $V_2$ .

**5-12. Triggering and Synchronization.**—The ideal triggering arrangement would include a switch which would be closed during the initial voltage step of the trigger, but which would then open to disconnect the multivibrator from the trigger source. In this way the multivibrator is freed from the reversing tendency of the trigger, which is now changing in the wrong direction, and from whatever loading the trigger source may present.

A series diode is an excellent way to accomplish this decoupling. The stray capacity across most diodes is very small, and by inserting the diode in the proper direction

triggers of either polarity can be injected. Very occasionally the leakage between heater and cathode of the diode becomes a matter of concern.

Examples of the use of diodes for trigger injection may be found in all of the monostable and bistable circuits which have been discussed. It should be noticed that the same diode can be used both for injecting the trigger and for catching the plate below the plate supply to reduce the recovery time; a bistable circuit of this sort, which makes the best simple scale-of-two circuit available, is shown in Fig. 5-36.

Triodes may also be used for triggering (see Fig. 5-37). The triggering tube should normally be biased off so that it will not load the multivibrator, and a positive trigger is placed on its grid, momentarily turning it on and effectively injecting a negative trigger into the multivibrator.

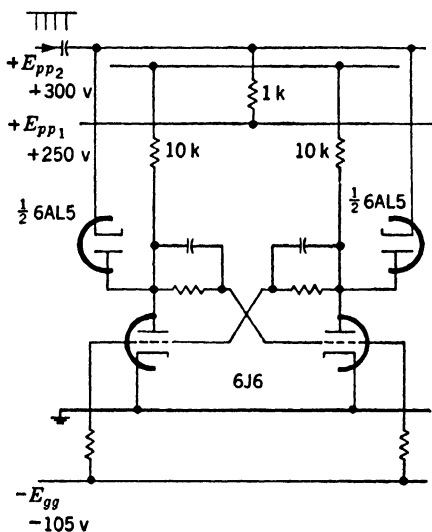


FIG. 5-36.—The use of diodes for both trigger injection and reduction of recovery time.

Where tube economy is so important that a diode cannot be afforded, the triggers may be coupled into the multivibrator directly through a condenser. The danger here is that the trigger will be differentiated and the resulting overshoot will turn the multivibrator off again as soon as it

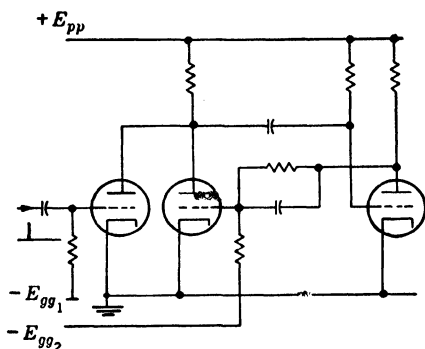


FIG. 5-37.—The use of a triode to trigger a multivibrator.

has begun to trigger. From this point of view it would be desirable to use a large coupling condenser for the trigger. However, a large capacity must not be connected to any point which will move fast during the transition. Occasionally there are grids or cathodes which do not move during transition and these make very suitable triggering points. An example is the circuit of Fig. 5-14, where a negative trigger can be placed upon the grid of  $V_1$  through an  $RC$ -network with an amply long time constant. Similarly, a negative trigger may be placed upon the suppressor of a conducting pentode. Cathodes are often good triggering points—for instance, an ordinary astable multivibrator can be synchronized with a train of positive pulses by injecting them at both cathodes across a small common cathode resistor, as in Fig. 5-38. This method is especially useful if the synchronizing pulses are the cathode current pulses from a blocking oscillator or gas tube since all three cathodes can then be tied together as shown.

As a last resort, the pulses can be brought to almost any point through a small condenser, for example, one of  $50\ \mu\text{f}$ . However, the additional capacitive loading on the multivibrator slows down both the transition and the recovery. When the triggers are inserted in this way they should be shaped like those of Fig. 5-39(a) and (b), since these waveforms will give little or no overshoot even when passed through a very small condenser. It will be recognized that waveform (b) is effectively the waveform obtained when (c) is injected through a series diode.

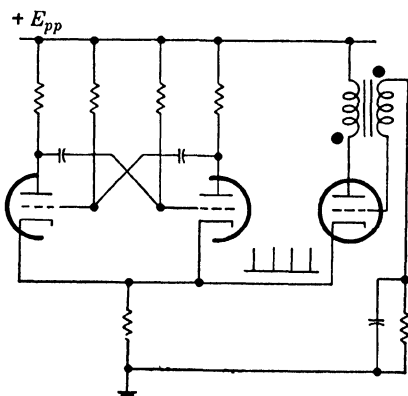


FIG. 5-38.—Synchronization of an astable multivibrator with low-impedance positive pulse from a blocking oscillator (or similar pulse generator).

At this point will be discussed very briefly the details of the synchronizing action by which an injected synchronizing pulse brings to an end a quasi-stable state in a monostable or astable multivibrator. This action is of great importance in the question of phase lock in pulse frequency dividers (see Chap. 16), can be discussed here with sufficient generality to apply to other types of relaxation oscillator besides the multivibrator, and is not so simple that it can be passed by.

The process of terminating a quasi-stable state in a relaxation oscillator with a synchronizing pulse is carried out essentially by adding the synchronizing pulse to the timing waveform on the grid of the "off" tube; therefore the pulse carries that grid above  $-E_c$ , the critical firing voltage, and initiates the flipover. Yet the *exact* moment of flipover is not usually at all well defined—that is, even though the synchronizing pulse ultimately brings about the transition, the exact time delay between synchronizing pulse and transition depends upon both the amplitude and duration of the pulse and may in fact vary so much as to render the circuit useless for an exacting application.

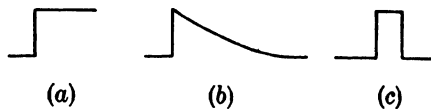


FIG. 5-39.—Good triggering waveforms (a) and (b) and poor triggering waveform (c) for insertion through a small condenser.

That this is so can be understood by considering an ordinary plate-to-grid-coupled astable multivibrator, so arranged that onto the grid of whichever tube is off can be put perfectly rectangular synchronizing pulses which will thus be added to the exponential timing waveform at that grid. Figure 5-40 shows a closeup of the waveform at that grid, under such conditions that the synchronizing pulse is just barely able to bring about the termination of the quasi-stable state. Before the pulse the grid is rising along an exponential curve. When the pulse arrives the grid is suddenly lifted  $V$  volts, which will be sufficient to carry it  $v$  volts above  $-E_c$ . The quantity  $v$  may be called the "effective synchronizing voltage," and depends upon the exact moment at which the trigger arrives. The "off" tube is now conducting somewhat, stray capacities are being charged, the grid of the "on" tube is dropping, and the total effect is to cause the transition to begin. This is indicated by the short rising portion of the grid waveform, which lasts until the synchronizing pulse ends. At this point the grid drops  $V$  volts. If now it is still at  $-E_c$  or higher, the transition will continue; otherwise it

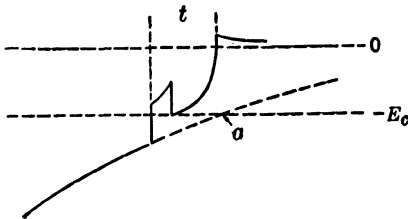


FIG. 5-40.—Closeup of a barely successful synchronizing action.

arrives the grid is suddenly lifted  $V$  volts, which will be sufficient to carry it  $v$  volts above  $-E_c$ . The quantity  $v$  may be called the "effective synchronizing voltage," and depends upon the exact moment at which the trigger arrives. The "off" tube is now conducting somewhat, stray capacities are being charged, the grid of the "on" tube is dropping, and the total effect is to cause the transition to begin. This is indicated by the short rising portion of the grid waveform, which lasts until the synchronizing pulse ends. At this point the grid drops  $V$  volts. If now it is still at  $-E_c$  or higher, the transition will continue; otherwise it

will not take place until the waveform has reached point  $a$ ,<sup>1</sup> at which time the exponential itself reaches  $-E_c$ . In the figure the grid rises exactly  $V - v$  volts during the pulse; hence it returns just to  $-E_c$  volts and the transition is barely able to proceed. The voltage slope at this instant is not zero, but approximately the slope of the exponential. The total triggering time is  $t$ . Clearly the total triggering time could be greatly reduced either if the effective synchronizing voltage  $v$  were increased, or if the pulse duration were increased. Waveforms illustrating these cases are shown in Fig. 5-41.

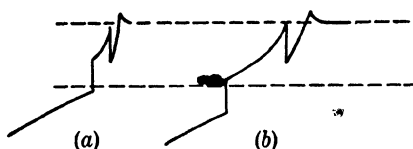


FIG. 5-41.—The reduction in triggering time obtained by increasing (a) effective synchronizing voltage and (b) synchronizing pulse width.

ing these cases are shown in Fig. 5-41.

The situation is thus seen to be a complicated one, with large variations in triggering time arising from very small variations in effective synchronizing voltage and pulse duration. Since  $v$  can scarcely be controlled (because it depends upon the exact moment when the synchronizing pulse arrives) it is generally best to make the pulse duration long enough to permit complete flipover even when  $v$  is small.

**5-13. Stabilizing the Duration of a Quasi-stable State.**—The duration of a quasi-stable state in a multivibrator depends upon the following four quantities:

1. The time constant  $\tau = RC$  of the timing network.
2. The initial voltage  $E_i$  from which the timing waveform begins.
3. The ultimate voltage  $E_u$  which the timing waveform would reach if it were permitted to do so.
4. The critical voltage  $E_c$  at which the transition occurs.

Any effect which a tube change or change in temperature, plate supply, or heater supply voltage, etc. may have upon the duration must occur by one of these four quantities. Stabilizing the duration is thus equivalent to stabilizing these four quantities, or at least making the effects of their change cancel out.

When Eq. (3) from Sec. 5-8 is rewritten in such a way as to permit  $E_i$ ,  $E_u$ , and  $E_c$  to take on either positive or negative values, the duration  $T$  of the quasi-stable state is

$$T = \tau \ln \frac{E_u - E_i}{E_u - E_c}.$$

<sup>1</sup> In practical frequency dividers it would be undesirable to have the transition begin from the exponential itself; therefore  $V$  is made large enough to insure that another trigger will arrive before point  $a$ .

In this form the equation is valid both for plate-to-grid-coupled types, in which  $E_u$  is positive and  $E_i$  and  $E_c$  negative, and for cathode-coupled types, in which  $E_u$  is negative (or zero) and  $E_i$  and  $E_c$  are positive. From this equation:

$$dT = d\tau \ln \frac{E_u - E_i}{E_u - E_c} + \tau \left( \frac{dE_u - dE_i}{E_u - E_i} - \frac{dE_u - dE_c}{E_u - E_c} \right).$$

Study of this equation leads to the following observations:

1. If  $\tau$ ,  $E_u$ ,  $E_i$ , and  $E_c$  were independent of each other, the only procedure which could stabilize  $T$  would be the stabilization of those four quantities individually. Such a procedure, though very difficult to carry out properly, would have the advantage of giving stabilization against any type of initial fluctuation.
2. In general, however,  $E_u$ ,  $E_i$ , and  $E_c$  change together; consequently it may be possible to stabilize by cancellation of their separate effects. Such a method is usually feasible, but it supposes a definite relationship between  $dE_u$ ,  $dE_i$ , and  $dE_c$ , which will probably hold for only one type of initial fluctuation. Thus it must be decided whether it is against tube change or supply voltage change, for example, that stabilization is desired, since the relations between  $dE_u$ ,  $dE_i$ , and  $dE_c$  will be different for those two cases.
3. Any good stabilization will have  $d\tau = 0$  since there is no relationship between  $\tau$  and the other variables. Stabilization of  $\tau$  against temperature changes is usually most important; this is achieved by making the temperature coefficient of  $R$  equal but opposite to that of  $C$ .
4. Perfect stabilization by cancellation, described above in 2, is obtained if  $d\tau = 0$  and  $\frac{dE_u}{E_u} = \frac{dE_i}{E_i} = \frac{dE_c}{E_c}$ ; that is, if  $\tau$  is stabilized and  $E_u$ ,  $E_i$ , and  $E_c$  all vary proportionately. Fortunately there is a tendency for this to happen when the line voltage changes, and for this reason an ordinary astable multivibrator can be made frequency-stable, without any special stabilizing networks, to better than 1 per cent against a 10 per cent change in line voltage.
5. Nevertheless, it is desirable to minimize the effect that a change in  $E_u$ ,  $E_i$ , or  $E_c$  would have if left uncanceled, and this is clearly accomplished by making  $\frac{\tau}{E_u - E_i}$  and  $\frac{\tau}{E_u - E_c}$  as small as possible.  $E_u - E_i$  and  $E_u - E_c$  should therefore be large. This is the reason for returning the grid in a plate-to-grid-coupled circuit to  $+E_{pp}$  instead of to ground, and for returning the cathode in a cathode-coupled type to  $-E_{kk}$  instead of to ground.

6. Other things being equal,  $dE_u$ ,  $dE_i$ , and  $dE_c$  should naturally be kept at a minimum. The remainder of this section will discuss a few practical ways of accomplishing this.

$E_u$  is usually either ground,  $+E_{pp}$ , or  $-E_{kk}$  (or some voltage obtained from these by division) and hence can be regulated to almost any desired degree. It should be realized, however, that if a circuit is supplied with both positive and negative voltages, regulating one supply against changes in line voltage without regulating the other may do more harm than good. In regulating both lines, a common voltage standard should be used for both—for example, the standardized negative line may be used as a reference for standardizing the positive line.

$E_c$ , for any given circuit, depends mainly upon the tube geometry, heater voltage, and cathode condition of the timing tube, and is very difficult to stabilize. Naturally, a tube with a short grid base should be used to reduce the magnitude of all these effects, and the heater voltage can be regulated, but these methods will not wholly eliminate the effects of tube change and aging. The best solution is to make the timing waveform as steep as possible at the moment of transition. This can be accomplished in several ways:

1. The amplitude of the timing waveform should be made as large as possible. This will require, in general, that the load resistors of the tubes be large so that a large step function may be fed into the timing network. There is accordingly the following dilemma to plague the designer: for fast waveforms the load resistors should be small, but for stability they should be large.
2. The voltage difference  $E_u - E_c$  should be made equal to  $\frac{1}{\epsilon} (E_u - E_i)$ .

This relation is derived in Chap. 16.

3. For operation at fixed durations, such as pulse frequency division to a constant frequency, tuned circuits of the desired frequency or some multiple thereof may be placed in the circuit to increase the effective slope at the moment of transition. Alternatively, delay networks can be used. These methods are discussed in detail in Chap. 16.

Stabilizing  $E_i$  may be accomplished either directly by placing a diode at the timing grid or cathode to establish the level from which the timing waveform starts out, or indirectly by stabilizing the amplitude of the step function produced at the other side of the timing condenser. An example of direct stabilization is shown in Fig. 5-42, where diodes are inserted in the grids of a plate-to-grid-coupled astable multivibrator

to set the initial level of the timing waveforms accurately at  $-E_{gg}$  volts. Thus the stabilization of  $E_i$  reduces essentially to the stabilization of  $-E_{gg}$ , which is an easy matter. Another advantage is that the negative overshoots in the waveforms of the ordinary version, shown in Figs. 5-16 and 5-17, are eliminated by these diodes. The value of  $-E_{gg}$  should be so chosen that as little as possible of the grid waveforms is cut off in order to permit the amplitudes of the timing waveforms to remain as large as possible.

Diodes may be similarly used at the cathodes of a cathode-coupled multivibrator, although the low output impedance of the cathode makes this difficult.

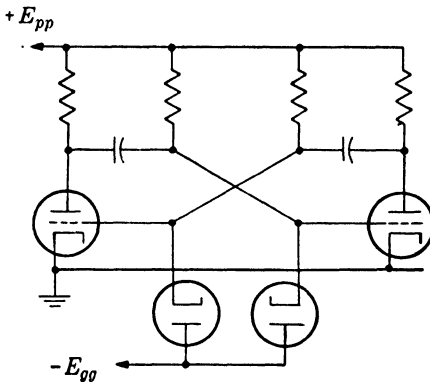


FIG. 5-42.—Use of the grid-catching diode to stabilize the initial level of the timing waveforms.

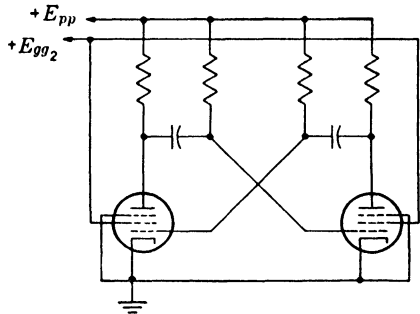


FIG. 5-43.—Use of the bottoming characteristics of pentodes to stabilize the amplitude of the timing waveform.

Similar methods are available for indirect stabilization. One method is to move the diodes in the circuit of Fig. 5-42 from the grid circuits to the plate circuits so that the plates will be prevented from dropping below a certain well-defined voltage. A stable negative supply is thus unnecessary; another advantage is that variations in  $+E_{pp}$  are partly compensated for if the plates of the diodes are returned to a voltage obtained directly by division from  $+E_{pp}$ . This voltage should be sufficiently lower than  $+E_{pp}$  to permit large timing waveforms to be formed at the grids.

In a similar method, pentodes are used instead of triodes, and advantage is taken of the "bottoming" of the plates against the knee of the plate characteristics (see Chap. 3). Figure 5-43 illustrates the connections for an astable circuit. Provided that the plate resistors are large enough to permit bottoming, the plates will always drop to a fairly well-defined voltage near ground. After the plate has bottomed, most of the cathode current goes to the screen; hence screen dissipation conditions impose a fairly low upper limit on  $E_{gg1}$ . Using a low screen



voltage also has the advantage of giving a smaller value of  $E_c$ , and thereby reducing the changes in that quantity with tube change.

A comparable bottoming effect is possible with triodes only when grid current is drawn and when the plate resistors are considerably larger than is necessary with pentodes. Good stability can be obtained with this sort of operation, but the recovery time of the various waveforms is long.

Jitter in the duration of the quasi-stable state, which is of special concern in time-modulation with monostable circuits, is closely akin to instability, though it refers to rapid fluctuations in duration instead of to slow ones. Usually, jitter will have two components: hum, arising from the alternating current in the power supply and occurring at the fundamental and harmonic frequencies of the line voltage; and microphonics, caused by mechanical vibrations in the chassis and tubes.

Hum can be reduced by: (1) filtering the plate supply voltage or in extreme cases using batteries; (2) using circuits in which the cathodes are grounded, to avoid the effects of heater-cathode capacity and leakage with a-c operated heaters, or in extreme cases using direct current for the heaters; (3) shielding of tubes; and (4) shielding of components at critical high-impedance points, especially in grid circuits. Occasionally hum can be canceled by the injection at the proper point of small a-c voltages at the line-voltage frequency. Also hum can be made harmless by operating the circuit at a frequency equal to the line-voltage frequency or some submultiple thereof. The fluctuations in value of high-resistance composition resistors may be rapid enough to cause effects very much like hum.

Microphonics can be reduced by: use of low-microphonic tubes; shock mounting of the entire chassis and the individual tube sockets; and packing of the tubes in Kimsul or some other deadening material.

**5-14. Varying the Duration of a Quasi-stable State.**—This process, when it is carried out with any monostable circuit (multivibrator, phantatron, or any other conceivable kind), is one of the methods by which the very important operation of time modulation (see Chap. 13) can be carried out. In the multivibrator it is clear that any of the four quantities  $\tau$ ,  $E_u$ ,  $E_i$ , and  $E_c$  might be used to vary the duration of the quasi-stable state. Examination will show that a similar statement can be made about any other monostable circuit.

Control by means of  $\tau$  has the often desirable property that the duration is a linear function of  $\tau$ , and hence of either  $R$  or  $C$ , provided the other variables are kept constant. By using a linear variable resistor or condenser, therefore, linear control of duration by a shaft rotation is possible. Capacity control is generally preferable to resistance control because (1) it leaves the quiescent state of the circuit more nearly con-

stant and (2) variable air condensers are smoother, more linear, and more stable than variable resistors.

By returning  $R$  to a variable voltage,  $E_u$  can be made the controlling variable but this method is rarely employed.

A satisfactory way to control the duration, although not linearly, is to vary  $E_i$ . This is most often done with the stabilized plate-to-grid-coupled circuits illustrated in the preceding section. In the circuit of Fig. 5-42, for instance, the duration is varied by making  $-E_{gg}$  variable, whereas in Fig. 5-43 the plate resistors are replaced by potentiometers, the movable center tap of which is coupled by the timing network to the grid of the other tube.

$E_c$  is not usually used, except in combination with  $E_i$  in the monostable cathode-coupled circuit of Fig. 5-12. As explained in Sec. 5-5, the duration of the quasi-stable state is found to be very nearly a linear function of the voltage impressed on the grid of  $V_1$ . This property is a consequence of the fact that  $E_i$  and  $E_c$  happen to vary in such a way with increasing grid voltage of  $V_1$  that the quantity  $\ln \frac{E_u - E_i}{E_u - E_c}$  increases almost perfectly linearly. The circuit is thus a useful and economical *voltage-controlled linear time-modulation circuit*.

### PHANTASTRON-TYPE CIRCUITS

**5-15. Introduction: Miller Sweep Generation.**—Work in recent years, especially in England, has brought about the development of a very important class of circuits, which have been given the names “phantastron,” “sanatron,” “sanaphant,” etc. These circuits can probably be best described as relaxation oscillators similar to multivibrators, but differing in this respect: whereas the multivibrator establishes its timing waveform (an exponential) by the use of only an  $RC$ -differentiator, phantastron-type circuits generate a linear timing waveform by means of the so-called “Miller sweep generator.” The use of a linear rather than an exponential timing waveform leads to a very important advantage, namely, the duration of the output rectangle can be made a linear function of an input control voltage. Accordingly, phantastron-type circuits are very useful for time modulation (see Chap. 13). Another advantage arises from the use of a linear waveform—increased timing stability—because the linear sweep (unlike the exponential) does not lose speed as it progresses.

Because Miller sweep generation is so pertinent to these circuits, it will be described here very briefly, although a more complete treatment appears in Chaps. 2 and 7. Special consideration will be given here to the mechanism by which the sweep is started and ended. The operation of the circuit of Fig. 5-44 is shown by the corresponding waveforms in

Fig. 5.45. Resistors  $R$  and  $R_1$  may be perhaps 1 megohm and several hundred kilohms, respectively:  $C$  may have any value from 50  $\mu\text{f}$  up.

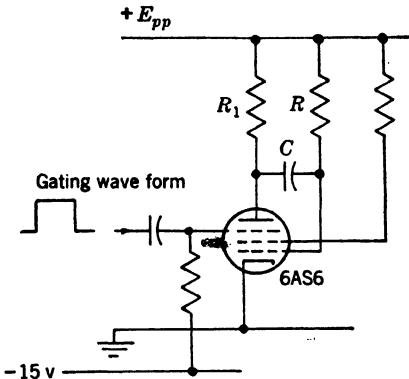


FIG. 5.44.—Miller-type linear sweep generator.

Initially the grid is at ground, and the suppressor at  $-15$  volts—a sufficient negative bias, in a 6AS6,<sup>1</sup> to cut off the plate current. Therefore the plate is at  $+E_{pp}$  volts, and all the cathode current is going to the screen, which may be at perhaps  $+60$  volts. When a positive gate is applied to the suppressor and is sufficient to raise it to about  $+5$  volts, current flows to the plate and the plate voltage immediately drops. Since the plate is coupled to the grid by  $C$ , the plate voltage drops only a few volts (about 5) before

the grid voltage is reduced and the plate current is reduced to just the few hundred microamperes that the plate load will permit. At the end of this initial step, therefore, the total cathode current has been greatly

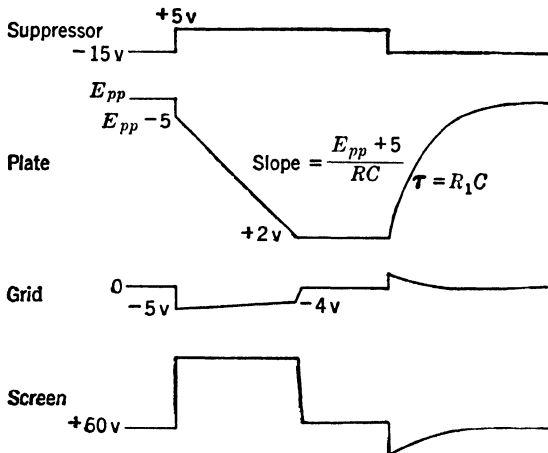


FIG. 5.45.—Waveforms of the circuit of Fig. 5.44.

reduced; the screen current has been so greatly reduced that a large positive wave appears at the screen; and a small plate current is flowing.

<sup>1</sup> A pentagrid converter, like the 6SA7, can also be used with the third grid taking the place of the suppressor in controlling the plate current. However, the 6AS6, having a higher suppressor-to-plate transconductance and more sturdy construction, is the best American tube for the purpose. The British VR116 is probably even better.

The next stage is what is properly called the Miller action. An electron current  $(E_{pp} + 5)/R$  is flowing to the plate of the tube, from left to right through  $C$ , and up through  $R$ . Therefore, the left side of  $C$  falls relative to the right side at a rate of  $(E_{pp} + 5)/RC$  volts per sec. This process continues, the grid rising very slightly to permit the plate to take the slightly increasing current needed for  $R_1$ , until the plate “bottoms”—that is, runs against the “knee” in the plate curve. At a grid voltage of about  $-4$  volts, this does not occur until the plate is within a volt or two of ground, and further drop is impossible. Since the necessary current through  $R$  can no longer pass through the tube, the right side of  $C$  rises exponentially toward  $E_{pp}$  at the same rate as the plate was previously falling<sup>1</sup> until the grid supplies the current. For this reason, and because of the transfer of the space current from the plate to the screen at bottoming, the screen current is again increased and the screen voltage returns almost to its initial level. This state will persist until the gate on the suppressor is removed, at which time the plate is released and rises toward  $E_{pp}$  with a speed limited mainly by  $R_1C$ . A more careful analysis reveals that, under typical circumstances, the departure from linearity in the rundown of the plate during the Miller portion of the operation is less than 0.1 per cent.

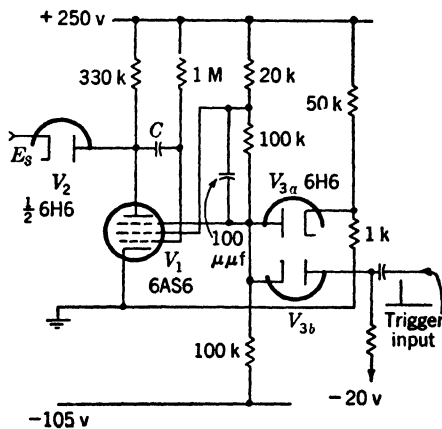


FIG. 5-46.—Monostable screen-coupled phantastron.

**5-16. The Screen-coupled Phantastron.**—Examination of the waveforms of Fig. 5-45 reveals that the positive gate, which in the circuit of Fig. 5-44 is injected externally at the suppressor, could be derived internally from the screen. Such a circuit, called a (monostable) “screen-coupled phantastron,”<sup>2</sup> is shown in Fig. 5-46, and photographs of its waveforms are shown in Fig. 5-47. Since it is internally gated, it requires

<sup>1</sup> Neglecting stray capacities from grid to ground.

<sup>2</sup> The British sometimes call this circuit a “Miller transitron,” or some similar name, reserving the name “phantastron” for what in this volume is called the “cathode-coupled phantastron.” The present circuit is reminiscent of the transitron family of circuits, which employ the screen-to-suppressor coupling used here, but which do not make use of the Miller feedback from plate to grid. This lack deprives the transitron of two important properties: it has no timing waveform other than the exponential on the suppressor; and without the feedback from plate to grid, the gain from suppressor to screen is so small that turnon and turnoff are slow.

only a positive trigger on the suppressor (or a negative trigger on the plate) to initiate the action. The turnoff of this circuit is somewhat different from that of Fig. 5-44. Just as in that circuit, as the plate bottoms, the screen current increases and causes the screen voltage to fall, but now this fall is coupled to the suppressor so that the plate current is reduced and the plate rises. This rise is transferred to the grid through  $C$  and the action is regenerative. Therefore, both the turnon and turnoff are regenerative, and the screen rectangle may have rise and fall times as

short as  $0.5 \mu\text{sec}$ .

The diode  $V_{3a}$  in the suppressor is not essential, but it insures that the suppressor will not be carried so high that it may "stick" because of secondary electron emission, and yet it permits the plate to be turned on fully during the rundown. It also permits a more rapid turnon and turnoff since the total movement of the suppressor is reduced. The small condenser between screen and suppressor is a speeding-up condenser. The diode  $V_2$  in the plate makes possible linear control of the rectangle and triangle length by the control, or signal, voltage  $V_s$ . The initial level of the plate is  $V_s$ , and the time necessary for it to run down to  $+2$  volts is therefore approximately

$$(V_s - 2)RC/(E_{pp} + 5) \text{ sec.}$$

Tube  $V_{3b}$  is a trigger-injecting diode;  $V_2$  might be used instead to inject a negative trigger at the plate.

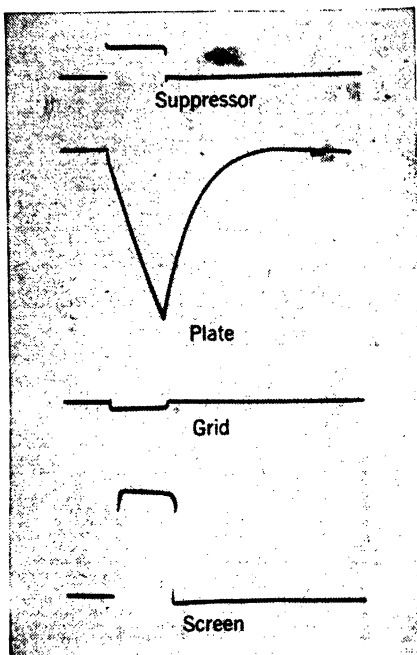


FIG. 5-47.—Waveforms of the circuit of Fig. 5-46. The trace was about 125 sec long; the amplitude of the suppressor waveform about 20 volts.

For many applications the severest fault of the circuit as it is shown in Fig. 5-46 is the long time necessary to recharge  $C$  through  $R_1$  and restore the plate to its initial voltage. This recovery time decreases rapidly as  $V_s$  is decreased because of the plate-catching action of the diode  $V_2$ , but even if the plate is caught at only 63% of  $E_{pp}$ , the recovery time will be about  $R_1C$  sec. For shorter recovery the timing network may be so arranged that the cathode follower  $V_3$  is used to provide a low-resistance recharging path for  $C$ , as in Fig. 5-48. It should be mentioned that this method of speeding recovery is of great generality and can be used with all circuits of this type.

The screen-coupled phantastron, like all the Miller sweep circuits, can exist in astable and bistable, as well as monostable, forms. Generally speaking, the bistable phantastrons offer no advantage over bistable multivibrators because it is only in the method of timing that multivibrators are inferior, and there is no timing operation in a bistable circuit. The astable phantastrons are, however, of considerable interest. For instance, the circuit of Fig. 5-46 can be made astable by leaving only a condenser between screen and suppressor. The diode  $V_{3a}$  is essential in this circuit. One part of the cycle is timed by the negative-going linear sweep generated at the plate, the other part by the positive-going exponential sweep at the suppressor. The speed of this latter waveform, and consequently the stability of the time interval which it establishes, is increased by returning the suppressor to  $+E_{pp}$  instead of to ground. A further improvement is to place perhaps a 5000-ohm resistor in the cathode and arrange a diode in the grid to prevent the grid from rising above +50 volts. In

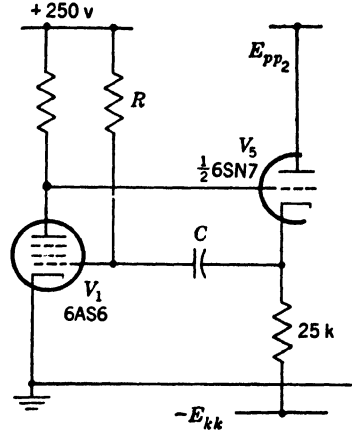


FIG. 5-48.—The use of a cathode-follower to speed the recharging of  $C$ .

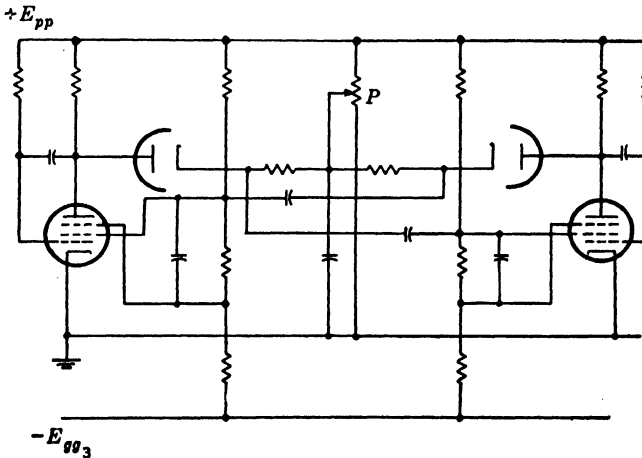


FIG. 5-49.—Double screen-coupled phantastron.

this way the screen current will be stabilized at 10 ma, and therefore the amplitude of the screen waveform and of the timing exponential on the suppressor will be stabilized.

Greater free-running frequency stability can be obtained by the use

of two cross-coupled monostable circuits. Such a double screen-coupled phantastron is illustrated in Fig. 5-49. Both parts of each cycle are timed by linear sweeps. The cross coupling between the two circuits is so arranged that each screen waveform is differentiated in a small condenser and applied to the other plate in such a way that the linear run-down of one plate is initiated at the instant the rundown of the other plate is finished. The potentiometer  $P$  provides a linear control over the period of the oscillations.

**5-17. The Sanatron and Sanaphant.**—Although somewhat more complex than the screen-coupled phantastron, the sanatron and sana-

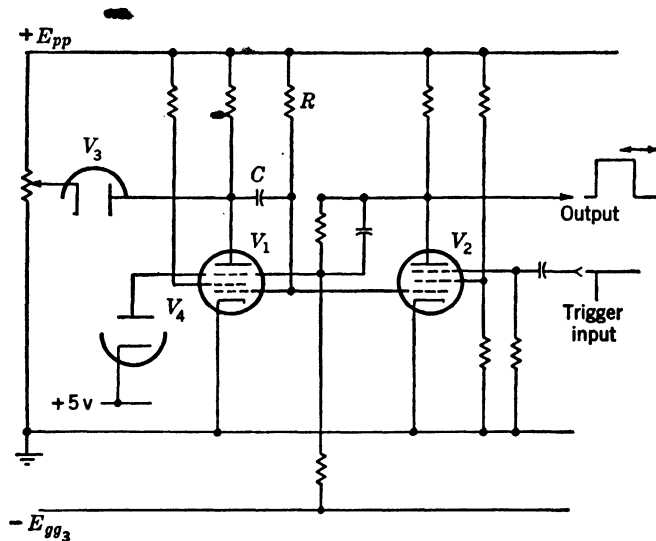


FIG. 5-50.—Monostable sanatron.

phant<sup>1</sup> can generate waveforms and, accordingly, rectangles as short as  $1 \mu\text{sec}$  whose length is nevertheless accurately defined by a linear waveform. Examination of the basic circuit of Fig. 5-44 reveals that, given a certain minimum value of  $C$ , the sweep speed is limited by the current-carrying capacity of the tube. The current is increased when  $R$  is made smaller, but as  $R$  is made smaller the screen current increases during both the quiescent and the active periods of the operation. Screen wattage is therefore usually the limiting factor in an attempt to increase the sweep speed. The purpose of the present circuits is to make possible the use of tubes that have a screen dissipation greater than that of the 6AS6, but may possess less effective suppressor control. By using another tube to amplify the gate before it is applied to the suppressor a

<sup>1</sup> See F. C. Williams and N. F. Moody, "Ranging Circuits, Linear Time-Base Generators, and Associated Circuits," I.E.E. Convention Paper, March 1946.

tube with a suppressor grid base of 60 volts or more can be used successfully. The 6AC7 has been used in this country in England the VR91 is usually employed.

The circuit illustrated in Fig. 5-50 is called the (monostable) "sanatron." In the figure,  $V_1$  is the Miller sweep generator and  $V_2$  amplifies the small negative gate on the grid of  $V_1$  into a large positive gate which is applied to the suppressor of  $V_1$  to permit the linear rundown to take place. The circuit may be triggered at any of several points, including, as shown in the figure, the suppressor of  $V_2$ . The initial level of the plate of  $V_1$ , and hence the duration of the rectangle, is set by the diode  $V_3$ . The output rectangle can be taken at an amplitude of one hundred volts or more from the plate of  $V_2$ . The voltage to which the suppressor of  $V_1$  is raised is defined by the diode  $V_4$ . It is generally desirable to have  $V_2$  completely cut off during the linear rundown and this can be accomplished in several ways.

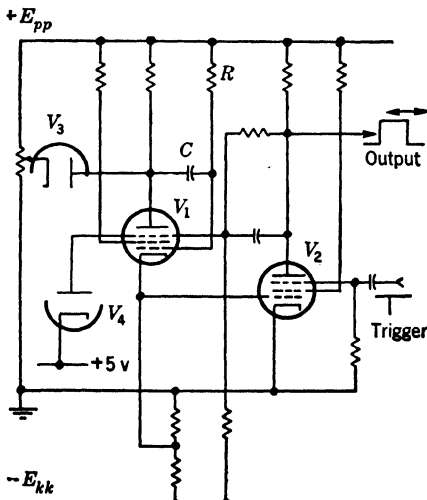


FIG. 5-52.—Monostable sanaphant.

way: namely, by inserting in the cathode of  $V_1$  an impedance across which the desired signal can be taken. This procedure has both an

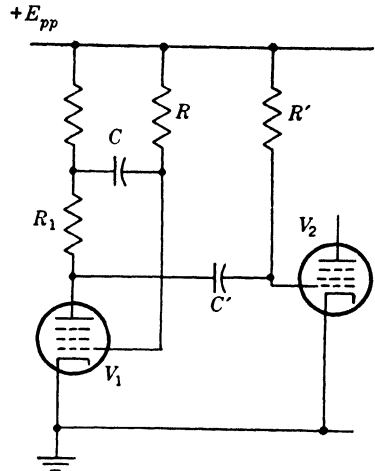


FIG. 5-51.—One method for deriving a suitable signal for the grid of the gate amplifier.

In the figure, the screen of  $V_2$  is not permitted to rise as far during the rundown as that of  $V_1$ ; hence the negative grid wave which will not quite cut off  $V_1$  will cut off  $V_2$ . Another method is to make  $V_2$  a different type tube from  $V_1$  and one with a shorter grid base. Or finally, the arrangement of Fig. 5-51 may be used, in which the entire current through  $R$  and  $C$  flows through  $R_1$  and provides the grid of  $V_2$  with a signal larger than that at the grid of  $V_1$  by the drop across  $R_1$ .

The sanaphant, illustrated in Fig. 5-52, derives the signal for the grid of  $V_2$  in a slightly different



advantage and a disadvantage. The advantage is that the signal which is produced at the grid of  $V_2$  can have both a larger amplitude and a lower impedance than in the sanatron. Since the impedance is lower,  $V_2$  is turned off and on more rapidly and hence the output rectangle has steeper edges. The disadvantage is that the initial negative step in the plate waveform is increased in amplitude with the result that changes in operating conditions cause larger changes in the amplitude and duration of this step, with larger consequent changes in the duration of the generated rectangle. One other advantage which should be noted is that there is a negative rectangular output available on the cathode of  $V_1$  as well as the positive outputs at the screen of  $V_1$  and the plate of  $V_2$ .

Other variations of the basic Miller sweep-generation circuit have been made for specific purposes. For instance, both the sanatron and the sanaphant suffer from the fact that there is always a small delay between bottoming and the turning on again of  $V_2$ . This delay is the time required for the grid of  $V_2$  to come up and cross the grid base, and because the grid base of different tubes varies somewhat, changing  $V_2$  may cause a noticeable alteration in the duration of the output rectangle. The following method has accordingly been used to minimize this delay. A pulse transformer is inserted in the screen of  $V_1$ , from the secondary of which can be taken the screen waveform differentiated and inverted—that is, a negative pulse at the moment of triggering and a positive pulse at the moment of bottoming. If the positive pulse is applied, through a diode, to the grid of  $V_2$ ,  $V_2$  will be turned on very shortly after bottoming, and the trailing edge of the output rectangle will very nearly coincide with the instant of bottoming. A precision sanatron using this device is described in detail in Vol. 20, Chap. 5, of this series.

Another variation, which has been used to produce rectangles with extremely fast trailing edges, differentiates the cathode waveform of  $V_1$  with either a transformer or a simple  $RC$ -network, and feeds the result, through a diode, back to the plate of  $V_1$ . The differentiated positive pulse speeds the plate snapback after bottoming.

The fundamental purpose of the sanatron and sanaphant—to remove as far as possible the limitation imposed on sweep speed by screen dissipation—can be carried still further by the so-called “screen-coupled” sanatron and sanaphant. The suppressor of  $V_1$  is not used at all (in fact, beam-power tubes with very high plate currents and rather small screen currents should be used for this purpose), and the positive gate generated at the plate of  $V_2$  is applied instead to the screen through a low-impedance a-c-d-c coupling. Sweep speeds of more than 100 volts/ $\mu$ sec are obtainable.

Astable and even bistable variations on all these circuits can be made.

**5-18. The Cathode-coupled Phantastron.**<sup>1</sup>—The screen-coupled phantastron discussed in Sec. 5-16 is not the only practical one-tube circuit of this general type. In the screen-coupled phantastron the positive suppressor gate is supplied by the screen. However, all or part of the positive gate on the suppressor may be replaced by a negative gate on the cathode, generated, as in the sanaphant, by inserting a resistance in the cathode. (Etymologically, the name “sanaphant” indicates that the circuit is halfway between a sanatron and a (cathode-coupled) phantastron.) An example<sup>2</sup> of a cathode-coupled phantastron is shown in

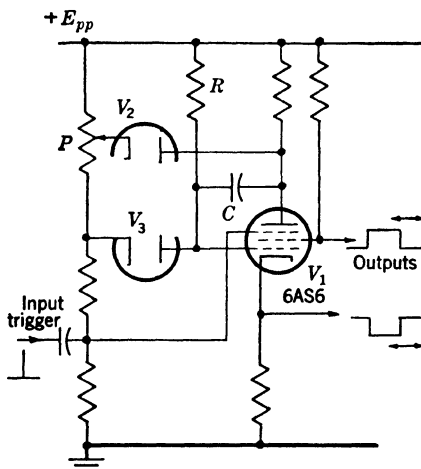


FIG. 5-53.—Monostable cathode-coupled phantastron.

Fig. 5-53. The diode  $V_3$  serves the important role of stabilizing the initial level of the grid and therefore the initial voltage across the timing condenser  $C$ . Since the duration of the quasi-stable state is the time necessary to discharge  $C$  through  $R$ ,  $V_3$  is very effective in stabilizing the duration of the output against changes in line voltage, etc. The diode  $V_2$  and the potentiometer  $P$  permit linear control over the duration of the output. It is interesting to note that there is approximately the same relation between the screen- and cathode-coupled phantastrons as between the plate-to-grid and cathode-coupled multivibrators.

The following are advantages that the cathode-coupled phantastron possesses: a monostable circuit can be built without a negative supply or without raising the cathode up on a bleeder; the rectangle on the screen

<sup>1</sup> See R. Kelner *et al.*, “An adaptation of the Phantastron Delay Multivibrator Circuit to the 6SA7 Tube,” RL Report No. 338 (Aug. 1943).

<sup>2</sup> Another example is discussed in detail in Vol. 20, Chap. 5.

is unloaded; outputs of both polarities are obtainable; and it is claimed that the linearity of time modulation is better at short ranges than in the screen-coupled phantastron. The main disadvantage is that the timing accuracy is not so good as in the screen-coupled phantastron. This is so partly because of the larger initial step in the plate waveform, and

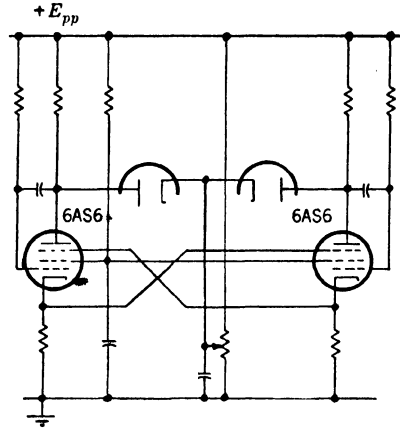


FIG. 5-54. Double cathode-coupled phantastron.

partly because the gain of the tube from grid to plate during the linear rundown is not so high as it would be if the degenerative effect of the cathode resistor were not present.

The cathode-coupled phantastron also lends itself, as illustrated in Fig. 5-54, to a very elegant analogue of the double screen-coupled phantastron.

## CHAPTER 6

### BLOCKING OSCILLATORS AND DELAY-LINE PULSE GENERATORS

BY E. F. MACNICHOL, JR. AND R. B. WOODBURY

**6-1. Blocking Oscillators.**—Blocking oscillators are transformer-coupled feedback oscillators in which plate current is permitted to flow for one-half cycle, after which cutoff bias is imposed upon the grid to prevent further oscillation. They are related to quenching or “squegging” oscillators which oscillate for several cycles before sufficient grid bias is developed to prevent further oscillation.

Most blocking oscillators are designed to produce nearly rectangular pulses of plate voltage or current, which are made possible by the special characteristics of the feedback transformer. In the ordinary feedback oscillator used to produce sinusoids, either the grid circuit, plate circuit, or both are tuned to resonance at the frequency of operation. In the blocking oscillator the resonant period of the transformer and associated stray capacitance is short compared with the duration of the pulse desired in the output and its “Q” is kept as low as possible. This results in a rapid rise of plate current when regeneration is initiated. The duration of the pulse is limited by the low-frequency response of the transformer, but it may be terminated sooner by the action of a delay network or feedback condenser.

The transformer is usually wound on an iron core of high permeability so that the coupling in the feedback circuit is made as high as possible to permit large grid currents. The high permeability which also permits fewer turns for a given inductance minimizes distributed capacitance and raises the resonant frequency. The coils are wound as closely together as possible to reduce leakage inductance that causes a delay in the feedback circuit and decreases the rate of rise and fall of the pulse.

The low-impedance feedback path and very short time lag in the transformer permit the generation of rapidly rising and falling pulse currents of very large magnitude. More than an ampere of current may be obtained from circuits employing small receiving tubes at rated plate potentials. Oxide-coated cathodes are entirely capable of emitting the required current, but the ratio of pulse length to repetition period must be kept small in order that the dissipation rating of the tube is not

exceeded. In no case should the average cathode current exceed that for which the tube is rated, although the peak current may be several hundred times this value.

Blocking oscillators are used as low-impedance pulse generators for triggering and switching where large currents are desired and tolerances in pulse width, shape, and amplitude are sufficiently broad to permit their use. It must be emphasized that the blocking oscillator is not a precision device and the characteristics of its output are influenced markedly by  $E_{pp}$ ,  $E_{on}$ ,  $E_f$ , the residual magnetism in the transformer core, and the age and condition of the tube. Like the thyatron pulse generator but unlike the multivibrator in which one tube must always be conducting and wasting power, it has the tremendous advantage of drawing plate current only during the pulse. Unlike the gas-tube pulse generator, which must deionize after each pulse, the recovery time of a blocking oscillator can be made very short.

*Types of Outputs.*—A typical blocking oscillator using a transformer with a 1 to 1 ratio and conventional plate-grid feedback is shown in Fig. 6-1a. The waveforms produced by this circuit are shown in Fig. 6-1b and c. Three types of output are obtainable: (1) A “voltage” pulse may be taken from the plate or from one or more added transformer windings. The number of turns on these windings may be adjusted to produce desired impedance and voltage levels. (2) A “current” pulse, that is, an  $IR$  drop, may be taken across a small resistor inserted in the plate, cathode, or grid circuit. (3) The output may be the waveform of the self-bias voltage.

The plate “voltage” pulse will have an amplitude of approximately  $E_{pp}/2$  at an impedance level of approximately 1000 ohms. The voltage and impedance of the tertiary winding are nearly those of the plate circuit, except as modified by the turns ratio of the transformer and the leakage inductance between windings. If the output winding is used to invert the plate waveform so that adjacent turns of the plate and output windings have large pulse potentials between them, the output pulse will be slowed up by the interwinding capacitance. The amplitude of the positive- or negative-“current” pulse from the cathode and plate circuits, respectively, varies with the magnitude of the series resistor, but it is generally impractical to make the amplitude of the pulse exceed  $E_{pp}/5$ . The output impedance is slightly less than the value of the series resistor which is usually less than 100 ohms. An output of this type owes its utility to its very low impedance and to the fact that the waveform has no overshoot. The self-bias voltage waveform, that is, the voltage across  $C$ , will have an amplitude of approximately  $E_{pp}/3$  when a feedback ratio of 1 to 1 is used. During the pulse the impedance across the condenser is low because of the large current flowing in the grid-

cathode circuit. When the tube is cut off, the impedance is merely that of the  $RC$  combination.

The time during which the blocking-oscillator tube conducts coincides with the current pulse, the positive part of the voltage pulse, and the

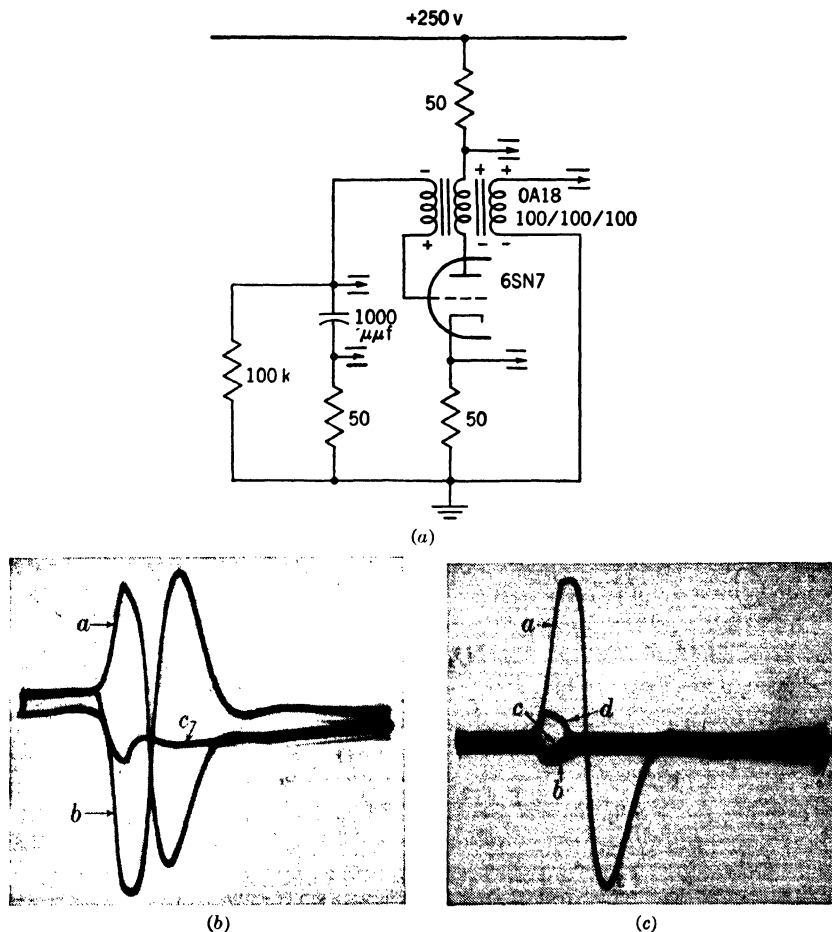


FIG. 6-1.—(a) Typical astable blocking oscillator using 1 to 1 ratio transformer and conventional plate-grid feedback; (b) grid  $a$ , plate  $b$ , and bias circuit  $c$  waveforms; (c) output-voltage  $a$ , plate-current  $b$ , grid-current  $c$ , and cathode-current waveforms  $d$ .

duration of the steep portion of the bias waveform (see Fig. 6-1b and 6-1c). This time may vary from less than one tenth microsecond to several hundred microseconds, depending upon the transformer and other circuit elements. With present transformer and circuit techniques the usual range of pulse widths in which blocking oscillators are useful is from 0.1 to 25 μsec.

*Types of Circuits.*—After the pulse has terminated, the grid is left highly negative because the condenser is charged. The grid voltage rises exponentially toward the potential to which the grid is returned. If this latter potential is higher than that at which the blocking oscillator will “fire,”<sup>1</sup> the grid will eventually reach this point, and a new pulse will be generated and cause a repetition of the cycle. A device operating in this manner will be referred to as an “astable” blocking oscillator. It is equivalent to the astable multivibrator, positive feedback being obtained from a transformer instead of from an amplifier stage. One time constant is that of the feedback circuit which determines the duration of the pulse. The other is the grid-recovery time constant. If the grid is not allowed to reach the firing voltage, a monostable circuit results. An external trigger must be applied to raise the grid voltage sufficiently to initiate regeneration before the blocking oscillator will fire. The monostable blocking oscillator is usually referred to as a “triggered” blocking oscillator and is equivalent to the monostable multivibrator.

Bistable blocking oscillators cannot be made since feedback is provided by the transformer, and positive grid voltage cannot be maintained unless current is changing in the transformer.

In blocking oscillators the  $RC$  grid-bias circuit may be replaced by an  $LC$ -circuit or a delay network, but each circuit must always perform the same function, namely, to maintain a negative potential on the grid so that conduction cannot take place until the network has been recharged or until the circuit is retriggered.

An astable blocking oscillator may be “fired” by inserting an external synchronizing pulse before the bias network has recharged. A blocking oscillator operating under these conditions will be referred to as a “synchronized astable” blocking oscillator.

*Applications.*—A blocking oscillator is employed to perform three general types of function. First, it may be employed to generate a pulse of very short duration when a slowly varying trigger voltage is applied. Appreciable spurious time modulation (jitter) of the output pulse may occur if the input waveform rises very slowly since the blocking oscillator is not a very stable amplitude comparator. For this purpose it is more economical than multistage squaring and differentiating circuits. Second, a blocking oscillator may be used to generate a pulse of appreciable peak power and a specified shape. It is most economical since plate current flows only during the pulse. Third, a blocking oscillator may be employed as a low-impedance switch. The circuit being switched is usually connected in the self-bias circuit of the blocking oscillator. The

<sup>1</sup> The firing point is the potential attained during the onset of current in the tube at which the  $g_m$  has increased to such a value that the gain around the feedback loop is greater than unity and regeneration commences.

switching action is used in frequency dividers and step counters to discharge the timing or counting circuits. The switch is closed when the grid potential reaches the firing voltage, and remains closed while the grid current is flowing. Circuits have also been developed in which the plate or cathode circuits are used as low-impedance switches. They are used in free-running time bases to replace the gas-tube switch. The blocking oscillator is frequently used to furnish low-impedance pulses to actuate external diode or triode switches for modulation, demodulation, or for the initiation of waveforms. It is very suitable for applying a switching voltage between ungrounded points since a transformer would have to be employed for isolation even if another type of circuit were used to generate the pulse.

*Theory of Operation.*—A complete explanation of a blocking oscillator by means of exact mathematical analysis has not yet been given. The tube characteristics in the positive-grid region are highly nonlinear, and the inductances of the windings of the pulse transformer are not only nonlinear but are also dependent upon the duration and spacing of the pulses. Most of the work with blocking oscillators has been largely of an empirical “cut-and-try” nature, and the mathematics developed has not proved itself useful in low-voltage, small power circuits using receiving tubes. In high-power applications where plate potentials in excess of 1 kv are used, and where beam tetrodes which produce large plate-power output with small grid-power input are used, assumptions may be made that permit the use of simplified mathematics for design purposes (see Vol. 32, Part III, of this series).<sup>1</sup>

The action of a blocking oscillator may be described qualitatively in the following manner. Initially, the plate current is cut off by grid bias. The grid potential is raised either by the application of a trigger or by the recharging of the grid-bias network. When cutoff bias is reached, plate current will start to flow. The changing plate current in the transformer induces in the grid winding a voltage that causes the grid potential to increase further in the positive direction. When the  $g_m$  of the tube has increased until the gain around the feedback loop is greater than unity, regeneration occurs. The grid voltage and plate current then increase more and more rapidly. The trigger is no longer necessary to maintain the action although it often adds an important component to the rate of rise of the grid voltage. Since there is very little leakage inductance in the feedback loop, the rate of fall of plate volt-

<sup>1</sup> Although an analysis of the precise operating conditions of the blocking oscillator has not been achieved, satisfactory transformers may be designed by the methods given in Vol. 32, Sec. 13-2. Once a transformer that will operate in the desired manner has been constructed, the exact pulse duration desired can be adjusted by experimentally changing the operating conditions; for example, by the adjustment of  $C_g$ .



age becomes very rapid. When the grid has become positive with respect to cathode, grid current starts to flow. When the grid has become positive by a few tenths of a volt, the grid impedance becomes of the order of a few hundred ohms imposing a heavy resistive load upon the transformer. Eventually, the power dissipated in the grid circuit, in internal losses, and in the external load becomes equal to that which can be supplied by plate circuit. This condition is accentuated by the fact that  $E_p$  has dropped to a value at which  $g_m$  is markedly less than it was in the earlier part of the cycle. A state of temporary equilibrium is reached in which the grid voltage is held constant by a linearly changing magnetizing current in the transformer. If the tuned circuit consisting of the transformer leakage inductance and stray capacitance has appreciable  $Q$ , it will be shock-excited by the rapid rise of the pulse. This excitation will be evidenced by a damped, high-frequency oscillation superposed on the flat top of the plate voltage pulse. If this oscillation is small, it will have little effect on the duration of the pulse.

The state of equilibrium is terminated by regenerative cutoff of the plate current and by a drop in grid potential initiated by three effects acting singly or in combination with one another. First, a delay network can be inserted in the circuit. A delayed step is produced and tends to start regeneration in the opposite direction.

Second, if a small grid condenser is used, the voltage across it

$$(e_c = 1/C_g \int i_g dt)$$

rises rapidly during the pulse. This voltage must be subtracted from the transformer output to give the actual grid driving voltage. Eventually, the voltage across the condenser becomes so large that the grid potential decreases more rapidly than it can be supplied by the transformer, and the grid starts to drop. As the grid drops, plate current is correspondingly decreased; a further decrease in grid potential results, and regeneration again takes place until the grid is driven beyond cutoff. At the end of the pulse the grid will be negative by an amount equal to the potential across  $C_g$ . The charge on  $C_g$  must be dissipated through a grid leak before the blocking oscillator can be reactivated.

Third, if  $C_g$  is very large, or if it is left out and bias is supplied from a low impedance supply, the equilibrium state will continue for a time determined by the transformer time constant in the following manner. When the plate potential has dropped until the equilibrium condition has been reached, the plate voltage cannot increase further and the grid potential starts to decay.<sup>1</sup> As the grid drops, plate current is decreased

<sup>1</sup> It might be expected that the grid potential would decay with a time constant

and the regenerative turnoff commences. When the tube cuts off, the plate voltage rises above the supply voltage as the core remagnetizes. Unless saturation has occurred, the area of the overshoot will be equal to the area of the pulse. Some shock-excited oscillations may be observed at the end of the pulse. These are due to the same cause as are the oscillations near the front of the pulse. Oscillations due to the resonance of the main inductance and stray capacitance are not observable since the  $Q$  of this tuned circuit is too low.<sup>1</sup>

### PULSE WAVEFORMS

**6-2. The Transformer.**—The most common types of pulse waveforms desired from a blocking oscillator are those that are very short, as nearly rectangular as possible, and that have high peak voltages or currents. The actual output pulse obtained is determined by the transformer, the tube and the constants, and the type of the circuit employed.

If it is desired to obtain an approximately rectangular waveform from a blocking oscillator, it is common practice to generate nearly the maximum pulse length by making  $C_o$  very large. A decrease in the duration of the transient periods relative to the duration of the equilibrium state results. Under these conditions the pulse length determines the selection of the proper pulse transformer. This transformer must have high- and low-frequency response sufficient for the desired pulse shape. The high-frequency response determines the rates of rise and fall of the pulse and the low-frequency response determines the pulse duration.

First the effects of the transformer will be considered. There are two salient characteristics of the transformer, its pass band, and its turns ratio. The high-frequency response of the transformer determines the maximum possible rates of rise and fall of the output pulse and is determined by the leakage inductance, stray capacitance, and core losses. To minimize the leakage inductance the transformer should have a large coefficient of coupling and as few turns as possible. The primary and secondary of the transformer should be on the same leg of the core. If windings must be wound on both legs of the core, both the grid and plate windings should be split.<sup>2</sup>

---

$L/R$  where  $L$  is the effective inductance of the transformer and  $R$  is the effective combination of grid, plate, and load impedances. Actually the waveforms indicate that the situation is more complicated. It can only be said that the pulse lasts for a time that is proportional to  $L/R$ .

<sup>1</sup> It is possible under some conditions to tune one of the windings by placing a large condenser across it. The result is a nearly sinusoidal oscillation which may have a large enough second overshoot to retrigger the oscillator, and thereby produce a train of oscillations that continue until quenching bias is built up.

<sup>2</sup> To produce the most rapidly rising and falling pulses the grid, plate, and output windings should each be a single layer winding.

The capacitances may be kept down by increasing the thickness of insulation between windings or between the windings and the core. This procedure, however, increases the leakage inductance and causes very little change in pulse shape within reasonable limits—except for the increase in the amplitude of the shocked oscillations on the pulse—since the relevant *LC* ratio is increased. The core losses may be reduced and the effective permeability increased by decreasing the thickness of the core laminations. The present limit is one mil, which is as thin as it is possible at present to roll the steel and maintain the proper crystalline structure for high d-c permeability.

TABLE 6-1.—~~SOME~~ COMMONLY USED LOW-POWER BLOCKING-OSCILLATOR TRANSFORMERS

Manufacturer	Type	Number of windings	Range of pulse widths
Utah Radio Products Co.*	OA-15(x-154-) series	4	1-30 $\mu$ sec
	OA-18(x-124-) series	6	0.2-15 $\mu$ sec
Westinghouse Electric and Manufacturing Co.	132 AW	3	0.2-5 $\mu$ sec
	132 BW	4	(0.2-5 $\mu$ sec (has extra low-impedance output winding)
	132 DW	3	0.1-2 $\mu$ sec
	145 EW	3	1-20 $\mu$ sec
General Electric Co.	68G-627	4	1-20 $\mu$ sec

\* Utah Radio Products Co. is no longer producing these transformers. They may now be obtained from Dunifon Engineering Co., 3649 Waveland Avenue, Chicago 18, Ill.

The primary and secondary inductances are the determining factors in the low-frequency response of the transformer because the magnetizing current increases directly with time and inversely with inductance. This requirement necessitates a high effective permeability if the number of turns is to be kept to a minimum for maximum high-frequency response, and the provision that the iron does not saturate. In some transformers the insertion of an air gap actually appears to increase the duration of the pulse. This effect is paradoxical and has not been satisfactorily explained. It is probable that without the gap a residual flux is built up from pulse to pulse. This flux biases the core toward saturation and reduces the effective inductance.<sup>1</sup> The difference in the pulse length produced by identical circuits with transformers that differ only because one has a wrapped

<sup>1</sup> Another explanation has been given. In some transformers the core losses are very high which makes the effective *L/R* time-constant small. Insertion of an air gap reduces *R* to a greater extent than it reduces *L*.

core while the other has a butt joint core are shown in the figures of Secs. 8, 9, and 10.

If maximum peak pulse current through the tube is desired, the turns ratio of the transformer should be adjusted to give an approximate impedance match between the plate output impedance and grid input impedance at the desired peak pulse amplitude. With low- $\mu$  triodes operating under pulse conditions, this implies a voltage stepup into the grid. If, however, maximum peak pulse voltage at the plate is required, the voltage should generally be stepped down going to the grid. With tetrodes and pentodes the grid current becomes equal to the plate current at small positive grid potentials so that a stepdown is necessary to obtain an impedance match.

A stepdown is also advisable if maximum pulse duration is desired from a given transformer since it permits the use of more of the available turns in the plate winding, and thus increases inductance of this winding and lowers the magnetizing current.

**6-3. The Tube.**—The tube employed in a blocking oscillator is a major factor in determining the characteristics of the output waveform. For positive-grid pulsed characteristics of a 6SN7 see Fig. 6-2. In general if a high-energy output pulse is required, the tube should exhibit a large value of  $I_p$ ,

$I_p/I_g$ ,  $\partial E_g/\partial I_g$ , and a small value of  $r_p$  over the portions of the characteristic curves corresponding to the peak of the pulse. There is a fundamental difference between triodes and pentodes or beam tetrodes operated as blocking oscillators. Medium- $\mu$  triodes exhibit large power gains in the positive grid region. With a 6SN7, for example,  $\partial I_p/\partial I_g = 3$  when the grid is driven from +50 to +75 volts, and  $E_p = 150$ . At low plate potentials it is necessary to operate in this region to obtain large current outputs, and this is a most favorable tube for operating in the far positive-grid region. The peak current obtainable is limited by the point at which more power is dissipated in the grid circuit than can be supplied, a condition brought about by the lowering of the plate potential and the raising of the grid potential until  $\partial I_p/\partial I_g < 1$  (when a 1 to 1 transformer is used). More current can, of course, be obtained by raising  $E_{pp}$  until safe values are exceeded.

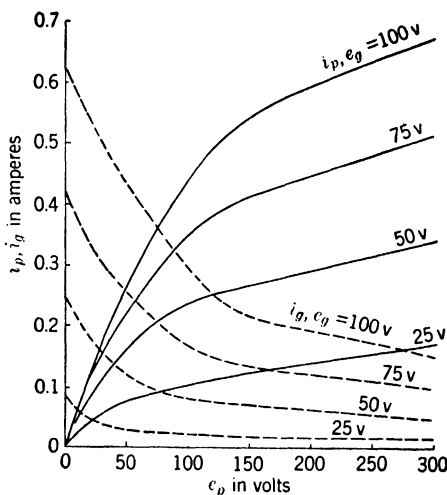


FIG. 6-2.—Positive-grid pulsed characteristics of a 6SN7.

With beam tetrodes and pentodes the operation of the blocking oscillator is quite different. As soon as grid current starts to flow,  $\partial I_p / \partial I_g$  becomes small; in the case of the 6AG7, which is one of the least favorable tubes for positive grid operation, as shown in Fig. 6-3, it is much less than unity when the grid has reached +25 volts. Therefore, the peak currents obtainable with tetrodes and pentodes are limited to those obtainable near zero bias. This means that if currents as large as those obtained with triodes are desired, the plate and screen potentials must be raised considerably above those for which tubes of the receiving type are normally rated. Since the voltage difference between zero bias and the potential at which limiting takes place is small, the regenerative

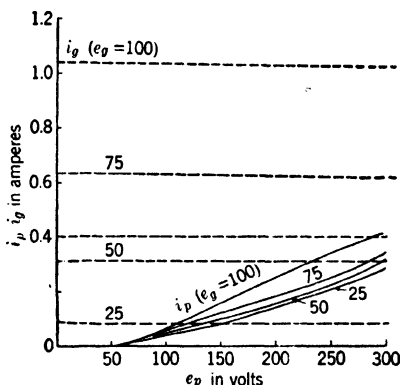


FIG. 6-3.—Positive-grid pulsed characteristics of a 6AG7.

region is passed through rapidly, and a steeper pulse than is obtainable with triodes results. In fact, the most rectangular pulses can be produced with a given transformer by using type 6AC7 or 6AG7 connected as pentodes. The peak currents will be much less than with 6SN7's—usually below 100 ma if rated potentials are applied to the plate and screen. Pentodes such as types 6AC7 and 6AG7 are frequently used as triodes to produce very rapidly rising and very short pulses because their  $g_m$  is higher

than that of most triodes, and there is consequently sufficient gain to produce regeneration even when transformers with very small inductance are used.

**Power Limitations.**—Beam tetrodes such as types 6L6, 6Y6, and 6V6 are frequently used as triodes when the duty ratio is large since their dissipation ratings are the highest of the receiving tubes. It is possible that the 6AS7 high-current regulator tube will give very high peak currents though no data are yet available.

The permissible peak current and voltage of a single pulse is set by the maximum voltage breakdown of the plate and grid of the tube. It must be remembered that the peak positive plate voltage is the sum of the positive supply potential and the inductive overshoot of the transformer, and that the peak negative voltage of the grid is the sum of the inductive overshoot, the charge on  $C_g$ , and the negative supply voltage.

For continuous operation, neither the maximum rated plate or grid dissipation nor the maximum cathode-current specifications should be exceeded. The grid-power rating of receiving tubes is seldom given

by the manufacturer, but is found to be roughly 0.2 watt for type 6SN7. If the grid-dissipation rating is exceeded, the grid may emit electrons which cause it to remain positive after the pulse. When the grid remains positive, very large steady plate current is drawn which soon ruins the tube.

Oxide-coated cathodes are capable of enormous emission, as shown in Fig. 6-2, and even with small tubes emission limiting of plate current is rarely obtained. If average emission ratings are exceeded, the structure of the cathode material is altered and loss of emission soon results. This loss shows up as a decay in the plate current during the pulse, and may also appear as a loss of average emission when measured by an ordinary commercial tube tester.

The shape of the pulse depends upon the type of limiting action that causes the quasi-stable state. If the state is brought about by heavy grid current when  $r_p$  is still high (current-limiting), a rectangular current pulse will result. If limiting takes place by "bottoming" of the plate (voltage-limiting), a rectangular voltage pulse will occur. In general, rectangular current and voltage pulses are not produced simultaneously in the same circuit.

A rectangular voltage pulse may be obtained with a 6SN7 if a large condenser is placed in the grid circuit. The  $r_p$  of the 6SN7 is small in the positive-grid region and the  $g_m$  is large.

The conditions for a rectangular current pulse are well met by a 6Y6 tetrode with 300 volts on the screen (see Fig. 6-4); it will be noticed that  $g_m$  is small and  $r_p$  is large over a large portion of the characteristic curves.

*Capacitance in the Grid Circuit.*—In a simple blocking oscillator having only a condenser  $C_g$  in the grid return, the effect of reducing  $C_g$  is to shorten the voltage pulse with the initial slope remaining nearly constant and the final slope decreasing. This effect is shown in Figs. 6-5a and 6-5b. Conditions in the two cases are identical in all respects other than the 400-fold change in  $C_g$ .

The shape of the current pulse undergoes similar changes as  $C_g$  is reduced; but in addition current decreases during the pulse, and the pulse

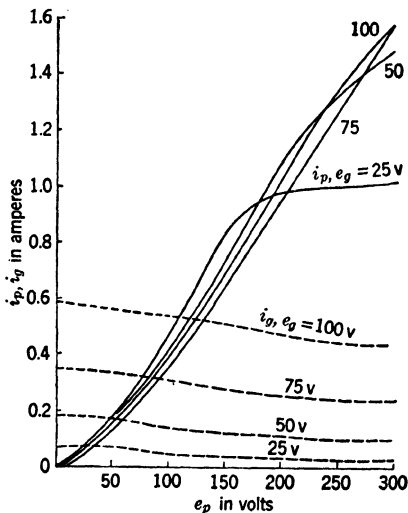


FIG. 6-4.—Positive-grid pulsed characteristics of 6Y6.

will become trapezoidal. If  $C_g$  is made so large that it presents a negligible impedance to the frequency components making up the pulse, or if it is omitted altogether, the pulse duration is determined by the low-frequency response of the transformer. In operation of this type the magnitude of the air gap in the core has a very marked influence on the pulse since it affects the inductance and the saturability of the core (see

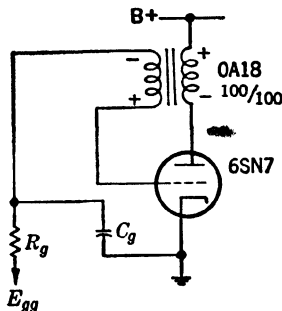
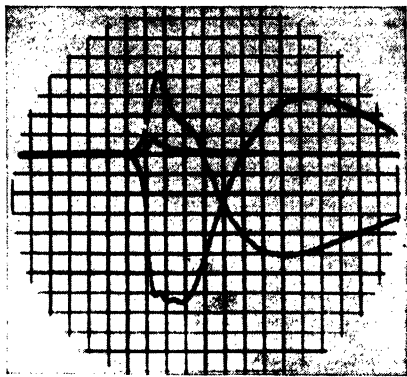


FIG. 6-5.—Monostable blocking oscillator with plate-grid feedback. Vertical deflection 25 volts/division. Connection: two windings in grid circuit; two windings in plate circuit. (a) Butt-joint core,  $C_g = 250 \mu\text{f}$ ;  $E_p$ ,  $E_g$ , and  $I_k$  waveforms; sweep speed  $0.15 \mu\text{sec/division}$ . (b) Butt-joint core,  $C_g = 0.1 \mu\text{f}$ ;  $E_p$ ,  $E_g$ , and  $I_k$  waveforms; sweep speed  $1.4 \mu\text{sec/division}$ . (c) Leading edge of pulse: butt-joint core,  $C_g = 0.1 \mu\text{f}$ ;  $E_p$ ,  $E_g$ , and  $I_k$  waveforms, sweep speed  $0.15 \mu\text{sec/division}$ . (d) Falling edge of pulse: butt-joint core,  $C_g = 0.1 \mu\text{f}$ ;  $E_p$ ,  $E_g$ , and  $I_k$  waveforms, sweep speed  $0.15 \mu\text{sec/division}$ . (e) Continuously wound core,  $C_g = 250 \mu\text{f}$ ,  $E_p$  waveform, sweep speed  $0.3 \mu\text{sec/division}$ . (f) Continuously wound core,  $0.1 \mu\text{f}$ ,  $E_p$  waveform, sweep speed  $0.3 \mu\text{sec/division}$ .

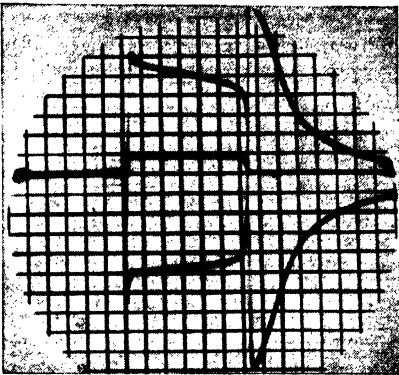
Sec. 6-2). In the Westinghouse "radio C" cores the butt joint produces a small but very uncertain air gap which results in characteristics that cannot be controlled in transformer manufacture. Operation with  $C_g$  very large or omitted altogether produces pulses with the highest possible ratio of duration to rise and fall time. The choice of a transformer that will give the desired pulse width when operating under these conditions will also permit the largest peak currents, provided the optimum turns ratio is used, since the impedance of the transformer will be a minimum. Unfortunately, the overshoots of the voltage pulses are at a maximum in this mode of operation since the core of the transformer becomes completely saturated by the end of the pulse and must demagnetize before another pulse can be produced.

The maximum duration obtainable from a particular transformer may be reduced by the residual magnetism in the core. In transformers employing very small air gaps (or none at all) the residual magnetism may accumulate from pulse to pulse and cause operation in a region of reduced permeability. The effective permeability may also be decreased by operating with such large magnetizing currents that the core actually is driven to saturation during the pulse. The d-c component of plate current increases this effect and may be reduced by employing parallel feed as shown in Fig. 6-6. The d-c plate current is applied to the tube through a separate inductance which is large compared with that of the transformer. The a-c component of plate current is applied through a condenser which is large enough to present negligible impedance to the frequency components of the pulse.

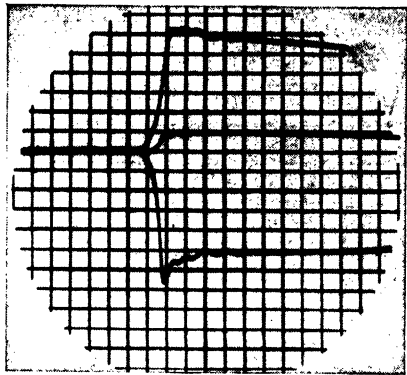
A direct current may also be introduced into any winding of the trans-



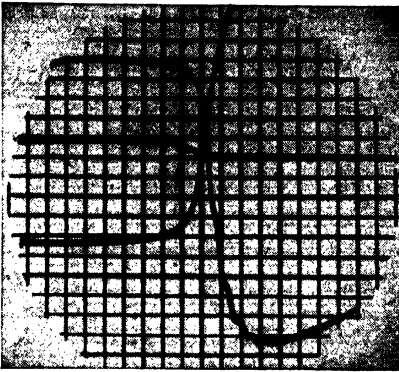
(a)



(b)



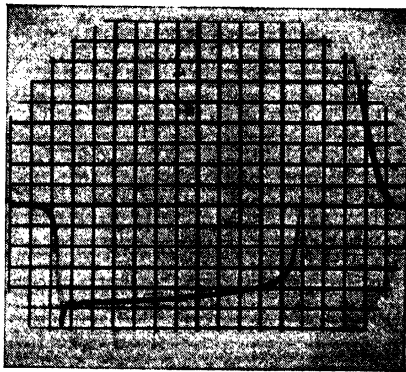
(c)



(d)



(e)



(f)

FIG. 6.5.—For legend see opposite page.



former to produce a magnetic bias in a direction opposite to saturation, a condition that permits the largest possible effective inductance and the longest pulse. Since the time constant is equal to  $L/R$ , the pulse can be

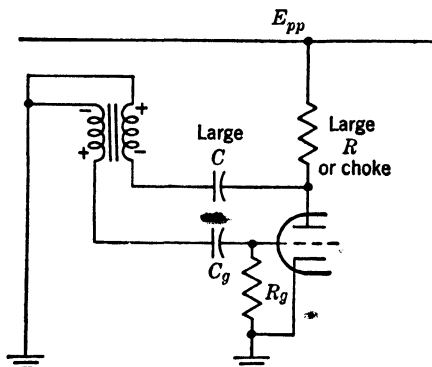


FIG. 6-6.—Parallel grid and plate current feed to remove direct current from transformer.

lengthened by loading one of the windings with resistance, a procedure almost never used since it is wasteful of power.

performance of the blocking oscillator and the least interference with the trigger source are produced. The difference between the time the trigger is applied and the time the blocking-oscillator pulse approaches full amplitude is a function of the trigger slope and amplitude. In applications where it is desired to keep this time difference to a minimum, the initial slope and peak amplitude of the trigger should be large.

The use of delay lines to terminate the pulse will be discussed later under "Delay-line Pulse Generators."

**TRIGGERING METHODS**

**6.4. Introduction.**—The problem of triggering a blocking oscillator resolves itself to one of inserting the trigger voltage into the grid-to-cathode loop in such a manner that the most favorable performance of the blocking oscillator pulse approaches full amplitude is produced.

The shape of the blocking-oscillator pulse depends to a very great extent upon the character of the initiating trigger. Usually the gain around the feedback loop is not very large even before heavy grid current is drawn by the tube. The gain is low because of the low impedance of the transformer. The rise in potential follows a positive exponential curve until limiting takes place. With a slow trigger the exponential must start in a region of very small slope. With a large trigger, on the other hand, the exponential buildup starts in a region of rapid potential change and the pulse is steeper. A comparison of the photographs of Figs. 6-1 and 6-5 shows the effects of trigger speed.

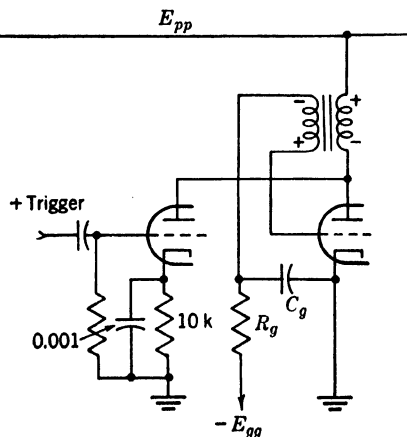


FIG. 6-7.—Parallel triggering with amplifier.

The astable circuit (Fig. 6-1) requires half the pulse length to rise to full amplitude. "Parallel" triggering was used in Fig. 6-5 so that the rise rate is greatly increased.

There are two basic methods of triggering a blocking oscillator, and these are shown in Figs. 6-7 and 6-8. They are called "parallel" and "series" triggering. The first requires a constant current source across some winding of the transformer. The second requires a constant voltage source in series with the grid-cathode loop.

*Parallel Triggering.*—When parallel triggering is employed, the ideal constant-current generator may be approximated by means of a pentode, but in most cases a triode can be employed. For example, a 6SN7 has a minimum  $r_p$  of about 7 k in the neighborhood of zero bias; this is large compared with the impedance of the blocking-oscillator tube and transformer. If desired, the effective  $r_p$  may be increased further by cathode degeneration, although this procedure is seldom necessary. Since sharp negative triggers are more easily obtained in the plate circuit of a triggering tube than positive triggers, it is common practice to apply a negative trigger to the plate of the blocking oscillator; this pulse will appear as a positive trigger on the grid because of the phase inversion of the transformer (see Fig. 6-7). This method of triggering requires that the trigger have a sufficiently steep edge to be effectively reproduced by the transformer.

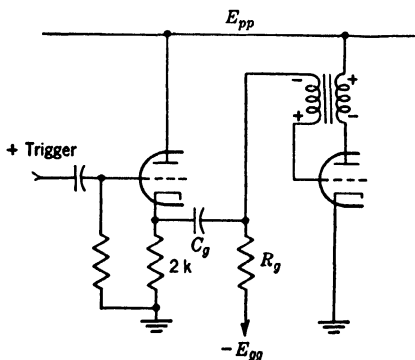


FIG. 6-8.—Series triggering with cathode follower.

If the trigger is of long duration, it will be partially "differentiated" since the transformer will not pass the low-frequency components. The transformer also introduces some time delay and somewhat decreases the initial slope of the trigger, but in most applications this effect may be considered negligible.

This method of triggering using a separate triggering tube has four important advantages:

1. It introduces the minimum interference with the blocking oscillator.
2. Reaction of the blocking oscillator upon the original trigger source is practically eliminated.
3. The time delay between the trigger and the blocking-oscillator output pulse is reduced since the slope and amplitude of the original trigger are increased by the gain of the trigger tube.

4. The amplitude of the trigger may be conveniently controlled by modifying the constants of the trigger amplifier circuit if this is desired. This method of triggering does, however, require an extra tube and a trigger with a fairly large initial slope.

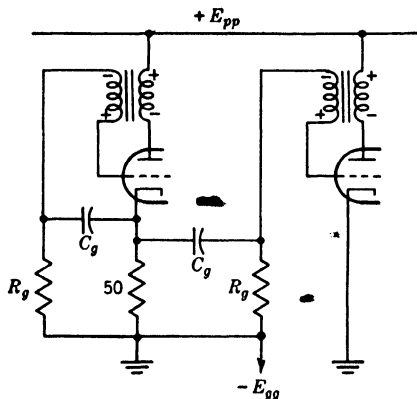


FIG. 6-9.—Series triggering from blocking oscillator.

*“Series” Triggering.*—When series triggering is employed, the constant-voltage generator may be approximated by the use of a cathode follower as in Fig. 6-8 or by use of any low-impedance trigger such as that from another blocking oscillator as in Fig. 6-9.

The series method of triggering has two advantages. The blocking oscillator may be fired with a very slow trigger since the trigger will not be appreciably “differentiated” with consequent loss in amplitude, and if a very fast trigger is avail-

able, it appears directly in the grid-cathode loop at its full amplitude, a condition that results in a minimum delay between the trigger and the output pulse.

Series triggering does not in practice provide a minimum interference with the blocking oscillator, and the blocking oscillator will interact back on the trigger source. If a cathode follower is used for triggering, severe interaction with the trigger source will be caused because the cathode follower will be made to draw grid current. If a slow trigger is being employed, the cathode follower can be prevented from drawing appreciable grid current by the insertion of a series resistance  $R_i$  of about 10,000 ohms in the grid circuit. An additional disadvantage of series triggering results from the insertion of the triggering impedance in series with the grid circuit, a procedure that wastes power in the feedback circuit. Another method of series triggering is shown in Fig. 6-10. A positive trigger is applied to  $C_g$  through  $R_i$  which is small compared with  $R_g$ . Since these resistors may be very large, the source impedance can

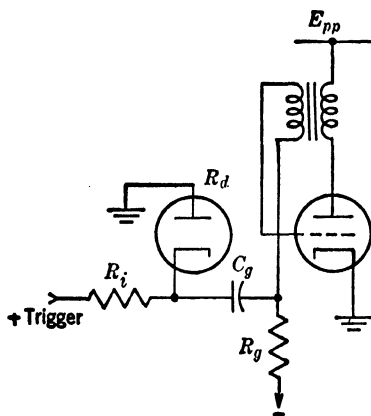


FIG. 6-10.—Series triggering using a diode.

be moderately high without very much trigger voltage being wasted. As soon as the tube starts to conduct, a negative pulse appears in series with  $C_g$ . The diode conducts, and thereby furnishes a very low-impedance path for the grid current; the blocking oscillator continues its cycle in the normal manner.

An example of the use of series and parallel triggers in a production equipment is shown in Fig. 6.11. It is desired to fire the first blocking oscillator at the end of a variable-width rectangular pulse. The second blocking oscillator is fired on the end of the pulse provided by the first blocking oscillator. The pulse-sharpening tube  $V_1$  amplifies and quasi-

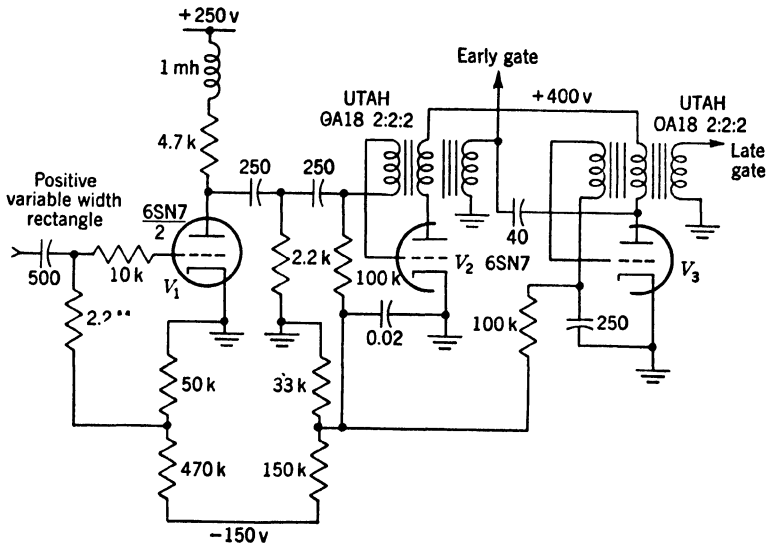


FIG. 6.11.—Range-gate generator in AN/APG-5.

differentiates the rectangle. A positive pulse produced by the trailing edge of the rectangle appears in the plate circuit. It is applied in series with the grid circuit of  $V_2$ . The voltage output pulse is applied to the plate of  $V_3$  through a small condenser which differentiates it. The negative pulse produced by the trailing edge of the pulse from  $V_2$  initiates regeneration in  $V_3$ . The negative plate pulse of  $V_3$  assists in terminating the pulse from  $V_2$ .

In some applications it is desired that the blocking oscillator fire when a slowly varying trigger reaches some externally applied reference level. This may be conveniently done by the circuit shown in Fig. 6-12. The bias on the tube is set low enough to cause the blocking oscillator to fire, but regeneration is prevented by the diode except when the applied voltage equals or exceeds the reference voltage. This circuit requires

that the applied voltage have a low source impedance and the blocking oscillator be prevented from firing more than once by the increase in self-bias or by distortion of the applied voltage. Regenerative amplitude

comparators are discussed in detail in Chap. 9.

If large-amplitude triggers are available and reaction of the blocking oscillator on the trigger source is unimportant, blocking oscillators may be triggered without the use of amplifiers or cathode followers as shown in Fig. 6-13. In fact, this method implies that waveforms equivalent to those obtainable at the output of the previously described trigger tubes are available. Parallel triggers may be inserted through resistors or small condensers connected to the grid or plate of the tube (points *c* and *d*).

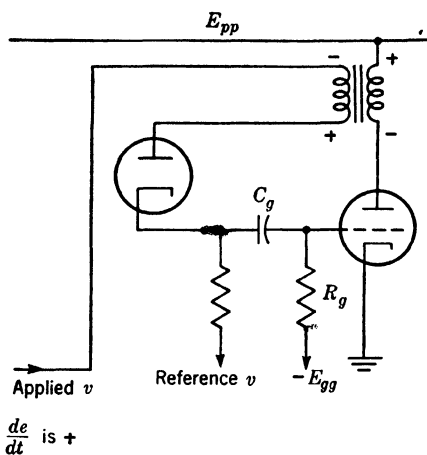


Fig. 6-12.—Blocking-oscillator amplitude selector.

They may also be supplied from a tertiary winding on the transformer (points *f* and *g*). Series triggers may be supplied to a small resistor in series with the grid winding (point *a*) or through a series transformer. If  $C_g$  can be made small or if the trigger voltage is large, a series method of triggering may be used which does not insert any resistance in series with  $C_g$ . The trigger is inserted across  $C_g$  by means of a condenser,  $C_g^2$  (point *b*). Capacitors  $C_g^1$  and  $C_g$  act as a capacitance divider so that the trigger is not slowed up although less voltage is available. The capacitor  $C_g^1$  will have an effect on the pulse length since it is in parallel with  $C_g$ . (For a further discussion of triggering methods see Chap. 16, "Frequency Dividers").

*Effect of the Trigger on Output Waveforms.*—As mentioned previously, the trigger as it actually appears in the blocking-oscillator circuit has a pronounced effect on the output waveform. The type of trigger may easily vary the time delay and the initial slope of the output pulse by a factor of 4. To obtain the minimum time delay and a maximum initial

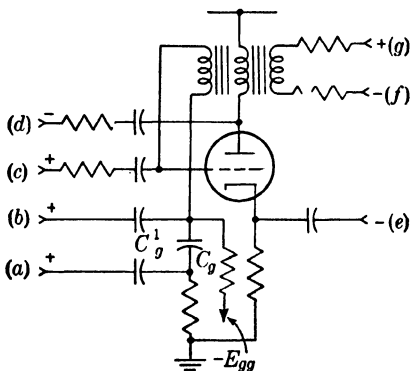


Fig. 6-13.—Direct methods of triggering blocking oscillator.

slope of the output pulse, the trigger should have a high initial slope and a relatively large amplitude as it appears in the grid-cathode loop.

Any pronounced variations in the amplitude of the trigger will appear in the output pulse. In extreme cases where the trigger is shorter than the output pulse, the end of the trigger may terminate the output pulse prematurely. The characteristic "spike" on the front of the pulse may sometimes be removed by applying a trigger which is carefully shaped. When series triggering is used, a long trigger may cause the blocking oscillator to refire several times until the trigger voltage is removed. Because of the differentiating property of the transformer, there is no danger of retriggering when parallel triggering is used. The ideal blocking-oscillator trigger for most applications is a rectangular pulse whose duration is slightly greater than that of the blocking oscillator. A trigger of this type may be approximated by using a triangular trigger whose initial slope is very large and whose amplitude decreases slowly after the peak amplitude is attained. In either case, the correct amplitude must be determined for the particular application.

#### RECOVERY TIME

**6-5. General Considerations.**—The self-bias that terminates the blocking-oscillator pulse also prevents the blocking oscillator from being triggered for a period of time after the pulse. This time interval is large compared with the pulse duration and will be referred to as the "recovery time." It places an upper limit on the repetition frequency of the blocking oscillator, but in most cases this is no more serious than the limitations due to tube dissipation.

If a constant PRF is used, the grid-bias voltage need not recover completely between triggers since triggering will always occur at the same bias potential. If the PRF is variable, recovery must be complete before retriggering, or spurious amplitude and time modulation will take place. If the average PRF is constant and the blocking oscillator is required to fire with uneven spacing, as in forming a multiple-pulse train,  $C_g$  may be made so large that the potential across it is changed negligibly during each pulse so that a constant bias is maintained. Under these conditions some other element must be varied to control the pulse width.

Several methods of biasing may be used in triggered blocking oscillators. With fixed grid bias through  $R_g$ , the value of  $R_g$  and the impedance of the bias supply must be kept low if rapid recovery is to be obtained. If  $R_g$  is made small, insufficient potential will be built up across  $C_g$  to terminate the action or, if parallel feed (Fig. 6-6) is used,  $R_g$  will load the transformer heavily. The low-impedance requirement may necessitate excessive current in the bias voltage divider. When a negative supply

is unavailable, cathode bias is often used as shown in Fig. 6-14a. Two time constants,  $C_g R_g$  and  $C_k R_k$ , must recover before the blocking oscillator will fire. The condenser  $C_k$  is charged by both the grid and cathode currents of the tube. It is possible to omit  $C_g$  and  $R_g$ ; in this case if  $C_k$  is small it determines the pulse length. An exponential sawtooth waveform may be obtained across  $C_k$  under these conditions. If  $R_k$  is

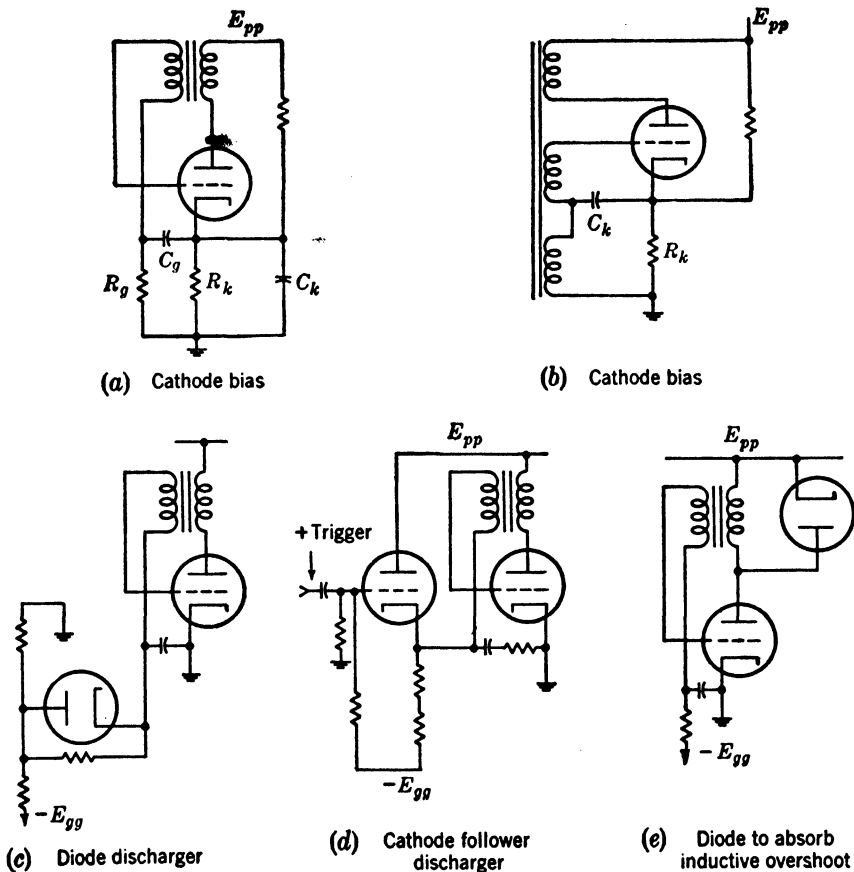


FIG. 6-14.—Methods of biasing blocking oscillator.

made very small,  $C_k$  may be omitted, and very rapid recovery results. In the grid-cathode, or grid-plate-cathode-coupled blocking oscillators (see Sec. 6-10), cathode bias may be obtained as shown in Fig. 6-14b.

To aid recovery, nonlinear elements may be inserted in the bias circuit for d-c restoration. In Fig. 6-14c a diode or a contact rectifier is used to discharge  $C_g$  after the pulse. The diode must be returned to a low-impedance supply which is not always conveniently obtained. In Fig. 6-14d a cathode follower is used in place of the diode. The cathode

follower cuts off during the pulse and conducts heavily during the overshoot. It is more economical than the diode because the low-impedance negative supply is eliminated. It also provides a convenient method of inserting a high-impedance trigger pulse.

If extremely close pulse spacing is required, the overshoot produced by demagnetization of the core may limit the minimum pulse spacing. If a condenser or delay line is used to terminate the pulse, the inductance of the transformer may be large so that the amplitude of the overshoot is small. If the inductance must be kept small, a diode or contact rectifier can be inserted across any winding of the transformer to absorb the overshoot of voltage, which would otherwise hold the grid biased off. The second pulse will probably differ in shape from the first since the magnetizing current will take a considerable time to fall to zero.

**6-6. Frequency Division.**—The trigger amplitude necessary to fire the blocking oscillator at any time is equal to the difference between the grid-to-cathode voltage at that time and the voltage at which the blocking oscillator will fire. This voltage difference decreases with time—exponentially in most cases. If triggers equally spaced in time and of the correct height are applied to the blocking oscillator, it is possible to make it fire on every  $n$ th trigger by modifying the waveform of the grid-to-cathode voltage. Stable operation can be obtained with integral values of  $n$  between 1 and 5. This process will be referred to as “pulse frequency division.”

In frequency dividers the usual exponential grid-to-cathode waveform is frequently replaced by a waveform that requires a much smaller trigger amplitude for the  $n$ th trigger than for any other, or a waveform which increases the rate of change of the grid-bias waveform around the  $n$ th trigger. In this case a stable division ratio of 10 or more is possible.<sup>1</sup> For a complete discussion of pulse frequency dividers see Chap. 16.

**6-7. Random Variations in PRF.**—In a free-running blocking oscillator there are small cycle-to-cycle variations in the repetition period. These variations appear to be caused by irregularities in the amplitude of the grid-to-cathode voltage waveform which are produced by a change in the residual magnetism of the core of the transformer from cycle to cycle. It is experimentally observed that this variation is most pronounced for small values of grid capacity, although certain very critical values of capacity may be found at which the variation disappears entirely. These values are, however, far too critical to be employed in

<sup>1</sup> Frequency dividers that divide by more than 100 in a single step have been used in radar equipment. The division ratio is not constant and the count may change by as much as  $\pm 10$  per cent. The phase lock between the divider pulse and the trigger can be made very precise which is often much more important than the accuracy of the division ratio.



the design of a blocking oscillator. It is best to employ a fairly large value of grid capacity if possible, in which case the variations will be consistent and generally less than  $\frac{1}{4}$  per cent.

The frequency of a free-running blocking oscillator is also affected by variations in pulse amplitude due to the variation of  $g_m$  with  $E_f$  and  $E_{pp}$  and tube aging and by fluctuations in the retriggering potential due to the same causes. In general, these fluctuations are the same as those found in frequency dividers. Accordingly, the reader is referred to Chap. 16 for a complete discussion.

If a free-running blocking oscillator is synchronized, the random cycle-to-cycle variation will disappear, but the amplitude of the grid-to-cathode waveform of a synchronized blocking oscillator is, however, a function of the amplitude of the synchronizing trigger, its initial slope, and its duration. Under certain conditions this may cause instability if the blocking oscillator is employed as a frequency divider (see Chap. 16).

### PRACTICAL CIRCUITS

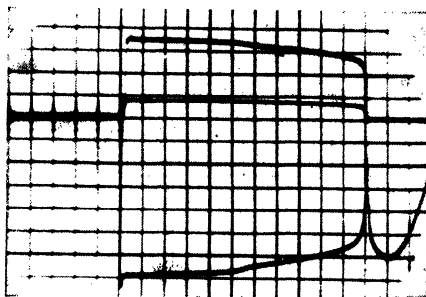
**6-8. General Considerations.**—To facilitate the comparison of the waveforms obtained from each of the various types of blocking-oscillator circuits, the output waveforms have been photographed and will be presented in the discussion of each type of circuit.

In all cases the blocking oscillator employed one section of a 6SN7, an OA18 pulse transformer (see Table 6-1), a 2- $\mu$ f, 0.1- $\mu$ f, or 250- $\mu$ f grid condenser, and  $E_{pp} = 250$  volts. Two series of waveforms are given, one with an OA18 with a continuously-wound core and the other with an OA18 with a butt-joint core to show the effect of core saturation on maximum pulse duration. This study illustrates that although the same components were used, the various inductances, leakage inductances, interwinding capacitances, and tube and stray capacitances are differently distributed, and have a marked effect on the pulse shape. The relative directions and the distribution of the windings in the 6-winding transformer are other variables. Obviously, since it would be unprofitable to discuss all possible permutations and combinations of the windings, this discussion is limited to only a few common circuits.

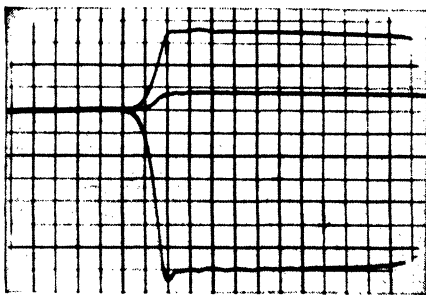
**6-9. Plate-to-grid Feedback.**—In a blocking oscillator of this type the primary of the transformer is placed in the plate circuit of the tube and the secondary in the grid-to-cathode loop in such a polarity that the grid will become positive as the plate is driven negative. The circuit is shown in Fig. 6-5, and indicates operation with two windings each in the grid, plate, and output circuits. The output may be a current pulse of either polarity, or a negative voltage pulse may be obtained directly at the plate without the use of a tertiary winding. These waveforms are shown in Figs. 6-5a through f. This circuit makes a fair approximation to a

rectangular pulse in all cases where  $C_g$  is large. The initial slope is large, and the pulse amplitude does not decrease greatly throughout its duration. It is evident, however, that as  $C_g$  is reduced the pulse waveform approaches a sinusoid.

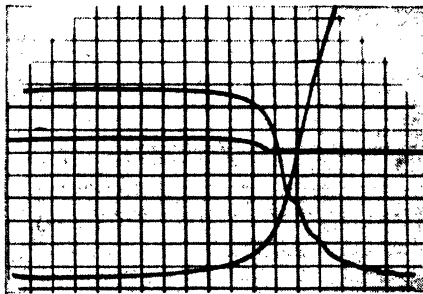
This is the most commonly employed type of blocking oscillator for several reasons aside from its simplicity. Since the circuit requires only two transformer windings, one end of grid-to-cathode loop can be con-



(a)



(b)

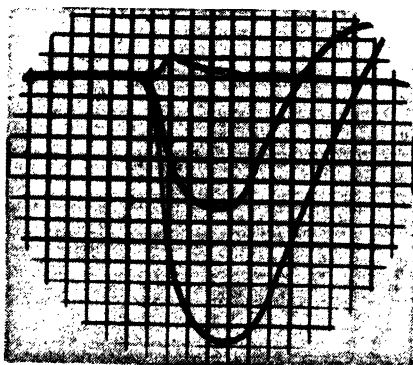
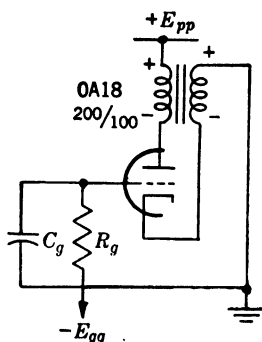


(c)

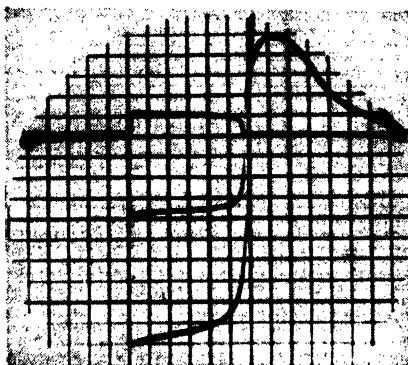
FIG. 6-15.—Grid-to-plate-coupled blocking oscillator with 2 to 1 ratio between plate and grid windings. Effect of changing turns-ratio of transformer. Compare with Figure 6-5. Butt-joint core. Plate-to-grid feedback. Windings—four in plate, two in grid circuit. Vertical deflection—25 volts/division.  $E_g$ ,  $E_p$ ,  $I_k$  waveforms.  $C_g = 2 \mu\text{f}$ . (a)  $1.4 \mu\text{sec/division}$ . (b) Leading edge of pulse:  $0.15 \mu\text{sec/division}$ . (c) Trailing edge of pulse:  $0.15 \mu\text{sec/division}$ .

nected to ground. This latter characteristic is necessary if series triggering is employed without resorting to a “floating” trigger source, and it is also convenient if the grid circuit of the blocking oscillator is being employed as a switch, since in many cases one side of the circuit to be switched must be returned to ground. The effect of varying the turns ratio is shown in Fig. 6-15. Conditions are identical to those in Fig. 6-5 except for the fact that four of the windings are connected in the plate circuit and two in the grid. The  $2\text{-}\mu\text{f}$  condenser in the grid circuit is needed to sustain the longer pulse.

**Plate-to-cathode Feedback.**—In this circuit (see Fig. 6-16), the primary of the transformer is placed in the plate circuit of the tube and the secondary in the cathode circuit. The feedback appears in both the grid-to-cathode and the plate-to-cathode loops; the polarity of the transformer is such that the cathode is driven negative as the plate potential drops. In this circuit it is necessary that the ratio of the number of turns in the plate winding to that in the cathode winding be greater than unity to enable the plate circuit to drive the lower-impedance cathode circuit, thus permitting a loop gain greater than unity. A turns ratio of 2 to 1 seems satisfactory for most applications. The output may be a



(a)



(b)

FIG. 6-16.—Plate-to-cathode feedback. Vertical deflections: 25 volts/division. Connection: two windings in cathode circuit, four windings in plate circuit. (a) Butt-joint core,  $C_g = 250 \mu\text{f}$ ;  $E_p$ ,  $E_k$ ,  $I_k$  waveforms; sweep speed  $0.15 \mu\text{sec/division}$ . (b) Butt-joint core;  $C_g = 0.1 \mu\text{f}$ ;  $E_p$ ,  $E_k$ ,  $I_k$  waveforms; sweep speed  $1.4 \mu\text{sec/division}$ . (c) Leading edge: Butt-joint core;  $C_g = 0.1 \mu\text{f}$ ;  $E_p$ ,  $E_k$ ,  $I_k$  waveforms; sweep speed  $0.15 \mu\text{sec/division}$ . (d) Trailing edge: Butt-joint core;  $C_g = 0.1 \mu\text{f}$ ;  $E_p$ ,  $E_k$ ,  $I_k$  waveforms; sweep speed  $0.15 \mu\text{sec/division}$ . (e) Continuously wound core;  $C_g = 250 \mu\text{f}$ ;  $E_p$  waveform; sweep speed  $0.3 \mu\text{sec/division}$ . (f) Continuously wound core;  $C_g = 250 \mu\text{f}$ ;  $E_k$  waveform; sweep speed  $0.3 \mu\text{sec/division}$ . (g) Continuously wound core;  $0.1 \mu\text{f}$ ;  $E_p$  waveform; sweep speed  $1.4 \mu\text{sec/division}$ . (h) Continuously wound core;  $0.1 \mu\text{f}$ ;  $E_k$  waveform; sweep speed  $1.4 \mu\text{sec/division}$ .

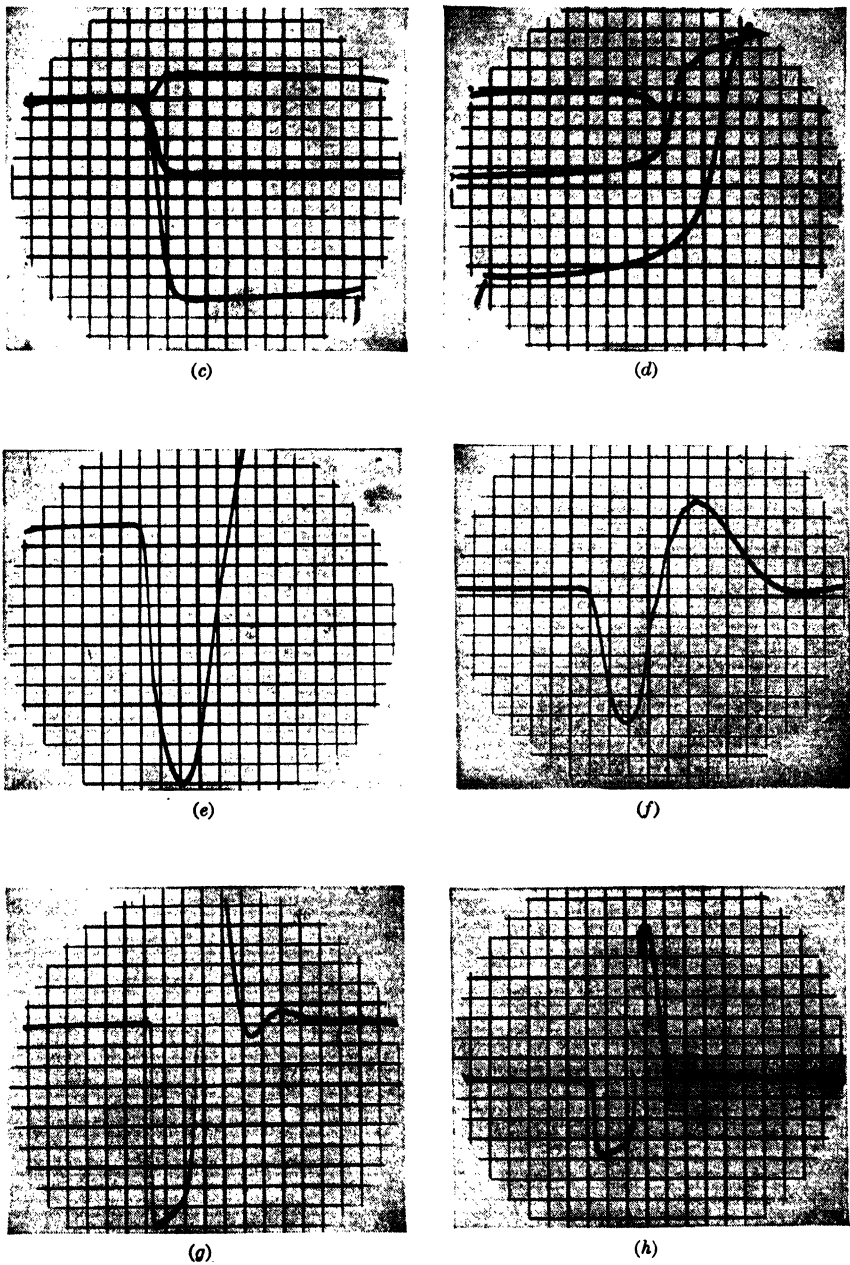
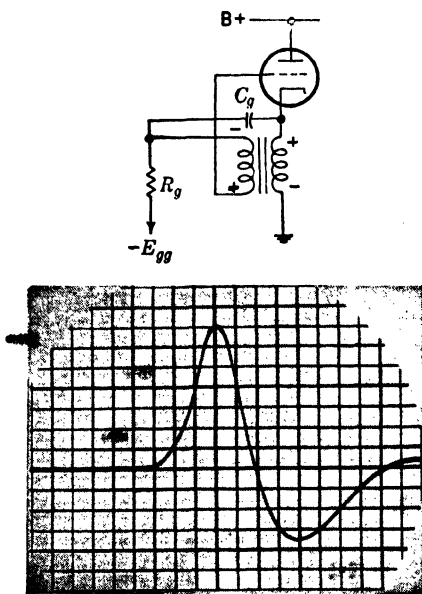
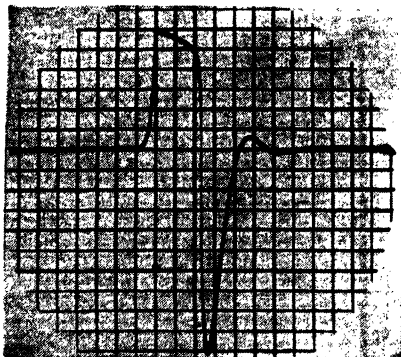


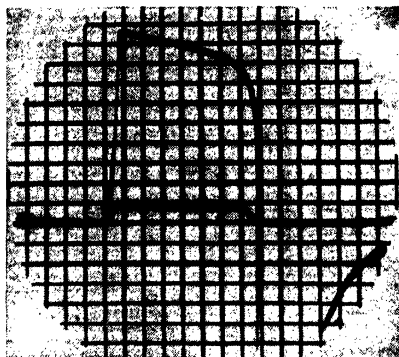
FIG. 6-16.—For legend see opposite page.



(a)



(b)



(c)

FIG. 6-17.—Cathode-to-grid feedback. Connection: two windings in cathode-ground circuit; two windings in cathode-grid circuit. Vertical deflection 25 volts/division. (a) Continuously wound core.  $C_g = 250 \mu\text{f}$ .  $E_k$  waveform; sweep speed  $0.3 \mu\text{sec/division}$ . (b) Continuously wound core.  $C_g = 0.1 \mu\text{f}$ .  $E_k$  waveform; sweep speed  $1.4 \mu\text{sec/division}$ . (c) Butt-joint core.  $C_g = 0.2 \mu\text{f}$ .  $E_k$  and  $I_k$  waveforms; sweep speed  $1.4 \mu\text{sec/division}$ .

current pulse of either polarity, a negative plate or cathode-voltage pulse, or the grid-bias waveform.

The plate pulse has a very large amplitude due to the turns ratio of the transformer and the fact that the plate-to-cathode potential does not decrease as rapidly as the plate-to-ground potential when the cathode is being driven negative.

This circuit owes its utility to the fact that the amplitude of the grid-bias waveform does not vary as rapidly with variations of heater voltage as the other types of blocking oscillators.<sup>1</sup> A change in the amplitude of the grid-bias waveform will manifest itself in a change of repetition frequency of a free-running blocking oscillator.

The waveform of the pulse does not approximate a rectangle so closely as in the plate-to-grid-coupled type since its initial slope is smaller and its amplitude decreases appreciably with time for pulses of long duration. There is a small choice of turns ratio available with a given transformer because the circuit requires a voltage stepdown from plate to cathode. Because of the above effect the circuit is useful in applications such as frequency dividers (see Chap. 16), and pulse-repetition-frequency generators.

*Cathode-to-grid Feedback.*—In this type of circuit (see Fig. 6-17), the primary of the transformer is placed in the cathode circuit instead of in the plate circuit and the grid is “bootstrapped,” so the primary of the transformer does not appear in the grid-to-cathode loop. This circuit is identical with that of Fig. 6-5 except that the ground point has been moved. The similarity of the grid-plate, cathode-grid, and grid-plate-cathode feedback circuits is illustrated in Fig. 6-18. The polarity of the transformer is such that the grid is driven positive as the cathode potential rises. A severe disadvantage is thus introduced: because the grid must rise nearly twice the cathode pulse amplitude, the effects of the stray capacity from grid to ground are serious. The similarity between this circuit configuration and that of the Hartley c-w oscillator is striking.

The only possible use for this circuit would arise from the fact that a large positive-voltage pulse can be obtained directly from the cathode without the use of a tertiary winding. The waveforms are shown in Fig. 6-18. Because of the increased effects of the stray capacity, this circuit has a pronounced tendency to act only as a regenerative amplifier if small values of  $C_g$  are employed (see Fig. 6-17a), and even if  $C_g$  is made large and added effects of the stray capacity are manifest in a very slowly rising pulse (see Fig. 6-17c). Since the grid-to-cathode loop of this circuit is not connected to ground only parallel triggering methods can be employed. This is a serious disadvantage since a large amplitude trigger with fast rise is necessary to insure that the circuit does not act as a regenerative amplifier only.

<sup>1</sup> This observation is purely empirical and has not been satisfactorily explained.

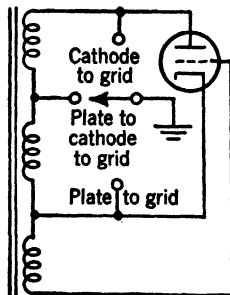


FIG. 6-18.—Schematic diagram illustrating the interconversion of three types of blocking oscillator by shifting the ground point.

*Plate-to-cathode-to-grid Feedback.*—This circuit (see Fig. 6-19) is obtained from that of Fig. 6-15 by moving the ground point to the center tap of the primary winding. In any circuit the leakage inductance and most of the stray capacity are in the transformer. In this circuit they are so divided between the plate and cathode circuits that a smaller time constant appears in each. Since these time constants are not added when the two voltages are combined to give the total primary voltage, the resultant time constant for the rise of this voltage is smaller than if the whole primary were placed in either the cathode or plate circuits.

Since the grid-to-cathode loop of this circuit is not connected to ground, parallel triggering must be employed, preferably by the use of a trigger amplifier.

This circuit provides both positive and negative voltage pulses without the use of an auxiliary winding. These voltage pulses are of smaller

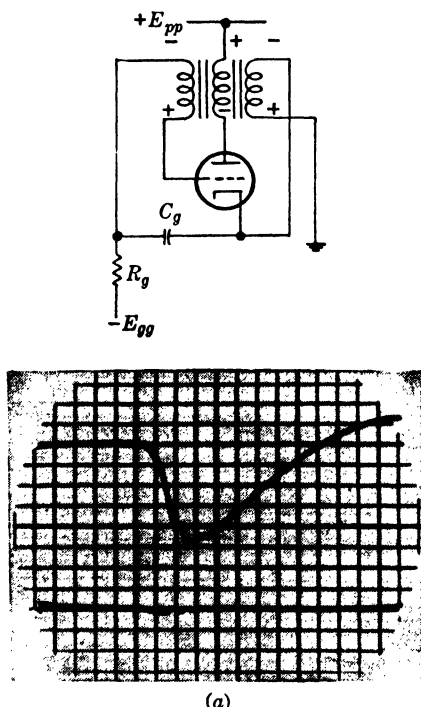


FIG. 6-19.—Plate-to-grid-to-cathode feedback. Connection: two windings in plate circuit; two in cathode circuit; two in grid-cathode circuit. Vertical deflection 25 volts/division. (a) Butt-joint core;  $C_g = 250 \mu\text{f}$ ;  $E_p$ ,  $I_k$  waveforms; sweep speed  $0.15 \mu\text{sec/division}$ . (b) Continuous core;  $C_g = 250 \mu\text{f}$ ;  $E_p$  waveform; sweep speed  $0.3 \mu\text{sec/division}$ . (c) Continuous core;  $C_g = 0.1 \mu\text{f}$ ;  $E_p$  waveform; sweep speed  $1.4 \mu\text{sec/division}$ . (d) Butt joint core;  $C_g = 2.0 \mu\text{f}$ ;  $E_p$  waveform; sweep speed  $1.4 \mu\text{sec/division}$ . (e) Butt joint core;  $C_g = 2.0 \mu\text{f}$ ;  $I_p$ ,  $I_k$  waveform; sweep speed  $1.4 \mu\text{sec/division}$ . (f) Leading edge: butt joint core;  $C_g = 2.0 \mu\text{f}$ ;  $I_p$ ,  $I_k$  waveforms; sweep speed  $0.15 \mu\text{sec/division}$ . (g) Falling edge: butt joint core;  $C_g = 2.0 \mu\text{f}$ ;  $I_p$ ,  $I_k$  waveforms; sweep speed  $0.15 \mu\text{sec/division}$ .

amplitude than those which may be obtained from other circuits. Either positive- or negative-current pulses, however, may likewise be obtained, although these will also be of smaller amplitude because of the adverse

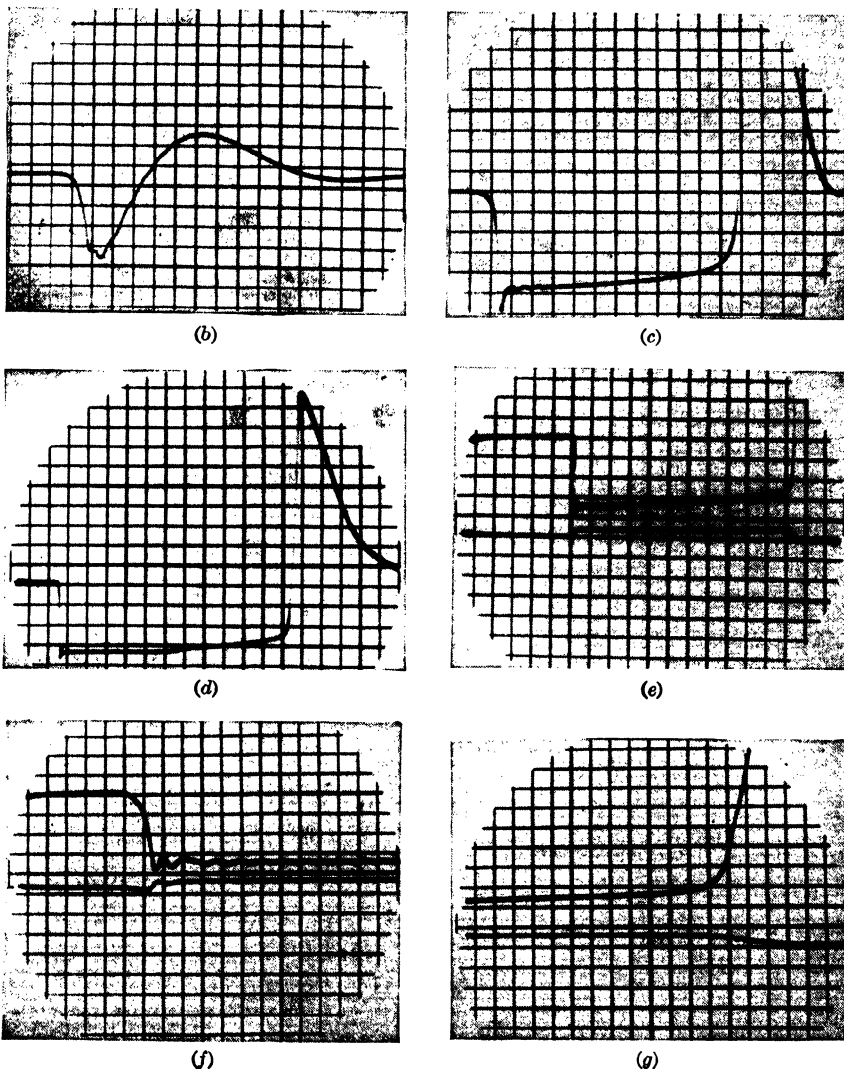
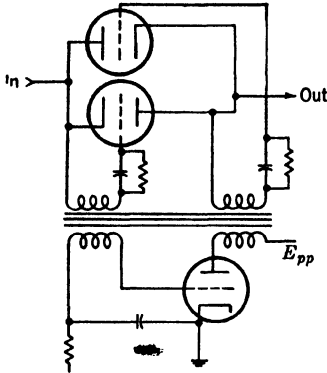


FIG. 6-19.—For legend see opposite page.

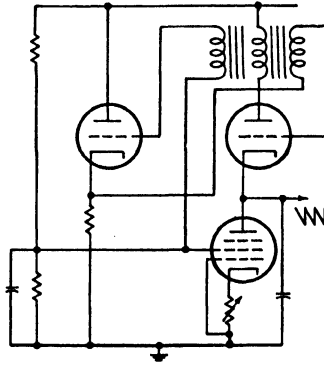
turns ratio used in this example. Larger current pulses can be obtained by using an over-all one-to-one ratio between primary and secondary.

**6-10. Some Applications of Blocking Oscillators.**—Figures 6-20a and 6-20b show the use of blocking oscillators in actuating bidirectional

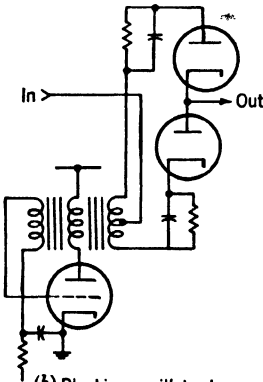




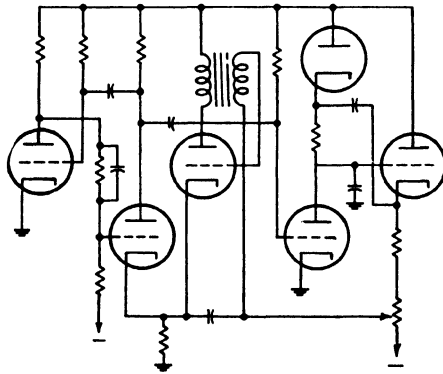
(a) Blocking oscillator to actuate triode switch



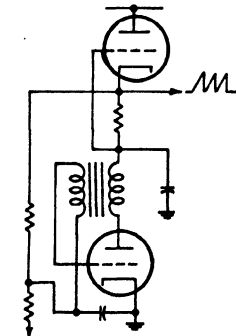
(d) Free running negative sawtooth



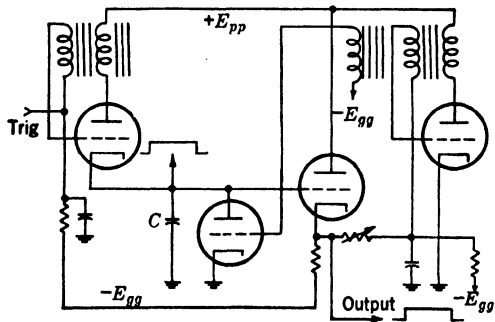
(b) Blocking oscillator to actuate diode switch



(e) Blocking oscillator to terminate triggered sawtooth



(c) Free running positive sawtooth



(f) Blocking oscillators for generating wide rectangular pulse

FIG. 6-20.—Some applications of blocking oscillators.

switches. Large-amplitude, low-impedance pulses which are isolated from the rest of the circuit are provided by the output windings. The voltage pulses must build up biases that are large enough to prevent conduction of the largest expected signals.

Figures 6-20c and 6-20d show a blocking oscillator used as a switch in a linear, free-running time base. The inductance of the transformer must be large enough to prevent the pulse from terminating before the condenser has charged. These circuits are capable of operating at much higher frequencies than those employing gas-tube switches.

In Fig. 6-20e a blocking oscillator is used as an amplitude comparator to terminate the action of a triggered time-base generator (see Chap. 7) at a predetermined amplitude. The time constant of the multivibrator gate generator should be made very long so that the blocking oscillator has control. The precision obtainable with a blocking-oscillator comparator (3 to 4 volts) is discussed in Chap. 9.

In Fig. 6-20f two blocking oscillators that are designed to give very rapidly rising pulses of very short duration are used to produce a variable-width rectangle. The first pulse rapidly charges the small condenser *C*. The step produced is quasi-integrated to produce a sawtooth waveform which delays the firing of the second blocking oscillator which discharges *C*.

*Quenching Oscillators.*—These are high-frequency oscillators using air-core transformers. A grid resistor and condenser that have a time constant large compared with one period of the oscillator are used. Bias is built up by grid current until the gain around the feedback loop is reduced below unity. The oscillator then blocks until the bias circuit has recharged. Quenching oscillators are used as self-pulsed transmitters in some radar sets such as the Mark-II ASV and ASB. They function as oscillator, modulator, and PRF generator combined. The PRF is not very stable since tuning and antenna loading affect the grid current and grid voltage. Quenching oscillators are also used as demodulators in some superregenerative receivers.

A quenching-oscillator PRF generator is shown in Fig. 6-21. The coils are wound on a polystyrene form and are ruggedly mounted and well shielded. Since an iron core is not used in the transformer, the stability is good. The circuit oscillates at about 20 Mc/sec. and the PRF is variable between about 50 cps and 5 kc/sec.

A quenching-oscillator PRF generator is used as an audio-frequency modulator in radiosonde equipment and is described in Vol. 20, Chap. 10, of this series.

*Cascaded Blocking Oscillators.*—It was mentioned previously that the steepness of rise of a blocking-oscillator pulse is dependent on the rate of rise of the initiating trigger. The shortest and most rapidly rising pulses

have been produced by using a blocking oscillator to produce a fast trigger for another blocking oscillator. Figure 6-22 shows a selector-pulse generator for accurate automatic time measurement. A fairly rapid trigger fires the first blocking oscillator which produces a 200-volt 0.16- $\mu$ sec pulse that is nearly triangular in shape. This pulse actuates the second blocking oscillator to produce a 0.12- $\mu$ sec pulse that is nearly rectangular. The 132DW transformer (see Table 6-1) uses the thinnest available hypersil core (0.0015 in.), and each winding consists of only 20 turns. The cathode followers used to prevent interaction

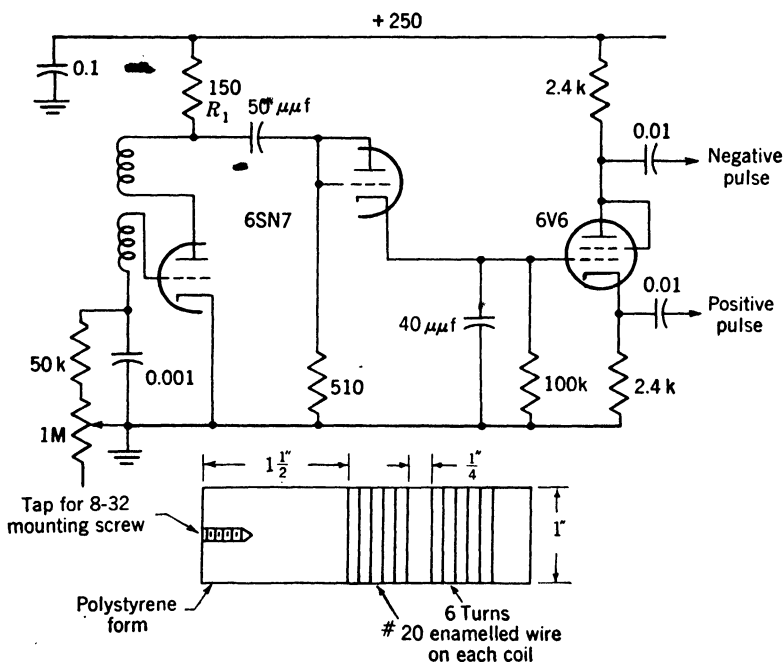


FIG. 6-21.—Quenching-oscillator PRF generator.

between the blocking oscillators and their trigger sources may not be necessary. The output pulses are nearly rectangular, rising and falling in 0.03  $\mu$ sec.

Pulses of the order of 0.1  $\mu$ sec may be generated without the application of exceptionally steep triggering waveforms by the use of a 132DW transformer (or the core of a 132AW with 16 turns instead of 32 turns on each winding) if a triode-connected 6AC7 is used. A 6AG7 should be used as a cathode follower to drive the grid condenser if series triggering is desired, or a 6AG7 should be used as a pentode for parallel triggering. The high  $g_m$  of the 6AC7 is necessary to permit regeneration with the very low impedance of the transformer and the high impedance of the very small grid condenser that are necessary to produce such a short pulse.

*Very Long Pulses.*—A circuit using a grid-plate-cathode-connected OA-15 pulse transformer for producing 25- $\mu$ sec pulses is shown in Fig. 6-23. The pulse is substantially rectangular and is used as a gate for the “R” sweeps in the Du Mont 256-B oscilloscope. It is necessary that the pulse be accurately flat on top since it is used as a gate for the

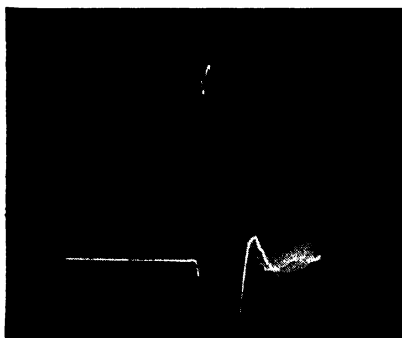
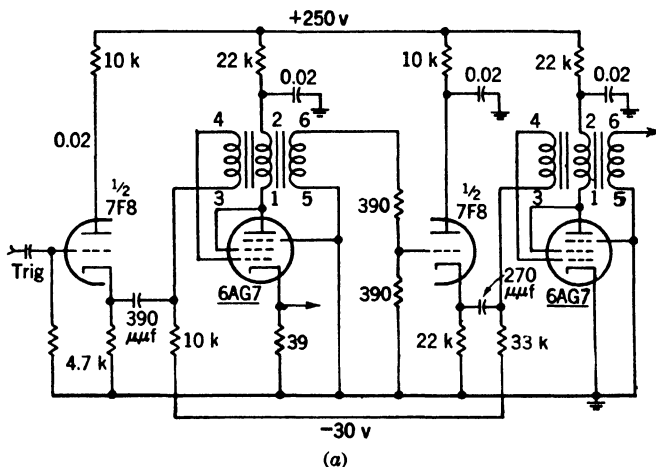


FIG. 6-22.—Cascaded blocking oscillator for very fast pulse. (a) Circuit; (b) waveform.

cathode-ray tube. Any variation in pulse amplitude would produce a corresponding change in brilliance of the trace.

It is possible to generate pulses as long as 50 or 100  $\mu$ sec by the use of special pulse transformers or audio transformers. Since the distributed capacitance and leakage inductance of these transformers are large, the pulses will rise fairly slowly, and ringing will be present after each edge of the pulse. The currents obtained will be smaller than those obtained with short-pulse transformers because the d-c resistances of the higher inductance windings are large. Since the number of turns is large, the

core will saturate at small values of current. Parallel feed should be used or d-c magnetic bias applied. In general, it will probably be found that multivibrators are more economical for generation of pulses wider than  $25\ \mu\text{sec}$ .

**6-11. Delay-line Pulse Generators.**—Delay lines are frequently used in the generation of rectangular pulses of fixed duration. They are used to produce a rectangle from a step function, to terminate a pulse produced by a regenerative device such as a multivibrator or a blocking oscillator, or they may be used to duplicate an existing pulse at a later time. They are simple, reliable, and permanent in their characteristics, and are accurately reproducible in manufacture. The distributed parameter types of delay lines produce the best waveforms and are simple to manufacture,

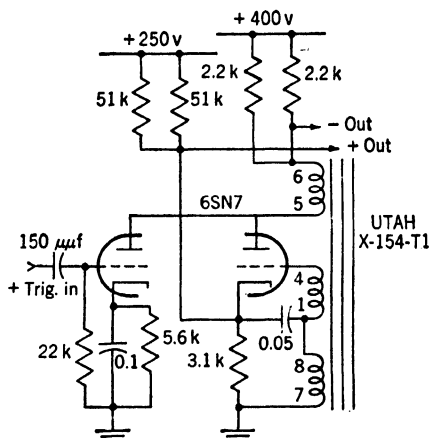


FIG. 6-23.— $25\ \mu\text{sec}$  blocking oscillator from 256B oscilloscope.

impedance,  $Z_0$ . Initially,  $I_0 = E_i/2Z_0$  and  $E_0 = E_{z_0} = E_i/2$ . The step function travels down the line charging up each section as it goes and maintaining a constant charging current. When the wave reaches the end of the line, it is reflected back in phase since there is no termination to absorb the energy. The reflected step function continues to charge the line at the same rate as previously so that the current in  $Z_0$  continues to be constant. When the reflected step reaches the end of the line, its energy is absorbed by  $Z_0$ . The impedance of the line suddenly becomes infinite so that  $I = 0$ .

An open-ended delay line, therefore, operates on a step function of voltage to produce a pulse of current equal in duration to twice the length of the line. The pulse across the characteristic impedance in series with the line has one half the amplitude of the step function.

In Fig. 6-24*b* a high-impedance source is used to provide a step func-

but networks composed of lumped constants are usually more compact and are capable of being temperature-compensated. For a complete discussion of the properties of electrical delay lines see Chap. 22 and Vol. 17, Chap. 6, of this series.

#### 6-12. Use of a Delay Line in Terminating a Step Function.

—In Fig. 6-24 two basic methods of using a delay line to terminate a pulse are illustrated. In the first, a low-impedance switch is used to produce a step function of voltage across an open-ended line in series with its characteristic

tion of current. Initially,  $I$  divides equally between the line and the terminating resistor  $R = Z_0$ . As a consequence, a voltage  $E_0 = (IZ_0)/2$  appears across the line which charges with constant current, and a constant-voltage drop is produced. The step of current is reflected in phase (the voltage is inverted) by the short circuit at the end of the line and travels toward the beginning. When the step reaches the beginning of the line, the energy is absorbed by  $Z_0$  and the impedance of the line suddenly becomes zero so that  $E_0$  is also zero.

Accordingly, a short-circuited delay line operates on a step function of current to produce a pulse of voltage equal in duration to twice the

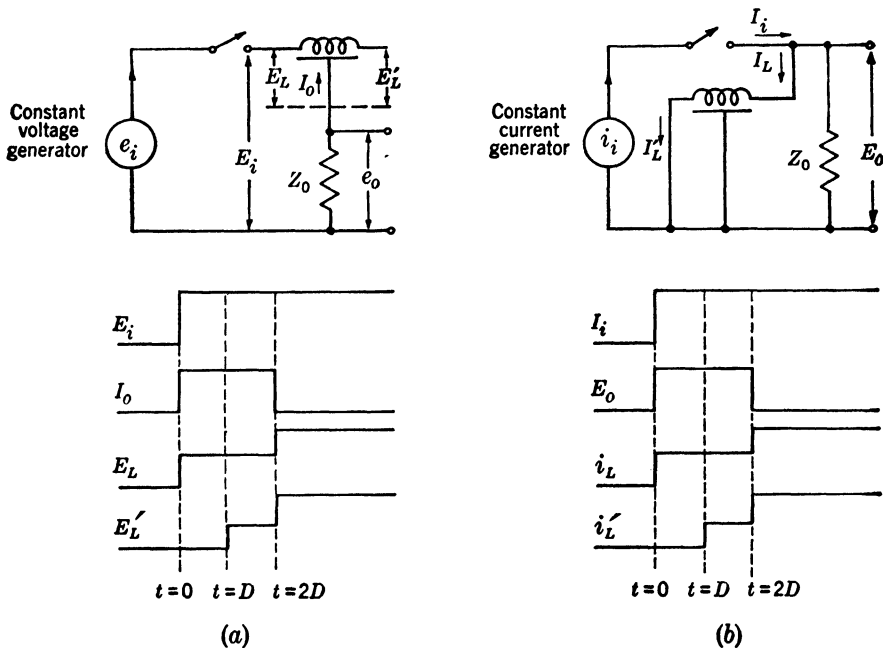


FIG. 6.24.—Basic delay-line pulse generators and idealized waveforms. (a) Open line type; (b) short-circuited line type.

length of the line. The voltage produced has half the amplitude of the step of current multiplied by the characteristic impedance.

Thus, there is a complete duality between open lines charged from a constant voltage source and short-circuited lines charged from a constant current source. The choice of the method depends upon the characteristics of the switch used to produce the step function. A thyatron switch has an impedance of less than 10 ohms and therefore effectively constitutes a constant voltage source. A pentode switch, on the other hand, may have an impedance of a megohm when closed, and yet switch appreciable currents.

In the above discussion ideal lines operated upon ideal step functions. In practice, the step function is not infinitely steep. Thyratrons operate in as little as  $10^{-8}$  sec, and hard tubes give results that depend upon

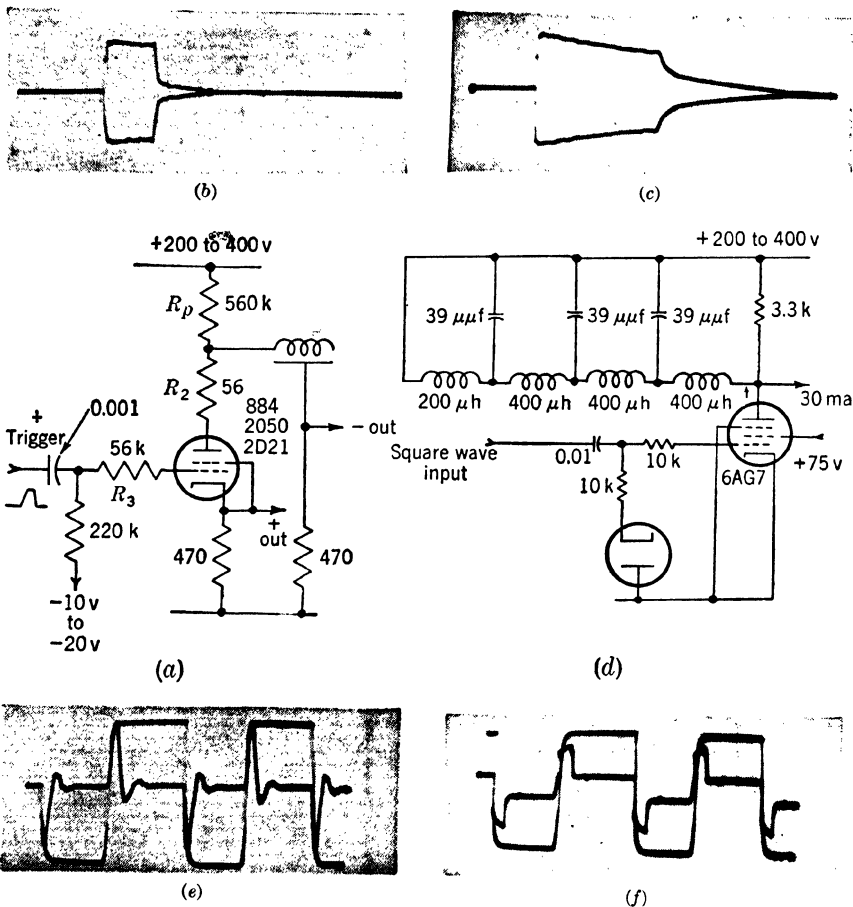


FIG. 6-25.—Delay-line pulse generators. (a) Circuit of open-line pulse generator. (b) Current waveforms from line and from the cathode of the thyatron. A 1- $\mu$ sec GE type YE4B line is used to produce a 2- $\mu$ sec pulse. (c) Delay line of (b) replaced by 4- $\mu$ sec line to produce an 8- $\mu$ sec pulse. Note the effects on the pulse produced by distortion in the longer line. (d) Circuit of shorted-line pulse generator. (e) Pulse produced by four-section lumped line shown in the circuit diagram. The exciting 50-kc/sec square wave is taken across a 2.2 k resistor that replaces the line and may be used for comparison. (f) Effect of replacing the lumped line with a 1- $\mu$ sec-type YE4B line. Note that the pulse is much squarer due to the superior response of the line but that a large pedestal is produced by the larger d-c resistance of the line.

steepness of the grid pulse and the effects of stray capacitance. The slope of the step function determines the slope of the leading edge of the pulse. The slope of the trailing edge is determined by the slope of the

step function and the characteristic response of the line. Amplitude and phase distortion have the same effect on the trailing edge of the pulse as they do in normal delay-line usage. Shock excitation of accidental resonances in the line may cause oscillation following both edges of the pulse. When thyratrons are used, leads of appreciable length may also act as tuned circuits that are shock-excited by the very rapid step that is produced. Under these conditions, it is best to make all leads as short and direct as possible and make necessarily long leads by properly terminated coaxial cables.

Since all delay lines have resistance associated with them, this resistance distorts the pulse; this distortion results in reduced current as the lines are charged and a consequent slope in the top of the pulse. In the case of the short-circuited line, the total lengthwise d-c resistance results in an impedance that is not zero after the pulse. The original step function therefore appears as a "tail" on the pulse of initial amplitude  $E_{(T)} = I_s(R_{d-c}Z_0)/(R_{d-c} + Z_0)$ , where  $R_{d-c}$  is the lengthwise resistance of the line and  $Z_0$  is the terminating resistance.

Typical circuits are shown in Fig. 6-25. In the thyatron circuit shown in Fig. 6-25a, the delay line is initially charged through  $R_p$ . Triggering of the gas tube switches a voltage step of amplitude  $E_{pp}$  across the line. Positive pulses can be taken from the cathode or negative pulses from the common terminal of the line. The total resistance in the discharge path should be  $Z_0$  or smaller. A small terminating resistance will reduce the output voltage and in practice will improve the shape of the pulse. After the gas tube deionizes, the line charges through  $R_p$ . Since the line is very short compared with the charging time, it appears as a pure capacitance, and hence the recharge curve is exponential. Since  $Z_0 \ll R_p$ , the step appearing in the output during the recharge time is of negligible amplitude. The plate-supply resistor must be sufficiently large to permit rapid quenching of the thyatron and depends upon the tube type. (See "Thyatron Frequency Dividers," Chap. 16.)

It must be emphasized that the protective resistors  $R_2$  and  $R_3$  must be mounted directly on the tube socket with a minimum of stray capacitance. Since the impedance of the gas tube is very low, the current drawn from even a small capacitance will ruin the cathode unless a current-limiting resistance is inserted. The lack of success that many engineers have experienced in the use of gas tubes is almost completely attributable to this cause.

A short-circuited-line pulse generator is shown in Fig. 6-25b. If a positive pulse is desired, the tube is initially conducting and is cut off by a fairly rapid negative step function derived from some other source such as the edge of a rectangular pulse from a multivibrator or other rectangle-generating circuit. The amount of current flowing in the line





function is applied to the grid of  $V_i$ , the plate voltage will be

$$\Delta E_p = E_i \frac{(g_m R_p)}{(1 + g_m Z_k)},$$

where  $Z_k$  is the net cathode impedance of  $V_1$ . Initially,  $Z_k = Z_0 = 1/g_m$ , and hence  $\Delta E_p = E_i(g_m R_p)/2$ . At time  $t = 2D$ , the impedance of the

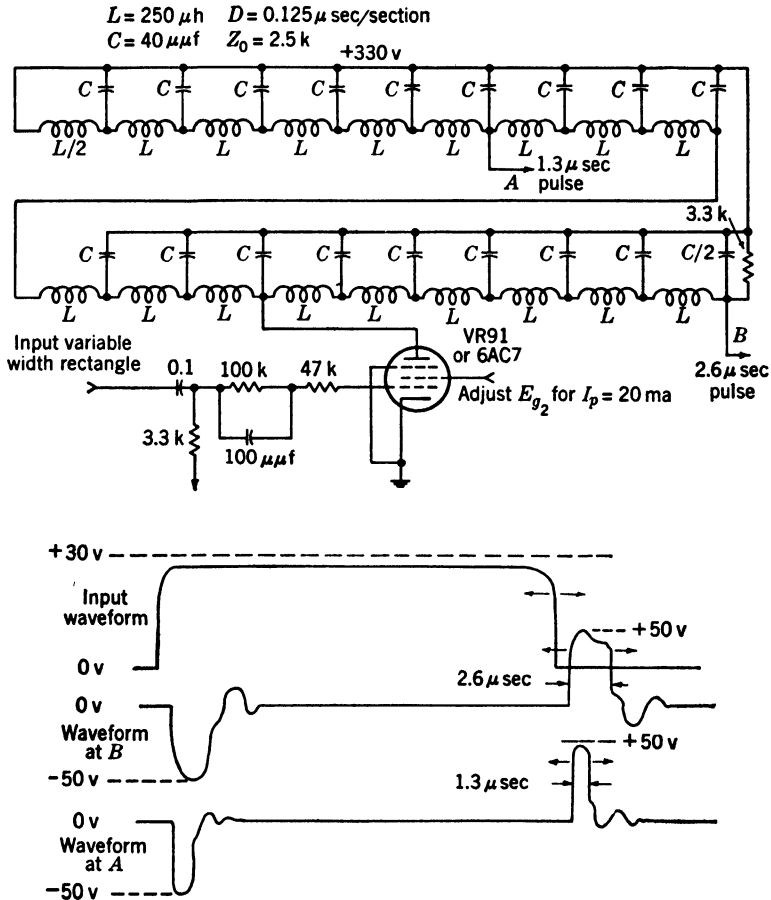


FIG. 6-27.—Delay-line pulse generator from ASV Mark 6.

open line becomes infinite; therefore, if  $V_2$  is truly a constant-current tube,  $\Delta E_p = (g_m R_p)/(1 + \infty) = 0$ . With normal receiving tubes

$$\frac{1}{g_m} = 100 \text{ to } 500 \text{ ohms,}$$

which is a convenient impedance for the construction of delay lines. Since the tube is conducting after the pulse, it is important that an exact

impedance match be made, or reflections will produce spurious pulses in the output. If a large negative supply is available, the constant-current tube may be replaced by a pure resistance  $R_k$  and a pedestal of magnitude  $(E_i g_m R_p)/(1 + g_m R_k)$  will be produced by the step function. An analogous circuit using a line short-circuited by  $C$  with voltage feedback might be used as shown in Fig. 6-28b. For this purpose a very high-impedance line must be used, since for proper termination,

$$Z_0 = \left( \frac{1}{g_m} R_p \right) / \left( \frac{1}{g_m} + R_p \right) = R_o + R_i,$$

and for gain greater than unity,  $Z_0 > R_o + R_i$ . A pedestal of magnitude  $E_i R_{d-c}/R_o$  will be produced by the step function. Since it is difficult to

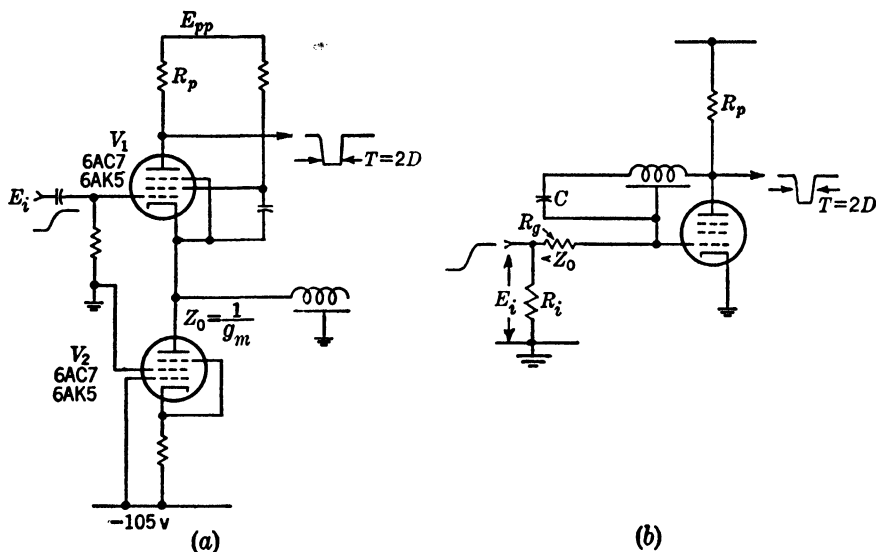


FIG. 6-28.—Delay line used in degenerative feedback networks. (a) Open-circuited delay line with current feedback; (b) short-circuited delay line with voltage feedback.

construct delay lines of high  $Z_0$  and low  $R_{d-c}$ , this circuit does not appear ever to have been used and is included only for the sake of completeness.

It is possible to construct a pulse generator in which the step function is passed through a time selector which is turned off by the inverted and delayed step function. An example of this technique is shown in Fig. 6-29a. The input waveform is applied to one control element of the selector circuit, and the inverted and delayed step to another. Conduction can take place only during the delay time. This circuit is capable of excellent waveform since, if a large input is used, the control elements will operate on a small portion of the rise of the waveforms and limiting will take place. Unlike the previous circuits, the pulse width will be

equal to the line length. Another circuit in which the pulse width is equal to the line length is shown in Fig. 6-29*b*. A switch applies a constant potential step across the terminated end of the line, and the pulse is taken across the ends of the winding. Initially, the impedance of the line is equal to  $Z_0$  and, after time  $t = D$ , it is equal to  $R_{dc}$ . The principal advantage of this circuit lies in the fact that the pulse amplitude is equal to the amplitude of the initial step function.

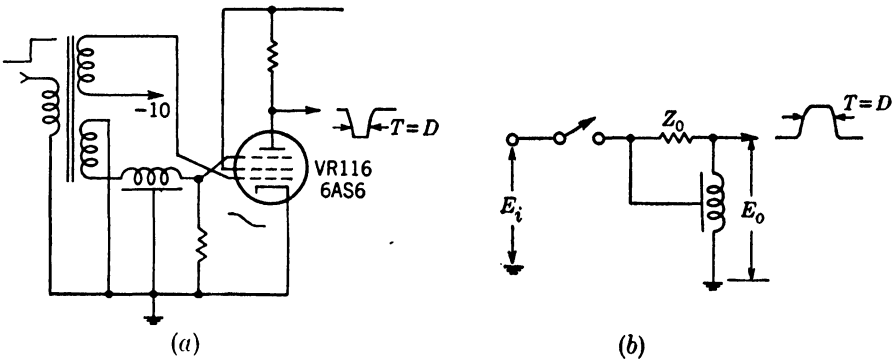


FIG. 6-29.—Circuit producing pulse duration equal to line delay. (a) Delay and coincidence; (b) another circuit to produce pulse of duration equal to line length.

**6-14. Delay Line Used to Terminate Regenerative Action.**—Delay lines are frequently used in regenerative rectangle generators to determine the width of the pulse. The regenerative device produces a step function which is applied to the line. The delayed step function which has traversed the line initiates reversal of the regenerative process; thus the pulse is terminated. Figure 6-30 illustrates this technique as applied to multivibrators and blocking oscillators. It should be emphasized that delay-line external control is the only method of insuring that a blocking oscillator will produce a pulse of accurately determined duration. In Fig. 6-30*a* the line appears as a “delayed short circuit” in parallel with the grid of the tube that is turned off during the pulse and turns this tube back on, and the cycle is terminated regeneratively. The line should have a fairly high impedance so that the grid can be driven well beyond cutoff by the tube that is conducting during the pulse, and  $R_p$  should equal  $Z_0$ . In Fig. 6-30*c* the line appears as a delayed short circuit across the pulse transformer, and the quasi-equilibrium state of the blocking oscillator is terminated. If the transformer has a turns ratio of 1 to 1, the impedance of the line should be fairly high ( $> 500$  ohms) so that it does not absorb too much energy from the pulse, but its d-c resistance must be small ( $< 100$  ohms) so that the transformer is very heavily loaded after the pulse. The turns ratio of the transformer may be adjusted to provide the desired impedance match with a given line.

In Figs 6-30*b* and *d* the line appears as a delayed open circuit in series with the grid of a tube. In Fig. 6-30*d* the line should have a low impedance ( $< 1000$  ohms if a triode is used) so that the tube may be driven into the grid-current region. If the impedance of the line is very low, however, it may appear as a pure capacitance to the grid circuit, and the pulse width will be controlled by the capacitance and not by the delay time of the line. The transformer must be capable of giving a pulse longer than  $2D$ .

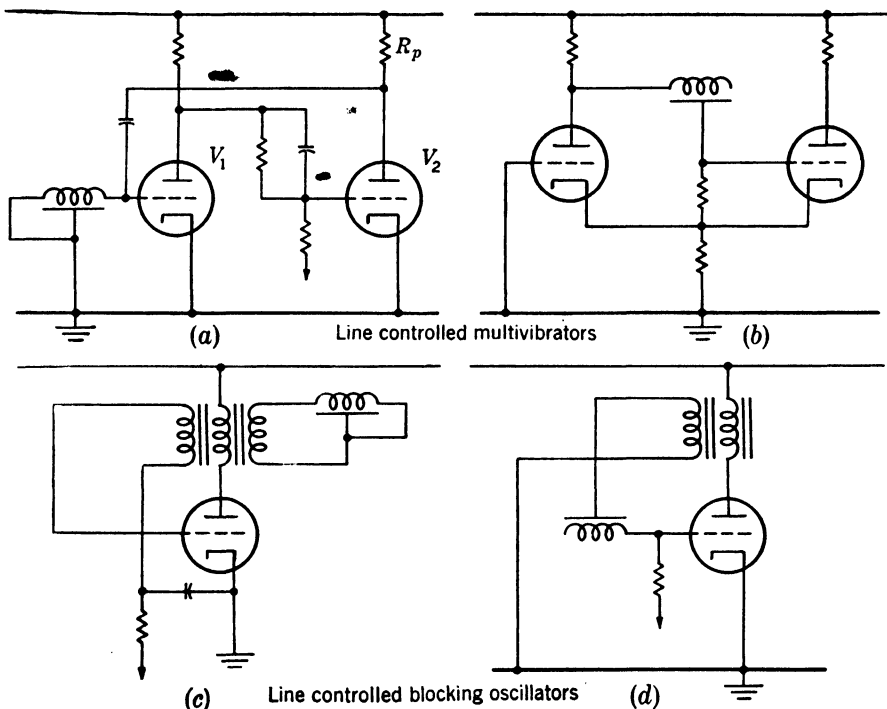


FIG. 6-30.—Delay line used to terminate the action of regenerative device.

Figure 6-31 shows a practical circuit using a delay-line-controlled blocking oscillator to form pulses of 0.5- or 2.5- $\mu$ sec duration. Since the shape of the output pulse is determined mainly by the characteristics of the transformer, nearly rectangular pulses may be obtained even if the delay line has very few sections.

A circuit for generating two adjacent 1- $\mu$ sec gates is shown in Fig. 6-32. The delay line controls both the width and spacing of the gates to insure that the second rises at exactly the time the first falls. The cathode-current pulse from  $V_{2a}$  is delayed by the line and causes conduction in  $V_{2b}$ . This conduction opposes the current in the transformer and causes the pulse to terminate.

**6.15. Duplication of Pulses by Means of Delay Lines.**—Combinations of delay lines are often used for generating pulse trains, and these pulses are attenuated and distorted by an amount depending upon the quality of the line. The reproduced pulses may be used in synchronization or time selection, as time markers, to form codes for identification or channel selection, etc. The pulses may have the same sign as that of

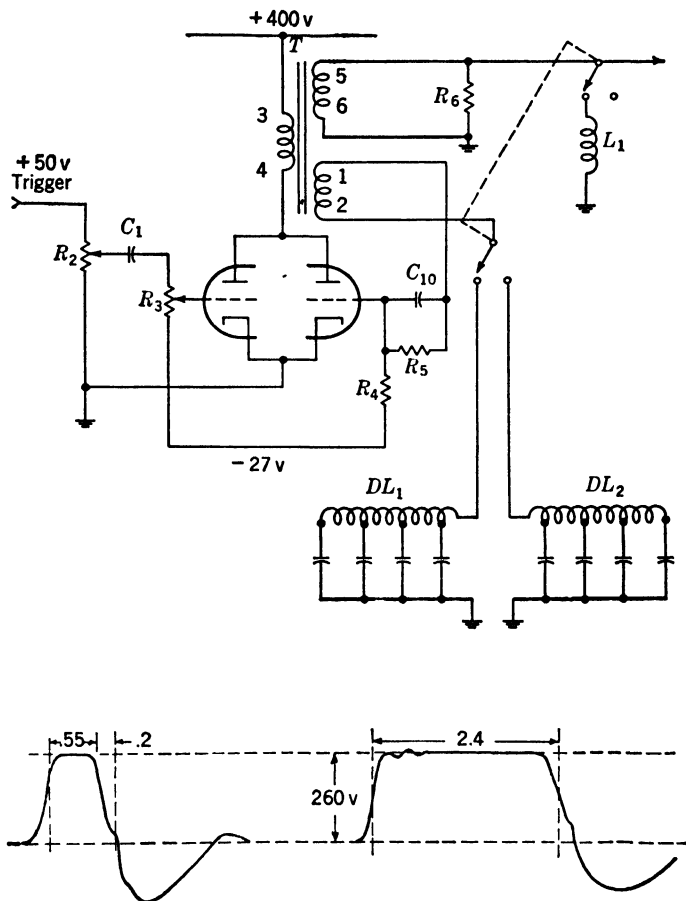


FIG. 6-31.—Delay-line-control blocking oscillator.

the input waveform, or they may be inverted in phase, depending upon the terminating impedances used. If the output end of the line is terminated in  $Z_0$ , one pulse will appear in the output. No other pulses will appear because all the energy will be absorbed by  $Z_0$ . The input need not be correctly terminated because no energy will be reflected back. If the input and output impedances are infinitely high, the pulse will be reflected back and forth between the ends of the line, and will be

reduced in amplitude only by the attenuation of the line during each transit. If the terminating impedances are finite and resistive the pulse will suffer attenuation on each reflection. If a terminating impedance is less than  $Z_0$ , the pulse will be inverted on each reflection and will suffer attenuation unless the terminating impedance is zero. Figure 6-33 shows the polarities of the reflections for various values of input and output impedances. If many equally spaced pulses are desired, the energy may be renewed by a regenerative circuit after each reflection as shown in Fig. 6-34. A blocking oscillator produces a pulse which travels down the line,

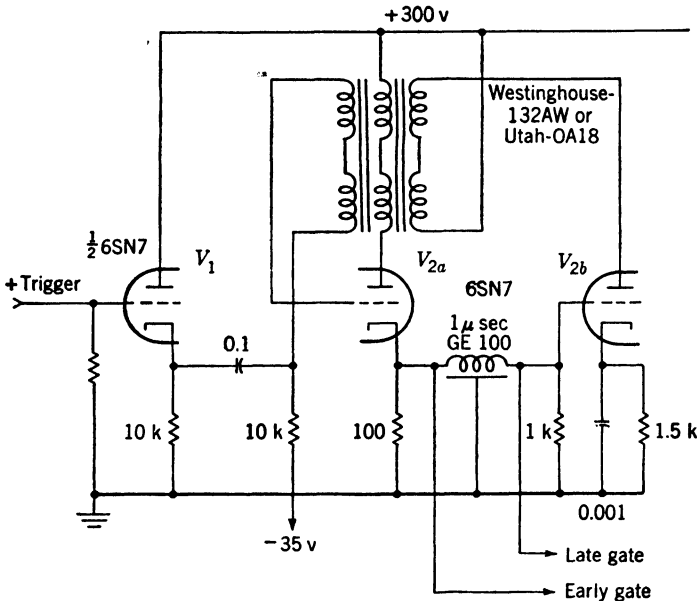


FIG. 6-32.—Delay-line blocking oscillator used to produce double gate in time demodulator.

is reflected back, and retriggers the monostable blocking oscillator. In the circuit shown, a trigger pulse initiates a train of pulses that are interrupted after a predetermined interval by a method similar to that employed in pulsed sinusoidal oscillators. The input trigger starts the gate multivibrator which removes cutoff bias from the suppressor of the blocking oscillator tube,  $V_2$ . The trigger is also differentiated and applied through  $V_2$  to the tertiary winding of the transformer to initiate the first pulse. Succeeding triggers are supplied by the reflections from the line. Clamp tube  $V_{3s}$  restores the initial bias to the grid of  $V_2$  after each pulse. If  $V_{3s}$  were not present, the accumulated bias would cause the blocking oscillator to trigger progressively later on each reflection, and would destroy the uniformity of the pulse spacing. At the end of the gate the suppressor of  $V_2$  is again cut off and the circuit returns to its

quiescent condition. This circuit is somewhat simpler than most shocked-oscillator pulse generators and produces excellently shaped pulses. The bulk, poor quality, and large temperature coefficients of available delay lines have prevented extensive use of this device.

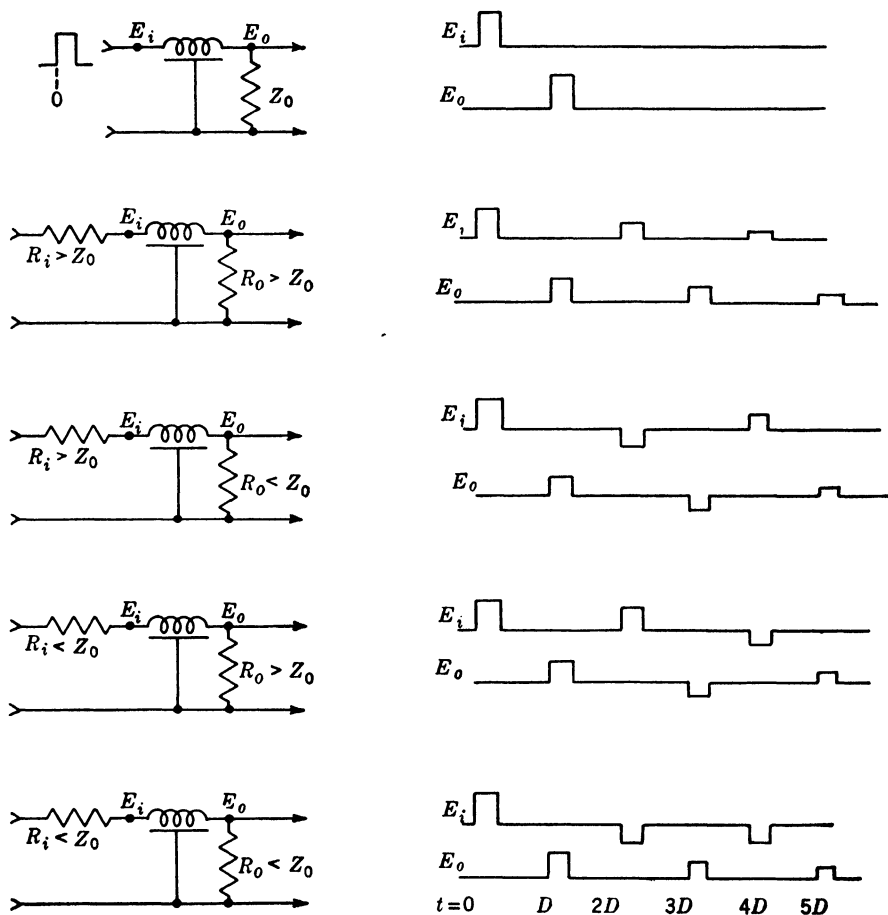


FIG. 6-33.—Delay lines and reflections.

Figure 6-35 shows the use of delay lines to produce irregularly spaced pulses. In Fig. 6-35a a series addition of the outputs of the lines is used. A fraction of the input to each line is passed on to the next line and a fraction to the load, because the first line is not correctly matched by the series combination of the second line and  $R_2$ ,  $R_4$  is added. If the reflection introduced by the omission of  $R_4$  is negligible, it is omitted. If no attenuation were present in the lines, the amplitude of each output pulse would be one third that of the input pulse. In practice,  $R_2$  and  $R_3$



are adjusted until the output pulses appear to be of equal amplitude. A similar circuit using parallel addition is shown at Fig. 6-35*b*. The impedance of the adding network should be high compared with that of the lines to prevent interaction. If very long lines are used, regenerative devices may be added after each delay to shape the pulse as shown at Fig. 6-35*c*. Each blocking oscillator produces a negative pulse which will not trigger the following blocking oscillator directly. Since the line is short-circuited, the positive reflection will trigger the next stage. The

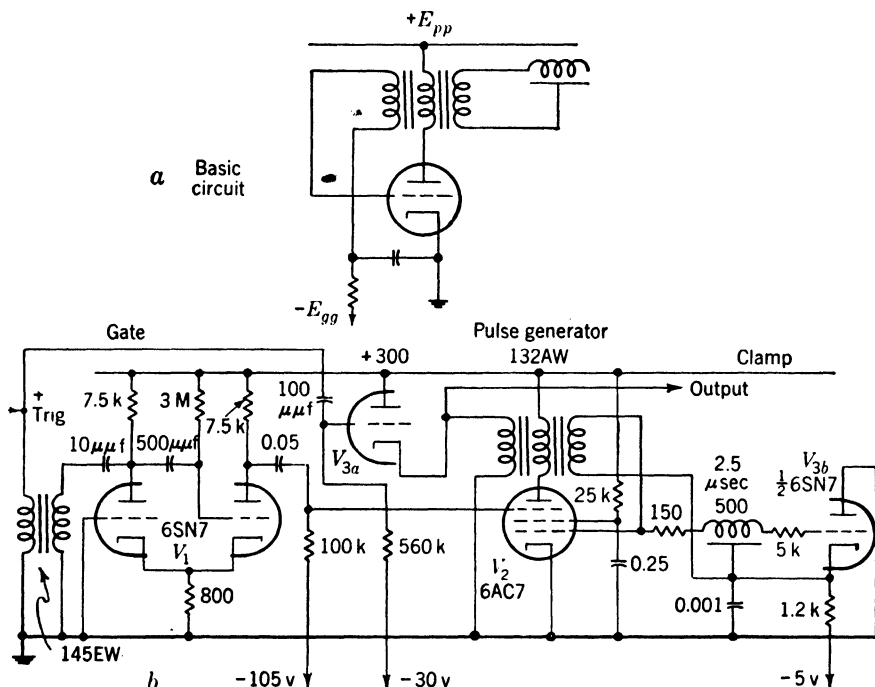


FIG. 6-34.—Pulsed marker generator using delay-line control of pulse spacing. (a) Basic circuit; (b) final circuit.

pulses are spaced by twice the line length. Any number of stages may be used and, if desired, the last stage may trigger the first so that a continuous train of controllably spaced pulses is produced.

An accurate circuit for producing a trigger pulse followed by a variably delayed, rectangular pulse of controllable duration is shown in Fig. 6-36. A thyatron relaxation oscillator supplies the trigger pulse which travels down a delay line. The first 10 sections of the line provide a delay of 0 to 3μ sec in 0.6-μsec steps. After the trigger has reached the 10th section it is amplified by  $V_2$  and fires the blocking oscillator  $V_3$ . The cathode follower  $V_{4a}$  charges a 400-μμf condenser, and produces a step function of voltage on the grid of the output cathode follower  $V_8$ .

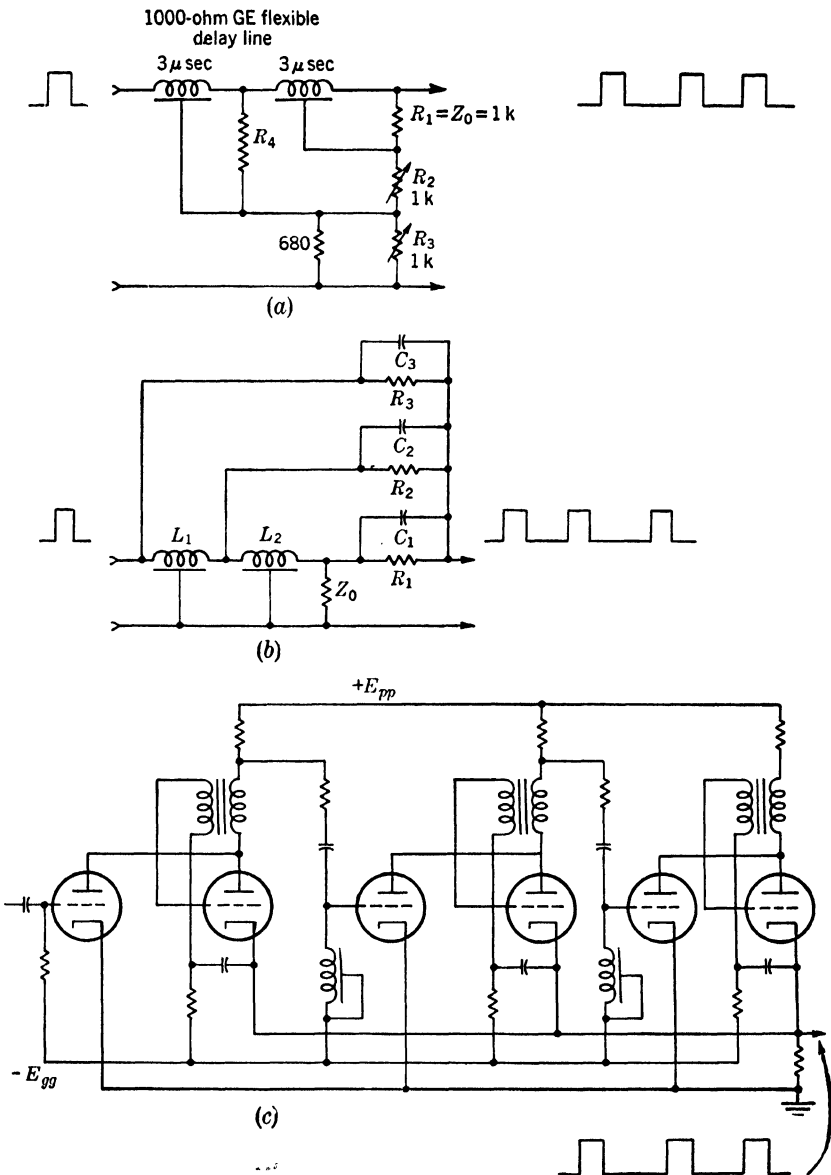


FIG. 6-35.—Delay-line coders.



The trigger pulse continues to travel down the line until it is absorbed by the termination at the end. When the pulse reaches the tap occupied by the pulse-length selector, it initiates the operation of the blocking oscillator  $V_6$  through the amplifier  $V_5$ . The cathode pulse of  $V_6$  drives the grid of  $V_7$  positive, so that the 400- $\mu\text{mf}$  condenser is discharged and the pulse is terminated. The pulse duration is adjustable in 0.6- $\mu\text{sec}$  steps from 0.6 to 3.0  $\mu\text{sec}$ . The pulse at the cathode of  $V_8$  rises and falls in 0.06  $\mu\text{sec}$ . The cathode follower,  $V_{4b}$ , is used to set the potential on the grid of  $V_8$  before and after the pulse. The widths of the pulses produced by the blocking oscillator are not critical, provided that they are great enough to insure substantially complete charging and discharging of the 400- $\mu\text{mf}$  condenser, and that the pulse produced by  $V_3$  is shorter than the minimum required output pulse length of 0.6  $\mu\text{sec}$ .

#### References for Design and Use

Design and construction of electrical delay lines: Vol. 17, Chap. 6. Theory of delay lines: Vol. 19, Chap. 22.  
(High-power) delay-line pulse generators: Vol. 5, Part II.  
High-power line-controlled blocking oscillators: Vol. 5, Chap. 4.  
Line-controlled coders and decoders: Vol. 20, Part II.

## CHAPTER 7

### GENERATION OF TRIANGULAR WAVEFORMS

By V. W. HUGHES AND R. M. WALKER

#### GENERAL CONSIDERATIONS

**7.1. Definition and Types.**—A triangular voltage waveform is a waveform of which one portion exhibits a linear dependence of voltage on time. Some examples of triangular voltage waveforms are given in Fig. 7.1. The voltage is linearly proportional to time during the portions  $AB$ ,  $A'B'$ , etc.; the voltage may either increase or decrease with time (Fig. 7.1a and 7.1f). The restoration or “flyback” portions of the

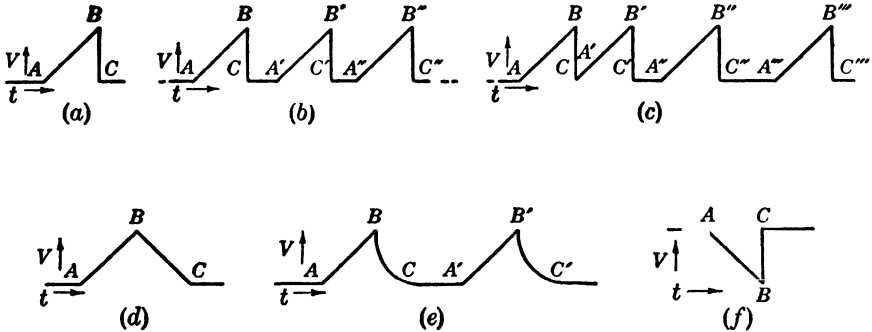


FIG. 7.1.—Types of triangular waveforms.  $AB$  is the portion of the waveform for which  $V$  is linearly dependent upon  $t$ .  $BC$  is the restoration or flyback portion of the waveform; it is of infinitesimal duration in (a), (b), (c), and (f). (b) A series of triangular waveforms occurring periodically. (c) A series of triangular waveforms occurring aperiodically. (d) A triangular waveform in which  $V$  is linear with  $t$  in  $BC$  as well as in  $AB$ . (e) A series of triangular waveforms whose restoration period is finite and is characterized by a nonlinear relation between  $V$  and  $t$ . (f) A triangular waveform in which  $V$  decreases linearly with  $t$  in the portion  $AB$ .

waveforms are  $BC$ ,  $B'C'$ , etc.; the durations of these portions are the restoration or flyback times. Occasionally, as shown in Fig. 7.1d, a linear relation may exist between  $V$  and  $t$  during the restoration time, but usually the relation is nonlinear (Fig. 7.1e). The triangular waveform may occur only once, or it may be repeated periodically or aperiodically (Figs. 7.1a, b, and c). Many types of waveforms other than those given in Fig. 7.1 are possible—for instance, a periodic series of triangular waveforms of the type shown in Fig. 7.1d, or an aperiodic series of triangular waveforms of the type shown in Fig. 7.1f. Triangular waveforms are

known as "sawtooth waveforms," "linear waveforms," "linear sweeps," or "time bases."<sup>1</sup>

**7.2. Characteristics of Triangular Waveforms.** *Durations.*—Great variations are possible in the durations, voltages, and accuracies associated with triangular voltage waveforms. Linear sweeps have been made with durations from  $10^{-7}$  sec to 10 min. The lower limit attainable is determined physically by the minimum values of tube and wiring capacitances, by the minimum values of leakage resistance, and by the maximum dissipation allowable in tubes and resistors; the upper limit is determined by the maximum values of capacitors (this is largely a matter of size and weight), by the maximum values of resistors, by the minimum values of leakage resistance, and by the minimum currents at which tubes operate satisfactorily. Restoration times as small as 5 per cent of the duration of the linear portion have been obtained, although it is more usual, when a triangular waveform is being generated periodically, to have the duration of the linear portion equal to less than one-half the repetition period.

*Voltages.*—The amplitudes of the linear sweeps ordinarily are between 10 and 1000 volts, although these figures do not represent the extremes attainable. Physically, the upper limit is determined by the peak voltage rating of tubes. For short sweeps the allowable dissipation in resistors may be of importance. Variations in clamping potentials due to variations in tube characteristics are more troublesome for low-amplitude linear sweeps than for high-amplitude ones and accordingly the latter are usually used. The voltage level of the start of the sweep can be set to any reasonable value.

*Linearity.*—The degree of perfection of the linearity of the sweep and the stability of the triangular waveform with respect to changes in supply and heater voltages, tube characteristics, and component values we consider as the two aspects of the accuracy of a triangular waveform.

The degree of linearity can be expressed as the deviation of the instantaneous voltage of the actual sweep from the instantaneous voltage of an assumed straight line which closely represents the actual sweep. This deviation is often expressed as a percentage of the amplitude of the actual sweep and is often called a "displacement error."<sup>2</sup> Linearities of about 0.01 per cent have been achieved over more than 99 per cent of the duration of the sweep; often the first one per cent of a sweep is nonlinear. The degree of linearity can also be expressed as the percentage deviation of the instantaneous slope of the actual sweep from the slope of the assumed straight line. This deviation is ordinarily considerably larger

<sup>1</sup> An excellent reference is *Time Bases*, by O. S. Puckle, Wiley, New York, 1944.

<sup>2</sup> Unless the contrary is stated, for this chapter for the computation of displacement and slope errors, the straight line chosen will be the one drawn from the point at the beginning (or near the beginning) of the sweep to the point at the end of the sweep.

than the displacement error. The linearity achievable is limited primarily by the finiteness of the gain and the nonlinearities of vacuum tubes.

*Stability.*—The degree of stability of the linear sweep can be expressed as the variation in displacement or slope due to a specified change in some circuit parameter. The variation in displacement is usually given as a percentage of the maximum amplitude of the actual sweep; the variation in slope is given as a percentage of the mean slope of the actual sweep. Zero error is a useful concept; it is the deviation of the beginning point of the sweep from the origin of the assumed straight line. A certain percentage change in the supply voltage ordinarily produces the same percentage change in slope; the same is true for changes in the most critical resistors and condensers. The percentage variation in displacement or slope can readily be kept to about  $\frac{1}{100}$  of any reasonable percentage change in heater voltage. Variations in the linear sweep due to variations in tube characteristics and in the values of the less critical fixed components can usually be made so that they are no more troublesome than instability due to the causes mentioned already. The variables that have been regarded as the cause of instability—i.e., heater and supply voltages, tube characteristics, and component values—are those most directly associated with the generator circuit, but often they are not the primary independent variables. Thus the stability of a triangular waveform is sometimes considered with respect to temperature, mechanical shock, and time. In a particular case with selected components the maximum displacement errors have been kept within  $\pm 0.1$  per cent for a temperature variation from  $-50^{\circ}\text{C}$  to  $+80^{\circ}\text{C}$ . With good circuit design microphonics are not troublesome.

The displacement and slope of the linear sweep are the most critical aspects of a triangular waveform; the stability of features associated with the restoration period is usually not of great concern.

*Generator Characteristics.*—Other characteristics associated more with the generator circuit than with the waveform are—

1. Output impedance.
2. Input requirements.
3. Engineering specifications such as reliability, ease of maintenance, safety, flexibility, weight, power consumption, and cost.

Often the output circuit of a triangular-waveform generator involves negative feedback, and an output impedance of several hundred ohms or less is presented; in other cases, the output impedance may be determined primarily by a condenser whose value is proportional to the duration of the linear sweep. In all cases, any value of output impedance can be achieved by the addition of several amplifier stages involving negative or positive feedback. A triangular-waveform generator often requires

either a trigger or a gating pulse as an input waveform. The engineering properties mentioned above vary considerably from generator to generator and are of great importance.

**7-3. Uses of Triangular Waveforms.**—The triangular waveform is a basic waveform of much value. Some of its applications are listed below.

*Measurement of Time Intervals Associated with Waveforms.*—The linear sweep is the most widely used time base for display purposes (Chap. 20). Furthermore it is used as a basis for the generation of time-modulated indices (Chap. 13 and Vol. 20, Chaps. 5 and 6). The use of linear sweeps as time bases in pulse-recurrence frequency dividers is a type of time measurement (Chap. 16).

*Generation of Other Basic Waveforms.*—Triangular voltage waveforms can be operated upon electronically to produce other basic voltage waveforms. Thus a parabolic waveform is produced by integration, and a rectangular waveform by differentiation, of a triangular waveform (Chap. 18). Often parabolic, trapezoidal, and hyperbolic generator circuits differ only slightly from prototype triangular-waveform-generator circuits (Chap. 8). A linear current waveform can be produced by applying a linear voltage waveform to a circuit passing a current that is proportional to the input voltage (Chap. 8).

*Functions Involving the Processes of Analysis and of Modulation and Demodulation.*—Many useful functions are performed by applying the processes of analysis and of modulation and demodulation to triangular waveforms. Thus data-transmission schemes sometimes carry their information in the form of time modulation on a triangular waveform (Vol. 20). Also, electromechanical amplitude modulation of triangular voltage waveforms or, more usually, of trapezoidal ones is useful in generating PPI radar sweeps electronically (see Chap. 12 of this volume and Vol. 22).

*Electronic Computation.*—It is frequently desirable to use a waveform with a linear voltage-time relationship in computer circuits. For example, electronic triangle solvers sometimes employ linear sweeps (Vol. 21, Part I).

**7-4. Methods of Generating Triangular Waveforms.**—Practical circuits for generating linear sweeps usually involve charging or discharging a condenser at approximately a constant rate. The change of the voltage across a condenser from its initial value at  $t = 0$  is given by

$$E_e = \frac{1}{C} \int_0^t i \, dt,$$

and, if the current  $i$  equals a constant  $I_0$ , then

$$E_e = \frac{I_0}{C} t.$$



The change of voltage with time is positive if  $I_0$  is positive and negative if  $I_0$  is negative. Some switching mechanism is always employed to determine the beginning and the end of the linear sweep.

Considered from this point of view, the problem of generating a linear sweep is one of obtaining a constant current with which a condenser can be charged or discharged. Methods for accomplishing this have been divided into four classifications (these methods are surveyed briefly in this section and discussed in detail in later sections). The condensers may be charged or discharged—

1. From a constant voltage source through a resistor.
2. From a constant voltage source through a high variational impedance of low d-c resistance.
3. With circuits involving positive and negative feedback.
4. With circuits involving negative feedback.

The first method is the most elementary. A voltage which varies as an exponential function of time is obtained. Only for those values of time, measured from the beginning of the sweep, which are small compared to  $RC$ , is a good approximation to a linear sweep obtained. This implies that only a small fraction of the total available voltage change, i.e., the constant voltage, exhibits a linear dependence on time.

The high variational impedance of the second method is often provided by an inductance or by a pentode. Many types of current-feedback devices can also be used. The circuit that uses an inductance is capable of providing an approximately linear voltage change which is greater than the supply voltage. In general, the linearity obtained by this method is somewhat less than that obtained by either of the last two methods; also, the switching problem is often more difficult and the restoration period is longer.

The “bootstrap” cathode-follower circuit is the primary example of the use of positive and negative feedback. Fundamentally, in this circuit a condenser is charged through a resistance from a supply voltage which varies in such a way as to maintain a constant voltage across the resistance. The cathode follower is a negative-feedback device, and positive voltage feedback to the resistance maintains a constant charging current. This is an excellent circuit for the generation of a linear sweep with a positive slope. By the addition of a compensating  $RC$ -network the linearity is improved by as much as a factor of 5 and becomes almost as good as that achieved with the best circuits employing negative feedback.

All negative-feedback circuits—these include the phantastron and sanatron—utilize the Miller effect, and the variations in these circuits consist in the number of stages used in the amplifier and in the switching

arrangements. Either positive- or negative-going linear sweeps can be generated. The ability of this type of circuit to generate sweeps of different amplitudes and durations is as great as that of the bootstrap cathode-follower circuit, and the best linearities and stabilities have been achieved with this circuit.<sup>1</sup>

#### DETAILED DISCUSSION OF METHODS OF GENERATION

##### 7.5. Condenser Charging through Resistor.—

The elemental method of charging or discharging a condenser from a constant voltage source through a resistor is shown in Fig. 7.2. The output voltage is an exponential sweep, whose first portion is approximately a linear sweep (see Chap. 8 for practical circuits). At  $t = 0$  the switch is opened and, thereafter, until the switch is closed again,

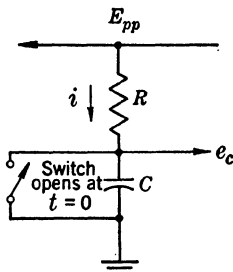


FIG. 7.2.—Elementary linear-sweep generator.

$$i = I_0 e^{-\frac{t}{RC}} \quad (t \geq 0).$$

The voltage waveform is given by

$$e_c = E_{pp}(1 - e^{-\frac{t}{RC}}), \quad (1)$$

and

$$\frac{de_c}{dt} = \frac{I_0}{C} e^{-\frac{t}{RC}}.$$

Expressed in series form,

$$e_c = E_{pp} \left[ \frac{t}{RC} - \frac{(t/RC)^2}{2!} + \frac{(t/RC)^3}{3!} - \dots \right]. \quad (2)$$

If the total time of generation of the sweep (i.e., the time the switch is open) is small compared to  $RC$ , then the charging current will be nearly constant during the charging period, and Eq. (2) can be written as

$$e_c = \frac{E_{pp}}{RC} t, \quad (3)$$

which is the expression for a linear sweep. Equation (3) implies that the maximum voltage of the generated waveform must be small compared to the supply voltage  $E_{pp}$ .

Expressions for slope and displacement errors are easily derived.

<sup>1</sup> See Sec. 2.6 for a discussion of the essential identity of the bootstrap and the Miller feedback sweeps.

For a total charging time  $t_1$  the ratio of the slope  $de_c/dt$  at the end of the charging period to that at the beginning is equal to<sup>1</sup>

$$\frac{i_1}{I_o} = e^{-\frac{t_1}{RC}} = 1 - \frac{e_{c1}}{E_{pp}}$$

There follows an expression for displacement error measured with respect to the straight line through the beginning point of the sweep with a slope equal to the initial slope of the actual sweep. The error is expressed as a percentage of the supply voltage, and

$$100 \frac{E_{pp} \frac{t}{RC} - e_c}{E_{pp}} = 100 \left[ -\ln \left( 1 - \frac{e_c}{E_{pp}} \right) - \frac{e_c}{E_{pp}} \right] \quad (4)$$

is plotted as a function of  $e_c/E_{pp}$  in Fig. 7-3. Other straight lines can be chosen which provide a better fit to the exponential waveform.

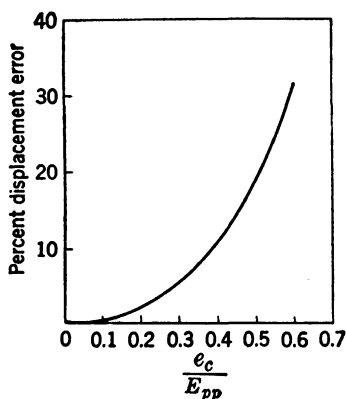


FIG. 7-3.—Percent displacement error vs.  $e_c/E_{pp}$  for circuit of Fig. 7-2. (The displacement error plotted here is the deviation of the exponential from  $(E_{pp}/Rc)t$ , expressed as a percentage of  $E_{pp}$ .)

In a practical circuit the imperfections of the switch introduce certain limitations. The nonzero impedance of the switch when closed causes  $e_c$  to be at a potential somewhat greater than 0 for  $t \leq 0$ , and, since this potential varies with the effective forward resistance of the switch, both the starting potential and initial slope of the sweep are unstable. Furthermore, the recovery time is usually determined primarily by the forward resistance of the switch through which  $C$  discharges. If insufficient time is allowed for the discharging process, the initial charging current will depend on the state of discharge of the condenser and will change with the duty ratio. The allowable peak voltage across the switch when open places a

limitation on the maximum amplitude of the sweep. Finally, the finite transition time of the switch results in additional transient phenomena both at the start and at the finish of the sweep.

The most serious disadvantage in the simple method of charging a condenser through a resistor from a fixed supply voltage is that the linearity is poor unless the sweep amplitude is restricted to a small fraction of the supply voltage. An advantage in this method is that, since the circuit consists only of a resistor, a condenser, and a switch, the

<sup>1</sup> Note that this is not the slope error defined in Sec. 7-2.

recovery time is limited only by the imperfections of the switch and, therefore, is generally superior to circuits using more elements. Moreover, this circuit can be used for as wide a range of sweep durations as can any other circuit. The maximum amplitude is determined by the value of  $E_{pp}$  and the allowable open circuit voltage across the switch. Very good stabilities can be achieved. The output impedance is essentially the parallel impedance of  $R$  and  $C$  (Fig. 7-2); the input requirement is a gate to operate the switch.

A practical circuit is given in Sec. 8-4, Fig. 8-16. The sweep duration is 300  $\mu$ sec and the amplitude is about one-third of  $E_{pp}$ .

#### USE OF HIGH VARIATIONAL IMPEDANCE

**7-6. Inductance in Series with Resistor.**—By placing an inductance in series with the charging resistor (Fig. 7-2), it is possible to obtain

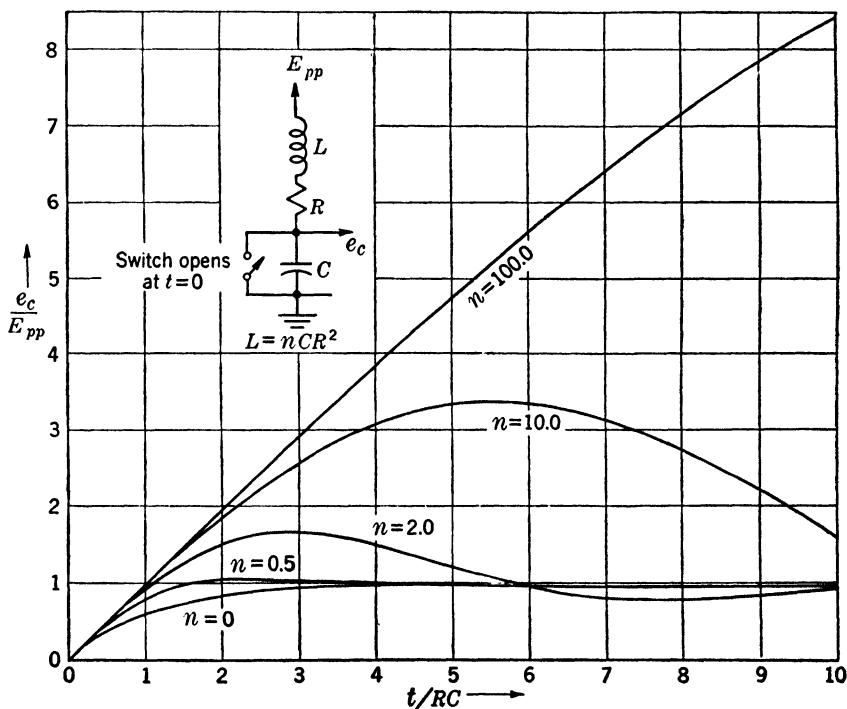


FIG. 7-4.—Basic circuit and output waveforms for  $R, L, C$  linear sweep.

considerable improvement in linearity for a given ratio  $e_c/E_{pp}$ . In addition, an output voltage larger than the supply voltage can be obtained. These effects are shown in Fig. 7-4, where the ratio  $e_c/E_{pp}$  is plotted against  $t/RC$  for different values of  $n$  where  $n = L/CR^2$ . The curve for  $n = 0$  corresponds to zero inductance and hence is the case discussed

in Sec. 7-5. If  $R$  and  $C$  are given fixed values and the inductance is increased, a sweep with better linearity and greater amplitude is obtained. The curves of Fig. 7-4 are illustrated in Fig. 7-5 by a photograph of the sweep output of an actual circuit.

The exact equations for the sweep voltage  $e_c$  can be derived easily. For sufficiently small values of  $t$ , a solution in the form of a power series in  $t$  is useful:

$$e_c = \frac{E_{pp}}{RC} t - \frac{E_{pp}}{6RLC^2} t^3. \quad (5)$$

The initial conditions assumed are  $e_c = 0$  and  $de_c/dt = E_{pp}/RC$ . The term in  $t^3$  represents the deviation from linearity; it obviously decreases as  $L$  is made larger.

If the circuit is operated at high repetition rates, initial conditions differing from those mentioned above will apply. With an ideal switch  $e_c$  is still 0, but

$\left. \frac{de_c}{dt} \right|_{t=0} \neq \frac{E_{pp}}{RC}$ : indeed, the value

of  $\left. \frac{de_c}{dt} \right|_{t=0} = \left( \frac{i}{C} \right)_{t=0}$  will vary with the repetition rate at which the sweep is being generated. The initial value of current can be determined from the equilibrium equation, which asserts that the decrease in current during the on period of the sweep is equal to the

increase in current during the off period of the sweep. During the restoration period the current is given by

$$i = i_o + \left( \frac{E_{pp}}{R} - i_o \right) \left( 1 - e^{-\frac{t}{L/R}} \right),$$

where  $i_o$  is the current at the beginning of the restoration period, and  $E_{pp}/R$  is the eventual steady-state current which will be attained. Hence there is associated with the restoration of the steady-state current a time constant of  $L/R$ . Still it is not necessary to provide a restoration time great compared to  $L/R$  in order to establish approximately the initial current  $E_{pp}/R$ , because only that amount  $(E_{pp}/R - i_o)$  by which the current at the beginning of the restoration period differs from  $E_{pp}/R$  is

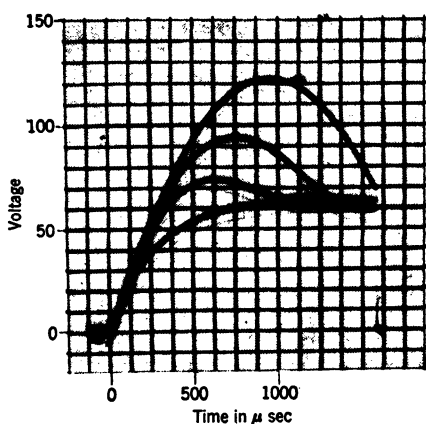


FIG. 7-5.—A waveform photograph illustrating the curves of Fig. 7-4 for an actual circuit. An inductance of 500 henrys and three resistor and condenser combinations each with a time constant of 500  $\mu$ sec were used. Waveforms are for  $n = 0, 0.5, 1$ , and 2.

being restored. A numerical example illustrating this point is given in Fig. 7-8 for the circuit of Fig. 7-7.

Voltage waveforms across the resistance of an  $RLC$  sweep circuit are shown in Fig. 7-6. The lower waveform and upper waveform are for

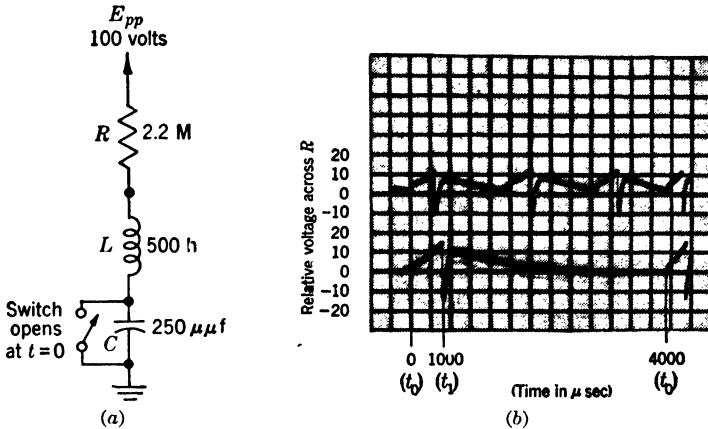


FIG. 7-6(a).— $R, L, C$  circuit used for waveforms of Fig. 7-6(b).

FIG. 7-6(b).—Current waveforms for  $R, L, C$  linear sweep of Fig. 7-6(a). Upper and lower waveforms are for operation at 750 cps and 250 cps respectively. (A change of +1 volt in voltage across  $R$  is equivalent to a change of  $-\frac{1}{2}$   $\mu$ m through  $R$ .)  $L = 500$ h,  $R = 500$ k,  $C = 1000$   $\mu\mu$ f. Unfortunately an exponential display sweep was used.

operation at 250 cps and 750 cps, respectively. During the on period of the sweep from  $t_0$  to  $t_1$  the current decreases. When the switch is closed at  $t_1$  the current suddenly increases. This effect can be explained by considering the capacity across the inductance and the finite resistance of the switch. It is apparent from a comparison of the lower and upper photographs that enough restoration time is not being allowed at the 750-cps repetition rate for the circuit to establish the initial value of  $E_{pp}/R$ .

A 300- $\mu$ sec sweep of about 250 volts amplitude is obtained from the circuit shown in Fig. 7-7. The value of  $n$  for this circuit is about 25. A linearity always better than 0.2 per cent displacement error is predicted by a calculation which takes into account the d-c resistance of the coil

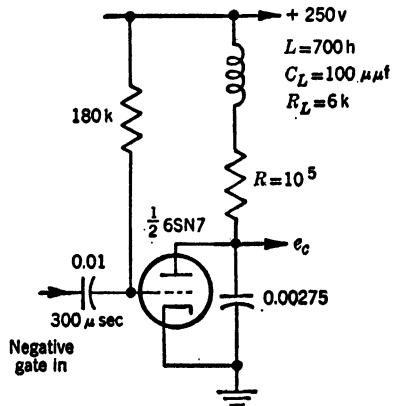


FIG. 7-7.—A practical circuit of an  $R, L, C$  linear sweep generator.

and the lumped value of the distributed capacity along the coil. For this calculation the assumed straight line was the one drawn between the

points of the actual sweep with abscissae of 50  $\mu\text{sec}$  and 200  $\mu\text{sec}$ . Accurate experimental studies confirmed the theoretical prediction on linearity.

The way in which the initial current into  $C$  varies with the restoration time is shown in Fig. 7-8. The on time of the sweep is 300  $\mu\text{sec}$ . This calculation was made by equating the decrease in current during the on period to the increase in current during the restoration period. It is noticed that a change in duty ratio from  $\frac{1}{2}$  to  $\frac{1}{10}$  causes a decrease in initial current of about  $\frac{1}{30}$ .

**7-7. Vacuum-tube Variational Impedances.**—High variational impedances can be achieved with vacuum tubes and these can be used in linear sweep generators. The variational plate resistance of a pentode is used in the “constant current” pentode linear sweep circuit. Even higher and more stable variational impedances can be achieved with certain current feedback circuits—for example, the cascode triode circuit. The constant current pentode circuit will be considered first.

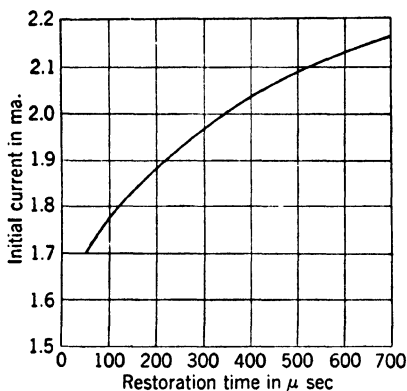


FIG. 7-8.—Calculated value of current flowing into  $C$  of Fig. 7-7 when switch is opened vs. restoration time. The on period of the sweep is 300  $\mu\text{sec}$ . The calculation assumed an ideal switch and inductance.

times the pentode plate current flowing during the quiescent period. In order for this to be true the assumption must be made that the plate current is given by

$$i_p = i_o + \frac{\Delta E_p}{r_p},$$

where

$i_o$  = plate current during quiescent period,

$r_p$  = variational plate resistance,

$\Delta E_p = E_p - E_{pp}$ .

#### *The Constant-current Pentode.*—

If a pentode tube is operated with its plate potential above the “knee” of the  $i_p$ ,  $e_p$  curves, its variational plate resistance is high; that is, its plate current varies only slightly with changes in plate potential. This fact is made use of in the circuit shown in Fig. 7-9 in order to charge  $C$  at an approximately constant rate. Actually, the charging current is an exponential function of time, and it is the same current that would be obtained by charging the condenser through a resistance equal to the variational plate resistance  $r_p$  of the pentode ( $\sim 1$  megohm) from a voltage source equal to  $r_p$

It is then true that

$$i_p = i_{o\ell} - \frac{t}{r_p C}. \quad (6)$$

Actually, since  $r_p$  is dependent on  $E_p$ , this relation gives only approximate results even when an average value of  $r_p$  is employed.

Fairly good linearity can be obtained for a sweep whose amplitude is a large fraction of the supply voltage. Thus, using a supply voltage of 300 volts and a 6SJ7 with its screen grid at 100 volts and its control grid at  $-2$  volts, a 200-volt sweep can be obtained for which the charging current at the end of sweep differs by 4 per cent from the charging current at the beginning of the sweep.

Often negative feedback is introduced by the insertion of an unby-passed cathode resistance. Provided the screen to cathode potential is maintained constant by the use of battery or condenser coupling the variational impedance from the plate of the pentode to ground is greatly increased and is  $r_p + (\mu + 1)R_K$ , where  $R_K$  is the cathode resistance. Variational impedances of 1000 megohms can easily be achieved, but they cannot be utilized fully due to the presence of leakage resistance (perhaps 100 megohms).

If the screen potential is fixed relative to ground or connected through a resistance to the supply voltage, variational plate to ground impedances approximately equal to  $r_p$  are obtained with cathode degeneration. The reason that the higher variational impedance of  $r_p + (\mu + 1)R_K$  is not obtained is that although the insertion of  $R_K$  reduces the change of cathode current with change in plate-to-ground potential, because of the redistribution of current between the plate and screen, the use of  $R_K$  does not appreciably reduce the change in plate current.

Stabilization of the value of quiescent plate current is achieved by the use of cathode degeneration whether or not the screen is bootstrapped to the cathode. Typical stability data follow. For a 6SJ7 with a 100,000-ohm cathode resistance a 10 per cent change in filament voltage results in a change in plate current of several tenths of one per cent, and upon change of tubes the current has not been observed to vary by more than  $\pm 0.5$  per cent.

A linear sweep circuit of an astable, rapid-flyback type suitable for oscilloscope use is shown in Fig. 7-10, in which  $V_1$  is a gas-tube switch and  $V_2$  is the constant-current pentode with cathode degeneration. Since the screen is not bootstrapped to the cathode, the cathode degen-

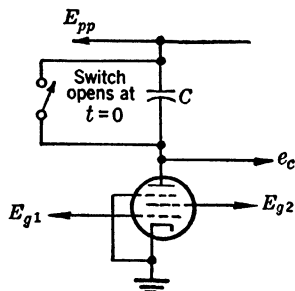


FIG. 7-9.—Constant current pentode linear sweep generator.



eration stabilizes the value of cathode current but does not improve the sweep linearity. A negative sawtooth waveform with an amplitude of approximately 200 volts is obtained; the amplitude can be changed by changing the potential to which the grid of  $V_1$  is returned.

**Triodes with Current Feedback.**—The variational impedance between plate and ground for a triode with cathode degeneration is  $r_p + (\mu + 1)R_K$ . For a 6SL7 tube with a 500-k cathode resistance and a +300-volt supply a variational impedance of some 30 megohms is realized. For two triodes in cascode as shown in Fig. 7-11 the variational impedance from the plate of  $V_2$  to ground is approximately  $(\mu + 1)^2 R_K$ . Using 6SL7's and a

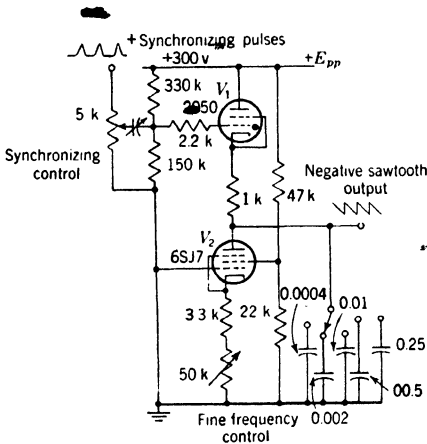


FIG. 7-10.—Sweep generator using a thyatron switch and a constant current pentode. Frequency from 5 to 50,000 cps.

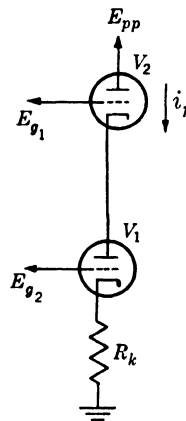


FIG. 7-11.—Two triodes in cascode used for achieving high variational impedance.

500-k cathode resistor an impedance of about 1000 megohms is calculated; however, leakage resistance reduces the effective value. Troubles due to heater-to-cathode leakage can be minimized by use of a separate heater winding for tube  $V_2$ , which is at the same potential as the cathode of  $V_2$ .

#### CIRCUITS INVOLVING POSITIVE AND NEGATIVE FEEDBACKS

By use of positive feedback a constant potential can be maintained across a resistor through which a condenser is being charged. This is achieved by the use of a unity-gain amplifier (ordinarily involving negative feedback), which takes its input signal from the condenser end of the resistor and impresses its output signal at the supply end (Fig. 7-12).

More generally, if the amplifier has a gain  $G$ , an infinite input impedance, and a zero output impedance,

$$i = I_0 e^{-\frac{t(1-g)}{RC}} = \frac{E}{R} e^{-\frac{t}{RC}(1-g)}, \quad (7)$$

$$e_c = \frac{E}{1-g} (1 - e^{-\frac{t}{RC}(1-g)}). \quad (8)$$

Hence by expansion

$$e_c = \frac{E}{RC} \left[ t - \frac{(1-g)}{RC} \frac{t^2}{2!} + \frac{(1-g)^2}{(RC)^2} \frac{t^3}{3!} - \cdots \right]. \quad (9)$$

And, if  $g = 1$ , the current will be constant and the voltage  $e_c$  will be a linear function of time. If  $g \neq 1$ , the current will be an exponential function of time with a positive or negative first derivative depending on whether  $g$  is greater than or less than unity; the voltage waveform will also be an exponential function of time. The effect of the positive feedback is the same as that which would be achieved by charging the condenser through a resistor  $1/(1-g)$  times as large as  $R$  from a supply voltage  $1/(1-g)$  times as large as  $E_{pp}$ .

**7-8. Use of the Cathode Follower.**—A cathode-follower type of amplifier is most commonly used.

It provides a nearly unity gain, a high input impedance, a low output impedance, and a wide bandwidth (Vol. 18). The differential gain of a cathode follower with a resistive load impedance  $R_K$  is

$$g = \frac{\partial E_{out}}{\partial E_{in}} = \frac{\mu R_K}{R_p + (\mu + 1)R_K}, \quad (10)$$

where

$\mu$  = amplification factor of tube, and

$r_p$  = dynamic plate resistance of tube.

If  $(\mu + 1)R_K \gg R_p$ ,  $g \approx \mu/(\mu + 1)$ . Since the  $\mu$  of a tube is almost constant over wide ranges of operating conditions, the gain of the cathode follower is rather independent of the operating condition. A medium- $\mu$  triode such as a 6SN7 with  $\mu$  of 20 has a ratio  $\mu/(\mu + 1) = 0.95$ . High- $\mu$  triodes and pentodes can be used to achieve unity gain even more closely. For example, a 6AC7 with a 50,000-ohm load resistance, with its screen bypassed to the cathode and with  $E_{pp} = 300$  volts, gives a gain of 0.995 over a 150-volt plate swing.

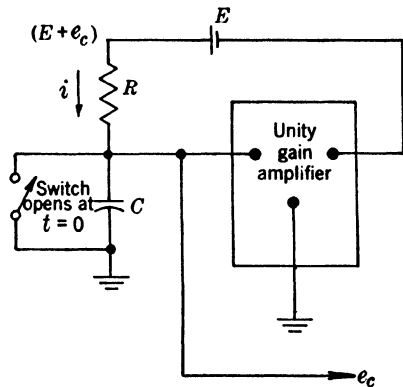


FIG. 7-12.—Method of generating a linear sweep using positive feedback.

Several possible circuit arrangements are illustrated in Figs. 7-13, 7-14, 7-15, and 7-16. A battery or floating power supply is required in the circuit shown in Fig. 7-13.

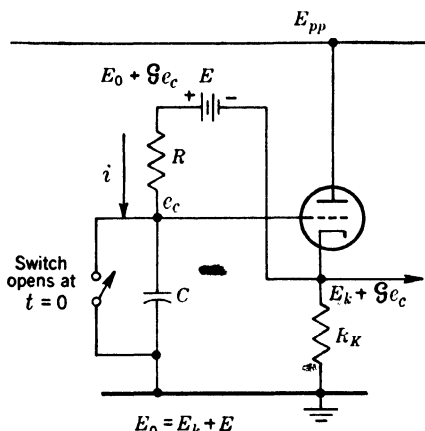


FIG. 7-13.—Method of generating a linear sweep using a cathode follower to achieve positive feedback.

the time constants  $R_D C_D$  and  $R C_D$  are large compared to the duration of the sweep. Quantitative relationships can be readily worked out. This form of the circuit is sensitive to variations in the repetition frequency of generation of the sawtooth waveform. The initial current flowing into the condenser can be computed for any particular repetition frequency of generation of the sweep by equating the loss in charge of  $C_D$  during the sweep generation period to the gain in charge of  $C_D$  during the restoration period. Figure 7-17a illustrates the change in slope of the linear sweep when the repetition frequency is varied.

A circuit arrangement which is less sensitive to repetition-frequency changes and permits a larger sweep amplitude is shown in Fig. 7-15. Figure 7-17b illustrates the smaller repetition-frequency sensitivity of this circuit. Here the resistor  $R_D$  is replaced by a diode which serves to set the initial voltage at the supply end of the charging resistor at essentially the supply potential  $E_{pp}$ . After the switch is opened,

In Fig. 7-14 the potential levels in the quiescent period are correctly maintained by use of the capacity  $C_D$  and the resistor  $R_D$ . If no current is flowing into the condenser  $C_D$  at the time the switch is opened, the initial current into  $C$  is  $E_{pp}/(R + R_D)$ . If the cathode follower has a unity gain and the condenser  $C_D$  does not discharge appreciably during the period of the sweep, this initial current into  $C$  will be maintained. The condenser  $C_D$  will not discharge appreciably provided  $C_D \gg C$ , and provided the

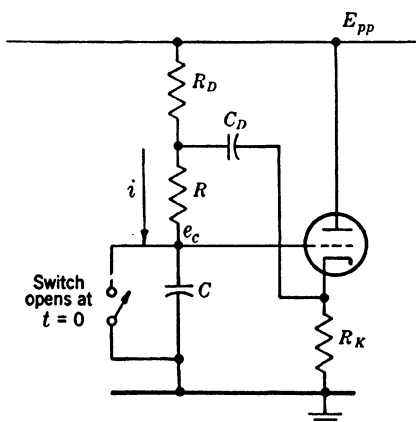


FIG. 7-14.—A variation of Fig. 7-13 which avoids the use of the battery or floating power supply.

the waveform from the output of the cathode follower raises the potential at the cathode of the diode above  $E_{pp}$ , so that the diode becomes non-conducting. The total charging current then flows through the coupling condenser  $C_D$ , reducing its charge. If a linear sweep is to be generated,  $C_D$  should be large enough to ensure that this loss of charge does not appreciably decrease the voltage across it. When the switch is closed  $C$  is discharged instantaneously to ground potential. Condenser  $C_D$  recharges through the diode and  $R_K$ . The cathode follower may or may not be cut off during the early part of the recovery period, depending upon how much the potential across  $C_D$  was reduced during the sweep period.

For this circuit as well as for that of Fig. 7-14 repetition-frequency sensitivity is present (though it is too small to be seen in Fig. 7-17b) because of the necessity to recharge  $C_D$  during the off period of the sweep. The initial current flowing into condenser  $C$  for any particular repetition frequency of generation of the sweep is

$$i_1 = \frac{E_{pp}}{R + R_D} - \frac{R_D}{R + R_D} \frac{E_a \left( \frac{C}{C_D} \right) e^{-\frac{\tau}{rC_D}}}{r \left[ 1 - (e^{-\frac{\tau}{rC_D}}) \right]}, \quad (11)$$

where

$i_1$  = initial current flowing into condenser  $C$ ,

$R_D$  = static resistance of diode, assumed constant,

$$r = R_D \left( 1 - \frac{R_D}{R + R_D} \right) + R_K \left[ 1 - \frac{R_K(\mu + 1)}{R_p + (\mu + 1)R_K} \right],$$

$E_a$  = amplitude of sweep voltage,

$R_p, \mu$  are constants of the cathode-follower tube, and

$\tau$  = duration of restoration period.

(The other quantities are defined in Fig. 7-15.) This equation was derived by equating the charge lost by the condenser  $C_D$  during the sweep-generation period to the charge gained by this condenser during the restoration period. It assumes that the cathode-follower current can be

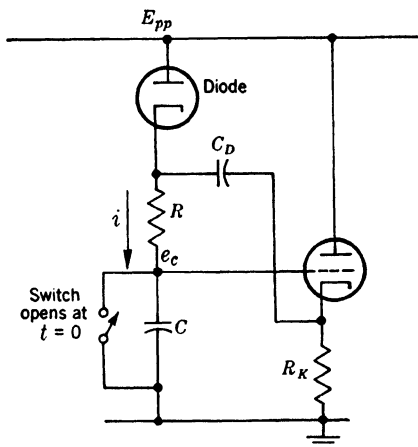


FIG. 7-15. A variation of Fig. 7-14 which is less sensitive to changes in the repetition frequency of generation of the sawtooth waveform.

represented by  $i_p = (E_p + \mu E_g)/R_p$ , and hence is not applicable if the cathode follower is cut off during the early portion of the restoration period. If the diode forward resistance  $R_D$  is zero, the initial current  $i_1$  is independent of recovery time; otherwise, it is apparent that  $i_1$  increases as the restoration period  $\tau$  is increased. If the time constant  $RC$  is to have a fixed value, it is desirable to make  $R$  as large as possible and  $C$  as small as possible in order to minimize the percentage change of  $i_1$  with  $\tau$ . From the point of view of minimizing the change in  $i_1$  due to change in  $\tau$  there is an optimum value of  $C_D$  for any given values of the other parameters. It is usually desirable to make  $R_K$  and  $R_D$  small and  $g_m$  large. Some advantage is often achieved by returning  $R_K$  to a negative potential.

In Fig. 7-16 the cathode follower feeds the charging circuit directly, its grid input being capacitively coupled by  $C_D$  to the point at which the

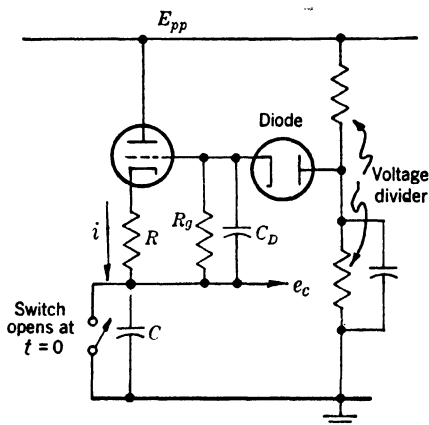


Fig. 7-16.—Another variation of Fig. 7-12.

linear sweep  $e_c$  appears. The diode and the voltage divider help to determine the potential levels in the quiescent condition of the circuit. This circuit permits the use of a smaller coupling condenser  $C_D$  than does the circuit of Fig. 7-15, since the only discharging in this case is through  $R_g$ , which can ordinarily be made as large as about one megohm before grid current affects the accuracy. To a first approximation the repetition-frequency sensitivity of this circuit is independent both of the values of  $R$  and  $C$  and

of the properties of the cathode follower. If a sufficiently low-resistance voltage divider can be used, this circuit can be designed to be much less sensitive to repetition-frequency changes than the circuits of Figs. 7-13 or 7-15.

Two examples of astable linear-sweep generators are shown in Figs. 7-18 and 7-19. As indicated in these figures, synchronizing pulses can be used but synchronization is possible over only a narrow range. The sweeps are of only moderate linearity, the displacement errors being at most about 2 or 3 per cent. Push-pull sweeps suitable for display purposes on a cathode ray oscilloscope are obtained from the circuit shown in Fig. 7-18. The gas-filled tube  $V_1$  serves as the switch and the sawtooth-waveform generator proper is of the form of Fig. 7-14,  $V_{2a}$  being the cathode follower. The output of the inverter stage  $V_{2b}$  is a negative sawtooth waveform of an amplitude approximately equal to that of

the positive sawtooth waveform from the  $V_{2a}$  cathode (see Chap. 2). The maximum amplitude of the sawtooth waveform is about 150 volts. The circuit can operate from repetition frequencies of a few cycles per second up to about 50 kc/sec with the upper frequency limit set by the deionization time of the gas tube. Flybacks that last for only several per cent of the repetition period are obtained.

In Fig. 7-19 the blocking oscillator  $V_{2b}$  (Chap. 6) is the switch and the sawtooth-waveform generator is essentially of the type of Fig. 7-16 in which  $V_{2a}$  is the cathode follower and the triode  $V_{2b}$  replaces the diode. A sawtooth waveform of about 100 volts amplitude is obtained. The

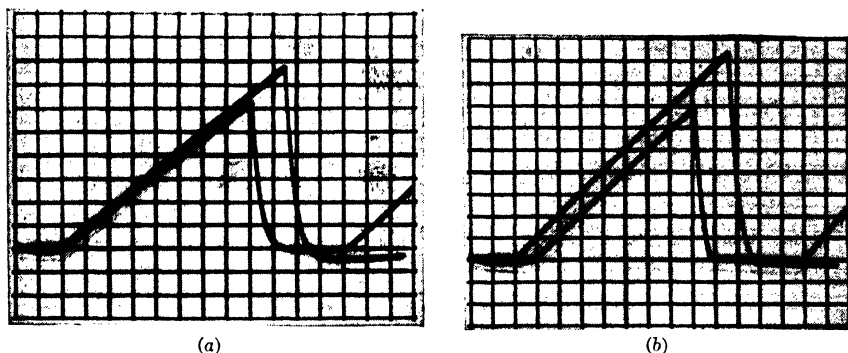


FIG. 7-17(a).—The change in slope of the linear sweep from the circuit of Fig. 7-14 when repetition frequency is varied. Sweep duration  $\approx 650 \mu\text{sec}$ . Repetition frequency of lower sweep is 1040 cps; that of upper sweep is 260 cps.

FIG. 7-17(b).—The change in slope of the linear sweep from the circuit of Fig. 7-15 when repetition frequency is varied. Sweep duration and repetition frequencies same as for Fig. 7-17(a). Sweeps have been displaced so their slopes can be more readily studied.

upper repetition-frequency limit is considerably higher for this circuit than for that of Fig. 7-18 since a blocking oscillator switch is used ( $\sim 1\text{-}\mu\text{sec}$  flyback time is achievable with an OA18 transformer).

A single-stroke push-pull linear-sweep generator is shown in Fig. 7-20. The switch  $V_1$  is chosen to be a pentode in order to minimize the capacity coupling of the input gating waveform at the grid of  $V_1$  to the output at the plate of  $V_1$ . The tube  $V_2$  is a pentode cathode follower and  $V_3$  is a paraphase amplifier. Push-pull output of 200 volts with a linearity of about one per cent, expressed in terms of displacement errors, is obtained. The push-pull output is shown connected to the CRT horizontal plates, whose centering control is the grid return of  $V_3$ . The minimum sweep duration of approximately  $1 \mu\text{sec}$  is obtained when the stray and tube capacities serve as  $C$ . (It should be noted that it is bad practice to have stray and tube capacities a large portion of  $C$  because the value of  $C$  is then not well defined.)

Figure 7-21 illustrates a single-stroke circuit in which the gating

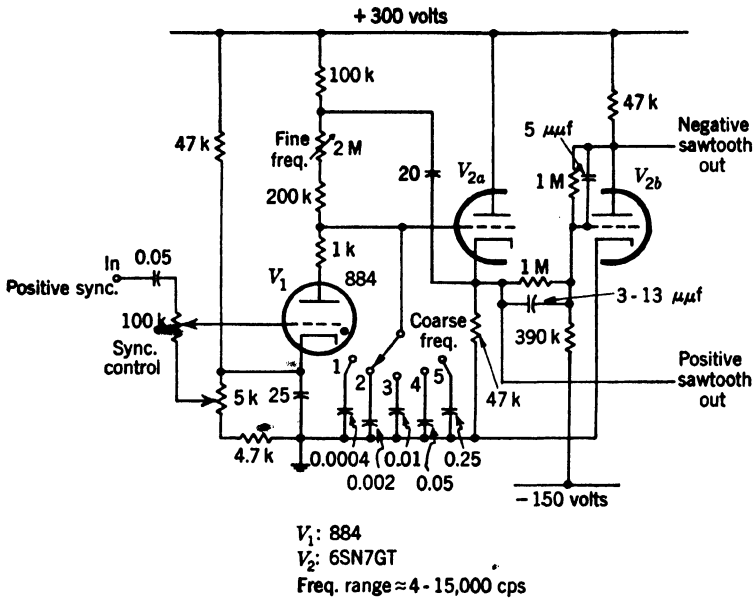


FIG. 7-18.—Astable linear sweep generator using cathode-follower positive feedback and a gas-tube switch.

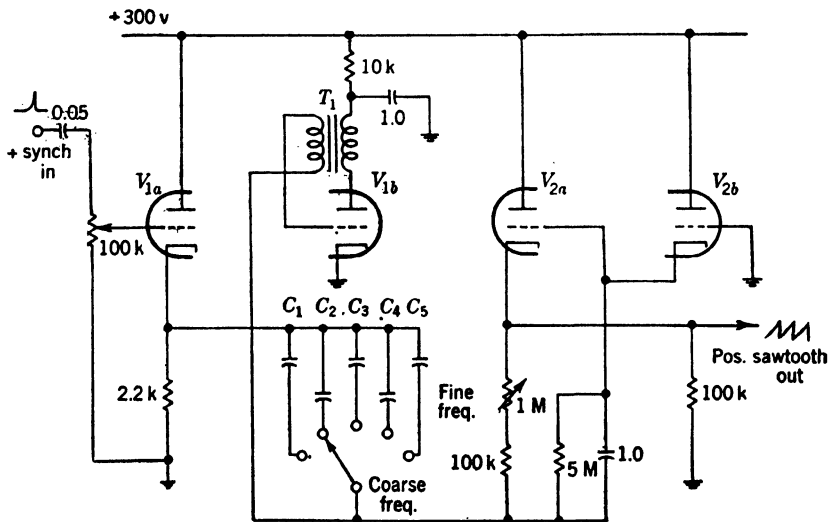
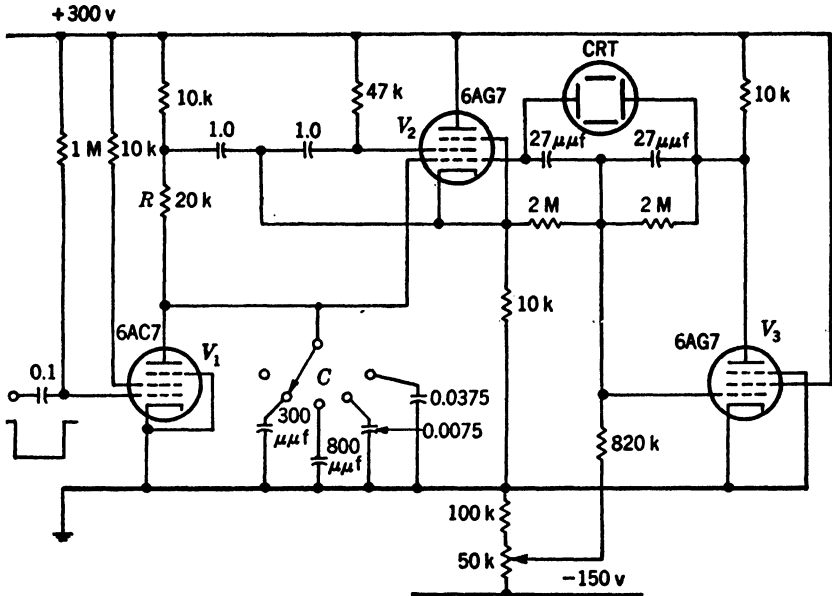
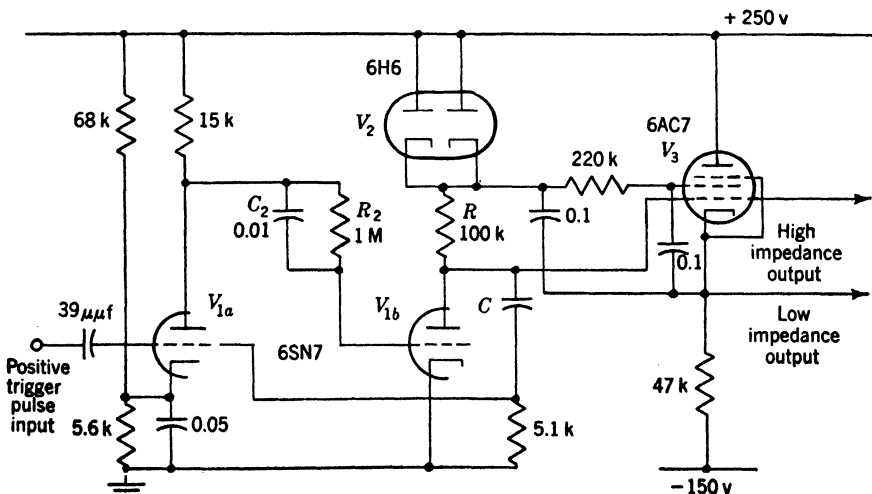


FIG. 7-19.—Astable linear sweep generator using cathode-follower positive feedback and a blocking oscillator switch.  $V_1$  and  $V_2$  are 6SN7 tubes.

waveform is derived from the sawtooth-waveform generator. This circuit can be so adjusted that the gate ends when the sawtooth waveform reaches a particular amplitude, and this property is sometimes of value. In the quiescent condition the switch tube  $V_{1a}$  is conducting and  $V_{1b}$  is biased beyond cutoff. A positive trigger pulse applied to the grid



**FIG. 7-20.**—High speed single-stroke synchroscope sweep using cathode-follower positive feedback and paraphase inverter.



**FIG. 7-21.—Medium precision single-stroke sawtooth generator with self-gating feature.**



of  $V_{1a}$  renders  $V_{1b}$  nonconducting and the current that was flowing through the switch tube flows through  $C$  and  $R_1$ . The resulting positive jump in potential at the grid of  $V_{1a}$  is amplified by  $V_{1a}$ , and the drop in potential at the plate of  $V_{1b}$  serves to hold off the switch tube  $V_{1b}$ . The switch tube will again conduct, either because the current through  $R_1$  has decreased appreciably, as it does when the sawtooth-waveform amplitude becomes so large that the cathode follower  $V_3$  is operating near zero bias, or because  $C_2$  has discharged sufficiently through  $R_2$ , as it does if the time constant  $R_2C_2$  is small enough. Sometimes both of these effects are important. The turning on of  $V_{1b}$  is a quick-acting regenerative process. After  $C$  has been discharged, the circuit is restored to its quiescent condition, and will remain in this condition until another trigger appears.

The sweep generator is essentially the circuit shown in Fig. 7-15. A pentode cathode follower  $V_3$  is used, and its screen supply resistor is connected to the cathode of diode  $V_2$ , thereby reducing somewhat the variation of screen potential with changing duty ratio. The output waveform is trapezoidal rather than triangular because the presence of  $R_1$  causes a jump in potential at  $t = 0$ . The initial potential jump is about 12 volts in amplitude and the sawtooth-waveform amplitude is about 125 volts. Often this initial potential jump is not troublesome and sometimes it is even desired in order to generate a trapezoidal waveform (Chap. 8).

**7-9. A Cathode-follower Circuit with a Compensating Network.**—A considerable improvement in linearity can be achieved by the use of the auxiliary network  $R'$ ,  $C''$ , as shown in Fig. 7-22. The condenser  $C$  of Fig. 7-15 is separated into two condensers,  $C'$  and  $C''$ , which are connected in series and are ordinarily about equal in value. A connection is made from their junction through a series resistor  $R'$  to the output of the cathode follower. It is possible to adjust  $R'$  so as to obtain a waveform that can be expressed as  $e_c(t) = K_1t + K_3t^3 + \dots$ , and it is by virtue of the elimination of the term in  $t^2$  that this circuit achieves its greater linearity. A diode is placed across  $R'$  to help maintain proper initial conditions independent of duty ratio. The diode does not conduct during the sweep period, but during the restoration period it provides a lower impedance path than does  $R'$  for the discharge of condensers  $C'$  and  $C''$ .

Qualitatively the action can be understood in the following way. Since the amount of current passing into  $C'$  and  $C''$  when the resistor  $R'$  is not present is a decreasing function of time, the voltage  $e_c$  has a decreasing rate of change. When  $R'$  is inserted, the amount of current passing into  $C''$  through  $R'$  is an increasing function of time and therefore the potential across  $C''$  due to this current has an increasing rate of change.

If  $R'$  is sufficiently small, a potential  $e_c$  with a positive second derivative is obtained, but if  $R'$  is very large  $e_c$  has a negative second derivative. Hence it is reasonable to expect that if the correct value of  $R'$  is chosen a potential  $e_c$  with a zero second derivative is obtained—and this result is actually possible.

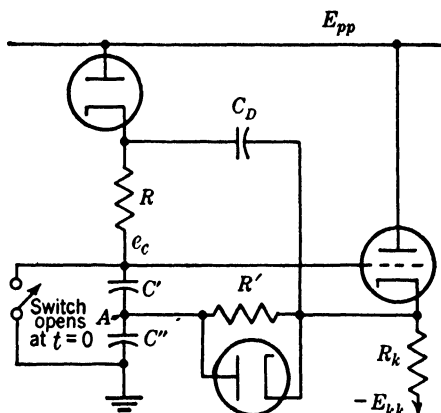


FIG. 7-22.—Second order compensation added to cathode-follower positive-feedback saw-tooth generator.

The differential equation for the voltage across the condenser is

$$\frac{d^2 e_c}{dt^2} = \left[ \frac{(1 - \mathcal{G})}{R \frac{C' C''}{C' + C''}} + \frac{1 - \mathcal{G}}{R' C''} + \frac{1}{R C_2} \right] \frac{de_c}{dt} + \left[ \frac{1 - \mathcal{G}}{R C' R' C''} + \frac{1 - \mathcal{G}}{R' C'' R C_2} \right] e_c = \frac{E_B}{R C' R' C''}.$$

The initial conditions taken are

$$e_c = 0$$

and

$$\frac{de_c}{dt} = \frac{E_B}{\frac{R C' C''}{C' + C''}}.$$

A useful form of solution for  $e_c$  is easily obtained by the use of Laplace transforms or by a series solution of the differential equation<sup>1</sup>

$$e_c = X_1 t + \frac{K - a_1 X_1}{2!} t^2 + \frac{a_1^2 x_1 - a_2 x_1 - a_1 K}{3!} t^3 + \dots, \quad (12)$$

<sup>1</sup> V. W. Hughes, "A Range Measuring System Using an RC Linear Sweep," NDRC 14-540, M.I.T. Radiation Laboratory, Sept. 18, 1944.

where

$$\begin{aligned} X_1 &= \frac{E_B}{R \frac{C' C''}{C' + C''}} \\ K &= \frac{E_B}{RC' R' C''} \\ a_1 &= \left( \frac{1 - g}{RC' C''} \right) + \frac{1 - g}{R' C''} + \frac{1}{RC_2} \\ a_2 &= \frac{1 - g}{RC' R' C''} + \frac{1 - g}{R' C'' RC_2} \end{aligned}$$

The virtue of the auxiliary network is that the term in  $t^2$  can be eliminated by setting

$$K - a_1 X_1 = 0.$$

This relation is satisfied if

$$R' = \frac{\frac{RC' C''}{C' + C''}}{\frac{RC' C''}{C' + C''} \frac{1}{C' + C''} \frac{C'(g - 1) + g C''}{C''}}, \quad (13)$$

$$(1 - g) + \frac{C' + C''}{RC_2}$$

and in this case

$$V_e = X_1 t \left( 1 - \frac{a_2}{3!} t^2 \right).$$

A practical circuit utilizing the compensating network is shown in Fig. 7.23.<sup>1</sup> Tube  $V_1$  supplies the gate to the switch tube  $V_{2a}$ . The linear-sweep generator is exactly similar in form to that of Fig. 7.22 except for the inclusion of the resistance  $R_2$ , which was found experimentally to improve the linearity near the start of the sweep. A sweep with an amplitude of about 125 volts and a duration of about 120  $\mu$ sec is obtained from the cathode or grid of  $V_{4a}$ . A linearity of 0.1 per cent in terms of displacement error is obtained over the range from about 2  $\mu$ sec to 120  $\mu$ sec. If the sweep voltage is taken at the grid of the cathode follower  $V_{4a}$ , the change in voltage at about 5  $\mu$ sec after the start of the sweep (zero shift) is about 0.03 per cent of the maximum sweep voltage for a 10 per cent change in the filament voltage of all tubes, and

<sup>1</sup> The circuit of Fig. 7.23 has been designed on the basis of the theory discussed above, even though the linearity achieved by the circuit is so good that the assumption that this theory makes, i.e., that the cathode follower has a constant gain, becomes of doubtful validity. However, the experimental results agree very well with the theory.

the change in voltage near the end of the sweep is about 0.15 per cent for this same change in filament voltage. The slope of the linear sweep is, of course, proportional to the value of  $E_{pp}$ . At all points of the linear sweep the change in voltage produced by a repetition rate change from 200 cps to 2400 cps is less than 0.1 per cent of the maximum sweep voltage. Microphonics corresponding to slight tapping of the tubes seldom cause a change of the sweep voltage at any point of the sweep by more than a few tenths of one per cent of the maximum sweep voltage.

The component values have been chosen so that no point of the sweep changes in voltage by more than 0.3 per cent of the maximum voltage

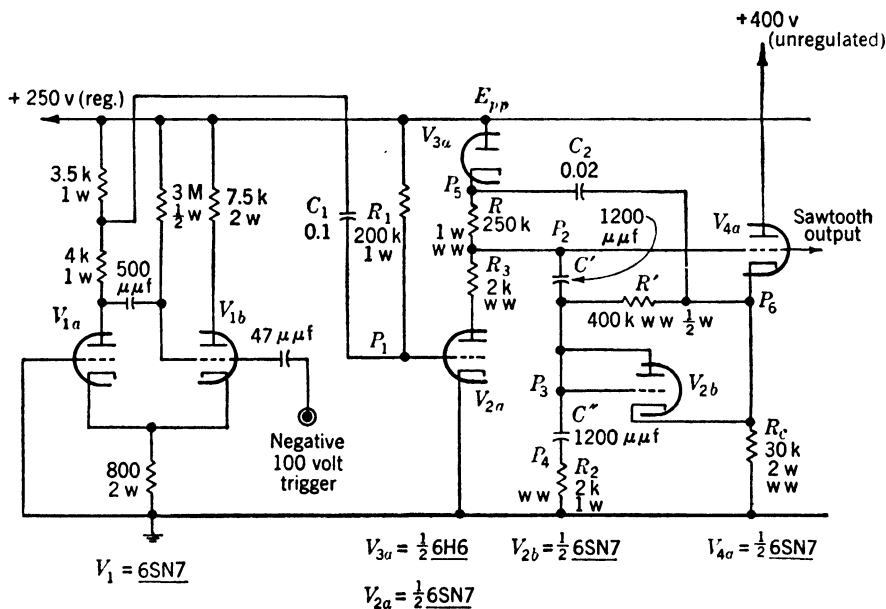


FIG. 7-23.—A 120- $\mu$ sec bootstrap linear sweep with a compensating network.

when the temperature of the surroundings are changed from  $-10^{\circ}\text{C}$  to  $+75^{\circ}$ . This is achieved primarily by choosing  $R$  and  $C$  so that the  $RC$  product is independent of temperature. A Nichrome wire-wound IRC resistor, ww-1, with a temperature coefficient of 0.017 per cent per  $^{\circ}\text{C}$  was chosen for  $R$ , and both  $C'$  and  $C''$  were a combination of ceramicon condensers manufactured by Erie Resistor Company. This combination has a temperature coefficient of  $-0.023$  per cent per  $^{\circ}\text{C}$  and includes a  $500\text{-}\mu\text{f}$  condenser with a temperature coefficient of  $-0.047$  per cent per  $^{\circ}\text{C}$ , a  $300\text{-}\mu\text{f}$  condenser with a temperature coefficient of  $-0.015$  per cent per  $^{\circ}\text{C}$  and a  $400\text{-}\mu\text{f}$  condenser with a zero temperature coefficient. The magnitude of the temperature coefficient of the condenser combination equals that of the resistor within the specifications

allowed on temperature coefficients. Of less importance is the necessity to keep the coefficient  $(K - a_1x_1)/2$  of the  $t^2$  term in Eq. (12) equal to zero for the entire temperature range encountered. The relations that must exist between the temperature coefficients of the various components to satisfy this latter condition as well can be readily determined.<sup>1</sup> In this circuit a wire-wound resistor with a temperature coefficient of 0.02 per cent per °C was used for  $R'$ , and a mica condenser was used for  $C_2$ .

The data on linearity and heater voltage sensitivity apply only if the sweep is taken from the grid of the cathode-follower tube  $V_{4a}$ . Sometimes it is desirable to use the sweep from the cathode of the cathode follower, because of the lower output impedance. It is then necessary

to readjust  $R'$ , which has been chosen to give the most linear sweep possible at the grid, in order to obtain the most linear sweep possible at the cathode. The heater-voltage sensitivity of the zero point of the sweep is greater when the output is taken from the cathode. This variation may be several tenths of a volt for a 10 per cent variation in filament voltage.

A variation of Fig. 7-16, which involves a compensating effect, and which can be designed to yield an output voltage of the form

$$e_c = K_1t + K_3t^3,$$

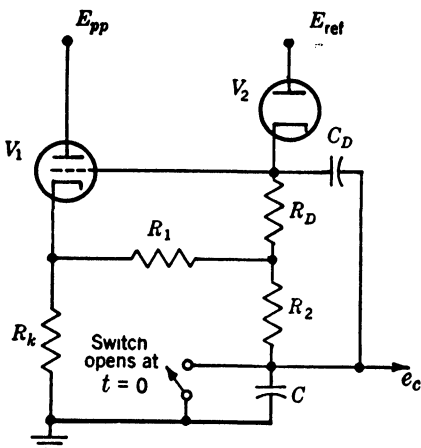


Fig. 7-24.—A variation of Fig. 7-16 capable of producing a highly precise linear sweep.

provided the cathode follower is assumed to have a constant gain, is shown in Fig. 7-24. The series combination  $R_1$  and  $R_2$  corresponds to  $R$  of Fig. 7-16.

## CIRCUITS INVOLVING NEGATIVE FEEDBACK

**7-10. General Theory and Classification.**—The Miller integrator circuit (Chaps. 2, 5 and 19) is the basic element of the linear-sweep generators employing negative feedback. The many variations of this type of circuit differ with regard to the switching method employed and the complexity of the amplifier. Among the possible variations of this class of linear-sweep generators are the single- and multiple-tube externally gated linear-sweep generators, the screen-coupled phantastron, the sanatron, and the phantastron.

<sup>1</sup> Hughes, *op. cit.*

*Miller Integrator Circuit.*—An idealized Miller integrator circuit is shown in Fig. 7·25a. We assume that the amplifier has an infinite input impedance, a zero output impedance, and a constant gain  $A$ , where  $A$

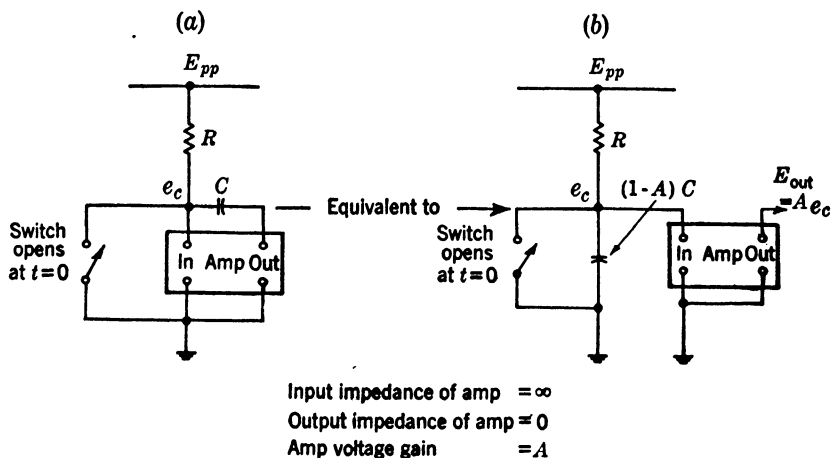


FIG. 7·25.—Basic negative-feedback linear-sweep generator.

is a negative real number. It is easily seen that

$$E_{\text{out}} = A e_c = A E_{pp} [1 - e^{-\frac{t}{(1-A)RC}}], \quad (14)$$

and if

$$\frac{t}{RC(1-A)} \ll 1, \quad (15)$$

$$E_{\text{out}} \cong E_{pp} \frac{A}{1-A} \left[ \frac{t}{RC} + \frac{t^2}{2(1-A)R^2C^2} + \dots \right],$$

$$E_{\text{out}} \cong -E_{pp} \frac{t}{RC} \quad \text{for } |A| \text{ large.} \quad (16)$$

Clearly, the higher the gain  $A$ , the more linear will be the sweep. For this circuit the ratio of the term in  $t^2$  to the term in  $t$  is  $1/(1-A)$  times the same ratio for the circuit in which  $C$  is discharged through  $R$  from  $-E_{pp}$ , although the amplitude of the term in  $t$  is approximately the same for the two circuits. Since the value of  $A$  cancels out of the final result to a first approximation, it need not be constant as a function of time or of input voltage.

Another circuit yielding an output voltage of the form of Eq. (14) is indicated in Fig. 7·25b. A condenser of value  $(1-A)C$  is charged through  $R$  from  $E_{pp}$  and the voltage across this condenser is amplified by  $A$ . This circuit is not recommended as an alternative method, because of the difficulty of generating a sweep at a low voltage level, but

is presented merely to indicate the relation of the Miller feedback circuit to the exponential generation discussed in Sec. 7-5.

**Types of Generators.**—The classification of the various types of negative-feedback sawtooth-waveform generators can be made on the basis of two properties: (1) the type of amplifier and (2) the type of switching arrangement. The single-tube amplifier is most common. For the achievement of high linearity a pentode with a resistive load impedance is normally employed; even higher gain can be achieved by the use of a load impedance consisting of a resistance and an inductance in series. A three-stage amplifier is also of value when a very high gain is desired. Circuits of both the astable and monostable types can be designed; this discussion will be mainly of monostable or single-stroke types. The multitube amplifier is usually gated by applying a pulse to the grid of the first stage. The single-tube amplifier is often gated in this way, but, if a pentode is employed, gating on the suppressor grid is common. Several circuits using suppressor-grid gating generate their own gate waveform after a trigger is applied to them. The sanatron does this by the use of an additional tube, and the phantatron accomplishes it in its own cathode or screen circuit (see Chap. 5).

In general, the linearity of the sweep is not appreciably affected by the switching arrangement used; the starting characteristics and the restoration time, however, are affected. When a single-tube pentode amplifier with a resistive load impedance is used, linearities of about 0.1 per cent, measured in terms of displacement errors, have been achieved for a sweep with an amplitude of about one-half the supply voltage. For a multitube amplifier or for a single pentode amplifier with a load impedance consisting of a resistance and inductance in series, linearities close to 0.01 per cent can be achieved.<sup>1</sup>

**7-11. Single-stage Amplifier Circuits, Externally Gated.**—The linear-sweep generator which employs a single-amplifier tube and is gated on its control grid is perhaps the simplest circuit of this type. Figure 7-26 illustrates such a circuit. The resistor  $R_c$  is inserted in order to minimize the positive jump which would otherwise occur in the plate potential when the switch is opened. The value of  $R_c$  required to avoid this transient in the output potential is approximately  $1/g_m$ , provided the amplifier was not biased off initially. The output waveform will be a trapezoid if  $R_c$  is larger than this.<sup>2</sup>

An example of a practical circuit of this type is shown in Fig. 7-27.

<sup>1</sup> Positive feedback to the top of the charging resistor can be used in any of the Miller feedback sweeps. This feedback can partially compensate for the rise in grid potential of the Miller tube, which always occurs as a result of limited amplifier gain, and it has been used successfully in high-precision circuits ( $\sim 0.1$  per cent linearity).

<sup>2</sup> See Fig. 7-33 and section 7-13.

This is an inexpensive, monostable push-pull time-base generator for driving an electrostatic cathode-ray tube. Basically it is the circuit of Fig. 7-26 with the addition of a switching tube  $V_1$  and an inverter tube  $V_{2b}$ . It is capable of generating up to 400 volts push-pull output with a 400-volt supply and is sufficiently linear for almost any visual use. The condenser  $C$  controls the slope of the linear sweeps. Of course, the triode is not as suitable as the pentode for precision linear sweeps.

To reduce the recovery time of the circuit of Fig. 7-26, which is mainly the time required for  $C$  to recharge through  $R_L$  and  $R_C$ , a cathode follower is often employed as shown in Fig. 7-28. The cathode follower changes the important recharging time constant of Fig. 7-26,  $R_L C$ , to  $R_L C_s$ , where  $C_s$  is the sum of the stray capacity from plate to ground of the amplifier tube and of the input capacity to the cathode follower. This reduces the restoration time by a large factor provided the cathode follower can supply sufficient current. The use of the cathode follower eliminates the need for the resistor  $R_C$ . The cathode follower can be used in this way to reduce restoration time in many of the circuits described in this section (see Chap. 5).

**Suppressor-grid Gating.**—Suppressor-grid switching of the amplifier tube is often useful because the switching circuit can be isolated from

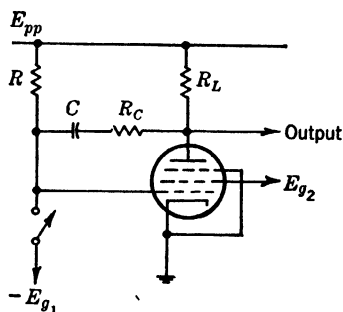


FIG. 7-26.—Linear sweep generator which employs a single amplifier stage and is gated on its control grid.

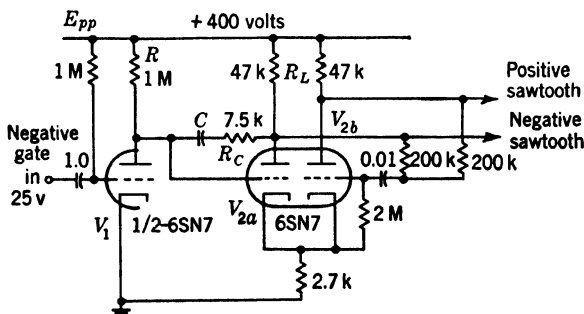


FIG. 7-27.—Inexpensive push-pull monostable sawtooth generator using negative feedback.

critical biasing circuits. Figure 7-29 shows the basic circuit and associated waveforms;  $V_2$  is the Miller integrator tube and  $V_1$  is the switch tube. In the quiescent condition  $V_1$  draws grid current via  $R_2$ . Because of the resulting low potential of the plate of  $V_1$ , the suppressor of  $V_2$  is held negative relative to its cathode—often in practice by about 100 volts.



The tube  $V_2$  draws grid current via  $R_9$ , which is connected to a positive voltage  $E_L$ ; the cathode current of  $V_2$  flows to the screen since the negative suppressor to cathode voltage cuts off substantially all anode current.

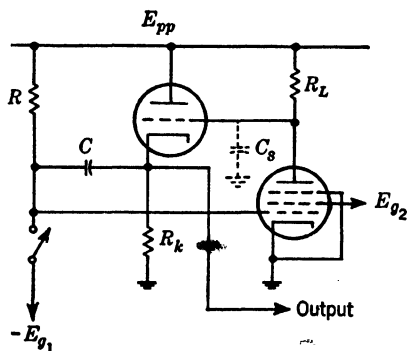


FIG. 7-28.—Use of cathode follower with negative-feedback sawtooth generator.

The space current in  $V_2$  is controlled by  $R_8$  to a value such that the screen wattage is not excessive. Since the potential  $E_1$  applied to  $V_6$  is assumed to be less than  $E_{pp}$ ,  $V_6$  is conducting a current  $I_o$  approximately equal to  $(E_{pp} - E_1)/R_7$ . The condenser  $C_2$  is charged to a voltage approximately equal to  $E_1$ .

Application of a negative triggering pulse to point  $P_1$  cuts off  $V_1$  because during the pulse the condenser  $C_1$  is discharged via  $V_3$ .

After the pulse is over,  $V_3$  is cut off and the recharging of  $C_1$  can take place only via  $R_2$ . When  $V_1$  is cut off, the suppressor of  $V_2$  is brought to ground level so that the plate of the latter tube is rendered conductive. In practice

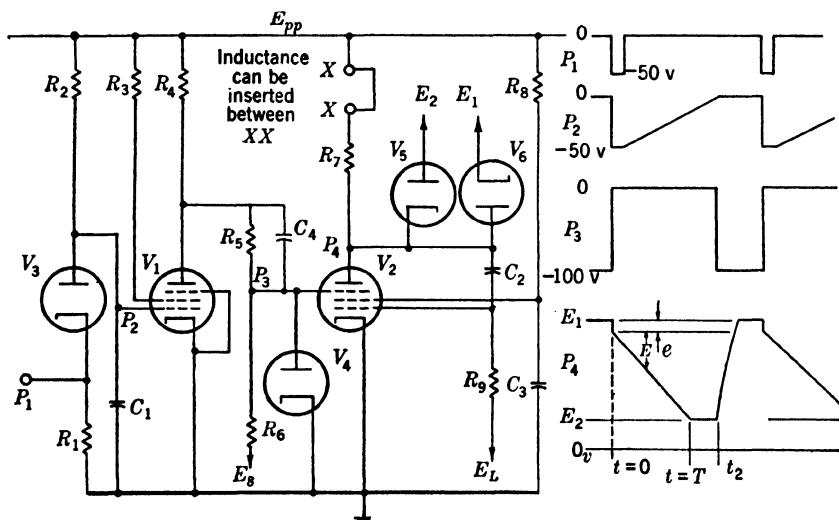


FIG. 7-29.—A suppressor-gated, negative-feedback linear-sweep generator and its waveforms.

it is convenient to choose the network  $R_4$ ,  $R_5$ ,  $R_6$  so that the suppressor of  $V_2$  would assume a positive potential during this period if its upper excursion were not limited to ground level by the diode  $V_4$ . Since the anode current that flows at  $t = 0$  is designed to be greater than the

current  $I_o$  that was flowing in diode  $V_6$  in the quiescent period,  $V_6$  cuts off and the anode potential of  $V_2$  falls. Since  $C_2$  cannot lose its charge instantaneously, any fall in the plate potential of  $V_2$  will be transferred to the control grid. An equilibrium condition will rapidly result such that the anode current is in excess of  $I_o$  by an amount which, when multiplied by  $R_7$ , gives rise to an increase in grid bias appropriate for this new operating condition of the tube. The cathode current will be much less for the new operating condition than it was for the quiescent operating condition. The initial fall  $e$  in plate potential at  $t = 0$  is often about 3 volts. This rapid initial fall merges rapidly into a decrease of anode potential which is a linear function of time.

For the analysis of the linear downward sweep Eq. (14) applies. The control grid of  $V_2$  is now at a voltage of  $-e + e_o = -e'$ , where  $e_o$  is the quiescent control-grid potential. Thus the effective voltage applied to  $R_9$  will be  $(E_L + e') = E'_L$ . If the potential by which the anode has moved from its starting level by time  $t$  (neglecting the rapid initial drop) is denoted by  $E$  and if the tube gain, assumed constant, is denoted by  $A$ , the grid will have moved  $-E/A$  volts. Hence, by Eq. (14),

$$E = -AE'_L \left\{ 1 - \exp \left[ -\frac{t}{C_2 R_9} (A + 1) \right] \right\}.$$

The sweep is terminated when the plate potential reaches the value  $E_2$ , where it is held by the diode  $V_6$ . The quiescent condition is restored after  $V_1$  turns on.

*An Inductance in Plate Load.*—A higher gain for the amplifier, and, hence, a greater linearity for the sweep, can often be achieved by the use of an inductance as well as a resistance in the plate circuit. The magnitude of the improvement is easily related to the values of the circuit parameters.

Suppose that a pentode amplifier is being used. Then the change in plate current is to a good approximation  $g_m \Delta E_g$ . Suppose further that the sawtooth waveform is of amplitude  $\Delta E$  at the plate of the pentode. As is evident from our previous analysis, the sweep would be perfectly linear if the grid potential did not change during the sweep, because in this case a constant current would be discharging the condenser  $C_2$  of Fig. 7-29. The change in grid voltage is necessary in order to allow the change in plate current which corresponds to  $\Delta E$ —that is,

$$\Delta i_p = \Delta I_L + \Delta I_c,$$

where  $I_c$  is the current which is discharging the condenser and  $I_L$  is the current through the plate-load impedance. The discharge current  $I_c$  is substantially constant. Suppose that the change in voltage at the plate is expressible as  $\Delta E \cdot t/T$ , where  $T$  is the duration of the sweep.

Then, if the plate-load impedance consists of  $R$  and  $L$  in series, it is easy to show that the change in  $I_L$  from  $t = 0$  to  $t = T$  is

$$\Delta I_L = \frac{\Delta E}{R} \left[ 1 - \frac{L}{RT} (1 - e^{-\frac{RT}{L}}) \right].$$

If the load impedance were simply a resistance  $R$ , the change in current would be  $\Delta E/R$ . The ratio of  $\Delta E/R$  to  $\Delta I_L$  is the increase in effective gain achieved by inserting the inductance  $L$  in the plate circuit. This ratio is

$$\frac{1}{1 - \frac{L}{RT} (1 - e^{-\frac{RT}{L}})},$$

which becomes for  $L/R \gg T$

$$2 \frac{L/R}{T}.$$

Therefore, when  $L/R$  can be made  $\gg T$ , a considerable improvement in the linearity of the sweep can be achieved by the insertion of the inductance  $L$  in the plate circuit. A practical example will be given in Sec. 7-13.

**7-12. Multistage Amplifier Circuits, Externally Gated.**—An externally gated Miller sweep generator using a multistage amplifier is shown in

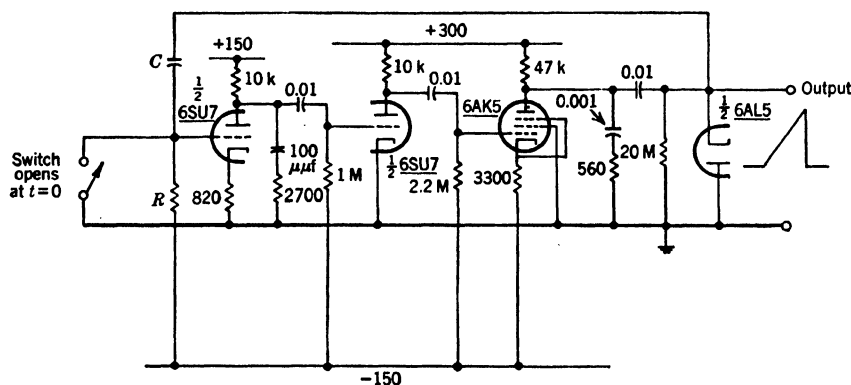


FIG. 7-30.—Gated, multistage amplifier Miller sweep generator. Sweep duration is approximately  $0.7 RC$ .

Fig. 7-30. The amplifier, which consists of two triode stages and one pentode stage, has a sufficiently high gain so that the nonlinearity of the sweep is less than 0.02 per cent (displacement error). The input grid of the amplifier is clamped except during the sweep generation.

A positive sweep is obtained at the output since the charging resistor is connected to the negative supply voltage. The output from the

pentode amplifier stage is taken through a  $CR$  level charger and diode in order that the initial level of the eventual output waveform shall depend on the clamping action of a diode rather than on the d-c characteristics of an amplifier. The amplitude of the triangular waveform is approximately 120 volts, its duration is 350  $\mu$ sec and its recurrence frequency is 1000 times per second. Since the time constants of the circuit are sufficiently small, the transients decay to less than  $\frac{1}{1000}$  of their initial amplitude during recovery.

The feedback amplifier has a gain of 2000 or 3000 at 1000 cps and its phase and amplitude characteristics are such that the amplifier is stable. The high-frequency cutoff occurs with an attenuation of 6 db per octave from 4 kc/sec to 88 kc/sec, followed by more rapid rate of attenuation which continues to a frequency slightly below that for which the loop gain equals unity. At frequencies for which the loop gain is less than unity there is a more rapid rate of increase of attenuation. Low-frequency stabilization is affected by the clamping of the circuit at the repetition frequency. It will be noticed that several  $RC$ -networks not included in ordinary  $RC$ -coupled amplifiers are employed; these are for the purpose of stabilization against oscillations.

Stability, not nonlinearity, is the primary source of inaccuracy in this circuit. The 6SU7 is used for the first stage because stable gain and low-grid current are necessary. The slope stability is improved if the charging resistor is returned to a larger supply voltage, because then instabilities in the switch (a double-diode type is used) are less troublesome. Slope instability is directly proportional to the instability of the negative supply voltage. The zero level of the triangular waveform is dependent upon the clamping action of the output diode and may vary by several tenths of a volt.

**7-13. Internally Gated Circuits.** *The Sanatron.*—The sanatron is a variation of the suppressor-gated Miller linear-sweep generator which itself produces the waveform employed for the suppressor gating by the use of an additional tube. Thus it is assured that the durations of the linear sweep and of the suppressor gate are equal. The component values given for the circuit of Fig. 7-31 represent a typical operating condition, for which a 200-volt sweep of 20- $\mu$ sec duration is obtained from the plate of  $V_2$ . Sweep speeds from 1 volt/sec to 50 volts/ $\mu$ sec or higher can readily be obtained with a circuit of this type. Without an inductance a linearity corresponding to a gain of about 100 is obtained with this particular circuit; with  $L = 20$  henrys the gain is increased to about 4000.

A detailed description of the operation of the circuit follows. In the quiescent condition  $V_1$  is conducting and plate current in  $V_2$  is cut off by suppressor-to-cathode bias. A negative trigger pulse of amplitude

greater than 6 volts is applied to  $P_1$ . The precise amplitude of the trigger is unimportant and, in any case, it is limited to 6 volts by diode  $V_5$ . This pulse cuts off  $V_1$  so that the suppressor to cathode bias of  $V_2$  is reduced to zero. Also the pulse causes a drop in potential at the point  $P_3$  in the anode load of  $V_2$  which in turn cuts off  $V_4$ . Hence the initial drop in potential at the plate of  $V_2$  due to the trigger is increased, since

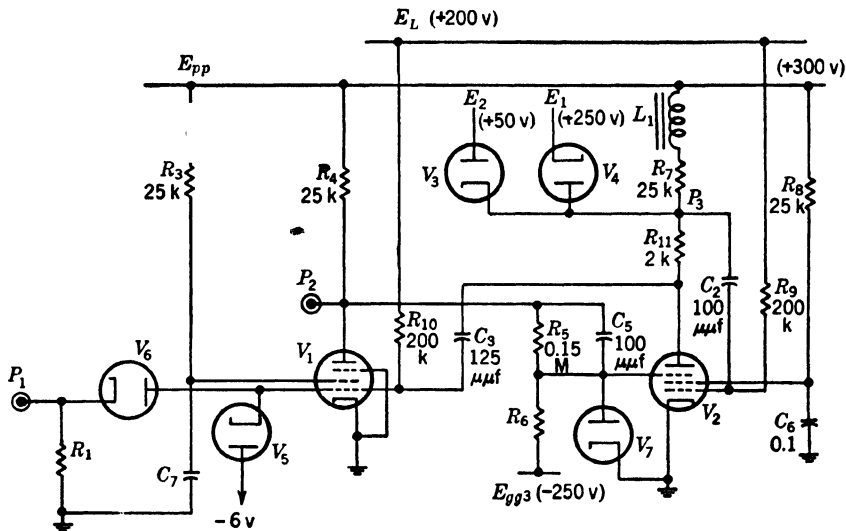


FIG. 7-31.—Sanatron linear-sweep generator. The tubes are British tube types. Tube  $V_2$  is a VR116 tube.

the quiescent current  $(E_{pp} - E_1)/R_7 = 50 \text{ v}/25 \text{ k} = 2 \text{ ma}$  is diverted through  $R_{11}$ . Moreover, the discharge current of  $C_2$ , which is

$$\frac{E_L}{R_9} \approx 1 \text{ ma},$$

begins to flow through this resistance, and the anode of  $V_2$  falls 6 volts below  $P_3$ . This drop in potential at the anode of  $V_2$ , which is about 9 volts, is applied via  $C_3$  to the grid of  $V_1$  and maintains  $V_1$  cut off for a short time after the triggering instant.

A linear fall in potential at  $P_3$  now commences. This fall is applied via  $R_{11}$  to one end of  $C_3$  and the current flowing in  $C_3$  will be

$$C_3 \frac{dE}{dt} = 1.25 \text{ ma},$$

where  $dE/dt$  is the rate of change of potential at  $P_3$ . Since only +1 ma flows through  $R_{10}$ , 0.25 ma must flow via  $V_5$ ; hence  $V_1$  remains cut off during the sweep with its grid at -6 volts. During the sweep the circuit is therefore in a stable condition and  $C_2$  continues to discharge.

When the potential at  $P_3$  reaches  $E_2$ , the clamping of the potential at  $P_3$  by  $V_3$  allows the grid of  $V_1$  to rise until it is conducting current. The resulting drop in potential at the plate of  $V_1$  results in a negative bias between suppressor and cathode of  $V_2$  which cuts off plate current in  $V_2$  and raises the grid of  $V_1$  so that a regenerative transition occurs. Since negative feedback between plate and grid of  $V_2$  is now stopped, the potential of the grid of  $V_2$  rises until grid current flows. When the plate of  $V_2$  has risen to  $E_1$  by the process of charging  $C_2$  through  $L_1$  and  $R_7$ , the quiescent conditions will have been reestablished.

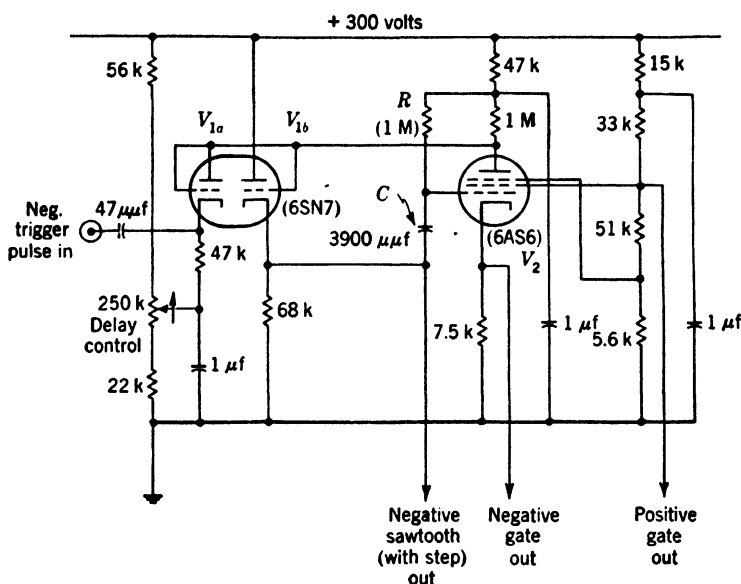


FIG. 7-32.—Cathode-coupled phantastron.

Times associated with the recovery process can be estimated as follows. First, it is not until the grid of  $V_1$  is at about  $-3$  volts that the regenerative process is well under way. This condition is reached about  $0.4 \mu\text{sec}$  after the cessation of the sweep, since the motion of this grid is due to the  $1 \text{ ma}$  flowing into  $C_3$  which results in a rate of change of potential of  $8 \text{ volts}/\mu\text{sec}$ . The longest portion of the recovery time is that required to recharge  $C_2$  through  $R_7$  and  $L_1$ . The condenser  $C_3$  is employed to avoid loss of speed in the transitrons from the quiescent to the operating state and vice versa.

**Phantastrons.**—Of the two principal types of phantastron circuit—the cathode-coupled phantastron and the screen-coupled phantastron—the former is sometimes less suitable as a linear sweep generator than the circuits already discussed because in its output there is a larger initial

jump in potential than there is in the outputs of the other circuits. Its principal virtue lies in its cheapness. A practical circuit is shown in Fig. 7-32. The phantastron tube  $V_2$  is triggered through the diode  $V_{1a}$ . Cathode follower  $V_{1b}$  is used to reduce the recovery time. The delay control varies the amplitude of the sweep but leaves its slope unchanged.

The screen-coupled phantastron avoids the large jump in potential which is objectionable in the cathode-coupled phantastron, and is comparable in excellence to the sanatron (see Chap. 5).

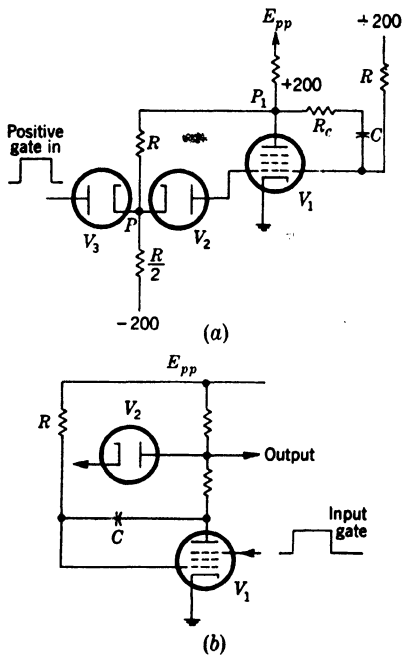


FIG. 7-33.—Methods of starting Miller sweeps without a step.

was flowing through the diode  $V_2$  during the quiescent period flows through the tube after the suppressor gate is applied. This method is inferior to that of Fig. 7-33a because it is difficult to arrange to have the diode current during the quiescent period equal to the plate current during the sweep-generation period. Indeed, this condition can never be exactly realized if the diode is to be cut off during the sweep generation period.

*Elimination of Initial Step.*—In most of the circuits given thus far a negative step appears at the start of the sweep. One method of avoiding this step by the use of a resistor in series with the charging condenser was illustrated in Fig. 7-26. This method required a switch which would hold the grid of the Miller tube during the quiescent period at the operating potential desired during the sweep-generation period. One such switch is indicated in Fig. 7-33a. With this switch d-c negative feedback stabilizes the potential  $P_1$  at +200 volts and  $R_c$  is the step-compensating resistor. Another method, which only partially avoids the step, is indicated in Fig. 7-33b. The current that

## CHAPTER 8

### GENERATION OF SPECIAL WAVEFORMS

By R. KELNER, W. PROCTOR, AND F. B. BERGER

**8-1. Introduction.**—The complex waveforms discussed in this chapter include exponential, hyperbolic, parabolic, and trapezoidal voltage waveforms and linear current waveforms. Most of these waves are initiated by triggers, follow a prescribed path in the voltage-time plane, and return to a quiescent condition considerably before the next trigger occurs. Voltage waveforms are seldom larger than a few hundred volts or smaller than 10 to 25 volts. Current waveforms involve currents as high as several hundred milliamperes. The duration of the useful portion of a

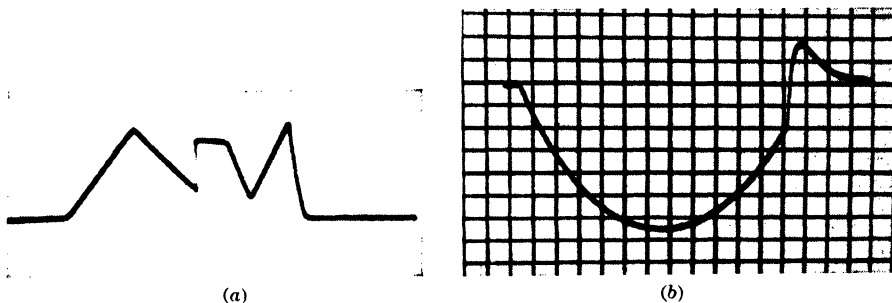


Fig. 8-1.—Complex waveforms: (a) linear segments; (b) parabolic and exponential segments.

waveform may vary from 1 to 1000  $\mu\text{sec}$ . The triggers usually occur at a constant rate of one hundred to a few thousand times per second although sporadic triggering is possible. These regions are not delimited by insuperable physical barriers but have, in general, been set by radar requirements.

Two complex waveforms are shown in Fig. 8-1. These waveforms are composed of two or more segments. Very often, a wave consists of the useful segment and a recovery segment that is exponentially shaped. The “flat” segment following recovery should be considered as a part of the waveform; in its absence the generator would be repetition-rate sensitive.

The difficulty of generating some specially shaped waveforms results in a slight decrease in the accuracy of these waveforms compared with the linearity of rise in a triangular wave. The displacement errors of most



of the waveforms of this chapter from their ideal curves is usually  $\pm 0.05$  per cent to  $\pm 2$  per cent. However, the shape of the exponential wave has a somewhat smaller deviation from the ideal curve.

*Applications.*—These waveforms are, at present, used in the following ways: (1) as elements and controlling waveforms in “model” computers,<sup>1</sup> (2) as timing waveforms, and (3) as elements for generation of other waveforms.

*Means of Generation.*—Only generators whose waveforms can be accurately controlled in shape and size will be considered here.

A designer of a triggered-waveform generator may assume that a trigger is available as well as the linear elements, curved elements, and nonconstant elements described in Chaps. 2 and 3. Those chapters also describe some operations that may be performed with these elements, and Chaps. 5 through 7 utilize these operations to produce rectangular pulses and triangular sawtooth waveforms. In this chapter, many of these methods are used.

The segmented appearance of complex waveforms is a result of the use of nonlinear elements. Each segment corresponds to one region of the nonlinear characteristic. The region of operation of a given element may be controlled by the waveform voltage across the element or by a separate waveform. Both means of segmenting are commonly utilized. In the analysis of complex waves, each segment is considered separately and represented by a separate equation. In the equivalent circuit, the nonconstant elements may be represented by constant elements and switches.

During each segment the shape of the waveform is determined by linear elements, or at least by elements without breaks in their characteristic. The step functions of voltage and of rate of change of voltage, for which means of generation have been described, may be modified in many ways by such elements. Laplace transform methods can be used to determine the transformation effected upon any waveform by a linear network with reactive components.<sup>2</sup> Integration and differentiation may be achieved by simple vacuum-tube circuits. Elements with curved characteristics produce similarly curved voltage or current waves if a triangular wave of the other variable is impressed.

**8-2. Special Triangles and Rectangles.**—Means for obtaining the simplest and most common triangular and rectangular waveforms are described in the preceding three chapters. This section deals with some uncommon types. Any number of the few elementary forms may be added together. By varying the duration, amplitude and starting time, a great variety of multisegment waves can be constructed from straight-

<sup>1</sup> See Sec. 6-5 and 6-6 Vol. 21.

<sup>2</sup> See Chap. 18 of this volume and Chap. 1, Vol. 18.

line segments. The elementary waves are, of course, limited in accuracy by the effects detailed in the preceding chapters.

*Simple Triangles.*—Figure 8·2a shows right triangles that “flyback” at the end of the triangle. In some instances, the “flyback” must occur at the beginning as in Fig. 8·2b. The requirements for rapid “flyback” are usually most restrictive in this case. The two cases merge when the interval between triangles becomes small. This type, shown in Fig. 8·2c, is used for oscillatory time-base generators.

A triangle generator of this type is shown in Fig. 8·3a. A capacitor is charged through a low-impedance triode and allowed to discharge through a high impedance triode. The upper triode is forced to conduct by a positive pulse at the grid that must be as large as the output triangle and of duration sufficient for the charging of the capacitor. The linearity of such triangular waves is discussed in Sec. 7·2, Chap 7.

In Fig. 8·3b a capacitor is discharged through a triode during the trigger and is charged through a resistor while the triode is held cut off by the grid current drawn during the trigger. The rise is “caught” by a diode at a voltage of  $+E$  and remains at that potential until another trigger appears.

The circuit in Fig. 8·3c is a saw-tooth waveform generator commonly used for generating time bases. A gas-filled tube fires when its plate voltage reaches a certain level or when a trigger is applied to its grid, and in either case the exponentially shaped charging curve of the RC-combination is restarted. The output waveform is that of Fig. 8·2. The departure from linearity of such an exponential is given approximately by the following expression:

$$\text{Per cent displacement error at } t \approx 10 \frac{t}{T},$$

where  $T$  is the effective time constant.<sup>1</sup> The circuit oscillates without

<sup>1</sup> See “Operating Instruction for Du Mont 208 Oscilloscope,” The Allen B. Du Mont Co., Passaic, N.J. If adjusted for 1000 sweeps per second, the time con-

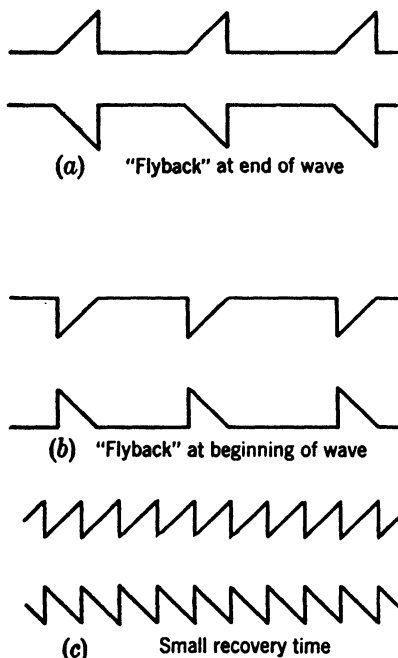


FIG. 8·2.—Simple right triangles. (a) “Flyback” at end of wave; (b) flyback at beginning of wave; (c) duty ratio 100 %.

triggers. In such a case, the gas-filled tube fires when the plate voltage reaches a certain level that is determined by the grid bias. Diodes could be used in the first two circuits to improve the accuracy with which the zero and slope of the waves are determined.

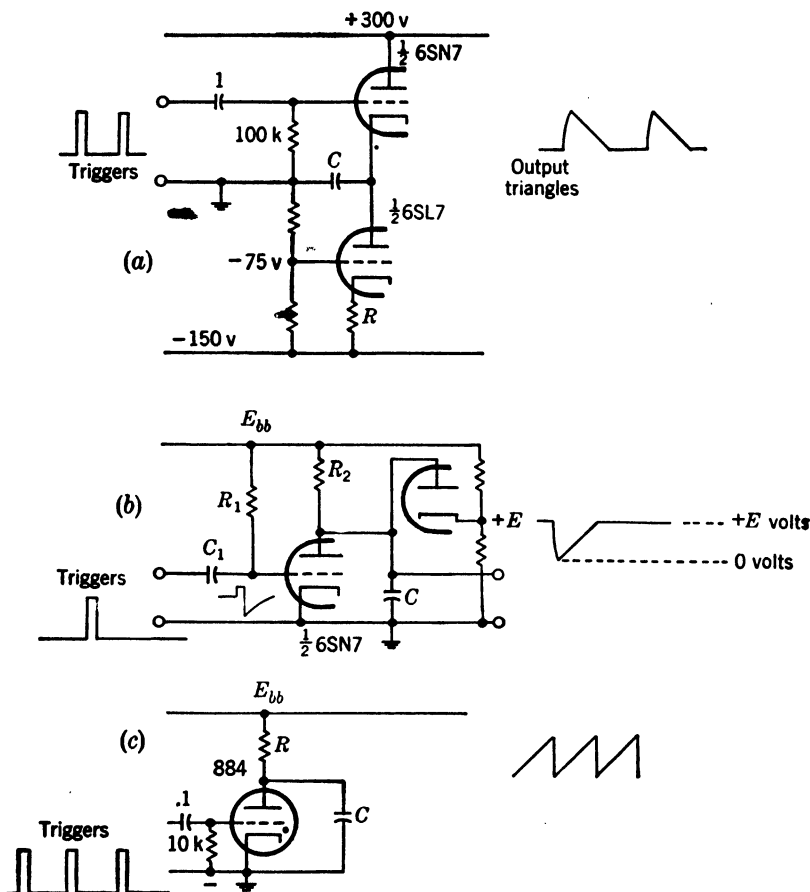


FIG. 8-3.—Triangular-waveform generators. (a) and (b) generate triangles of types of Fig. 8.2b; (c) generates the waveform of Fig. 8-2c. In (a) the heater potential of the upper tube should be maintained at cathode level to minimize leakage.

The cathode follower with a constant-current cathode load (Fig. 8-3a) can be used to produce several types of waveform. If a positive rectangle is applied to the grid of the 6SN7 triode, the same rectangle is reproduced in the output of the circuit except that the return to the

stant is 10,000  $\mu$ sec, assuming that the fine frequency control is set at its central position. The deviation of the exponential curve from the best straight line that can be passed through it is not greater than 1 per cent.

quiescent level is a linear fall at a rate determined by the constant current and the charging condenser. The resultant waveform is shown in Fig. 8-4a. This circuit is suitable for following an arbitrary wave by a linear fall, provided only that the wave terminates in a fall that is faster than the one to be generated. (See Fig. 8-4b for the output with a triangular input wave.) The errors of this circuit are the same as for cathode-following of a waveform plus some nonlinearity in the voltage fall.

*Staircase Waveforms.*—The staircase waveform may be considered as the sum of a number of rectangles of different heights. Its use in

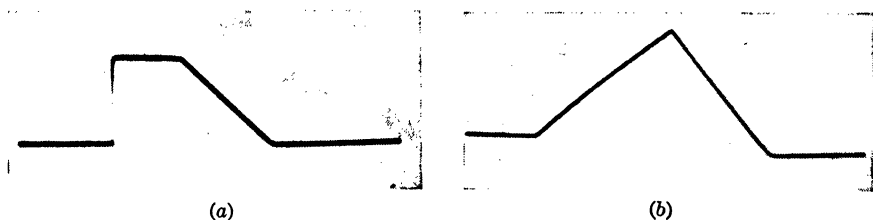


FIG. 8-4.—Rectangular wave followed by triangular wave; (b) triangular wave followed by triangular wave.

counter circuits is described in Sec. 17-6. A photograph of a staircase waveform is shown in Fig. 8-5.

Several means of generation of the staircase waveform are shown in Fig. 8-6. The first shows the adding in a resistance network of the square-wave outputs of several monostable multivibrators. The resistances in the adding network must be large compared with the source impedances of the multivibrators if interactions are not to occur. On the other hand, the resistances cannot be increased beyond the point where the delaying action of stray capacitances affects the waveform rises. The output waveform is at a comparatively high impedance. The output may be a rising or a falling staircase according to whether the positive or negative multivibrator output is used. Adding with a network of resistors connected to the virtual ground of a feedback amplifier is an excellent method.

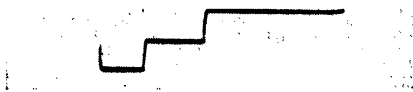


FIG. 8-5.—Staircase waveform.

The addition may also be done as in Fig. 8-6b. Each component square wave changes the conduction of one tube by a certain number of milliamperes. The accuracy of the action is increased by providing current feedback in the cathode circuit of each tube.

Still another type of circuit is shown in Fig. 8-6c. The output voltage approaches the maximum amplitude of the input pulses via a staircase waveform. This circuit is analyzed in Sec. 17-8. The true integration of pulses provides a staircase with a linear envelope. Particular atten-

tion must often be paid to elimination of heater-cathode leakage in the inverted diode in order to assure a flat top for the steps. The circuit action is ended or restarted by the discharge of  $C_2$  through a switch.

*Display System.*—Another use for step waves occurs in the control of cathode-ray-tube displays. Frequently, it is necessary to sweep the electron beam horizontally across the face of the tube at a succession of vertical levels. In addition to the other signals impressed between the

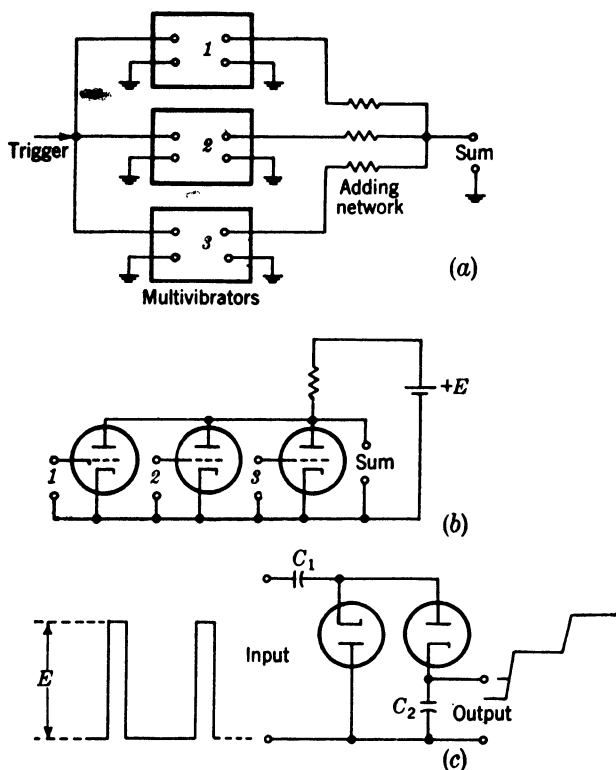


FIG. 8-6.—Staircase-waveform generators.

vertical deflection plates, there must occur a staircase waveform. In television or radar B-scope displays, the number of steps is so large and their amplitude is so small that the staircase is approximated by a smooth sweep, the envelope of the staircase. When the number of horizontal sweeps is small and the desired separation is larger, a true staircase must be used. The functional diagram of such a system is shown in Fig. 8·7 and the details of the circuits in Fig. 8·8. A two-tube vacuum-tube adder follows multivibrator square-wave generators. A sum of triangular waves of varying slopes must be applied to the horizontal plates of the

cathode-ray tube in Fig. 8.7. The high slope triangles provide expanded displays.

*Triangle Adders.*—A multiple-sawtooth waveform may be produced in a variety of ways. Several sawtooth-waveform generators may be

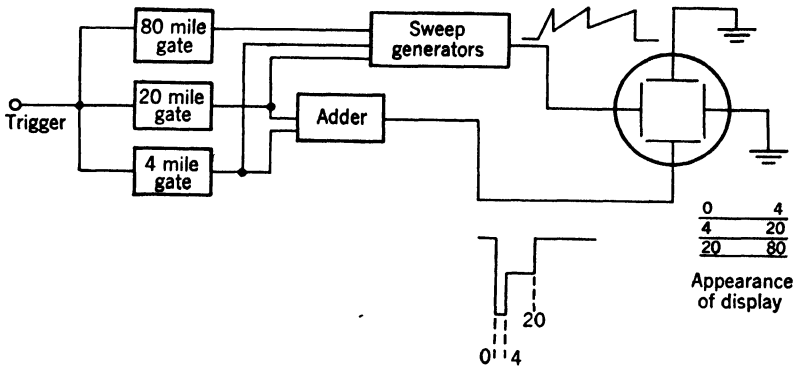


FIG. 8-7.—Display system. (1 mile corresponds to about 12  $\mu$ sec.)

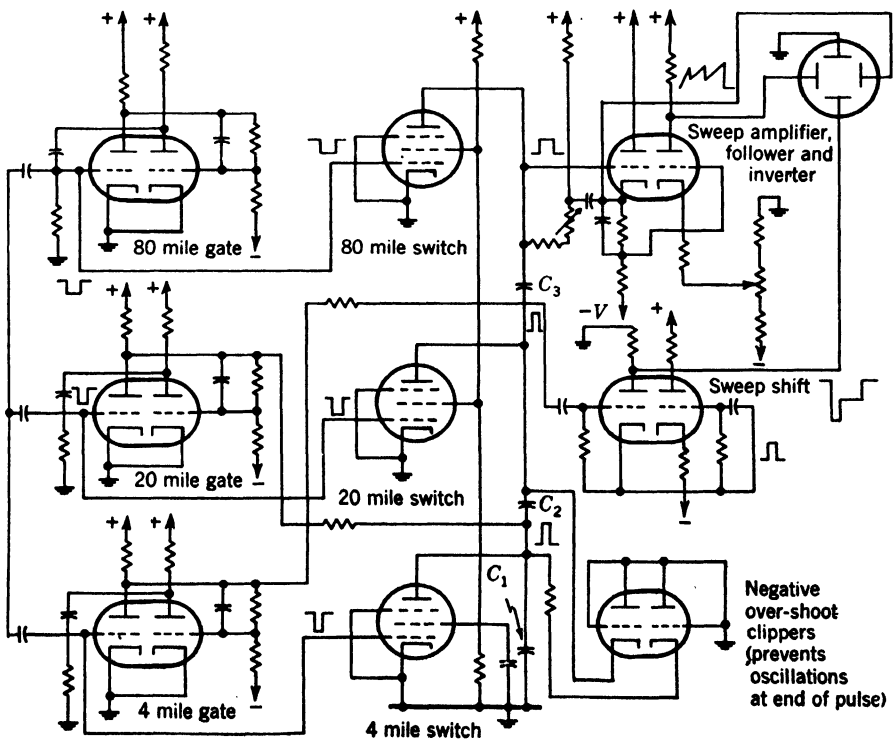


FIG. 8-8.—Details of display circuits.

gated at the appropriate times and their outputs added. Or a slope-determining element in a single generator may be switched in value.

Figure 8-9 illustrates the use of the "bootstrap" circuit for a multiple-sawtooth waveform. The two sawtooth-waveform generators interact

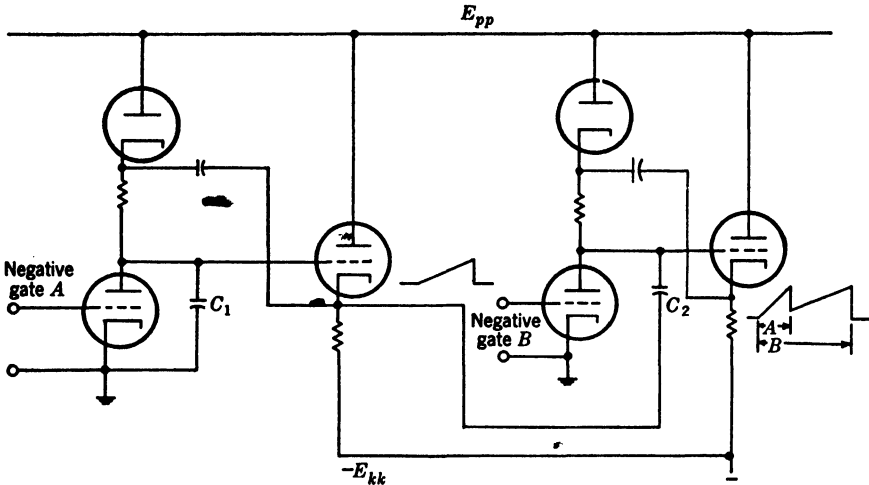


FIG. 8-9.—Triangle adder.

although this would not be true if the cathode followers had zero output impedance. The interaction is small and may be neglected for a first-order approximation. The output of the circuit is nearly the triangle from the first cathode follower plus the voltage across condenser  $C_2$ .

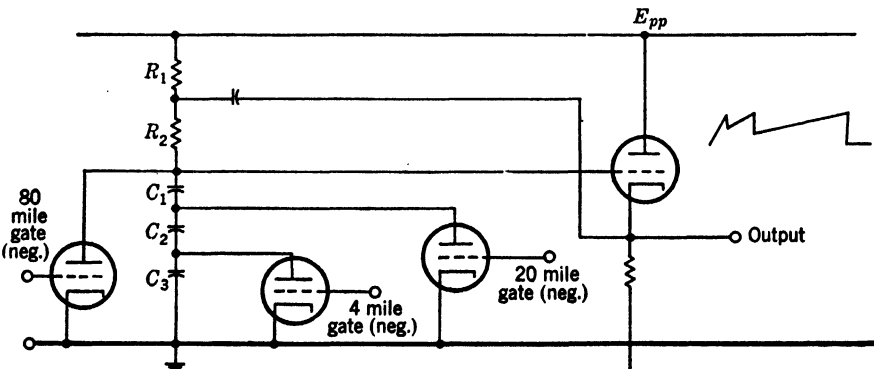


FIG. 8-10.—Triangle adder of Fig. 8-8.

In Fig. 8-10 the value of the charging condenser  $C$  is switched to provide the multiple triangles. The gating arrangement is suitable for the display of Fig. 8-7. The bootstrap circuit differs from the previous type by the substitution of  $R_1$  for a diode. The rapidity of fall of the

discharge sections of the grid wave is determined by the capacitance and the resistance of the switch tube through which it is discharged.

**8-3. Trapezoids.**—A trapezoid is a quadrilateral with two parallel sides. This is only a special case of the wave shapes described in the last section since a quadrilateral is formed of straight lines. The trapezoidal waveform is of considerable use in self-gating triangle generators and current sawtooth-waveform drivers but will be only briefly considered in this section because detailed circuits are given in Chap. 7 (bootstrap and phantatron circuits), and Sec. 8-15.

A trapezoid may be generated by addition of a rectangular and triangular waveform or by the use of a special trapezoidal waveform generator. The most common and useful shape of trapezoid is illustrated in Fig. 8-11.

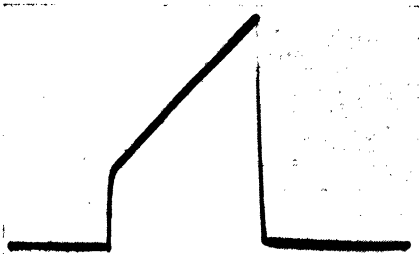


FIG. 8-11.—Trapezoidal waveform.

Some self-gating triangle generators give rise to output waveforms that are actually trapezoidal, consisting of a triangle mounted on a step (Chap. 7). The means employed for generating the step is a resistor in series with the condenser of an  $RC$ -sawtooth waveform generator. (The wave of Fig. 8-11 is generated by the circuit of Fig. 8-12.) This method of generating trapezoids is simple and permits accurate control of the step size.

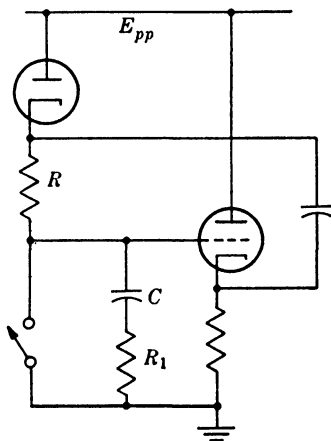


FIG. 8-12.—Trapezoidal-waveform generator. The step of voltage is equal to  $(E_{pp}/R)R_1$ .

The circuit is simple. Any exponential wave may be represented by

$$y = Ae^{t/T} + B, \quad (1)$$

where  $T$  is determined by a resistance and a reactance, and  $A$  and  $B$  are determined by the initial conditions. The deviations of an actual wave from its ideal shape are caused by variable leakage across the clamp tube,



by "soaking" effects in capacitors (see Vol. 17), or by distributed or stray capacitances and inductances. Good quality resistors and capacitors are available for which these effects are small.

*Simple Exponential-waveform Generators.*—The "linear"-sawtooth-waveform circuits (Figs. 8-3b and c) actually produce exponential waves. The waveforms of Figs. 8-13a, b, and c are taken across condenser *C* of Fig. 8-3b. They have a constant duration, the time constant of expo-

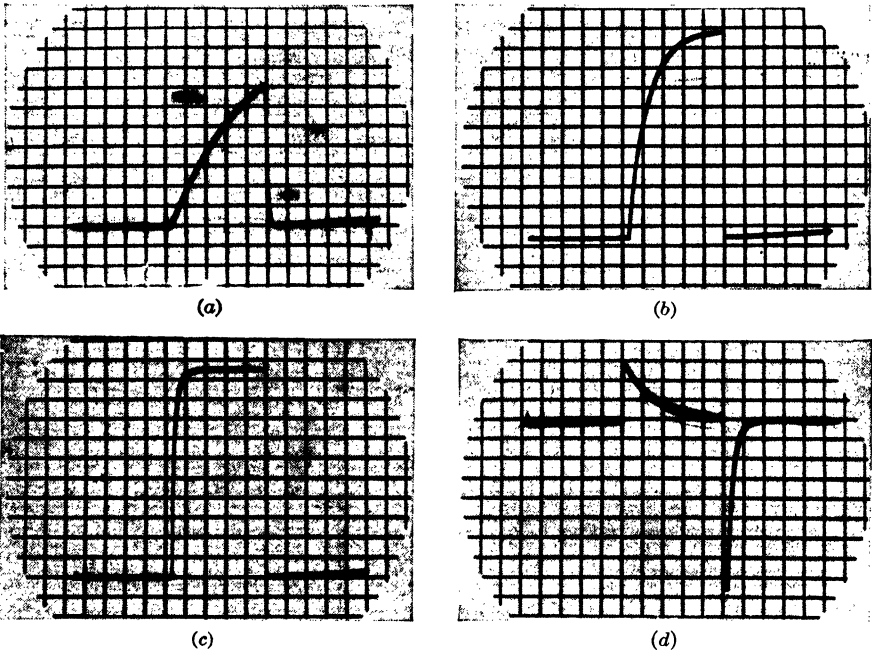


FIG. 8-13.—Exponential waveforms. The durations are fixed and the time constant is varied; (d) is the current waveform corresponding to (b).

ponential rise being varied. The waveform which is the derivative of the waveform of Fig. 8-13b is shown in Fig. 8-13d.

The grid waveforms of multivibrators and blocking oscillators are exponentially shaped. The amplitude is not as well controlled, in general, as for the circuits of Figs. 8-3b and c but can be set by means of diode "catchers."

*General Exponential Generator.*—A more versatile circuit is that of Fig. 8-14. It will be seen that by the choice of  $\mathcal{G}$  the exponent can be made positive. The voltage across the condenser is, ideally,

$$e = \frac{1}{C} \int_0^t \frac{E + e(\mathcal{G} - 1)}{R} dt \quad (2)$$

$$= \frac{E}{1-g} \left(1 - e^{-\frac{t}{RC/(1-g)}}\right) \quad (3)$$

$$= E \left( \frac{t}{RC} - \frac{(1-g)t^2}{2!R^2C^2} + \frac{(1-g)^2}{3!R^3C^3} t^3 + \dots \right). \quad (4)$$

The simple exponential generators may be considered to be circuits for which  $\mathfrak{G}$  equals zero.

The rate of change of  $e$  with time increases with increasing time if  $\mathfrak{G}$  is greater than unity and positive. If  $\mathfrak{G} < +1$ , the rate of change

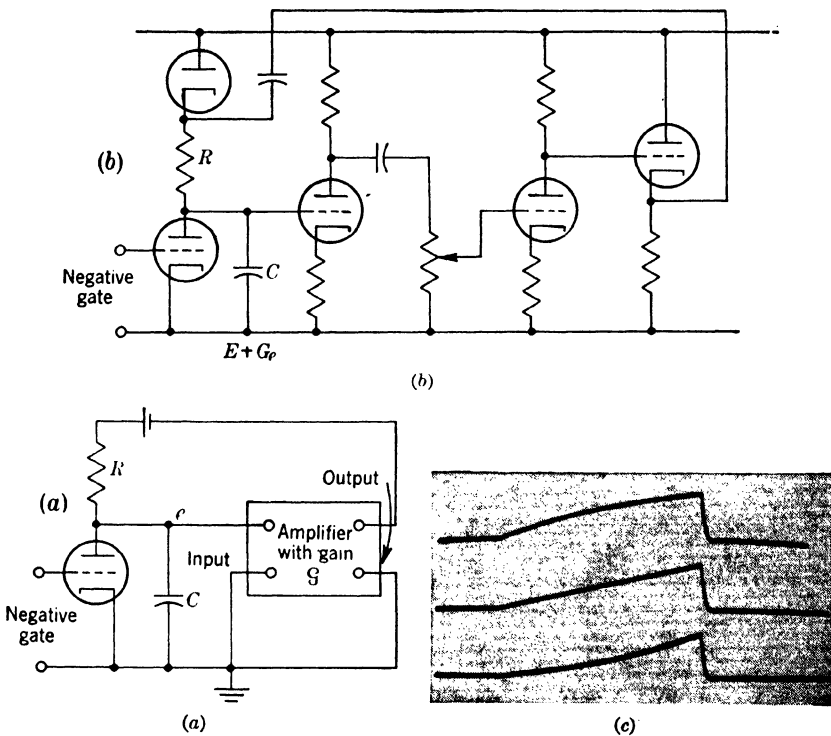


FIG. 8.14.—(a) Generator of exponentials with positive or negative exponents; (b) circuit details; (c) wave forms: Line 1—positive exponent, Line 2—zero exponent, Line 3—negative exponent.

decreases to zero exponentially. If  $+g$  equals unity, the waveform is linear as is indicated by Eq. (4). This case is that of the bootstrap triangle generator, which is discussed in Chap. 7.

The waveform of Fig. 8-14c is generated with the circuit of Fig. 8-14b for which  $\mathfrak{G}$  is approximately 0 for the highest curve, 1 for the center curve, and 2 for the lowest curve. The output swing of the amplifier may be nearly as large as the supply voltage. The stability and linearity of these amplifiers may be increased by local negative feedback.

*Time-measurement Circuit.*—A simple time measurement circuit which uses a cathode-ray tube, an exponential sweep, and an exponentially shaped card potentiometer is shown in Fig. 8-15. An exponential rise occurs across  $C$  and deflects the electron beam. The

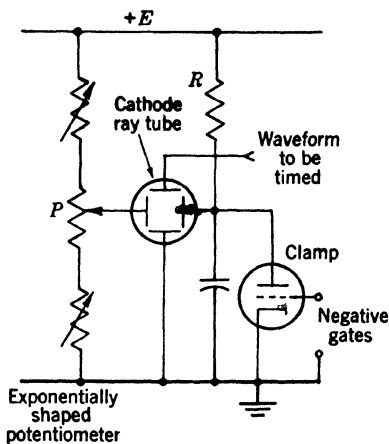


FIG. 8-15.—Exponential time-base generator—use in time measurement.

phenomenon to be timed is caused to deflect the beam vertically when it occurs. The reading of  $P$ , for which the pulse is at an index on the tube, is a measure of the time interval between the start of the exponential and the pulse. In order to correct for the shape of the exponential sweep,  $P$  should be an exponentially shaped potentiometer with a linear scale.

*Time-modulation Circuits.*—A crude form of an exponential-sweep delay circuit is a conventional monostable mult vibrator using a variable capacitor in the time constant. The delay increases with increase in the

time constant, which varies linearly as the capacitor shaft is turned.

Another type of delay circuit uses an exponential potentiometer to provide a voltage for comparison with a sawtooth waveform. A prac-

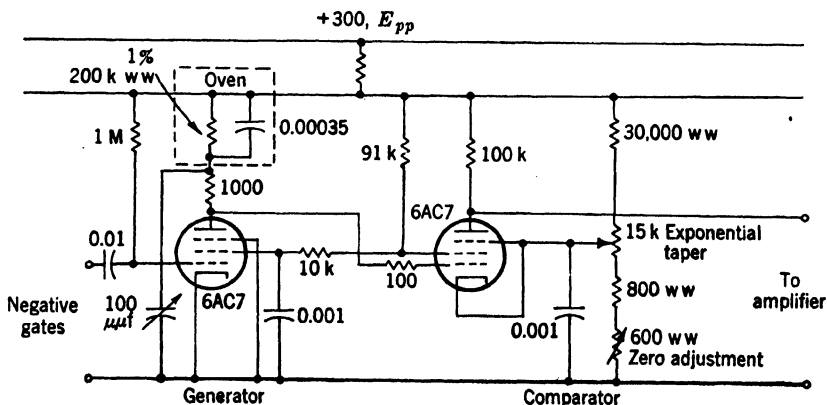


FIG. 8-16.—Exponential sawtooth-waveform generator—use in time modulation.

tical circuit using this scheme is presented in Fig. 8-16. A negative gate is applied to a clamp tube for the duration of the exponential waveform for which the shape is determined by a voltage and a resistance-capacitance combination which is maintained at a constant temperature.

Small adjustments of the capacitance and the starting potential of the wave are provided. The waveform is provided with an initial step to minimize the effects of distributed capacitance at the start.

The exponential waveform is applied to an amplitude selector which utilizes the cutoff characteristic of a pentode. The resultant rise is amplified to form a marker. The circuit provides a maximum delay of 300  $\mu\text{sec}$ . The time constant of the rise is 720  $\mu\text{sec}$ , and a rise of about 94 volts occurs in 300  $\mu\text{sec}$ . The accuracy is limited by the clamp and amplitude selector characteristics, not by the exponential portion of the wave or by the potentiometer.

Means of approximating hyperbolic waves by subtracting several exponentials from a trapezoid are described in Sec. 8-6. The exponentials that are used for the summation are of the transient type, for which  $T$  is negative.

**8-5. Hyperbolas.** *General Considerations.*—The type of hyperbolic voltage waveform to be discussed is shown in Fig. 8-17. The voltage

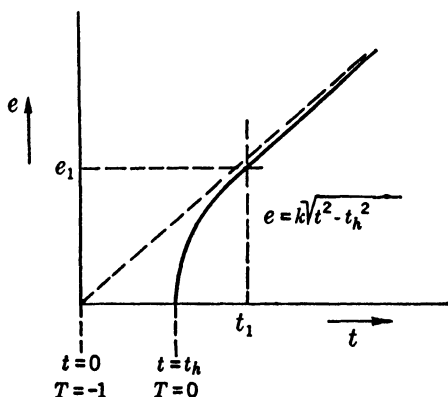


FIG. 8-17.—Hyperbolic voltage waveform.

as a function of time is expressed by the relations

$$\begin{aligned} e &= 0, & t &< t_h \\ e &= k \sqrt{t^2 - t_h^2}, & t &> t_h, \end{aligned} \quad (5)$$

where  $t_h$  is a constant that is equal to the interval between a reference time ( $t = 0$ ) and the time instant at which the hyperbolic portion of the waveform starts.

A common use for such a waveform may be considered as a special case of “triangle solving.” Referring to the right triangle shown in Fig. 8-18,

$$r = \sqrt{s^2 - h^2}. \quad (6)$$

This equation has the same form as Eq. (5). In one of the applications

the parameter  $t_h$  is made proportional to one side of the triangle in question, and the amplitude of a hyperbola like that shown in Fig. 8-17 is determined at a fixed time  $t_1$ , which is made proportional to  $s$ . The amplitude  $e_1$  so measured will be proportional to  $r$ . Alternatively, the time  $t_1$ , at which the amplitude reaches a fixed value  $e_1$ , gives a measure of  $s$ . Another common application of such a hyperbolic waveform is as a time base.

Hyperbolic waveforms for use in radar have been generated in a variety of ways, most of them giving very rough approximations to the ideal hyperbolic waveform. Three methods capable of the greatest

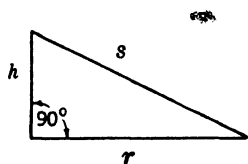


FIG. 8-18.—Triangle for slant-range problem.

accuracy (of the order of  $\frac{1}{10}$  of 1 to 1 per cent) will be discussed here. One method consists of generating the hyperbola by a series of electronic circuits performing the algebraic functions of squaring and square-root extracting as suggested by Eq. (5). The other two methods make use of *RC*-networks which give rise to voltage waveforms approximating the desired hyperbola by giving the

difference between the sum of several exponential waveforms and a trapezoid.

**8-6. Hyperbolic Waveforms by Algebraic Operations; by Charge Compensation.** *Algebraic Operations.*—Equation (7), describes the

$$e = k \sqrt{t^2 - t_h^2}, \quad (7)$$

desired voltage waveform. One method that has been used to generate such a waveform is first to generate a parabolic waveform

$$e_1 = E_1(t^2 - t_h^2), \quad t > t_h, \quad (8)$$

and then, by use of a square-root-extracting circuit, with  $e_1$  as the input, to derive  $e$  of Eq. (7). Chapter 19 is devoted to a discussion of the basic squaring and square-root-extracting circuits; Chap. 18 describes electric integration. This method is difficult and costly (Fig. 8-19).

*Charge-compensation Method.*—Another method for generating a hyperbolic waveform is shown in Fig. 8-20. It consists of a "height-correction" circuit which supplies a nonlinear current to the condenser of a sawtooth waveform generator which adds to the ordinary constant current such that a hyperbolic waveform is obtained. The variation with the parameter  $t_h$  is of such a nature that  $k$  of Eq. (7) does not vary as  $t_h$  does. A detailed description of the operation of the circuit follows.

Tube  $V_1$  is cut off except during the time from 0 to  $t_h$ . It follows that immediately preceding time  $t_0$ , diodes  $V_2$  and  $V_3$  are conducting, and the condensers  $C_2$ ,  $C_3$ ,  $C_4$ , and  $C_5$  are all charged to about 105 volts, the grid of  $V_6$  being at  $-5$  volts. From 0 to  $t_h$ ,  $V_1$  is on and its plate

bottoms; hence, current flows out of the condensers through the 500-K resistor,  $V_2$  being nonconducting. The total charge that flows out during this period is closely proportional to  $t_h$ , since the cathode of  $V_2$  does not depart far from 100 volts. The discharge is proportioned among the condensers in a manner dependent on  $t_h$ ; for small values of  $t_h$  it comes mainly from the short-time-constant arm; for large  $t_h$  mainly from the long-time-constant arm. The time constants given on the diagram have been chosen to suit a range of  $t_h$  from 10 to 60  $\mu\text{sec}$ . At the time  $t_h$ ,  $V_1$  is cut off, and simultaneously the switch  $V_5 + V_4$  is opened to permit the

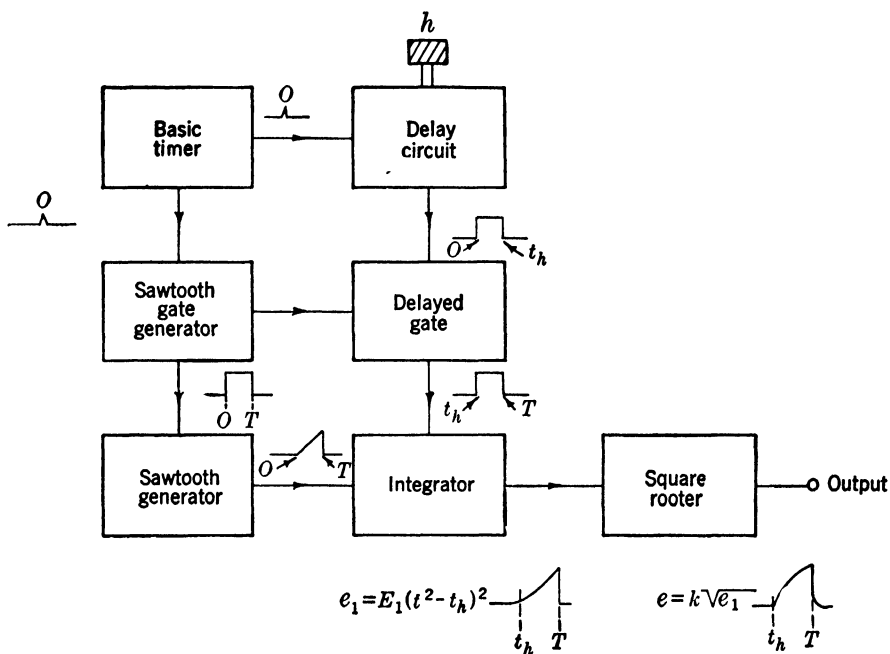


FIG. 8-19.—Hyperbolic waveform by algebraic manipulation.

sweep to start. The pulse generated across the inductance  $L_1$  is maintained at a delay proportional to  $h$  by an external circuit. Through  $V_2$  the network is returned to 100 volts (at cathode of  $V_2$ ), and the charge that left the condensers through the 500-K resistor during the period from zero to  $t_h$  is replaced by charge flowing through  $V_2$  into  $C_1$  by feedback action in  $V_6$ . This charge flows onto  $C_1$  in addition to the charge flowing through  $R_2$  and results in an increased rate of fall of the potential of the plate of  $V_6$ . In other words, the charge lost by the network in the time from 0 to  $t_h$  is effectively transferred to the feedback condenser  $C_1$  during the first part of the hyperbolic portion of the wave. The time scale of the increased rate of change of plate voltage is determined

by  $t_h$  and the network time constants; the total amount is set by  $t_h$  and the 500-K network discharging resistor. The total additional charge to be supplied to  $C_1$  by the network is  $(200 \text{ volts}/1 \text{ megohm}) \cdot t_h$ ; this is the charge lost to  $C_1$  by delaying the start of the time base. If just this amount of charge is replaced, all hyperbolas (i.e., for all  $t_h$ ) will, at large values of time, assume the same value. The charge received by  $C_1$  is the charge lost by the network during the period from 0 to  $t_h$ , which is approximately  $(100 \text{ volts}/0.5 \text{ megohm}) \cdot t_h$ ; the two quantities of charge are equal for any  $t_h$ . In practice, because the value of 100 volts is not

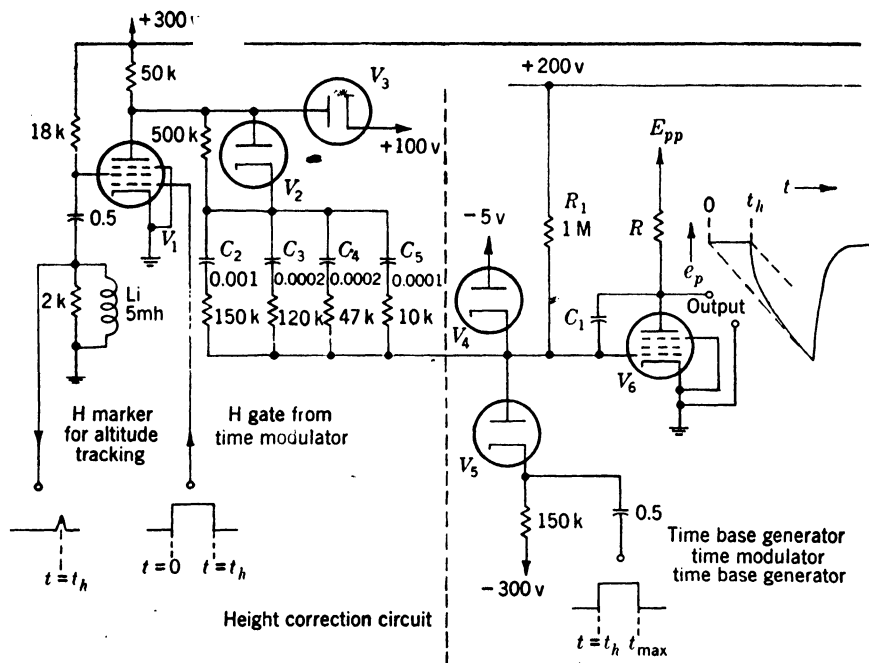


FIG. 8-20.—Hyperbolic waveform by charge compensation.

maintained during the discharge period, it is found necessary to reduce the 500 k to a somewhat lower value.

**8-7. Hyperbolic Waveforms by Summing Exponentials.**—In order to generate the hyperbolic waveform described by Eq. (7) and Fig. 8-17, the trapezoid generator of Sec. 8-3 may serve as the fundamental circuit. The step of the trapezoid is to be “rounded” so as to approximate a hyperbolic wave (Fig. 8-21). The circuit forces a constant current through this network after time  $t_h$ . The voltage across the network rises according to the various time constants involved (an exponential wave is associated with each) and the output waveform is a hyperbola. In the design of these networks, difficulties arise if  $t_h$  must be variable for then the shape must vary. The effect of varying all the resistances is

to change the amplitude of the exponential terms. If

$$T = \frac{t - t_h}{t_h} \quad (9)$$

is substituted in Eq. (7), the desired waveform becomes

$$\begin{aligned} e &= 0, & \text{for } T < 0 \\ &= kt_h \sqrt{T^2 + 2T}, & \text{for } T > 0 \end{aligned} \quad (10)$$

This is a hyperbola with vertex at  $T = 0$ . This waveform can be modified properly for varying  $t_h$  by varying the amplitude and time constant of each exponential term in proportion to  $t_h$ , which is achieved in practice, by varying all the resistances by a  $t_h$  shaft. Instead of starting the current step exactly at  $t = t_h$ , it has been found that fewer  $RC$  sections will serve if the step is started somewhat before  $t_h$ .

The design of the network is the geometrical problem of adding several exponential curves and a linear curve to approximate a hyperbolic curve. This is often done graphically.

When the design of the network in the form shown in Fig. 8-21 has been completed, it can be changed into any equivalent  $RC$ -network demanded by practical considerations such as element size, stray capacitance, etc. The illustrations in Figs. 8-22a and b show several equivalent forms of the networks in question. The figures show the error in fit as a function of ground range for various altitudes. The amount of prestart and maximum sweep speed are given in each case;  $\theta$  is the angle  $OPQ$  in Fig. 8-18. The data are given for  $h$  and  $r$  in feet.<sup>1</sup> These curves indicate the extremes of accuracy that have been used.

**8.8. Parabolas.**—The solid curve in Fig. 8-23 is the type of parabolic waveform we consider. Such a parabola is represented analytically by

$$y = k_1 t^2. \quad (11)$$

A repeated parabolic waveform is shown in Fig. 8-24.

<sup>1</sup> Altitude  $h$  is proportional to  $t_h$  and ground range is proportional to  $e$  in Equation (7).

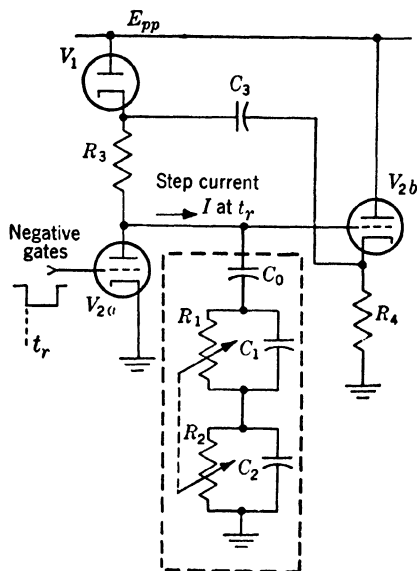


FIG. 8-21.—Hyperbolic waveform by summing a trapezoid and two exponentials.



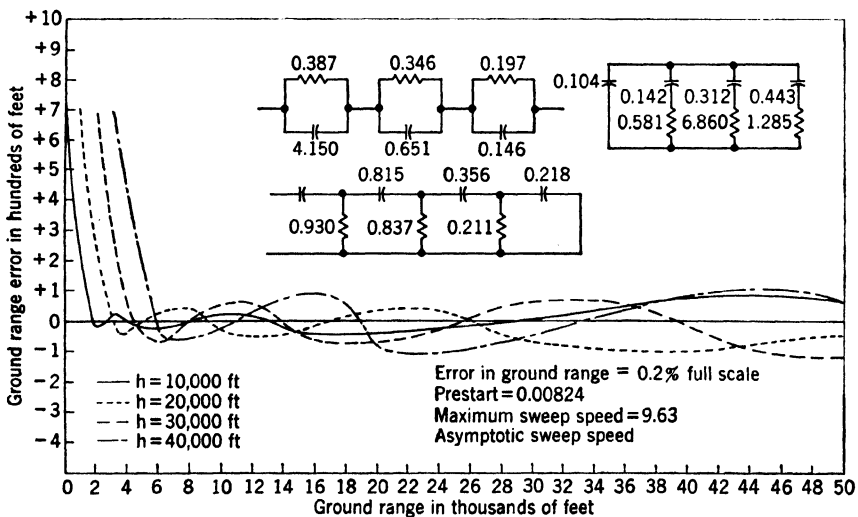
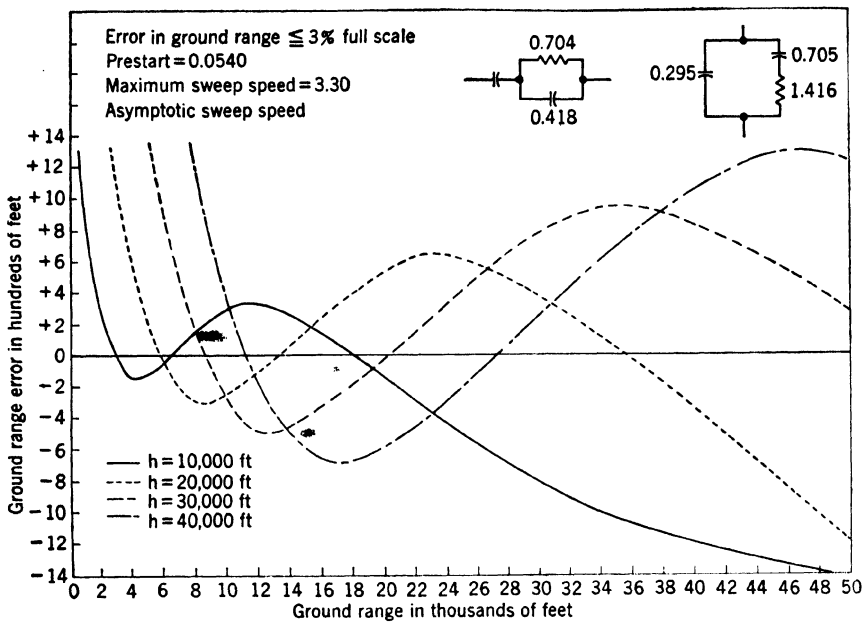


FIG. 8-22.—Error curves for ground-range sweep networks. (2000 yds corresponds to about 12  $\mu\text{sec.}$ )

*Means for Obtaining Parabolic Waveforms.*—The several means of obtaining a parabolic waveform that are described here all involve operations upon a linear waveform. See Chap. 7. The operations that will produce a parabolic segment of waveform from a linear segment are integration, multiplication, and squaring (see Chaps. 18 and 19).

A portion of a triangular waveform can be represented by

$$y = k_2 t. \quad (12)$$

The integral is

$$\int y dt = y_1 = \frac{k_2}{2} t^2 + k_3. \quad (13)$$

The electrical integrator approximates this process to various degrees of precision (see Chap. 18).

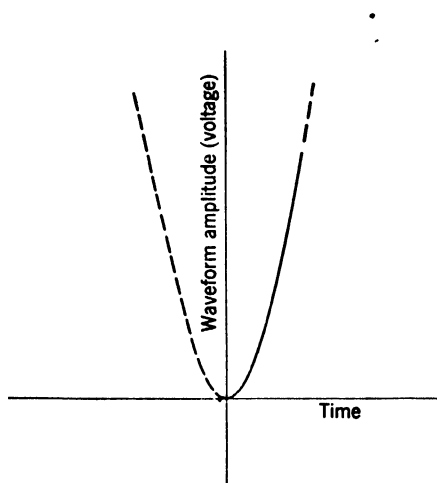


FIG. 8-23.—Useful parabolic segment.

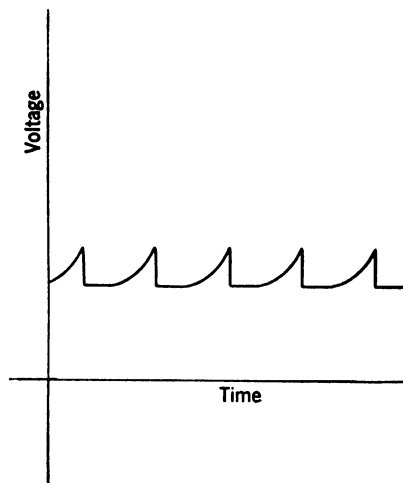


FIG. 8-24.—A "parabolic" waveform.

The simplicity and accuracy of integrating circuits have obviated to some extent the development of parabolic-waveform generators that depend upon squaring processes. Many of the multiplication and squaring circuits of Chap. 19 can be applied as parabola generators. A triangular wave applied at the single input of a squarer or at both inputs of a multiplier produces a parabolic waveform at the output.

Descriptions follow of a bootstrap generator and a Miller integrator-generator.

*Double-bootstrap-integrator Parabola Generator.*—A circuit that has been used considerably for parabola generation is illustrated in Figs. 8-25 and 8-26. The voltage is maintained constant by the bootstrap circuit involving  $CF_1$  and the voltage across the charging resistor  $R_2$  is con-



The switches are opened simultaneously by a gate occurring at  $t = 0$ . The current  $E/R_1$  starts to flow into  $C_1$  and is maintained nearly constant by the feedback through  $C_3$ . The voltage across  $R_2$  is a linearly increasing function of time. Hence the voltage  $e_2$ , which is the integral of the current through  $R_2$  divided by  $C_2$ , is parabolic.

There follows a mathematical analysis, for which the vacuum-tube switches are assumed perfect and the cathode followers have constant gains  $g_1$  and  $g_2$ . The current into  $C_2$  may be represented by

$$i_{e_1} = \frac{g_1(g_2 e_2 + e_1) - e_2}{R_2}, \quad (14)$$

from which follows

$$\frac{de_2}{dt} + \frac{(1 - g_1 g_2)}{R_2 C_2} e_2 - \frac{g_1 e_1}{R_2 C_2} = 0. \quad (15)$$

The current into  $C_1$  may be found from the following relation that sums the voltage drops along its path:

$$g_2 e_2 + e_1 + \frac{de_1}{dt} R_1 C_1 - \frac{C_1}{C_3} \int \frac{de_1}{dt} dt = g_1 (e_1 + g_2 e_2). \quad (16)$$

by rearrangement of these terms and application of the following assumptions at  $t = 0$ ,

$$\begin{aligned} e_1 &= 0 \\ e_2 &= 0 \\ \frac{de_1}{dt} &= \frac{E}{R_1 C_1}, \end{aligned} \quad (17)$$

we derive

$$\frac{de_1}{dt} + \frac{(1 - g + C_1/C_3)}{R_1 C_1} e_1 + \frac{g_2(1 - g_1)}{R_1 C_1} e_2 = \frac{E}{R_1 C_1}. \quad (18)$$

If two solutions in power series are assumed for  $e_1$  and  $e_2$ , together with the initial conditions, and if the coefficients are determined by substituting the assumed solutions in Eqs. (15) and (16) and by equating coefficients of like powers, it is found that

$$g_2 e_2 = g_1 g_2 \frac{E}{R_1 C_1 R_2 C_2} \left[ \frac{t^2}{2!} - \frac{t^3}{3!} \left( \frac{1 - g_1 + C_1/C_3}{R_1 C_1} + \frac{1 - g_1 g_2}{R_2 C_2} \right) \right]. \quad (19)$$

In order to produce the waveform of Eq. (19), the initial current through  $R_2$  must be zero. This would be true only if ideal switches and cathode followers were available. Otherwise a first-power term is added. The coefficient for this term may be calculated from the new initial condition. Any additional first-power term moves the parabola on the time

voltage plane but does not change its shape. Equation (19) becomes the following expression for the circuit of Fig. 8-26:

$$g_2 e_2 = 1.4 \times 10^{+10} (t^2 - 440t^3). \quad (20)$$

The cubic term is about 2 per cent of the square term when

$$t = 50 \mu\text{sec} \left( \frac{t}{R_1 C_1} = \frac{1}{4}, \frac{t}{R_2 C_2} = 1 \right).$$

A reduction of this term by a factor of 10 may be produced by the use of a pentode cathode follower for the feedback.

According to Eq. (20) the parabola from the above circuit will have the proper ordinate to within 0.2 per cent from 0 to 50  $\mu\text{sec}$ . This accuracy is approximately realized although there are sources of error not taken into account by the above analysis. Thus the initial current through  $R_2$  and the nonconstant gain of the cathode follower have not been considered.

The ratio of the amplitude of the linear rise  $e_1$  to that of the parabolic rise  $e_2$  may be adjusted by means of  $R_1 C_1$  and  $R_2 C_2$ . By maintaining fixed the product of the two time constants, the output parabola amplitude is fixed. Higher accuracy results from a small linear sawtooth waveform and a large parabolic sawtooth waveform. The circuit of Fig. 8-26 is not optimal in this respect. The size of the output is limited by the characteristics of cathode followers at allowable supply voltages. The output impedance is a few hundred ohms.

The limiting errors of the circuit may total to several per cent, but by calibration, such as adjustment of the potentiometers of Fig. 8-26, they are reduced to less than  $\frac{1}{2}$  per cent. The sources of error are the same as for the triangle generator, but they are more numerous in this more complicated circuit. An initial delay from the trigger start to the parabola start of the order of 1  $\mu\text{sec}$  is caused primarily by the capacities associated with the switch tubes. The transients that follow the end of the sawtooth waveform should be of negligible amplitude by the beginning of the next sawtooth waveform if repetition frequency sensitivity is to be avoided.

The circuit of Fig. 8-26 was operated as shown to provide the parabola of Fig. 8-27. Figure 8-28 corresponds to a modification of this circuit which provides a nonzero initial current through  $R_2$ . For each waveform, the derivative is shown; it is seen to be nearly linear.

*Double-Miller-integrator Parabola Generator.*—This circuit is shown in Fig. 8-29. It is designed to accept a negative-going sawtooth waveform that can start at any voltage and to produce as output a positive-going parabola. If the input voltage is represented by

$$e = kt, \quad (21)$$

the parabola is, approximately,

$$e = \frac{kt^2}{2RC} \quad (22)$$

To avoid a linear term, no current can be flowing into  $C$  at  $t = 0$ . The diode ensures this condition. The grid-coupling time constant is

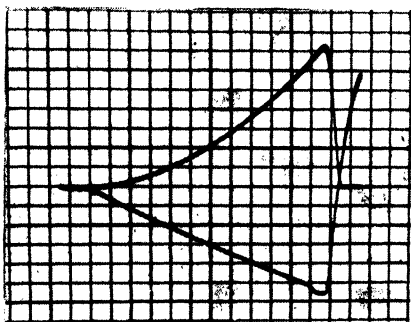


FIG. 8-27.—Parabolic waveform and its derivative. The parabolic waveform was generated by the circuit of Fig. 8-26.

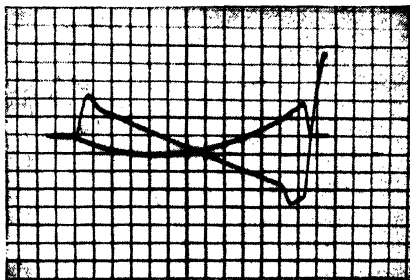


FIG. 8-28.—Parabolic waveform with non-zero initial slope and its derivative.

much larger than  $RC$ . Capacitive coupling is used in order to avoid current through  $R$  at  $t = 0$ , whatever the quiescent voltage at the input. This integrator is capable of very good accuracy, particularly if a pentode is used. In general the Miller circuit is more suitable for accurate parabola generation than is the bootstrap circuit.

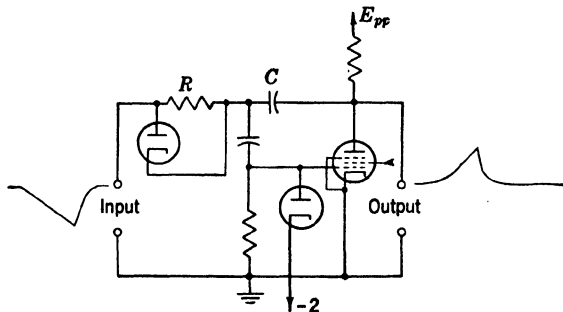


FIG. 8-29.—Miller feedback integrator for converting a linear fall to a parabolic rise.

*Other Methods.*—Another type of integrator that may be used for parabola generation is shown in Fig. 8-30. The current across the cathode resistor of a pentode is varied linearly by applying a linear sawtooth waveform to the grid. The plate current which is nearly proportional to the cathode current is integrated in a condenser, the only element connected to the plate of the tube drawing the sawtooth current.

The changing plate voltage of the pentode has little influence upon the plate current.

The generation of parabolas by multiplication and squaring is developed in Chap. 18, where several complete circuits are given.

**Measurement.**—The exact waveforms resulting from these circuits can be analyzed by the comparison methods described in Chap. 9. This analysis is described in Chap. 20 and is usually required for accuracies of observation better than  $\frac{1}{2}$  per cent.

Another means of examining the waveform is differentiation (see Chap. 20). The derivative of a parabola is a triangle, and a triangle is

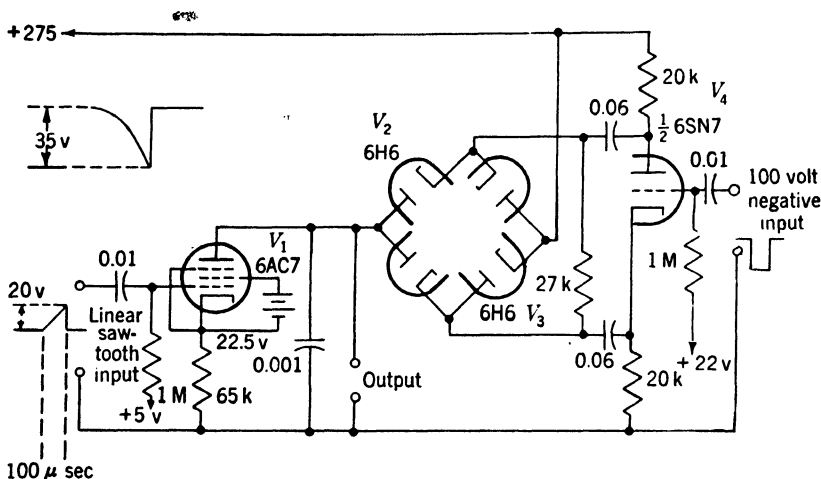


FIG. 8-30.—Constant current pentode integrator for producing a parabolic fall when modulated by a linear rise.

easier to analyze than a parabola. The differentiator that was used for the waveforms of Figs. 8-27 and 8-28 is described in Chap. 18.

**8-9. Higher Powers and Series Approximations.**—One of the simplest means of generating linear and parabolic waveforms is integration. Integration of a constant voltage produces a linearly changing voltage; integration of the linear waveform yields a parabolic wave; another integration leads to the cubic, and the process is limited only by the increase in complexity of the generator. This method produces simple terms of the form  $a_n t^n$  if the constants of integration are adjusted to zero in each integrator. This fact suggests that exceedingly complex waveforms might be synthesized by a summation of terms with integral exponents, since it is well known that a large class of functions can be approximated over a certain interval by a few terms of a power series,

$$y = a_0 + a_1 t + a_2 t^2 + a_3 t^3 + \cdots + a_n t^n. \quad (23)$$

**8-10. The Sums of Sinusoids.**—The conventional approach to analyzing the effect of a network upon a nearly sinusoidal waveform is to consider the waveform as the sum of the fundamental and harmonics. The logical inverse of this problem, the synthesis of a network to produce a given effect upon a waveform or to produce a given waveform can be attacked by the same method, although it is not often profitable to do so.

A wide variety of periodic waves can be represented by Fourier series and often to a useful degree of accuracy by only a few terms. The generation of sinusoids carefully controlled in purity, amplitude, and frequency is a familiar and easily solved engineering problem. From these two facts it might be surmised that the summation of sinusoids to form complex waveforms is common. This is, of course, not the case since simpler means are available for generating most waveforms. The resonant stabilized frequency divider of Sec. 16-12 is one example, however, where a wave is formed by the summation of sine waves. A second example is in the simulation of musical tones by electrical circuits and mechanical transducers.

**8-11. Pulse Shaping.**—It is often convenient for the testing of video amplifiers or indicators to have a video pulse whose shape is like that of a pulse that has passed through a radar receiver consisting of single-tuned stages, staggered pairs, or double-tuned circuits, and it is inconvenient to use a complete receiver for the purpose. A series of *RC*-low-pass sections acting upon a square video pulse distort it so as to give the effect of a set of single-tuned circuits upon the envelope of a square i-f pulse. This effect occurs, however, only if the sections of the *RC*-filter are separated by tubes or otherwise arranged so that each filter section is not affected by currents in following sections. One method of accomplishing this isolation is to increase the *RC*-ratio in each section by a factor of three or more while keeping the *RC*-product the same. Figure 8-31 shows such an arrangement.

The cathode impedance of the first cathode follower is about 130 ohms and, in parallel with the 150-ohm cathode resistor, makes the effective resistance of the first section of the filter 180 ohms, giving the first section a time constant of 0.1  $\mu$ sec. The other sections have an increasingly higher impedance but the same time constant. The last section uses the effective input capacity of the 6SN7 amplifier to give it the same time constant. The second set of filter sections is the same, but the last section has a lower capacity and a higher resistance since the last 6SN7 section is used as a cathode follower and therefore has no Miller effect. The relation for the bandwidth of this filter is the same as for single-tuned-circuit i-f amplifiers if the effect of each section on the preceding one is neglected, namely,



$$\Delta F = \frac{1}{2\pi RC} \quad (24)$$

and

$$\frac{\text{Bandwidth per section}}{\text{Over-all bandwidth}} = 1.2 \sqrt{N},$$

where  $N$  is the number of sections and  $\Delta F$  is the bandwidth per section. For eight sections, as in this circuit,  $\Delta F$  equals 1.6 Mc/sec, and the over-all

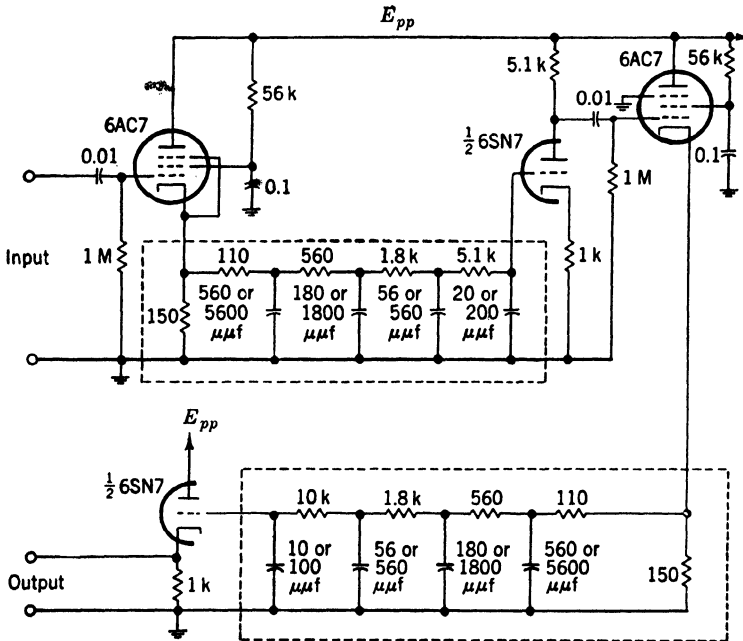


FIG. 8-31.—Filter and amplifier for linear shaping of rectangular waves to simulate output of multistage receiver.

bandwidth equals 0.475 Mc/sec. A similar filter is shown with the same resistors but with the condensers ten times larger.

With the circuit of Fig. 8-31 pulses were passed through the filter with the larger condensers that give a 47-kilocycle bandwidth. The results are shown in Fig. 8-32. An input pulse 10  $\mu$ sec long was used (see Fig. 8-32a). Figure 8-32b shows the output from the circuit. The whole pulse has been delayed nearly 3  $\mu$ sec at its foot, and very rounded corners are evident. If a 1- $\mu$ sec pulse is used (Fig. 8-32c), the output is too small to observe (see Fig. 8-32d). By increasing the input pulse considerably a noticeable output is obtained (see Fig. 8-32e) and it can be seen that although this pulse is delayed about the same amount as the output from the long pulse, its peak occurs much earlier. If a

$\frac{1}{4}$ - $\mu$ sec pulse is used, the output is still smaller, but upon further raising the input-pulse amplitude an output is obtained like that shown in Fig. 8-32*f*. This pulse is very like the one shown in Fig. 8-32*e*. Thus for input pulses of 1  $\mu$ sec or shorter, the output has a constant shape.

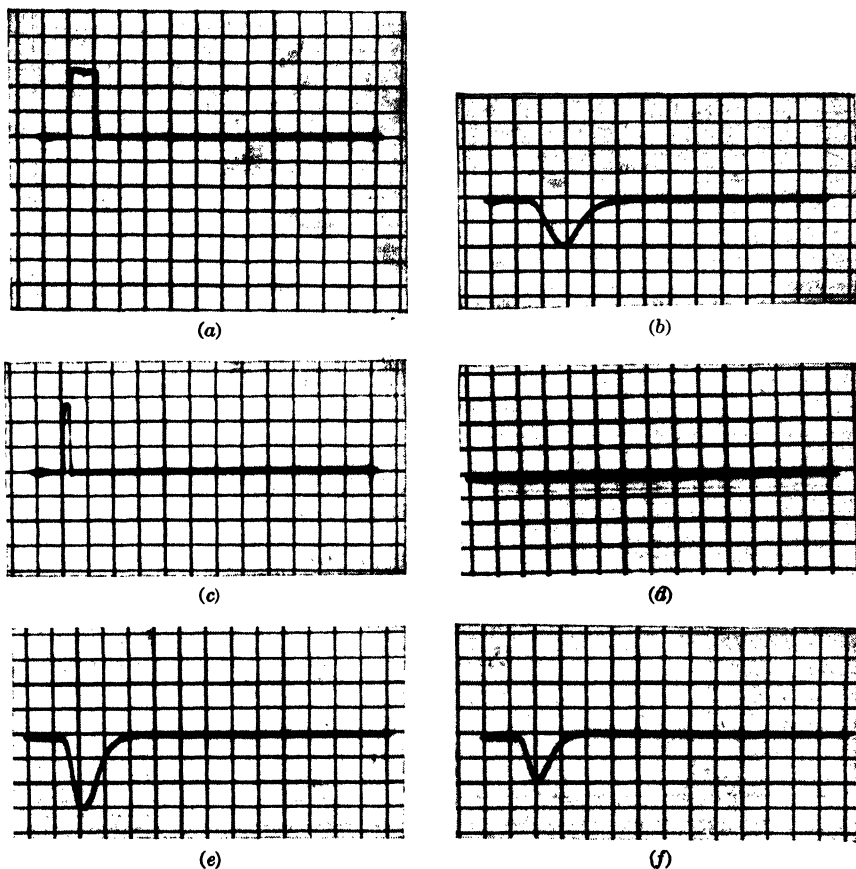
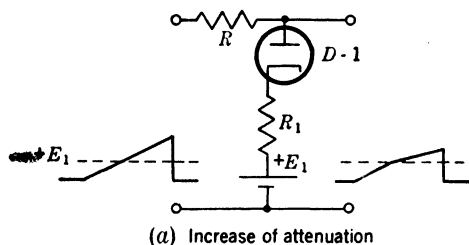


FIG. 8-32.—Filtered square waves.

**8-12. Approximation of Curves by Segments.**—This method may find applications where a wave shape is required which cannot be synthesized by simple operations, such as integration. No experimental tests on the circuits of this section have been made.

*Straight-line Segments.*—Curve-fitting can be done to any desired degree of accuracy by the combination of a sufficient number of straight-line segments. To apply this principle to waveform generation, the simple circuits shown in Fig. 8-33 are used. A linear rise of voltage is applied to the circuit. The output is equal to the input so long as the

diode is effectively an open circuit. When the rise equals the diode bias, the tube becomes a resistance of a few hundred ohms, which may be made effectively a closed switch. The output then rises more slowly than the input (in circuit *a*). The degree of attenuation is set by the ratio  $R_1/(R + R_1)$ . A two-segmented wave is produced with its boundary



As above with  
reversed diode

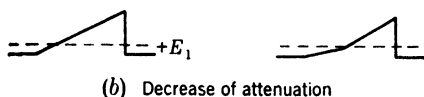


FIG. 8-33.—Two-segment elements.

a voltage set by a supply voltage and the diode broken-line characteristic. In circuit *b*, the diode is conducting at first and becomes nonconducting. Thus, the slope of the output wave can be made to increase or decrease.

Curves whose main trend resembles a straight line may be constructed by this means. As an example, the circuit of Fig. 8-34 is shown.

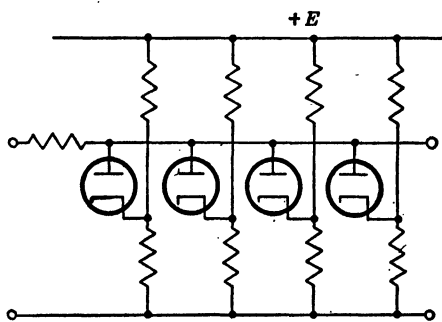


FIG. 8-34.—Circuit for producing a four-segment waveform.

Several branches are successively connected across the output terminals, thus producing an irregular output voltage which may be made to follow a smooth curve rather closely.

*Curved Segments.*—Since many empirical curves can be more closely represented by segments of a parabola or exponential curve than by linear segments, it should

be noted that these curved waveforms may be supplied at the input of the circuit of Fig. 8-33 in place of a linear rise.

**Other Voltage-defined Segments.**—A direct nonlinearity or broken-line characteristic is employed in the preceding examples to vary the attenuation of a waveform. Another way in which the waveform can be altered while its value lies between a pair of boundary voltages is to modify the waveform generator itself. Thus feedback networks within the generator may be disconnected or additional elements may be connected into them. The amplitude-selection process is the basis for this type of segmenting.

**Timed Segments.**—Clearly, the nonlinearities that have been used to produce segments may be operated by gates occurring at fixed instants rather than by fixed voltages. This method was exemplified in the multiple-triangle generators of Sec. 8-2. The circuit of Fig. 8-35 shows a circuit that will provide a large variety of exponential segments with various time constants.

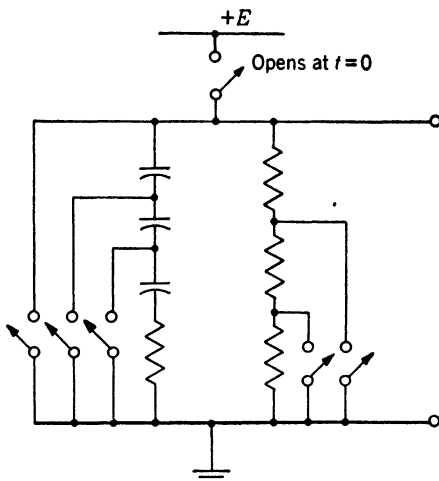


FIG. 8-35.—Circuit for producing timed segments.

## SPECIAL CURRENT WAVEFORMS

### INTRODUCTION

The foregoing material has outlined the methods for generating linear and nonlinear voltage waveforms. In a number of important applications corresponding current waveforms must be reproduced in the magnetic-deflection coil of cathode-ray oscilloscopes, and a number of special techniques for this purpose have been developed. They are treated in detail in Vol. 22, Chaps. 11 and 17, but a few of the basic methods of obtaining linear current waveforms are summarized here.

#### 8-13. Derivation of a Current Waveform from a Voltage Waveform.—

The most common method for obtaining a current waveform is to generate a voltage waveform of the desired shape and then to drive an amplifier whose current output is proportional to the input voltage. A basic circuit for this purpose is illustrated in Fig. 8-36. An approximately linear sawtooth waveform is generated by the switch tube and resistance-capacitance network  $R_1C_1$ . If the cathode resistor  $R_2$  is large enough to give linear operation,<sup>1</sup> amplifier  $V_1$  will give an approximately linear current through  $L_1$  in response to the input voltage.

<sup>1</sup> See Vol. 18 for discussion of the pentode cathode follower.

A practical example is shown in Fig. 8-37. Since the positive pulse applied to the cathode of  $V_1$  is controlled in duration by the signal on the cathode of  $V_1$ , the amplitude of the triangular voltage waveform generated in  $V_1$ ,  $V_8$ , and  $V_9$  is constant. The duration is variable from 60 to 2400  $\mu\text{sec}$ . For triangular waveforms of durations longer than 720  $\mu\text{sec}$ , the gain of amplifier  $V_9$  is made greater than unity to compensate for the poor low-frequency response of  $T_1$ .<sup>1</sup>

The current amplifier consists of tubes  $V_3$  to  $V_8$ , and ensures a linear current waveform in the cathode resistor of  $V_7$  and  $V_8$  and, hence, through the primary of  $T_1$ . The high-frequency response of the amplifier is, however, limited by the resistance-capacitance network in the grid of

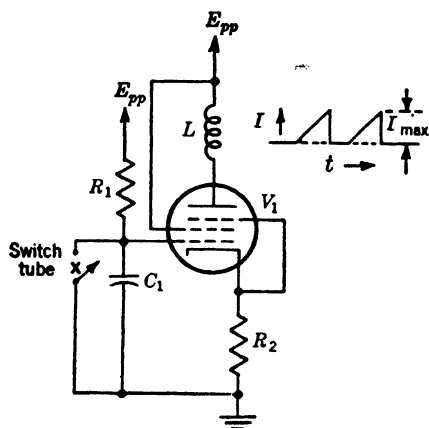


FIG. 8-36.—Simplified current amplifier for a triangular waveform.

$V_4$ . Diode  $V_6$  sets the level of the amplified signal applied to  $V_8$  at a considerably negative potential to ensure that  $V_7$  and  $V_8$  are cut off in the absence of the sawtooth wave. The cathode follower  $V_6$  drives the grids of  $V_7$  and  $V_8$  far enough positive to achieve a reasonably high transconductance. The performance of this circuit is fairly good, and the linearity of the current waveform through a synchro of the Diehl FJE44-1 type is  $\pm 3$  per cent.

#### 8-14. Current-waveform Generators.—

In some circuits the current waveform is directly generated through the inductive load. A few of the important types of current-waveform generators are discussed below.

**Switched Inductance Type.**—Figure 8-38 gives a simplified circuit of a sawtooth-current generator. Initially the plate current is cut off, and, on applying a rectangular waveform to the grid, the plate “bottoms” and considerable screen current is drawn. The plate voltage will increase linearly according to the equation

$$E_{pp} - e_p = L \frac{di}{dt} \quad (25)$$

If the change of  $e_p$  is much less than  $E_{pp}$ , the current is to a first approximation,  $i = (E_{pp}/L)t$ . The inductance  $L$  is usually shunted by a

<sup>1</sup> The frequency response of synchros and other inductive loads is discussed in detail in Vol. 22, Chap. 11 and 17. A complete circuit is shown in Fig. 12-28.



damping resistor to prevent too high voltage at the termination of the rectangular pulse.

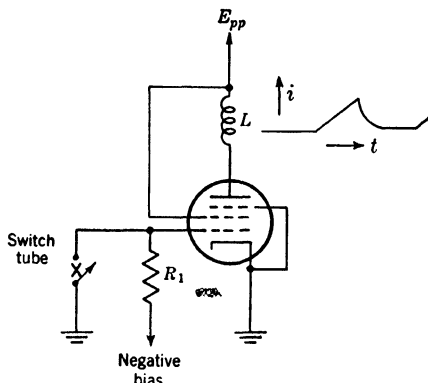


FIG. 8-38.—A simplified triangular current generator.

A practical circuit is shown in Fig. 8-39. The inductance is, however, in the cathode circuit rather than in the plate, and two parallel pentodes are required to supply sufficient current through the inductance  $L$ . A negative rectangle applied to amplifier  $V_1$  gives a very large positive pulse on the negatively biased grids of  $V_2$  and  $V_3$ . The cathode potential of  $V_2$  and  $V_3$  rises rapidly to slightly above the grid potential and then drops slightly as the current

rises through the inductance in a linear fashion. This drop together with any resistive loss in the coil can be compensated by replacing the

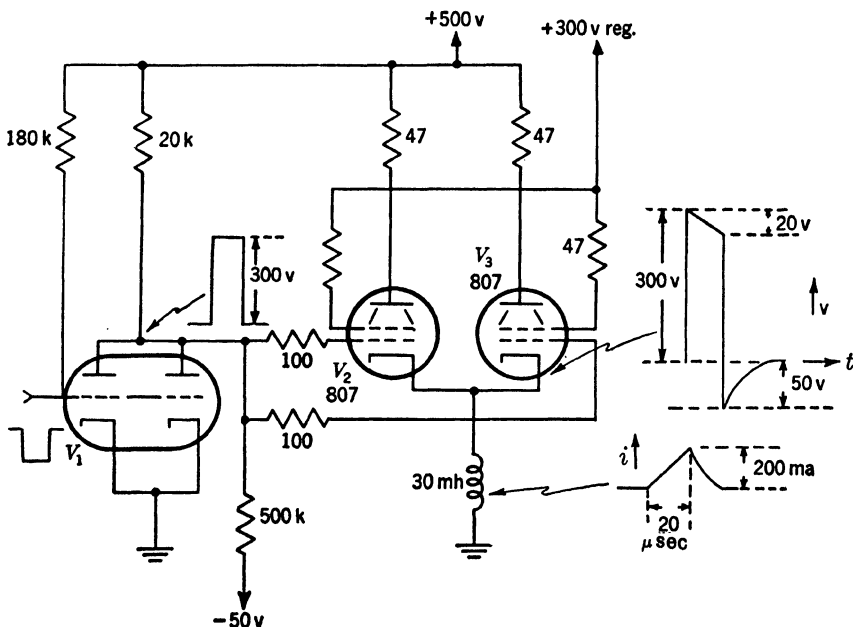


FIG. 8-39.—A practical circuit of the type of Fig. 8-38.

input rectangle by a trapezoid at the grids of  $V_2$  and  $V_3$ . For the particular constants shown, a sawtooth of 20- $\mu$ sec duration and a peak current of 200 ma are obtained.

**Voltage Feedback.**—Instead of current feedback, one may take advantage of voltage feedback for generating a linear current waveform, as indicated in Fig. 8-40. The condition for obtaining a linear sawtooth current wave in  $L$  with a constant input voltage  $e_i$  is

$$\frac{L}{R_L} = R_1 C \frac{R_L g_m + 1}{R_L g_m}; \quad (26)$$

otherwise the sawtooth becomes exponential. Providing the term  $R_L g_m$  is large, the character of the output wave depends little upon  $g_m$ . The principal difficulty is due to stray capacitance (neglected in this equation) which causes a small delay in the initiation of the current wave.<sup>1</sup> The strays have a

minimum effect in this circuit since the tube current is large.

A related circuit is shown in Fig. 8-41 in which the load current  $i_L$  is proportional to the input voltage  $e_i$ . If Eq. (26) is satisfied, then,

$$i_L(t) = a e_i(t), \quad (27)$$

where  $a$  is a constant.

**8-15. Level-setting of Current Waveforms.**—Precise cathode-ray-tube displays, especially those using mechanical grids or overlays, require that the positioning of the cathode-ray-tube display be maintained constant. Therefore, the d-c level of the current waveform must be constant in spite of changes of duty ratio. Also the display pattern must start at the center of the tube (PPI).

Two methods of accomplishing this constancy are possible. First,

d-c restoration may be used. Although this is relatively simple with voltage waveforms, where diode detectors may be used to establish the

<sup>1</sup> A detailed discussion of voltage-feedback amplifiers is given in Chap. 2 of this volume, in Vol. 18, and in Vol. 22. A practical example is given in Fig. 12-26.

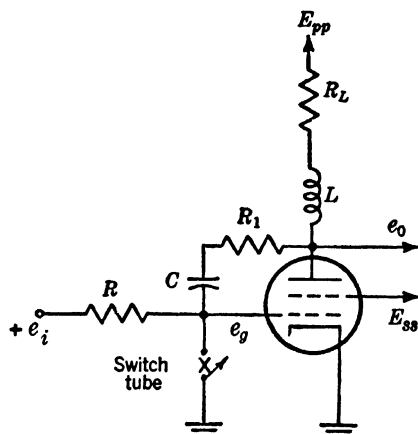


FIG. 8-40.—A triangular-current generator using voltage feedback.

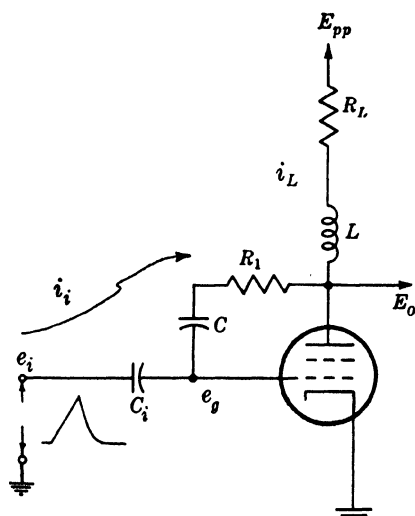


FIG. 8-41.—A variation of Fig. 8-40.



level, it is difficult with low-impedance current waveforms. Impedance changing devices must often be used in the latter case.

Second, a circuit may be employed to initiate the phenomena displayed on the cathode-ray tube at the moment the current wave passes through zero. Shown in Fig. 8-42 are three typical current waveforms which might be used for the display sweep on a CRT. One may have a free choice of the moment at which the waveform to be displayed is initiated, and for these three types of waveforms one may obtain a display that is initiated on the same portion of the cathode-ray tube by starting the unknown event at the moment the rising portion of the

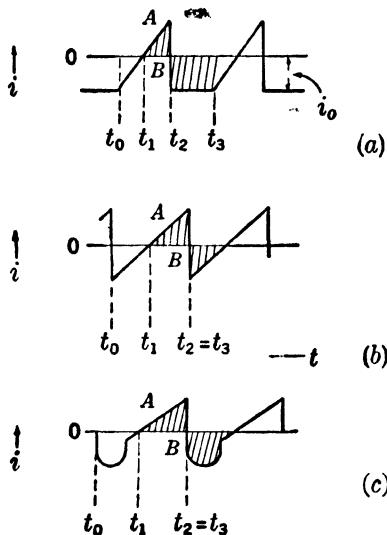


FIG. 8-42.—Various types of current waveforms indicating the area-balancing that may be obtained by initiating the display waveforms at the moment when the current waveform equals zero.

current waveform is equal to zero. This process therefore avoids the necessity for establishing the level of the displayed waveform, and instead at the appropriate time derives the trigger for the phenomenon to be displayed. Amplitude-comparison circuits (see Chap. 9) are specialized for the purpose of accurately defining the moment of equality of two voltages and may therefore be employed here.

This second method has, however, some limitations. The first and most important is that the display circuits must trigger the waveform to be displayed. The second difficulty is indicated in Fig. 8-42b, which shows that the maximum duty ratio is 50 per cent for a sawtooth waveform. A more complicated waveform, as indicated in Fig. 8-42c, will reduce this difficulty. A third objection is the

difficulty of obtaining a voltage waveform of sufficient amplitude from the current waveform to permit accurate amplitude comparison. This requirement is usually avoided by employing a voltage-waveform generator and a linear-current amplifier (Fig. 8-37). If the current waveform is triggered by the same trigger that initiates the waveform to be observed then it is necessary that the area of the recovery portion of the current wave equal that of the useful portion in order that the sweep shall start from the center of the tube. A straightforward method of adding to the triangular current waveform an area which exactly balances the forward portion of the triangle is indicated in the block diagram of Fig. 8-43. This method permits area balancing in spite of changes of amplitude, dura-

tion, or repetition rate of the time base. As, for example, in the circuit of Fig. 8-37, a triangular waveform is generated. The area of the forward portion of the triangle is then measured with an area detector (see Chap.

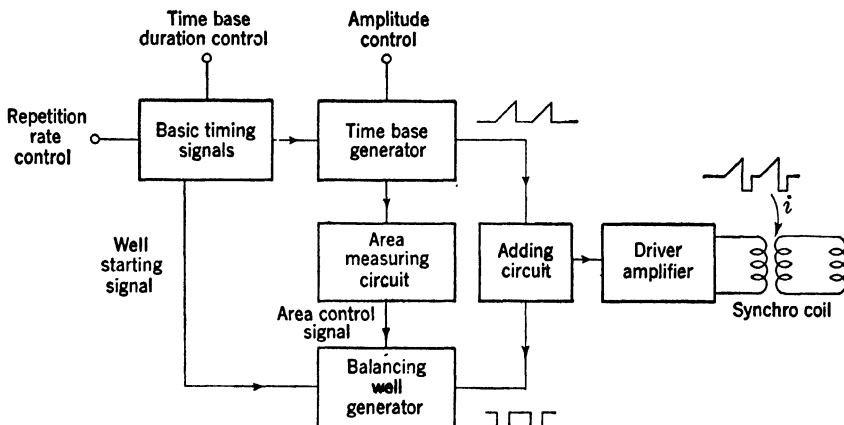


FIG. 8-43.—Block diagram of an area-balanced current-waveform generator.

14). The duration of a negative rectangular wave is controlled in accordance with the output of the area detector and the rectangular waveform added to the triangular waveform. The negative rectangle

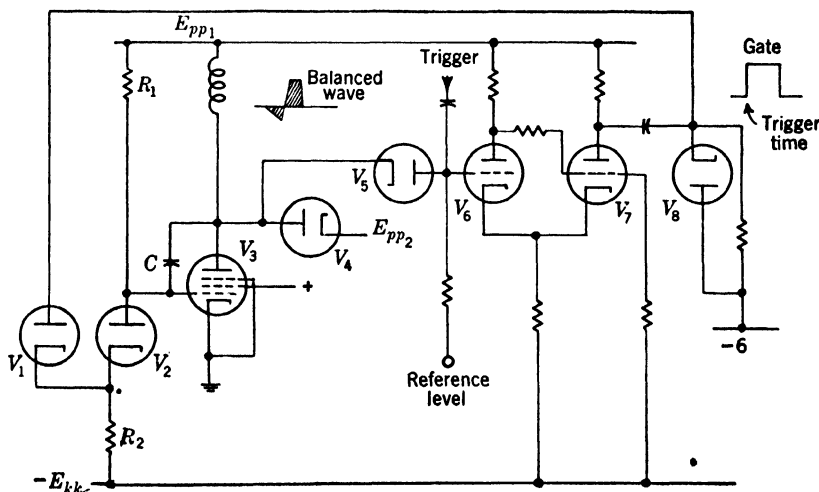


FIG. 8-44.—Circuit involving a Miller integrator for producing a balanced voltage waveform.

is phased appropriately with the triangular wave so as to coincide with its falling edge. A circuit is given in Fig. 12-28.

A Miller integrator with an inductive plate load is a convenient means

for generating an area-balanced voltage wave. Such a circuit is shown in Fig. 8-44 together with circuits for linearizing the flyback, limiting the rise of the pulse at flyback, and gating the Miller integrator. After a trigger is applied, a positive gate appears at the cathodes of diodes  $V_1$  and  $V_2$ . The integrator grid ( $V_3$ ) has been previously held at  $-6$  volts but now starts to rise and the plate runs down linearly at a rate determined by  $R_1$ ,  $C$ , and  $E_{pp1}$ . When diode  $V_5$  conducts, the integrator grid starts to fall since the current through  $R_2$  is larger than that through  $R_1$ . A linear plate rise results which ends only when  $V_4$  conducts. The circuit reverts to its quiescent state as the grid of  $V_3$  falls to  $-6$  volts and the plate voltage returns rapidly to the quiescent level.

Other methods, including automatic ones, of producing area-balanced waves are discussed in Vol. 22, Chap. 17.

## CHAPTER 9

### AMPLITUDE, SELECTION, COMPARISON AND DISCRIMINATION

By R. KELNER, J. W. GRAY, E. F. MACNICHOL, JR.

**9-1. Introduction.**—The processes of amplitude selection and amplitude comparison (see Chap. 3) have been extensively used in many vacuum-tube devices. All relaxation oscillators, for example, contain one or two amplitude comparators. The point of view that leads one to analyze the circuit action in terms of waveform shaping processes also brings about explicit formulation of these processes. Thus, the circuits of this chapter are presented as selectors and comparators although they were developed as components within complex waveform generators.

These processes have another application: the analysis of waveforms requires amplitude-sensitive devices. For many purposes, a waveform may be plotted with sufficient accuracy on the face of a cathode-ray tube (see Chap. 20). Grids and other means of measurement permit some increase in the accuracy of examination. Amplitude comparison, followed by time-interval measurement is considerably more accurate, however, as a method for obtaining the voltage-time curve that defines a waveform.

Amplitude discrimination (see Chap. 3) is similar to the other two processes in its concern with the relative amplitudes of two voltages. The time scale is somewhat different since discriminator input signals vary comparatively slowly and continuous information is required in the output.

**9-2. Amplitude Selection.**—The process of amplitude selection is derived from nonlinear elements. If a waveform and a boundary (reference) voltage are applied to a selector, the output from the selector is usually that portion of the waveform that lies beyond (above or below) the boundary amplitude. The selector may provide amplification or attenuation of the selected wave. The linearity of the selector is generally required to be good. A *quasi-selector* distorts the selected waveform but is suitable for the purpose of amplitude comparison.

The most common selector is the diode-series-resistance circuit that is illustrated in Chap. 3. The importance of the size of the waveform with respect to the voltage region over which the diode characteristic is exponential (a few tenths of a volt) is shown in Fig. 9-1, which consists of two photographs of selected portions of sine waves of different ampli-

tudes. In addition to the greater distortion of the low-amplitude selected wave, the boundary uncertainty caused by drifts in the break of the diode characteristic is a much larger percentage of the maximum amplitude of the smaller wave.

*Applications.*—Selection provides a means for generating waveforms containing segments parallel to the horizontal axis (flat regions), such as trapezoids or square waves. Thus, square waves may be made by selecting the central portion of a sinusoidal wave.

A curved waveform may sometimes be profitably selected from another which has a simpler analytic representation. Thus, a hyperbolic segment correctly shaped for the time base of an interval delayed from  $t_A$  (in an airborne radar) could be selected from the hyperbolic time-base wave that starts at the time of return of the altitude signal

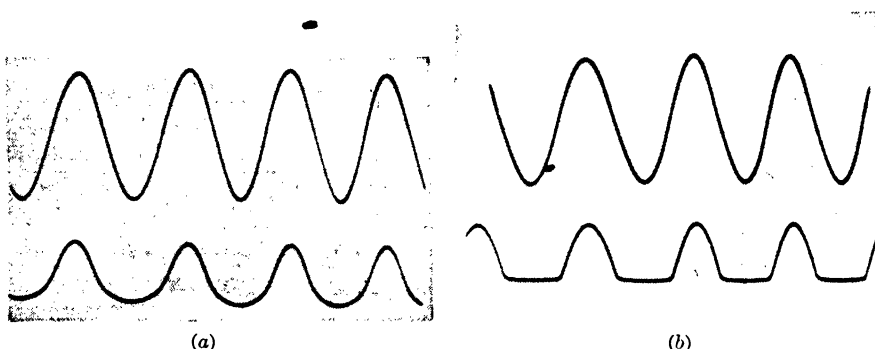


FIG. 9-1.—Effective sharpness of break in a selector (broken-line characteristic) with two sizes of input waveform: (a)  $\frac{1}{2}$  volt rms; (b) 50 volts rms.

(see Sec. 8-5). The selected segment is amplified and applied to the CRT. Figure 9-2 shows the original and selected waveforms.

Modulation of a carrier with an electrical signal may be accomplished by selecting portions of the carrier above, below, or within amplitude bounds set by the signal (see Chap. 11).

Amplitude selection is analogous to time selection on the other waveform axis (Chap. 10). Amplitude comparison may be considered as quasi-selection above or below a reference amplitude followed by distortion of the selected wave into a step or fast pulse.

*Methods.*—The broken-line characteristic is the basis for amplitude selection (see Chap. 3). More generally, any means of instantaneous indication of amplitude correspondence may be used to operate a selector switch. Auxiliary means for linearization, disconnection, or isolation of the selector may be used, but the accuracy of the selection boundary is determined solely by the stability and sharpness of break of the broken-line element.

The characteristics of many nonlinear elements and the factors that

cause them to deviate from the ideal are discussed in Chap. 3. For a diode in addition to the disadvantage of the curvature at the break of the characteristic, the entire characteristic moves along the voltage scale by several tenths of a volt with changes in heater voltage, tube age, and tube sample. A germanium-crystal characteristic breaks somewhat more sharply and has no heater voltage as a source of error, but the effective break moves along the voltage axis with temperature changes. All contact rectifiers are inferior to the diode in back characteristic. Other broken-line elements such as grid-controlled tubes have similar faults. By comparing the approximate magnitude of the curved segment of the characteristic with the maximum waveform amplitude that is usually realizable, the errors of selection may be estimated at  $\frac{1}{1000}$  to  $\frac{1}{200}$  of the

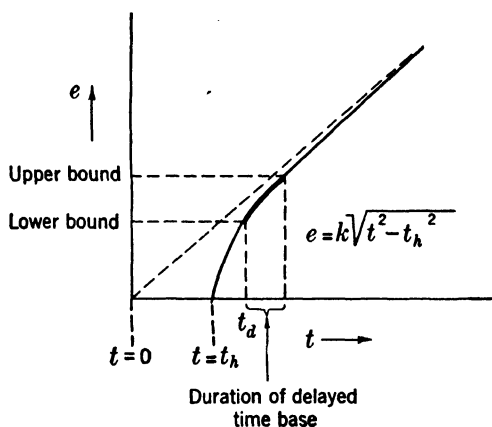


FIG. 9.2.—Selection of a delayed hyperbolic time base.

maximum amplitude. The drift may be considerably reduced by the compensation methods of Sec. 9.6.

The linearity of the selector in regions away from the boundaries is achieved in diode selectors by the addition of a linear series resistance (see Fig. 3.27). For multielectrode elements the nonlinearity is a severe handicap that nullifies in most cases the advantage of amplification within the selection circuit. Negative feedback may be used to linearize the selection at the expense of a loss in gain.

*Other Properties of Selectors.*—The selector may have undesirable effects upon the waveform generator or may provide undesired coupling between the waveform and the output circuit. It is often desirable to minimize such effects by *isolating* the selector from the waveform generator. A cathode follower may be interposed as a buffer stage, but this does not remove stray capacitance coupling (across a diode selector, for example) and introduces drift errors. A pentode selector is excellent in these respects: the input impedance may be very high, and the undesired

capacitance from grid circuit to plate circuit is comparatively low. The germanium crystal is shunted by  $\frac{2}{10}$  to  $\frac{5}{10} \mu\text{mf}$ , a factor of 10 smaller than the diode shunt capacitance. Often the capacitance effect can be balanced out in symmetrical diode circuits or by "neutralization" capacitances.

The impedances that a selector presents to a waveform generator may be different for the selection and the rejection (antiselection) periods; if this is true, capacitance coupling causes rectification. This property is not always objectionable, particularly if the selector impedance is large compared with that of the generator. Very often, the effective impedance of a selector circuit is determined by that of the load. Selectors must not be allowed to distort the waveform at the generator terminals.

The *recovery time* of a selector is always of interest if repetitive waveforms are to be selected. If the time constants associated with the selector circuits are not small compared with the repetition period, the effective boundary voltage will be a function of the repetition frequency. For large time constants, *rectification* may occur with broken-line characteristics. This fact usually precludes capacitance coupling to the selector unless the level of the waveform is reset once per cycle (d-c-restored) on the same side of the capacitor as the nonlinear element. Moreover, rectification does not occur if no current is drawn by the selector as, for example, in selectors using the cutoff characteristic of a grid tube.

The economy of the diode amplitude selectors is an important consideration. The use of diodes for waveform shaping is common throughout this volume. Other elements are relatively more expensive, if only because more electrodes must be biased properly.

**9-3. Diode Selectors.**—A diode selector is described in the previous section to illustrate the importance of a large waveform amplitude in "sharpening" the break in a broken-line characteristic. The shape of the break and the effect of the series resistance in linearizing the transmission segment of the characteristic (a large linear resistance is in series with a small nonlinear resistance) is shown in Sec. 3-14. Other connections of this simple type of selector are possible with which selection above or below a boundary voltage, between or outside of two boundary voltages, and between adjustable limits may be carried out. These circuits present various input and output impedances and voltage levels.

The fundamental idealized circuits are shown in Fig. 9-3. Other possible variations are effected by placing the battery and the source of reference voltage elsewhere in the loop of wave generator, diode, and resistor. These variations, as well as adjustments in the size and polarity of  $E$ , change the level of selection and the level of the output waveform.

The four circuits shown may be subdivided according to whether the output voltage is taken across the diode or the resistor. This classi-

fication corresponds to the shunt and series switches of Chap. 10. The two types have somewhat different properties: the series-switch circuits provide a low series impedance during selection and a very high input impedance during antiselection; the shunt switches give a high series impedance during selection and a comparatively low input impedance during antiselection. For these reasons, the series selectors (c) and (d)

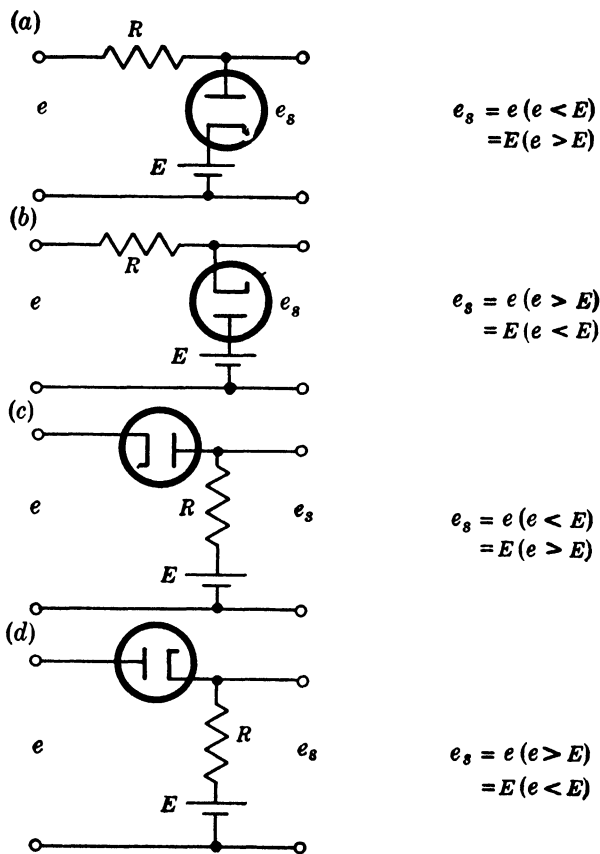


FIG. 9·3.—Fundamental diode selector circuits.

in Fig. 9·3 are commonly used, except in special cases. The series-switch circuits increase the impedance level of the selected signal only by the resistance of a conducting diode. Both the input and output impedances during antiselection are higher than for the corresponding shunt circuits. The series switches have one main fault: the shunt capacitance of the diode provides a transmission path for fast signals during the antiselection time. This undesired signal can be cancelled by such means as are shown in Sec. 9·9 for the quasi-selector circuits used in



comparison. Another consideration, if thermionic diodes are used, is the allowable heater-cathode potential, which must be as large as the waveform amplitude for the series circuits, unless separate filament windings are used. This expedient is not usually necessary since some diodes are designed for 300 volts between heater and cathode.

The ideal circuits require a battery of zero or comparatively low impedance except when the battery and the resistance have a common

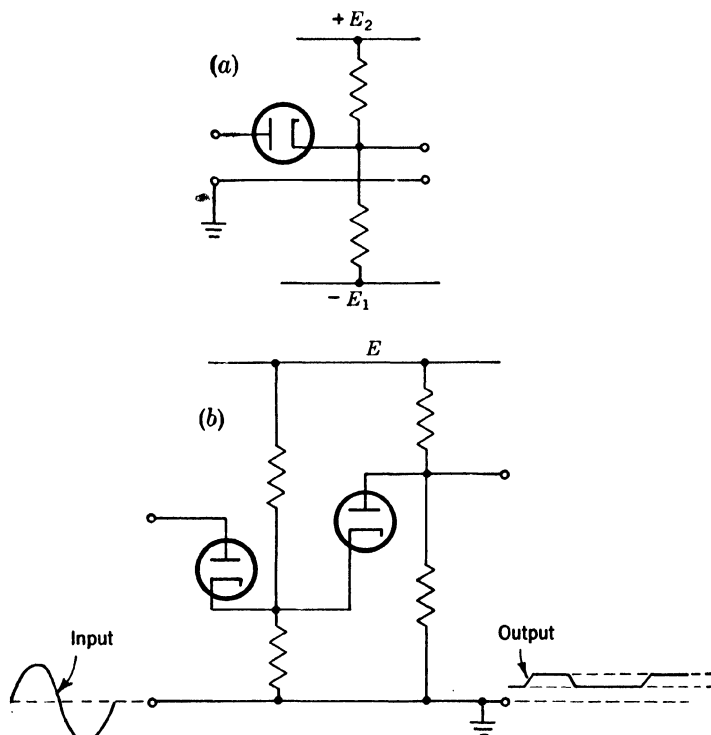


FIG. 9-4.—Practical diode selector circuits. (a) One-bound selector. (b) Two-bound selector. The transfer characteristic for this type of circuit is given in Fig. 3-60.

terminal, since in the latter case,  $R$  can be made up partly of the source impedance of  $E$ . In this case,  $E$  can be obtained from a voltage divider between a supply voltage and ground without drawing excessive current. Thus, the circuit of Fig. 9-4a is an economical practical realization of Fig. 9-3d. The positive or negative supply voltage may be used alone unless the boundary voltage must be adjustable to values above and below ground.

Selection within two boundary voltages may be accomplished by combinations of circuits from Fig. 9-3. A practical circuit combining

Figs. 9-3c and d is shown in Fig. 9-4b. The combination of two shunt switches may be simplified by using a single series resistor and connecting both diodes to the same output point.

**9-4. Germanium-crystal Selectors.**—The contact rectifier may be substituted for the diode as a broken-line element in the circuits of the previous section. The two elements cannot be considered to be interchangeable, however, and fairly severe limitations upon the size of waveform and the impedance of the waveform generator are imposed by the crystal characteristic (see Sec. 3-15). The most suitable contact rectifier is the high-voltage germanium crystal operated at a constant temperature.

For precision selection with crystals the series-switch circuits of Figs. 9-3c and d are preferable to the shunt-switch circuits, as is evident from the previous section, particularly since the capacitance coupling is smaller than for the diode. The back resistance of the crystal may be less than 100 k so that the series resistance  $R$  cannot be made very large, since the transmission during the antiselection time is determined by  $R/(R_{back} + R)$ . If  $R$  must be so small that the break instability becomes intolerable, temperature control may be used, but unit-to-unit variation remains. The maximum back voltage that can be applied is small enough to limit the size of waveform in many cases, and tends to nullify the increased sharpness in crystal break over diode break. The presence of crystal reverse conduction imposes a load upon the waveform generator.

In Sec. 9-19, a special selector using germanium crystals is described. The circuit uses two crystals to limit mutually the applied back voltage, but it is not suitable for the undistorted reproduction of the output waveform. At the present stage of crystal development, the uses of germanium crystals are mostly for quasi-selection where some distortion of the waveform is permissible. In these cases, the economy of the crystals is realized because temperature control is unnecessary.

**9-5. Triode and Pentode Selectors.**—The diode selector is almost universally used for the accurate selection and reproduction of a portion of a waveform. If the wave is to be amplified, however, and if accurate reproduction and boundary setting are of secondary importance, a grid tube is desirable. The various broken-line characteristics that may be achieved with a grid tube are described in Chap. 3. The break instabilities are larger than those of the diode, in general.

**Cathode-follower Circuits.**—A selector that uses the cutoff break of a triode and selects all input voltages above the boundary thus defined is given in Fig. 9-5. This circuit provides a low output impedance for the selected wave and may provide a boundary definition only slightly inferior to that of a diode. At a given plate voltage a high- $\mu$  tube is

better for sharpness of boundary than a low- $\mu$  tube (see Sec. 3-17). The cutoff break in the triode characteristic is not as stable as that for the diode. Hence, this circuit is somewhat less precise than the diode selectors.

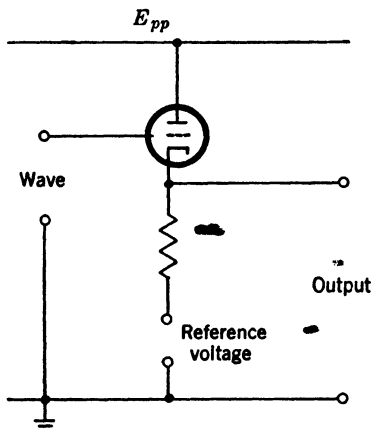


FIG. 9-5.—Cathode-follower selector.

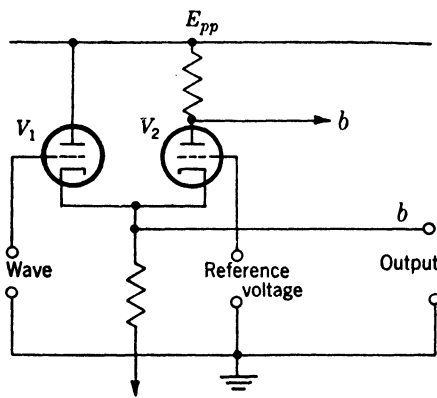


FIG. 9-6.—Double-triode selector.

If the reference voltage is applied to the cathode of the selector tube through a second and identical tube as in Fig. 9-6, the stability of the boundary is increased. For the 6SU7 tube the instability in boundary is smaller than  $\frac{1}{10}$  volt. Unfortunately  $V_2$  acts as a low impedance load (less than 1 k) upon  $V_1$  during the first part of the selected wave; a distorted output waveform is produced until  $V_2$  is cut off.

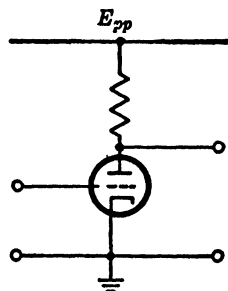


FIG. 9-7.—Triode amplifier selector.

**Amplifier Selectors.**—The plate output of the circuit of Fig. 9-6 provides an amplified selected wave. Another amplifier selector is shown in Fig. 9-7. If a waveform is applied between the grid and cathode, the portion corresponding to the grid base is selected. The lower bound is set by cutoff; no upper bound is present unless the flow of grid current reacts upon the waveform generator. By adding a series-grid resistor, an upper bound is provided, and the circuit selects only those portions of the input wave that lie

within the grid base of the tube. Two circuits and their characteristics are given in Chap. 3, Fig. 3-38.

The use of negative feedback to linearize the transmission segment of an amplifier selector is feasible, but the usual procedure is to use an accurate diode selector and a separate linear amplifier. In many of the applications of these amplifier selectors, wave-shape reproduction is not important.

*Other Selectors from Grid-controlled Tubes.*—Any of the broken-line characteristics from a grid-controlled tube may be used for a more or less precise amplitude selection. For particular applications these may be of interest, but in general the accuracy of selection is inferior to that for the circuits that have been listed here.

**9-6. Compensation of Cathode Drifts.**—The dependence of all of the vacuum-tube selectors upon the heater voltage (the cathode temperature) is sufficiently large so that compensation of this source of error by special circuits is often necessary. A common method is to balance the drifts in one cathode against those of a similar cathode supplied with the same heater voltage. The effects of aging tend also to compensate in such a circuit. The ideal is to use the same cathode for both elements. The 6X5 diode pair have a common cathode, and a few tests have shown that good compensation is achieved. The 6J6 type of construction may be of interest although no data is available.

*Compensating Diode Drifts with a Second Diode.*—Any circuit utilizing this device for increasing accuracy depends upon the attainable similarity between diodes. The uncompensated drift figure, 100 mv for 10 per cent filament-voltage change, can be reduced by a factor of 5 or 10 by using the two diode sections of a single tube. Best results are achieved by the use of a 6SU7, diode-connected.

A circuit for stabilizing a series-switch selector against drifts is shown in Fig. 9-8. In this case the boundary voltage is determined by the combination of three resistors. The analogous circuits for stabilizing shunt-switch selectors are shown in Fig. 9-9. The added circuit in each case is a source of current of the proper polarity to maintain one diode

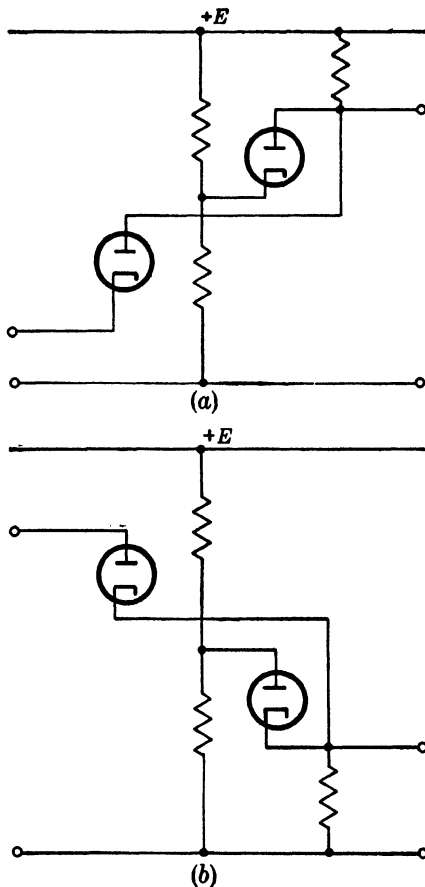


FIG. 9-8.—Stabilization of boundary voltage of a series-switch selector with a second diode.

in conduction at all times. The current should be adjusted to the current of "effective break" in the other diode. The added circuit presents a high impedance during selection.

*Compensation of Triode or Pentode Plate-current Cutoff with a Diode.*—This subject is discussed in Chap. 12, Vol. 18. The circuits used there may be adapted to the corresponding selector circuits. As an example, the means of compensation for the triode selector of Fig. 9-5 is shown in

Fig. 9-10.

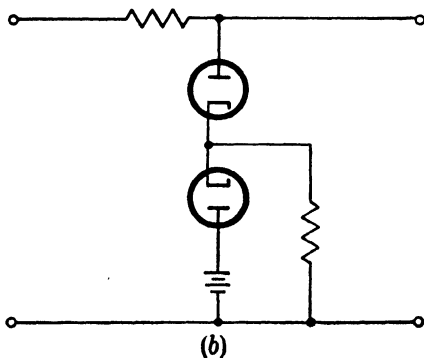
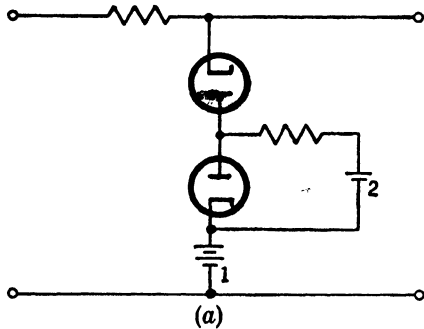


FIG. 9-9.—Stabilization of a shunt-switch selector with a second diode.

*Compensation of Triode Pairs.* This type of selector circuit has other advantages that have been described in Sec. 9-5. The compensation against cathode drifts may be high since identical tubes or sections may be used. Tube selection for symmetry may be desirable if extreme accuracy is necessary. The effect of this type of stabilization is only to remove drifts from the effective boundary at the input waveform. The drifts are still effective in changing the d-c level of the output selected wave.

**9-7. Quasi Selectors.**—The amplitude selectors that are described in the preceding sections deliver a portion of the input waveform in the ideal case. The output wave is composed of segments of constant voltage during the rejection times and a segment corresponding to the portion of the input waveform that is selected.

Ideally, the break between these two segments of the waveform is abrupt; there is a discontinuity in slope. Actually, the sharpness of break is limited by that of the nonlinear characteristic, as has been shown.

The abrupt rise of the selected portion of the waveform identifies a time instant with some precision so a selected waveform may be used as a marker or a trigger. The initial rise is the only part of the selected waveform which is of interest in such cases and the major part of the selected wave need not follow the input wave. A high value of volts/ $\mu$ sec at a time corresponding to the instant when the waveform reaches the

reference voltage is the requirement of an amplitude comparator. Hence some circuits, often called "quasi selectors," which are inferior selectors because they reproduce the input waveform only approximately, are of interest as elements in comparator circuits.

Quasi selection can be accomplished by any element with a broken-line characteristic. The characteristic property of quasi-selection circuits is the comparative unimportance of the transmission segment as compared with the sharpness and stability of the break. The quasi selector often involves an amplifier.

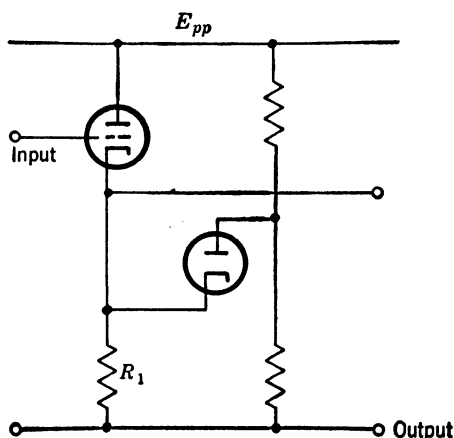


FIG. 9-10.—Stabilization of a cathode-follower selector.  $R_1$  is important in determining the boundary voltage and acts as cathode resistor for the cathode follower.

**9-8. Amplitude Comparison.**—The process of amplitude comparison is accomplished by quasi selection and amplification. By amplification the initial rate of change of the selected wave is to be made as large as the timing accuracy requires. Rises with a total duration of  $0.005 \mu\text{sec}$  have been used.

The mechanism of comparators is simple if an ideal selector is postulated. The selected waveform, which starts at a perfectly defined time instant, is amplified in a linear device (Fig. 9-11a). In practice, the exponentially curved break in most selector elements makes the "instant" of output rise *dependent upon the amplifier gain* (Fig. 9-11b). The marker time is defined here as the instant at which the amplifier output rises to a fixed voltage.

**9-9. Amplifiers for Comparators.**—The broken-line characteristic that is essential for amplitude comparison may exhibit a gain during the transmission segment. Diode circuits provide no gain, and many elements provide insufficient gain for a marker so that auxiliary amplification is necessary.

The comparator may profitably be regarded as a quasi selector and

an amplifier even when these functions are provided by a single element such as a gas-filled triode (see Chap. 3). The amplifier is a "rise-rate amplifier" and often a pulse former. The most economical rise-rate amplifiers use regenerative feedback to obtain very high gains, which are limited by the stray reactances present rather than by the amplification factor of the tubes. Regeneration may be used in any stage of the amplifier, in the entire amplifier, or around the entire loop of amplifier

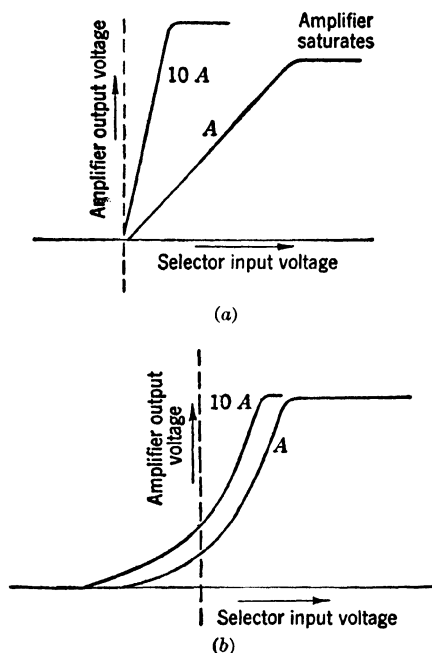


FIG. 9-11.—Effect of linear amplification upon selector output. (a) With ideal selector. The output waveform approaches a step function as amplification is increased. The discontinuity occurs at a well-defined value of input voltage, the voltage at which the ideal selector "switch" closes. (b) With diode selector. The effective boundary voltage varies with amplification.

and selector. The requirement for an output pulse rather than a step often makes it convenient to use a blocking oscillator as a regenerative output stage. Each intermediate amplifier stage should be operated within the high- $g_m$  region near zero bias. The gain of these stages must be sufficient to ensure stable triggering of a blocking oscillator.

The differentiation or quasi differentiation of a selected wave may be used for wave shaping. A pulse may be formed from a step by this means. An  $RC$ -network or a pulse transformer may be used to accomplish quasi differentiation. The pulse transformers are convenient since they provide for level changing and impedance changing and may be

used as inverters so that each stage operates in a phase that may be determined by other considerations. The polarity of output or of feedback is also conveniently controllable with pulse transformers.

An example of a rise-rate amplifier is given in Fig. 9-12. The input waveform is a negative gate which cuts off  $V_1$ . The end of the gate turns this tube on, and a negative signal appears at the plate. This is quasi-differentiated and inverted by the pulse transformer and used to fire the blocking oscillator,  $V_2$ . The first section of  $V_2$  is used to amplify the trigger further and to apply it to the plate of the blocking-oscillator tube. The positive-pulse output is about 20 volts in amplitude but may be increased somewhat by increasing resistor  $R_1$ . The pulse rises 20 to 40

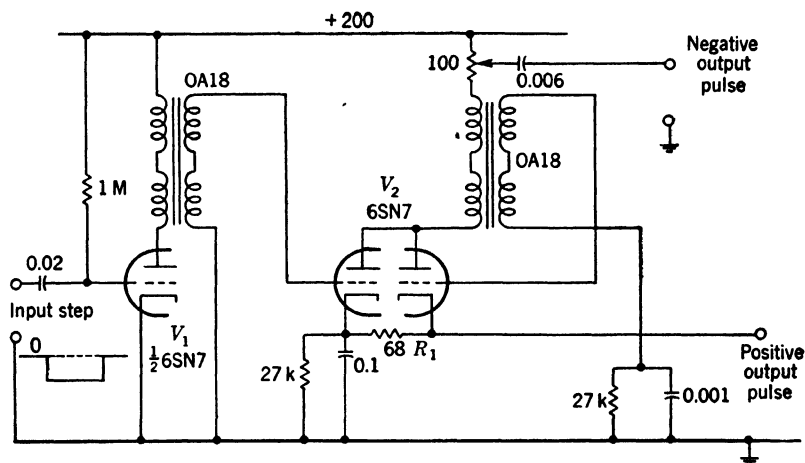


FIG. 9-12.—Rise-rate amplifier. A quasi-differentiating amplifier plus a blocking oscillator.

volts in a few tenths of a microsecond. The circuit is a special design for firing the blocking oscillator at the rising portion of a negative rectangular wave. A grid return to a voltage near the center of the grid base would make the circuit responsive to a positive-going selected waveform preceded by a constant voltage.

It is sometimes necessary to compensate the effect of capacitance shunted across the selector. This may be done by a "neutralization" capacitance connected from the waveform generator to the amplifier at such points that the neutralization signal and the undesired signal are of opposite polarity. An example of this device is shown in Fig. 9-13. The input waveform is a trapezoid. The output of the diode-selector circuit is a selected upper portion of the trapezoid plus a component contributed by the capacitance across the diode. This is canceled in the grid circuit of the second stage by the adjustable capacitor coupling to the waveform



generator. The waveform generator must have a sufficiently low output impedance so that the additional capacitance produces no distortion. The capacitor  $C$  is chosen to minimize the undesired output signal.

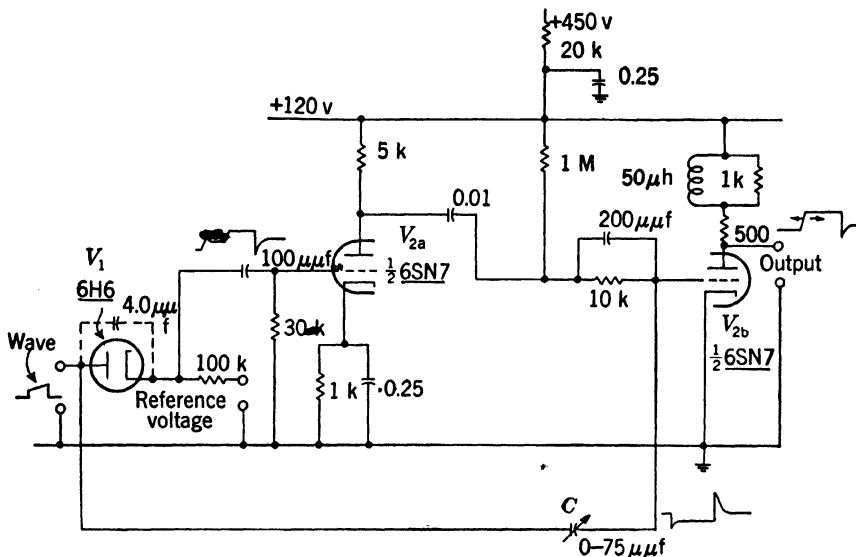


FIG. 9-13.—Comparator with neutralization of the effect of the capacitance shunting the diode selector.

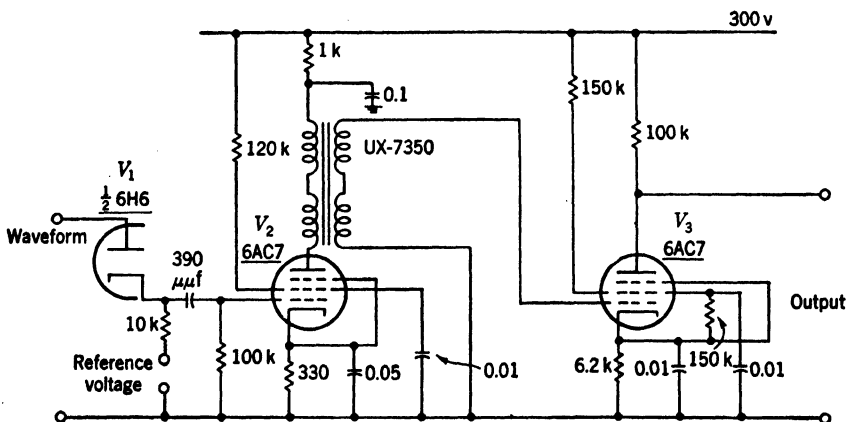


FIG. 9-14.—Simple diode comparator.

**9-10. Simple Diode Comparator.**—The example of Fig. 9-14 is a representative application of diodes in amplitude comparison. The amplifier illustrates the use of pulse transformers for coupling elements.

The diode selects a portion of a triangle above a reference voltage, and the selected wave is amplified and shaped to form a trigger. The

triangle input waveform rises 150 volts in 300  $\mu\text{sec}$ . A pulse is obtained which rises 100 volts in 1 or 2  $\mu\text{sec}$  depending upon stray capacitances. The delay through the amplifiers is less than a microsecond. The accuracy of comparison depends primarily upon the definition of conduction of the diode. In order to compensate for the diode drifts, a second diode may be added (see Sec. 9-6).

An attenuated portion of the triangle appears at the cathode of the diode. This positive signal is quasi-differentiated in the grid circuit of the first tube and again by the transformer at the plate. The second stage is cut off by the screen-divider current through the cathode resistor. Thus, it does not respond to negative signals and amplifies only the trigger corresponding to the time of conduction of the diode.<sup>1</sup> The transformer is connected to invert the polarity of this trigger so that it is positive at the grid of  $V_2$ . A sharp negative drop at the plate of  $V_2$  is followed by a somewhat slower rise.

### 9-11. Grid-controlled Comparators.

The grid-tube elements that are described in Chap. 3 are suitable for both quasi selection and amplification within a single unit. Their chief disadvantages as comparators using cutoff are the loss of sharpness and stability in the break of their characteristics compared with that for a diode, and the difficulties in operating the cathode at a variable potential with respect to plate or screen, since these relative potentials determine  $E_{g1,k}$  at cutoff.

In Fig. 9-15 a single triode is ordinarily held cut off by the difference voltage between the wave and the reference potential. The waveform raises the grid until the tube conducts. Further rise of the grid will finally cause grid conduction. The diode d-c restorer is included to reset the level of the wave during recovery. The negative-output signal is amplified and shaped to form a marker. The circuit will operate only for the positive-going portions of a waveform.

If a falling waveform is to be compared with a reference, their differ-

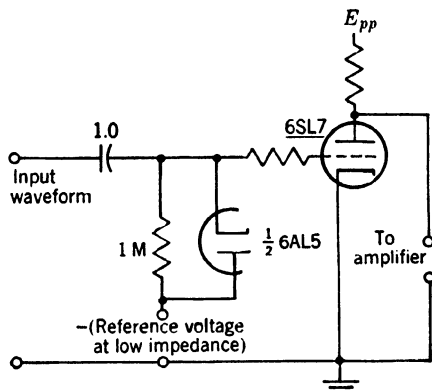


FIG. 9-15.—Simple triode selector for comparison. Plate-current cutoff provides the nonlinearity or comparator point.

<sup>1</sup> In general, maintaining a stage of amplification beyond cutoff is bad practice since it introduces a small delay in the amplifier. The need for this quasi selection may be eliminated by the capacitance-balancing circuit described in the preceding section.

ence can be applied to the cathode of the tube. With this connection, the input waveform may be distorted by the plate current which flows after the comparison. It is also possible to apply a falling signal to the cathode and the reference voltage to the grid. If the reference voltage is applied to the cathode or to the grid, the effect of the varying plate-cathode voltage upon the cutoff point may be appreciable.

Comparators (or at least their selector component) are similar to direct-coupled amplifiers. One problem of direct-coupled difference-amplifier design is the rejection of common-mode signals. In the immediately preceding example (Fig. 9-15) this was accomplished by applying the reference and the waveform voltages to the same electrode,

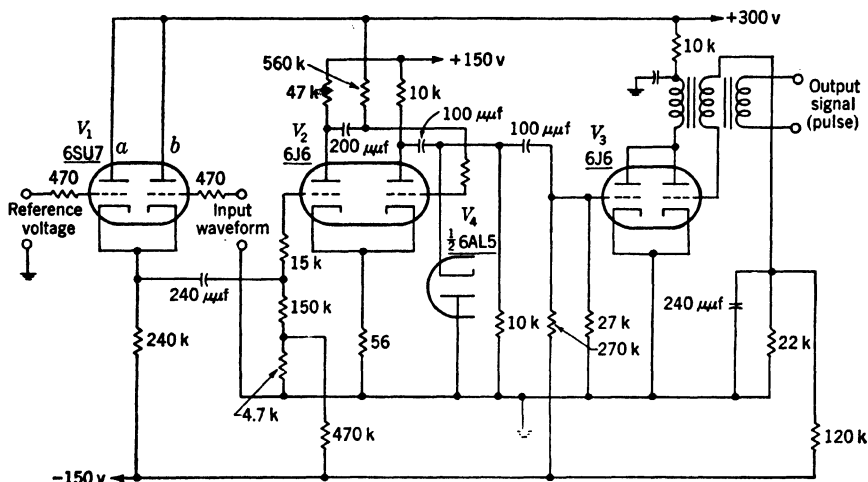


FIG. 9-16.—Double-triode comparator.

thereby eliminating the common-mode signal.<sup>1</sup> However the superposition of the waveform on a level equal to the negative of the reference voltage is not always convenient.

The double-triode circuit of Fig. 9-16 rejects common-mode signals in another way. This selector is discussed in Sec. 9-5. The cathode signal here is applied to a two-stage amplifier with some regeneration through the cathode resistor. A rapid rise from this 6J6 is differentiated, its negative overshoot is eliminated by  $V_4$  and the rise is used to trigger a blocking oscillator. The wave that was applied to this circuit was a triangle which rose 120 volts in 350  $\mu$ sec. The rise of the blocking-oscillator pulse is about one thousand times faster. The circuit might require some additional gain if a slower waveform were used. This comparator is used in a time modulator described in Sec. 5-4, Vol. 20.

<sup>1</sup> See Vol. 18, Chap. 12.

**9-12. Multivibrator Comparators.**—The monostable or bistable multivibrator may be used as a comparator. In most multivibrators, regeneration is initiated when a rising grid reaches a grid base. An example is shown in Fig. 9-17. Tube  $V_1$  is ordinarily conducting, and acts as a cathode follower for the input waveform. Tube  $V_2$  is cut off by the high cathode potential. As the waveform falls, the cathode of  $V_2$  falls, and  $V_2$  eventually starts to conduct when the grid of  $V_1$  is slightly above that of  $V_2$ . Conduction in  $V_2$  completes a positive-feedback circuit from plate to cathode of  $V_1$  with  $V_2$  acting as a cathode follower. A regenerative action rapidly turns  $V_1$  off and  $V_2$  on. The rapid rise of plate current in  $V_2$  is quasi-differentiated by the plate inductance, across which the output

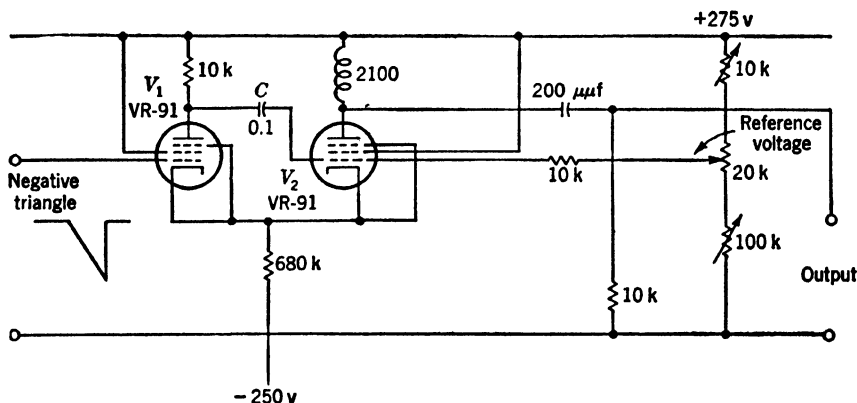


FIG. 9-17.—Monostable multivibrator comparator. Often called “long-tailed pair.” The VR91 is a British pentode resembling the 6AC7.

is taken. The reference voltage may be obtained at a potentiometer and applied to the grid of  $V_2$ . No voltage appears across the 10 k resistor before the regeneration starts. The portion of the waveform that appears on the plate of  $V_1$  slightly modifies the effective reference voltage.

The circuit is fairly accurate since the effects of filament-voltage variation from the two tubes and other drifts tend to cancel. The proportion of the total supply voltage through which the reference voltage can be varied is somewhat limited. In some cases, the subtraction of some portion of the reference voltage from the waveform may be used to remove this limitation. The feedback during regeneration is more effective if a very high cathode resistance and a negative-supply voltage are used. Since a high variational resistance is required, a triode with cathode degeneration is sometimes used in place of a cathode resistor. The common-cathode circuit is particularly advantageous because of the drift cancellation.

Multivibrator circuits with other feedback connections are inherently

less accurate but could be used in special cases. The difference between the wave and the reference can be applied to any two electrodes that provide sufficient control of the loop gain. Ordinarily these are the first control grid and cathode, but the second control grid in a multigrid tube could be used.

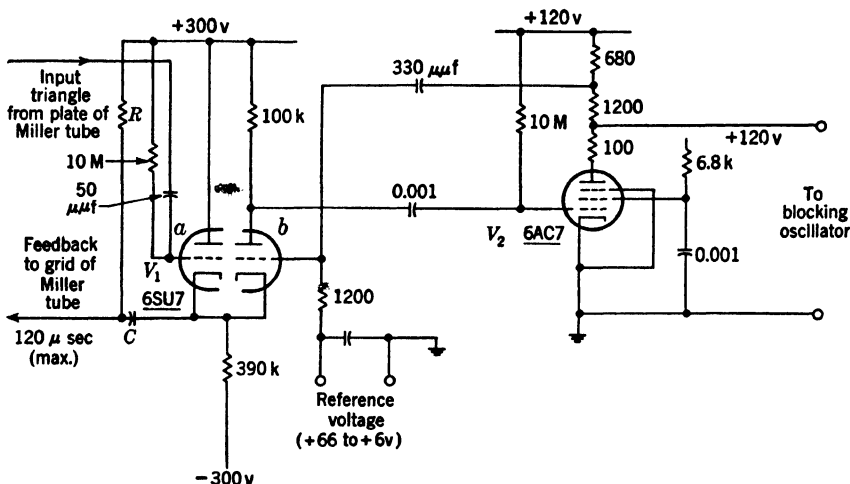


FIG. 9-18.—Double-triode multivibrator comparator with additional gain in the regenerative loop.

A variation of the above circuit involving a pair of triodes in a single envelope, chosen for balance, is shown in Fig. 9-18. It gives high accuracy. This circuit includes part of the waveform generator. The cathode follower  $V_{1a}$  applies a negative-going triangle to the cathode of  $V_{1b}$ . The grid of  $V_{1b}$  is held at the reference potential. When the cathode of  $V_{1b}$  reaches the reference voltage plus the cutoff voltage of the tube, conduction starts. The action is speeded up by the amplifier  $V_2$ , which amplifies the fall at the plate of  $V_{1b}$  and produces its positive derivative at the grid of  $V_{1b}$ . When the common cathode rises, the grid of  $V_{1a}$  falls rapidly. The turn-on of  $V_{1b}$  occurs in about  $\frac{1}{10}$

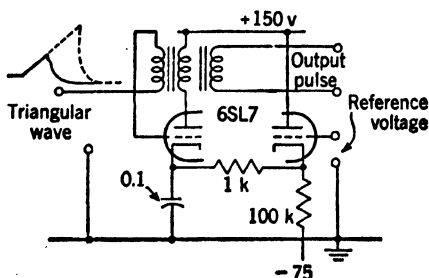


FIG. 9-19.—Blocking-oscillator comparator.

$\mu\text{sec}$ . The output signal at  $V_2$  is a step that is used to trigger a blocking-oscillator pulse generator.

**9-13. Blocking-oscillator Comparator.**—If a blocking oscillator such as is described in Sec. 6-1 is maintained in a nonoscillatory state by a negative grid bias and a positive-going wave is superimposed upon this

voltage, the circuit will fire when the tube starts to conduct plate current. A practical example is shown in Fig. 9-19. The triangle rises 50 volts in approximately 30  $\mu\text{sec}$ . Variations of the heater voltage by  $\pm 0.2$  volt and of the B-supply voltage by  $\pm 1$  volt resulted in less than  $\pm 0.15\text{-}\mu\text{sec}$  change in the timing of the output pulse. The reaction of the comparator resets the waveform generator.

**9-14. The Multiar.**—A most simple and accurate amplitude-comparison circuit is the “multiar,” for which a practical circuit is shown in Fig. 9-20. The accuracy of selection depends only upon a single diode, and the amplifier that follows is an economical regenerative device which provides a nearly instantaneous pulse and step at the instant of diode conduction.<sup>1</sup> The principles that underly the design of this device are widely applicable to the problems of amplitude comparison.

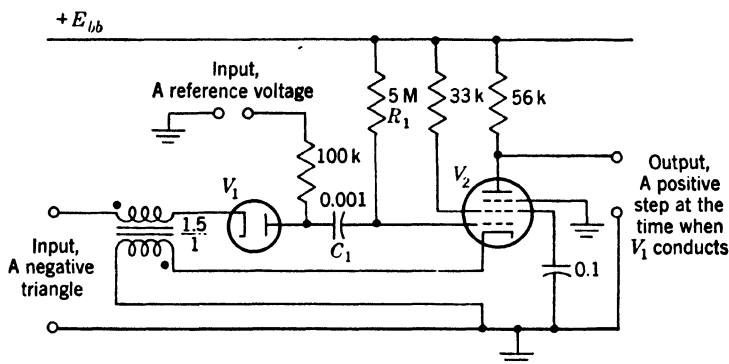


FIG. 9-20.—The multiar circuit. A diode selector and a regenerative amplifier with loop broken until the diode conducts.

**Circuit Operation.**—For the multiar of Fig. 9-20, the pentode is ordinarily conducting strongly. The plate of this tube,  $V_2$ , may be bottomed. A small grid current is flowing through the grid leak which is returned to the positive supply. The plate of the diode,  $V_1$ , is at the reference voltage. Its cathode is higher being at the quiescent level of the input waveform. Tube  $V_1$ , therefore, is not conducting and the feedback path through the transformer is not complete. The negative input waveform, in this case a triangle, lowers the voltage at the cathode of  $V_1$ . When this voltage reaches the reference voltage, the diode conducts. The feedback path is now completed, and since the transformer is connected for positive feedback, the pentode is rapidly cut off. The circuit is returned to its quiescent condition by the voltage rise at the end of the triangle.

<sup>1</sup> See F. C. Williams and N. F. Moody, “Some Remarks on ‘Ranging Circuits, Linear Time Base Generators and Time Discriminators,’” I.E.E. Convention Paper, March 1946, p. 13.

A distorted reproduction of the portion of the triangle below the reference voltage occurs at the plate of the diode. This wave tends to carry the pentode grid negative and, thus, acts as a trigger for the regeneration. The grid of the pentode is driven several volts below ground by the regeneration. If the input terminal were held at a constant potential after the start of regeneration, the grid of the pentode would rise with a time constant determined by the charging rate of the stray capacitances at the grid circuit. The pentode would again conduct and be cut off by regeneration when the grid rise permitted the diode to conduct. This relaxation oscillation or "bouncing" is accentuated by any quasi differentiation in the transformer operating upon the overshoot of the cathode wave. A short grid base for  $V_2$  is desirable to prevent this effect. Proper transformer design also is helpful. If the input waveform is a negative-going triangle, the triangle continues its fall after the comparison thus tending to suppress bouncing, and finally maintains the grid of the pentode beyond cutoff. It is clear that some other solution of this problem may be necessary when a positive-going or slowly falling triangle is used.

*Design.*—The considerations that should be applied to the design of a transformer for this circuit are like those for the pulse transformers that are used in blocking-oscillator circuits (see Sec. 9-20). In addition some attention must be paid to low-frequency response in order to prevent bouncing, since the tube should be cut off after the input waveform has passed the comparison point. The interwinding capacitance of the transformer shunts the waveform generator and must be minimized.

The tube is chosen to deliver sufficient power so that the output rise may be of the size and speed desired. The pentode has several advantages over the triode for this application including the low Miller effect, the independence of plate potential of the cutoff voltage, and the short grid base. The grid time constant and the resistance through which the reference voltage is applied are chosen so as to load the triangle generator as little as possible. By making the loading sufficiently small, the triangle may be applied to several comparison circuits with independent reference voltages. The multiar is insensitive to repetition-rate changes except for  $R_1C_1$  averaging effects.

**9-15. Other Forms of the Multiar.**—The advantages of the multiar are twofold: (1) the stable and sharp break of the diode is used to define the equality of voltages by firing a regenerative circuit, and (2) the gain of the circuit is obtained in a single regenerative loop.

*Drift Compensation.*—The largest source of error that remains for most multiar circuits is the cathode drift of the diode. This may be compensated by another diode according to the methods of Sec. 9-6. The multiar-circuit modification is shown in Fig. 9-21.

**Sine-wave Comparator.**—It is often desirable to produce a square wave whose rise and fall instants are stably timed with respect to a sine wave. This “squaring” is easily done with a circuit of the multirar type. Such a circuit is shown in Fig. 9-22, and the relevant waveforms in Fig. 9-23.

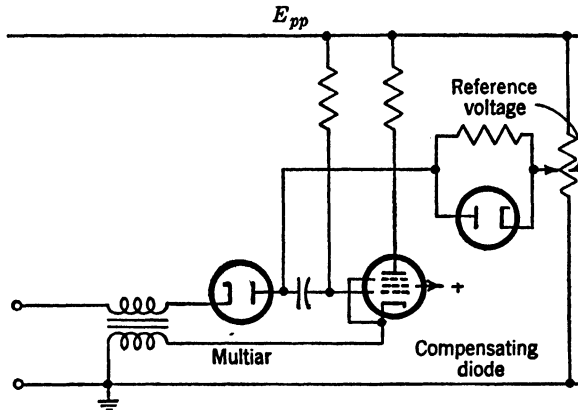


FIG. 9.21.—Stabilization of diode in multiar.

The pulse spacing and the square wave are not symmetrical since the turning on of the triode occurs when the sine wave reaches the cutoff voltage instead of zero. The waveform may be made more nearly symmetrical by increasing the sine-wave amplitude or by using a tube with a shorter grid base. The accuracy of relating the positive-pulse

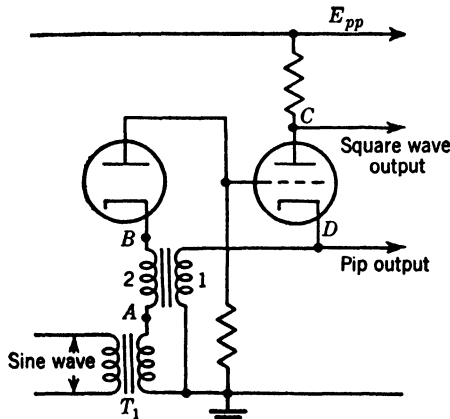


FIG. 9-22.—Multiar for conversion of sinusoids to square waves.

output to a fixed phase of the sine wave depends, in the main, upon the diode characteristic. The instant of the negative pulse is less accurately determined.

**Regenerative Azimuth-marker Generator.**—A type of amplitude comparison that operates at a slower time scale than the preceding methods



producing a pulse of a few milliseconds duration at a fixed phase of a low frequency sinusoid is sometimes required (see Fig. 9-24). The 24 rpm sinusoid appears as modulation upon a carrier of a higher frequency. The steepest portion of the wave which is near the null is chosen as the operating point for comparison, and a regenerative circuit is used for amplification. The modulated carrier waveform shown in Fig. 9-24 is derived from a synchro system connected to a radar scanner. The envelope nulls do not go to zero amplitude, since an unmodulated component of carrier, phase-shifted  $90^\circ$  from the modulated component, is present.

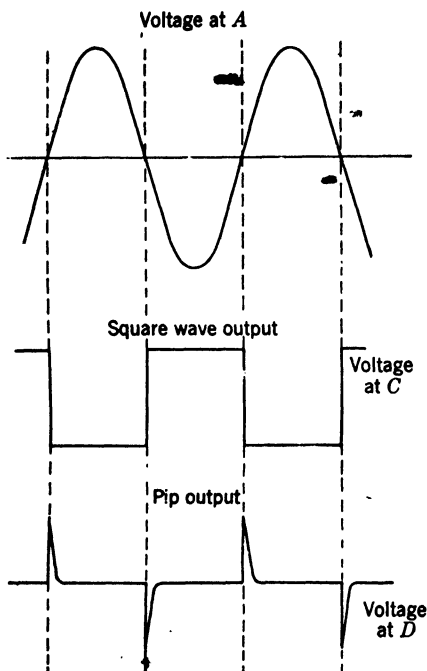


FIG. 9-23.—Waveforms for Fig. 9-22.

component of carrier, phase-shifted  $90^\circ$  from the modulated component, is present.

A circuit for performing this operation when a 400-cps carrier is used is shown in Fig. 9-25. The input waveform is amplified by a factor of 100 or more in the input transformer and push-pull amplifier. The two outputs are applied to the grids of a full-wave plate detector. The connected plates of these triode sections rise toward the supply voltage at the null. The output of the detector operates the quasi-selector stages (a cathode-follower cutoff by 50 volts bias). During the selected portion of the waveform, a regenerative loop is connected through the center tap of the input transformer. The marker is formed by a multivibrator-like circuit.

By adjusting the bias on the quasi-selector stage, the start of the pulse may be adjusted relative to the null. The center of the pulse must occur at the center of the null if a variation in marker time with polarity of input signal previous to the null is to be avoided. Thus, for one bias of the quasi selector, the circuit is a fairly accurate two-way comparator (see next section). The duration of the pulse may be adjusted by the time constant of the feedback network. The uncertainty of the 400-cps phase at the null introduces some jitter (a time equal to  $\frac{1}{4}$  of a 400-cps period, at the most). Any variation in amplifier gain or in the scan rate will require a readjustment of the selection boundary and the duration of the pulse. The waveforms at the input to the selector are shown in Fig. 9-26.

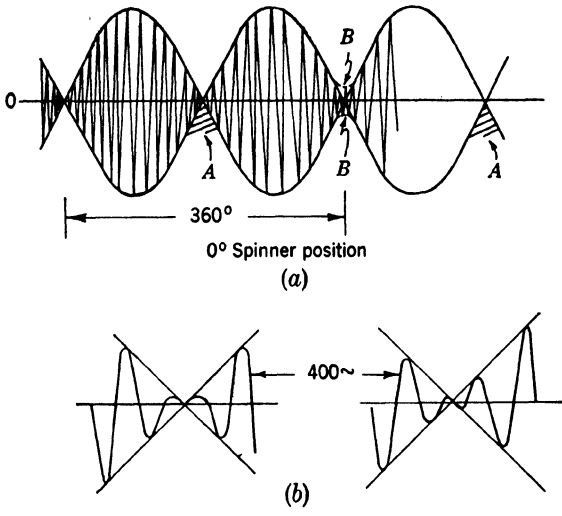


FIG. 9-24.—Input waveform to azimuth-mark generator.

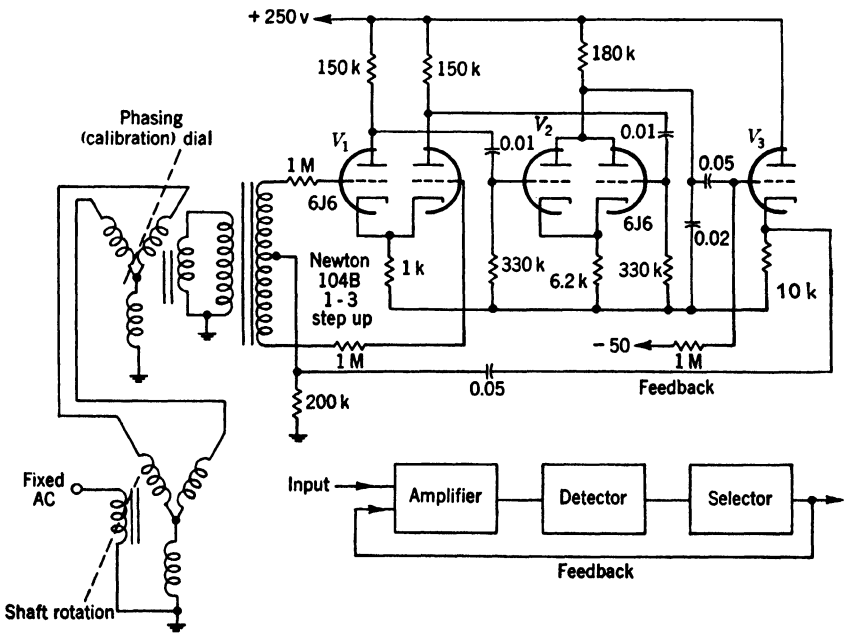


FIG. 9-25.—Azimuth-mark-generator circuit.

The  $90^\circ$ -shifted unmodulated carrier component that prevents perfect nulls may be discriminated against by a phase-detector action. The null must be good even with such a circuit, in order to avoid overloading the amplifier.

**9-16. Two-way Comparators.**—If a marker is desired whether a waveform approaches a reference voltage from larger or smaller values, a two-way comparator must be used. A satisfactory solution is to provide two circuits, each sensitive to one direction of approach. Or one seeks a discontinuous characteristic as shown in Figs. 9-27 and 9-28. The instability of the effective boundary is large for both circuits, and they are designed for use with slow waveforms.

Figure 9-27a shows a circuit that is to operate as a two-way comparator. Its characteristic is simply adjusted for maximum slope without

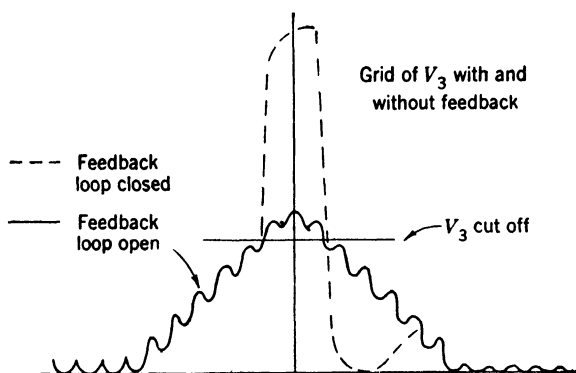


FIG. 9-26.—Detector output in azimuth-mark generator.

hysteresis, as is illustrated in Fig. 9-27b. Figure 9-28 exhibits the use of a high variational resistance as a cathode resistor in a double-triode comparator involving a conductive regeneration connection to produce the desired characteristic.

**9-17. Sine-wave Comparators.**<sup>1</sup>—Comparators to produce a marker when a sinusoid equals a fixed voltage are necessary to many high-precision timing circuits. This process is sometimes called “peaking” or “squaring.” The methods are identical with those for any comparison, selection, or quasi selection followed by amplification. A broken-line characteristic is clearly required, because no operation on sine waves with linear elements can produce any wave except another sinusoid.

The quality required of the marker, which is usually a pulse, is that its time instant shall correspond to a fixed phase of the sinusoid. Except for the zero-voltage points, the phase corresponding to a given voltage depends upon the maximum amplitude. As a result, comparison with

<sup>1</sup> Sec. 9-17 to 9-20 by R. Kelner and E. F. MacNichol, Jr.

zero voltage is capable of the greatest accuracy. Another advantage in zero comparison is that the slope of the wave is greatest at this point and small changes in the reference level from the nominal value of zero and in the sine-wave amplitude have the least effect upon the phase of the marker. Furthermore the least amplification is required to increase this rate of rise to that of a suitable marker.

The waveforms resulting from peak selection and linear amplification are shown in Figs. 9-29b and *d*. This wide pulse can be used with a time-selector circuit to select a narrower and more accurate pulse which

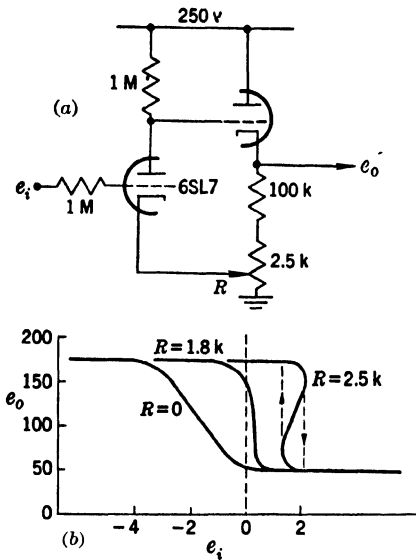


FIG. 9-27.—Two-way comparator for operation at a fixed reference level.

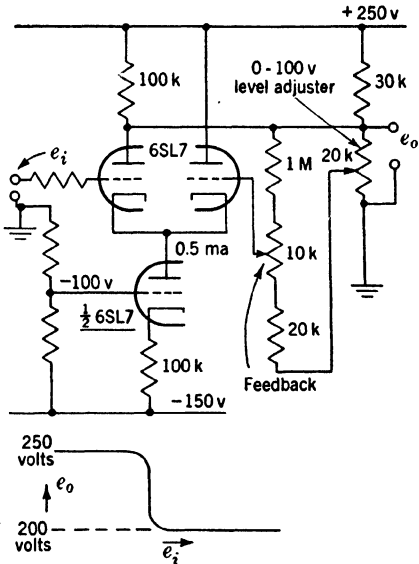


FIG. 9-28.—Another two-way comparator. The feedback adjustment permits adjustment of the characteristic to maximum slope without hysteresis.

occurs near the peak of the sinusoid. The center of the selected pulse is not affected by shifts in the sine-wave amplitude or the reference level, and small symmetrical variations in its width are unimportant.<sup>1</sup> The edges of the selected peak could be amplified to form markers, but the amplification required is comparatively large, and the dependence of marker phase upon amplitude relationships is excessive. Still with complex circuits a marker can be derived from the peak of the wave fairly accurately.

Zero comparison followed by double differentiation is shown in Figs. 9-29c and *e*. A single-bound selector is biased to select the positive

<sup>1</sup> See Vol. 20, Chap. 6.

half cycle. A sinusoid may be marked at four accurately determined points by a combination of peak and zero selection as shown in Fig. 9-30. By amplitude comparison at amplitudes intermediate to the peak and

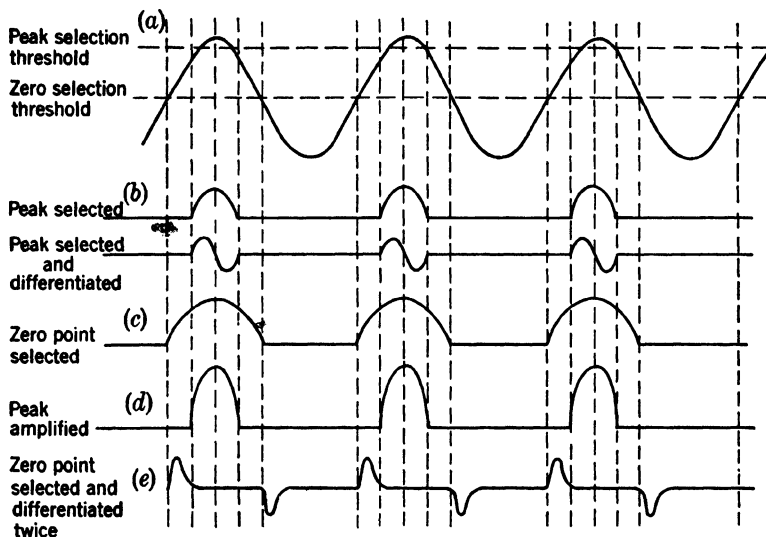


FIG. 9-29.—Peak and zero selection.

zero, interpolation, or variable pulse spacing, and smaller fixed delays are possible. The additional necessity of controlling the amplitude of the sinusoid is troublesome.

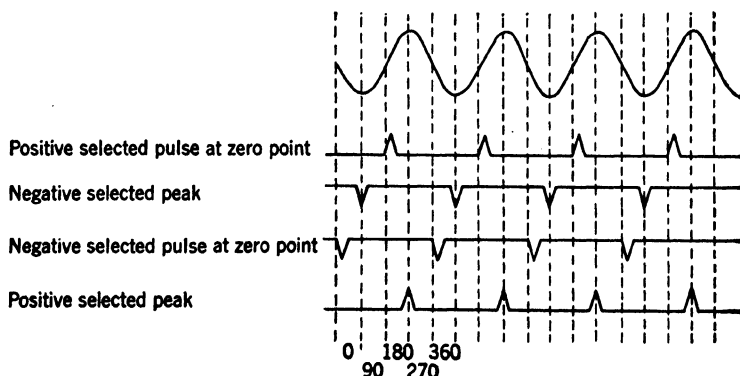


FIG. 9-30.—Phase relationships of pulses formed from a sinusoid.

**9-18. Sine-wave Peak Comparison.**—Peak selection is usually accomplished in Class C amplifiers or oscillators. The grid of the selector tube is biased off so that conduction takes place only on the peak of the wave. The output pulse appears across a small resistance or inductance in the

plate circuit. Figure 9-31 shows two typical circuits for peaking the output of crystal oscillators. In both circuits the oscillator operates with

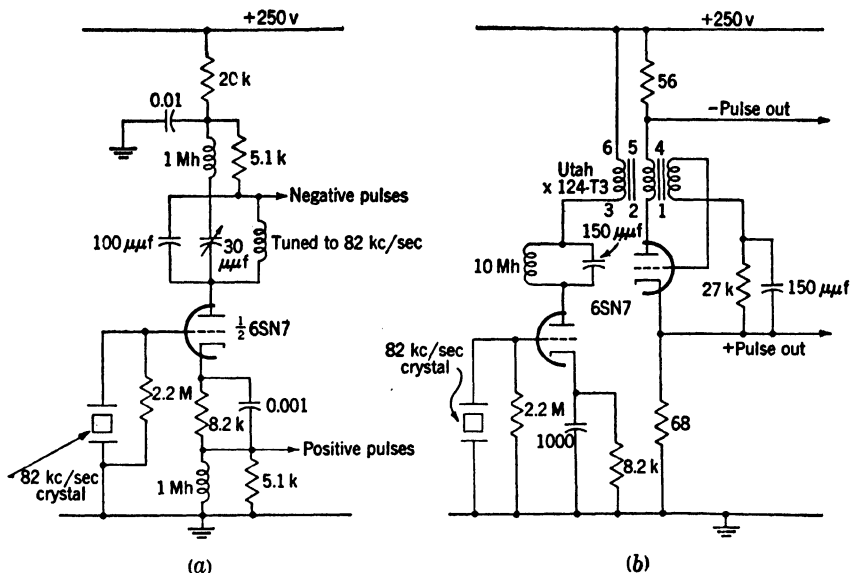


FIG. 9-31.—Crystal-oscillator peakers. (a) TS-100 1AP; (b) 256B oscilloscope.

very large cathode bias so that plate current flows only on peaks. In *a*, pulses are taken across 1-mh inductors in the plate and cathode circuits. These coils have negligible impedance at the 82-kc/sec fundamental frequency, but they have a high impedance for the pulses of plate current so that pulses of approximately 25 volts of about 1-μsec duration are developed across them. The 5.1-k resistors overdamp the oscillations that are shock-excited in the coils. In *b*, the plate-current pulses pass through one winding of a pulse transformer which has negligible impedance for the fundamental frequency. The heavy pulse current synchronizes a blocking oscillator which would free-run at a frequency slightly lower than 82 kc/sec. Pulses of 1-μsec duration are taken at very low impedance level from the plate and cathode circuits.

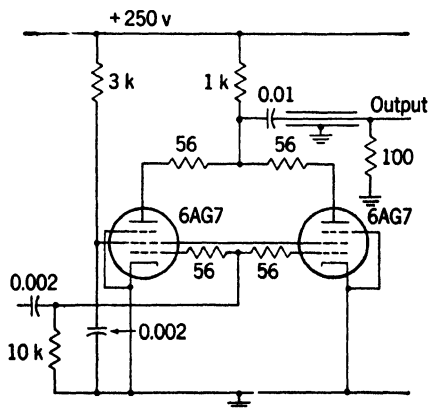


FIG. 9-32.—Squaring amplifier for peak selection.

A circuit for producing timing marks from a 1-Mc/sec sine wave is shown in Fig. 9-32. The input sine wave has a peak amplitude of 150 volts. The tubes conduct over a  $70^\circ$  region near the peak, producing nearly rectangular pulses of 30 volts amplitude and  $0.02\text{-}\mu\text{sec}$  duration which rise and fall in  $0.003\text{ }\mu\text{sec}$ . Two tubes are used in parallel to provide the necessary  $g_m$  and dissipation. The output is taken through a 95-ohm cable correctly terminated at the deflecting plates of the CRT.

**9-19. Sine-wave Zero Comparison.**—Since selection takes place at a fixed level, triodes and pentodes are frequently used as selectors as shown in Fig. 9-33. The amplitude of the input wave must be large compared with the grid base of the tube so that linear amplification takes place over a very small portion of the waveform. In the circuits shown, a large grid resistor is used so that grid limiting takes place. The average

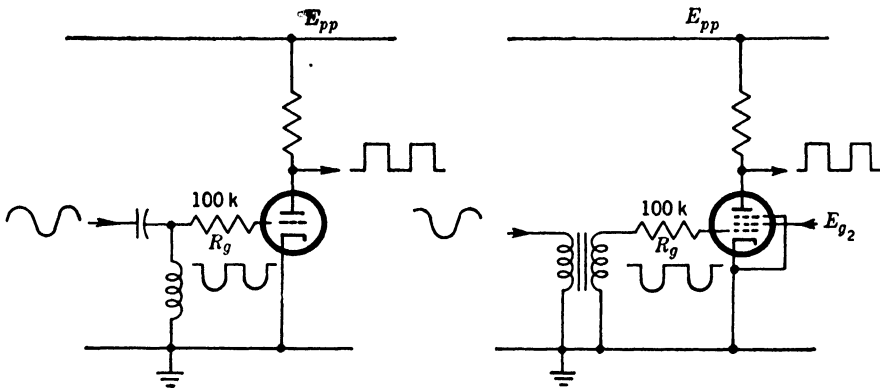


FIG. 9-33.—Sine wave zero comparison circuits.

current and the length of the grid base are adjusted by varying  $E_{pp}$  or  $E_{g2}$ . The pentode circuit will give the most nearly rectangular output because it will bottom on positive half cycles of the input as well as cut off on the negative half cycles. The d-c resistance in the grid-cathode circuit should be kept as small as possible to prevent shifts in the selection threshold with amplitude or frequency of the input signal. This is particularly important if a pulsed oscillator is used as a source since the duty ratio will be variable. In Fig. 9-33 inductances are used for this purpose as they have a low d-c resistance but a high impedance for the sinusoid.

If  $RC$ -coupling must be used, diodes should be inserted for d-c restoration as shown in Fig. 9-34. In *a*,  $R_d$  and  $R_g$  are equal and large compared to the tube resistances  $r_d$  and  $r_g$ , which are also nearly equal. The current drawn will therefore be the same on positive and negative halves of the cycle, and the average level at point *A* will be zero. In *b*,  $R_d$  is very much smaller than  $R_g$ . The diode cuts off on positive halves of

the cycle so that no grid current will flow. There will be a slight shift in level since current is drawn through  $R_g$  on negative half cycles only.

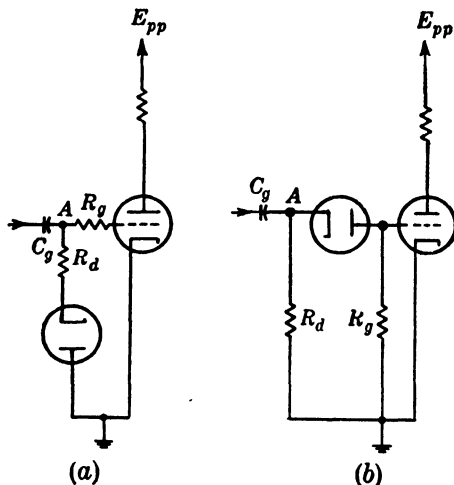


FIG. 9-34.—Sine wave zero comparison circuit with diode d-c restorers.

It is sometimes advantageous to stabilize the level of the output waveform in a manner that makes it independent of the tube characteristics. This may be accomplished by inverse feedback as shown in Fig. 9-35. Inverse feedback is applied from the plate to the grid through the diode  $V_2$ . The level is adjusted so that the grid is slightly negative when no input signal is present. On negative half cycles  $V_1$  conducts, breaking the feedback loop and permitting the tube to cut off rapidly.

An example of a regenerative comparator is the cathode-coupled bistable multivibrator (see Fig. 9-36a). It should be so designed that the first control grid never draws current and is biased in the center of the unstable region.

An oscillator that produces square waves that are accurately phased with respect to the sine-wave output is shown in Fig. 9-36b. A large cathode resistor is used so that the tubes draw equal currents during their conduction time and

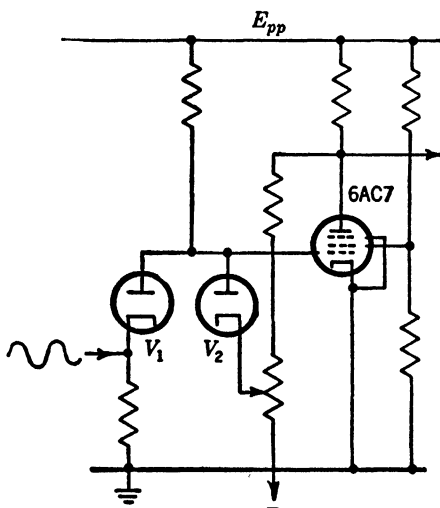


FIG. 9-35.—Comparison circuit with inverse feedback to maintain the output level constant.



this current value is maintained by degeneration. The tuned circuit receives a square wave of current of accurately determined amplitude and duration so that high stability is achieved.

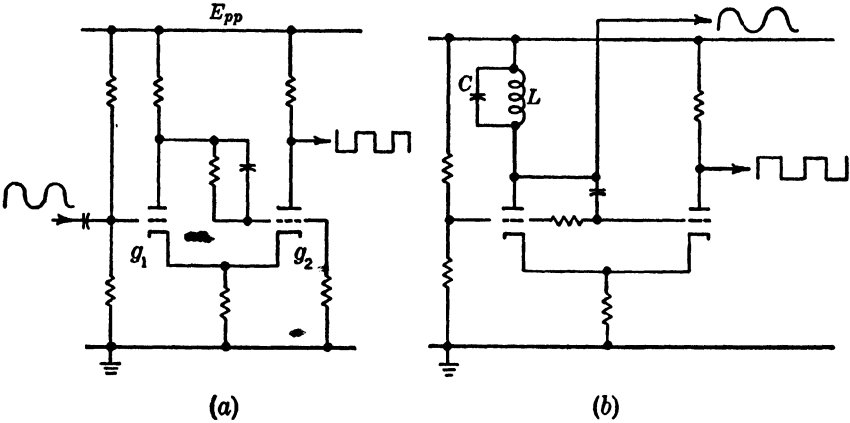


FIG. 9-36.—Multivibrator-type comparators.

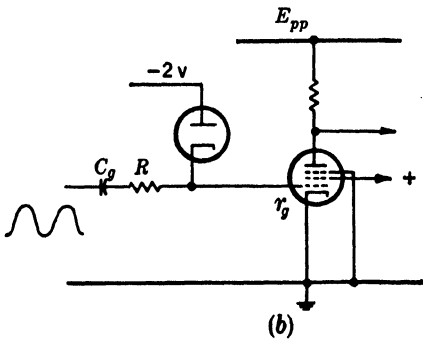
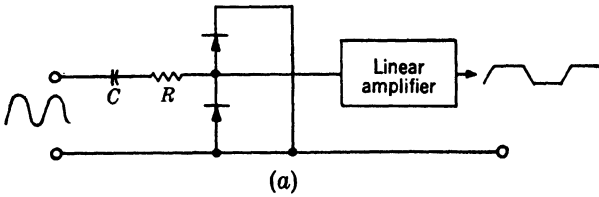


FIG. 9-37.—Accurate two-bound selectors.

None of the circuits shown above produces a waveform that has the same spacing from negative edge to positive edge as from positive edge to negative edge; also, the slope of one edge is greater than that of the other. Hence upon differentiation the negative-going pulses will be of a

different size and shape than the positive-going ones. This is brought about by the fact that the  $g_m$  of the tube is greater near zero bias than near cutoff so that the negative-going edges are amplified more than the positive-going ones. If identical pulses are wanted from both the positive- and the negative-going edges, accurate, symmetrical squaring must be used. This can best be accomplished by diode-amplitude selection. Figure 9.37a shows how symmetrical squaring can be accomplished by two-contact rectifiers or diodes. A single, symmetrical, nonlinear element, such as thyrite or a saturable transformer, might be used in place of the rectifiers. In Fig. 9.37b the grid current of the pentode amplifier is used as the upper bound and a diode is used to define the lower one. Since grid current starts at  $-0.5$  volt and the diode conducts at  $-1.5$  volts, the grid base has been effectively shortened to 1.0 volt. The change in  $g_m$  between these limits is small so that both the rising and falling edges are sharp. As the operation on the input wave is symmetrical, condenser coupling may be used in both circuits. If the wave must be very greatly steepened, several stages may be used, each selector being followed by a linear amplifier.

**9-20. Sine-wave-comparator Amplifiers.**—If pulses are to be produced from the steep-edged waveforms discussed above, some form of

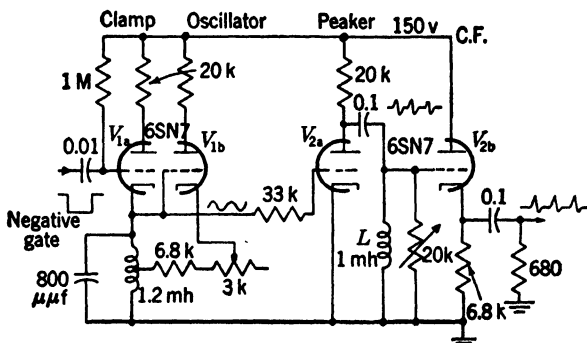


FIG. 9-38.—Pulsed-oscillator and peaker circuit.

pulse shortening must be used. If accurate rectangular pulses are required, the steep edges may operate the switch tube in a delay-line pulse generator or actuate a blocking oscillator or a multivibrator. For many purposes a simple quasi differentiation will suffice. This may be an  $RC$ ,  $LR$ , or transformer differentiator. A complete pulsed sine-wave oscillator-peaker circuit is shown in Fig. 9-38. The pulsed oscillator  $V_1$  is actuated by a negative gate and produces a sinusoidal wave train. The limiter  $V_{2a}$  selects only negative half cycles. The plate current in  $V_{2a}$  is applied to the inductance  $L$  through the bypass condenser  $C$ . The resonant frequency of the combination is too low to be shock-excited

by the plate-current pulses. Pulses of appreciable amplitude appear at the plate of  $V_{2a}$  only when  $V_{2a}$  is cut off. The output pulse is applied to the cathode follower  $V_{2b}$ , which passes only the positive pulses. With the oscillator tuned to 163 kc/sec and  $L = 2$  mh, the output pulses are 15 volts in amplitude, nearly triangular, and about  $0.75 \mu\text{sec}$  in duration at the base. A diode may be used in place of the damping resistor so that nearly complete attenuation of the negative pulses will occur.

Pulse transformers may be used as excellent quasi differentiators and will produce outputs at any desired impedance or voltage level. Closed-core transformers such as are used in blocking oscillators are not satisfactory. Very satisfactory transformers using straight cores are easily

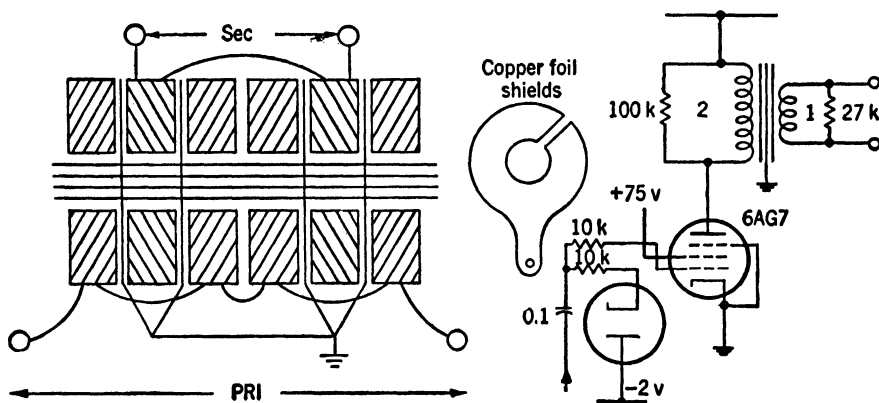


Fig. 9-39.—Quasi-differentiating amplifier and transformer.

constructed.<sup>1</sup> Figure 9-39 shows how such a transformer is constructed using pies from standard RF chokes and laminations cut from a type Utah OA-15 pulse transformer. The core material is not critical, as practically all the reluctance is in the air gap. The core increases the inductance of the transformer by a factor of approximately 4 depending upon the shape of the coils. The coils are cut from 4-pie 1-mh RF chokes and, with the core in place, the inductance is approximately 7 mh. The primary and secondary coils are separated by copper-foil faraday shields to minimize capacitance. With a 10-k load in the primary and a 2.7-k load in the secondary, which is stepped down 2 to 1, the effective load is approximately 5.6 k, yielding a time constant of  $L/R = 1.2 \mu\text{sec}$ .

The waveforms in a two-stage squaring and differentiating amplifier are shown in Fig. 9-40. The circuit is two stages resembling that of Fig. 9-39 with a resistance or the above transformer in the plate circuit of the second stage.

<sup>1</sup> F. N. Moody, I.E.E. Convention Lecture, March 1946.

**9-21. Amplitude Discrimination.**—Indication of either the equality of two voltages or of the sense and approximate magnitude of their inequality is termed amplitude discrimination (see Chap. 3). Subtraction of the two voltages and amplification of their input difference is suitable for

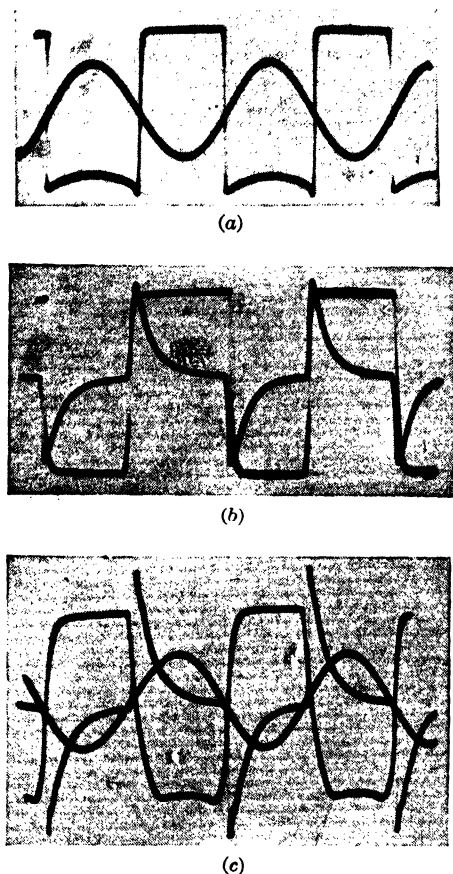


FIG. 9-40.—Squaring or differentiating amplifier waveforms. Two stages were used, identical with the one shown in Fig. 9-39, except that the first stage had a 22-K plate resistor. The 6AG7 tube was used for the second stage in all cases. (a) 6AC7 first stage: sinusoid input and plate voltage. (b) Outputs from second stage with a resistor load and with a transformer load. (c) Input wave and first and second stage outputs with 6AG7 first stage and transformer load in second stage. The concave bottoms of the square waveforms result from the positive-grid characteristics of the first tube.

this operation. The amplified signal must be in a form acceptable in signal amplitude, d-c level, and wave shape to some recording, indicating, or controlling device. In order to avoid common-mode interference (i.e. variation of the d-c. level common to both the inputs) with stability, the entire discriminator and indicator may be “floated” upon one of the

input voltages. Extensive use of amplitude discrimination is made in servo follow-ups.<sup>1</sup>

The slowly varying input voltages need not be d-c, but may be the slowly varying amplitudes of a-c carriers. If the carriers are in phase, subtraction and amplification suffice. The sign of the input difference is indicated by an error signal in phase or out of phase with one of the carrier waves. This type of discrimination may replace the discrimination of d-c voltages in servo follow-ups and has the advantage of permitting the use of a-c amplifiers in the discriminator. The error signal may be rectified or used as alternating current.

Even in cases where the input signals are d-c, a-c amplification can be used if the subtractor is replaced by a modulator that develops an alternating current proportional to the difference voltage. The particular requirements for such modulators are described in Sec. 9-23. The stability of the discriminator depends primarily upon the modulator characteristics. For some mechanical-switch modulators, the characteristics are such that the stability of discrimination may be increased by a factor of 1000 over the stability of devices using only vacuum tubes.

Subtraction in d-c discriminators may be by use of a passive<sup>2</sup> network, but the common-mode component cannot be eliminated by a passive network alone except in special cases. Certain so-called "difference amplifiers," however, can accept two d-c voltages at two grids, amplify their difference, largely reject common-mode variation, and also compensate for the effect of cathode drifts, thereby attaining fairly good stability. This circuit and other d-c amplifier discriminators are discussed in the next section.

For all of these discriminators, the linearity and constancy of gain may be increased by negative feedback. Local feedback in the amplifiers or, with modulation-demodulation systems, feedback from the d-c output back to the d-c input should be used.

**9-22. Direct-coupled Discriminators.**—These circuits are special d-c amplifiers with the unusual property that they amplify the difference between two d-c voltages but not the sum. Their outputs are single-ended or push-pull voltages measured from a reference potential that is fixed with respect to ground. Good rejection of the common mode, and stable indication of zero input difference are usually the important properties of a discriminator.

Some considerations that affect the design of direct-coupled discriminators are given below:

<sup>1</sup> See Vol. 21, Part II.

<sup>2</sup> See Vol. 18, Chap. 18. See also Chap. 18.

1. Input common-mode variation—the degree to which the output should be independent of the d-c level of the two inputs, and the range through which this level will change.
2. Nature of output—whether the output voltage is single-ended or push-pull, and, if it is the latter, whether its central value must be independent of the input common mode.
3. Linearity—how nearly perfect a measure of the input difference is desired.
4. Range—the extremes of the input difference to which the output should respond.
5. Gain.
6. Stability—effect upon zero point and upon gain of time, heater voltage, etc.

*Difference Amplifier Stages.*—The simplest discriminating amplifier is a triode with inputs to both grid and cathode, as in Fig. 9-41. A certain offset of the inputs is required in practice,  $e_1$  being somewhat below  $e_2$  for the “central” value of output. Also, common-mode input variation affects the output  $1/\mu$  times as much as does the difference input. The input  $e_2$  must be at a comparatively low impedance.

The latter two conditions are avoided in Fig. 9-42a, where  $e_2$  is attenuated and shifted by the appropriate amounts. With proper adjustment, the zero shift caused by common-mode variation is the

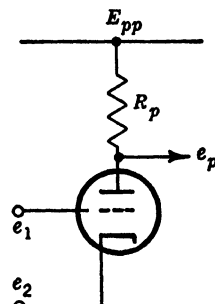


FIG. 9-41.—Single-triode discriminator.

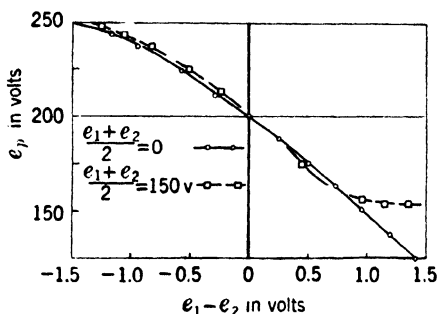
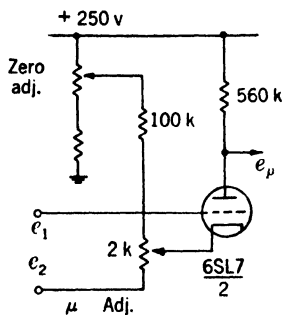


FIG. 9-42.—Improved single-triode discriminator.

result only of the change of  $\mu$  with respect to plate-cathode potential, which, at any one value of plate current, is usually small. The zero shift caused by an input common-mode level change from zero to 150 volts was found to be not more than that due to 10 mv of  $e_1 - e_2$  signal, for the several 6SL7's tested (with proper adjustment of the potentiometers for each tube). The gain and shape of the output curve are somewhat dependent on input level, as shown by Fig. 9-42b.

The above circuit will suffer considerable zero shift if the cathode temperature changes; a 10 per cent increase of heater voltage demands

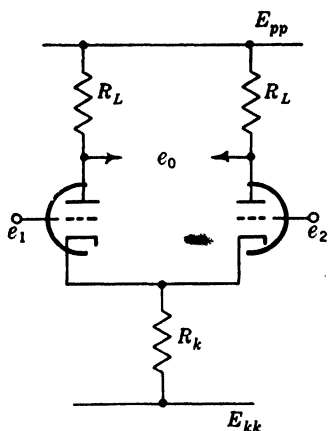


FIG. 9-43.—Double-triode discriminator.

about a 100-mv decrease of  $e_1 - e_2$  for a fixed output. In the differential arrangement of Fig. 9-43, the effect of heater-voltage variation is canceled in so far as the two cathodes are similar. For two triodes in the same envelope this cancellation is generally better than  $\frac{1}{10}$  effective, or, in other words, the zero shift at the inputs will be less than 10 mv for a 10 per cent change of heater voltage. Another advantage of the differential amplifier is that both inputs are to high impedance grids.

The output of the differential amplifier is via two terminals, and is in terms of the voltage between them. Assuming, for the moment, exact similarity of the triodes,

the output difference will be zero when the input difference is zero regardless of input level. The output level, however, will be a function of input level; it will, in fact, vary approximately  $-R_L/2R_k$  times the input-level variation. This effect is reduced by increasing  $R_k$  in comparison with  $R_L$ .

The resistor  $R_k$  may be made higher, without reduction of current, by the substitution of a triode constant-current circuit as shown in Fig. 9-44. The output level is approximately +200 volts, and will change by only two volts as the level of the inputs is changed from -50 to +150 volts, the change being caused by a 4 per cent variation of the total current.

Where the plate currents are constant at null output as in Fig. 9-44 the percentage difference zero shift resulting from the common mode signal is equal to  $1/(\mu + 1)$  of the percentage inequality of the two triode  $\mu$ 's. That is if the input level is changed by  $e$  volts, the difference in input levels required to maintain the output zero is given by:<sup>1</sup>

<sup>1</sup> Vol. 18, Sec. 12-10.

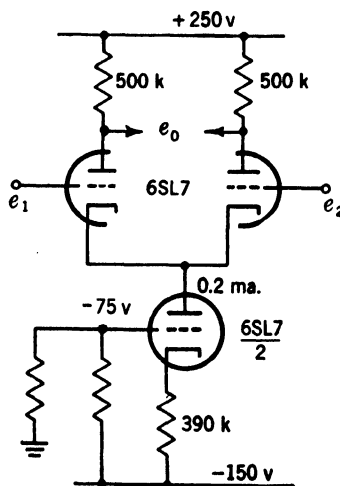


FIG. 9-44.—Double triode discriminator with a constant-current cathode load.

$$\frac{\Delta(e_1 - e_2)}{e} = \frac{1}{\mu + 1} \frac{\mu_2 - \mu_1}{\mu},$$

where  $\mu_1, \mu_2$  are the  $\mu$ 's of two triodes and  $\mu = \frac{\mu_1 + \mu_2}{2}$ .

Thus, for example, if the  $\mu$ 's of the two triodes in a certain 6SL7 differ by 3.5 per cent, the above expression will be 0.5 per cent ( $\mu$  is about 70) and the zero shift in Fig. 9-44 will be 0.1 volt if the input level changes by 200 volts. Nearly all 6SL7's are even more closely matched than this, as has been shown by actual tests. A potentiometer between the cathodes for the purpose of a zero adjustment does not affect the above equation. If plate current is permitted to vary appreciably, as it will in Fig. 9-43

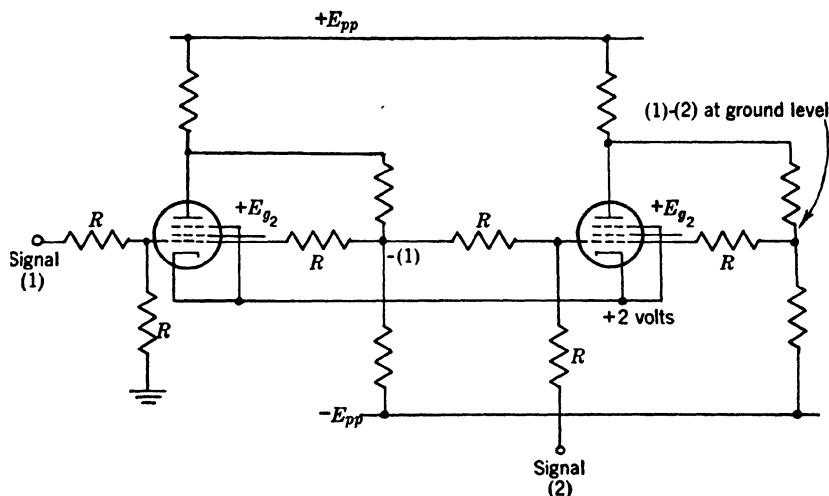


FIG. 9-45.—Improved balanced discriminator.

due to common-mode variation, plate resistance differences affect the above expression as well as  $\mu$  differences. Another restriction upon the utility of this formula is that the analysis does not apply to pentodes since the assumption is made that the variational resistance of the cathode element is very much larger than the plate resistance of the tubes. The increased  $\mu$  of a pentode does not increase the insensitivity to common-mode signals. A pair of 6SJ7 pentodes ( $\mu > 1000$ ) has been found to give no better rejection than two triodes (6SL7).

A fundamentally different type of discriminator circuit is shown in Fig. 9-45. One input is applied to an amplifier which inverts it about ground. This result is added to the second input in a resistor adding network. The output of this stage is the difference of the two signals, and the output level (ground) is independent of input level. The balanced circuit tends to cancel out filament variations and other tube



drifts. This circuit also utilizes negative feedback for linearization and gain stabilization. The output signal is independent of supply-voltage changes, which was not true of the previous discriminators.<sup>1</sup>

**9-23. Modulated-carrier-amplitude Discriminators.**—The advantages of a-c amplification may be employed by impressing the magnitude of the difference of the input signals upon a carrier and the sense of the difference upon the phase of the carrier.<sup>2</sup> Zero carrier amplitude is a useful indication of equal inputs for many purposes. If the output of the discriminator is required to be a slowly varying voltage rather than the amplitude of a carrier, a subsequent demodulation stage may be used.

*Mechanical-switch Modulator Circuits.*—The stability of output corresponding to zero input difference is determined largely by the modulating circuit. Vacuum-tube and contact-rectifier modulating circuits introduce errors of zero drift only slightly smaller than the similar errors for a d-c discriminator. If a mechanical-switch modulator is used, however, the zero stability is increased by a large factor. This device provides the most accurate discrimination that is available at present. It is often convenient to use a mechanical-switch demodulator after sufficient a-c amplification. This combination is suitable for very high accuracy discrimination with feedback and for discrimination at very low values of input difference.

Other combinations of mechanical-switch modulators and vacuum-tube circuits may be convenient. The design of such modulators and the characteristics of some switches are given in Chap. 11. The main restrictions on the applicability of the device are: introduction of spurious signals into high-impedance circuits,  $< 0.01$  of a microvolt of uncertainty in the voltage between switch contacts, the restriction of input differences to less than a few volts in order to avoid injury to the contacts, and the limited upper frequency at which mechanical switches can be vibrated. Where these restrictions are not binding and the requirement for small weight and size is not paramount, this discriminator far surpasses all others.

*Electrical-modulator Circuits.*—An important feature of electrical modulators is that they can be used at frequencies above those for which the mechanical-switch modulator will operate. The stability of zero indication of electrical discriminators is such that drift rates of less than  $3 \mu\text{v}/\text{min}$ , shifts from tube change of less than 50 mv, and sensitivity to heater-voltage change (5 to 7 volts) of less than 25 mv have been observed.

<sup>1</sup> For the design of the stages of a d-c discriminator following the difference amplifier see Chap. 12, Vol. 18.

<sup>2</sup> See Chap. 11 for modulation circuits and Vol. 21, Part II for phase-sensitive modulators used in servos.

The linearity and constancy of gain may be made as good as for the mechanical-switch discriminator by the use of negative feedback.

Only bidirectional electrical modulators are suitable; bidirectional discrimination is necessary for a modulated, carrier-amplitude discriminator.

*Amplifiers and Detectors.*—The amplifiers used with these modulators need satisfy no difficult requirements. The bandwidth and gain stability desirable in the amplifier vary according to whether or not negative feedback is provided around the complete modulator-demodulator loop. The demodulator operates at a comparatively high signal level so that its d-c drifts are not effective as sources of error in the output signal. Phase-sensitive demodulation is necessary in most cases.

## CHAPTER 10

### TIME SELECTION

BY BRITTON CHANCE

**10-1. Introduction.**—There are three important analytical processes, time selection, time discrimination, and time comparison, that may be applied to the time axis (abscissa) of a waveform;<sup>1</sup> they are analogous to the processes of amplitude analysis described in Chap. 9. The first function is analogous to amplitude selection and may be defined similarly as the process of selecting a portion of a waveform that occurs within a given interval or before or after a given time relative to a repeated time reference. Time selectors have been called “coincidence,” “separator,” “strobe,” “gating,” and “interval-selector” circuits. These time selectors have three important uses: (1) the selection of a desired waveform to the exclusion of other nonsimultaneous waveforms which may interfere, as, for example, in radar systems; (2) the selection of a member of a train of timing pulses for the precise initiation of a lower-frequency waveform, as, for example, in frequency division or multiple-scale range circuits (see Chap. 16), and (3) the selection of a portion of a waveform for the purposes of phase discrimination (phase-sensitive detection), time discrimination, or time comparison (see Chap. 14).

Time discrimination is defined as the process of indicating the relative time of occurrence of two electrical events by zero output if they are simultaneous or, if nonsimultaneous, by an output that indicates the sense and approximate magnitude of the time difference. This process depends upon both time selection and detection and is therefore the subject of a separate chapter (Chap. 14). Time comparison, analogous to amplitude comparison but operating on the time axis instead of the amplitude axis, gives in the output the amplitude corresponding to a given value of the abscissa of the waveform. It too requires detection since a constant output is desired, and is also discussed in Chap. 14.

The discussion of the various time-selector circuits follows a pattern

<sup>1</sup> The abscissa of the waveform need not always represent time; for example, it may represent quantities such as mechanical position, temperature, pressure, etc. The general principles of the three processes here designated as “time operations” are equally applicable to waveforms whose abscissa has the other representations. The selector waveform must, however, be controlled in accordance with these other quantities.

dictated not only by the type of circuit element employed but also by its effectiveness. The circuit elements are, of course, those described in Chap. 3 and may be two-variable, three-variable, or multivariable. A time selector should fulfill the following conditions. First, an undesired signal in excess of the amplitude of the selector pulse should not be passed through the time selector. Second, the amplitude of the output pulse should not be dependent upon the amplitude of the selector pulse applied to the time selector. Time selectors employing addition of signal and selector pulse and followed by amplitude selection violate the first proviso, and the conditions of the second are fulfilled only by three-variable elements such as multigrid tubes. A large number of circuits, including multidiode switches, satisfy the first and the second requirements unless the signal exceeds the selector pulse amplitude.

This chapter also includes a somewhat different category of time selectors. These devices are definitely time-sensitive in that a pulse response is produced which is dependent upon the duration or time of occurrence of the input wave. These devices do not, however, reproduce the input wave and are therefore called "quasi time selectors."

Another type of time selector is useful in time discrimination and may consist of a pair of time selectors giving a two-terminal output or a pair of phase-reversing time selectors giving a single-ended output. Their use in time demodulation is presented in Chap. 14.

**10-2. Amplitude Selectors.** *Diodes.*—The characteristics of nonlinear circuit elements and the basic principles of amplitude selection have been given in Chaps. 3 and 9. The use of nonlinear circuit elements in time selection stresses wideband circuits and requires that the signals, selector pulses, and nonlinear circuit elements shall all have a low impedance.

Figure 10-1 indicates the addition and amplitude selection of positive pulses. The first line of the figure shows the train of input pulses, the second line the selector pulse, and the third the output of the amplitude selector. The time selection of the second pulse of the top line is indicated in the third line. Since the selector pulse is slightly larger than the input signals, only the coincident pulse appears in the output. Satisfactory time selection requires that the selector pulse be precisely equal to the bias ( $E_{kk}$ ), which in turn must equal the amplitude of the largest interfering signal to be rejected. A slight decrease of the bias ( $E_{kk}$ ) would cause not only the unwanted signal but also a portion of the selector pulse (a pedestal) to appear in the output. Pedestal would also be caused by a slight increase in the amplitude of the selector pulse. In order to avoid excessive sensitivity to variations in signal, selector pulse, and bias, the voltage scale of the whole operation must be large compared with the voltage scale of the nonlinearity. Operation under these

conditions minimizes the effects of variation of contact potential of the nonlinear element with heater voltage and time. Since low-impedance wideband circuits are desirable for time selection, the germanium crystal in its present form appears desirable for time selection because of its excellent stability, the sharp break in its characteristic, and its low shunt capacitance. These factors also permit operations at somewhat lower levels than with thermionic-diode amplitude selectors.

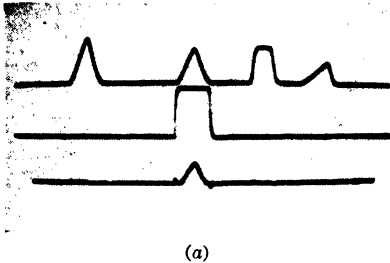
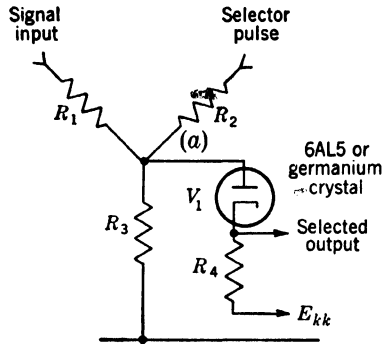


FIG. 10-1.—Addition and amplitude selection of positive pulses. The first line shows the signal input, the second the selector pulse, and the third the selected output. The waveforms of Fig. 10-1a were obtained with  $R_1 = R_2 = 27k$ ,  $R_3 = 220k$ ,  $R_4 = 43k$ ,  $V_1$  = type 6SN7.  $E_{kk}$  is obtained from a low-impedance source. The sweep duration is 120  $\mu\text{sec}$ .

*Triodes and Pentodes.*—Time selection depending upon grid-cathode addition and amplitude selection in triodes and pentodes has been employed in a number of circuits in the interests of expediency. Not only is the characteristic more curved than in the diode, but the maximum signal voltage cannot exceed the grid base of the tube. Also drift is somewhat greater than in the diode. This method is, however, employed in a number of “decoders” described in the next paragraph. In this case fidelity is not required; the circuits are quasi time selectors.

*Quasi Selectors Employing Delay Lines.*—An electric, supersonic, or cathode-ray-tube delay device (see Chaps. 21, 22, and 23) may be used to delay an early member of a train of pulses and thereby permit the time selection of a late member by the delayed early member. This process is called “decoding.” Reasonably secure identification of a particular pulse train may be obtained if it contains three or more pulses, and delay devices are cascaded to make the

early pulses coincide with the last one. Time selection gives a single pulse free from interference.

The various circuit connections for electric delay lines have already been discussed (see Sec. 6.15), and some practical applications of these “decoders” are given in Vol. 20, Secs. 10.6 and 11.4, and in Vol. 3.

An example of a double-pulse selector employing a delay line and grid-cathode addition in a triode is indicated in Fig. 10.2. A pair of

low-impedance negative pulses of duration  $D$  microseconds is connected to the input terminal. The bias of  $g_1$  prevents conduction of  $V_1$  provided the initial pulse is not too large. The delay line  $L_1$  is matched by a resistor  $R_2$  at its input end, is short-circuited at the other end, and has a tap at  $D$  microseconds from the input end. The tap may not be closer to the input than the width of the input pulse. The first pulse travels through the line, is reflected as a positive pulse, and  $2L - D$  microseconds later arrives at point  $D$ , where  $L$  represents the total delay of the line and  $D$  represents the displacement of tap  $D$  from the input end. If the spacing between the two pulses has this value ( $2L - D$ ), conduction of  $V_1$  will occur since a positive pulse is applied to the grid coincident with the negative second pulse on the cathode. This process may be repeated in a number of stages in series to give selection of any reasonable number of pulses.

The second member of the coded pulse train may be time-modulated. The duration of the output pulse then varies in response to this time modulation and may be demodulated by the methods of Sec. 14-5.

Sometimes selectors are designed to give a pulse output when the duration of a rectangular input pulse lies within certain values or is less or greater than a certain value. These decoding circuits are widely used in radar beacons (see Vol. 3). The beacon receives a pulse of a prescribed waveform, and the time selector gives a pulse output if the input lies within required time limits. Figure 10-3 shows a typical circuit for selecting pulses of duration in excess of  $1.6 \mu\text{sec}$ . The negative input signal is connected to the grid of  $V_2$  by means of diode  $V_1$ , which removes the positive overshoot from the input signal. The positive output from the plate of  $V_2$  is connected to open-circuited delay line,  $L_1$ . This positive pulse is reflected with the same polarity and,  $1.6 \mu\text{sec}$  later, adds to the input wave. If the duration of the positive pulse exceeds  $1.6 \mu\text{sec}$ , the input and the reflected pulse will overlap and give at the grid of  $V_2$  a positive pulse which is twice the amplitude of the input.

Time selection occurs in  $V_2$  by addition and amplitude selection, and the bias of  $V_2$  is adjusted so that no conduction occurs for either one of the

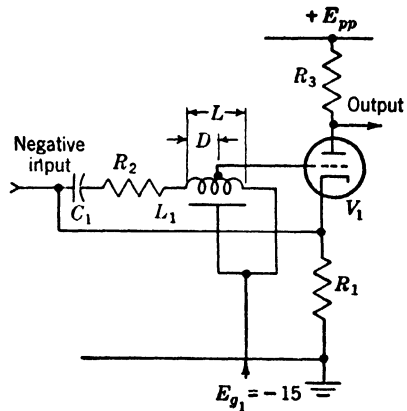


FIG. 10-2.—Double-pulse selector. The first member of a pair of negative pulses is reflected as a positive pulse with a delay  $= 2L - D$  and acts as selector pulse for the second member of the pair.  $R_2$  is adjusted to match the characteristic impedance of the delay line  $L_1$ .  $V_1$  may be type 6SN7.

positive pulses connected to its grid. The sum of the pulses will exceed the bias of the amplitude selector and cause triggering of blocking oscillator  $V_4$ . Therefore, a negative output is obtained for pulses which exceed  $1.6 \mu\text{sec}$  in duration.

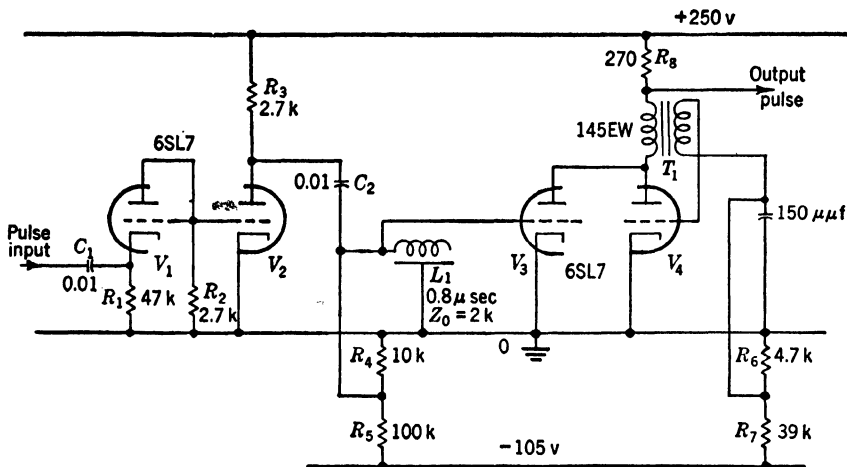


FIG. 10-3.—Pulse-width selector using a delay line and an amplitude comparator. The circuit selects pulses in excess of  $1.6\text{-}\mu\text{sec}$  duration. The overlap of the trailing edge of a pulse in excess of  $1.6\text{-}\mu\text{sec}$  duration is added to the leading edge of this pulse delayed  $1.6 \mu\text{sec}$  by  $L_1$ . The output triggers blocking oscillator  $V_4$  through  $V_3$ .

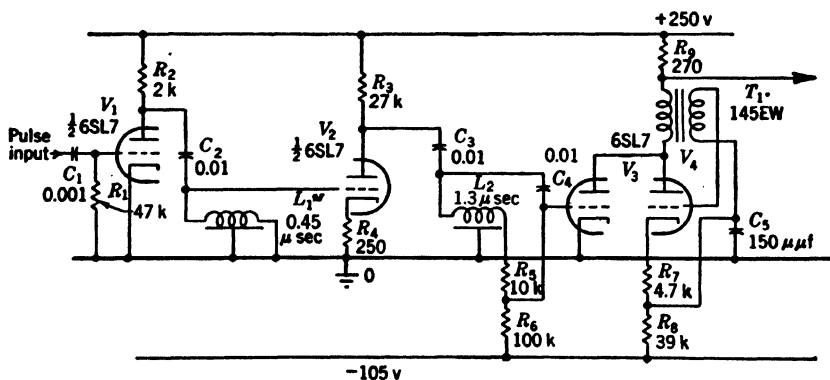


FIG. 10-4.—Pulse selection in an interval between  $1.9$  and  $3.3 \mu\text{sec}$ . Pulses of durations between these limits give sufficient overlap at the grid of  $V_3$  to cause triggering of  $V_4$ .

A time selector responsive to signals having a duration of  $1.9$  to  $3.3 \mu\text{sec}$  are shown in Fig. 10-4, in which short-circuited delay lines are employed. A negative input pulse applied to the grid of  $V_1$  causes a positive pulse to travel down  $L_1$ . The pulse is then reflected and returned to the input with the opposite polarity with the result that pulses in

excess of  $1\ \mu\text{sec}$  give two pulses of opposite polarity, each  $0.9\ \mu\text{sec}$  long. These pulses, amplified by  $V_2$  and connected to the second short-circuited delay line  $L_2$ , give for each of the input pulses another pair of positive and negative pulses spaced by  $2.6\ \mu\text{sec}$ . At the grid of the time selector,  $V_3$  there are, therefore, four  $0.9\text{-}\mu\text{sec}$  rectangular pulses; the first and fourth are negative, the second and third are positive. No single pulse will exceed the bias of amplitude selector  $V_3$ . Input pulses to  $V_1$  of durations between  $1.9$  and  $3.3\ \mu\text{sec}$  give sufficient overlap of the second and third pulses at the grid of  $V_3$  to cause triggering of  $V_4$ .

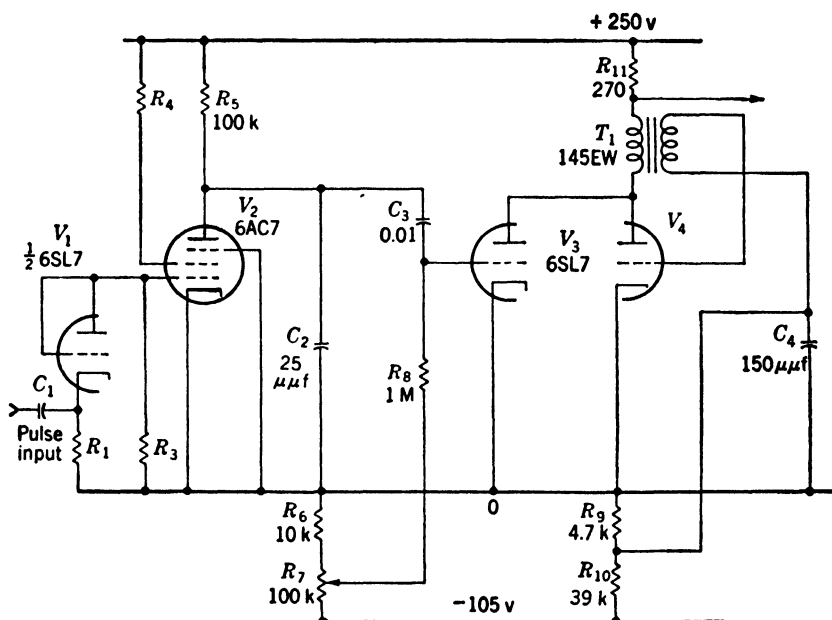
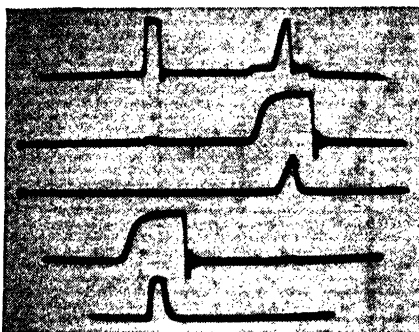
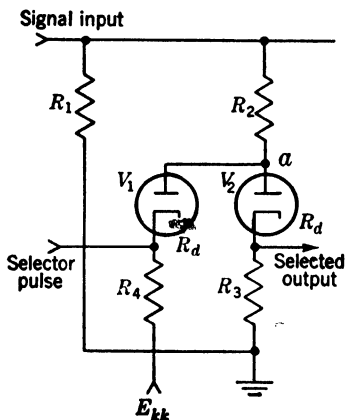


FIG. 10-5.—Pulse-width selector using a sawtooth generator and an amplitude comparator. The circuit responds to pulses in excess of  $1.5\ \mu\text{sec}$ . The duration of the input pulse determines the amplitude of an exponential wave at the plate of  $V_2$ . Adjustment of  $R_7$  causes triggering of  $V_3$  and  $V_4$  in response to pulses in excess of  $1.5\ \mu\text{sec}$ .

*Quasi Selectors Employing a Timing Waveform.*—Pulse-width selection may be accomplished by converting the input pulse to a triangular waveform of constant slope but of a duration depending upon that of the input signal. An amplitude comparator set to operate when the triangular waveform reaches a given amplitude indicates the reception of a pulse in excess of a predetermined width. An example of this circuit is shown in Fig. 10-5, where a negative input pulse is applied to the grid of  $V_2$  through diode  $V_1$ . This diode,  $V_1$ , eliminates positive overshoots of the input signal and also prevents any positive bias from accumulating upon  $C_1$ , a process which would displace the potential of the plate of  $V_2$  at the moment of reception of the input pulse. The negative signal then



generates at the plate of  $V_1$  a positive exponential waveform whose slope is determined by  $R_5C_2$ , a time constant of  $2.5 \mu\text{sec}$ . Since the grid of  $V_2$  is biased negatively by roughly 100 volts, amplitude selection of a portion of the triangular wave rising above this potential causes triggering



(a)

FIG. 10-6.—Series diode switch for positive pulses. The waveform diagrams of Fig. 10-6a were obtained with the following component values:  $V_1 = V_2$  = Western Electric germanium crystal type D 171612,  $R_1 = 240$ ,  $R_2 = 550$ ,  $R_3 = 1\text{k}$ ,  $R_4 = 1\text{k}$ ,  $E_{kk} = -9\text{v}$ . The signal input is shown on the top line of the waveform diagram and the selector pulse on the second and fourth lines. The outputs corresponding to these two selector pulses are shown on the third and fifth lines respectively. The sweep duration is  $12 \mu\text{sec}$ .

of the blocking oscillator  $V_4$ . Adjustment of the grid bias of  $V_2$  will cause triggering earlier or later, as may be desired. Termination of the input pulse discharges  $C_2$  to a value of several volts because of the “bottoming” of pentode  $V_2$ . The circuit is then ready to operate again.

**10-3. Switch Circuits.**—Switch circuits are much more useful for time selection than the circuits described in Sec. 10-2 since one may employ a three-variable characteristic such as that of multidiode and multigrid switches (see Chap. 3), and hence there is no critical dependence upon the amplitude or shape of the selector pulse. There are, however, two other less stringent requirements for the selector pulse: it must exceed the value of the signal voltage in multidiode switches, or it must exceed the grid base of a multigrid switch.

*Diode-switch Circuits for Unipolar Signals.*—The circuit of Fig. 10-6 indicates a diode-switch circuit suitable for positive pulses.

The signal amplitudes, the circuit impedances, and the bias  $E_{kk}$  are chosen so that the potential of point  $a$  does not exceed ground in the absence of a selector pulse.

A positive selector pulse applied to

With a switching waveform of a low impedance—for example, 500 ohms—and a type 6AL5 diode or germanium crystal giving a value of  $R_d$  equal to a few hundred ohms,  $R_2$  may be as low as a few thousand ohms. The cathode resistor of  $V_2$  should be somewhat greater than  $R_2$  to prevent undue attenuation of the signal during the selection interval.

The diagrams of Fig. 10-6a were obtained by using germanium crystals and indicate on the top line the positive signals applied to the plates of  $V_1$  and  $V_2$  through  $R_2$ . The first three lines indicate the time selection of the second input signal by the selector pulse shown on the second line. The last two lines indicate the time selection of the first input signal. The waveform diagrams indicate several characteristics of this type of circuit: (1) the linearity is reasonably good since the abruptly broken-line characteristics of the germanium crystal is used; (2) there is no noticeable pedestal associated with the selector signal; (3) there is very little leakage of the anticoincident signals caused by capacitance coupling; (4) there is some reaction of the selector pulse upon the input signal (see the first line of Fig. 10-6a).

An example of the practical use of this diode switch in a multiple-coincidence circuit is given in Fig. 10-19.

A limitation of these circuits is, of course, that they respond to unipolar signals only. Another difficulty is the fact that the capacitance coupling between the input and output is not balanced as it is in the four-diode-switch circuits discussed in the next paragraph.

**Diode-switch Circuits for Bipolar Signals.**—Figure 10-7 shows a series diode switch that will accept either positive or negative input signals. A bias developed across  $R_1C_1$  and  $R_4C_2$  from the previous selector pulses

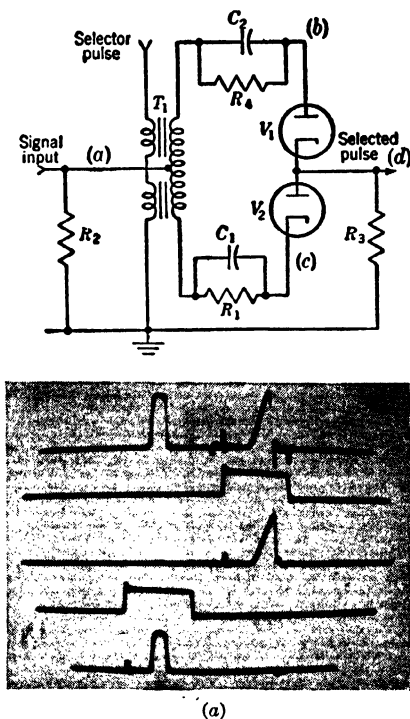


FIG. 10-7.—Bidirectional switch. The waveforms of Fig. 10-7a were obtained with the following component values:  $T_1 = 0A18$ ,  $R_2 = 250$  ohms,  $C_1 = C_2 = 0.1$ ,  $R_1 = R_4 = 510k$ ,  $R_3 = 550$  ohms. The input signals are displayed on the top line and the selector pulse on the second line. The outputs corresponding to these two selector pulses are shown on the third and fifth lines respectively. The sweep duration is 12  $\mu$ sec.

is of sufficient magnitude to maintain  $V_1$  and  $V_2$  nonconducting over the desired excursions of the signal input voltage. Therefore, no output except that due to stray capacitance coupling will appear at  $d$ . A selector pulse applied by transformer  $T_1$  gives a positive and a negative voltage on the plate of  $V_1$  and on the cathode of  $V_2$  respectively. The signal will then be conducted through the leakage inductance of the secondary windings of the transformer and through  $V_1$  for positive signals and  $V_2$  for negative

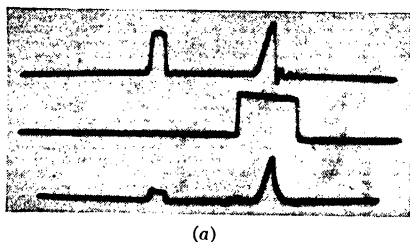
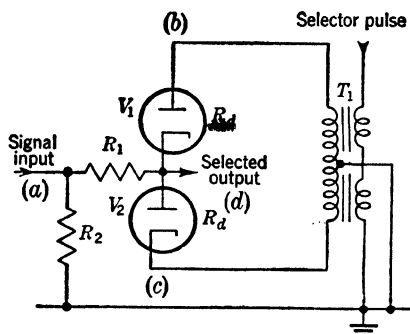


FIG. 10-8.—Shunt diode switch—bidirectional operation. The waveforms of Fig. 10-8a were obtained with the following component values:  $R_2 = 240$  ohms,  $R_1 = 1k$ ,  $T_1 = 0A18$ ,  $V_1 = V_2 =$  Western Electric germanium crystal type D 171612. The first and second lines represent the signal and selector pulses. The coincident signal and the leakage of the anticoincident signal are indicated on the third line. The sweep duration is  $12 \mu\text{sec}$ .

negative signals is similar to that shown for positive ones.

A similar connection of this circuit for shunt or normally conducting operation is indicated in Fig. 10-8 where, in the absence of a selector pulse, the signal output is effectively short-circuited through  $V_1$  and  $V_2$ . The selector waveform appears negatively at  $b$  and positively at  $c$ , and hence disconnects the short circuit. The response of the circuit of Fig. 10-8 to coincident and anticoincident pulses is shown in Fig. 10-8a. Since the diode short circuit is not completely effective ( $R_d \approx R_1$ ), a portion of the anticoincident pulse appears in the output. With a

signals. At the same time the capacitances  $C_1$  and  $C_2$  are recharged to the peak value of the selector pulse and thereby maintain disconnection of  $V_1$  and  $V_2$  in the absence of the selector pulse. Thus, there are two requirements for the selector pulse: (1) sufficient charge must be accumulated in capacitances  $C_1$  and  $C_2$ , and (2) the current through the diodes  $V_1$  and  $V_2$  must be in excess of the signal current through  $R_3$ .

The waveform diagrams of Fig. 10-7a indicate on the first line the input signals and the selector pulse on lines 2 and 4. Outputs obtained on coincidence of the selector pulse with either one of the input pulses are shown on the third and fifth lines. Considerable distortion of the input signal results from the ringing of the transformer which is excited by the selector pulse in the position indicated by the second line. The linearity of the circuit is good, and the response to negative

larger value of  $R_1$  the anticoincident output would be nearly completely attenuated.

The transformer coupling of the selector pulses is not always necessary, as is indicated in Fig. 10-9, where the output signal is short-circuited to the positive and negative power supplies by the diodes  $V_1$  and  $V_2$ . The impedance of the diodes in the region where the signal current does not exceed the current through either tube is approximately  $500\ \Omega$  (see Sec. 3-14). Negative selector pulse  $b$  and positive selector pulse  $c$  disconnect the short circuit and give selected output at  $d$ .

The circuit of Fig. 10-9 has the severe limitation that the output potential in the absence of selector pulse is dependent upon the equality of the positive and negative voltage supply, the resistors  $R_1$  and  $R_2$ , and the diodes  $V_1$  and  $V_2$ . A considerable improvement in this respect is obtained by the configuration of the circuit of Fig. 10-11. In addition, a lower resistance is obtained.

The waveforms of Figs. 10-10*a* and 10-10*b* show the response of the four-diode-switch circuit to positive and negative coincident and anticoincident pulses. In the first line is shown the selector pulse, in the second and fourth lines the input signal, and in the third and fifth lines the coincident and anticoincident outputs. The diagrams indicate that pedestal is completely eliminated and all that remains is capacitance coupling of the switching waveform. A more accurate balancing of the stray capacitance of the diode bridge would equalize any residual effect. The anticoincident signals give no output except for a small capacitance coupling.

The impedance of 200 ohms obtainable with type 6AL5 may be reduced to approximately 100 ohms with germanium crystals. Figures 10-10*c*, 10-10*d*, and 10-10*e* represent operation with selected samples of Western Electric crystals. Figures 10-10*c* and 10-10*d* respectively represent response to coincident and anticoincident negative signals. The linearity of response of the switch to a triangular signal shown in the second line of Fig. 10-10*e* is indicated in the third line. Equal fidelity is obtained for negative signals.

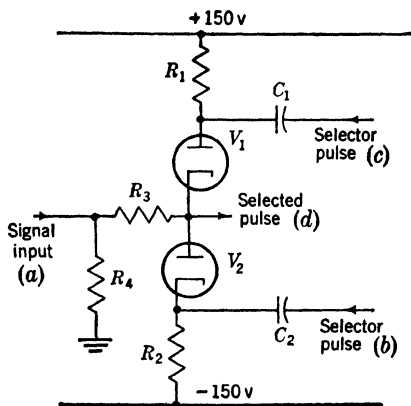


FIG. 10-9.—Shunt diode switch for bi-directional operation. Negative and positive selector pulses applied to the plate and cathode of  $V_1$  and  $V_2$  respectively release the short circuit at point  $d$  and give a selected pulse in the output. Currents of 5 to 10 ma through  $V_1$  and  $V_2$  are usually employed. The resistor  $R_4$  includes the source resistance of the signal. Also  $R_1 = R_2$ .

Figure 10-11 indicates a shunt-diode switch that employs resistance-capacitance coupling of the selector pulses. The normally conducting diode bridge carries roughly 10 ma, and selector pulses of the appropriate

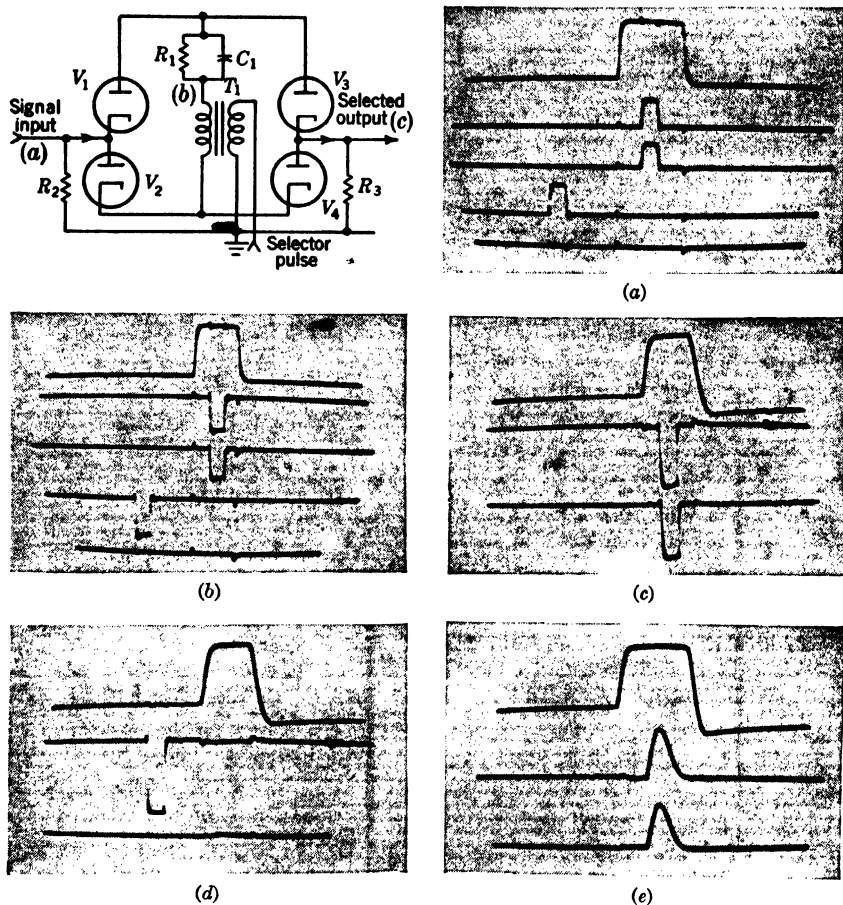


FIG. 10-10.—Four-diode switch. The waveform diagrams indicate operation with thermionic diodes, 10-10a and 10-10b, and with germanium crystals, 10-10c, 10d, and 10e. The circuit values are,  $R_1 = 600k$ ,  $R_2 = 200$  ohms,  $R_3 = 1k$  (for germanium crystals,  $R_3 = 300$  ohms),  $T_1 = 0A18$ ,  $C_1 = 0.01$ . In 10-10a and 10b, the top waveform represents the selector pulse, the second and fourth the input signal, and the third and fifth the coincident and anticoincident outputs. In waveforms 10-10c, 10d, and 10e the top line represents the selector pulse, the second line the signal, and the third line the output. The waveforms are displayed on a sweep of 12- $\mu$ sec duration except for the waveform of Fig. 10-10e that is displayed upon a 120- $\mu$ sec sweep.

polarity release the short circuit from  $R_3$  and permit the selected pulse to appear in the output. As the waveform diagram of Fig. 10-11a indicates, the linearity and absence of pedestal are excellent. Similar results are obtained from negative signals.

The circuit of Fig. 10-11 has an advantage over that of Fig. 10-9 in that the output potential in the absence of selector pulse is set at ground by the diodes  $V_2$  and  $V_4$ . The configuration of Fig. 10-11 is useful since a high-impedance selector pulse may be conveniently used. The advantage of a high-resistance input for the selector pulse is not great in wideband circuits, although it is useful in case the amplitude of the input wave is large. A more significant advantage is that additional signals occurring at the same time may be selected by the addition of only two diodes (duplicating  $V_1$  and  $V_3$ ) to the circuit of Fig. 10-11. If this is attempted with the circuit of Fig. 10-10, addition of the signals occurs in the output.

*Double-triode Switches Giving Bidirectional Operation.*—Figures 10-12 and 10-13 give series- and shunt-connected double-triode switches which provide two-way operation. These circuits resemble those of Figs. 10-7 and 10-9, respectively, except that advantage is taken of the three-variable property of the grid of the triode. In Fig. 10-12 the input waveform is normally disconnected from the output because of the bias developed across networks  $R_1C_1$  and  $R_2C_2$  by the previous selector pulse. A positive selector pulse  $b$  applied to the grids of  $V_1$  and  $V_2$  causes conduction for positive and negative signal inputs. In this case the necessary amplitude of the selector pulse is determined by the grid base of  $V_1$  and  $V_2$  and not, to a first approximation, by excursions of the signal input.

In order to avoid capacitance coupling between transformers  $T_1$  and  $T_2$ , it is desirable that separate transformers be used. If, however, the same transformer is used, the winding should be on different legs of the common core.

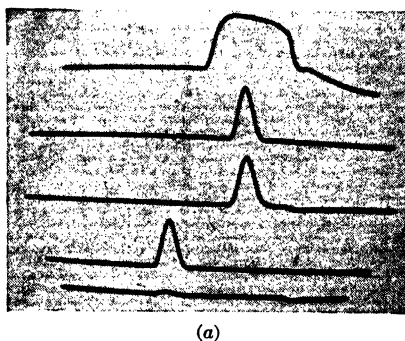
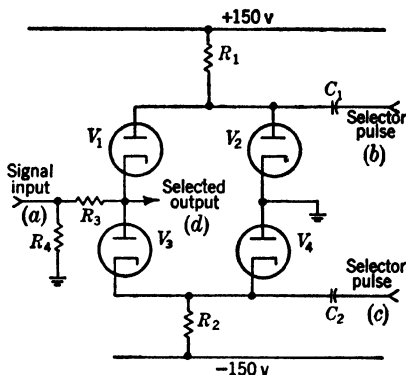


FIG. 10-11.—Four-diode bidirectional switch-shunt operation. The waveforms were obtained using germanium crystals with 10-ma quiescent current. For the particular conditions of Fig. 10-11a,  $R_4 = 200$  ohms,  $R_3 = 1k$ ,  $R_1 = R_2 = 15k$ ,  $C_1 = C_2 = 0.01$ . The selector pulses were generated at an impedance of roughly 200 ohms. The top line indicates the selector pulse, the second and fourth lines signal inputs, and the third and fifth lines coincident and antioincident outputs. The waveforms are displayed on a sweep of 120- $\mu$ sec duration.

The response of the circuit of Fig. 10-12 is shown in the waveform diagrams of Figs. 10-12a and 10-12b. The response to positive and negative coincident and anticoincident signals is shown in the third and fifth lines respectively. The capacitance coupling of the anticoincident signal to the output through the pulse transformer and stray inter-electrode capacitances is evident in the bottom line of these two figures.

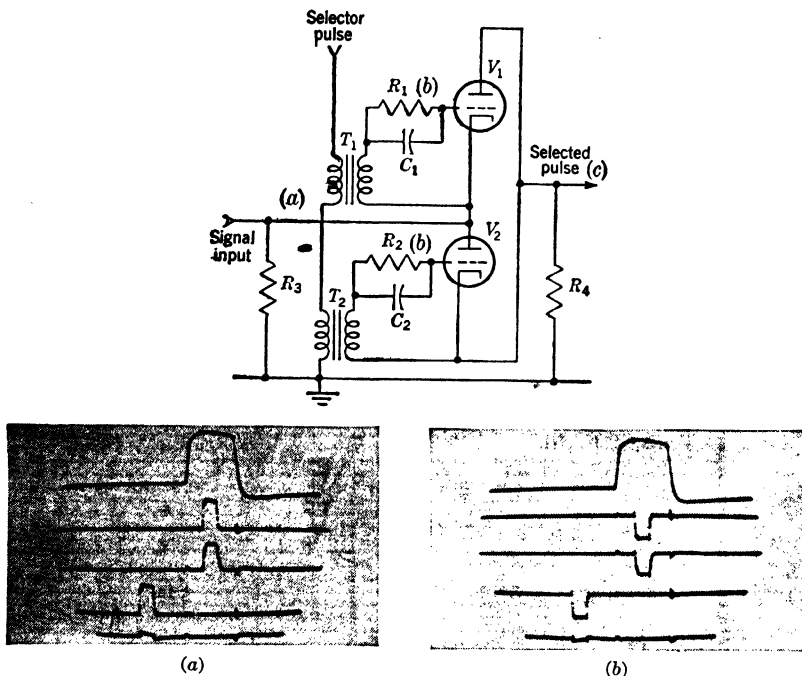


FIG. 10-12.—Double-triode bidirectional switch. The circuit values for the particular waveforms shown are  $V_1 = V_2 =$  type 6SN7;  $T_1$  and  $T_2$  represent separate legs of the same transformer, type 0A18.  $R_3 = 200$  ohms,  $R_1 = R_2 = 620k$ ,  $C_1 = C_2 = 0.01$ ,  $R_4 = 5.1k$ . The waveform diagrams of Figs. 10-12a and b show the selector pulse on the top line, coincident and anticoincident signals on the second and fourth lines, and the output on the third and fifth lines. The sweep duration is approximately 12  $\mu$ sec.

The cancellation of the switching pulse and the linearity are, however, excellent.

A normally conducting circuit is shown in Fig. 10-13; a negative selector pulse in excess of the excursions of the input signal is applied to the grids of  $V_1$  and  $V_2$  and permits disconnection of the short-circuiting action of these tubes and conduction of the desired signals into the output circuit.

This circuit has a severe disadvantage compared with the transformer-coupled circuit of Fig. 10-12. The output resistance is unequal for positive and negative signals. With positive signals the plate resistance

of a triode  $V_2$  is obtained, and with negative signals the cathode-follower resistance of  $V_1$  is obtained.

Although these circuits permit a high-impedance selector pulse, some grid current (5 to 10 ma) must flow to obtain a reasonably low-impedance switch circuit. In most cases the desired selector pulses are generated from blocking oscillators at impedances of 100 or 200 ohms, and the possibility of employing a high-impedance selector pulse is of little practical advantage except, of course, for the time selection of slowly varying waveforms.

*Parallel Cathode Followers or Pentodes.*—A well-known switch circuit for time selection is indicated in Fig. 10-14. This circuit is, however, suitable only for negative pulses which have no positive parts since the circuit shows no time selectivity whatsoever for positive signals. It consists of a pair of normally conducting cathode followers arranged in such a way that disconnection of one permits the conduction of the input waveform through to the output terminals. Since the tubes  $V_1$  and  $V_2$  are normally conducting, their dissipation may be exceeded if  $R_3$  is reduced to give good response for short pulses.

The waveform diagram of Fig. 10-14a indicates on the top line a negative selector pulse applied to the control grid of  $V_2$ . Two negative signals are applied to the control grid of  $V_1$ , the first anticoincident and the other coincident, and the output is indicated on the third line. The low impedance of cathode follower  $V_2$  maintains the output potential relatively constant in spite of the cutoff of  $V_1$  due to the anticoincident signals. The very small back swing of this signal, however, does appear in the output. The slight pedestal due to the selector pulse is also indicated. The linearity of this circuit is excellent as the third line of the diagram indicates.

A similar connection using parallel pentodes is indicated in Fig. 10-18. Here both pentodes are conducting with the result that a negative selector pulse applied to the grid of  $V_2$  will not cause a change of the output potential, unless a negative signal is simultaneously applied to the grid of  $V_1$ .

The operation of this circuit is indicated by the waveform diagram,

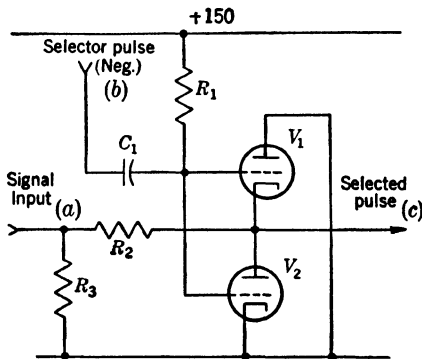


FIG. 10-13.—Double-triode bidirectional switch. The grids of  $V_1$  and  $V_2$  are biased positively and draw several milliamperes in the absence of a selector pulse. A negative selector pulse applied at (b) will release the short circuit at the point c giving a selected pulse in the output.



Fig. 10-15a, the first line representing the negative selector pulse applied to the control grid of  $V_2$ , and the second line representing coincident and anticoincident negative pulses applied to the control grid of  $V_1$ . The output is represented in the third line, and for the particular value of  $R_3$  used, appreciable selector pulse and anticoincident signal appear

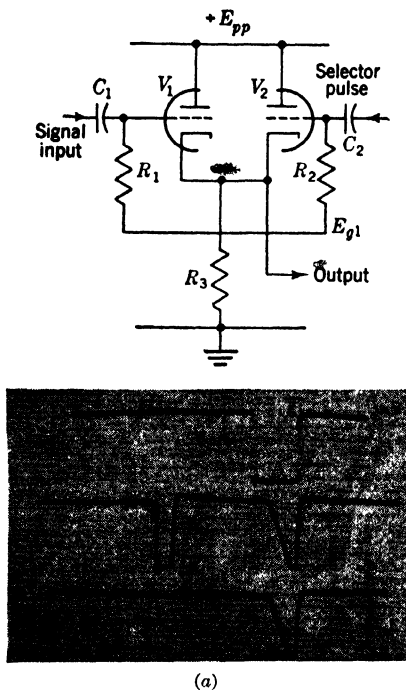


FIG. 10-14.—Time-selector circuit using parallel cathode followers. The waveform diagrams of Fig. 10-14a were taken with  $V_1 = V_2 =$  type 6SN7,  $R_3 = 10k$ ,  $C_1 = C_2 = 0.1$ ,  $R_1 = R_2 = 1M$ ,  $E_{g1} = +90$ ,  $E_{pp} = +300$ . The first and second lines indicate the inputs to the control grids, and the third line indicates the output at the cathode. The sweep duration is approximately 1200  $\mu\text{sec}$ .

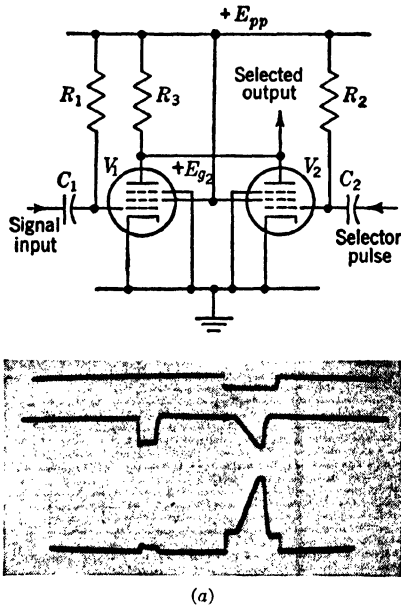


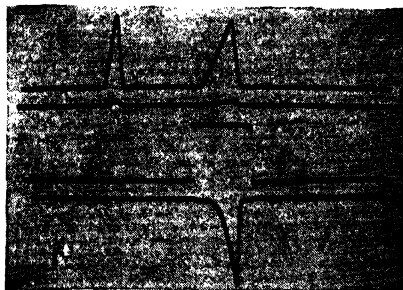
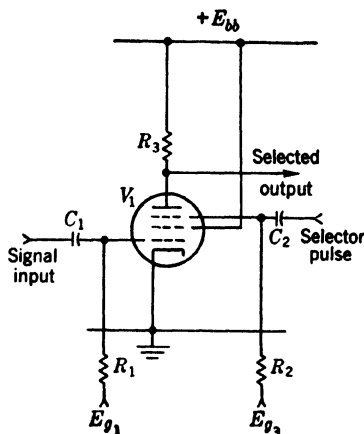
FIG. 10-15.—Time selector using parallel pentodes. The waveforms were obtained with  $V_1 = V_2 = 6AK5$ ,  $R_3 = 18k$ ,  $C_1 = C_2 = 0.1$ ,  $R_1 = R_2 = 1.5M$ ,  $E_{g2} = +40$ ,  $E_{pp} = +120$ . The first and second lines represent the signals applied to the control grids, and the third line represents the selected output. The sweep duration is approximately 1200  $\mu\text{sec}$ .

in the output. The rejection of pedestal and anticoincident signals can be increased by increasing  $R_3$ , but at the expense of speed of response. The tubes in Fig. 10-15 are not "bottomed," since this condition would lead to nonlinear operation.

One advantage of these circuits is that high-impedance input signals may be employed and that a number of units may be connected in parallel for multiple-coincidence operation (see Sec. 10-4).

**Pentodes and Multigrid Switches.**—The most useful time selectors for high-impedance signal and selector pulse employ the pentode or multigrid switch, and the selector pulse is applied to the suppressor grid of a pentode or control grid,  $g_3$ , of the multigrid tube. The use of type 6AS6, developed specifically for this purpose, is indicated in Fig. 10-16, where a positive selector pulse is applied to the suppressor grid and the signals are connected to the control grid. Because of the characteristic of the suppressor grid of this tube, the amplitude of the selector pulse is not critical providing it carries the grid positive with respect to the cathode; and under normal operating conditions, a selector pulse of 5 or 10 volts is adequate. Some tubes require a resistance in series with  $g_3$  to avoid a decrease of plate current at positive suppressor voltages. The short grid base of this tube permits the use of a small signal. The screen grid is, however, conducting in the absence of a selector pulse, and a sizable current must be maintained in order to have an adequate plate current at the time of the selector pulse. Type 6AS6 has an especially high screen-current rating<sup>1</sup> for this purpose.

The operation of this circuit is indicated in the waveform diagram of Fig. 10-16a where the top line indicates a scaled-up version of the signals applied to the control grid of the multigrid selector. The actual amplitudes of the input signal, the selector pulse, and the selected output are

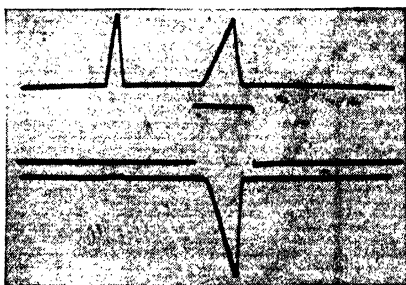
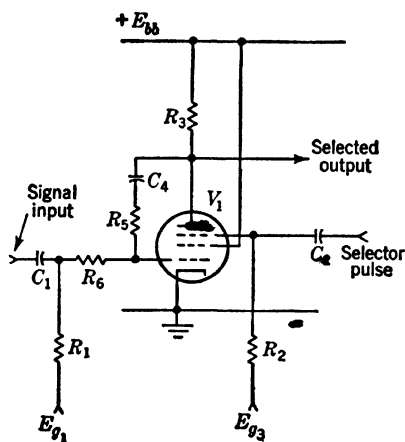


(a)

FIG. 10-16.—Pentode time selector. Signals applied to the control grid coincident with the selector waveform applied to the suppressor grid are selected. The waveforms of Fig. 10-16a were obtained with  $V_1 = 6AS6$ ,  $C_1 = C_2 = 0.1$ ,  $R_1 = R_2 = 47k$ ,  $R_3 = 15k$ ,  $E_{pp} = +120$ ,  $E_{g1} = -6v$ ,  $E_{g2} = -42v$ . The signal applied to the control grid is shown on the second line and that applied to the suppressor grid is shown on the third line. The first line indicates the signal input at a higher scale factor. The last line represents the selected output. The sweep duration is approximately 1200  $\mu sec$ .

<sup>1</sup> In some circuits additional screen voltage is applied before and after the occurrence of the selector pulse in order to achieve higher transconductance and avoid exceeding the screen dissipation.

shown in the second, third, and fourth lines, respectively. It is evident that there is nearly a complete absence of leakage of the anticoincident signal and only a small amount of pedestal from the selector pulse. The



(a)

FIG. 10-17.—Pentode time selector with negative feedback. The output waveform shown on the third line of Fig. 10-17a indicates the improvement of linearity due to the addition of the negative-feedback network  $C_4$ ,  $R_4$ , and  $R_5$ . The first and second lines indicate the signals applied to the control grid and suppressor grid respectively. The waveforms were obtained with the following component values:  $C_4 = 0.1$ ,  $R_5 = 62k$ ,  $R_4 = 30k$ . Other conditions of the circuit of Fig. 10-16 were unchanged; the sweep duration was 1200  $\mu\text{sec}$ .

of the input and output waveforms indicates. The gain is closely represented by the ratio  $R_5/R_4$ .

There is, of course, some feedthrough of the input signal to the output circuit in the absence of a selector pulse because of the feedback network.

linearity of the circuit is poor since  $g_1$  is biased nearly to cutoff in order to obtain freedom from pedestal. The triangular signal input is converted into a much narrower curved signal. Types 6AS6 and 6AC7 have a relatively sharp cutoff of  $g_1$ ; in other pentodes and multigrid tubes—for example, types 6L7 and 6SA7—the curvature is more severe.

Greater linearity may be obtained by increasing the screen current in the absence of selector pulse. This leads to an increase in the pedestal and may be objectionable in this time-selector circuit. On the other hand, pedestal may be tolerated in the double time selectors used in time discrimination, and under these circumstances the screen rating of the multigrid tube is of importance.

A significant improvement of linearity is provided by the circuit of Fig. 10-17, where negative feedback between the output and input of the time selector is obtained by the network,  $C_4$ ,  $R_4$ , and  $R_5$ . The performance of this circuit, shown in Fig. 10-17a, indicates the accurate reproduction of the input wave as represented by the strictly linear fall of the output voltage. This circuit has the well-known property of negative-feedback circuits—a low but known gain—as the size

This pulse is, however, of opposite sign to that obtained from coincident signals and is therefore unlikely to cause difficulty.

Except for the necessity of maintaining a reasonable screen dissipation, these multigrid circuits give performance on a par with the four-diode-switch circuits shown in Figs. 10-10 and 10-11.

**10-4. Multiple-coincidence Circuits.**—There are many ways in which satisfactory multiple-coincidence circuits may be made by a combination of the circuits described previously. For example, network addition and amplitude selection are always possible—though these have numerous difficulties. More practical circuits employ the multigrid tube as indicated in Fig. 10-18, where a selector pulse has been applied to the screen grid of type 6AS6 as well as to its suppressor grid. Although this arrangement is unsatisfactory for some purposes since pedestal is introduced and the output current depends upon the amplitude of the pulse applied to the screen, it has the advantage that considerably higher screen voltage may be used than when a continuous screen current is passed.

A most efficient and satisfactory arrangement is shown in Fig. 10-19, which is a combination of the multigrid time selector with the simple diode-switch of Fig. 10-6. The input pulse and selector pulse *c* are short-circuited through normally conducting diodes  $V_1$  and  $V_2$ . Pulses can reach the control and suppressor grids of the time selector only after positive selector pulses *b* and *d* have been applied to the cathodes of  $V_1$  and  $V_2$  and thereby the positive waveforms *a* and *c* are allowed to vary the control and suppressor grid potential, respectively.

The first four lines of Fig. 10-19a give the input signals and the three selector pulses, two of which are coincident with the desired signal, and the third of which is anticoincident. The output contains no trace of the signal or selector pulse. Coincident operation is indicated in Fig. 10-19b, where the input wave is reproduced with high fidelity.

Operation for multiple coincidences can be obtained by the addition of a number of diode switches in parallel with  $V_1$  and  $V_2$  in such a way that the waveforms *a* and *b* cannot reach the control electrodes of  $V_3$  until the desired number of positive waveforms have coincided.

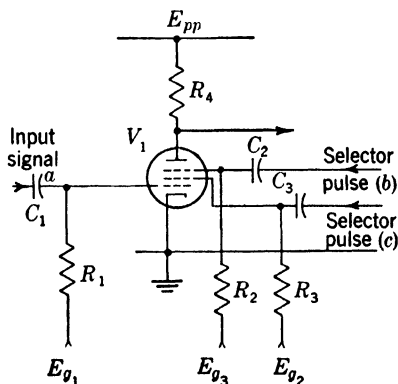


FIG. 10-18.—Triple-coincidence circuit for positive pulses. Positive selector pulses are applied to the suppressor and screen grids of  $V_1$ , and the input signal is connected to the control grid. The pulse applied to the screen should be capable of supplying 10 or 20 ma.

Similar combinations of circuit elements can be made suitable for negative pulses by the addition of more tubes in parallel with those indicated in Figs. 10·14 and 10·15. In this case, however, the average current drain from the power supply will be large.

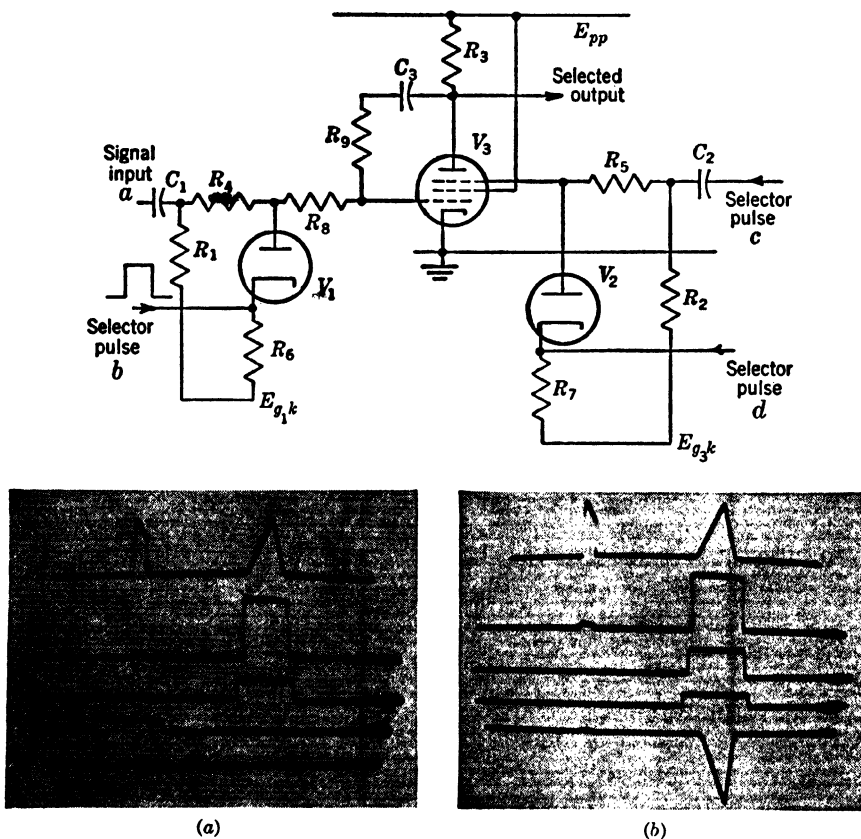
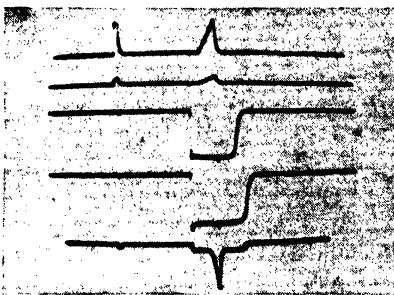
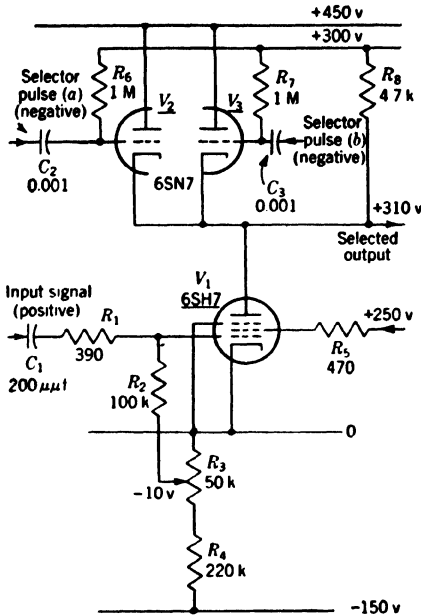


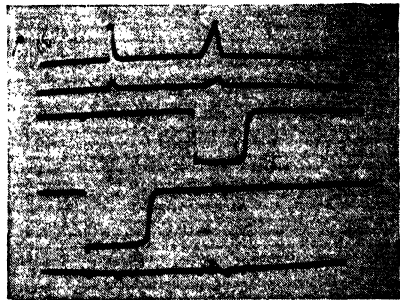
FIG. 10-19.—Quadruple-coincidence circuit for positive pulses. The output waveforms were obtained with the following component values:  $V_3 = 6AS6$ ,  $V_1 = V_2 = \frac{1}{2}6AL5$ ,  $C_1 = 0.05$ ,  $R_1 = 47k$ ,  $C_2 = 0.1$ ,  $R_2 = 47k$ ,  $R_3 = 5k$ ,  $R_4 = 15k$ ,  $R_5 = 1k$ ,  $R_6 = 30k$ ,  $R_7 = 62k$ ,  $C_3 = 0.1$ ,  $E_{pp} = 130$ ,  $E_{q_1k} = -9v$ ,  $E_{q_2k} = -10v$ . The waveform diagrams indicate on the top line the signal applied at point  $a$ , on the second line the selector pulse applied at point  $b$ , on the third line the selector pulse applied at point  $d$ , and on the fourth line the selector pulse applied at  $c$ . The bottom line shows the anticoincident and coincident outputs. The sweep duration is  $1200 \mu\text{sec}$ .

Figure 10-20 shows another triple-coincidence circuit. The tubes  $V_2$  and  $V_3$  are conducting and passing a small plate current through  $V_1$ , since its grid bias is set at the negative end of its linear range. Under these conditions a positive pulse on the control grid of  $V_1$  will result in an increase of current through  $V_2$  and  $V_3$  and a negligible change of potential

drop in  $R_8$  because of cathode-follower action. Similarly, if a negative selector pulse is applied to the grid of either  $V_2$  or  $V_3$ , a positive pulse on the control grid of  $V_1$  will have a negligible effect upon the output. On



(a)



(b)

FIG. 10-20.—Triple-coincidence circuit using a pentode as load resistance for parallel cathode followers. The waveforms were taken with the component values and voltages indicated in the figure. The top two lines show the input signal (amplified and direct), and the third and fourth the selector pulses. The bottom lines indicate the coincident and anticoincident output. The sweep duration is 120  $\mu\text{sec}$ .

the other hand, if both  $V_2$  and  $V_3$  are cut off, a negative pulse is obtained at the plate of  $V_1$ .

The waveform diagrams of Fig. 10-20a show on the second line the actual input signal, and on the top line a scaled-up version of it. The two

selector pulses are shown on the third and fourth lines, and a coincident output is shown on the fifth line. The circuit has three obvious faults: (1) the feedthrough of the anticoincident signals, (2) the portion of the selector pulse appearing in the output, and (3) the obvious nonlinearity. The response obtained with the second selector pulse in anticoincidence is shown in Fig. 10-20b, and the transmission of the input signals is still visible. In view of the complexity and poor performance of this circuit in comparison with that of the multigrid coincidence circuit, it seems desirable to use the latter wherever possible.

**10-5. Adjacent Time Selectors.**—It is often desired to determine not only whether two pulses coincide but the accuracy with which they coincide. This is a part of the important process of time discrimination described in Sec. 14-7. A pair of tubes supplied with adjacent selector pulses are suitable for this purpose, and a typical example is shown in Fig. 10-21.

This circuit consists of two multigrid time selectors identical with those employed in Fig. 10-17. As is shown in the top line of waveform diagram Fig. 10-21a, positive input signals are connected to the parallel-connected grids of  $V_1$  and  $V_2$ . Adjacent selector pulses shown in the second and third lines are centered with respect to the signal, and are of slightly greater total duration. These pulses are connected to the suppressor grids of  $V_1$  and  $V_2$ . The fourth line shows the difference of the output obtained between the plates of  $V_1$  and  $V_2$ . The difference was obtained by connecting the outputs of  $V_1$  and  $V_2$  to the opposite plates of an oscilloscope, and indicates an initial response to the overlap of the first selector pulse and the signal, and then to the second selector pulse and the signal. For the relative timing of signal and selector pulses shown, the sum of the areas is nearly equal to zero. The output is, however, sensitive to a small displacement of the selector pulses with respect to the signal. As Fig. 10-21b indicates, an increase of the delay of the selector pulses with respect to the input signal results in an output that is predominantly negative. Similarly an earlier occurrence of the selector pulses gives an output that is predominantly positive. Detection of the area of the output by the difference detectors of Sec. 14-6 gives a sensitive indication of the relative time of occurrence of the signal and selector pulses.

It is often desired to select the whole signal itself in addition to the differential signal for the purposes of automatic volume control, etc. (see Vol. 20, Sec. 8-11). The common output of the tubes  $V_1$  and  $V_2$  is taken by summing the differential outputs in resistance networks.

A wideband version of Fig. 10-21 for selecting 0.1- $\mu$ sec pulses is indicated in Fig. 10-22. In this case, type 6AC7 tubes are used with suppressor control in order to obtain higher transconductance. As the

circuit indicates, a bias of 130 volts is necessary to ensure nonconduction of limit tubes in the absence of a selector pulse. The positive input signal is applied to the parallel-connected control grids of pentodes and is d-c-restored by  $V_2$ . Cathode resistors,  $R_1$  and  $R_2$ , are employed to improve the linearity of the time selector. Especial attention is paid

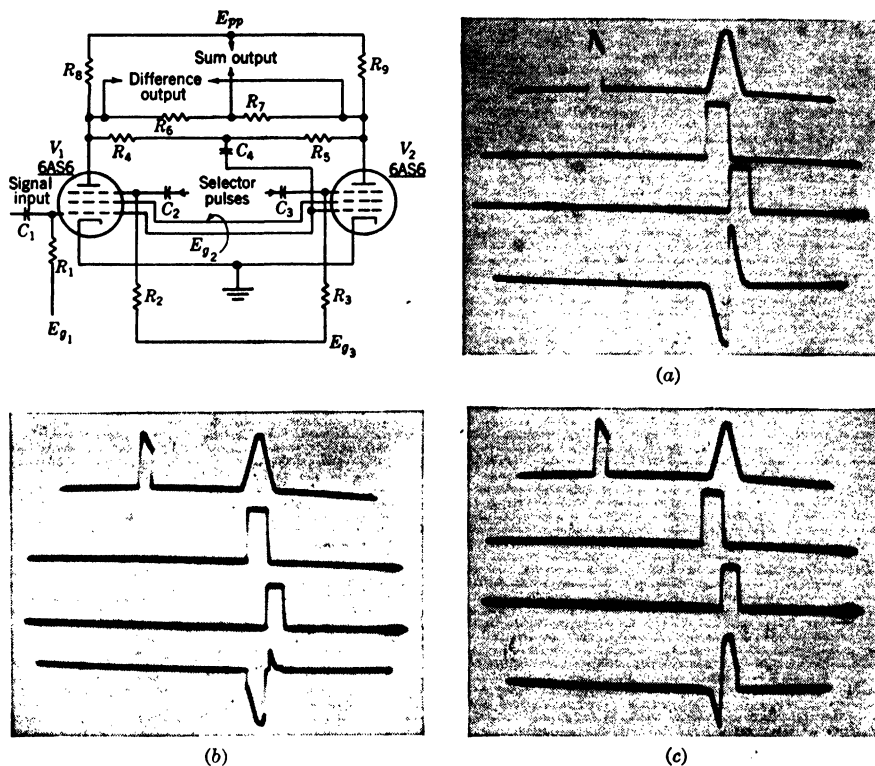


FIG. 10-21.—Adjacent time selectors. The waveforms indicate on the top line the signals, on the second and third lines the selector pulses, and on the fourth line the variations of the differential output at the plates of  $V_1$  and  $V_2$  depending upon the relative times of occurrence of the input signal and the selector pulses. These waveforms were obtained with the following component values:  $V_1 = V_2 = 6AS6$ ,  $R_1 = R_2 = R_3 = 47k$ ,  $C_1 = C_2 = C_3 = C_4 = 0.1$ ,  $R_4 = R_5 = R_6 = R_7 = 62k$ ,  $R_8 = R_9 = 15k$ ,  $E_{pp} = 130$ ,  $E_{g1} = -3.5$ ,  $E_{g2} = -32$ . The sweep duration was 120  $\mu\text{sec}$ . The output waveforms were attenuated by  $\frac{1}{4}$ .

to the series and shunt peaking of the plate circuit in order to obtain maximum bandwidth ( $\sim 16$  Mc/sec) and to adjust the response properly for the capacitance of the difference-detector circuit to which the output is usually connected (see Sec. 14-6 of this volume and Sec. 8-14 of Vol. 20).

A novel<sup>1</sup> time selector for giving current outputs is indicated in

<sup>1</sup> F. C. Williams *et al.*, "Linear Time Base Generators, Delay Generators and Time Discriminators," I E.E. Convention Paper, 1945.



Fig. 10-23. As a time selector, this circuit has no great advantages over the previous circuits, but it has very important features for time discrimination (see Vol. 20, Sec. 8-13). Although the configuration might appear to be similar to that of Fig. 10-20, in this case,  $V_2$  and  $V_3$  are *nonconducting*, and the current caused by a positive signal on the grid of  $V_1$  is carried by diode  $V_4$ , which maintains the cathodes of  $V_2$  and  $V_3$  at ground potential. If a positive signal is coincident with a selector pulse on  $V_2$ , the current set up in  $V_1$  traverses  $V_2$  and the current transformer

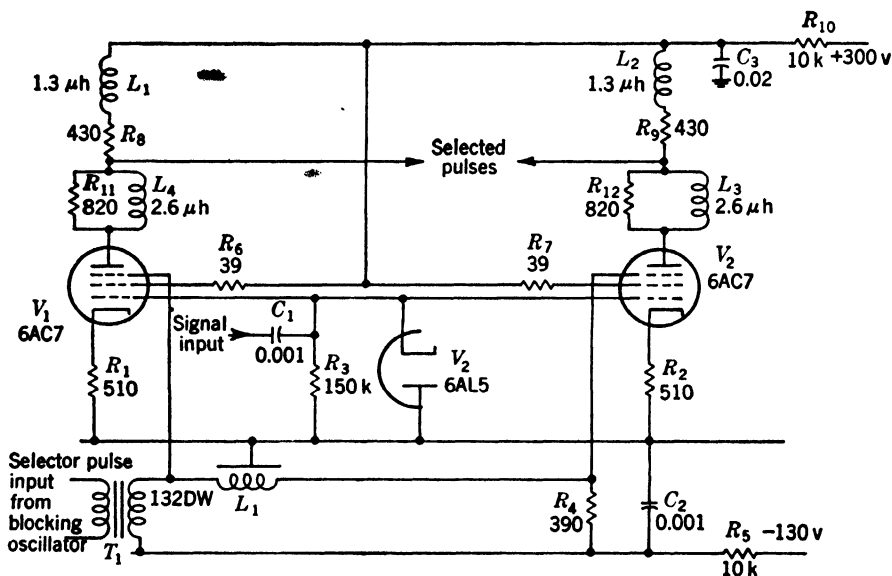


FIG. 10-22.—Adjacent time selectors for 0.1- $\mu$ sec pulses. Two suppressor-gated pentodes giving selected outputs rising and falling in roughly 0.05  $\mu$ sec are employed in this circuit. The particular circuit constants in the output are adjusted to operate into the stray capacitance of a type 6AL5 differential detector circuit.  $L_1$  is a delay line of duration approximately equal to that of the input selector pulse.

$T_2$  to produce a current in  $R_9$ . Similarly conduction of  $V_3$  coincident with  $V_1$  will give a current in the opposite direction. But conduction of  $V_1$  while both  $V_2$  and  $V_3$  are conducting will give a cancellation of the current in  $T_2$ . As in Fig. 10-21, a signal proportional to the amplitude of the input signal may be obtained through current transformer  $T_1$ , which is placed in the common supply to  $V_2$  and  $V_3$ .

The circuit above obtained reversal of the output current by means of the transformer. A circuit which combines an amplifier and cathode follower in a series-triode switch, is indicated in Fig. 10-24. In this case, the selector pulses are applied to the plates of  $V_1$  and  $V_2$ , and the signal is connected to the control grids. Furthermore, only one selector pulse is applied, and the signal, instead of the selector pulse, is split into two portions.

If it is assumed that a positive selector pulse is applied to the plates of  $V_1$  and  $V_2$  in the absence of a signal input, equal currents flow in  $V_1$  and  $V_2$ , and, for similar tubes and resistances, the potential of point  $d$  will remain constant. If, for example, a positive signal that coincides with the selector pulse is present, at first  $V_1$  conducts and thereby raises the potential of point  $d$ . Three-tenths of a microsecond later,  $V_2$  conducts and lowers the potential of point  $d$ . The shape of the pulses at  $d$  are therefore related to the overlap of the signal and the selector pulse.

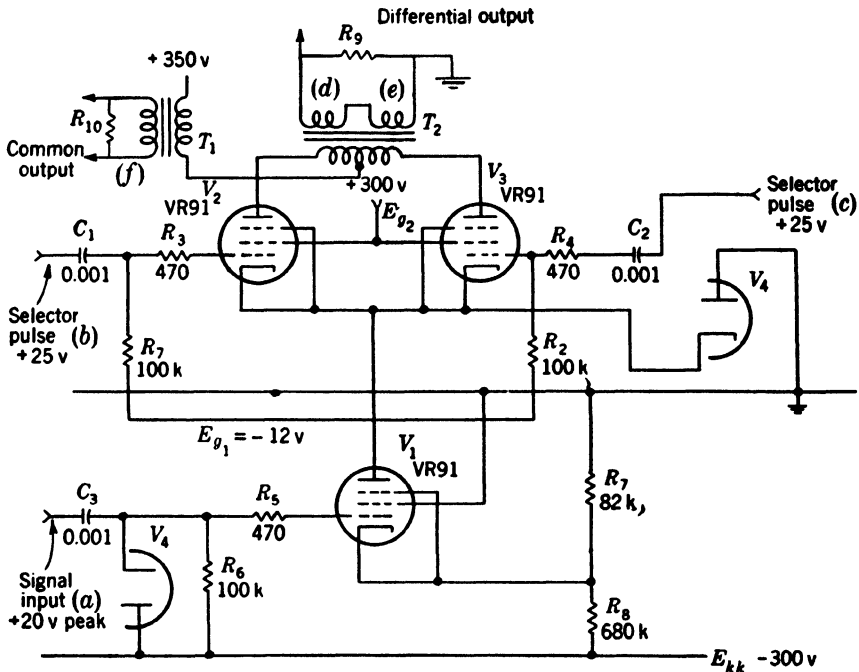


FIG. 10-23.—Adjacent time selectors.  $V_2$  and  $V_3$  are normally nonconducting, and the current through  $V_1$  is diverted through  $V_4$  unless  $V_2$  or  $V_3$  is conducting. The circuit constants are adjusted for British type VR-91 but, with small adjustments of the bias and screen voltages, satisfactory operation may be obtained with types 6AK5 or 6AC7.

If  $d$  is connected to a storage condenser, the circuit functions as a time discriminator (see Sec. 14.7).

In certain cases it is desirable that no output for small signals or for noise be obtained from the time selector, and, therefore, positive bias is provided for the cathodes of  $V_1$  and  $V_2$  by pulse  $e$ , which precedes and lasts longer than the selector pulse.

**10-6. Cathode-ray-tube Displays.**—Cathode-ray-tube displays are extensively used in radar systems for visual time selection. A triangular waveform is applied to the horizontal plates of the scope, and the pulses to be selected are applied to the vertical plates or to the control grid. An observer may then concentrate his attention upon any desired pulse.

Alternatively a photocell may be placed in front of the desired signal, and electrical signals containing the selected pulse are obtained at the output. Although this method has not been widely used, it presents an extremely flexible, but bulky, method of time selection—that is, a

variation of the sweep speed or the use of a mask in front of the phototube will vary the duration of the sensitive interval. With the phototube an intensity-modulated signal is much more useful than a deflection-modulated signal.

Several practical systems have been made that use the cathode-ray-tube-photocell system in this manner. In a particular case, a type 2AP5 cathode-ray tube was operated at 1.7 kv, and approximately unity gain from the control grid of the cathode-ray tube to the output of the photo-multiplier was obtained, using a total voltage of 1 kv and an output resistor of 100,000 ohms. The sweep speed was 0.5 in./ $\mu$ sec and the input pulses had a duration of 0.3  $\mu$ sec. With the high value of load resistor, the output pulses had a duration of roughly 10  $\mu$ sec. (For further details of a time demodulator using this principle, see Sec. 14-9.)

A considerably more rapid response is obtained if the output resistor is reduced and an amplifier is added. If the negative-capacitance amplifier of App. A were employed, a reasonable reproduction of a 1- $\mu$ sec pulse may be obtained.

In another method, time selection may be obtained by the application of a small electrode to the face of the cathode-ray tube. The discussion of cathode-ray-tube storage devices in Chap. 21 indicates that an electrode attached to the outer glass surface of an ordinary cathode-ray tube gives signals of approximately 300 mv for 1- $\mu$ sec input signals.

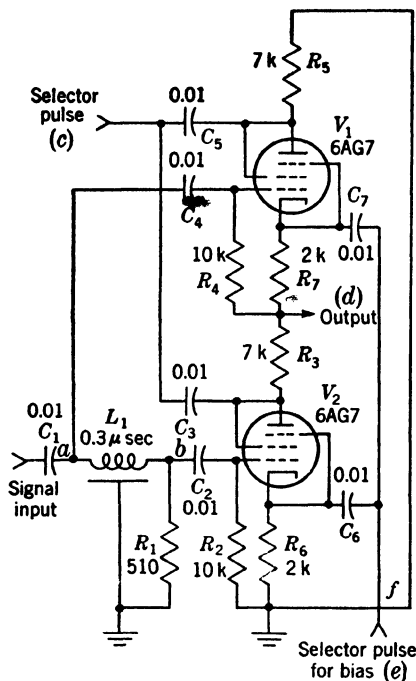


FIG. 10-24.—Adjacent selectors using series pentodes. Positive selector pulses and positive signal inputs applied to the plates and grids of  $V_1$  and  $V_2$  respectively give at the output  $d$  the difference of the overlap between the selector and signal input. The latter is split by a delay line equal to the duration of the input signal. A bias pulse which controls the amount of conduction of  $V_1$  and  $V_2$  in the absence of signal input is applied to their cathodes by waveform  $e$  which starts before, and lasts longer than, the selector pulse. For operation as a difference detector (see Chap. 14), point  $f$  is returned to a slightly negative potential and a condenser is connected to  $d$ .

## CHAPTER 11

### ELECTRICAL AMPLITUDE MODULATION

BY BRITTON CHANCE

**11.1. Introduction.**—This chapter makes no attempt to survey the field of amplitude modulation as used in communication but presents a number of methods especially suited to certain requirements of circuit design and electronic instrumentation. Information on processes of importance in communication, such as the conversion of audio or video signals to suitable bands for radio transmission, is found in a number of standard texts.<sup>1</sup>

The usual definition of amplitude modulation, a process by which the amplitude of a waveform is varied in accordance with a signal, includes modulation in response to both electrical and mechanical signals. The modulation of electrical waves with electrical signals is the subject of this chapter, and modulation with mechanical signals is the subject of Chap. 12.

Demodulation methods giving electrical outputs are presented in Chap. 14, and those giving mechanical outputs are discussed in considerable detail in Vol. 22 of this series, Part II.

An important use of electrical amplitude modulators is in the conversion of low-frequency signals to modulated carriers, with a-c amplification and subsequent demodulation as a more stable substitute for d-c amplifiers. Other important applications use electrical modulation for obtaining lower output impedance or transformer-isolated d-c signals through carrier amplification, transformer coupling, and demodulation.

For the latter two applications, the level of the input signal is so high that the thermionic-vacuum-tube modulator may be employed without difficulties due to drift. But for low-level signals numerous experimental data indicate that most modulator circuits represent a relatively small increase in stability over a carefully designed d-c amplifier. In fact, experimental tests have indicated that the relative drift rate of a diode modulator using type 6AL5 is only about one fourth that of a differential amplifier using type 6SU7 (see Chap. 9). Although there is, therefore, no major reason for replacing a stable d-c amplifier by an electrical amplitude modulator, other requirements of the circuit design may make

<sup>1</sup> F. E. Terman, *Radio Engineers' Handbook*, McGraw-Hill, New York, 1943, Sec. 7; M.I.T. E. E. Staff, *Applied Electronics*, The Technology Press, 1943, Chap. 7.

this desirable; for example, stabilized supply voltages may not be available, or an a-c output may be desirable—for example, to operate a two-phase servomechanism. Also greater flexibility is permitted in the design of the modulator stage since its voltage gain is not important and specialized conditions favoring high input resistance are feasible. Once the modulated signal is obtained, the remaining amplifier stages are of simple design.

A significant gain of stability is obtained from amplitude modulators which employ mechanical devices giving capacitance, inductance, or resistance variation. A well-known example of this class is the mechanical-switch (Brown Converter); its drift is a few tenths of a microvolt over a long period of time and the carrier level (hum) is about a microvolt. These devices are of such great importance in circuit design that a considerable portion of the chapter is devoted to their characteristics.

Electrical amplitude modulation is often used for modulation of rapidly varying waveforms used in PPI or type B cathode-ray-tube displays (see Vol. 22 of this series) or for the simulation of amplitude-modulated echoes observed in scanning-radar systems. In these circuits the waveform of the carrier is nonsinusoidal.

In most of the examples of this chapter the carrier waveform is not reproduced in the output, but a few examples are given of circuits that preserve a sinusoidal carrier. The latter circuits, which usually depend upon the curvature of the characteristic of a vacuum tube, are often of low precision. Those giving accurate operation and still preserving the carrier waveform may be more precisely described as multiplying circuits and are therefore discussed in Chap. 19.

The frequency spectrum of the modulated wave is not discussed in detail since many data are already available in textbooks.<sup>1</sup> Also this approach is of less value in the modulation of complex waveforms. The various methods of frequency selection used to remove the modulating signal or carrier from the output of a modulator are not discussed in this chapter since complete information on electric filters is also obtainable in standard texts. Some very useful frequency selectors employing the twin-T are described in Vol. 18, Chap. 10, of this series.

Applications of amplitude modulation and demodulation for obtaining large current outputs or transformer-isolated signals will not be discussed separately because the methods of modulation and demodulation presented in this and the following chapters may be combined with a suitable transformer to make a satisfactory system.

**11.2. Signal-controlled Amplitude Selectors.** *Unbalanced Half-wave Circuits.*—The possibility of amplitude modulation by amplitude selection has already been mentioned in Sec. 3.7. A typical example is indicated

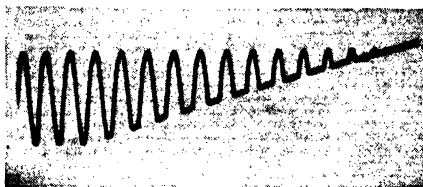
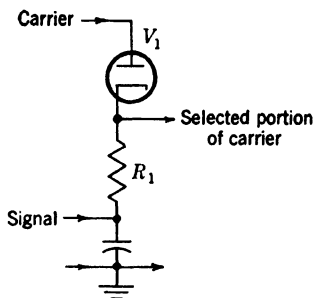
<sup>1</sup> Terman, *loc. cit.*

in Fig. 11-1, where a diode amplitude selector is used to select portions of a sinusoidal carrier that exceed its cathode potential and thus to give an amplitude-modulated wave. Alternatively the load impedance  $R_1$  can be put in the plate circuit; the modulated output would then represent portions of the carrier that were less than the cathode potential. Thus in the first case, the negative excursions of the carrier would be modulated, whereas in the second case the positive excursions of the carrier would be modulated.

The circuit of Fig. 11-1 illustrates some important features of modulators employing amplitude selection. First, the amplitude of the modulated wave is linearly related to the amplitude of the modulating signal, provided that the carrier voltage is much greater than the slope discontinuity of the broken-line characteristic of the diode. Linear modulation is therefore obtained with 20- or 30-volt carriers for thermionic diodes, and somewhat smaller values may be used with contact rectifiers. The linearity of modulation is, however, of little importance in modulation-demodulation systems employing negative feedback. Second, the range of linear modulation is approximately equal to the peak-to-peak value of the carrier, although this higher range is rarely used with low-level modulating signals. Third, the stability is entirely dependent upon the characteristics of the diode as an amplitude selector, and these have been discussed in detail in Secs. 3-14 and 9-3. For highest stability one would, of course, apply a signal voltage roughly equal to the carrier, but this is not possible in low-level applications.

The waveform diagram of Fig. 11-1 clearly indicates the weaknesses of this modulator circuit, since there is no cancellation of the signal or carrier. In addition, the circuit is not responsive to bidirectional signals, as is often required in amplitude discrimination.

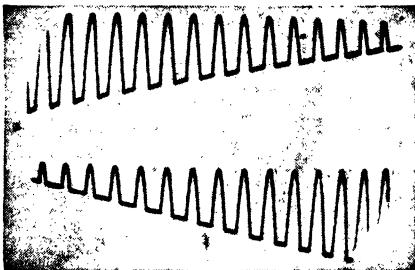
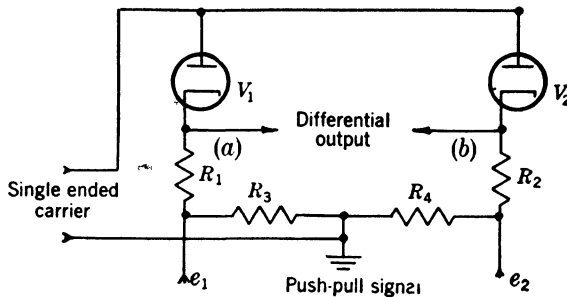
*Carrier-balanced Half-wave Circuits.*—A circuit of the type shown in Fig. 11-2 permits the use of a push-pull signal and a single-ended carrier and gives a considerable increase in usefulness.



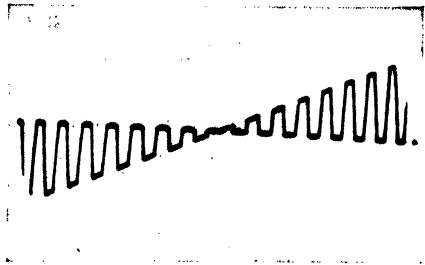
(a)

FIG. 11-1.—Half-wave diode amplitude selector. For the particular waveform shown:  $R_1 = 4.3 \text{ k}$ ,  $V_1 = 6\text{AG7}$  diode-connected, carrier = 22 kc/sec. The carrier is sinusoidal; the signal is a positive sawtooth waveform.

The waveform diagram (a) indicates the individual outputs at the cathodes of  $V_1$  and  $V_2$ . Subtraction of these outputs by means of a push-pull or differential amplifier gives the balanced output waveform (b). In the strict sense of the word this output is not push-pull since the output waveforms are neither symmetrical nor of equal amplitudes. Since both outputs must be connected to a push-pull or differential amplifier in order to obtain balanced operation, the designation "differential" will be used consistently throughout this chapter.



(a)



(b)

FIG. 11·2.—Carrier-balanced half-wave diode modulator. The waveforms are displayed on an oscilloscope the vertical plates of which are connected between the output terminals; the circuit employs values of  $R_1 = R_2 = 4.3 \text{ k}$ ;  $R_3 = R_4 = 500 \text{ ohms}$ ;  $V_1 = V_2 = 6\text{AG7}$  diode-connected. Carrier = 22 kc/sec. The carrier waveform is sinusoidal; the signal is a push-pull sawtooth waveform.

For equal tubes and resistors,  $R_1$  and  $R_2$ , the carrier gives equal voltages in these resistors when the signal is zero. The carrier is therefore suppressed in the differential output. The resulting circuit is a carrier-balanced modulator.

Another important property of this modulator is indicated by the waveform diagrams of Fig. 11·2. As in Fig. 11·1, the output voltage at the cathodes of  $V_1$  and  $V_2$  contains portions of the carrier which exceed the reference voltages  $e_1$  and  $e_2$ . The separate waveforms at points  $a$  and  $b$  are clearly indicated in Fig. 11·2a. Subtraction of these waveforms is shown in Fig. 11·2b, which clearly indicates that the phase of the output voltage depends upon the sign of  $e_1 - e_2$ . At equality, the phase of the

output shifts  $180^\circ$ . This is an extremely important characteristic of amplitude modulators that accept push-pull or differential input signals and is termed "bidirectional modulation." Operation of this type is, of course, not restricted to modulators employing amplitude selection but is also characteristic of other types to be described.

*Signal-balanced Circuits.*—In Fig. 11-3 is indicated a modulator employing a single-ended signal and a push-pull carrier with the output taken differentially between the cathodes of  $V_1$  and  $V_2$ . The operation

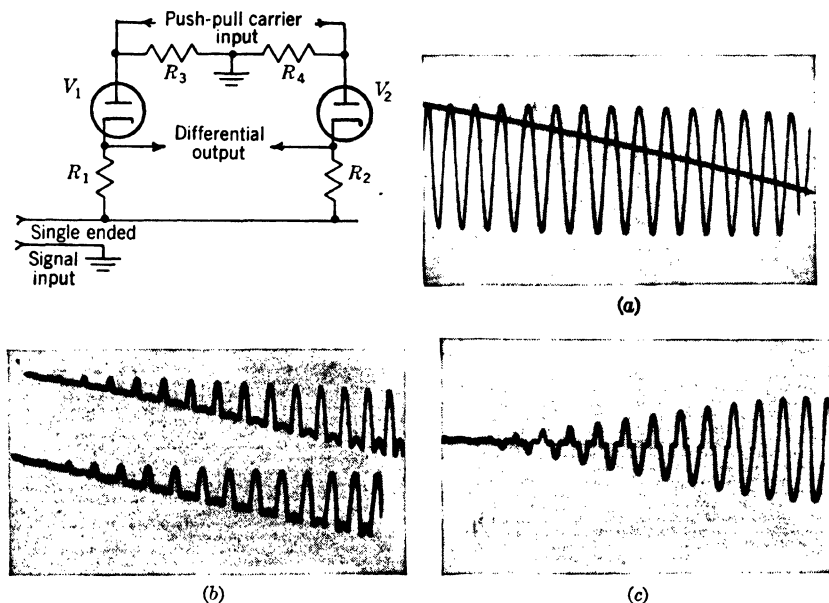


FIG. 11-3.—Signal-balanced diode modulator. The signal and carrier are superimposed in (a). The separate outputs at the cathodes of  $V_1$  and  $V_2$  are shown in (b) and the differential output in (c). The component values are  $R_1 = R_2 = 4.3 \text{ k}$ ,  $R_3 = R_4 = 500 \text{ ohms}$ ;  $V_1 = V_2 = 6\text{AG7}$  diode-connected. Carrier =  $22 \text{ kc/sec}$ .

of the circuit is depicted by the waveform diagrams. In Fig. 11-3a are shown the carrier and signal waveform superimposed, and in Fig. 11-3b are shown the separate outputs from the cathodes of  $V_1$  and  $V_2$ , each tube operating similarly to the circuit of Fig. 11-1 on alternate half cycles of the carrier wave. Subtraction of these outputs gives the modulated wave shown in Fig. 11-3c, which represents modulation in a full-wave fashion—that is, both negative and positive excursions of the carrier are modulated by the signal. In contrast to the previous example, the modulated output does not reverse phase since the signal is single-ended. Also carrier is not balanced out. Bidirectional modulation is obtained with the full-wave version of this circuit (see Fig. 11-5).



**Signal- and Carrier-balanced Circuits.**—Figure 11-4 indicates the third possible combination of signal, carrier, and output connections. Here a push-pull carrier and signal are used, but the output is taken in a single-ended fashion. The effects of neither the signal nor the carrier voltage appear across the output resistor  $R_5$ , provided balanced components are used. But the sidebands of the modulated carrier are obtained. In addition, the output contains a considerable amount of second harmonic

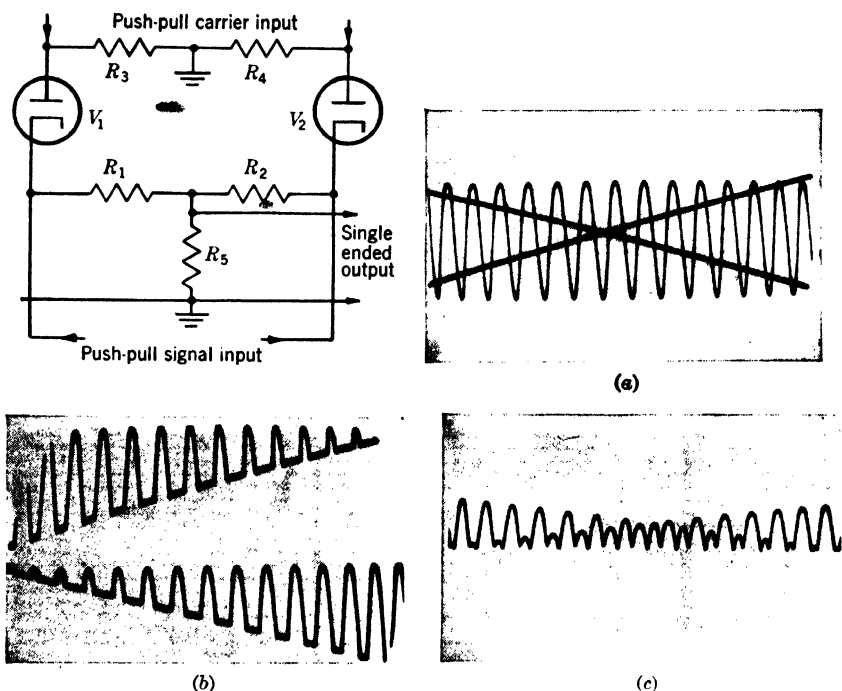


FIG. 11-4.—Signal and carrier-balanced half-wave modulator. The signal and carrier are superimposed in (a). The separate outputs at the cathodes of  $V_1$  and  $V_2$  are shown in (b), and the sum of the two waves appearing across  $R_5$  is indicated in (c). The waveforms were obtained with the following component values:  $R_1 = R_2 = R_3 = R_4 = 500$  ohms,  $R_5 = 1$  M. Carrier = 22 kc/sec,  $V_1 = V_2 =$  diode connected 6AG7.

of the signal and carrier (shown in the waveform diagram) since the circuit is a full-wave rectifier for either signal or carrier. In most cases it is relatively simple to remove the double-frequency component.

In waveform diagram, Fig. 11-4a, the push-pull signal voltages applied to the cathodes of  $V_1$  and  $V_2$  are shown superimposed upon the carrier. Amplitude selection occurs in  $V_1$  and  $V_2$  on alternate half cycles of the carrier wave and gives the two outputs at their cathodes shown at Fig. 11-4b. Addition of these two waveforms across the cathode resistor  $R_5$ , indicated in waveform diagram Fig. 11-4c, gives the signal- and carrier-

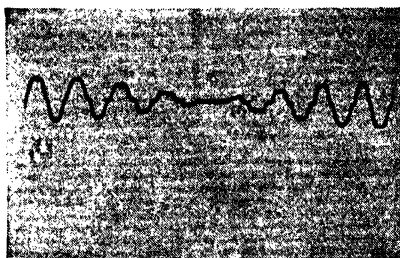
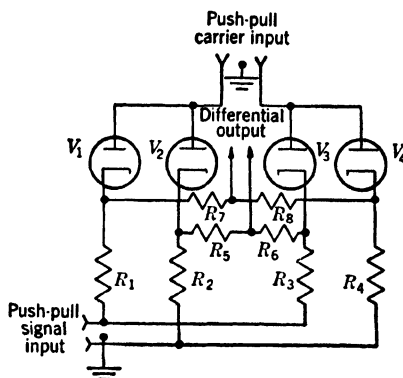
balanced output waveform, and the phase of the modulated output reverses with a reversal of the sign of the difference of the input signals.

Circuits employing push-pull carrier, signal, and output combine the features of the previous examples and give balanced operation for signal and carrier and, in addition, full-wave modulation. As indicated in Fig. 11-5, the outputs from  $V_1$  and  $V_4$  and from  $V_2$  and  $V_3$  are added together and then the sums are subtracted to give the differential output. The phase of the output wave reverses when the sign of the input signals reverses, and modulation occurs for both polarities of the carrier. Thus this modulator has the advantages of being balanced for both signal and carrier, and, in addition, gives bidirectional modulation. The second harmonic content of the output of the modulator of Fig. 11-5 is small.

The circuit of Fig. 11-6 represents a simplification that is possible provided the push-pull input does not reverse. As is evident from Sec. 9.3, this circuit represents amplitude selection between two bounds, the bounds in this case being set by the push-pull signal inputs. The operation of this circuit is restricted to signal voltages  $e_2 > e_1$ , since modulation ceases as these two voltages become equal, as is indicated by the waveform diagram. The upward deflection of the base line of the waveform diagram is due to the unbalance between the source impedances for the positive and negative signals.

Except for the limitation to the polarity of the signal voltages, this modulator has all the advantages of the much more complicated circuit of Fig. 11-5.

**Summary.**—The preceding circuit arrangements indicate the use of amplitude selection in certain types of modulation and some balanced circuits for suppression of the signal and carrier. A number of combinations of connections exist, but the useful ones employ a differential output to eliminate a single-ended input. In the circuits using four diodes,

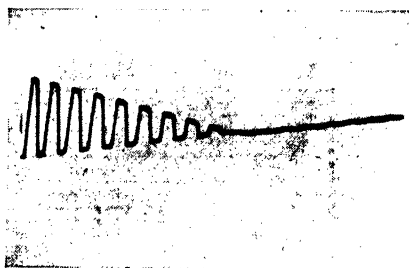
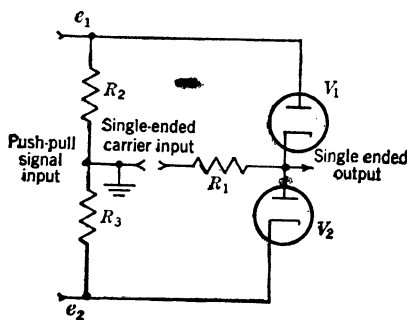


(a)

FIG. 11-5.—Signal and carrier-balanced full-wave modulator. For the particular waveforms shown:  $V_1, V_2, V_3, V_4 = 6AG7$  diode-connected.  $R_1, R_2, R_3, R_4 = 4.3$  k,  $R_5, R_6, R_7, R_8 = 56$  k. Carrier = 12.2 kc/sec.

push-pull inputs do not appear in the differential output. Thus outputs containing only the sidebands of the modulated carrier and harmonics of the signal and carrier are obtained. These relations may be derived mathematically for modulators employing curvature.<sup>1</sup> The results of this analysis do not apply to these modulator circuits that employ amplitude selection, and for this reason the explanation of their circuit operation has relied heavily upon the waveform diagrams.

Few detailed data on the performance of these modulator circuits



(a)

FIG. 11-6.—Signal- and carrier-balanced full-wave modulator for  $e_2 > e_1$ . For waveforms indicated,  $R_1 = 39$  k,  $R_2 = R_3 = 500$  ohms,  $V_1 = V_2 = 6\text{AG7}$  diode-connected. Carrier = 22 kc/sec.

angular-signal waveform diagram. Figure 11-7a indicates the sinusoidal signal applied to  $V_1$  and the rectangular carrier applied to  $V_2$ . Alternate half cycles of the signal wave are short-circuited by diode  $V_1$  and give the interrupted waveform of Fig. 11-7b. In Fig. 11-7c a negative-going sawtooth waveform is applied to the plate of  $V_1$ , and linear modulation is observed for positive values of the signal. Capacitance feed-through of diode  $V_1$  gives a visible differentiation of the carrier waveform at low signal levels.

<sup>1</sup> See M.I.T. E. E. Staff, *Applied Electronics*, The Technology Press, 1943, Chap. 7, p. 689.

in the conversion of low-level d-c voltages to modulated carriers are available. The data on the stability of amplitude selectors given in Sec. 3-14 and 9-3 apply to these circuits, and there is no reason why excellent stability may not be obtained.

**11-3. Carrier-controlled Switches.**—Amplitude modulation may be carried out by interrupting the signal waveform with a series switch or by short-circuiting it with a parallel switch at the carrier frequency. In each case high accuracy may be achieved if complete disconnection or complete short-circuiting is accomplished. Suitable vacuum-tube switches for these purposes have been described in detail in Secs. 3-6, 9-3, and 10-3.

A typical example of the employment of a half-wave diode is indicated in Fig. 11-7 and shows modulation of a sinusoidal- and triangular-signal waveform diagram.

Figure 11-7a indicates the sinusoidal signal applied to  $V_1$  and the rectangular carrier applied to  $V_2$ . Alternate half cycles of the signal wave are short-circuited by diode  $V_1$  and give the interrupted waveform of Fig. 11-7b. In Fig. 11-7c a negative-going sawtooth waveform is applied to the plate of  $V_1$ , and linear modulation is observed for positive values of the signal. Capacitance feed-through of diode  $V_1$  gives a visible differentiation of the carrier waveform at low signal levels.

Although this example should not be regarded as a practical modulator circuit, it indicates some limitations of a circuit of this type. The carrier amplitude must be in excess of the signal amplitude in order to ensure nonconduction of  $V_1$  during positive excursions of the carrier. On negative excursions of the carrier, the signal is attenuated by the factor  $(R_2 + R_d)/(R_1 + R_2 + R_d)$ . Therefore,  $R_2$  and  $R_d$  must be small compared with  $R_1$ . Reasonably accurate operation is obtained if the value of  $R_1$  is several hundred thousand ohms and if that of  $R_2$  is a few thousand

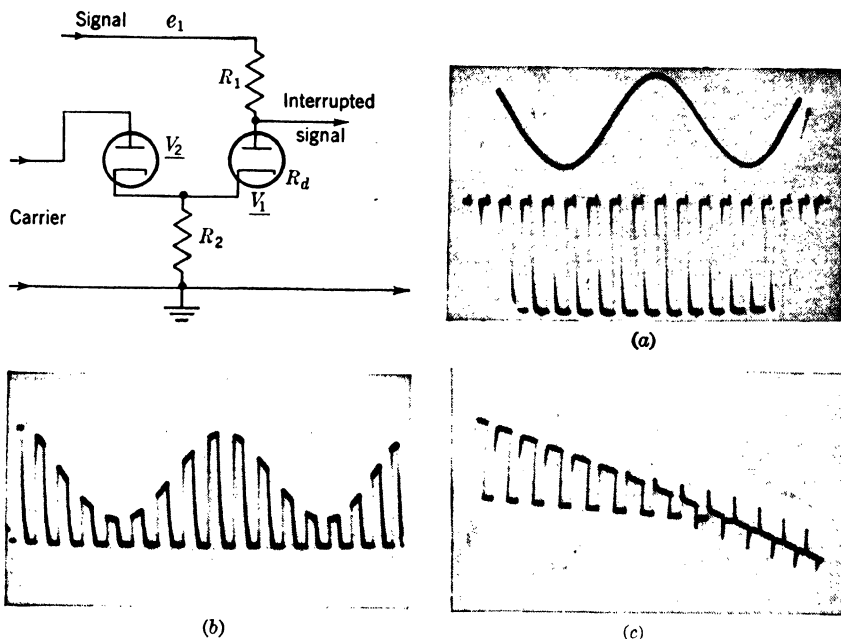


FIG. 11-7.—Half-wave diode-switch modulator. Waveforms (a) and (b) indicate modulation in accordance with a sinusoidal signal, whereas (c) indicates modulation in accordance with a triangular waveform. The effect of diode capacitance is especially noticeable in (c). For these waveforms, component values are:  $R_1 = 50$  k,  $R_2 = 500$  ohms,  $V_1 = V_2 = 6\text{AG7}$  diode-connected. Carrier = 22 kc/sec.

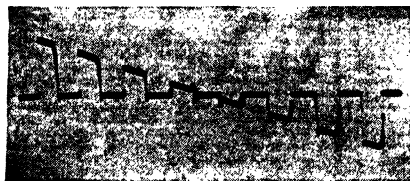
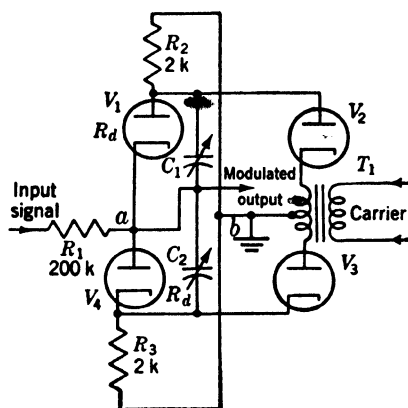
ohms, but the modulation of rapidly varying waveforms may require values of 1000 and 100 ohms respectively. The effect of plate-cathode capacitance of  $V_1$  is clearly shown in the waveform of Fig. 11-7c.

The single-diode circuits are of little practical importance since they operate with signals of only one polarity and, in addition, give half-wave operation. There are, however, a number of important circuits that operate with signals of both polarities and give some cancellation of capacitance-coupling of the carrier.

*Half-wave-switch Modulators—Bidirectional Operation.*—Figure 11-8 indicates a carefully tested diode modulator circuit, the "Diamod."

Operation for both polarities of the signal voltage is obtained by a combination of two of the elements shown in Fig. 11-7, and bidirectional modulation is achieved by the methods shown in the waveforms of Fig. 11-8.

On a particular half-cycle of the carrier, the output of the transformer  $T_1$  gives a negative signal at the cathode of  $V_2$  and a positive signal on the plate of  $V_3$  and prevents conduction of  $V_1$  and  $V_4$ . Under these conditions



(a)

FIG. 11-8.—Half-wave-switch modulator for positive and negative input signals, "The Diamod." For the waveform illustrated,  $R_2 = R_3 = 2\text{ k}$ ,  $R_1 = 24\text{ k}$ ,  $V_1$ ,  $V_2$ ,  $V_3$ ,  $V_4 = 6\text{AG7}$  diode-connected. Carrier = 12 kc/sec. A value of  $R_1$  of 200,000 ohms or more is desirable to minimize the effects of differences of  $V_1$  and  $V_4$ .

secondary winding of  $T_1$  to ground are not troublesome, one of the diodes,  $V_2$  or  $V_3$ , may be removed and the other inserted between the two parts of a split secondary winding for  $T_1$ . Better results are, however, usually obtained from the arrangement shown in Fig. 11-8.

Figure 11-9 indicates the excellent reproducibility and stability of this circuit. From the curves it is seen that 90 per cent of the thirteen tubes tested gave a shift of the zero point of less than 30 mv on changing tubes, less than 12 mv on varying the heater voltage from 5 to 7 volts, and less than 3  $\mu\text{volt/min}$  drift at reduced heater voltage. The error

the value of the output rises to the peak value of the input. On the opposite half-cycle of the carrier, current will flow to ground through  $V_1$  or  $V_4$ , depending upon the polarity of the signal. As before, the signal is attenuated by the factor  $(R_2 + R_d)/(R_1 + R_2 + R_d)$ . The carrier voltage does not appear in the output and bidirectional modulation is obtained, but the signal voltage is not cancelled.

A spurious signal equal to one half the difference of the contact potentials of  $V_1$  and  $V_4$  appears at the output. If the heater voltage of the tube having the higher contact potential is reduced, the potentials may be equalized. It appears that this equalization has the additional benefit of considerably reducing the differential effects of heater-voltage variation.

Residual unbalance due to different stray or tube capacitances is equalized by a variation of  $C_1$  or  $C_2$ .

If the stray capacitances from the

due to changing tubes and varying heater voltage is comparable to that obtainable with the best type of direct-coupled amplifier using type 6SU7. The drift rate is roughly one quarter that obtainable with such direct-

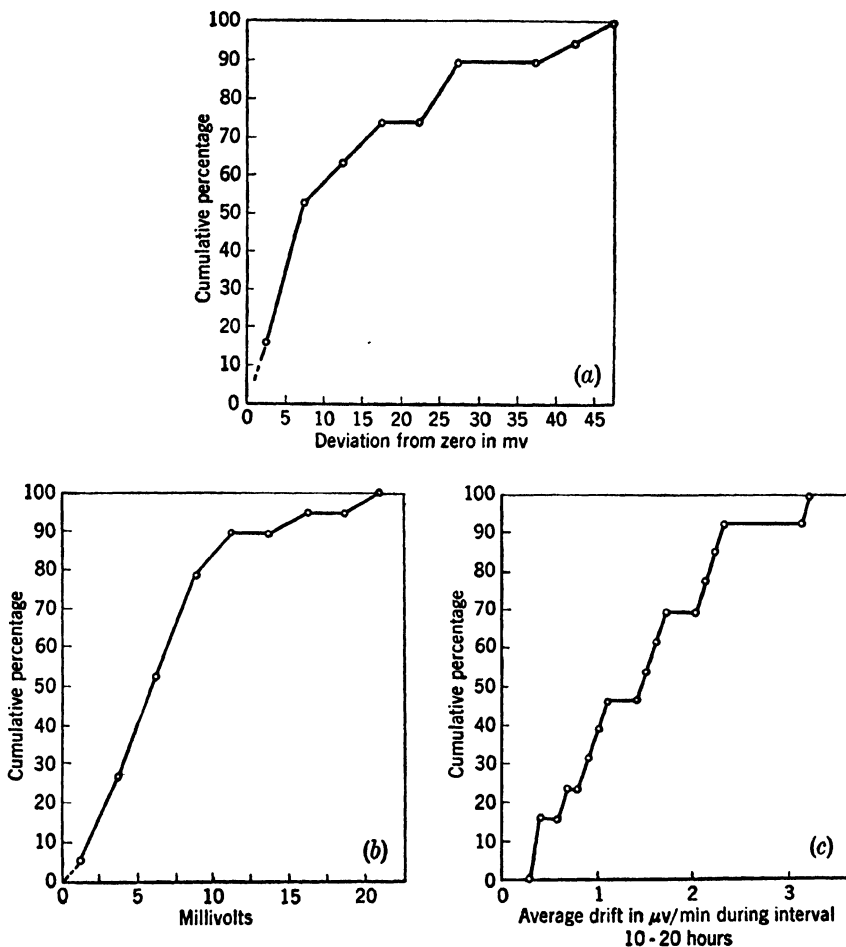


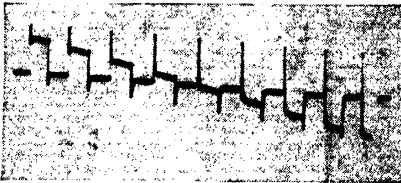
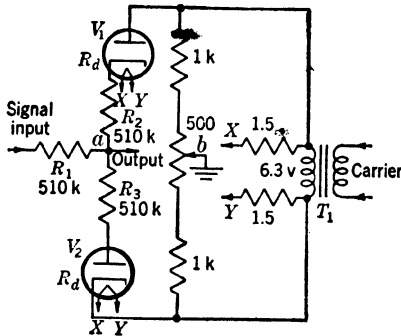
FIG. 11-9.—Performance of diode modulator of Fig. 11-8 using type 6AL5 double diode. (a) Indicates the millivolts change of the zero point for 13 samples of Hytron type 6AL5, (b) the effect of heater-voltage variation from 5 to 7 volts, (c) the drift rate at 10 hr after inserting the tubes ( $E_f = 5.0$  volts).

coupled amplifiers. Even better stability has been obtained with a germanium-crystal modulator circuit as shown in Fig. 11-19.

A more economical but less stable diode modulator circuit is shown in Fig. 11-10. In this circuit a particular half-cycle of the carrier at the output of  $T_1$  makes the voltage supplied to the plate of  $V_1$  and to the

cathode of  $V_2$  negative and positive respectively. Under these conditions the output voltage will assume the full value of the signal. With the opposite half-cycle of the carrier waveform, the signal voltage will be reduced by roughly one third its value with the components indicated. But the potential of point  $a$  will depend upon the accuracy of the resistive center tap of  $T_1$ , the actual values of  $R_2$  and  $R_3$ , and the shapes of the waves applied to  $V_1$  and  $V_2$ .

The large "swamping" resistors,  $R_2$  and  $R_3$ , minimize the effects of differences in the conductance of diodes  $V_1$  and  $V_2$ . These resistances



(a)

FIG. 11-10.—Half-wave-switch modulator. For the particular waveform indicated,  $R_1 = 24 \text{ k}$ ,  $R_2 = R_3 = 4.3 \text{ k}$ ,  $V_1 = V_2 = 6\text{AG7}$  diode-connected. Carrier = 12 kc/sec. The higher values indicated in the circuit diagram are desirable to reduce dependence on the characteristics of  $V_1$  and  $V_2$ .

In this circuit and in the previous one, operation has been indicated for a single ended input, and in both cases the point  $b$  has been grounded. But disconnection of the ground gives satisfactory operation for differential signals. These circuits are therefore extremely useful for amplitude discriminators since the level of the input signals is not critical.

Figure 11-11 gives the circuit of another half-wave diode-switch modulator which represents some improvement over the previous circuit for modulating rapidly varying waveforms. The signal is short-circuited by diode bridge  $V_1$  to  $V_4$ , which carries several milliamperes because of the

are, however, so large compared with the input resistor  $R_1$  that the amplitude of the modulated output is much smaller than the input voltage—smaller than is desirable. The potential of point  $a$  during closure of the switch depends upon many more factors than in the circuit of Fig. 11-8. In that circuit the emission potential of the diodes themselves was used to close the switch and, hence, did not depend upon an external waveform. In this circuit the switching wave is used to close the diode switch, and therefore the balance depends upon the circuit components and the shape of the carrier wave.

With proper adjustment of point  $b$ , the residual from a 6.3-volt carrier voltage for zero signal input can be reduced to approximately  $50 \mu\text{v}$ . Smaller values would be obtained by capacitance-balancing such as is indicated in Fig. 11-8.

fixed potentials applied to the plates of  $V_1$  and  $V_2$  and to the cathodes of  $V_3$  and  $V_4$ . The junction of the plate and cathode of  $V_2$  and  $V_4$  is connected to ground, and the potential of point  $a$  is substantially zero. A push-pull carrier is applied at the points  $b$  and  $c$ , and negative and positive excursions respectively cut off the diodes and allow the output to assume the full value of signal.

The effect of the diode capacitance is balanced by the two diodes  $V_1$  and  $V_3$ . This particular circuit has two additional advantages. First, a high-impedance switching voltage may be used, since the potential of point  $a$  in the absence of switching voltage is accurately established at ground by diodes  $V_2$  and  $V_4$ . Secondly, this circuit has the advantage of the circuit shown in Fig. 11-8 for modulating a number of electrical signals in that the diodes  $V_2$  and  $V_4$  need not be duplicated for additional signal inputs.

These three half-wave-switch modulator circuits are representative examples of a number of combinations of diode switch circuits that give similar effects. That of Fig. 11-10 is the simplest and requires fewer tubes than the others. Its operation, however, depends to a large extent upon the many associated resistors and differences in the shape of the switching waveforms. The circuit of Fig. 11-8 represents a definite improvement in stability over the direct-coupled amplifier and may be used where a factor of 4 is of critical importance. The third circuit, that of Fig. 11-11 is, as has already been stated, specialized for the modulation of rapidly varying waveforms.

A significant gain in stability is achieved by employing a mechanical-switch modulator. Since nearly all the available types of mechanical switches have single-pole, double-throw contacts, they are suitable for full-wave modulation and will, therefore, be discussed in the next section.

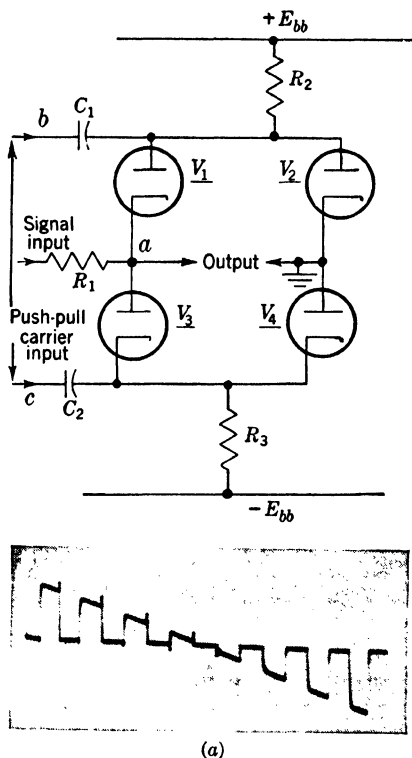


FIG. 11-11.—Diode-switch modulator for rapidly varying waveforms. The waveform was taken with  $R_1 = 10k$ ,  $R_2 = R_3 = 500$  ohms;  $V_1$ ,  $V_2$ ,  $V_3$ ,  $V_4 = 6AG7$  diode-connected. Carrier = 12 kc/sec.



**Full-wave-switch Modulators.**—There are several manufacturers of mechanical switches for precision modulation. The Brown Instrument Company makes a 60-cps “Converter” on which performance data are available. This device is illustrated in Fig. 11-12. The commercially available unit has a resonant frequency of approximately 90 cps and is designed to operate from 50 to 60 cps at 6.3 volts excitation. Both the outer contacts are connected to the reed for 7 per cent of the operating cycle, but the convenient adjusting screws permit alteration of the position of the contacts to give non-short-circuiting operation. The life of the contacts of a particular converter is indicated in the table immediately below. For this experiment the given potential was applied to a pair of contacts of the converter through a 10-K resistor. The times given represent the interval required for the duty ratio of the contact to alter appreciably.

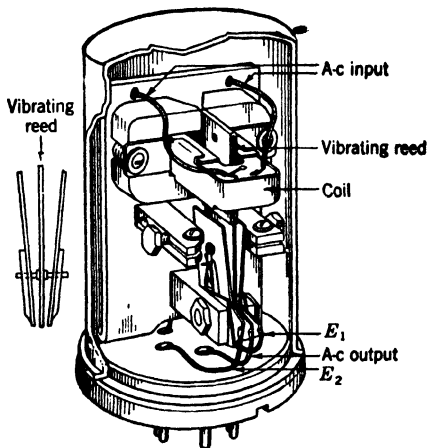


FIG. 11-12.—Brown Converter for 60-cps operation.

Supply potential	Hours
6.4	>> 2100
17	1500
45	40

In low-impedance circuits the stability of the Brown Converter is known to be better than  $1 \mu\text{v}$  over a period of several weeks. The amount of carrier voltage picked up by the signal circuit depends to some extent upon the impedances used. For low-impedance circuits, the pickup is about  $1 \mu\text{v}$ . Considerable reduction of pickup in high-impedance circuits is obtained by grounding an adjustable center tap across the exciting voltage for the electromagnet of the converter, and values of the order of magnitude of  $1 \mu\text{v}$  are obtainable in circuit impedances of  $\frac{1}{2}$  megohm. In addition, it has been found desirable to modify the converter so that the excitation for the electromagnet is brought out through the top of the case in shielded leads. Satisfactory measurements have been made in circuits having a resistance of 3 or more megohms, although the pickup may set a limitation under these conditions.

If hum is present in the converter output at null, the constancy of the duty ratio or “dwell time” of the contacts is of importance in circuits where narrow-band amplification at the carrier frequency is employed. No detailed data are available on such variations, but wideband ampli-

If hum is present in the converter output at null, the constancy of the duty ratio or “dwell time” of the contacts is of importance in circuits where narrow-band amplification at the carrier frequency is employed. No detailed data are available on such variations, but wideband ampli-

fication and switch detection (Sec. 14-5) within the limits of the dwell time give independence of duty-ratio variations over reasonable limits.

A second converter designed for frequencies of 400 cps and resonant at 600 to 700 cps has been made in experimental quantities by the Minneapolis-Honeywell Company. It is illustrated in Fig. 11-13. Considerably fewer performance data are available for this modulator, but with similar contact materials, the properties should be equal to those of the Brown Instrument Converter.

The Western Electric mercury relay D 168479, although not specifically designed for low-level operation, has been used satisfactorily for these purposes. The limitation to the signal level is set by the carrier pickup.

Other types of mechanical switches for low-level signals have employed rotating machinery to operate the contacts. An experimental model constructed by British-Thompson-Houston for Telecommunications Research Establishment has a bank of more than ten modulate-demodulate switches for an application requiring a large number of channels. A cam-operated contactor of extremely high performance in low-resistance circuits has been recently described.<sup>1</sup> The measured noise level with an input resistance of 5 ohms and a bandwidth of roughly 1 cps is  $3 \times 10^{-9}$  volts

peak to peak and may be compared with a theoretical value of roughly  $3 \times 10^{-10}$  volts rms. The stability with time is outstanding, and the drift over a 4-hour period is only  $4 \times 10^{-9}$  volts corresponding to  $1 \times 10^{-6} \mu\text{V}/\text{min}$ —a factor of roughly one million better than that obtainable with the thermionic vacuum tube. Operation at levels as low as this requires especial precaution to eliminate spurious thermal and magnetic effects in the input circuit and in the mechanical switch. In addition, microphonics, flicker effect, and other noises associated with the first amplifier tube may set a limit to the obtainable noise level. In the

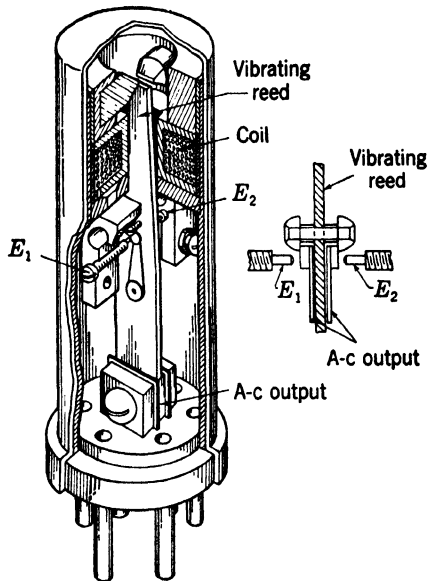


FIG. 11-13.—Minneapolis-Honeywell vibrator.

<sup>1</sup> M. D. Liston *et al*; "A Contact Modulated Amplifier to Replace Sensitive Suspension Galvanometers," *Rev. Sci. Instruments*, **17**, 194 (1946).

particular circuit, the effect of tube noises was considerably reduced by a 320-to-1 stepup transformer.

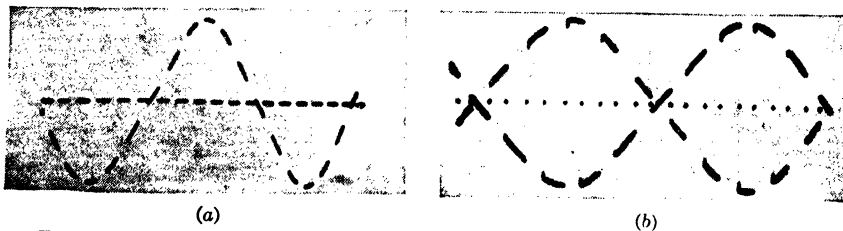
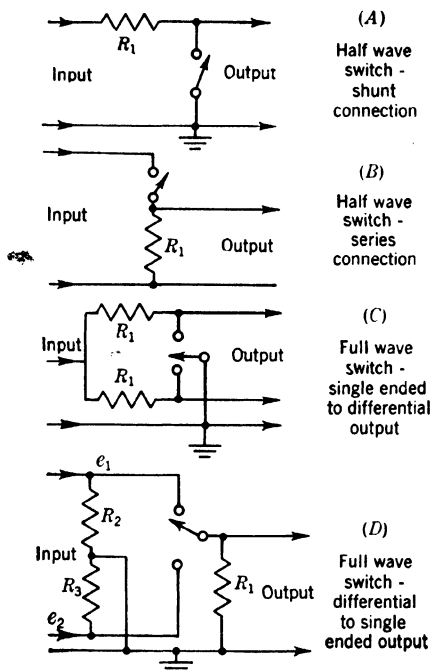


Fig. 11-14.—Configurations of switch modulators. *A* and *B* represent shunt and series connections of a half-wave switch and *C* and *D* represent connections for full-wave switches giving respectively single-ended-to-differential operation and differential-to-single-ended operation. Waveform diagram (a) indicates the operation of circuit configurations *A* and *B*, and the signal is connected to the output for only  $\frac{1}{2}$  the switching period. Waveform diagram (b) indicates the operation of circuit configuration *D*. One or the other input signal lead is connected to the output over the entire period of switch operation except for the brief transient indicated by the dot on the horizontal axis. The waveforms were obtained with  $R_1 = 11 \text{ k}$  and a carrier frequency of 720 cps, using the Minneapolis-Honeywell vibrator.

Figure 11-14 gives four typical circuit connections for mechanical-switch modulators. *A* and *B* represent shunt and series connections similar to those already indicated by the half-wave thermionic-switch mod-

ulators of the previous section. Since single-pole, double-throw contacts are available for all the modulators mentioned above, connections *C* and *D* are preferred, the first for operation with single-ended signals where differential output is desired and the second where push-pull signals are available but single-ended output is desired. Since most of the a-c amplifiers for the modulated carrier are single-ended, circuit *D* is highly desirable because it accomplishes the conversion from differential to single-ended operation. The operation of these circuits is explained by the waveform and the circuit diagrams. The contact resistance of these modulators is very low, and correspondingly small values of  $R_1$  may be used.

A typical input circuit for the use of this mechanical switch in thermoelectric measurements is indicated in Fig. 11-15, where  $R_1$  and  $R_2$  may represent the resistances of a reference and a measuring thermocouple. Since these are of low resistance, advantage may be taken of transformer coupling to the amplifier, and stepup ratios in  $T_1$  of several hundred are desirable. The single-ended output is desirable for economical a-c amplification.

Two precautions should be observed with these modulators. First, the resistance of both signal inputs of circuit type *D* should be equal lest variations of the grid current of the amplifier be measured. Second, when large by-pass condensers are shunted across the contacts, non-short-circuiting operation should be used or a large loss of signal voltage will occur. In low-level circuits where the maximum excursions of the signal are not likely to exceed the grid base of the amplifier tube, there is no objection to direct coupling to the grid provided later stages are *RC*-coupled in order to avoid the effect of slow drifts of the input tube.

Another important laboratory use of this mechanical switch is as part of a visual null indicator for potentiometric measurements. If, for example, it is desired to compare the linearity<sup>1</sup> of two potentiometers with a high degree of accuracy, the mechanical switch is connected as indicated in Fig. 11-16; the output of the converter is connected to the high-gain amplifier of an oscilloscope. When a sweep synchronized with the carrier frequency is used, the null may be detected with considerable accuracy. It is found convenient to build one of these converters into a commercially available oscilloscope.

<sup>1</sup> In this case an alternating wave could be connected directly to the two potentiometers and, providing inductive effects were negligible, the same measurement procedure would be satisfactory without the use of the modulator.

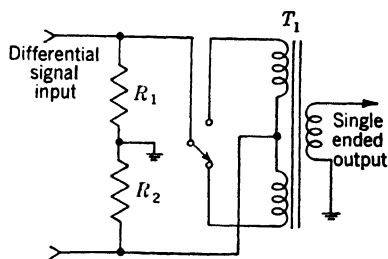


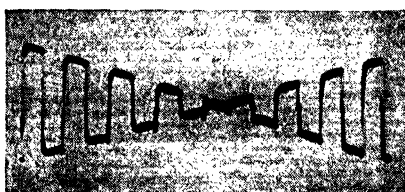
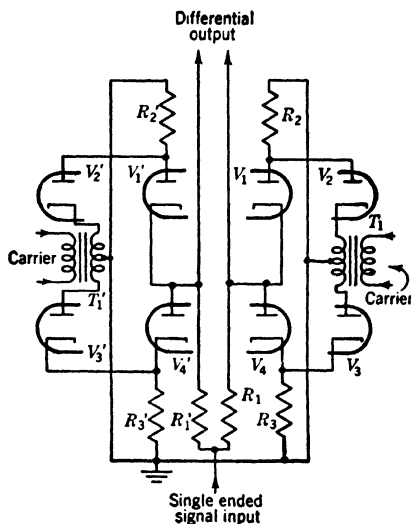
FIG. 11-15.—Typical transformer input circuit for a low-impedance signal.



if the bandwidth of the carrier amplifier is maintained relatively wide (1 kc/sec) and the bandwidth is controlled after phase detection. No less signal-to-noise ratio results from this procedure since phase-sensitive detection resembles frequency conversion from the noise standpoint. A microvoltmeter for precision measurements of the difference of two photocurrents has been constructed and employs 0.5-megohm resistors at the input to the Brown Converter followed by an a-c amplifier of a gain of  $10^6$ . Phase-sensitive detection is accomplished by another Brown Converter whose contacts are adjusted to operate within the interval of the original modulation in order to avoid any error due to small variations in dwell time. The output voltage, after being amplified and passed through several simple  $RC$ -filter sections (see Sec. 8-11), is connected to an Esterline-Angus recorder having a bandwidth of roughly 0.5 cps. The hum level of the carrier at the input was of the order of several microvolts, provided the balance of the exciting voltage was correctly adjusted. The noise output corresponded closely to the thermal agitation noise in the input resistors, and the drift over a period of 5 hr corresponded to  $0.02 \mu\text{V}/\text{min}$ .

Similar, but much less stable, operation may be obtained over a much wider range of carrier frequencies by a combination of the half-wave diode modulator circuits of the previous section. For example, Fig. 11-18 shows two units of the circuit of Fig. 11-8 combined according to C, Fig. 11-14.

Another full-wave circuit based on two elements of Fig. 11-10 is shown in Fig. 11-19. This circuit illustrates the application of germanium crystals to modulator circuits. The long time stability of the



(a)

FIG. 11-18.—Full-wave diode-switch modulator. This circuit represents a combination of two units of the circuit of Fig. 11-8 connected according to D of Fig. 11-14. In a practical circuit,  $T_1'$  may be eliminated. For the particular waveform shown,  $R_1 = R_1' = 24 \text{ k}$ ;  $R_2 = R_2' = R_3 = R_3' = 3.9 \text{ k}$ . All the tubes are 6AG7 diode-connected. The source impedance for the carrier is 500 ohms. Carrier = 12 kc/sec. It is usually desirable to employ values of  $R_1$  and  $R_1'$  of 200 k. The carrier voltages from  $T_1$  and  $T_1'$  are phased at  $180^\circ$ .

circuit is indicated by the accompanying graph. A drift rate of approximately  $1 \mu\text{volt}/\text{min}$  is obtained after a relatively short operating period, and hence represents an improvement of a factor of 2 or 3 over the average 6AL5 performance shown in Fig. 11-9. In addition, there is no effect of heater-voltage variation. A serious disadvantage of the germanium crystal is the fact that, since the rms noise voltage of the order of  $150 \mu\text{v}$  is observed over a bandwidth of roughly  $50 \text{ Kc}/\text{sec}$ , the circuit is rendered unsuited for low-level measurements. Another drawback is low back resistance of the crystals, which prevented the use of input

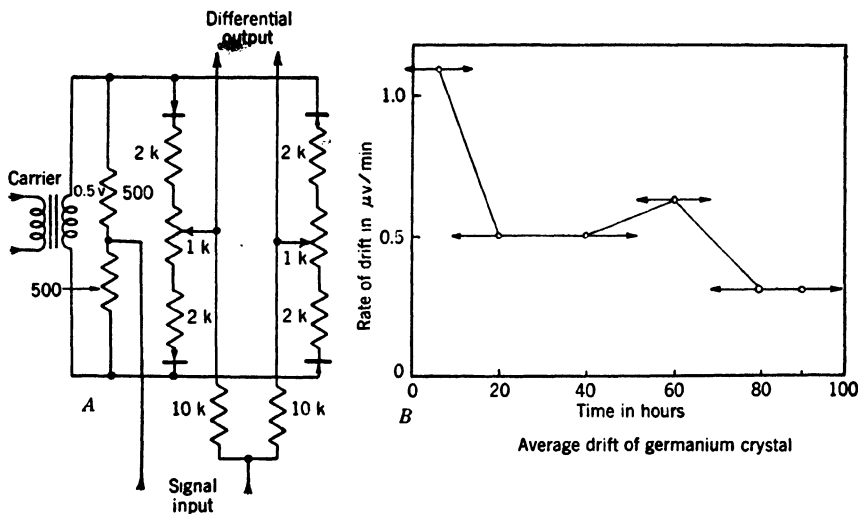


FIG. 11-19.—Full-wave modulator using germanium crystals. The potentiometers are for obtaining satisfactory balance with zero signal inputs. The performance data were obtained with experimental samples of germanium crystals having characteristics similar to those commercially available from Western Electric or Sylvania.

resistors much larger than those shown in the circuit diagram. But some recent samples have a back resistance in excess of 1 megohm at a voltage of  $-40$ . Forward resistances of less than 200 ohms are usually obtainable. Crystals of poorer quality give considerably higher drift rates (several  $\mu\text{volts}$  per minute) and noise voltages up to 1 mv. These tests were made with selected experimental samples of germanium crystals obtained from Purdue University, and it is believed that the performance is representative of units currently available from Western Electric<sup>1</sup> or Sylvania. Some especially selected crystals obtained from Bell Telephone Laboratories gave considerably smaller noise voltages.

The effect of temperature upon the back resistance of germanium crystals may amount to a factor of 3 to 10 over a range of  $100^\circ\text{C}$ , and the

<sup>1</sup> J. H. Scaff and H. C. Theurer, "Final Report on Preparation of High Back Voltage Germanium Rectifiers," NDRC 14-555, Bell Telephone Laboratories.

operation of this modulator circuit should therefore be restricted to low-impedance input signals.

Similar bridge-modulator circuits have employed thermionic diodes, and the signal resistance could, of course, be raised to the order of  $\frac{1}{2}$  megohm or greater. However, a variation of heater voltage of 10 per cent gave an equivalent d-c unbalance of 1.2 mv. The unbalance at the null point for a carrier voltage of several volts could easily be reduced to an equivalent of  $100\ \mu\text{v}$  direct current.

The full-wave diode circuits are not frequently used in circuit design because the large number of elements makes them somewhat cumbersome and they show no great advantage over the half-wave circuits. The availability of push-pull input affords no practical advantage over the half-wave circuits having transformer-coupled carrier since the whole modulator may "float" between the terminals of a differential input signal.

*Copper-oxide Modulators.*—By way of contrast, a distinctly different use of similar modulator configurations is presented. These depend upon the copper-oxide rectifier or varistor and are widely used for modulation and demodulation in telephone communication circuits. Here the objectives of the design are different, and the efficiency of signal-power conversion, the modulator bandwidth, and frequency spectrum are of importance. The latter is of especial importance in multiple-channel communication systems where the harmonics of the modulated output frequencies from several systems may cause mutual interference. These requirements lead to a different approach to the design and performance criteria for modulator operation, and many data are available on the relation between signal and carrier power and the power appearing at various unwanted harmonics. Thus, in the data that follow, the results are expressed in terms of decibels below the carrier power. These data may be converted into voltage, since the effective resistance of the modulating elements is roughly 200 ohms. Although the use of copper oxide elements and low-impedance input and output circuits leads to high-power conversion, the operation of these circuits is extremely sensitive to both temperature and carrier levels.<sup>1</sup> Much has been done, however, to control the quality of varistor modulator elements in order that a consistent, although not high, ratio of signal to carrier power may be obtained at the output of balanced-modulator circuits.

The modulator configurations used in these circuits closely resemble the diode switches previously described, and three configurations of diode bridge, double-balanced, or ring circuits are in common use and are illustrated in Fig. 11-20. The illustration shows in (a) a bridge circuit

<sup>1</sup> R. S. Caruthers, "Copper Oxide Modulators in Carrier Telephone Systems," *Elec. Engr.*, **58**, 253 (1939).



used as a shunt switch and in (b) a bridge circuit used as a series switch. Configuration (c) is clarified by the schematic switch of (d). This diagram indicates the correspondence of (c) to modulation obtainable

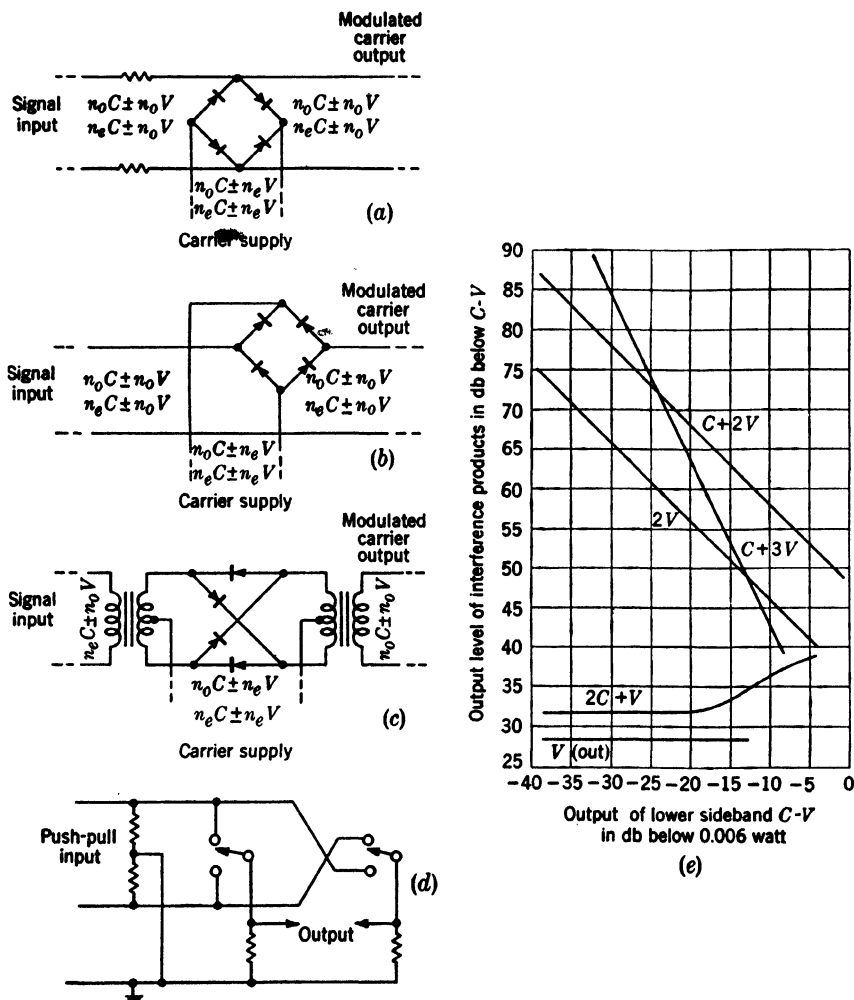


FIG. 11-20.—Copper-oxide bridge modulators. (a) Indicates a shunt switch, (b) a series switch, and (c) a single-pole double-throw reversing switch as explained by schematic diagram (d). The components of the signal frequency ( $V$ ) and carrier frequency ( $C$ ) appearing at the input and output are indicated in the appropriate places;  $n_o$  represents an odd number, and  $n_e$  represents an even number. The frequency spectrum of the output for particular values of harmonics is given in the graph (e).

with a pair of synchronous single-pole, double-throw switches based upon circuit D of Fig. 11-14. The configuration (c) of this figure gives therefore a push-pull output from a push-pull input signal.

As seen from Fig. 11-20, the carrier power in the output is roughly 30 db below that at the input. This is a desirable property in these modulating elements since it determines the minimum necessary signal power. Typical production units give an output balance of 20 to 30 db with reference to a 1-mw carrier input. Experimental circuits have been balanced to a much better precision—in a particular case, to 110 db.<sup>1</sup>

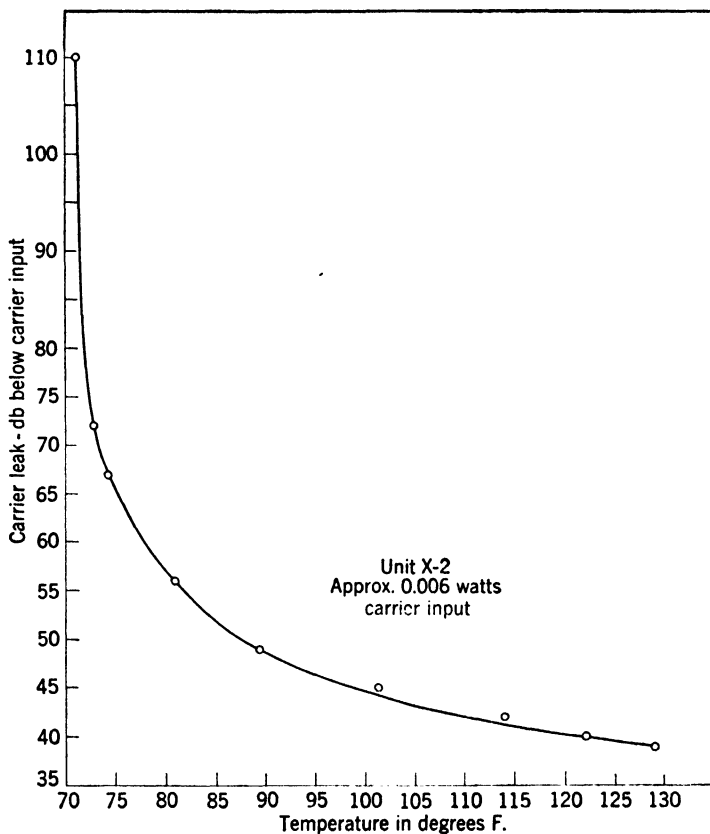


FIG. 11-21.—Variation of carrier leak balance with change of temperature. Original balance adjustment of 71°F left unchanged as temperature varied.

This high value of balance in the copper-oxide modulator was obtained only with the proper values of resistance in series and capacitance in shunt with one of the bridge arms. If these values are converted to volts, it is seen that the optimum performance of the balanced copper oxide bridge compares favorably with that obtainable from the other circuits—the unbalanced carrier voltage is approximately several microvolts, but the following effects make this value impractical to obtain

<sup>1</sup> R. S. Caruthers, Bell Telephone Laboratories, personal communication on these tests of varistors.

under reasonable operating conditions. The effect of temperature and carrier voltage upon this high value of balance is extremely large—a temperature change of 2°F reduced the balance from 110 to 72 db. Similarly a slight deviation of carrier power, 2 db, from that giving an optimal balance (in this case 80 db) reduces the balance to roughly 60 db. These data are amplified by Figs. 11·21 and 11·22.

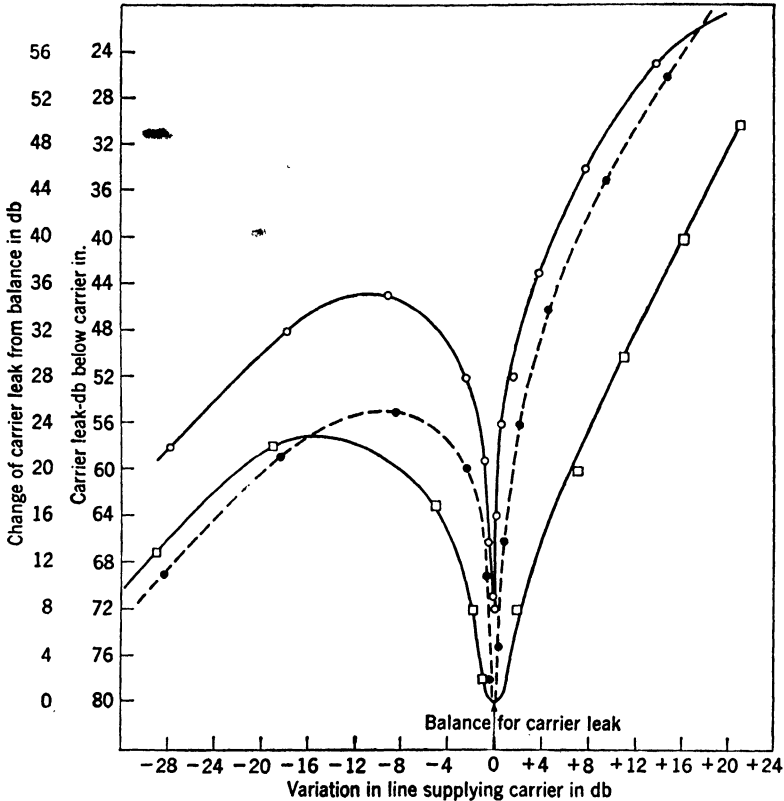


FIG. 11·22.—Variation of carrier leak with variation of carrier input for several circuit conditions.

Other factors of importance in determining the stability of the balance are time, harmonics in the carrier waveform, variations in impedance of the carrier supply, and a slight heating of the varistor units on application of the carrier voltage.

Although the stability of the nonlinearity in copper oxide is not so high as that of the circuit elements discussed previously in the chapter, greater stability against variations due to the variables mentioned above may be obtained by inserting resistors in series with the nonlinear circuit elements as indicated in some of the previous circuit diagrams. In

applications where the efficiency of the modulator must be represented in terms of signal power, this will represent no improvement since the signal power corresponding to carrier unbalance is similarly increased. For the usual applications of the conversion of direct current to alternating current for precision measurement, the signal output power is not usually of any importance.

Figure 11-20e also represents a typical example of the frequency spectrum of the output of the circuit of (c) employing  $\frac{3}{8}$ -in.-diameter disks in each bridge arm. The frequency components due to the signal frequencies  $V$  and the carrier frequency  $C$  are indicated at the appropriate place in (a), (b), and (c);  $n_o$  is any odd number—1, 3, 5, etc., and  $n_e$  is any even number—0, 2, 4, 6, etc. It is observed that a decrease of the signal power for constant carrier input gives a considerable improvement in the ratio of the output of the lower sideband to components  $2V$ ,  $C + 3V$ , and  $C + 2V$ . The rejection of the circuit to  $V$  is, of course, independent of the signal voltage. This diagram emphasizes the desirability of operating these modulators with small signals if these sidebands are to be avoided. Sidebands are, however, rarely of importance in the simple conversion of direct current to alternating current where a single channel is employed.

#### 11-4. Balanced Triodes, Tetrodes, and Multigrid Tubes.—The

following section contains several examples of balanced modulator circuits in which the signal and carrier are connected to high-impedance electrodes, and some gain may be obtained in the modulator. These circuits are not so stable as those of the previous section which employ diodes or mechanical switches, and they represent, in general, no improvement in stability over that obtain-

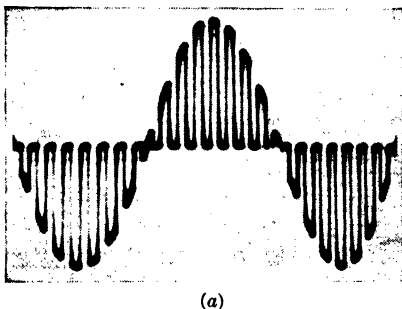
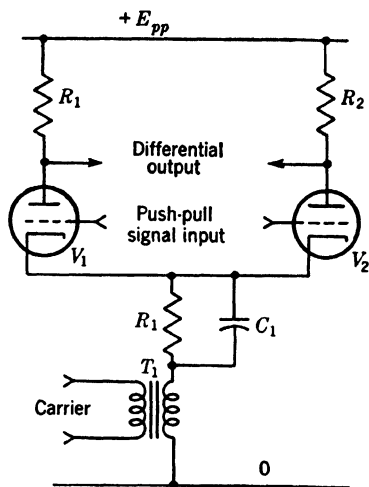


FIG. 11-23.—Balanced triode modulator. The bias provided by  $R_1C_1$  permits the input signal to be balanced with respect to ground. The waveforms represent the performance obtained with  $R_1 = R_2 = 16k$ ;  $V_1 = V_2 = 6SN7$ ; carrier source impedance = 500 ohms; carrier frequency = 15 kc/sec. The carrier waveform is sinusoidal.

able with the direct-coupled amplifier. They are, however, of considerable use where high stability is not required but where gain and high-impedance input are desirable.

*Balanced-triode Modulator.*—The circuit of Fig. 11-23 is a balanced-triode modulator patterned after the circuit of Fig. 11-2. A push-pull signal is connected to the grids and a single-ended carrier to the cathode. A differential output may be taken from the plate circuit. A circuit of this form is particularly satisfactory where the carrier employed is at the

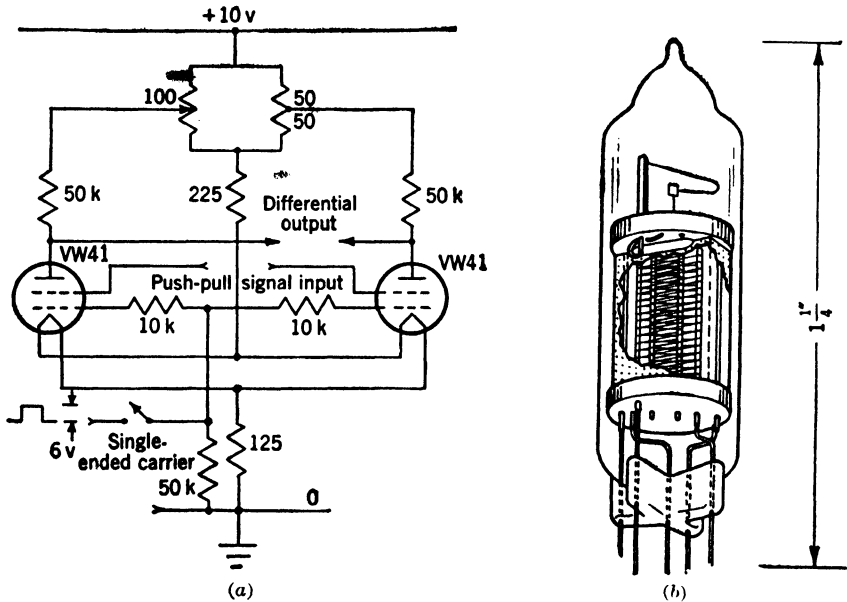


FIG. 11-24.—Tetrode modulator circuit for electrometer application. Manufacturer's data indicate that stability of  $\frac{1}{2}$  mv and a grid current in the signal electrode of  $10^{-14}$  amp are obtainable. The perspective view indicates the small size of the electrometer tubes. For the particular circuit constants, the signal input should be balanced with respect to ground.

power-supply frequency, and a low-impedance drive for the cathodes is available.

The waveform diagram indicates the bidirectional modulation obtained with this circuit. The carrier amplitude was made so large that switching operation was obtained with consequent grid current. Smaller carrier amplitudes, though giving less grid current, would give modulation by curvature with attendant nonlinearity.

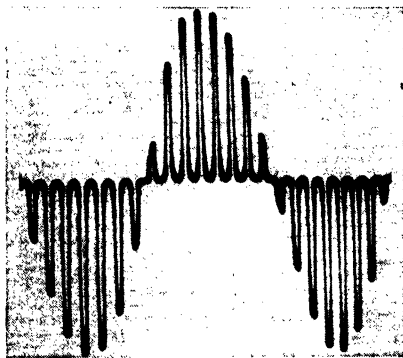
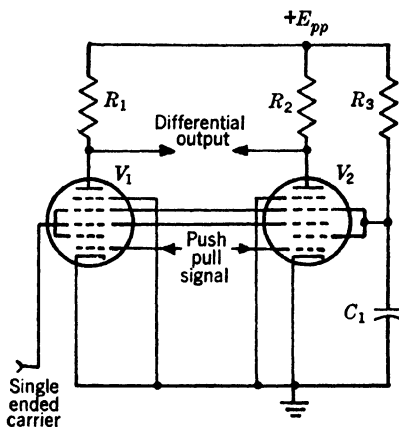
*Tetrode Modulator for Electrometer Application.*—A very high input impedance for the signal is obtained by the connections of Fig. 11-24. Low-grid-current Victoreen tetrodes (VW-41) (Fig. 11-24b) are used in a balanced modulator circuit by employing  $g_2$  for the signal and  $g_1$  for the carrier. These particular tubes have, in addition to a high input

impedance, a low filament current—between 10 and 15 ma—permitting accurate electronic stabilization of the filament voltage to minimize drift and pickup.

The circuit design of Fig. 11-24 is supplied by the tube manufacturers.<sup>1</sup> When a rectangular carrier of 6 volts is applied to the normally cut-off  $g_1$  of the two tetrodes, approximately  $250 \mu\text{a}$  flow in each one from  $g_1$  to cathode. This causes switch operation of the two tetrodes in a manner similar to that indicated in the previous figure. Most of the carrier voltage is canceled from the differential output, and more complete rejection is obtained by a plate-circuit-balancing control which compensates for inequalities in the tubes and components. Either a push-pull or single-ended input may be used, and in the latter case one of the input leads is grounded. The output of this modulator may be connected in a feedback circuit as shown in Sec. 11-6.

The manufacturers' data on the performance of the circuit give a stability of  $\frac{1}{2}$  mv at the input terminals over a period of 24 hr ( $0.3 \mu\text{v}/\text{min}$ ). The grid current of the single electrode is less than  $10^{-14}$  amp. A switch is included in the carrier circuit as a result of the manufacturers' tests, which indicate that the stability of the cathode is impaired by current flow before the operating temperature is reached. This unusually high stability was not observed in preliminary tests at Radiation Laboratory.

These tubes (VW-41) have excessive microphonics for applications requiring rapid response: when the tube is gently tapped, fluctuations



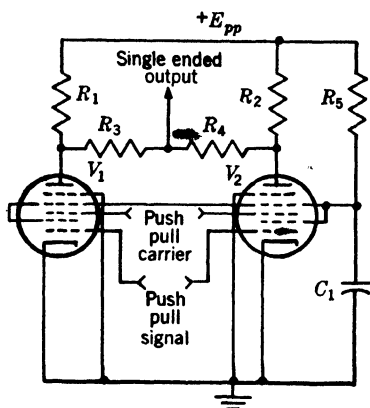
(a)

FIG. 11-25.—Carrier-balanced modulator using multigrid tubes and supplied with a single-ended carrier and a push-pull signal. The circuit constants used to obtain the waveform diagram are:  $R_1 = R_2 = 7 \text{ k}$ ,  $R_3 = 10 \text{ k}$ ;  $C_1 = 4 \mu\text{f}$ ;  $V_1 = V_2 = 6\text{SA}7$ . The bias for  $g_1$  was set at  $-5.5$  volts, and for  $g_2$  at  $-3.8$  volts. The carrier frequency is  $15 \text{ kc}/\text{sec}$ .  $E_{pp} = 250$  volts.

<sup>1</sup> Victoreen Instrument Co., Cleveland, O. A low-microphonic tube is now being advertised (1948).

equivalent to values from 0.3 to 1 volt amplitude at the grid lasting several seconds have been observed.

*Balanced-multigrid Modulator.*—Convenient forms of balanced modulators giving high-impedance inputs for both signal and carrier are indicated in Figs. 11-25 and 11-26. In the type shown in Fig. 11-25, the application of a push-pull signal gives carrier-balanced operation and a



(a)

FIG. 11-26.—Signal- and carrier-balanced modulator using multigrid tubes and supplied with a push-pull signal and carrier. The waveform diagram corresponds to component values,  $R_1 = R_2 = 13k$ ,  $R_3 = R_4 = 18k$ ; carrier and signal are biased at  $-5$  and  $-4$  volts, respectively.  $R_5 = 15k$ ;  $C_1 = 0.1$ ,  $V_2 = 6SA7$ .  $E_{pp} = 250$  volts; carrier frequency,  $15$  kc/sec.

The operation of this circuit is substantially the same as that of Fig. 11-5 with the important exception that there is continuous conduction of  $V_1$  to  $V_4$  throughout positive and negative excursions of the carrier. The modulation depends upon the variation of the plate resistance of the triodes with grid bias. This feature is of considerable advantage as far as carrier distortion is concerned, although the linearity of modulation is not so good as that obtainable with amplitude selection. In this particular case, the amplitude modulator is designed for use as an element in the negative-feedback system, and linearity is of considerably

differential output. As the waveform diagram shows, the carrier amplitude is sufficient to cause the multigrid tubes to act as carrier-controlled switches. In Fig. 11-26, signal- and carrier-balanced operation is obtained, and the output waveform is seen to resemble closely that shown in Fig. 11-4.

These circuits also make satisfactory curvature modulators since type 6SA7 tubes act as approximate multipliers (see Sec. 19-3), and the value of the signal voltage determines the carrier amplitude. Operation of this type is indicated in Fig. 11-27, where typical waveforms are shown for the two circuits. One advantage of this type of operation is, of course, that the distortion of the carrier waveform is minimized and a simpler filter may be used to remove unwanted harmonics. A more satisfactory circuit for obtaining small carrier distortion is, however, given in the next section.

*Full-wave Balanced-triode Modulator Giving Small Carrier Distortion.*

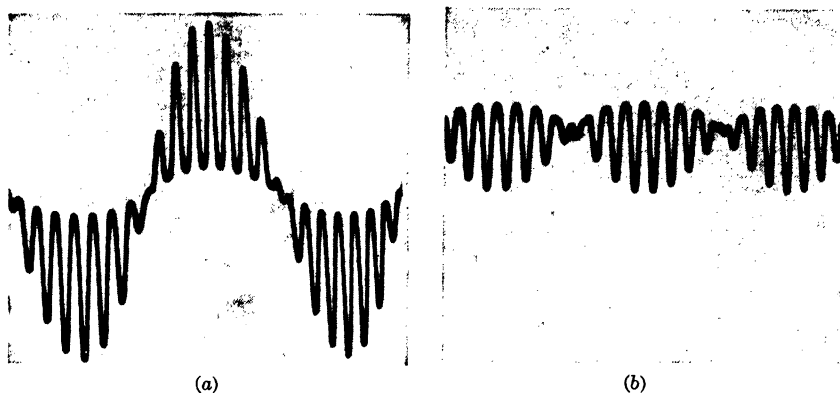


FIG. 11-27.—Output waveforms for balanced curvature modulator. These waveforms indicate, in (a) and (b) respectively, the operation of Figs. 11-25 and 11-26 for smaller values of the carrier. Modulation depends upon variation of the transfer characteristic in response to the signal amplitude.

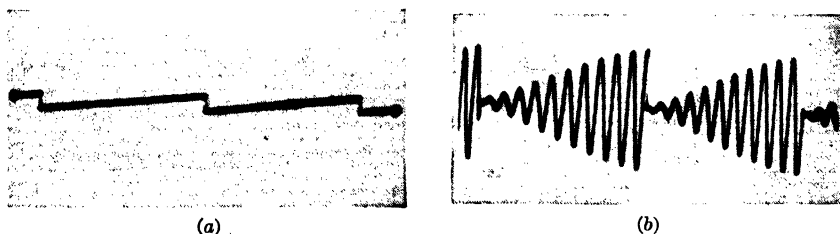
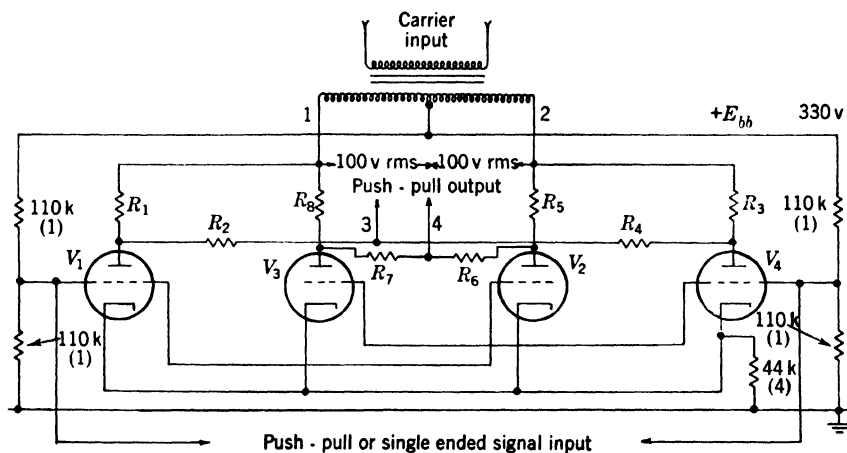


FIG. 11-28.—Balanced triode modulator giving small distortion of the carrier.  $R_1, R_2, R_3, R_4, R_5, R_6, R_7, R_8 = 47 \text{ k} (\pm 5 \text{ per cent})$ . (a) and (b) are signal and output waveforms respectively. Carrier frequency, 2400 cps.



less importance than carrier distortion and phase shift. The cathode resistor for the modulator tubes is so large that a single-ended signal may be satisfactorily inverted; in fact, the input waveform shown in Fig. 11-28*a* is single-ended and gives the push-pull output waveform of Fig. 11-28*b*, as distinct from the previous modulator circuits which require a push-pull input and give a differential output.

The output of this modulator contains some second harmonic components, and in a particular application it was found necessary to employ a twin-T selector circuit to reject the second harmonic component and to give a wave with negligible phase shift (see Vol. 20, Sec. 11-7).

**11-5. Variable-capacitance Modulators.**—Just as the mechanical-switch modulator appears to be outstanding for the potential measurement in low- and medium-resistance circuits (to  $10^6$  ohms), the variable-capacitance modulator appears to be ideally suited to the potential measurement in high-resistance circuits ( $10^6$  to  $10^{12}$  ohms). These modulators are, however, not of the switch type, since the variation of the amplitude of the input signal by capacitance variation rarely approaches 100 per cent. These modulators are nonlinear and are, therefore, nearly always used in negative-feedback systems.

A particular design has been highly developed for electrometer applications.<sup>1</sup> The variable-capacitance modulator is isolated from the current source by a high value of input resistor (around  $10^{11}$  ohms). The variable capacitance itself is roughly 40  $\mu\text{mf}$  and has a conversion efficiency (rms voltage out)/(d-c voltage in) of approximately 0.2. In one type of construction the input plate of the variable capacitance is fixed and the other plate is vibrated at 60 cycles by an electromagnetically driven reed. The input plate of the variable capacitance is, however, shielded from the electromagnet. For optimum stability the vibrating reed and the input plate of the condenser are made of hardened steel, are optically polished on one face, and are gold-plated and gold-evaporated in pairs. The entire assembly is then sealed and filled with argon at atmospheric pressure. This treatment is required to obtain the high stability mentioned below.

In a particular application, type 954 was used as a first-stage amplifier because of its low input capacitance,<sup>2</sup> low grid current, and freedom from microphonics. The output of this amplifier is connected directly to the standard a-c amplifier and two-phase servomotor of the Brown Instru-

<sup>1</sup> H. Palevsky, R. K. Shwank, and R. Grenshik, "Design of Dynamic Condenser Electrometer," Report No. CP3440, Metallurgical Laboratories, University of Chicago.

<sup>2</sup> Advantage may be taken of a positive-feedback circuit for nullifying the stray capacitance of the input circuit and for greatly increasing the effectiveness of the capacitance variation (see Appendix A).

ment recorder. The output potentiometer of the servomechanism balances the input, in order to achieve high linearity and freedom from gain variation in the amplifier.

The performance of this electrometer is excellent, the input resistance being in excess of  $10^{16}$  ohms and the background current less than  $10^{-16}$  amps. The drift over a period of 24 hrs is less than  $100\text{ }\mu\text{v}$  corresponding to  $0.07\text{ }\mu\text{v/min}$ . With a time constant of roughly 1 sec, over a bandwidth of roughly 1 cps, the short-period fluctuations appear to be somewhat less than  $50\text{ }\mu\text{v}$ . Since the input capacitance of the present instrument is  $40\text{ }\mu\text{mf}$ , the time constant is 4 sec. With a modified design, the input capacitance may be made as low as  $10\text{ }\mu\text{mf}$ . The stability of this instrument appears to be much better than that obtainable with thermionic vacuum tubes, and the associated circuits are simple and compact.

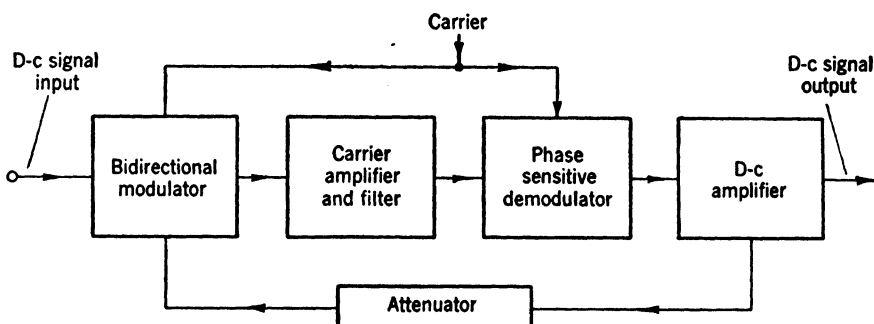


FIG. 11-29.—Block diagram of a negative-feedback modulator-demodulator system.

Another variable-capacitance modulator was developed by RCA. In this unit, operation at the high carrier frequency (2615 cps) is obtained by a loudspeaker voice coil which drives a diaphragm. There is capacitance variation between this diaphragm and four pickup electrodes or probes. Each probe is mounted in a shielded compartment which contains the series resistor for the signal voltage and the coupling capacitor for the a-c output. In actual usage, the amplitude of oscillation of the diaphragm is maintained by a feedback circuit which is controlled from the output of one of the four probes and which adjusts the exciting current in the voice coil to maintain a constant amplitude.

A similar modulator employs a tuning fork for the vibrating element and therefore also serves as a frequency standard. In this case, long and narrow probes parallel to the tines of the tuning fork are employed to give a sizable area and a higher sensitivity.

In contrast with the first example, these variable-capacitance modulators were used with signal voltages in excess of 100 volts. An a-c output of only 0.5 volt is obtained, but the linearity of modulation is extremely

high—better than 0.1 per cent. Thus this modulator serves as a precision multiplier.

**11-6. Negative-feedback Diode Modulator.**—It is often desirable to use modulation-demodulation systems for precise measurements of small voltages. Although the linearity of the diode-switch modulators of Sec. 11-3 is excellent, the use of negative feedback over the whole modu-

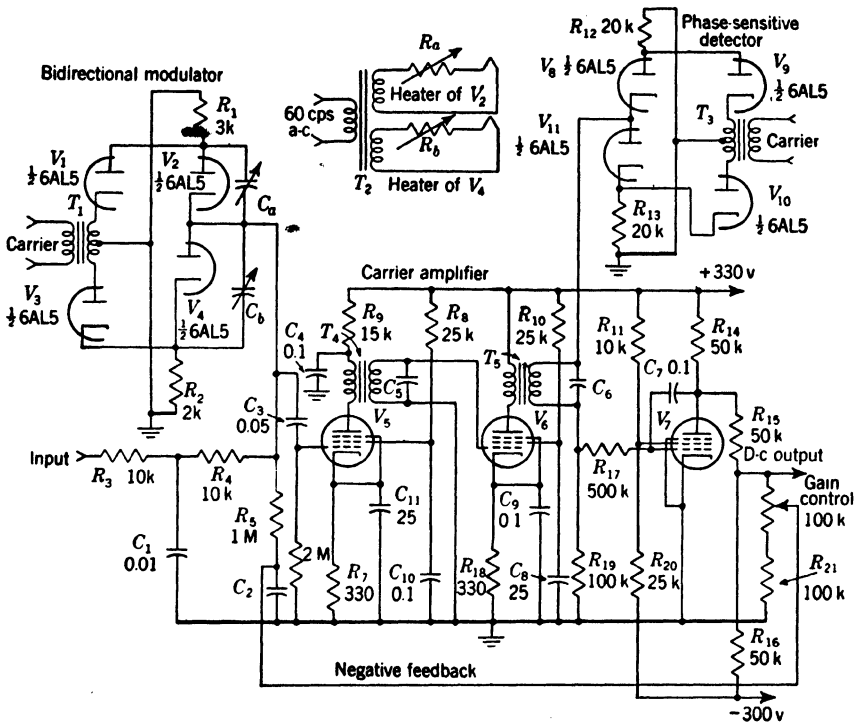


FIG. 11-30.—Negative-feedback modulator employing the circuit of Fig. 11-8 for modulation and demodulation. The particular circuit was designed for operation with a 10-ke/sec carrier. Adjustments  $C_a$  and  $C_b$  and  $R_a$  and  $R_b$  are provided to equalize stray capacitance and contact-potential differences respectively.  $C_2$  and  $C_7$  are chosen to give the desired response speed. The bias networks for  $V_5$ ,  $V_6$ , and  $V_7$  are suitable for British type VR-91, but a small adjustment will give satisfactory operation with type 6SJ7, etc.

lator-demodulator system is used to ensure constancy of gain in spite of wide variations of the characteristics of the carrier amplifier. The block diagram of Fig. 11-29 illustrates the use of phase-sensitive demodulation for this purpose. The output of the modulator is amplified, filtered, and detected. The output of the direct-coupled amplifier following the detector is fed back and subtracted from the input signal ensuring constancy of gain and linearity. The demodulator circuits for these purposes are discussed in detail in Sec. 14-5.

Figure 11-30 shows a practical circuit employing a pair of diode switches for modulation and demodulation. The modulator short-circuits the input voltage at the carrier frequency. The modulated output is connected to a two-stage 10-kc/sec amplifier of gain of  $10^5$ . The output is connected to a phase-sensitive demodulator (see Sec. 14-5) which converts the carrier to direct current by synchronously switching it to ground. A negative-feedback memory circuit (integrator) (see Sec. 14-6 and 18-7) is used to remove the carrier voltage and give a low-impedance output suitable for feeding back to the input stage. The feedback ratio is set by the setting of the gain-control potentiometer and the ratio of  $R_3/(R_3 + R_4)$ , provided the signal input is of negligible impedance. Thus a gain of roughly 50 to 100 is obtainable with excellent stability and linearity. For higher-impedance signals a resistor between point *a* and ground would be desirable to fix the feedback ratio. The stability and the effect of tube and heater voltage change are given in Fig. 11-9.

Although this particular system was designed for a specialized application, wide use of this principle has been made for precision measurements. The over-all stability is, of course, set by that of the phase-sensitive modulator, especially  $V_2$  and  $V_4$ , and complete characteristics of this modulator were given in Sec. 11-3.

**11-7. Modulation with Nonlinear Magnetic Circuits.**—Nonlinear magnetic circuits<sup>1</sup> may be used in negative-feedback modulation systems and give a high stability and linearity in the measurement of potentials obtained from low-resistance sources. The transformers used have a ferromagnetic core and are operated near saturation for greater sensitivity and stability. The hysteresis loop should have a very steep slope as, for instance, in the case of Mo-permalloy, mu-metal, etc. Whenever a pure sine wave of angular frequency,  $\omega$ , is applied to the primary of such a transformer, the potential on the secondary will contain the same frequency and odd harmonics. This is true for any magnitude of the input potential as long as the hysteresis loop is symmetrical with respect to the origin. If, however, this symmetry is disturbed by superimposing a d-c magnetic field and thus displacing the hysteresis loop along the *H*-axis, then even harmonics will appear in the output. The amplitude of these even harmonics will, to a first approximation, be proportional to the superimposed d-c magnetic field. This d-c magnetic field can be produced by a direct current passing through a separate coil wound on this transformer or, in the case of the magnesyn (see Sec. 12-6), by a rotatable permanent magnet.

In order to separate the even harmonics—for instance, the second harmonic—from the fundamental and odd harmonics, it is customary

<sup>1</sup> H. S. Sack *et al.*, "Magnetic Amplifier," NDRC 14-437, Cornell University.

to use two identical transformers and to connect them as indicated in Fig. 11-31. In this figure it is assumed that all the windings are wound in the same sense;  $W_p$  is the primary winding and  $S_1$  and  $S_2$  the d-c input and second harmonic output windings. Under these conditions the

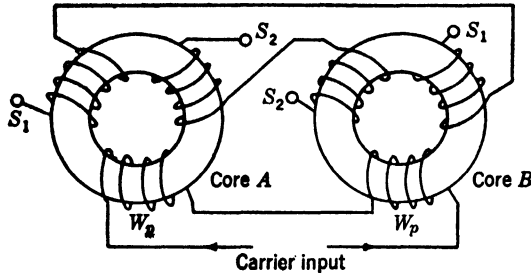


FIG. 11-31.—Nonlinear transformer for amplitude modulation. The two transformers form a balanced circuit eliminating the carrier frequency from the secondaries  $S_1$  and  $S_2$ .

fundamental component cancels out across the two output secondaries, whereas the second harmonic component due to the direct current adds up in the two transformers. This is true, of course, only if the two transformers are ideally matched.

Since the relation between d-c and a-c amplitude is nonlinear, linearity and constancy of gain are obtained by the use of negative feedback as

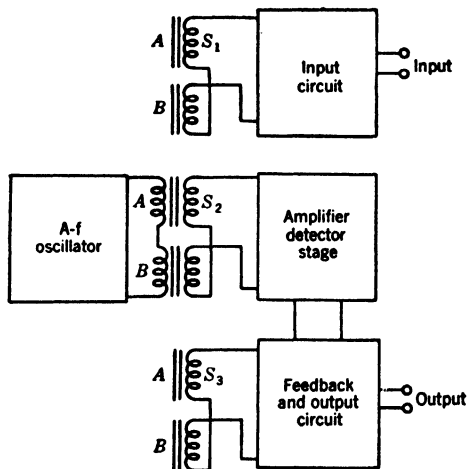


FIG. 11-32.—Block diagram of negative-feedback modulator using nonlinear transformer. As many as five independent windings may be wound on the same pair of cores.

shown in Fig. 11-32. The transformers are provided with another set of windings  $S_3$  similar to the output windings  $S_2$ . The second harmonic appearing on the output winding is amplified, phase-detected, and gives a direct current which is fed into the compensation or feedback windings  $S_3$  in such a way that it opposes the effect of the input direct current.

If the amplification is sufficiently high, the compensation current will then be proportional to the bias current with very high precision.

Let us denote  $I_1$  the bias current,  $I_c$  the compensating current, and  $A$  the over-all amplification of the system. The latter is defined as the ratio of the output current of the amplifier system to the bias current if the compensating coils are not connected. If, furthermore, the number

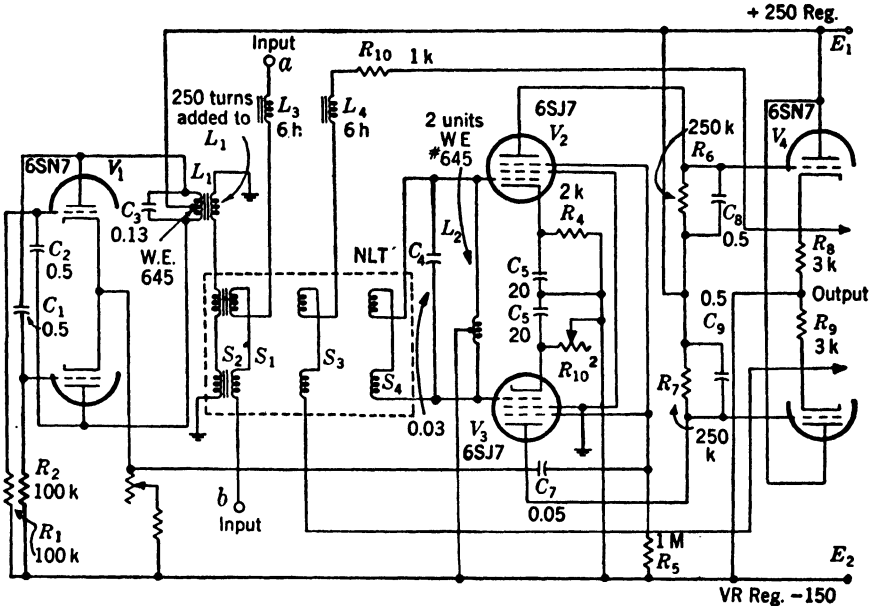


FIG. 11-33.—Typical circuit suitable for use with negative-feedback modulator.  $V_1$  is a 1000-cps oscillator,  $V_2$  and  $V_3$ , a phase detector, and  $V_4$  a pair of cathode followers.

of turns on the bias winding is  $N_1$ , and that on the compensation winding is  $N_c$ , then the following relation holds:

$$I_c = \frac{I_1}{\frac{1}{A} + \frac{N_1}{N_c}}$$

If  $A$  is very large,  $I_c$  will be equal to  $\frac{N_1}{N_c} I_1$ . It is evident that such a system does not require a strictly linear relation in the transformer or a very high stability of the gain of the amplifying system.

Figure 11-33 gives a practical circuit design employing amplitude modulation of this type. Numerous modifications of this circuit may be made for specialized applications, but for most uses this particular design is satisfactory and economical. The oscillator circuit consisting of  $V_1$  and inductor  $L_1$  operates at approximately 1000 cps. This particular

circuit satisfies the requirements of the magnetic circuit since it gives low second-harmonic output (roughly 0.07 per cent). But the second-harmonic signal, later needed for phase detection, is readily available from its cathode circuit. The coil  $L_1$  is Western Electric No. 645, modified by the addition of a 250-turn secondary which is of satisfactory impedance for driving the magnetic circuit to saturation.

The nonlinear transformers were obtained from Bell Telephone Laboratories and, in a particular case, consisted of 250 turns of No. 32 Formex wire for the primaries and five windings of 800 turns each of No. 36 Formex wire for the secondaries. The resistance of the 800-turn windings is 90 ohms. These were all wound on a core made of 0.002 by 0.25 in. of Mo-Permalloy strip and having inner and outer diameters of roughly 1 and 1.5 in. The sensitivity is roughly 35 mv rms/ $\mu$ a with no load. Each transformer is adjusted for optimum cancellation of the fundamental. For practical applications magnetic shielding and shock mounting are desirable.

The output of the windings  $S_4$  is connected to circuit  $L_2C_4$  which is tuned to 2000 cps and then to the phase-sensitive detector consisting of  $V_2$  and  $V_3$ . If a pair of type 6SJ7 is used, a gain of 70 is obtainable (the gain is represented in terms of the ratio of the d-c output potential to the input rms potential). A gain of 120 may be obtained with a pair of type 6AS6. A 40-volt 2000-cps signal is satisfactory for the suppressor grids of type 6SJ7, and 10 volts may be employed for type 6AS6. Any of the other types of phase-sensitive detectors discussed in Sec. 14-4 are applicable here.

The output of the phase detector is connected to the compensating coils by means of the cathode follower  $V_4$ .

The open loop gain  $A$  of the circuit of Fig. 11-33 is roughly 5000. This results in excellent input-output linearity, and the over-all gain is set by  $N_1/N_c$ , a current gain of 1. The corresponding voltage gain is 1000. In fact, experimental tests indicate that there are no measurable deviations from linearity and that the limitation is set by short-period fluctuations. For  $A = 5000$ , the mean deviation between input and output is  $0.026 \mu$ a ( $2 \mu$ v) or 0.0025 per cent of a maximum current of 1.1 ma. Tests extended over a period of a week (at room temperature) indicate a drift of the order of magnitude of  $0.1 \mu$ a ( $1 \times 10^{-3} \mu$ v/min). As a potential-measuring device the performance of this circuit is poor since the short-period fluctuations correspond to a voltage of 30 mv through an impedance of 1 megohm. This is large compared with that expected from well-stabilized direct-coupled amplifiers employing high-quality vacuum tubes—for example, type 6SU7. On the other hand, the long-time stability surpasses that obtainable with direct-coupled amplifiers. Its extremely good linearity and stability recommend its

use where signals from the required source resistance are available. Because of the availability of several independent transformer windings, the flexibility of this circuit makes it a very important device for the addition of voltages and currents of considerably different d-c levels. This circuit has also been used for precision differentiation and integration (see Vol. 21, Secs. 4-4 and 4-8).

**11-8. Summary.**—In view of the foregoing discussion, certain recommendations may be made. Few modulating circuits employing thermionic vacuum tubes give stabilities which are greatly in excess of those obtainable with carefully designed direct-coupled amplifiers. But the important advantage of the modulation system is that reasonable stability may be obtained with very few precautions since not much can go wrong with a simple diode modulator circuit and its associated a-c amplifier. This is not the case with direct-coupled amplifier circuits. Table 11-1 summarizes the characteristics of the modulators which have been discussed. In most cases the performance data were obtained at Radiation Laboratory. In other cases the source of the data was given in the circuit discussion.

Where high stability in voltage measurement in low- to medium-resistance circuits is required and rapid response is not needed, the mechanical-switch modulator is unconditionally recommended, and wherever possible this device should be used in computing and measuring circuits.

For measurements in high-resistance circuits, the variable-capacitance modulator appears to be superior to thermionic electrometer tubes. In connection with the measurement of small photocurrents, it should be remembered that the photocell itself is an excellent switch modulator when supplied with the proper waveform (see Sec. 3-16).

Although the saturable magnetic transformers have no great advantage of sensitivity, they are very convenient for summing a large number of input currents with excellent long-time stability. They also permit a higher carrier frequency and have no moving parts.

Negative feedback in modulation-demodulation systems offers the important advantage of gain stabilization. In addition, negative feedback will correct for nonlinearity in a modulator or a demodulator. Negative feedback should, therefore, be used wherever practicable.

Balanced operation is directly obtainable in modulation circuits employing switches and can also be achieved by cancellation schemes in modulators employing amplitude selection or curvature. In addition to the advantage of eliminating the signal and carrier, balanced operation gives greater stability since the drift of one tube tends to cancel that of the other.

In the various applications of modulation to impedance-changing or



TABLE 11-1.—SUMMARY OF PERFORMANCE OF MODULATION CIRCUITS

Type of modulator	Drift, $\mu\text{V}/\text{min}$	Input re- sistance, ohms	Fluctua- tion, $\mu\text{V}$ (noise or carrier level)	Band- width, cps	carrier fre- quency, cps
<b>High-resistance circuits</b>					
Balanced-triode modulator (6SU7) .....	3	$\sim 10^{10}$			
Balanced-tetrode modulator .....	0.3	$\sim 10^{11}$			$< 10^5$
Variable-capacitance modula- tor .....	$7 \times 10^{-2}$	$10^{11}$	100	0.04	$< 10^2$
<b>Medium-resistance circuits</b>					
Diode-switch modulator .....	$\frac{1}{2}$ to 3	$\sim 2 \times 10^5$	$> 50$	$\sim 100$	$< 10^5$
Germanium-crystal modula- tor .....	0.2 to 1	$\sim 1 \times 10^4$	$\sim 150$	$10^4$	$< 10^5$
Mechanical switch (Brown) ..	$2 \times 10^{-2}$	$\sim 5 \times 10^5$	0.2	$\sim 0.5$	$< 10^2$
<b>Low-resistance circuits</b>					
Saturable magnetic circuits ..	$1 \times 10^{-3}$	90"	2	$\sim 1$	$< 10^4$
Mechanical switch (G.M.) ...	$1 \times 10^{-5}$	5	.003	$\sim 1$	$< 10^2$
Mechanical switch (Brown) ..	$1 \times 10^{-5}$	$\sim 5$			$< 10^2$

level-shifting, nearly any modulator will be found to be satisfactory and may be chosen in the interests of economy rather than in view of the requirements mentioned above. In this connection, gain is often desirable in the modulator stage, and some of the simple double-triode modulators will be found to be of advantage.

Some preliminary data are available on an important use of thermionic switch modulators for multiple-channel data transmission, communication, and computation. In an experimental TRE computer, it was desired to modulate electromechanically a number of different quantities representing range, velocity, etc. by the same element. It was also desired to pass voltages representing these quantities through the same amplifiers. Instead of employing multiple frequencies as in communication practice where phase shift, pickup, and unwanted modulation frequencies may cause difficulties, a train of amplitude-modulated pulses was generated by switch circuits. These pulses were later separated by time selection (see Chap. 10). Modulation and demodulation techniques accurate to better than  $\frac{1}{4}$  per cent are readily available by the methods presented in this chapter and in Chap. 14. By employing appropriate time selection in demodulation, errors due to pulse distortion may be avoided by demodulating after the effects of transients have disappeared.

## CHAPTER 12

### ELECTROMECHANICAL MODULATORS

By F. B. BERGER AND E. F. MACNICHOL, JR.

**12.1. Introduction.**—Mechanical amplitude modulation is the process of converting a mechanical displacement into a variation of electrical potential or current. The elements used in the conversion are known as “electromechanical transducers.” The conversion is accomplished

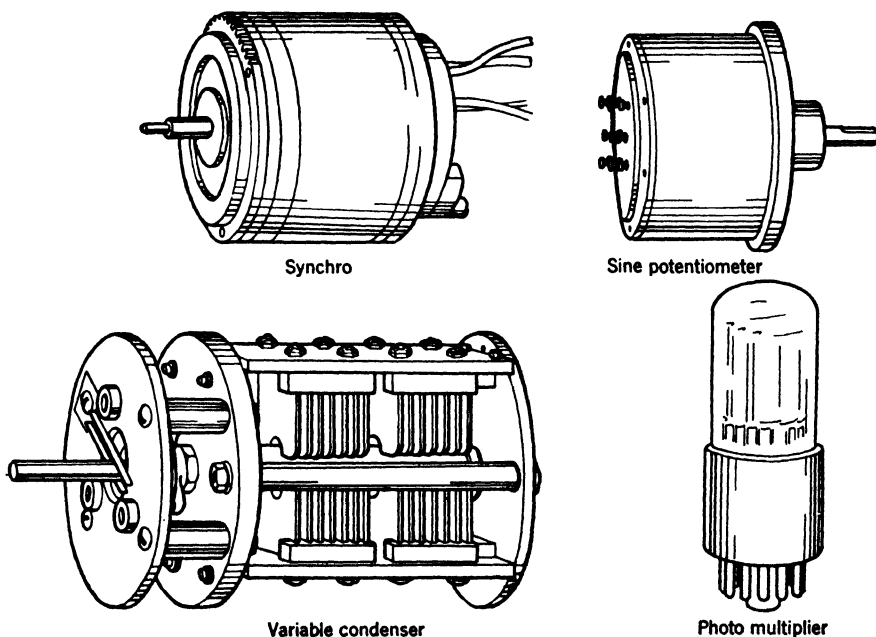


FIG. 12-1.—Electromechanical modulators.

through photoelectric, piezo-electric, magneto-strictive, or other properties of materials, or by change in the electrical capacitance, magnetic flux, or resistance produced by a change in the mechanical configuration of the system. Devices for converting very small mechanical motion into electrical variations such as microphones, phonograph pickups, and strain gauges are well covered in the existing literature. This chapter will confine itself to devices in which the input signal is the rotation of a shaft and the maximum angle of rotation is unlimited or is at least a few

degrees. Unlike most types of microphones, the devices discussed are capable of sustained output at zero frequency of the input data, high accuracy, and a wide range of modulation. Devices with the above characteristics are suitable for use in remote data transmission (Vol. 20, Chap. 10; Vol. 22, Chap. 5), torque amplification (Vol. 21, Part II), and in computing devices (Vol. 21, Part I). Four types of conversion device are considered here:

1. Potentiometers, that is, devices in which a contact is moved over a resistance element.
2. Transformers with variable coupling between windings.
3. Variable capacitances.
4. Photoelectric devices in which a beam of light is mechanically modulated and the light variation converted into an electrical modulation.

The relative merits of these devices are summarized in Table 12-1. Typical examples are shown in Fig. 12-1.

### POTENTIOMETERS

**12-2. Fundamental Characteristics.**—A potentiometer<sup>1</sup> is a variable-resistive voltage divider. Practically all precision potentiometers are constructed by winding wire around a supporting form with the variable contact sliding along the form at right angles to the wire direction at all points. Because of this method of construction, the voltage appearing on the movable arm when a fixed potential is applied across the ends of the potentiometer winding will not vary continuously as the arm is moved, but will change by discrete amounts corresponding to the potential drop across one turn. Some of the undesirable effects resulting from the step nature of the output voltage of a moving potentiometer arm are eliminated or reduced by filtering the output voltage. Figure 12-2 shows the effects of filtering the output of a potentiometer as contrasted with the effects of filtering and demodulation of the output of a transducer employing an a-c carrier.

Another and sometimes serious problem which is encountered with potentiometers is the "noise" or spurious electrical signals arising from fluctuations in brush-to-wire contact resistance, dust on the contacts, or other causes that will be discussed later.

**Linear Potentiometers.**—A potentiometer in which the variation in resistance between a sliding contact and an end is proportional to the displacement of the sliding contact is said to be a linear potentiometer.

<sup>1</sup> Considerable information on construction and available types of potentiometers will be found in Vol. 17, Chap. 8. Applications of potentiometers are discussed in Vol. 21, and Vol. 22.

TABLE 12-1.—ELECTROMECHANICAL MODULATORS

	Torque required	Life	Speed of operation	Short-time stability	Output level	Carrier frequency
Potentiometers	Largest (electrical contact to rotor always necessary)	Wear of contact changes proper-ties. Not more than $5 \times 10^6$ operations permitted even with best designs	Excessive wear if motion of variable contact exceeds 5 in./sec in best instruments	Excellent; may have very low temperature coefficient	Preferably low. Output resistance of precision types usually limited to 50 k by wire size	Zero frequency may be used. Maximum frequency limited by capacitance and inductance of windings
Variable trans-formers	Large in those de-vices requiring slip rings	Indefinite in those devices that do not require slip rings (at least as long as well-de-signed motor for all types)	May be as high as in similarly de-signed electric motor. Depends only upon carrier frequency in types that do not require electrical contact with ro-tor	Fairly large tem-perature coefficient of resistance in windings and of reluctance in magnetic circuit	Upper limit de-termined by wire size and inter-winding capaci-tance	Commercial de-vices 30 cps to 100 kc/sec
Variable capa-citances	May be v e r y small; some types require contact to rotor	Indefinite in those types that do not require contact to rotor	Depends only up-on carrier fre-quency in types that do not re-quire electrical contact with ro-tor	May be made very high if correctly designed	Depends upon fre-quency of carrier; capacitance range $\approx 5$ to 1000 $\mu\text{mf}$	Generally imprac-tical below 1 kc; upper frequency at least several Mc/sec
Photoelectric devices	None; no contact to rotor required	No mechanical wear; photo cell and light source may change prop-erties after 100 to 1000 hr	Limited only by high-frequency response of am-plifier when emis-sive cells are used below 1000 cps in photovoltaic and photoresistive types	Photovoltaic and resistance cells have large tem-perature coefficient; amplifiers subject to drift	Impedance above 10 <sup>6</sup> ohms in emis-sive photocells; current amplifica-tion required; low voltage, low im-pedance in photo-voltaic and photoresistive cells	Zero frequency to limits imposed by bandwidth of am-plifier and transit time in emissive cell. Voltaic and resistive cells cut-off above 1 kc

This is the most familiar type of potentiometer and the one made in the greatest variety of forms. Almost all of the composition-type and a majority of the wire-wound ones are designed for uses in which the linearity need be only approximate. Sometimes because of restricted rotation, and more often because of the accuracy required, these potentiometers are unsuited for many applications as modulators. There are, however, a few linear potentiometers that are designed for precision applications.

*Sinusoidal Potentiometers.*—For some applications, particularly as resolvers, potentiometers in which the output voltage varies as the sine

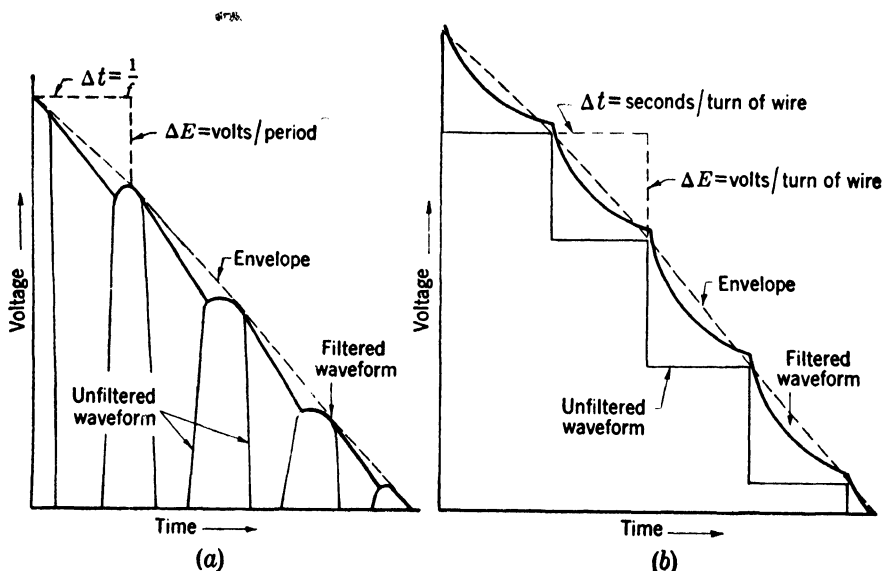


FIG. 12.2.—Comparison of filtered and unfiltered waveforms. (a) Illustrates the peak detected output of an amplitude-modulated sinusoidal carrier. (b) Illustrates the output of a Gibbs micropot before and after filtering.

of the angle of rotation of the brush arm are required. Special potentiometers have been designed for such applications and several models are in production. The cards for such devices are wound similarly to those for linear potentiometers, the output being sinusoidal because of the way the brush is constrained to move over the card.

*Nonlinear Potentiometers.*—A nonlinear potentiometer is one for which the output voltage is a nonlinear function of brush displacement. Many cheap nonlinear potentiometers for low-precision applications are available but, as is the case with linear potentiometers, they are unsuited to most applications as modulators. Units of very high precision for use primarily in computing circuits have been produced. Nonlinear output

voltage as a function of shaft rotation is achieved in eight ways: specially shaped mandrel, controlled wire spacing, control of wire size, special contact arrangement,<sup>1</sup> cam control to shift the contact with respect to the shaft, electrical loading of the output, step potentiometers (contacts plus fixed resistors), and tapped winding with shunts. (Volume 17, Chap. 8.)

*Accuracy.*—By the accuracy of a potentiometer is meant the accuracy with which the observed output signal follows the desired or ideal variation with displacement of the movable arm; for a linear potentiometer the ideal output signal varies linearly with the shaft rotation; any departure from this behavior constitutes an error or inaccuracy. The over-all accuracy depends on a multitude of factors. In the construction of the potentiometer itself, consideration must be given to the extent and nature of the brush contacts, nonuniformity in the resistivity and spacing of the wire and tolerances of mechanical components, to name a few of the most important factors. Some electrical considerations are those pertaining to noise, filtering, loading, and driving. An accurate output demands also that the voltage level of the output be appropriate. “Zero-setting” or establishing this level is accomplished either mechanically by adjusting the relative position of brush and winding or electrically by adjusting the voltages at one or both ends of the winding. For a well-built potentiometer, the accuracy often approaches the resolution.

In most of the applications of linear potentiometers as modulators a fixed potential is applied across the winding, and the output is a slowly varying (with shaft rotation) d-c signal. The potentiometer used in this way is an electromechanical modulating device in which the “carrier wave” is a d-c potential.

**12.3. Linear Potentiometers.** *Applicability.*—When a voltage proportional to a shaft rotation is desired, a linear potentiometer is generally the most satisfactory electromechanical modulating device to use.

An examination of the specifications on available types of potentiometers shows that they can be used if the speed of rotation does not exceed 1 rps and if a life of the order of  $10^6$  cycles and a resolution of the order  $\frac{1}{3}^\circ$  are adequate (see Table 12-1).

Linear potentiometers can be used in circuits in such a way as to give an output voltage that varies other than linearly with the shaft rotation. Such applications will be discussed under nonlinear potentiometers.

*The Carrier.*—In high-resistance potentiometers such as the Helipot,

<sup>1</sup> An example is the sine potentiometer, which is being considered here as a separate type.

Micropot, or in the RL270 series, phase shifts due to inductance and capacitance effects in the windings would appear to make operation unreliable above 1000 cps.<sup>1</sup>

The reader is referred to Vol. 17, Chap. 8 for a discussion of the manufacture of potentiometers and a listing of available types. In Vol. 21, Chap. 5 will be found a discussion of potentiometers as elements in computing circuits. Other pertinent material will be found in Vol. 22, Chap. 3.

Many linear potentiometers, particularly the Beckman Helipot and Gibbs Micropot<sup>2</sup>, have been used in computers. The use of a carrier of

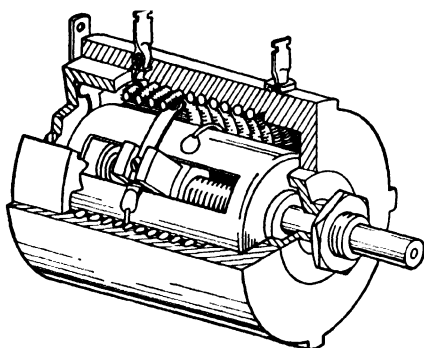


FIG. 12-3.

FIG. 12-3.—The Gibbs Micropot. The Beckmann Helipot is an equivalent device.

FIG. 12-4.—A linear potentiometer designed for data transmission in a radar set. The following data specify the operating conditions: Maximum rate 1 cps, linearity of middle 60°,  $\pm \frac{1}{2}$  per cent; linearity of rest of winding,  $\pm 3$  per cent; life,  $0.5 \times 10^6$  cycles; 505 turns of 0.00275-in. nichrome wire; 130 wires/in.; resolution 0.37°; size,  $2\frac{1}{8}$  in. long  $\times$   $3\frac{1}{8}$  in. diameter; brush force  $80 \pm 10$ ; torque 5 in.; brushes are lubricated.

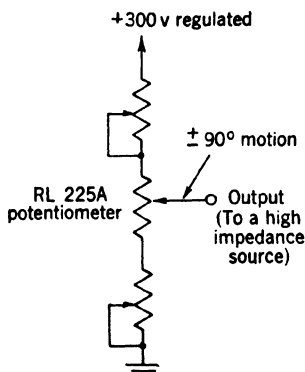


FIG. 12-4.

400 to 500 cps with potentiometers having a resistance of the order of 20,000 ohms is satisfactory. The lower inductance and distributed capacitance of a lower-resistance potentiometer would permit the use of higher-frequency carriers.<sup>3</sup>

*Simple Potentiometer Modulator.*—An example of a potentiometer especially designed for use in data transmission in a radar system is shown in Fig. 12-4. The mechanical signal is a shaft rotating back and forth in a sector of 180° or less. The information obtained from the potentiometer is a d-c voltage that varies linearly with the angle of rotation of the potentiometer shaft. The greatest accuracy is

<sup>1</sup> An experimental device has been constructed in which a rapid sawtooth waveform has been applied directly to a precision potentiometer. (See Vol. 22.)

<sup>2</sup> See Vol. 17, Chap. 8 for description.

<sup>3</sup> A helical potentiometer of 40 ohms resistance made by Minneapolis-Honeywell should be ideal for high frequency use.

obtained in the central 60° section of the winding. The rheostats are provided to adjust the sensitivity (volts/degree) and the d-c level of the output.

*Potentiometer Modulator with Feedback Amplifier.*—A second example of an application of a linear potentiometer to a data-transmission system requiring a linear output is shown in Fig. 12.5.

The potentiometer, type RL 255, is a General Radio 433A<sup>1</sup> 5-in. unit modified to turn continuously through 360° and is supplied with special contactors and slip rings. In this particular application half a 6SN7 is used as a cathode follower to afford a low-impedance output and the

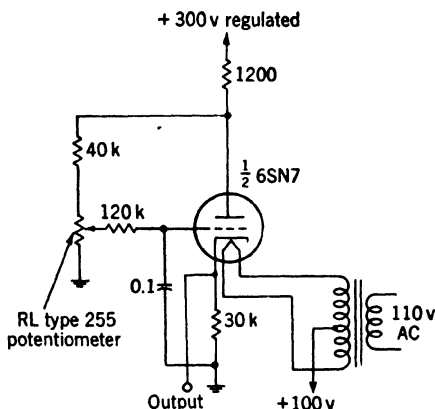


FIG. 12.5.—A potentiometer modulator with a feedback amplifier. The following data apply to the potentiometer: type RL 255; rate 18 rpm; linearity  $\frac{1}{10}$  per cent; rotation, continuous; winding, 250 turns/in. of number 41 nichrome wire extending over 322°, total resistance 10,000 ohms; power, 25 watts; life,  $10^7$  rotations at 60 rpm.

output is utilized only when it exceeds 60 volts. To compensate for the nonlinearity of the cathode follower,<sup>2</sup> the potentiometer is driven not from a fixed-potential source but from the plate of the triode. As the potentiometer output goes more positive with respect to ground the grid volts/degree decreases correcting for the increasing cathode-follower gain. This principle of driving the potentiometer from a source whose voltage is a function of the output can be extended, of course, to introduce a desired departure from linearity. The data are smoothed and the little noise present is reduced by use of the RC-filter section on the potentiometer output. This particular potentiometer is designed to operate without lubrication on the sliding electrical contacts since the electrical noise is thereby reduced. Both the resolution and the linearity of the potentiometer are about 0.1°.

<sup>1</sup> The Muter Co. makes an almost identical potentiometer.

<sup>2</sup> Discussed in Vol. 22, Chap. 4.



The linear potentiometer is very well suited to what is known as "multiple-scale modulation."<sup>1</sup> Figure 12-6 illustrates such a modulator. The total input resistance is  $4R$ . An output voltage anywhere from zero up to  $e_{in}$  can be obtained by proper positions of the potentiometer shaft and the switch  $Sw_1$ . If the fixed resistors are precise, then the system has the advantage of a resolution as great as would be obtained with a potentiometer with a winding extending over four times the angle of the present one. In general, a multiple-scale system has definite advantages as far as accuracy is concerned; it does, however, require some

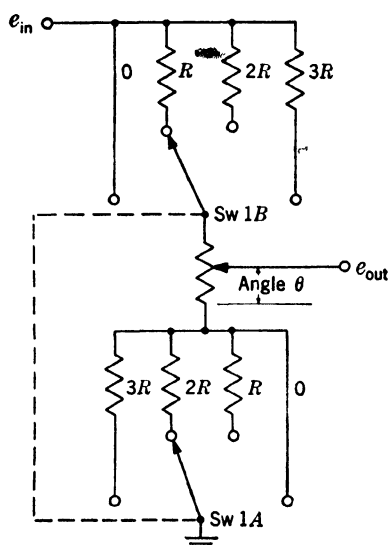


FIG. 12-6.—A multiple-scale potentiometer modulator.

type of synchronizing element to tell which cycle of the high-speed scale is being used. In Vol. 20, Chap. 6, such a system is discussed.

Several types of ingenious mechanisms for coordinating the "fine" and "coarse" scales of the two-scale system have been made with the result that a single control will give a continuous potential variation over the entire range. Such mechanisms operate, in general, by employing for the fine scale a potentiometer that covers very nearly  $360^\circ$ —perhaps  $359\frac{1}{2}^\circ$ . As the potentiometer nears the  $359\frac{1}{2}^\circ$  point, a switch is arranged which moves the taps of the coarse scale to the next pair of contacts. The potentiometer continues to move through  $360^\circ$ , starts over again, and gives substantially continuous motion except for the  $\frac{1}{2}^\circ$  gap.

Numerous examples of multiple-scale systems are available in laboratory potentiometers and bridges. In these, however, there is no coordination of the two scales.

**12-4. Sinusoidal Potentiometers.**—The primary function of these potentiometers<sup>2</sup> is to provide from one to four d-c potentials which vary sinusoidally with the angle of rotation of the shaft of the potentiometer. When there are four outputs, they have the same amplitude and are phased at  $90^\circ$  intervals with each other. Most of these potentiometers function continuously through more than  $360$  degrees of rotation in either

<sup>1</sup> Multiple-scale modulation is discussed in Chap. 13, and in Vol. 20, Chaps. 3 and 6.

<sup>2</sup> The reader is referred to Vol. 17, Chap. 8 for a more detailed discussion of the construction of these units.

direction. Although sinusoidal potentiometers were originally designed for use as sine-cosine resolvers in radar systems having plan-position indicators, they have found other applications, particularly in computers. A "midget" potentiometer that had a card  $1\frac{1}{8}$  in. wide was developed, and a "giant" unit using a 6-in. card was developed for high accuracy and high resolution applications. One of the most widely used of the sinusoidal potentiometers, RL 14 (Fig. 12-7), will be described in some detail.

The sinusoidal variation of the output voltage of the potentiometer is obtained by moving an essentially point-contact brush in a circle upon a

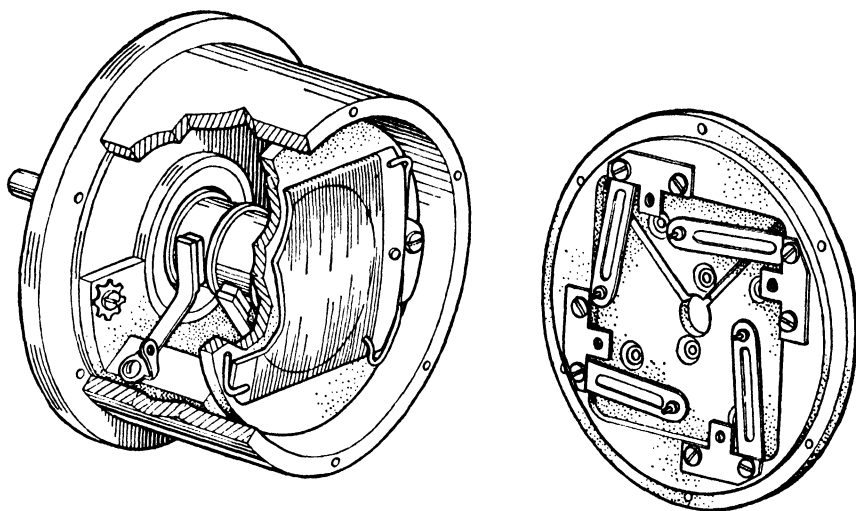


FIG. 12-7.—Sinusoidal potentiometer type RL-14. The performance is indicated by the following data: angular resolution  $\pm 1^\circ$ ; life  $5 \times 10^6$  revolutions at speeds up to 120 rpm; weight 1 lb, 6 oz; diameter  $4\frac{1}{2}$  in.; length  $4\frac{1}{2}$  in.; winding resistance 32,000 ohms; applied voltage 300 volts or less; 305 turns/in. of 0.0025-in. diameter nichrome wire; formex insulation; brush force 30; resolution 0.3 per cent of peak voltage.

family of straight parallel wires which lie approximately in a single plane and which have a constant potential gradient. Four brush contacts rotate in the same circle and are always  $90^\circ$  separated from each other.

Among the more important features of design of the potentiometer are: the cambered wire-wound resistance card; the material, size and shape, and method of mounting of the four brushes that contact the wire-wound card; the almost point contact obtained with a relatively wide brush; and the absence of lubrication. Also since the card is rotated against the brushes rather than vice versa, fewer slip rings are required.

The resolution expressed in terms of rotation angle varies from  $0.17^\circ$ , when the brush is moving at right angles to the turns of wire, to  $4^\circ$ , when the brush is moving parallel to the wire. The resolution that is generally

of interest, however, is the angular resolution of the rotation of the vector whose components constitute the outputs, that is, the angle of the small but finite step with which the vector rotates. This angle varies from  $0.17^\circ$ , when two of the brushes are moving normally to the wires, to  $0.24^\circ$ , when all four are at  $45^\circ$  with respect to the wires. (See Vol. 20, Chap. 5.)

One circuit in which this potentiometer was used is shown in Fig. 12.8.

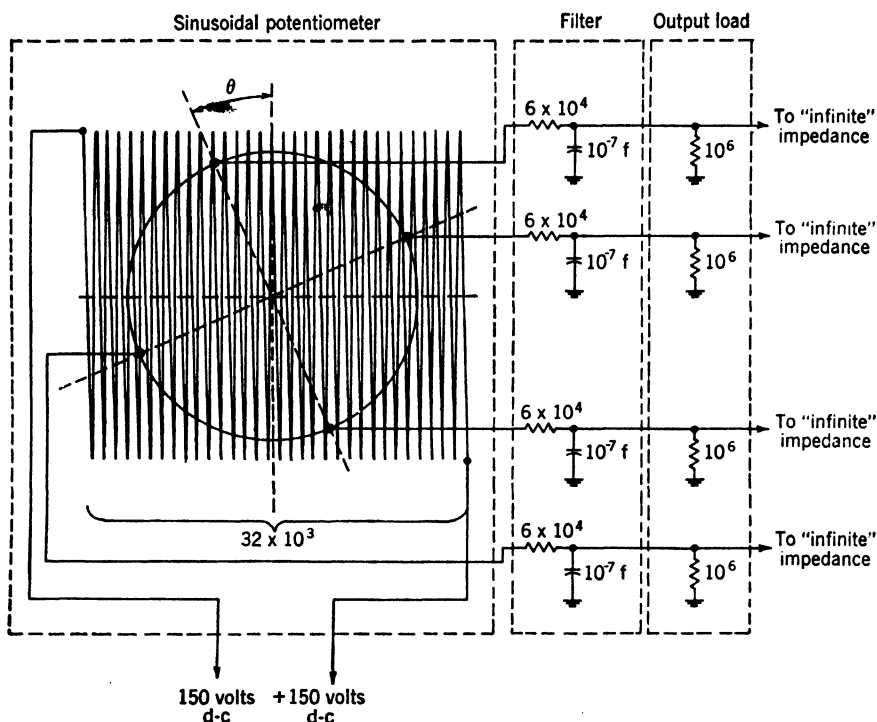


FIG. 12.8.—Sine potentiometer with filtered output.

A simple single-section  $RC$ -filter is included in series with each output lead as shown. The filter, of course, introduces a delay between the shaft rotation and the rotating-output vector. For the values of  $R$  and  $C$  shown in Fig. 12.8 ( $60 \text{ k}$  and  $0.1 \mu\text{f}$ ) at  $10 \text{ rpm}$  the lag is  $0.36^\circ$ .

**12.5. Nonlinear Potentiometers.** *Nonlinear Output Signals Obtained by Use of Inherently Linear Potentiometers.*—In the discussion of Fig. 12.5 in the section on linear potentiometers, a means was indicated in which, by driving a physically linear potentiometer from a source whose voltage is a function of the output signal, this output signal can be made to depart from linearity in a prescribed fashion. Another approach to obtaining a nonlinear output is illustrated in Fig. 12.9 where two linear

potentiometers are ganged, the output of one being the input to the other. If  $R_2 \gg R_1$  or if an isolating linear amplifier is inserted between the output of the first potentiometer and the input of the second, then the output is proportional to the square of the common shaft displacement.

In Fig. 12-10 is shown a method of obtaining a resistance variation proportional to the square of the rotation of the shaft of a single linear potentiometer. Let the rotation  $\theta$  be measured from the center of the

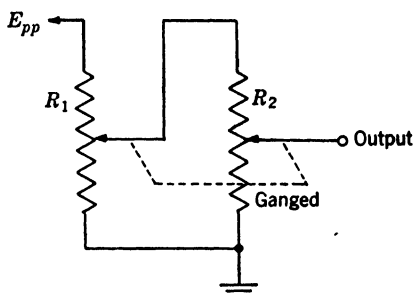


FIG. 12-9.—A means of obtaining an output voltage proportional to the square of a shaft rotation with a dual linear potentiometer.

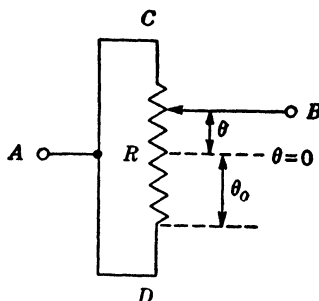


FIG. 12-10.—A method of obtaining a resistance variation proportional to the square of the rotation of the shaft of a single linear potentiometer.

winding of resistance  $R$ . The resistance between points  $A$  and  $B$  will be given by

$$\frac{1}{R_{AB}} = \frac{1}{R_{ACB}} + \frac{1}{R_{ADB}}, \quad (1)$$

where  $R_{ACB}$ , the resistance above the sliding contact, is equal to

$$\frac{R}{2} \left( 1 - \frac{\theta}{\theta_0} \right),$$

and  $R_{ADB}$ , the resistance below the brush, is  $R(1 + \theta/\theta_0)/2$ ; and where  $\theta_0$  is the maximum angle, which corresponds to  $R/2$ . Expressed as a function of  $\theta$  then

$$R_{AB} = \frac{R}{4} \left[ 1 - \left( \frac{\theta}{\theta_0} \right)^2 \right]. \quad (2)$$

An application of this “quadratic potentiometer” to approximating the secant function is shown in Fig. 12-11. A simple calculation shows that

$$\frac{E_{out}}{E_{in}} \approx \frac{r_1}{r_1 + r_2} \sec \left( \frac{\delta}{\Delta} \right) \sqrt{\frac{2r_2}{r_1 + r_2}}. \quad (3)$$

The approximation is in error by only  $\frac{1}{24}$  of the fourth power of the argument. If the maximum angle  $\Delta$  is 1 radian ( $\pm 57^\circ$ ) and if  $r_1 = r_2$ , the

circuit in Fig. 12-11 gives an approximation to the secant of the shaft rotation good to 1 per cent or better in the range  $\pm 40^\circ$ .

Figure 12-12 shows another useful circuit using a linear potentiometer, this one giving an output voltage proportional to the reciprocal of the shaft displacement as measured from the proper zero.<sup>1</sup>

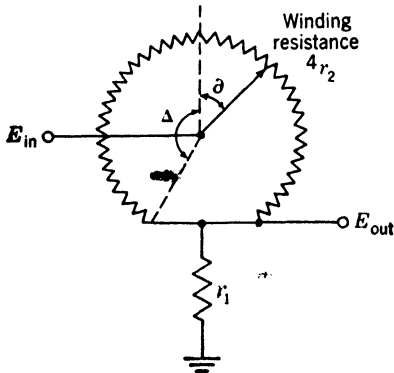


FIG. 12-11.—An application of linear potentiometer to approximate the secant function.

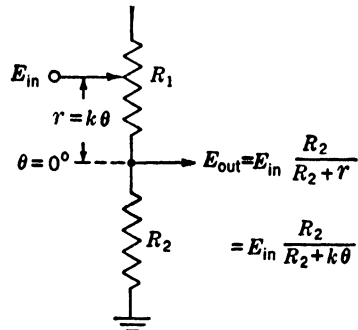


FIG. 12-12.—Use of a linear potentiometer to obtain a voltage inversely proportional to the shaft displacement.  $R_2$  corresponds to an angle of  $(R_2/k)^\circ$ .

Another circuit, shown in Fig. 12-13, is an example of a loaded output. It can be shown that if  $\frac{R}{2R + r_0} \frac{1}{\theta_0^2}$  equals  $\frac{1}{3}$ , the output approximates

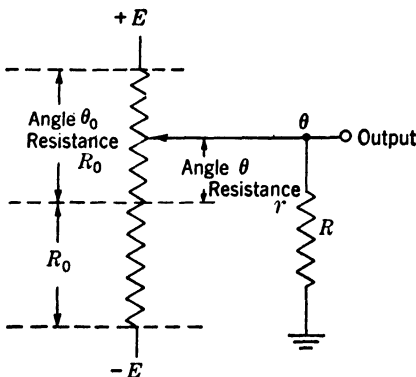


FIG. 12-13.—Use of linear potentiometer to obtain an output approximating the tangent function.

tangent  $\theta$  to within  $\theta^5/45 + \dots$ . If  $\theta_0 = 1$  radian, for example, this condition is satisfied for  $r_0 = R$ .

By the methods illustrated and by combinations of these techniques, a great variety of nonlinear outputs can be derived by employing inherently linear potentiometers.

*Nonlinearly Wound Potentiometers.*—Potentiometers are available in which the resistance between the sliding contact and one end of the winding is a nonlinear function of the displacement of the sliding contact.<sup>2</sup> They are made in various

ways enumerated in Sec. 12-2. One example of the application of such a potentiometer will now be discussed.

<sup>1</sup> The proper zero is  $(R_2/k)^\circ$  less than  $\theta = 0$ .

<sup>2</sup> See Vol. 17, Chap. 8.

In one type of CRT display, it is desirable that the electron beam be displaced linearly with a potentiometer shaft rotation. A direct drive of the CRT deflection coil is employed in the present case, which is illustrated in Fig. 12-14. The load, represented by  $R_L$ , "turns through" an angle  $\theta$  of  $\pm 75^\circ$ . It can be shown that if the current through  $R_L$  is to be proportional to  $\theta$ , the potentiometer must be wound so that

$$\theta = \frac{\pi r}{2R} \frac{1}{1 + \frac{R}{R_L} \left(1 - \frac{r^2}{R^2}\right)} \quad (4)$$

If  $R/R_L$  is chosen to be large, for example  $= 1$ , the width of a card that would satisfy Eq. (4) would change by a factor of 7 over a  $90^\circ$  range. Not only is such a tapered card difficult to wind, but it is also more difficult to approximate with several linear sections (stepped card) than if  $R/R_L$  were smaller. From these considerations and from consideration of power drain and power dissipation, the value of  $\frac{1}{2}$  for  $R/R_L$  was chosen as being optimum. A composition resistance element is not suitable for the present use because manufacturing tolerances are too broad, humidity and temperature would affect it unduly, and it would wear too rapidly. The potentiometer as manufactured is wound with a single size and type of wire with uniform spacing on a toroidal frame (see Fig. 12-15) which is stepped to give a number of linear resistance sections. These different linear sections afford a sufficiently close approximation to the required resistance taper. The production unit has four linear sections in each  $90^\circ$  segment. The potentiometer resistance  $R$  was chosen to be 100 ohms. The load, which should be 200 ohms, is not too critical; the current in  $R_L$  departing by an amount equivalent to  $1.2^\circ$  at  $0.45^\circ$  if  $R_L$  is 220 ohms. The brush contacts three or four wires at one time.

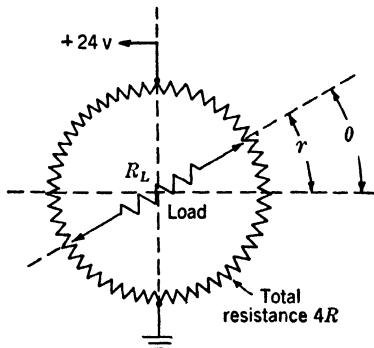


FIG. 12-14.—A nonlinear potentiometer.

**Low-torque Potentiometers.**—A special low-torque potentiometer is shown in Fig. 12-16. The small diameter of the winding and slip ring at the points of contact, the small brush area and pressure, and the very small bearings reduce the torque sufficiently to permit the potentiometer to be used as a data take off from a sensitive aircraft instrument. (Giannini Microtorque Potentiometer.)

**12.6. Synchros.**—Synchros are rotary-variable transformers which generally have two or three windings on the stator and one, two, or three

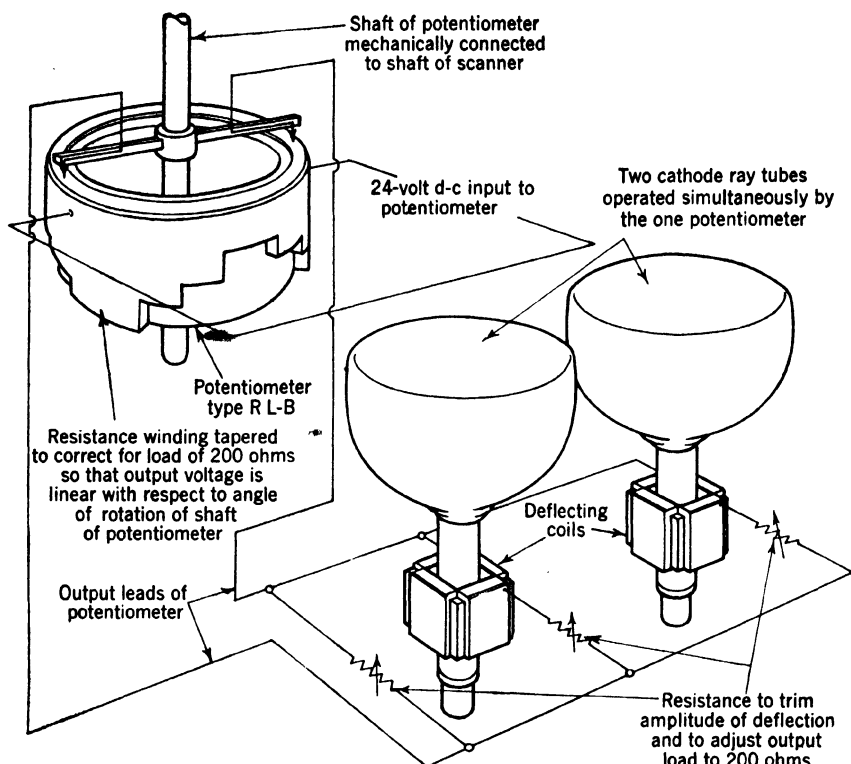


FIG. 12-15.—Nonlinear potentiometer RL-B: resistance  $R$ , 100 ohms, linearity 1.8°; 70 wires/in.; 520 wires total, resolution 0.7°; wire 0.012 in. nichrome; torque 5 in.; life  $10^8$  cycles; applied potential 24 volts.

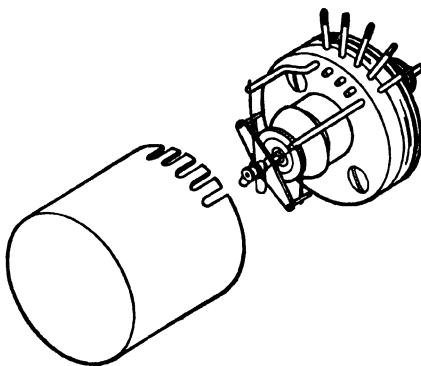


FIG. 12-16.—The Giannini Microtorque Potentiometer, a 360° type requiring extremely low torque.

windings on the rotor. When synchros are used as electromechanical modulators, the rotor winding is generally the primary of the transformer and the stator windings the secondary.

*Available Types.*—"Synchro" is a generic term applying to a multitude of similar devices manufactured by several companies, many of

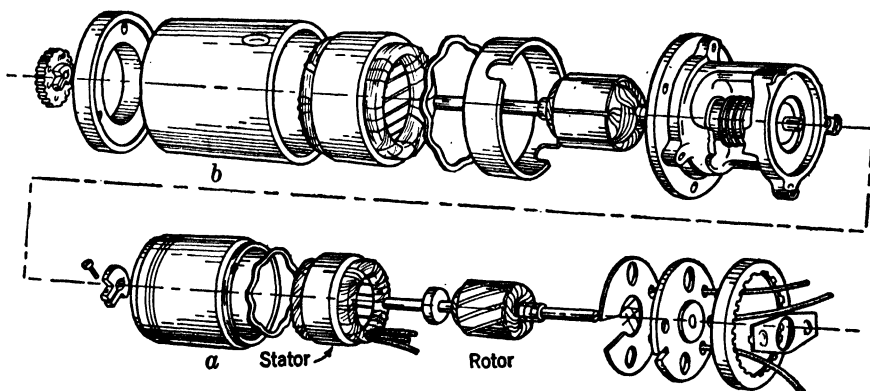


FIG. 12-17.—Miniature precision synchros 2-phase stator 2-phase rotor. (a) Bendix AY 120D accuracy  $\pm 0.25^\circ$ . (b) Special highly accurate resolver (Bendix) accuracy  $\pm 0.1^\circ$ .

which have trade names for their products: for example, the General Electric "Selsyn," the Kollsman Instrument "Teletorque," and the Pioneer-Bendix "Autosyn." Chapter 10 in Vol. 17 of this series discusses the available types in detail. Synchros considered as elements in data-transmission systems are discussed in Vol. 20, Chap. 10 and Vol. 22, Chap. 5. Typical small synchro resolvers are shown in Fig. 12-17.

If a sinusoidal waveform of fixed amplitude, is applied to the rotor winding of a synchro, the waveform observed on the stator or output terminals (open circuit) will, ideally, be a sinusoid of the same frequency as the input waveform, but with an amplitude which varies as the sine of the displacement angle between rotor and stator (see Fig. 12-18). If the stator has a second winding  $90^\circ$  displaced from the first winding, a second sinusoidal-waveform output whose amplitude varies as the cosine of the shaft displacement may be obtained. The modulation envelopes of two output waveforms may be said to differ in phase by  $90^\circ$  with respect to the posi-

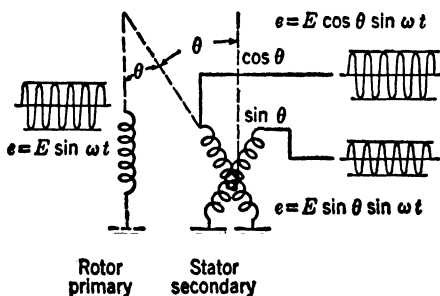


FIG. 12-18.—A 2-phase synchro used as an electromechanical modulator.



tion of the shaft. It is to be pointed out that the electrical phase of the two outputs and of the input or carrier are all the same;<sup>1</sup> they differ only in amplitude. For some rotor positions, of course, one or both output amplitudes will be negative, and this is equivalent to a 180° shift in electrical phase.

*Physical Characteristics.*—The life of most synchros is limited only by wear of the bearings and slip rings. Most of the available types will stand the standard Navy shock and vibration tests,<sup>2</sup> they will operate satisfactorily from -65° to +95°C, and, when the windings are properly impregnated, they will withstand moisture. Synchros vary considerably in size and weight. The Bendix Autosyn AY-100, for example, weighs 5 oz., whereas Navy synchro 7DG weighs 18 lb.

*Angular Accuracy.*—There are several factors to be considered in specifying the accuracy of a synchro. As has been mentioned, the output amplitude should be, ideally, a constant times the sine of the angle of rotation of the rotor shaft. The actual departure from such an ideal output gives a measure of the inaccuracy of the device. The accuracy so measured depends not only on the synchro itself but also on the impedance loading the stator windings, the output impedance of the source, and upon the amplitude of the input. Since synchros have both leakage inductance and stray capacitance, which in general depend on shaft position, the frequency chosen for the carrier or the Fourier components of a complex-waveform carrier will have a determining effect on the accuracy. The inaccuracy is sometimes stated as an angular error; namely, the difference between an actual shaft displacement and the displacement that would ideally give the observed output. In all statements concerning angular accuracy some normalization procedure is, of course, implied. The angular errors observed in practical applications frequently show a tendency to vary periodically with shaft rotation. For example, the error is a maximum at 60° intervals for most 3-phase synchros. The absolute accuracy obtainable varies widely, being confined to less than 0.1° in the case of the Bendix AY-400 Autosyn and being as large as 7° for an Army Mark XVII synchro. If the device is improperly used, much larger errors will sometime result. The nature and magnitude of the angular error, inasmuch as they are determined by the synchro itself, are dependent on numerous design factors. Some of the most important of these factors are: the number of poles on the stator and rotor; whether or not the slots are diagonal; the uniformity of the stator to rotor air gap; the method in which the coils are wound and the degree to which they are matched; and the degree of magnetic isotropy

<sup>1</sup> There is a small quadrature component caused by leakage inductance and stray capacitance (see Vol. 22, Chap. 5).

<sup>2</sup> See Vol. 17, Chap. 10.

of the iron. When the rotor is turned to null output there are residual components left that cannot be completely eliminated. These are induced by electrostatic coupling, and consist of harmonics and a fundamental component in quadrature with the exciting signal. The harmonics may be removed by filtering and the quadrature component disappears in the process of phase detection. The angular accuracy of a synchro modulator used in practical systems depends upon two factors: (1) the intrinsic accuracy of the synchro itself expressed in degrees, and (2) the number of degrees of rotation corresponding to full scale. In single-scale systems the full scale is, of course,  $360^\circ$ . Multiple-scale systems employing two synchros geared together so that they operate at different speeds may be used in which the fine scale may cover any reasonable number of degrees desired. For example, two-speed systems at 36 to 1 are employed as standard Army-Navy data-transmission systems. In this way, a 36-fold increase of accuracy is achieved. Not only does the use of two synchros permit the great increase of accuracy, but it often enables a decrease in the tolerance of the synchro and the use of a cheaper or more readily available design. A drawback of the multiple-scale system is, of course, the need for synchronization to indicate which sector of the slow-speed shaft is being represented by the high-speed shaft.

*Generator Effect.*—A synchro is not essentially different from an a-c generator. In view of this, it is readily seen that if the primary current has a d-c component, there will be a component of the output voltage that is proportional in magnitude and frequency to the speed of rotation superimposed on the desired modulated output.

*Waveform Distortion.*—The above paragraphs discuss errors that are characteristic of synchros used as rotating devices. The performance of synchros considered as transformers must also be borne in mind, that is, the output waveform differs in several respects other than amplitude from the input waveform, frequently in ways that are independent of rotor-stator displacement. Because of the leakage inductance between rotor and stator and because of distributed capacitances, an induced sinusoid will, in general, be shifted in phase with respect to the primary sinusoid. This is a consequence of importance in some applications. Complex waveforms, such as a triangular wave, will be distorted on passing through a synchro in a way dependent on the frequency-response characteristics of the device and on the amplitude of the waveform. Waveform distortion is, of course, dependent upon output loading and driver characteristics as well as upon the synchro itself.

*Applicability.*—Because of their essential sinusoidal nature, synchros as modulating or as data-transmission devices are particularly adapted to the role of sine-cosine resolvers, that is, to obtaining outputs proportional to the sine and cosine of the shaft displacement. Synchros can

be used and have been used as modulators where the required electrical signal is some function other than the sine or cosine of the mechanical displacement. One approach is to use a nonlinear mechanical link preceding the synchro, for example, a suitable cam arrangement on the synchro shaft. The other approach is to synthesize the required electrical signal by using additional available electrical signals such as the sines and cosines of angles that are multiples of the primary rotation angle. In this way outputs that vary approximately as the tangent of the angle, etc. can be obtained.<sup>1</sup> Another method for obtaining other than a sinusoidal output and which is possible for certain applications is to distribute the rotor and stator windings in such a way that the synchro output is the desired function of shaft rotation.

Frequently when a synchro is used as a resolver, the output information is desired in the form of two orthogonal components. When the

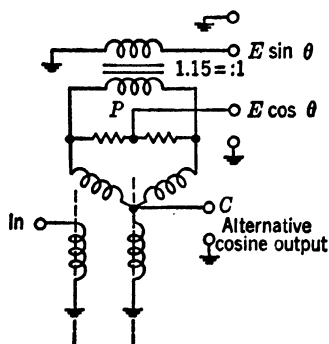


Fig. 12-19.—Conversion of 3-phase output to 2-phase output.

synchro secondary has a 2-phase winding, the intelligence is in this form (see Fig. 12-18). Many of the available synchros have 3-phase windings, however, and although 3-phase information can frequently be utilized, 2-phase output signals are often required. Figure 12-19 shows one method in which the desired outputs can be obtained. The center tap (C in Fig. 12-19) is not brought out on any of the standard synchros. If the tap P is made adjustable, the cosine output can be rotated a few degrees while retaining practically constant amplitude. This procedure

is of value as an alternative to a mechanical zero-set adjustment if only one component is needed. Another way of accomplishing this phase transformation is by the use of "Scott connected" transformers.<sup>2</sup>

The most convenient way to classify synchros for further discussion is on the basis of the nature of the carrier waveform. The following three sections will discuss the use of synchros with sinusoidal carriers, their use as complex voltage-waveform modulators, and their use as complex-current-waveform modulators.

**12-7. Use With Sinusoidal Carriers.**—Sinusoidal waveforms are usually used when wave shape is not a characteristic of primary impor-

<sup>1</sup> See Vol. 22, Chap. 5.

<sup>2</sup> A transformer with a center-tapped primary is connected between two windings. A second transformer is connected between the center tap and the third winding. The sine and cosine components are taken from the secondaries of the transformers.

tance since sinusoids are easily generated and are the waveforms passed with minimum distortion by synchros.

**Applicability.**—Synchros have been employed in applications using a carrier frequency as low as 30 cps and as high as 20 kc/sec; most applications, however, employ carrier frequencies of 60, 400, or 1000 cps. The

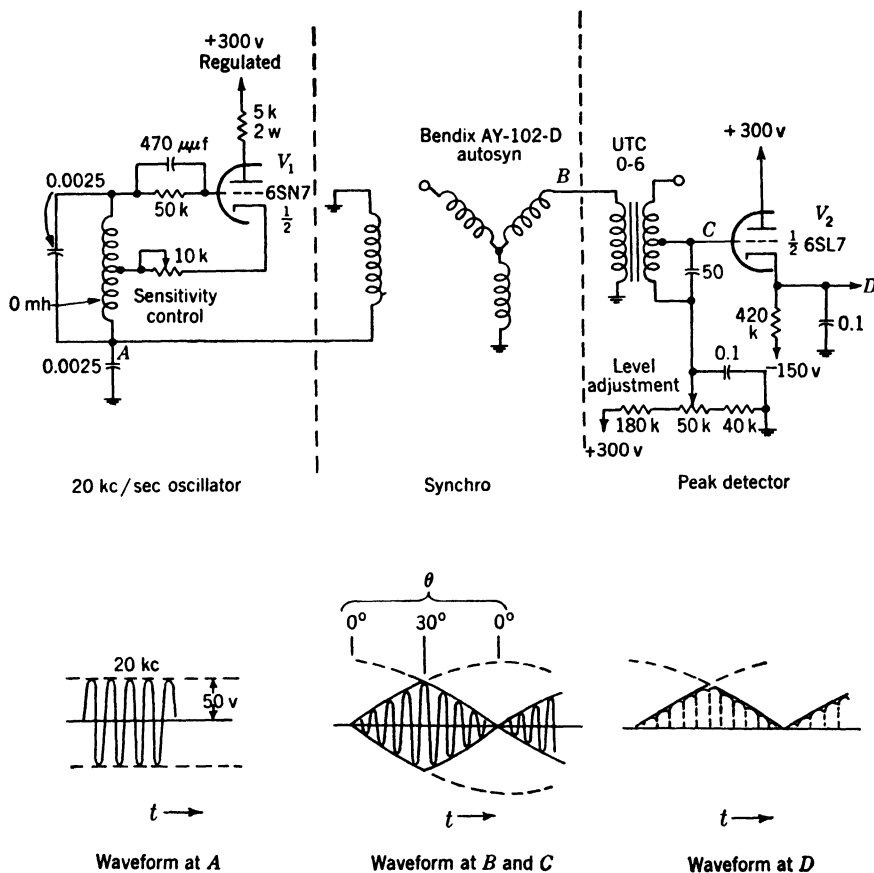


FIG. 2-20.—A simple data-transmission system designed to operate in one quadrant only.

angular velocities occurring in various applications range from zero (hand set) up to more than  $360^\circ/\text{sec}$ , and angular accelerations as high as  $16,000^\circ/\text{sec per sec}$  have been normal in some systems.

**Driving and Demodulating.**—Synchros have been driven with their primaries as plate load, cathode load, or as part of the tank circuit of the oscillator. The examples will illustrate several different circuits that have been used. Practically every type of detector discussed in Chap. 14 has been employed in conjunction with synchro modulators.

Synchros with sinusoidal carriers are very widely used as sine-cosine

resolvers. In such applications, it is also common practice to rotate the coordinate system by interposing a differential synchro.

*Synchro Modulator Employing a Peak Detector.*—A simple data-transmission system designed to operate in one quadrant only ( $0^\circ$  to  $30^\circ$  actually used) is shown in Fig. 12-20. The synchro stator winding forms part of the 20-kc oscillator tank circuit. The leads to and from the synchro were 50 ft long in the system from which this example is taken. Both the Autosyn (at maximum coupling) and the U.T.C. 0-6 are roughly 1-to-1 transformers. The  $50\ \mu\text{f}$  condenser across the transformer secondary tunes the transformer to approximately 20 kc to pro-

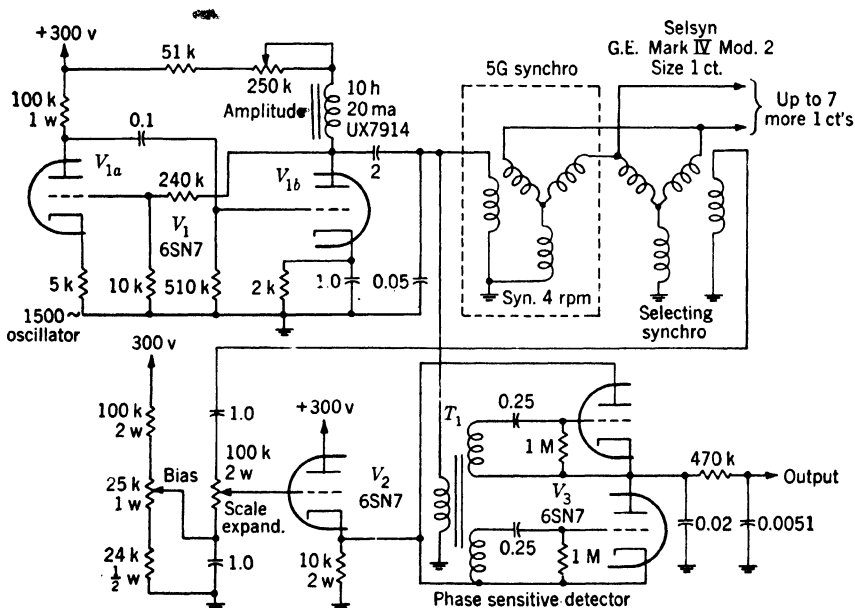


FIG. 12-21.—A synchro modulator and a phase-sensitive detector.

duce a better waveform and somewhat more amplitude than is obtained without the condenser; the amplitude is observed to be only very slightly dependent on frequency over a useful operating range.

At an angular velocity of the rotor of  $150^\circ/\text{sec}$  the time constant of the detector<sup>1</sup> gives a maximum peak-to-peak ripple in the demodulator output of  $\frac{1}{4}$  volt.

*A Synchro Modulator and a Phase-sensitive Detector.*—Figure 12-21 shows a somewhat more complicated example from a radar set in which a synchro<sup>2</sup> turns continuously at 4 rpm. The synchro primary forms part of the tank circuit of the 1500-cps driving oscillator.

<sup>1</sup> Chap. 14 and Vol. 22, Chap. 5.

<sup>2</sup> The 5G in Fig. 12-21 is a Navy synchro designed for 60-cycle operation at 115

The secondary output is not utilized directly, but is fed into a second synchro<sup>1</sup> which serves as a sector selector, that is, it serves to select a sector out of the complete 360° which is represented by the output data. The phase (with respect to the mechanical data) of the output is the sum of the angles of the two synchros. For any fixed shaft position, this synchro may be regarded as a transformer. A fraction of the output of the second synchro is put onto the grid of the cathode follower  $V_2$ . This fraction is chosen by the "scale expand" potentiometer to give the desired volts output per degree of rotation. The reference d-c level of the output is determined by the setting of the "bias" potentiometer. The switch detector composed of  $V_3$  and associated components is a type described in Chap. 14, Sec. 14.4. The 5G synchro, which is geared to the radar scanner, turns continuously in one direction, and the output information is utilized only during a time corresponding to 50° each side of the zero at which the output voltage is increasing.

During the remainder of the cycle the video signals are not sent to the cathode-ray tube on which the information is displayed. The input power to the 5G synchro is sufficient to drive as many as eight selector synchros and outputs.

**12-8. Complex-voltage-waveform Modulation—The Problem.**—It is frequently desirable to control the amplitude of a complex waveform in accordance with a mechanical signal as, for example, in a fixed-coil PPI. This can be done by supplying a d-c control signal obtained from a potentiometer, for example, to an appropriate waveform generator (Fig. 12-22) or to an electronic modulator following the waveform generator. For many applications, it is preferable to generate the desired complex waveform initially and then pass it through an electromechanical modulator; the output is then the required waveform of an amplitude determined by the mechanical signal (Fig. 12-23).

In radar applications, the complex waveform is nearly always a time base and generally a linear time base. In those applications in which the time base is modulated by means of a synchro, it is generally from about 20  $\mu$ sec up to 2500  $\mu$ sec in duration. If the windings of the synchro have extremely low inductance, it is feasible to pass even faster sawtooth waveforms. Longer-duration waveforms can be transmitted if the time constant of the input circuit (effective  $L/R$ ) is made very long. It is not feasible with present techniques, however, to make any one synchro

---

volts input and 90 volts output. The primary can dissipate 6 watts, weight 5 lb; average angular error, 0.2°; peak angular error, 0.6°.

<sup>1</sup> This synchro is a GE Mark IV Model 2 size 1CT instrument designed for 60 cps operation. With 90 volts on the primary (stator) the maximum rotor voltage will be 55 volts. This Selsyn is rated at 1.5-watt dissipation, it weighs 1.5 lb and has average and maximum errors of 0.2° and 0.6° respectively.

suitable at both extremes. A block diagram of such a system as that under discussion is shown in Fig. 12·24. The time-base generator is of no particular concern for the present discussion. The synchro driver is

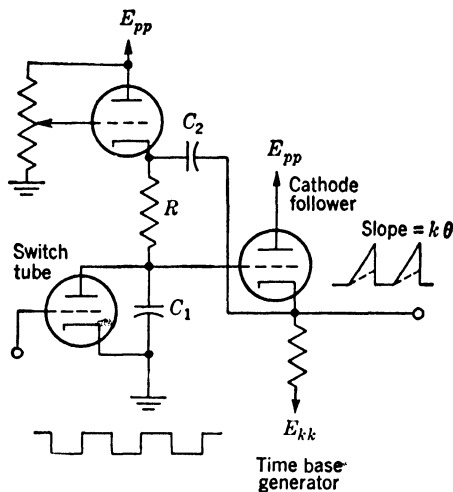


FIG. 12·22.—Generation of an amplitude-modulated sawtooth waveform with a potentiometer modulating a d-c carrier. The modulated carrier in turn controls the sawtooth waveform amplitude.

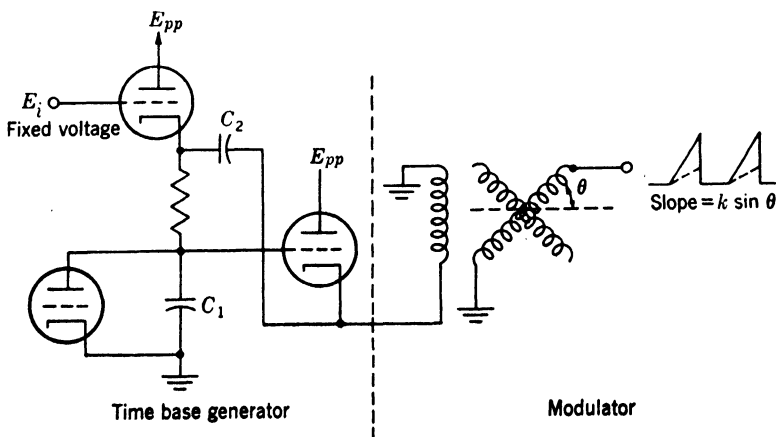


FIG. 12·23.—Generation of an amplitude-modulated sawtooth waveform by passing a constant-amplitude sawtooth waveform through a synchro.

generally distinct from the time-base generator, but sometimes the functions of both the generator and the driver are performed by one circuit. Its function, in any case, is either to impress the proper voltage waveform across the synchro primary or to force the proper current waveform through it. In some applications the synchro output may be

utilized directly; more often amplifiers are used. In a majority of the applications the synchro is used as a resolver, that is, components proportional to the sine and to the cosine of the shaft rotation are both utilized.

*Delay.*—In passing “sweep” or time-base waveforms through synchros and associated circuit elements, some delay in the start of the output waveform is observed. This delay is due largely to the fact that the synchros, transformers, and deflection coils are not purely inductive elements, but they have resistance losses, distributed capacitance, and leakage inductance. In some applications employing fast-sweep waveforms, for example, a sawtooth waveform of 50- $\mu$ sec duration the commonly encountered delay of 3 or 4  $\mu$ sec is excessive.<sup>1</sup> In such cases it is customary to prestart the sweep waveform generator with respect to the basic timing signal to compensate for the delay, that is, to start the sawtooth waveform generator some 3 or 4  $\mu$ sec earlier than would otherwise be done.

*Voltage-waveform Drivers.*—The remainder of this section will be devoted to applications in which the voltage waveform is of primary interest. The following section (12-9) will discuss those applications in which the current waveform is the foremost consideration. Radar has made considerable use of both current and voltage-waveform synchro modulators. Volume 22, Chaps. 5 and 10 discuss such applications in considerable detail. Methods of obtaining the desired waveforms are discussed in Chaps. 2 and 8.

If the desired synchro output is a voltage waveform similar to the output of the time-base generator, it is necessary that the voltage waveform across the synchro primary have this same shape. The simplest form of driver circuit for accomplishing this is illustrated in Fig. 12-25a. It is essentially a cathode follower with the (primarily) inductive load of the synchro as the cathode impedance. The cathode waveform is approximately the grid waveform but attenuated somewhat. If the synchro-secondary load impedance is high, the induced or output voltage will be of nearly the same waveform as that across the primary, but of an amplitude proportional to the sine of the synchro shaft rotation. Figure 12-25b shows a similar method of drive in which preceding the synchro is a transformer used as an impedance matcher. Figure 12-25c shows a simple plate-drive circuit with voltage feedback. The voltage gain from

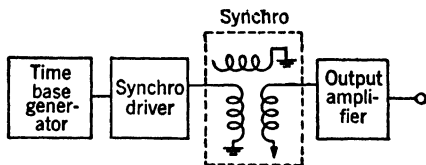


FIG. 12-24.—Use of synchros to modulate triangular waveforms.

<sup>1</sup> The term “delay” is somewhat misleading as used here. Due to the reactance of the synchro system the sawtooth starts out with zero slope. The delay is the time required for the slope to become nearly constant.



input to plate is  $R_2/R_1$ . A transformer could be used in this circuit to drive the synchro analogously to the circuit shown in 12-25b. Voltage-feedback amplifiers are discussed in Chap. 2, in Vol. 22, Chap. 10, and in Vol. 18, Chap. 6.

Figure 12-26 shows the circuit for a plan-position indicator used in radar. It makes use of a linear-time-base voltage waveform which is modulated by a synchro. The functions of most of the circuit elements

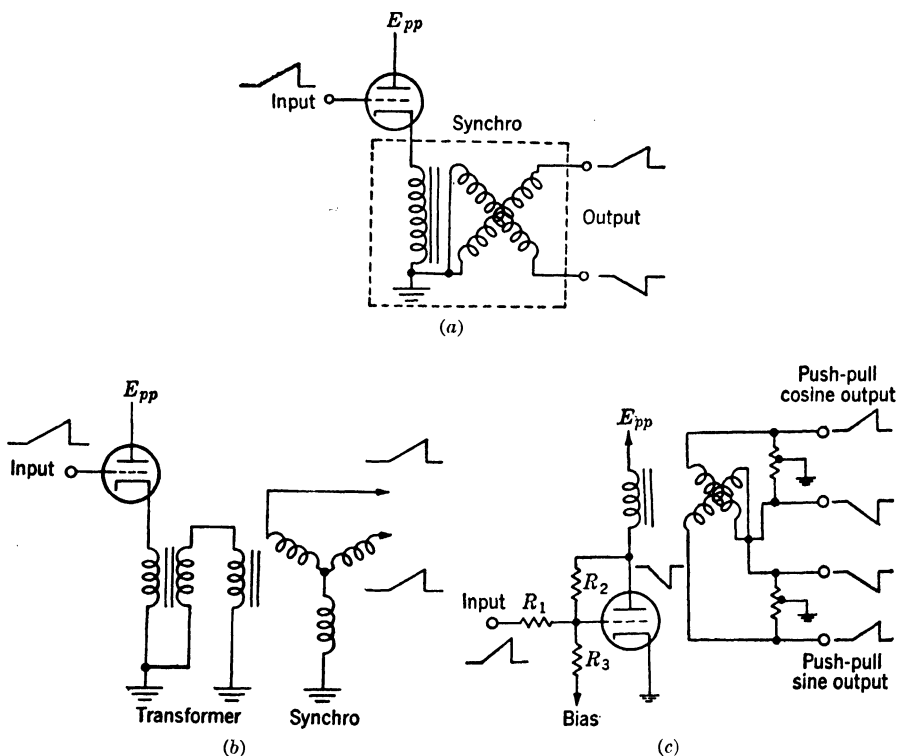


FIG. 12-25.—(a) Cathode synchro drive. Voltage waveforms are shown for a given shaft position. (b) Cathode drive with transformer. A 3-phase synchro is illustrated. (c) Plate-drive amplifier with voltage feedback. Push-pull synchro output shown.

are indicated on the diagram. The circuit is an elaboration of that shown in Fig. 12-25a together with auxiliary timing circuits and circuits for establishing the level of the current in the deflection coil.

**12-9. Complex-current-waveform Modulation.**—It is often necessary to force a certain current waveform to flow in a given load. (See Chap. 8.) One very commonly encountered requirement of this type is that presented by the deflection coil for a magnetic-deflection cathode-ray tube. The waveform, like the voltage waveform previously discussed, is used as a time base. If such a current waveform need be controlled in amplitude

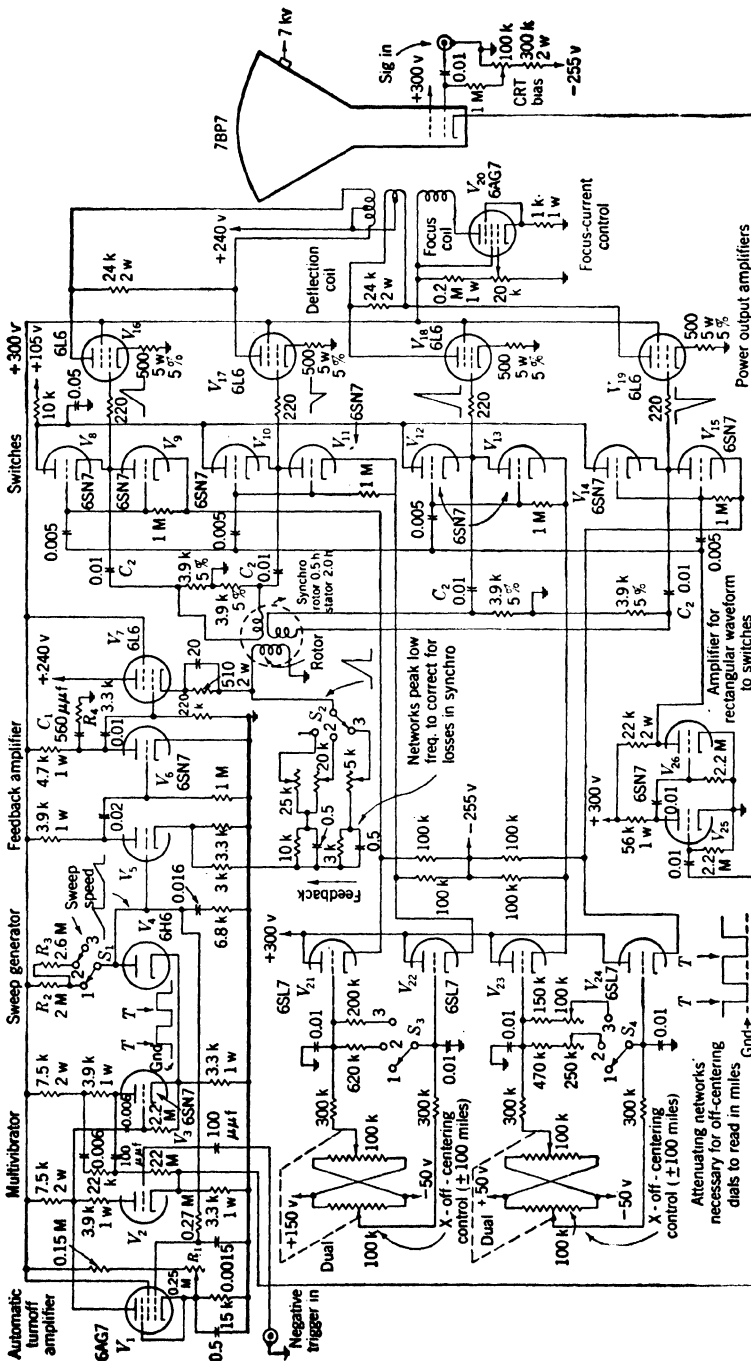


FIG. 12-26.—Circuit for PPI used in radar.

by a mechanical signal, a current-feedback driving amplifier can be used with an appropriately controlled voltage waveform. An alternative to this procedure is to drive the deflection coil or other load directly from the synchro output, in which case the synchro acts as a power transformer and not, as above, simply as a voltage transformer. Figure 12-27a shows

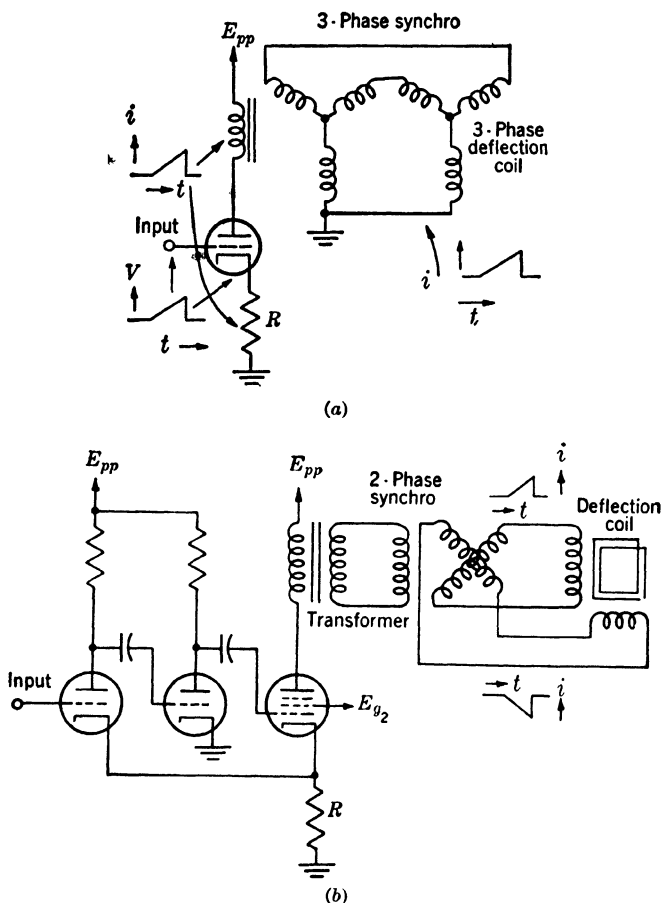


FIG. 12-27.—(a) Simple direct synchro drive for magnetic cathode-ray tube deflection coil. (b) Direct synchro drive with current-feedback amplifier and transformer.

a very simple driver of this type. Figure 12-27b illustrates a somewhat more complicated system using a three-stage current-feedback amplifier and transformer coupling. In a circuit of this type the load presented to the driver tube is not simply the synchro or transformer primary but it is this primary shunted by the transformed impedances of the rotor and the load. The problem of direct synchro drive is much the same as that of

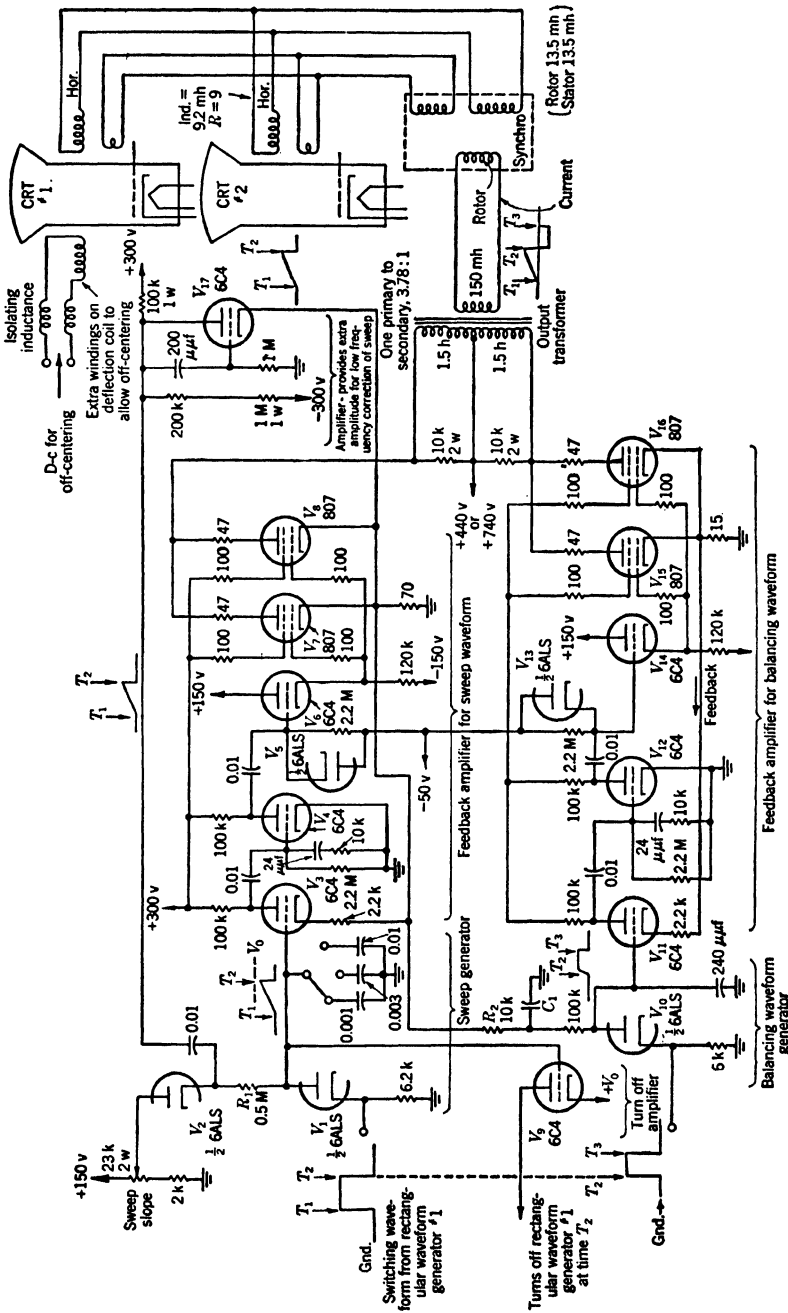


FIG. 12-28.—Area-balanced driving circuit for RTB display. Two magnetic deflection CRT's can be operated in parallel. One-radius off-centering is possible.

deflection-coil drive. The latter, together with coil-design information that is pertinent to the present problem, is discussed in Chap. 2 of Vol. 22.

**D-c Level.**—When amplifiers are used to drive the load following a synchro modulator, the proper d-c reference for the driving waveform is established by clamps or restorers (see Chaps. 3 and 14); in the present case, however, there are no amplifiers through which the waveform passes, and other methods of establishing the reference level must be employed. This problem is considered in Chap. 8, and Vol. 22, Chap. 10.

**An Example.**—An example from a radar set in which the deflection coil controlling the CRT beam is driven directly from a synchro is shown in Fig. 12-28.

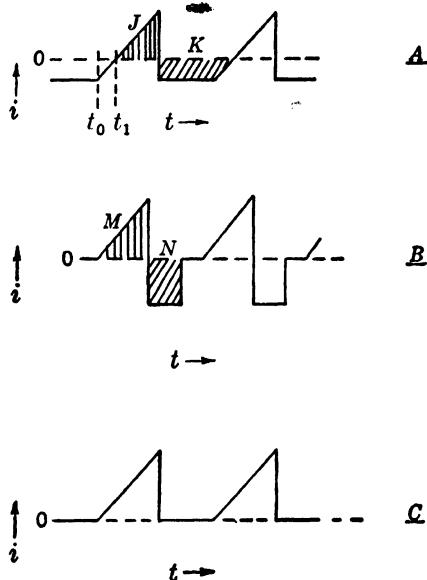


FIG. 12-29.—Triangular current waveforms illustrating ways of establishing a reference level.

the triangular-waveform area by switching the grid of  $V_{11}$  with  $V_{10}$  alternately to ground and to the output of the sawtooth-averaging filter  $R_2C_1$ . Further discussion of this same example will be found in Vol. 22, Chaps. 5 and 13, and Vol. 17, Chap. 10.

**Modulator Requiring Very Low Torque.**—Ordinary synchro devices are not suitable in applications in which very small torque is available since slip rings must be used to make electrical connection to the rotor and these introduce considerable friction. The Magnesyn is a device in which the rotor is a bar magnet, and consequently the jewel bearings provide the only friction. The stator consists of a laminated ring made of easily saturable magnetic material, on which is wound a toroidal coil,

The method is an elaboration of the one illustrated in Fig. 12-29b in which a second current-feedback amplifier ( $V_{11}$  to  $V_{16}$  inclusive) generates a rectangular current waveform of area equal to that of the triangular sweep waveform. The rectangular and the triangular waveforms are mixed in the transformer. The synchro resolver is a Diehl FJE-44-1 which was designed for this application in which sweep waveforms between 60- and 2400- $\mu$ sec duration are modulated.  $V_1$  and  $V_2$  comprise the sawtooth-voltage-waveform generator, and  $V_3$  through  $V_8$  constitute the current-feedback synchro-driver amplifier. The balancing waveform amplitude is made proportional to

tapped at the  $120^\circ$  points. The permanent magnet is pivoted concentrically with the core and rotates inside the coil as shown schematically in Fig. 12-30. The coil is excited by an alternating current producing a magnetization that completely saturates the core. The permanent magnet produces a magnetic bias which causes even harmonic components to appear across the windings. (The core functions exactly as in the magnetic amplifier of Chap. 11.) The relative magnitude of these components in each  $120^\circ$  sector is proportional to the sine of the direction of the bar magnet with respect to the center of the sector. The output from each tap contains both the fundamental and the even harmonic components. The fundamental is removed by adding an equal and

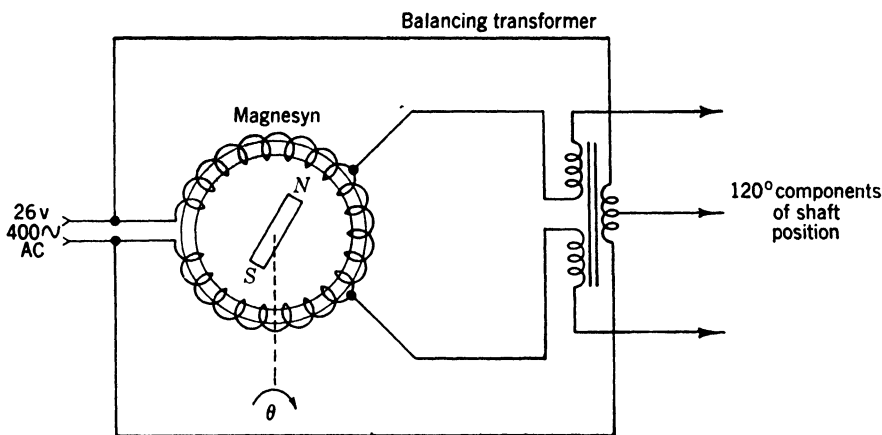


FIG. 12-30.—Magnesyn and energizing circuit.

opposite component to each output from a transformer. The outputs of the transformer windings in series with the Magnesyn windings contain only the harmonic components. Thus, the Magnesyn not only modulates the signal but also doubles the frequency of the carrier. The smallest synchros (Bendix Autosyn) require a torque of 0.04 in.-oz whereas the Magnesyn requires only about  $\frac{1}{10}$  as much.

Other devices that require very small torque are Microsyns and Telecons. For details see Vol. 21, Part II.

**12-10. Variable Condensers.**—A variable condenser, used generally as part of a voltage-divider circuit, serves as a modulator that changes a mechanical signal into an electrical signal. The simplest and most common case is illustrated in Fig. 12-31a. If an alternating-voltage signal  $e_1$ , for example, a sinusoid, is applied across  $C_1$  and  $C_2$  in series and the output  $e_2$  taken across  $C_2$ , then

$$\frac{e_2}{e_1} = \frac{C_1}{C_1 + C_2} \quad (11)$$

The desired output as a function of the shaft rotation  $\theta$  of the variable condenser is expressed by

$$e_2 = [A + kf(\theta)] \left( \frac{e_1}{2A} \right), \quad (12)$$

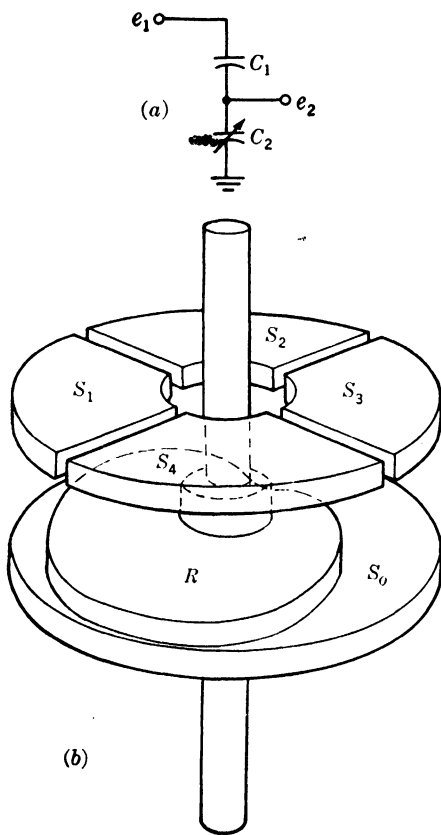
where  $A$  and  $k$  are constants. Equation (11) shows that this output will be obtained if

$$C_2 = C_1 \frac{A - kf(\theta)}{A + kf(\theta)}. \quad (13)$$

The way in which  $C$  depends on  $\theta$  is determined by the shape and size of the condenser rotor and stator plates. In designing a condenser for a precision application, edge effects must be taken into consideration, and particular care must be given to the mechanical design. Chapter 9 of Vol. 17 discusses the design problems in detail.

*Applicability.*—The variable condenser as an electromechanical modulator has certain advantages and certain limitations compared with other electromechanical devices. For applications involving high shaft speeds condensers are decidedly better than potentiometers and are better than most synchros since friction can be made smaller. The condensers, which in most precision applications have been designed specifically for the job in question, are built to stand high accelerations. They withstand shock, vibration, humidity and long use very well. Unlike synchros, condensers can readily be designed to give almost any desired variation of output as a function of shaft rotation.

FIG. 12-31.—(a) Condenser-voltage divider.  
(b) Phase-shifting condenser.



A variable condenser, if it is to be kept a reasonable size and is to be a good mechanical design, cannot have a maximum capacitance greater than a few hundred micromicrofarads. Because of the small capacity of the device, considerable care must be exercised in the wiring, and the use of short leads to and from the condenser is almost imperative.

Stray and lead capacitances may cause undesirable variations in output with angle and will result in attenuation of the output signal.

**12-11. Use with Sinusoidal Carrier.**—It is possible with condensers, as with synchros, to use any a-c waveform as the input or carrier to be amplitude-modulated. For example, to obtain a variable-speed linear time base, a variable condenser may be used as the control device in either of two ways. A constant-amplitude sinusoidal carrier may be used as the input and the demodulated output may be used to control the time-base generator. In the alternative method, a sawtooth or other time-base waveform may be attenuated directly by the condenser divider. Either the first method or a combination of the two methods is generally used because any practicable condenser divider presents a very high impedance to the lower frequencies that are present in most time-base waveforms.

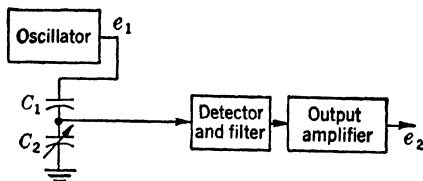


FIG. 12-32.—Block diagram of a condenser-divider data transmission system including oscillator, modulator, and detector.

Figure 12-32 shows a block diagram of a data-transmission system employing a sinusoidal carrier wave and a variable-condenser divider. If the condenser is driven directly by the oscillator (e.g., Fig. 12-36) the frequency shifts somewhat as  $C_2$  is varied, but if the circuit has a fairly high  $Q$  the amplitude will remain constant. The slight frequency shift is of no consequence in most applications.

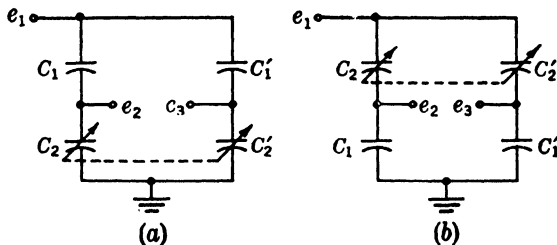


FIG. 12-33.—Push-pull condenser-voltage dividers.

**Push-pull Network.**—Two push-pull condenser networks are shown in Fig. 12-33 in which the total capacitance, and hence the frequency, does not change. The capacitances are designed to follow the relationships

$$C_2 = C_1 \frac{B + kf(\theta)}{A - kf(\theta)}, \quad (14)$$

$$C_2' = C_1 \frac{B - kf(\theta)}{A + kf(\theta)}, \quad (15)$$



where  $A$  and  $B$  are constants. The outputs for Fig. 12-33a are

$$e_2 = [A - kf(\theta)] \left( \frac{e_1}{A + B} \right) \quad (16)$$

$$e_3 = [A + kf(\theta)] \left( \frac{e_1}{A + B} \right).$$

For Fig. 12-33b  $A$  and  $B$  in Eq. (16) are interchanged. The total capacitance,

$$C_T = \frac{C_1 C_2}{C_1 + C_2} + \frac{C_1 C'_2}{C_1 + C'_2} = C_1 \frac{2B}{A + B}, \quad (17)$$

is seen to be constant. The analysis shows that Eq. (17) holds for both networks of Fig. 12-33a and b. The network of Fig. 12-33b is generally preferred in practice because cable and other stray capacitances from the

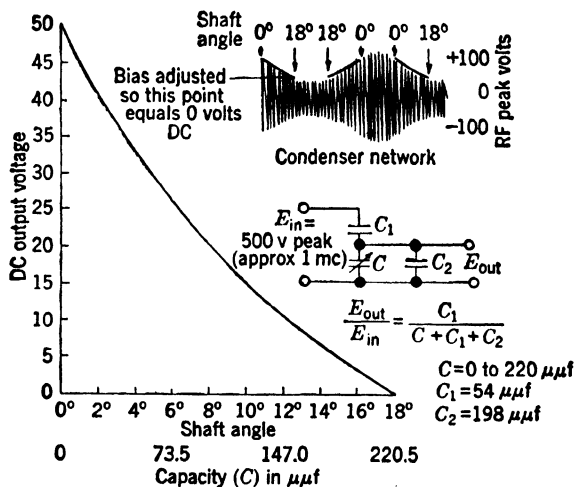


FIG. 12-34.—Capacitance network for nonlinear function.

outputs to ground are generally much larger than stray capacitance between input and output. Strays across the outputs of Fig. 12-33b may be considered a part of  $C_1$ . Work with a push-pull network of this type led to the conclusion that in practice it is not capable of the accuracy obtainable with a single divider, primarily because of the great difficulty of accurate alignment.

*Another Network.*—The condenser network shown in Fig. 12-34 has been found useful in producing output voltages that are certain nonlinear functions of condenser shaft rotation. For this network

$$\frac{e_{out}}{e_{in}} = \frac{C_1}{C + C_1 + C_2} \quad (18)$$

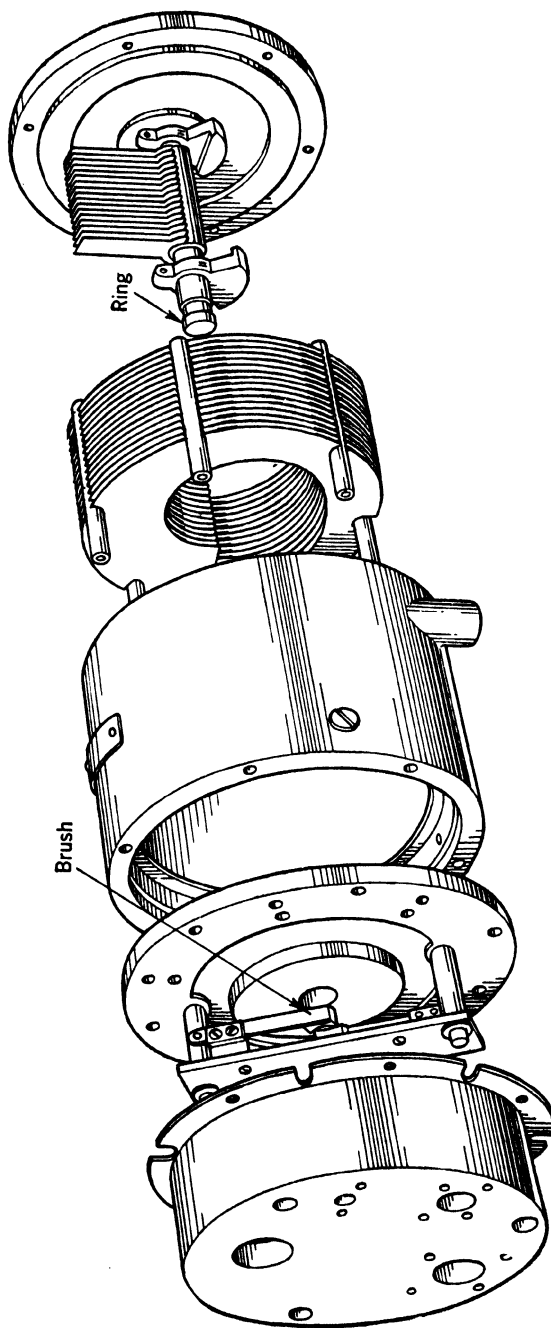


FIG. 12-35.—The Rauland CV-11 variable condenser. The following data describe the condenser: temperature coefficient of capacitance 100 parts per million  $^{\circ}\text{C}$ ; linearity  $\frac{1}{2}$  per cent; operable from  $-40^{\circ}\text{C}$  to  $70^{\circ}\text{C}$  and at 95 per cent humidity at  $45^{\circ}\text{C}$ ; stands 10 g shock test; designed for 400 volts rms input; life 10,000 at speeds from 10 to 2000 rpm; torque 4 in.; shaft, continuous rotation.

from which  $e_{out}$  as a function of  $\theta$  may be determined when  $C$  as a function of  $\theta$  is specified. A condenser,<sup>1</sup> for which  $C = A + k\theta$ , has been used in this way to produce a desired nonlinear output. In one such radar application  $C_1 = 122 \mu\mu\text{f}$ ,  $C_2 = 194 \mu\mu\text{f}$ , and  $C$  varies linearly with  $\theta$  from nearly 0 to  $110 \mu\mu\text{f}$ . Other condenser networks with still different characteristics can, of course, be used. A condenser for which  $f(\theta)$  in Eqs. (14) and (15) is  $\sin \theta$  has been designed but was not put into production.<sup>2</sup>

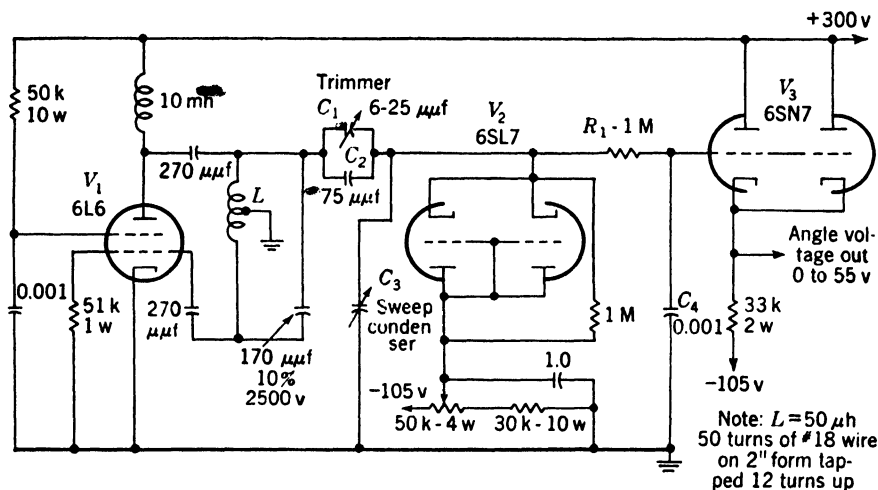


FIG. 12-36.—SCR 598 angle-sweep generator.

*Example.*—Two condensers have been designed that yield an output for which  $f(\theta)$  in Eq. (12) is linear in  $\theta$ , that is,

$$e_2 = A + k\theta. \quad (19)$$

One is the Bendix OAR 971-30-1; the other is the Rauland CV-11. They are constructed (see Fig. 12-35) of 17 fixed stator plates and one adjustable stator plate which are  $0.160 \text{ in.} \pm 0.001 \text{ in.}$  apart, and of 17 rotor plates, each plate being  $0.04 \text{ in.}$  thick. The capacitance varies from  $50$  to  $200 \mu\mu\text{f}$  in the usable  $320^\circ$  of rotation.

*A Circuit.*—In Fig. 12-36 a circuit (SCR-598)<sup>3</sup> is shown which makes use of a condenser divider such that Eq. (19) is satisfied. The condenser divider forms part of the tank circuit of a 1-Mc/sec Hartley oscillator ( $V_1$ ). The peak-to-peak output of 575 volts does not change appreciably as the heater supply varies from 4 to 8 volts. The tank circuit and all

<sup>1</sup> Bendix condenser No. 74747-1.

<sup>2</sup> See Vol. 17, Chap. 9.

<sup>3</sup> Fire Control Radar MPG-1. H. A. Strauss *et al.*, *Electronics*, 92 (December 1945).

radiating components are shielded in copper, and the entire oscillator is mounted only a few inches from the variable condenser and is connected to it by a shielded cable. The trimmer condenser  $C_1$  is adjusted so that  $C_1$  plus  $C_2$  is equal to  $C_3$  for  $\theta = 0^\circ$ . The proper adjustment is ascertained by comparing the observed output vs. angle curve with the calculated curve. The 6SL7,  $V_2$ , serves as a peak detector (see Chap. 14).

Tube  $V_3$  is a cathode follower which affords the low output impedance necessary in this case to drive several feet of cable. Both the detector and the cathode follower are mounted very close to the slip rings of the variable condenser to minimize the stray capacity. When the Rauland condenser is used, the output is from 0 to 55 volts for a variation in shaft rotation from  $-160^\circ$  to  $+160^\circ$ . The calculated peak-to-peak carrier ripple in the output is less than 0.05 volt, and the calculated phase shift for 10 rps is about  $4^\circ$ . Replacing  $R_1$  by a 0.25-mh choke reduces the phase shift to  $0.02^\circ$ .

**12-12. Complex-waveform Modulation.**—If a time-base waveform is to be attenuated by a condenser divider, frequencies as low as the PRF of the time base must be passed. With available condensers with PRF's of a few hundred pps this means that the divider has an impedance of approximately one megohm for the low-frequency components. At this level, leakage resistance becomes troublesome. Consequently, variable condensers are not used for most such applications, synchros being most often employed. Laboratory models that perform satisfactorily, however, have been constructed. Another laboratory system was tried which used a synchro and a sinusoidal condenser in parallel as a modulator for a linear time base. The system operates satisfactorily, but it appears that switching to a lower-inductance synchro when fast sawtooth waveforms are used is a better procedure.

*Use of High-frequency Carriers.*—Modulated-time-base systems that employ high-frequency carriers have been built in the laboratory and have performed satisfactorily. Two such systems will be briefly described. Figure 12-37a shows the block diagram and Fig. 12-37b the circuit of one such system using Cardwell sinusoidal condensers. Section  $C_1$  is the cosine condenser, and  $C_2$  is the sine condenser. Its rotor is  $90^\circ$  out of phase with that of  $C_1$ . The condenser  $C_1$ , together with  $C_3$  and  $C_4$ , constitutes a push-pull voltage-divider network similar to that shown in Fig. 12-33. For the Cardwell condenser  $C_1 = A + k \sin \theta$  and  $C'_1 = A - k \sin \theta$ . Making use of Eq. (11) it is seen that the difference in the outputs

$$e_3 - e_2 = e_1 \frac{2kC_1 \sin \theta}{(C_1 + A)^2 - k^2 \sin^2 \theta} \quad (20)$$

If  $C_1$  is about 10 times as large as  $k$  (as in Figs. 12-35a and b), the

$\sin^2 \theta$  term introduces a departure from true sinusoidal push-pull output of less than 1 per cent. Condensers  $C_3$  and  $C_4$  are made adjustable so that balanced output can be obtained. The input waveform is a modulated sinusoid of about 2-Mc/sec frequency. The envelope of the waveform is a sawtooth waveform, and the modulation is accomplished by applying a triangular wave to the screen of the

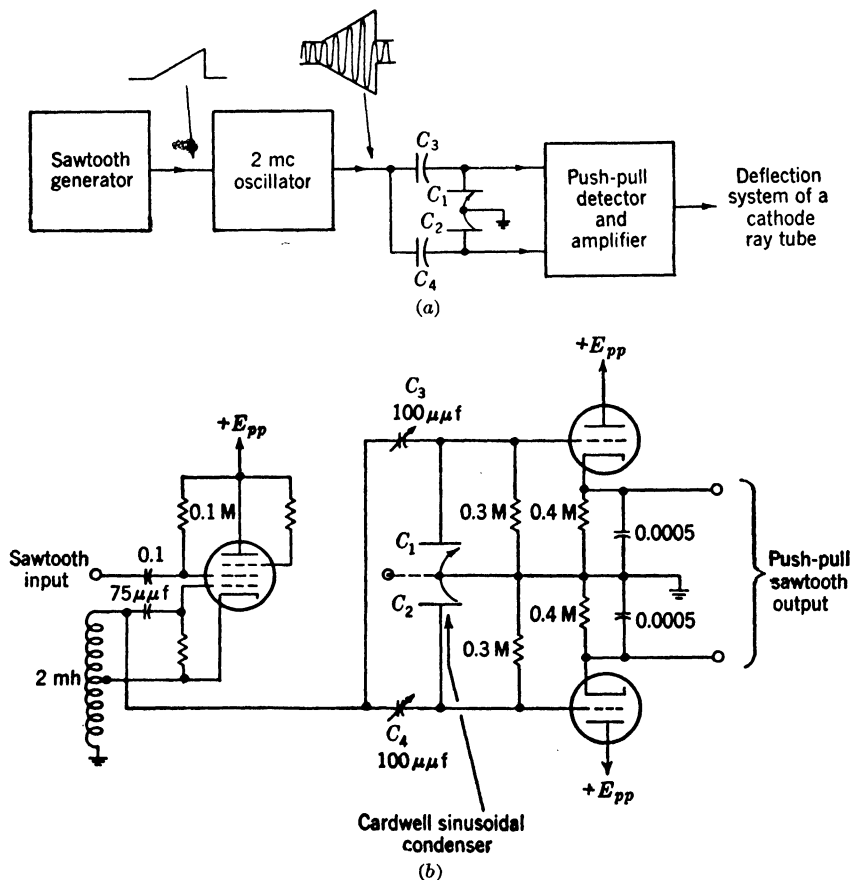


FIG. 12-37.—(a) Block diagram of a variable-condenser time-base waveform modulator employing a carrier of high frequency. (b) Circuit diagram.

oscillator.<sup>1</sup> An automatic-amplitude-control circuit has been used successfully with this oscillator, the control voltage being applied to the suppressor grid. The detectors are bypassed cathode followers which are described in Chap. 14. The outputs are push-pull sawtooth waveforms varying in amplitude as the sine and cosine of the condenser-shaft

<sup>1</sup> A linear electrical modulator is required. See Chap. 11 for a discussion of appropriate circuits.

displacement. The circuit shown (Fig. 12-37b) was operated satisfactorily with shaft rotations as high as 30 rps. Additional intelligence can be transmitted by frequency modulation of the carrier.

*A System Using Frequency Modulation.*—Figure 12-38 is the block diagram of another system for amplitude-modulating a time base that employs a carrier—in this case, a carrier that is amplitude-modulated by a sawtooth waveform as in the above example is also frequency-modulated by the variable condenser. A frequency-sensitive detector gives push-pull sawtooth waveforms of amplitude proportional to the frequency deviation; hence, the frequency varies linearly with  $C_1$ , which is proportional to  $\sin \theta$ . Since the output is proportional to the input amplitude also, the wave envelope is preserved. If such a circuit is used with no amplitude modulation of the carrier, the system reduces to one in which the carrier is frequency-modulated only.

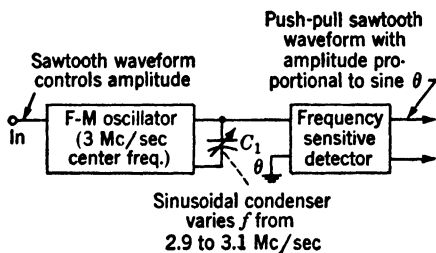


FIG. 12-38.—Fm-am time-base modulator.

Both the examples are best suited for use as resolvers since, in the form described, the outputs vary as sine and cosine of the input.

**12-13. Variacs.**—Variacs are variable autotransformers in which a single layer of wire is wound on a toroidal iron core. A slider makes contact with a single turn as in a potentiometer. Since variacs are reactive devices, they may be used to transform power without loss. In potentiometers most of the input power must be dissipated in the windings. Most variacs are designed as line-voltage compensators and are not precision devices. The British Admiralty Mark I potentiometer, however, is a device designed for use in a computer. It is 6 in. in diameter and operates at 50 cps with a linearity of  $\pm 0.1$  per cent. Variacs are discussed in detail in Vol. 17, Chap. 10.

**12-14. Photomechanical Modulators.**—Photoelectric devices offer particular advantages when extremely low torque is available or for operation at very high speeds. In operation, a shutter is actuated by the mechanical data to modulate the amount of light falling on a photocell. The light is supplied from a constant-intensity source. The shutter may be made from very light-weight material and can be cut to provide nearly any mathematical function. Very sharply discontinuous functions may be produced by photoelectric devices. Angle marks for PPI displays are produced by a slotted disk rotated between a light source and a photocell as shown in Fig. 12-39.

The 6AC7 is normally conducting so that the cathode rises to about +50 volts and thereby provides bias for the phototube. The plate is at

"bottom" with most of the space current flowing to the screen. Illumination of the phototube causes the grid to go negative and thus cuts off the 6AC7 and causes an abrupt rise in plate voltage. The  $0.05\text{-}\mu\text{f}$  cathode-bypass condenser steepens the edge of the marker pulse by pre-

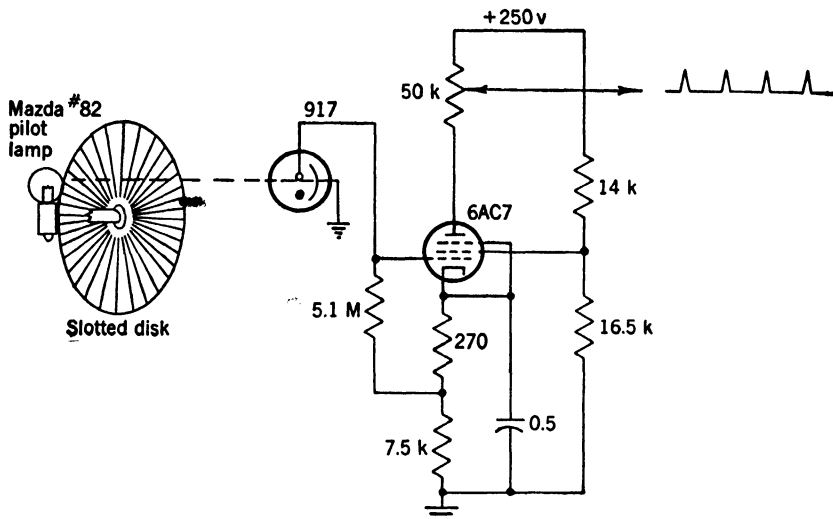


FIG. 12-39.—Photomechanical azimuth-mark generator.

venting degeneration at high frequencies. (See Vol. 22, Chaps. 6 and 15, Radiation Laboratory Series.)

In the above circuit abrupt pulses that are limited in amplitude are produced. When it is desired to obtain an output accurately proportional to the area of illumination, accurately linear amplifiers must be

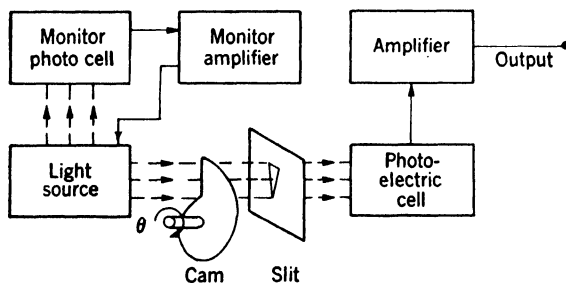


FIG. 12-40.—Circuit for producing a potential accurately proportional to the area of an aperture.

used. Refer to Fig. 12-40. Errors may arise from changes in the output of the light source or from drift in the amplifier. The light source may be stabilized by operation from a regulated power supply, or better, an auxiliary photocell may be used to measure the light intensity and correct

the output of the light source. Alternatively the auxiliary photocell may be used to vary the gain of the amplifier in accordance with changes in light intensity. With a light source of fixed intensity the gain of the amplifier should be stabilized by means of inverse feedback. Since d-c amplifiers are subject to drift, a-c amplifiers may be used when greatest stability is desired. To provide the a-c carrier, the light source may be modulated, the potential supply to the photocell may be an a-c carrier, or a mechanical vibrator-modulator may be used to modulate the output of a photocell operated on DC.

Photomechanical devices are frequently used as null indicators in torque-amplifying systems. A beam of light is made to subtend equal areas on two adjacent photocells by amplifying the difference between their outputs and applying it to a servomechanism that moves the beam.<sup>1</sup>

<sup>1</sup> For details of typical devices see: Strong, J., *Procedures in Experimental Physics*, Prentice-Hall, New York, Chap. 10; Chance, B., *Electronics Engineering Manual*, McGraw-Hill, New York.



## CHAPTER 13

### TIME MODULATION

BY D. SAYRE

**13.1. Introductory Remarks.**—Waveforms define time intervals—that is, a value can be assigned to the time that elapses between the occurrence of an identifiable portion of a waveform and the occurrence of another identifiable portion of the same or a different waveform. This chapter is concerned with the important class of circuits that can alter, or modulate, this time interval in accordance with a signal. If the time interval is  $T$  and the value of the signal is  $x$ , then a time-modulation (t-m) circuit establishes the relationship  $T = F(x)$ . The function  $F$  is called the transfer function of the t-m circuit.

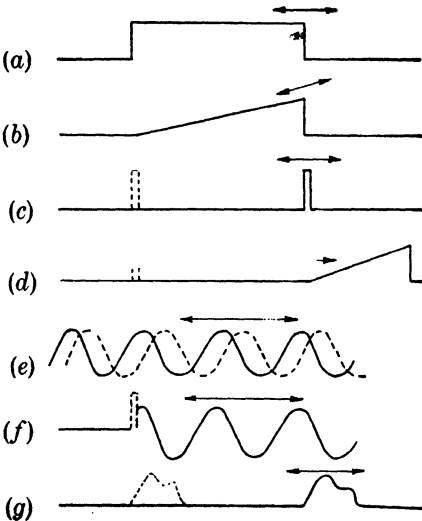


FIG. 13.1.—Typical time-modulated waveforms: (a) rectangle, trailing edge variable with respect to the leading edge; (b) triangle, trailing edge variable with respect to the start; (c) pulse, variable with respect to a reference pulse; (d) triangle whose start is variable with respect to a reference pulse; (e) continuous sine wave, capable of being phase-shifted with respect to a reference sine wave; (f) pulsed sine wave, capable of being phase-shifted with respect to the initiating pulse; (g) arbitrary waveform, output of an ideal variable delay device, variable with respect to the input.

#### GENERAL PROPERTIES OF T-M WAVEFORMS

**13.2. Examples of T-m Waveforms.**—Figure 13.1 gives several typical examples of t-m waveforms. They may occur either periodically or sporadically; their recurrence frequency may be anything up to several hundred kilocycles per second. In several cases there are two waveforms involved at different points of the circuit—a reference pulse to mark the beginning of the time interval and the movable waveform itself.

Waveforms with rise and fall times less than 0.01 to 0.05  $\mu\text{sec}$  are difficult to obtain. For this reason the time intervals involved in TM at present are not likely to be much less than 1  $\mu\text{sec}$ . Under such circum-

stances the recurrence frequency cannot exceed the few hundred kilocycles per second mentioned above.

More common, at least in radar applications, are time intervals from 1  $\mu$ sec to 1000  $\mu$ sec—that is, times that correspond to target ranges from about 100 yd to 100 miles. Recurrence frequencies seldom exceed 2500 cps, and then, of course, only when the time interval is less than 400  $\mu$ sec.

Finally, time intervals from 0.001 sec to 1 sec or even to 100 sec are perfectly possible, with very low recurrence frequencies.

The recurrence frequency is of importance in setting an upper limit to the frequency at which the time interval may be usefully modulated. Generally speaking, the modulating frequency should be less than one half the recurrence frequency. This is equivalent to the situation in AM, where the carrier frequency must be high compared with the signal frequency.

Often it is desired to transform one t-m waveform into a similarly t-m waveform of different shape. For instance, waveform (a) can be converted into (c) by differentiation, (c) can be used to trigger a triangle generator to obtain (d), etc.

**13-3. Fundamental T-m Methods.**—Figure 13-2 illustrates, in highly compressed form, the three most useful methods for TM. Considerations concerning the accuracy of these methods will be given in Sec. 13-7.

In Method (a), called TM with a voltage-sawtooth waveform, the time interval is the time necessary for the sawtooth waveform to rise from its initial voltage to the comparison voltage. The comparison voltage is the signal, since varying it changes the time interval.

Method (b) is really time modulation by phase modulation. The pulse generators are arranged to fire on some definite portion of the sine waves, probably the point of greatest slope, since that can be most accurately defined. The phase-shifting device is usually either a synchro or a special phase-shifting condenser; these devices require a shaft-rotation input as a signal.

Method (c) is usually carried out either with sonic waves in a liquid or solid medium, or with an artificial electrical line. Variation in the time interval is obtained by moving the pickoff element along the medium of propagation; some mechanical means for altering the path length is thus the signal.

These are the principal methods that have been used. They will be described in detail in later portions of this chapter. Also Vol. 20, Chaps. 5 and 6 of the Radiation Laboratory Series presents a number of practical t-m circuits of all the basic types, together with a discussion of the problems of incorporating these circuits into more complicated systems.

There are a few other methods that might sometimes be useful, such

as frequency modulation of a sine-wave oscillator to vary the interval between successive zeros of the wave, but these are mostly of insufficient importance to merit discussion. One curious method involving storage tubes permits a type of operation upon arbitrary waveforms which can be performed, for all practical purposes, in no other manner; this matter is accordingly discussed in the final section of this chapter.

Two simple t-m circuits can be combined to form a multiple-scale circuit. In such an arrangement one circuit provides a sort of coarse

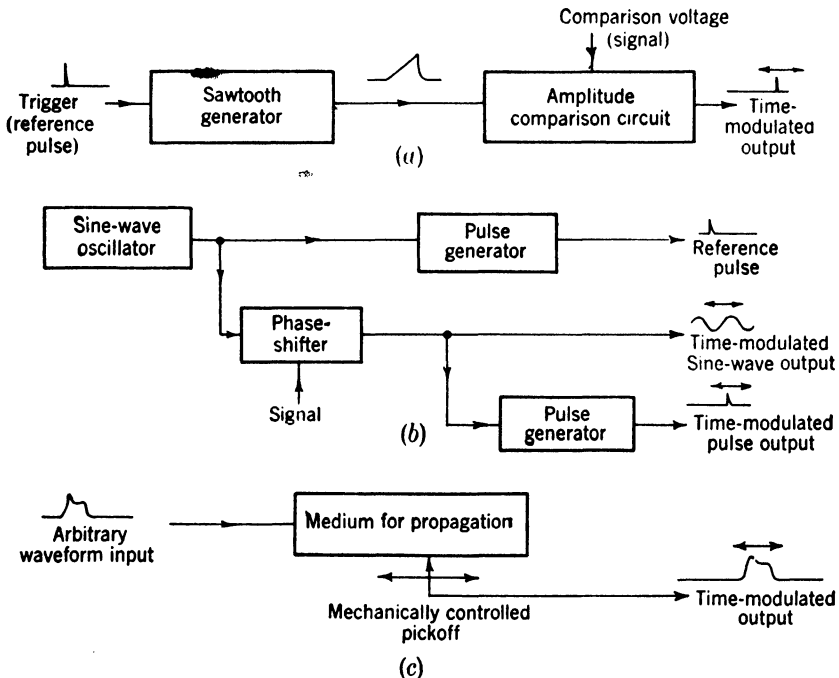


FIG. 13-2.—Three basic methods for TM: (a) TM with a voltage sawtooth; (b) TM by phase modulation of a sine wave; (c) TM by propagation velocity.

scale and is used to establish the time interval approximately, the other one being the fine scale and determining the time interval more exactly. For example, the phase modulation circuit of Fig. 13-2b together with a coarse circuit to select just one of the train of t-m pulses would comprise a double-scale t-m circuit. The usefulness of such a system is that TM over long time intervals (corresponding to the length of the coarse scale) can be carried out with the same absolute accuracy as TM over a much shorter time interval (that of the fine scale), resulting in very small fractional errors. If desired, three or even more scales can be used. The subject of multiple-scale systems is treated in detail in Vol. 20, Chaps. 3 and 6 of the Series.

All t-m devices may be classified as externally or internally synchronized, according to whether they accept or establish the initial instant of the time interval. The externally synchronized circuit accepts a trigger or other initiating waveform and after a certain length of time is free to accept another. This sort of circuit is useful for use with randomly occurring events that cannot be initiated at will. An internally synchronized circuit sets its own initial instant, simultaneously delivering a pulse that can be used to synchronize other circuits.

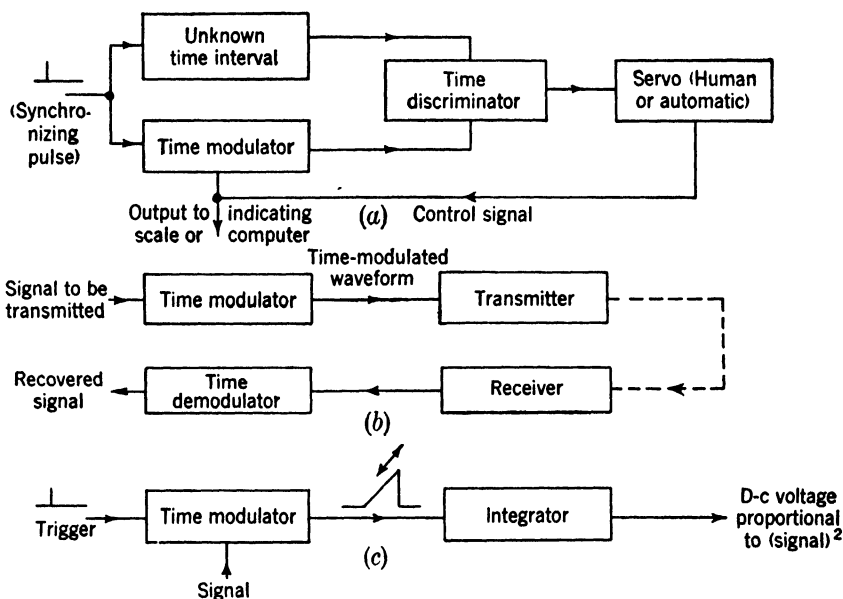


FIG. 13-3.—Several applications of TM: (a) to measure unknown time intervals; (b) to transmit intelligence; (c) to obtain a voltage proportional to the square of a signal.

**13.4. Applications.**—It has already been stated that TM permits the establishment of a time interval  $T$  as a definite function of  $x$ , the value of the control signal. By the techniques of TM, therefore, a new property of waveforms is brought under the control of the designer. Several important applications result, among them being—

1. Measurement of unknown time intervals—for instance, the measurement of radar range. One method, shown in block form in Fig. 13-3a, consists of the following: synchronizing in a t-m waveform; adjusting it, by means of a time discriminator and a servo loop, until its time interval is equal to the unknown time interval; and finally reading off the value of the control signal thus obtained, from which can be determined the value of the time interval if the

function  $F(x)$  is known. (This and other methods of time-interval measurement are discussed in Chap. 14).

2. Transmission of intelligence—that is, the reproduction, at a distance, of a signal. One possible method is to use the signal as the control signal for a t-m device; transmit the t-m waveform at a recurrence frequency high in comparison with the highest frequency component in the signal; and finally recover the original signal by means of a time-demodulation device (see Chap. 14). Figure 13-3*b* represents this schematically. The well-known pulse-width modulation is an example of this method.
3. Control of displays. The usefulness of a cathode-ray-tube display can often be greatly enhanced by the use of t-m circuits in conjunction with the sweep-generating circuits (see Vol. 22 of this series). For instance, if the waveform shown in Fig. 13-1*d* is applied to the horizontal deflecting plates of a cathode-ray tube, a “delayed A-sweep” or “R-sweep” is obtained.
4. Computing. Time-modulation circuits are often important components in complex computing networks. A simple example may illustrate this. Suppose it is desired to obtain a d-c voltage proportional to the square of a signal, for instance, to convert slant range (from an aircraft to a ground target) to ground range. One method, illustrated in Fig. 13-3*c*, is to use the signal to time-modulate a sawtooth waveform as in Fig. 13-1*b* and then integrate. The peak output of the integrator will be the desired voltage, since the area under the sawtooth waveform increases as the square of the duration of the sawtooth waveform.
5. Simulation of more complex time-varying waveforms. Many test and training equipments use t-m circuits to simulate more complex waveforms which vary with time—for example, the waveform of Fig. 13-1*c* might be used to simulate the radar echo of a moving target.

**13-5. Transfer Functions—Linear and Nonlinear.**—Thus far it has been tacitly assumed that  $F(x)$  is linear, but this need not be so. Exponential, hyperbolic, parabolic, and other kinds of special transfer functions can be obtained with the voltage sawtooth method simply by generating the proper shape of sawtooth waveform (see Chap. 8), the exponential being obtained with particular simplicity and accuracy. Alternatively, special potentiometers, gears, cams, etc. can be used to derive any desired transfer function from any of the three basic t-m methods.

Linear TM offers many obvious advantages and is, in fact, the most generally used. In the measurement of time intervals it supplies the answer in what is usually the most useful form. It is used in the trans-

mission of intelligence when distortion must be kept small. An example has been given of its usefulness in automatic computation.

Nonlinear TM is especially useful for automatic computation. An example will make this clear. It is possible to construct a t-m circuit with a hyperbolic transfer function—that is, with  $T^2 = x^2 + h^2$ , where  $h$  is an adjustable parameter. Such a circuit is obviously useful in the solution of the slant-range ground-range problem with an airborne radar.

**13-6. Control Signals.**—Regarding the control signal the following remarks are pertinent.

1. Some t-m circuits require a mechanical signal, usually either a linear or angular displacement; others require an electrical signal, which may be a circuit parameter such as resistance, capacitance, or inductance, but which is most commonly a voltage.
2. If a given control signal is of the wrong kind to be used with a certain t-m circuit, it can usually be converted to the proper kind by some sort of electromechanical device. A potentiometer voltage divider, for instance, converts a shaft rotation to a voltage. A great many such interconversions are known; the properties of some of the more important of these are given in Chap. 12.
3. The electromechanical device can be used to alter the transfer function of the t-m circuit in some desired way. Thus an exponential potentiometer with an exponential sawtooth waveform gives  $T$  as a linear function of the input shaft rotation, or a sine potentiometer may be used with a linear sawtooth waveform to give  $T$  as a sine function of shaft rotation. Similarly, special cams or gears can be used with any of the methods to give any desired transfer function.
4. Errors may be introduced by these electromechanical devices either because they are not perfectly linear, exponential, sinusoidal, etc., or because their inertia prevents them from following rapid changes in the input signal. Errors of the former type can sometimes be made unimportant by placing the device within a servo loop (like that of Fig. 13-3a), because the gain around the loop is effective as negative feedback.
5. Mechanical signals have the advantage of being subject to direct manual control, of providing force or torque for a visible scale or counter, and of having good long-time stability. This last property makes them especially useful for conveying very slowly varying quantities, but obvious mechanical limitations usually impose rather severe restrictions on the upper end of their useful frequency spectrum.
6. Voltage signals can easily be transmitted over considerable dis-

tances and have virtually no upper-frequency limit, but the difficulty of designing direct-coupled networks with adequate stability tends to make electrical signals inferior to mechanical at very low frequencies, unless the signal is modulated on a carrier.

7. For good accuracy and stability, the signal should vary over as large a range as other considerations will permit. It may be desired to multiply or divide the signal by some appropriate constant. This can be done for mechanical signals with gears. Electrical signals can be divided by impedance dividers, but multiplication (amplification) is not accurate unless feedback is employed.
8. Signals should preferably be delivered at an impedance low compared with the input impedance of the t-m circuit. Cathode followers are useful, low-distortion impedance transformers for electrical signals; for a mechanical signal a servomechanism capable of delivering sufficient power might be used.

**13·7. Errors—General Accuracy Considerations.**—The purpose of a t-m circuit is to set up a desired relationship  $T = F(x)$ . Any deviation from this desired characteristic is an error. These errors will be of two sorts: (a) original errors, which will exist even immediately after calibration and which arise from some fundamental inability of the circuit to generate exactly the required waveform (this inability may be due to the nonlinearity of some important component, or to an approximation—for example, the approximation that a cathode follower has unity gain); and (b) drift errors, which are removed by each calibration but which thereafter begin to appear again, arising from the inevitable instability of the circuit elements. Drift errors are accentuated by large changes in temperature and humidity, mechanical shock, etc., but will be observed even when these factors are eliminated, since the mere existence of a vacuum tube or a composition resistor alters its properties. One of the most important tasks of the designer is to find circuits that will depend for their accuracy only upon components that can be made with nearly ideal characteristics, and upon as few of those as possible.

Freedom from original errors is called “fidelity”; freedom from drift errors is called “stability.” Definitions of the terms “limiting error,” “probable error,” and “linearity” which are useful in describing the performance of t-m circuits are given in Vol. 20, Chap. 5 of this series.

The bulk of this section will be devoted to an examination of the basic t-m circuits in order to point out, in each case, which are the critical components—that is, upon which components the responsibility of determining the time interval rests—and to acquaint the reader with the

approximate accuracies that may be expected from each class of component.<sup>1</sup> The basic facts can, however, be stated in advance.

1. The vagaries of certain elements, such as amplifiers, can be greatly reduced by feedback.
2. By calibrating against a high-precision circuit, drift errors can be temporarily removed.
3. There is no substitute, however, for certain standard elements that present constant electrical or sonic characteristics. Thus, the circuit must be so arranged that the time interval is a function of only the high-quality components.

*Propagation-velocity Method.*—If the path length is  $d$  and the velocity of propagation is  $v$ , then  $T = d/v$ . Accuracy thus depends upon the exactness with which the position of the pickoff element can be indicated and the constancy of the propagation velocity.

The precision with which a linear or angular position can be mechanically transmitted and indicated is not one of the factors that limit the accuracy of any t-m system. For example, the limiting error, for one direction of rotation, in the indication of the position of the tool in a precision lathe is less than 5 parts in 100,000 for a 10-in. range. Since other errors are comparatively large regardless of the t-m method employed, the ultimate accuracy of mechanical components is not ordinarily utilized.

The question of velocity changes with temperature in supersonic delay lines is discussed in Vol. 17, Chap. 7 of this series. The delay time in mercury is  $17.52 \mu\text{sec/in.}$  at  $20^\circ\text{C}$ , with a temperature coefficient of  $+0.0052 \mu\text{sec/in.}$  per degree centigrade at that temperature, or about  $+300$  parts per million per degree. Water at room temperature shows a temperature coefficient of sign opposite to that of mercury (and most other liquids investigated) but at  $72.5^\circ\text{C}$  its coefficient is zero, the velocity of propagation being a maximum there. By using an oven to keep the temperature within  $1^\circ$  of  $72.5^\circ\text{C}$ , a tank can be built which is stable to better than 1 part in 20,000. The temperature at which the velocity coefficient is zero can be made lower than  $72.5^\circ\text{C}$  by mixing ethylene glycol into the water.

Electrical delay lines have not been so carefully studied from the point of view of their stability. Changes in temperature cause changes in both the  $L$ 's and  $C$ 's of lumped-constant lines and, in distributed-constant lines, cause alteration of the geometry of the structure and the dielectric constant of the core, which bring about changes in the inductance and capacitance per unit length. Distributed lines show a wide variation of

<sup>1</sup> More detailed information on components will be found in Vol. 17 of this series.



temperature coefficients, the smallest being a change in delay time per unit length of +0.02 per cent/°C (General Electric YE4B type line).

Changes with time in propagation velocity of electrical or sonic media cause drift errors, not original errors.

*Voltage Sawtooth Method.*—The time interval depends upon the shape of the sawtooth waveform, the initial level  $E_i$  at which it starts, and the level  $E_s$  at which the amplitude comparison, or pickoff, is made. Thus, for a linear sawtooth waveform of slope  $K$ ,  $T = (E_s - E_i)/K$ . Accuracy is therefore dependent upon a sawtooth generating circuit ( $K$ ), a switching circuit ( $E_i$ ), and an amplitude comparator ( $E_s$ ).

Switching circuits, which are discussed in Chaps. 3 and 9, are electronic switches that lock the quiescent level of the sawtooth to some well-defined voltage, and that can be opened when it is desired to permit the sawtooth to start. The accuracy with which clamping may be accomplished is limited by the stability of the vacuum tubes available.

Chapter 3 contains a good deal of information on this subject. Diodes, and triodes during grid conduction, both of which may be used as switching elements, exhibit a voltage across the switch which is small and constant to within a few tenths of a volt. This is probably a reasonable figure for switching accuracies with simple circuits. More complicated arrangements (described in Chap. 9), in which two tubes are used in such a way that the effects of aging and heater-voltage change will tend to cancel, are constant to considerably better than 0.1 volt. Change of tubes, however, may cause 0.1-volt changes in the initial voltage of the sawtooth.

Recently much attention has been turned toward the possibility of using germanium crystals instead of thermionic diodes for switching and amplitude comparison. The hope has been that the crystals would show better stability than diodes. To date, however, this is only partly true, temperature changes being particularly serious. Also, it has not yet been possible to make crystals that have a high back resistance at voltages greater than 50 volts. A comparator circuit has been invented (see Sec. 9-5) which obviates this difficulty, but as yet there is no really satisfactory switching circuit.

Amplitude comparison circuits are discussed in detail in Chap. 9. The limitations are again imposed by the instability of available nonlinear elements, and the accuracy of comparison may be considered to be about the same as that of switching.

It may be noticed that errors in switching and comparison are drift errors, and not original errors. This is true at any rate for linear sawtooth waveforms; for a nonlinear sawtooth waveform, however, there may be an original error, since the comparator must work with an input waveform whose slope changes with the time interval.

The shape of the sawtooth waveform is determined, in all the circuits described in this book, primarily by a network of  $R$ 's and  $C$ 's. It is true that the properties of the tubes employed play some role, and both original and drift errors are found which could be removed if amplifiers with ideal characteristics were available. These matters are discussed in Chaps. 7 and 8. But, in most of the circuits employed, there is enough feedback to make these errors less serious than drift errors arising from instability of the fundamental timing resistors and condensers.

The carbon resistors and paper condensers which are common in radio receivers are ordinarily specified to within only 5 per cent, 10 per cent, or 20 per cent, depending upon the degree of selection that is practiced. The variation of these components with a 50°C temperature change amounts to many per cent of the nominal values. These units may, however, be made so that they are reliable in the sense that they do not fail completely.

Somewhat more predictable are the values of mica-dielectric condensers and wire-wound resistances. The original value may be specified as closely as 1 per cent, and the temperature coefficients may result in only a few tenths of a per cent increment with a rise of 50°C. Moreover, there is the possibility of matching temperature coefficients so that the product of a resistance and a capacitance is constant even though each varies with temperature. The coefficients themselves are not sufficiently controllable so that the product may be fixed to closer than one part in one thousand of the initial value with a 50°C temperature change. Certain types of resistors are wound with very thin wire, and special precautions against failure are necessary.

The best resistance and capacitance stability which has been obtained utilizes control of the ambient conditions to which the units are subjected. Hermetically sealed units are protected from humidity and any reagents in air. Temperature control in the interior of a small container or a complete chassis is entirely feasible. The constancy of an  $RC$ -product may be made considerably better than 1 part in 1000 by such methods. The original values of the components may be exactly set by certain industrial control processes. The improved quality is expensive and will presumably not be common.

Two other factors that affect the accuracy of a sawtooth t-m circuit are the d-c power supply and the potentiometer which is used when it is desired to control the time interval with a mechanical signal.

The subject of stabilized d-c power supplies is treated in great detail in Vol. 21, Chaps. 13 and 14 of this series. For a 250-volt supply, stabilization to about 50 mv is about the best that can be done. In general, however, such stability is quite unnecessary, provided the control voltage is suitably derived from the same supply that serves the t-m

circuits, for any change in the slope of the sawtooth waveform is accompanied by a compensating change in the control voltage. For this reason it is usually unwise to regulate the negative supply unless the positive supply is also regulated, and when both are regulated a single standard should be used.

Among potentiometers, one of the most accurate linear types is the RL 270 series, designed by the Radiation Laboratory. They are available in sizes from 20 to 50,000 ohms, with departures from linearity of resistance vs. shaft rotation as small as 1 to 10 parts per 10,000. The Gibbs Micropot and the Beckman Helipot are linear to better than 1 part per 1000, and permit 10 complete shaft rotations to cover the full range. Special nonlinear potentiometers are also available, with errors from 1 to 10 parts per thousand. A full discussion of potentiometer design, with names of manufacturers and specifications of their products, is given in Vol. 17, Chap. 8 of this series.

*Phase-modulation Method.*—If the frequency of the sine wave is  $f$  cycles per second and the phase shift is  $\phi$  radians, then  $T = \phi/2\pi f$ . Usually  $\phi$  is some function of an input shaft rotation. Thus, the accuracy is dependent upon a sine-wave oscillator and a phase-shifting device.

The frequency of sine-wave oscillators, discussed in Chap. 4, can be held constant to a few parts per million by the use of crystals, or at lower frequencies to about 0.1 per cent by the use of  $RC$ -oscillators with properly stabilized timing components. Since the per cent error in  $T$  is equal to the per cent error in  $f$ , the oscillator is not likely to become the limiting factor in accuracy.

The best phase-shift devices are special inductances (synchros) or condensers, which are described in Secs. 13-15 and 13-16 and in Chap. 12, and in Vol. 17, Chaps. 9 and 10 of the Series. The phase shift of both these devices can be made linear with respect to shaft rotation to about  $\frac{1}{2}^\circ$ , the synchros at present being slightly the more accurate. Out of  $360^\circ$ ,  $\frac{1}{2}^\circ$  amounts to 1 part in 720, but the errors due to the phase shifter are not cumulative, since each full turn of the shaft increases  $T$  by  $1/f$ , regardless of nonlinearities during the turn. Thus, the absolute error due to the phase shifter is a cyclic error and is no greater for large  $T$  than for small. Any original error resides in the phase shifter, and the sine-wave oscillator, provided it puts out truly sinusoidal waves, can contribute only to the drift error.

If a  $t$ - $m$  pulse is to be formed from the phase-modulated sine wave, as in Fig. 13-2*b*, a comparator circuit is involved. It is the function of the comparator to form a pulse when the sinewave attains some definite value, usually zero (since that is the point where the sine wave has the greatest slope). Circuits especially designed for this purpose, whose drift errors can be kept lower than 0.1 volt, are given in Chap. 9.

### VOLTAGE SAWTOOTH METHOD

**13-8. Introduction.**—The unique advantage of this method is that it is voltage-controlled; there are no moving parts and very fast signals can therefore be accepted. Simplicity, low cost, and convenience are other advantages that have caused this method to be widely used even when shaft-rotation control is permissible. Accuracy of 0.1 per cent or slightly better is possible even with single-scale circuits; this is adequate for most purposes, though not as good as is possible with the other t-m methods. A disadvantage is that time must be wasted in permitting the circuit to recover after each cycle. As previously stated, the method is especially convenient for obtaining nonlinear transfer functions.

The time intervals obtainable with this type of circuit range from about 1  $\mu$ sec to many seconds. For time intervals shorter than a few microseconds, special small tubes and low-capacitance circuits are necessary. Very slow sweeps can be made by driving the center tap of a potentiometer with a constant-speed motor.

It may be noticed that another way of obtaining TM with a sawtooth-waveform method is to vary the slope of the sawtooth waveform, leaving the pickoff voltage constant. The fact that the pickoff will occur at slightly different levels for sawtooth waveforms with different slopes prevents this method from having great accuracy; nevertheless, it has often been used, especially with multivibrators, when an adjustable time interval is required.

It is a curious fact that the t-m circuits that employ the most tubes are the easiest to analyze. The operation of a large number of components is not difficult to understand if each unit is performing a single function. If, however, the same tube is used for generating the sawtooth waveform, performing the amplitude comparison, and generating a step function for the t-m output—as is the case in a multivibrator or other internally gated circuit—the transition periods between the several modes of operation are exceedingly difficult to represent analytically. Non-linearities in the tube characteristics and the various stray capacities usually become the decisive factors. The system becomes easier to represent by simple circuits and is often more accurate if a component is inoperative during all except a single stage of the circuit action. Thus a diode may conduct briefly at the time of pickoff and be tolerably well represented by an open circuit at other times. For this reason the internally gated circuits of Sec. 13-12 are more difficult to understand than the less compact circuits which will be treated earlier.

#### **13-9. Representative Circuit. Switching and Comparison Methods.**

A representative sawtooth t-m circuit is shown in Fig. 13-4, and sketches of its waveforms are shown in Fig. 13-5. The circuit is a simplification

of the circuit of Vol. 20, Sec. 5-7 of this series. A nearly linear positive-going sawtooth waveform is generated by the compensated bootstrap circuit (see Chap. 7) consisting of  $V_2$ ,  $V_3$ ,  $V_4$ , and their associated components. The simple triode switch  $V_1$  is opened and initiates the

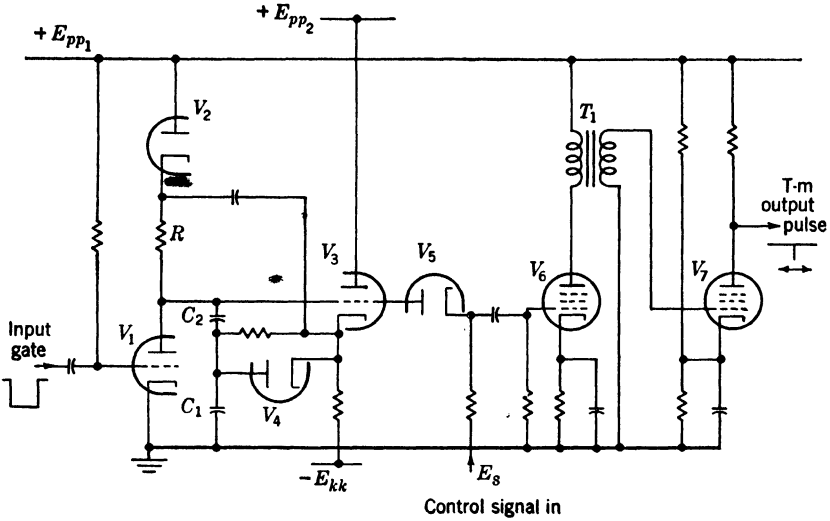


FIG. 13-4.—Simplified circuit diagram of a typical linear sawtooth t-m circuit.

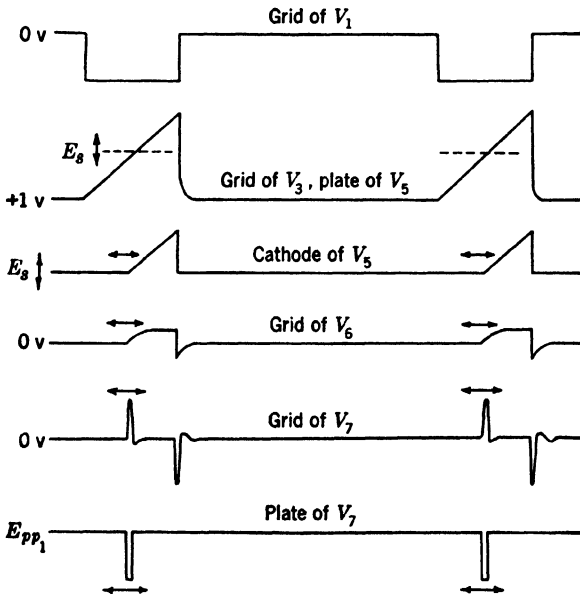


FIG. 13-5.—Timing diagram of the t-m circuit of Fig. 13-4.

sawtooth waveform when a negative gate is applied to its grid. The sawtooth waveform begins at about 1 volt above ground; its slope is about  $E_{pp}/RC$ , where  $C = (C_1 C_2)/(C_1 + C_2)$ ; its useful amplitude depends upon the design but may typically be 200 volts. The diode amplitude selector, or pickoff diode,  $V_5$  is so arranged that on its cathode appears only that portion of the sawtooth waveform above  $E_s$  volts. The diode  $V_5$ , together with the amplifiers  $V_6$  and  $V_7$ , forms an amplitude comparator, the output of which is a pulse marking the instant at which the sawtooth attained the voltage  $E_s$ .

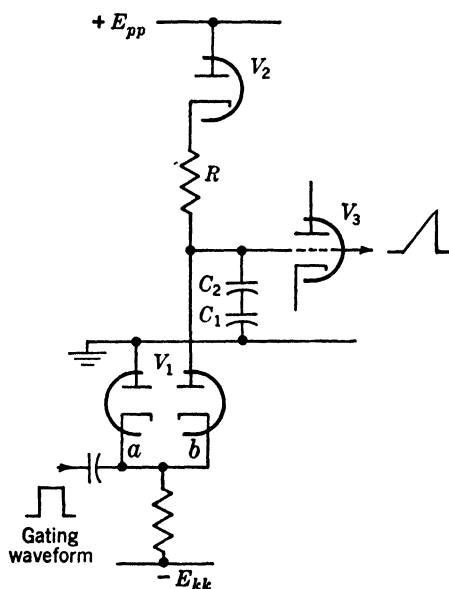


FIG. 13-6.—Double diode self-stabilizing switch.

Data presented in Vol. 20, Sec. 5-7 of this series indicate that the most serious single cause of error, amounting to about 0.5 per cent, is tube change or the gradual drift of tube characteristics. It may be supposed that these errors are mainly zero errors and not slope errors—that is, that they are due to inexact switching and comparison rather than to any changes in the shape of the sawtooth waveform. There are several methods for minimizing or reducing zero errors.

There are better types of switch than the gated triode; one which shows very good freedom from drift is the self-stabilizing double-diode circuit shown in Fig. 13-6. Here the voltage to which the sawtooth waveform is clamped depends not upon the absolute characteristics of  $V_{1a}$  and  $V_{1b}$  but upon the balance between them. Provided they drift together, the clamping voltage is unchanged. By using diodes in a

single envelope, the drift can be reduced to about 20 millivolts per week. The clamping voltage is altered by only about 40 mv by a 10 per cent change in heater voltage. Changing tubes, however, can still cause a change of 0.1 volt or even more. A disadvantage is that the input gating waveform must be as large as the desired amplitude of the sawtooth waveform.

Extremely bad definition of the initial level of the sawtooth would be obtained if the sawtooth were taken from the cathode of  $V_3$  instead of the grid, for in that case no amount of care in stabilizing the initial level of the grid would prevent the cathode level from changing with time, heater voltage, and tube change. The only condition under which use of the cathode waveform is justifiable is when, for any reason, the control voltage  $E_s$  must be fed into the cathode of  $V_5$  through a cathode follower. In this case it might be hoped that  $E_s$  and the initial level of the sawtooth would drift together.

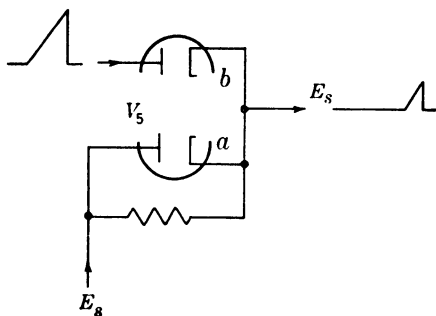


FIG. 13-7.—Double diode self-stabilizing amplitude selector.

Similarly there are more stable comparators than the single diode. A double-diode circuit (see Fig. 13-7), analogous to the switching circuit just described, has the same property of subtracting the drift of  $V_{5a}$  from that of  $V_{5b}$ . The resistor across  $V_{5a}$  plays the same role as that played by the common cathode resistor in the preceding circuit; it is returned to  $E_s$  and not to some lower voltage in

order to avoid drawing any current from the source of  $E_s$ . This and other comparators are described in Chap. 9.

The fact that  $V_6$  is partly, and  $V_7$  completely, nonconducting in the quiescent state means that there will be some slight delay between the moment when  $V_5$  begins to conduct and the moment when the output pulse is formed. Variation in operating conditions may cause some change in this delay and therefore some zero error. In general it is much better design if at least the first amplifier in the comparator is normally on, so that full gain will be realized right from the start.

Another way to cancel out the drift in the single comparator diode is to switch with a similar single diode (as in Fig. 13-8a). The effect of an increase in cathode emission in both these diodes would be to lower the level of the sawtooth waveform slightly and also to lower the effective control voltage by a similar amount. A small slope error is introduced by this method, however, since the initial current through  $R$  increases slightly with increased cathode emission. This method requires a zero-

impedance gating waveform, but an approximation to this is provided by the cathode-follower arrangement of Fig. 13-8*b*. The resistor  $R_1$  should be made as small as the cathode follower will permit.

Another method for zero-error cancellation is possible when the system can be internally synchronized. In this case the sawtooth is initiated by some local recurrence-frequency generator and is picked off not once but twice, the first pickoff providing the synchronizing pulse that is delivered to the external equipment, and the second pickoff forming the pulse that is time-modulated with respect to the first. Usually the first pickoff is at a constant voltage and the second pickoff voltage is the one that is varied. In this way the time interval depends only upon the *difference* between the two pickoff voltages; the initial level

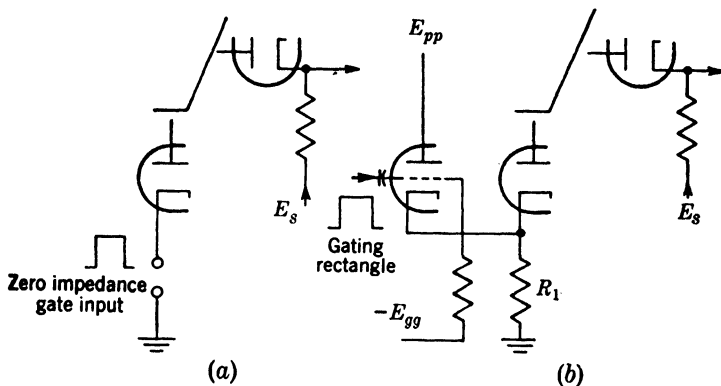


FIG. 13-8.—Zero error cancellation with single diodes: (a) ideal case with zero-impedance gating waveform; (b) approximation with a cathode follower.

of the sawtooth waveform becomes unimportant, and the drifts in the two pickoffs subtract. The difficulty arises from the loading that the first pickoff imposes upon the sawtooth waveform. This difficulty can be met by using high-impedance comparators (see Chap. 9) or by using a sawtooth waveform from a low-impedance point of the circuit. For such an application therefore the sawtooth waveform from the cathode of  $V_3$  might be used.

Probably the most satisfactory method of all is the following one, which completely eliminates any zero error and which can be applied to a large number of time-measurement problems, though its application to the transmission of intelligence or automatic computation is not easy, since the reference and t-m pulses never exist both in the same cycle. A linear sawtooth waveform, whose initial level is not important, is picked off by a single diode (or other simple comparator) sometimes at a voltage  $E_s$ , and sometimes at a higher voltage  $E_2$ . The signal voltage may be switched from  $E_s$  to  $E_2$  at 60 cps by a vibrating switch like the Brown



converter; there is no need to have the switching rate bear any special relation to the recurrence frequency of the sawtooth waveform. Now  $E_{s1}$  corresponds to the time interval  $T_1$ , and  $E_{s2}$  corresponds to  $T_2$ ; the zero error is cancelled out so that  $T_2 - T_1 = K(E_{s1} - E_{s2})$  and depends only upon the stability of the slope constant  $K$ . Usually  $E_{s1}$  will be held constant and control is obtained through  $E_{s2}$ . The diagram of Fig. 13-9 illustrates one way in which this circuit can be used to measure unknown time intervals. The circuit is internally synchronized and the unknown time delay device is triggered by the output pulses from the sawtooth waveform. The output pulses and the output from the unknown delay device are displayed on the cathode-ray tube, and  $E_{s2}$  is adjusted until coincidence is obtained between the pulse from the

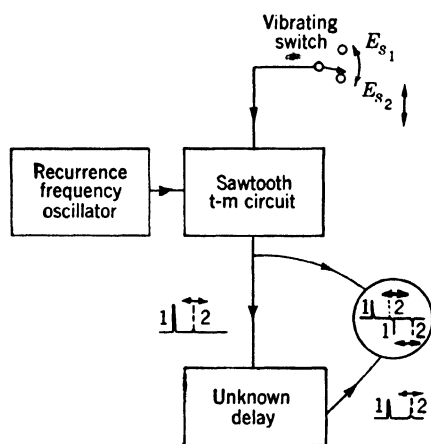


FIG. 13-9.—The use of a vibrating switch in the measurement of time intervals without zero error.

unknown delay corresponding to  $E_{s1}$  and the pulse from the sawtooth corresponding to  $E_{s2}$ .

In order to make the unavoidable errors in switching and pick-off as unimportant as possible, the sawtooth waveform should be large. If the difference between initial and pickoff voltages can change by as much as 0.2 volt, the change in  $T$  can nevertheless be held to only 0.1 per cent by making the sawtooth waveform 200 volts in amplitude. Some preliminary work has been done on sawtooth waveforms with amplitudes of several kilovolts. The

generation of the sweep can be accomplished, but the principal need is for clamping and pickoff diodes that can withstand the large inverse voltages to which they will be subjected.

Earlier in this section it was assumed that most of the errors arising from tube change in the circuit of Fig. 13-4 are zero errors and not slope errors. Naturally this is not exactly true. A change in the initial voltage alters the initial current through  $R$  and hence the slope with which the sawtooth starts out. More important is the effect of changing  $V_s$ , since very small changes in the gain of the bootstrap cathode follower can cause noticeable changes in the shape of the sawtooth. Some work has been done on the use of high- $g_m$  pentodes for this stage (see Chap. 7), but in general the bootstrap sweep is abandoned in favor of the Miller sweep when precision greater than 0.1 per cent is required.

For other details on the performance of this type of circuit see Vol. 20,

Sec. 5·7 of this series. Other errors, which have not been discussed here, are due to temperature changes, recurrence-frequency changes, and nonlinearity of the potentiometer which may be used to derive the control voltage.

**13·10. Problems with Miller Negative-going Sweeps.**—Miller negative-going sweeps can be generated with greater linearity and at lower cost than can bootstrap positive-going sweeps. Yet their use in *t-m* circuits is in some respects more difficult, when the greatest precision is desired, because of the switching and comparison problem.

It was stated in the preceding section that in the case of a positive-going sweep a single-diode switch and single-diode comparator would give good freedom from drift and heater voltage sensitivity because the effects of the two tubes subtract. The analogous Miller circuit is shown in Fig. 13·10. In the Miller tube  $V_1$  the plate is normally cut off by negative bias on the suppressor and is turned on for the duration of the sawtooth waveform by the gating rectangle. Tube  $V_2$  is the diode which sets the initial level of the sawtooth;  $V_3$  is the pickoff diode. Now if the cathode emission in both  $V_2$  and  $V_3$  increases, the level of the sawtooth drops slightly, and pick-off occurs at a slightly higher voltage. These effects add and do not cancel, and  $T$  therefore decreases with increasing heater voltage. The change is a zero change.

A further source of difficulty is the Miller tube  $V_1$  itself. If its cathode emission increases, the quiescent level of the grid drops slightly, and when the gate is applied, the negative step on the grid, although the same size as formerly, carries the grid to a slightly lower voltage, increasing the current through  $R$  and hence through  $C$ . The slope of the sawtooth will therefore increase with heater voltage—that is, there will be a decrease in the slope of  $T$  vs. the control voltage.

Fig. 13·11 shows two ways of overcoming this slope change. In *a* the level of the grid is kept constant by the compensating diode  $V_4$ , very much as in the self-stabilizing switch and pickoff of the preceding section. In *b* the level of the grid is permitted to change, but the voltage to which the timing resistor  $R$  is returned is made to change in the same way by the

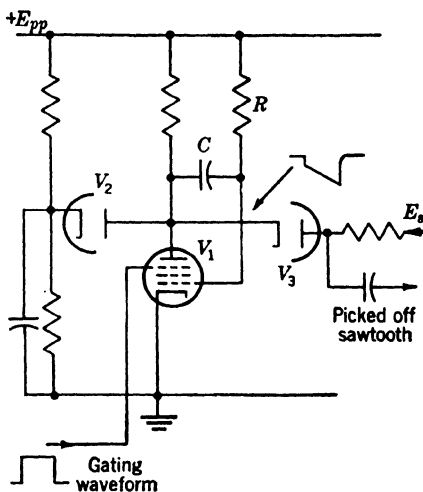


FIG. 13·10.—A *t-m* circuit using a Miller negative-going sawtooth.

diode  $V_4$ . The voltage across  $R$  is thus made independent of heater voltage, and the slope of the sawtooth remains constant. It may be remarked that all these methods of self-stabilization depend upon the fact that a change in heater voltage merely alters the effective potential of the cathode of the tube, and by the same amount, whether the tube is a diode, triode, or pentode.

It still remains to discuss the methods for reducing the zero errors. As in the case of the bootstrap sweep, an effective method is to pick off twice with matched pickoff elements from the same sawtooth, and an even more accurate method is to use a single pickoff element, switching the control voltage rapidly between two values. Other than these two

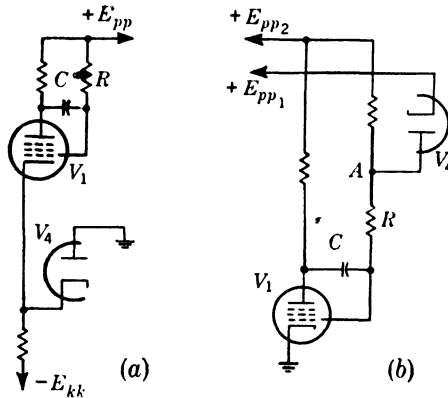


FIG. 13-11.—Methods of stabilizing the slope of the sawtooth against changes in heater voltage. In (a) the level of the grid of  $V_1$  is kept constant; in (b) the voltage at the point  $A$  changes in the same way as the grid voltage changes.

methods, the only suitable way to reduce the zero errors is to use self-stabilizing switches and pickoffs like those of Figs. 13-6 and 13-7.

The problem of accurate zeroing is especially troublesome when the Miller sawtooth generator includes a cathode follower to permit rapid recovery. In this case the sawtooth waveform from the cathode of the cathode follower is more linear and at a lower impedance than that from the grid; its level, however, cannot be set accurately. This is no disadvantage when the double pickoff or vibrating-switch methods can be used, but in other cases it is a difficult problem. The best solution, shown in Fig. 13-12, is to insert another condenser  $C_1$ , large compared with  $C$ , in the feedback loop, so that the point between  $C$  and  $C_1$  describes an accurate sawtooth but at a completely indeterminate level. The desired level can then be inserted by a single diode, as in the figure, or by a self-stabilizing switch.

The methods described thus far are of no use in reducing the effects of tube change of  $V_1$ . Changes in the size of the negative step at the

grid are to be expected and with them both zero and slope changes. The only way to reduce these errors is to eliminate the step. Several methods for accomplishing this are known; they are discussed in Chap. 7.

**13-11. Slow and Nonlinear Sweeps—Regenerative Pickoffs.**—When very slow or highly nonlinear sweeps are used, the problem of reducing

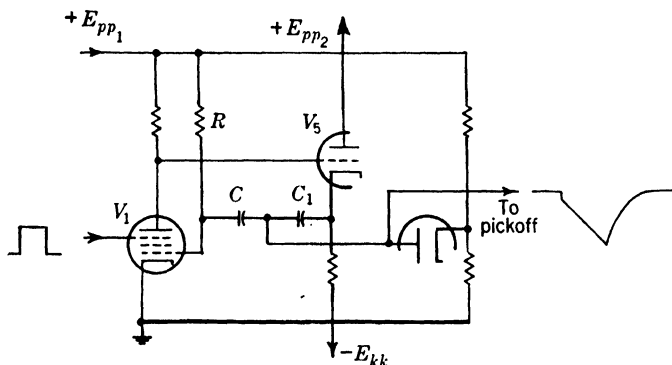


FIG. 13-12.—Illustrating how accurate zeroing of the sawtooth may be obtained when cathode follower coupling is used for rapid recovery.

the lag between the instant of voltage equality (of the sweep and  $E_s$ ) and the pulse formation becomes important. Failure to solve this problem means drift errors in the case of the linear sweeps and both original errors and drift errors with the highly nonlinear sweeps. A simple diode comparator plus several stages of amplification is one answer;

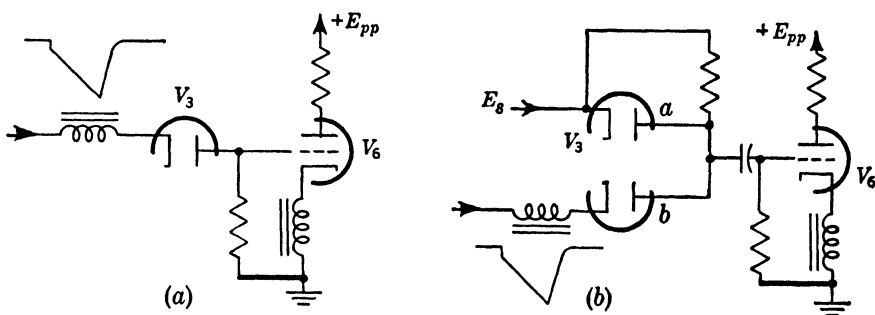


FIG. 13-13.—Self-stabilization in a Multiar pickoff. In (a) the grid and cathode of  $V_6$  act as a diode to stabilize  $V_3$ . In (b) the control signal  $E_s$  can be introduced through  $V_{3a}$  which also serves to stabilize  $V_3$ .

a simpler answer is the use of regenerative pickoffs. These circuits are treated in detail in Secs. 9-12 to 9-15.

Briefly, any regenerative device can be made to act as a regenerative comparator, but the stability, depending as it does upon the cutoff characteristics of a triode or pentode, is not very good. One circuit, however, the Multiar pickoff, is controlled by a diode and accordingly

shows much better stability. Several variations in the circuit arrangement exist, giving different degrees of stability. If the diode can be conductively coupled to the grid of the triode, as in Fig. 13-13a, the circuit is self-stabilizing and shows very good freedom from drift. If it is desired to place the control voltage on the plate of the diode, then capacity coupling must be used which will remove the self-stabilizing feature. It can be regained, of course, by using two diodes, as in Fig. 13-13b.

The Multiar with a stabilized Miller sweep generator probably represents the most economical method for obtaining the greatest accuracy possible at present. In Vol. 20, Sec. 5-3 of this series a circuit of this type is described as giving linearity of 0.05 per cent, with a 5 per cent change in line voltage causing less than 0.04 per cent change in zero and 0.1 per cent change in slope.

**13-12. Internally Gated Circuits.**—The circuits of the preceding sections have all required, as the gating waveform, a rectangle at least as long as the maximum time interval desired. Since there is usually only a pulse available, these circuits must be preceded by a monostable multivibrator or similar circuit. When a t-m circuit is operated in this way, it is said to be externally gated. There are two other possibilities, however, which will now be treated very briefly.

If the t-m output pulse from the sawtooth waveform is fed back to the gating multivibrator in such a way as to shut it off immediately, the circuit yields not only a t-m pulse, but also a t-m rectangle and a t-m triangle like those of Figs. 13-1a and b. Furthermore, all three outputs are time-modulated in exactly the same way, a property that is often very convenient. For this purpose an ordinary bistable multivibrator should be used, with both the initial triggers and the t-m terminating triggers being injected. A monostable multivibrator has the disadvantage that the exponential waveform on the grid makes the circuit harder to terminate when  $T$  is short than when  $T$  is long.

The other possibility is that of producing the gating rectangle from the sawtooth waveform itself, thus making a separate gate generator unnecessary. Essentially, the sawtooth waveform is differentiated to obtain a rectangle and the rectangle is fed back to the gating electrode of the sawtooth generator. In this way a positive-feedback loop is obtained which makes the circuit respond to a trigger alone without any need for an externally generated gate. In fact, the circuit has become a monostable relaxation oscillator with a linear timing waveform. A circuit operating in this fashion is said to be internally gated. The important fact about these circuits is that they contain, in very compact form, all the elements for a complete sawtooth t-m circuit: gating mechanism, sawtooth-waveform generator, and regenerative pickoff mech-

anism. Circuits can be mentioned which perform all these operations in a single envelope. Hence this class of circuits is extremely economical, and, in accordance with the statements made in Sec. 13-8, very difficult to analyze precisely. The present section will deal with the most important of these circuits.

*Internally Gated Bootstrap Circuits.*—Chapter 7 describes how bootstrap sweep generators can be made internally gated, and an example of such a circuit is shown in Fig. 13-14. A small resistor  $R_1$  is inserted in series with  $C_1$  and  $C_2$  and differentiates the sawtooth waveform. The rectangle appearing across the resistor is amplified and inverted in a

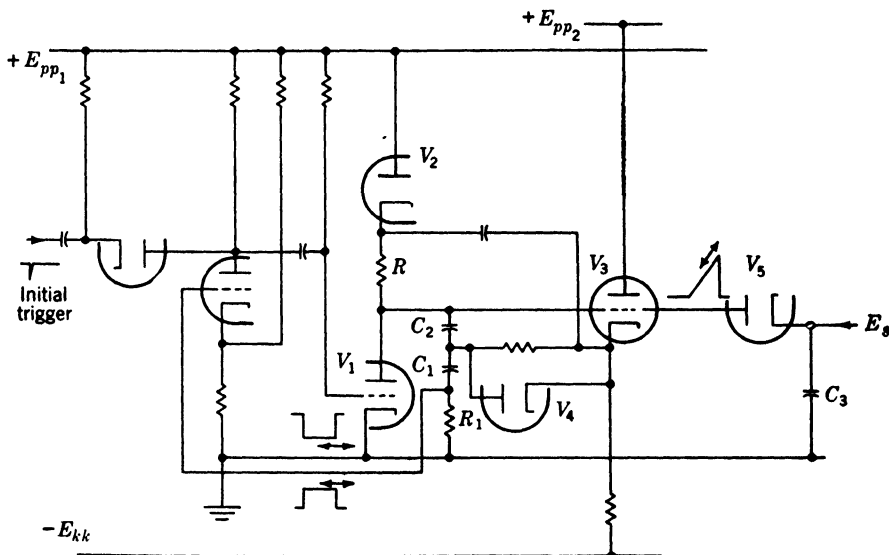


FIG. 13-14.—Internally gated bootstrap sweep, terminated by loading with the diode  $V_4$  and the condenser  $C_3$ .

single-triode section and placed on the grid of  $V_1$ , the clamping triode. The circuit is now internally gated and can be triggered with a negative trigger on the grid of  $V_1$ . The pickoff mechanism is provided by  $V_3$ , the bootstrap cathode follower. The grid of  $V_3$ , rising linearly with the sawtooth waveform, sooner or later begins to draw grid current. When it does, the load on the sawtooth waveform suddenly increases, the slope of the sawtooth waveform decreases, the amplitude of the gating rectangle decreases, and very shortly afterward the entire circuit snaps back to its initial quiescent condition.

The moment of grid-current flow in  $V_3$  is very poorly defined—furthermore, it cannot be controlled easily and linearly. Therefore, the sweep is never permitted to terminate itself in this way, a pickoff diode or other comparator being used. Two methods are, in fact, in use. One is to use

a comparator in the ordinary way, in which case economy is the only advantage in making the sawtooth-waveform generator internally gated. The other method uses a diode to apply a sudden load to the sawtooth waveform when it reaches  $E_s$ , thus simulating the grid-current action of  $V_s$  but with much better accuracy. This is the method illustrated in Fig. 13-14. A t-m rectangle and t-m triangle are the outputs.

*Internally Gated Miller Circuits.*—By far the most important internally gated circuits are those employing a Miller sweep generator. Several types are in frequent use and have such names as “phantastron,” “sanatron,” “sanaphant,” etc. They were all invented and mainly developed in England. At their best they undoubtedly offer the highest ratio of performance to cost now available. The briefness of the treatment here is no reflection on their importance; it simply results from the fact that these circuits have already been treated in Chap. 5 of this volume and several engineered examples will be discussed in detail in Vol. 20, Chap. 5 of the Series.

A high-precision sanatron is described in Vol. 20, Sec. 5-6 of this series. There it is stated that the linearity of  $T$  vs.  $E_s$  is 0.05 per cent and that the addition of a suitable inductance in the plate circuit of the Miller tube could improve this to 0.0006 per cent. The largest error caused by change of any one tube is 0.2 per cent.

Screen-coupled sanatrons permit the use of heavy-current beam-power tubes which can provide a very large integrating current and hence very fast sweeps. Linear t-m circuits with a maximum  $T$  of 1 or 2  $\mu$ sec can be built in this way.

The screen-coupled phantastron probably offers the best ratio of performance to cost now possible. The following data apply to the circuit shown in Fig. 5-46 of this volume: linearity, 0.05 per cent; tube change, 0.3 per cent;  $T$  decreases 0.2 per cent for 10 per cent increase in heater voltage;  $T$  increases 0.2 per cent for 10 per cent increase in the positive and negative lines.

Cathode-coupled phantastrons have given accuracies somewhat better than 1 per cent in the field.

In circuits of this sort, in which the sweep is always terminated at the same voltage—namely the voltage at which the plate bottoms—the control over  $T$  must be obtained by varying the initial level of the sweep. This can be done with a simple diode switch as in Fig. 13-15a. Two faults are apparent in this arrangement, however, and Fig. 13-15b illustrates the simplest methods for minimizing them.

One of the difficulties is that current will be drawn from the source of  $E_s$  so that unless that source has zero internal impedance the effective value of  $E_s$  will be too high. The plate resistor  $R_1$  can be made very large, but this seriously increases the recovery time of the timing con-

denser  $C$ . Various solutions have been used. One way is to introduce  $E_s$  through a cathode follower; this provides a low-impedance control signal, but it introduces a new source of nonlinearity and drift errors. The rather ingenious method shown in Fig. 13-15*b* makes use of a simple compensating element. The resistor  $R_2$  is made equal to  $R_1$  and the

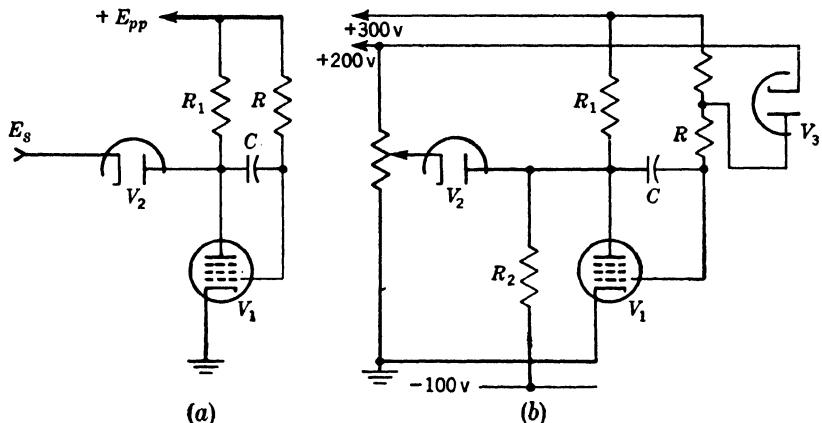


FIG. 13-15.—(a) Simple method of introducing  $E_s$ . (b) Improved circuit, including a correcting resistor  $R_2$  to reduce the current drawn from the source of  $E_s$ , and a compensating diode  $V_3$  to reduce the effects of heater voltage change.

voltage to which it is returned is chosen so that for  $E_s$  near the middle of its range the drops across  $R_1$  and  $R_2$  are equal. Then at this point no current is drawn from the potentiometer or other source of  $E_s$ , and the error in  $E_s$ , as plotted in Fig. 13-16, is considerably reduced.

The other fault in the circuit of Fig. 13-15*a* is that no provision is made against a slope error with heater voltage change. Two methods were shown in Fig. 13-11 for accomplishing this: in the method of Fig. 13-11*a* the bottoming voltage is unchanged with heater voltage change, whereas in that of Fig. 13-11*b* the bottoming voltage decreases with increased heater voltage. The latter method is used here because the decrease in bottoming voltage exactly compensates for the decrease in the initial level of the sawtooth caused by the increased cathode emission of  $V_2$ ; if the method of Fig. 13-11*a* were used, a self-stabilized switch would have to be used in place of  $V_2$ .

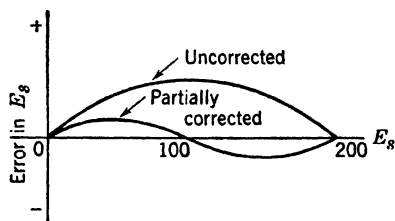


FIG. 13-16.—The reduction in loading error obtained with the correcting resistor  $R_2$  in Fig. 13-15*b*.

**Multivibrators.**—Section 5-14 discussed methods of varying the duration of a multivibrator square wave—that is, of carrying out TM with a



multivibrator. The only one of those methods that has been extensively used is voltage control of the cathode-coupled monostable multivibrator. The method is inexpensive but not very accurate. Linearity can be as good as 0.1 or 0.2 per cent, but tube change can alter  $T$  by 10 per cent, and a 10 per cent change in line voltage can alter  $T$  by 2 per cent.

### PHASE-MODULATION METHOD

**13-13. Introduction.**—The circuits to be described in this part of the chapter are designed to produce phase-shifted sine waves, either continuous sine waves as in Fig. 13-1e or pulsed sine waves as in Fig. 13-1f.

Variable phase-shifting devices for sine waves fall into two groups: limited phase-shifting types, which are restricted to varying the phase shift over a range of only a finite number of degrees (usually  $180^\circ$ ); and continuous phase-shifting types, which are not so limited. The simple networks consisting of a variable resistor with a condenser or inductance are examples of the first class of circuits—these are discussed in Chap. 4 and will not be further described here. A synchro, in which the phase-shifting depends upon the mechanical rotation of a pickoff element in a rotating field, is an example of the second class of circuits, which will form the subject of the next few pages. The importance of continuous phase-modulators in TM stems from the fact that the phase shift can be made very nearly linear with respect to shaft rotation, whereas with the limited phase-shifting types this is distinctly not so.

As a method of TM, continuous phase-modulators offer the advantage of determining  $T$  with an absolute accuracy which is virtually as good for  $T$  large as for  $T$  small, though with an ambiguity equal to the period of the sine wave being used. The phase-modulation method of TM is, therefore, most often used in high-precision double-scale systems, in which a less precise t-m circuit (usually a sawtooth and comparator) selects the correct cycle of the phase-modulated sine wave and thereby removes the ambiguity. In this way unknown time intervals, under proper circumstances, can be measured with an accuracy of better than 10 parts per million. This accuracy is possible because, although the phase-shifting element may contribute a cyclic error of 0.1 or 0.2 per cent of the period of the sine wave, this error, being cyclic, is not cumulative. The only cumulative error is the frequency error of the oscillator that supplies the sine waves. The error in properly designed crystal-controlled oscillators can be kept well below 10 parts per million.

The presence of the cyclic error is, however, a serious drawback for some purposes. Circuits of this sort are commonly used in radar when very good absolute range accuracy is required even out to large ranges. When rapidly moving targets are tracked with such circuits, however, the cyclic error in the phase-shifter makes the rate data uneven, and great

pains must be taken to filter out the unwanted fluctuations, often with a serious loss in ability to follow target accelerations. Both the sawtooth and propagation velocity methods are free from this defect. The phase-modulation method is also restricted to rather low modulating frequencies since the control is by means of a shaft with sufficient inertia to filter out all high frequencies.

The problem of deriving t-m pulses, if they are desired, from the phase-modulated sine waves is essentially a problem in amplitude comparison with special emphasis on the stability of comparison to keep the point of the sine wave at which the pulse is formed as constant as possible. The basic methods are given in Chap. 9. Practical examples of these methods will be found throughout Chaps. 5, 6, 7, 9, and 11 of Vol. 20 of this series.

An important property of these phase-modulators, to which some attention should be given, is their behavior with pulsed sine waves. The point here is that the discontinuity in the envelope of the sine wave can produce in the phase-shifted output a very undesirable additive transient. Most of the phase-modulators to be described below require polyphase sine-wave inputs; the problem of designing pulsed polyphase sources without transients for phase-modulators is discussed in Chap. 4, and in this chapter it will be assumed that the input sine waves come from such sources. In cases where the transients may arise in the phase-modulator itself, methods for reducing them will be given in this chapter.

**13-14. Phase-modulating Potentiometer.**—An economical, though not very accurate, method is provided by the phase-shifting potentiometer shown in Fig. 13-17. If the potentiometer is linear, the output in the first quadrant is  $\frac{2}{\pi} A \left[ \theta \sin \omega t + \left( \frac{\pi}{2} - \theta \right) \cos \omega t \right]$ . Thus the phase angle of the output is defined in the first quadrant by

$$\tan \phi = 2\theta/(\pi - 2\theta).$$

It is therefore seen that the phase shift is not truly linear with respect to the shaft rotation of the potentiometer. Actually, if  $\phi$  is plotted against  $\theta$ , a curve like that of Fig. 13-18 will be obtained. The greatest error will be found when  $\theta$  differs from  $0^\circ$ ,  $90^\circ$ ,  $180^\circ$ , or  $270^\circ$  by  $21.5^\circ$  (not  $22.5^\circ$ ) and at these points the error amounts to about  $4^\circ$ , or about 1.1 per cent of the full  $360^\circ$ . The amplitude of the output, in the first

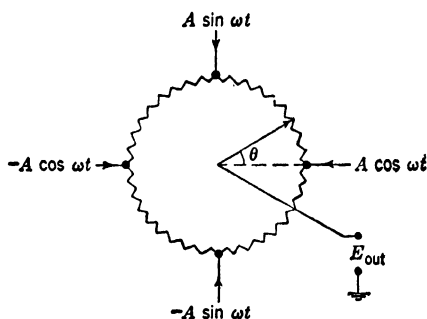


FIG. 13-17.—Schematic diagram of the phase-shifting potentiometer.

quadrant, is  $A \sqrt{1 + \frac{4\theta}{\pi} \left( \frac{2\theta}{\pi} - 1 \right)}$ . If the output amplitude is plotted against  $\theta$ , a curve like that of Fig. 13-19 will result.

From the preceding material two main disadvantages appear: the linearity is good to only  $\pm 1.1$  per cent, and the output amplitude is far

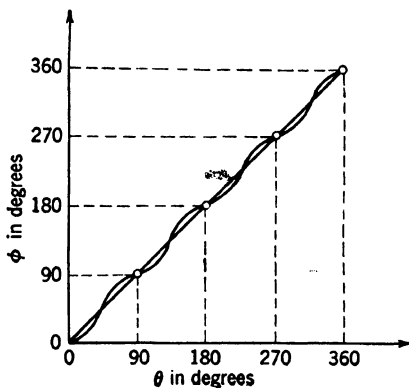


FIG. 13-18.—The departure from linearity in the variation of phase shift  $\phi$  with shaft rotation  $\theta$  in the potentiometer phase shifter of Fig. 13-17.

from constant. Both of these faults can be reduced by increasing the number of inputs (to 8, for example) and using an 8-phase source of sine waves. Also the nonlinearity in the phase shift can be removed completely by deliberately inserting the correct nonlinearity into the potentiometer winding. Another disadvantage is the limitation on life inherent in all sliding-contact devices. The method has, however, the great advantage of economy because the necessary driving circuit is very simple, because it introduces little attenuation, and because

it can be used with pulsed sine waves, provided that a suitable source of pulsed polyphase inputs exists. Figure 13-20 shows a typical practical circuit of this type. The  $150 \mu\text{f}$  condensers and  $3.3 \text{ k}$  resistors are the phase-splitting network to provide the 4-phase inputs.

**13-15. Phase-shifting Condensers.**—Considerably better accuracy than with the phase-shifting potentiometer can be obtained with the phase-shifting condensers to be described here, which can set up a rotating electrostatic field and pick off a phase-shifted signal from it with an error as small as  $\pm \frac{1}{4}^\circ$ . Two types of condenser have been developed, differing in the number of inputs.

The 4-phase condenser, which may be represented schematically in either of the ways shown in Fig.

13-21, consists of four variable condensers, each one of which has one plate in common with the others and one plate free to accept one phase of the 4-phase sine wave input. Let the input to  $C_1$  be  $A \sin \omega t$ , that to  $C_2$  be  $-A \cos \omega t$ , that to  $C_3$  be  $-A \sin \omega t$ , and that to  $C_4$  be  $A \cos \omega t$ .

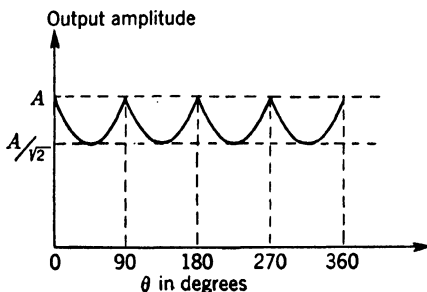


FIG. 13-19.—The departure from constant amplitude with shaft rotation  $\theta$  in the potentiometer phase shifter of Fig. 13-17.

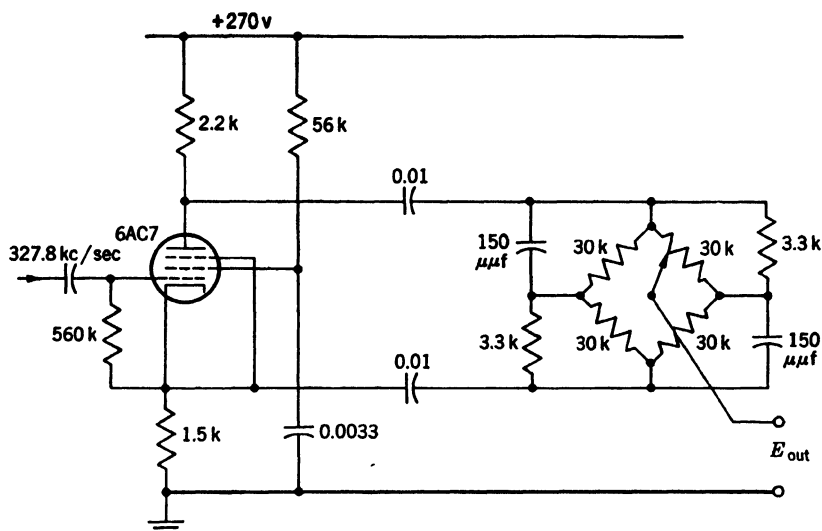


FIG. 13-20.—Practical circuit using a phase-shifting potentiometer.

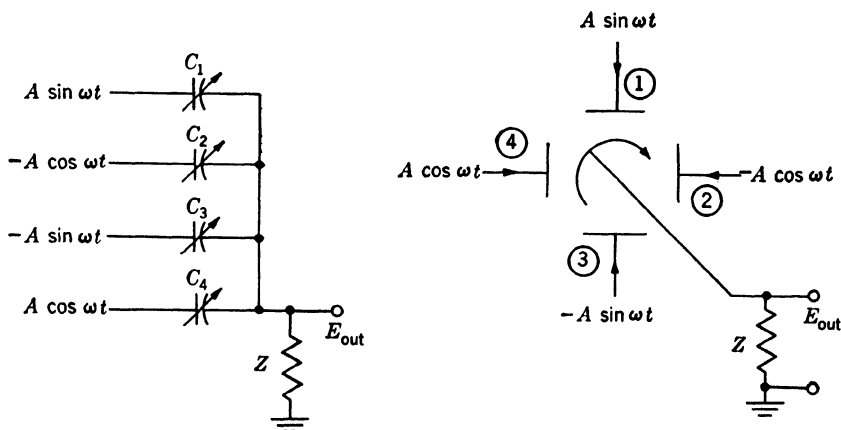


FIG. 13-21.—Equivalent schematic representations for a 4-phase phase-shifting condenser.

Also suppose that the capacities are so arranged that they are sine functions of some shaft rotation  $\theta$  as follows:

$$C_1 = D + G \cos \theta$$

$$C_2 = D + G \sin \theta$$

$$C_3 = D - G \cos \theta$$

$$C_4 = D - G \sin \theta,$$

where  $D$  and  $G$  are positive constants ( $D > G$ ). Then it can be shown that

$$E_{out} = \frac{2AG}{4D + \frac{1}{j\omega Z}} \sin(\omega t - \theta). \quad (1)$$

Thus the phase-shifting condenser gives constant output amplitude and perfect linearity of phase shift.

The 3-phase condenser is shown in Fig. 13-22. If  $C_1 = D + G \cos \theta$ ,  $C_2 = D + G \cos(\theta + 120^\circ)$ , and  $C_3 = D + G \cos(\theta + 240^\circ)$ , and if the inputs are respectively  $A \sin \omega t$ ,  $A \sin(\omega t + 120^\circ)$ , and  $A \sin(\omega t + 240^\circ)$ , it can be shown that

$$E_{out} = \frac{3AG}{2 \left( 3D + \frac{1}{j\omega Z} \right)} \sin(\omega t - \theta). \quad (2)$$

Constant output amplitude and perfect linearity of phase shift are again obtained. Notice that with either type of condenser, even when  $Z$  is infinite, the output is attenuated from the input by a factor  $2D/G$ , a quantity that can never be smaller than 2, since  $D > G$ .

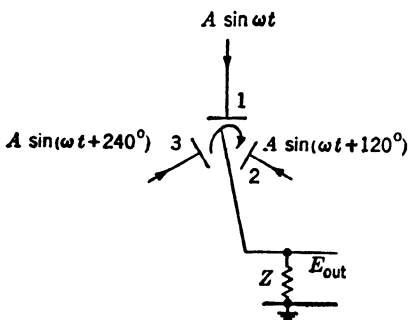


FIG. 13-22.—Schematic representation of a 3-phase phase-shifting condenser.

Phase-shifting condensers have been constructed mainly in three ways. (For details of construction, see Vol. 17, Chap. 9, this series.) The Cardwell KS-8533 resembles very closely the ordinary variable air condenser, except that there are two sets of stationary ones, and these

plates are shaped and placed in such a way as to give the proper sinusoidal variation in capacity with shaft rotation. Its main disadvantages are its bulk, the lack of shielding for the output, and the large values of the capacities, which make it difficult to drive. No 3-phase condenser of this type is available.

A much more compact method of construction is embodied in the Western Electric D-150734 4-phase condenser and the similar 3-phase condenser manufactured by the P. J. Nilsen Company, Oak Park, Illinois. Here the input plates are the sectors of a circle and the output plate is another circle, parallel to the first and displaced from it by a small distance. Between the two circles is a slab of dielectric (micalex), mounted on a shaft which lies along the axis of the circles and shaped in such a way that the capacities from the sectors of the upper circle to the lower circle are the desired functions of  $\theta$ , the angular position of the

shaft. The proper shape for the micalex rotor is given by the polar equation  $\rho^2 = A + B \cos \theta$ , but for reasons which will be given later, the 4-phase condenser can use an off-center circular rotor without serious loss in accuracy.

A third method of construction, used in both 3-phase and 4-phase condensers now under development, uses a metal instead of a micalex rotor, which itself serves as the output plate. This arrangement results in an increase of the ratio of  $G$  to  $D$  and a consequent reduction in the attenuation.

Finally, a fourth method that shows promise is to use two concentric metal cylinders, the outer one of which is cut along lines parallel with the axis to form the three or four input plates, while the inner one, which can be rotated about its own axis, and which will serve as the output plate, is a truncated cylinder to provide the sinusoidal variation of capacitance.

The error in phase shift cannot be held to  $\frac{1}{2}^\circ$  unless considerable care is taken to provide inputs to the condenser accurately equal in amplitude and exactly  $90^\circ$  or  $120^\circ$  apart in phase. The 4-phase condenser thus requires six independent adjustments; the 3-phase condenser requires four.

One very simple method for performing the adjustment depends upon the fact<sup>1</sup> that, provided the condenser itself is perfectly made, the correct settings of amplitudes and phases will be those for which the amplitude of the output is independent of  $\theta$ . The method is to display  $E_{out}$  on an oscilloscope and adjust the inputs until the envelope of  $E_{out}$  shows no amplitude modulation when the rotor of the condenser is spun. This method is apparently suitable for use with either 3- or 4-phase condensers.

Somewhat better accuracy can be obtained by another method which can be applied only with 3-phase condensers. If the micalex rotor is removed from the condenser, and if the amplitudes of the three inputs have been made exactly equal with the aid of a voltmeter or oscilloscope, then the correct phase adjustments for the inputs will clearly be those for which there is zero output from the condenser. The possibility of using this method is the chief advantage of the 3-phase over the 4-phase condenser.

Of interest to the reader may be a careful theoretical study<sup>2</sup> of the errors in the 4-phase condenser. The errors studied arise from the following causes: inequality of the input amplitudes; failure to have the inputs exactly  $90^\circ$  apart in phase; presence of harmonics in the input signals; transients produced in the polyphase source and in the condenser itself when the sine waves are pulsed; and departures from a true sinusoidal

<sup>1</sup> The author has never seen this statement proved.

<sup>2</sup> See G. R. Gamertsfelder, "Errors in the Condenser Type Continuous Phase Shifter," RL Report No. 633, Dec. 6, 1944.

variation of the capacities with  $\theta$ . In connection with this source of error, it is shown that if the capacity is expressed in terms of  $\theta$ ,  $2\theta$ ,  $3\theta$ , etc. by a Fourier series, then no errors will arise from the terms in  $2\theta$ ,  $4\theta$ ,  $6\theta$ , etc. This is not true with the 3-phase condenser; hence, an off-center circular rotor can be used in the 4-phase condenser in place of the special rotor which must be used in the 3-phase condenser.

In Eqs. (1) and (2) it is seen that the amplitude of the output  $E_{out}$  is attenuated from the amplitude  $A$  of the input by a factor of  $\left| \frac{\left(4D + \frac{1}{j\omega Z}\right)}{2G} \right|$

for the 4-phase condenser and  $\left| \frac{2\left(3D + \frac{1}{j\omega Z}\right)}{3G} \right|$  for the 3-phase condenser.

In general,  $Z$  will be made up of the output capacity  $C'$  of the phase-shifting condenser, the input capacity  $C$  of the next stage, and the input resistance  $R$  of the next stage, all in parallel. Hence,

$$Z = \frac{1}{\left[ \frac{1}{R} + j\omega(C + C') \right]},$$

and the attenuation factors can be written as  $\left| \frac{\left(4D + C + C' + \frac{1}{j\omega R}\right)}{2G} \right|$

and  $\left| \frac{\left(6D + 2C + 2C' + \frac{2}{j\omega R}\right)}{3G} \right|$ , respectively. If  $C$  were 0 and  $R$  were

$\infty$ , then in the case of the D-150734 4-phase condenser, the attenuation factor would be 12.5 since  $D = 1.5 \mu\text{mf}$ ,  $C' = 12.7 \mu\text{mf}$ , and  $G = 0.75 \mu\text{mf}$ . Actually, of course, both  $C$  and  $R$  have finite values, so that the attenuation is greater. The presence of the term  $1/j\omega R$  is especially bad at the lower frequencies, as is clearly illustrated in Fig. 13.23, in which the attenuation in the D-150734 4-phase condenser is plotted as a function of frequency for  $R = 10^7$  ohms,  $C = 1 \mu\text{mf}$ , and for  $R = 10^6$  ohms,  $C = 11 \mu\text{mf}$ . The very rapid increase of attenuation at low frequencies should be noted. Fortunately there is no need to extend the useful range of frequencies below 10 to 15 kc/sec, since the synchro phase-shifters are satisfactory below those frequencies.

Practical examples of the use of phase-shifting condensers will be found in several chapters of Vol. 20, especially Chaps. 6 and 11. Figure 11-21 in that volume is of special interest, since it demonstrates recent techniques for the production of pulsed sine wave for the condenser inputs. Reference should also be made to Chap. 4 of this volume.

**13.16. Synchro Phase-modulators.**—Precision synchros probably offer the highest accuracy possible, the errors in certain of these instruments being only about 10 minutes of arc (for details see Vol. 17, Chap. 10). They also make possible the accurate phase-shifting of sine waves in the frequency range below 15 to 20 kc, where the phase-shifting condenser is unsuitable.

Synchros may be used for phase-modulating in either of two ways. One method depends upon the establishment of a rotating field and is quite analogous to the potentiometer and condenser methods. As is shown in Fig. 13-24, two inputs of equal amplitude but 90° out of phase are placed on the stators to produce the rotating field, which is picked off with the rotor.

The voltage induced in the rotor is  $M_1 \frac{di_1}{dt} + M_2 \frac{di_2}{dt}$ , where  $M_1 = M \cos \theta$ ,  $M_2 = M \sin \theta$ ,  $i_1 = I_o \sin \omega t$ , and  $i_2 = I_o \cos \omega t$ . Thus the output from the rotor is  $M\omega I_o$

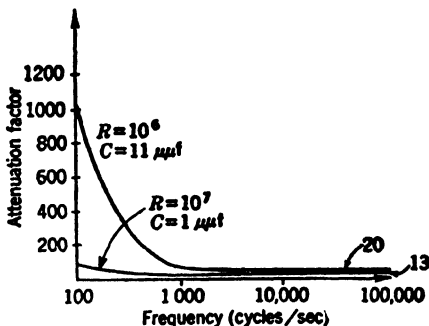


FIG. 13-23.—Attenuation vs. frequency in the D-150734 4-phase condenser, plotted for two input impedances to the following stage.

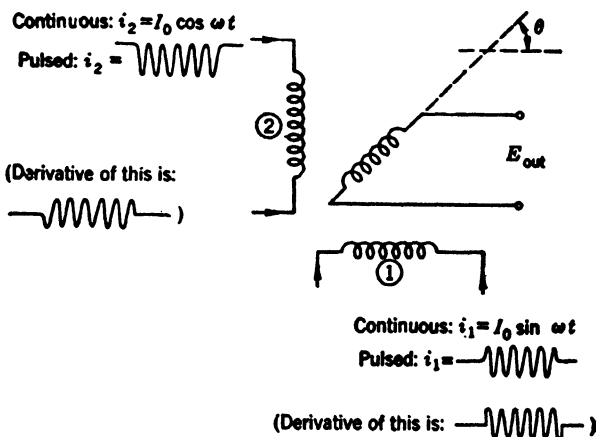


FIG. 13-24.—Rotating field method for phase-shifting with a synchro. Notice the form of the input current waveforms necessary for transientless operation under pulsed conditions.

$\cos(\omega t + \theta)$ , and it is seen to be constant in amplitude and linearly phase-shifted.

The problem of operating a synchro with pulsed sine waves is solved by using pulsed current waveforms of the forms shown in the figure.



The voltages induced in the rotor are the derivatives of these currents and will, as it is shown in the figure, have no transient. Reference should be made to Sec. 4-18 for a practical circuit that can be used to

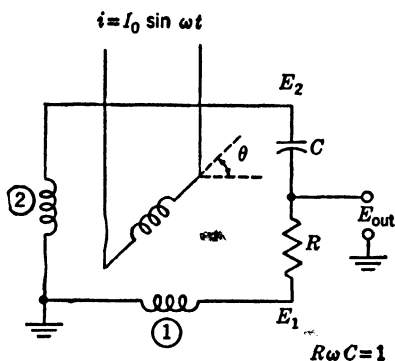


FIG. 13-25.—Resolution method for phase-shifting with a synchro.

supply the stators with these currents. The rotor should be made to work into a high impedance, especially under pulsed conditions, because the current in the rotor will produce a transient if it is not small.

The other method is illustrated in Fig. 13-25. Here a single sine wave  $I_o \sin \omega t$  is fed into the rotor, and across the stators appear two waves,  $E_1 = M\omega I_o \cos \omega t \cos \theta$  and  $E_2 = M\omega I_o \cos \omega t \sin \theta$ . The RC-network, where  $R\omega C = 1$ , simultaneously shifts the phases of these

two waves  $+45^\circ$  and  $-45^\circ$  respectively and adds them, yielding as output

$$E_{out} = \frac{M\omega I_o}{\sqrt{2}} \sin(\omega t + \theta + 45^\circ).$$

Thus this circuit is also seen to provide constant output amplitude and

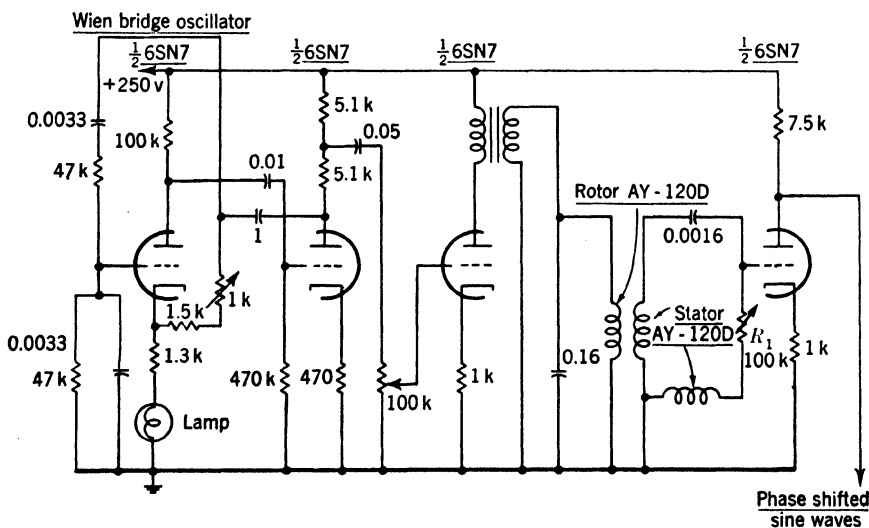


FIG. 13-26.—Practical synchro phase-shifting circuit (resolution method) for continuous 1 kc sine waves.

linear phase shift. Figure 13-26 shows a practical circuit of this sort for 1000 cycle sine waves, using a Bendix AY 120D synchro.

This latter method, which may be called the resolution method to distinguish it from the rotating-field method, is very much the simpler and more reliable of the two, since it requires only one input current of arbitrary amplitude, whereas the rotating-field method will give erroneous phase-shifting unless both inputs are of equal amplitude and exactly  $90^\circ$  out of phase. A disadvantage, however, of the resolution method is its behavior with pulsed sine waves. The difficulty lies not in the synchro, since  $E_1$  and  $E_2$  can be made transientless by using the proper current waveform for the input, but in the  $RC$ -network, which, as is shown in Sec. 4-16, produces an additive transient with a time-constant  $RC = 1/\omega$ . The transient is, therefore, rather short-lived, decaying to less than  $e^{-6}$  of its initial value after one cycle of the sine wave, but for some purposes it may still prove troublesome.<sup>1</sup>

Lining up the circuit involves, for the rotating field method, the adjustment of one amplitude and one phase; for the resolution method, an adjustment of either  $R$  or  $C$  to make  $R\omega C = 1$ . In either case, the rotor-spinning technique described in the preceding section is accurate enough to make errors smaller than  $\pm \frac{1}{2}^\circ$  with high-quality synchros.

Because their internal impedance rises with frequency, synchros become less useful at high frequencies very much as condensers become less useful at low frequencies. Below about 15–20 kc/sec, iron-core synchros are perfectly satisfactory; air-core synchros can be used at much higher frequencies.

### STORAGE-TUBE METHOD

**13-17. Storage Tubes.**—In a storage tube (see Chap. 21) a signal can be stored at any instant on that point of the tube face where the electron beam is then directed, and it can be picked up again at any later time by bringing the electron beam back to that same point. Thus, it is clear that the storage tube, unlike the electrical or acoustical delay line, has no time base inherently associated with it, and that any such time base must be applied externally by the deflection plates. This has the disadvantage of complexity but the advantage of permitting greater flexibility.

Time modulation with a storage tube thus depends upon varying the time interval between successive sweeps, and, as implied above, this in

<sup>1</sup> It has been pointed out that the transient can be removed by negative feedback. If the point between  $R$  and  $C$  is placed on the grid of a high-gain tube, the plate of which is fed back to the grid, then the grid will be a virtual ground (see Chap. 2) and at the plate will appear a transientless phase-modulated wave. The impedance placed between the plate and grid of the tube should probably be a parallel  $R_1C_1$ , where  $R_1\omega C_1 = 1$ , since such an impedance will leave the phase of the output wave the same (though inverted) as without feedback. It is probably necessary to drive the rotor with a current waveform like that on stator 2 of Fig. 13-24.

turn reduces to varying the time interval between twice impressing the same waveforms on the deflecting plates or coils of the tube. Figure

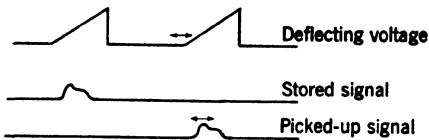


FIG. 13-27.—Use of a storage tube to perform TM upon an arbitrary waveform.

13-27 illustrates this procedure for a storage tube with a linear sweep. The upper waveform is the voltage applied to the deflection plates, the middle waveform is the one that is to be stored, and the bottom waveform is the one that is

picked up from the tube face—that is, the t-m output. More complex deflecting waveforms might, of course, be used to make more efficient use of the tube-face area.

Time modulation of a unique sort can be carried out by varying not the interval between sweeps but the sweep speed. Figure 13-28 illustrates the waveforms that will be picked up when different sweep speeds are used. This method is the only one available for TM of this sort, except in the case of

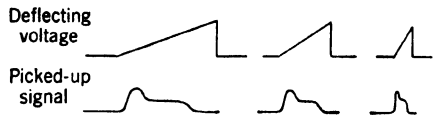


FIG. 13-28.—The type of TM obtained with a storage tube when the sweep speed is varied.

certain special waveforms, such as rectangles. It may, of course, be combined with variations of the time interval between sweeps to give very complex forms of TM.

## CHAPTER 14

### AMPLITUDE AND TIME DEMODULATION

BY BRITTON CHANCE

**14.1. Introduction.**—Demodulation of radio waves for communication purposes is discussed in a number of standard texts.<sup>1</sup> The emphasis of this chapter is upon methods for the demodulation of pulse trains of extremely low duty ratio (about 0.1 per cent). A number of specialized detector circuits give extremely rapid response to the value of the input pulse and maintain this output constant over a much longer interval than the usual type of detector of equally rapid response. These detector circuits are extremely efficient for demodulating pulse trains representing distance and angular information in radar systems. Also their rapid response makes these circuits extremely useful in the demodulation of amplitude-modulated waves in which the signal frequency is comparable to the carrier frequency.

The methods for the demodulation of signal information impressed upon a pulse carrier by means of time modulation are also presented in this chapter. Some of the methods are very similar to those used in amplitude demodulation in that the time-modulated carriers are first converted into amplitude-modulated carriers. In other cases a detector responsive to the area of the input signal is employed. The discussion of methods for converting time-modulated pulse trains into waveforms of variable amplitude or area is given in Sec. 14.7. The most useful methods of time demodulation depend upon negative-feedback systems employing time modulation, time discriminators, and control. An introductory discussion is given in this chapter, and the full discussion of practical systems is presented in Chaps. 8 and 9, Vol. 20, of this series.

In amplitude demodulation, peak detection is emphasized, whereas in time demodulation, area detection is commonly used. Since ordinary detector circuits are readily converted from peak to amplitude detectors by the mere addition of a resistance, the basic circuits will be discussed without regard to their specialization for amplitude and time demodulation, although desirable properties for either purpose will be pointed out in the course of the discussion.

The demodulation of amplitude-modulated waves, obtained from

<sup>1</sup> F. E. Terman, *Radio Engineers' Handbook*, McGraw-Hill, New York, 1943, Sec. 7.

bidirectional modulators, requires phase-sensitive detectors or phase discriminators. These circuits are similar to those used for time discrimination but usually are supplied with sinusoidal switching waveforms and may have a narrow bandwidth. The phase-sensitive detection of amplitude-modulated sinusoids obtained from the electromechanical amplitude modulators of Chap. 12 is also treated.

In those systems where output is required as a shaft rotation, a negative-feedback demodulator employing a servomechanism may be used. A complete discussion of electronic servomechanisms is given in Vol. 21, Part II, of the Series.

Often the cathode-ray-tube display is used as a part of a negative-feedback demodulator including a manually operated tracking system. Such use of these displays is fully presented in Vol. 20, Chap. 7, and in Vol. 22.

**14.2. Types of Amplitude Demodulation.**—Depending upon the intent, an amplitude demodulator may be made to indicate a number of

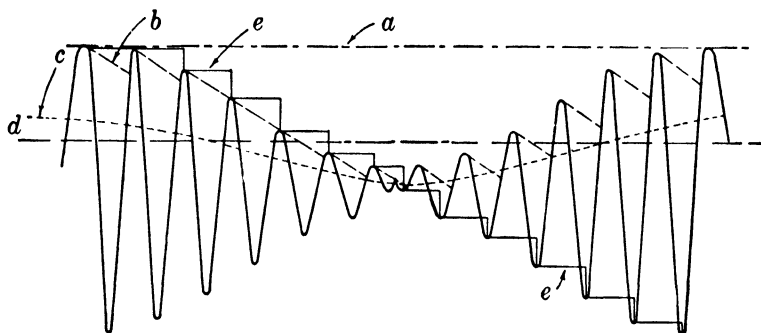


FIG. 14-1.—Illustration of various types of demodulation. Peak detection is illustrated in (a) and is obtained, for example, by a vacuum-tube voltmeter. Detection obtained from a short-time-constant peak detector is shown in (b). The output that would be obtained from an average detector is shown in (c), and (d) represents the output of a long-time-constant average detector, while (e) represents phase-sensitive demodulation by the switch circuits of Secs. 14.4 and 14.5.

completely different values for a given modulated carrier. An example of this is shown in Fig. 14-1 which indicates an amplitude-modulated carrier obtained from a bidirectional modulator.

If, for example, a peak vacuum-tube voltmeter having a time constant of several seconds is employed, an output corresponding to the peaks of the amplitude-modulated wave is obtained as indicated by curve *a*. But if the time constant of the peak detector is shorter, the envelope of the amplitude-modulated wave is obtained as indicated by curve *b*; this is called “short-time-constant peak detection.” If an average detector is used, its output represents the mean value of the positive excursions of the modulated carrier as shown in curve *c*. The output

of this detector smoothed over a time long compared with the amplitude modulation gives output  $d$ , which is representative of the peak value of the mean or unmodulated carrier.

The bulk of the important information has been missed by these demodulators because they are not phase-sensitive and do not respond to the change of sign of the modulating signal which occurs when the amplitude of the modulated carrier passes through zero. The output of a phase-sensitive demodulator gives curve  $e$ , which, instead of going to zero and rising again, passes through zero and reverses sign in accordance with the modulated signal.

Peak vacuum-tube voltmeters, audio detectors, and AGC detectors for communication have been treated extensively elsewhere.<sup>1</sup> No attempt will be made to emphasize properties of detector circuits specialized for those purposes.

**14-3. Amplitude Selectors.** *Half-wave Diode Peak Detector—Unidirectional Operation.*—The series diode peak detector (shown in Fig. 14-2) consists of diode  $V_1$  and output circuit  $R_1C_1$ . The following remarks also

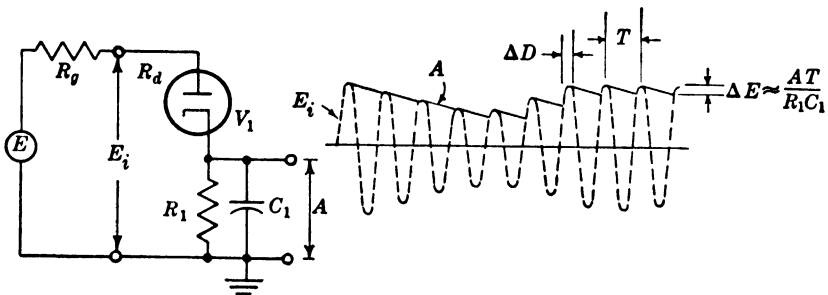


FIG. 14-2.—A half-wave peak detector for unidirectional operation employing a diode amplitude selector and a resistance-capacitance output circuit. The waveform diagram shows that the conduction interval  $\Delta T$  of the amplitude selector is short compared with the carrier repetition interval  $T$ . The fractional carrier content of the output voltage in the absence of modulation is approximately  $T/R_1C_1$  provided  $(R_g + R_d)C_1 \ll \Delta T$ .

apply to the shunt diode detector. Under ideal conditions, diode  $V_1$  is operating essentially as an amplitude selector (see Sec. 9-3). For example, if the diode impedance is small compared with that of the output circuit  $R_1C_1$ , the output potential will rapidly assume the peak value of the input voltage. Providing the product  $R_1C_1$  is long compared with the carrier period, the output will be maintained at the peak value of the last cycle of the modulated carrier. Because of this property, the detector output circuits are often termed “memory circuits.” The operation of diode  $V_1$  on the next positive cycle of the modulated carrier depends upon the relative potentials of the modulated carrier and the

<sup>1</sup> F. E. Terman, *Radio Engineers' Handbook*, McGraw-Hill, New York, 1943, Sec. 7.

voltage on the output circuit  $R_1C_1$ . The diode is therefore operating essentially as an amplitude selector; it selects portions of the modulated carrier that exceed the output potential and increases the output potential until it equals the peak value of the modulated carrier. Thus, the discussion of Chaps. 3 and 9 concerned with the broken-line characteristic of thermionic vacuum tubes and contact rectifiers applies here. Linear and stable operation is obtained only when the peak value of the modulated carrier exceeds 10 or 20 volts and is preferably of about 100 or 200 volts. An important distinction from the discussion of Chap. 9 is, however, that the forward resistance of the amplitude selector should be a minimum, and therefore low-resistance thermionic diodes such as type 6AL5 or germanium crystals are recommended in order that large values of  $C_1$  may be charged rapidly. The latter, however, are not suitable for large output voltages because of the decrease of their back resistance.

The unidirectional characteristic of the simple diode detector necessitates discharging the output circuit at a rate exceeding the maximum rate of decrease of the modulated signal in order that none of the modulating information be lost, and thereby determines the choice of  $R_1C_1$  (Fig. 14-2). If  $T$  is the carrier repetition interval and is small compared with  $R_1C_1$ , the discharge may be considered linear; its rate is  $A/R_1C_1$ , where  $A$  is the modulated carrier amplitude.

A more exact formula has been derived for a sinusoidal modulating signal:<sup>1</sup>

$$\frac{1}{\omega C_1 R_1} = \frac{m}{\sqrt{1 - m^2}}, \quad (1)$$

where  $\omega$  is the angular frequency of the modulating signal,  $R_1C_1$  the time constant of the detector circuit, and  $m$  the degree of modulation.

The effect of an unfortunate choice of output time constants is indicated in Fig. 14-3a. A more appropriate choice of time constant is indicated in Fig. 14-3b, but considerable distortion is still apparent.

The use of a short-time-constant peak detector leads to a large amplitude of the carrier in the output which, for a number of applications, is undesirable. For an unmodulated sinusoidal carrier, the fractional carrier content is simply expressed by the formula  $T/\pi R_1C_1$  where  $T$  is the carrier-repetition interval. It is assumed that the conduction time of the detector is negligible compared with  $T$  and, for diodes of reasonably low resistance, this is a valid assumption.

The operation of the short-time-constant peak detectors may be unsatisfactory in the presence of noise and interference. If, for example, it is desired to demodulate the rectangular waveform of Fig. 14-4a by means of a short-time-constant detector, the three superimposed

<sup>1</sup> F. E. Terman, *Radio Engineering*, 2d ed., McGraw-Hill, New York, 1937.

interfering pulses will have undesired prominence in the output. More satisfactory operation is indicated in Fig. 14-4b where sufficient resistance is added to make the charge and discharge time constants roughly equal. Although there is considerable delay in the response to the rectangular pulse in the output, the effect of interference is considerably reduced.

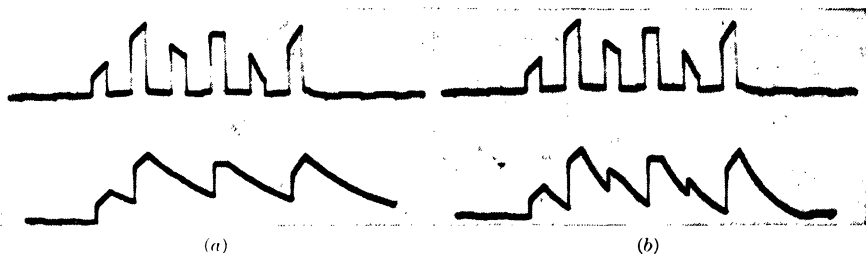


FIG. 14-3.—Effect of time constant upon detector response. Fig. 14-3a indicates the response of a diode detector and a resistance-capacitance output circuit to a pulse train modulated with a rapidly varying signal. The long time constant results in a nearly complete loss of the signal information. Fig. 14-3b represents detection with a shorter time constant and improved fidelity. The ratio of the two time constants is 3 to 1. The waveforms are displayed on a sweep of duration of 12  $\mu$ sec.

Thus the possibility of a large interfering signal charging the output voltage to such a high value that much of the subsequent modulation would be lost is avoided.<sup>1</sup>

The efficiency and simplicity of the simple peak detector under certain conditions must not be underestimated. If the input waveform is

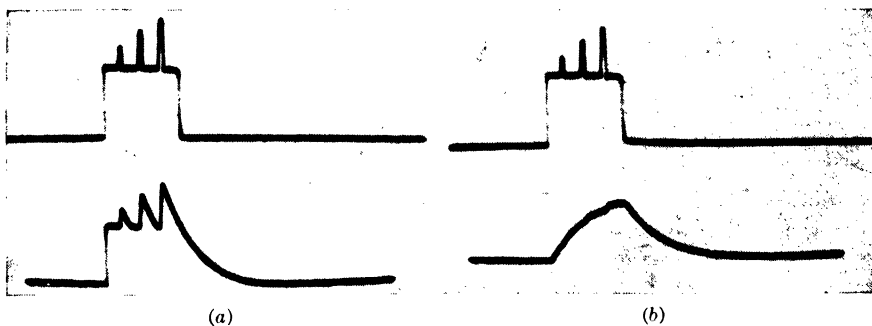


FIG. 14-4.—The effect of detector time constant upon interference reduction. Fig. 14-4a represents on the top line the envelope of a signal to be detected and on the bottom line the output of a short-time-constant peak detector. The second line on Fig. 14-4b represents the effect of increasing the charging resistance from 500 to 100,000 ohms, resulting in reduction of the effects of interfering waveforms. The sweep duration is 12  $\mu$ sec.

similar to the transient response of the detector, the carrier content is much less than that indicated previously for a steady signal, and response time is very small as indicated in Fig. 14-5. The first portion of the

<sup>1</sup> A discussion of the relative merits of various types of detectors in the presence of interference is given in RL Report No. 833 by R. S. Phillips.



envelope of the modulated wave is a transient with exponential decay, and the detector output shown in Fig. 14-5b has zero carrier content. On the other hand, there is appreciable carrier content in the response of this detector to the subsequent linear rise of the modulated wave and con-

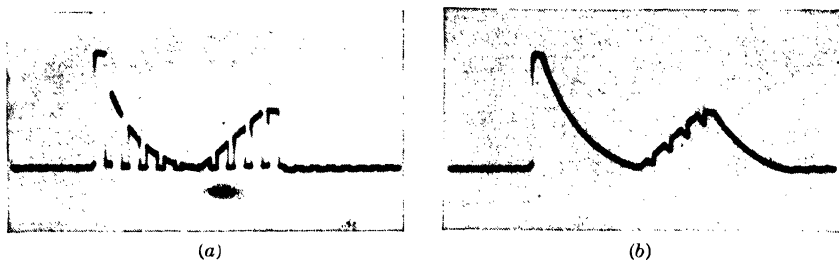


FIG. 14-5.—The response to an exponential decay in a peak detector with a resistance-capacitance output circuit. Fig. 14-5a shows an amplitude-modulated wave train in which the first portion represents an exponential decay. Fig. 14-5b shows that the carrier content of the output is zero for an appropriate value of the time constant. Response to the rise of the modulating signal and the sharp decay is, of course, extremely poor. These waveforms are displayed on a sweep of 1 2- $\mu$ sec duration.

siderable delay and distortion in its response to the rapid fall of the output.

The average current through the resistance-capacitance-coupling network may cause an error in precision detectors as indicated in Fig. 14-6. The potential of point A may be reduced by the product  $R_1 i_{av}$ , and

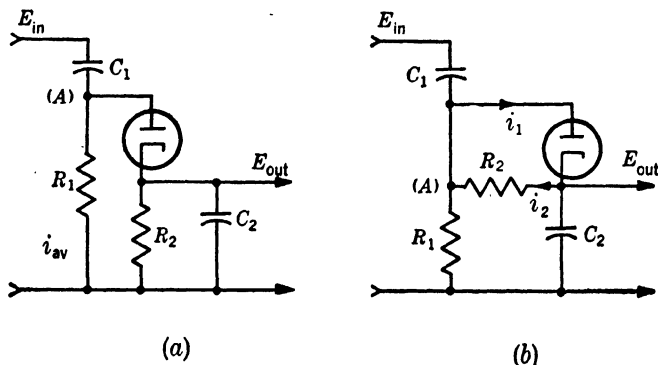


FIG. 14-6.—Precision peak detector with high input impedance. The error due to the average current through  $R_1$  in (a) adds a voltage  $R_1 i_{av}$ . This error is avoided by returning  $R_2$  to point A as indicated in (b) which maintains the average potential of A at zero.

this voltage will add to the input voltage and give an error in the measurement of the peak value of the input. Usually this difficulty is avoided by the use of a transformer-coupled input to the detector. But the use of a special circuit connection, shown in Fig. 14-6, will avoid this difficulty in resistance-capacitance-coupled circuits. The resistor of the output

time constant is connected to point *A* instead of to ground, as it usually is. The net current in  $R_1$  is then zero and the error is avoided.

A practical circuit for the detection of a slowly varying push-pull amplitude-modulated carrier is indicated in Fig. 14-7. Cathode followers  $V_1$  and  $V_2$  are employed to avoid loading of the modulated carrier, and the push-pull input is applied to the full-wave peak detector. The steady voltage due to the quiescent current of the cathode follower is removed by condenser  $C_1$ , which is much larger than  $C_2$ ; therefore, the peak voltage of the input signal appears across the latter. The charge of

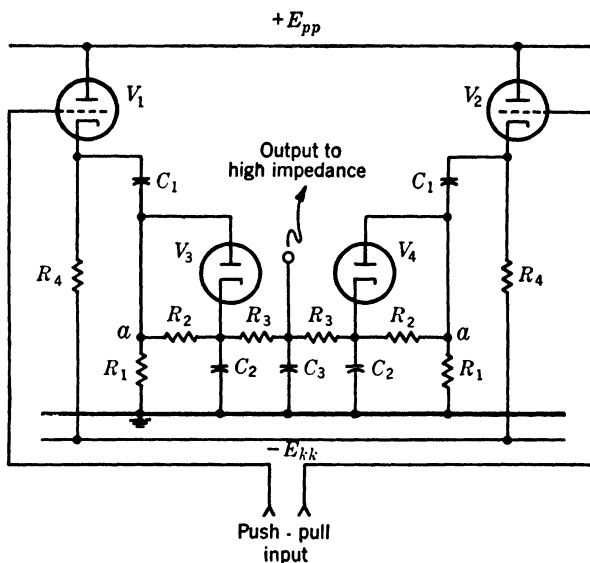


FIG. 14-7. —A push-pull detector employing the basic circuit of Fig. 14-6. For a carrier frequency of 500 cps the following component values are used:

$$\begin{aligned} R_1 &= R_3 = 1\text{M}, R_2 = 3\text{M}, R_4 = 0.1\text{M} \\ C_1 &= C_3 = 0.1\ \mu\text{f}, C_2 = 0.01\ \mu\text{f} \\ E_{pp} &= +300\text{ v}, E_{kk} = -100\text{ v} \end{aligned}$$

$C_2$  is shared with  $C_3$ , and  $C_3$  gives additional filtering at the output. The potential of point *a* is maintained at zero by the method indicated in the previous figure.

If the output is connected to a high-impedance circuit, for example, a cathode follower, the performance of this circuit is excellent, being linear over a range of 5 to 100 volts to an accuracy of  $\pm 0.1$  per cent. Operation of the diodes  $V_3$  and  $V_4$  at reduced cathode temperature is desirable to minimize the drift.

*The Cathode-follower Detector.*—A considerable increase in the charging current obtainable with a high-impedance signal is achieved through the use of a cathode follower instead of a diode, as shown in Fig. 14-8. A

typical cathode-follower circuit can charge a 200- $\mu\text{f}$  condenser in 1 or 2  $\mu\text{sec}$ , even though the impedance of the modulated carrier is relatively high.

As the circuit diagram indicates, the cathode potential of  $V_1$  is returned to a negative voltage. This connection applies equally well to the diode detectors described previously and gives a constant rate of decay of the output voltage independent of the amplitude of the input signal. Therefore, less difficulty is encountered because of high rates of decay at low signal amplitudes. Where accurate detection is required, the nonlinearity of this detector for small signal voltages may offset

the advantages obtained by impedance changing. It is but slightly more complicated to insert a diode between a linear cathode follower and the memory circuit to achieve more linear and stable detection as already shown in Fig. 14.7.

*A Constant-output Detector with Recycling.*—Although the use of a long-time-constant resistance-capacitance output circuit gives a constant output voltage approximately equal to the peak value of the input waveform, the response of the circuit to decreases of input amplitude is often inadequate and much information may be lost (see Fig. 14.3). A much more satisfactory solution to the problem completely replaces the exponential decay of the detector output by an abrupt and intentional reduction of the output voltage to

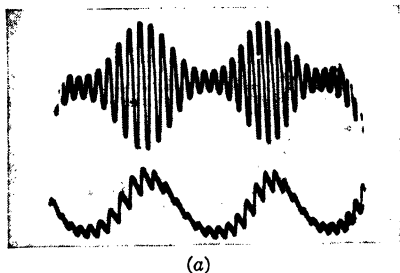


FIG. 14-8.— The cathode-follower detector: For the particular waveform shown,  $R_1 = 120 \text{ k}$ ,  $C_1 = .007 \text{ } \mu\text{f}$ . The carrier frequency is 7.6 kc/sec.

zero just before the next cycle of the carrier waveform is received. This circuit and those depending upon the bidirectional switches described in Sec. 14.5 are the most efficient types for pulse demodulation. They have a number of advantages which may be summarized as follows:

1. The detector output does not decay exponentially, but instead remains constant and thus permits a large increase in signal voltage; for pulse circuits this may approach the reciprocal of the duty ratio.
2. The carrier frequencies may be nearly eliminated from the output.
3. The output voltage is independent of the repetition frequency.

The generalized circuit, shown in Fig. 14-9, indicates cathode-follower detector  $V_1$  charging  $C_2$  up to peak value of the input signal. Since there is no intentional resistance shunted across  $C_2$ , it should maintain the peak value of the input signal with a time constant determined by the leakage of the capacitor and heater-cathode leakage of  $V_1$ . Just previous to the next recurrence of the pulse carrier, a positive recycling pulse (often called the "dunking" pulse) is applied to the control grid of  $V_2$  in such a way that the potential of  $C_2$  is reduced almost to zero. Immediately thereafter the next cycle of the input wave charges  $V_1$  to the new value of the modulating signal.

This circuit has several limitations in demodulating microsecond pulses. The impedance of  $V_1$  at zero bias is such that a condenser no

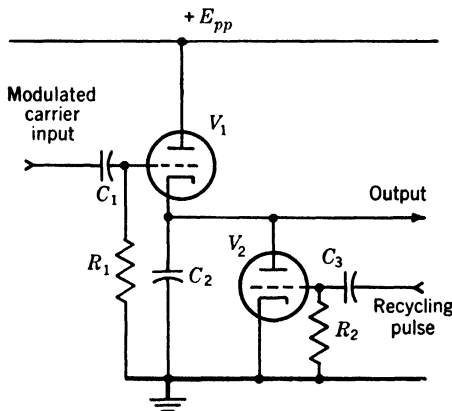


FIG. 14-9.—The basic circuit of recycling detector.

larger than  $500\ \mu\text{mf}$  can be charged in  $1\ \mu\text{sec}$ . With usual values of heater-cathode leakage, there may be as much as 5 per cent decay of the output voltage at pulse-recurrence frequencies of 500 cps. In addition, the hum due to the heater-cathode leakage of  $V_1$  may amount to 50 mv.

A considerable improvement upon this circuit and an example of a general principle in pulse-amplitude demodulation is illustrated by Fig. 14-10. Tube  $V_1$  is a cathode-follower detector with short-time-constant network  $R_2C_2$  which may be easily charged to the peak value of the input signal in  $0.3\ \mu\text{sec}$ . The time constant of this circuit is sufficient to sustain the peak value of the input wave for several microseconds and thus to permit cathode-follower detector  $V_2$  to charge a condenser as large as  $5000\ \mu\text{mf}$ . The performance of this circuit is correspondingly better since the decay of the output is less than 1 per cent at a pulse-recurrence frequency of 500 cps. Likewise the hum level is less than 10 mv.

The double-time-constant detection illustrated by this circuit is of

great value in pulse demodulation circuits. Its use in this connection is indicated by examples in Sec. 14-5.

The carrier content of a constant-output circuit of this type may be calculated on the assumption that the leakage resistance shunting  $C_3$  is negligible and that the interval  $\Delta T$  from the beginning of the recycling pulse to the beginning of the signal pulse is small compared with the carrier repetition interval  $T$ . The fractional value of carrier content is simply that of a pulse of duration  $\Delta T$  at the carrier frequency:  $2\Delta T/T$ .

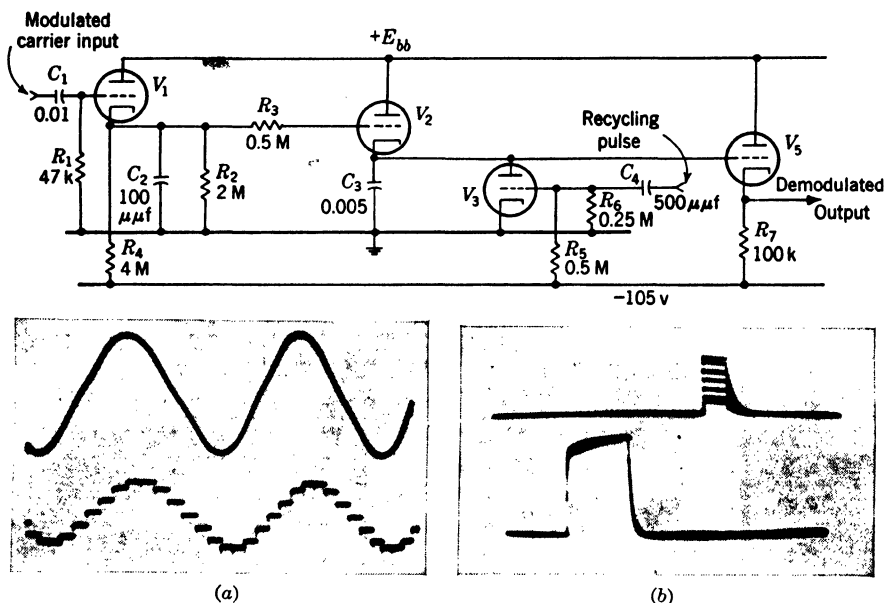


FIG. 14-10.—A double time-constant detector with recycling: The waveforms were obtained with the component values indicated on the circuit diagram. Figure 14-10a shows the sinusoidal modulating signal at the input to a modulator and at the output of the recycling detector. Figure 14-10b shows the recycling pulse on the lower line and the amplitude-modulated pulse on the upper line. The modulating frequency was 60 cps. The sweep duration of Fig. 14-10b is roughly  $12\text{ }\mu\text{sec}$ . The carrier repetition frequency is 800 cps.

The phase shift of the output of this detector in terms of the signal frequency is  $\omega_m T/2$ , where  $\omega_m$  is the signal frequency. In other words, the averaged output from a detector circuit of this type lags the signal voltage by one-half the carrier period.

In contrast with the operation of a detector circuit employing exponential decay, there is no preferred direction of operation for the constant-output detector, and the transient response is independent of the sense of the rate of change of the modulating signal.

The performance of this circuit, although much more satisfactory for pulse-amplitude demodulation than one using an exponential decay,

still has definite drawbacks, since the carrier content is directly proportional to the effective duration of the recycling pulse and is usually removed by additional filtering.

In comparison with some of the switch circuits described in Sec. 14.5, this circuit has two fundamental weaknesses. An appropriate timing of the recycling pulse requires a foreknowledge of the time of occurrence of the signal pulse. This may cause difficulty where the signal pulse is time-modulated over a large fraction of the repetition interval since the recycling pulse must be similarly modulated in order to avoid a serious variation of the interval  $\Delta t$  with consequent effects upon the carrier content. The more serious difficulty with this circuit is its lack of time selectivity; even though a pulse must be applied to the circuit for recycling, no benefits of time selectivity are obtained as in the switch circuits. Since the recycling detector requires as many components as these switch circuits, there is little to recommend its use in place of a switch circuit.

**14.4. Phase-sensitive Detectors.**—This class of detector circuits is used to demodulate waveforms obtained from the bidirectional modulators of Chaps. 11 and 12. Phase selectivity may be obtained by direct

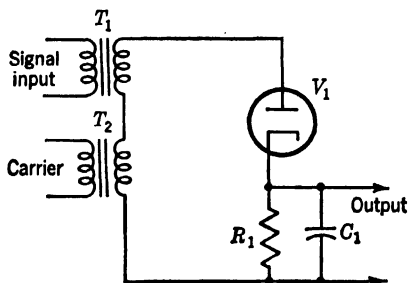


FIG. 14.11.—Unbalanced phase-sensitive detector employing addition of signal and carrier.

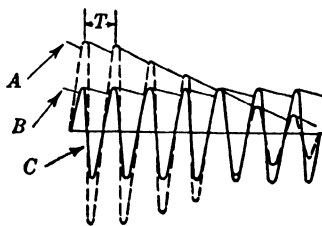
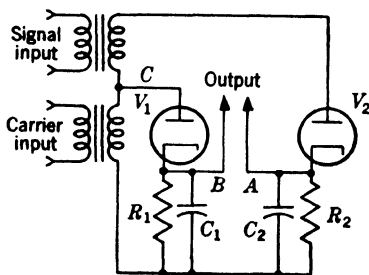


FIG. 14.12.—Unbalanced phase-sensitive detector employing additional diode to give a bidirectional output: The waveform diagram indicates the output at points A and B, and the carrier at C.

addition of modulated carrier and unmodulated carrier followed by amplitude selection (see Fig. 10.1). In general, the circuits to be described are employed only with sinusoidal carriers, and the switch detectors discussed in Sec. 14.5 are suitable for use with rectangular carrier waveforms. Like the circuits of amplitude modulators, these

circuits may be balanced or unbalanced, depending upon whether a push-pull input is employed.

Figures 14.11 and 14.12 illustrate two forms of phase detectors depending upon the addition of the modulated and unmodulated carrier followed

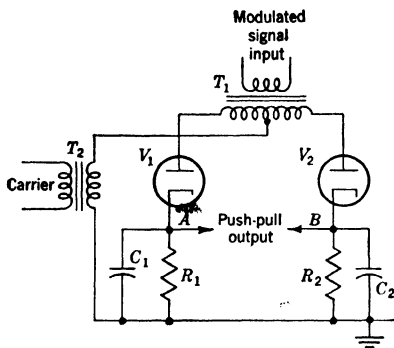


FIG. 14.13.—Carrier-balanced half-wave phase-sensitive detector: The single-ended carrier and push-pull signal are added to give push-pull output between A and B.

by amplitude selection. Figure 14.12 shows a subsidiary diode rectifying the carrier in order to obtain a differential output which is balanced with respect to variations of carrier amplitude. The circuit is not, however, a balanced demodulator.

*Carrier-balanced Half-wave Phase-sensitive Demodulator.*—The circuit of Fig. 14.13 is identical in operation to the carrier-balanced half-wave modulator of Chap. 11, Fig. 11.2. A single-ended carrier is added to a push-pull input signal

and the sum is applied to the plates of  $V_1$  and  $V_2$ . The addition of these two voltages causes amplitude selection in  $V_1$  and  $V_2$  on alternate half cycles of the carrier wave, provided, of course, that the carrier waveform is large compared with the input signal. The sign of the output voltage reverses with the sign of the modulating signal.

Stability considerations are rarely as important in detector circuits as they are in low-level modulator circuits since the amplification at the carrier frequency may be made sufficient to give sizable output voltages. Therefore detectors employing double triodes are much more popular.

Figure 14.14 shows an example of a carrier and input signal added in a transformer and applied to the grids of a push-pull amplifier having resistance-capacitance networks  $R_1C_1$  and  $R_2C_2$  in the plate circuits. As is usual for proper amplitude selection, the carrier is made large compared with the input signal which is limited to the grid base of  $V_1$  and  $V_2$ . Bias is obtained from  $R_3C_3$ .

In the demodulation of signals from systems in which no steady volt-

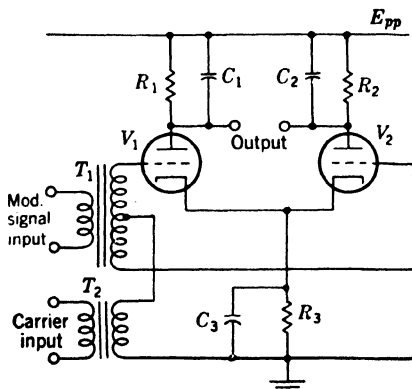


FIG. 14.14.—Balanced triode demodulator employing transformer addition of signal and carrier.

age for plate supply may be available, such as synchros, it is possible to use the carrier for this purpose—for example, as shown in the phase-sensitive demodulator of Fig. 14-15. A single-ended carrier is applied to the plates of  $V_1$  and  $V_2$ , and the push-pull signal input is applied to the grids. The output may be taken differentially between the cathodes. Bias is provided by  $R_3C_3$ .

*Carrier-balanced Full-wave Phase-sensitive Demodulators.*—A full-wave circuit which accepts as input a push-pull modulated signal and gives push-pull output is indicated in Fig. 14-16. Its operation is similar to the full-wave balanced modulator described in Fig. 11-16.

#### 14-5. Demodulators Employing Switching.

*Time selectivity* in detector circuits is obtained from a carrier-operated switch. There are a number of advantages of operation of this type. The rejection of unwanted interference is accomplished, and this is of special importance

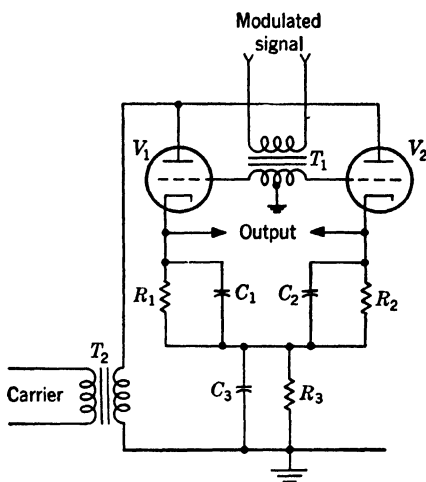


FIG. 14-15.—Balanced triode demodulator in which a single-ended carrier is applied to the plates and a push-pull signal is applied to the grids.

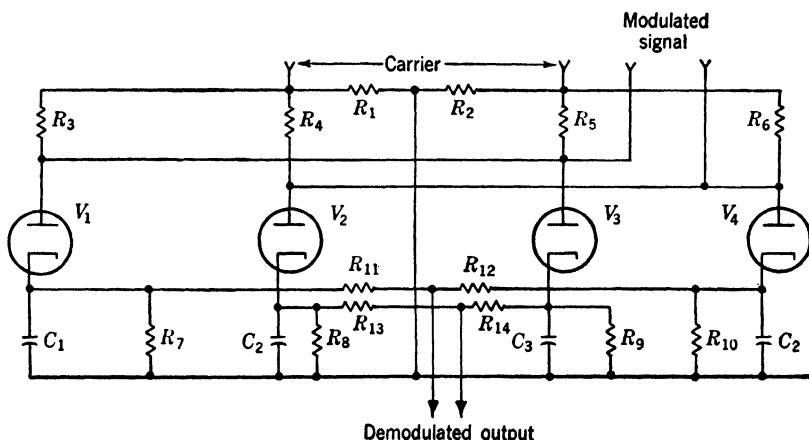


FIG. 14-16.—Carrier-balanced full-wave diode detector.

in demodulating an amplitude-modulated pulse train where the spacing between the desired pulses is large compared with the carrier-repetition interval. The most important advantage of the two-way switch detector



is the possibility of employing a constant-output circuit—a subject discussed in the next section.

Switch detectors are also time- or phase-sensitive since the output may represent the overlap of signal and selector pulse. In Fig. 14-17 the time of occurrence of the input signal shown on the first line is modulated



FIG. 14-17.—The use of time selection for conversion of a time-modulated pulse indicated on the first line, to a duration-modulation pulse indicated on the third line, by a selector pulse indicated on the second line.

with respect to the selector pulse shown on the second line, and the selected output is shown on the third line. The maximum range of input modulation that can be linearly demodulated is limited to the duration of the signal pulse. Demodulation of this signal requires a detector time constant long enough to give average, instead of peak, detection. Methods for converting various wave trains into pulses of variable amplitude are given in Sec. 14-7.

*Half-wave Unidirectional Switch.*—Figure 14-18 shows a simple circuit based on the half-wave diode switch discussed in Sec. 10-3. In this case the positive excursions of the carrier connect the modulated input to the resistance-capacitance network  $R_1C_1$ , and the capacitance charges up to the peak value of the input signal. During the interval between positive excursions of the carrier waveform, the output decays exponentially. The circuit is, therefore, similar to the half-wave diode except that time selectivity is obtained. The circuit is phase-sensitive to unidirectional modulated signals but the output does not pass through zero.

This switching technique applied to the ordinary differential amplifier makes an excellent phase-sensitive differential detector as shown in Fig. 14-19. Positive values of the carrier raise the cathode above the maximum excursion of the grid potential and cause complete cutoff in both  $V_2$  and  $V_3$ . Negative excursions of the carrier wave leave the differential amplifier operating under the ordinary conditions, and a potential is accumulated upon  $C_1$  and  $C_2$ . The output is taken differentially between

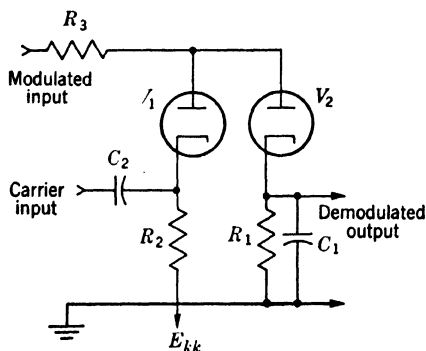


FIG. 14-18.—Half-wave unidirectional switch detector.

the two condensers and represents phase-sensitive demodulation, the polarity of which reverses with the sign of the modulating signal. This detector is useful in servomechanisms where the modulated signal from

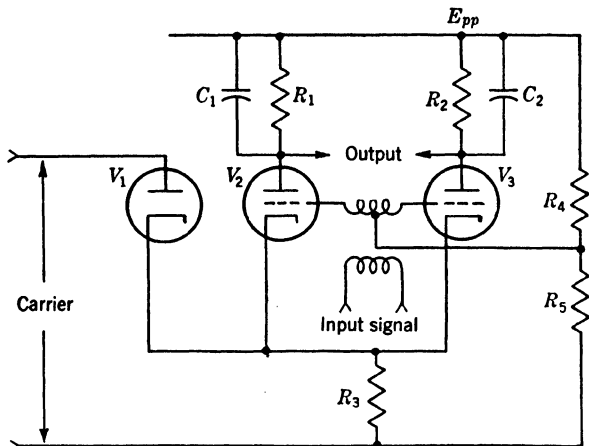


FIG. 14.19.—Phase-sensitive detector employing diode switch  $V_1$ .

synchros and other devices is available, and detection at relatively high level is possible. Another advantage of this circuit is, of course, that some gain is obtained in the phase detector.

A cathode follower<sup>1</sup> may be used in place of the diode, as shown in

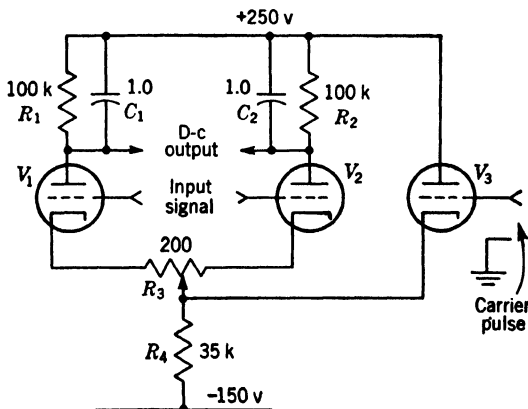


FIG. 14.20.—Phase-sensitive detector employing cathode-follower switch  $V_1$ . The signal is balanced with respect to ground.

the circuit of Fig. 14.20, and the following performance is obtained for the component values shown. In the demodulation of a 400-cycle carrier,

<sup>1</sup> H. S. Sach, A. A. Oliner, "An AC-voltage Equalizer and Phase Detector," NDRC 14-513, Cornell University.

the gain is approximately 35 (in terms of rms input and d-c output), and the operation is independent of amplitude of the carrier wave in excess of that required to cut off  $V_1$  and  $V_2$  by conduction of  $V_3$ —roughly 12 volts rms. For a limited number of type 6SJ7, the reported effect of tube change and the drift of an average tube is 20 mv, and the reported effect of a 10 per cent heater-voltage variation is 3 mv, each voltage expressed in terms of equivalent shift in rms potential at the grids. Results approaching these may be obtained for a larger number of tubes by employing type 6SU7 (see Sec. 3-17).

Higher gain may be obtained by the circuit of Fig. 14-21 in which the carrier voltage is connected to the suppressor grid of a pentode or multi-grid switch.<sup>1</sup> The gain is approximately 70 for type 6SJ7, 120 for type

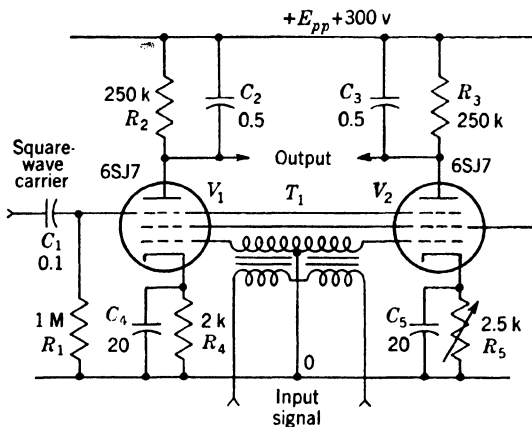


FIG. 14-21.—Phase-sensitive detector employing suppressor control of pentode switches  $V_1$  and  $V_2$ .

6AS6. An advantage of type 6AS6 is that a 10- or 15-volt carrier is sufficient, whereas a 40-volt carrier is required for type 6SJ7. Thus the pentode detector has roughly 4 times the gain of the double-triode circuit and requires no larger carrier signal. The reported stability is roughly the same as that of the double triode if type 6SJ7 is used.

A pentode-switch detector circuit is shown in Fig. 14-22. This circuit is often called a "strobed diode." In the absence of a positive carrier pulse there is no conduction of the pentode and, hence, no detection. A positive carrier pulse causes conduction of  $V_1$ , and the bottoming of the plate causes  $C_1$  to be charged to the peak value of the input as the waveform diagrams indicate. The charge from  $C_1$  leaks through  $R_1$  and  $C_2$ , and after several cycles brings the latter to a potential proportional to the peak value of the carrier. Excessive discharge of  $C_2$  during conduc-

<sup>1</sup> H. S. Sach *et al.*, "Magnetic Amplifier," NDRC 14-437, Cornell University.

tion of  $V_1$  is prevented by  $R_2$ . This circuit is much more often used as an average detector by inserting a resistance in series with  $C_1$ .

Time selection and peak detection may be accomplished separately as indicated in Fig. 14-23. Tube  $V_1$  is a multigrid time selector, for example,

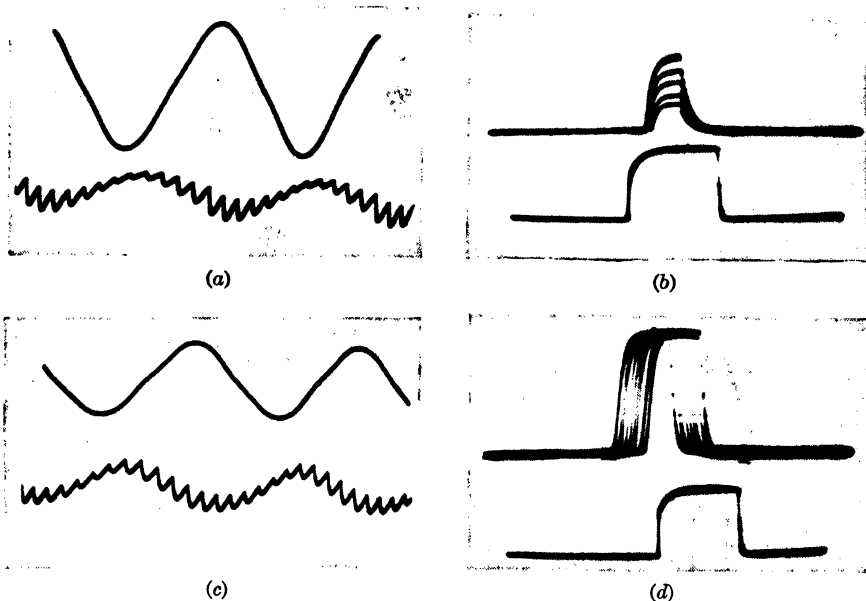
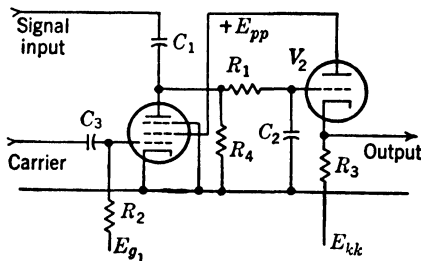


FIG. 14-22.—Pentode-switch detector (strobed diode). Amplitude demodulation is indicated in (a) and (b). The sinusoidal modulating signal is indicated on the upper line of (a) and the output of the detector on the lower line. The amplitude-modulated pulse is indicated on the upper line of (b) and the selector pulse on the lower line. Time demodulation is indicated in (c) and (d). On the upper line of (c) is shown the sinusoidal modulating signal and on the lower line the demodulated output. On the upper line of (d) is shown the time-modulated signal and on the lower line the selector pulse.

type 6SA7, and  $V_2$  is a diode detector with an extremely high-impedance time constant in order to give satisfactory operation with short pulses at low duty ratios.<sup>1</sup> The separate diode detector has several advantages, the most important being that the lack of cutoff of  $V_1$  will not cause

<sup>1</sup> A complete report on this circuit is available: J. Kurshan and B. Rossi, "Analysis of the 6SA7 Gated Amplifier," NDRC 14-158, Cornell University.

discharge of the output condenser  $C_2$ . Another advantage is that the d-c level of the output may be set at any value desired by breaking the circuit at point  $b$  and inserting an arbitrary voltage suitably bypassed to

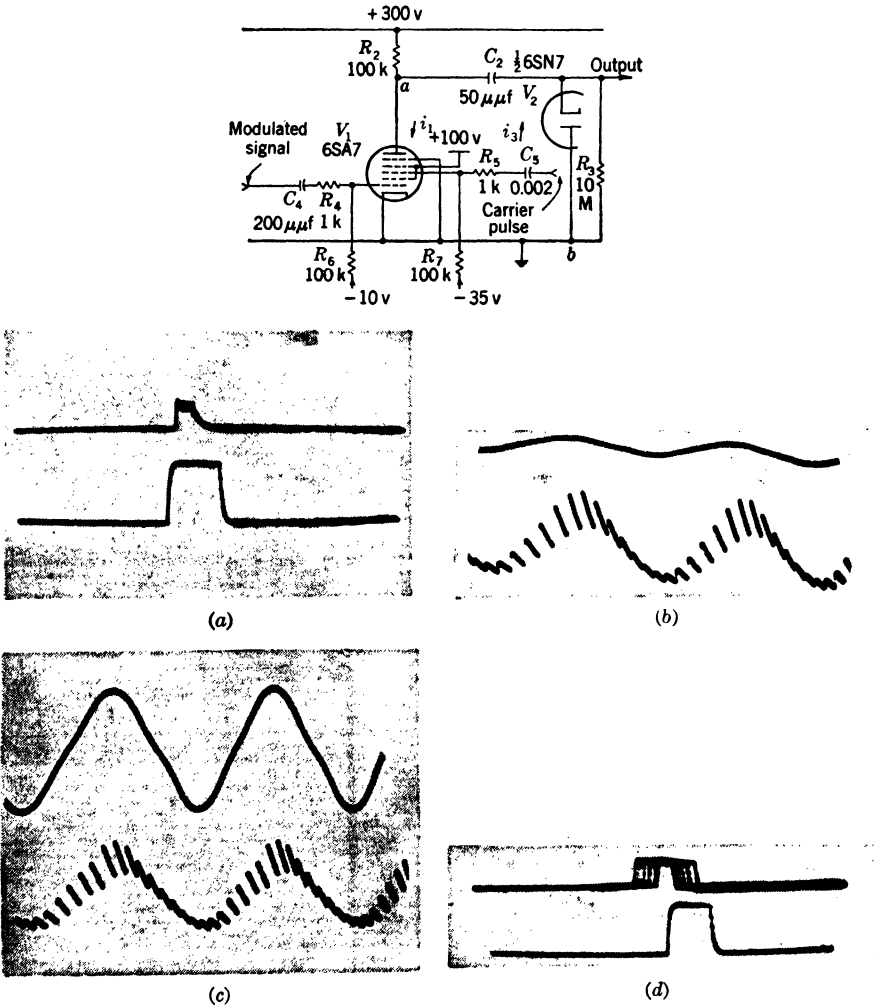
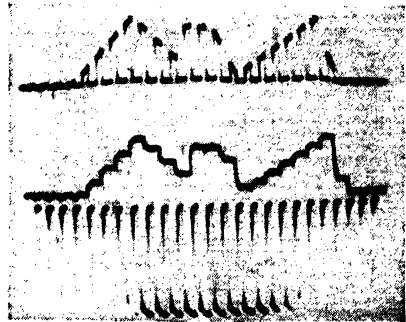
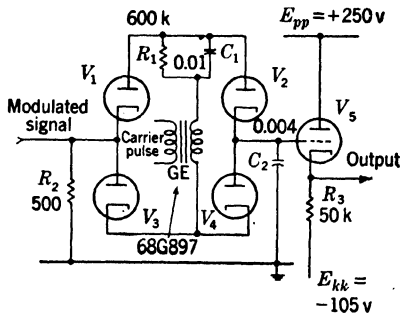


FIG. 14-23.—A multigrid-tube time selector and diode detector. This circuit is also suitable for detecting the area of overlap of time modulated and selector pulses. The waveforms in (a) show the amplitude-modulated pulse on the top line, and the selector pulse on the bottom line; in (b) are shown the modulating and output waveforms. In (c) and (d) are shown similar waveforms for time modulation.

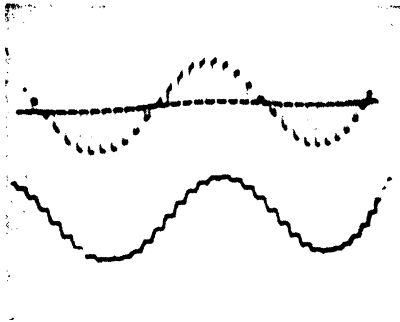
ground. Also, either sense of output voltage is obtained by a shunt or series diode connection. For the component values indicated, the operation of the circuit is relatively independent of the impedance of  $V_1$  and  $V_2$  and gives relatively stable operation in spite of tube changes.

The sensitivity, however, depends upon the pentode characteristics. Furthermore, the requirements of this circuit for low heater-cathode leakage in  $V_2$  may be difficult to meet for a large number of tubes.

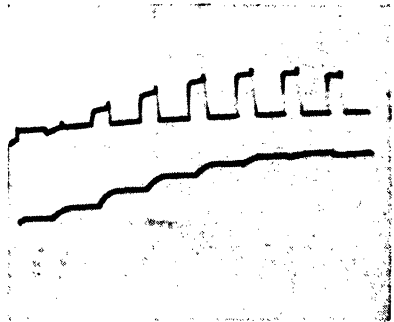
*Half-wave Bidirectional Switch.*—The two-way-switch circuits of Sec. 10-3 permit a radical departure in detector operation that gives



(a)



(b)



(c)

FIG. 14-24.—Four-diode bidirectional-switch demodulator: The waveforms were taken with the component values indicated in the circuit diagram.  $V_1 - V_4$  6SN7. The waveforms are displayed on a 1.2-msec sweep. Figure 14-24a shows, on the top line, an irregular modulating signal applied to a 40 kc/sec carrier. The second line shows the detector output and the third line shows the switching waveform: its positive excursions close the switch. Figures 14-24b and 14-24c show the response of the detector to a sinusoidally modulated signal obtained by bidirectional modulation. The modulated signal is shown on the top line of Fig. 14-24b, and the bottom line shows the detector output. Figure 14-24c shows, on the top line, the modulated carrier and on the bottom line the detector output on a 120- $\mu$ sec sweep.

nearly complete elimination of the carrier content of a slowly varying signal and an extremely good transient response.

When a bidirectional switch is employed, the memory circuit will be connected to the input at the time of the pulses of the carrier waveform and will therefore be made to respond not only to the increase of the signal amplitude as the one-way detector circuits do, but also to the decrease of the signal amplitude. The only limitation of the time

constant of the memory circuit is, therefore, the ability of the switch to make the output circuit respond to the signal voltage during the carrier pulse. When, for example, the excellent four-diode bidirectional-switch circuit shown in Fig. 14-24 is used, unique operation in demodulation is obtained, as the waveform diagrams indicate. Fig. 14-24a shows the response of this detector circuit to a modulating signal that is varying rapidly compared with the carrier frequency. The switch connects the input to the memory circuit in synchronism with the carrier pulses. The output waveform clearly indicates that the response of the circuit is equally good for increases and decreases of the signal intensity. Furthermore, it shows that the output voltage remains nearly constant in the interval between positive cycles of the carrier waveform. The 200- or 300-ohm impedance of the diode bridge is sufficiently low to charge the

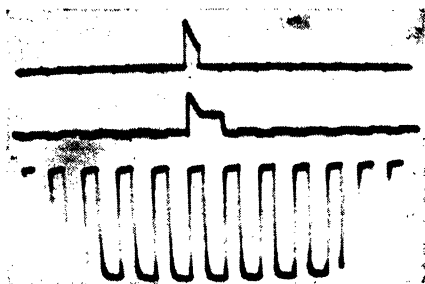


FIG. 14-25.—The response of a bidirectional switch with constant output to variations of the modulated signal occurring during the carrier pulse. The top line shows such a modulating signal, the next line the output of a bidirectional detector, the third the carrier pulse. The sweep duration is 12  $\mu$ sec.

output condenser adequately during a fraction of the conducting time of the switch (25  $\mu$ sec). The charge accumulated on the network  $R_1C_1$  holds the switch open in the absence of a carrier voltage. The bias accumulated on this network must, of course, exceed the excursions of the output voltage; otherwise, conduction of the switch in the absence of a carrier pulse will result in nonlinear operation.

The response of this circuit to a modulated wave train obtained from bidirectional modulation is

shown in Fig. 14-24b. The nearly complete absence of carrier voltage in the output is shown. The operation of the demodulator at phase reversal of the input wave is shown on an expanded sweep in Fig. 14-24c.

When a rectangular carrier waveform and a conduction interval for the switch less than the duration of the carrier pulse are used, the carrier content of the output is negligible for a slowly varying signal. If, however, a sinusoidal carrier is used and the conduction interval of the switch includes an appreciable portion of the curvature of the sinusoid, the fractional value of carrier content is approximately  $\frac{2}{3\pi^2} (\Delta T/T)^2$  for small values of  $\Delta T/T$ , which is small compared with that of the constant-output circuit employing recycling (see Sec. 14-3). But the phase shift of the output in degrees of the signal frequency is the same:  $(\omega_m T)/2$ . The two-way detector gives rapid response to the changes of signal

voltage, but does not overload in the presence of noise and interference. Although the output may be charged to a large value by a single noise pulse, it will immediately recover on the next cycle of the carrier wave.

An interesting feature of the two-way detector is indicated by the waveform diagram of Fig. 14-25 which shows an expanded view of the response of the detector to a single carrier pulse. The detector output shown in the second line clearly indicates the response to the decay of the amplitude of a single pulse, and then the output remains constant until the next carrier pulse. This constancy of output is of considerable value in the demodulation of intermittent data in which the wave shape is significant and the signal-to-noise ratio is high.

The ideal detector would, of course, maintain the rate of change of the signal voltage during the interval between carrier pulses. This operation is not readily obtainable in electric circuits, although operation of this type has been approached in some types of automatic time-measuring devices (see Chaps. 8 and 9, Vol. 20 of the Series). The characteristic may, however, be readily and simply obtained by manual demodulation methods employing aided tracking on a much slower time scale. These are briefly mentioned in Sec. 14-8 and are discussed in more detail in Vol. 20, Sec. 7-15.

Demodulation with constant output may be obtained with any bidirectional switch. Although the four-diode switch shown in Fig. 14-24 is best suited for the demodulation of rapidly varying inputs, the four-diode switch previously discussed as the "Diamod" (Sec. 11-3) is also satisfactory for demodulation of this type and is known to be relatively stable. This circuit is shown in Fig. 14-26 as a series switch with square-wave carrier and is nearly identical to that used in amplitude modulation. A shunt connection of this switch is preferred for operation with a pulse carrier.

The simple two-diode switch and the double-triode switch (see Secs. 10-3 and 11-3) may also be used for demodulation of this type, and special configurations are applicable depending upon the particular requirements. It may be mentioned that the double-triode switch with both grids con-

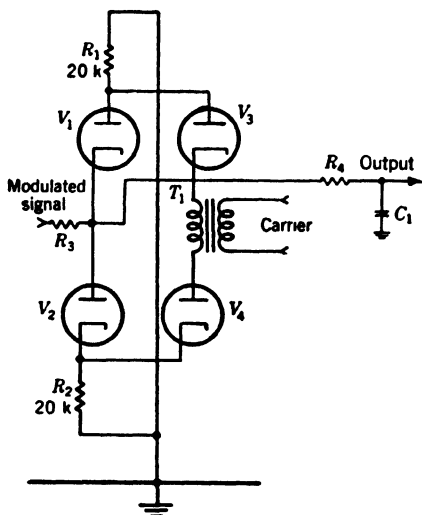


FIG. 14-26.—The two-way diode-switch detector. (Averaging type.)



nected to a negative bias is a simpler circuit and may be useful in some instances.

For the demodulation of short pulses recurring in a long interval, for example, half-microsecond pulses occurring every 3000  $\mu\text{sec}$ , it is often desirable to employ the same principles of double-time-constant detection that were mentioned in Sec. 14-3. The same circuit as that shown in Fig. 14-10 is recommended except that the output of the cathode follower  $V_2$  should drive a two- or preferably a four-diode-switch circuit and the output circuits of Fig. 14-24. This circuit results in an extremely efficient detection system and is considered definitely superior to that of Fig. 14-10 because of the lower carrier content of the output. In a particular case, response to the full value of the input signal is obtained

in less than a microsecond, and the output can be made to remain constant for several milliseconds.

The constancy of output is, however, limited by heater-cathode and capacitor leakage. This difficulty may easily be avoided by a combination of several switch detectors, each having progressively longer time constants and switching pulses. In this way the output may be maintained constant until the reception of the next signal pulse.

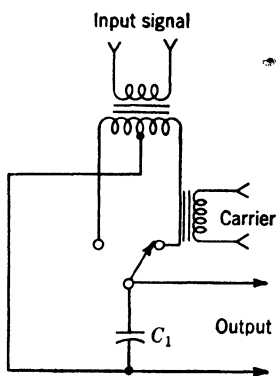


FIG. 14-27.—A full-wave bidirectional-switch demodulator employing a mechanical switch.

*Full-wave Bidirectional-switch Demodulator.* The mechanical switches described in Sec. 11-3 may be employed as a phase-sensitive demodulator for symmetrical square waves by using the circuit connection shown in Fig. 14-27.

For one phase of the signal input, the output condenser is connected to one terminal, and vice versa. The phase of the closure of the contacts must, of course, be adjusted accurately to correspond to the phase used in the modulation; the duration of the closure, however, must be shorter than that used in modulation. Unfortunately, the precision mechanical-switch modulators are unsuitable for output currents in excess of a few milliamperes. The Western Electric mercury relay<sup>1</sup> and numerous mechanical vibrators made for power-supply service are more suitable. The former has a high-impedance driving coil and can give peak output currents of several amperes provided proper contact protection is employed. It has, however, one difficulty: the center arm connects to both contacts on passing from one side to the other. Therefore, full advantage of the low impedance of the switch may not be taken, and

<sup>1</sup> The type number of this relay is D168479, and it is manufactured by the Western Electric Co. It has a frequency limit of roughly 100 cps.

a small resistor should be inserted in series with  $C_1$  to avoid discharge of the output voltage.

The circuit of Fig. 14-28 represents a combination of two of the half-wave switches of Fig. 14-26 that gives a thermionic-switch demodulator operating as the mechanical switch of Fig. 14-27.

A simplified circuit of fewer components is indicated in Fig. 14-29. Although the output impedance is considerably increased, satisfactory operation is obtained if the restrictions noted in the figure legend are observed.

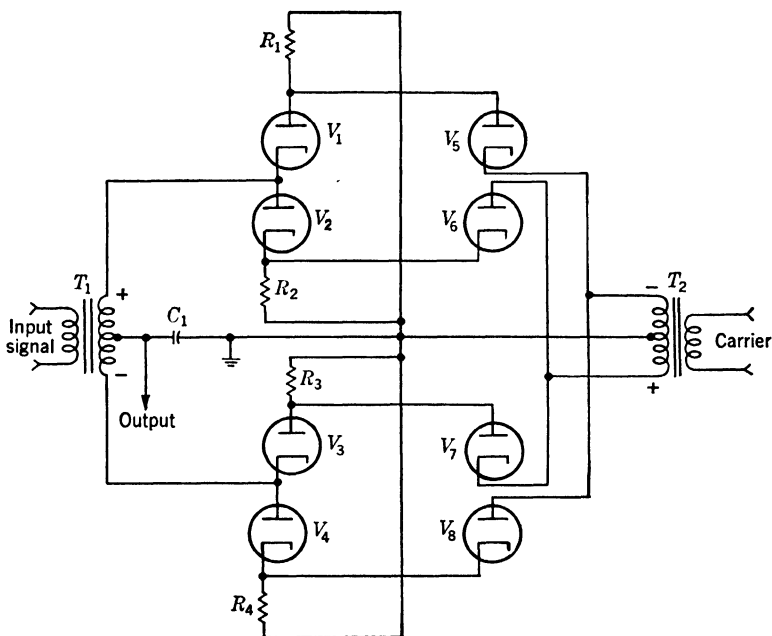


FIG. 14-28.—A full-wave bidirectional-switch demodulator using diodes. The circuit is composed of two elements of the circuit of Fig. 14-26.

*Summary.*—If the carrier frequency is large compared with the signal frequency and if the carrier wave is sinusoidal and free from interference, the simple peak detector is extremely useful. But in systems where phase-sensitive demodulation is required and where the duty ratio of the carrier is low, the two-way-switch demodulator gives phase sensitivity, rapid response, and minimal carrier content. The recycling detector, suitable only for pulse demodulation, has a larger carrier content than the bidirectional-switch detector and requires nearly the same number of components.

Multistage switch detectors involving time constants and selector pulses of progressively increasing duration are of extreme importance in

the demodulation of short pulses of low duty ratios. Peak detection is most efficient and can be employed where the input signals are free from interference. However, in peak detection the potential stored in the output circuit represents the last portion of the received signal pulse, and in cases where interference is heavy, a fictitious result may be obtained. This difficulty is avoided by area detection which is easily obtained by adding an appropriate resistance in series with the storage condenser. Thus the response time is made greater than the duration of the received pulse but less than the interval between pulses. This area detector

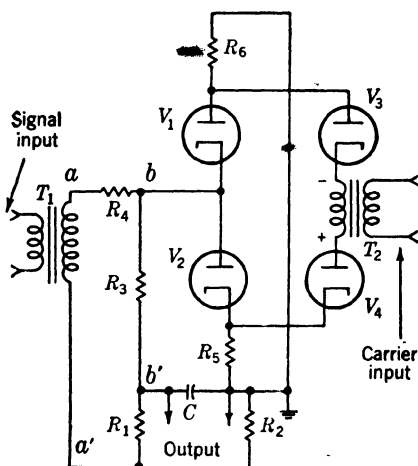


FIG. 14-29.—Full-wave bipolar-switch demodulator: This represents a simplification of the circuit of Fig. 14-28. Provided  $R_2 \gg R_6 = R_8$  and  $R_3 + R_1 \gg R_2 \gg R_4$  and  $R_3 = R_1$ , the output voltage will approach one-half the peak value of the input.

may then be followed by peak detectors, preferably of the bidirectional switch type. This combination would appear to give optimal efficiency and freedom from the effects of interference.

**14-6. Difference Detectors with Constant Output.**—Constant output detection in response to the difference of the areas of two pulses is sometimes required for time discrimination (see Sec. 14-7). In negative-feedback time-demodulator systems the output voltage from the difference detector must remain constant in the absence of signal and, in spite of large amounts of interference, proper operation must be resumed as soon as the signal reappears.

In the following discussion it will

be assumed that the input to the difference detector is obtained from adjacent time selectors (Sec. 10-5).

The requirements for constancy of output vary greatly depending upon the application and the type of negative-feedback time-demodulation system. For example, if single or double integration (see Sec. 18-7 and Vol. 20, Sec. 8-6) is performed before controlling the time demodulator, a difference detector of exponential decay may be satisfactorily employed, for example, as shown in Fig. 14-30. Transformer coupling of the peak-detected and stretched output of a pair of time selectors gives pulses of opposite sign which are area-detected in  $V_1$  and  $V_2$ , and potentials of opposite sign are obtained at  $A$  and  $B$ . Resistance addition in equal resistors  $R_1$  and  $R_2$  gives the desired potential difference. The output, however, decays exponentially in the absence of signal.

Detection with constant output may be obtained with the circuit of Fig. 14-31. Pulse transformer  $T_1$  inverts  $P_1$  and causes conduction of  $V_1$ , a process which results in an increase of the potential of  $C_3$  proportional to the area of  $P_1$ . The potential accumulated upon  $C_3$  as a result of this pulse maintains  $V_1$  nonconducting at the termination of  $P_1$ , yet

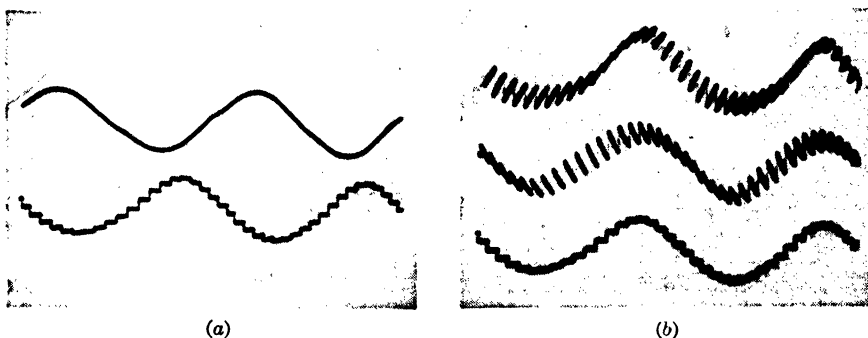
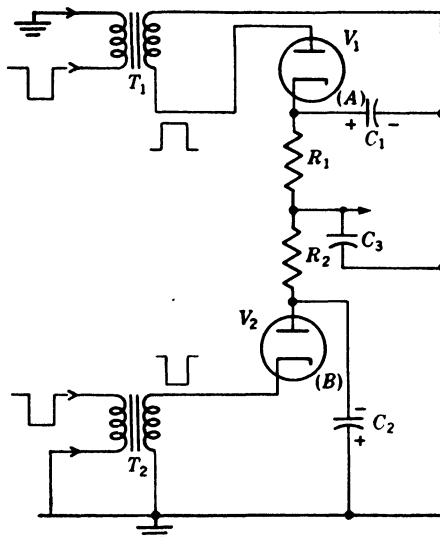


FIG. 14-30.—Difference detector consisting of two area detectors with exponential decay. The waveforms shown in Fig. 14-30a represent the response to the output of a pair of time selectors operating on a time-modulated pulse. The top line shows the input modulation to a time modulator; the bottom line shows the output of the difference detector. The top two waveforms of Fig. 14-30b indicate the separate outputs of the detectors, and the bottom line, the difference of their outputs.

this potential must not be large enough to cause conduction of  $V_2$ . Negative pulse  $P_2$  is applied to the cathode of  $V_2$ , and a decrease of the potential of  $C_3$  proportional to the area of  $P_2$  is obtained. If, for example, the area of  $P_1$  is slightly larger than that of  $P_2$ , the condenser  $C_3$  will be left with a net positive charge and, because of the bias between the plate

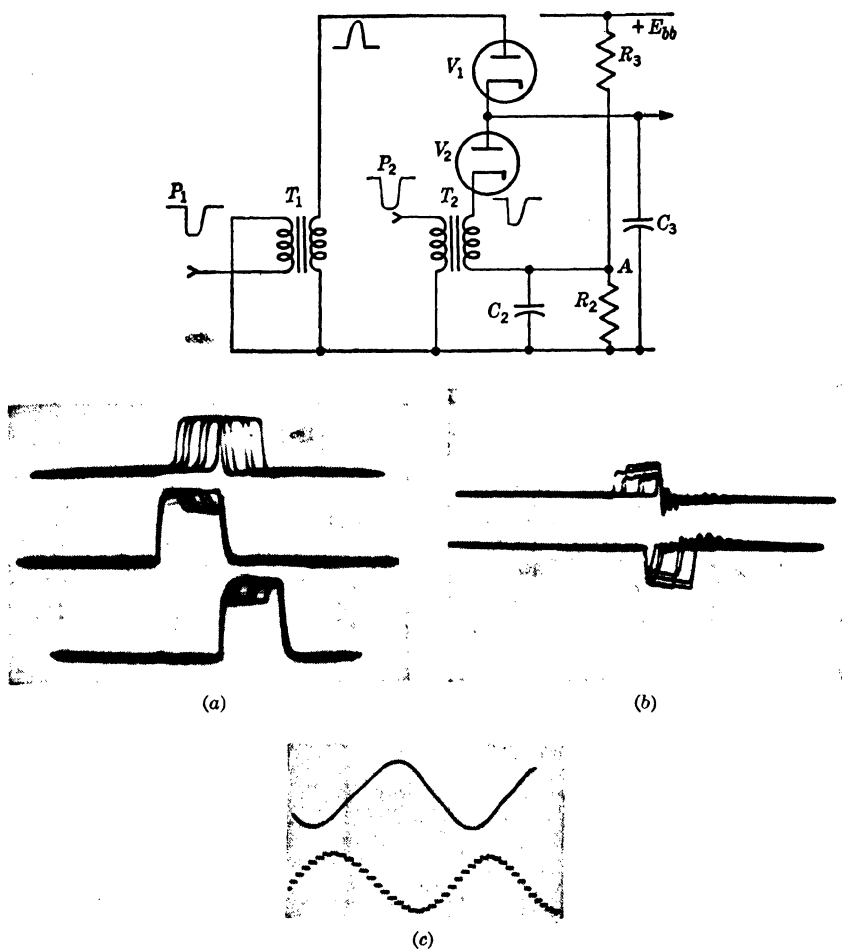


FIG. 14-31.—Difference detector with constant output. Figure 14-31a indicates on the top line the time-modulated pulse and on the second and third lines the selector pulses. The amplitude modulation of the selector pulses is due to loading in the time selector. Figure 14-31b indicates on the top line the output of each time selector applied to the difference detector by  $T_1$  and  $T_2$ . These pulses are modulated in both duration and amplitude. Figure 14-31c indicates on the top line the sinusoidal signal which was applied to the time modulator and on the lower line the output of the time demodulator. In the actual circuit  $T_1$  and  $T_2$  approximated current transformers making possible the large output voltage shown. The sustaining condenser is therefore charged with constant increments of current, independent of output voltage.

of  $V_1$  and the cathode of  $V_2$ , a constant output will be maintained until the next pair of input pulses.

The circuit has, therefore, characteristics similar to those of the two-way-switch circuits of the previous section. But there are several important differences. In the first place, the circuit must be an average

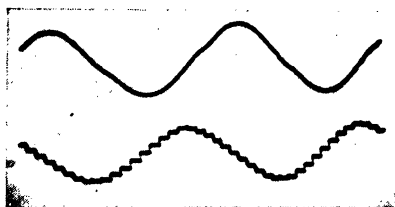
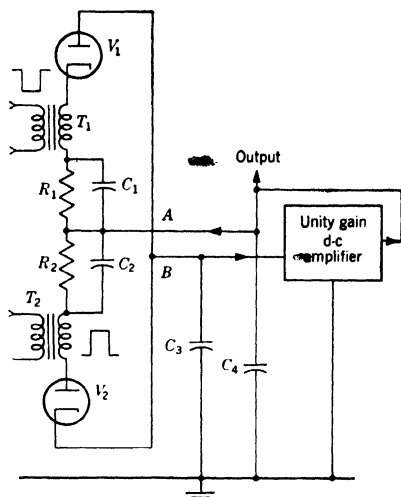
detector since the second pulse would completely discharge the output condenser if peak detection were employed. Average detection is easily obtained by the use of a large condenser or by adding a resistance in series with the condenser. Second, the circuit must have a certain "dead" space or threshold which the input must exceed; in the circuit of Fig. 14-31 this is on the average equal to one-half the potential of the point  $A$ . In other words, the signal amplitude required to cause conduction of  $V_1$  or  $V_2$  depends upon the potential of  $C_3$ . Third, the circuit exhibits two-way operation only so long as neither  $P_1$  or  $P_2$  is zero; if either becomes zero, the circuit will no longer be responsive to a decrease in the amplitude of the larger pulse.

In practical circuits it is often required that the potential of  $C_3$  be maintained even though  $P_1$  and  $P_2$  represent equal amounts of noise or pedestal such as may be obtained from adjacent time selectors. The circuit of Fig. 14-31 would not give constant output under these conditions since pulses of equal areas will cause the output potential to return rapidly to approximately one-half that of the potential of the point  $A$ .

The dead space in the operation of this circuit may be completely eliminated if  $T_1$  and  $T_2$  are used as current transformers by supplying them from high-impedance sources (pentodes). The same amount of charge will be delivered to  $C_3$  for pulses of equal areas regardless of small variations of the potential of  $C_3$  and of the potential of the point  $a$ . Another advantage of current-transformer feed is that the potential of  $C_3$  will be maintained constant in the presence of equal amounts of noise or pedestal in contrast to the operation obtained with voltage feed. A third advantage of this circuit is the fact that unbalance in the diodes has little effect upon the circuit operation. It is usually desirable to connect the output of this circuit to a Miller integrator (see Sec. 18-7) in which case the diodes are reversed and the potential  $E_{pp}$  is made negative.

An alternative arrangement is indicated in Fig. 14-32. The basic differential detector circuit is identical to that shown in Fig. 14-31 since it contains diodes  $V_1$  and  $V_2$  which are actuated by negative and positive pulses from transformers  $T_1$  and  $T_2$  respectively. Conduction of  $V_1$ , initiated by a negative pulse on its cathode, will cause a decrease in potential of  $C_3$ . But at the same time bias is developed across  $R_1C_1$  which will serve to maintain  $V_1$  nonconducting in the absence of a pulse. The conduction of  $V_2$  gives similar effects except that the potential of  $C_3$  is raised. The resistance-capacitance networks  $R_1C_1$  and  $R_2C_2$  provide bias and thus take the place of the fixed potential  $A$  of Fig. 14-31, and the potential of the whole difference-detector circuit may be adjusted with respect to the potential of  $C_3$  by variation of point  $A$  of Fig. 14-32. If the potential of point  $A$  is maintained equal to that of  $B$  by a unity-gain

direct-coupled amplifier, then a variation of the potential of  $C_3$  will have no effect upon the characteristics of the difference detector. Thus the output range of point  $a$  is theoretically as great as the linear range of the d-c amplifier. As a consequence, the operation of  $V_1$  and  $V_2$  in the presence of noise pulses or pedestal of equal amplitudes should be substantially independent of the potential of the condenser and dependent only upon the balance between  $V_1$  and  $V_2$  and  $R_1C_1$  and  $R_2C_2$ .



(a)

FIG. 14-32.—Difference detector giving constant output over a wide range of the output voltage. The potential of point  $A$  is maintained equal to that of point  $B$  by the unity-gain direct-coupled amplifier. The output waveforms indicated in Fig. 14-32a were obtained using the same input pulses as in Fig. 14-31.

substantially independent of the potential of the condenser and dependent only upon the balance between  $V_1$  and  $V_2$  and  $R_1C_1$  and  $R_2C_2$ .

Where bias is obtained from resistance-capacitance networks, the output of the time selectors must be sufficient to maintain the potential drop across these networks in the absence of signal input to the time selector. Usually a small amount of pedestal is generated in the time selector and is sufficient. Of course, this pedestal must be balanced so that conduction of  $V_1$  and  $V_2$  occurs equally and no net change of the potential of  $C_3$  occurs. Another important advantage of an ideal unity-gain amplifier is that the required potential across  $R_1C_1$  and  $R_2C_2$  need only be sufficient to render the diodes nonconducting since the amplifier will maintain the potential difference between points  $A$  and  $B$  near zero, as in Fig. 14-31, provided current transformers are used in the difference detector and the output is connected to a Miller integrator (see Sec. 18-7).

The circuits of Figs. 14-31 and 14-32 are related in the same sense as are the Miller and the bootstrap integrator (see Sec. 2-6). The so-called "unity gain amplifier" of Fig. 14-32 suffers the weakness described in detail in Sec. 7-8. However, a combination of the principles of Fig. 14-31 with those of 14-32 is interesting. In this case, current-transformer feed of the diodes is again employed, but the difference detector is connected to a cathode follower as in the latter circuit. In this way the current trans-

formers would make up for the inadequacies of the cathode follower, and yet a large range of output voltage would be obtainable. In general, however, a large variation of the potential drop across  $C_3$  is objectionable because of the increased leakage current. Such large potential differences are usually avoided by a bootstrapping arrangement similar to that shown in Fig. 14-32. For details see Chap. 18.

Three other configurations of this circuit are shown in Figs. 14-33a, 14-33b, and 14-33c. In Fig. 14-33a is shown difference detection with resistance-capacitance coupling of the negative output from the time discriminator. It is usual practice to employ for  $R_1C_1$  and  $R_2C_2$  time con-

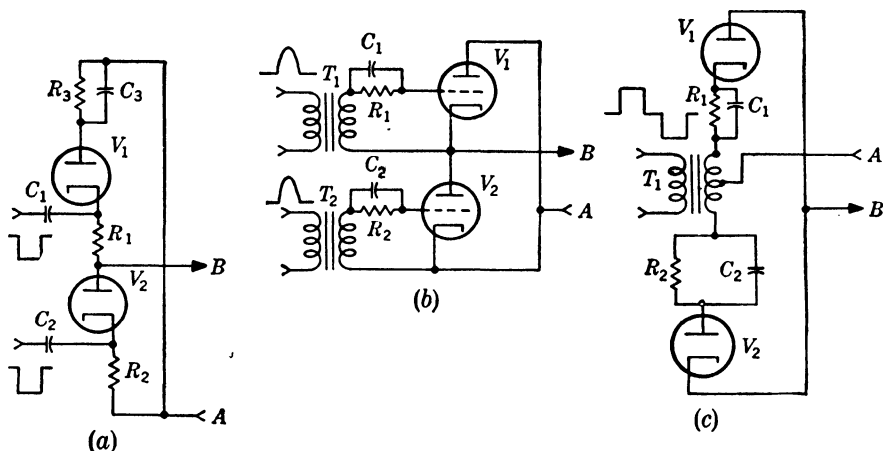


FIG. 14-33.—Various connections of difference detectors: Figure 14-33a represents capacitance coupling suitable for negative pulses. Figure 14-33b represents the use of a triode switch with pulse-transformer coupling of positive or negative signals. Figure 14-33c represents a circuit taking the difference of successive positive and negative pulses connected to the same transformer  $T_1$ . In each case the arrows indicate the proper connection to the output condenser and from a unity-gain amplifier, as shown in Fig. 14-32.

stants that are short compared with the time constant of  $R_3C_3$ . A similar circuit, which employs triodes, is shown in Fig. 14-33b. The polarity of transformers  $T_1$  and  $T_2$  is arranged to apply positive pulses to the grids of  $V_1$  and  $V_2$ . Disconnection of  $V_1$  and  $V_2$  from the condenser is obtained by the negative grid bias accumulated across  $R_1C_1$  and  $R_2C_2$  during the selector pulse. As is usual with grid control, some difficulties due to improper cutoff of  $V_1$  and  $V_2$  may be encountered, and performance inferior to that obtained with the diode circuits is to be expected. However, the input pulses may be of somewhat higher impedance and smaller amplitude.

In certain instances positive and negative pulses which have already been added may be connected directly to a circuit indicated in Fig. 14-33c. Negative excursions of the input cause conduction of  $V_1$  and



positive excursions cause conduction of  $V_2$ . Bias to maintain  $V_1$  and  $V_2$  nonconducting in the intervals between input pulses is obtained from  $R_1C_1$  and  $R_2C_2$ . This circuit is most useful when current feed is used.

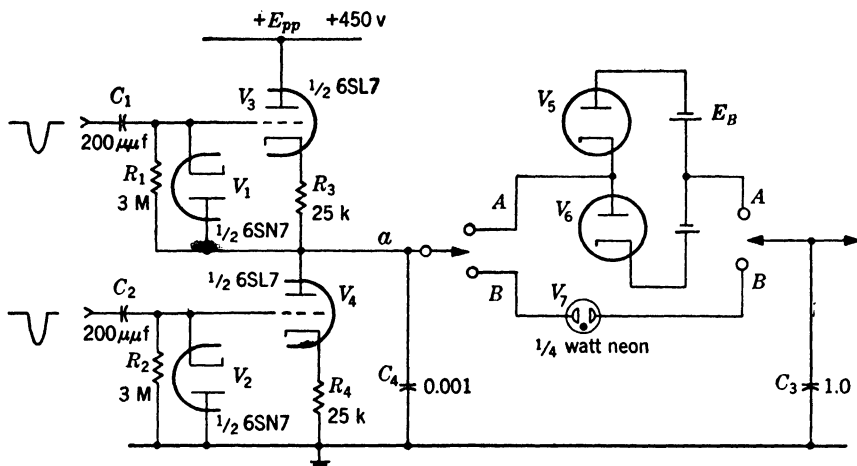


FIG. 14-34.—Difference detector employing short-time-constant detection, subtraction, and difference detection. The figure indicates suitable component values for the demodulation of 0.3- $\mu$ sec pulses at a PRF of 2700. Two types of amplitude selectors  $A$  and  $B$  are shown interposed between the difference voltage and the output voltage.

A differential detector of high sensitivity<sup>1</sup> and constant output in the

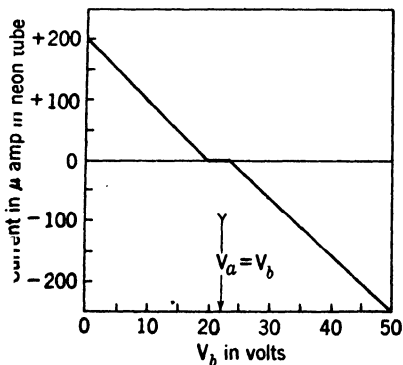


FIG. 14-35.—Static characteristics of difference detector. This curve represents the relation between the steady potential  $V_a$  on the grid of  $V_4$  and the current through the neon tube of Fig. 14-34. The potential of the grid of  $V_3$  was fixed at 22 volts in this measurement.

presence of equal amounts of noise or interference is indicated in Fig. 14-34. The static characteristic of the difference amplifier composed of  $V_3$  and  $V_4$  is given in Fig. 14-35 and shows that a small differential potential on the grids of these two tubes will result in an output voltage which is large compared with the breakdown voltage of the neon tube  $V_7$ . The gain of the stage is roughly 10. For equal voltages applied to the grids of  $V_3$  and  $V_4$ , the neon tube does not break down, and the output condenser is completely disconnected from the input and its potential is constant for a reasonable length of time.

When used as a differential detector, the negative outputs of adjacent

<sup>1</sup> B. Rossi, K. Greisen, "Range-tracking Circuit with Position Memory," NDRC 14-160, Cornell University.

time selectors are connected to  $C_1$  and  $C_2$ . Diodes  $V_1$  and  $V_2$  give peak detection of the applied pulses and develop a positive bias on the grids of  $V_3$  and  $V_4$ . The current that flows into condenser  $C_3$  is therefore representative of the difference of the amplitude of the pulses applied to  $C_1$  and  $C_2$ , which is in turn proportional to the overlap of the signal and selector pulses.

The performance of a typical circuit operating with a  $0.3\text{-}\mu\text{sec}$  input pulse at a PRF of 2700 cps is indicated in Fig. 14-36, which shows the current output from a neon tube in response to the signal obtained from adjacent time selectors (a typical circuit using type 6SA7 multigrid switches) for four values of signal input amplitude.

In this particular test,  $R_1C_1$  and  $R_2C_2$  were  $15\text{ }\mu\text{f}$  and  $20\text{ M}$ ; consequently operation of the heater voltage of  $V_1$  and  $V_2$  at  $4\frac{1}{2}$  volts was necessary. With the potential of the cathode of  $V_1$  averaging 100 volts above ground, the heater-cathode leakage at normal heater temperature would be roughly  $0.02\text{ }\mu\text{a}$ . The reduction of heater temperature reduces this by a factor of 10 (see Sec. 3-14).

Difficulties are encountered because of the variability of different samples of the neon tubes, their large temperature coefficient, and the irregularity of their starting characteristics. More predictable operation is obtained by the bidirectional amplitude selector biased by a battery or, preferably, a floating power supply obtained from a transformer and rectifier. On the other hand, the heater-cathode leakage of the diodes is undesirable.

The difference amplifier  $V_3$  and  $V_4$  serves a purpose similar to that of the current transformers of Fig. 14-31. This particular circuit is, however, somewhat more efficient than the previous one since the pulses are first peak-detected in diodes  $V_1$  and  $V_2$  previous to subtraction and integration in  $V_4$ . The use of the neon tube or diode amplitude selector following integration in condenser  $C_4$  appears at first sight to be extremely attractive for obtaining a constant output voltage in the absence of signal information and in the presence of equal amounts of pedestal and noise.

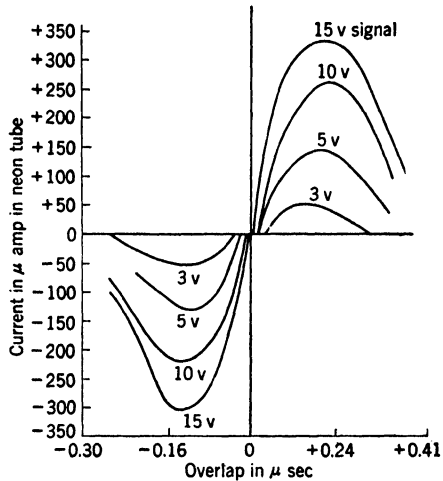


FIG. 14-36.—The over-all response of the differential detector of Fig. 14-34 used with a multigrid time selector for several values of the input pulse. The curves represent operation with  $0.3\text{-}\mu\text{sec}$  pulses and a PRF of approximately 2700.

If the dead space due to either of these amplitude selectors is to be kept small, very accurate balancing of the amplitudes of pedestal and noise applied to the diodes  $V_1$  and  $V_2$  is essential.

**14-7. General Considerations in Time Demodulation.**—Many of the circuits discussed previously are suitable for demodulation of duration-modulated signals providing the output circuits measure the area of the

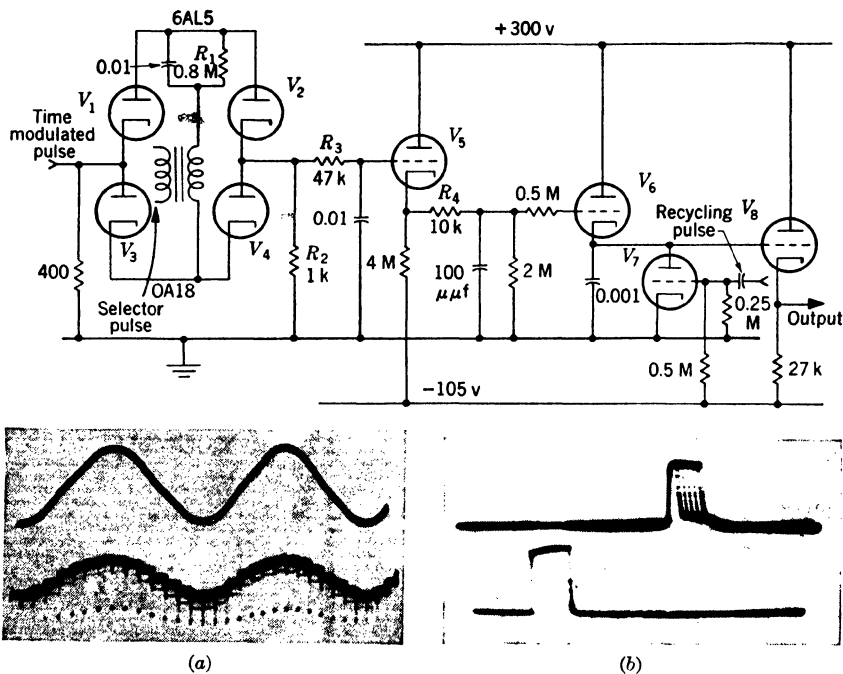


FIG. 14-37.—Recycling detector modified to give detection of the overlap of the time-modulated pulse and the selector pulse. Waveform diagram (a) indicates the sinusoidal signal applied to the time modulator used in this experiment and the bottom line indicates the demodulated output. Figure 14-37b indicates on the top line the duration-modulated pulse from the time selector and on the bottom line the recycling pulse. The series resistor  $R_3$  is employed to obtain area instead of peak detection.

input signal instead of its peak value. Frequently the time-modulated input signal may be represented by the spacing between a pair of pulses. If the range of modulation of the second member of a pair of pulses is less than its duration, a duration-modulated rectangle may be readily obtained by a suitable time selector (see Sec. 10-3). The waveform diagrams of Fig. 14-17 indicate a typical method of accomplishing this with time selection. Usually the range of time modulation is large compared with the duration of the time-modulated pulse. When this is so, simple overlap methods for converting the time-modulated pulse to a

width-modulated pulse are no longer satisfactory, and different methods are used as is indicated below.

*Time Demodulation by Unidirectional-switch Circuits.*—The unidirectional switch circuits of Sec. 14·5 provide satisfactory time demodulators for excursions of the time-modulated pulse that are small compared with the duration of the pulse. Usually, a resistance is inserted in series with the switch in order that the output voltage may not rise to the peak value of the width-modulated pulse. Often a pentode switch is desirable, since then a nearly constant current will flow for the duration of the pulse.

An approximation to constant output may be obtained from recycling detectors, as described in Sec. 14·5, and a demodulation circuit employing

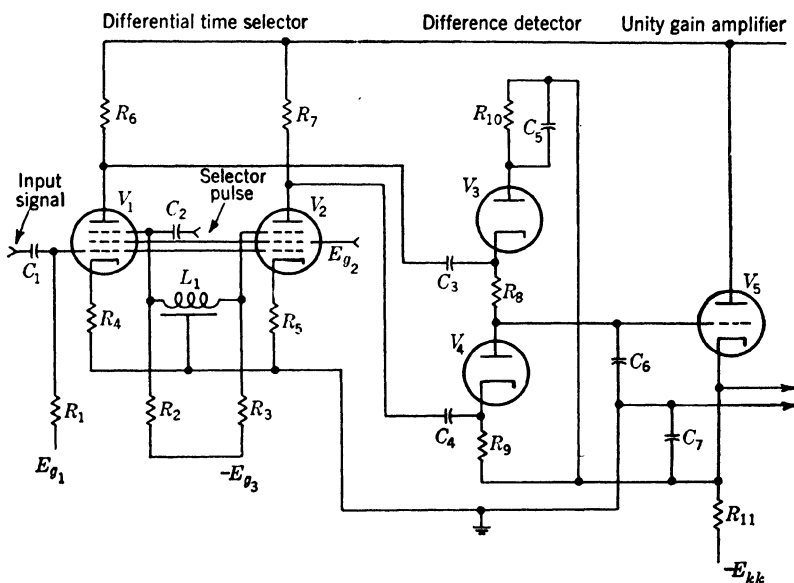


FIG. 14·38.—Time discriminator using separate tubes for time selection and differential detection.

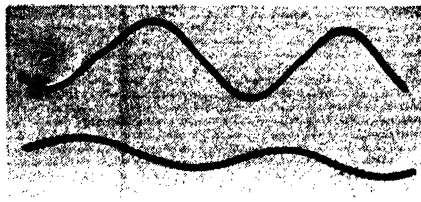
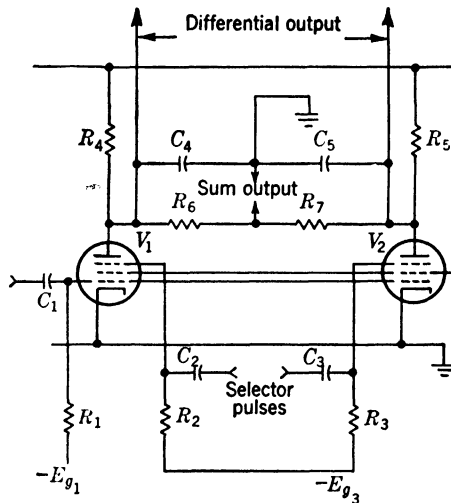
this principle based upon the circuit of Fig. 14·10 is indicated in Fig. 14·37.

Since area detection is required in these circuits, the bidirectional feature of switch circuits is not needed. The output voltage of the area detector is so small that only one diode operates, and hence the other is unnecessary.

*Conversion of a Width-modulated Rectangle to an Amplitude-modulated Triangle Followed by Amplitude Demodulation.*—The width-modulated pulse may be connected to the switch tube of any triangular-waveform generator, and the output will be an amplitude-modulated wave train. This train may be demodulated by any of the peak detectors described in

Secs. 14.3 and 14.5; those having constant output depending upon recycling or bidirectional switching circuits are most useful. These two types require a “dunking” and a time-selector pulse, respectively.

*Use of Adjacent Time Selectors and a Difference Detector.*—Constant output and time selectivity may be obtained by using adjacent time selectors (Sec. 10.5) and the difference detectors of Sec. 14.6. The time-modulated pulse split by the two time selectors gives two width-modu-



(a)

FIG. 14.39.—Time discriminator using parallel pentodes. The waveform diagram indicates on the top line the sinusoidal signal applied to a time modulator and on the bottom line the differential output between the plates of the time discriminator.

lated pulses which may be used to charge and discharge the output condenser of the difference detector as shown in Fig. 14.38. This method gives good performance in the presence of noise and interference.

Two other circuits that combine the functions of time selection and detection are indicated in Figs. 14.39 and 14.40. They represent variations of Fig. 14.38. In the first circuit, detection is accomplished in the two time selectors, and in the second circuit, time selection is accomplished in the difference detector.

In Fig. 14.39, resistance-capacitance networks are shunted across the

plates of two time selectors  $V_1$  and  $V_2$ . In addition, considerably larger plate resistors  $R_4$  and  $R_5$  are used to give a reasonable time constant. The differential output obtained from this circuit with  $1\text{-}\mu\text{sec}$  input pulses is indicated in Fig. 14·39*a*. A steady voltage corresponding to the sum of the two differential signals is obtained by addition of the two outputs through  $R_6$  and  $R_7$ .

The triode difference detector of Fig. 14·40 can be rendered non-conducting by the potential developed across  $R_3C_4$ , and conduction is achieved by selector pulses applied to the plates of  $V_1$  and  $V_2$  through transformers  $T_3$  and  $T_4$ . As in the previous circuits, the potential of point  $A$  is made to follow that of  $B$  in order to obtain a large range of output voltage.

The output of these circuits does not follow the signal variations with extreme linearity, and these time discriminators are usually employed as an element of the negative-feedback time demodulators discussed in the next paragraphs.

*Pulse-spacing Modulation—Large Excursions.*—Here the excursions of the time-modulated pulse are large compared with its duration. This is the most usual case of time modulation, and is, of course, the one found in all radar systems. There are two general methods of time demodulation and they vary considerably in their ability to reject interference.

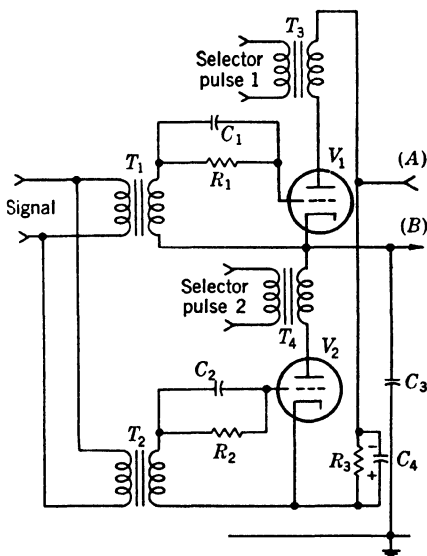


FIG. 14·40.—Time discriminator using series triodes.

The simplest method, which is indicated in Fig. 14·41, represents an application of "time comparison," which was presented briefly in Sec. 10·1. The time-modulated pulse connects a bidirectional switch circuit to a triangular timing wave so that the output voltage represents the potential of the triangular waveform at the time of occurrence of the modulated pulse. This is a simple, direct, and accurate method of time demodulation; it suffers from a great drawback if the time-modulated pulse is mixed with noise and interference, for then the output circuit is connected to the triangular timing wave at a number of different times and accurate demodulation is impossible.

This difficulty is avoided by negative-feedback time-demodulation

systems that employ the output of a differential time selector and difference detector to control another time modulator which, in turn, controls the time of occurrence of the selector pulse. As the block diagram of Fig. 14-42 indicates, the output of the difference detector varies the reference voltage of the amplitude comparator of an electrical time modulator. In a mechanical time modulator, the electrical output may

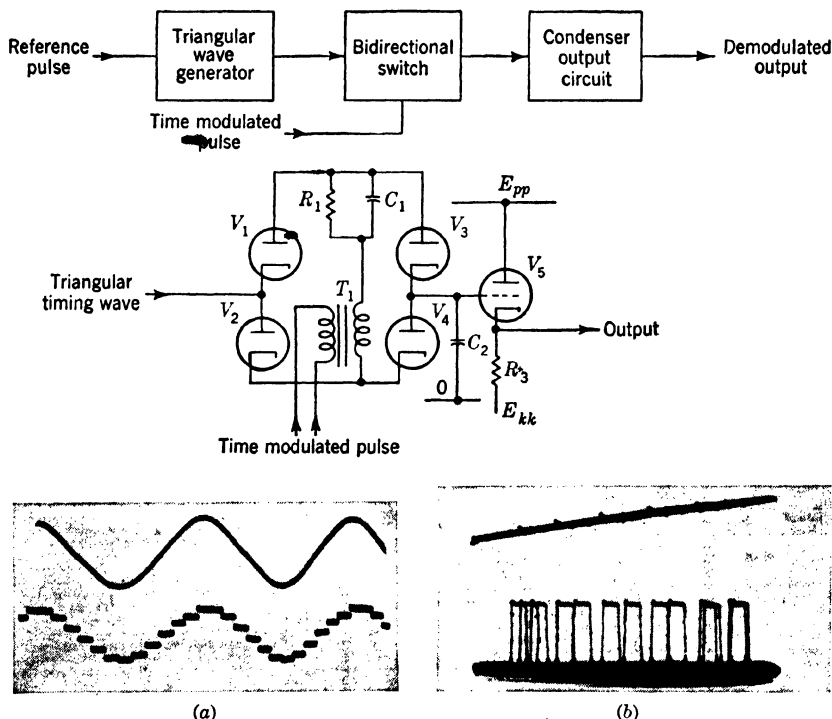


FIG. 14-41.—Time demodulation by time comparison. The time delay of the modulated pulse is represented by the amplitude of the output voltage obtained by connecting condenser  $C_2$  to a triangular waveform. In Fig. 14-41a the waveform diagrams indicate the sinusoidal signal applied to the time modulator on the top line. On the bottom line is indicated the output of the time demodulator. The top line of Fig. 14-41b indicates the triangular timing wave and the bottom line indicates the time modulated pulse.

be converted into a mechanical shaft rotation by a servomechanism. The sense of the output is, of course, arranged to give negative feedback. The combination of adjacent time selectors and difference detectors is called a "time discriminator."

It is essential to provide a band-shaping network between the difference detector and the amplitude comparator for the purpose of giving the negative-feedback loop adequate stability. These networks are discussed in detail in Vol. 20, Sec. 8-4 and are called "function units."

This method of time demodulation has a number of basic advantages. The first and most important is that the accuracy of demodulation depends, to a first approximation, upon the linearity of the time-modulation system. Second, the automatic following of a time-modulated pulse by the time-selector pulse rejects a large amount of interference and noise. Third, the adjacent time selectors and difference detector act as a null indicator, and the requirements for their linearity and constancy of gain are greatly reduced. There are, however, still strict requirements for their balance in the presence of equal amounts of noise or in the presence of rapidly fluctuating signals.

Since the time discriminator is sensitive only to a portion of the full range of time modulation—a portion often as small as 0.1 per cent—its

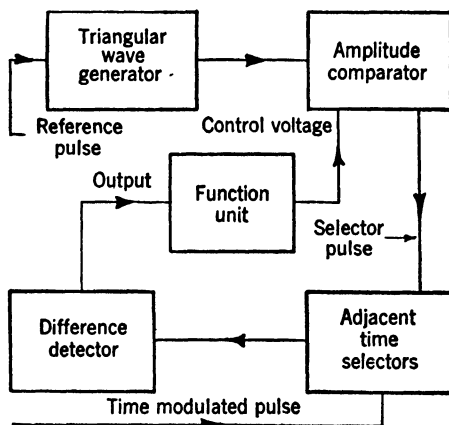


FIG. 14·42.—Block diagram of a negative-feedback time demodulator.

operation cannot, therefore, be initiated by the appearance of a signal anywhere in the range of modulation. In radar systems, where the signal may cover the full range only once, the selector pulses must be brought into initial coincidence with the desired signal. This is usually accomplished manually by a cathode-ray-tube display. This method is discussed in Sec. 14·8, but a number of automatic “search” methods are available (Vol. 20, Sec. 8·17). If, during a momentary disappearance of the signal, the selector pulses and the signal cease to overlap, the operation must be reinitiated manually or automatically. Many important characteristics of these circuits are given in the detailed discussion of Vol. 20, Chap. 8.

**14·8. Simplified Negative-feedback Time Demodulator.**—The discussion of highly precise time demodulators is beyond the scope of this chapter, but an example of a simplified circuit is included here.

Figure 14·43 indicates the use of the double-triode delay multivibrator





terminated  $\frac{1}{2}$ - $\mu$ sec delay line  $L_1$ . In this way, the time-modulated signal is split into two adjacent portions each  $\frac{1}{2}$   $\mu$ sec in duration. Coincidence of these two pulses and the selector pulse obtained from  $V_4$  energizes the differential detector composed of  $V_6$  and  $V_7$  to give a potential at point  $c$  which depends upon the difference of the areas of the overlap of selector pulse  $a$  and the split pulses  $d$  and  $e$ .

For usual values of the potential of point  $c$ ,  $V_6$  and  $V_7$  are nonconducting since the cathode of  $V_7$  is maintained positive with respect to its plate by the grid bias of  $V_8$ , and the plate of  $V_6$  is held negative with respect to its cathode by the difference of potential between point  $c$  and ground. In the absence of a time-modulated signal coincident with the selector pulse  $a$ , negligible conduction of  $V_6$  and  $V_7$  occurs since a positive pulse  $b$  is applied to the cathodes of  $V_6$  and  $V_7$  at the same time as the selector pulse  $a$  is applied to their plates, and sufficient bias is developed to maintain  $V_6$  and  $V_7$  very nearly nonconducting. Therefore, the potential of point  $c$  is relatively undisturbed in the absence of a coincident input signal. On the other hand, a coincident signal causes a decrease of grid bias in  $V_6$  and  $V_7$  and conduction of either one of these tubes for a time determined by the overlap of the split signal and selector pulse. A charge then accumulates on  $C_1$  which represents the integral of the time error. If the selector pulse exactly bisects the split input signal, that is, there is no time error, then the potential of  $C_1$  is unchanged since equal conduction will occur in  $V_6$  and  $V_7$  for balanced components. This potential of  $C_1$  is therefore connected through the cathode follower to the control grid of the time modulator and adjusts the position of the selector pulse to follow exactly the modulation of the input signal.

For demodulating pulses of a relatively high intermittency, heater-cathode leakage in  $V_6$  would discharge the storage condenser  $C_1$ . Therefore, the heater of this tube is operated at 5 volts and is maintained at a constant negative potential with respect to the cathodes by connection to the cathode follower at point  $f$ . In this way, leakages of  $3 \times 10^{-3}$   $\mu$ a are obtained in this particular circuit.

The gain of the time-demodulator circuit is not very high, and, hence, no difficulty arises due to instability. The bandwidth of the demodulator is not high; it is suitable for following signals which cover the full range of modulation in several seconds. The speed of following could, however, be considerably increased by reduction of  $C_1$ .

**14-9. Mechanical Demodulation by Cathode-ray-tube Display.**—Amplitude- or time-modulated waves, containing signal frequencies of the order of magnitude of 0.1 cps, are accurately demodulated by amplitude or time discrimination and manual or servo control. The most important application of these methods is to the time demodulation of the range information of radar signals, in which case the methods are

called "range tracking" (a detailed discussion is given in Vol. 20, Chap. 7, and in Vol. 22). As shown in Fig. 14·44, a triangular wave is applied to the horizontal plates of a cathode-ray tube and a rectangular wave is applied to its control grid with the result that only the rising portion of the triangular wave is visible. A train of radar echoes is displayed on the linear sweep. If, however, the particular echo *a* is an aircraft signal that is moving in a radial direction with respect to the radar system, the received pulse is time-modulated. The displacement between the vertical mechanical index and the position of the echo *a* gives the operator a measure of the sense and magnitude of the time error—in other words, permits time discrimination. Manual control of the index to reduce this error to zero and to maintain it at zero gives mechan-

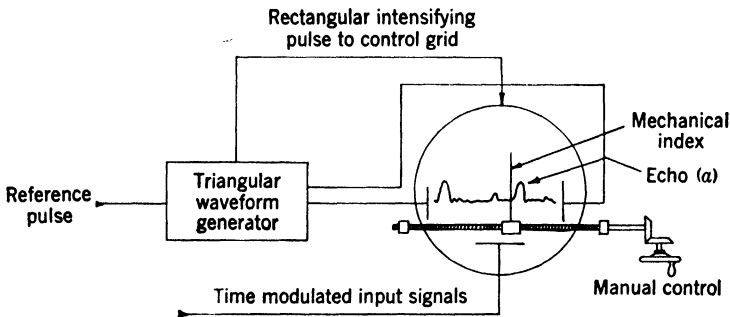


FIG. 14·44.—Time demodulation by manual control of a mechanical index on a cathode-ray-tube display.

ical demodulation of the information on the target range, and the position of the control shaft represents the desired output.

The method is analogous to that shown in Fig. 14·42 since the accuracy depends upon (1) the linearity of the timing waveform as displayed upon the cathode-ray tube, (2) the time discrimination of the cathode-ray tube, and (3) the ability of the operator.

In some scanning radar systems, a group of approximately 12 pulses is received in a period of 0.03 sec while the beam scans the desired target. The beam is, however, pointed in other directions for approximately 30 sec until it again scans the target. A rapidly moving target (one moving at 400 mph) covers the full range of time modulation (200 miles) in a very short time (30 min), and consequently only 120 groups of the selected pulses are observed in this interval. Highly accurate demodulation under these circumstances is difficult. In a simple case the operation of the constant-output detectors of Sec. 14·6 may be simulated. Every time the group of time-modulated pulses appears on the cathode-ray-tube display, the mechanical index is moved to reduce the error to zero. When the group of pulses terminates, the operator maintains the shaft

stationary and immediately resets the output on reception of the next group of pulses. Thus, an output time constant that is large compared with that readily obtainable by electric circuits may be attained. A better-trained operator would attempt to remember the rate at which the signal was moving and to rotate the control shaft continuously in the interval between groups of input information. In this way, the displacement error of the next group of pulses is kept to a minimum. Provided the rate memory is obtained from the average of the past information, this process represents the "ideal demodulation" briefly discussed in Sec. 14·5. A number of tracking "aids" assist the manual controller in remembering the target velocity in the interval when no information is available. These may consist of a controllable speed drive which is

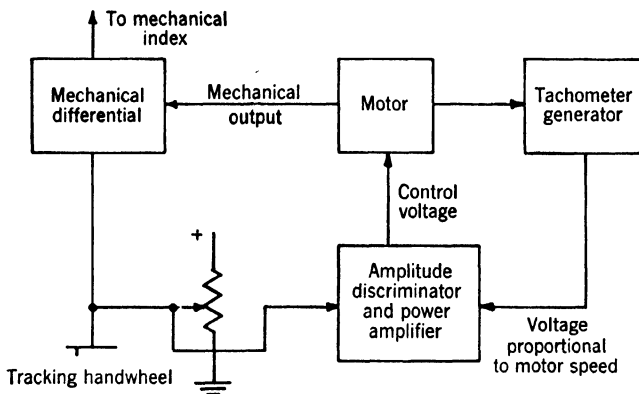


FIG. 14·45.—Block diagram of mechanical aided-tracking system.

automatically adjusted to the previous values of the target velocity in the course of reducing displacement error. This mechanism is called "an aided-tracking system," and is indicated in Fig. 14·45. Other more complicated tracking aids may take into account known factors which may be expected to vary the rate of movement of the echo in a predictable manner and alter the speed of the mechanical drive for the index in accordance with the computed rate. The tracking process adds corrections to the input rate for unknown or unaccountable factors. These devices are called "regenerative tracking" systems. The properties and typical examples of these systems are given in Vol. 20, Sec. 7·15.

*Photoelectric Controllers Used with Cathode-ray-tube Display.*—A photo-cell and servomechanism may replace the human controller and mechanical index. An experimental system is shown in Fig. 14·46. A circular sweep is applied to the four plates of a cathode-ray tube, the time-modulated signal is applied to the control grid, and an intensified spot corresponding to the time of occurrence of the received signal is displayed

on the trace. Time discrimination is accomplished by the two photocells, which receive light from the intensified spot on the cathode-ray-tube trace by means of a pair of prisms. The prisms divide the spot equally at the null position. The whole frame for the photocells is movable

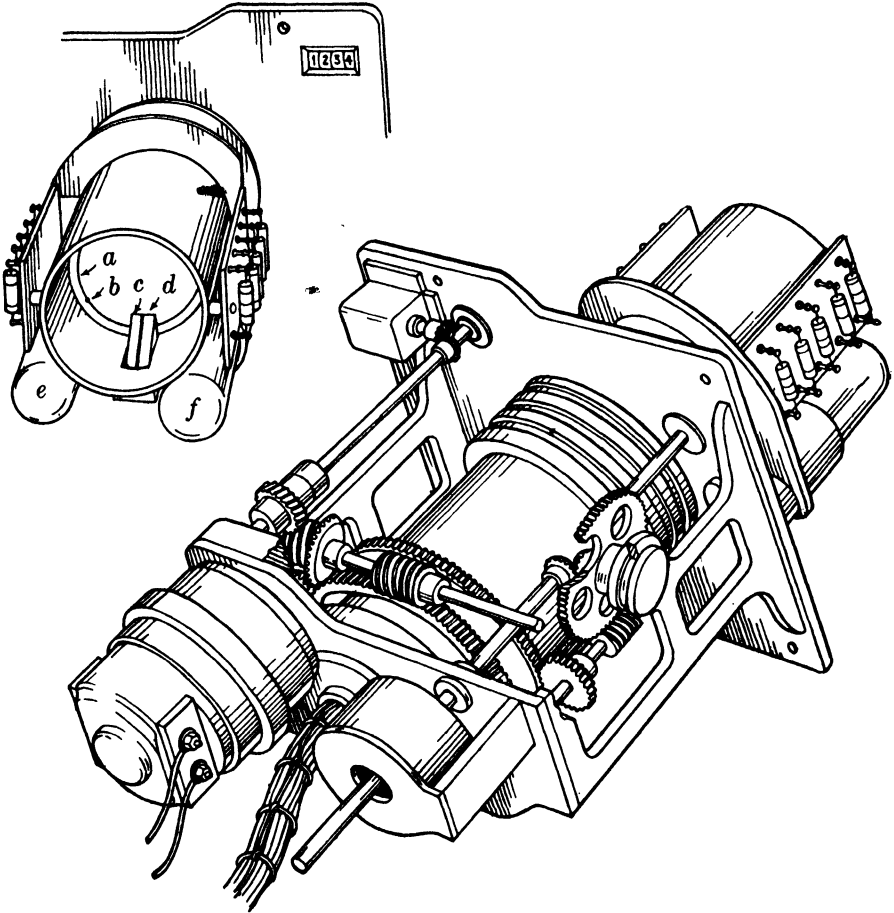


FIG. 14-46.—Perspective view of an automatic range-tracking mechanism employing photocells. Intensity-modulated signal *b* is displayed upon circular trace *a* of a 2-in. cathode-ray tube. Split prisms *c* and *d* reflect light onto type 931 photomultipliers *e* and *f*. The photomultiplier assembly is rotatable about the fixed cathode-ray tube by means of a motor-driven worm gear, and the output voltage is obtained through slip rings. The total range is displayed upon a Veeder Root counter.

about the center of the circle displayed on the cathode-ray tube, and its position is controlled by a small motor. The electrical signals from the photocell output are amplified and connected to a thyatron controller for driving the motor. The motor then maintains the light from the intensified spot equally divided by the two photocells. In this way a

sensitive and accurate indication is obtained because the sensitivity depends upon the gain of the photoelectric system and the accuracy depends upon the precision of the circular trace.

If the photocells and servomechanism are accurately balanced, this system will exhibit properties of a constant-output difference detector and maintain its position in spite of fading or interference which would obliterate the signal. Also, integrating circuits that cause the output to maintain the past value of the input rate for a reasonable period of time may be included in the servomechanism. It is, however, usually difficult to obtain the extremely long memory which is possible with the aided-tracking devices mentioned in the paragraph above.

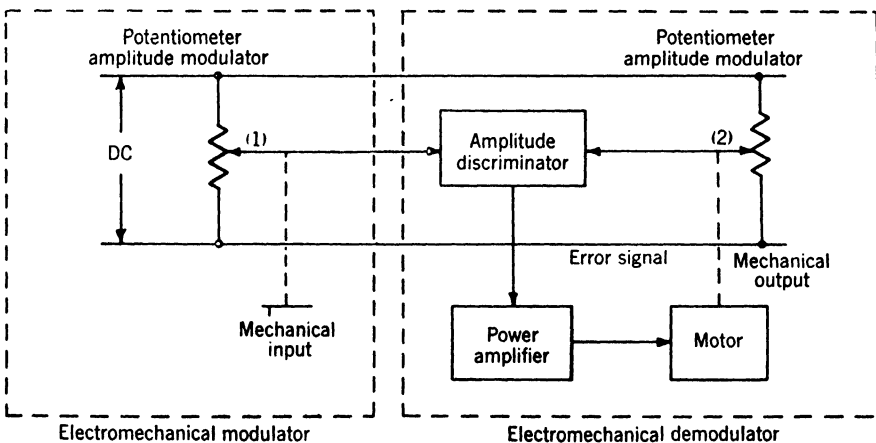


Fig. 14-47.—Block diagram indicating mechanical demodulation by a servomechanism.

Another feature of this method is its flexibility. The scale factors of the system are readily varied over wide limits by simply changing the frequency of the circular sweep. For example, the circular trace of Fig. 14-46 may cover anything from 1  $\mu$ sec to 0.1 sec. The apertures, of course, still correspond to the same percentage of the timing waveform. On the other hand, the speed of response of the system is independent of the time range it covers and, in fact, cannot be readily varied. Furthermore, it cannot be increased above 10 or 20 cps, even with the best electronic servomechanism design.

A method of time demodulation depending upon the storage tube is presented in Sec. 21-10.

#### 14-10. Amplitude Demodulation by Electronic Servomechanisms.—

The demodulation of mechanical signals converted into electrical information by the methods of Chap. 12 may be accomplished by the system indicated in Fig. 14-47, which indicates the components of a mechanical modulation-demodulation system using a d-c or a zero-frequency carrier.

The signal from the amplitude modulator, obtained in accordance with the methods in Chap. 12, is connected to an amplitude discriminator as described in Sec. 9-22. The amplitude discriminator is also connected to the output of the motor-driven potentiometer, and a signal indicating the sense and approximate magnitude of the error voltage between the two is connected to a power amplifier which in turn controls the motor for the reduction of the output of the amplitude discriminator to zero. The precision of the demodulation depends upon the linearity of the potentiometer, and the stability and sensitivity depend upon the characteristics of the amplitude discriminator and the gain of the negative-feedback system. When a zero-frequency carrier is used, the input data are continuous except for any discontinuity in the modulator or demodulator.

In order to obtain greater stability, the amplitude discriminator may use an electrical amplitude modulator and demodulator employing, for example, a mechanical switch (see Sec. 9-23). The operation is, however, similar. But if an alternating carrier is used, for example, by applying alternating current directly to the two potentiometers, a phase discriminator (phase-sensitive detector) must be employed. The demodulated output of this device, however, will control the power amplifier as in the previous case.

## CHAPTER 15

### SINUSOIDAL FREQUENCY MULTIPLIERS AND DIVIDERS

BY E. B. HALES AND J. V. HOLDAM

Many precision timing systems require synchronized waveforms whose frequencies are integral multiples or rational ratios of some fundamental frequency. This chapter deals with devices that give out a sine wave whose frequency is some integral multiple or rational ratio of the fundamental frequency of the input waveform. Other waveforms at that frequency can usually be initiated by a train of pulses.

An example of a timing system that requires synchronized waveforms at different frequencies occurs in those radar range units that trigger the modulator at an exactly constant repetition rate and that use as a timing reference a sine wave whose frequency is an integral multiple of the repetition frequency (Vol. 20, Chap. 4). Such a frequency relation can be obtained by using a standard oscillator at the higher frequency and obtaining the lower frequency by frequency division. It can also be obtained by making the standard oscillator at the lower frequency and getting the higher frequency by frequency multiplication. Preference for one method or the other depends on the practical details of the problem at hand. The examination of a large number of timing systems shows that the use of frequency division usually, but not invariably, leads to simpler and less costly circuits for a given degree of precision.

#### SINUSOIDAL FREQUENCY MULTIPLIERS

**15-1. Introduction.**—One important use of frequency multiplication arises in the calibration or testing of crystal-oscillator controlled timing units. A time scale of greater precision than that of the range unit is necessary for accurate testing. A synchronized time scale of almost any desired precision can be obtained by multiplying the timing frequency of the range unit and applying the output frequency as the drive to a suitably designed J-scope or other sine-wave controlled time scale.<sup>1</sup>

Sine-wave frequency multipliers have long been used in radio transmitters to generate very stable frequencies which are higher than those

<sup>1</sup> This statement does not imply that the accuracy of the crystal-controlled oscillator is increased by frequency multiplication. The object of the calibrating device is to provide a vernier time scale that is used to check the accuracy of a time modulator in the ranging device.



that can be obtained directly from a crystal oscillator. They have also been used in frequency standards to generate exact harmonics of precisely determined frequencies and thus greatly to extend the range over which standard frequency outputs are available.

In the applications of the preceding paragraphs a moderately good sine-wave output is necessary. In setting up a synchronized timing system it is essential that the multiple frequency be a pure sine wave, but it is also essential that the multiple frequency have fixed phase with respect to the input waveform. These simultaneous requirements are stringent specifications on the circuits employed; and much of this discussion is devoted to meeting them.

There are two essentials to the process of frequency multiplication. The first is the generation of a waveform that is synchronized with the input and that has a component of the desired output frequency. In general this cannot be done without also generating undesired frequency components. The second essential in the process is the use of a suitable bandpass filter to select the desired frequency component from all the components generated. Because of these filters, frequency multiplication is useful only if the sine waves are to be generated continuously. These frequency multipliers are not suitable for pulsed operation because bandpass filters do not have sufficiently good transient response.

**15-2. Harmonic Generation.**—A Fourier analysis of any nonsinusoidal periodic waveform shows that it is made up of sinusoidal components whose frequencies are integral multiples of the fundamental frequency of the nonsinusoidal periodic waveform. The components that are present and their relative amplitudes depend on the exact time course of the waveform. It is clear that when a sine-wave input is applied to a circuit that has a nonlinear transfer characteristic the output is nonsinusoidal and contains synchronized harmonics of the sine wave.<sup>1</sup> The problem is to choose the type of distortion—that is, nonlinear transfer characteristic—which will give a waveform rich in the desired component.

Three types of nonlinear devices have been used extensively for harmonic generation: iron-core inductances, diodes, and nonlinear amplifiers. Since iron-core inductances have a nonlinear relation between magnetizing current and magnetic flux, a properly designed inductance driven by a current generator is a good source of voltage harmonics. It is particularly good at high harmonics. A new inductance design is usually required for each application. This fact and the fact that they are often low-impedance devices requiring considerable driving power make it inadvisable to use them in most simple synchronizing systems.

<sup>1</sup> Peterson, Manley, and Wrathall, "Magnetic Generation of a Group of Harmonics," *Bell Sys. Tech. J.*, **437**, (October 1937); D. G. Tucker, "The Generation of Groups of Harmonics," *Electronic Eng.*, **242**, (November 1942).

Diodes or contact rectifiers can be used in various combinations to obtain waveforms with harmonic content. The output of a single-phase full-wave rectifier contains all the even harmonics of a sine-wave input. Such a rectifier is often used in a frequency doubler.

The harmonic generator offering the greatest flexibility is the nonlinear amplifier. A class C amplifier can be made to have a small conduction angle if the grid bias and sine-wave drive are made sufficiently large. With a pentode amplifier tube the pulse of current in the plate circuit can be made nearly rectangular. In any case, a rectangular pulse may be used as an approximation to give a qualitative idea of how the harmonic content depends on the width of the current pulse.

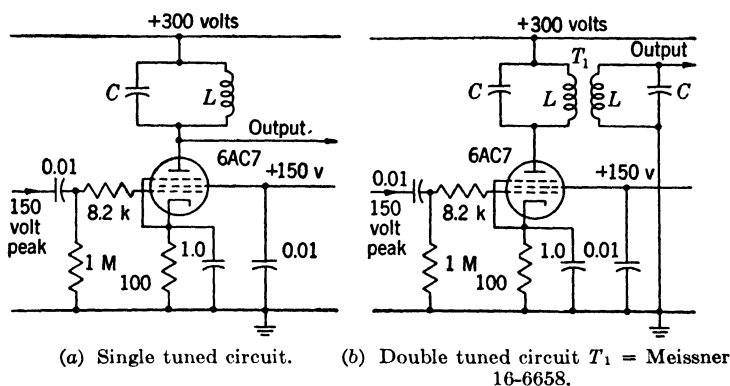


FIG. 15-1.—Class C multiplier amplifiers.

Let the input voltage be of the form  $e = E \cos 2\pi f_0 t$ , where  $e$  is instantaneous voltage,  $E$  is peak voltage,  $f_0$  is the frequency of the input, and  $t$  is time. If the peak voltage is considerably larger than the grid base of the amplifier tube of Fig. 15-1, the current occurs in pulses. Assume that the bias and driving voltages are such that the current pulse is rectangular, with an angular width  $2\alpha$  starting at  $-\alpha$  and ending at  $+\alpha$ . These pulses are repeated once every cycle of the input wave. If  $I$  is the peak value of the current pulse,  $i(t)$  is the current as a function of time, and  $n$  is any positive integer, the Fourier series for this continuous train of pulses is

$$i(t) = 2I \left[ \frac{\alpha}{2\pi} + \frac{\sin \alpha}{\pi} \cos 2\pi f_0 t + \frac{\sin 2\alpha}{2\pi} \cos 4\pi f_0 t + \frac{\sin 3\alpha}{3\pi} \cos 6\pi f_0 t + \cdots + \frac{\sin n\alpha}{n\pi} \cos 2\pi n f_0 t + \cdots \right]. \quad (1)$$

The general term  $\cos 2\pi n f_0 t$  has a frequency  $n f_0$ . The output has a component with a frequency equal to every integral multiple of  $f$  except for those terms for which the amplitude coefficient  $\sin n\alpha/n\pi$  is equal to

zero. This can happen only if  $n\alpha$  is some integral multiple of  $\pi$ . Consequently, if the conduction angle  $\alpha$  is properly chosen, a rectangular train of pulses can be made to have a component of any frequency that is a harmonic of  $f_0$ . The amplitude of the  $n$ th harmonic is  $2I \sin n\alpha/n\pi$ . The maximum amplitude occurs when  $\sin n\alpha = 1$ —that is, when  $n\alpha = \pi/2$ , or  $3\pi/2$ , etc. Actually, the practical case is the one for which  $n\alpha = \pi/2$ . Then  $\alpha = \pi/2n$  and the conduction angle  $2\alpha = \pi/n$  for maximum output in the  $n$ th harmonic. The largest possible amplitude for the  $n$ th harmonic is  $2I/n\pi$ . This makes it clear why it is difficult to get large outputs at high harmonics.

**15-3. Frequency-selecting Filters.**—The previous section shows how a current waveform can be generated which contains a component of the desired frequency. The waveform also contains undesired components. These can be reduced to an acceptable level by proper filtering. Throughout this discussion it is assumed that the input impedance of the filter is low in comparison with the plate resistance of the multiplying tube. This condition is usually met with pentodes, and the consequent constant current driving conditions lead to a great simplification of the analysis without invalidating the qualitative results. Triodes can be employed as frequency-multiplying tubes. The extent to which this analysis is applicable to triode circuits is considered in the section on practical circuits.

The frequency selection arguments developed here can be applied to any continuously generated periodic waveform whose Fourier-series representation is known. Specifically, for the train of rectangular pulses represented by Eq. (1), the current at the  $n$ th harmonic is

$$i_n = 2I \frac{\sin n\alpha}{n\pi} \cos 2\pi n f_0 t.$$

The transfer impedance of a filter is a complex function  $Z(f)$ , where  $f$  is the frequency of any input to the filter. The output voltage of the filter at the  $n$ th harmonic is equal to  $i_n Z(nf_0)$ . The most desirable filter is one having a large transfer impedance at the  $n$ th harmonic and zero transfer impedance at all other harmonic frequencies. Any type of bandpass filter can be designed so that it has a very small transfer impedance for the undesired components.

Because of their simplicity and the large outputs that can be obtained,  $LC$  resonant circuits with lumped constants are most often employed as frequency-selective circuits over the range of frequencies from approximately 100 cps to 100 Mc/sec. Outside this range simple resonant circuits do not have sufficiently good  $Q$  to function satisfactorily. At higher frequencies resonant elements with distributed constants are employed, and at very low frequencies tuned amplifiers employing feedback are used

as bandpass filters (Vol. 18, Chap. 10). Since the range covered by lumped constant resonant circuits includes all the frequencies commonly employed in synchronized timing systems, only these circuits are considered in detail here.

The simplest circuit with the desired pass band is a parallel resonant circuit used as the load impedance for a multiplier tube, as shown in Fig. 15-1. An idealized parallel resonant circuit is shown in Fig. 15-2. It is assumed in the discussion to follow that the shunt resistance  $R$  represents all the losses in the circuit. For frequencies in the neighborhood of resonance this represents the losses in the circuit well enough for practical purposes. At the resonant frequency  $f_r = 1/2\pi \sqrt{LC}$ , the parallel  $LC$ -combination offers an infinite impedance to the input. The resulting impedance is just equal to  $R$ . The amplitude of the impedance at a frequency  $f$  in the neighborhood of resonance is given by

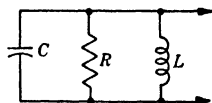


FIG. 15-2.—Idealized parallel resonant circuit with all losses in  $R$ .

$$Z = \frac{R}{\sqrt{1 + Q^2 \left( \frac{f}{f_r} - \frac{f_r}{f} \right)^2}}, \quad (2)$$

where  $Q$  is defined as equal to  $\frac{R}{2\pi f_r L}$ .

The phase angle of the impedance is given by

$$\tan \phi = Q \left( \frac{f_r}{f} - \frac{f}{f_r} \right). \quad (3)$$

A plot of Eq. (2) shows that the impedance at any of the nonresonant frequencies can be made a smaller fraction of  $R$  as long as  $Q$  can be increased. Consequently if the only requirement on the output waveform is that it be a good sine wave, the resonant circuit should have as high a value of  $Q$  as it is possible to get.

In the timing systems which are of primary interest here, it is also necessary that the phase of the impedance remain fixed. From Eq. (3) the phase angle of the impedance is zero when  $f = f_r$ . Suppose that, because of small changes in  $L$  or  $C$ , the resonant frequency is changed by a very small amount  $\Delta f_r$ . The resulting small change in phase angle is

$$\Delta \phi = \frac{2Q}{f_r} \Delta f_r. \quad (4)$$

Hence very large  $Q$  makes it difficult to maintain good phase stability.

<sup>1</sup> See F. E. Terman, *Radio Engineering*, McGraw-Hill, New York, 1937, Chap. III, for graphical representation of characteristics of tuned circuits.

The requirements of good phase stability and a pure sine wave are hard to meet simultaneously. Every design must be a compromise between these two factors.

At a given  $Q$  the phase stability can be improved by using components that are stable and temperature-compensated. Designs involving excessively small values of  $C$  should be avoided because of the possibility that microphonics or slow changes in tube and wiring capacitances may seriously affect the phase.

If it is found that a single circuit of high  $Q$  giving sufficient attenuation at the undesired frequencies causes excessive phase instability, the condition may be greatly improved by cascading the attenuation of two circuits of moderate  $Q$ . It can be shown by applying Eqs. (2) and (4) to most practical cases, that this gives much less phase shift in the neighborhood of resonance for the same amount of attenuation at the adjacent harmonics. Simple one-way coupling from the first tuned circuit to the second can be accomplished by the use of an isolation stage. Such a tuned amplifier usually has to be neutralized.

A better method for most purposes is to use two tuned coils with mutual inductance coupling as the frequency selector. This arrangement is shown in Fig. 15-1b. Such a double-tuned transformer with both primary and secondary tuned to the desired pass frequency is like the intermediate-frequency transformers employed in most superheterodyne radio receivers. A complete description of their attenuation and phase characteristics is too lengthy to be included here but can be found in many radio engineering text books.<sup>1</sup> The most pertinent facts for the purposes of this section are noted here. For simplicity, only the transformer with exactly equal primary and secondary is considered: that is,  $R$ ,  $L$ ,  $C$ , and  $Q$  are the same for both circuits. The coupling factor between two equal inductances of value  $L$  is defined as  $K = M/L$ , where  $M$  is the mutual inductance between the two inductances. Maximum voltage output is obtained at the critical coupling factor  $K = 1/Q$ . Under these conditions a given change in the resonant frequency of both primary and secondary coils has the same effect on the phase of the output as the same change in resonant frequency has on a single-tuned circuit of the same  $Q$ , but the transformer has much larger attenuation at the undesired frequencies than has the single-tuned circuit. Although increasing the coupling factor beyond the critical value increases phase stability, it decreases the output voltage, decreases the attenuation of undesired components, and produces two peaks in the resonance curve. This last effect makes adjustment difficult. In this application it is recommended that the critical coupling factor be chosen in designing tuned transformers having equal primary and secondary circuits.

<sup>1</sup> Terman, *loc. cit.*

These transformers can be designed with good enough characteristics for most practical frequency multipliers. More elaborate passive filters or selection feedback amplifiers can be designed for special purposes to give even more desirable attenuation and phase characteristics (see Vol. 18, Chap. 10). It must be borne in mind that, if good phase stability is required, the bandpass filter should be no more narrow than is necessary for good output waveform, since all bandpass filters have at least  $\pm 90^\circ$  phase shift at frequencies that differ considerably from the center frequency of the passband.

### FREQUENCY MULTIPLIERS

**15-4. Practical Multiplier Circuits.**—Because of their low plate resistance the plate currents in triode multiplier tubes are greatly affected by the load impedance. During the time the tube is on, it acts as a

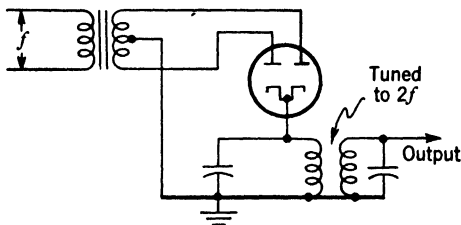


FIG. 15-3.—Resonant filter and diode frequency doubler.

shunt on the plate load, which has effectively a different value of  $Q$  during different portions of the cycle. The relations between  $Q$  and the attenuation and phase given in the previous section can still serve as a qualitative guide, but numerical results can be obtained only by very laborious methods. Practical design is usually empirical. Because of the large cutoff voltage of triodes, they require very large sine-wave grid drive to obtain current pulses of small conduction angle. For relatively small multiplication factors or under conditions where narrow pulse waveforms are used to drive the grid properly, a triode makes a satisfactory frequency multiplier.

Diodes are frequently used in the circuit of Fig. 15-3 as frequency doublers. With a perfectly balanced circuit there is no output at the fundamental frequency. The undesired output is at the even harmonic frequencies above the doubled frequency. The filtering can be accomplished with a very-low- $Q$  circuit and does not lead to serious phase shifts. The  $Q$  should be selected just high enough to give an acceptable sine wave.

The 6AC7 Class C amplifier of Fig. 15-1 has a nearly rectangular current pulse of about 35-ma amplitude and a conduction angle of about  $40^\circ$  when the input is a sine wave from a low impedance source of 150

volts peak. The input may vary considerably in amplitude without much effect on the current wave. The bypassed cathode resistor is included to protect the tube in case the grid drive fails. Since a 6AC7 is nearly cut off at  $-4$  volts, it is relatively easy to get a small angle conduction. This arrangement gives fairly good output for many harmonics, but is specifically designed to multiply by five. The currents at the fourth, fifth, and sixth harmonics are about 5.6 ma, 4.5 ma, and 3.2 ma respectively. Current and voltage values given here and in Table 15-1 vary considerably with the transconductance of the tube, but the relative values are still correct.

If practical circuit considerations make it necessary to operate with a much smaller grid drive or a high impedance driving source, the series grid resistor should be removed. With less effective grid bias, the output will be smaller, and because of the greater conduction angle, the lower-frequency harmonics will be relatively larger. This circuit is arranged to give best output at the fifth harmonic. Coupling and bypassing values are chosen for an input frequency of from 80 kc/sec to 1 Mc/sec.

The same Class C amplifier is shown in Fig. 15-1a with a single resonant circuit and in Fig. 15-1b with a double-tuned circuit. Table 15-1 compares the characteristics of the two circuits with typical design values for a frequency multiplication of five. It is assumed that the double-tuned circuit has identical primary and secondary circuits and critical coupling between the two coils. The double-tuned circuit clearly has an advantage both as to attenuation of undesired harmonics and stability of phase. In many practical cases it may be difficult to obtain a  $Q$  as high as that specified for the single resonant circuit. The simpler circuit is used only if the requirements for purity of output waveform and phase stability are not great. The specific values of  $L$  and  $C$  given in the table

TABLE 15-1.—CALCULATED OUTPUTS FROM SINGLE AND DOUBLE-TUNED CIRCUITS OF  
FIG. 15-1

(Same current waveform for each)

	Fig. 15-1a	Fig. 15-1b
$Q$ primary .....	100	30
$Q$ secondary .....	.....	30
Reactance of $L$ in ohms at resonant frequency ..	400	1,333
Peak voltage at fourth harmonic .....	5	1.3
Peak voltage at fifth harmonic .....	180	90
Peak voltage at sixth harmonic .....	3.5	1.1
Phase shift in degrees for 0.1 per cent change in resonant frequency .....	11.6	3.4
Inductance in $\mu$ h for 410-kc output .....	151	503
Capacitance in $\mu$ mf for 410-kc output .....	943	283

are those required for an output frequency of 410 kc/sec and the impedance levels given in the table. For these resonant circuits and all others discussed in this section it is usually most convenient to use fixed inductors and capacitors whose values are close to the calculated ones and to make adjustment to exact resonance by the use of a small variable capacitor shunted across each fixed capacitor.

Oscillators that are operated with large grid drive have plate current flowing in pulses in a manner similar to the Class C amplifiers that have been described here. Oscillators employing pentodes or tetrodes can be so arranged that the oscillations in the grid circuit are maintained almost independent of the load impedance in the plate circuit. It is then possible to tune the plate load to a harmonic of the oscillator frequency. This arrangement is often used with crystal oscillators to generate stable frequencies that are higher than those of available crystals.<sup>1</sup> This method is seldom used for multiples greater than five. Figure 15·4 is a crystal oscillator with the plate circuit tuned to a harmonic of the crystal frequency.

If two Class C amplifiers are driven in push-pull, as shown in Fig. 15·5*b*, each has a train of current pulses which are identical except that they differ in phase by one-half cycle of the input wave. If the two plates are connected in parallel to drive a single load impedance as in Fig. 15·5*a* (sometimes called a "push-push" connection), the output contains only the even harmonics of  $f$ . If the difference of the two currents is applied to the load impedance in the push-pull plate connection of Fig. 15·5*b*, the output contains only the odd harmonics. Of course if the circuit is not exactly balanced this separation of harmonics is not complete. Since in these circuits the harmonics are spaced twice as far apart in frequency as they are in the single-tube multipliers, the tuned circuits are not required to have such large values of  $Q$  and the resulting phase stability is much better. It is considerably easier to generate good sine waves at high harmonics by this method.

Class C multipliers with a multiplication as high as 20 in a single stage

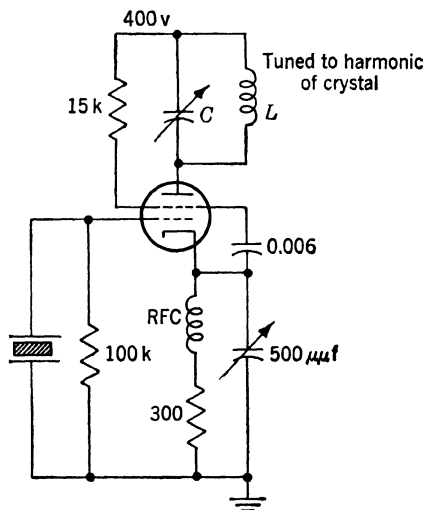


FIG. 15·4.—Crystal oscillator with plate circuit tuned to harmonic.

<sup>1</sup> *The Radio Handbook*, 1942, p. 161.



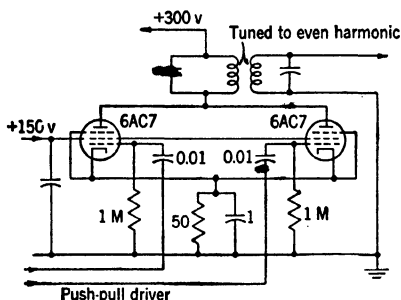
can be made to give an output of a few volts. For large multiplications it is usually necessary either to cascade several stages of lower multiples or to add an amplifier to bring the output to a usable level.

Attempts have sometimes been made to synchronize oscillators by introducing large synchronizing signals at some submultiple of the oscillator frequency into some point of the oscillating circuit. Superficially this proposal appears to be particularly attractive when the desired output is some nonsinusoidal waveform, because the oscillator can often be

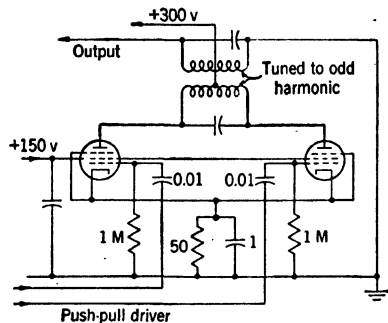
made to generate the desired waveform directly. These attempts have usually led to unsatisfactory results. The free-running characteristics of the oscillator and the synchronizing input are competing for control of the output waveform. Any change in the free-running frequency of the oscillator, the gain of the oscillator tube, or the size of the synchronizing signals greatly affects the output. This type of multiplier is not recommended when the waveform is required to be stable in phase, amplitude, or wave shape.

Figure 15-6 is a practical circuit for multiplying 100 kc/sec by 100 in steps of 5, 4, and 5. Each multiplier stage is operated Class C, and the selective filters are double tuned. The use of 6AC7's gives each stage sufficient gain to make up the loss in the filter.

Figure 15-7 is a block diagram of a reactance-tube-controlled



(a) Multiplier for even harmonics.



(b) Multiplier for odd harmonics.

FIG. 15-5.—Balanced multipliers.

frequency synchronizer, and Fig. 15-8 is a circuit that employs this principle to multiply a 100-kc/sec sine wave by 10 to obtain 1 Mc/sec. In Fig. 15-8 the input is a low-level (about 2 volts) 100-kc/sec sine wave and the output is a 1-Mc/sec sine wave. Tube  $V_4$  is a free-running oscillator at approximately 1 Mc/sec; its exact frequency is controlled by the reactance tube  $V_5$  and can be varied by changing the grid bias on  $V_5$ . Amplifier  $V_1$  operates at 100 kc, and  $V_2$  is a Class C amplifier with a conduction angle of approximately  $90^\circ$ . The delay line in the plate circuit generates short square voltage pulses at the leading and trailing edges of the conduction cycle. Tube  $V_3$  is a time selector with inputs of the 0.3  $\mu$ sec

gate ( $A$  in the figure) from the delay line and the output of the 1-Mc/sec oscillator. The output of  $V_3$  ( $E$  in the figure) is rectified in  $V_7$  and smoothed and is used to control the reactance tube  $V_5$ , which, in turn, controls the frequency of the 1-Mc/sec oscillator. In this way the 1-Mc/sec oscillator is kept in synchronism with the input 100 kc/sec. The output  $B$  is used to select a pulse from the 1 Mc/sec oscillator.

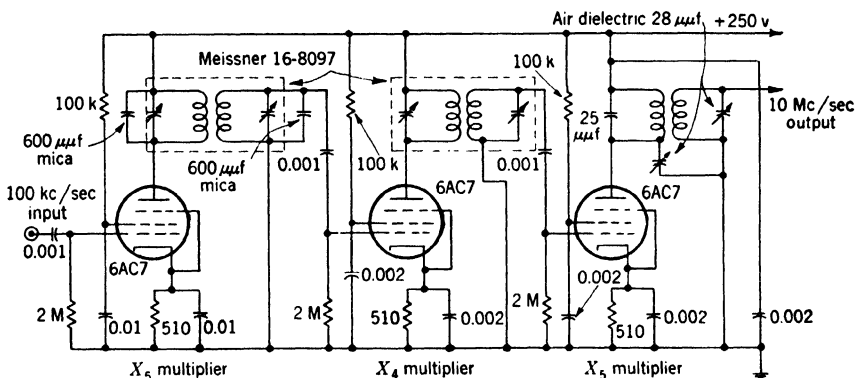


FIG. 15-6.—100-kc/sec to 10-Mc/sec multiplier.

The voltage diagram  $D$  on the figure indicates the amount that the 1-Mc/sec oscillator can be controlled by the reactance tube. For the 1-Mc/sec frequency, diagram  $E$  shows the plate voltage of  $V_3$  when the phase is lagging, correct, and leading. When the frequency and phase are correct, the selector pulse from the 100-kc/sec source overlaps the second

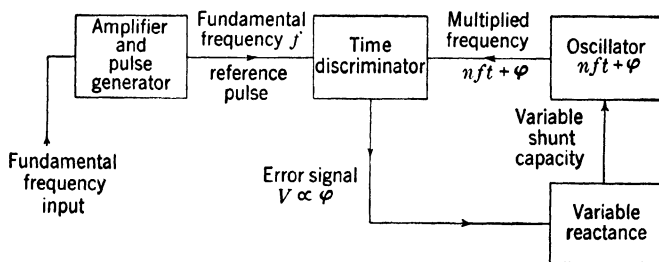


FIG. 15-7.—Block diagram of reactance-tube-controlled frequency synchronization.

$90^\circ$  interval of the 1-Mc/sec sine wave; if the frequency is too high, the overlap provides less output at  $V_3$ ; and if the frequency is too low, the overlap provides more output. The rectified current from a correct overlap is balanced against the voltage from  $R$  in the stable condition, and hence the time discriminator  $V_3$  and  $V_7$  control the reactance of the reactance tube  $V_5$ .



Frequency division has essentially the same uses as frequency multiplication in the production of synchronized wave trains of harmonically related frequencies. One use is in frequency standards where submultiples of the master-oscillator frequency may be developed.<sup>1</sup> In this case phase lock is not essential but the waveform should be good and frequency ratio should be stable. In this application, dividers deriving the submultiple frequencies from a high-frequency standard have one marked advantage over multipliers operating from a low-frequency standard. If the output waveform is imperfectly filtered the stray components from a divider are all harmonics of the required output. The stray frequencies from a multiplier are restricted only to rational ratios of the required output frequency. Hence the number of possible stray frequency components is much less in the output of a divider than in the output of a multiplier.

Division is used as a synchronizing method for multiple-scale timing systems. For this use precise phase lock is usually required between input and output waveforms. If the required low-frequency waveform is not sinusoidal, it can usually be obtained more simply and reliably by the synchronization of relaxation oscillators (Chap. 16). Although there are some multiple-scale systems employing sine-wave references throughout, the majority of the radar and television timing systems employ pulses as the low-frequency time reference. For this reason the problem of good phase lock in sinusoidal dividers has not been given the consideration that the problem has had with respect to frequency multipliers or dividers employing relaxation oscillators. The information from publications or other available sources is not very complete. Only the regenerative modulator divider has been treated thoroughly. The characteristics of divider circuits are summarized here without an exhaustive treatment.

In a limited sense frequency division is analogous to frequency multiplication. That is, a waveform must be generated which has a component of the desired output frequency. Then, since the required output is sinusoidal, a frequency selector is required to select the desired frequency from all the components generated. It is desired that this filtering should not introduce variable phase shifts into the output. Because of the limited transient response of the filters that must be used, sinusoidal division is applicable only to continuously generated sine waves.

One method of generating waveforms with subharmonic content is to apply a sine wave to a nonlinear inductance through a suitable auxiliary circuit. The behavior of these circuits is critically dependent on driving

<sup>1</sup> For instance, crystal clocks. See F. R. Stansel, "Secondary Frequency Standard," *Proc. I.R.E.* **30**, 157 (April 1942).

voltages and initial conditions in a manner not generally understood. The method is at present of little more than academic interest.<sup>1</sup>

Division may be performed by comparing the phase of an oscillator output with a synchronizing signal at a harmonic of the oscillator. The signal depending on the phase error between the two sine waves is used to control the tuning of the oscillator in such a direction as to reduce the phase error. In the block diagram shown in Fig. 15-7 the reactance tube can just as well be connected to the lower-frequency oscillator, in which case the time discriminator controls its frequency to be an exact submultiple of the reference frequency. The limit of the division ratio is determined by the time discriminator (Chap. 14) whereas the stability problems are characteristic of electronic servos. A divider of this type is probably capable of larger division ratios, in one step, than any other circuit discussed in this chapter.<sup>2</sup>

The practical methods of generating subharmonics are methods of synchronizing oscillators. A relaxation oscillator can be synchronized at subharmonics of a control frequency. Since relaxation oscillators always have a definite recovery time and are often employed as time bases, they are referred to as "dividers using a time base." Regenerative oscillators can be synchronized (though not very stably) by introducing a harmonic frequency-control signal at a suitable point in the circuit. These are called "regenerative dividers." A third type of divider operates regeneratively and includes modulation devices in the feedback circuit; these are referred to as "dividers using regeneration and modulation."

Certain general relations between the waveform of an oscillator and its frequency stability and synchronizing characteristics have been demonstrated. The presence of harmonics in the output of a free-running oscillator produces frequency instability.<sup>3</sup> Synchronization of an oscillator at a subharmonic of an input signal depends on interactions between the input signal and harmonics of the oscillator. Consequently, regenerative oscillators with sinusoidal output are very stable in frequency but are comparatively hard to synchronize. Relaxation oscillators, which usually have complex waveforms, are relatively instable in frequency but are easier to synchronize both in frequency and phase.

A frequency-dividing circuit must have enough frequency stability

<sup>1</sup> C. F. Spitzer, "Sustained Subharmonic Response in Nonlinear Series Circuits," *J. Applied Phys.*, **16**, 105 (February 1945).

<sup>2</sup> F. C. Williams and T. Kilburn, "Time Discriminators, Automatic Strokes, and Pulse-recurrence Frequency Selectors," Part II, I.E.E. Convention Paper, March 1946.

<sup>3</sup> J. Groszkowski, "The Interdependence of Frequency Variation and Harmonic Content," *Proc. I.R.E.*, **21**, 958—981 (July 1933).

so that changes in tube gain and supply voltages do not cause it to operate at the wrong submultiple. It must, at the same time, be sufficiently easy to synchronize so that small changes in the free-running frequency do not cause the divider to fall out of synchronization.

**15-6. Dividers Using a Time Base.**—Many divider circuits are made with relaxation time bases (Chap. 16). In addition to the natural waveform of the divider, it may be desirable to have a sine wave of the same frequency. When the waveform contains a sizable component of the fundamental frequency, that component can be selected by a filter designed to pass the desired frequency. The cases of most practical interest occur when the waveform to be filtered is either a symmetrical square wave from a multivibrator or a sawtooth from a gas-tube relaxation oscillator or from the grid circuit of a blocking oscillator. These waveforms contain very small components of the even harmonics; hence it is possible to separate the fundamental frequency with a relatively broad filter having small phase shift. Three things can produce variable phase shift in the sine wave: variable time delays in the operation of the relaxation oscillator, changes in the waveform from the oscillator which may result in relative phase shift of the sine-wave component, and changes in the filter transfer impedance. The time delays of the divider are discussed in Chap. 16. An example of the second difficulty occurs when the duty ratio of a multivibrator waveform is not exactly 50 per cent. The difficulty in this case is removed by making the multivibrator waveform symmetrical. The phase shifts in the filter depend on stability and bandwidth in the same way that they do in frequency multipliers (Sec. 15-3).

Selection of the desired sine-wave component is accomplished by applying the complex waveform from the relaxation time base to the grid of an amplifier whose plate load is tuned to the desired frequency. A practical circuit of this sort using a multivibrator divider is used in the SCR-584 circular-sweep display circuits shown in Fig. 15-9.

Synchronized relaxation oscillators can be greatly improved in frequency stability by incorporating tuned circuits in a suitable manner (Chap. 16). Builder<sup>1</sup> has described an ingeniously stabilized gas-tube relaxation oscillator in which the same tuned circuit serves to stabilize the free-running frequency and to select the sine-wave component for the output. It has been used as a frequency divider for division ratios up to ten.

The frequency range, possible frequency ratios, and stability ratios are essentially the same for these circuits as for the circuits of Chap. 16 inasmuch as the actual division is done by the relaxation oscillator. They are useful because they can be synchronized either with sine waves

<sup>1</sup> G. Builder, "A Stabilized Frequency Divider," *Proc. I.R.E.*, **29**, 177 (1941).



between the synchronizing signal and the output is smallest when  $E_{syn}$  is large,  $Q$  is small, and  $f_{syn}$  is equal to  $f_0$ .

Resistance-capacitance oscillators of the phase-shift type or of the bridge type have synchronizing characteristics similar to those of oscillators with resonant feedback circuits in which the resonant circuit has a  $Q$  of about one, and are particularly easy to synchronize. This type of synchronized oscillator can be considered as a "divider" with a one-to-one frequency ratio. As such, it has little use in synchronizing systems, although it is used as an oscillator limited to give large, constant output at a frequency determined by a small, variable amplitude input. The properties of this device do shed considerable light on the method of synchronization of true dividers.

If the synchronizing signal is of frequency  $nf_{syn}$  approximately equal to  $nf_0$ , where  $n$  is a positive integer and  $f_0$  is the free running frequency, synchronization can occur at the frequency  $f_{syn}$ . This synchronization arises because cross modulation between the frequency  $nf_{syn}$  and harmonics of the oscillator produces a component of frequency  $f_{syn}$ .<sup>1</sup> This serves the oscillator as a synchronizing signal with a one-to-one frequency ratio. In the strictest sense, synchronization is due to a combination of regeneration and modulation, but there is no element in the circuit specifically designed to perform the modulation operation. The amplitude and phase of the synchronizing signal depends in an exceedingly complex manner on the amplitude distortions and the frequency response of the oscillator. In general it may be said that operating the oscillator at low output level with sharply tuned elements, which is the necessary condition for frequency stability and sinusoidal output, will lead to nearly zero amplitude of the synchronizing voltage at the frequency  $f_{syn}$ ; hence small variations in operating conditions can lead to excessive phase shift or even to total failure of synchronization. The oscillator continues to give an output in the absence of all synchronization. For these reasons this type of divider is not useful where stability is important. Even when used for division ratios not greater than three, its phase errors can be large and variable. The "design" is experimental, because the non-linear analysis is so difficult and because the optimum stability conditions are seldom realized.

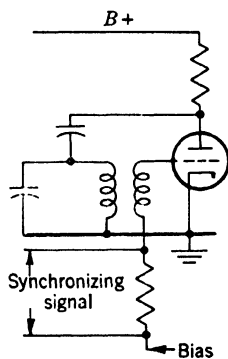


FIG. 15-10.—Syn-  
chronized sine wave os-  
cillator.

<sup>1</sup> R. L. Fortescue, "Quasi-stable Frequency Dividing Circuits," *J. Inst. Elec. Eng.* (June 1939).



One example of a regenerative oscillator<sup>1</sup> that can be directly synchronized at a subharmonic of a control frequency and that has no output in the absence of synchronizing signal is shown in Fig. 15-11. Its limitations are as stated in the previous paragraph. This is a conventional oscillator except that the plate supply is not a direct current but an alternating voltage at the synchronizing frequency. The resonant

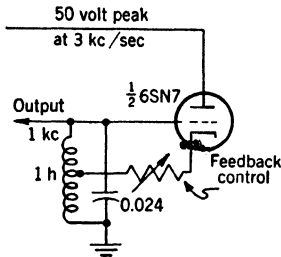


FIG. 15-11.—Regenerative divider.

circuit is tuned to the desired output frequency and the feedback is adjusted to maintain oscillation. The output can be at any frequency  $m/n$  times the control frequency, where  $m$  and  $n$  are small integers. This means that the circuit can divide or multiply the frequency by rational numbers as well as by integers. The frequency ratio should not exceed 3. About the only advantage of this circuit is extreme simplicity in construction. It is not sufficiently reliable for most purposes.

**15-8. Dividers with Regeneration and Modulation.**—The previous section has shown that in simple synchronization of a regenerative oscillator at a subharmonic of the control frequency, those factors that aid frequency selection in the regenerative loop make it more difficult for a satisfactory synchronizing signal to be generated by cross modulation. The necessary conditions for a good divider can be met by performing the regeneration and modulation functions in different parts of the circuit. Each function can then be performed with optimum efficiency without in any way interfering with the other. A block diagram of one method<sup>2</sup> is shown in Fig. 15-12. The oscillator has a free-running frequency  $(f + \epsilon)$ , where  $\epsilon$  is small compared to  $f$ . Its output is multiplied by  $(n - 1)$  to  $(n - 1)(f + \epsilon)$  by the frequency multiplier. This frequency and the frequency  $nf$ , which is to be divided by  $n$ , are applied to the square-law modulator. In addition to the input frequencies the output contains the sum and difference frequencies  $[nf + (n - 1)(f + \epsilon)]$  and  $[f - (n - 1)\epsilon]$ . The difference frequency is selected by a filter and is applied as a synchronizing signal to the oscillator in the manner suggested by Fig. 15-10 of Sec. 15-7. The synchronizing signal tends to decrease  $\epsilon$ , and the stable state of the system is that in which the synchronizing signal frequency is equal to the oscillator frequency—that is,  $\epsilon = 0$ —and the output frequency is exactly  $f$ . Thus the frequency  $nf$  has been divided by  $n$ . If the frequency multiplier has a multiplication  $(n + 1)$ ,

<sup>1</sup> J. Groszkowski, "Frequency Dividers," *Proc. I.R.E.*, **18**, 1960 (1930).

<sup>2</sup> D. G. Tucker, "The Synchronization of Oscillators," *Electronic Eng.*, Part III, 26 (June 1943).

the difference frequency is  $[f + (n + 1)\epsilon]$  and the system has no stable state.

Dividers of this sort have been operated successfully. They are self-starting and may be operated with very large division ratios. One objection is that the oscillator continues to give an output even if the synchronization fails entirely. Another objection is that in addition to the phase shifts introduced by the filter element, there can be a sizeable

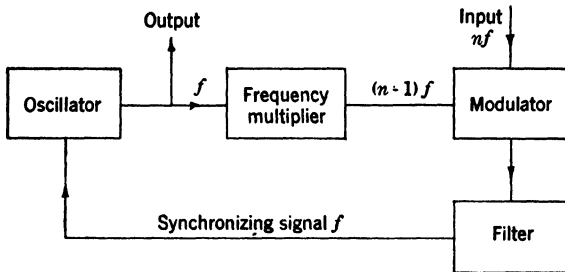


FIG. 15-12.—Oscillator synchronized at subharmonic of control frequency.

phase shift between the fed-back synchronizing voltage and the oscillator output.

The block diagram of an arrangement that eliminates these difficulties is shown in Fig. 15-13. Here the oscillator of Fig. 15-12 is eliminated and the difference frequency is fed directly into the frequency-multiplying circuit. If the gain around the loop through the modulator and frequency multiplier and back to the modulator input exceeds one, the output builds up as in any regenerative oscillator. The regeneration is independent of the phase shifts in the system. To assure that the divider give only the desired frequency, it is necessary that the loop gain be less than one for other subharmonic frequencies. If the input is absent there is no output, since the conversion gain of the modulator is proportional to the amplitude of the input at the control frequency. The circuit cannot operate without a sufficiently large input at both frequencies,  $nf$  and  $(n-1)f$ , to give unity gain in the feedback loop. The divider may not be self-starting because frequency multipliers are nonlinear and that portion of the loop may have very low gain for small signals. Many circuits will have sufficiently large transients from the application of plate voltages and control signal to start them. In the designs of dividers

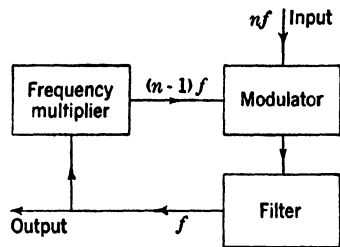


FIG. 15-13.—Regenerative divider using square-law modulation.

that are not self-starting, it is necessary to introduce sizeable starting voltages.<sup>1</sup>

The phase relations with respect to the input sine waves are easily determined. Assume zero phase for the input sine wave. Let  $\phi$  be the phase at the output of the modulator filter. Let  $\theta_1$  and  $\theta_2$  be the phase shifts produced by the frequency-selecting circuits at frequencies  $f$  and  $(n - 1)f$  respectively. The output phase of the frequency multiplier is then  $(n - 1)\phi + \theta_2$ , and the output phase at the modulator filter is  $-(n - 1)\phi - \theta_2 + \theta_1$ . By definition  $\phi = -(n - 1)\phi - \theta_2 + \theta_1$ , or  $\phi = \theta_1 - \theta_2/n$ . The phase shift in the filter circuits can be made nominally zero. The variable phase shifts in the output are equal to the difference in variation of the filter phase shifts divided by  $n$ . They can be made very small. Dividers of this sort have shown phase shifts too small to measure with reasonable changes in control-signal amplitude. Shifts of the order of  $2^\circ$  have been observed with changes of more than 30-db control-signal amplitude. A divider of this type has a phase stability superior to that of all other types considered in this chapter.

So far the discussion has assumed that a square-law modulation is used. If a higher-order modulation is used—that is, modulation that depends on current components that vary as powers of grid voltage higher than the second power—other frequency ratios can be obtained. Another possibility is to select the  $m$ th harmonic in the frequency multiplier as an output frequency. By these means an output of frequency  $m/n$  times the input frequency may be obtained, where  $m$  and  $n$  are positive integers. It is thus theoretically possible to divide (or multiply) by any rational ratio. Large ratios imply the necessity of very selective filters to prevent the possibility of output at the wrong subharmonic.

Design methods and the results of theoretical and experimental investigations for these dividers have been published by R. L. Miller.<sup>2</sup> It is shown there that if certain linearity requirements are met in the frequency-multiplying and modulating circuits, the output amplitude is a linear function of input amplitude over a considerable range.

Many of the practical designs included in the literature employ contact rectifiers as modulators and harmonic generators. Selenium and germanium rectifiers seem to be particularly suited to this application.

Dividers with regeneration and modulation have certain advantages over relaxation-oscillator dividers. There is no output unless there is a synchronizing input. If the frequency response of the feedback loop is chosen so that oscillation can be maintained at only one subharmonic, the

<sup>1</sup> R. L. Fortescue, "Quasi-stable Frequency Dividing Circuits," *J. Inst. Elec. Eng.* (June 1939); R. L. Miller, "Fractional Frequency Generators Utilizing Regenerative Modulation," *Proc. I.R.E.* **27**, 438 (1939).

<sup>2</sup> Miller, *loc. cit.*

output, if present, must be synchronized at the proper subharmonic. The gain must be large enough for the circuit to regenerate, but when that condition is met the only effect of gain changes in the circuit is to change the size of the output. In contrast, a relaxation-oscillator divider may change its division ratio with changes in tube characteristics and supply voltages. The frequencies at which these dividers can operate is limited only by the frequency range over which amplifiers, modulators, and frequency multipliers can be built. Relaxation oscillators are limited to about 1 Mc/sec, at which frequency they are not very easy to synchronize. By the use of narrow and stable filters and good harmonic generators (possibly cascaded multipliers), dividers employing regeneration and modulation may be extended over almost any desired frequency

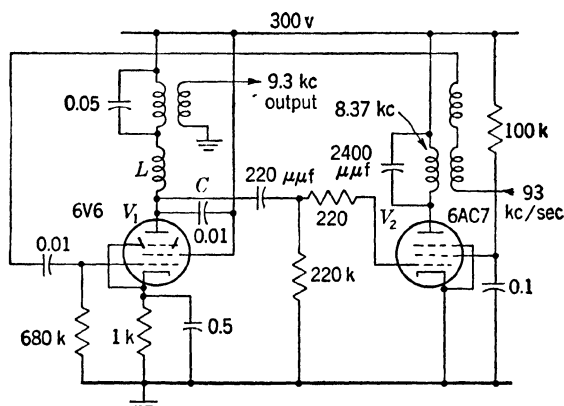


FIG. 15-14.—Regeneration and modulation divider, AN/APN-3.

ratio. The chief disadvantages are relative complexity and the fact that some designs require special starting devices.

A regeneration and modulation divider circuit<sup>1</sup> that was employed in the AN/APN-3 range unit is shown in Fig. 15-14. It can give considerable power in the output and divides from 93 kc/sec to 9.3 kc/sec. With division ratios no larger than this, a considerable range of values is possible in the resonant coupling circuits without producing outputs at incorrect frequencies. The output power obtained and the input amplitude necessary to control operation depends on the values in these circuits. The components  $L$  and  $C$  in the figure and the “scrambling” pulse (not shown, see Vol. 20, Chap. 6) assure that the divider will be selfstarting. Tube  $V_1$  serves to produce modulation products of the input and the output of the frequency multiplier. The output transformer is tuned to the difference frequency. Tube  $V_2$  serves as a fre-

<sup>1</sup> The AN/APN-3 is the airborne part of a precision-radio-navigation equipment manufactured by RCA, Camden, N.J.

quency multiplier to produce the 83.7-kc/sec component (nine times 9.3 kc/sec). Exact values of phase variation depend on the stability and bandwidth of the resonant circuits employed.

When the division ratio is 2, a simple modulation scheme such as that of the previous circuit should not be used. Direct feedback of the frequency  $f/2$  would occur in the modulator tube and would usually exceed the component of that frequency produced as a modulation product and would take over control of the circuit. This introduces the possibility of free oscillation in the divider. If a balanced modulator is used the circuit can be made to operate stably. For division by 2, it is self-starting. Dividers using contact rectifiers in a balanced square-law modulator and one vacuum tube as the feedback amplifier are described in the literature.<sup>1</sup> Modulators of this type can be made to operate as higher-order modulators. This makes other division ratios available without the use of frequency multipliers. Circuits using two vacuum tubes in a balanced modulator for division by 2 or 3 are described by Sterkey.<sup>2</sup> These circuits require complex transformers of special design.

<sup>1</sup> Tucker, *loc. cit.*; Miller, *loc. cit.*

<sup>2</sup> H. Sterkey, "Frequency Division," *Proc. I.R.E.*, **25**, 1153 (1937).

## CHAPTER 16

### PULSE-RECURRENCE-FREQUENCY DIVISION

By A. H. FREDERICK, V. W. HUGHES, AND E. F. MACNICHOL, JR.

#### GENERAL CONSIDERATIONS

**16-1. Definition.**—Pulse-recurrence-frequency division is the process of producing equally spaced pulses recurring at a frequency  $f_2$  from equally spaced synchronizing or controlling pulses recurring at a higher frequency  $nf_2 = f_1$  where  $n$  is an integer. The requirement of equal pulse-spacing distinguishes pulse-divider circuits from pulse-counting circuits,<sup>1</sup> which can also function as pulse-recurrence-frequency (PRF) dividers. The controlling pulses  $f_1$  may recur continuously or they may

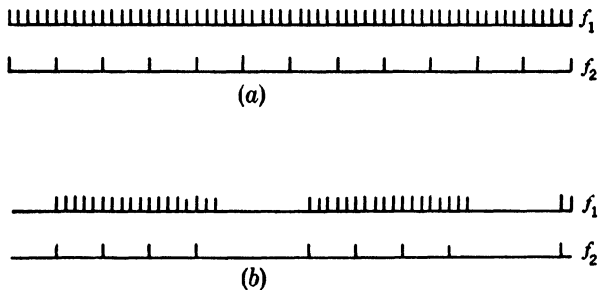


FIG. 16-1—(a) Continuous pulse recurrence frequency division. (b) Intermittent pulse recurrence frequency division.

recur in finite groups separated by intervals during which no pulses occur. In the former case, the  $f_2$  pulses occur continuously and the division is said to be continuous. In the latter case, the  $f_2$  pulses as well as the  $f_1$  pulses occur in groups spaced from one another, and the division is intermittent. These differences are illustrated in Fig. 16-1. In all cases intermittent-PRF-divider circuits are capable of continuous-PRF division although they may be more elaborate than is necessary for continuous division.

**16-2. Characteristics of Pulse-recurrence-frequency Dividers.**—Great variations are possible in the characteristics of pulse-recurrence-frequency dividers. For the practical circuits to be given in this chapter

<sup>1</sup> See Chap. 17 for a discussion of pulse-counting circuits.

the input pulses upon which the frequency divider operates will ordinarily be rectangular pulses about one microsecond in duration and 10 to 100 volts in amplitude, yet widely different input pulses can be treated with the general circuit types discussed. The output pulses from a frequency divider are ordinarily generated in the frequency-divider circuit and are often, though not always, very similar to the input pulses. The division ratio—that is, the ratio of the recurrence frequency of the input pulses to the recurrence frequency of the output pulses—is anywhere from two to several thousand or more; there is theoretically no limit to the division ratio for continuous frequency division. Practical limitations on circuit complexity and requirements on the uniformity of output-pulse spacing usually necessitate that the division ratio be less than 20 per divider stage. If considerable nonuniformity in output-pulse spacing is tolerable, division ratios of several thousand can be used.

Of primary concern is the question of the accuracy of the frequency divider and there are two types of errors to which frequency dividers are subject. First, the division ratio may not be constant; the resulting variation in the recurrence frequency of the output pulses is called “frequency jitter.” In a divider circuit with a single stage, if the division ratio is as large as 1000, this ratio may vary by several per cent over short periods of time under normal laboratory conditions. Second, there may be a delay between an input pulse to the divider and the output pulse initiated by it. This so-called “phase delay” is caused by finite response speed of the divider and finite rise times of the input pulses. It may vary with time; the jitter so produced is called “phase jitter.” For most of the dividers discussed, including those with high division ratios, phase delays are less than 1  $\mu$ sec; some precision circuits have phase delays of 0.1  $\mu$ sec or less. The stability of the division ratio and of the phase delay with respect to changes of circuit parameters, such as the supply voltages, tubes, and components, is a matter of great importance.

The input requirements of frequency dividers—that is, the amplitude and source impedance of the input pulse—vary considerably and are often critical.

**16-3. Uses of Pulse-recurrence-frequency Dividers.**—The main application is in electronic timing circuits. Often timing operations require a number of synchronized pulse-wave trains of different pulse spacings. Figure 16-2 shows a pulse-wave group typical of those often associated with radar timing systems and with calibrators.<sup>1</sup>

<sup>1</sup> A discussion of time-marking pulses as applied to cathode-ray-tube measurement is found in Chap. 20 and Vol. 20, Chap. 7; synchronizing systems employing frequency dividers are discussed in Vol. 20, Chap. 4. Test oscilloscopes containing frequency dividers are discussed in Vol. 21, Chap. 18.

**16·4. Methods for Accomplishing Continuous Pulse-recurrence-frequency Division.**—*Astable Relaxation Oscillators.*—There are two widely used fundamental methods of pulse-recurrence-frequency division. The first involves the synchronization of an astable pulse-generating oscillator at a frequency somewhat higher than its normal frequency. Relaxation oscillators—for example, multivibrators, blocking oscillators, and gas discharge tube (“gas tube”) oscillators—are the basis of nearly all such dividers. The output of these relaxation oscillators may have to be shaped into appropriate pulses. The principal advantages of these oscillators are the ease of synchronization, the simplicity, and the ability to produce pulse-output waveforms or waveforms that can easily be converted to pulses. Some representative circuits and their waveforms are indicated in Fig. 16·3.

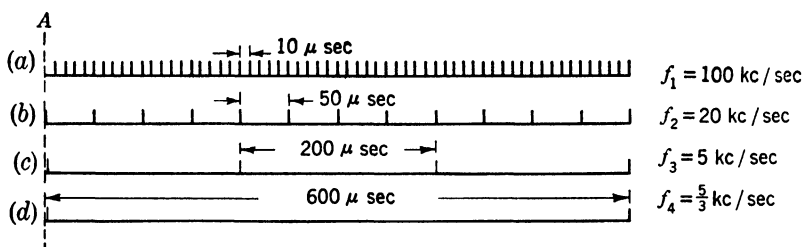


FIG. 16·2.—Typical synchronized pulse wave trains for electronic timing.

*Monostable Oscillators.*—The second fundamental method involves the use of a monostable oscillator that can be triggered by the first input pulse appearing after the end of its active period. Two basic circuits are shown in Fig. 16·4. The duration of the “on” period of the monostable oscillator must be greater than the time between  $n - 1$  of the input pulses and less than the time between  $n$  of the input pulses, where  $n$  is the division ratio. When these conditions are fulfilled, the oscillator will be triggered only by every  $n$ th pulse. The leading edge of the output from the oscillator can be used to produce the output pulse. Multivibrators and Miller feedback rectangle generators of the type discussed in Chap. 5 are often used in this type of frequency division.

*Use of Time Selectors.*—An important variation that is particularly valuable in the reduction of phase jitter and that can be employed with either of these methods involves the use of a time-selector circuit. A selector pulse that is sufficiently long to span the first pulse after the pulse that initiates it is generated by either type of divider at the time of every  $n$ th pulse. This selector and the input pulses are applied to a time-selector circuit whose output then consists of uniformly spaced pulses with frequency  $1/n$  times that of the input pulses.



**Frequency Tracking.**—Still another type of divider employs the principle of frequency tracking. In Chap. 15 it was shown that a frequency multiplier could be produced by synchronizing the phase of an oscillator operating at a multiple of the input frequency by use of a time-discrimi-

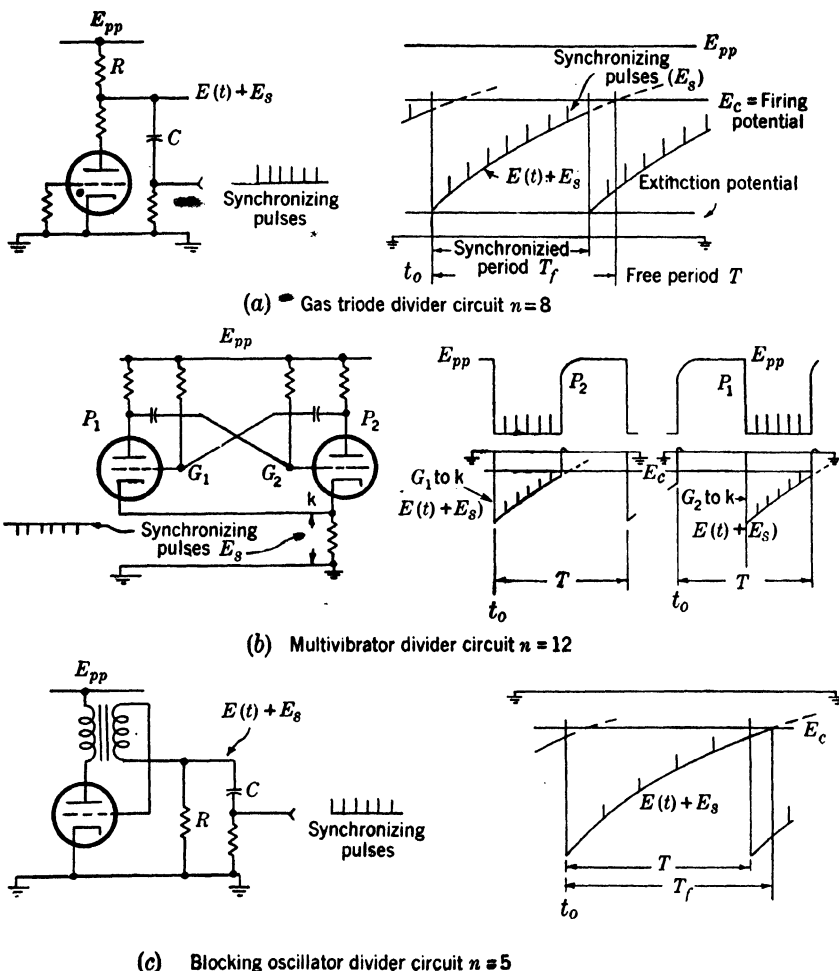


FIG. 16-3.—Synchronized relaxation oscillator frequency dividers. (a) Gas tube divider circuit,  $n = 8$ . (b) Multivibrator divider circuit,  $n = 12$ . (c) Blocking oscillator divider circuit,  $n = 5$ .

nator circuit which controls a frequency modulator. The same principle may be used in frequency division as shown in Fig. 16-5.

A stable oscillator is set to operate approximately at frequency  $f_2$  when no input is present. From the output of the oscillator a pair of

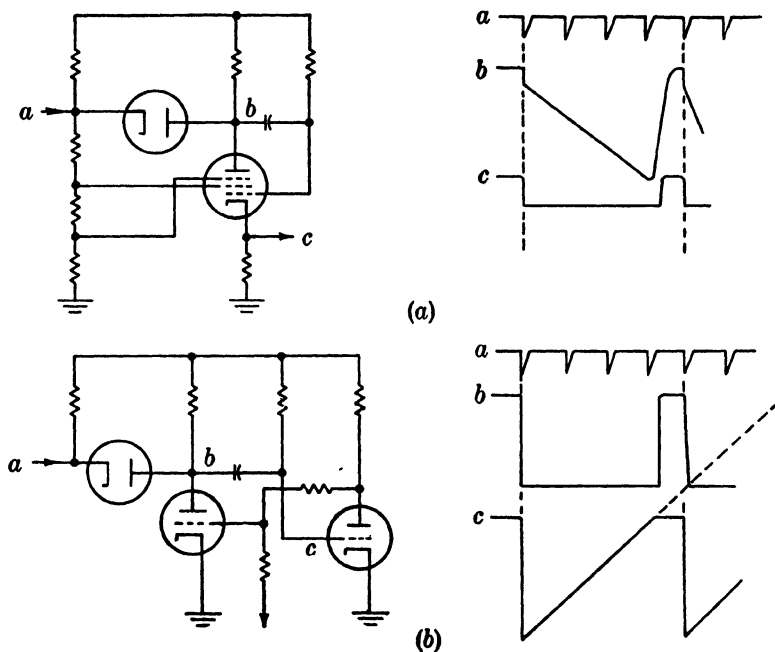


FIG. 16-4.—Monostable frequency dividers. (a) Phantastron. (b) Multivibrator.

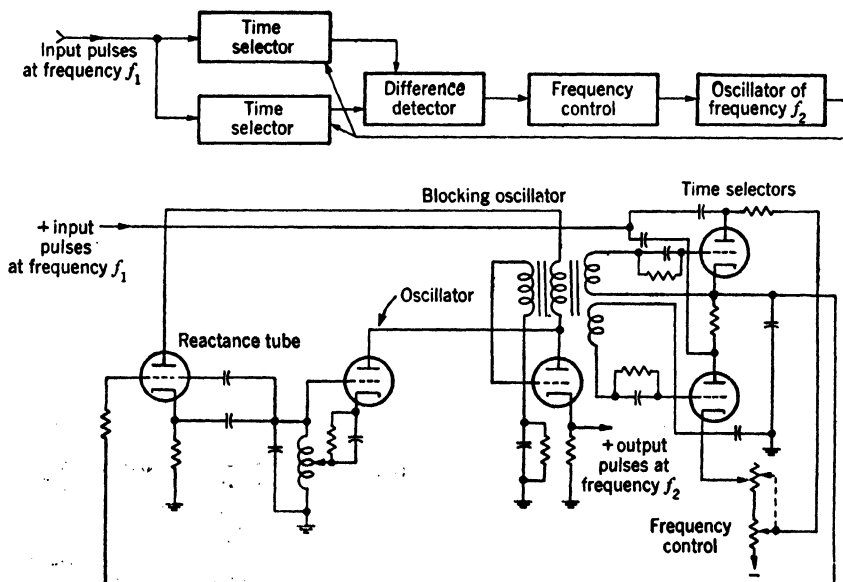


FIG. 16-5.—Block diagram and circuit for frequency tracking divider.

time-selector pulses is obtained by means of a blocking oscillator. In this case the second pulse is formed by the overshoot of the blocking-oscillator pulse. The input pulse of frequency  $f_1$  and the two selector pulses of approximate frequency  $f_2$  are applied to a time discriminator whose d-c error signal operates on a reactance tube which controls the frequency of the oscillator. This frequency will be maintained at  $f_2 = f_1/n$  because the tracking loop forces the selector pulses to span equal areas of the input pulse.<sup>1</sup>

### SOME FUNDAMENTAL CIRCUITS AS CONTINUOUS FREQUENCY DIVIDERS

**16-5. Monostable Multivibrators.**—The monostable multivibrator is often used as a frequency divider. Essentially the operation depends on the fact that while the multivibrator is in its unstable state the input triggers are ineffective, but as soon as the multivibrator has returned to its stable state the next pulse will trigger it. A typical circuit and its waveforms are shown in Fig. 16-6.

In the stable state, the tube  $V_2$  is conducting and its grid is held by diode  $V_4$  at  $-1.5$  volts with respect to its cathode potential. The current of  $V_2$  flowing through  $R_k$  biases off  $V_1$ . The plate of  $V_1$  is held at about 100 volts below  $E_{pp}$  by the current flowing through  $R_1$ ,  $V_3$ ,  $R_3$  and the potential divider. A negative trigger of about 25 volts amplitude will trigger the multivibrator to its unstable state in which  $V_1$  is conducting and  $V_2$  is nonconducting. Both diodes  $V_3$  and  $V_4$  will also be nonconducting, and hence the triggers are isolated from the multivibrator in the unstable state. The capacitor  $C$  charges through  $R$  until the potential at the grid of  $V_2$  rises to the critical potential at which  $V_2$  begins to conduct. A regenerative action then restores the multivibrator to its stable condition. The first trigger that appears after the circuit has been restored to its stable state will now switch the multivibrator back to its unstable state. The positive rectangles that appear at the anode of  $V_2$  start at the time of an input trigger and can be differentiated to generate the train of low-frequency pulses.

The stability of this circuit as a frequency divider is determined mainly by the stability of the period taken for the multivibrator to return to its stable state after being triggered. Variations in the initial charge across  $C$ , in the current that flows through  $V_1$  during the unstable period, or in the cutoff potential of  $V_2$  will cause a variation in this period.

<sup>1</sup> See Vol. 20, Chap. 4, for a further discussion of dividers and many practical circuits.

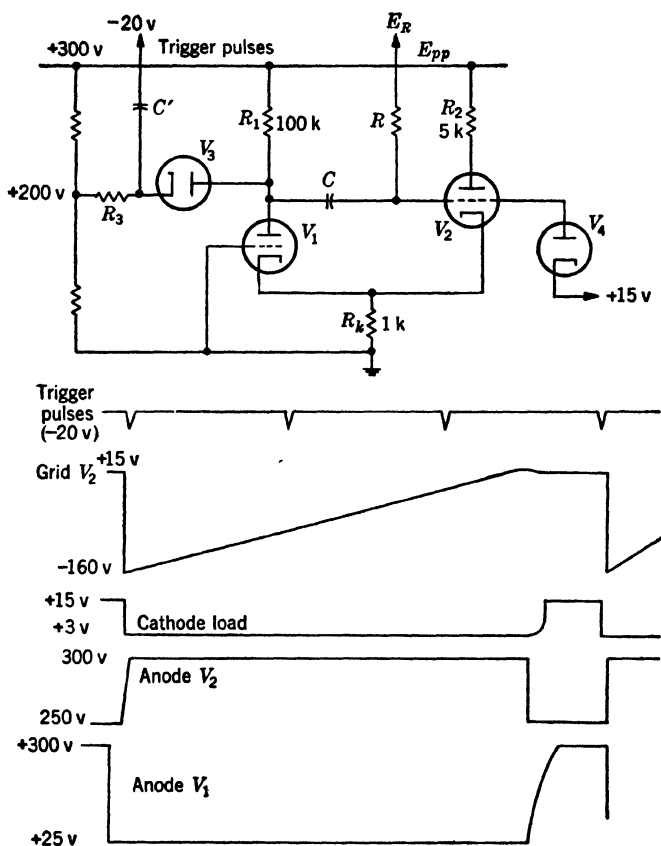


FIG. 16-6.—Typical circuit of monostable multivibrator frequency divider.  $V_1$  and  $V_2$  are 6SN7's.  $V_3$  and  $V_4$  are 6AL5's.

The expression for the period  $T$  is given implicitly by

$$E_c + i_1 R_k = (E_R - E_p)(1 - e^{-\frac{T}{RC}}) - E_1 e^{-\frac{T}{RC}} + E_p \quad (1)$$

where  $E_c$  = critical grid to cathode potential

$i_1$  = current in  $V_1$

$E_R$  = potential of grid return

$E_p$  = potential at plate of  $V_1$

$E_1$  = initial potential across  $C$ .

The potential  $E_1$  is defined by the diodes  $V_3$  and  $V_4$ . The potential  $E_p$  and  $i_1 R_k$  are dependent on the current flowing in  $V_1$  and are ordinarily the most variable quantities. Assuming linear triode characteristics this current is given by  $\frac{E_{pp}}{R_1 + R_p + (\mu + 1)R_k}$ , where  $R_p$  is the plate resistance

of the tube. Hence  $R_1$  and  $R_k$  should be given large values in order to reduce the dependence of the current upon the characteristics of the tube. An optimum size for  $R_1$  and  $R_k$  will exist because  $R_p$  itself is not a constant but becomes larger if smaller currents are drawn through the tube. The critical grid-to-cathode potential  $E_c$  at which  $V_2$  begins to conduct is an important variable, which is dependent on heater voltage.

For the most stable design it is usually desirable that the grid waveform at  $V_2$  have the largest possible slope when it reaches the potential at which  $V_2$  conducts, in order that changes in this critical potential shall have as small an effect as possible on the duration of  $t$ ; this implies that the grid-return voltage  $E_R$  should be as large as possible. But if changes in  $E_p$  as well as changes in  $E_c$  are considered, it can be shown that there is an optimum finite value for  $E_R$ . This question is discussed in the section on blocking oscillators (Sec. 16-8) since for them the choice of an optimum  $E_R$  is of more critical concern.

The transition time between the unstable and stable states is determined by the time constant  $R_1C$  in conjunction with the potentials to which the diodes  $V_3$  and  $V_4$  are returned. By the use of a cathode follower with its grid connected to the plate of  $V_1$  and its cathode connected to  $C$ , this recovery time can be reduced, although the potential across the condenser in the stable state is less well defined. The period required for the transition from the stable state to the unstable state is of the order of 1  $\mu$ sec. It is these transition times that limit to several megacycles the maximum frequency of the output pulses from a multivibrator.

It is reasonable to expect under laboratory conditions to keep  $T$  to within 1 per cent of its mean value so that stable division by 20 to 25 can be expected when the transition times are small compared with  $T$ .

The phase delay between the input trigger and the output trigger at the plate of  $V_2$  is dependent upon the rate of rise of this output trigger and is kept small by the use of a small load resistor in the plate of  $V_2$ . At sufficiently low frequencies the output impedance is approximately that of the load resistor of  $V_2$ .

One of the principal advantages of this monostable type of divider is that it is relatively insensitive to the characteristics of the input triggers, since they have no influence upon the duration of the period during which the multivibrator is in its unstable state.

A practical circuit using subminiature triodes is shown in Fig. 16-7a; waveform photographs are presented in Fig. 16-7b. The normally-off tube  $V_2$  is biased off by the use of the potential divider  $R_2$  and  $R_3$  and the negative supply rather than by the bias due to the plate current of the normally-on tube flowing in a common cathode resistor, as was done in Fig. 16-6. This circuit is preferred to the cathode-coupled variety when an accurately regulated positive and negative supply are avail-

able because the transition grid potentials are better defined. This circuit provides an output pulse at a frequency of about 16 kc/sec. The 5 to 1 division ratio is maintained when the heater voltage is varied from 3.5 to 8.0 volts and when the supply voltage is varied from 40 to 250

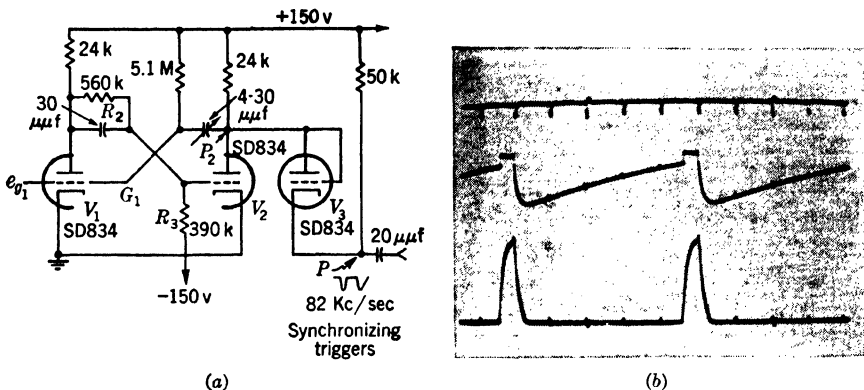


FIG. 16-7.—(a) A 5 to 1 monostable-multivibrator frequency divider. (b) Photographs of waveforms at  $P$ ,  $G_1$ , and  $P_2$ .

volts. Also no readjustment of the circuit was required for 90 per cent of the 150 tubes tried. The phase delay is less than  $0.1 \mu\text{sec}$ .

**16-6. Astable Multivibrator Dividers.**—Astable multivibrators (see Chap. 5) are suitable only for continuous PRF division. They have been used extensively in the past in frequency standards and in television equipment.

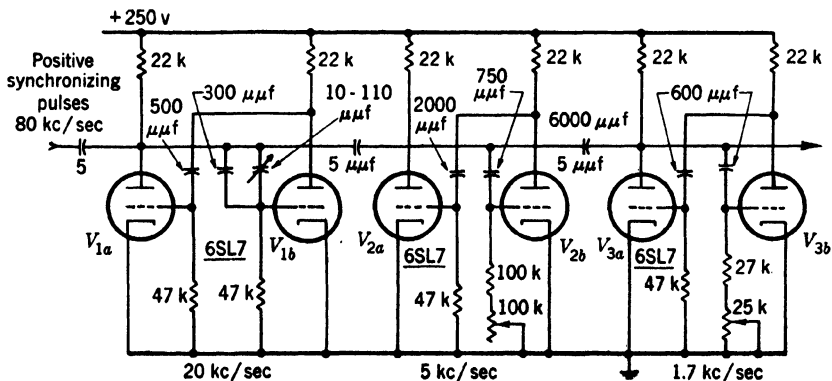


FIG. 16-8.—Astable-multivibrator divider chain (SCR-584).

A typical divider chain (from the SCR-584 radar) is shown in Fig. 16-8. Positive synchronizing pulses are supplied at 81.94 kc/sec to the plate of  $V_{1a}$ . These pulses add to the grid exponential of  $V_{1b}$  causing synchronization with every fourth pulse at approximately 20 kc/sec.

The plate waveform of  $V_{1a}$  is differentiated and synchronizes the grid of  $V_{2b}$  on every fourth pulse or at approximately 5 kc/sec. By a similar process  $V_3$  divides by 3 to approximately 1.7 kc/sec. This divider chain has been used extensively in field equipment and operates reliably at the small division ratios required, though the circuit constants may require readjustment for limit tubes.

This circuit does not, however, represent the best design practice. In the first place, the 22-k plate resistors are too low and permit only 100 volts of plate swing. If 250-k plate resistors are used, 200 volts of swing is available. Large plate resistors are, however, objectionable for high frequency operation. Secondly, the grid resistors should be increased to at least 1 megohm to prevent loading of the plate circuits, and they should be returned to  $E_{pp}$  so that the grid waveforms will have maximum steepness when crossing the critical bias.

The values of the time base condensers can be calculated from the formula for the period  $T$ , given in Sec. 5-8:

$$T = (R_1C_1 + R_2C_2) \ln \frac{E_{pp} + E_i}{E_{pp} + E_c}, \quad (2)$$

where  $R_1C_1$  and  $R_2C_2$  are the grid time constants,  $E_i$  is the amplitude of the plate waveform, and  $-E_c$  is the bias level at which regeneration takes place. For a 6SL7 with  $E_{pp} = 250$  volts and  $R_p = 250$  k,  $E_i = 200$  volts and  $E_c = 5$  volts. For the duty ratio to be 50 per cent the unsynchronized time base should have a natural period of one half or somewhat less than one half the total period, and the synchronized time base should have a natural period longer than half the total period. In the redesign of the first 4 to 1 divider of Fig. 16-8 the unsynchronized period is taken as 0.45 of the total period. Its time constant is given by

$$R_1C_1 = 0.45T \frac{1}{\ln \frac{E_{pp} + E_i}{E_{pp} + E_c}} = 0.64T.$$

For the synchronized time base, transition occurs when the sum of the exponential waveform and the synchronizing pulses reaches  $E_c$ . It is a general design principle for astable dividers that the trigger amplitude at the grid should be sufficiently large so that it is assured that transition occurs at the time of one of the triggers. This can be achieved by choosing a trigger amplitude equal to the increase of the time base between two successive triggers that occur near the time of transition. Furthermore the firing potential should correspond to the half amplitude of the firing trigger. There is no advantage in using a trigger greater than this.

Often a somewhat larger trigger is chosen to allow for tolerances in the circuit. For our design then approximately a 45-volt trigger is required, since  $E_s = (E_i - E_c)/4.5$ .

The time constant for the synchronized time base is given by

$$R_2 C_2 = \frac{0.5T}{\ln \frac{250 + 200}{250 + 27.5}} = 0.99T,$$

in which  $E_c + E_s$  has been substituted for  $E_c$  of equation (2).

A 10 to 1 divider circuit designed according to the principles mentioned above is shown in Fig. 16-9. This astable multivibrator is synchronized by pulses of 81.94 kc/sec to a frequency of about 8 kc/sec. The synchronized time base is 0.55 of the total period of the multivibrator, the unsynchronized time base is 0.45 of this period. The divider has been observed to maintain its division ratio when the heater voltage was varied from 3.5 to 7.8 volts rms, and the supply voltage was varied from 180 volts to greater than 350 volts. The rise time of the output pulse was from 6 to 8  $\mu$ sec. When 15 k plate load resistors were used, the circuit maintained its division ratio only over a heater-voltage range from 4.3 to 7.8 volts and a supply-voltage range from 235 to 265 volts.

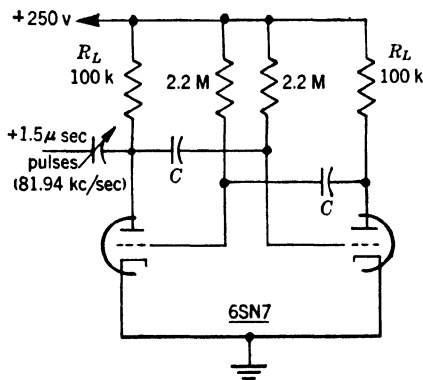


FIG. 16-9.—A 10 to 1 astable multivibrator divider.

**16-7. Phantastron-type Dividers.**—Any of the phantastron or sanatron circuits discussed in Chap. 5 can be used as frequency dividers. Usually monostable circuits are used. A circuit of a 5 to 1 phantastron divider together with some of its waveforms is shown in Fig. 16-10.

**A 5 to 1 Divider.**—The phantastron is switched from its stable state by a negative input pulse of 33-volt amplitude applied to the plate of  $V_1$  through  $V_s$ . The plate of  $V_1$  drops as regeneration starts, disconnecting  $V_1$  from further input pulses. The rundown continues until the plate “bottoms,” at which time the grid rises, bringing the cathode positive with respect to the suppressor and cutting off plate current. The plate potential rises until it is caught by  $V_s$ . As soon as a pulse appears on the cathode of  $V_s$ , the action will be repeated. Retriggering may even occur before the plate of  $V_1$  has reached its quiescent state, if a pulse is present on the cathode of  $V_s$  near the end of recovery period; this type of operation should be avoided.



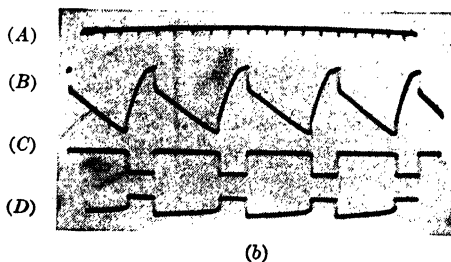
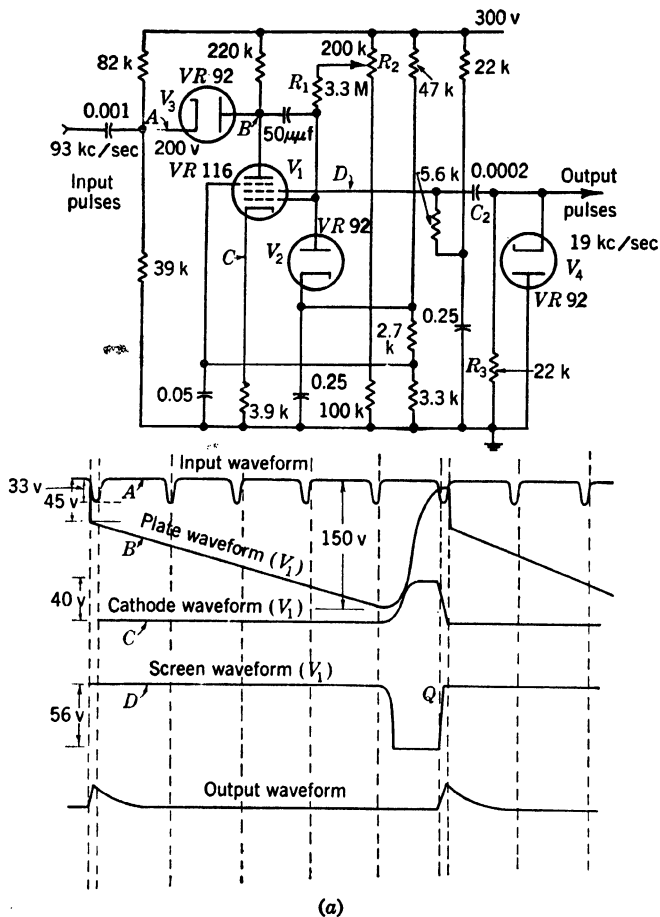


FIG. 16-10.—(a) 5 to 1 phantatron divider and waveforms. (b) Photographs of waveforms at Points A, B, C, and D of circuit of Fig. 16-10a.

As indicated in the waveform diagram, the initial edges of the cathode and screen waveforms coincide with the front edge of every trigger pulse. The screen waveform is differentiated by  $R_3$  and  $C_2$ , the negative pulses being removed by the diode  $V_4$ . The cathode waveform may be differentiated—for example, by the insertion of a small inductance between cathode resistor and ground—and used as an output waveform if negative pulses are desired. These pulses may be used to trigger an identical divider in the next stage of a chain. The division ratio of this divider is determined mainly by  $R_1C_1$  and the setting of potentiometer  $R_2$ , which varies the grid-leak return potential.

*Maximum PRF of Phantastron Dividers.*—Ordinary phantastrons will divide from triggers occurring at about 250 kc/sec. The stages of opera-

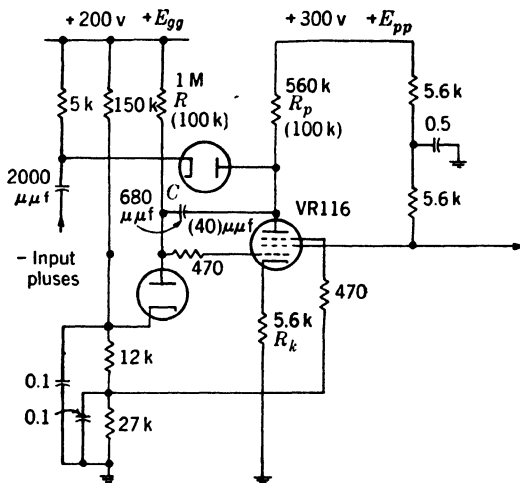


FIG. 16-11.—Circuit of phantastron used in stability tests.

tion which are important are: the linear-sweep time,  $t_s$ ; the flyback time,  $t_f$ ; the quiescent time,  $t_q$ ; and the time between trigger pulses,  $t$ . For highest-frequency operation, the resistances and capacitances should be made as small as is consistent with reliable operation. A typical circuit is shown in Fig. 16-11. For a division by 2 from 324 kc/sec,  $R_p = R = 100$  k, and  $C = 40$   $\mu\mu\text{f}$ . By neglecting strays, it can be shown that  $t_s = 4$   $\mu\text{sec}$  and  $t_f = 5$   $\mu\text{sec}$ . In the design,  $t_q$  is made equal to  $t/2$  and  $t_f = \frac{5}{8}t$ . For division ratios greater than 2,  $t_f$  may be made larger than  $t$  provided the circuit returns to its quiescent condition before it is retriggered, and provided the amplitude of the input pulses is well enough controlled so that retriggering occurs only on the desired pulse. The amplitude of the plate waveform may also be reduced to shorten both  $t_s$  and  $t_f$  but this implies a sacrifice in stability. An output frequency of about 500 kc/sec is at present the upper limit.

**Triggering.**—The trigger pulse, which is most often applied to the plate of a phantastron through a diode, must have sufficient amplitude to initiate regeneration, but it should not be much larger than the step on the plate waveform or it will interfere with the action of the circuit. It must also be small enough so that a trigger appearing during  $t_f$  will not trigger the circuit. The quiescent period  $t_q$  must exist for stable operation. If suppressor or grid triggering is used, the duration of the trigger must be less than  $t_s$ . In Fig. 16-11 the minimum trigger width is 0.25  $\mu$ sec.

**Stability.**—The stability of the divider then is determined by the constancy of the time during which the phantastron is in its unstable state. The factors that determine this time are discussed in Sec. 13-12. In general, it can be expected that this period will remain constant to a few tenths of one per cent under laboratory conditions. Hence division ratios of several hundred should be possible. With stable voltage supplies, reliable division by 30 has been achieved (Oboe calibrator). Under adverse conditions, 10 appears to be a safe limit.

A summary of tests of the stability of the circuit of Fig. 16-11 is presented below. For these tests  $R = 1$  megohm,  $C = 680 \mu\mu$ f,  $E_{gg} = +200$  volts,  $E_{pp} = +300$  volts, and  $R_p = 560$  k.

TABLE 16-1

The variable	Its change	Change in $t_s$ (expressed as a percentage of its nominal value of 490 $\mu$ sec)
$E_{pp}$	-10 %	+0.5 %
	+10 %	-0.25 %
Filament voltage	+20 %	+0.1 %
Phantastron tube	6 tubes	Maximum $\pm 2$ % Average (of absolute values) $\pm 0.7$ %
$R_k$	+20 %	+0.25 %
$R_p$	+20 %	-0.25 %
Trigger amplitude	16-70 v	0

With good components and reasonable voltage stabilization jitter is less than 1 part in 20,000.

Hence it is seen that the most serious instability tabulated above is that due to dependence on the properties of the phantastron tube. It is the variation in "bottoming" potential which is most serious. Other first-order instabilities not tabulated are those due to dependence of  $t_s$  on  $R$  and  $C$  and on  $+E_{gg}$ . Diode contact potentials are also important. Second-order instabilities are caused by variations in  $E_{pp}$ ,  $E_f$ ,  $R_p$ ,  $R_k$  and trigger amplitude and duration.

*Triggering Phantatron Divider Chains.*—Several methods of triggering successive phantastrons in a chain divider are shown in Fig. 16-12. In the first method *a*, the cathode waveform is differentiated and applied to the diode at the plate of the following stage. In *b*, the screen waveform is differentiated and applied to the suppressor. In *c*, the cathode of one

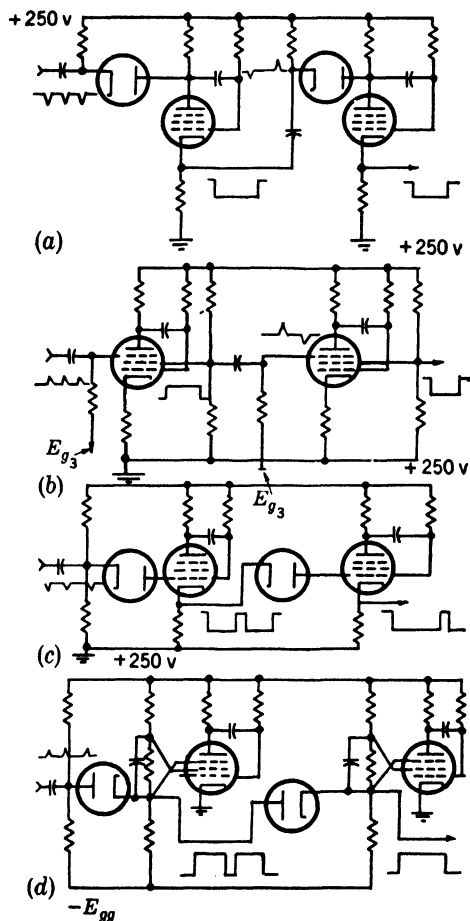


FIG. 16-12.—Methods of triggering phantatron divider chain.

stage is coupled directly through a diode to the grid of the succeeding stage. The grid-cathode bias developed in each stage is sufficient to keep the diode disconnected during the rundown. In *d*, diodes are used to couple the suppressors of consecutive screen-coupled phantastrons. The circuits in *c* and *d* should provide very small phase delay between the input and output pulses, since the selected input pulses travel through the entire chain without appreciable slowing up and appear directly

at the output of the last stage. (Monostable multivibrator chains may be triggered similarly by connecting diodes directly between negative-going plates.) Triggering on control grid or suppressor grid, unlike triggering on the plate, suffers from the disadvantage that triggers appearing during the flyback time will interfere with the timing waveform.

**16-8. Blocking Oscillator Dividers.**—Blocking oscillator frequency dividers are valuable particularly because of their ability to generate narrow pulses at a low impedance level. The upper frequency of operation is limited by tube dissipation ratings. For a 6SN7 generating

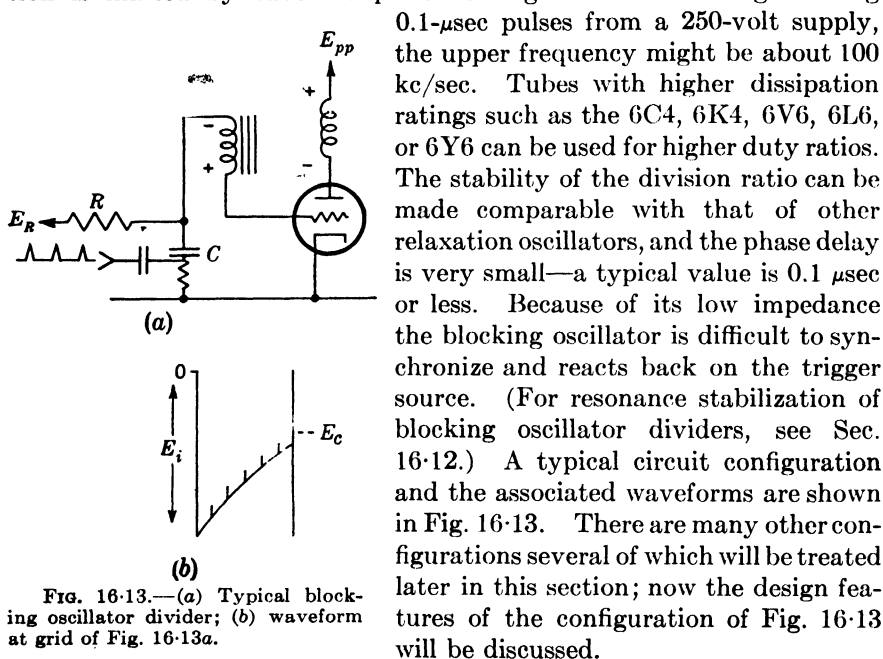


FIG. 16-13.—(a) Typical blocking oscillator divider; (b) waveform at grid of Fig. 16-13a.

**Theory of Design.**—Normally the grid-leak is returned to a sufficiently high potential  $E_R$  so that the blocking oscillator will be astable. The input triggers, which are shown originating from a very-low-impedance source, are applied to the grid of the blocking oscillator, and hence the firing of the blocking oscillator is synchronized with one of the input triggers. The time between output pulses from the blocking oscillator will be somewhat less than when it is synchronized free-running.

Suppose that the blocking oscillator is to be designed to divide by  $n$  and to have a synchronized period  $T$ , and that the tube, the supply voltage, the transformer, and condenser are chosen so that the desired form of output pulse is obtained. The latter condition implies that both  $E_i$  and  $E_c$  are fixed. There are two main sources of instability: variations in the time-base amplitude  $E_i$ , and variations in the firing potential  $E_c$  (see Fig. 16-13).

Ordinarily the potential  $E_i$  is the most unstable aspect of this circuit because it is determined by a highly variable quantity—the grid current that flows during the pulse. The firing potential  $E_c$  is the grid potential at which the triode begins to conduct and is a function of heater voltage and tube aging, but ordinarily its instability is not as troublesome as that of  $E_i$ . The stability of  $E_i$  cannot be greatly improved by the use of a diode because of the very low impedance of the circuit when the tube is conducting. The stabilization of  $E_R$  and  $E_{pp}$  is easily accomplished, and the variations in the lumped-constant elements are relatively inappreciable.

The choice of  $R$  and  $E_R$  for achieving maximum stability can be made with the criterion that the divider shall not fire on the  $(n - 1)$ st pulse because of decrease in the absolute magnitude of  $E_i$  (only variation in  $E_i$  is considered at the moment). There is clearly a maximum allowable variation in  $E_i$ ,  $\Delta E_{i_{\max}}$ , before the divider begins to fire at the  $(n - 1)$ st pulse, and  $R$  and  $E_R$  are chosen to maximize this allowable variation. It will appear from the succeeding discussion that the smaller  $E_R$  is the more stable the divider is with respect to variations in  $E_i$ .

The value of  $R$  is related to  $E_R$  by the condition that the timing waveform reach the proper potential by time  $t$ ,

$$\left(E_c - E_i - \frac{E_s}{2}\right) = (E_R - E_i)e^{-\frac{t}{RC}}, \quad (3)$$

where the synchronizing pulse amplitude  $E_s$  is considered to be constant. Actually,  $E_s$  would probably be chosen to equal the increment in the timing waveform between the  $(n - 1)$  and  $n$ th pulses and hence is a function of  $E_R$ , but this dependence has no effect on the general conclusions. A reasonable value to choose for design purposes might be  $E_s = (E_c - E_i)/n$ .

It is easy to see that  $E_R$  should not have an infinitely large value. For any given value of  $E_R$ , three factors determine  $\Delta E_{i_{\max}}$ .

1. The change,  $\Delta E_i$ , in the starting point of the timing waveform.
2. The change in the difference of the values of the timing waveform at  $t = T_{n-1}$  [time of  $(n - 1)$ st pulse] and at  $t = 0$ , due to  $\Delta E_i$ .
3. The maximum allowable change in the value of the timing waveform before firing occurs at the  $(n - 1)$ st pulse.

Point 1 is independent of  $E_R$ ; Point 2 decreases as  $E_R$  increases; Point 3 increases as  $E_R$  increases. For very large values of  $E_R$ , Point 2 is more important than Point 3, and hence  $\Delta E_{i_{\max}}$  decreases as  $E_R$  increases in the neighborhood of large values of  $E_R$ .

This can be shown mathematically as follows:

$$\Delta E_{i_{\max}} - \Delta E_{i_{\max}} [1 - e^{-\frac{t(1/n)}{RC}}] = (E_R - E_i)[-e^{-\frac{t}{RC}} + e^{-\frac{t(1-1/n)}{RC}}]$$

Equation (4) simply states that the maximum allowable change in the value of the timing waveform before firing occurs at the time of the  $(n - 1)$ st pulse [the right-hand side of Eq. (4)] is equal to the change in value of the timing waveform at the time of the  $(n - 1)$ st pulse evaluated for  $\Delta E_i = \Delta E_{i_{\max}}$  [the left-hand side of Eq. (4)]. The left-hand side of Eq. (4) is obtained by using the equation of the timing waveform  $E(t)$ :

$$E(t) = E_i + (E_R - E_i)(1 - e^{-t/RC}).$$

Using Eq. (3), Eq. (4) yields

$$E_{i_{\max}} = (E_R - E_i) - (E_R - E_i)^{(1-1/n)}(E_R - E_c)^{1/n}.$$

By differentiation,

$$\frac{\partial \Delta E_{i_{\max}}}{\partial E_R} = 1 - \frac{(1 - 1/n)}{x^{1/n}} - \frac{1}{n} x^{(1-1/n)},$$

where  $x = (E_R - E_i)/(E_R - E_c)$  and is always greater than 1 since  $E_R > E_c$ . Under this condition,  $\partial \Delta E_{i_{\max}} / \partial E_R < 0$ ; hence, the best design in order to make  $\Delta E_{i_{\max}}$  greatest is to make  $E_R$  smallest.

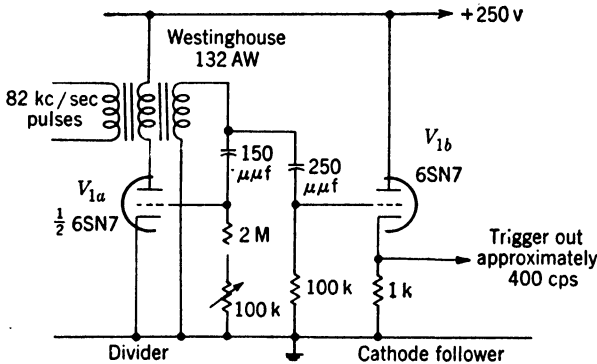


FIG. 16-14.—Practical 200 to 1 blocking-oscillator divider.

The conclusion, then, is that a blocking-oscillator circuit of the type shown in Fig. 16-13a should be designed with a small grid-leak return voltage in order to avoid instability of division ratio due to the variations in the grid current that flows during the blocking-oscillator pulse. In terms of our symbols,  $E_R$  should be given its smallest possible value in order to avoid instability due to variations in  $E_i$ .

But there is a limitation to how small  $E_R$  should be made. The smaller  $E_R$  is made, the smaller will be the difference between the value of the timing waveform at the time of the  $n$ th pulse and its value at the time of the  $(n - 1)$ st pulse. Hence, small variations in  $E_c$  or in  $E_i$  can more easily cause synchronization by a pulse other than the  $n$ th one. If  $E_i$  were constant and only  $E_c$  were subject to variations, then it would be

desirable to have  $E_R$  infinitely large, because in this case we would have the maximum difference between the value of the timing waveform at the time of the  $n$ th pulse and at the time of the  $(n - 1)$ st pulse.

In practice, the grid-leak return voltage must be chosen on a compromise basis. It must not be too large—otherwise, variations in  $E_i$  are too troublesome; it must not be too small—otherwise, variations in  $E_c$  and  $E_s$  are too troublesome. In a particular circuit in which the instability of  $E_i$  and  $E_c$  is known, the value of  $E_R$  is often chosen so that the divider instability due to  $E_i$  variations will equal its instability due to  $E_c$  variations (see Chaps. 3 and 9 for  $E_c$  instability—ordinarily several tenths of a volt for any given tube—and Chap. 6 for  $E_i$  instability). For instance, a value of  $E_R$  can be chosen midway between the value that would just avoid firing due to maximum  $\Delta E_i$  [use Eq. (4)] and the value that would just avoid firing due to  $\Delta E_c$  [use Eq. (3)].<sup>1</sup>

Often variations in  $E_i$  and  $E_c$  are related, and, indeed, their effects on instability tend to compensate one another. The extent of this compensation must be considered in any practical design. Variations in  $E_s$ , like those in  $E_c$ , are less troublesome if  $E_R$  is large. They also may be related to the variations in  $E_i$  and  $E_c$ . In view of these complexities it is often easiest to make the final adjustment of  $E_R$  experimentally.

<sup>1</sup> A similar argument can be applied to the design of multivibrator dividers. In Sec. 16-6 it was assumed that all errors are due to changes in  $E_c$ . Actually the variation in plate potential ( $\Delta E_p$ ) of the conducting tube will have the same effect as in the case of the blocking oscillator. When small plate resistors are used the variation  $E_i$  will become very serious.

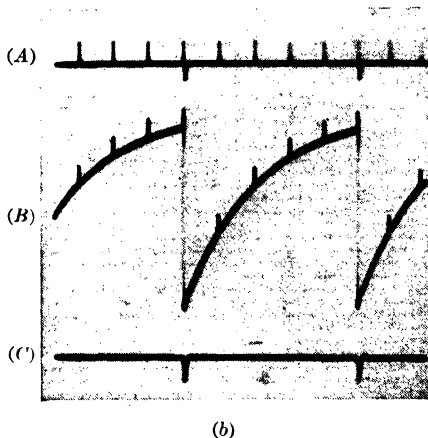
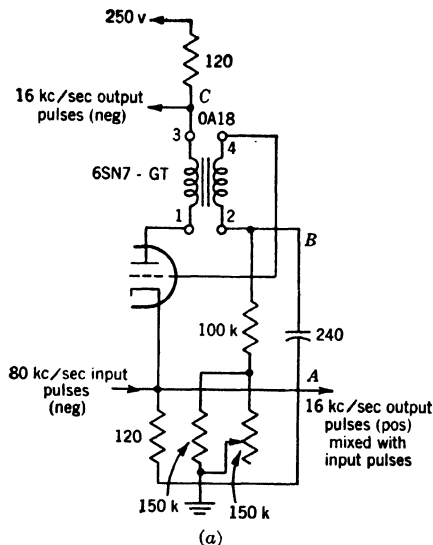


FIG. 16-15.—(a) 5 to 1 blocking oscillator divider. (b) Photographs of input (A), grid (B), and output (C) waveforms.



*Practical Circuits.*—A 200 to 1 blocking-oscillator-divider circuit is shown in Fig. 16-14. This circuit takes as its input 82-kc/sec triggers and gives as its output pulses occurring at a frequency of 400 cps. Synchronization is effected by applying the triggers to the plate of the blocking oscillator via transformer coupling, and a 1- $\mu$ sec output pulse is obtained from a cathode follower. This is not a high-stability frequency divider, and a heater-voltage change of 20 per cent causes a 5 per cent change in the counting ratio. However, phase jitter is small, because the delay between the input trigger and the corresponding output trigger is only about 0.1  $\mu$ sec. It is to be noticed that the grid-leak resistor is returned to ground rather than to a higher potential, which is in accordance with the remarks made in the previous paragraphs.

The 5 to 1 blocking-oscillator divider shown in Fig. 16-15 maintains its division ratio under a  $\pm 10$  per cent variation in line voltage without the use of regulated supplies. Readjustment of the circuit is seldom required even when tubes are changed.

*Variations Associated with Circuit Configuration.*—The various blocking-oscillator circuit configurations discussed in Chap. 6 have the same advantages for divider use as they have for pulse generation. For example, the grid-to-plate-coupled type [(1) of Fig. 16-16] is useful in generating wide pulses at low PRF; often this is suitable for a selector gate in pulse-selecting dividers. Greatest stability of division ratio is obtained with the plate-to-cathode coupled type [(2) of Fig. 16-16]. Some data indicating that type 2 has a greater stability than type 1 were obtained with the test setup shown in Fig. 16-16 and are summarized below.

The count of 10 was maintained under the following conditions for the two dividers:

Divider No. 1— $E_f$  varied from 5.5 to 8.0 volts;  $E_{pp}$  varied from 235 to 290 volts.

Divider No. 2— $E_f$  varied from 4.9 to 8.0 volts;  $E_{pp}$  varied from 200 to 290 volts.

*Synchronization of Single-stage Blocking-oscillator Dividers.*—The low impedance of the blocking oscillator makes it difficult to synchronize. Not only is it difficult to produce large triggers at the appropriate points of the blocking oscillator, but also the output of the blocking oscillator reacts on the source unless decoupling stages are employed. The low impedance does offer the advantage that the blocking oscillator is not easily loaded by the trigger source (see Chap. 6 for discussion of triggering of blocking oscillators). If a low-impedance source of triggers is available, so-called "series triggering" at the grid or cathode is usually

employed (see Fig. 16-17). Blocking oscillator, gas tube, and cathode-follower trigger sources are shown.

If the driver is of high impedance—for example, the output from some crystal oscillators—large amplitude triggers are needed. Several so-called “parallel triggering” methods are shown in Fig. 16-18. The synchronizing pulses are applied to the grid or plate via capacity or

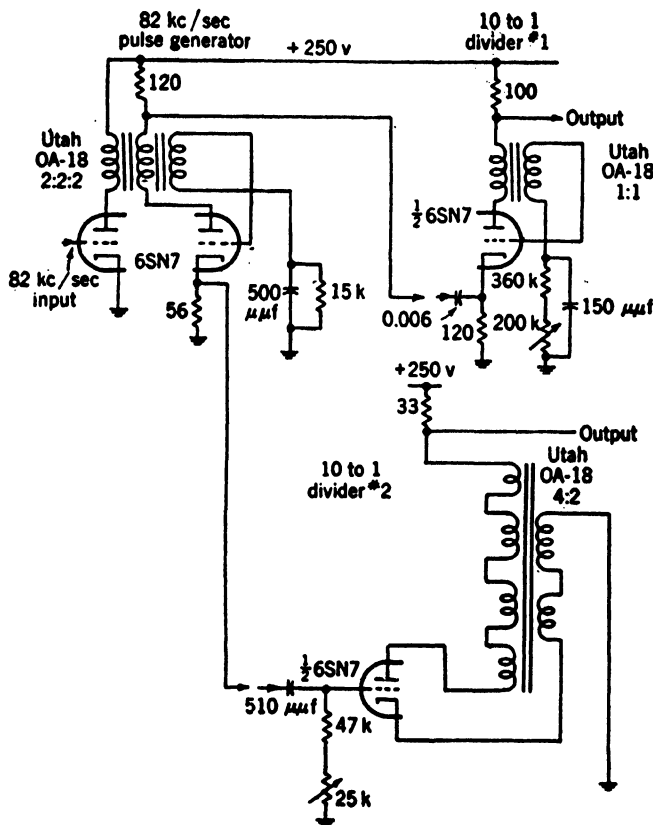


FIG. 16-16.—Blocking oscillator dividers used in stability tests.

transformer coupling. Back coupling of the blocking oscillator output to the source is particularly troublesome for high-impedance sources.

To reduce back coupling, buffers, cathode followers, or diodes may be used as shown in Fig. 16-19. Care must be exercised in the use of decoupling circuits to insure that stray capacity coupling is kept low and that they do not unduly load the blocking oscillator. Thus loading of the transformer core—flux biasing (see Chap. 6)—prevents the use of the direct-coupled buffer (Fig. 16-18a) for wide pulses. Also any variation

in the current of the direct-coupled buffer results in changes in the time-base amplitude due to the effect of variable flux bias.

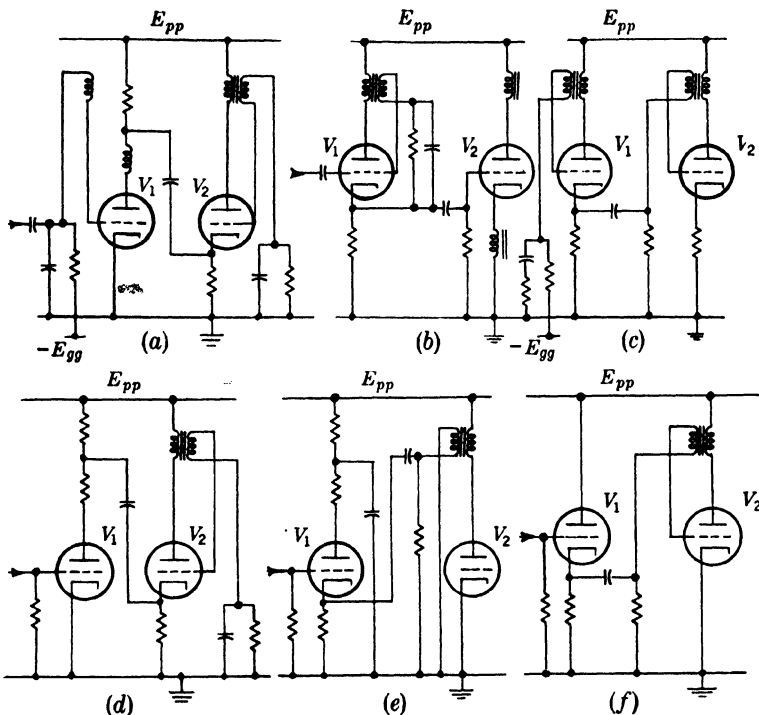


FIG. 16-17.—Synchronization of blocking oscillator dividers from low impedance sources.

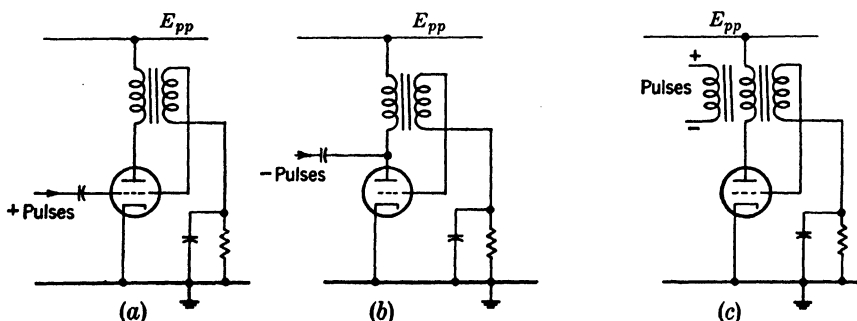


FIG. 16-18.—Synchronization of blocking oscillator dividers from high impedance sources.

**16-9. Blocking Oscillators in Divider Chains.**—When blocking-oscillator dividers are cascaded, the firing of the synchronizing divider may disturb the operation of the synchronizing divider. Several methods for eliminating this reaction have been devised.

The simplest of these methods makes use of the overshoot voltage of the pulse transformer to synchronize the following divider (Fig. 16-20), and, since the synchronized divider fires after the synchronizing divider,

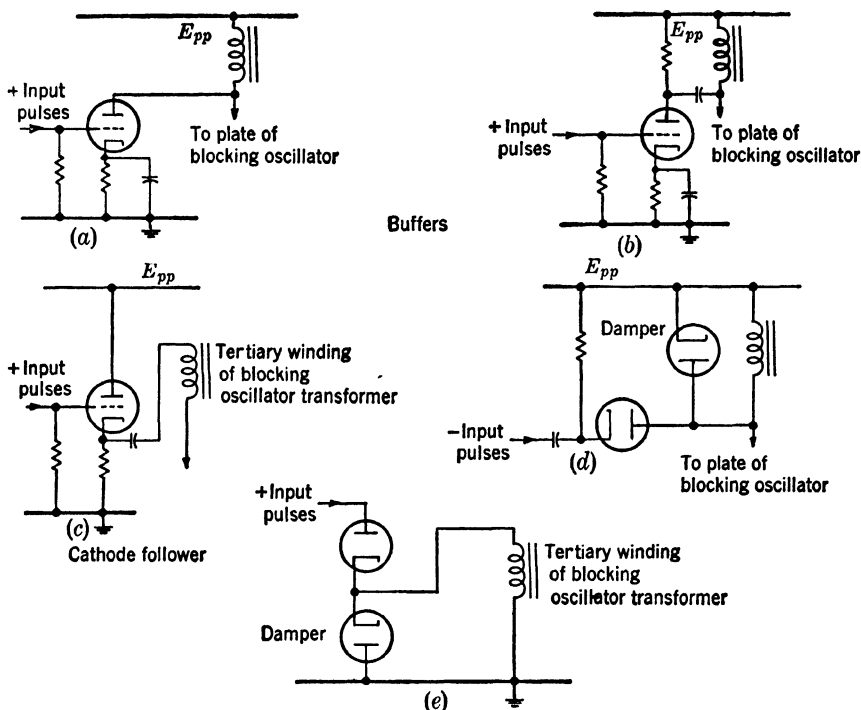


FIG. 16-19.—Decoupling circuits.

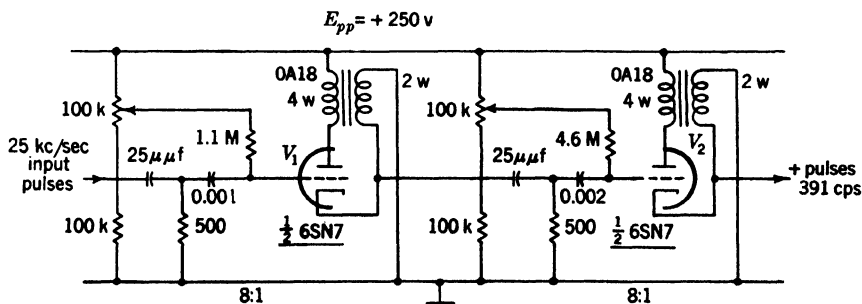


FIG. 16-20.—Divider chain with overshoot synchronization.

reaction is negligible. This method is only applicable when phase delays somewhat greater than one pulse width per stage can be tolerated. When smaller synchronizing delays are required, the method of Fig. 16-17a is often satisfactory. The two blocking oscillators are  $V_1$  and

$V_2$ . There is a small reaction due to the change in the effective  $E_{pp}$  for  $V_1$  when  $V_2$  fires.

Almost complete elimination of reaction can be obtained by the neutralizing scheme of Fig. 16-21. In this circuit the negative plate

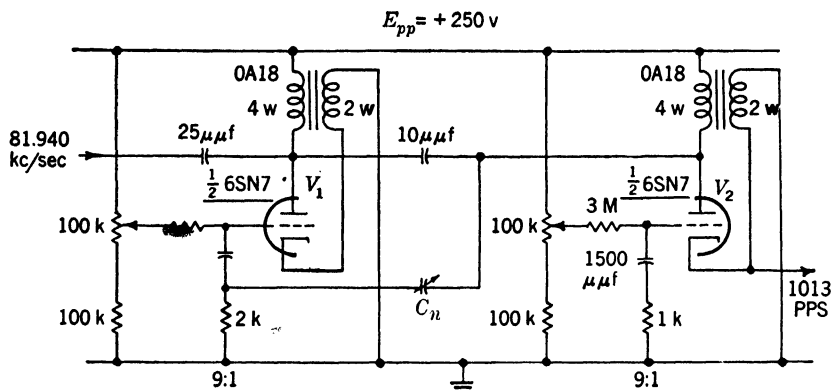


FIG. 16-21.—Divider chain with neutralization.

voltage pulses of  $V_1$  are used for synchronization of  $V_2$ . The back-coupled plate signal from  $V_2$ , which would result in a larger time base for  $V_1$ , is neutralized by a fraction of the negative plate pulse of the  $V_2$

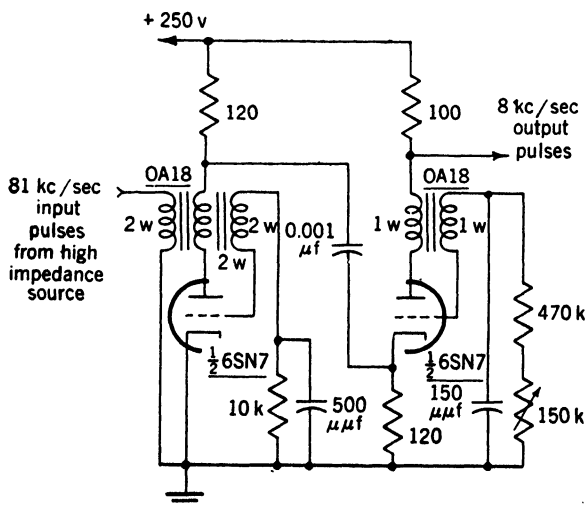


FIG. 16-22.—Two-stage 10 to 1 divider chain.

synchronized divider, which is fed back to the time-base circuit of  $V_1$  through  $C_n$ . This circuit can be effective but it is very critical to the adjustment of  $C_n$  and to charges in tubes.

A two-stage divider chain operating between 82 and 8 kc/sec is

shown in Fig. 16-22. This circuit will maintain its division ratio of 10 when the heater voltage is varied between 5.0 and 7.1 volts and the supply voltage is varied from 200 volts to 500 volts. The total phase shift introduced by these variations is less than  $0.2 \mu\text{sec}$ . Of the tubes tried in this circuit, 95 per cent gave the division ratio of 10 without the necessity for any readjustment of the grid-circuit time constant.

**16-10. Gas-tube Dividers.**—Frequency dividers that use gas tubes are simple and can provide low impedance output pulses of rectangular shape. Their most severe limitation is the maximum frequency of operation. Primarily because of deionization time, this frequency is limited to about 20 kc/sec; and, since deionization time is a variable quantity, stability requirements may necessitate keeping the upper frequency less

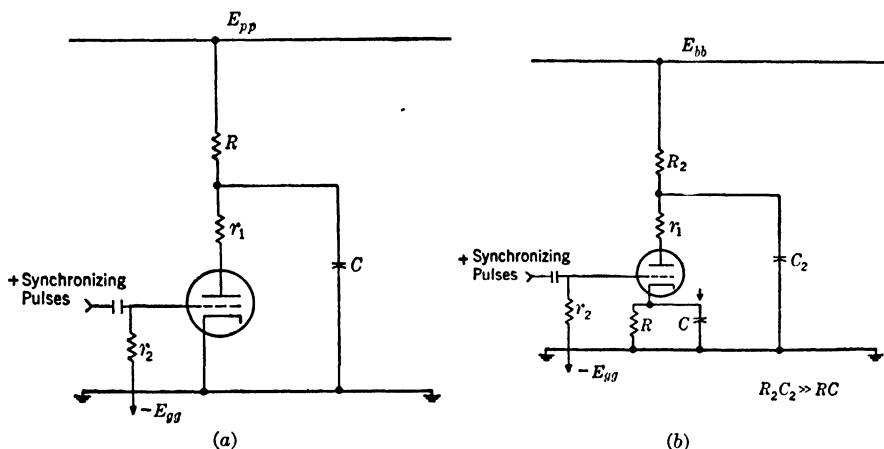


FIG. 16-23.—(a) Thyatron frequency divider with timing  $R, C$  in plate circuit. (b) Thyatron frequency divider with timing  $R, C$  in cathode circuit.

than 10 kc/sec. A second limitation is the phase delay introduced by the finite time required for complete breakdown ( $\approx 1 \mu\text{sec}$ ). Third, the life of a gas tube is only about one thousand hours as compared to several thousand hours for vacuum tubes.

The thyatron arc-discharge tube has been the basis for most gas-tube frequency dividers, but a cold-cathode glow-discharge tube can also be used. Ordinarily the gas tubes are operated as astable relaxation oscillators that are synchronized with the input pulse (see Chap. 3 of this volume for a discussion of the properties of gas tubes).

**Thyatrions.**—Two basic forms of the thyatron relaxation oscillator used as a frequency divider are shown in Fig. 16-23. Both are astable oscillators that are synchronized with the input triggers. In the circuit of Fig. 16-23a the time-base waveform appears at the plate of the gas tube, and the synchronizing triggers are applied to the grid. Instability of division ratio is caused by variations of the firing and extinction

potentials of the thyatron. By putting the time-base condenser and resistor in the cathode circuit (Fig. 16-23*b*), the stability of division ratio is improved, because now a timing waveform of the same amplitude as in the previous circuit appears at the cathode rather than at the plate. The waveform at the cathode is more effective for firing the gas tube because of the  $\mu$  of the tube. A 10 to 1 divider with its timing waveform in the cathode has been designed to operate with 20-kc/sec input pulses. The division ratio was maintained when the heater voltage was varied from 3.5 to 7.0 volts and the supply voltage was varied from 250 to 450 volts.

**Cold Cathode Gas-tubes.**—The basic circuit of the gas-diode frequency divider is shown in Fig. 16-24. The primary limitation of the gas diode for this application is the smallness of the difference between the breakdown and extinction potentials, which necessitates a small amplitude timing waveform. In addition, the breakdown voltage is unstable.

Consequently it is seldom possible to realize division ratios of greater than 4 with suitable stability.

Although cold-cathode gas triodes (1C21 and OA4-G) and the tetrode (631-P1) have not yet been used for frequency division, they appear to have desirable properties for this application. Of first importance is the fact that they are without heaters and, hence, are not subject to the variations of firing and extinction potentials with heater voltage observed for thyatrons. Secondly, the peak anode currents are as large as those of thyatrons. Finally the breakdown voltage may be more stable than it is for gas diodes because of the control anode glow.

Further investigation should be made of dividers using cold-cathode gas triodes and tetrodes.

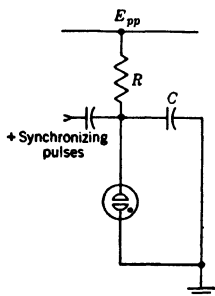


FIG. 16-24.—Gas diode relaxation oscillator frequency divider.

#### MORE ELABORATE DIVIDER SCHEMES, AND INTERMITTENT-FREQUENCY DIVISION

**16-11. Pulse-selection PRF Dividers.**—Instability in the time delay between the input pulse and the output pulse can be very considerably reduced by the use of the so-called “pulse selection” method of pulse-recurrence-frequency division. A timing diagram illustrating this method is shown in Fig. 16-25. A selector pulse *c* is derived from the output *b* of a divider and is used in a time-selector circuit to select the high-frequency input pulse following the one corresponding to the divider output. If a multigrid tube or a properly designed diode switch time selector is used, there will be a phase delay that is negligibly small for most purposes. Usually, in the interests of economy, time selectors employing addition and amplitude selection have been used; this is a poor

method of time selection since it requires an accurately rectangular selector pulse and careful adjustment of bias levels (see Chap. 10 for discussion of time selectors). Although phase jitter can be stabilized

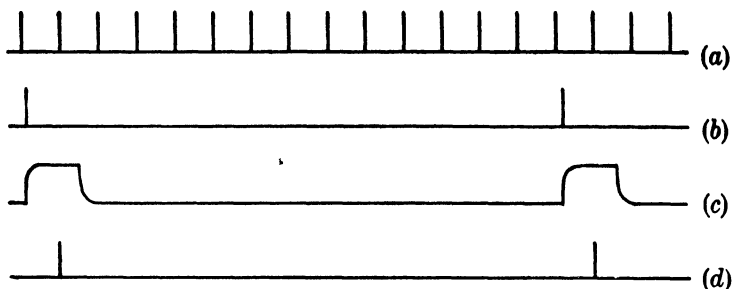


FIG. 16-25.—Timing diagram for pulse-selecting frequency divider. (a) Input pulses. (b) 14 to 1 divider output pulses. (c) Time selector gates initiated by b. (c) *a* pulses selected by gate c.

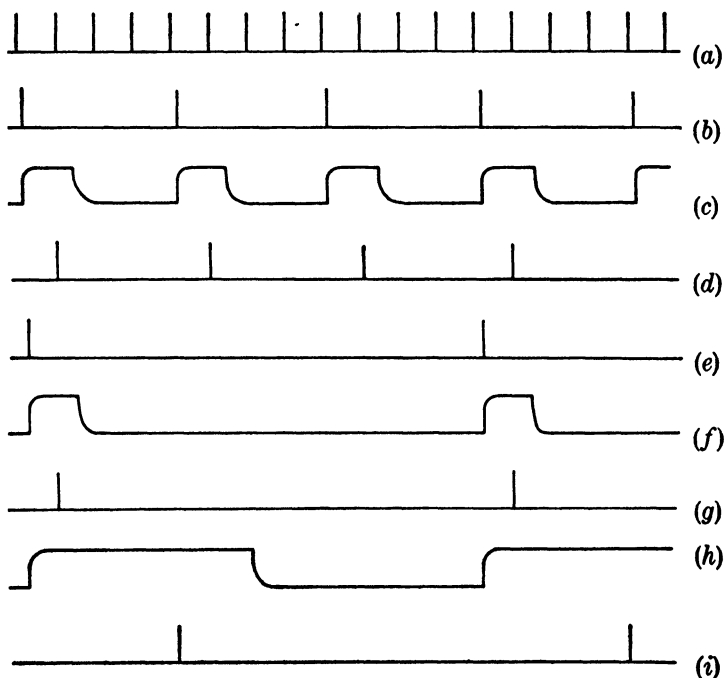


FIG. 16-26.—Timing diagram for cascaded pulse-selecting frequency divider. (a) Input pulses. (b) Output of 4 to 1 divider. (c) Selector gate initiated by b. (d) *a* pulses selected by c. (e) 3 to 1 divider synchronized from c. (f) Short selector gate initiated by e. (g) *a* pulses selected by f. (h) Long selector gate initiated by e. (i) *b* pulses selected by h.

by the pulse-selection method, the actual delay between the output pulse and the synchronizing input pulse has been increased to the period between two successive input pulses. This method of pulse selection





**16-12. Frequency Division Using Resonant Stabilization.**—By the use of resonant circuits it is possible to change the time base of a frequency divider in such a way as to increase its stability. This method has been applied to continuous frequency division only, because transient conditions make this method difficult to apply to intermittent pulse-recurrence-frequency division.

Resonant stabilization has been employed in blocking-oscillator and multivibrator-divider circuits, but, as will appear in the discussion of the method, its application can be extended to other circuits. The principles of resonant stabilization will be illustrated by a discussion of

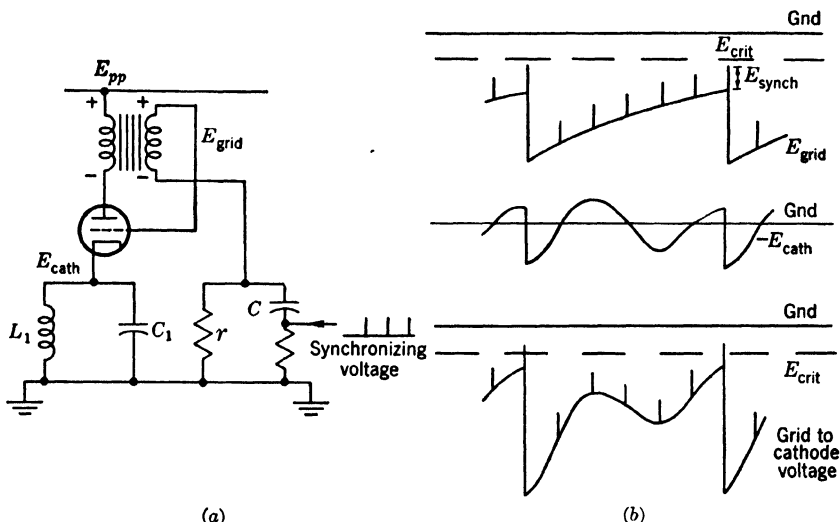


FIG. 16-28.—(a) Basic circuit of blocking oscillator divider using resonant stabilization. (b) Typical grid, cathode, and grid to cathode waveforms for circuit of (a). ( $E_{\text{crit}}$  on the grid waveform diagram is the potential the grid would have to reach for firing to occur under the assumption that the cathode is grounded.)

its application to blocking-oscillator dividers. The use of only one or two resonant circuits will be treated first; then the extension of the method to the use of delay lines, which can be considered as structures with an infinite number of resonant circuits, will be given.

A resonant-stabilized blocking-oscillator-divider circuit is shown in Fig. 16-28a, and the corresponding waveforms are shown in Fig. 16-28b. It is seen that this circuit differs from that of an ordinary blocking-oscillator divider only in that there is a resonant circuit in the cathode of the blocking oscillator. During the pulse the condenser  $C_1$  is charged to a positive voltage, say  $E_1$ . The tube is cut off after the pulse. The grid potential then approaches ground exponentially, and the cathode potential oscillates sinusoidally with a frequency  $f = 1/2\pi \sqrt{L_1 C_1}$ . The

frequency  $f$  is so chosen that the cathode potential will equal  $-E_1$  at the time  $T$  of the  $n$ th pulse when the blocking oscillator again fires. The cathode potential will be raised to  $E_1$  during the pulse, and the cycle will repeat itself. If the frequency of the resonant circuit is chosen so that the cathode potential at  $t = T$  is the negative of its value at  $t = 0$ , it is reasonable physically to expect that the equilibrium operating condition described will be realized.

Increased probability of firing at the time of the  $n$ th pulse is achieved by resonant stabilization, as is indicated by a comparison of the first and last waveforms of Fig. 16-28*b*. The grid-to-cathode potential is lower at the time of the  $(n - 1)$ st pulse in the last waveform than it is in the first; hence there is less probability of firing on the  $(n - 1)$ st pulse in a circuit with resonant stabilization than there is in one without this feature. This is not strictly a fair comparison, since, because of the division of the total charge flowing during the pulse between  $C_1$  and  $C$ , the first waveform is of lower amplitude than the grid waveform on a blocking oscillator with no resonant circuit in its cathode. However, the nature of the stabilization achieved is correctly indicated. The ratio of the amplitude of the exponential waveform at the grid to the amplitude of the sinusoidal waveform at the cathode is an important design consideration which will be discussed later.

The criterion for stability is that firing at the  $(n - 1)$ st pulse must be avoided. Actually, firing by earlier pulses also is to be avoided and in order to accomplish this two or more resonant circuits of different frequencies are sometimes inserted in series in the cathode (see Fig. 16-30*a*).

The design and operating characteristics of the two practical circuits shown in Figs. 16-29*a* and 16-30*a* will now be discussed. If the frequency of the output pulses is  $f$ , the frequencies of the resonant circuits must be chosen to equal  $(n + \frac{1}{2})f$ , where  $n = 0, 1, 2 \dots$ . This condition will assure that the phase of the cathode voltage at the time of the  $n$ th pulse will be the reverse of the phase to which it was brought by the 0th pulse—that is, the previous firing pulse. If this situation exists, an equilibrium condition will result.

A possible design procedure is first to choose the number and frequencies of the resonant circuits and the relative amplitudes of the sinusoidal voltages associated with them by plotting the cathode waveform for various combinations of resonant circuits. Ordinarily not more than two resonant circuits are used, and a choice can be made which will make it fairly certain that the divider shall not fire at certain pulses preceding the  $n$ th one, often the  $(n - 1)$ st and the  $(n - 2)$ nd. Then the relative amplitude of the exponential waveform is chosen to ensure that the divider will not fire at any other pulse; for instance, this might

be the  $(n - 3)$ rd pulse. The amplitude of the exponential voltage is inversely proportional to the condenser in the grid circuit and directly proportional to the grid current. The sinusoidal voltages are inversely proportional to the capacities associated with them and directly proportional to the cathode current. The total value of the series capacity in the cathode-grid circuit is often determined by the duration of the output pulse required from the blocking oscillator. Often the peak-to-peak value of the waveform at the cathode is made approximately equal to the amplitude of the timing waveform at the grid. The 2 to 1 divider of Fig. 16-29 is an elementary example of stabilization using a single resonant circuit. The frequency of the resonant circuit is 20.5 kc/sec, whereas the frequency of the output pulses is twice this or 41 kc/sec.

For the 5 to 1 divider with the two resonant circuits, the two resonant frequencies are 20 kc/sec and 12 kc/sec, whereas the output pulse frequency is 8 kc/sec and the input pulse frequency is 40 kc/sec. The 20-kc/sec resonant circuit favors firing at the 5th pulse over firing at the 4th pulse, but does not distinguish between firing at the 3rd pulse and the 5th pulse. The 12-kc/sec resonant

circuit favors firing at the 5th pulse over firing at the 3rd pulse or 4th pulse. Hence, by the use of the two resonant circuits, the probability of firing at the 3rd or 4th pulse is reduced considerably. The grid waveform prevents firing at the first or second pulses. Waveform photographs are shown in Fig. 16-30b. The effect of the 10mh, 0.0062  $\mu$ f resonant circuit in stabilizing the division ratio is indicated in Fig. 16-30c.

Stable division ratio is maintained with both these circuits when tubes are changed and when the heater voltage is varied from 4.5 to 7.0 volts and the supply voltage is varied by  $\pm 40$  per cent of its stated value. A compensation for the effects of changes in heater voltage is present in both these circuits. This is explained as follows: An increase in heater voltage will reduce the amplitudes of the exponential in the

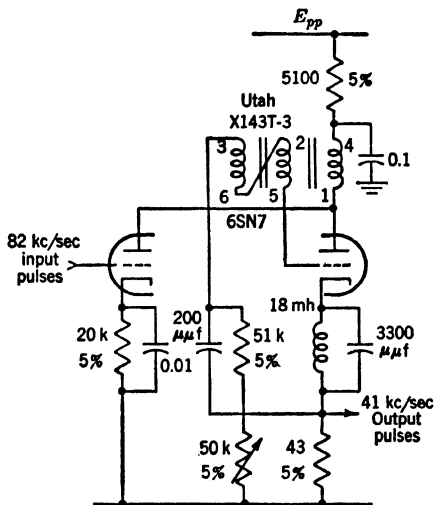
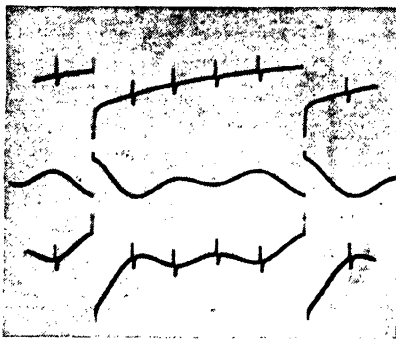
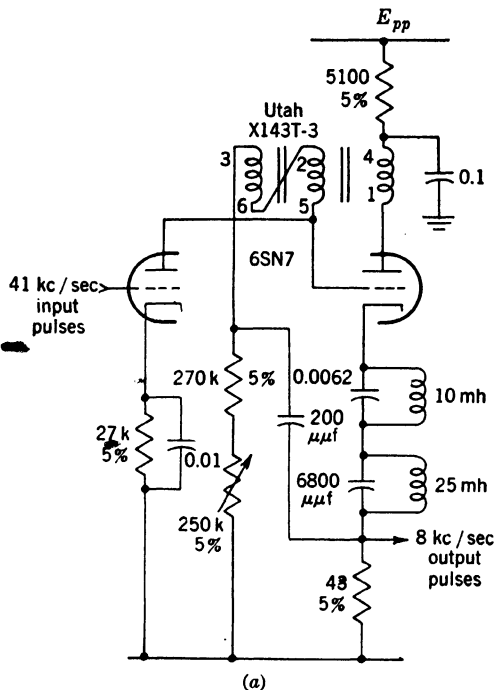
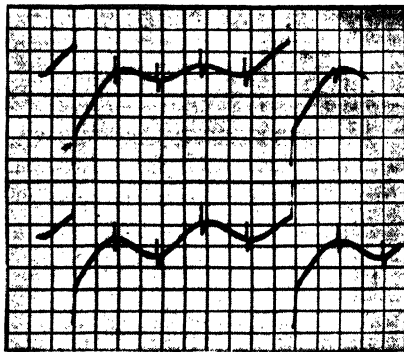


FIG. 16-29.—2 to 1 blocking-oscillator frequency divider using a single resonant circuit.



(b)



(c)

FIG. 16-30.—(a) 5 to 1 blocking-oscillator frequency divider using two resonant circuits. (b) Photographs of waveforms of circuit of Fig. 16-30. Top line: grid to ground. Middle line: cathode to ground. Bottom line: grid to cathode. Top line: same as bottom line of 16-30b. (c) Bottom line: grid to cathode waveform with 10 mh and 0.0062  $\mu$ f removed.

grid circuit and of the sinusoids in the cathode circuit and these two effects tend to cancel each other.

The  $Q$ 's of the resonant-circuits are sufficiently high (approximately 10 to 20) so that the damping of the sine waves during the periods between

firing can be disregarded. If the  $Q$  is low, it is necessary to increase the amplitude of the exponential to achieve the desired stability. In a good divider design the input trigger amplitude should vary as the amplitudes of the timing waveforms.

*Delay-line Stabilization.*—A short-circuited delay line can be inserted in the cathode circuit of a blocking oscillator in place of the resonant circuit. A negative pulse will be developed at the cathode at a time equal to twice the line length and this pulse can then be used to select the desired synchronizing pulse. Alternatively, an open line may be connected across the grid or plate winding to obtain similar results (see Chap. 6). The line impedance should be adjusted to give a waveform equal in amplitude to the grid-timing waveform. Since electrical lines are usually impractical for delays above 10  $\mu\text{sec}$ , they can be used only for fairly high frequency division.

**16-13. Divider Chains with Feedback.**—Up to this point the only division ratios obtainable are those that can be achieved by single dividers or by divider chains. Yet in practice this does not include all division ratios that may be desired. For example, a division ratio that is a large prime number may be too large to be obtained by a single divider stage, and cannot be achieved by a divider chain because the prime number cannot be factored. Also, a division ratio that can be factored only into a large prime number and some other number or numbers is not obtainable by the methods thus far discussed. A method that may be called “addition by feedback” makes possible the achievement of any frequency-division ratio.

This method is illustrated in the circuit of Fig. 16-31. The VR116 tubes  $V_4$  and  $V_7$  are astable phantatron dividers which are cascaded in a divider chain. The output from the second divider  $V_7$  triggers a phantatron delay circuit  $V_8$ , whose output gate is applied to the suppressor of the first phantatron divider  $V_4$ , thus returning it to its stable state for the duration of the gate. In this circuit the gate is of duration less than the spacing between two of the input pulses so that the second input pulse will retrigger the first divider. This divider now operates as a normal 7 to 1 divider until the second divider chain is again triggered.

The effect of this injection of a gate back to the first phantatron divider is thus to extend the period between the output pulses from the second phantatron divider by an amount equal to the period between two successive input pulses. Hence, if the divider chain were dividing by 100 without feedback, after the introduction of feedback it would be dividing by 101. Additional periods of the input pulses can be added to the output period by widening the injection gate. The circuit shown can be adjusted to divide from 16 kc/sec to the range from 90 to 150 cps (see Chap. 4, Vol. 20, for a more complete discussion of this circuit).

This principle of addition by feedback is, of course, applicable to other circuits as well as the phantatron (see Chap. 17, "Counters").

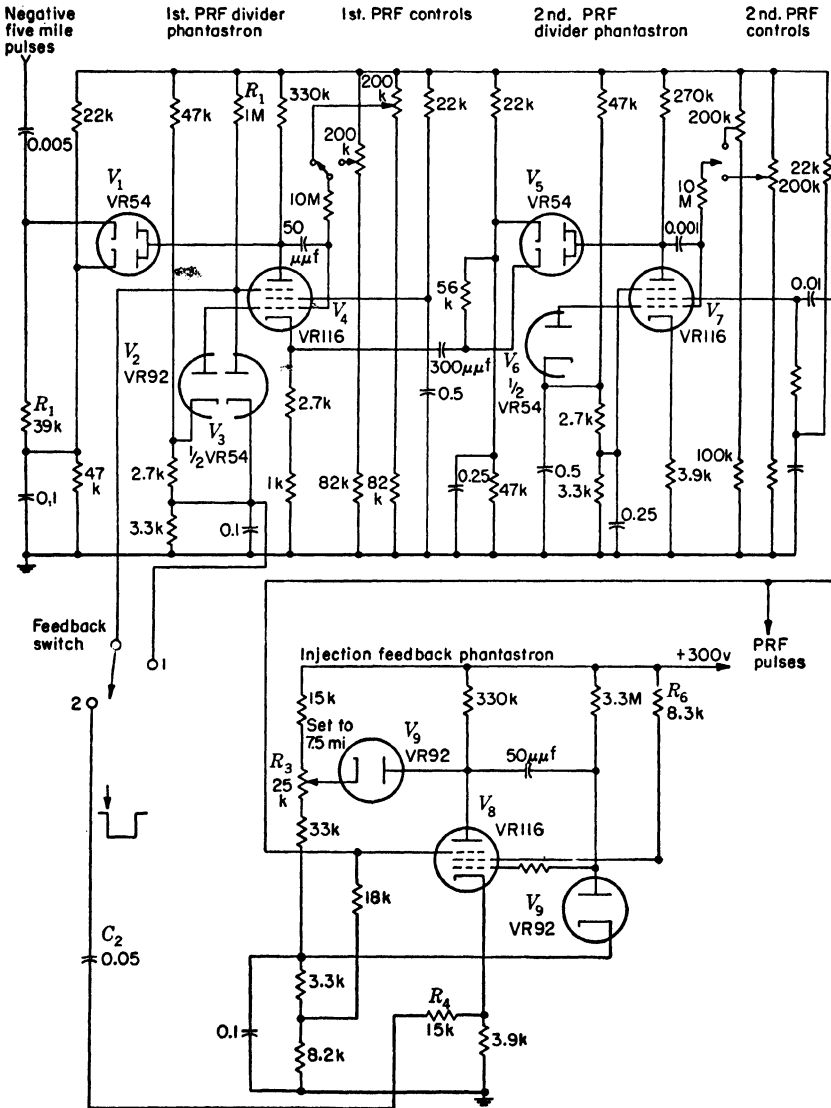
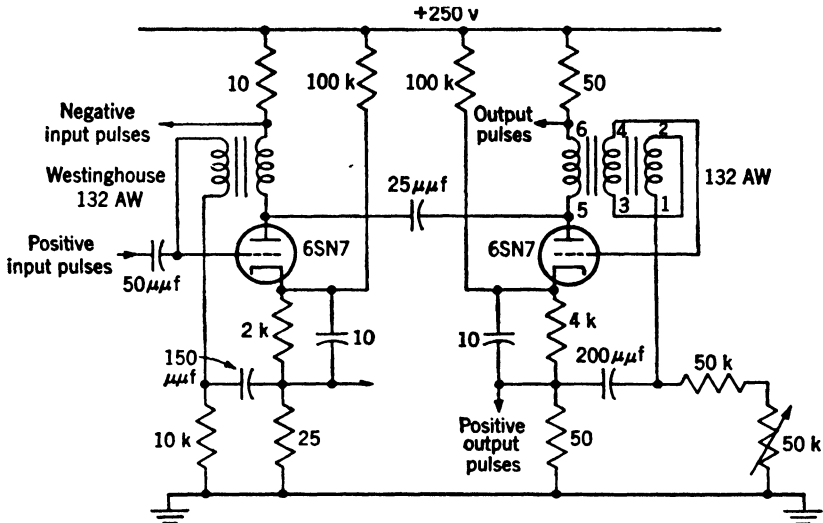


FIG. 16-31.—Phantatron divider chain with feedback.

**16-14. Intermittent Pulse-recurrence-frequency Division.**—Intermittent frequency division, as defined in Sec. 16-1, requires that the divider shall be nonoperative in the absence of the input signal and then shall start to operate at the appearance of the first pulse of the train of pulses.

This requirement usually makes it desirable that the divider shall not operate as an astable oscillator, since this would require that the time interval between the trains of pulses be constant and the proper multiple of the spacing between pulses. Hence monostable oscillators are used for intermittent frequency division.

Any properly designed monostable divider can be used. Multivibrators and phantastrons require no modification whatever. Dividers employing grid-controlled gas-tubes and blocking oscillators can be rendered monostable by applying sufficient bias to the grids to prevent conduction in the absence of a trigger pulse.



**FIG. 16-32.**—Intermittent blocking-oscillator frequency divider. 1 to 1 pulser and 5 to 1 divider.

An example of an intermittent blocking-oscillator divider is shown in Fig. 16-32. From the 82-kc/sec input triggers, tube  $V_1$  generates large amplitude pulses which are used to trigger the divider tube  $V_2$ . In the absence of triggers, tube  $V_2$  is biased off by its high cathode potential. The first input pulse appearing on the plate of  $V_2$  triggers the oscillator, which then operates as a synchronized blocking-oscillator divider as long as triggers are applied to its plate. Unlike most of the monostable dividers discussed previously, this circuit is triggered before it completely returns to its monostable state. This circuit requires high amplitude triggers and is sensitive to variations in trigger amplitude.

The pulse-selection method and the method of addition can be applied to intermittent frequency division as well as to continuous frequency division. Resonant stabilization is not easily applied because of transient phenomena.



## CHAPTER 17

### COUNTING

By R. B. WOODBURY AND J. V. HOLDAM

#### INTRODUCTION

**17.1. The Problem.**—Counting is a logical extension of frequency division. Where frequency division is discussed in Chaps. 15 and 16 as applied to sinusoidal and periodic pulse waveforms, counting is applied to nonperiodic waveforms. In some special cases periodic pulse waveforms may be divided by counters rather than by dividers. Whether a circuit is considered a counting circuit or a nonperiodic divider depends on the particular application. If the output is continuous it is generally considered to be a divider; if the output is measured over a discrete time interval it is considered to be a counting circuit.

Counting circuits are used extensively in nuclear-physics experiments. Such applications are characterized by the random time distribution of the pulses, thus making it necessary to count large numbers to improve the statistical average. Rather than count for long periods of time it is more efficient to count at high rates. Consequently, electronic scaling or dividing circuits are employed to reduce the rate so that it can be followed by a mechanical counter.

In radar, counting circuits have been used to divide from a variable PRF and/or to obtain a division ratio that is variable in small steps. The Loran system, explained in Vol. 20, Chap. 7, is an example of the latter application.

Although counters are designed to operate on random pulses, there is always a lower limit to the time interval between two pulses below which the counter will respond to only the first pulse. In some types of counters there is also a maximum allowable time interval for  $n$  pulses where  $n$  is the number the circuit counts in each complete cycle of operation.

**17.2. General Method.**—All practical counter circuits may be classified as either the sequence-operated type or the energy-storage type. Both types are designed to recycle automatically after a given number of input pulses, and both types produce an output pulse by the resetting process. Hence it is apparent that both types divide the number of input pulses by the number of pulses necessary to cause resetting.

Most sequence-operated counting circuits are in the form of a ring

counter. A block diagram of a ring-of-six—i.e., a count of six per cycle of the counter—is shown in Fig. 17.1. A ring counter is composed of  $n$  identical units,  $n$  being equal to 6 in this case. Each unit has two stable states, which we will designate by “on” and “off.” The pulses to be counted are applied simultaneously to all units and the units are so interrelated that a pulse will turn a unit “on” only if the unit immediately preceding it is “on” at the time the pulse is applied, and, moreover, the interrelation makes it possible for only one unit to be “on” at a time. At the time each pulse is received, the “on” unit will become the next unit around the ring. If means are provided to indicate the “on” unit and if provisions are made to insure that the  $n$ th or zero unit<sup>1</sup> is on at the beginning of the time interval up to  $n$  pulses may be counted. If it is desired, an output may be obtained for every  $n$ th pulse by taking an output when the  $n - 1$  unit goes from “on” to “off.”

Sequence-operated counters may be of either the electrical or the electromechanical type. In most cases they have the advantage that there is no upper limit on the time interval between successive pulses. The most common type of electrical sequence-operated counters is the scale-of-two shown in Fig. 17.3. It is the simplest form of ring counter and has been used extensively. It is explained in detail in Sec. 17.3.

A counter of the energy-storage type consists of four parts: a unit to store energy, a device to add a fixed increment of energy at the time of each input pulse, a means of determining when the energy reaches some known level, and a means of recycling by removing the stored energy when it reaches this level.

The stored energy of a circuit counting by six is shown in Fig. 17.2, plotted as a function of time. In this diagram equal amounts of energy are added at equal increments of time. The increments of time in most cases will not be equal, and in numerous circuits the amounts of energy added for each received pulse depend upon the amount of stored energy at that time; hence, although all increments of energy may not be equal,

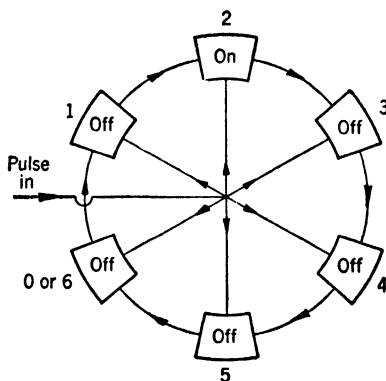


FIG. 17.1.—Ring counter.

<sup>1</sup> A complete cycle of the counter coincides with  $n$  pulses and  $n$  indicated counts, and, as it is necessary to indicate a count of zero, the  $n$ th pulse must be considered as establishing an indication of zero pulses rather than  $n$  pulses. This introduces no ambiguity if it is kept in mind that an output is obtained from the counter for every  $n$ th pulse.

the corresponding ones in each cycle of operation of the counter are equal. If the  $n$ -energy levels are numbered, six in the case shown in Fig. 17-2, the  $n$ th pulse starts to add its energy, but when approximately half of the energy is added, it passes the threshold and the energy is removed, returning the counter to the zero-energy level.

If there are means provided to indicate the energy level, up to  $n$  pulses may be counted in an interval of time provided the energy was at the zero level at the beginning of the time interval, or an output may be obtained for every  $n$ th pulse if the output coincides with the removal of the stored energy.

In most energy-storage counting circuits, a condenser is charged to a fixed potential by each input pulse and discharged into another condenser that is used to store the charge. An amplitude comparator is used to determine when the potential or the storage condenser has reached

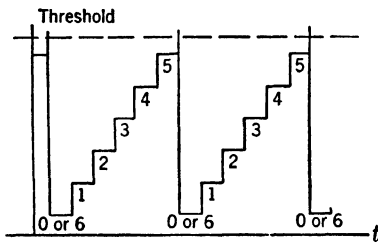


FIG. 17-2.—Energy waveform.

the level produced by the  $n$ th pulse. The amplitude comparator then operates an electronic switch that discharges the storage condenser to the “zero” level. This type of circuit has the advantage of employing a small number of components, but rate of leakage of charge from the condenser places an upper limit on the period of a complete cycle of the counter.

If a larger counting ratio is desired than can be obtained with either a sequence-operated or an energy-storage counter, multiple counters may be operated in series or parallel. If the desired counting ratio is not obtainable in this manner, additional interconnections must be added between counters. These interconnections will be referred to as “feedback loops,” since pulses are generally transmitted from a counter back to one which precedes it. These techniques will be discussed in detail in Sec. 17-8.

## SEQUENCE CIRCUITS

**17-3. Scale-of-two. Principles of Operation.**—A multivibrator with two stable states as described in Secs. 5-12 to 5-22 may be employed as a sequence-operated ring-of-two counter circuit. This type of circuit is the most frequently employed counter circuit because of its reliability and simplicity.

The basic scale-of-two circuit is shown in Fig. 17-3. This circuit meets the requirements for a ring-of-two, since the pulses to be counted may be applied to both tubes and only one tube can conduct at a time

because of the interconnection between tubes by  $R_4$  and  $R_5$ . Each time a trigger pulse is applied the conducting and nonconducting tubes are interchanged. This action is brought about by applying a negative pulse to the cathodes of  $V_1$ . The circuit is so arranged that the conducting section of  $V_2$  will be cut off and regeneration initiated. This results in a rectangular waveform at the plate of either tube which may be used directly or after differentiation as the output pulse.

The circuit shown in Fig. 17.3 is designed to operate as one of a series of scales-of-two to make up a counting divider of  $2^r$ , where  $r$  is the number

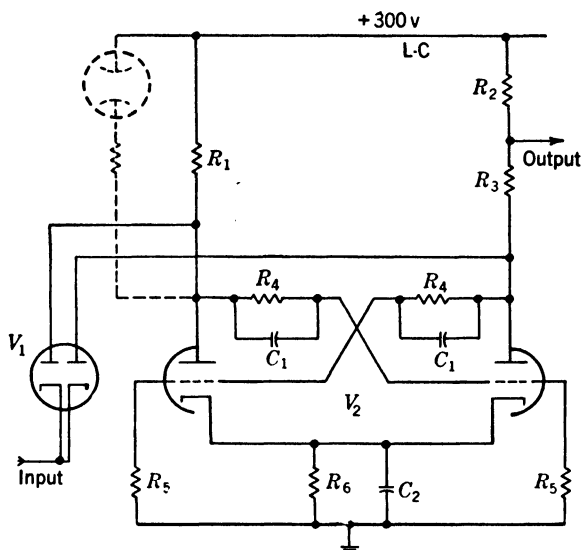


FIG. 17.3.—Scale-of-two.

(a) 6SN7 Unit

$C_1 = 50\mu\text{f}$ ;  $C_2 = 0.01\mu\text{f}$ ;  $R_1 = 20\text{k}$ ,  
 $2\text{w}$ ;  $R_2 = 5\text{k}$ ,  $\frac{1}{2}\text{w}$ ;  $R_3 = 15\text{k}$ ,  $2\text{w}$ ;  $R_4 =$   
 $200\text{k}$ ,  $\frac{1}{2}\text{w}$ ;  $R_5 = 510\text{k}$ ,  $\frac{1}{2}\text{w}$ ;  $R_6 = 10\text{k}$ ,  $1\text{w}$ ;  
 $V_1 = 6\text{H}6$ ;  $V_2 = 6\text{SN}7$ .

(b) 6SL7 Unit

$C_1 = 40\mu\text{f}$ ;  $C_2 = 0.01\mu\text{f}$ ;  $R_1 = 100\text{k}$ ,  $1\text{w}$ ;  
 $R_2 = 25\text{k}$ ,  $\frac{1}{2}\text{w}$ ;  $R_3 = 75\text{k}$ ,  $1\text{w}$ ;  $R_4 = 1\text{M}$ ,  
 $\frac{1}{2}\text{w}$ ;  $R_5 = 500\text{k}$ ,  $\frac{1}{2}\text{w}$ ;  $R_6 = 40\text{k}$ ,  $\frac{1}{2}\text{w}$ ;  $V_1 =$   
 $6\text{H}6$ ;  $V_2 = 6\text{SL}7$ .

of such circuits in series. The constants are apportioned for satisfactory series operation when the output connection of one circuit is connected directly to the cathodes of the trigger diode of the next circuit. The self-bias in the cathode circuit can be replaced by fixed bias on the grids but this makes the operation more sensitive to tube changes.

*Characteristics as a Counter.*—This circuit places no upper limit on the time interval between pulses, and with no special precaution it can be made to count pulses separated by only  $0.5\mu\text{sec}$ . The values shown in the figure result in a resolving time for random pulses of  $5\mu\text{sec}$  for the 6SN7 unit and  $20\mu\text{sec}$  for the 6SL7 unit.

The limit counting rate of the circuit is set by the time of rise of the

plate tube which is being cut off. This time can be reduced in two ways—by reducing  $R_1$  and  $R_2$ , a method that demands greater plate currents, or by reducing the amplitude of the voltage variation at the plates. This waveform is obviously larger than it need be; it is required only that the fraction of this voltage variation transferred to the grid of the other tube should cut off the plate current, i.e., about 10 volts for safety, whereas in Fig. 17-3 100 volts were transferred. It is not convenient simply to reduce  $R_a$  in order to reduce the transfer, for then the relative values of the positive and negative supply voltages would become too critical. The termination of the plate rise at +200 volts in the previous case limited the reset time to one plate-circuit time constant. By termination at a lower voltage, this can be reduced to a small fraction of the plate-circuit time constant. The remaining fault of the first circuit is due to the time required to restore the grid voltage; this also can be eliminated by suitably disposed diodes.

In the circuit of Fig. 17-4a the plate excursion is held between the limits of 60 and 80 volts by diodes and the grid excursion to between 0 and -3 volts by the grids and diodes. The cross-connecting networks and voltages are chosen so that with the one plate at 70 volts, the grid of the other tube is at -1.5. Thus the grid of the conducting tube is tending toward 7 volts but is caught at ground, while the cutoff grid is tending to -10.5 volts but is caught at -3 volts by a diode. The effective grid base<sup>1</sup> of each tube will be about 0.4 volts symmetrically disposed about -1.5 volts. In drawing the waveform diagrams (Fig. 17-4c) it has been assumed that  $C = 20 \mu\text{f}$  transfers two thirds of the plate voltage variation to the opposite grid, i.e., that the input capacity is  $10 \mu\text{f}$ . It has further been assumed that no change in the plate potential of  $V_{1a}$  due to tube current occurs until the grid potential of  $V_1$  has reached ground and is drawing grid current; in fact, this potential will start to fall parabolically sooner than this—when the grid potential of  $V_1$  approaches -1.5 volts. Note that when the trigger pulse ends, the plate potential of  $V_2$  has to change from 75 to 80 volts before the circuit can be retriggered. If the input pulse is appropriately shorter, there will be no “flat” in the rising waveform at the plate of  $V_2$ . It must not be made shorter than  $t_1 \approx \frac{2}{3} R_p C_s$  ( $\approx .01 \mu\text{sec}$ ), where  $C_s$  is the stray capacity, or the regeneration will not have started. The minimum duration of the action is less than  $\frac{2}{3} R_p (C_s + C) = .08 \mu\text{sec}$ , so that the counter should work up to 12 Mc/sec at least. It has been assumed that the potentials of the plates fall faster than they rise, that is, that  $R_p I_o > 500$  volts or  $I_o > 20$  ma, where  $I_o$  is the anode current in the tube being turned on during transition. The circuit requires accurate

<sup>1</sup> The effective grid base is the grid voltage variation for which the plate voltage moves between the limiting diode voltages.

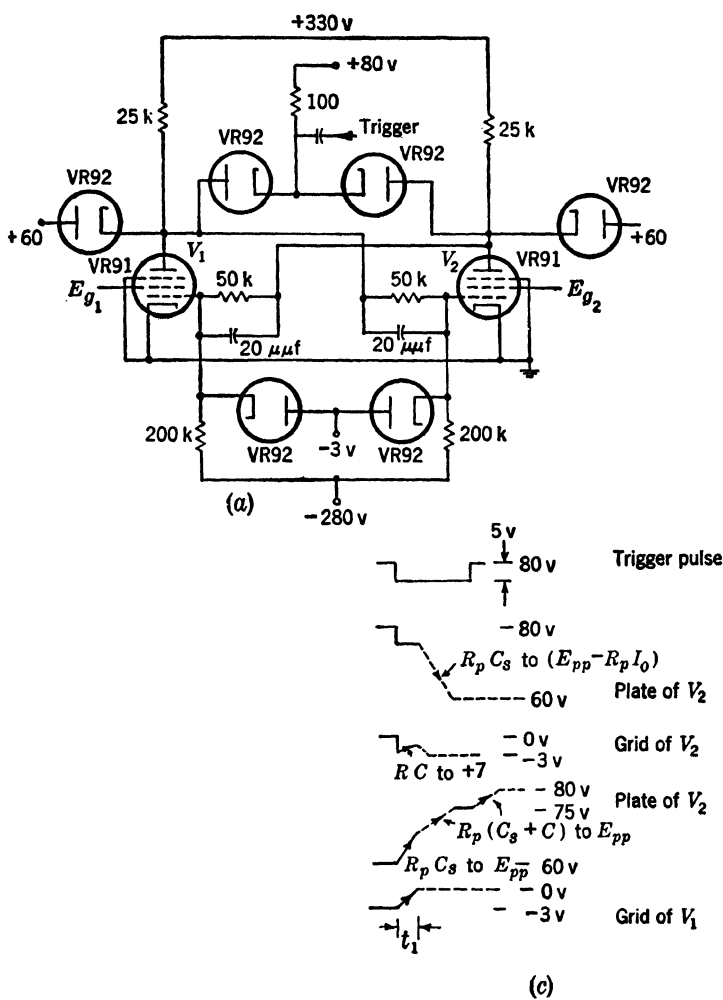


FIG. 17-4.—High-speed scale-of-two. The circuit diagram is shown at (a). The triggering waveform and one plate waveform are shown at (b). The trigger is 6 pulses at 8 Mc/sec. The waveforms drawn at (c) illustrate the triggering action: the notation " $E_p$  ( $C_1 + C_2$ ) to  $E_{pp}$ " indicates exponential approach to  $E_{pp}$  with time constant  $R_p(C_1 + C_2)$ . The full lines show the direct effect of the trigger; the broken lines show the regenerative action.

resistors in the cross-connecting networks and positive and negative voltage supplies that have a proportional voltage variation.

In an experimental circuit using the values shown in Fig. 17-4a, the maximum counting rate was found to be 8 Mc/sec;<sup>1</sup> the photograph (Fig. 17-4b) shows the counting of a group of pulses at this frequency.

The causes of this discrepancy between calculated and observed maximum rates were not ascertained but they may be attributed to increased stray capacity, poorly shaped trigger, and the assumption of ideal diodes.

Considerable improvement might be expected by replacing the diodes with germanium crystals since these have much less capacitance, both interelectrode and to ground. Also they have lower forward resistance. Their poor back resistance would not be important and the reverse voltage they are called upon to withstand is only 20 volts.

The time delay between an input and an output pulse of the counter is determined by the same factors as the minimum allowable time interval between pulses, and it can generally be reduced to about one third of this value. Since these circuits have two stable states, they represent a count of zero or one; hence, it is only necessary to ascertain which tube is on to determine the count. This can be done by placing a neon bulb in the plate of the first tube as shown by dotted lines in Fig. 17-3.

The various methods of triggering are shown in order of preference in Figs. 17-3 to 18-6. Triggering by use of diodes is shown in Fig. 17-3. In this circuit the negative trigger is applied to the cathodes of both diodes, the trigger consisting of the voltage waveform at the plate of the preceding counter. Diode coupling precludes the possibility of misfiring by disconnecting the input circuit during the differentiated overshoot of the trigger. The only time the diode cathodes are driven negative is when the preceding circuit has counted two input pulses. The amplitude of the trigger is approximately one fourth of the voltage appearing across the preceding plate resistor. This is not large enough to change the state of the two triodes but is enough to start the regenerative process that completes the change-over.

In applications where it is not feasible to direct-couple the proper voltage waveform, the negative trigger can be coupled to the diode cathodes by a resistance-capacitance network. The transition time of the circuit may be improved by returning the diode cathode to a voltage somewhat less than  $B+$ . In this case the plate of the "off" tube rises only to this voltage, where it is clamped, with a resultant improvement in transition time. This circuit gives good reliability.

<sup>1</sup> This rate was achieved for regularly spaced input pulses. The resolving time for randomly spaced pulses was not measured but is presumably somewhat greater than the 0.125  $\mu$ sec indicated.

In cases where more rapid transition is required the stray capacity may be reduced by replacing the diodes with germanium crystal elements. The very small capacitance prevents loading of the scaling circuit, and the ratio of front-to-back resistance is sufficient to allow good triggering.

In the circuit shown in Fig. 17-5 a positive trigger is applied to both cathodes through  $C_T$  across  $R_T$ . The cathode resistor  $R_T$  should be reasonably small to reduce degenerative effects. The trigger when applied to the cathodes reduces the grid-to-cathode potential of both tubes directly. To operate reliably, this circuit requires a low-impedance triangular trigger with a fast rise and a slow fall. The advantage of cathode triggering is that the capacitive loading of the cathode circuit does not interfere with the regeneration.

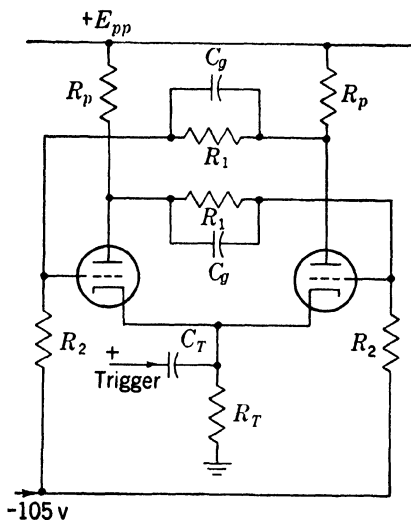


FIG. 17-5.—Cathode triggering.

In the circuit shown in Fig. 17-6 the triodes have been replaced by tubes with two control grids, in this case 6AS6's. The negative trigger is then applied through  $C_T$  to the second control grid, in this case the suppressor. The interrupted plate current in the "on" tube causes the plate voltage to rise and turns the first control grid of the other tube "on." This sequence causes plate current to flow only if the original negative trigger on the suppressor has terminated. The original negative trigger must therefore be of shorter duration than the transition time of the circuit. Because the amplified or inverted trigger of the "on" tube cannot be used to cancel the effect

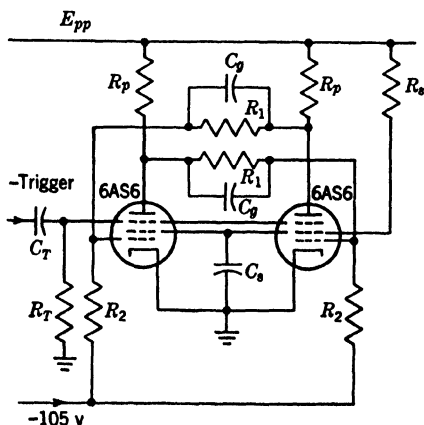


FIG. 17-6.—Suppressor triggering.

of the negative trigger on the "off" tube, this method of triggering is unreliable and should be used only in cases where the source impedance of the trigger is too high to employ other methods.

Feedback may be added to either half of the counter stage by any



of the triggering methods described. In cases where the feedback trigger must cancel the effect of an existing trigger, the circuit shown in Fig. 17-7 is recommended. In this circuit a positive trigger is applied to a "biased off" amplifier which is direct-coupled to half of the scale-of-two circuit. No difficulty will be experienced with this circuit if a triangular trigger is employed.

*Stability.*—In choosing the circuit components for a scale-of-two circuit, resistors and condensers with a tolerance of 5 per cent should

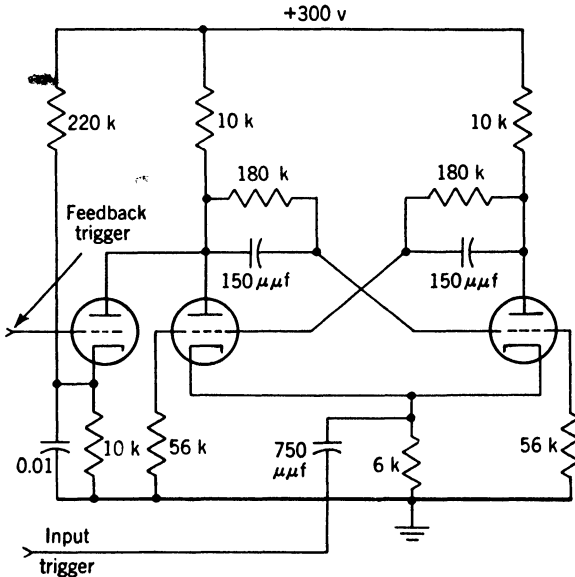


FIG. 17-7.—Feedback with amplifier.

be employed, particular care being taken to duplicate corresponding components in each half of the circuit.

If these precautions are taken and the recommended method of triggering employed, the circuit shown in Fig. 17-3 can be made to operate with a  $\pm 20$  per cent variation in heater voltage or a  $\pm 30$  per cent variation in plate voltage. The same figures hold if the cathodes are grounded and the grids are returned to a negative supply whose variations are proportional to those of the positive supply; however, if a fixed negative supply is employed the allowable variation in plate voltage is reduced to  $\pm 20$  per cent and that for heater voltage to about  $-15$  per cent or  $+18$  per cent. The allowable variation for the circuit of Fig. 17-3 may be further increased by selecting the tubes for "balanced" characteristics (for example, type 6SU7).

*Special Circuits.*—It is frequently desired to use scale-of-two circuits to obtain counting ratios other than  $2^n$  because of their rapid response and

reliability. This may be done by employing feedback in conjunction with cascaded scale-of-two circuits.

A common application of feedback in cascaded scale-of-two circuits is to obtain a scale-of-ten—a procedure that is often advantageous since it establishes a decade counting system. Figure 17-8 shows the application of the circuit in Fig. 17-3 with feedback to make a scale-of-ten. Manual operation of the RESET switch causes the right triode in each pair to become conducting. The first seven pulses count in the normal way. The eighth pulse restores the first three pairs to the original condition,

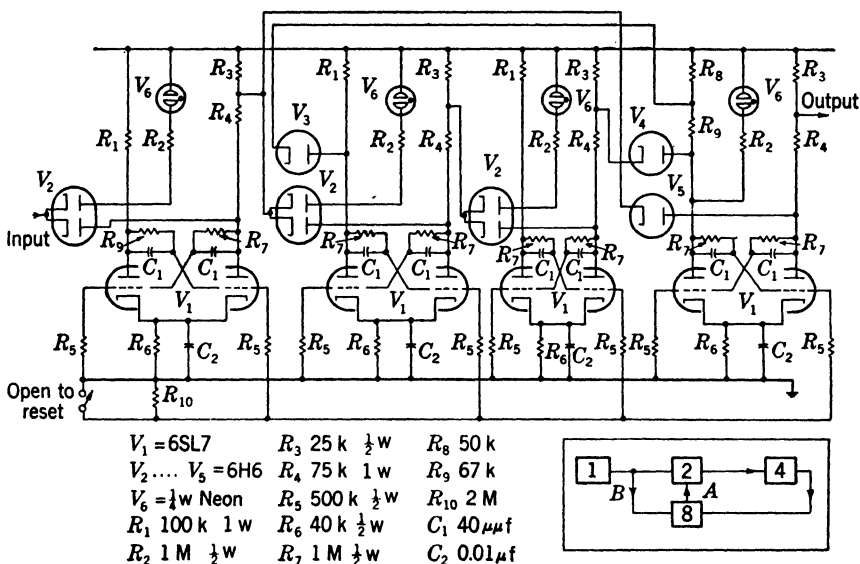


FIG. 17-8.—Scale-of-ten.  $V_1 = 6SL7$ ;  $V_2 \dots V_5 = 6H6$ ;  $V_6 = \frac{1}{4}\text{ w Neon}$ ;  $R_1 = 100\text{ k } 1\text{ w}$ ;  $R_2 = 1\text{ M } \frac{1}{2}\text{ w}$ ;  $R_3 = 25\text{ k } \frac{1}{2}\text{ w}$ ;  $R_4 = 75\text{ k } 1\text{ w}$ ;  $R_5 = 500\text{ k } \frac{1}{2}\text{ w}$ ;  $R_6 = 40\text{ k } \frac{1}{2}\text{ w}$ ;  $R_7 = 1\text{ M } \frac{1}{2}\text{ w}$ ;  $R_8 = 50\text{ k}$ ;  $R_9 = 67\text{ k}$ ;  $R_{10} = 2\text{ M}$ ;  $C_1 = 40\mu\text{mf}$ ;  $C_2 = 0.01\mu\text{f}$ .

causing the left tube of the last pair to become conducting, and, by means of the feedback through  $V_3$ , biases off the “off” tube of the second pair. Hence the second pair is not allowed to change state until the last pair is recycled. The ninth pulse turns on the left tube of the first pair, and the tenth pulse turns off the left tube of the first pair and, through  $V_6$ , the left tube of the last pair. Hence ten pulses cause a complete recycling and produce one output pulse.

It can be shown that scales-of-two can be added in series with the proper feedback to recycle for any integral number of pulses. However, few applications that count random pulses require a specific over-all counting ratio; in the interests of simplicity it is generally sufficient to reduce the counting rate so that it can be followed by a mechanical counter.



$R_P C$  larger than the deionization time. The values of  $R_B$  and  $R_A$  are chosen to make the grids sufficiently negative to prevent firing of the thyatron except when a positive trigger is applied through  $C_T$ .

To explain the operation of this circuit let us consider the plate waveform of tube  $V_1$  of the circuit in Fig. 17-9 as shown in Fig. 17-11. In time interval of  $t_1$  to  $t_2$  tube  $V_1$  is conducting. At time  $t_2$  a positive trigger is applied to the grids of both tubes firing  $V_2$ . Its plate then drops nearly to ground forcing the plate of  $V_1$  down to nearly  $-E_{PP}$  because of the capacity  $C$ . Tube  $V_1$  then deionizes and its plate starts rising toward  $+E_{PP}$  with  $\omega$  time constant equal to  $R_P C$ . This completes a cycle of operation.

The operation of the circuit shown in Fig. 17-10 is identical with that shown in Fig. 17-9 except that the quenching circuit is placed in the cathode circuits rather than in the plate circuits. The plate supply is limited to 100 volts to prevent the cathode voltage from exceeding the maximum allowable heater-cathode voltage rating of the tubes.

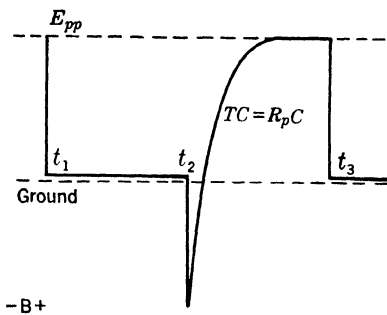


FIG. 17-11.—Thyatron scale-of-two waveform.

*Ring-of-n Counter.*—Thyratrons may be employed to give a reliable ring-of- $n$  counter.<sup>1</sup> A typical circuit of this type is shown in Fig. 17-12. Although this circuit is a scale-of-three, it may be extended to a scale-of- $n$ .

The method of quenching the tubes employed in this circuit is identical with that in the circuit shown in Fig. 17-10. The resistor  $R_A$  in the bias voltage network is returned to the cathode of the previous tube rather than to ground as in Fig. 17-10. The values of  $R_A$  and  $R_B$  are so chosen that a tube will not be fired by a trigger unless the tube immediately preceding it in the ring is conducting. By reducing the bias on the next tube the firing sequence is determined. All the necessary conditions for a ring counter are then met by this circuit.

The same type of circuit may be employed in a slightly modified form if gas tetrodes (type 2050) are employed. In this case the "priming" circuit of  $R_A$  and  $R_B$  is connected to the shield grid rather than to the control grid and sequence switching is assured.

by experience with gas tubes. References for thyatron ring counters include H. J. Reich, *Theory and Applications of Electron Tubes*, 2nd ed., McGraw Hill, New York, 1944, pp. 486-487, in which the various circuits are discussed, and for the original work, C. E. Wynn-Williams, *Proc. Roy. Soc.*, **132**, 295 (1931); **136**, 312 (1932); A. W. Hull, *Gen. Elec. Rev.*, **32**, 399 (1929).

<sup>1</sup> See H. J. Reich, *loc. cit.*, in which the various circuits are discussed, and, for the original work, C. E. Wynn-Williams, *loc. cit.*, and A. W. Hull, *loc. cit.*

**Characteristics of Thyatron Ring Counters.**—Whereas hard-tube ring counters are usually triggered by turning an “on” tube off, thyatron ring counters are triggered by turning an “off” tube on. After a thyatron begins to conduct, the grid has practically no control; hence the positive trigger is applied to the grid of the “off” tubes. If the trigger is of proper height, only the primed tube fires and the preceding tube is turned off by plate or cathode coupling.

If triggering delay is to be kept to a minimum a negative trigger is applied to the cathodes. Grid-plate or grid-shield capacity slows the

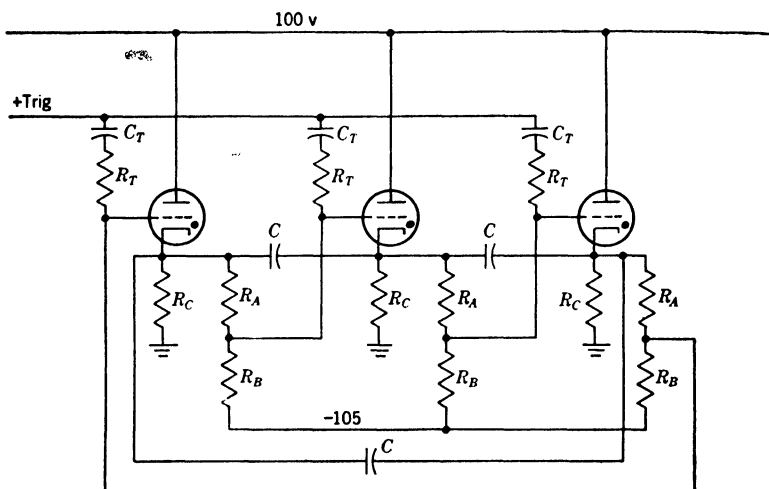


FIG. 17-12.—Thyatron scale-of-three.

rise time of a positive trigger applied to the grid. The negative trigger can be applied across a small resistor in the common ground return of all the cathodes.

The thyatrons employed are either 884 or 6D4 triodes, or 2050 or 2D21 tetrodes. The triodes have a distinct advantage in that they may be made to deionize in 20  $\mu$ sec whereas 50  $\mu$ sec is required for the tetrodes. The triodes extinguish when the plate current drops below 5 ma, and the tetrodes when the plate current drops below 2 ma, although the latter is quite irregular. By proper design the life of a thyatron in a counter circuit can always be made to exceed one thousand hours of operation (see Sec. 17-7).

## ENERGY STORAGE COUNTERS

**17-5. General Considerations.**—As is stated in Sec. 17-2 energy-storage counters are frequently employed since a larger counting ratio may be obtained with a given number of components than with sequence-operated counters. Because of the limitations placed on the maximum

allowable time interval of  $n$  pulses, an energy storage counter may be used only to count regularly spaced pulses or pulses whose spacings never exceed a predetermined upper limit. The major use of this type of counter is to obtain over-all counting ratios of regularly spaced pulses that cannot be factored into  $n_1 \cdot n_2 \cdot \cdot \cdot n_r$  where  $n$  is less than ten. Such an application is clearly frequency division, but counters are employed when feedback is required since feedback is more difficult to introduce into frequency dividers.

**17.6. Storage Circuits.**—The energy-storage element in most electronic counters of this type is usually a condenser. Since  $E = CV^2/2$  or

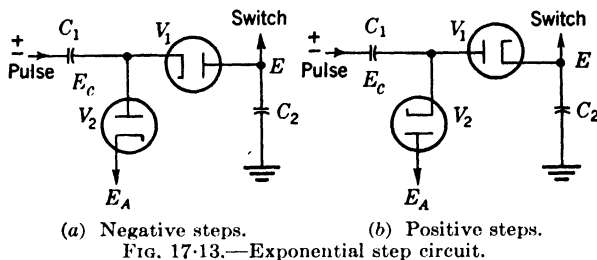


FIG. 17-13.—Exponential step circuit.

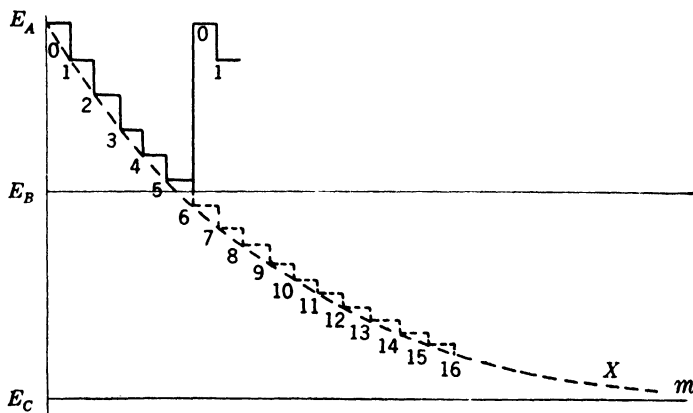


FIG. 17-14.—Waveform of exponential steps.

$V = \sqrt{2E/C}$  the voltage  $V$  defines the energy  $E$  for any value of capacity  $C$ . The use of a condenser has an advantage in that the energy may be stored for relatively long periods of time and a condenser is the most stable storage element with respect to temperature and aging effects.

**Exponential Voltage Steps.**—A simple and effective energy-storage circuit is shown in Fig. 17-13. The type of switch employed determines the choice of voltage step polarity. In these circuits  $C_2$  is the energy-storage condenser and  $C_1$  is a relatively small condenser for adding energy.

In Fig. 17-13a  $E_A$  is a fixed positive voltage and  $E_C$  is the amplitude of the trigger pulse (positive or negative). Figure 17-14 shows the voltage

waveform on  $C_2$  for the circuit shown in Fig. 17-13a. If  $E_B$  is the critical voltage of the recycling switch connected to  $C_2$  six counts are required to give one output pulse. The steps that would exist if the switch did not operate are dotted in; the number  $n$  of each step is indicated on the diagram.

When the recycling switch is operated,  $E$  is returned to  $E_A$  where it is held by the diodes. Step 1 is generated when a pulse  $E_c$  is applied to the input. Since  $E = E_A$  just before the pulse, the upper diode conducts immediately and a negative step  ${}_0\Delta E_1$  of amplitude  $E_c \frac{C_1}{C_1 + C_2}$  appears on  $C_2$ . On succeeding pulses (until the voltage on  $C_2$  is recycled)  $E_c$  must drop to  $E$  before the upper diode conducts. Hence the voltage change for the  $n$ th step is

$${}_{n-1}\Delta E_n = [E_c + (E_A - E_{n-1})] \frac{C_1}{C_1 + C_2}. \quad (5)$$

This expression holds for positive or negative input pulses.

Since  $\Delta E$  is proportional to  $E$  the general expression for  $E_n$  must be of the form

$$E_n = Ae^{-Kn} + B. \quad (6)$$

The constants  $A$  and  $B$  are determined by the boundary conditions, and  $K$  is determined by Eq. (5) and the continuity equation

$$E_n = E_{n-1} + {}_{n-1}\Delta E_n. \quad (7)$$

After the determination of  $A$ ,  $B$ , and  $K$ , Eq. (6) becomes

$$E_n = E_A + E_c - E_c \left( \frac{C_2}{C_1 + C_2} \right)^n \quad \text{where } K = \log \left( \frac{C_1 + C_2}{C_2} \right) \quad (8)$$

which, being general, gives the voltage after any pulse whether the pulses are uniformly spaced or not.

In order to permit  $C_2$  to charge completely, it is essential that the trigger supplied to this circuit be of long enough duration, that it have a large controlled amplitude, and that its source impedance be low. Ideally the trigger should be rectangular but other types will suffice providing the termination is rapid enough to prevent overlapping of successive triggers.

If  $E$  is held at  $E_A$  at the end of each cycle the circuit can be made completely self-compensating for variations in the supply voltages by making  $E_A$ ,  $E_B$ , and  $E_c$  vary in proportion to the supply voltages. The critical components are condensers and the effects of temperature on the circuit are not serious.

The most serious difficulty experienced with this circuit is maintaining the variation of  $E_B$  proportional to that of  $E_c$ . Both  $E_b$  and  $E_c$  should be as large as possible to minimize the effects of variations in the amplitude

selection process. Equation (8) shows the amplitude of the last step is considerably smaller than the initial one unless  $E_A - E_B \ll E_C$ . Also since it is not desirable to reduce  $E_A - E_B$ , the trigger height must be made large and even then only partial compensation can be obtained. This reduction in step amplitude with count constitutes a major limitation of this type of circuit.

In most cases the counter may be adjusted by adding a trimmer condenser to  $C_1$ . If the value of the trimmer condenser required is too large the adjustment may be made by varying  $E_B$ . This latter method is less desirable since some of the available voltage is sacrificed.

*Linear Steps of Voltage.*—Waveforms of this type are described in Chaps. 2, 7, and 8. In Fig. 17-13a, if the voltage  $E$  is fed to the grid of a cathode follower whose cathode supplies  $E_A$ , the result is the circuit shown in Fig. 17-15. The circuit in Fig. 17-13b may also be modified in the same manner. If the gain of the cathode follower is unity  $E_{n-1} \equiv E_A$  and Eq. (5) becomes

$$n-1\Delta E_n = E_C \frac{C_1}{C_1 + C_2}, \quad (9)$$

and all steps are of equal amplitude.

The allowable tolerance on the variation of  $E_B$  is increased and the requirement for a very large trigger is removed. However, the clamping action of the lower diode is removed by the cathode follower making the initial value of  $E$  depend on the electronic switch unless a third diode is added as a clamp.

Negative linear steps may be generated by a constant-current pentode as shown in Fig. 17-16.

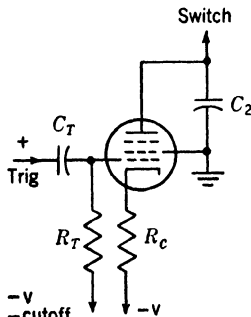


FIG. 17-16.—Linear step circuit.

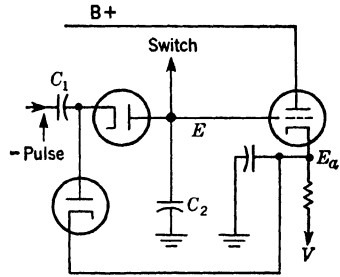


FIG. 17-15.—Linear step circuit.

The amplitude of each step is  $\frac{1}{C_2} \int_0^T i_p dt$ , where  $T$  is the duration of the trigger. This circuit generates very linear steps with a high-impedance trigger; however, both the width and amplitude of the trigger must be controlled. Although the

tube has cathode degeneration the value of  $\int_0^T i_p dt$  is still subject to tube variation and only partial cancellation for variations in supply voltage is possible. The count may be adjusted by varying the grid and cathode return voltages, the trigger amplitude, or  $R_C$ .



Positive linear steps cannot be generated by integrating cathode current. If  $C_2$  is connected to the cathode rather than to the plate, it is extremely difficult to maintain constant screen potential and, consequently, use cannot be made of the constant-current characteristics of the pentode. Although this method is not recommended it is sometimes employed with triodes to generate nearly linear steps.

Linear steps may be obtained from the circuits shown in Fig. 17-13 if  $C_2$  is used as a Miller feedback condenser as shown in Fig. 17-17.

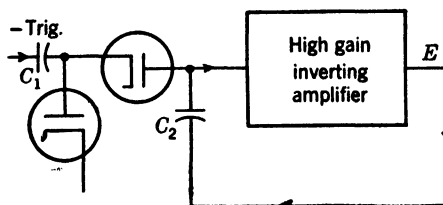


FIG. 17-17.—Miller feedback linear step circuit.

The steps in  $E$  are positive and have an amplitude equal to  $E_T \frac{C_1}{C_2}$ , where  $E_T$  is the trigger amplitude. The electronic switch may operate at either end of  $C_2$ , or this function may be performed by trigger action in the amplifier (see Fig. 17-22). In any case it should be remembered that both of these points are at a low impedance due to the negative voltage feedback in the amplifier provided by  $C_2$ . The negative feedback also stabilizes the operation of the amplifier. The amount may be adjusted by varying  $C_1$  or the threshold of the amplitude selector.

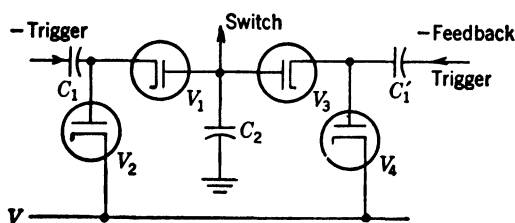


FIG. 17-18.—Conventional feedback.

*Methods of Introducing Feedback.*—Feedback is accomplished by duplicating the circuit that feeds the pulses to  $C_2$  to provide a separate input for the feedback pulse. The circuit shown in Fig. 17-13a modified in this manner results in the circuit shown in Fig. 17-18. In this circuit  $C_1$  may be adjusted to give a step on  $C_2$  at the time of a feedback pulse equal in amplitude to  $n''$  steps produced by pulses through  $C_1$ . This is exactly equivalent to feeding back  $n''$  pulses through  $C_1$  for each pulse actually fed back through  $C_1'$ . The adjustment of  $C_1'$  then provides a

convenient means of changing the over-all counting ratio of a chain of dividers in unit steps.

In most applications the diode  $V_4$  may be replaced by a resistor since the feedback occurs infrequently. The value of the resistor must be large enough to prevent differentiation of the feedback pulse and small enough to allow  $C_1$  to recover completely between feedback pulses. The removal of the diode does not interfere with the clamping of the voltage on  $C_2$  as this function is still performed by  $V_2$ .

The addition of feedback in this manner is equally applicable to the circuits shown in Figs. 17-15 and 17-17. The same type of modification may be introduced into the circuit shown in Fig. 17-16 by adding a second constant-current pentode to introduce the feedback pulse.

*Methods of Reading the Count.*—If the grid of a cathode follower is connected to the point in the circuit where the step-voltage waveform appears, the count may be read from a meter connected to the cathode of the cathode follower provided the meter is correctly calibrated.

It will be noticed that if this procedure is followed with either of the circuits shown in Fig. 17-13, the meter must have a nonlinear calibration. The use of a cathode follower for meter isolation permits linear step operation without additional tubes and gives a linear calibration.

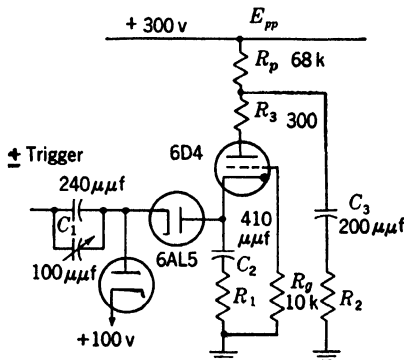


FIG. 17-19.—Thyatron counter.

The use of energy-storage counters in applications where it is necessary to count the number of pulses in an interval of time is severely limited by the leakage of charge from  $C_2$  since the reading of the count drifts while no pulses are being received. If  $C_2$  is small the drift may be so rapid that it is impossible to obtain a reading.

**17-7. Energy-storage Counter Circuits. Thyatron Counter Circuits.** A counter circuit employing thyatrons and the energy-storage circuit of Fig. 17-13 is shown in Fig. 17-19. In this circuit  $R_1$ ,  $R_2$ , and  $R_3$  are all small-value resistors and  $C_3 = C_2/2$  in most cases. Negative steps are generated on the cathode by the incoming triggers until the critical firing voltage of the tube is passed. At this time  $C_3$  has charged to  $E_{pp}$  through  $R_p$ ; consequently  $C_2$  will rise to +100 volts, and  $C_3$  will drop 200 volts to approximately +100 volts because of the charge-sharing action of the condensers.

After this action is over the thyatron deionizes since the only current

it can now draw is through  $R_p$  and this is not sufficient to maintain the discharge.  $C_3$  must then recharge to  $E_{pp}$  through  $R_p$  before the tube fires again. The condenser  $C_3$  performs two functions in this circuit: it prevents the tube from raising its cathode temporarily to  $E_{pp}$ , and it provides a 200-volt negative pulse which may be used as a trigger for a subsequent counter. During the period of conduction by the tube the peak current is limited only by  $R_1$ ,  $R_2$ , and  $R_3$ , the primary limiting being done by  $R_3$ . The resistors  $R_1$  and  $R_2$  are not necessary but may be inserted to obtain low-impedance positive or negative pulses of short duration.

The resistance  $R_p$  should be greater than 60  $K$  for triodes and 150  $K$  for tetrodes to permit deionization, and  $C_3$  must be greater than 200  $\mu\text{f}$  to allow a plasma to be formed in the tube during conduction.

Although this circuit employs the energy-storage system shown in Fig. 17-13, it may be used in conjunction with those shown in Fig. 17-15 or Fig. 17-16. The action of the thyatron switch will be unaffected except that the positive rise of  $E_c$  will not be limited by the diode but will be equal to  $(E_{pp} - E_2) \frac{C_3}{C_2 + C_3}$ , where  $E_2$  is the firing voltage.

One of the chief advantages of this circuit is that the extent of the sudden rise of  $E_c$  and the sudden drop of  $E_c$  is unaffected by the type of trigger, the adjustment of the counter, and interaction from other circuits. This is due to the fact that the plate-to-cathode voltage of the tube always drops to about 12 volts during the period of conduction.

The maximum allowable spacing for  $n$  pulses is determined primarily by  $C_2$  and the cathode-to-heater resistance ( $R_{HK}$ ) of the tube, since  $E_c$  decays with a time constant of  $R_{HK}C_2$ . The minimum spacing between pulses must be greater than the deionization time, and the minimum spacing for  $n$  pulses must be great enough to allow  $C_3$  to recharge to  $E_{pp}$  through  $R_p$ . Since the deionization time is never less than 20  $\mu\text{sec}$  and  $R_p > 60 K$  and  $C_3 > 200 \mu\text{f}$ , the requirement on minimum allowable pulse spacing seriously restricts the use of this circuit.<sup>1</sup>

The time delay between an  $n$ th input pulse and an output pulse is generally only a few tenths of a microsecond; however, for incorrect values of the count adjustment it may become several microseconds.

Feedback may be introduced by the circuit shown in Fig. 17-18. If feedback is applied immediately after the counter has fired and while the thyatron is still ionized, the effect of the feedback is totally unreliable. For reliable operation it is necessary to apply the feedback after the tube has deionized. In the case of a series divider chain a convenient method of doing this is shown in the block diagram of Fig. 17-20. The output

<sup>1</sup> Satisfactory operation using 6D4 tubes has been obtained with a frequency of firing of the thyatron up to 20 kc/sec.

of the counter chain generates a gate which is applied to a time selector. This circuit selects the next pulse to be applied to the chain that is to be fed back to the first counter. The feedback then occurs at the time of the next pulse after the one that fired the chain, and hence the tube in the first counter is deionized.

The circuit shown in Fig. 17-19 will count by 10 reliably in field use and by 20 in laboratory use. The count may be adjusted by means of a trimmer condenser on  $C_1$  or by varying the d-c grid voltage to change the critical value of the cathode voltage.

If all the voltages in this circuit vary proportionally, nearly complete cancellation against variation in supply voltages may be obtained, the tube drop being negligible. The amplitude of the incoming trigger may be made to vary in this manner by generating it in a similar circuit with the same voltage supply. The voltage to which the lower diode is returned should be obtained from a bleeder to  $+E_{pp}$ , and the effects of variations in firing voltage of the tube cancel in any tube with a constant control ratio. Variations in heater voltage are manifest in variations in tube drop and control ratio and the latter of these is the more serious. A counter of this type counting by ten will maintain its count with a  $\pm 50\%$  variation in  $E_{pp}$  and with heater voltage from 4.3 to 7.5 volts.

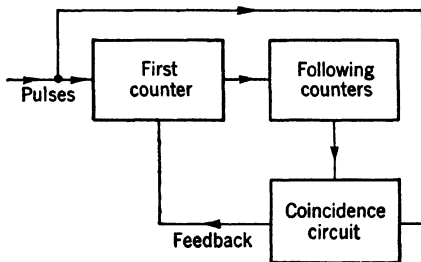


FIG. 17-20.—Feedback in thyratron counter chain.

The use of triodes such as the 884 or 6D4 is preferred as they deionize in about  $20\ \mu\text{sec}$ ,  $R_p$  need only be greater than 60 k, and triodes usually have less heater-to-cathode leakage. With tetrodes such as the 2050 or 2D21 the deionization time is about  $50\ \mu\text{sec}$ , and  $R_p$  should be greater than 150 ohms. However, tetrodes have much steeper grid-cutoff characteristics and can be fired reliably with smaller triggers.

The tube may have a life well over 1000 hours if the following precautions are taken. Resistor  $R_o$  should be increased to 50 k and  $R_s$  to 1 k ohms.  $R_o$  must be large enough to prevent grid-to-cathode arcs, and  $R_s$  must limit the peak current to 0.3 amp.

**Blocking-oscillator Counter Circuits.**—Blocking oscillators are described in detail in Chap. 6. It is only necessary to replace the bias circuit by an energy-storage circuit to provide a counter. Figure 17-21 shows a blocking oscillator of the type described in Sec. 6-9 and the energy-storage circuit in Fig. 17-13. The energy-storage circuit in Fig. 17-15 can also be used, as can blocking oscillators of any other type. In general it is unwise to use negative steps and to place the energy-storage

circuit in the cathode since the blocking-oscillator tube can draw some current before it fires and this current interferes with the last step applied to the cathode before the blocking oscillator fires.

When blocking-oscillator counters are arranged in a chain each counter may be triggered from the tertiary winding of the plate transformer of the preceding counter.<sup>1</sup>

Unfortunately the value of the maximum negative voltage on  $C_2$  is a function of the portion of the fall of the last step on which the blocking oscillator fires. This action can give rise to the same type of instability as that experienced in blocking-oscillator frequency dividers.

Another undesirable characteristic is the reaction of the firing of one counter on the one that precedes it. This is a common characteristic of blocking-oscillator counters and frequency dividers (see Chap. 16 for discussion).

As a result of the interaction between counters and the variation in the maximum negative grid swing the proper adjustment of any counter is dependent on the adjustment of the rest of the counters in the chain. In all cases

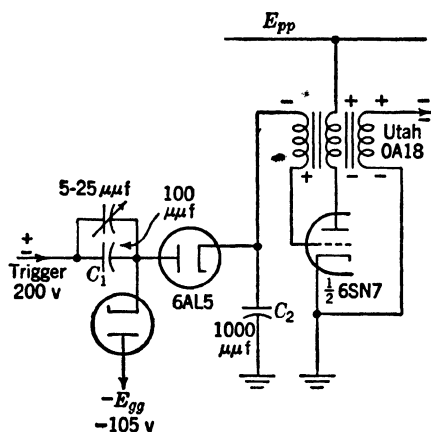


FIG. 17-21.—Blocking-oscillator counter.

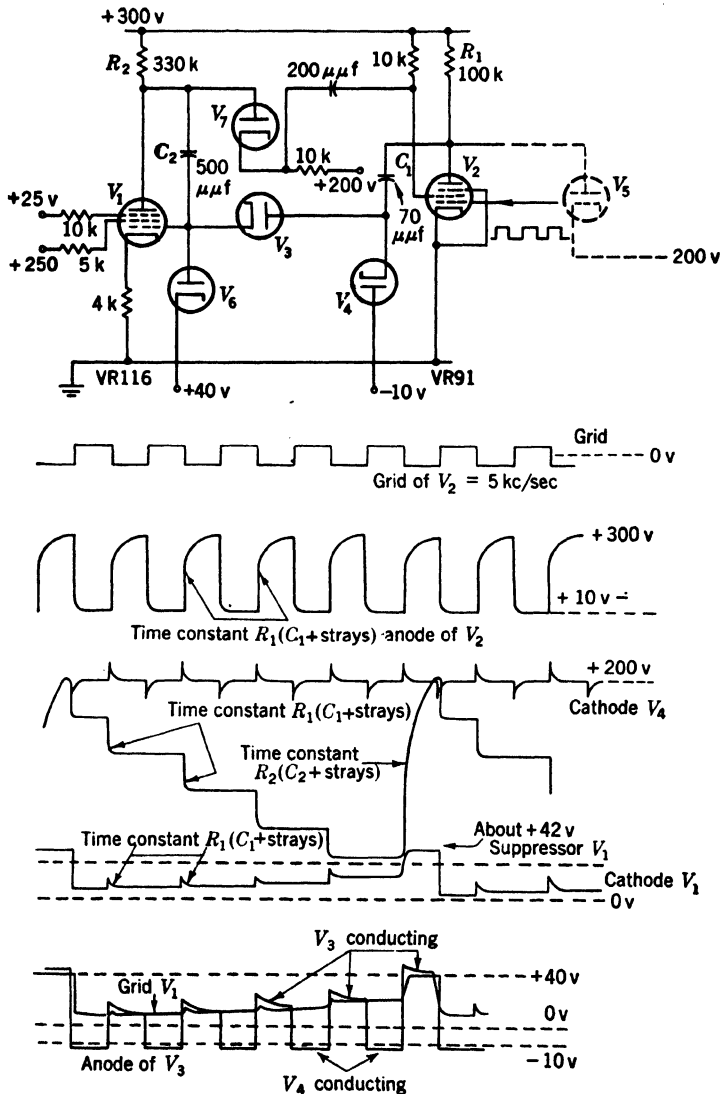
extreme care is necessary in design to minimize these undesirable characteristics.

The maximum allowable time interval for  $n$  pulses is determined by  $C_2$  in conjunction with the heater-to-cathode resistance ( $R_{HK}$ ) of the upper diode, since  $E_{C_2}$  will decay exponentially with a time constant equal to  $C_2 R_{HK}$ . The minimum allowable spacing between pulses is determined solely by the recovery of  $C_1$ ; the minimum allowable spacing for  $n$ -pulses is determined only by the tube dissipation.

The time delay between an  $n$ th input pulse and an output pulse is the same as for a normal blocking oscillator and is generally only a few tenths of a microsecond.

<sup>1</sup> When counters are connected by plate coupling,  $C_1$  and  $C_2$  load the plate of the preceding counter during the conduction period of the upper diode. This loading has a marked effect on the performance of the blocking oscillator and limits the size of  $C_1$  to a small value. When exponential steps are employed, the current through the upper diode is determined by the number of the step and, consequently, the loading on the preceding counter varies with the number of the count. This effect may be so serious as to cause variations in the count from cycle to cycle.

Feedback presents no special problem and any of the conventional methods may be employed, since the normal time delay in the counter



either case,  $n$  should not be greater than five for field use or ten for laboratory use.

The negative voltage to which the grid is driven when the blocking oscillator fires is a function of heater voltage,  $E_{pp}$ , and the characteristics of the particular tube. In general the variation of  $E_c$  is not proportional to variations in  $E_{pp}$ . If stability for variations in heater voltage and  $E_{pp}$  is required, a third diode is employed to clamp the negative excursion of  $E_c$  to some voltage that varies proportionally to  $E_{pp}$ .

*Phantastron Counter Circuit.*—Figure 17-22 is a phantastron counter circuit employing Miller feedback in the manner described in Fig. 17-17. The functions of  $C_1$ ,  $C_2$ ,  $V_1$ , and  $V_2$  of Fig. 17-13*b* in the energy-storage system are performed by  $C_1$ ,  $C_2$ ,  $V_3$ , and  $V_4$ . Condenser  $C_2$  is also the feedback condenser.

The operation during a complete cycle is shown by the waveform diagrams in Fig. 17-22. The negative input pulses are inverted by  $V_2$ , and  $C_1$  couples a small amount of energy through  $V_3$  to  $C_2$ . Feedback through  $C_2$  from the plate of  $V_1$  to the grid prevents the grid from rising very far with each pulse. However, each pulse reduces the plate potential so the plate voltage waveform is a series of negative steps. When the plate has dropped to the level of the suppressor, the transconductance of  $V_1$  is so low that the positive pulses on the grid are no longer fed back through  $C_2$ . Hence the grid goes positive with the last pulse. This cuts off the plate current since the cathode also rises with the last pulse and since the suppressor, at a fixed potential, cuts off the plate current. The plate voltage then rises and the circuit is recycled.<sup>1</sup>

The size of each step in the plate voltage is proportional to  $C_1/C_2$  and to the plate supply voltage of  $V_2$ . Hence the counting ratio can be varied either by  $C_1$ ,  $C_2$ , or by the plate potential of  $V_1$ . The minimum time between pulses is determined by  $R_1C_1$  and can be made very short by including a fifth diode ( $V_5$ ) on the plate of  $V_2$  to limit the positive swing of the plate voltage on  $V_2$ . The maximum time for  $n$  pulses is determined by  $R_{HK}C_2$ , where  $R_{HK}$  is the heater-to-cathode resistance of  $V_3$ .

**17-8. Combinations of Counters.**—In many applications it is desirable to count a large number of pulses or to obtain an output for every  $n$ th pulse where  $n$  becomes large. In energy-storage counters the value of  $n$  must always be less than 20 and in most cases not greater than 10 to meet stability requirements. In sequence counters,  $n$  is usually 2 and never larger than 3 for hard tubes and never larger than 10 for gas tubes.

*Cascading Counters.*—When counters are connected in cascade—that is, the output of one is the input of the next as in Fig. 17-23—the over-all

<sup>1</sup> The operation of phantastrons is explained in more detail in Chap. 5. In the step counter, plate current must be initiated by a trigger through  $V_7$  after recycling. This trigger can be supplied from an external source so that the circuit can be used to signal the time of arrival of the  $n$ th pulse after the trigger.

scaling or dividing ratio  $N$  is the product of the individual counter scaling ratios.

$$N = n_1 n_2 \cdots n_r. \quad (1)$$

If the counter chain is used to count a given number of pulses rather than to divide a continuous pulse train it is often necessary to know the remainder as well as the quotient. If there is a method of determining the number of times the counter chain has recycled (for instance, a mechanical counter) and a method of determining the number of pulses stored in each counter (for instance, neon count-indicating lights), the total number of pulses received is given by

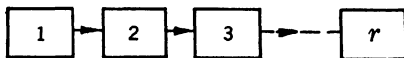


FIG. 17-23.—Series divider chain.

$$N_{\text{in}} = N'_1 + n_1 N'_2 + n_1 n_2 N'_3 + \cdots (n_1 n_2 \cdots n_r) N_{\text{out}} \quad (2)$$

where the prime indicates the number of “held” counts in the counter with appropriate subscript. The last term in Eq. (2) is the number of times the counter chain has recycled.

As the over-all counting ratio is the product of the individual counting ratios rather than their sum, it is possible to achieve a great saving in the number of circuit components. It should be noted, however, that this is possible only when the over-all counting ratio can be factored into  $n_1 \cdot n_2 \cdots n_r$ . Thus the counter chain establishes a decimal system if the  $n$ 's are all 10.

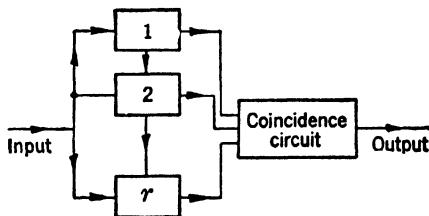


FIG. 17-24.—Parallel dividers.

**Parallel Counters.**—Counter circuits may be arranged to operate in parallel as indicated in Fig. 17-24. In this case the pulses to be counted are fed directly into each counter. The outputs of all the counters are fed to a coincidence circuit that gives an output

only when outputs are received from all counters simultaneously.

The over-all counting ratio of this system is equal to the lowest common multiple of  $n_1, n_2, n_3$ , etc. If each  $n$  is broken down to its prime factors and no prime factors of any  $n$  are repeated in any other  $n$ , the over-all counting ratio is again  $n_1 \cdot n_2 \cdot n_3 \cdots n_r$ .

In this circuit, the time delay between the  $n$ th pulse and the output is approximately equal to the largest time delay of any of the counters. If, however, the counters are connected in series, the over-all time delay is equal to the sum of the time delays for all the individual counters. The decrease in over-all time delay achieved by connecting the counters in parallel is a major factor in some applications.



If energy-storage counters are employed, the parallel connection has another advantage over the series connection. When counters are connected in series the energy must be stored in the  $r$ th counter until  $n_1 \cdot n_2 \cdot n_3 \cdot \dots \cdot n_r$  pulses appear at the input of the system, but when the counters are connected in parallel, the energy need be stored only until  $n$  pulses appear at its input where  $n$  is the counting ratio of that particular counter.

Parallel operation has disadvantages other than the restriction placed on  $n_1, n_2, n_3$ , etc. The system provides only an output pulse for every  $n$ th input pulse and does not give a direct indication of the number of pulses that have been received at any time. The circuit is also considerably complicated by the coincidence circuit, which becomes involved if a large number of counters are employed.

*Feedback in Cascaded Counters.*—Equation (1) shows that the over-all counting ratio of a series of cascaded counters is given by

$$n_1 \cdot n_2 \cdot n_3 \cdot \dots \cdot n_r,$$

where the values of the  $n$ 's are integers and are generally not greater than 10. This places a serious limitation on the flexibility of this type

of counter circuit as we may desire an over-all counting ratio that can not be factored in this manner. In numerous cases it is desired to utilize a single counting circuit to give any one of a series of over-all counting ratios by changing the

circuit, in which case some of the desired counting ratios are unobtainable because they cannot be factored.

It is sometimes found advisable to construct a counting circuit in which the value of  $n$  for all individual counters is the same. Equation (1) gives the over-all counting ratio for a system of this type as  $n^r$ . This places an even more serious limitation on the obtainable counting ratios. Many of these difficulties may be circumvented by the addition of feedback loops.

*Feedback in Energy-storage Counters.*—A counter chain of energy-storage counters with feedback is shown in Fig. 17-25. In this diagram the entire counter chain is broken down into three parts: those counters that precede the feedback loop, the ones within the feedback loop, and the ones that follow the feedback loop. Let the counting ratios of these subdivisions be represented by  $n_A, n_B$ , and  $n_C$  respectively, and let  $n'_B$  be the counting ratio of section  $B$  without feedback. The effect of feedback in this type of counter chain is the same as if  $n''_B$  pulses were added or subtracted from the input of section  $B$  every time an output is

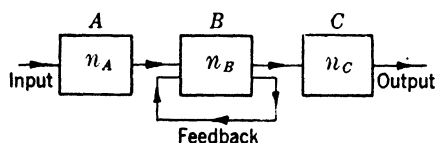


FIG. 17-25.—Series divider chain with feedback.

obtained from section *B*. Consequently, it is seen that  $n'_B = n_B + n''_B$  or  $n_B = n'_B - n''_B$ . Therefore the over-all counting ratio for the whole chain is

$$n = n_A n_B n_C = n_A n_C (n'_B - n''_B)^1. \quad (3)$$

If section *B* is composed of only one counter this is the same result as would be obtained by changing the counting ratio of this stage. However, section *B* may be any number of counters in series, and  $n'_B$  may therefore be very large. Feedback provides a means of changing the over-all counting ratio of section *B* in unit steps.

If feedback is employed from the output of the entire chain back to the input—that is,  $n_A$  and  $n_C$  equal unity—Eq. (3) becomes

$$n = n' - n''. \quad (4)$$

In this case the over-all counting ratio may be changed in steps of unity. Practical circuit considerations do, however, place an upper limit on the magnitude of  $n'$  and for this reason circuits may have multiple feedback loops. In this case Eq. (3) is still valid if the feedback loops are considered separately and if  $n'_B$  represents the counting ratio without the feedback loop being considered. The value of  $n$  for a circuit of this type may then be found by considering the feedback loops as being added one at a time and assigning  $n'_B$  its successive values.

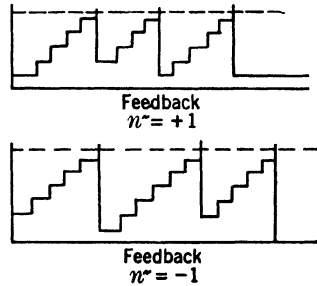


FIG. 17-26.—Energy feedback.

If multiple feedback loops are employed in addition to varying the counting ratios of the individual counters, any desired over-all counting ratio may be obtained. Moreover, if the number of individual counters in the chain is varied, a wide variety of over-all counting ratios may be obtained even if severe restrictions are placed on the values of  $n_1, n_2$ , etc.

It was stated that the effect of the output pulse of section *B* (see Fig. 17-25) was to produce the same effect as if  $n$  pulses were either added to or subtracted from the input of section *B*. This effect may be accomplished in either of two ways. Considering the first counter in section *B* and referring to Fig. 17-2 the feedback pulse may be made to add or subtract  $n''$  increments of energy from the stored energy (see Fig. 17-26) or the feedback pulse may change the threshold value at which the stored energy is removed (see Fig. 17-27). The result in either case is to change the counting ratio of the first counter in section *B* from  $n$  to  $n - n''$  during the cycle when the feedback pulse is received.

<sup>1</sup> The term  $n''_B$  is positive if pulses are added, and negative if they are subtracted.

*Feedback in Sequence Counters.*—This same type of feedback may be employed in a chain or sequence-operated ring counters by utilizing the output pulse of section *B* (see Fig. 17·25) to turn “on” a particular unit of the first counter in section *B* (see Fig. 17·1). In this case,  $n''$  equals the number of the unit turned on and must always be positive.

There are other types of interconnections possible in a counter chain of this type since one may obtain the output that is to be fed back from

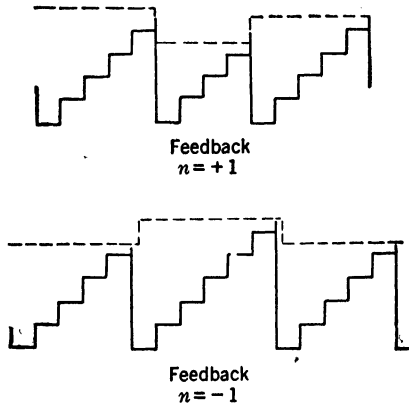


FIG. 17-27.—Threshold feedback.

any unit of a ring counter, and the feedback may be used to turn a unit of a counter “off” rather than “on.” In the latter case, the pulse will be effective only if it is applied when this particular unit is “on.” The use of either of these interconnections necessitates the use of multiple feedback loops. In some instances pulse selectors may be inserted in the feedback loops to produce the same effect. The number of these combinations possible are, however, too numerous to analyze.

## CHAPTER 18

### MATHEMATICAL OPERATIONS ON WAVEFORMS—I

BY D. MACRAE, JR., A. H. FREDRICK, AND A. S. BISHOP

The operations to be considered in this chapter are addition, subtraction, differentiation, and integration. These operations have in common the property of being performable, at least approximately, by means of networks of linear passive elements. To present lower output impedance or provide more accurate computation, feedback amplifiers may be used. These operations are thus special cases of the process of linear waveform-shaping discussed in Chap. 2.

Although the methods of performing these operations are similar, there are some obvious differences among the operations. In addition and subtraction, waveform shaping is usually not desired; differentiation and integration, however, represent attempts to shape the input waveforms in particular ways. Addition and subtraction can be done very accurately by means of linear passive elements, whereas in the case of differentiation and integration with passive networks accuracy is obtainable only at the expense of decreased output amplitude.

In this chapter some of the applications of these operations will be pointed out; general circuit types for performing the operations will be described; some of the equations governing the action of these circuits will be derived; and practical circuits with design data will be given.

#### ADDITION AND SUBTRACTION OF VOLTAGES AND CURRENTS

**18-1. General Considerations.** *Uses of Addition and Subtraction.*—Addition and subtraction are operations that are frequently used in electronic circuits although in many cases the operations performed are not considered to be addition and subtraction. A number of operations accomplished entirely or in part by addition and discussed elsewhere in this volume, are the following:

1. *Signal mixing at d-c, audio, video, or radio frequencies* usually refers to the addition of similar waveforms at approximately the same frequency. Examples are heterodyning in receivers, addition of input to a fraction of output in feedback amplifiers, addition of a carrier to a modulated wave for demodulation (Chap. 14), the addition of waveforms to produce deflection or intensity modula-

tion on cathode-ray tubes (Chap. 20 of this volume and in Vol. 22 of the Series, Chap. 4), and the production of sum-waveforms such as staircase waveforms or trapezoids (Chap. 8).

2. *Addition of a d-c level to an a-c waveform* is done, for example, in varying the bias of variable-gain tubes in AVC circuits, and in the addition of a d-c modulating signal to a carrier (Chap. 11).
3. *Injection of triggers or synchronizing pulses into relaxation oscillators* is treated in Chap. 5 for multivibrators, in Chap. 6 for blocking oscillators, and in Chap. 16 for frequency dividers using relaxation oscillators. A typical problem is the addition of pulses to an exponential recovery waveform.
4. *Amplitude discrimination or comparison* (Chap. 9) may be accomplished by subtracting one signal from another; the difference then indicates the sign of inequality, or a time index may be produced at the instant of zero difference.
5. *Time selection by addition* (Chap. 10) may be performed by adding a rectangular waveform to the waveform of which a part is to be selected and applying the resulting waveform to a nonlinear element which has no response below a certain input level.

*Characteristic Problems.*—In some of these operations a generalized sort of addition in which the output is a linear function of the inputs rather than simply their sum or difference is performed. Thus if the inputs are  $e_1$  and  $e_2$  and the output  $e_o$ , the general operation considered can be represented by

$$e_o = ae_1 + be_2.$$

The constants  $a$  and  $b$  will be called the “weighting factors” for the operation. This generalized addition also includes subtraction, that is, the case in which  $a$  and  $b$  have opposite signs.

The accuracy of the summation of voltages or currents is not of prime importance in the operations listed above, as it is in the process of addition for electronic computation. There must still be consideration of the dependability of the operation performed, however, and this usually introduces accuracy requirements that must be met by procedures similar to those used for more accurate circuits.

In some applications (time selection, for instance) one of the input waveforms is rectangular and therefore has only two significant values. In this case the requirement of linearity with respect to this variable no longer exists.

Addition may be followed by limiting; one example is signal mixing at the input to a cathode-ray tube, in which case the sum must be limited in order to avoid “blooming” on the tube face. Addition is sometimes preceded by limiting; an example of this occurs in time selection, when

a rectangular wave is added to a series of pulses and it is desired to reject pulses that do not coincide with the rectangle but are of greater amplitude than the rectangle.

The waveforms to be added may be shaped by the adding device. In some cases this is desired, for integration or differentiation may be used to accentuate or subdue certain features of the input waveforms. In other cases undesired shaping occurs, as when a rapid rise is slowed down or the amplitude of a narrow pulse is decreased because the adding device has insufficient speed of response. Undesired transients may also be excited in an adding network by an input waveform with a sharp edge.

The interaction of the inputs and outputs with the adding device and with each other must be considered, for example when an undesired pulse might trigger a multivibrator or blocking oscillator. The interaction between two sources may be measured in terms of the *transfer admittance* which gives the ratio of the current increment produced at one input to a voltage increment at the other input in question. In the case of linear networks the reciprocity theorem shows that this factor is independent of the order in which two terminals are taken; it may therefore be called a "mutual coupling factor."

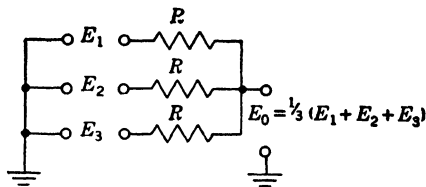


FIG. 18-1.—Example of parallel adding network.

*Methods of Addition and Subtraction.*—The properties generally desired in an adding or subtracting device are that it produce the sum or difference of the inputs with little distortion or with the desired shaping; that it have high input impedance relative to the waveform sources, and low output impedance relative to the load; that the output amplitude be not attenuated excessively with respect to the input; that the interaction of the sources through coupling in the device be tolerable; and that the device be simple and easy to construct.

The simplest method of addition involves the use of linear passive networks. A parallel adding network in which resistances are used to add three voltages is shown in Fig. 18-1. Capacitances or any like impedance elements may also be used in this way. A network of this sort inevitably introduces attenuation.

If it is desired to use networks for subtraction, it is usually necessary to employ an additional inverting element such as a tube or transformer.<sup>1</sup>

<sup>1</sup> It is also possible to invert a sine wave by the use of networks; an example is the use of three resistance-capacitance stages in a phase-shift oscillator. See Ginzton and Hollingsworth, "Phase-shift Oscillators," *Proc. I.R.E.*, **29**, 43 (February, 1941). See also Sec. 4-4 on phase-shift oscillators.

Transformers provide a floating output whose polarity can be reversed, and thus permit subtraction directly without attenuation.

Single vacuum tubes may be used for addition and subtraction if the inputs are to different electrodes. With inputs to grid and cathode, for example, approximate subtraction is performed; a multigrid tube with inputs on the control grid and the screen will produce an approximate sum. Combinations of vacuum tubes with a common cathode or plate load can also perform the operation of addition.

The use of feedback with vacuum tubes makes possible more precise addition and at the same time provides less mutual coupling than does a parallel adding network with passive elements alone.

These methods will now be considered in more detail. In Sec. 18.4 there is a tabular summary comparing the various methods from the standpoint of the properties desired in adding and subtracting devices.

**18.2. Linear Passive Networks. General Equations.**—The superposition theorem as applied to resistive networks states that any output voltage or current is a linear function of the inputs. The mesh or nodal equations<sup>1</sup> may be used for calculation of the weighting factors. These equations show that any purely resistive network may be used for addition. Similarly, a network of pure capacitances or inductances will produce an undistorted sum of several waveforms. In practice there is difficulty in obtaining such networks; at high frequencies, stray capacitances may have effect in resistive adding networks; inductances have resistance and stray capacitance which may prevent ideal operation; capacitive adding networks may produce distortion if the waveform sources have resistive output impedance.

It is possible to obtain undistorted addition, however, in another way: parallel adding networks in which each element is a series  $RC$ -combination, or in which each is a parallel  $RC$ -combination, may be used, provided the time-constants are the same. Thus in a parallel adding network if there is stray capacitance from the output node to ground, its effect may be compensated by making each element in the network a parallel  $RC$ -combination. This is done by inserting a small condenser in parallel with each resistive branch, and a resistance in parallel with the stray capacitance, in such a way that the  $RC$ -products are all the same.

More generally, the condition necessary for undistorted addition of any waveforms is that the operational expressions in the transfer function of the network cancel and thereby leave a ratio that does not involve  $p$ . If feedback amplifiers are used to produce a "virtual ground," such cancellation can be obtained with networks that do not involve the same types of elements; for example, an  $LR$ -differentiator might cancel the effect of an  $RC$ -integrator, except for constants of integration.

<sup>1</sup> For a detailed treatment of linear network analysis see Vol. 18, Chap. 1.

The mesh or nodal equations for a network may also be used for calculating the impedance between any pair of input or output terminals, and for calculating the mutual coupling between the inputs. This method will be used below in connection with resistive adding networks.

*Parallel Adding Networks.*—Much voltage and current addition is accomplished in parallel, series, or bridge networks or in networks resolvable by equivalence theorems to these forms. The networks which will be considered first are those that are made up of like elements—usually resistances but occasionally capacitances—and are used to add waveforms whose frequency spectra are in roughly the same region.

A parallel adding network is shown in Fig. 18-2. The input voltages  $E_1, E_2, \dots, E_n$ , and the output voltage  $E_o$ , are measured with respect to a common reference node, usually ground. Each input voltage has associated with it a source impedance  $z_i$  and has in series with it a network element having impedance  $Z_i$ . It is convenient to define for the  $j$ th input node an admittance

$$\bar{Y}_i = \frac{1}{z_i + Z_i}$$

In terms of this admittance the nodal analysis gives

$$E_o(\bar{Y}_1 + \bar{Y}_2 + \dots + \bar{Y}_n) = E_1\bar{Y}_1 + E_2\bar{Y}_2 + \dots + E_n\bar{Y}_n,$$

or

$$E_o = \frac{\sum_{i=1}^n E_i \bar{Y}_i}{\sum_{i=1}^n \bar{Y}_i}. \quad (1)$$

The weighting factor for any particular input  $E_k$  is then

$$\frac{\bar{Y}_k}{\sum_{i=1}^n \bar{Y}_i}.$$

If, for example, there are  $n$  identical branches, so that all the  $\bar{Y}_k$ 's are

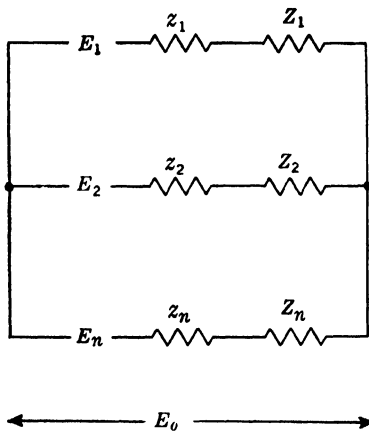


FIG. 18-2.—Parallel adding network.



equal, the weighting factor for each voltage will be  $1/n$ . If it is desired to combine three voltages in the ratio 1 to 3 to 4 or

$$E_o = \text{const.} \times (E_1 + 3E_2 + 4E_3),$$

it is necessary to let the  $\bar{Y}_k$ 's have the ratio 1 to 3 to 4, or the impedances  $z_k + Z_k$  have the ratio 1 to  $\frac{1}{3}$  to  $\frac{1}{4}$ . According to Eq. (6), the corresponding weighting factors will then be  $\frac{1}{8}$ ,  $\frac{3}{8}$ , and  $\frac{4}{8}$ .

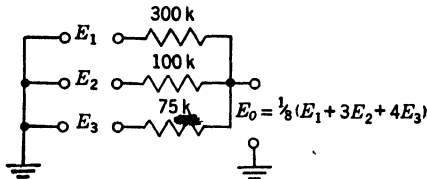


FIG. 18-3.—Adding network with specified weighting factors.

The loading impedance seen at the  $k$ th input is equal to the sum of the series  $Z_k$  and the parallel combination of the other impedances:

$$Z_{kk} = Z_k + \frac{1}{\sum_{i=k} \bar{Y}_i} \quad (2)$$

For the ratio 1 to 3 to 4, a possible circuit (Fig. 18-3) is

$$Z_1 = 300 \text{ kilohms}$$

$$Z_2 = 100 \text{ kilohms}$$

$$Z_3 = 75 \text{ kilohms.}$$

Neglecting the internal resistances  $z_k$ , the loading resistance presented to the first generator of internal impedance  $z_1$  is then

$$Z_1 + \frac{1}{Y_2 + Y_3} = \left[ 300,000 + \frac{1}{10^{-6}(1 + \frac{4}{3})} \right] \text{ ohms} = 343 \text{ kilohms.}$$

The mutual coupling factor (transfer admittance) between one source and another is the ratio of current produced through the second source to the voltage at the first which produces it. This ratio may be expressed for the  $k$ th and  $l$ th sources with the aid of Eq. (1). The contribution of the  $l$ th source to the current passing through the  $k$ th source may be found by multiplying the contribution of the  $l$ th source to the voltage at the output node by the admittance of the  $k$ th branch:

$$\begin{aligned} \frac{\Delta i_{kl}}{\Delta E_l} &= \frac{\Delta E_o}{\Delta E_l} \times \frac{\Delta i_{kl}}{\Delta E_o} \\ &= \frac{\bar{Y}_l}{\sum_{i=1}^n \bar{Y}_i} \times \bar{Y}_k. \end{aligned} \quad (3)$$

This is a symmetrical expression, its value being unaffected by the interchange of the subscripts  $k$  and  $l$ ; hence the use of the term "mutual." [For a network consisting of  $n$  equal impedances, the transfer admittance is  $\bar{Y}/n$ .]

The voltage produced across the internal impedance of the  $k$ th source is

$$z_k \Delta i_{kl} = \frac{z_k}{z_k + Z_k} \times \frac{\bar{Y}_l \Delta E_l}{\sum_{j=1}^n \bar{Y}_j},$$

where the last factor is  $\Delta E_l$  multiplied by its weighting factor from Eq. (1). Suppose that in the previous example (Fig. 18.3) it is desired to find the effect of  $E_1$  on  $E_3$ , and that  $E_3$  has an internal impedance  $[z_3]$  which is 5 per cent of the total impedance  $z_3 + Z_3$ . Since the source  $E_1$  has a weighting factor  $\frac{1}{8}$ , the voltage produced across  $z_3$  by a voltage  $\Delta E_1$  at the first source is given by

$$\frac{z_3 \Delta i_3}{\Delta E_1} = \frac{z_3}{z_3 + Z_3} \times \frac{\bar{Y}_3}{\sum_{j=1}^3 \bar{Y}_j}$$

$= 0.05 \times \frac{1}{8} = 0.006 = 0.6$  per cent of the voltage change at the first source. If the coupling is excessive in a parallel adding network, it may be reduced by lowering the corresponding weighting factor or the internal impedance of the generator.

A convenient way of reducing weighting factors is to introduce an impedance between the output terminal and ground. By this means all the weighting factors may be lowered together and their relative values left unchanged.

The addition of currents in parallel networks can be treated similarly to that of voltages because any voltage generator  $E$  with a series impedance  $Z$  is equivalent<sup>1</sup> to a current generator  $E/Z$  with a parallel impedance  $Z$ .

**Series Adding Networks.**—Figure 18.4 shows a series adding network for voltages. All the sources except one must be floating with respect to the reference node. In this case the weighting factors are all the same: the output voltage is equal to

$$\frac{(E_1 + E_2 + \cdots + E_n)Z_L}{Z_1 + Z_2 + \cdots + Z_n + z_1 + z_2 + \cdots + z_n + Z_L}.$$

When the load impedance  $Z_L$  is very large, the output is the sum of the inputs with each weighting factor equal to unity. Transformers are most frequently used for series adding; a schematic circuit is shown in

<sup>1</sup> See, for example, H. W. Bode, *Network Analysis and Feedback Amplifier Design*, Van Nostrand, New York, 1945, p. 12.

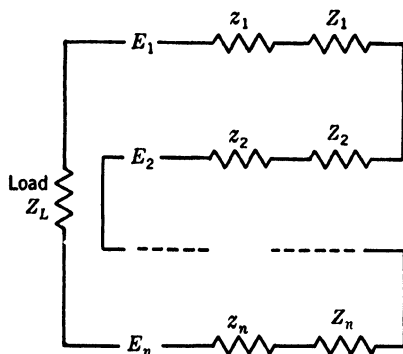


FIG. 18.4.—Series adding circuit.

Fig. 18-5. D-c voltage supplies such as batteries, tachometers, or rectifiers with floating reference levels are also used. In any of these cases the weighting factors may be varied by means of potentiometers across the outputs of the voltage sources.

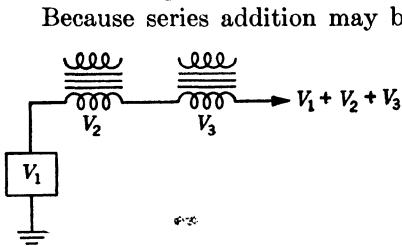


FIG. 18-5.—Addition by means of transformers.

Because series addition may be done conveniently with alternating voltages, modulation-demodulation methods may be used to add d-c voltage differences when the d-c levels are inconvenient for the use of resistive networks. Two such methods are shown in Fig. 18-6; in case (a) series addition with transformers is used, and in case (b) floating rectifiers are used.

*Bridge Adding Network.*—Figure 18-7 shows a bridge adding network. The principal advantage of using bridge networks is that the mutual coupling between the inputs may be eliminated if the bridge is balanced and the inputs are at pairs of opposite corners of the bridge. Here again a floating voltage source is required for one of the inputs.

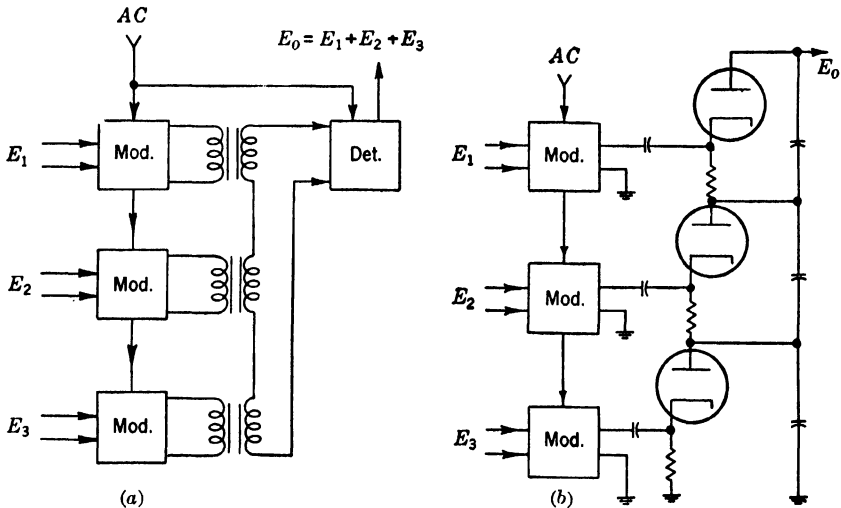


FIG. 18-6.—Carrier methods of adding d-c voltages independent of level.

The input impedance of a balanced bridge at either pair of terminals ( $E_1$  or  $E_2$ ) may be calculated by series-parallel analysis on the assumption that no current flows in one input branch as a result of the other input voltage. Thus for purposes of analysis one branch may be considered an open circuit or short circuit.

A useful special case of the balanced bridge is the equal-arm bridge

shown in Fig. 18-8. This circuit permits relatively easy analysis and because of its symmetry may be used with a balanced voltage source such as a push-pull amplifier. The analysis suggested shows that the loading impedance at either input is simply  $Z$ . The output voltage and

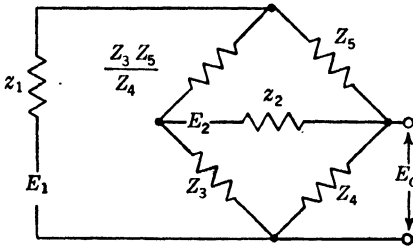


FIG. 18-7.—Balanced bridge.

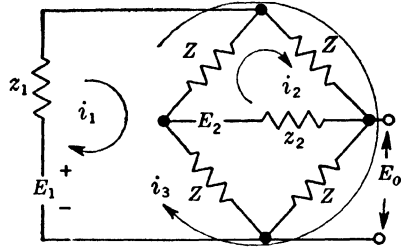


FIG. 18-8.—Equal-arm bridge.

the weighting factors may be found by setting up the mesh equations as indicated in Fig. 18-8:

$$\begin{aligned}(2Z + z_1)i_1 - Zi_2 - 2Zi_3 &= E_1 \\ -Zi_1 + (2Z + z_2)i_2 + 2Zi_3 &= -E_2 \\ -2Zi_1 + 2Zi_2 + 4Zi_3 &= 0.\end{aligned}$$

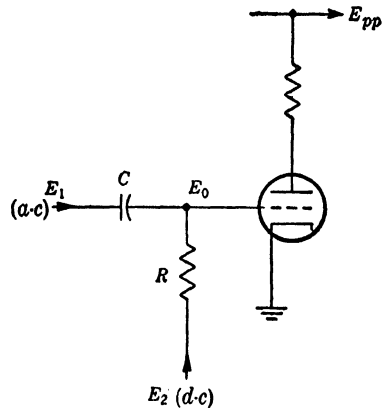
The output is  $E_o = i_3 Z$ . Solution of the equations gives

$$E_o = \frac{Z}{2} \left[ \frac{E_1}{Z + Z_1} + \frac{E_2}{Z + Z_2} \right]. \quad (4)$$

Moreover, it may be seen from the above equations that the mutual coupling is zero, since the minor formed from the coefficients of  $i_1$  and  $i_3$  in the second and third equations, which is the coefficient of  $E_1$  in the solution for  $i_2$ , vanishes.

#### Addition of Different Frequencies.

If the waveforms to be added are of sufficiently different frequency, parallel networks may be used in such a way that the weighting factor for each input is nearly unity. An example is the use of an  $RC$  coupling network to add an a-c voltage to a d-c voltage in a variable-bias amplifier as shown in Fig. 18-9. Since for d-c voltages the condenser is an open circuit, the weighting factor for the bias voltage is unity; for a-c voltages the condenser is a short circuit, and if the grid leak resistance is much greater than the output impedance of the source, this weighting factor is also nearly unity.

FIG. 18-9.— $RC$  coupling network.

The injection of triggers and synchronizing pulses into relaxation oscillators (Chap. 5) is another case in which the frequency spectra of the two waveforms to be added are in different regions. Resistance-capacitance coupling networks are also commonly used to perform this addition, the synchronizing pulse being fed in through a condenser to the grid of a multivibrator and superimposed on an exponential recovery waveform.

*Transient Response.*—A limitation of adding networks—especially when the input waveforms have sharp edges—results from the possibility of undesired transients. These transients may be due to the presence of stray capacitance or to interaction between reactances in the sources or load and the resistances of the network.

A type of waveform which is often affected by the transient response of the adding circuit is one having a short rise time, either a rectangular waveform or a narrow pulse. The output rectangular waveform may not rise rapidly enough, and as a result may not define precisely the desired time interval; a short pulse may be decreased in amplitude by the effect of a time constant in the adding network. In each case the limitation results from the time required to charge the stray capacitance. The capacitance to be considered will vary between wide limits, depending on construction practice and on the output circuit. As an example, suppose that a resistive network is to be used to add 1- $\mu$ sec pulses to rectangular gates having a rise time of 0.1  $\mu$ sec. The adding network will be assumed to consist of two 100,000-ohm resistances, and to have a capacitance of 20  $\mu$ f from the output terminal to ground. For each waveform there is a circuit which is equivalent on the basis of Thévenin's theorem and which has half the output resistance (i.e., 50,000 ohms) in series with a generator producing a waveform of half the amplitude. The corresponding time constant is  $(20 \times 10^{-12} \times 5 \times 10^4)$  sec. = 1.0  $\mu$ sec. The gates will reach 90 per cent of peak value in 2.3  $\mu$ sec (the network will have a similar effect on the trailing edge); the pulses will reach only 63 per cent of the peak amplitude in 1  $\mu$ sec. If a sharper rise or greater output amplitude is desired, it may be necessary to lower the mixing resistances. The extent to which these resistances may be lowered is limited by the loading of sources which may occur when the mixing resistances are low.

For some purposes, when an extremely short rise time is desired, a resistor in the mixing network may be bypassed with a small condenser and rapid changes thereby permitted to pass through. This device is used, for example, in multivibrators. It increases the mutual coupling for rapid pulses however. Better performance can be obtained by also inserting a resistance in parallel with the stray capacitance; each branch of the network will thus consist of a parallel resistance and capacitance, and if the time constants are made equal the distortion will be minimized.

Another sort of undesired response is the overshoot that occurs when an  $RC$  coupling network is used to add bias to pulses or rectangles. This overshoot is particularly objectionable in high-gain video amplifiers.<sup>1</sup> It results from the tendency of the coupling condenser to discharge rather than maintain its charge for the duration of the waveform.

A third type of undesired transient is the shock-excited oscillation, which may exist if the network has an underdamped resonant frequency and if rapid changes occur in the operation of the circuit. These conditions are present, for example, when a transformer is used for subtraction and the load is a diode rectifier (see Fig. 18-10). The sudden start of conduction in the diode produces a train of damped oscillations in the transformer secondary and thereby slightly increases the rectifier output voltage.

Some general methods of reducing the effects of transients are (1) reduction of stray capacitances by improved layout or choice of different components; (2) in the case of stray capacitances, reduction of charging time by lowering the resistance through which the capacitance charges; (3) in the case of oscillation, damping by means of resistance; (4) compensation by means of additional network elements.

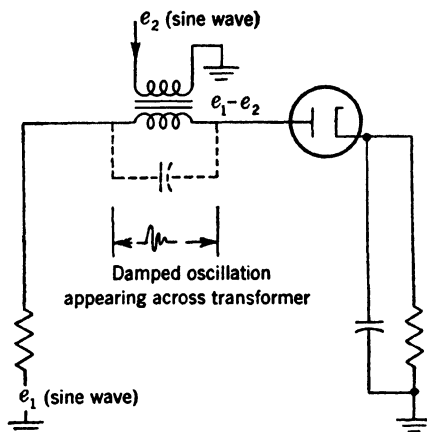


FIG. 18-10.—Transient oscillation produced by transformer and diode.

It is not possible to obtain immediately useful solutions for the response of a network to general transient voltages or currents since each input function and set of initial conditions determines a different solution. The general transient behavior of networks<sup>2</sup> is described in Vol. 18, Chap. 1 of this series; the Laplace-transform method can be used to determine the response of a specific network to a specific input waveform. The effort involved, however, may be great, and it will be wise to consider whether an exact transient solution is needed. Often it is merely necessary to obtain an approximate solution if it can be shown that the network is adequate for the specific problem.

The following rules are useful in determining whether a network behaves adequately for specific transient conditions when addition without distortion is desired:

<sup>1</sup> Vol. 18, Chap. 3, "High-gain Pulse Amplifiers."

<sup>2</sup> These equations apply only to linear networks. Often source generators and loads do not meet this requirement.

1. The network must have a uniform pass band accommodating the highest and lowest frequency components of the input waveform.
2. The network should not have any underdamped resonant frequencies.
3. The source loading and mutual couplings must not exceed the driving capabilities of the source.
4. The network must be capable of driving its load in any of its states if the load is nonlinear.
5. If a transient exists, its amplitude must be sufficiently reduced before the sum is to be observed.

Waveform shaping by deliberate use of transients can be performed simultaneously with adding. The coupling network of Fig. 18-9, for example, will differentiate the input  $E_1$  if the time constant  $RC$  is small relative to the interval of variation of  $E_1$ ; it will also integrate  $E_2$  over intervals small relative to the time constant.

**18-3. Addition and Subtraction by Means of Vacuum Tubes.**—In the design of adding circuits with passive networks, it is sometimes difficult to lower input mutual couplings to the required degree without decreasing the weighting factors to a point where the sum voltage is unreasonably

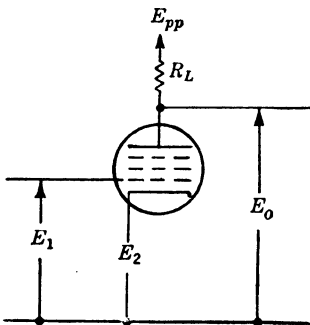


FIG. 18-11.—Double input vacuum tube.

small; at other times it is difficult to obtain the required bandwidth or transient response without increasing the source loading excessively. Vacuum tubes provide means for isolating the network from the source voltages and for changing impedance levels between the network and the source voltages. They may also be used directly as adding devices or in feedback loops for addition. If the inputs are to grids that are not drawing current, they can be affected by the adding circuit only through inter-electrode and stray capacitances.

**Multiple-input Vacuum Tubes.**—Circuits utilizing multiple-input tubes are suitable for adding with moderate or low accuracy, depending on the particular tube or circuit used. Double input triode, tetrode, and pentode amplifiers, in which the control grid and cathode are the input terminals, are moderately linear. An example is shown in Fig. 18-11; in this case  $E_0$  is the amplified difference between  $E_1$  and  $E_2$ . The magnitude of  $E_0$  and the input impedances of  $E_1$  and  $E_2$  may be calculated on the assumption of linear tube characteristics (see, for example, Vol. 18, Chap. 11). When a triode is used for subtraction by letting the control grid and cathode be the two input terminals, the low input impedance at

the cathode (approximately  $1/g_m$ ) makes it necessary to supply the cathode from a low-impedance waveform source. In time selection a low-impedance rectangular waveform is sometimes used as a gate in the cathode circuit. A particular example is a type of blocking-oscillator frequency divider in which input pulses are effectively added to the grid recovery waveform by introducing negative pulses in the cathode circuit.

In general, each grid of a vacuum tube can receive a signal voltage that is capable of altering the flow of plate current. However, the relationship between the plate current and the various inputs may be far from linear. Generally, an operating point that permits all grids to affect the plate current can be found, provided the input signals are not too large.

*Parallel-plate Addition.*—The parallel-plate adding circuit shown in Fig. 18-12a has the advantages of high input impedance and almost zero

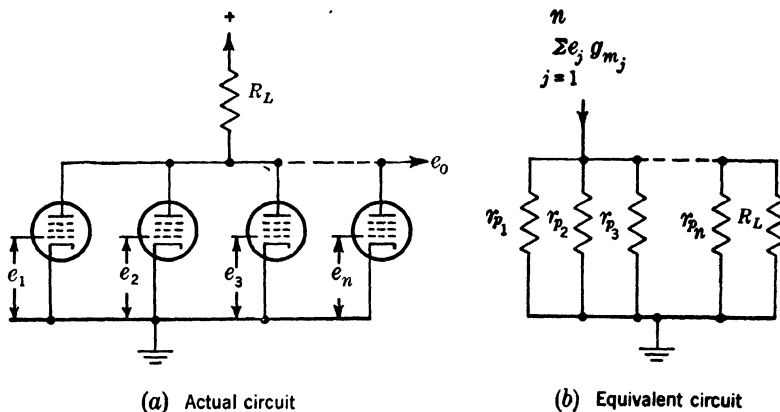


FIG. 18-12.—Parallel-plate adding circuit.

coupling between inputs (except for capacitance effects). The weighting factors can be altered by means of input potentiometers although these potentiometers increase the source loading, or by adjusting the amplifier gain by means of cathode resistors. The parallel form of the equivalent-plate-circuit theorem may be used to put the parallel-plate adding circuit of Fig. 18-12a in the form shown in Fig. 18-12b.

In this equivalent circuit the total current

$$g_{m1}e_1 + g_{m2}e_2 + \cdots + g_{mn}e_n$$

flows through the parallel combination of the plate resistances and the load resistance. If the reciprocal of the plate resistance  $r_{pj}$  is written  $Y_j$ , and the load admittance  $Y_L$ , the output voltage is



$$e_o = \frac{\sum_{j=1}^n g_{mj} e_j}{Y_L + \sum_{j=1}^n Y_j} \quad (5)$$

For pentodes the  $Y_j$ 's are usually small enough to be negligible relative to  $Y_L$  ( $r_p \gg R_L$ ); consequently

$$e_o = R_L \sum_{j=1}^n g_{mj} e_j.$$

If the  $g_m$ 's are alike, the weighting factors are all equal.

For rapid addition of waveforms low input capacitance is usually desired. For this reason pentodes are preferable to triodes. It may be

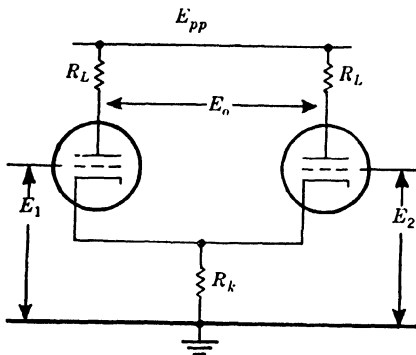


FIG. 18-13.—Differential amplifier.

desirable to perform more precise addition with relatively slow waveforms, however; in this case cathode degeneration may be used to make the operation less dependent on tube characteristics ( $g_m$  variation). In this case triodes are preferable because cathode degeneration in pentodes produces undesired transfer of current between the screen and the plate.<sup>1</sup>

*Cathode Coupling.*—A combination of two amplifier tubes with a common cathode impedance, shown in Fig. 18-13, is known as a “differential amplifier.” Such a circuit involves feedback as does any circuit with impedance between cathode and ground. This circuit produces a voltage proportional to the difference of  $E_1$  and  $E_2$ . The theory and practical details of this circuit are given in Chap. 9 and Vol. 18, Chap. 11. The output voltage difference is given by the equation

$$E_o = \frac{\mu R_L (E_1 - E_2)}{r_p + R_L}, \quad (6)$$

<sup>1</sup> For a discussion of this effect, see Chap. 7.

subject to the assumption that the triodes have identical linear characteristics given by

$$i_p = \frac{e_{pk} + \mu e_{gk}}{r_p}.$$

If a single-ended output is desired, the voltage with respect to ground may be taken from either plate. In this case the two inputs have slightly different weighting factors (Vol. 21, Chap. 3 of this series), but by introduction of a constant-current triode in series with the cathode resistor the weighting factors may be made more nearly equal. The difference in weighting factors is a measure of the common-mode variation, since

$$ae_1 - be_2 = \frac{(a+b)}{2}(e_1 - e_2) + \frac{(a-b)}{2}(e_1 + e_2).$$

Over the same range of inputs for which  $E_o$  measures the difference of  $E_1$  and  $E_2$ , the cathode voltage  $E_k$  measures approximately half their sum (plus a constant). This adding property is a special case of a general common-cathode adding property, shown in Fig. 18-14. By means of this circuit as many voltages as desired may be added by connecting the cathodes of the triodes together. For the circuit of Fig. 18-14, straight-forward analysis assuming linear characteristics shows that for variational voltages

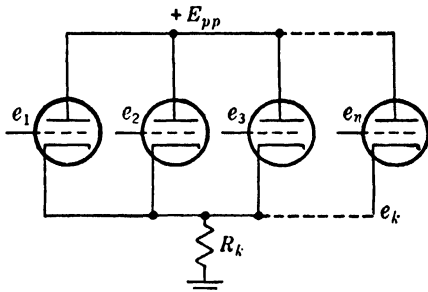


FIG. 18-14.—Addition using common cathode resistor.

$$e_k = \frac{\mu \sum_{j=1}^n e_j}{n(\mu + 1) + \frac{r_p}{R_k}} \approx \frac{\sum_{j=1}^n e_j}{n}, \quad \text{if } \mu \text{ is large.} \quad (7)$$

This is essentially the same result as for a passive parallel network with  $n$  equal resistances except that there is no mutual coupling between sources other than that due to interelectrode capacitances. The output impedance is very low—approximately  $1/(ng_m)$ . The weighting factors may be varied by inserting resistors between the cathodes and the common output node; this, however, increases the output impedance. The amplitude of each input voltage is limited to approximately the grid base if linear operation is desired.

**Parallel Adding with Feedback.**—One of the most useful methods of addition uses negative feedback in connection with a passive network.

In the circuit of Fig. 18-15, a parallel adding network is connected to add a number of inputs to the output of an amplifier; the sum of these voltages is the input to the amplifier grid.<sup>1</sup> An expression for the output voltage

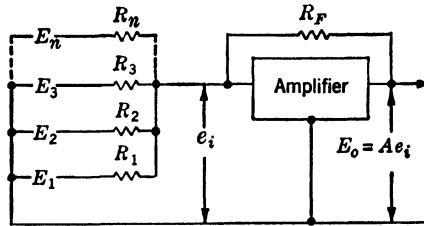


FIG. 18-15.—Parallel network with feedback.

can be derived<sup>2</sup> by means of Eq. (6) for the parallel adding network and the equation

$$e_o = Ae_i$$

for the action of the amplifier. This expression is

$$e_o = \frac{-\sum_{j=1}^n e_j Y_j}{Y_f - \frac{\sum_{j=1}^n Y_j + Y_f}{A}}, \quad (8)$$

where the  $Y_j$ 's are the admittances in the respective input branches as before, and  $Y_f$  is the admittance in the feedback branch. For sufficiently large values of  $A$ , a simplified expression may be written:

$$e_o = \frac{-\sum_{j=1}^n e_j Y_j}{Y_f}. \quad (9)$$

The weighting factors are nearly the same in magnitude as for parallel adding, but negative. An amplifier of this sort can thus be used to produce the negative of a voltage sum, or to invert a voltage prior to subtraction (Sec. 2-5). The input admittance for the  $j$ th source is approximately  $Y_j$  if  $A$  is large, since the grid node is nearly at a constant potential. High impedances (or low  $Y_j$ 's) may be used without the danger of bad transient response; the input capacitance of the first stage

<sup>1</sup> The operation of this circuit is discussed in Sec. 2-5 for the case of a single input voltage.

<sup>2</sup> A similar derivation taking into account the output impedance of the amplifier is given in Vol. 18, Sec. 92 of this series.

has hardly any effect since the grid voltage changes very little. This may be considered to result from the high input admittance at the first grid,  $(1 - A)Y_f$ . Stray capacitance from portions of the resistors to ground, however, still has effect.

The mutual coupling factors may be derived in a manner similar to that in which these for the passive parallel-adding network were derived. The current increment in the  $k$ th branch resulting from a voltage increment in the  $j$ th is

$$\frac{\Delta i_k}{\Delta e_j} = \frac{\Delta e_g}{\Delta e_j} \times Y_k = \frac{\Delta e_o}{\Delta e_j} \times \frac{Y_k}{A}.$$

Substituting the weighting factor  $\Delta e_o/\Delta e_j$  from the approximate Eq. (9) gives an expression for the coupling,

$$\frac{\Delta i_k}{\Delta e_j} = \frac{-Y_j Y_k}{A Y_f} = \frac{-Z_f}{A Z_j Z_k}. \quad (10)$$

Because this mutual transfer admittance tends to zero as  $A$  increases, the inputs are nearly independent.

A circuit of this type then gives an output practically the same as that of the passive parallel-adding network, but inverted in polarity. The feedback circuit has the advantage that the output amplitude may exceed that of the input. If a multistage feedback amplifier is used for extremely sharp pulses, delays within the amplifier itself may have the effect that the first grid is not returned to its equilibrium voltage until, for example,  $0.1 \mu\text{sec}$  after a step function at the input. During this time the amplifier may be overloaded.

An advantage of this circuit as compared with other vacuum-tube adding circuits is that it requires only one amplifier, regardless of the number of inputs to be added. If a large number ( $n$ ) of similar inputs is used, the loop gain goes down as  $1/n$ , and extra gain may be necessary. For an example of a circuit of this type see Fig. 19-27.

Instead of an a-c or d-c amplifier, a carrier amplifier (see Chap. 9) may be used for this method of addition. For example, a mechanical modulation-demodulation system with amplification may be used as the amplifier in Fig. 18-15.

Another amplitude-discrimination device that may be used is the "magnetic amplifier."<sup>1</sup> The speed of computation of this device is also limited by the frequency of the a-c carrier.

*Subtraction by Vacuum Tubes.*—It is possible to subtract voltages by means of vacuum-tube circuits<sup>2</sup> having high input resistance. Two

<sup>1</sup> H. S. Sack *et al.*, "Electronic Computers for Division, Multiplication, Squaring, etc.," NDRC 14-435, Cornell University, 1944; see also Sec. 11-7 of this volume.

<sup>2</sup> J. W. Gray and D. MacRae, Jr., "Differential to Single-ended Potential Converters," RL Report No. 457, November 1943.

such circuits designed to operate with d-c voltages are shown in Fig. 18-16. The first (Fig. 18-16a) is a symmetrical circuit producing two outputs which vary as  $(E_1 - E_2)/2$  and  $(E_2 - E_1)/2$  and have an additive constant voltage. Over a range of about 80 volts for each input, the output is accurate to within 0.5 per cent of the peak output variation; change of tubes varies the d-c level by less than one per cent. If calibration potentiometers are provided for varying the 750,000 ohm resistors, the effects of tube change and resistor unbalance can be compensated for laboratory purposes.

The second circuit (Fig. 18-16b) operates over a range of about 140 volts for  $E_1$  and 100 volts for  $E_2$ . The output potentiometer tap may

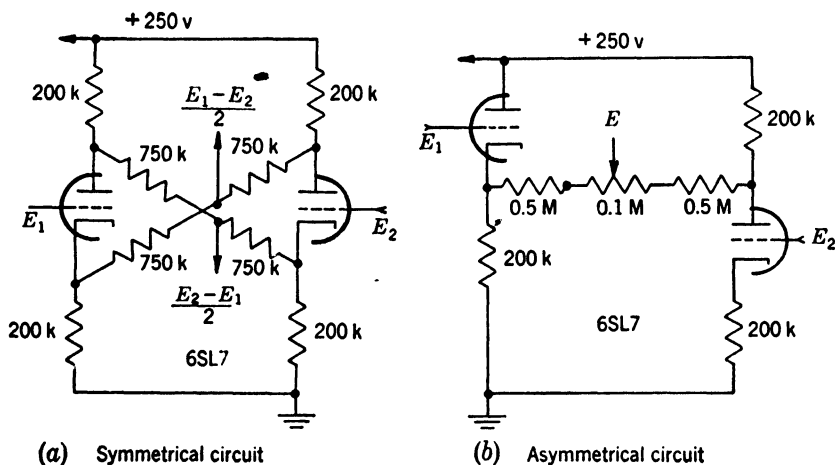


FIG. 18-16.—Difference-to-potential converters.

be adjusted to vary the weighting factors of  $E_1$  and  $E_2$ . The accuracy of computation is similar to that of circuit (Fig. 18-16a); the principal source of error (1 to 2 per cent) is a drift of the constant d-c level, but if calibration controls are permissible the residual errors from linearity are less than 0.5 per cent of the output range. As compared with differential amplifiers, these circuits have the disadvantages of requiring adjustment and not providing amplification. For amplitude discrimination, differential amplifiers are preferable, but for fairly accurate subtraction over a wide range of inputs, these circuits depend less on tube characteristics.

Combinations of the methods discussed may of course be used for addition and subtraction. A combination series-parallel network may be used, for example, when only one of the waveforms to be added is available from a floating source; series addition may also be used in the input or feedback path of an amplifier to produce addition or subtraction.

**18-4. Summary.**—The following methods of addition and subtraction have been discussed: (1) Linear Passive Networks: parallel, series, bridge. (2) Vacuum-tube Circuits: multiple input, common plate, common cathode, parallel adding with feedback. Some general conclusions may now be stated which will indicate what methods are appropriate for particular applications. The use of vacuum tubes introduces problems of maintenance that might not otherwise arise, but stability problems, except for slow drifts, may be solved by the use of feedback even though vacuum-tube parameters may vary considerably (Chap. 3).

In Table 18-1 the various passive networks are compared from the standpoint of desirable properties. In order to express the input and output impedances and the coupling admittances conveniently, values are given for the case when all inputs are alike; the impedance  $Z$  is defined here to include the internal impedance of the source.

Subtraction with resistive networks always requires a separate inversion of one input.

The effect of resistive networks on pulses or step functions depends on the output impedance of the network and the input impedance of the following element. An important source of delays is stray capacitance, either input capacitance of vacuum tubes or strays from components and wiring to ground.

The most significant data in Table 18-1 are that a parallel network requires no floating inputs, and that a bridge network or a series network operating into infinite impedance has no coupling between inputs.

TABLE 18-1.—COMPARISON OF PASSIVE ADDING NETWORKS

Property	Parallel	Series	Bridge
Number of possible inputs	Any number	Any number	Two
Floating inputs needed	None	All but one	One (may be push-pull resp. ground if bridge is symmetrical)
Weighting factors	Easily adjustable; $1/n$ if inputs are alike	Easily adjustable; may be all unity	Adjustable
Mutual transfer admittance between inputs	$\frac{1}{nZ}$	Decreases with increasing load; zero if load is an open circuit	Zero if bridge is balanced
Input impedance	Approx. $Z$	$nZ$ plus load; infinite if load is an open circuit	Approx. $Z$
Output impedance	Approx. $\frac{Z}{n}$	$nZ$	Approx. $Z$

Table 18-2 shows a similar comparison for vacuum-tube adding circuits. In all the circuits listed in the table, inputs are measured with respect to ground.

TABLE 18-2.—COMPARISON OF VACUUM-TUBE ADDING CIRCUITS

Property	Multiple input	Common plate	Common cathode	Parallel adding with feedback
Number of inputs	Limited by number of electrodes	Any number; each input requires one tube section	Any number; each input requires one tube section	Any number; additional inputs do not increase number of tubes
Weighting factors	Depend on tube	Adjustable if series resistors are used	Adjustable if series resistors are used	Easily adjustable; depend on network
Transfer admittance between inputs	$g_m$ for grid and cathode inputs; low for grid-to-grid	Zero with exception of interelectrode capacitance	Zero with exception of interelectrode capacitance	$\frac{1}{AZ}$ ( $A$ = gain of amplifier; $Z_i = Z_j$ )
Input impedance	$\frac{1}{g_m}$ at cathode; high for grids unless the electrode draws current	Due to interelectrode capacitance (large)	Due to interelectrode capacitance (small)	$Z$
Output impedance	Approx. $r_p$	Approx. $\frac{r_p}{n}$	$\frac{1}{ng_m}$	$\frac{Z_{out}}{A}$ ( $Z_{out}$ = output $Z$ without feedback)
Possibility of subtraction	Yes, with cathode input	Yes, direct to plate	No	Yes, direct to plate

## DIFFERENTIATION AND INTEGRATION

**18-5. Methods of Differentiation and Integration.**—The circuits to be considered in Secs. 18-5 to 18-7 are those that produce waveforms approximately proportional to the derivative or integral of the input waveform. The required accuracy varies considerably among the applications; more elaborate circuits are required for higher accuracy. Emphasis will be placed on purely electrical devices; a number of mechanical and electro-mechanical devices are available,<sup>1</sup> but their response time is generally much longer than the duration of the waveforms considered in this volume.

There are a number of applications in which only certain properties

<sup>1</sup> See, for example, Vol. 21, Chap. 4.

of the derivative or integral are desired, and the operations need not be performed with high precision. For example, if it is desired to produce pulses from a periodic rectangular waveform, an  $RC$  “differentiating” circuit can be used for this purpose (Fig. 18-17). If the duration of the pulse is not of critical importance, a relatively large time constant may be used; in this case the departure from true differentiation is considerable.

The process of filtering to remove alternating components from waveforms may be done by means of an  $RC$  integrating network. This is commonly used with rectifiers. It may also be used to produce an approximately triangular waveform from a rectangular wave (Fig. 18-18).

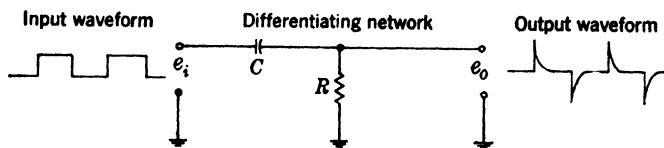


FIG. 18-17.—Differentiation of a rectangular waveform.

Here also the requirement may be not accurate integration, but only reduction of ripple by a specified amount.

One important application of accurate differentiation and integration is in automatic computation (Vol. 21, Chap. 4). Integrating circuits are used to produce triangular and parabolic waveforms (Chaps. 7 and 8), and differentiating circuits afford a convenient method of testing the accuracy of these waveforms (Chap. 20). The differentiation of triangular waveforms is used to produce rectangles in “self-gating” triangular-waveform generators (Chap. 7). Accurate integrating circuits

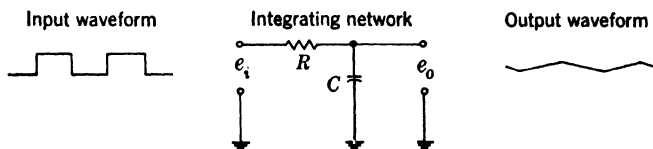


FIG. 18-18.—Integration of a rectangular waveform.

have had considerable use in automatic-tracking devices (Vol. 20, Chap. 8).

The most common methods of performing differentiation and integration make use of the fact that the current through a condenser is proportional to the derivative of the voltage across it. These methods employ, first, the simple  $RC$ -networks mentioned above; second, circuits using a resistance and a capacitance with feedback (Fig. 18-19a and b) for higher accuracy. In each case negative feedback tends to hold the grid at a constant potential; if the grid did not move at all, the output would be exactly proportional to the negative derivative or negative integral of the input. Inductances and resistances may be used in a



similar way (Fig. 18-20); the resistance of inductors introduces errors, but the differentiation is satisfactory for many purposes. Another method of performing approximate differentiation, which is of interest but not widely used, involves a delay line. The effect is to subtract from the value of a waveform at time  $t$  its value at some previous time  $t - \Delta t$ ; the result is then a differencing process resembling differentiation.

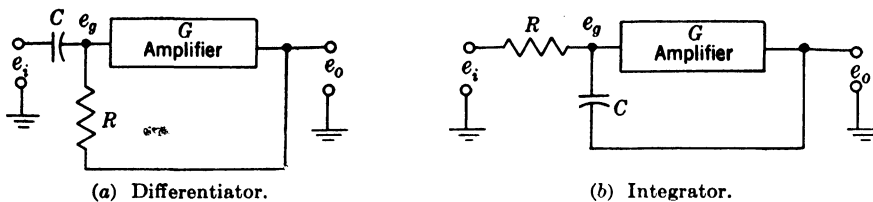


FIG. 18-19.—Feedback circuits for differentiation and integration.

**18-6. Theoretical Approaches. Fourier Analysis.**—The response of any linear network, and of differentiating and integrating networks in particular, to an arbitrary input waveform may be expressed in terms of the response to sine waves of all frequencies. A more convenient expression is possible if the response to the complex exponential  $e^{j\omega t}$  is considered; in this case the phase- and amplitude-response functions of the network are given together by a complex transfer ratio. The ratio of output to input amplitude for a perfect differentiating circuit would then be

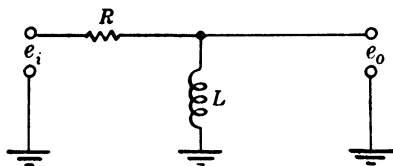


FIG. 18-20.—Simple  $LR$  differentiating network.

$$\frac{e_o}{e_i} = \frac{d}{dt} (e^{j\omega t}) = j\omega.$$

This implies that the amplitude response of a differentiating circuit should be proportional to frequency, and the phase response should be a constant  $90^\circ$  phase lead. The response of an  $RC$  “differentiating” network of the type shown in Fig. 18-17 is

$$\frac{e_o}{e_i} = \frac{R}{R + \frac{1}{j\omega C}} = \frac{j\omega RC}{1 + j\omega RC},$$

which is nearly equal to  $j\omega RC$  for small values of  $\omega RC$ . This necessitates making the time constant  $RC$  small, however, and a corresponding decrease in the output results. The effect of the network corresponds to that of a perfect differentiator (the numerator of the fraction) plus an  $RC$  integrating network (the denominator).

Similarly, the response of a perfect integrating circuit is

$$\frac{e_o}{e_i} = \frac{\int e^{j\omega t} dt}{e^{j\omega t}} = \frac{1}{j\omega},$$

and that of the  $RC$  integrating network of Fig. 18-18 is

$$\frac{1}{R + \frac{1}{j\omega C}} = \frac{1}{1 + j\omega RC},$$

which is nearly equal to  $1/j\omega RC$  for large values of  $\omega RC$ . Again the region of accurate operation corresponds to small output. This can be remedied by amplification, but a more stable output can be obtained if feedback is used.

If the input waveform is periodic, the output may be calculated by multiplying each of the Fourier components of the input by the corresponding value of the transfer ratio and adding; if the input is not periodic, an analogous process may be carried out using the Fourier integral.<sup>1</sup> Either of these procedures usually involves considerable labor.

*Laplace Transform.*—A similar result may be obtained by taking the Laplace transform<sup>2</sup> of each term in the differential equation of the network; the result is an algebraic expression giving the ratio<sup>3</sup> of the transform of the output to the transform of the input in terms of the complex variable  $p$ . This expression has the same form as that arrived at by Fourier analysis, except that  $p$  replaces  $j\omega$ . The output waveform may be found by multiplying the transfer ratio by the transform of the input waveform and finding the inverse transform. This procedure is commonly done with the aid of tables of direct and inverse transforms.

The transfer ratio of the  $RC$  “differentiating” circuit of Fig. 18-17 is

$$\frac{\mathcal{L}(e_o)}{\mathcal{L}(e_i)} = \frac{p}{p + \frac{1}{RC}} \quad (11)$$

where  $\mathcal{L}(e_o)$  = Laplace transform of output waveform.

$\mathcal{L}(e_i)$  = Laplace transform of input waveform.

This may be compared with the transfer ratio of a perfect differentiator; the latter is simply  $p$ .

<sup>1</sup> See, for example, E. A. Guillemin, *Communication Networks*, Vol. II, Wiley, New York, 1935, pp. 461–470.

<sup>2</sup> See Vol. 18, Chap. 1 and Sec. 2-7 of this volume.

<sup>3</sup> The following analysis applies only to zero initial values of  $e$  or  $i$ .

For the  $RC$  “integrating” circuit of Fig. 18-18 the transfer ratio is

$$\frac{\mathcal{L}(e_o)}{\mathcal{L}(e_i)} = \frac{1}{1 + pRC}, \quad (12)$$

as compared with  $1/p$  for a perfect integrator.

*Analysis of Feedback Differentiator and Integrator.*—The differentiating circuit of Fig. 18-19a may be analyzed by combining the three equations<sup>1</sup>

$$\begin{aligned} e_o &= -Ge_o \\ \frac{e_o - e_g}{R} &= -i \end{aligned}$$

and

$$e_i - e_o = \frac{1}{C} \int i \, dt,$$

where  $i$  is the current flowing through the  $RC$  from the input terminal to the output terminal. The result is

$$-\frac{e_o}{G} = e_i + \frac{G+1}{GRC} \int e_o \, dt.$$

By application of the Laplace transform, the transfer ratio is

$$\frac{\mathcal{L}(e_o)}{\mathcal{L}(e_i)} = - \frac{Gp}{p + \frac{G+1}{RC}}. \quad (13)$$

This has the same general form as the ratio for an  $RC$  “differentiating” network without feedback [Eq. (11)]. The time constant is effectively divided by  $G+1$ , however; this would ordinarily imply a corresponding decrease in the output amplitude, but the factor  $(-G)$  in the numerator effectively compensates for this decrease. The result is an improvement in accuracy corresponding to the decreased time constant, without the attenuation of the output that results from decreasing the time constant of a simple  $RC$ -network. It is assumed here that  $G$  is constant for the application at hand. Variation of  $G$  with frequency<sup>2</sup> is a further source of error in the differentiation of rapid waveforms.

The effect of this circuit may also be considered to be that of a perfect differentiator with gain  $G$ , followed by an  $RC$  integrating network with a time constant  $RC/(G+1)$ .

The integrating circuit of Fig. 18-19b may be analyzed in a similar manner. The transfer ratio is

<sup>1</sup> In the following derivation,  $-G$  is used for the gain of the amplifier without feedback.

<sup>2</sup> The response of amplifiers to pulses is sometimes better expressed in terms of rise time and overshoot. See Vol. 18, Chap. 3.

$$\frac{\mathcal{L}(e_o)}{\mathcal{L}(e_i)} = - \frac{G}{1 + pRC(G + 1)}. \quad (14)$$

Comparison of this expression with that of Eq. (12) shows that the use of feedback has effectively multiplied the time constant by  $G + 1$ , and at the same time multiplied the output amplitude by  $(-G)$ . The result again is an increase in accuracy such as would have been obtained by the use of a simple  $RC$ -network with a larger time constant, without the attendant decrease in output amplitude.

*Superposition Integral.*—A convenient physical picture of differentiation and integration may be obtained by means of the superposition theorem,<sup>1</sup> as applied to a succession of voltage impulses following one another in time. This theorem expresses the output voltage of a network as a function of the input voltage and of the response of the network to a step function.

If the output voltage of the network in response to an input step function is  $A(t)$ , the output in response to an arbitrary waveform  $e_i(t)$  can be expressed in terms of  $A(t)$ , provided the input waveform is replaced by an infinite number of infinitesimal step functions, as shown in Fig. 18-21. The amplitude of the step at time  $\lambda$ , for example, is  $\frac{d}{d\lambda} e_i(\lambda) \cdot d\lambda$ . The output waveform is then obtained by superimposing the effects of these step functions; it takes the form of an integral. If the output voltage at time  $t$  is desired, the effect of a previous step  $de_i$  at time  $\lambda$  is  $\frac{de_i}{d\lambda}(\lambda) \cdot A(t - \lambda)d\lambda$ ; consequently, the response is

$$e_o(t) = e_i(0)A(t) + \int_0^t \frac{d}{d\lambda} e_i(\lambda) \cdot A(t - \lambda) d\lambda, \quad (15)$$

where the term  $e_i(0)A(t)$  takes account of any initial step in  $e_i$ . Integration by parts makes possible the alternative expression

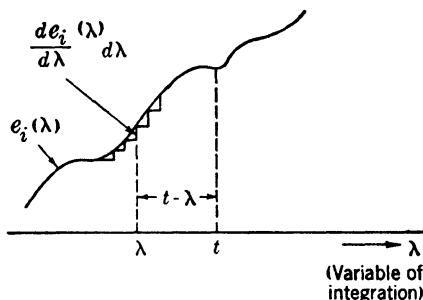


FIG. 18-21.—Replacement of input waveform by step functions.

<sup>1</sup> See, for example, V. Bush, *Operational Circuit Analysis*, Wiley, New York, 1937, p. 56 ff.; M. F. Gardner and J. L. Barnes, *Transients in Linear Systems*, Wiley, New York, 1942, p. 231 ff.; Vol. 18, Chap. 1, Radiation Laboratory Series. The same result may be arrived at through the "convolution theorem" of Laplace transform theory, but only the "physical" explanation is given here. Readers not interested in the mathematical details may skip to the end of this derivation, where the results are summarized.

$$e_o(t) = e_i(t)A(0) + \int_0^t e_i(\lambda) \frac{d}{d(t-\lambda)} A(t-\lambda) d\lambda. \quad (16)$$

In connection with differentiating circuits it is convenient to use the form of Eq. (15). For a perfect differentiating circuit the response to a step function,  $A(t)$ , is given by the delta function.<sup>1</sup> This is simply a weighting function which, if multiplied by a function and integrated, causes the value of the integral to be equal to the value of the function at the point where the delta function has a nonzero value. If a delta function is used for  $A(t-\lambda)$  in Eq. (15), then for  $t \neq 0$ , the first term drops out; the integral assumes the value of  $\frac{d}{d\lambda} e_i(\lambda)$  at  $\lambda = t$ , so that

$$e_o(t) = \frac{d}{dt} e_i(t).$$

For either the simple  $RC$  "differentiating" network or the feedback differentiating circuit, the transfer ratio has the form

$$\frac{\mathfrak{L}(e_o)}{\mathfrak{L}(e_i)} = \frac{Bp}{p + \frac{1}{T}},$$

where  $B$  and  $T$  are constants, and the response to a unit step function<sup>2</sup> is

$$A(t) = Be^{-\frac{t}{T}}.$$

For small  $T$  this resembles a delta function in that most of its area is concentrated in a small region along the  $t$ -axis. In the case of the feedback differentiator [Eq. (13)],  $B = -G$  and  $1/T = (G+1)/RC$ ; as  $G$  increases, the area under the curve remains nearly constant, but the area of the function is concentrated more closely about  $t = 0$ .

If this function is substituted in Eq. (15), the result is

$$e_o(t) = e_i(0) \cdot Be^{-\frac{t}{T}} + \int_0^t \frac{d}{d\lambda} e_i(\lambda) \cdot Be^{-\frac{(t-\lambda)}{T}} d\lambda. \quad (17)$$

This means that the output voltage at time  $t$  is in error by an amount depending on the weight given to the derivatives of the input voltage at *previous* times  $\lambda < t$ . The weighting function is shown in Fig. 18-22 together with an input waveform which is a linear sawtooth waveform

<sup>1</sup> Defined to be zero if  $x \neq 0$  and infinite at  $x = 0$  in such a way that  $\int_{-\infty}^{\infty} \delta(x) dx = 1$ .

1. See for example H. S. Carslaw and J. C. Jaeger, *Operational Methods in Applied Mathematics*, Clarendon Press, Oxford, 1941, p. 251.

<sup>2</sup> Provided that, in the case of the feedback differentiator, it is small enough not to drive the tubes out of the linear region.

starting at  $t = t_0$ . Since the weighting function is a function of  $(t - \lambda)$ , it is plotted backward along the  $\lambda$ -axis from  $\lambda = t$ . The deviation from the correct output voltage at time  $t$  may be considered to be due to the weighting of the zero derivative, at  $t < t_0$ , in the integral of Eq. (17).

A delay-line circuit may be made to produce an output voltage equal to  $e_i(t + \Delta t) - e_i(t)$ . The response to a step function is then a narrow rectangle. This is another way of producing a weighting function that has values only near  $t = 0$  and resembles a delta function.

The superposition integral in the form of Eq. (16) may be used to show the action of an integrating circuit. The response of a perfect integrating circuit to a unit step function should be a linear waveform, that is,  $A(t) = t$ . If this function is substituted in Eq. (16), the result is

$$e_o(t) = \int_0^t e_i(\lambda) d\lambda,$$

for  $A(0) = 0$  the term  $e_i(t)A(0)$  vanishes and the weighting function

$$(d/d(t - \lambda))A(t - \lambda)$$

is identically equal to unity. For the  $RC$  integrating network or the corresponding feedback circuit the transfer ratio has the form

$$\frac{\mathcal{L}(e_o)}{\mathcal{L}(e_i)} = \frac{B}{1 + pT},$$

where  $B$  and  $T$  are constants, and the response to a step function is

$$A(t) = B(1 - e^{-\frac{t}{T}}).$$

The weighting function is equal to the derivative:

$$\frac{d}{dt} A(t) = \frac{B}{T} (e^{-\frac{t}{T}}).$$

If this function is substituted in Eq. (17), the result is

$$e_o(t) = \int_0^t e_i(\lambda) \cdot \frac{B}{T} e^{-\frac{(t-\lambda)}{T}} d\lambda. \quad (18)$$

If  $T$  is large relative to the time interval of integration, the weighting function is nearly a constant. For the feedback integrator,  $B = -G$  and  $T = RC(G + 1)$ ; consequently for  $t \ll T$  and  $G \gg 1$  the magnitude of the weighting function is approximately equal to the constant,  $1/RC$ .

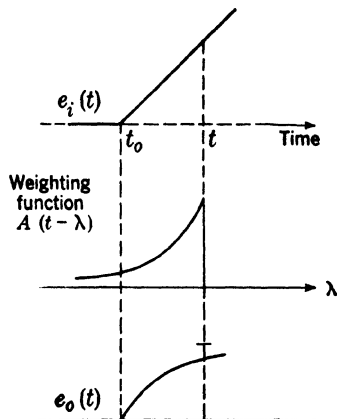


FIG. 18-22.—Weighting function and differentiation of a linear waveform. The voltage scales of  $e_i$  and  $e_o$  are not necessarily the same. The departure of  $e_o(t)$  from the derivative corresponds to the portion of the weighting function that coincides with the zero-slope region of  $e_i(t)$ .

Figure 18-23 shows the weighting function, plotted backward along the  $\lambda$ -axis as before, together with a rectangular input waveform. The deviation of the output from the integral corresponds to the departure of the weighting function from a constant. As the integration proceeds to increasing values of  $t$ , the weight associated with the initial values of the integrand gradually decreases, as if the integrator were slowly forgetting the old input information. In the case of slow-acting integrators this is caused more often by leakage in the storage condenser itself than by the finite gain of the amplifier.

The superposition-integral treatment thus provides an explanation for the errors of differentiation and integration by networks and feedback amplifiers, and a method of computation of these errors; this treatment is applicable to any input waveform encountered in practice,

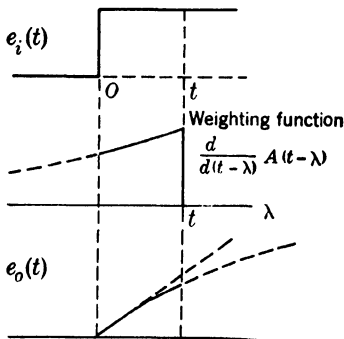


FIG. 18-23.—Weighting function and integration of a rectangular waveform. The departure of  $e_o(t)$  from the integral corresponds to the departure of the weighting function from constancy.

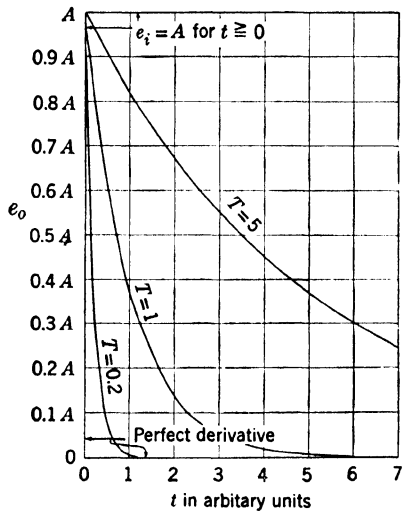


FIG. 18-24.—Waveform resulting from differentiation of a step function by an  $RC$ -network. The time constants  $T$  are measured in the same units as the horizontal axis.

including those that cannot be described by simple algebraic expressions. The explanation of the errors is this: a differentiator, by weighting past derivatives in the output, “remembers” values of the input derivative that it should not have “remembered”; an integrator “forgets” past values of the integrand to some extent. The computation of errors by means of these integrals has not been carried out to any great extent, but it is believed that for small errors a convenient estimate can be obtained by a series expansion of the weighting function in Eq. (17) or Eq. (18).

The behavior of the output of an  $RC$  “differentiating” network may be associated with a “direct-coupling” term, for when there is a constant-voltage input the output tends asymptotically toward that value rather

than increasing indefinitely. If there is a constant nonzero input voltage to a feedback integrator, the output will start toward an asymptote of approximately  $(-G)$  times the input, but the amplifier will usually saturate long before this is reached.

*Differentiation and Integration of Typical Waveforms.*—Figure 18-24 shows the waveform resulting from “differentiation” of a step function<sup>1</sup> by an  $RC$ -network: a sharp rise at  $t = 0$  followed by an exponential decay. The three curves shown correspond to time constants of 5, 1,

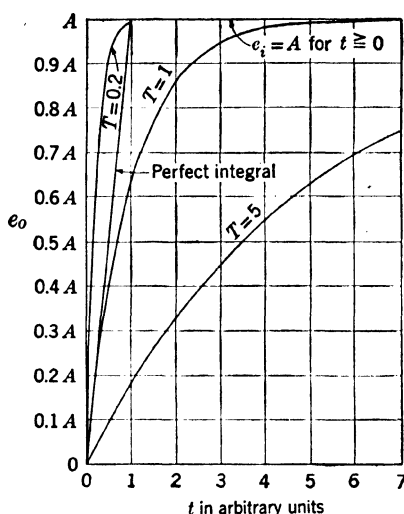


FIG. 18-25.—Integration of a step function.

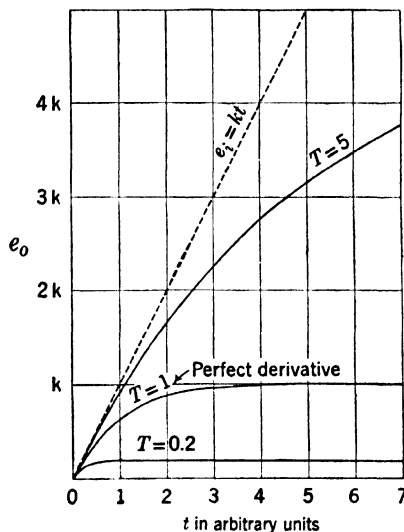


FIG. 18-26.—Differentiation of a linear waveform.

and 0.2 times the time unit on the horizontal scale. The result of integration of a step function by a similar network is shown in Fig. 18-25.

The waveform resulting from “differentiation” of a linear waveform is shown in Fig. 18-26. This method is used to check the linearity of such waveforms. The Laplace transform of this waveform has the same form as that of the “integrated” step function. For “integration” by a passive network the ratio of transforms has the form  $1/(1 + pT)$ , and the step function has the transform<sup>2</sup>  $1/p$ ; therefore, the transform of the output waveform is  $1/p(1 + pT)$ . Similarly, the “differentiation” of a

<sup>1</sup> A graphical treatment of this operation is given by G. P. Ohman, “Square-wave Differentiating Circuit Analysis,” *Electronics*, **18**, 8, 132 (1945). The input is assumed to be a rapid exponential rise. Shunt capacitance is considered, and a number of graphs are given.

<sup>2</sup> The Laplace transforms of waveforms differ from the Heaviside expressions by a factor  $1/p$ .



linear waveform of slope  $1/T$  produces

$$\frac{pT}{1 + pT} \times \frac{1}{p^2T} = \frac{1}{p(1 + pT)}$$

The difference is that in "integration" the initial transient of the output waveform is important, whereas in differentiation as a slope-finding process the steady state to which the network settles is the desired output. Figure 18-27 shows the result of "integration" of a linear waveform with various time constants.

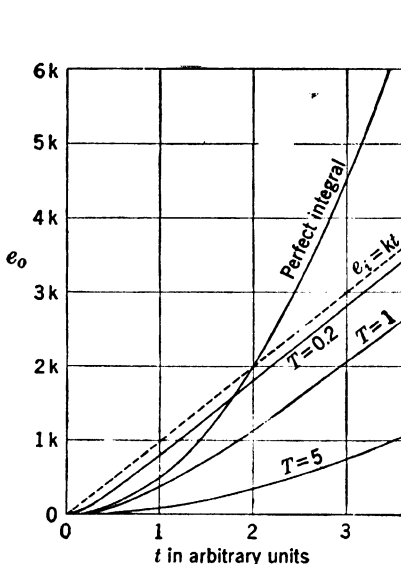


FIG. 18-27.—Result of integration of a linear waveform with various time constants.

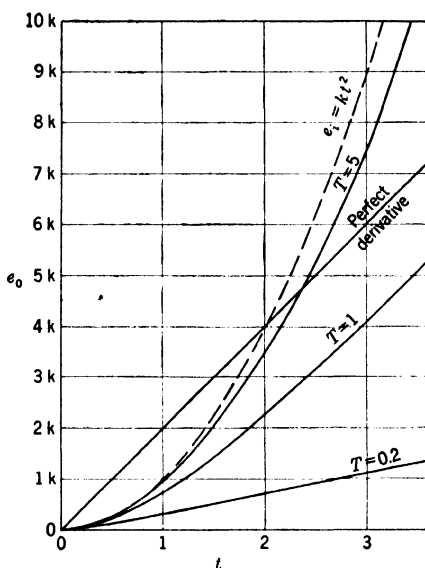


FIG. 18-28.—Differentiation of a parabolic waveform.

Figure 18-28 shows the result of "differentiation" of a parabolic waveform. This procedure is used as a rough check on the accuracy of parabolic waveforms. The transform of this waveform has the same form as that of the integrated linear waveform.

In the case of integration the errors, which are always smallest at the start, increase with time. For differentiation the opposite is true: a short time is required before the output waveform reaches its correct value, after which it maintains that value as long as the input derivative is constant.

**18-7. Practical Circuits.**—The errors discussed above, which are due to the departure of  $RC$ -circuits from perfect differentiators and integrators, are important when feedback is not used. If a feedback loop with sufficiently high gain is used, however, these errors become small

relative to the errors caused by departure of components from the ideal properties assumed in deriving the equations. In differentiating circuits, stray capacitances cause a time lag around the feedback loop; such a delay limits the rate of response of the circuit. If the input is a rapidly rising waveform, the amplifier may be overloaded at first; the flow of grid current in the input condenser may introduce serious overshoot effects. In integrating circuits, especially those operating over time intervals of several minutes, the effect of dielectric absorption in the integrating condenser may cause errors.<sup>1</sup> Another important source of error in such integrators is leakage across the integrating condenser. If the theoretical time constant  $(G + 1)RC$  is sufficiently large, the limiting effect will be determined by the leakage time constant. The leakage conductance may be decreased by special mounting, insulation, or cooling of the condenser. The effect may also be reduced by adjustment of d-c levels in the circuit so that at the center of the output range there is no voltage across the condenser (Fig. 18-29). If this circuit is used, the drift will always be toward the center of the output range, rather than being always a decrease in voltage, as in the case of the single-stage Miller integrator.

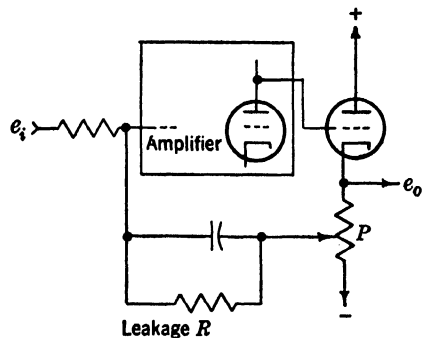


FIG. 18-29.—Compensation for leakage at center of output range. The potentiometer  $P$  may be adjusted to make the drift rate zero at the center of the range of output voltage.

By means of a more elaborate circuit, compensation over the entire output range may be obtained. The leakage resistance of the condenser contributes a current proportional to the voltage across the condenser; in order to compensate for this it is necessary to withdraw an equal current from the grid node. This can be done by means of an appropriate resistance if a voltage is available which is proportional to the negative of the voltage across the condenser. The circuit of Fig. 18-30 may be used for this purpose; the feedback amplifier connected to the plate of the Miller integrator produces a voltage  $(-e_p/k)$  which withdraws through the adjustable resistance  $R_L/k$  a current equal to the leakage current. The effect is that of a negative resistance<sup>2</sup> in parallel with the positive leakage resistance.

In feedback differentiators and integrators there are several methods

<sup>1</sup> See Vol. 21, Chap. 4.

<sup>2</sup> See E. L. Ginzton, "Stabilized Negative Impedance," *Electronics* (July–September, 1945).

which the designer may use to increase the loop gain and correspondingly reduce the variation in potential of the first grid. The most obvious is to use more than one stage of amplification. Another, shown in Fig. 18-32 below, is the use of a constant-current tube as the plate load of a pentode. A third is the use of a large inductance in the plate circuit of an amplifier. Examples of this method are given in Chap. 7 and in Vol. 21, Sec. 6-6.

*Feedback Differentiators.*—Figure 18-31 shows a differentiating circuit designed to operate with relatively rapid changes of the input voltage. Its response time is of the order of magnitude of several microseconds; this means that if the input waveform is triangular, the output waveform will be a rectangle whose front edge is an exponential with a time constant

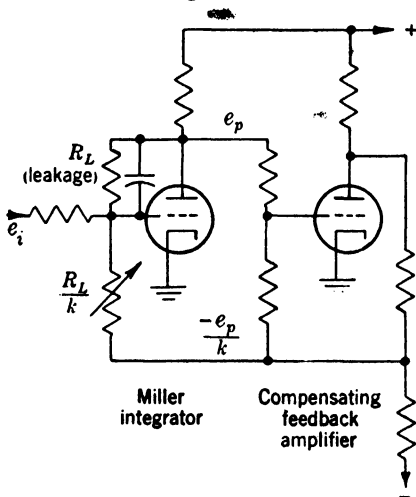


FIG. 18-30.—Compensation for leakage in storage condenser over entire output range.

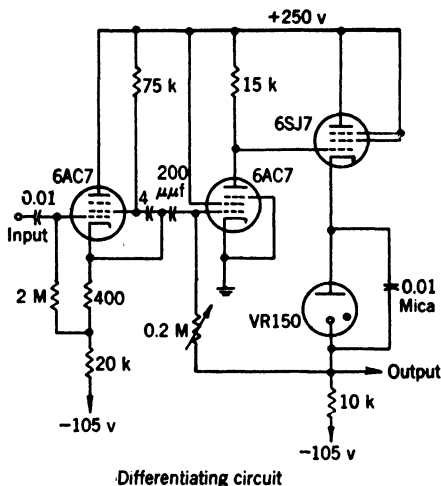


FIG. 18-31.—Feedback-differentiating circuit.

of several microseconds. The first stage is a cathode follower, for the differentiator has an input impedance approximately equal to that of the input capacitance. The differentiator itself has one stage of amplification, followed by a cathode follower with a VR tube in the cathode circuit to correct the d-c level. The adjustable 200,000-ohm-feedback resistor permits variation of the over-all gain as the input-rise rate varies from one waveform to another. With a value of 200,000 ohms in the circuit, an input rate of 25 volts/msec produces one volt at the output. Input and output voltage amplitudes of at least 50 volts can be accommodated.

Figure 18-32 shows another design in which several improvements have been made. The power supply provides a higher voltage (+575 volts). A decoupling filter is included in the plate circuit of the first cathode follower. In addition to the rheostat gain control, a switch is



voltage. Only positive output voltages (negative input rates) are provided by this circuit. The output voltage is increased by feeding back only part of it; an input rate of only 0.4 volt/min suffices to produce an output of one volt. The network  $R_1R_2R_3$  feeds back a fraction of the output voltage and at the same time sets the d-c level to that of the first grid. The input condenser must be chosen carefully, because in some makes of condensers dielectric absorption causes errors in differentiator operation.

Current feedback may also be used for differentiation and integration. If an amplifier has a capacitance in the cathode circuit and a resistance

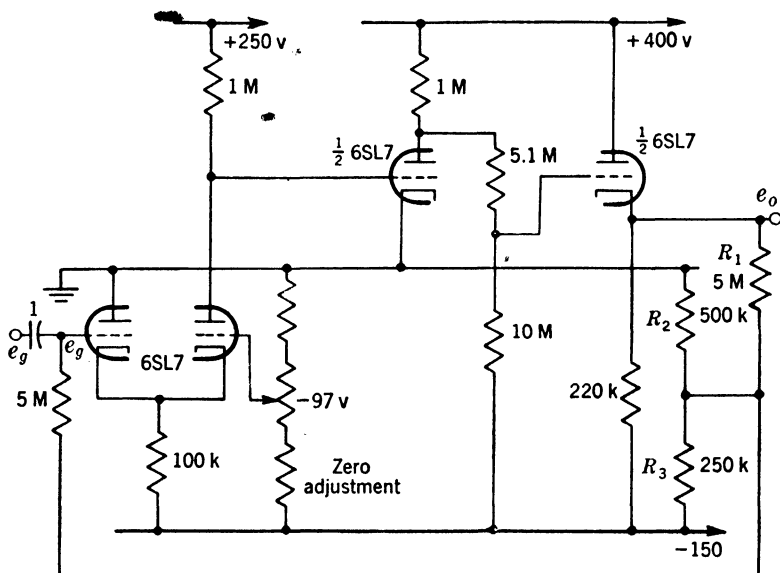


FIG. 18-33.—Example of feedback amplifier type of  $RC$ -differentiator.

in the plate circuit, for example, it will resemble a differentiator, for the cathode voltage is proportional to the integral of plate current. The feedback forces the cathode voltage to be approximately equal to the input voltage; the plate current therefore varies as the derivative of the input voltage. A number of other variations of the cathode-follower circuit for differentiation and integration are given in Vol. 21, Chap. 4.

**Bootstrap Integrators.**—One method of reducing the error that is characteristic of the simple  $RC$  integrating network is shown in Fig. 18-34. The input current may be made independent of the voltage on the integrating condenser by adding the condenser voltage to the source voltage. A circuit of this type, in which the voltage difference between two terminals is maintained constant by feedback from one terminal to the other, is known as a “bootstrap” circuit. A floating source (certain types of

detectors, for example) is necessary if this method is to be used. A further refinement is to use a unity-gain amplifier instead of a cathode follower.

Figure 18-35a shows another circuit type that makes use of feedback from one terminal of an element to another. The feedback is from the grid of the triode to the junction of the integrating condensers  $C_1$  and  $C_2$ , although the action of the circuit is not such that a constant voltage is maintained across a condenser. This circuit performs approximately the operation of double integration of an input current. It has been used in automatic range-tracking loops,<sup>1</sup> the object being to provide "memory" of position and velocity. In order to make a tracking circuit "remember," it is necessary that during intervals when there are no input data the output voltage shall continue from its last known value at a rate equal to that previously established. This property makes it possible for tracking to continue when the intermittent input data again appear.

The operation of the circuit may be described fairly easily, subject to the simplifying assumption that the cathode follower is a unity-gain

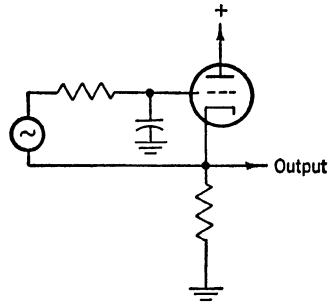
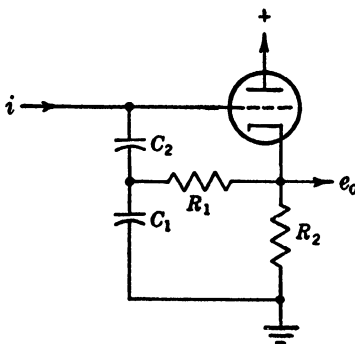
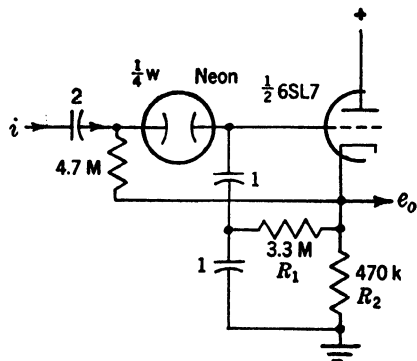


FIG. 18-34.—Integrator using floating voltage source and feedback.



(a) Schematic diagram.



(b) Typical memory circuit.

FIG. 18-35.—Double-integrator memory circuit.

amplifier. In this case a relation between the input current  $i$  and the output voltage  $e_o$  may be found by straightforward network analysis:

$$R_1 C_1 C_2 \frac{d^2 e_o}{dt^2} = i + R_1 (C_1 + C_2) \frac{di}{dt} \quad (19)$$

If there is no input information ( $i = 0$ ,  $di/dt = 0$ ), the output voltage  $e_o$

<sup>1</sup> Automatic range tracking is discussed in Vol. 20, Chap. 8.

will continue to vary linearly with a slope and zero determined by the preceding tracking operation. A more exact equation taking into account the gain  $G$  of the cathode follower shows that the actual curve is a slow exponential having a time constant  $(GR_1C_1)/(1 - G)$ . Although the performance of the circuit as an integrator is good when there is zero input, a serious departure from the double integral is introduced when

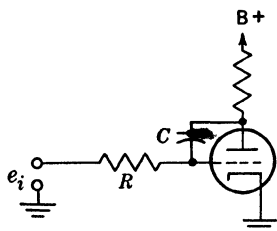


FIG. 18-36.—Miller circuit.

there is an input  $i$  because of the linear combination of  $i$  and  $di/dt$  on the right-hand side of Eq. (19). In a tracking loop this departure from double integration is not objectionable and is often necessary for stability of the loop; this circuit, however, is not suitable for precise integration in computers.

Figure 18-35b shows a typical circuit of this type. A neon tube is incorporated in the input circuit to prevent spurious signals from being integrated during the intervals when there are no data. The neon tube acts as an amplitude selector. The 4.7-megohm feedback resistor keeps the potential difference across the neon tube small during these intervals. The resistances used are typical in that  $R_1$  is usually considerably greater than  $R_2$ . An input condenser can be used because the current  $i$  is supplied in pulses.

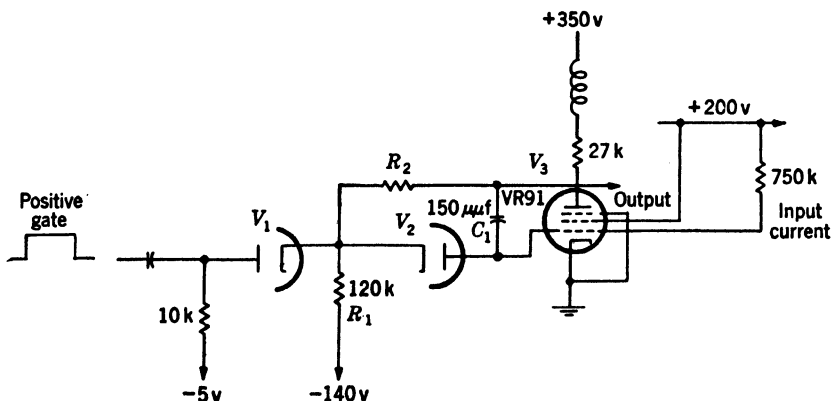


FIG. 18-37.—Diode switch for establishing starting level of integrator. The VR91 is a British tube type.

**Miller Integrators.**—A number of feedback-integrating circuits designed to produce specific waveforms are discussed in Chaps. 7 and 8. One of the most generally applicable circuits and one of the simplest is a single-stage amplifier with capacitive feedback from plate to grid (Fig. 18-36). This is known as “the Miller circuit” because of the

resemblance of its operation to an effect described by J. M. Miller,<sup>1</sup> which concerns a similar feedback resulting from the grid-plate capacitance of a triode. The analysis of Eq. (14) is applicable. In the generation of periodic waveforms it is frequently desirable to start the output waveform from a predetermined level.<sup>2</sup> Figure 18-37 shows a method by which this can be done. Normally  $V_1$  is cut off and  $V_2$  is conducting. The plate of  $V_2$  is then set at a potential determined by the resistive feedback network consisting of  $R_1$  and  $R_2$ . When a positive gate is impressed on  $V_1$ , current begins to flow through the integrating condenser  $C_1$  (150  $\mu\text{f}$ ) and thereby generates a negative sawtooth waveform at the plate.

An important application of the Miller integrator is in automatic tracking.<sup>3</sup> Figure 18-38 shows two such circuits used for this purpose.

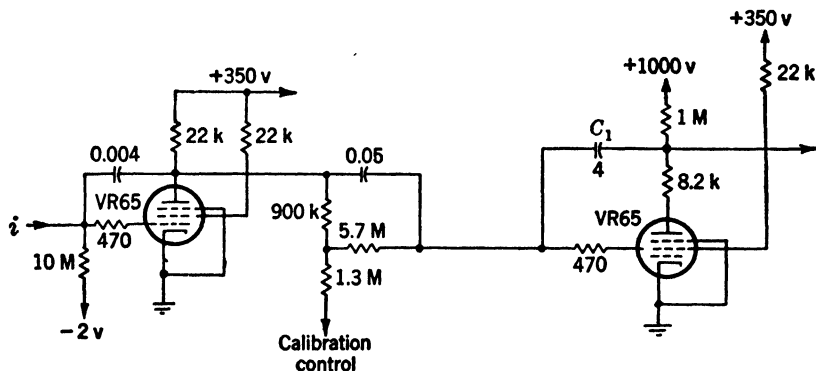


FIG. 18-38.—Integrators from Oboe tracking circuit. The VR65 is a British tube type.

The network between the two integrators contains an additional condenser necessary to the stability of the feedback loop of which these circuits are a part.

Figure 18-39 shows an integrator designed to operate over longer periods of time. The principal feature which makes this possible is the mounting of the resistance and capacitance and other input components in a hermetically sealed container to minimize leakage. The second differential-amplifier stage is provided with positive feedback by the resistors from each plate to the opposite grid. The positive feedback must be carefully adjusted, however, for "over-regeneration" produces errors. A push-pull output was desired for this particular application; positive and negative output voltages, symmetrical with respect to ground, are produced. A switch is provided for adjusting the starting

<sup>1</sup> J. M. Miller, "Dependence of the Input Impedance of a Three-element Vacuum Tube upon the Load in the Plate Circuit," *Nat. Bur. Standards Sci. Paper* 351.

<sup>2</sup> See Chap. 7.

<sup>3</sup> Vol. 20, Chap. 9.



level, or integration constant. The output rate is 50 volts/hr for an input of 2.3 volts. Critical factors in the design of circuits of this type are grid current, which must be small relative to the input current; and differential tube drift, which may produce undesired integration. In this circuit a change of grid current of  $0.00056 \mu\text{a}$ , or a differential drift of the 6SU7 of 23 mv, will give an error of 0.5 volt/hr.

*Magnetic Amplifier.*—A nonlinear core of magnetic material<sup>1</sup> may be used in place of a differential amplifier as an amplitude discriminator.

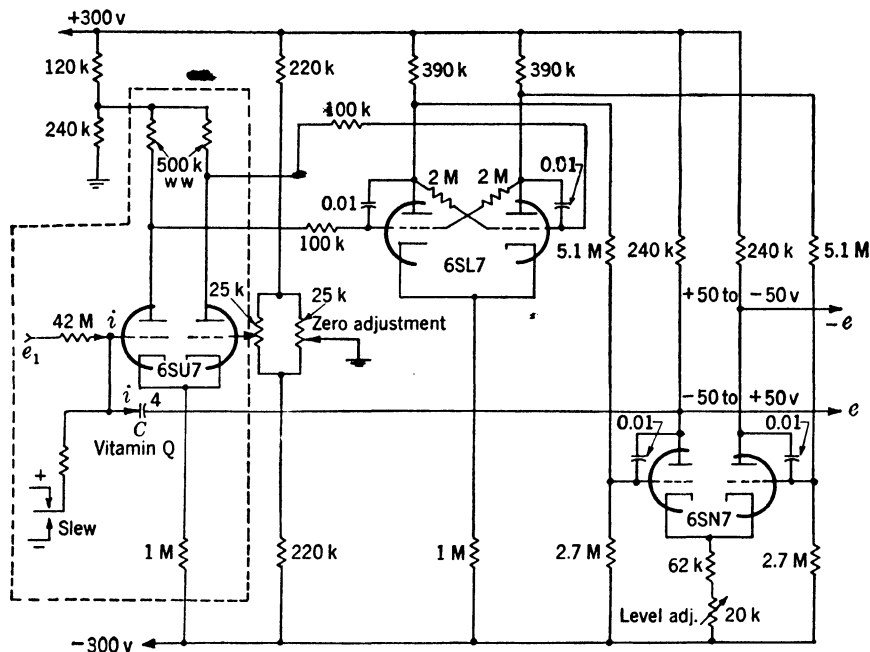


FIG. 18-39.—Electronic integrator for slowly changing output voltages. The dotted line includes components that are hermetically sealed.

One winding supplies a carrier frequency to the core, and several other windings carry currents whose sum is to be made equal to zero. If there is a net d-c flux in the core, a second-harmonic output is produced; this is used as an error signal in a feedback amplifier which restores the d-c flux to zero by adjusting one of the currents. By the use of a condenser in series with one of the d-c windings, differentiation or integration is possible. The carrier frequency limits the speed with which differentiation can be performed. Tests of a differentiating circuit of this type with an exponential input having a time constant of about 0.3 sec showed a mean error of 0.6 per cent of maximum output.

<sup>1</sup> H. S. Sack *et al.*, NDRC 14-437; H. S. Sack *et al.*, "Use of a Specially Designed Magnetic Amplifier in Computing Circuits," Cornell University, May 10, 1945. See also Sec. 11.7 for a more detailed treatment.

## CHAPTER 19

### MATHEMATICAL OPERATIONS ON WAVEFORMS--II

BY F. B. BERGER AND D. MACRAE, JR.

**19.1. Introduction.**—The operations to be considered in this chapter are multiplication, division, squaring, and the extraction of square roots. These operations are difficult to perform with linear circuit elements, even with the aid of feedback amplifiers. The methods used, therefore, involve either nonlinear or multivariable elements.

In selecting devices for these operations, the designer usually has a choice between accuracy and speed of computation. The most accurate multiplying methods use electromechanical devices<sup>1</sup> (e.g., potentiometers) and feedback systems with carrier waveforms (Sec. 19.5). Either of these methods may give accuracy of the order of magnitude of 0.1 per cent of the range of output, but both are limited in speed of response—the electromechanical devices being limited by inertia to response in about  $10^{-2}$  sec, the carrier-type amplifier being limited by the period of the carrier waveform (response times as low as  $10^{-5}$  sec have been obtained). On the other hand, there are multiplying devices having “instantaneous” response (within a few tenths of a microsecond), such as logarithmic circuits and multiple-input vacuum tubes. The accuracy obtainable with these devices depends directly on the characteristics of the elements used and is rarely better than about 1 per cent of the range of output. The variation of characteristics with temperature and with change of elements is an additional source of error.

Among squaring devices there is also a choice between accuracy and speed. Sections 19.6 to 19.9 will be concerned chiefly with “instantaneous” squaring; this is done, for the most part, by means of the nonlinear characteristics of vacuum tubes. The best accuracy measured has been about 0.5 per cent of the range of output, and careful calibration is required to realize this. “Noninstantaneous” squaring may be done with considerable accuracy but less speed by means of a repetitive parabolic voltage waveform generated by integration (Chap. 8); a voltage varying as the square of an input may be produced from it by time selection.

An aspect of the problem that might be considered further is the development of vacuum tubes having more nearly the desired character-

<sup>1</sup>Vol. 21, Chap. 3.

istics. Another subject that remains to be investigated is the nature of fundamental limitations on computing speed in these devices. For devices making direct use of tube or crystal characteristics, the speed is probably limited by stray capacitances; for carrier-type multipliers the maximum carrier frequency may be limited by stray capacitive coupling from one circuit element to another.

## MULTIPLICATION AND DIVISION

### 19-2. Relation of Multiplication and Division to Other Operations.—

The process of amplitude modulation is in many cases a process of multiplication in which the carrier amplitude after modulation is proportional to the modulating signal and to the amplitude of the input carrier. In other types of modulation the output amplitude is proportional to the product of input carrier amplitude and some prescribed function of

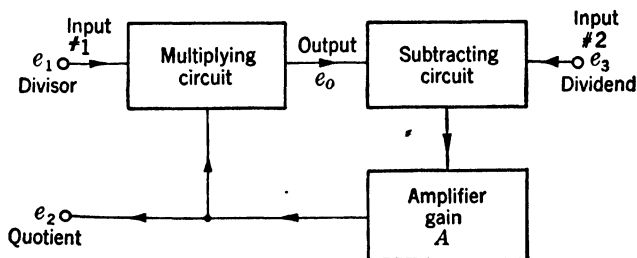


FIG. 19-1. —Division performed by the use of a multiplying circuit and a feedback loop.

input signal—for example, the output of a synchro is equal to  $e_i \sin \theta$ , where  $e_i$  is the input voltage and  $\theta$  is the shaft rotation. Any precision modulator of these types may, therefore, be considered as a multiplier. Electrical and electromechanical modulators are discussed in Chaps. 11 and 12 respectively.

Squaring<sup>1</sup> is a special case of multiplication in which the multiplier and multiplicand are equal or proportional. Thus multiplying devices may be used as squarers. Conversely, squaring circuits may also be used as multipliers by means of the relation

$$(x + y)^2 - (x - y)^2 = 4xy. \quad (1)$$

Logarithmic devices may be used for multiplication by means of the relationship

$$\log x + \log y = \log xy. \quad (2)$$

A multiplying device may be used to divide, by means of feedback, as shown in Fig. 19-1. The output of the multiplying circuit is  $e_o = ke_1e_2$ ; the operation of the amplifier is described by the equation  $A(e_o - e_3) = e_2$ .

<sup>1</sup> Squaring and the extraction of square roots are discussed in Sec. 19-6 to 19-9.

These relations give

$$e_2 = \frac{e_3}{ke_1 - \frac{1}{A}}, \quad (3)$$

which for large  $A$  is approximately equal to  $e_3/ke_1$ . A similar method is discussed in Sec. 19.8 where square-root extraction is accomplished by this type of circuit and a squaring unit replaces the multiplying unit of Fig. 19.1.

With the use of logarithmic devices, division may be performed analogously to multiplication by means of the relationship

$$\log x - \log y = \log \frac{x}{y}.$$

**19.3. Multipliers Using Tube Characteristics.**—In order to make a vacuum tube serve as a multiplier, the output signal must be proportional

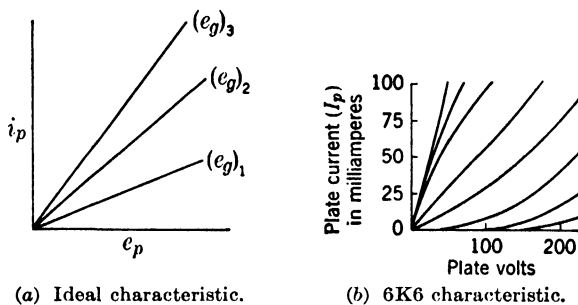


FIG. 19.2.—Multiplier characteristics.

to each of two parameters independently—for example, if a triode is used, the plate current should obey the relation

$$i_p = ke_e e_p, \quad (4)$$

which is illustrated in Fig. 19.2. No available triode satisfies Eq. (4) over a very wide range of values of the variables. For the 6K6 connected as a triode, in the range where  $e_p$  is less than 25 volts and  $e_g$  is between 0 and +20 volts, Eq. (4) is approximately satisfied if  $e_g$  is measured from an appropriate reference level. Figures 19.3a and 19.3b show two ways in which this property can be utilized to get an output voltage proportional to the product of two independent input voltages. If a circuit of type *a* is used, input  $e_2$  must be able to supply the tube current and the transformer must have a response suitable for passing the output waveform without undue distortion. The output transformer must have a low-impedance primary winding, to avoid superimposing the output voltage on the plate voltage. Circuit type *b* is essentially a

cathode follower,<sup>1</sup>  $V_2$ , with the multiplying tube  $V_1$  as the cathode impedance. This circuit eliminates the difficulty encountered in type *a* by making it possible to measure the output at a different point from the  $e_2$ -input. The cathode of  $V_2$  (plate of  $V_1$ ) will assume a voltage approximately equal to  $e_2$ ; the plate current through  $V_1$  (and  $V_2$ ) is then proportional to  $e_1 e_2$ . The source of input voltage  $e_1$  must have low impedance if the grid is to be operated at positive potentials. The circuit may be used for d-c inputs as well as for a-c inputs.

Other tubes, for example the 6L6 and 6V6, roughly satisfy Eq. (4), but none are very good over a wide range.

A second relationship that is approximately satisfied for some tubes and that may be used for multiplication is

$$i_p = ae_{g_1}e_{g_2}, \quad (5)$$

where  $i_p$  is plate current and  $e_{g_1}$  and  $e_{g_2}$  are the voltages on two grids of the tube. Of the available multigrid tubes the 6SA7 and the 6AS6 most nearly satisfy Eq. (5),  $e_{g_1}$  and  $e_{g_2}$  being the voltages on the first and third grids respectively.<sup>2</sup> In the case of the 6AS6 it has been

found that more accurate multiplication is possible if the voltage  $e_{g_2}$  is measured with respect to  $e_{g_1}$ —that is, the relation satisfied is more nearly

$$i_p = ae_{g_1}(e_{g_2} - e_{g_1}).$$

**19.4. Logarithmic Devices.**—Contact rectifiers and diodes have been found under some conditions to have very nearly exponential variation of current with voltage, or logarithmic variation of voltage with current. According to Eq. (2) these devices can be used for multiplication. After two logarithms are produced and added, the antilogarithm of the sum must be computed. This may be done either by employing an exponential characteristic directly, or, if this is inconvenient, by using a feedback loop.

A fundamental limitation of logarithmic devices in waveform multiplication is their inability to handle inputs that go through zero. A possible but untried remedy for this is to add constants to the inputs until the

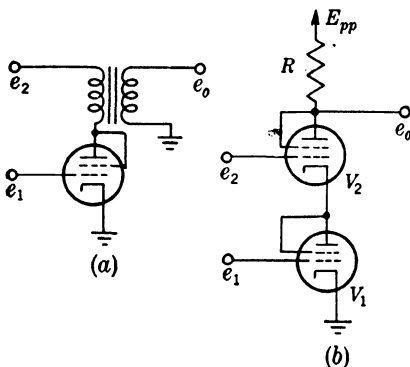


FIG. 19-3.—Multiplying circuits employing a vacuum tube for which  $i_p = ke_{g_1}e_{g_2}$ . (a) Transformer-coupled output, (b) cathode-follower type.

<sup>1</sup> For theory of cathode follower see Vol. 18, Chaps. 9 and 11.

<sup>2</sup> See Sec. 19.7 (multigrid squarers), Fig. 19-19.

resulting quantities are positive throughout the region to be used, then to multiply and subtract out the undesired terms.

Obviously, by adjustment of scale factors, a logarithmic multiplying device can be used to compute the function  $xy^b$ , where  $a$  and  $b$  are arbitrary real exponents. The difficulty in practice is to keep it from doing this since careful calibration is required to set the exponents at the desired values.

**Contact Rectifiers.**—It has been observed that the impedance of certain contact rectifiers<sup>1</sup> follows the law  $E = r \log i$  over a substantial range of their forward characteristics. Commercial copper-oxide rectifiers of various makes and sizes were found to follow that law consistently for a current range of 1 to 50 above a potential of about 0.070 volt per contact layer. Certain microwave mixer-type crystal detectors follow the logarithmic law through a current range of at least five decades, from the lowest measured value of  $1 \mu a$  (with 0.16 volt) up to about 10 ma (0.50 volt) in any circuit, and up to about 0.25 amp. if the linear contribution to the IR drop in the semiconductor is canceled.

The simplest electrical circuit for obtaining logarithms is the voltage-divider circuit shown in Fig. 19-4. The output of this voltage divider is strictly logarithmic only if—

1. The ohmic resistance  $R_i$  within the rectifier is negligible compared with the logarithmic contact resistance  $Z$ .
2. The source, or series resistance  $R_s$ , is large compared with  $Z$ .
3. The load, or meter resistance  $R_m$ , is large compared with  $Z$ .

An alternative circuit for the production of logarithms is the bridge circuit shown in Fig. 19-5. For convenience, symmetry will be assumed, with  $R_1 = R_2$ ,  $R_3 = R_4$ ,  $Z_3 = Z_4$ .

Nonlinear bridges of this type are known to have an output-vs.-input characteristic as plotted in Fig. 19-6 for negligible load current ( $R_m = \infty$ ). All curves were plotted with  $R_1 = R_2 = 100$  ohms, with  $Z_3$  and  $Z_4$  each consisting of two layers of 0.85-in.<sup>2</sup> copper-oxide rectifiers in series, and with values of  $R_3 = R_4$  varied from 0 to 100 ohms as indicated. The larger are these resistances, which are in series with the rectifier contacts, the higher is the input voltage at which the bridge balances ( $E_m = 0$ ).

<sup>1</sup> This material is taken from H. E. Kallmann, "Three Applications of Nonlinear Resistors," Report Ja-5, Part III (Oct. 19, 1945).

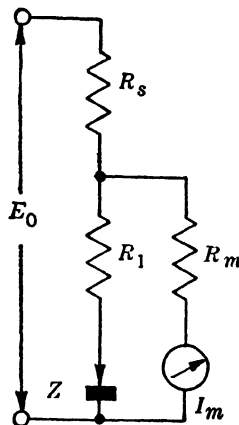


FIG. 19-4.—Voltage divider.  $R_i$  is the ohmic component of the rectifier resistance;  $Z$  is the logarithmic contact resistance;  $R_s$  = source resistance;  $R_m$  = meter resistance.

In particular, when  $R_1 = R_2 = R_3 = R_4$ , the output voltage  $E_m$  no longer goes through zero. It then presents an exact replica of the voltage on the copper-oxide rectifiers, rising logarithmically with rising bridge input. This result will be seen more clearly if the curve

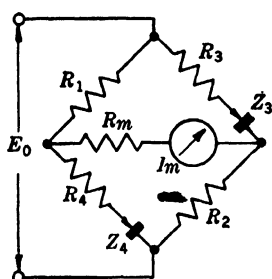


FIG. 19-5.—Bridge circuit.

$$R_3 = R_4 = 100 \text{ ohms}$$

is replotted on a semilogarithmic scale as in Fig. 19-7. The straight line indicates a strictly logarithmic relation over an input range of 34 db.

An evident merit of the bridge circuit is that the residual resistivity  $R_i$  of the contacts can be allowed for in the adjustment of the resistances  $R_3$  and  $R_4$ . As in the voltage-divider circuit, the output of the bridge circuit departs from the desired law at the low-current end of the range when  $Z$  grows comparable to  $R$ .

Logarithmic circuits lend themselves to combinations for the purpose of electrical multiplication or division. Figure 19-8 shows, as an example, the combination of two logarithmic bridges. Their outputs are connected in series and fed, with opposite sign, to a meter,

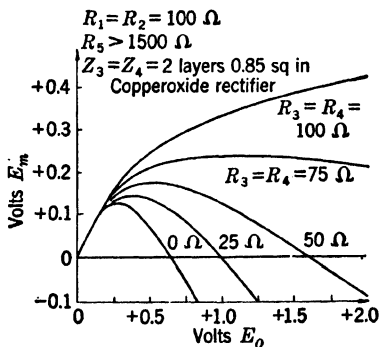


FIG. 19-6.—Characteristics of bridge circuit.

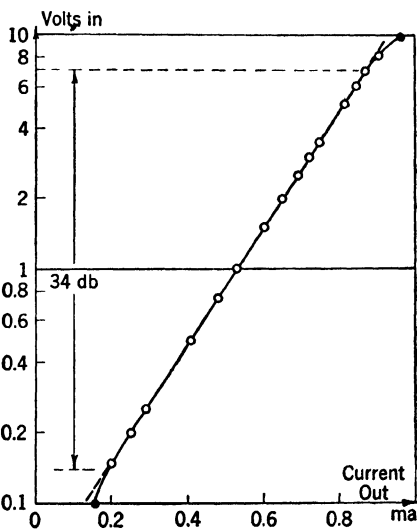


FIG. 19-7.—Logarithmic plot of bridge characteristic.

which thus reads the difference of their output currents. The current is then

$$i_{m1} - i_{m2} = A \log E_{01} - A \log E_{02} = A \log \left( \frac{E_{01}}{E_{02}} \right),$$

which is proportional to the logarithm of the ratio of the two bridge inputs. The meter may thus be calibrated directly in decibels of quo-

tient with a linear scale. Two small resistors  $\rho$  with adjustable taps are shown in Fig. 19-8 for the initial adjustment of bridge balance. A model with each  $R = 200$  ohms, each  $Z$  one layer of 0.85-in.<sup>2</sup> copper oxide,  $\rho = 5$  ohms and a meter for 0.1 ma full scale with  $R_m = 1800$  ohms was found reliable within  $\pm 2$  per cent of full scale for either input voltage varying from 0.14 volt to 7 volts—that is, up to ratios of  $\pm 35$  db. (For the temperature-sensitivity of crystal characteristics, see Chap. 3.)

If circuits of this sort are to be used to obtain the product of rapidly varying waveforms, it is necessary to compute automatically the antilogarithm of the output current.

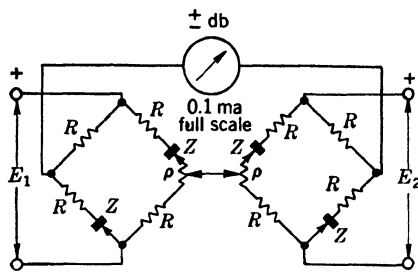


FIG. 19-8.—Combination of logarithmic bridges for division.

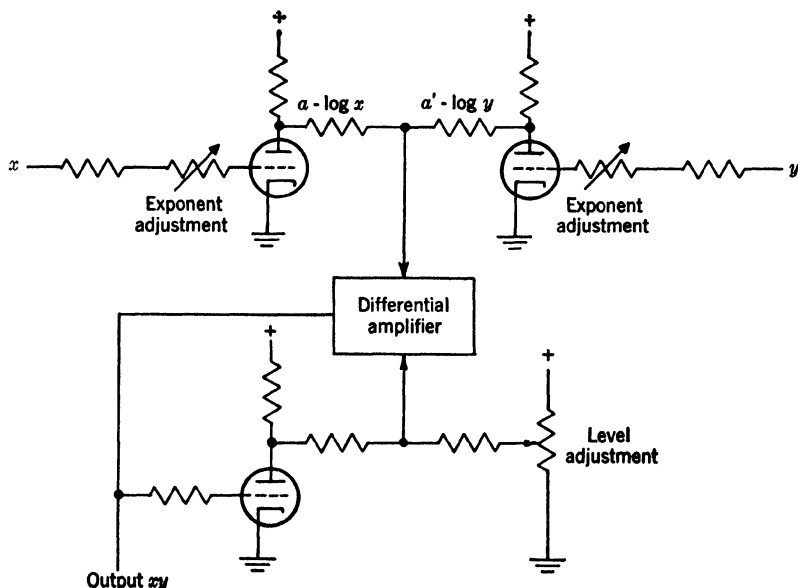


FIG. 19-9.—Use of logarithmic diode characteristic for multiplication. The grid voltage of each triode varies logarithmically with grid current.

**Diodes.**—For a diode at low-current values the variation of current with voltage is very nearly an exponential. By the use of a large series resistor the current may be made the independent variable, the voltage output then being a logarithmic function of current. This property



has been used<sup>1</sup> in a multiplying device; the grid-cathode current characteristic of a triode is used to produce a logarithmic variation of grid potential, and the grid-plate characteristic to amplify this variation. Three such devices may be combined in a feedback loop as shown in Fig. 19-9. Errors may result from variation of contact potential of the diodes, or from variation of heater voltage.

**19-5. Multiplying Devices Using Carrier Waveforms.** *Variation of Waveform.*—One method of multiplication is to vary the amplitude and duration of a rectangular waveform. If the bottom of the rectangle is

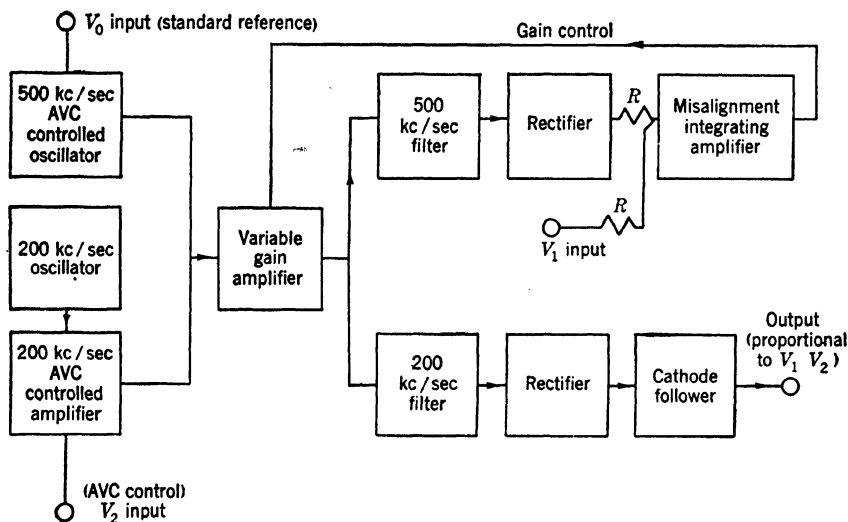


Fig. 19-10.—Block schematic of "carrier" multiplier circuit.

held at zero potential, the average or integral of the waveform is proportional to the product of amplitude and duration. Several computers using this principle have been designed<sup>2</sup> at Cornell University. A feedback circuit is employed in such a way that some errors cancel out. Multiplication of two voltages has been accomplished with errors of 0.2 per cent or less of maximum output. The inputs cannot, however, go through zero.

A similar procedure using triangular waveforms could conceivably be used to produce the function  $xy$ , the amplitude being varied as  $y$  and the duration as  $x$ .

*Gain Control Using Feedback at Carrier Frequency.*—A multiplying circuit developed at TRE makes use of a variable-gain amplifier whose

<sup>1</sup> For a more detailed treatment see Vol. 21, Chap. 3.

<sup>2</sup> H. S. Sack *et al.*, "Electronic Computers for Division, Multiplication, Squaring, etc." NDRC 14-435 Cornell University, 1944; Vol. 21, Chap. 3.

gain is controlled in accordance with an input signal by means of a feedback loop. A block diagram is shown in Fig. 19.10. A standard reference signal of 500 kc/sec is put through a variable-gain amplifier. The 500-kc/sec output component of the amplifier is compared with one of the input signals,  $V_1$ , and the difference is integrated and fed back to control the amplifier gain. The result is that when the loop is in equilibrium the gain of the amplifier is proportional to  $V_1$ . A second signal  $V_2$  modulates a 200-kc/sec wave, which is also fed to the input grid of

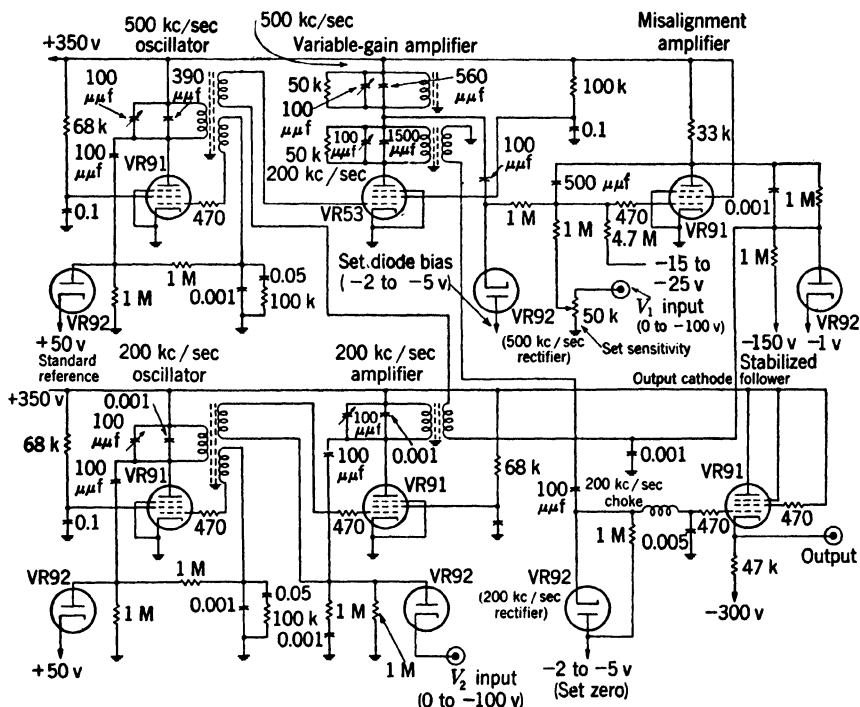


FIG. 19.11.—“Carrier” multiplier circuit. The tube types indicated are British.

the amplifier. The output at 200-kc/sec is then proportional to the product  $V_1 V_2$ . The two outputs of the amplifier are separated by tuned circuits. Figure 19.11 shows a circuit of this type which was found to operate satisfactorily. The two signals entering the variable-gain amplifier (VR53) are regulated in amplitude (the 500-kc/sec signal amplitude being kept constant, the 200-kc/sec signal varying proportionally to  $V_2$ ) by means of feedback loops in which the output is rectified and varies the gain of a tube. Additional  $RC$ -networks are provided to stabilize the AVC loops. The “misalignment amplifier” is a Miller integrator<sup>1</sup>

<sup>1</sup> For a discussion of the use of integrators in feedback loops see Vol. 20, Chaps. 8 and 9.

(Sec. 18·7). Controls are provided for the region of operation of the integrator and for the sensitivity of the entire feedback loop. For proper operation it is necessary that the variable-gain amplifier remain in its linear region—that is, the output signals of the amplifier cannot exceed about 50 volts. The output measuring  $V_1V_2$  is rectified and the d-c output is taken from a cathode follower. The output level is adjustable by variation of the level of the final rectifier; thus the output can be set to zero at zero input.

The chief advantages of this method of multiplication are that it does not depend to a first order on tube characteristics, and does not require special tubes. A similar method has been used at Bell Telephone Laboratories to linearize the characteristics of the 6AS6 as a multiplier. Time selection rather than frequency selection might be used in a multiplier of this sort; one pulse train might set the gain of the amplifier, and another measure the second input signal.

*Multiplication by the Method of Coincidences.*—A method making use of probability<sup>1</sup> may be used to compute the product of any number of inputs. It is a well-established result of probability theory that if several events occur with a random distribution in time, the probability of simultaneous occurrence of all of them is the product of their separate probabilities. This result may be extended to periodic waveforms whose periods have no common divisor. In particular, if rectangular waveforms of independent frequencies are superimposed, the time during which all the waveforms are positive will be proportional to the product of the duty ratios of the waveforms. One method of making use of this principle is to adjust the d-c levels of the rectangular waveforms which are to be added in such a way that a tube will be turned on only during the time when all the input waveforms are positive. The result will be that the average current drawn by this tube is proportional to the product of the input duty ratios.

It is first necessary to produce at each frequency rectangular waves of variable duration. This may be done by means of a time-modulation device and a prf generator (see Chaps. 5 and 13). The method actually used in the equipment constructed was to generate a triangular wave (see Fig. 19·12) and to select a portion of it by means of a variable bias level. The resulting amplitude-selected wave was converted to a square wave by amplification and limiting. The duration of the positive portion of the rectangular wave then varied linearly with the input bias level.

These rectangular waves were added by means of a resistance network and the sum fed to the grid of a pentode (Fig. 19·13). The d-c

<sup>1</sup> This method of multiplication was described by Professor A. C. Hardy of M.I.T. at the M.I.T. Physics Colloquium on Jan. 31, 1946. It was used in connection with the solution of three simultaneous third-order equations (Vol. 21, Chap. 3).

levels were so adjusted that the tube conducted only when all three waves were positive. When this coincidence occurred the tube was driven to zero grid bias. The current flowing in this case could be adjusted to a predetermined value by means of the screen potential. The average current in the tube then measured the product of the inputs.

The three trains of rectangular waves used to multiply three quantities in this equipment were generated at frequencies of approximately 18, 21, and 24 kc/sec. The computation of a product could be completed in approximately 500  $\mu$ sec. The errors of computation in a computer using 24 of these devices ranged from 1 to 4 per cent of maximum output.<sup>1</sup> These figures for speed and accuracy, however, are not determined by fundamental limitations; the design was so made that the performance was satisfactory for the problem at hand. Furthermore, these figures do not include errors due to time modulation. Reference should be made to Chaps. 5 and 13 for more precise methods of performing this operation. The principal accuracy limitations seem to be those resulting from linear time modulation and from variation with time of the current through the vacuum tube at zero grid bias. If the input

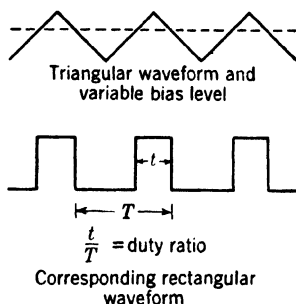


FIG. 19-12.—Generation of rectangular wave of variable duration.

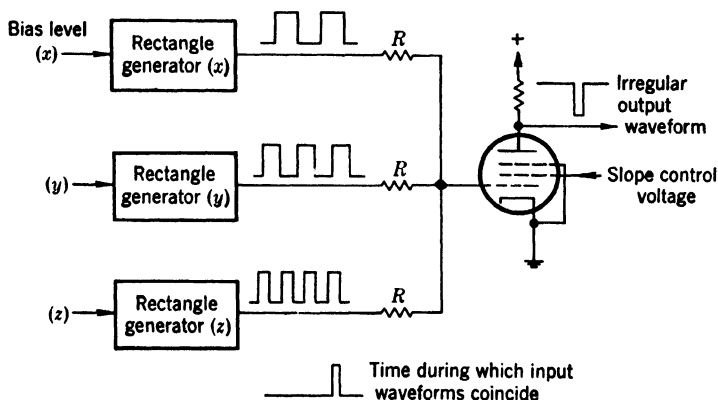


FIG. 19-13.—Superposition of rectangular waves for multiplication.

variables are measured by the averages of the corresponding rectangular waves, the time-modulation errors are irrelevant.

A distinguishing characteristic of this method of multiplication is

<sup>1</sup> These results were obtained from work done at the research laboratories of the Interchemical Corporation, New York City.

that any number of inputs may be used. Moreover, the operation of multiplication itself does not depend on the characteristics of vacuum tubes or nonlinear elements. The method does not, however, provide for a change of sign of the inputs.

### SQUARES AND SQUARE ROOTS

**19-6. Circuits for Producing Squares and Square Roots.**—By a squaring or square-root-extracting circuit is meant a circuit the output of which is proportional to the square or square root respectively of the input signal. The duration of the waveforms used in these circuits ranges from about 30  $\mu$ sec to several thousand microseconds. The response to very rapid input rates is limited chiefly by stray capacitances.

Most of the circuits to be discussed are amplifiers whose output signals are proportional to either the square or the square root of the input signals. For these circuits the input is usually to a grid, and the input impedance is high. The peak input signals range from 3 to 50 volts, depending on how much of the tube characteristic may be used. The errors of these circuits when properly calibrated range from 0.5 to 10 per cent of maximum output. The circuits that depend directly on vacuum-tube characteristics require calibration controls, for the output may vary considerably with heater voltage or aging, or from one tube to another.

Squaring and the extraction of square roots may be done by means of other mathematical operations. A multiplying circuit in which the inputs are equal has an output proportional to the square of this input. Similarly, a dividing circuit in which the "quotient" and "divisor" are somehow made proportional to each other serves to extract the square root of the "dividend." A voltage waveform proportional to the square of the time elapsed since its start may be produced by actually squaring a waveform in which the voltage is a linear function of time, but it may also be obtained by integrating the linear waveform.<sup>1</sup> By means of time selection a voltage proportional to the square of a time interval may be obtained from a parabolic waveform.

A squaring circuit can serve as a frequency doubler (Chap. 15),

$$\cos^2 \omega t = \frac{1}{2} + \frac{1}{2} \cos 2\omega t.$$

This equation may be used for squaring if two sine waves are available, one of which has twice the frequency of the other. By amplitude comparison of a cosine waveform with an input variable  $x$ , a time interval proportional to the inverse cosine of  $x$  may be defined. This time interval is then used for time selection of the double-frequency sine wave, and a voltage proportional to the amplitude of the double-frequency sine wave, or to  $2x^2 - 1$ , is generated.

<sup>1</sup> See Chap. 8; and Chap. 4, Vol. 21.

*Uses.*—The ground-range sweep for a radar cathode-ray-tube display requires a hyperbolic voltage waveform<sup>1</sup>

$$e = \alpha \sqrt{t^2 - h^2},$$

where  $\alpha$  and  $h$  are constants and  $t$  is time. One method of generating this waveform has been to take the square root of a delayed parabolic wave of the form  $t^2 - h^2$ .

Whereas the ground-range sweep application requires computation of a function within the repetition interval of the radar, other applications may require only a single value of the function.

Another use for quadratic amplifiers is in “triangle-solving” computers;<sup>2</sup> voltages are given which are proportional to two legs of a right triangle, and it is required to generate a voltage proportional to the hypotenuse. Methods other than quadratic amplifiers, however, are generally more suited to this application.<sup>3</sup>

Approximate square-root response for video amplifiers is sometimes desirable in radar applications.<sup>4</sup> In the synthesis of certain radar displays<sup>5</sup> quadratic functions are employed.

**19-7. Squaring Circuits.** *Direct Use of  $e_g$ - $i_p$  Characteristic.*—If the grid voltage  $e_g$  of a triode or pentode is plotted against the plate current  $i_p$  at constant plate voltage, the curve resembles that shown in Fig. 19-14. The characteristic curve may be expressed by the series<sup>6</sup>

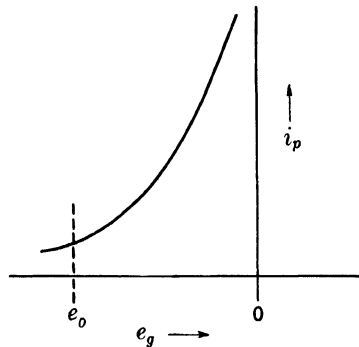


FIG. 19-14.—Typical  $i_p - e_g$  curve.

$$i_p = \alpha + \beta(e_g - e_0) + \gamma(e_g - e_0)^2 + \delta(e_g - e_0)^3 + \cdots, \quad (6)$$

where  $\alpha, \beta, \gamma, \dots$  are constants of the vacuum tube and  $e_0$  is a reference value from which the input is measured. A similar expression is possible for a triode with a constant plate load. The linear term  $\beta(e_g - e_0)$  may always be eliminated by proper choice of  $e_0$  (i.e., by a shift of the zero of

<sup>1</sup> See Sec. 8-5 to 8-7.

<sup>2</sup> The above example (hyperbola) may be considered as a special case of “triangle solution.”

<sup>3</sup> See Vol. 21, Chap. 6.

<sup>4</sup> This is to compensate for the quadratic response of a square-law detector.

<sup>5</sup> M. A. Starr, RL Report No. 678.

<sup>6</sup> See, for example, M.I.T. E.E. Staff, *Applied Electronics*, Wiley, New York, 1943, p. 672 ff.  $\beta = \frac{de_g}{di_p}$ ;  $\gamma = \frac{1}{2} \frac{d^2e_g}{di_p^2}$ ; etc.

the horizontal axis). If a vacuum tube could be found such that all constants beyond  $\gamma$  were zero, then its characteristic could be put in the form

$$i_p = \alpha + \gamma(e_g - e_0)^2. \quad (7)$$

This tube could be used as a squaring circuit: an output signal proportional to  $i_p$  could be obtained across a plate resistor,<sup>1</sup> this output signal being a constant plus a signal proportional to the square of the input signal (see Fig. 19-15). If the required range of operation of the squaring circuit for a given application is from  $e_{g1}$  to  $e_{g2}$ , where the range  $e_{g2} - e_{g1}$  is not large relative to  $e_{g1} - e_0$ , it is not difficult to find a tube that will come rather near satisfying Eq. (7) over the required range (see Fig. 19-16). This condition

is equivalent to saying that the region of operation shall not be near the vertex of the parabola. If this restriction cannot be imposed, as in the case where  $e_g - e_0$  must go to zero, no tubes are available that will meet the requirements.

The plate-current characteristics as a function of screen voltage for pentodes or tetrodes with fixed grid bias can, of course, be expressed by equations analogous to Eqs. (6) and (7).

If the characteristic of a vacuum tube cannot be expressed by Eq. (7) for the range of operation desired, but can be expressed by the equation

$$i_p = \alpha + \beta(e_g - e_0) + \gamma(e_g - e_0)^2, \quad (8)$$

methods can be devised which eliminate the contribution of the linear term and permit operation near  $e_g = e_0$  (i.e., near the vertex of the parabola). If the proper amplitude of input signal is subtracted from the plate signal, the resultant voltage will be, within a constant value,

<sup>1</sup> For a pentode the  $i_p$  vs.  $e_g$  curve is practically independent of  $e_p$  over a wide range of values for  $e_p$ ; for a triode Eq. (6) may be considered as determined with a given plate load.

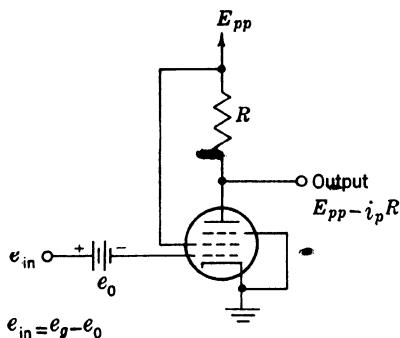


FIG. 19-15.—Simple squarer.

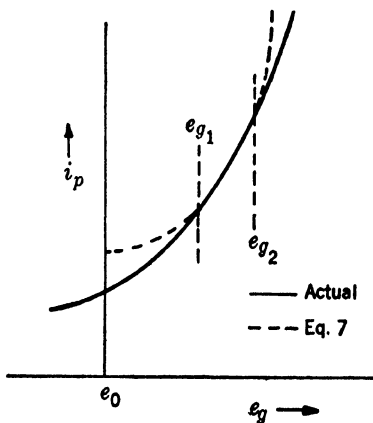


FIG. 19-16.—Approximation to ideal characteristic by actual curve.

proportional to the square of the input signal. Figure 19-17 illustrates a way of doing this, provided both  $R_2$  and  $R_3$  are much larger than  $R$ . The output impedance will of course be correspondingly higher.

*Suitable Tubes.*—Of the tube types available a few are much better suited to this application than the others. The desirable feature in a tube is that the  $i_p$  vs.  $e_g$  characteristic have a parabolic shape. Since  $g_m = \partial i_p / \partial e_g$ , it follows that  $g_m$  will be a linear function of  $e_g$  for those tubes that are of interest here. This relationship is one that may be detected reasonably well by inspection of  $g_m$  vs.  $e_g$  curves in a book of tube characteristics.<sup>1</sup> Figure 19-18 shows the curves for a 6B8 pentode. It is seen that  $g_m$  is approximately a linear function of  $e_g$  over the range

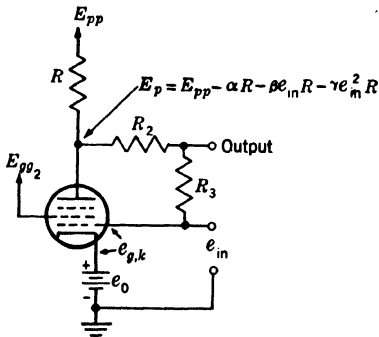


FIG. 19-17.—Linear compensation.

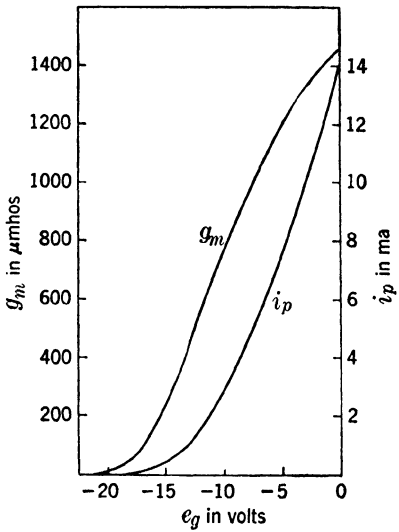


FIG. 19-18.—6B8 characteristics.

of  $e_g$  from  $-8$  to  $-15$  volts. Some recommended tube types are listed in Table 19-1.

TABLE 19-1

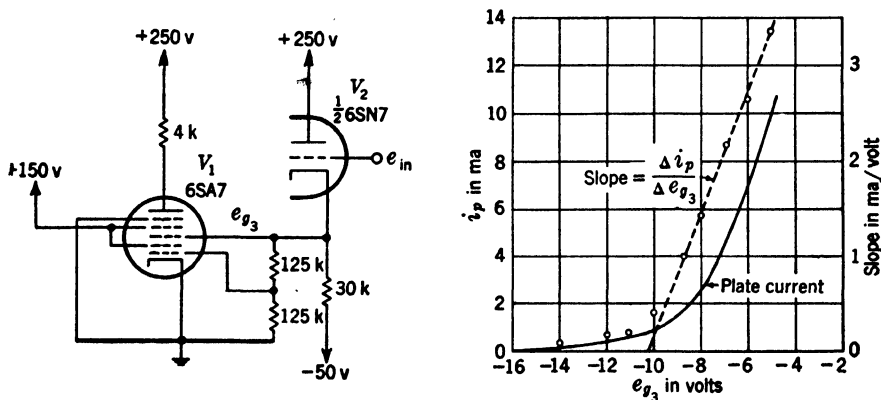
Type	Characteristic of interest	Remarks
6B8	$i_p$ vs. $e_g$	small linear contribution; 7 v useful grid swing
1S5	$i_p$ vs. $e_g$	small linear contribution; only 2 or 3 v useful grid swing
6SN7	$i_p$ vs. $e_g$	fair with 10 k plate resistor
6D6 } 6U7G }	$i_p$ vs. $e_{gk}$	40 v swing usable
38	$i_p$ vs. $e_g$	30 v swing usable
Sylvania 1205	$i_p$ vs. $e_g$	small linear contribution

<sup>1</sup> See, for example, RCA Tube Handbook HB-3.



In designing a squaring circuit of the simple type just discussed, one must consider that the shape and position with respect to the origin of the characteristic curves varies from one tube to another.<sup>1</sup> It is found that for the 6SN7, for example, both the shape and “cutoff” of the tubes vary considerably with the sample (see Chap. 3). For the 6B8, on the other hand, the shape is reasonably consistent, with the curve shifting within a range of about a volt along the  $e_g$  axis from tube to tube.

It should be pointed out that the plate voltage-plate current characteristics of some triodes (e.g., the 6SQ7) are approximately of the form  $i_p = \gamma(e_p - e_0)^2$  and thus can be used for squaring (see Sec. 19·8). Also for some pentodes<sup>2</sup>  $e_p$  is, except for a constant difference, almost



(a) Circuit diagram.  
 (b) Performance of circuit.  
 FIG. 19-19.—Multigrid squaring circuit. Circles are experimental points for the slope of  $i_p - e_{g3}$  curve.

proportional to the square of the plate current measured from an appropriate reference value.

**Multigrid Squarer.**—In Sec. 19·3 the multigrid tube as a multiplier is discussed. To operate such a tube as a squarer places similar but much less stringent restrictions on the characteristic. If the  $g_m$  of the tube is varied in proportion to the change in  $e_{g1}$ , if the change in plate current is proportional to  $\Delta e_{g1}$ , times  $g_m$ , and if  $e_{g1}$  and  $e_{g3}$  are proportional, then  $\Delta i_p = k \Delta e_{g1}^2$ , when  $k$  is a constant.

Tube types that have been found most suitable for this application are the 6SA7, 6AS6, and 7A8. Figure 19·19 demonstrates a typical circuit and a curve showing the accuracy attained in that case. The derivative of the output, which should be a linear function, is compared with a straight line.

<sup>1</sup> The effects of variation of tube characteristics are discussed in Vol. 18, Chap. 11, “D-c Amplifiers.”

<sup>2</sup> For example, 6B8, 33, 6Y6G.

*Push-pull Squaring Circuit.*—A principle that has been used in electronic wattmeters<sup>1</sup> has been successfully applied to a squaring circuit.

If in Fig. 19-20 the input voltage to tube  $V_1$  is defined by  $e_{g1} - e_0 = e_{in}$ , Eq. (6) may be rewritten

$$i_{p1} = \alpha + \beta e_{in} + \gamma e_{in}^2 + \delta e_{in}^3 + \epsilon e_{in}^4 \cdots \quad (9)$$

If now  $e_{g2} - e_0$  is made equal to  $-e_{in}$ —that is, if the grid of  $V_2$  is driven from the reference voltage,  $e_0$ , by an amount equal in magnitude but of opposite sign to the signal on the grid of  $V_1$ —we have

$$i_{p2} = \alpha - \beta e_{in} + \gamma e_{in}^2 - \delta e_{in}^3 + \epsilon e_{in}^4 - \cdots \quad (10)$$

If the plate currents of  $V_1$  and  $V_2$  flow through a common plate resistor  $R$ , as in Fig. 19-18, the common plate voltage  $e_p$  will be

$$e_p = E_{pp} - iR = E_{pp} - 2R(\alpha + \gamma e_{in}^2 + \epsilon e_{in}^4 \cdots). \quad (11)$$

It is assumed in Eqs. (9), (10), and (11) that the plate voltage does not materially affect  $i_p$ ; this will be true if  $V_1$  and  $V_2$  are pentodes, if  $R$  is very small, or if the constants are determined for the tubes operating together (Fig. 19-18). In the last case, even when there is interaction, it can be shown from symmetry considerations that the output will be a function containing only even powers of  $e_{in}$ .

If a tube is used for which  $\epsilon$  and all succeeding coefficients of even power terms are small enough to be ignored, Eq. (11) gives for the a-c output voltage

$$\Delta e_p = -2R\gamma e_{in}^2, \quad (12)$$

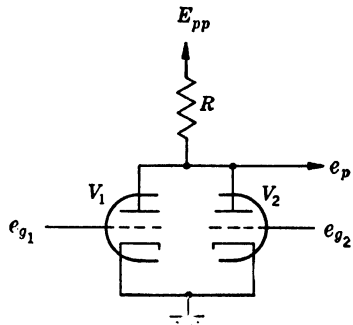


FIG. 19-20.—Push-pull squaring circuit.

which shows that the change in output voltage varies as the square of the input signal. The tube types listed in Table 19-1 are those best suited for use with this type of circuit.

It is to be noted that the present circuit, as contrasted to those discussed above, will give an output signal proportional to the square of an input signal of either sign, the circuit of Fig. 19-17 being the only other mentioned so far which has this property.

D-c tests were made on pairs of 6B8's with the suppressors tied to the cathodes, with 105 volts on the screens, and with a 300-volt plate

<sup>1</sup> H. G. Reich, *Theory and Application of Electron Tubes*, McGraw-Hill, New York, 1939, pp. 582-583.

supply. With 11.1 k as plate resistor, for a typical 6B8 it was found<sup>1</sup> that

$$i_p = 0.265 + 0.101\Delta e_g + 0.051(\Delta e_g)^2 \quad (13)$$

where  $\Delta e_g$  is measured in volts and  $i_p$  in milliamperes. The reference potential  $e_0$  for this tube was  $-12.6$  volts. The absence of interaction was measured as follows: the static characteristic for another 6B8 was

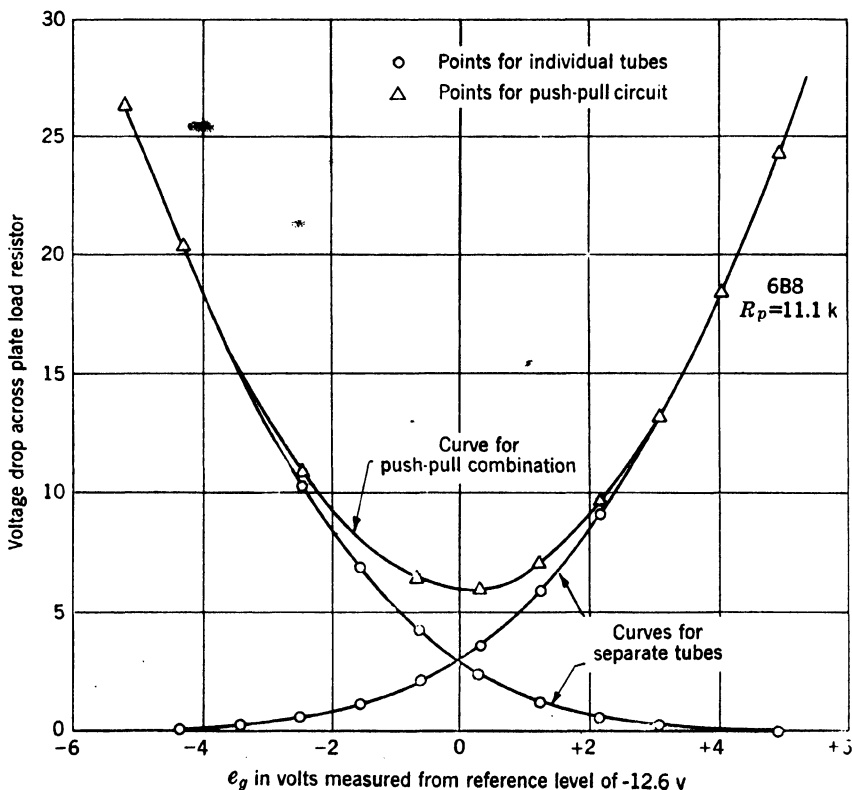


FIG. 19.21.—Output vs. input for push-pull squaring circuit.

determined; the expected output of the pair, connected as in Fig. 19.20 and driven push-pull, was calculated. Actual measurements on that pair connected in that way were made. Figure 19.21 shows that the calculated and observed results are in excellent agreement. This means that the plate currents add with little interaction. Over a range of  $\pm 5$  volts for the input, the output varied parabolically to within  $\frac{1}{2}$  per cent of maximum output.

<sup>1</sup> This was done by fitting the measured characteristic curve at three points. The term in  $(\Delta e_g)^4$  was unfortunately omitted.



between the plate and the screen effectively decreases the impedance seen at the plate. A screen battery might also be used to reduce the effect.

**19-8. Square-root-extracting Circuits.** *Direct Dependence on Tube Characteristics.*—One method of constructing an amplifier whose output voltage is proportional to the square root of the input voltage makes use of the fact that for some pentodes the plate current varies roughly as the square root of the plate voltage. Such a circuit is shown in Fig. 19-23, where  $V_2$  is the pentode the  $i_p$  vs.  $e_p$  characteristic of which is being relied on, and  $V_1$  is a cathode follower that serves to make  $e_{p1}$  approximately equal to  $e_{in}$ . If  $i_p$  for  $V_2$  is proportional to  $\sqrt{e_{p1}}$ , then the

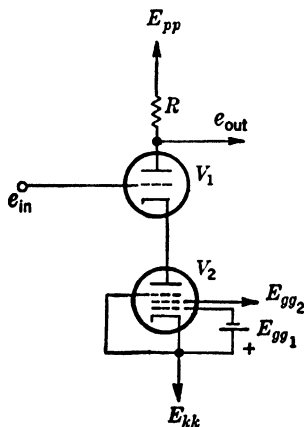


FIG. 19-23.— $e_p$  -  $i_p$  square-root-extracting circuit.

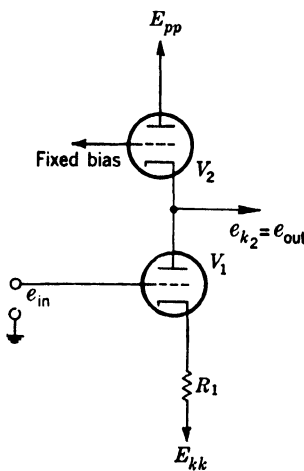


FIG. 19-24.— $e_g$  -  $i_p$  simple square-root-extracting circuit.

cathode current in  $V_1$  will also be proportional. Actually, however, since the best  $e_p$ - $i_p$  curves obey the ideal square-root relationship over only a small range, this method is of only very limited usefulness. For example, the  $e_p$ - $i_p$  curve of the 6L7 at  $e_g = -5$ , from 0 to 50 volts input, fits a parabola to within 10 per cent of maximum output. Additional errors are caused by variation of tube characteristics.

Another equally direct method makes use of the fact that for some tubes the change in plate current varies approximately as the square of the change in grid voltage [see Eq. (7)]. If current is made the independent variable and if voltage is made the output or dependent variable, a square root is produced. In Fig. 19-24 the tube having the parabolic characteristic is  $V_2$ . The plate current of  $V_2$  is controlled by the constant-current tube  $V_1$  so as to be proportional to  $e_{in}$ . The grid-cathode drop of  $V_2$  assumes the value consistent with this value of plate

current. Since  $e_{g_2}$  is fixed,  $e_{k_2}$  is the desired output signal. Inasmuch as for all tubes tried the contribution to plate current of the term that is linear in  $e_g$  [see Eqs. (6), (7), and (8)] is not negligible, this amplifier has an output signal only very roughly approximating the square root of the input signal.

*Methods Employing Cancellation of Odd-power Terms.*—An elaboration of the method just discussed, which is capable of much greater precision, consists of replacing the quadratic element ( $V_2$  in Fig. 19-24) by a push-pull squaring element of the type discussed under "Squaring Circuits" (see Fig. 19-25). The greatest drawbacks to this circuit are the difficulty

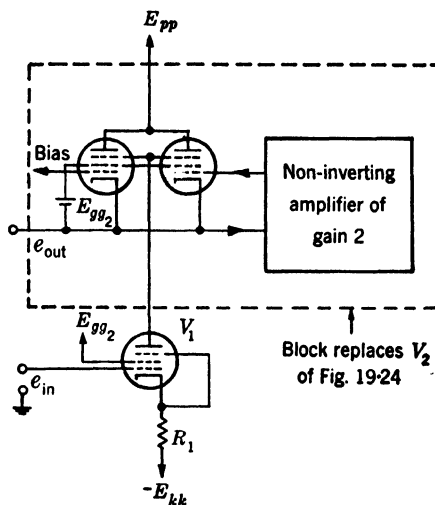


FIG. 19-25.—Square-root-extracting circuit with push-pull quadratic element.

in maintaining the proper grid biases for the squaring pair and the necessity of a noninverting amplifier of gain 2 in order to achieve the push-pull operation.

The inadequacy of the simple circuit shown in Fig. 19-24 led to the development of a circuit that can make use of tubes for which Eq. (8) is true—that is, instead of requiring that  $\Delta i_p$  be proportional to the square of  $\Delta e_g$ , it requires only that

$$\Delta i_p = \beta(e_g - e_0) + \gamma(e_g - e_0)^2. \quad (14)$$

This will permit more freedom in the choice of  $e_0$ .

The discussion will refer to the circuit shown in Fig. 19-26. Rewriting Eq. (8) in terms of  $\Delta e_{k_2}$ , the grid-cathode voltage of  $V_2$ , the plate current is

$$\Delta i_{p_1} = \beta(-\Delta e_{k_2}) + \gamma(-\Delta e_{k_2})^2. \quad (15)$$

The voltage at the grid of  $V_1$  is given by

$$\Delta e_{g1} = e_{in} + b(-\Delta e_{k2}), \quad (16)$$

and for the cathode follower  $V_1$

$$\Delta i_{p1} = \Delta i_{p2} = \frac{\Delta e_{g1}}{R}, \text{ ignoring screen currents.}$$

Substitution of Eqs. (15) and (16) into this last relationship yields

$$R\Delta i_{p2} = -R\beta\Delta e_{k2} + R\gamma(\Delta e_{k2})^2 = e_{in} - b\Delta e_{k2}. \quad (17)$$

If now the attenuation factor  $b$  is chosen to be equal to  $R\beta$ , Eq. (17) reduces to

$$e_{(out)} = \Delta e_{k2} = \sqrt{\frac{e_{in}}{R\gamma}},$$

which shows that the circuit response is of the desired form.

Figure 19-27 shows a practical circuit embodying the principle just discussed. It is designed to accept waveforms of duration of about

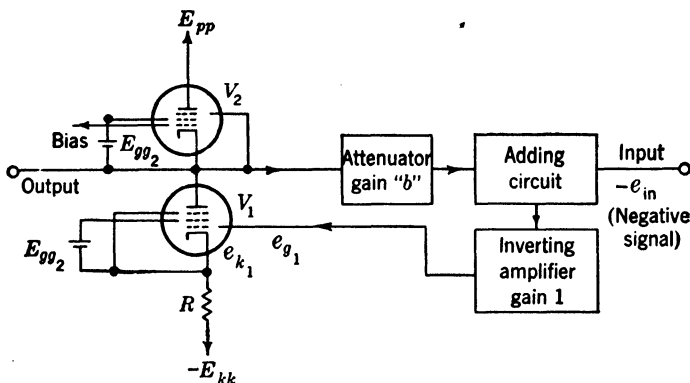


FIG. 19-26.—Square-root circuit employing as quadratic element a tube for which  $\Delta i_p = \beta e_{in} + \gamma e_{in}^2$ .

100  $\mu$ sec. The output for a 40-volt input signal is about 40 volts in amplitude. As an example, if the input is a parabolic waveform ( $e_{in} = k_1 t^2$ ) of 100- $\mu$ sec duration and 40-volts amplitude, the output will be a sawtooth waveform ( $e_{out} = k_2 t$ ) of the same duration and peak amplitude.

The cathode follower  $V_2$  has its grid bias established by  $R_4$ , the diode insuring that the effective bias is independent of input waveform (see Chap. 3 for a discussion of d-c level restoration). The quadratic element is the 6D6 ( $V_1$ ), the screen voltage-plate current characteristic of which is approximately expressed by Eq. (15) for a fixed grid bias. The cathode follower  $V_4$  affords a low-impedance output circuit and supplies the grid bias for  $V_1$ . The high-frequency response of the circuit is improved by

using the cathode follower, which isolates the cathode of  $V_1$  from other stray capacitances.

Tube  $V_3$  serves as the adding circuit discussed in connection with Fig. 19-26. The resistance  $R_3$  is adjusted to secure the proper bias for

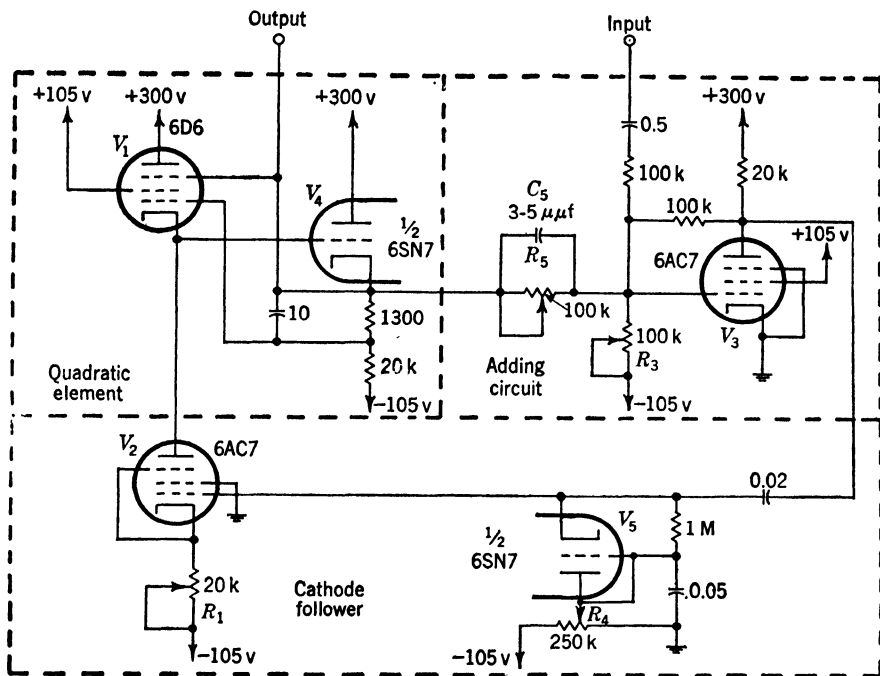


FIG. 19-27.—Square-root-extracting circuit.

the adding tube. The variable input resistor  $R_5$  serves as the attenuator shown in Fig. 19-26. The capacitance  $C_5$  can be shown to compensate partially for the stray capacitance from the cathode of  $V_1$  to ground.

Another method of designing a square-root-extracting circuit consists of using feedback in such a way as to force the output of a squaring circuit to be equal to the signal whose square root is sought—the input to the squaring circuit then being the desired output signal. Consider the block diagram of such a circuit shown in Fig. 19-28. Assume a perfect squaring circuit that gives an output signal  $-ax^2$  with an input signal  $x$ , where  $a$  is a constant. Let the input signal, the square root of

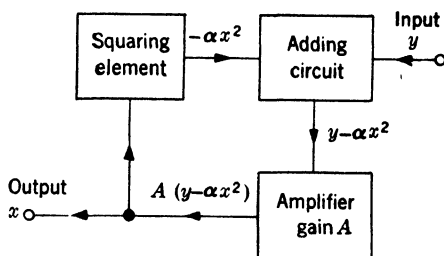


FIG. 19-28.—Block diagram of feedback square-root-extracting circuit.



which is desired, be  $y$ . An adding circuit is employed to give a signal equal to the difference between the magnitude of the input,  $y$ , and the output  $ax^2$  of the squaring element. This difference, amplified by a factor  $A$ , is supplied to the input terminal of the squaring circuit, but this input signal is also  $x$ . The amplifier output,  $x$ , is then determined by the condition that

$$x = A(y - ax^2). \quad (19)$$

By rewriting in the form

$$y = ax^2 + \frac{x}{A}, \quad (20)$$

it is readily seen that for sufficiently large gain,  $A$ , the term  $x/A$  can be neglected, giving for the approximate output

$$x = \sqrt{\frac{y}{a}} \quad (21)$$

as desired.

More exactly, Eq. (20) yields

$$x = -\frac{1}{2aA} + \sqrt{\frac{1}{4a^2A^2} + \frac{y}{a}}. \quad (22)$$

If the input waveform is parabolic ( $y = bt^2$ ), the output will be approximately linear. For relatively large values of  $t$  the actual output is nearly

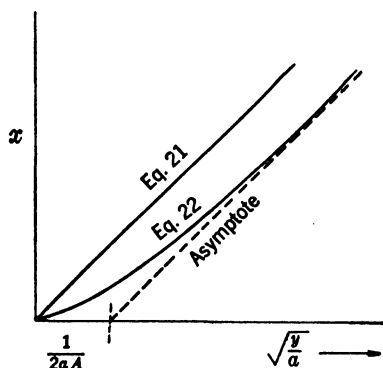


FIG. 19-29.—Output of feedback square-root circuit.

a straight line parallel to the ideal output function (Fig. 19-29); the output waveform is effectively delayed in time by a small amount.

A practical circuit is shown in Fig. 19-30. The 6B8's,  $V_1$  and  $V_2$ , constitute the quadratic element (Sec. 19-7), which is driven push-pull from the plates of the differential amplifier  $V_3$  and  $V_4$ . The cathode resistance  $R_1$  is chosen so that the amplifier is not driven beyond the range over which it is nearly linear. The diode return potentials  $-E_1$

and  $-E_2$  are adjustable around the level of  $-12$  volts. The circuit was generally operated with a negative parabolic waveform ( $e = -kt^2$ ) of 30-volt peak amplitude and  $100\mu$  sec duration as the input. Optimum operation under these conditions is achieved for  $-E_{cc}$  within a volt or two of ground, with  $R_3$  between 5 and 15 k, and with  $R_2 = 10$  k. If the loop gain is made too great (e.g., if  $R_3$  exceeds 25 k), the circuit oscillates.

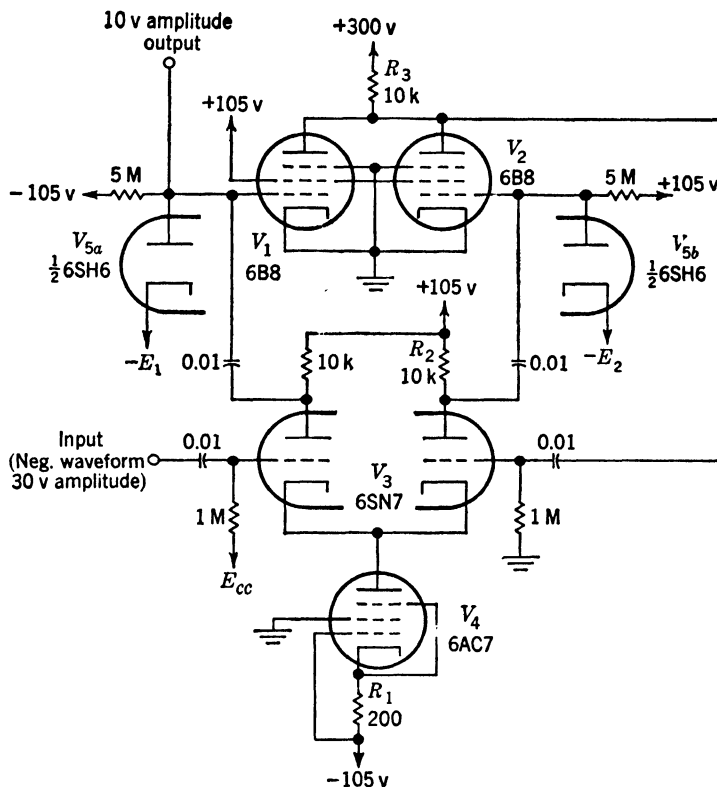


FIG. 19-30.—Feedback push-pull square-root circuit.

The designer should be cautioned that the establishment of the d-c level of the input waveform to a square-root-extracting circuit is very important. At the start of the waveform an error of 1 per cent of the peak amplitude will result in a 10 per cent error in the output ( $\sqrt{1/100} = 1/10$ ).

**19-9. Other Quadratic Elements. Magnetron.**—Consider a simple magnetron consisting of a long straight wire emitter surrounded by a coaxial cylindrical plate, both placed in a uniform magnetic field directed along the electrode (Fig. 19-31). If the current as a function of the plate potential for a given field  $H_1$  is measured, it is found that the current increases from almost zero to a saturation value for a small increase in

plate voltage, the higher the field strength the higher being this critical or "cutoff" voltage (see Fig. 19-32). It is found that the relationship between the magnetic field strength and the plate potential at "cutoff" is expressed by an equation of the form<sup>1</sup>

$$V_{co} = kH^2. \quad (23)$$

Since the field is proportional to the current in a solenoidal coil producing the field, the magnetron together with the solenoid can form the nucleus

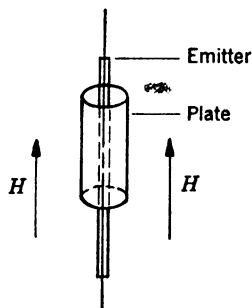


FIG. 19-31.—Magnetron.

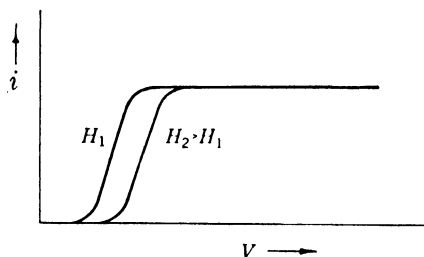
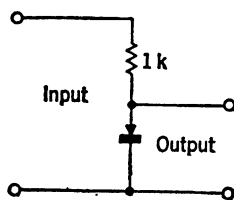


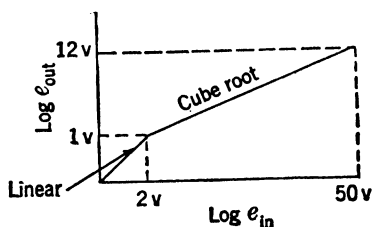
FIG. 19-32.—Magnetron current vs. plate potential.

of a quadratic circuit. The chief difficulty with such a device is encountered in trying to secure a magnetron in which the  $i$  vs.  $V$  curve (Fig. 19-32) is steep enough and for which the cutoff is complete enough. It is difficult also to produce rapid changes in the magnetic field  $H$ .

*Crystals.*—The nonlinearity of the voltage-current curve for crystals may be utilized in various ways.<sup>2</sup> For example, the circuit shown in



(a) Schematic circuit.



(b) Idealized characteristic.

FIG. 19-33.—Crystal circuit with idealized nonlinear characteristic.

Fig. 19-33a may give roughly a square-root or cube-root response, the exact nature of the response depending on the crystal used. Figure 19-33b shows the response of the circuit in Fig. 19-33a for a 1N21B

<sup>1</sup> See, for example, G. P. Harnwell, *Principles of Electricity and Electromagnetism*, McGraw-Hill, New York, 1938, p. 285; J. G. Brainerd et al., *Ultra-High-Frequency Techniques*, Van Nostrand, New York, 1942, p. 312.

<sup>2</sup> See Chap. 11; also Sec. 19-4, "Logarithmic Devices."

crystal.<sup>1</sup> This circuit has a pass band extending up to about 1 Mc/sec.

Thermistors, varistors, diodes, photoelectric cells, and other devices involving nonlinear relationships between the parameters have been used as the basis of circuits designed to give various nonlinear responses (Chap. 3).

**19-10. Testing of Circuits Producing Squares and Square Roots.**—For direct-coupled circuits designed for operation with slowly varying input signals, quadratic circuits may be tested simply by measuring with d-c instruments the output voltages corresponding to a series of input voltages. By plotting the square of one variable against the other variable or by plotting the log of one against the log of the other, the quadratic nature or departure therefrom may be ascertained.

In the case of circuits designed for rapidly varying input signals, however, this procedure is not necessarily applicable. Methods are available (see Chap. 20) for accurately measuring the input and output waveforms. For some applications and in most preliminary design work, the more rapid testing methods of Chap. 20 are useful.

<sup>1</sup> For characteristic see Vol. 16, Chap. 2.

## CHAPTER 20

### OSCILLOSCOPE TECHNIQUES IN WAVEFORM MEASUREMENT

BY BRITTON CHANCE

**20-1. Introduction.**—The testing and calibration of the circuits described in the previous chapters require apparatus for the viewing and measurement of the waveform. The properties of the cathode-ray oscilloscope are of outstanding importance in the study of these circuits. The following material will attempt to summarize oscilloscope techniques of proved usefulness or extreme novelty that have been applied in the course of the development of the circuits described in this book. In doing so, the material of this chapter anticipates the content of Chap. 7, Vol. 20, and Vol. 22 of the Radiation Laboratory Series. But in nearly all cases the treatment of the subject material differs greatly. Furthermore, the description of complete oscilloscopes is deferred to the appropriate chapters in Vol. 21, Part IV.

**20-2. Oscilloscopes and Meters.**—The two-coordinate intensity-modulated display, the good frequency response, and the high input impedance of the electrostatic cathode-ray oscilloscope make it extremely versatile for the display and measurement of a large amount of information. On the other hand, it is insensitive, inaccurate for direct measurement, fragile, dangerous in view of the high voltages employed, expensive, and bulky. Conventional meters when used with vacuum-tube input circuits have extremely high input impedance, are sensitive, accurate, relatively rugged, and compact. The frequency response of ordinary meters is low, and they do not permit the observation or measurement of more than one quantity at a time. Furthermore, their operation is adversely affected by the extremely low and variable duty ratios encountered in pulse techniques, polarity effects, and confusion due to lack of time selectivity. The inadequate frequency response and the resulting lack of time selectivity make the ordinary meter unsuitable for measurements of rapid and complex waveforms. If external time-selective circuits are added to a vacuum-tube metering circuit, however, the equipment becomes nearly as complex as the oscilloscope. Even then metering circuits lack the most useful attribute of the oscilloscope—its apparently simultaneous display of many waveforms. Further discussion of these devices will therefore be omitted. However, their usefulness in standardized test procedures based on meters should not be belittled.

**20-3. Amplitude Measurements.** *Direct.*—The amplitude of a rectangular waveform may be measured by connecting the waveform directly to the vertical plate of an oscilloscope. The deflection sensitivity of the 5-in. tube, although roughly twice that of the 3-in. tube, is only between 60 and 70 volts/in. for type 5CP1 operating with an accelerating voltage of 2 kv (for a single plate). Although the sensitivity may be increased by reducing the accelerating voltage, the consequent loss in focus and intensity greatly offsets this advantage, and therefore wideband amplification of the input waveform is employed where necessary.

The input capacitance of the deflecting electrode brought out through the base is approximately  $7\ \mu\text{f}$ . Those tubes having the deflecting plates brought out directly through the side wall of the tube (5JP1) permit a reduction of this value to  $3\ \mu\text{f}$ .

The electron current to the deflection plate may limit the permissible value of the source resistance for low-frequency signals. Usual specifications on this characteristic indicate that a 10-megohm resistance in series with one deflecting plate should give less than a 10-mm deflection. A conversion of this specification to equivalent current gives approximately  $2\ \mu\text{a}$ , a factor that must be taken into account in narrow-band amplifiers employing large plate resistors.

In the absence of stray magnetic fields, the linearity of the deflection characteristic of an oscilloscope can usually be relied upon to be somewhat better than 1 per cent. A much more significant error is likely to be the variation of deflection sensitivity with accelerating voltage or the variation of the zero point of amplitude measurement due to variations of the spot-positioning voltages. The drift of the spot with time or with mechanical vibrations is not known, but it is usually essential to check the zero point of amplitude measurements every time the oscilloscope is used.

Often the amplitude of a particular member of a pulse train is required, and in this case a linear time base is applied to the horizontal axis of the oscilloscope in order to give time selectivity as shown in Fig. 20-1. This figure clearly demonstrates that the amplitude of the separate parts of the waveform may be easily determined. This measurement represents a distinct improvement compared with the operation of the vacuum-tube voltmeter which would, of course, give only the amplitude of the third pulse if it were peak-reading or the average amplitude of all four if it were average-reading. In the cathode-ray-tube display variations in duty ratio affect only the intensity of the trace; polarity is immediately indicated; and confusion with other parts of the waveform is eliminated as indicated in the figure.

*Substitution.*—The amplitudes of the pulses of Fig. 20-1 may be measured by substituting a steady potential that has a known value and

is adjusted to be equal to the amplitude of any particular pulse to be measured—for example, the first. Also the amplitudes of the other pulses may be determined directly in terms of the deflection sensitivity calibrated in this manner.

*Subtraction.*—A more convenient method is indicated in Fig. 20-2,

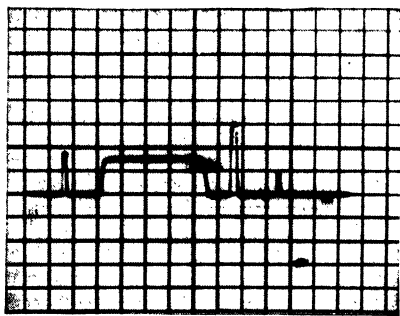


Fig. 20-1.—Oscilloscope display of waveform amplitude.

where a voltage of polarity opposite to that to be measured is connected to the opposite deflecting plate and adjusted until the amplitude of the input signal is returned to the base line (the position of the trace in the absence of signal). The accuracy of this procedure is, of course, independent of the deflection sensitivity of the cathode-ray tube and depends upon the equality of the sensitivity of the two plates, the linearity of the potentiometer, and the accuracy of

the voltmeter. These three factors are stable and accurate.

*Amplitude Selection.*—Instead of depending upon subtraction between the two plates of the oscilloscope, amplitude selection may be used and an example is shown in Fig. 20-3. The particular configuration is

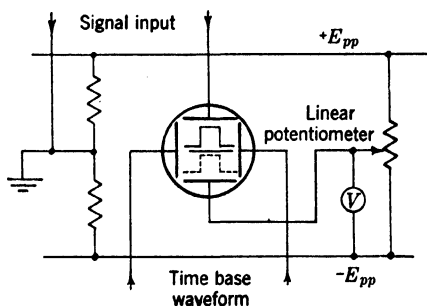


Fig. 20-2.—Amplitude measurement by subtraction.

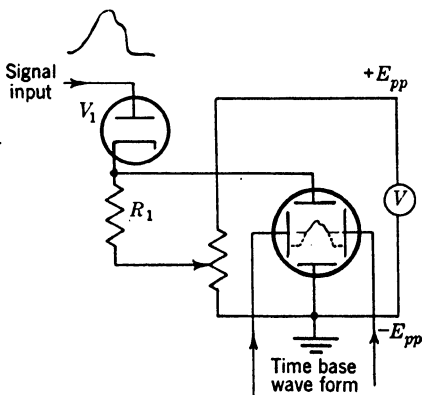


Fig. 20-3.—Amplitude measurement by selection.

operative for positive signals only. The bias of the cathode of  $V_1$  is adjusted so that the peak of the input waveform is selected and is displayed on the oscilloscope. The point at which the waveform disappears from the display indicates that the potentiometer has been moved through an amount corresponding to the peak voltage of the desired waveform.

The potentiometer should, of course, be of low impedance compared with  $R_1$ . Amplitude selection with thermionic diodes is accurate only for signals of the order of 200 or 300 volts since errors of  $\frac{1}{2}$  volt may be expected. Amplification of the waveforms to a high level is, therefore, desirable. A reversal of the diode connections will give operation suitable for negative signals.

*Amplitude Discrimination.*—If it is desired to indicate the equality of two voltages, they may be directly connected to the plates of the oscilloscope and subtraction will be accomplished; equality of the voltages is indicated by the fact that no displacement of the spot occurs on their connection. Greater sensitivity may be obtained by employing those amplitude discriminators described in Sec. 9·22 that have appreciable gain. Care must then be taken, however, lest the variation of the level of the two signals alter the balance point of the amplitude discriminator. The plates of the cathode-ray tube are insensitive to level as far as balance is concerned, but considerable defocusing will occur if the level of one pair of plates deviates much from the potential of the other pair or of the third anode.

Several examples of the use of the cathode-ray tube for subtraction of two waveforms have been indicated in Chap. 11, where the differential output of modulators is displayed on the screen. A typical example is shown in Fig. 11·2.

*Summary.*—For signals producing an appreciable deflection on the oscilloscope, there is little to choose between subtraction and selection. Smaller signals require amplification previous to subtraction or selection. But amplification may follow the latter process. This method gives a much more sensitive indication of equality of the two voltages, and differences of a few millivolts may be detected. Under these conditions, the stability of the amplitude selector and of the reference voltages may become the limiting factor.

**20·4. Time Measurements.** *Direct Displays.*—If a triangular waveform is applied to the horizontal plates of an oscilloscope, the duration or spacing of portions of a waveform connected to the vertical plates may be obtained as indicated in Fig. 20·4. The deflection sensitivity along the horizontal axis may now be represented in time units per division, and time-delay measurements between any two points may be made directly. The deflection sensitivity in time units may be computed

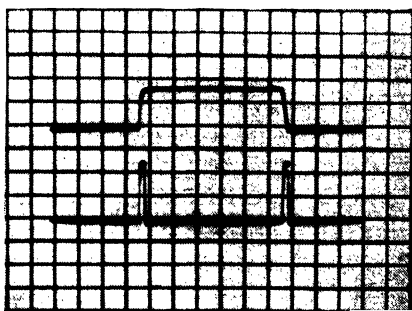


FIG. 20·4.—Measurement of waveform duration by display on a linear time base.



from the known slope of the waveform (volts/ $\mu$ sec) and the deflection sensitivity of the oscilloscope in volts per division. A subtraction method similar to that shown in Fig. 20-2 may be employed to return the rise or fall of the pulse to some reference line on the vertical scale; in this way the effects of variation of deflection sensitivity are avoided. But the other important variable in this case is the slope of the timing waveform, and this may be calibrated by the method described in the next paragraph.

*Substitution of Fixed Pulses.*—A train of fixed pulses of known period may be substituted for or superimposed upon the unknown waveform, and its duration may be obtained by interpolation as indicated in Fig. 20-7.

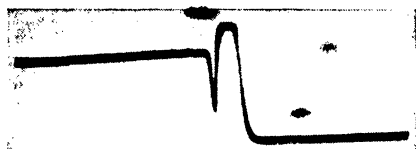


FIG. 20-5.—Measurement of the duration of a rectangular wave by setting a movable mark to the trailing edge.

number of methods for accurately setting the coincidence of marker and pulse is given in Vol. 20, Chap. 7.

*Time Selection and Discrimination.*—Instead of matching the overlap of the pulse from a time modulator and the unknown waveform upon the cathode-ray tube, these two waveforms may be connected to a time selector (Sec. 10-3) and the outputs displayed upon the cathode-ray tube. Similarly, the inputs may be connected to a time discriminator (Sec. 14-5), and the output of the discriminator connected to the vertical plates of the oscilloscope. The first method gives no appreciable gain in accuracy as compared with direct display. The output of the second is more often indicated on a meter and is, of course, more sensitive, provided adequate amplification follows the discriminator.

*Expanded Sweeps.*—Occasionally greater accuracy may be obtained through expansion of the time base. If, for example, the waveform to be measured is initiated by one of a series of crystal-controlled pulses, another member of this pulse train may be selected just previous to the termination of the unknown waveform and made to initiate the display waveform. The number of pulses intervening between the start of the unknown waveform and the start of the display waveform is counted, perhaps on a cathode-ray-tube display, the time increment from the start of the expanded display to the termination of the unknown waveform is added, and a highly accurate total value of the time interval is obtained (see Sec. 13-3; also Vol. 20, Sec. 7-24).

Much more convenient than the selection of one of a member of a train of fixed pulses is the employment of a high-frequency circular sweep.

The unknown waveform is initiated in synchronism with the circular sweep, and the terminal portion is displayed by means of a radial-deflection cathode-ray tube (3DP1). The integral number of oscillations to the termination of the input waveform is determined by direct display on a linear time base or by means of a crude time-modulation circuit employed to intensify the particular cycle of the circular sweep on which the termination of the unknown waveform is displayed. The remainder of the time delay may be obtained by direct interpolation on the face of a cathode-ray tube that is provided with a circular scale. Circular sweeps of a variety of frequencies may be obtained by the methods of Chaps. 4 and 15, of Vol. 20, Chap. 7, of Vol. 21, Part IV, and Vol. 22. Lower-frequency circular sweeps may be employed to obtain the integral value of oscillations of a sweep of higher frequency. The advantages of the circular-sweep system are the accuracy of the scale—roughly 0.5 per cent, the independence of the scale factor from changes of accelerating voltage, and the ease with which the sweep may be generated. Although the deflection sensitivity of type 3DP1 is extremely low—roughly 100 volts for  $\frac{1}{4}$  in., the input capacitance is only  $2\ \mu\text{f}$ . The calibration of the circular sweep is much simpler than that of the linear sweep, and simply adjusting the pattern to appear circular gives a display linear to 0.5 per cent. It is, however, necessary to ensure that the display and scale are concentric.

The deflection sensitivity of the central electrode is unfortunately a function of circular diameter, and, for a given circle diameter, a nonlinear function of deflecting voltage. The display is therefore of little use for amplitude measurement, but is wholly satisfactory for time measurements. A typical display is shown in Fig. 20-13.

*Pulse-sharpening Circuits.*—For the precise measurement of a slowly varying waveform, it is essential to obtain sharply rising pulses marking its initiation and termination in order to obtain accurate measurements on expanded sweeps. Practical pulse-sharpening circuits are given in Sec. 9-14, for example, the Multiar circuit. The influence of pulse-rise time on the accuracy of measurement is described in Vol. 20, Sec. 7-8. Usually a timing accuracy of one twentieth of the rise time of the pulse is obtainable.

**20-5. Waveform Measurements.**—The linear, exponential, or hyperbolic character of voltage or current waveforms may be determined by oscilloscope displays.

*Direct Displays.*—A well-known method for the determination of waveforms involves direct display against a linear time base as shown in Fig. 20-6. The accuracy of the resultant curve depends not only upon the linearity of deflection but also upon the linearity of the time base. At best the accuracy of this method does not exceed 2 per cent. If the unknown waveform has a shape other than linear—for example, para-

bolic—it may be compared to a suitable overlay having this characteristic. In both cases, parallax between the trace and the scale must be avoided. Scales applied by direct inking or by optical projection are most satisfactory.

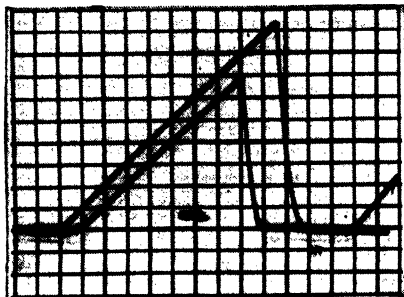


FIG. 20-6.—Waveform determination by display on a linear time base.

*Fixed Time Indices.*—If, for example, the unknown waveform is applied directly to the horizontal plates of an oscilloscope, and if timing indices of a fixed spacing are applied to the vertical plates, a constant spacing will verify linearity of the waveform as shown in Fig. 20-7a. Figures 20-7b and 20-7c indicate that other waveforms may be studied in this manner but with considerably more difficulty. This method is not,

however, independent of the characteristics of the cathode-ray tube since the deflection linearity of the horizontal axis is still a determining factor. In fact, this method is often used as a means for determining linearity of deflection in cathode-ray tubes (see Vol. 22).

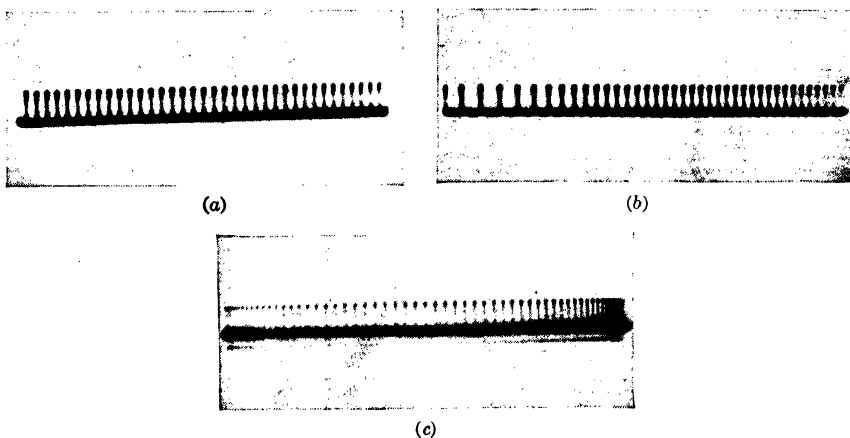


FIG. 20-7.—Waveform determination by display on a linear time base and superposition of fixed time markers; in (a) on a triangular waveform, in (b) on a hyperbolic waveform, and in (c) on a sinusoidal waveform. In (a) and (b) the spacing of the pulses is approximately  $2.4 \mu\text{sec}$ . In (c) the spacing of the pulses is  $12 \mu\text{sec}$ .

*Differentiation.*—A simple and straightforward method<sup>1</sup> of determining the character of triangular and parabolic waveforms depends upon differentiation once in the first case and twice in the second case to obtain

<sup>1</sup> Unfortunately, the accuracy of the differentiators used for this purpose is rarely greater than that of the integrators used in waveform generation.

a rectangular waveform of constant amplitude if the waveforms are in accordance with the required functions. Single differentiation of a triangular and a parabolic waveform is shown in Figs. 20-8 and 20-9. A differentiating circuit of good transient response with sufficient gain is a

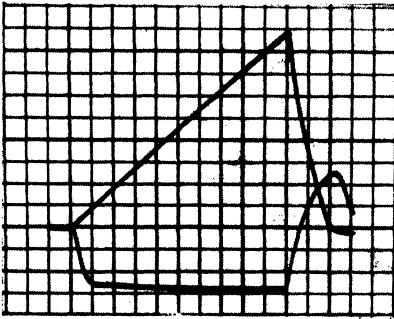


FIG. 20-8.—Differentiation of a triangular waveform to obtain a rectangular waveform. The constancy of amplitude of the rectangular waveform displayed in the lower trace is indicative of the linearity of the triangular waveform. The sweep duration is approximately 120  $\mu$ sec.

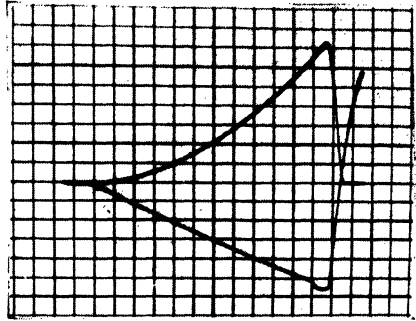


FIG. 20-9.—Differentiation of a parabolic waveform to obtain a linear waveform. The linear waveform may be differentiated again to produce a rectangle as in Fig. 20-8.

sensitive indicator of the waveform. In addition to this, the deflection of the oscilloscope may be calibrated in terms of speed of the waveforms in volts/ $\mu$ sec, provided the values of resistance and capacitance employed in differentiation are known. Such differentiation devices are described in Sec. 18-7. Alternatively, a triangular waveform of known speed may be employed for calibration. Although this method of waveform measurement is more sensitive than that employing fixed pulses described in the preceding section, it has not been used so extensively, and it is not so precise as the methods that follow.

**Amplitude Comparison.**—Precision methods of waveform determination depend upon amplitude comparison and time demodulation (see Sec. 9-8) as indicated in Fig. 20-10. The pulse output of the amplitude comparator occurs at the moment of equality of its reference voltage with the unknown waveform. The time delay with respect to the initiation of the waveform may be determined by synchronizing it with any accurate time-measuring system—for example, a circular-sweep

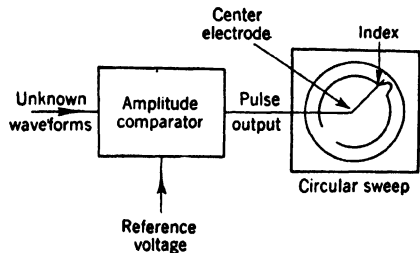


FIG. 20-10.—Waveform determination by amplitude comparison and time demodulation. The unknown waveform must be synchronized with the circular sweep.

display. The readings of the circular-sweep oscilloscope, which are then plotted against the reference voltage, give an exact reproduction of the input waveform. The accuracy of a circular-sweep timing system is sufficient for these purposes (see Vol. 20, Sec. 7-18), and the over-all accuracy of this method of measurement may be easily 0.01 per cent.

**Time Comparison.**—Alternatively, the voltage of the unknown waveform corresponding to a known time may be determined as shown in Fig. 20-11 (see Sec. 14-5). In this case the unknown waveform is again synchronized with an accurate time-modulation system. The pulse of accurately known time delay with respect to the initiation of the unknown

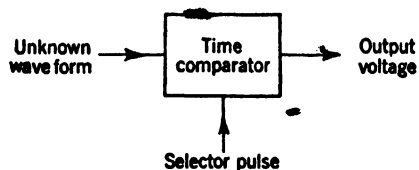


FIG. 20-11.—Waveform determination by time comparison.

waveform is connected to the time comparator which gives as a steady output the voltage of the unknown waveform at the moment of the selector pulse. This output voltage may then be measured by a voltmeter or a potentiometer. This method has, however, the drawback

that the output is of very high impedance and has a slight but perceptible carrier content.

**Summary.**—For qualitative observations the direct display upon a cathode-ray tube is satisfactory. But all quantitative measurements of triangular and other waveforms made in this laboratory have been carried out by means of amplitude comparison and display upon a circular-sweep timing system. This is in every way an extremely precise, simple, and satisfactory method.

**20-6. Frequency Measurements.** *Continuous Oscillators.*—The frequency of continuous oscillators may be readily measured by direct comparison with the frequency of a standard oscillator. The two frequencies are applied to the plates of the cathode-ray oscilloscope to produce the Lissajous or roulette figures.<sup>1</sup> Where a circular sweep is available, the unknown frequency may be applied to the center electrode. The ratio of the two frequencies is equal to the quotient of the number of waves displayed upon the circular pattern and the number of revolutions that the cathode-ray-tube spot makes in completing this display. This pattern is difficult to interpret for large frequency ratios or for unstable patterns.

Since a number of the oscilloscopes used in the calibration of timing circuits contain accurate time-modulation circuits that may be externally triggered (see discussion of DuMont type 256B, Vol. 20, Sec. 7-24), time measurement may be used for a simple and exact method of frequency

<sup>1</sup> See H. J. Reich, *Theory and Application of Electron Tubes*, 2nd ed., McGraw-Hill, New York, 1944, p. 644.

determination as shown in Fig. 20-12. The sinusoid of unknown frequency is converted into pulses by amplitude comparison (see Sec. 9-8). The spacing of these pulses is precisely equal to the period of the sinusoid. If these pulses are connected to a scale-of-two, or, in fact, to the gate generator of most oscilloscopes, the display will be triggered at a fraction of the period of the sinusoid. A few pulses will, therefore, be displayed on the time base, and the delay between them may be measured with an accuracy of 0.1 per cent by the time modulation circuit. The calibration of the latter may be referred to pulses from a crystal-controlled calibrating oscillator.

*Pulsed Sinusoids.*—The Lissajous pattern or other patterns employing sinusoidal time bases have been found to be of little value for the frequency measurement of pulsed sinusoids. Often the duty ratio of the pulsed waveform is so low that the intensity of the pattern is small. Furthermore, starting and stopping transients may very nearly completely obliterate the desired figure, and the phase deviation in the starting transient may be of considerable interest. In addition, the spacing of pulses derived from the pulsed oscillator is usually required. The most simple and accurate method is to display pulses obtained from the oscillator by amplitude comparison upon a circular sweep by means of radial deflection. The adjustment is made most conveniently if the two frequencies are equal, since the majority of the pulses from the pulsed oscillator coincide as indicated in Fig. 20-13a. The following important data may be determined by this method:

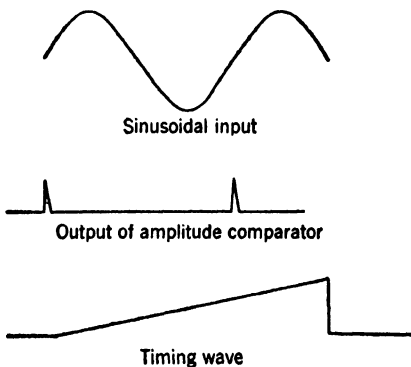


FIG. 20-12.—Frequency determination by time measurements.

1. Alignment of all members of the pulsed oscillator ensures equality of frequency to an accuracy  $1/200n$ , where  $n$  is the number of pulses of the oscillator displayed on the circular sweep.
2. The delay of the output pulses with respect to the trigger pulse may be measured.
3. The error of the first few pulses that is due to the starting transient may be observed.

The indication is similar for integral multiples of the circular sweep as shown in Fig. 20-14.

Another method of comparable sensitivity and time selectivity is

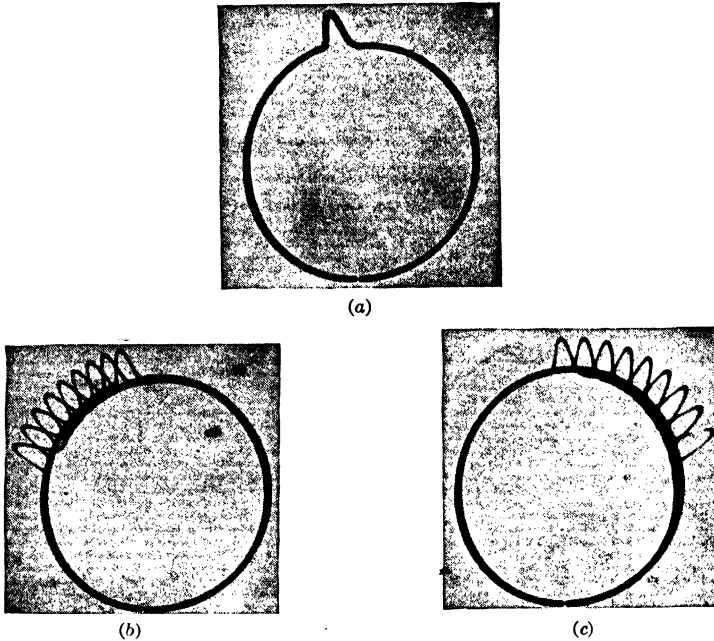


FIG. 20-13.—Frequency determination by display on a circular sweep. Figure 20-13a indicates the output of an 82-kc pulsed oscillator, adjusted to the frequency of the 82-kc circular sweep; (b) indicates that the frequency of the pulsed oscillator is too high and (c) indicates that the frequency of the pulsed oscillator is too low.

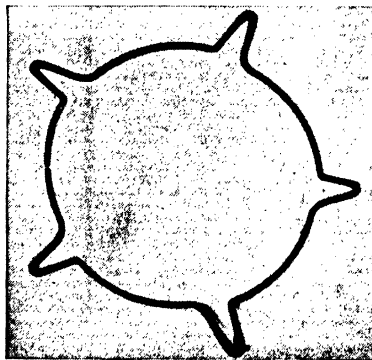


FIG. 20-14.—Display of pulses from a 410-kc pulsed oscillator on a 82-kc sweep. The frequency of the pulses is adjusted to an exact multiple of 82 kc/sec.

indicated in Fig. 20-15. The sinusoids of unknown frequency are displayed upon a linear time base, and calibration markers are superimposed by intensity modulation. For equal frequencies the calibration markers intersect the sinusoids at the same point on each cycle. This method does not, however, indicate the delay of pulses derived from the oscillator

with respect to a trigger, and it does not indicate the error due to the starting transient so clearly as does the circular-sweep method. Greater sensitivity is obtained if pulses derived from the unknown waveform are displayed instead of the sinusoids.

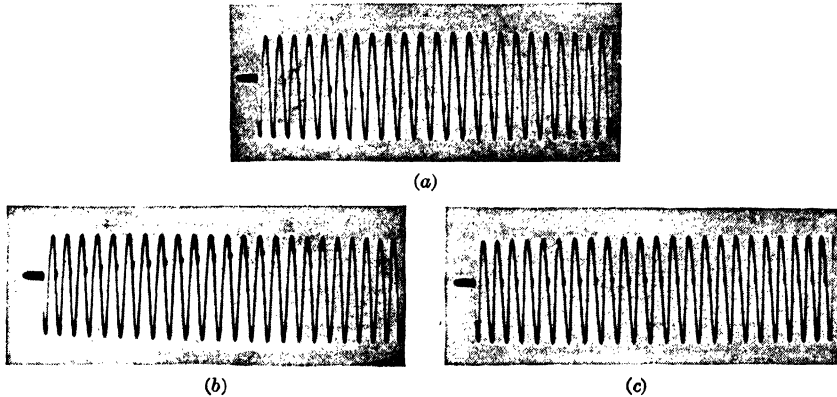


FIG. 20-15.—Frequency determination of a pulsed sinusoidal oscillator by display on a linear time base in comparison with fixed intensity markers. In (a) the pulsed sinusoid is too fast, in (b) too slow, and in (c) exactly on frequency. The frequency is 82 kc/sec.

**20-7. Phase Measurements.**—Rough measurements of the phase of two sinusoids may be obtained directly by applying the two voltages, separately adjusted to give equal deflection, to the plates of the oscilloscope. The direction of the major axis of the ellipse gives relative phase shift between the two voltages as indicated in Fig. 20-16. The accuracy of this method, of course, depends upon the deflection linearity of the oscilloscope.

A method that employs this pattern as the null indicator uses the phase modulators of Sec. 13-16 to reduce the phase shift between the two sinusoids to zero. The oscilloscope pattern is then a straight line. The accuracy of this method is limited by the phase shifter and at best is approximately  $1^\circ$ .

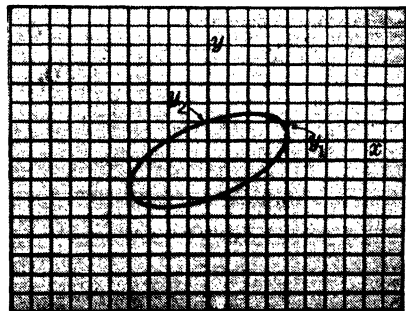


FIG. 20-16.—Phase measurement by a Lissajou figure. The phase angle  $\phi$  is equal to  $\tan^{-1} Y_2/Y_1$ , where  $Y_2$  is the intersection of the ellipse with the ordinate at  $X = 0$  and  $Y_1$  is the intersection of the ellipse with the ordinate corresponding to the maximum value of  $YX$ .

When pulses are derived from the two sinusoids by amplitude comparison, one pulse train may be made to trigger a time-modulation system similar to that shown in Fig. 20-12 for frequency measurements. The other pulse train is displayed upon the oscilloscope, and one of its pulses



will appear upon the cathode-ray-tube display. The time-modulation circuit may be used to measure the phase shift accurately. In this case measurement may be good to 0.1 per cent or  $0.4^\circ$ . Considerably better accuracy may of course be obtained with multiple-scale systems (see Vol. 20, Chaps. 3 and 7).

**20-8. Impedance Measurements.**—The characteristics of an unknown impedance may be directly determined by phase and amplitude measurement. First, the two deflecting amplifiers of an oscilloscope are adjusted so that they have equal gain (by adding a sinusoidal voltage and adjusting the relative gain until a  $45^\circ$  line is obtained on the face of the oscilloscope). An alternating voltage is connected to a variable resistor in series with the unknown impedance. The variable resistor is adjusted until

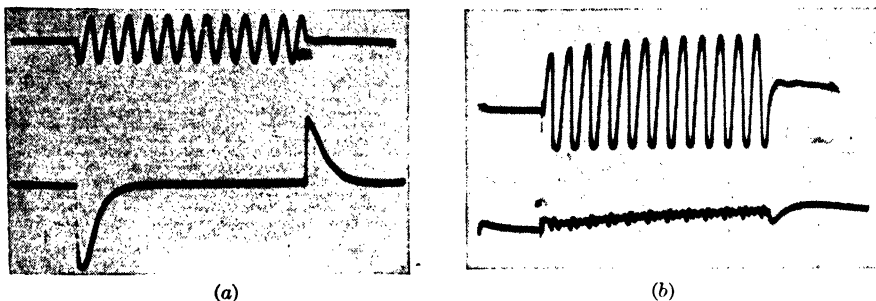


FIG. 20-17.—Determination of harmonic distortion of a pulsed oscillator by a frequency-selective circuit. In (a) the distortion of the pulsed oscillator is negligible even though the output displayed upon the scope has been considerably amplified. The effects of the starting and stopping transients are clearly indicated. In (b) is indicated the output of the selective circuit due to the distorted sinusoid of the upper trace, and the lower trace shows, with no further amplification, considerable harmonic distortion.

the figure on the oscilloscope has equal horizontal and vertical amplitude. Under these conditions the value of the resistance is equal to the unknown impedance. The phase angle of the voltage across the impedance is determined directly by measurements of the geometry of the pattern as mentioned previously in Fig. 20-16. The advantages of this method are that the measurements can be made over a wide range of frequencies and that the technique is extremely simple.

**20-9. Harmonic Distortion in Pulsed Sinusoids.**—It is often of considerable importance to measure the harmonic distortion of a pulsed sinusoidal oscillator. None of the commercial harmonic analyzers is suitable for these measurements since the harmonics generated in the starting transient of the sinusoidal waveform would obscure those which follow. If a frequency-selective circuit (twin-T) is added to the input to the oscilloscope to discriminate against the fundamental frequency, the output indicates the harmonics as shown in Fig. 20-17.

## CHAPTER 21

### STORAGE TUBES

#### INTRODUCTION

By P. R. BELL, G. D. FORBES, AND E. F. MACNICHOL, JR.

**21.1. General Definition of a Storage Tube.**—A storage tube may be defined as a cathode-ray tube containing a surface which may be charged by the electron beam to provide a record of information over the length of one sweep, and which may later be discharged to obtain the stored information in the form of voltage variations, or may be recharged by the beam with a second set of information in such a manner as to obtain an output containing only the difference between the first and second sets of information.

**21.2. General Methods, Applications.**—Storage methods are used in television pickup equipment of the Iconoscope and Orthicon varieties. In these tubes the storage surface is charged by the electron beam, and the charge is modified by photoelectric emission. The most satisfactory photoemitters are metals or semiconductors. Hence the storage surface must be broken into a mosaic of photosensitive particles to prevent conduction across the surface. In the storage tubes described here, photoemission plays no part. The metallic mosaic is therefore unnecessary and the storage surface consists of a plate of uniform highly insulating material. The only requirements imposed on this material are the conditions that it must emit more than one secondary electron for each primary electron striking it, and that it must have extremely high resistivity.

In addition to the storage surface, the storage tube comprises an electron gun, a deflecting system, a secondary electron collector, and a signal plate capacitively coupled to the storage surface. In operation, electrons from the gun strike the storage surface and cause emission of secondary electrons. These electrons redistribute themselves until a condition of equilibrium is reached. Information is stored by modulating one of the electrodes of the CRT when the surface is scanned by the electron beam and recovered when the surface is again scanned. The stored signal is recovered in the process of redistributing the charge on the storage surface to fit the conditions imposed by the second scan.

Although the Iconoscope and Orthicon have been successfully used

for several years, techniques for storage of electrical signals are still in the early experimental stage. Most work to date has been directed toward their use in pulse-to-pulse amplitude cancellation of radar video signals.

Supersonic delay lines have been successfully used for this purpose, but their use requires that the delay of the line be exactly equal to the pulse-repetition interval of the radar, a condition difficult to maintain in some systems. Supersonic lines also become very large and complicated when low PRF's are used (see Vol. 20, Chap. 12).

Storage tubes have also been applied to equipment in which it is desired to obtain output signals only when two signals have appeared consecutively with the same delay with respect to a fixed reference pulse. This application may be considered the inverse of pulse-to-pulse amplitude cancellation and has been employed to increase the signal-to-noise ratio in radar systems<sup>1</sup> and to eliminate unsynchronized interfering pulses from responder-beacon displays.

Some synchronization systems have been proposed in which it is desired to compare waveforms at incommensurable recurrence frequencies and on different time scales. The externally synchronized crystal-controlled range-mark generator described later is an example of this use. Several methods have also been proposed for using storage tubes to record randomly occurring high-speed transients, which are then played back repetitively at a slower speed for photography or observation. Methods are also under development for using storage tubes as memory devices in pulse-operated computers.

In most of the work described the storage tube is a standard electrostatic cathode-ray tube of the 3BP-, 3FP-, or 5CP-type, with or without phosphors. The glass wall of the tube and the phosphor are used as the storage surface. Modulation has been applied to the grid, focus electrode, second anode, and deflecting systems with varying results. A special high-voltage Orthicon-type storage tube has been used by Radio Corporation of America.<sup>2</sup> In this tube modulation is applied to the signal plate. Before describing the results obtained with these tubes the theory of operation of the storage surface will be discussed.

<sup>1</sup> Delay lines were actually used for this purpose.

<sup>2</sup> At the time this chapter was written storage tubes were in a very early developmental state and their action was very imperfectly understood. Since that time a great deal of work has been done. References: "A Storage System for Use with Binary Digital Computing Machines" (a report by the Electro-Technical Laboratories of the University of Manchester, England). Haeff, "A Memory Tube," *Electronics*, **20**, p. 80 (1947); Forgue, "The Storage Orthicon," *RCA Review*, **8**, p. 633 (December 1947); McConnell, "Video Storage by Secondary Emission," *Proc. IRE*, **35**, p. 1258 (1947). A storage tube designed especially for digital computation is described by J. A. Rajchman in IRE Convention Paper #49, February 1947.

**21.3. Theory of Storage Action.—Intensity Modulation.**—There is no comprehensive theory that explains the action of the cathode-ray-tube storage device. In its place a tentative physical argument based upon the observed experiments on these tubes and upon data on the secondary-emission coefficient of glass has been evolved.

When a constant intensity electron beam is swept across a glass surface in a storage tube, secondary electrons are emitted from the glass. By this action and by the redistribution of the emitted secondary electrons a charged condition of the surface is obtained.

The secondary-emission coefficients of glass depend somewhat upon the type of glass. For Pyrex, the secondary-emission coefficient at 200° to 300°C is as shown in Fig. 21-1.<sup>1</sup> It is assumed that this curve holds roughly for the glass in an ordinary CRT at room temperature. The secondary-emission coefficient is greater than one for the voltages used. The spot under the electron beam, therefore, will receive positive charge. Eventually the field due to the positive charge will attract as many electrons as escape to other parts of the tube and steady state potential distribution will be attained. At this time no further change of charge will occur at the spot. Some of the secondaries that are attracted back to the spot strike the surface near the spot and, since the glass is an insulator, they are unable to escape. The result will be somewhat as shown in Fig. 21-2, which represents a positively charged spot surrounded by a negative hill of charge.

If the beam is caused to move across the surface, a different situation is found. In front and to each side of the spot there is a negative hill of charge, but behind it there is the distinctly positive track left by passage of the spot. Some of the secondaries fall into this track and reduce its positive charge. After a number of repetitions of the sweep, there will remain a positively charged track with a more positive spot at its end where the beam was suddenly shut off and no secondaries were available to fall back into this portion of the trace and discharge it. Surrounding this track on all sides will be the negative charge hill, so negative that no secondary electron will be able to reach the surface in that region. The charged condition of the section of this trace along its center is shown in Fig. 21-3a. When the next trace starts (Fig. 21-3b),

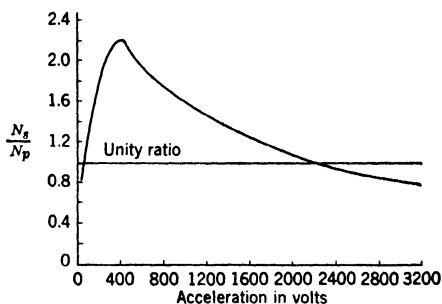


FIG. 21-1.—Ratio of secondary electrons emitted to primary electrons striking Pyrex-glass surface plotted as a function of accelerating potential.

<sup>1</sup> The data for this curve were taken from C. W. Mueller, "The Secondary Emission of Glass as a Function of Temperature and Voltage," Sc.D. Thesis, M.I.T., 1942.

the beam suddenly charges the beginning of the trace more positive, and many of the secondaries escape to the anodes since a negative hill surrounds three sides of the spot. When the beam has advanced well out on the trace, electrons are falling on the trace both before and behind the spot, but, since the passage of the spot leaves the trace in the original condition, there is no output from the signal plate since there is no net change of charge instant by instant, as shown in Fig. 21·3c.

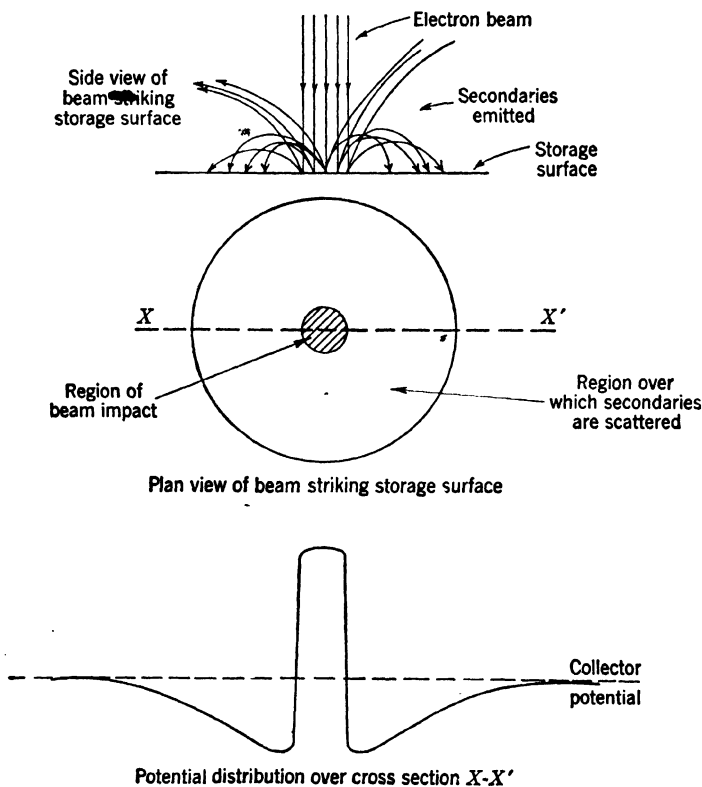


FIG. 21·2.—Potential distribution around charged spot on storage surface.

As the spot approaches the very positive region at the end of the trace, many of the secondaries fall into it causing a negative output voltage, since more of the electrons of the beam appear to “stick” somewhere on the surface (Fig. 21·3d). Finally, when the beam reaches the end of the trace, the secondary electrons cannot fall ahead of the spot on account of the negative hill at that point, and the output goes positive, then falls to zero as the beam is turned off (Fig. 21·3e).

If the electron beam is intensified for a short interval during the sweep, the output voltage and charge conditions appear on the first sweep, as

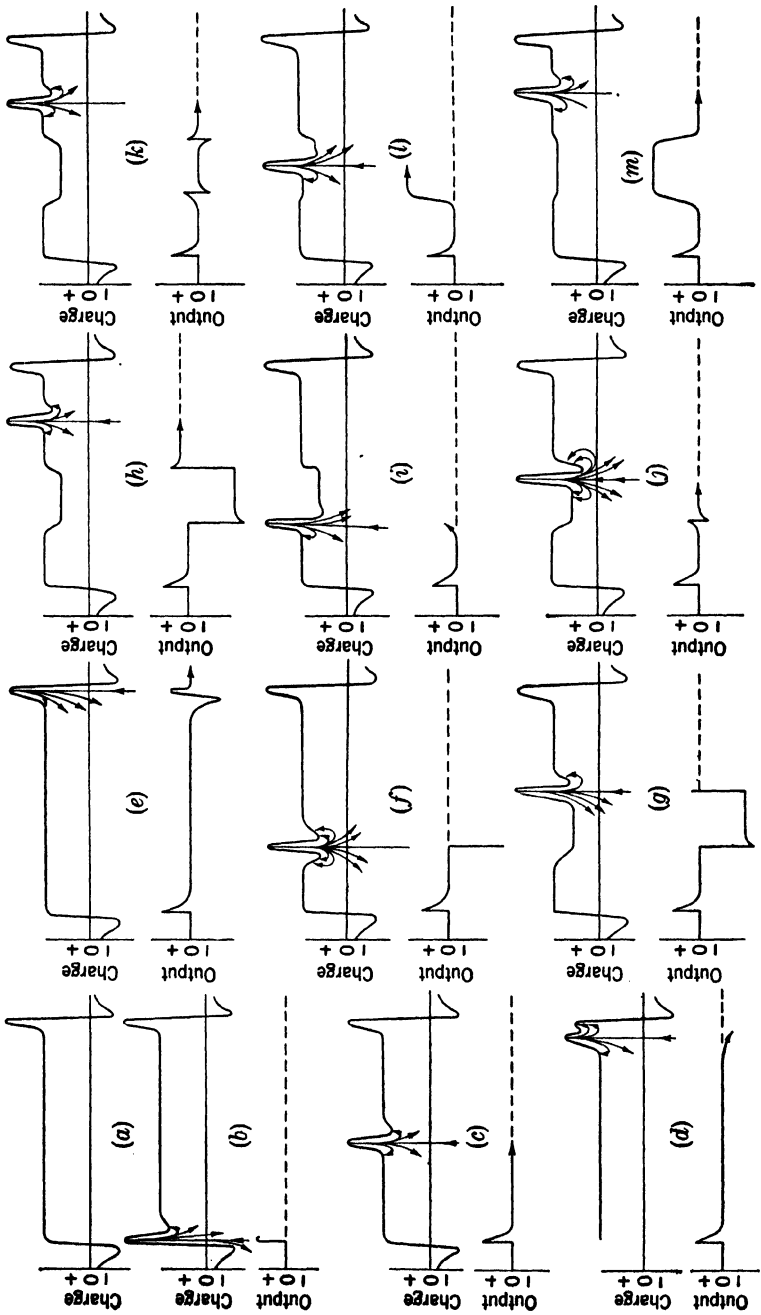


FIG. 21-3.—Charge and output pattern of storage surface under moving beam.

shown in Fig. 21·3*f*. The increased beam current gives an increased number of secondary electrons, and more of them fall on the charged trace discharging it to a greater extent than the weak beam. More electrons return to the surface near the beginning of this intensified region because of the more positive trace close to the spot than near the end of the intensified region where there is a less positive region of trace behind the spot<sup>1</sup> (Fig. 21·3*g*).

After the intensified pulse ends and the weaker beam passes over the end of the less positive region left by the intensified beam, the output voltage is positive because of the decreased tendency of the secondaries to fall into the trace behind the spot. It falls to zero as the spot gets far away from the intensified region (Fig. 21·3*h*).

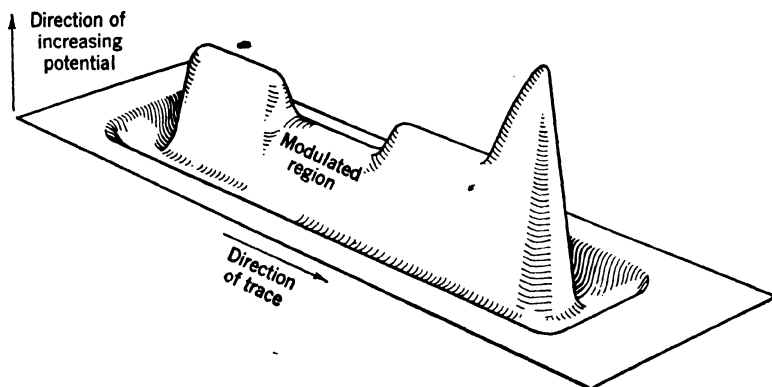


Fig. 21·4.—Model of potential distribution produced by moving beam on storage surface.

During the next sweep, when the beam spot approaches the previously intensified portion of the surface, a positive output voltage is obtained because of the decreased tendency of secondaries to fall into the less positive region (Fig. 21·3*i*). When the beam is suddenly intensified this time, there is a sudden change to a negative output voltage since the greater flux of secondaries finds the trace behind the spot more positive than it would be in the center of a long trace made by a beam of this intensity. As the spot approaches the center of the intensified region, the output voltage is more nearly zero since the charge on each side of the spot has almost reached a steady state (Fig. 21·3*j*). The output has a similar form near the other end of the intensified region, but in reverse sequence (Fig. 21·3*k*). During the third sweep the action is quite similar to that during the second. Nearly complete equilibrium is reached with the result that the center of the intensified region produces little output. If on the next sweep there is no intensity-modulated region, the output

<sup>1</sup> The large negative pulse in the output when the intensity of the beam is changed is due to the charge induced in the pickup plate by the "electron cloud" passing over it.

signal will contain a positive pulse with smooth edges because of the smaller tendency for secondaries to return to the screen in the region where the track is less positive (Figs. 21-3*l* and *m*); this is the main stored signal. The track is not returned entirely to the normal charged condition for the weak beam because of the slightly greater number of secondaries produced as the surface is charged positively. The result will be that on the following sweep another smaller stored output will be obtained. A three-dimensional model of the potential distribution on the storage surface after scanning is shown in Fig. 21-4.

In some applications the cancellation of signals which do not vary from pulse to pulse is desired. For this purpose deflection modulation in ordinary cathode-ray tubes and signal-plate modulation in the SDT-5 appear to be satisfactory (see Secs 21-4 and 21-5). In other applications storage of the video signals without cancellation is desired. For some purposes, such as pulse computation and time-mark generation, fidelity of output amplitude vs. input amplitude is not important. In other applications good linearity is required. The most effective noncanceling method thus far used is grid modulation of the electron gun (intensity modulation). The stored signal is a very nonlinear function of the modulating potential because the beam current is a nonlinear function of this potential, and because the stored signal is also a nonlinear function of the beam current.

**21-4. Deflection Modulation.**—When the electron beam is swept across an insulator surface but is kept at constant intensity and is deflected perpendicularly to the direction of the sweep with a rectangular pulse, only a very small output is obtained after the surface has come to equilibrium (reached a steady state). This small output occurs at the beginning and at the end of the pulse, and its form can be seen from Fig. 21-13*b* as the signal produced by the large, fixed-amplitude pulse. When the pulse height is changed a positive pulse is obtained. This positive output is obtained every time there is a difference in deflection amplitude from trace to trace. It appears even when alternate traces are identical, so that only two tracks are produced on the surface with the beam tracing first one then the other. It is evident that the action is distinctly different from that with intensity modulation, since in that case there were two separate processes, each giving an output of opposite sign depending upon whether the surface accumulated or lost a net charge. Figure 21-5 is taken from an experiment in which amplitude modulation was used. The output from the pickup plate is plotted as a function of the separation between the two traces (difference in modulation intensity). The solid line shows the results when two paths are traced alternately. The dotted line was obtained when the deflection was modulated sinusoidally at a frequency incommensurate with the PRF. This resulted in a pattern having many different traces that did not superpose.



The presence of the two traces side by side must therefore affect the way in which secondary electrons return to the storage surface so that secondary electrons will fall back into the region of the two closely spaced traces although they are emitted from other parts of the trace ahead of and behind the space occupied by the double trace. When the two traces are more widely spaced, the probability of attracting extra secondary

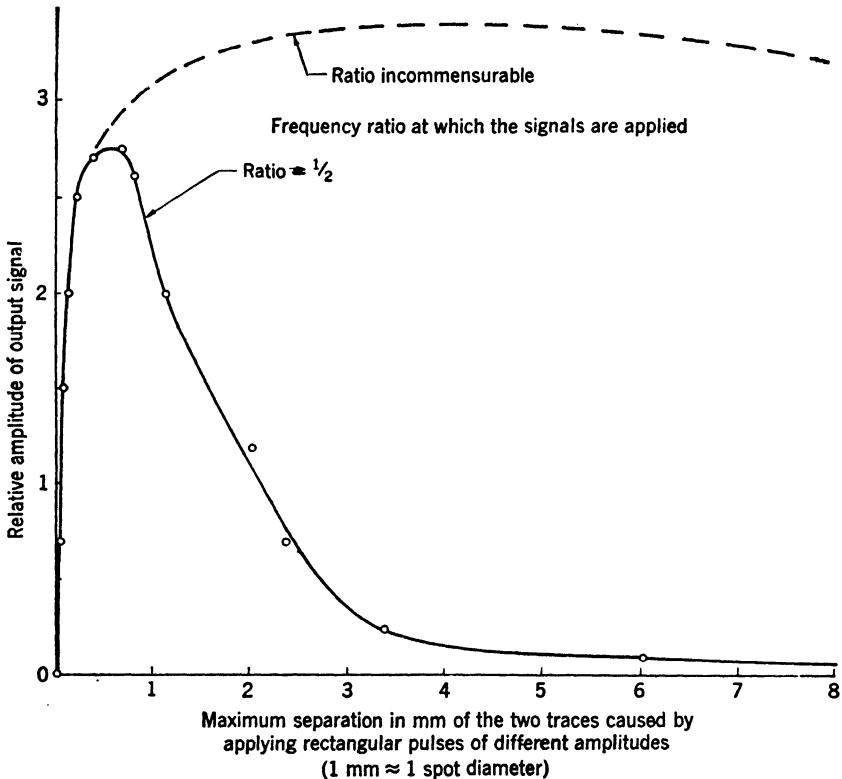


FIG. 21-5.—Output of deflection-modulated storage tube as a function of deflection-amplitude difference between two successive traces.

electrons falls rapidly with increased spacing; there is, therefore, little extra charge to be removed by the beam and to give positive output. At considerable distances the field from a positively charged line bordered by two negatively charged lines falls away as the inverse fourth power of the distance away from the lines. The field produced by the combination when measured at a moderate distance will decrease as the spacing between the lines is decreased, even though the charges are adjusted so that the field appears constant at a great distance. This effect might allow the closely spaced double trace to cause more secondaries to return to it from distant parts of the screen than would return

to the traces if they were at such a distance that one had little effect upon the other.

The experimentally measured variation of output with separation of the double trace (Fig. 21-5) agrees qualitatively with such a theory.

**21-5. Signal-plate Modulation.**—Modulation of the electrode behind the storage surface has been attempted and appears to be successful under certain conditions. In the first method tried, the signal plate was modulated by the incoming video pulses while the charging current was measured. If equilibrium exists between the beam and the emitted secondary electrons, no charging current will flow. If the signal amplitude changes, a pulse of charging current appears. This method was unsuccessful because of the difficulty of removing the high-level video signal from the low-level output.

Attempts have also been made to modulate the signal plate and obtain the stored signal from the Aquadag coating on the inside of the CRT. This method was unsuccessful for two reasons. First, most of the secondary electrons emitted from the surface fall back onto other parts of the surface; few of them reach the Aquadag coating directly. Second, there is sufficient capacity coupling between the signal plate and the Aquadag coating to produce a direct signal which is much larger than the stored signal.

The only device which successfully uses signal-plate modulation is the RCA type SDT5. This is a tube of the Orthicon type in which the electrons are constrained to travel down the tube by means of an axial magnetic field. Deflection is accomplished electromagnetically. Unlike the ordinary Orthicon, the accelerating potential is high enough to cause a secondary-emission ratio greater than unity. The tube operates as follows: An unmodulated electron beam is made to trace across an aluminum-oxide insulator surface behind which there is a metal back plate and in front of which there is a fine wire-mesh screen through which the electron beam penetrates. The signal to be stored is applied between the back plate and the wire screen (screen on ground end of signal). The incident beam charges the spot it strikes to about the voltage of the wire mesh. If the spot is more positive than the screen, most of the secondary electrons produced return to the spot making it more negative. If the spot is more negative than the screen, most of the secondaries are accelerated toward the screen. Because of the action of the axial magnetic field, the emitted secondary electrons travel back down the tube in nearly straight lines. Those electrons which are not collected by the screen travel the entire length of the tube and are collected and amplified by a five-stage electron multiplier which surrounds the electron gun.

When the video signal changes, the spot now under the beam is

charged to a new potential with respect to the back plate, but it is charged to the same potential with respect to the wire mesh. When the surface is retraced by the beam, the surface touched by the beam is point by point the same potential as the wire mesh (assuming complete equilibrium on the first sweep) if the video signal is exactly the same as before. If, however, at some point the video signal is not the same height as on the previous trace, the insulator surface will be above or below screen potential and more or fewer secondaries will have to leave to restore the voltage of the surface to screen potential. The secondaries penetrating the screen are amplified by the electron multiplier and appear as an output signal.

The output current is constant and proportional to primary beam current as long as the insulator surface being hit is at screen potential, but it increases or decreases when the surface is differently charged and is restored to screen potential by the action of the secondaries.

For some purposes this is a satisfactory tube, which gives a good cancellation ratio even on sweeps that are very long compared with the pulse, but complete equilibrium is not established on each trace; some tubes require perhaps six traces to reach a steady state. This charging time is undesirable in applications involving cancellation although it may be desirable for some other purposes.

**21.6. Focus Modulation.**—Focus-modulation storage has been tried briefly with only moderately successful results. In this method the spot area is changed by the video signal, and the output signal is obtained from a pickup plate behind the insulator surface being scanned by the beam. When the same set of signals is applied on successive sweeps, the output contains some pulses that occur at the beginning and end of the signals. The output obtained when a modulated pulse is used as a signal is larger than these pulses, but the difference is only about two to one in voltage, although under some conditions a difference of ten to one has been obtained. The ten-to-one cancellation was obtained when the storage surface was surrounded by a short solenoid. The field from this solenoid apparently changes the distribution of the secondary electrons that return to the surface.

**21.7. Frequency-modulated Carrier with Intensity Modulation.**—Where the stored signal must reproduce the input signal with good fidelity it has been proposed to impress the video signals upon a high-frequency carrier by means of frequency modulation. The frequency-modulated carrier would then be applied to the grid of the storage tube producing a series of spots of variable spacing on the screen. The stored carrier would then be recovered by retracing the surface with a constant-intensity beam. The output carrier is then amplitude limited to get rid of amplitude variations and applied to an f-m discriminator which demodulates

it. The output signal should then be a faithful reproduction of the original signal. The principal disadvantage of the method lies in its requirement of a higher rate of sweep on the CRT. The minimum resolvable signal on the storage surface will be at least a spot width long. If a carrier is used, it must be several times the frequency of the highest frequency component in the stored signal. A resolvable spot must be produced for each cycle of the carrier, so that the sweep speed must be several times that which would be required if the signal were stored directly.

#### DESCRIPTION OF APPARATUS USED IN STORAGE-TUBE EXPERIMENTS

**21.8. Intensity Modulation Tests.**<sup>1</sup>—Ordinary electrostatic cathode-ray tubes were used and the power supply and positioning circuits were

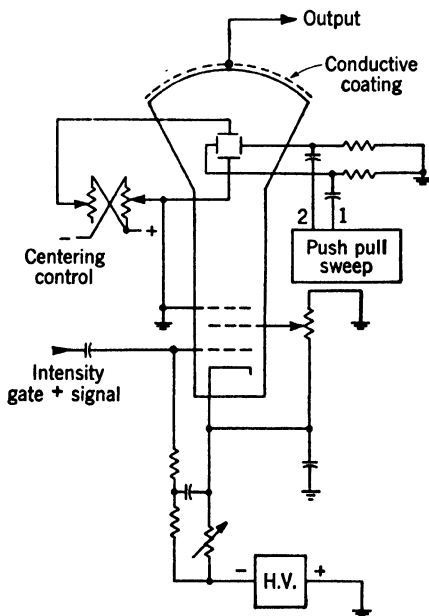


FIG. 21-6.—Connections to intensity-modulated storage tube.

conventional as shown in Fig. 21-6. Horizontal deflection was provided by a conventional linear sweep. The accelerating voltage used was about 1500 volts.

The time sequence of the intensity-gate voltage, the voltages of the sweep, and the signal output are shown in Fig. 21-7.

Tubes containing various insulator targets were prepared by Allen B. Du Mont Laboratories, and from these it was found that mica yields as large a signal as glass, but on account of the presence of bubbles and

<sup>1</sup> For a description of sonic-delay-line cancellation system see Vol. 20, Chap. 12

surface irregularities no satisfactory large surface has been obtained; it does not seem to give any greater output than glass. Tubes with P1 and P11 phosphors give the same result as glass, although in some samples of P11 screens one or more small points were found on the screen that gave an output whenever the beam struck them; P7 phosphors were

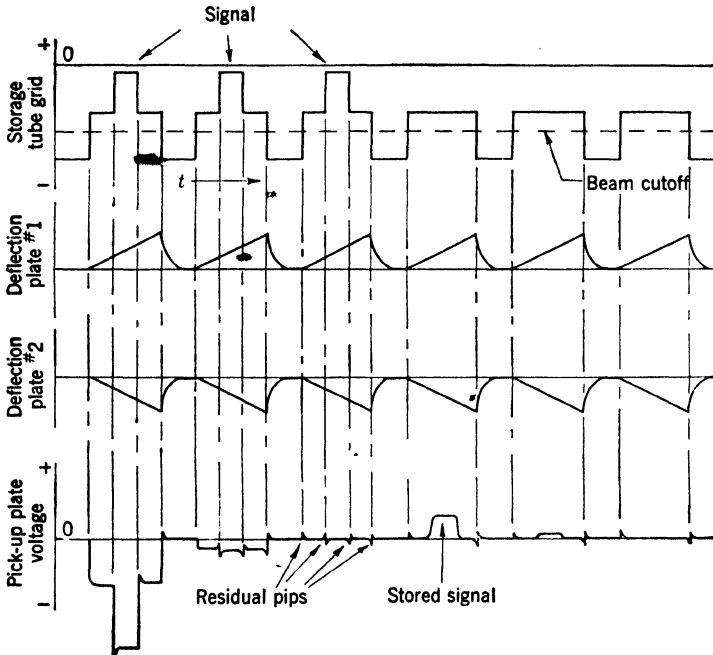


FIG. 21-7.—Timing diagram of signals used in intensity-modulated storage-tube tests.

much more irregular than P1 phosphors or glass. The antiarc coating used as a surface insulator between sections of conductive coating inside high-voltage cathode-ray tubes gives no stored signal whatever.

One tube had samples of glass of various thickness from 0.001 to 0.25 in.; no difference in stored output was obtained when the different thicknesses were used.

Some tubes were made with ground and polished-end faces similar to type 4AP-10. When these were tried there was no noticeable difference between them and ordinary cathode-ray tubes.

As a result of these tests, ordinary 3BP-1 tubes were used for much of the later work.

A 1- $\mu$  sec-pulse output can be made as large as 0.2 volt through a 1-megohm input circuit with a  $\frac{1}{2}$ -Mc/sec bandwidth using a 5CP1A tube

with a trace speed of 10  $\mu\text{sec}/\text{in.}$ , provided that the special negative-capacitance amplifier described in Appendix I is connected to the signal plate.

Many types of pickup plates outside the tube end were tried and almost any type of conductive coating on the tube face seems to be satisfactory. If an Aquadag (colloidal graphite) stripe is painted across the face of the tube and contact to it made by a bit of copper foil attached to it by scotch tape, a satisfactory output can be obtained. If the trace of the electron beam is moved so as to be parallel to the conducting stripe, but above or below it on an uncoated section of the tube face, very little reduction in output is found until the beam is about  $\frac{1}{2}$  in. away from the edge of the conducting stripe.

A flat metal plate near the glass or not more than  $\frac{1}{8}$  in. away will do as a pickup, although a smaller output is obtained as the section of glass being touched by the beam becomes progressively farther from the metal plate.

A cell containing an electrolyte (salt water), which allows a free view of the tube face, has been used and found to be satisfactory. A coarse metal screen was tried, but was found to produce considerable wiggles in the base line on account of the crossing of the screen wires by the trace. A fine metal screen 100 meshes per inch gave satisfactory results when made flat and, although it was not tried, it is believed that a thinly sputtered transparent film of chromium or platinum would be equally satisfactory. It is very desirable to have a somewhat transparent pickup plate to allow the beam to be centered and focused by eye, thus permitting quicker adjustment of the tube. The effect of varying the total accelerating potential was tried over the range of 500 to 2200 volts. It is unfortunate that voltages up to 3000 volts were not used, because no change in stored signal resulted other than a small change in character due to defocusing near 500 volts. Some change of results could have been expected on the basis of the present theory of operation if the total accelerating voltage had reached about 2500 to 2600 volts, since above some voltage in this region the number of secondary electrons emitted by the glass of the tube is believed to become less than the number of primaries striking it (see Fig. 21.1).

The stored signal is a nonlinear function of the intensity of the storing beam and is also a function of the intensity of the reading beam used to take off the stored signal. In particular, the degree to which the stored signal is "wiped off" by the reading beam is greatly influenced by the intensity used; when a very weak reading intensity is used, the stored signal is only partly removed, and up to 200 outputs can be obtained from one stored signal before the signal becomes too small to be discerned

in the thermal noise<sup>1</sup> of the output circuit. If the reading-beam intensity is high, less than 10 per cent of the stored signal may remain after a single passage over the screen.

As might be expected, the spot focus has considerable effect on the output and sharpness of the stored signals; and it is most important to maintain a *uniform* degree of focus from one part of the screen to another, or the output pulse will contain a large varying voltage from one end of the sweep to the other. Figure 21-8 shows this effect.

As a consequence, a push-pull sweep must be used, and the average voltages of the deflection-plate sets and the second and third anodes

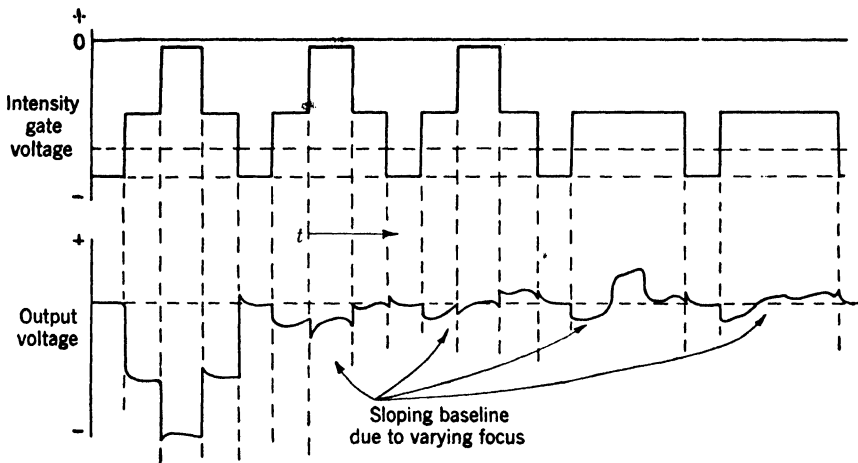


FIG. 21-8.—Effect of focus variation along trace.

must be distributed properly to maintain uniform focus over the tube face. Different CRT's require slightly different voltage distributions, and astigmatism controls should be provided to adjust them (see Fig. 21-9).

It was found that the most satisfactory reading intensity was different for different sweep speeds, and it was observed that the optimum intensity for different sweep speeds gave approximately the same visual brilliancy of trace; this seems to indicate an approximately constant current density for optimum results. The output pulse obtained with the same signal was larger for faster sweeps. This fact might be expected; since the storage effect is obviously some change of the charged condition of the screen surface and since the optimum condition involves approximately a constant current density, the output could be expected to be greater for a greater number of inches per microsecond covered by the trace.

<sup>1</sup> For a discussion of noise in video amplifiers see Vol. 18.

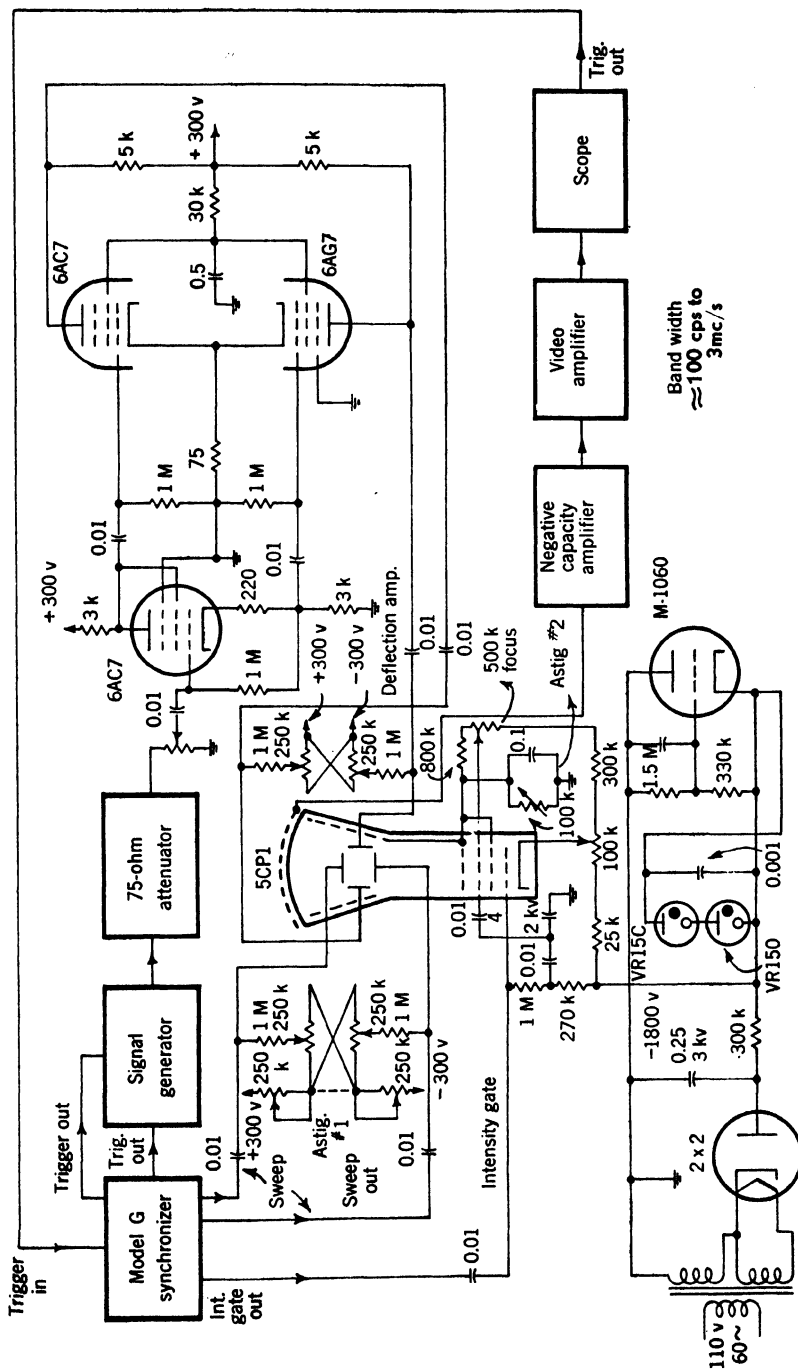


Fig. 21.9.—Test setup for deflection-modulated storage tube.



No change in the output was found with any phosphor or glass when the repetition rate of the sweep was varied from 20 to 2000 cps. This seems to indicate that the effect of conduction along the surface of the glass or phosphor is negligible, at least for  $\frac{1}{20}$  sec.<sup>1</sup>

To obtain cancellation of signals of constant intensity one set of signals is compared with another, with the result that only the difference between them is left.

One could, for example, store the first set of signals, and then when the second set was being received, read off the stored signals and subtract them, instant by instant, from the incoming signal; thus only the part of the signal that was different would give any output. Unfortunately, the stored signal is a nonlinear function of the initial signal, and a complex signal could, therefore, not be completely canceled by the stored signal. It was necessary, therefore, to store the first signal in one storage tube and the second signal in another identical tube, then read off the two stored signals together, trusting that the two tubes would have similarly nonlinear outputs. It is possible to do this and leave uncanceled residues about 25 to 30 db smaller than the signal, but considerable equipment is needed and the adjustments are complex and difficult.

**21-9. Deflection Modulation Tests.**—Deflection modulation was next tried since cancellation of fixed signals occurs directly on the storage surface as explained in Sec. 21-4. Here a beam of constant intensity is deflected in a direction perpendicular to the trace motion as in the ordinary A-scope. When a signal of constant height is impressed upon the vertical deflecting plates, a very small output is found on the pickup plate; when the height of this signal is changed, an output is obtained; this output is always positive at the pickup plate, whether the signal be increasing or decreasing (see Fig. 21-10).

A cathode-ray tube used in this way performs the complete function of a signal canceler; that is, the output contains almost nothing except the differences between successive sets of signals fed into it. This produces a much simpler arrangement than the intensity-modulated method, and considerable work was done to find the best conditions for signal cancellation.

A signal generator was constructed giving both a positive or negative pulse of adjustable duration and amplitude and a modulated pulse of adjustable duration, amplitude, and modulation frequency. The two pulses could be made coincident in time or not, at will. The modulated pulse varies in amplitude from a positive to a negative maximum in a

<sup>1</sup> The University of Manchester group reports a leakage time-constant of  $\frac{1}{2}$  sec for commercial British cathode-ray tubes.

sinusoidal manner so as to represent the radar return from a moving target on a system equipped with a coherent oscillator. The circuit diagram of this signal generator is shown in Fig. 21-11. A complete test setup for deflection modulation is shown in Fig. 21-9. Several 3FP1 and 5CP1A tubes were tested with this equipment.

One RCA 5CP1 was found that gave very poor results and later another RCA tube was found that was unsatisfactory. All Du Mont 5CP1A tubes tried were satisfactory. Any hum voltage applied to the deflecting plates, of course, gives a large hum output from the pickup plate. Alternating magnetic fields have the same effect. The storage tube must therefore be shielded by a mu-metal shield (or its equivalent) and even then must not be exposed to strong fields. A voltage-regulating

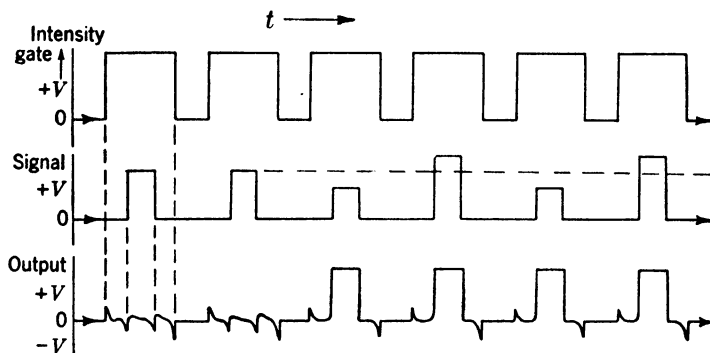


FIG. 21-10.—Timing diagram of signals used in deflection-modulation tests.

transformer several feet away caused serious effects even with a shield. The power supply for the video amplifiers supplying the deflecting plates and for centering voltages must be well filtered and preferably regulated. Any hum voltage on the accelerating voltage supply also gives hum in the output with the result that the supply must be extremely well filtered. The intensity of the beam has an optimum value, and a change in accelerating voltage will increase or decrease the amplitude of the output signals undesirably. It was found necessary, therefore, to regulate this voltage.

Figure 21-12a shows the maximum modulated-signal output and residual pip height obtained with best adjustment as a function of sweep speed for 17, 46, and 160  $\mu\text{sec/in.}$  Figure 21-12b shows the product of peak output due to the moving target and the square root of sweep in microseconds per inch plotted against the length of the pulse in inches on the tube. Multiplying by the square root of sweep speed seems to correct for the increase of output due to the use of more storage surface per microsecond and leaves only the effect of geometrical factors. Since the intensity was always set so that the uncanceled residue due to the



fixed signal is equal to that of the modulated one, although when the fixed signal is more than three times as long as the modulated one there is no change in the output whether the fixed signal is present or absent.

The modulated signal input was decreased until the output it produced was equal to the maximum positive value of the uncancelled residue of the large unmodulated signal. The ratio of the fixed signal amplitude to the modulated signal amplitude, under these circumstances, is called the cancellation ratio. The value of the cancellation ratio (in decibels) obtained at various sweep speeds is shown in Fig. 21-12c. The modulated signal amplitude is measured from the base line to either the positive or negative maximum. The fixed signal amplitude was about  $\frac{3}{8}$  in. for these results.

The output is a distinctly non-linear function of the input amplitude and also depends greatly upon the ratio of modulation frequency to repetition rate of the sweep. When the ratio of the modulation frequency to repetition rate is exactly  $\frac{1}{2}$ , so that one pulse is positive and the next negative, the output rises rapidly as the deflection modulation increases and then falls smoothly to a very small value. Figure 21-5 shows this effect for frequency ratios,  $\frac{1}{2}$  and an incommensurable ratio near  $\frac{1}{2}$ . The output is in arbitrary units of signal potential; the input is in millimeters of signal height peak-to-peak on the tube face. There seems to be no other explanation of these output curves except that the presence of two traces close to each other affects the way in which secondary electrons return to the screen from more distant parts of the trace. The pulse length for this test is about 7.4 mm, and the output for the two-trace patterns has passed through the peak and fallen off to  $\frac{1}{2}$  when the traces are separated by 2.5 mm. The effect, therefore, is not simply one of the geometric relations of the pulse-top regions to the parts of the base line before and behind the trace; the multiple-trace pattern obtained when the modulation frequency is substantially incommensurable

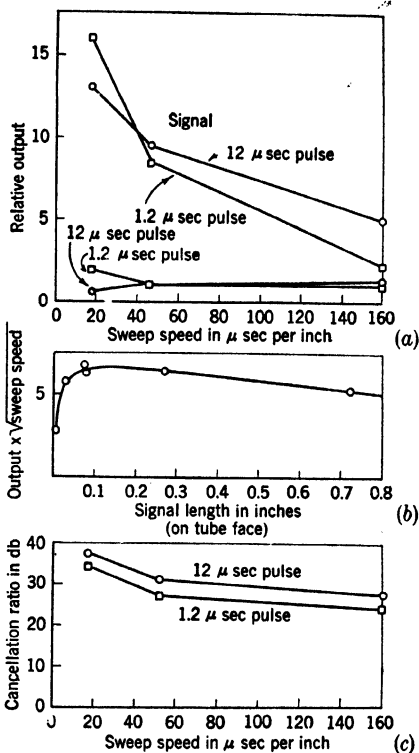


FIG. 21-12.—Output and cancellation ratio as functions of signal length and sweep speed.

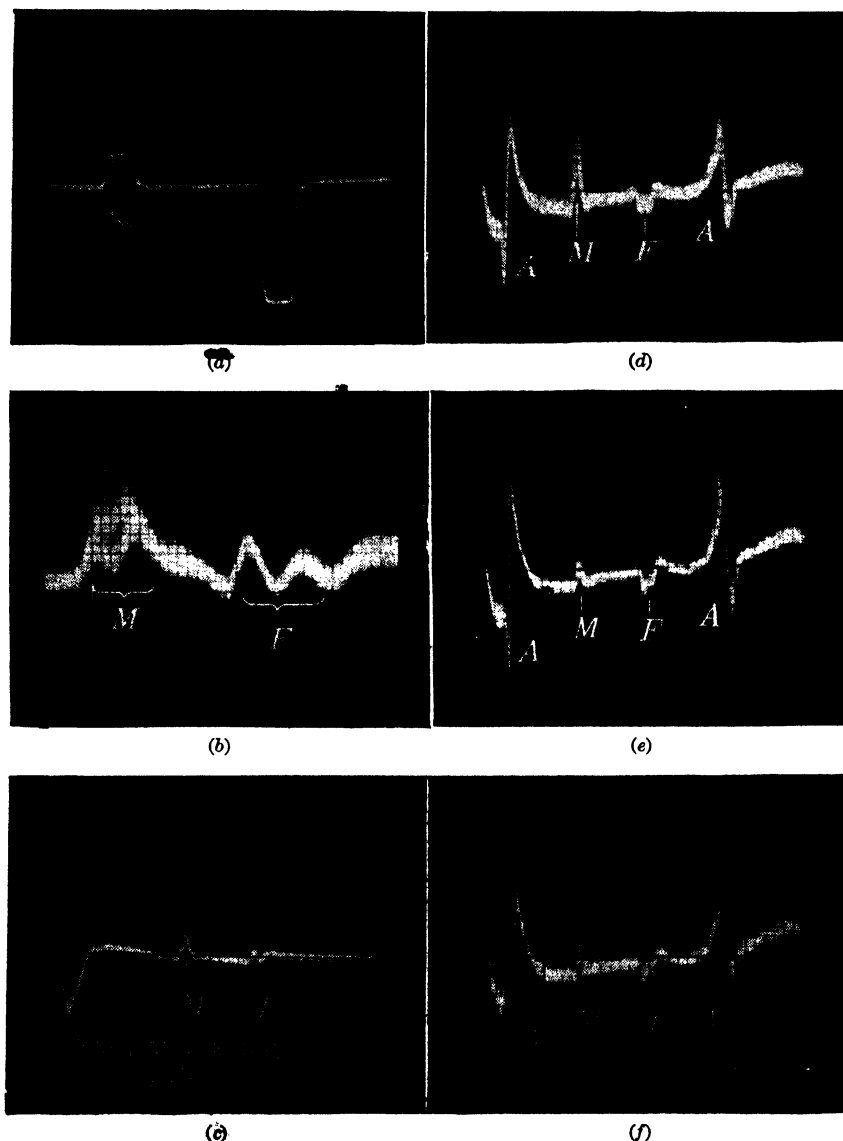


FIG. 21-13.—Waveform photographs obtained with deflection-modulated storage tube. *A* indicates transients due to the starting and stopping of the sweep; *M* is the output due to the modulated signal; *F* is the uncanceled residue of the fixed signal.

measurable with the sweep repetition rate also gives a large output that does not decrease much even for large amplitudes.

Photographs of the signal input and 5CP1A storage-tube output as seen on an A-scope are shown in Fig. 21-13. Figure 21-13*a* shows the input signals, each about one microsecond long and spaced about  $5\ \mu\text{sec}$

from each other. The ratio of modulated to unmodulated signal is 10 db. Figure 21-13b shows the storage-tube output as shown on the same oscilloscope. The storage-tube sweep speed is about  $46 \mu\text{sec/in.}$  The fuzziness of the base line is caused by thermal agitation voltage in the resistor attached to the pickup plate. Figure 21-13c shows the same signals displayed on a scope trace ten times slower. The pulses have been spaced about  $50 \mu\text{sec}$  apart for greater clarity.

The next photograph (Fig. 21-13d) has the same signal input and scope sweep, but the storage-tube sweep has been changed to about  $17 \mu\text{sec/in.}$  The modulated-signal output is now much larger compared with the amplitude of the uncanceled residue. In Fig. 21-13e the modulated signal is 32 db smaller than the fixed unmodulated signal yet the output signals are of equal amplitude indicating a cancellation ratio of 32 db. Figure 21-13f shows a signal ratio of 30 db, but the pickup video bandwidth has been made three times as wide and the amplifier has been adjusted to be slightly overpeaked. From these tests it was concluded that the storage-tube system using deflection modulation was feasible for use in a radar moving target indicator as a replacement for sonic delay lines. Such a system was built and tested. Cancellation of fixed signals of about 25 db was obtained and moving aircrafts were clearly indicated. In a practical system the trace length would have to be increased to cover the full range of the radar equipment. This could be accomplished by using a multiple scan of vertically displaced traces or by use of a spiral sweep.

**21-10. Storage-tube Synchronizing Devices.** *Externally Synchronized Crystal-controlled Time-mark Generator.*—In many time-measurement applications it is desirable to produce a train of accurately spaced time marks which can be initiated by a phenomenon which occurs more or less at random. Pulsed *LC*-oscillators have been used successfully but their stability is not high (Chap. 4 and Vol. 20, Chap. 4). Pulsed crystal oscillators have also been used, but transient effects cause the first two or three marks to appear with incorrect spacing. A storage-tube technique has been developed that permits the use of a continuously running crystal-controlled oscillator to determine the spacing between the marks in a discontinuous pulse train while a randomly occurring pulse determines their phase. This method is shown in Fig. 21-14.

The crystal oscillator and phase splitter produce 2-phase sinusoids which are applied to the deflecting system of the storage tube and cause the spot to follow a circular trace. This circular trace causes no output from the signal plate provided precautions are taken to minimize capacity coupling between the pickup circuits and the deflecting circuits. Since sharp pulses are desired in the output, a high-pass filter that attenuates the circular-sweep frequency may be placed in the pickup amplifier circuit without detriment to the desired output signals. The beam is momen-

tarily intensified by the input pulse and a positive spot is thereby caused to appear on the circular trace. The next time the weak beam passes the spot a pulse will appear on the signal plate as the steady state is gradually restored. By making the intensified beam very strong and the normal trace very weak a large number of output pulses may be produced, each trace discharging the intensified spot by only a very small amount. In an experimental setup, using an 82-kc/sec circular sweep on a 3BP-1 tube, triangular pulses  $1\text{ }\mu\text{sec}$  wide at the base were obtained. By proper adjustment of the beam, the 100th pulse had  $\frac{1}{3}$  the amplitude of the first stored pulse. The amplitude of the 100th pulse was about 5 times the noise level (thermal noise and pickup from the deflecting system). The negative-capacitance amplifier was not used in this test though it is believed that its use would have greatly improved the operation. Attempts were made to erase the pulses that remain after the desired

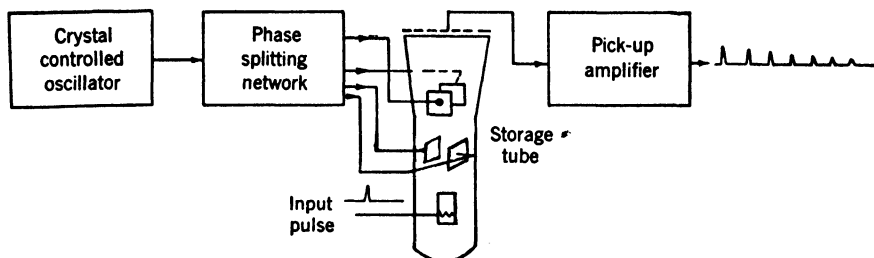


FIG. 21-14.—Storage-tube time-mark generator.

number of pulses are obtained. Modulation of the beam with a pulse having a sharp rise and a slow exponential fall that lasts for at least two cycles of the circular trace appears to be partially effective for this purpose. To reduce pickup from the deflecting system magnetic deflection appears to be desirable.

**21-11. Storage-tube Time Demodulator. Sensitive Time Discriminator Employing Storage Tube.**—The desirable characteristics of signals and indices for visual time discrimination are described in detail in Vol. 20, Chap. 7, and a number of practical displays for accurate time measurement are included. A particular configuration of signal and index called "superposition" gives much more sensitive discrimination than any of the other types. In this method the shapes of the signal and index are identical, and their superposition to give the appearance of a single trace gives a sensitive indication of time difference. A more sensitive indication, however, is obtained by displacing the two traces by a line width and adjusting the point of contact between the two nearly superposed traces. With pulse-rise times of  $20\text{ }\mu\text{sec}$ , an accuracy of time discrimination of  $0.002\text{ }\mu\text{sec}$  was obtained visually when optimal sweep speeds were used (see Vol. 20, Sec. 7-12).

An electrical method of simulating the visual-matching process is shown in Fig. 21-15. The signals *A* and *B* modulate alternate traces of the storage tube in accordance with the following sequence which is repeated in a four-pulse cycle operated by a scale-of-four circuit. On the first trace, signal *A* is selected by selector  $A_1$  and applied as vertical deflection. On the second trace signal *B* is selected by selectors  $B_1$  and  $B_3$ . The separation between the two traces produces an output in the pickup amplifier which is applied to the rms detector and filtered. On

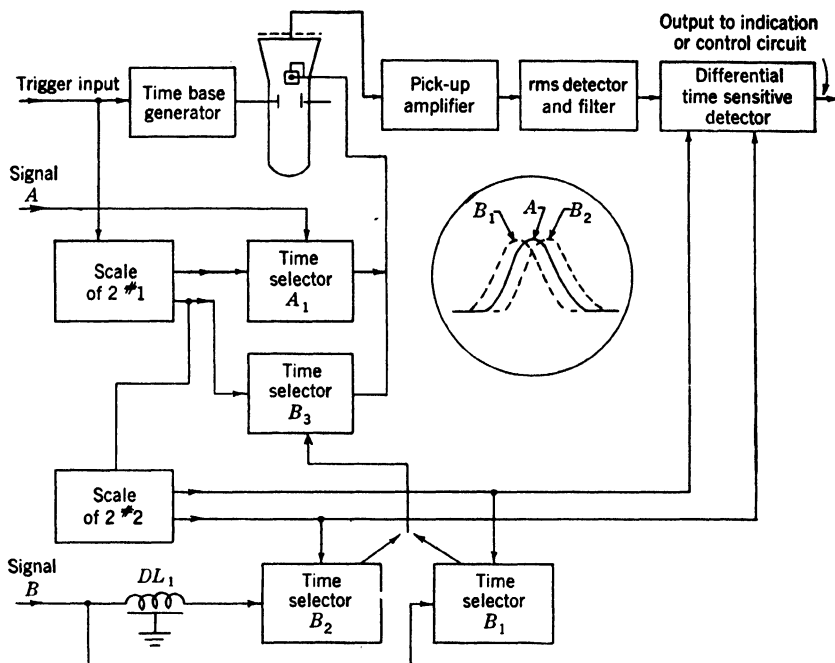


FIG. 21-15.—Use of storage tube for sensitive time discrimination.

the third trace signal *A* is again selected by selector  $A_1$ , and another pulse proportional to the average separation between *A* and *B* is obtained. On the fourth trace signal *B* is delayed by  $DL_1$ , an amount slightly greater than two trace widths, and selected by selectors  $B_2$  and  $B_3$ . A pulse proportional to the separation between  $B_2$  and  $A$  is produced and detected. On the fifth trace a pulse is produced which is again proportional to the separation of  $B_2$  and  $A$ , and the cycle repeats. The pulses proportional to the separation of  $B_1$  and  $A$  and  $B_2$  and  $A$  are compared in a differential time-sensitive detector which gives a null output when  $A$  is half way between  $B_1$  and  $B_2$ . Experimental tests of this device have not been made, but the data already presented indicate its feasibility.



## CHAPTER 22

### ELECTRICAL DELAY LINES

By VERNON HUGHES

**22-1. Introduction.**—Electrical networks can be used for delaying electrical signals because of the finite propagation time of the signals. Such “delay lines” can delay video signals faithfully for periods of time ranging from a fraction of a microsecond to about  $10\ \mu\text{sec}$ . Rise times of the output pulse of a few hundredths of a microsecond can be achieved although  $0.1\ \mu\text{sec}$  or greater is the more usual figure; rise time is proportional to delay time. Signals with a peak-to-peak amplitude of 200 volts or less are easily handled. The input and output impedances of electrical delay lines are between several hundred and several thousand ohms.

In general, electrical delay lines are of one of two types: (1) lumped-constant lines, which consist of combinations of inductors and capacitors; (2) distributed-constant lines, which are continuous structures. Both these types are low-pass filters. The first type is illustrated in Fig. 22-1 by a simple  $LC$ -filter. A common type of distributed-constant

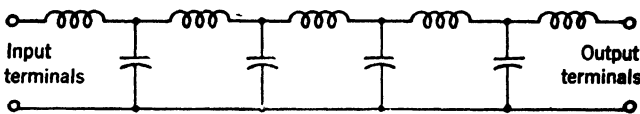


FIG. 22-1.—A low-pass  $LC$  filter type of lumped-constant electrical delay line.

delay line consists of a cylindrical-shell conductor with longitudinal slots on which is wound insulated wire in the form of a solenoid. A layer of dielectric may be placed between the solenoid and the inner cylinder. The equivalent circuit of this continuous line is a single  $LC$ -section of Fig. 22-1, where  $C$  is the capacity between the solenoid and the inner conductor and  $L$  is the inductance of the solenoid. In Vol. 17, Chap. 6 there is a detailed discussion of the design of electrical delay lines of both types.

The uses of electrical delay lines for the synchronization of waveforms and for marker generation are treated in 22-11. A more detailed discussion of rectangular-pulse generators using electrical delay lines is in Chap. 6; coder and decoder applications are treated in Chap. 10, Vol. 20. Some theoretical considerations concerning electrical delay lines will now be discussed.

## THEORY OF ELECTRICAL DELAY LINES

**22-2. Propagation Function and Characteristic-impedance Function.**

**Importance.**—It is both possible and useful to discuss the behavior of electrical delay lines in terms of three complex functions of frequency—the propagation function,  $\gamma(\omega)$ , and two image-impedance functions,  $Z_{01}(\omega)$  and  $Z_{02}(\omega)$ .

The lumped-constant delay line involves no sources of emf, and its components are ordinary lumped constants. Hence it is a passive linear network. It is in general a four-terminal network; accordingly, its behavior can be described<sup>1</sup> in terms of  $\gamma(\omega)$ ,  $Z_{01}(\omega)$ , and  $Z_{02}(\omega)$ . Usually the delay line is symmetrical; that is, two pairs of terminals cannot be distinguished. In this case  $Z_{01}(\omega)$  and  $Z_{02}(\omega)$  are equal and their common value,  $Z_0(\omega)$ , is called the “characteristic-impedance function.”

The distributed-constant delay line also is in general a linear, passive symmetrical four-terminal network, and it will be found that the prediction of the behavior of a distributed-constant delay line based on a use of  $Z_0(\omega)$  and  $\gamma(\omega)$  is in good agreement with the experimental results.

**Definitions.**—The definitions of the functions  $\gamma(\omega)$ ,  $Z_{01}(\omega)$ ,  $Z_{02}(\omega)$ , and  $Z_0(\omega)$  can be given with the aid of Fig. 22-2, in which the box with four terminals represents an electrical delay line. Under steady-state conditions<sup>2</sup>

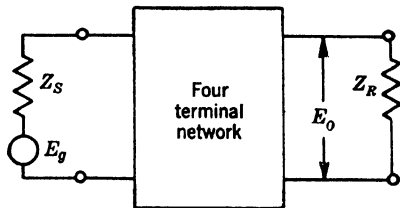


FIG. 22-2.—A four-terminal network representing an electrical delay line.

$$E_o = \frac{E_g(Z_{01}e^\gamma + Z_{02}\gamma_R e^{-\gamma})}{(Z_s + Z_{01})(e^\gamma - \gamma_s \gamma_R e^{-\gamma})}, \quad (1)$$

where

$Z_{01}$ ,  $Z_{02}$  are the image-impedance functions,

$\gamma$  is the propagation function,

$Z_s$  is the sending-end impedance,

$Z_R$  is the terminating impedance,

$$\gamma_R = \frac{Z_R - Z_{01}}{Z_R + Z_{02}},$$

$$\gamma_s = \frac{Z_s - Z_{02}}{Z_s + Z_{01}}.$$

In the figure  $E_g$  is a single-frequency voltage that equals  $|E_g|e^{j\omega t}$ . The image-impedance function  $Z_{01}$  is the impedance looking into an

<sup>1</sup> See E. A. Guillemin, *Communication Networks*, Vol. II, Wiley, New York, 1942, Chap. 4.

<sup>2</sup> *Ibid.* p. 165.

infinitely long chain of identical structures, all of which are oriented with their Ends 1 on the left and Ends 2 on the right. There is a similar physical interpretation for  $Z_{02}$ . If the box is symmetrical with respect to terminals 1 and 2,  $Z_{01}$  and  $Z_{02}$  are equal and their common value,  $Z_0$ , is the characteristic impedance. If  $Z_R = Z_{01}$ , Eq. (1) reduces to Eq. (2).

$$\left. \begin{aligned} E_0 &= E_g \frac{Z_{01}}{Z_s + Z_{01}} e^{-\gamma} \\ &= |E_g| \frac{Z_{01}}{Z_s + Z_{01}} e^{j\omega t - \gamma} \end{aligned} \right\} \quad (2)$$

If  $Z_{01}$  and  $Z_s$  are pure resistances, as is usually approximately true, the following physical interpretation of  $\gamma$  can be made. If  $\gamma = \gamma_1 + j\gamma_2$ , where  $\gamma_1$  and  $\gamma_2$  are real functions of frequency, then except for the constant factor  $Z_{01}/(Z_s + Z_{01})$ ,  $e^{-\gamma}$  is the ratio of the amplitude of the output voltage  $E_0$  to that of the input voltage  $E_g$ , and the function  $\gamma_2$  is the phase angle of  $E_0$  relative to  $E_g$ .  $\gamma_1$  is called the "attenuation function" or "amplitude function," and  $\gamma_2$  is called the "phase function."

*Usefulness.*—The primary interest is in the response of electrical delay lines to video pulses, and the usefulness of discussing delay-line operation in terms of  $\gamma$ ,  $Z_{01}$ , and  $Z_{02}$  is due to the fact that this response can be deduced from a knowledge of these three functions. It will be shown later that for any line these functions can always be determined experimentally and can sometimes be determined theoretically.

#### RESPONSE OF NETWORKS WITH PARTICULAR $\gamma$ AND $Z_0$ FUNCTIONS

The response of a network to a step function is an important indication of the response of a network to video pulses, since a rectangular pulse can be considered as the superposition of two step functions of opposite polarity and equal amplitude whose steps are separated by a time interval equal to the duration of the pulse. In the following sections there is presented the response of certain idealized networks to step-function or pulse inputs; a study of these responses is most useful in predicting the behavior of actual delay lines.

**22-3. Ideal Transmission Network and Distortion.**—In Fig. 22-2  $Z_R$  is taken equal to  $Z_{01}$ ,  $Z_s$  and  $Z_{01}$  are pure resistances, and  $E_g$  is a step-function voltage. According to the well-known methods of Fourier analysis<sup>1</sup> the output voltage  $E_0$  is

$$E_0 = \int_{-\infty}^{\infty} g(\omega) H(\omega) e^{j\omega t} d\omega \quad (3)$$

<sup>1</sup> See E. A. Guillemin, *op. cit.*, Chap. 2; and Vol. 18, Chap. 1.

where

$$H(\omega) = \frac{Z_{01}}{Z_s + Z_{01}} e^{-\gamma}, \text{ the network function,}$$

$$g(\omega) = \frac{E}{2\pi\omega}, \text{ the Fourier transform of a step-function voltage, } U(t)$$

$$U(t) = \begin{cases} 0, & t < 0. \\ E, & t > 0. \end{cases}$$

If  $\gamma = K + j\omega t_d$ , where  $K$  and  $t_d$  are real constants,<sup>1</sup> it will be seen that this is a distortionless network. Since  $Z_{01}$  and  $Z_s$  are resistances,

$$\left. \begin{aligned} E_0 &= \frac{Z_{01}}{Z_s + Z_{01}} e^{-K} \int_{-\infty}^{+\infty} g(\omega) d\omega e^{j\omega(t-t_d)} \\ &= \frac{Z_{01}}{Z_s + Z_{01}} e^{-K} U(t - t_d) \end{aligned} \right\} \quad (4)$$

Therefore, except for the reduction in amplitude by the factor

$$\frac{Z_{01}}{Z_s + Z_{01}} e^{-K},$$

the output voltage is also a step-function voltage, but the step does not appear at the output until a time interval  $t_d$  after it is impressed on the input. Thus a delay of  $t_d$  with faithful reproduction is achieved with a network having an attenuation or amplitude function, which is a constant, and a phase function, which is a linear function of frequency. When a network has a  $\gamma_1$  that is not constant or a  $\gamma_2$  that is not a linear function of frequency, it is said that the network has amplitude distortion or phase distortion. In practice, most networks involve both amplitude and phase distortion.

**22-4. Amplitude Distortion. Idealized Low-pass Filter.**—The idealized low-pass filter characteristics are shown in Fig. 22-3. It will be noticed that only amplitude distortion is present. The response of a network with such a propagation function is<sup>2</sup>

$$E_0 = E' \left\{ \frac{1}{2} + \frac{1}{\pi} S_i[\omega_c(t - t_d)] \right\}, \quad (5)$$

where

$$\begin{aligned} S_i[\omega_c(t - t_d)] &= \int_0^{\omega_c(t-t_d)} \frac{\sin u}{u} du \\ E' &= e^{-K} \frac{Z_{01}}{Z_s + Z_{01}} E_g \end{aligned}$$

The output is a delayed and distorted reproduction of the input (see

<sup>1</sup> This is a physically realizable form of propagation function.

<sup>2</sup> E. A. Guillemin, *op. cit.*, p. 479.

Fig. 22-4), If the delay time is defined as the time interval between the time of appearance of the step at the input and the time at which the output pulse attains one-half its final value, it equals  $t_d$ , which is the slope of the characteristic. The step at the output has a finite rise time which it is convenient to define as

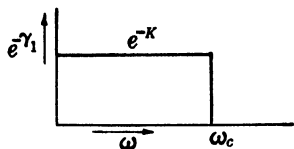


FIG. 22-3.—Amplitude and phase characteristics of ideal low-pass filter;  $\omega_c$  = cutoff frequency.

$$\tau_a = \frac{E'}{\left(\frac{dE_0}{dt}\right)_{t=t_d}}$$

Hence, by Eq. (5),

$$\tau_a = \frac{\pi}{\omega_c}$$

The rise time is thus inversely proportional to the width of the pass band of the low-pass filter. For an actual low-pass network the pass band is not sharply defined; if the 3-db bandwidth is chosen and the rise time from 0.1 to 0.9 amplitude is taken, then  $\tau$  times (bandwidth) = 0.25 to 0.3.

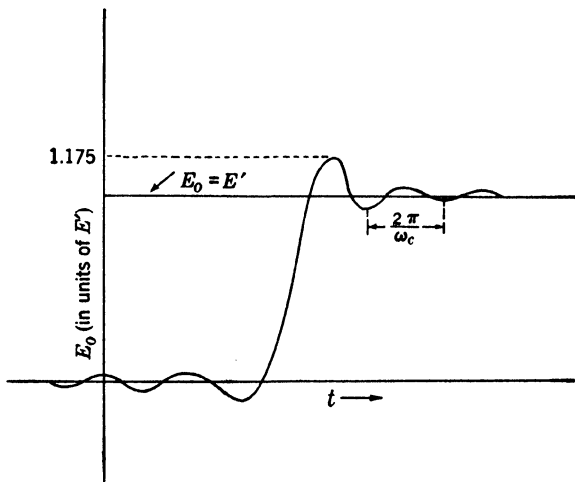


FIG. 22-4.—Response of ideal low-pass filter to a step function.

The ripples appearing on the top of the pulse have a frequency of approximately  $\omega_c$ . The existence of a response before  $t = 0$  is, of course, a physical impossibility and is an indication that the  $\gamma_1$  and the  $\gamma_2$  assumed are incompatible.<sup>1</sup>

<sup>1</sup> See Vol. 18. Despite the physical unrealizability of the ideal low-pass filter, a study of its behavior is valuable in understanding the response of actual

*Other Cases of Amplitude Distortion.*—The attenuation characteristic of distributed-constant delay lines is often well represented by  $\gamma_1 = K\omega$ . If a network has  $\gamma = K\omega + j\omega t_d$ , then the response to a unit step function is (see Fig. 22-5)

$$E = \frac{Z_{01}}{Z_s + Z_{01}} \left[ \frac{1}{\pi} \arctan \frac{t - t_d}{K} + \frac{1}{2} \right].$$

As for the ideal low-pass filter, the delay time is  $t_d$ . The rise time, defined as the maximum amplitude of the output voltage divided by the rate of change of voltage at  $t = t_d$ , is  $K\pi$ . There are no overshoots or ripples in this case.

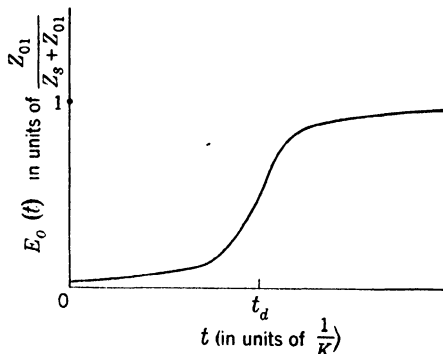


FIG. 22-5.—Response of network with  $\gamma = K\omega + j\omega t_d$  to a unit step function applied at  $t = 0$ .

The step function has an odd symmetry with respect to the time at which the discontinuity occurs, and the single pulse has an even symmetry with respect to the time corresponding to the center of the pulse. It is easily seen by an application of Fourier analysis that these symmetries are not affected by amplitude distortion alone. It is evident in Figs. 22-4 and 22-5 that these symmetries are not affected by passage through the networks with amplitude distortion. More generally, it can be shown by Fourier analysis that amplitude distortion alone does not affect the symmetry of any signal. It will be seen in the next section, however, that phase distortion does introduce asymmetry.

**22-5. Phase Distortion. Some Examples.**—Networks having only phase distortion, like those having only amplitude distortion, are not encountered, but a consideration of certain networks of this type is

---

low-pass filters whose characteristics approximate those of the ideal filter. This is true because by only slight modifications in the assumptions about the characteristics of the ideal low-pass filter a physically realizable structure is obtained; it is very reasonable to suppose that these modifications will not materially affect the main features of the response.

instructive. In Figs. 22-6 and 22-7 are shown the outputs from a network with  $\gamma = j \left( b_0 \omega + b_1 \sin \frac{\omega}{2f_h} \right)$ , where  $f_h$  is the highest frequency considered in the input signal (a 1- $\mu$ sec pulse). Both cases considered involve phase distortion that is larger than that ordinarily exhibited by delay lines. Ripples and asymmetry are introduced by the phase distortion. In the case for which the slope of the phase characteristic decreases with frequency, high-frequency ripples appear before the dis-

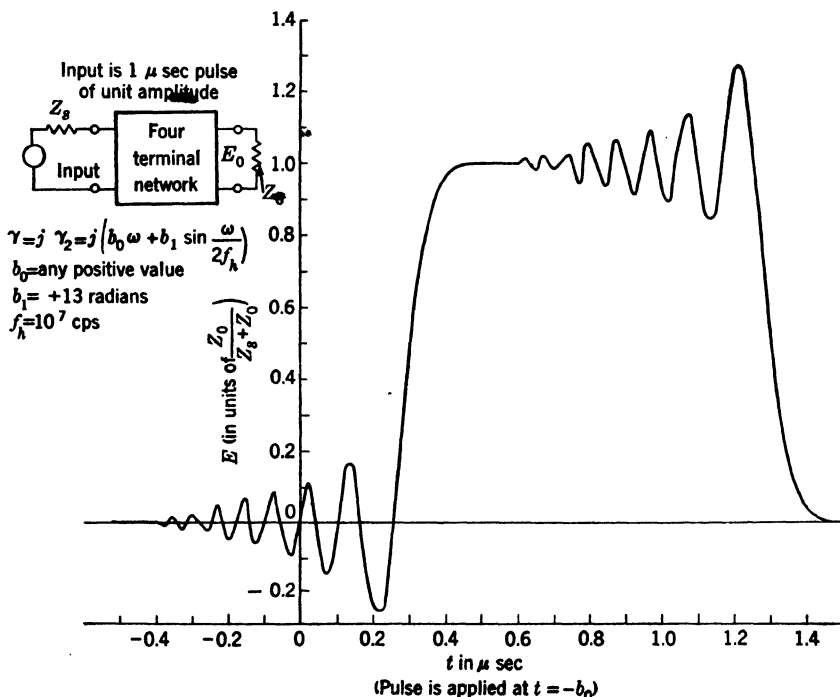


FIG. 22-6.—Output voltage vs. time (positive  $b_1$ ).

continuities of the pulse (Fig. 22-6). In the other case these ripples appear after the discontinuities of the pulse (Fig. 22-7).<sup>1</sup>

It can be shown in general for small phase distortion that when the phase function is convex upward, ripples appear before the discontinuities and the asymmetry is as shown in Fig. 22-7, and, when the phase function is convex downward, ripples appear after the discontinuities and the asymmetry is as shown in Fig. 22-6. Proof is readily given by the method of "paired echoes,"<sup>2</sup> according to which

<sup>1</sup> These graphs were computed with the approximation that 10 Mc/sec is the highest frequency present in the 1- $\mu$ sec input pulse.

<sup>2</sup> H. A. Wheeler, "Paired Echoes," *Proc. I.R.E.*, **27**, 359 (June 1939).

$$E_0(t) = J_{-1}(-b_1) U_0\left(t - b_0 - \frac{1}{2f_h}\right) + J_0(-b_1) U_0(t - b_0) \\ + J_1(-b_1) U_0\left(t - b_0 + \frac{1}{2f_h}\right),$$

where

$E_0(t)$  is the output voltage for a 1- $\mu$ sec pulse input voltage

$U_0(t)$  is a unit-amplitude 1- $\mu$ sec pulse,

$$\gamma(\omega) = j\left(b_0\omega + b_1 \sin \frac{\omega}{2f_h}\right); b_1 \ll 1,$$

$f_h$  = highest frequency considered in 1- $\mu$ sec pulse,

$J$ 's are Bessel functions.

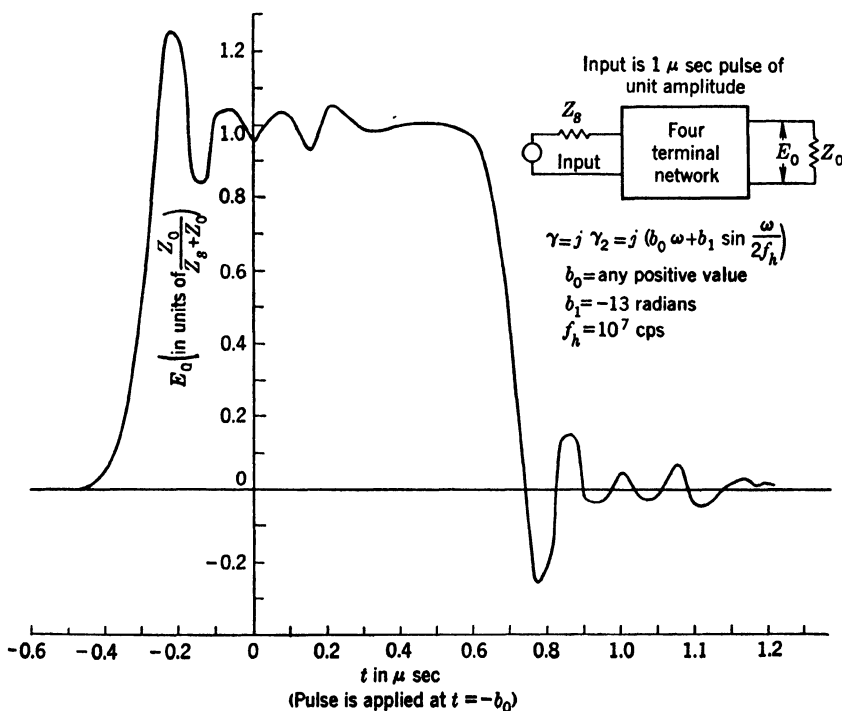


FIG. 22-7.—Output voltage vs. time (negative  $b_1$ ).

Since  $b_1$  is small,  $E_0(t)$  can be written

$$E_0(t) = +\frac{b_1}{2} U_0\left(t - \frac{1}{2f_h}\right) + U_0(t) - \frac{b_1}{2} U_0\left(t + \frac{1}{2f_h}\right). \quad (6)$$

These three terms and their sum are plotted in Fig. 22-8. The case plotted is for  $b_1$  positive, which implies a  $d\gamma/d\omega$  that decreases with fre-



quency. This is seen to have asymmetry of the same type as that shown in Fig. 22-6. In a similar way it can be shown that if  $b_1$  is a small negative number, the type of asymmetry shown in Fig. 22-7 will be obtained.

*A Qualitative Approach.*—A useful way of regarding phase distortion, which can be justified rigorously, is merely suggested here.<sup>1</sup> The Fourier integral expression for the response of a network to a step function, is

$$E_0 = \int_{-\infty}^{+\infty} \frac{1}{j2\pi\omega} e^{j\omega t} e^{j\theta(\omega)} d\omega,$$

where  $\theta(\omega)$ , a nonlinear function of frequency, is the phase characteristic of the network, whose amplitude characteristic,  $e^{-\gamma_1}$ , is assumed to be

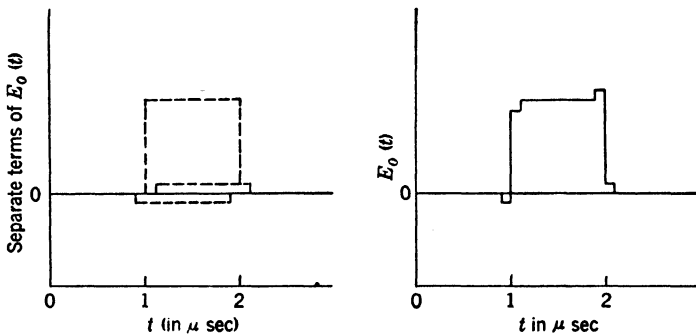


FIG. 22-8.—Paired-echoes method of analyzing phase distortion. [Equation (1);  $b_1 = 0.1$ ,  $b_0 = 1 \mu\text{sec.}$ ]

1 for all frequencies. The integral is difficult to evaluate because  $\theta(\omega)$  is a nonlinear function of frequency. It can be written as the sum of a large number of integrals of the form

$$\int_{+\omega_i}^{+\omega_i + \Delta\omega} \frac{1}{j2\pi\omega} e^{j\omega t} e^{j\theta(\omega)} d\omega,$$

in which  $\Delta\omega$  is so small that it is a good approximation to regard  $\theta(\omega)$  as a linear function of  $\omega$  in the range from  $\omega_i$  to  $\omega_i + \Delta\omega$ , and to regard  $1/\omega$  as a constant. This elemental integral indicates that frequency components in the neighborhood of  $\omega_i$  will be delayed by a time  $\left. \frac{d\theta}{d\omega} \right|_{\omega=\omega_i}$ .

Applying this concept of the delay of a single frequency component to the type of network with a phase characteristic  $\gamma_2 = b_0\omega + b_1 \sin \omega/2f_h$  ( $b_0, b_1$  positive), it is seen that the higher-frequency components are delayed a shorter time than the low-frequency components; hence if a pulse is put into this network, a high-frequency ripple preceding the discontinuous portions of the pulse is expected (Fig. 22-7). For the

<sup>1</sup> E. A. Guillemin, *op. cit.*, p. 492.

network with  $\gamma_2 = b_0\omega - b_1 \sin \omega/2f_h$  ( $b_0, b_1$  positive), high-frequency ripples appearing after the discontinuous portions of the pulse (see Fig. 22-6) are expected.

**22.6. Amplitude and Phase Distortion.**—All practical delay lines exhibit both amplitude and phase distortion and generalizations about

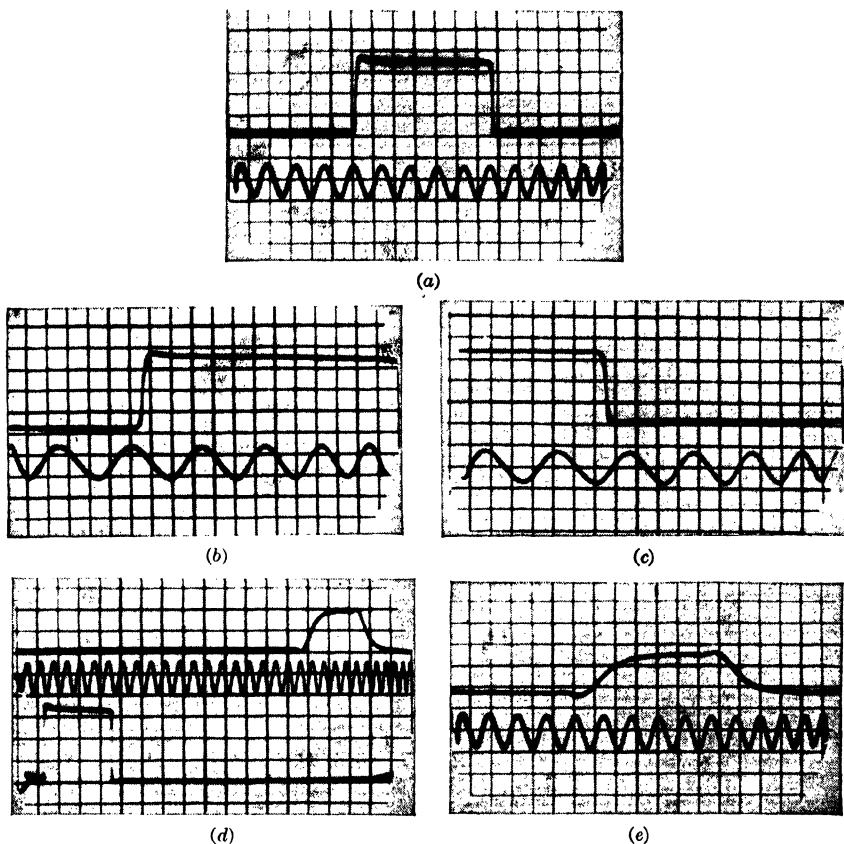
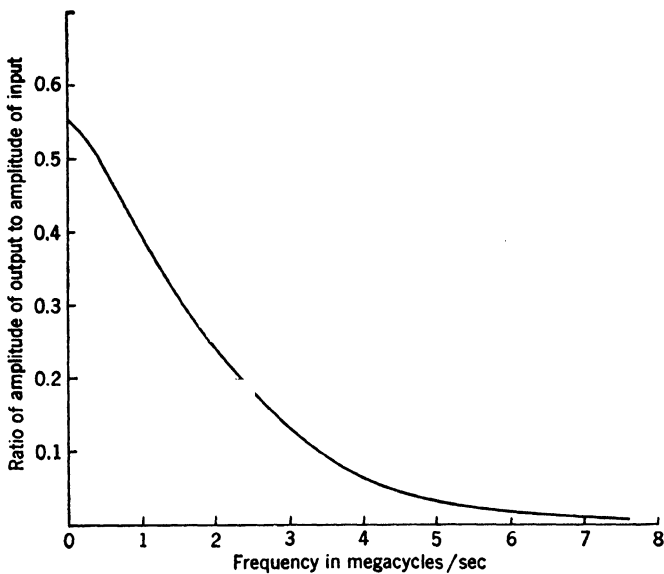
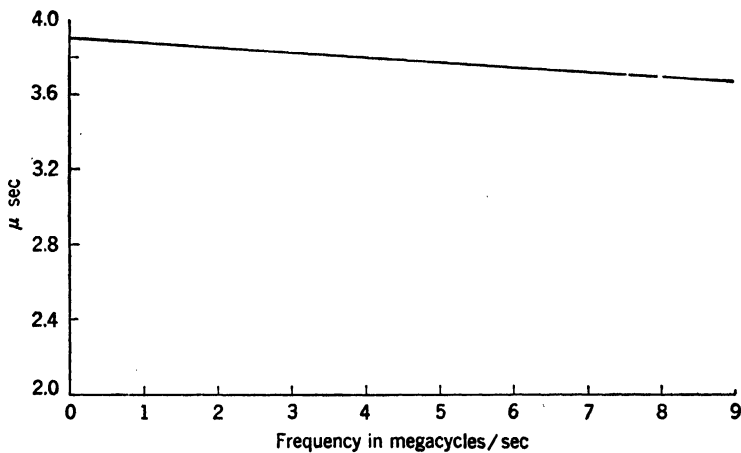


FIG. 22-9.— Photographs of input and output pulses for 4- $\mu$ sec delay line. (a) 1- $\mu$ sec input pulse and 5-Mc/sec. calibrating sine wave, (b) leading edge of input pulse and 5-Mc/sec-calibrating sine wave, (c) falling edge of input pulse and 5-Mc/sec-calibrating sine wave, (d) input pulse, delayed output pulse, and 5-Mc/sec-calibrating sine wave, (e) output pulse and 5-Mc/sec-calibrating sine wave.

the response are difficult to make. In some cases it is apparent that either amplitude or phase distortion alone is the more important and in this case the results of the previous sections can be applied. Often, however, a numerical solution must be undertaken, or crude estimates of the distortion are made on the basis of idealized cases such as were considered in the previous sections. These estimates usually neglect the



(a)



(b)

FIG. 22-10a.—Amplitude characteristic of 4- $\mu$ sec delay line. FIG. 22-10b.—Phase characteristic,  $\theta(\omega)$ , divided by  $\omega$  vs. frequency for 4- $\mu$ sec delay line.

interaction of phase and amplitude distortion. It is often possible to specify the limits within which the amplitude and phase distortion must be kept in order that the distortion of the pulse shall be within certain limits. For example, the 3-db bandwidth may be specified in order that the rise time shall be less than a certain value.

*Response of Line with Large Amplitude and Phase Distortion.*—The results of a numerical calculation on a high-distortion 4- $\mu$ sec delay line will now be presented. Figure 22·9 shows a number of photographs taken on the input and output pulse. It is seen from Figs. 22·9*b* and 22·9*c* that the rise and fall times of the input pulse are about 0.02  $\mu$ sec.

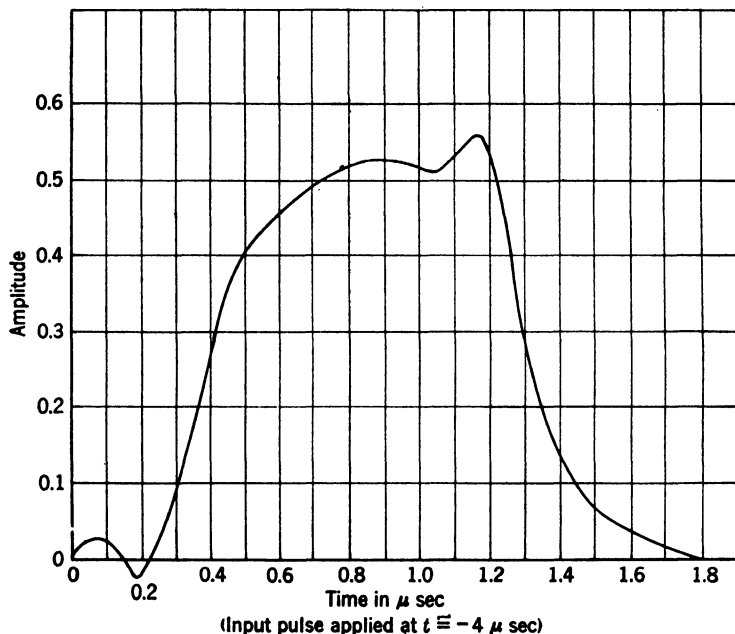


FIG. 22-11.—Computed output pulse from line with characteristics shown in Fig. 22-10 for a 1- $\mu$ sec unit-amplitude input pulse.

The output pulse is very much distorted. The rise and fall times are about 0.3  $\mu$ sec; the pulse is attenuated to about one-half its original amplitude and an undershoot and overshoot appear at the beginning and end of the pulse, respectively. The amplitude and phase characteristics of the 4- $\mu$ sec delay line are plotted in Fig. 22-10; these characteristics were measured experimentally as described in Sec. 22-13 and 22-14. In Fig. 22-11 is shown the output pulse to be expected when a perfect 1- $\mu$ sec pulse is put into a delay line with such characteristics.<sup>1</sup> It can be seen that the computed output pulse agrees very well with the observed out-

<sup>1</sup> The long and laborious computation was made by the method of multiple echoes. See H. A. Wheeler, *op. cit.*, Appendix.

put pulse; indeed, quantitative measures of the salient features of the two agree within a few per cent. This example illustrates the adequacy of the phase and amplitude characteristics for specifying the behavior of a delay line.

**22-7. Reflection.**—The only case that has been considered thus far is that in which the delay line is perfectly matched at its receiving end and in which  $Z_s$  and  $Z_{01}$  are pure resistances. In practice it is usually possible to terminate the delay line nearly perfectly with a resistance; that is,  $Z_{01}$  is a resistance and  $Z_s$  is often a resistance.

If the termination is perfect, that is,  $Z_R = Z_{01}$ , no energy of the input pulse will return to the input terminals, or, equivalently, there is no reflection of energy at the output terminals. If  $Z_{01}$  or  $Z_s$  are not pure resistances, there will still be no reflection if  $Z_R = Z_{01}$ , but the results of the last section would have to be modified to take into account the frequency dependence of  $Z_{01}$  and  $Z_s$  [see Eqs. (2) and (3)]. If the termination is not perfect, a fraction of the energy of the input pulse that reaches the output will be reflected. The ratio of the amplitude of the reflected wave to the amplitude of the incident wave is<sup>1</sup>

$$\frac{Z_{02}(Z_R - Z_{01})e^{-2\gamma}}{Z_{01}(Z_R + Z_{02})}.$$

The shape of the pulse at the output will be affected by a mismatch at the receiving terminals [see Eq. (2)]. If  $Z_s \neq Z_{02}$ , another reflection at the input terminals will occur.

The reflection phenomenon is illustrated in Fig. 22-12. It is seen that when the output is terminated in its characteristic impedance of 1150 ohms, no reflected wave is observed at the input  $a$ . If the output is terminated in a resistance greater than the characteristic impedance, a reflected pulse of the same polarity as the input pulse is observed at the input. On the other hand if the output is terminated in a resistance less than the characteristic impedance, a reflected pulse of polarity opposite to that of the input pulse is seen at the input. The magnitude of the reflected pulse depends on the amount of mismatch at the output terminals. A series of reflected pulses is present at the input and output when both input and output are improperly terminated (Fig. 22-12*h*.)

One important use of reflection is in the formation of a series of pulses from one pulse (Chap. 6). This is closely related to the coding problem. Secondly, reflection can be considered to double the effective length of a delay line.

### TYPES OF DELAY LINES

Since the design of various types of delay lines is treated in great detail in Vol. 17, Chap. 6, only a very brief discussion will be included

<sup>1</sup> E. A. Guillemin, *op. cit.*, p. 165.

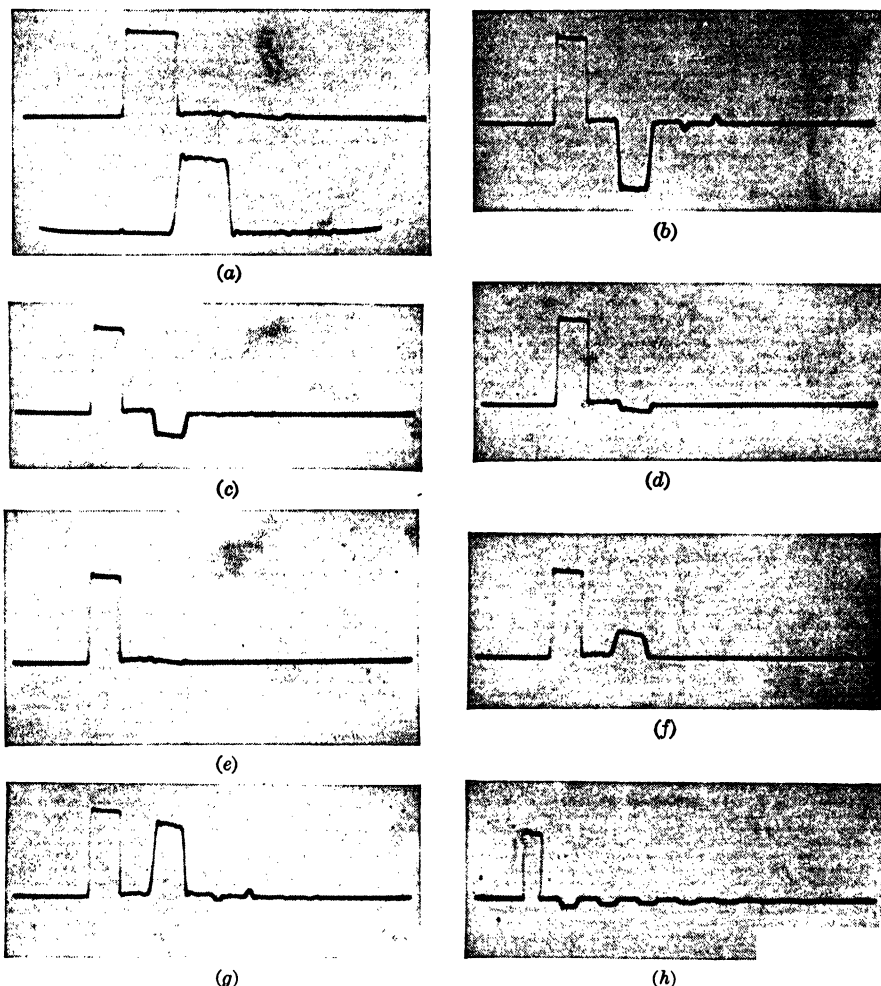


FIG. 22-12.—Series of pictures involving 1- $\mu$ sec input pulses and a 1- $\mu$ sec line with various types of termination.  $Z_0 = 1150$  ohms for the line. (a) Input and output waveforms. Line properly terminated at both input and output. (b) Waveform at input with output short-circuited and input properly terminated. (c) Waveform at input with output terminated in 575 ohms and input properly terminated. (d) Waveform at input with output terminated in 950 ohms and input properly terminated. (e) Waveform at input with output and input properly terminated. (f) Waveform at input with output terminated in 2300 ohms and input properly terminated. (g) Waveform at input with output open-circuited and input properly terminated. (h) Waveform at input with output short circuited and input terminated in 100 ohms.

here. As has been mentioned, delay lines are of one of two types: lumped constant or distributed constant.

**22-8. Lumped-constant Lines.**—Any low-pass filter constructed of lumped-constant elements can serve as a delay line. By employing the

well-known techniques of conventional filter theory,<sup>1</sup> it is possible to design lines with widely varying characteristics.

The simplest type of delay line is the constant- $k$  low-pass filter whose

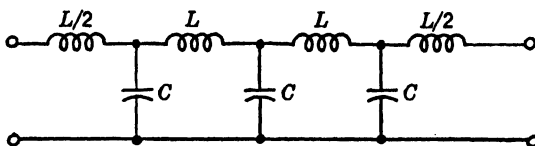


FIG. 22-13.—Constant- $k$  low-pass filter with half- $T$  section terminations.

form is indicated in Fig. 22-13. The propagation and characteristic-impedance functions are given by

$$\left. \begin{aligned} \gamma_1 &= 0 \\ \gamma_2 &= 2n \sin^{-1} \left( \frac{\omega}{\omega_c} \right) \end{aligned} \right\} \quad (0 \leq \omega \leq \omega_c)$$

$$\left. \begin{aligned} \gamma_1 &= 2n \cosh^{-1} \left| \frac{\omega}{\omega_c} \right| \\ \gamma_2 &= \pi n \end{aligned} \right\} \quad \omega_c \leq \omega$$

where

$n$  = number of sections of filter,

$\omega_c = \frac{2}{\sqrt{LC}}$  = cutoff frequency,

$$Z_0 = \sqrt{\frac{L}{C}} \sqrt{1 - \left( \frac{\omega}{\omega_c} \right)^2}.$$

Thus there is no attenuation over the pass band, and the delay of a frequency group centered at  $\omega$  is

$$\tau = \frac{d\gamma_2}{d\omega} = \frac{2n}{\omega_c} \frac{1}{\sqrt{1 - \left( \frac{\omega}{\omega_c} \right)^2}} = n \sqrt{LC} \frac{1}{\sqrt{1 - \left( \frac{\omega}{\omega_c} \right)^2}}.$$

For  $\omega/\omega_c \ll 1$  this time is a constant and is inversely proportional to  $\omega_c$ . With this same approximation,  $Z_0 = \sqrt{L/C}$ .

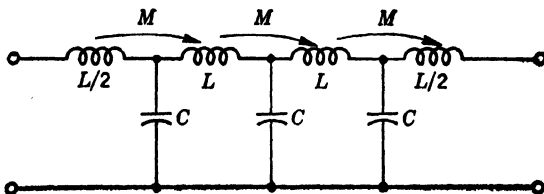


FIG. 22-14.—Low-pass  $LC$  filter with mutual inductance between adjacent coils.

The low-pass  $LC$  filter with mutual coupling shown in Fig. 22-14 can exhibit considerable improvement over the constant  $K$  low-pass  $LC$ -filter

<sup>1</sup> See E. A. Guillemin, *op. cit.*, Chap. 9.

as regards constancy of delay as a function of frequency. If the coefficient of coupling between adjacent coils is 0, the structure is a low-pass filter that has a convex phase characteristic; if the coefficient of coupling is 1, the structure is an all-pass filter with a concave phase characteristic. It has been found that for a coefficient of coupling of about 0.36 the most linear phase characteristic is achieved.<sup>1</sup> This result assumes that there is appreciable coupling only between adjacent coils.<sup>2</sup>

**22-9. Distributed-constant Lines.**—The distributed-constant line consists of a conductor, often of cylindrical shape, on which is wound a solenoidal conductor. The two conductors are separated by a dielectric layer, and the inner conductor has lengthwise longitudinal slots or is otherwise constructed so that the magnetic flux of the solenoid can penetrate the entire area within the solenoid. Roughly speaking, the line can be regarded as a transmission line along which the “guided wave” follows the solenoid. It is useful to consider the equivalent circuit shown in Fig. 22-15 for the distributed-constant line.<sup>3</sup> In this figure  $C$  is the capacity between the turns of wire and the cylindrical conductor and  $L$  is the total inductance of the solenoid. The total inductance of the solenoid is computed under the assumption that the cylindrical conductor is absent. The turn-to-turn capacity along the line is neglected.

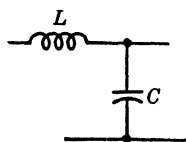


FIG. 22-15.—  
Equivalent circuit  
of distributed-constant delay line.

The capacitor  $C$  is independent of frequency, but the value of the inductance is a decreasing function of frequency. At low frequencies the inductance is

$$L = 10^{-9} \cdot \pi^2 \cdot n^2 d^2 k \quad \text{henrys,}$$

where

$d$  = diameter of coil,

$k$  = Nagaka's correction factor for coils of finite length (see Vol. 17),

$n$  = number of turns.

To obtain this value of inductance it is assumed that the actual solenoid is a current sheet along which all the currents are of the same phase. This is approximately true at low frequencies, but at higher frequencies the wavelength is comparable to the length of the coil and the currents along the line are out of phase. It is clear that this will result in a reduction of the inductance at high frequencies.

The delay time is given by  $\tau = \sqrt{LC}$  and the impedance by

$$Z_0 = \sqrt{\frac{L}{C}}.$$

<sup>1</sup> E. L. C. White, I.E.E. Convention, March 1946.

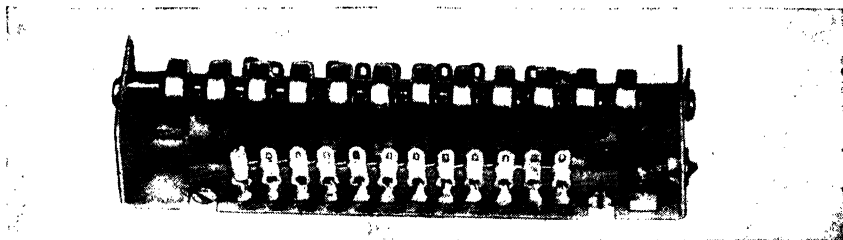
<sup>2</sup> See Vol. 17 of the Series for construction details and a further discussion.

<sup>3</sup> No attempt is made to prove the validity of the equivalent circuit.

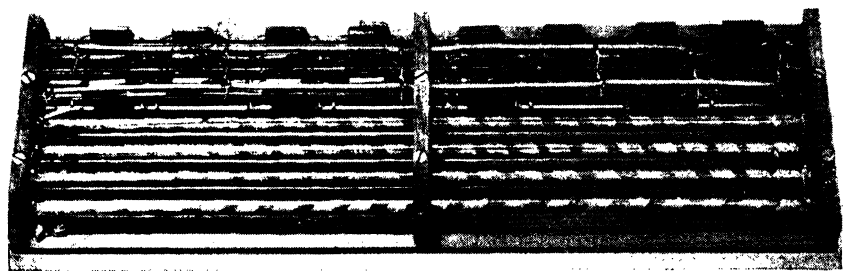




The amplitude attenuation can be corrected by the use of amplifiers. A form of amplifier that was used to boost the high frequencies relative to the low frequencies is shown in Fig. 22-17. A 30- $\mu$ sec delay line was constructed by the use of some ten elemental structures of the type shown in the figure. This 30- $\mu$ sec delay line did not produce much more distortion than did one of its component delay lines.



(a)



(b)

FIG. 22-18a.—Lumped-constant 1- $\mu$ sec electrical delay line.FIG. 22-18b.—Distributed-constant 4- $\mu$ sec electrical delay line with compensating networks.

Photographs of a 1- $\mu$ sec distributed-constant line with internal phase correction and of a 10- $\mu$ sec lumped-constant line employing mutual inductance are shown in Figs. 22-18a and 22-18b.

### USES OF DELAY LINES

This subject is treated in various parts of this volume and other volumes. Reference will be made here to these treatments, and a brief discussion will be given of applications not mentioned elsewhere.

**22-11. Synchronization and Generation of Waveforms.**—The synchronization of waveforms is an obvious application. One important aspect is to delay waveforms appearing near the time at which the operation of a measuring instrument is initiated so that they can be examined at a time when the measuring instrument is operating properly. Test oscilloscopes and radar-range-measuring systems often use delay lines in this way

Delay lines providing a variable time delay can be used for time modulation (Chap. 13).

The generation of waveforms is a second general category for applications of delay lines. Their use in pulse generation is treated in Chap. 6. Circuits are described in which rectangular pulses are generated from step functions and short pulses are derived from long pulses. The generation of a series of pulses is also discussed. Many coder systems utilize electrical delay lines to generate series of pulses with various characteristics (see Chap. 6 of this volume and Chaps. 10 and 11 of Vol. 20). Decoders sometimes use delay lines to analyze a series of pulses (see Chap. 10).

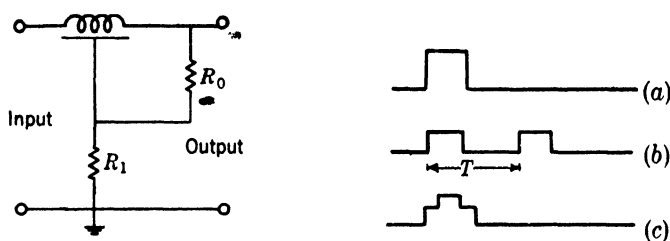


FIG. 22-19.—Example of waveform generation with a delay line of characteristic impedance  $R_0$ . (a) Input pulse; (b) output pulse when delay time  $\tau$  of line is greater than pulse width; (c) output pulse when  $\tau$  is less than pulse width.

An example of the generation of waveforms with delay lines is given in Fig. 22-19. If a pulse of duration shorter than the delay time of the line is applied to the input terminals, two pulses separated by the delay time of the line are observed at the output. If, on the other hand, the input pulse has a duration greater than the delay time of the line, a waveform of the staircase type will be observed at the output. These cases are illustrated in Fig. 22-19b. Many other waveforms can be built up by cascading other sections similar to the one shown and by varying the value of  $R_1$ .

**22-12. High-impedance Cable.**—Occasionally, certain types of delay lines are used as high-impedance connecting cables (see Vol. 17, Chap. 1). This application does not utilize the delaying property of the line; indeed, it is usually desirable to have the delay introduced by the line as small as possible. Ordinary coaxial cables have impedances of 50 to 100 ohms; their capacities vary from 10 to 30  $\mu\text{mf}/\text{ft}$ , and their inductances vary from about 0.01 to 1  $\mu\text{h}/\text{ft}$ . These coaxial cables would impose an undesirable loading upon many video circuits. Distributed-parameter delay lines have been especially designed to serve as high-impedance connecting cables for video-circuit work. These lines have high impedances because of their high inductance and low capacitance per unit length.

A typical line has an impedance of 950 ohms. Its capacitance is

42  $\mu\text{f}/\text{ft}$ ; its inductance is 42  $\mu\text{h}/\text{ft}$ . The delay introduced is about 0.042  $\mu\text{sec}/\text{ft}$ ;<sup>1</sup> this figure is to be compared with 0.003  $\mu\text{sec}/\text{ft}$ , which is as large a delay as would ordinarily be obtained with a coaxial cable. The attenuation of the high-impedance line at 5 Mc/sec is 0.14 db/ft. Its outer diameter is 0.340 in.

### MEASUREMENT OF PROPERTIES OF DELAY LINES<sup>2</sup>

**22-13. Attenuation Function  $\gamma_1$ .**—The attenuation function  $\gamma_1$  can be most readily determined by means of the experiment indicated in Fig. 22-20. The line is terminated at both ends in its characteristic impedance, and the voltage across the input and that across the output are measured. The ratio of the voltage across the output to that across the input is  $e^{-\gamma_1}$  [Eq. (2)].

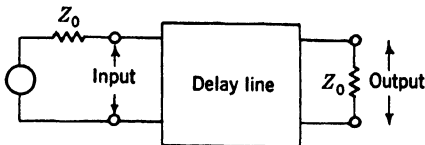


FIG. 22-20.—Illustrating a method of measuring attenuation of delay line.

Another method of measuring  $\gamma_1$ , which does not require perfect termination of the line, is based on the formula<sup>3</sup>

$$\gamma = \frac{1}{2} \ln \left( \frac{\sqrt{Y_{11}Z_{11}} + 1}{\sqrt{Y_{11}Z_{11}} - 1} \right). \quad (7)$$

where  $Z_{11}$  is the open-circuit impedance of the line seen from the input, and  $Y_{11}$  is the short-circuit admittance of the line seen from the input. The attenuation function  $\gamma_1$ , of course, is the real part of this expression. A radio-frequency bridge can be used to measure  $Z_{11}$  and  $Y_{11}$ . This method is more complicated than the first method and is seldom used.

Finally, if only a measure of the attenuation in the pulse amplitude is required, the oscilloscope or a peak-reading vacuum-tube voltmeter can be used.

**22-14. Phase Function  $\gamma_2$ .**—The Lissajous-figure method of determining the phase function  $\gamma_2$  is perhaps the most satisfactory method. A line is terminated at both ends in its characteristic impedance and driven by a variable-frequency generator. The signals across the input and output terminals of the line are applied respectively to the horizontal and vertical deflecting plates of a cathode-ray tube. The frequencies at which the phase shift between input and output signals is an integral multiple of  $\pi$  radians can be determined with considerable precision because the Lissajous figure, which is an ellipse in general, degenerates into a straight line in this case.

<sup>1</sup> This is the delay at 5 Mc/sec.

<sup>2</sup> H. Kallmann, "Equalized Delay Lines," RL Report No. 550, June 3, 1944.

<sup>3</sup> F. A. Guillemin, *op. cit.*, p. 175.

A measurement of the open-circuit and short-circuit impedances and a use of Eq. (7) provides another method of measuring  $\gamma_2$ :  $\gamma_2$  is the imaginary part of

$$\frac{1}{2} \ln \left( \frac{\sqrt{Y_{11}Z_{11}} + 1}{\sqrt{Y_{11}Z_{11}} - 1} \right).$$

**22·15. Characteristic Impedance.**—The simplest method of measuring characteristic impedance,  $Z_0$ , is to vary a calibrated resistor inserted across the output of the line until no reflections are observable at the input when a pulse is sent down the line. This method determines only the resistive component of  $Z_0$ , but this is the most important component.

The substitution method is a somewhat more precise way of measuring the resistive component of  $Z_0$  (Fig. 22·21).

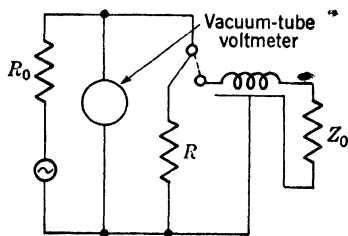


FIG. 22·21.—Substitution method of measuring characteristic impedance of delay line.

The line is terminated in its characteristic impedance approximately, by adjusting the terminating resistor in order to minimize the reflection of pulses sent down the line. Then the sine-wave generator  $E_0$  is used to drive the line, and the voltage across the input is measured with a vacuum-tube voltmeter. The line and its termination are then replaced by a resistance  $R$  which is

adjusted so that the vacuum-tube voltmeter reads as it did when the line was used. This value of  $R$  is a good approximation to  $Z_0$ .

Finally, the open-circuit and short-circuit impedances of the line can be measured.<sup>1</sup>

$$Z_0 = \sqrt{\frac{Z_{11}}{Y_{11}}}.$$

This is a precise method for determining the reactive as well as the resistive component of  $Z_0$ .

<sup>1</sup> See Guillemin, *op. cit.*

## CHAPTER 23

### SUPERSONIC DELAY DEVICE

By V. W. HUGHES and H. B. HUNTINGTON

**23.1. Introduction.**—In the last chapter electrical delay lines were discussed. Essentially, the delay that is achieved for the signal is attributable to the finite velocity with which the electromagnetic wave travels along the line. It is also possible to utilize the finite velocity of propagation of acoustical waves to achieve delays for electrical signals. The electrical signal is transformed into an acoustical wave by means of an electromechanical transducer, and the acoustical wave then travels through a medium to an electromechanical transducer that reconverts the acoustical wave into an electrical signal. Piezoelectric crystals serve as the electromechanical transducers. In this chapter there is an introduction to the theory of supersonic delay lines and a description of some lines that were built. In Vol. 17 there is further discussion of supersonic delay lines, particularly with regard to detailed description of lines that have been used in radar systems. In Vol. 20 there is a treatment of the use of supersonic lines in delay and cancellation systems. For a complete treatment of the theory, reference is made to a journal article by Huntington, *et al.*<sup>1</sup>

The most important property that distinguishes a supersonic from an electrical delay line is its ability to delay signals faithfully by much longer times than it is possible to do with electrical lines. This is because phase and amplitude distortions are much less for the propagation of acoustical waves than they are for the propagation of electromagnetic waves. Thus, whereas with electrical delay lines it is usually impractical to achieve delays much greater than  $10\ \mu\text{sec}$ , with supersonic lines delays anywhere from several microseconds to several milliseconds are realizable.

The types of signals a line can handle and the distortion introduced are important considerations. In general it is readily possible to build systems with sufficiently small distortion so that pulses of approximately  $1\ \mu\text{sec}$  can be reproduced faithfully. Because of the bandwidth limitations of the transducer it is often necessary to impress the waveform to be delayed as a modulating signal on a high-frequency carrier (1 to 30 Mc/sec) in order to avoid undue distortion. Signals with amplitudes up to several hundred volts have been applied across the crystal; it is often desirable to use even larger amplitude signals to achieve larger

<sup>1</sup> Huntington, H. B., A. G. Emslie, and V. W. Hughes, "Ultrasonic Delay Lines I," *Jour. Franklin Inst.*, **245**, 1, 1948.

output signals, but the breakdown voltage of the crystal provides a limitation.

The instability of a supersonic delay line, particularly with respect to shock and to changes in temperature, is often troublesome. Such practical considerations as size, power consumption, and ease of construction are treated in Vol. 17.

There have been three classes of uses for supersonic delay lines:

1. The delay of a trigger. Fidelity of reproduction of the input signal at the output is of no concern. The first delay line discussed in Sec. 23-6 is an example.
2. The time-modulation system in which the delay of a trigger is accurately proportional to a shaft rotation. The range unit treated in Sec. 23-6 is an example.
3. The faithful and stable delay of a signal. In this case, which is perhaps the most important, amplitude and phase distortion in the line must be kept small (Sec. 23-7).

In order to discuss later the over-all properties of a supersonic delay system in terms of its design parameters it is necessary to consider now the properties of electromechanical transducers, of the electrical circuits associated with the transducers, and of the media in which the acoustical waves travel.

### THEORY OF SUPERSONIC DELAY DEVICE

**23-2. The Quartz Crystal as an Electromechanical Transducer.**—A most useful transducer is the piezoelectric quartz crystal.<sup>1</sup> Some of the important properties of the quartz crystal as an electromechanical transducer are listed below.<sup>2</sup>

1. Type of cut: x-cut
2. Type of vibration: thickness vibration, usually at lowest resonant frequency of crystal
3. Relation of resonant frequency to dimensions:

$$f_r = \frac{2.86}{d},$$

where  $f_r$  = resonant frequency (in Mc/sec)

$d$  = thickness of crystal in millimeters

<sup>1</sup> This discussion is confined to the piezoelectric quartz crystal, which is the only transducer with which Radiation Laboratory has had experience. Other piezoelectric crystals such as Rochelle salt, tourmaline, and magnetostriuctive devices may also be useful. It was largely because of their mechanical strength and availability that quartz crystals were used.

<sup>2</sup> Cgs esu units are employed.

4. Range of frequencies: crystals with their lowest resonant frequencies much greater than 30 Mc/sec are inconveniently thin (0.1 mm). However, crystals can be operated at harmonics of their lowest resonant frequency. Frequencies as low as about 1000 cps are available, but for delay line applications several hundred kilocycles is ordinarily the lowest frequency desired.
5. Dielectric constant: 4.55
6. Piezoelectric constant:  $14.3 \cdot 10^4$  (cgs esu).<sup>1</sup>

Two alternative equivalent circuits for the quartz piezoelectric transducer are shown in Figs. 23-1 and 23-2. The values of the elements in

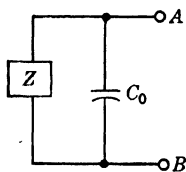


FIG. 23-1.—Equivalent circuit of x-cut quartz crystal as transmitter or receiver.  $A$  and  $B$  are the plate terminals of the crystal. Where  $C_0$  = electrostatic capacitance between plates of crystal =  $\frac{KA}{4\pi L_x}$ ;  $K$  = dielectric constant of quartz = 4.55;  $A$  = area of either crystal face in contact with medium;  $L_x$  = thickness of crystal in  $x$  direction;  $Z = \frac{16\pi^2 L_x^2}{D^2 K^2 \omega A F \beta L_x}$ ;  $\beta = \frac{2\pi}{\lambda}$ ;  $\lambda$  = wavelength in crystal;  $D$  = piezoelectric constant =  $14.3 \cdot 10^4$ ;  $\omega$  = angular frequency =  $2\pi f$ ;

$$F(\beta L_x) = \frac{2Y\beta[\cos(\beta L_x) - 1] + j(Y_1\beta_1 + Y_2\beta_2) \sin \beta L_x}{Y\beta(\beta_1 Y_1 + \beta_2 Y_2) \cos \beta L_x + j[\beta_1 Y_1 \beta_2 Y_2 + (Y\beta)^2 \sin \beta L_x]}$$

$Y$  = elastic modulus of quartz =  $8.63 \cdot 10^{11}$ . Subscripts 1 and 2 refer to media on either side of crystal;  $Y_1, Y_2$  = appropriate elastic moduli.

these circuits depend upon the properties of the crystal (dielectric, elastic, and piezoelectric constants) and of the acoustic media on either side of the crystal.<sup>2</sup> If the transducer is being used as a transmitter, the voltage is applied across the terminals  $AB$  and acoustic waves are radiated into the media (represented by the impedances  $Z_1$  and  $Z_2$ ) on either side of the crystal. The amplitude of these waves can be determined from the equivalent circuits. If the transducer is being used as a receiver, a generator is inserted in series with the impedance representing the medium through which the incoming acoustic wave is traveling. Thus in Figs. 23-1 and 23-2 a generator is inserted in series with either  $Z_1$  or  $Z_2$ , depending upon whether the wave is incident through Medium 1 or

<sup>1</sup> See W. G. Cady, *Piezoelectricity*, McGraw-Hill, New York, 1946, and W. Mason, *Electromechanical Transducers and Wave Filters*, Van Nostrand, New York, 1942, for detailed discussions of transducers.

<sup>2</sup> See Sec. 23-2 for a short discussion of acoustic media.



**Medium 2.** The output voltage across  $AB$  can be found from the equivalent circuits.

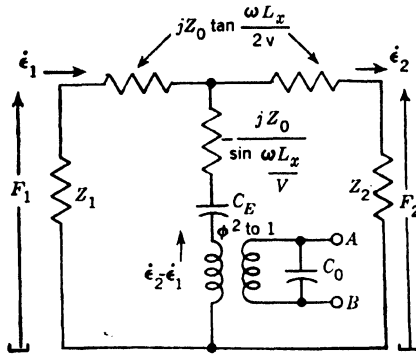


FIG. 23-2. A second equivalent circuit for x-cut quartz crystal where  $A$  and  $B$  are plate terminals of crystal;  $v$  = velocity of propagation of wave motion in crystal =  $\sqrt{\frac{Y}{P_0}} = 5.71 \cdot 10^5$ ;  $P_0$  = density of quartz = 2.65;  $\phi = \frac{DKA}{4\pi L_x}$  = turns ratio of electrical to mechanical transformer;  $Z_1, Z_2$  = acoustic impedances presented to the crystal by Medium 1 and Medium 2 respectively;  $Z_0 = A\sqrt{P_0 Y} = 15.1 \cdot 10^5 A$ ;  $C_E = -\frac{C_0}{\phi^2}$ ;  $\dot{\epsilon}_1, \dot{\epsilon}_2$  = velocities of particles in crystal at ends 1 and 2 respectively;  $F_1, F_2$  = forces exerted on the faces of the crystals at ends 1 and 2 respectively;  $\omega = 2\pi f$ ;  $f$  = frequency.

The assumptions underlying the derivations of each of these two equivalent circuits are largely the same:

1. The simple piezoelectric equations apply.

$$-X_x = Y \frac{\partial \epsilon}{\partial x} + Dq$$

$$E_x = \frac{4\pi q}{K} + D \frac{\partial \epsilon}{\partial x},$$

where  $X_x$  is the stress in x-direction,

$E_x$  = potential gradient in crystal,

$\epsilon$  = displacement of any particle of crystal in x-direction,

$Y$  = appropriate modulus of elasticity,

$$q = \frac{D'_x}{4\pi},$$

$D'_x$  = x-component of the electric displacement,

$K$  = dielectric constant of crystal,

$D$  = piezoelectric constant of crystal.

2. The x-cut crystal vibrates only in the thickness mode at a single frequency. Lateral displacements are negligible with respect to displacements in the thickness direction and there are no edge effects due to clamping of the crystal.

3. Newton's law applies within the crystal.
4. There is no free charge within the crystal; hence the divergence of the electric displacement is zero.
5. There is no internal friction within the crystal.

In addition to these assumptions that are common to both circuits, the assumption that the admittance of the electrostatic capacity  $C$  across the crystal is large compared to admittance  $1/Z$  is made for Fig. 23·1.

The power absorbed by the crystal is  $V^2G$ , where  $V$  is the voltage across the crystal and  $G$  is the conductance of the crystal.

From Fig. 23·1 the conductance equals  $R_c$  ( $1/Z$ ) and is given by

$$G = \frac{1}{4} \frac{\{2Z_0^2(\cos^2 \beta L_x - \cos \beta L_x) + (Z_1 Z_2 + Z_0^2) \sin^2 \beta L_x\} (Z_1 + Z_2)}{Z_0^2(Z_1 + Z_2)^2 \cos^2 \beta L_x + [(Z_1 Z_2 + Z_0^2) \sin \beta L_x]^2}. \quad (1)$$

Actually all this power is radiated into the acoustical media on either side of the crystal and none is dissipated in the crystal. The frequency response for this power absorption is obtained by computing  $G$  as a function of  $\beta L_x$ .

Examples of the use of these equivalent circuits will be given in Sec. 23·5.

**23·3. Acoustical Media.**—The acoustical media on either side of the crystal have been represented solely by the impedances  $Z_1$  and  $Z_2$ , which can almost always be considered as purely resistive. A few words of explanation about this representation can be made.<sup>1</sup>

The specific acoustic impedance of a medium at a point in the medium is the ratio of pressure to velocity at that point. If this impedance is the same at all points at which the medium is in contact with the crystal, it is possible to speak of the impedance presented to the crystal by the medium. This condition is satisfied if only plane waves travel in the media. Since the dimensions of the transmitter are large compared with the wave length of the radiation, the wave emitted by the transmitter is nearly plane. The radiation incident at the receiver crystal is often far from being a plane wave, but for investigations of most phenomena of interest it has been found suitable to assume that there is incident a plane wave that exerts the same force on the receiver crystal as does the actual wave.

For  $Z_1$  and  $Z_2$  to be resistive it is necessary in addition that there be no reflections. This means that at the transmitter only the emitted plane wave shall be present, and at the receiver only the plane wave directly from the transmitter shall be present. There are reflected waves in a delay line but ordinarily they are small and their effect on  $Z_1$  and  $Z_2$  is neglected. Also the operation of the transmitter or receiver is often

<sup>1</sup> See P. Morse, *Vibration and Sound*, McGraw-Hill, New York, 1936.

considered only over short intervals of time during which reflected waves are not present at either crystal. For, instance, the transmitter crystal will often have ceased vibrating before the earlier portion of its radiated wave is reflected from the receiver and returns to the transmitter.

The following properties are desirable for an acoustical medium.

1. It should be such that efficient transfer of energy from the electrical to the acoustical form or vice versa can be made both at the transmitter and at the receiver. This ordinarily implies that its impedance shall be fairly small. Also it must be possible to make good mechanical contact between the crystal and the medium.
2. The medium must damp the crystal sufficiently so that good bandwidth is obtained. This requires that the impedance of the medium be rather high. (See simplified equivalent circuit of Sec. 23-4.)
3. The velocity of propagation for the acoustical wave should be low.
4. This velocity should be independent of temperature.
5. The attenuation of the acoustical wave should be small.

TABLE 23-1.—PROPERTIES OF ACOUSTICAL MEDIA

Medium	Velocity, (cm/sec.)	Temperature coefficient of velocity† (parts per °C at 10 Mc/sec)	Impedance, ohms	Attenuation* (at 10 Mc/sec) nepiers/cm†
Water.....	$1.5 \cdot 10^5$	$2 \cdot 10^{-3}$ at 15°C	$1.43 \cdot 10^5$	$0.78 \cdot 10^{-3}$
Mercury.....	$1.5 \cdot 10^5$	$-2.0 \cdot 10^{-4}$ at 20°C	$19.8 \cdot 10^5$	$0.090 \cdot 10^{-3}$
Fused quartz..	$5.45 \cdot 10^5$	$1.1 \cdot 10^{-4}$ at 20°C	$14.4 \cdot 10^5$	$2.3 \cdot 10^{-2}$
Air (standard conditions)...	$0.331 \cdot 10^5$	.....	43	.....
Steel.....	$5.05 \cdot 10^5$	$4 \cdot 10^{-4}$ at 20°C	$39.3 \cdot 10^5$	$\sim 40 \cdot 10^{-2}$
Lead.....	$1.2 \cdot 10^5$	.....	$13.7 \cdot 10^5$	Very high
Glass.....	$(4.5 \text{ to } 5.6) \cdot 10^5$	.....	$(11.2 \text{ to } 14) \cdot 10^5$	.....
Rubber.....	$0.03 \cdot 10^5$	.....	$0.03 \cdot 10^5$	Very high
Mixture of H <sub>2</sub> O (100 parts by volume) + Ethylene gly- col (15.8 parts by vol- ume)	$1.5 \cdot 10^5$	0 at 155°F	$1.43 \cdot 10^5$	$0.78 \cdot 10^{-3}$

\* It has been fairly well established experimentally that the attenuation varies as  $f^2$  for liquids and more nearly as  $f$  for many solids.

† Data on fused quartz and steel furnished by D. Arenberg. Remainder of data from Wood, *A Textbook of Sound*, Macmillan, New York, 1941, and Vol. 17.

Table 23-1 summarizes these properties for a number of media. Like air, all gases have such very low impedances that the damping of the

crystal is inadequate. Solids in general present several disadvantages: the velocity of propagation is rather high, the attenuation is high, and contact between the crystal and the solid is difficult to establish. Solids often offer mechanical advantages, however, and give delays that are more stable with respect to changes in temperature. Fused quartz is a particularly useful solid. Water and mercury have been most widely used. Water can be used for trigger delays in which fidelity is not important; mercury with its relatively higher impedance has been used for wideband delay lines. There is less transducer loss for a water line than for a mercury line.

**23.4. Radiation and Propagation.**—The spreading of the acoustical beam radiated by the transmitter depends both upon the transducer and the medium, and is determined primarily by the ratio of the size of the transmitter crystal to the wavelength of the radiation in the medium. Beam spreading is important in determining how large the crystals must be and how far apart they can be placed, since the distortion introduced by the spreading of the beam in a tube is often troublesome. Also beam spreading introduces loss.

The first problem is to compute the beam pattern when a vibrating disk is radiating into a medium of infinite extent; ordinary radiation theory is applicable (see Fig. 23.3). If the medium is a fluid, both the disk and the medium are usually contained within a tube. The tube is often sufficiently large so that only a small portion of the radiated energy reaches the walls of the tube, and in this case it is justifiable to consider the "free space" beam. At distances between the transmitter and the observation point that are sufficiently large so that terms can be neglected which involve the square of the ratio of a dimension of the transmitter to this distance, the Fraunhofer theory is applicable. At smaller distances, for which the term in the square of the ratio cannot be neglected but higher powers can, Fresnel theory applies. For still smaller distances higher-order terms would have to be considered, but there is little interest in this region. Important general conclusions can be reached by considering the case of a circular disk.<sup>1</sup>

Fraunhofer theory is an excellent approximation for distances greater than  $a^2/\lambda$  from the transmitter, where  $a$  is the radius of transmitter and

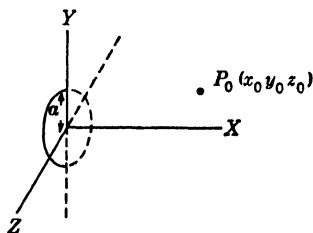


FIG. 23.3.—Radiation problem: A circular disk of radius  $a$  is vibrating piston-like with frequency  $f_1$ . Wavelength of radiation is  $\lambda$ . Wave disturbance at an arbitrary point  $P_0(x_0, y_0, z_0)$  is sought.

<sup>1</sup> See P. Morse, *Vibration and Sound*, McGraw-Hill, New York, 1936; or any physical optics book on diffraction.

$\lambda$  is the wavelength. In this region the square of the amplitude of the disturbance  $A^2$  is given by

$$A^2 \propto \left[ \frac{I_1 \left( \frac{2\pi}{\lambda} a\psi \right)}{\left( \frac{2\pi}{\lambda} a\psi \right)} \right]^2$$

where  $\psi$  is the sine of the angle with respect to the x-axis in which the observation is made and  $I_1$  is a first order Bessel function of the first kind. In this region the semiangle of the first minimum of intensity is  $\sin^{-1} 0.61 \frac{\lambda}{a}$ . A useful rule of thumb is that as long as the wall of the tube at the position of the receiver is at a distance from the axis of the tube greater than the distance of the first minimum from the axis, no appreciable amount of energy is incident upon the walls. In order to utilize the major portion of the energy radiated by the transmitter, the radius of the receiver crystal should extend out to the first minimum in the Fraunhofer pattern. In the Fraunhofer region the intensity on the axis varies as  $\sin^2 (\pi a^2 \lambda / 2x)$ . Eventually then the intensity is proportional to  $1/x^2$ , which can be interpreted as indicating that the radiation is diverging in the form of a cone with its vertex at the center of the transmitter.

The Fresnel theory applies for distances from the transmitter as small as a few diameters of the transmitter crystal and can be replaced by the Fraunhofer theory at large distances. In this Fresnel region the major portion of the radiation is confined within an imaginary cylinder whose axis is through the center of the transmitter and whose radius is equal to the transmitter radius; hence a receiver crystal with a radius equal to that of the transmitter will pick up the major portion of the energy. The amplitude and phase of the wave disturbance vary along any diameter of this imaginary cylinder, the variation being particularly rapid at distances close to the transmitter where many maxima and minima of intensity are observed. Experimental evidence and a few theoretical calculations indicate that in the Fresnel region the total force on a receiver with the same radius as the transmitter varies by only a few decibels at most at different distances between the transmitter and receiver. Hence the distance between the transmitter and receiver can be varied, thereby changing the delay time but not the amplitude of the output signal.

The loss due to these radiation pattern effects can be computed by comparing the actual force on the receiving crystal, computed by Fraunhofer or Fresnel methods, with the force that would be present if an ideal plane wave traveled from the transmitter to the receiver. For the case of a 500- $\mu$ sec mercury delay line using 10-Mc transmitter and receiver

crystals of 1-cm radius this loss was found by calculation to be about 10 db.

*Attenuation.*—Values of attenuation for various media are given in Table 23·1. These are experimental values for the attenuation of a plane wave in a medium of effectively infinite extent. It was mentioned in the table that for liquids this attenuation varies as the square of the frequency.

In practice the wave usually travels in a tube, and because of viscosity of the fluid the tangential velocity at the walls is zero. Another source of attenuation thus arises because of the gradient of velocity in the direction perpendicular to the direction of propagation. For any particular medium this attenuation varies as  $\sqrt{f}/a$  where  $a$  is the radius of the tube and  $f$  is the frequency of the radiation.

**23·5. Some Special Cases of Transducer Equivalent Circuits and Associated Electrical Circuits.**—The resonant condition for the crystal is that its width be an odd number of half wavelengths or  $\beta L_z = n\pi$ , where  $n$  is odd. At these frequencies,  $Z$  of Fig. 23·1 reduces to

$$Z(n\pi) = \frac{4\pi^2 I_x^2}{D^2 K A} (R_1 + R_2), \quad (n \text{ odd})$$

where  $R_1$  and  $R_2$  are the acoustic impedances of the loading media. The actual resonant frequency of the transmitter or receiver system—that is, the frequency at which maximum power is transferred to the media from a constant voltage source—does not vary appreciably from the crystal resonant frequency in the examples considered here. The resonant frequency for a receiver system with a particular electrical output circuit will depend upon the loading impedances. The equivalent circuits to be presented for the transmitter and receiver systems are valid in the neighborhood of the resonant frequency of the systems—that is,  $(f - f_r)/f_r^2$  is neglected with respect to 1 in their derivation.

*Symmetrical Loading.*—For the case in which the same medium is on both sides of the crystal, Figs. 23·1 and 23·2 reduce to Fig. 23·4 in the neighborhood of the resonant frequency. The efficiency of transfer of energy from the electrical to the acoustical form at the transmitter or from the acoustical to the electrical form at the receiver, and the phase and amplitude characteristics of the transmitter and the receiver systems depend on the electrical circuits inserted at  $AB$ .

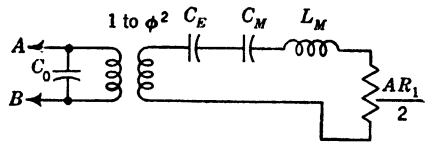


FIG. 23-4.—Circuit to which Figure 23·2 reduces in the neighborhood of the resonant frequency for the case of symmetrical loading.

$$L_M = \frac{Z_0 L_z}{8\sigma}; \quad C_M = \frac{8L_z}{\pi^2 Z_0 V}; \quad \omega_0 \text{ (resonant frequency)} = \frac{\pi V}{L_z}$$

If a generator is inserted across  $AB$ , Fig. 23-4 is the equivalent circuit of the transmitter; if a receiver circuit is placed across  $AB$  and a generator  $E$  is inserted in series with  $AR_1/2$  to represent the plane wave incident on the receiver, Fig. 23-4 becomes the equivalent circuit of the receiver. The case in which a low-impedance driver circuit and a low impedance receiver circuit is used across  $AB$ <sup>1</sup> is of great importance because wide-band systems are obtained. If a low-impedance source is inserted across  $AB$ , the characteristic of the system is simply that of the series resonant circuit of Fig. 23-4 consisting of  $C_E$ ,  $C_M$ ,  $L_M$ ,  $AR_1/2$ . The  $Q$  of this circuit<sup>2</sup> is given by

$$Q = \frac{\pi R_0}{4 R_1},$$

where  $R_0 = \rho_0 v$ , the specific acoustic impedance of quartz, where  $\rho_0$  is the density of quartz, and  $v$  is the velocity of propagation of waves in quartz. The bandwidth of this circuit is  $B = f_0/Q$ , where  $f_0$  is the resonant frequency of the crystal. If water is used as the loading medium,  $Q = 8.3$ ; if mercury is used as the loading medium,  $Q = 0.60$ .<sup>3</sup> The over-all bandwidth of a delay system with low-impedance driver and receiver circuits and including both a transmitter and receiver is that of two series resonant circuits isolated from one another and in cascade.

The over-all loss between input voltage and output voltage at the resonant frequency is given by

$$\frac{E_{out}}{E_{in}} = \frac{2R_1R_r}{(2R_1 + R_t)(2R_1 + R_r)}, \quad (2)$$

where  $R_t$  and  $R_r$  are the internal resistances of the transmitter and receiver circuits placed across  $AB$ , and  $R_1$  is the acoustical resistance of the medium expressed in electrical units. The conversion factor from acoustical to electrical units is  $(4\pi^2 L_x^2 / D^2 KA)$ . In general  $R_t$  and  $R_r$  are small compared to  $R_1$  so

$$\frac{E_{out}}{E_{in}} = \frac{R_r}{2R_1}. \quad (3)$$

The main loss takes place at the receiver and is due to the mismatch between the acoustic impedance of the medium and the internal resistance  $R_r$  of the receiver circuit.

If higher-impedance driving and receiving circuits are employed, the over-all voltage loss will be less [see Eq. (2)]. A series resonant circuit

<sup>1</sup> The driver often includes an inductance that is shunted across  $AB$  and resonates with  $C_0$  at the resonant frequency of the crystal.

<sup>2</sup> This expression for  $Q$  can also be derived from Eq. (1).

<sup>3</sup> For the case of mercury,  $Q$  is sufficiently low so that the relationship between  $B$  and  $Q$  is a poor approximation.

alone no longer represents the crystal and load since the impedance of the source and of the crystal capacity must be considered.<sup>1</sup> The bandwidth is less with these higher-impedance circuits.

*Asymmetrical Loading.*—If an infinitely high-impedance medium is placed on one side of the crystal and a medium of any impedance  $R_2$  is placed on the other side, Fig. 23-5 shows the equivalent circuit to which Figs. 23-1 and 23-2 reduce.

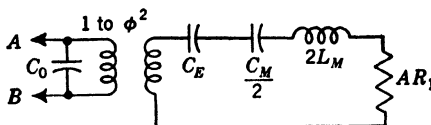


FIG. 23-5.—Circuit to which Figure 23-2 reduces in the neighborhood of the resonant frequency for the case in which infinite impedance loading is used on one side of the crystal.

$$\omega_0(\text{resonant frequency}) = \frac{2\pi V}{L_x}$$

It should be noticed that for this case the resonant condition for the crystal is that its thickness be  $(n + 1)(\lambda/4)$ ,  $n = 0, 2, 4, \dots$ . If low-impedance driving and receiving circuits are used, the  $Q$  of this circuit is the same as that for Fig. 23-4 and the over-all voltage loss is

$$\frac{E_{\text{out}}}{E_{\text{in}}} = \frac{R_r}{4R_1}$$

For other cases of asymmetrical loading the equivalent circuit has not been reduced to a simple form. However, the amplitude characteristic can be computed from Eq. (1), and the over-all voltage loss is given by

$$\frac{E_{\text{out}}}{E_{\text{in}}} = \frac{2R_1R_r}{(R_1 + R_2 + R_l)(R_1 + R_2 + R_r)}$$

*Choice of Circuits.*—The circuits chosen depend, of course, on the application to which the delay line will be put. If it is desired to use the line as a trigger delay so that large bandwidth is usually not required, any fairly low-impedance pulse generator is adequate for the driver circuit (see Chap. 5). If the line is required to delay a group of video pulses without much distortion, it is necessary to modulate a high-frequency carrier, perhaps 10 to 30 Mc/sec, with the video pulses (see Chap. 12 of Vol. 20).

Generally the receiver circuit consists of a coil and a resistor shunted across the capacity  $C_0$  of the crystal and followed by an amplifier system. The coil resonates with  $C_0$  to the resonant frequency of the crystal. The size of the resistor is determined by a compromise, since the larger the

<sup>1</sup> See W. Mason, *Electromechanical Transducers and Wave Filters*, Van Nostrand, New York, 1942.



resistor is the greater is the output voltage and the smaller is the bandwidth. The amplifiers may be video amplifiers or wide-band i-f amplifiers depending upon the signal to be amplified (see Vol. 18).

*Reflections.*—In general a signal that reaches the receiver will be partially reflected; this reflected signal may itself be partially reflected again when it reaches the transmitter. Thus, at a time equal to twice the delay time of the line after the direct signal appeared, a reflected signal may appear at the receiver. Additional reflections may, of course, also occur. Often, particularly in short lines, it is desirable to eliminate these reflections; this can be done effectively if symmetrical loading and absorbing end cells are used (see Vol. 17). In long lines attenuation of the signal as it travels along the line often makes these measures unnecessary.

### SOME EXAMPLES OF DELAY LINES

**23.6. "Trigger" Delays.**—As was mentioned in the introduction, the object of a trigger delay system is not to reproduce the input signal faithfully at a later time, but rather merely to provide a sharp change in voltage—a trigger—at a certain definite time after the input signal is applied. For the synchronization of waveforms and for time measurement, the usefulness of performing such a function is obvious (see Vol. 20, Chap. 5). If the trigger delay time is accurately proportional to a shaft rotation, the line can serve as a time-modulation system.

The input signal should contain strong frequency components in the neighborhood of the resonant frequency of the crystal because what is actually transmitted is a damped oscillation whose frequency is the resonant frequency of the crystal, and this oscillation is more readily excited by a signal with frequency components in the neighborhood of the resonant frequency. The amplitude of the input signal can have any value which is not so large that it exceeds the breakdown voltage of the transmitter crystal or so small that noise is troublesome at the receiver.

A brief description of three trigger delay lines follows.

*A Variable 1200- $\mu$ sec Delay Line.*—A detailed presentation of the characteristics of this line together with a picture of the line is given in Vol. 17. It is sufficient to mention here that this line employs x-cut 10-Mc/sec quartz crystals, 1 in. in diameter. The crystals are loaded on both sides with water. The transmitter crystal is driven from the cathode of a blocking oscillator (Chap. 6), and the receiving circuit consists simply of a 47-k resistor shunted across the crystal and tied between grid and ground of the first video amplifier. Delays from 10 to 1200  $\mu$ sec settable to within 0.1  $\mu$ sec can be obtained by moving the transmitter cartridge with respect to the receiver. The stability of delay is limited mainly by the temperature coefficient of velocity of the supersonic waves in water.

*A Precision Range Unit.*—This line is treated in detail in Vol. 17 and in Chap. 13 of this volume. It employs x-cut 1.4-Mc/sec quartz crystals,  $\frac{7}{8}$  in. square. Both crystals are soldered on one side to brass blocks, and the propagating medium is a mixture of water and ethylene glycol. The transmitter crystal is driven from a low output impedance multivibrator (Chap. 5). The receiving circuit is shown in Vol. 17.

Delays from 2 to 240  $\mu$ sec can be obtained. The delay is changed by turning a lead screw connected to the transmitter-crystal cartridge and is linearly proportional to the shaft rotation of the lead screw to within  $\pm 0.1$  per cent of maximum delay, or  $\pm 0.24$   $\mu$ sec. Stability of delay is good because the unit is thermostated to  $155^\circ \pm 1^\circ\text{F}$ , a temperature at which the mixture of water and ethylene glycol has a zero temperature coefficient of velocity.

*A 6- $\mu$ sec Glass Line.*—This line is used to delay pulses for a time of 6  $\mu$ sec. No attempt is made to eliminate multiple echoes nor is high quality of pulse reproduction required. The unit consists of a rectangular prism of plate glass to which are attached 30-Mc/sec crystals on opposite faces. These faces are flat, parallel, and polished. The parts are encased in a short piece of brass tubing which can be bolted to the chassis in which the delay line is a component. The crystals are waxed on to the glass by a thin uniform layer of paraffin wax, and end blocks and springs support the crystals in position. A series of reflected pulses from this line are shown in Fig. 23-6.

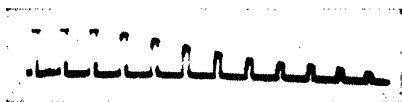


Fig. 23-6.—A series of reflected pulses from the 6- $\mu$ sec glass line. Line is in contact with transmitter crystal at one end and is terminated at other end. Distance between pulses is 12  $\mu$ sec.

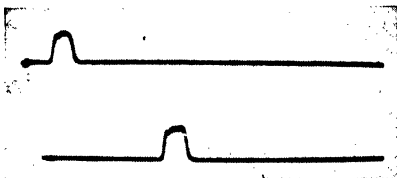


Fig. 23-7.—Input and output pulses from 600- $\mu$ sec line (SCR 584). Top line: 4- $\mu$ sec input pulse. Bottom line: Output pulse, which is delayed by 586  $\mu$ sec.

**23-7. Delay Lines Providing Faithful Reproduction.**—The delay lines used for delaying pulses faithfully must have a wide pass band and must keep all subsidiary echoes negligibly small.<sup>1</sup> The former matter has been discussed briefly in Secs. 23-2 and 23-5. It was noted that high impedance media should be used. The frequency-dependent attenuation of the propagating wave sometimes introduces distortion that must be compensated for at some stage in the amplifier system. Considerations on echoes are treated in some detail in Chap. 12 of Vol. 20. There it is

<sup>1</sup> These lines are used in delay and cancellation devices (Vol. 20).

pointed out that the subsidiary echoes can either be absorbed into the material backing the crystal or attenuated in transit (or both).

A brief description of three lines giving faithful reproductions is given below. (For more detailed discussions see Vols. 17 and 20.)

*A 600- $\mu$ sec Mercury Line.*—A mercury line built for the SCR-584 system employs a 30-Mc/sec carrier and provides a delay of 586  $\mu$ sec. The 30-Mc/sec transmitting and receiving crystals are in contact with mercury on both sides. The over-all attenuation into a 70-ohm load is  $80 \pm 2$  db and the bandwidth is about 8 Mc/sec. Subsidiary echoes are attenuated by the high attenuation in the transmitting medium at this frequency. The length of the line is variable and the delay can be adjusted to match the repetition interval. Input and output pulses are shown in Fig. 23-7.

*A 3000- $\mu$ sec Mercury Line.*—This line was used for delaying 2- $\mu$ sec pulses by 3333  $\mu$ sec. The carrier frequency and the crystal resonant frequency was 10 Mc/sec. The crystals are backed by steel on the sides not in contact with mercury. Subsidiary echoes are lost by attenuation in the long path in the transmitting medium. The path of the beam is folded once by a reflector block which presents two 45° reflecting surfaces to the path of the beam. The beam then travels back through a parallel pipe so that the delay line is of shorter length; transmitting and receiving crystals are within 6 in. of each other. An extra line is employed to delay the trigger that controls repetition rate and the length of either line is variable so that they can be adjusted to exact synchronization. Both lines are placed close together so that changes in temperature have the same effect on both.

*A 2000- $\mu$ sec Water Line.*—A delay line with water for the transmitting medium and a 10-Mc/sec carrier has been used to provide a delay of 2000  $\mu$ sec. The attenuation of the 10-Mc/sec supersonic wave traveling in water is about  $0.8 \cdot 10^{-2}$  nepers/cm compared to  $0.09 \cdot 10^{-2}$  nepers/cm for mercury. The bandwidth is somewhat less than 1 Mc/sec. One corner reflector is employed to reduce the required length of the line. The water is held at a temperature of  $72\frac{1}{2}^{\circ}\text{C} \pm 1^{\circ}\text{C}$ . At this temperature the temperature coefficient of velocity is low; hence refraction effects due to temperature variations throughout the cross section of the tube can be made small.

#### BIBLIOGRAPHY

- Hughes, V., "A Theory of the Supersonic Delay Line," RL Report No. 733, Sept. 15, 1945.
- Huntington, H. B., "The Theory and Performance of Liquid Delay Lines," RL Report No. 792, Sept. 21, 1945.
- Huntington, H. B., A. G. Emslie, and V. W. Hughes, "Ultrasonic Delay Lines I," *Jour. Franklin Inst.*, **245**, 1, 1948. These first three references present the details of work at the Radiation Laboratory.

- Mason, W., *Electromechanical Transducers and Wave Filters*, Van Nostrand, New York, 1942. A most useful text treating all aspects of the subject. Extensive use of circuit analysis.
- Wood, A. B., *A Textbook of Sound*, Macmillan, New York, 1941. An excellent book which treats all aspects of the subject.
- Rayleigh, J. W. S., *The Theory of Sound*, Vols. I and II, Macmillan, New York, 1877. The standard text on the theory of the propagation of sound waves.
- Richards, "Supersonic Phenomena," *Rev. Mod. Phys.*, January 1939. Summary article on propagation phenomena. Gives extensive references.
- Bergmann, *Ultrasonics and their Scientific and Technical Applications*, translated by Dr. Hatfield, Wiley, New York, 1938. Covers experimental aspects of the subject.
- Willard, G., "Ultrasonic Absorption and Velocity Measurements in Numerous Liquids," *J.A.S.A.*, January 1941, p. 443.
- Series of articles on crystals in *Bell Syst. Tech. J.*, 1942, 1943, and 1944.



# APPENDIX A

## NEGATIVE-CAPACITY AMPLIFIER

By P. R. BELL

The pickup-plate video amplifier used in the tests of Chap. 21 deserves more than casual mention since satisfactory results have not been obtained without using an amplifier of this type. The kind used is the so-called "negative capacity" type. The circuit diagram of the one used is shown

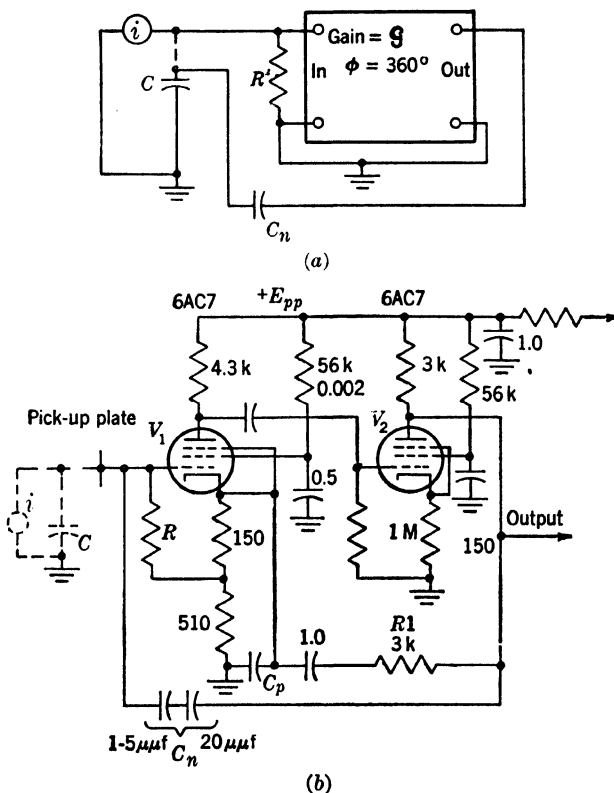


FIG. A-1.—Negative-capacity amplifier.

(a) Block diagram.

(b) Circuit diagram.

in Fig. A-1a and b. This is a two-stage amplifier whose gain is stabilized by negative feedback from the plate of Stage Two to the cathode of Stage

One by the resistors,  $R_1$  and  $R_2$ . The gain ( $\mathcal{G}$ ) of this amplifier is

$$\mathcal{G} = \frac{A}{1 + g_m R_2 + \frac{R_2 A}{R_1 + R_2}}$$

where  $A$  is the gain from the grid of  $V_1$  to the output with the feedback path removed and cathode of  $V_1$  bypassed to ground. The total cathode mutual conductance of  $V_1$  is  $g_m$ . For the constants in the circuit, the gain with feedback is about 4.

Because of the feedback, the effective input resistance  $R'$  is

$$R' = R \left( \frac{1}{1 - \frac{A - \mathcal{G}}{A} N} \right),$$

where  $N$  is the fraction of the resistor  $R_2$  by which the grid resistor  $R$  is tapped up from the ground end, in this case  $N = 0.77$ ; so for the constants given

$$R' = 4.2R.$$

The condenser  $C_n$  is connected in a positive-feedback manner. The block diagram of Fig. A-1b shows this arrangement simplified. Let us suppose that the total input capacity  $C$  (which includes the input capacity of the first tube, the stray capacity, and the output capacity of the storage tube or other signal source) is for the moment disconnected from the input lead. Then the signal current  $i$  flows into the input resistance  $R'$  giving a voltage

$$e = R'i.$$

The voltage appearing at the output of the amplifier will be

$$e_o = \mathcal{G}e.$$

The voltage ( $e_c$ ) appearing at the junction of  $C$  and  $C_n$  will be

$$e_c = e_o \frac{\frac{1}{C}}{\frac{1}{C} + \frac{1}{C_n}} = e_o \frac{C_n}{C_n + C}.$$

If  $C_n$  is so chosen that  $e_c = e$ , then if the junction of  $C$  and  $C_n$  were reconnected to the input terminal, no current would flow from the signal source into these capacitors and hence the effect of  $C$  would have been removed from the input of the amplifier. For this condition

$$e = e_o \frac{C_n}{C_n + C}.$$

Therefore,

$$C_n = \frac{C}{g - 1};$$

and, for an input capacitance of  $20 \mu\mu\text{f}$  and an effective gain of 4,

$$C_n = 3.3 \mu\mu\text{f}.$$

Unfortunately, this does not mean that the amplifier displays infinite bandwidth in its input circuit since the output of the amplifier does not rise immediately after a signal is applied to its input; consequently, some signal current flows into the input capacity thus reducing the signal

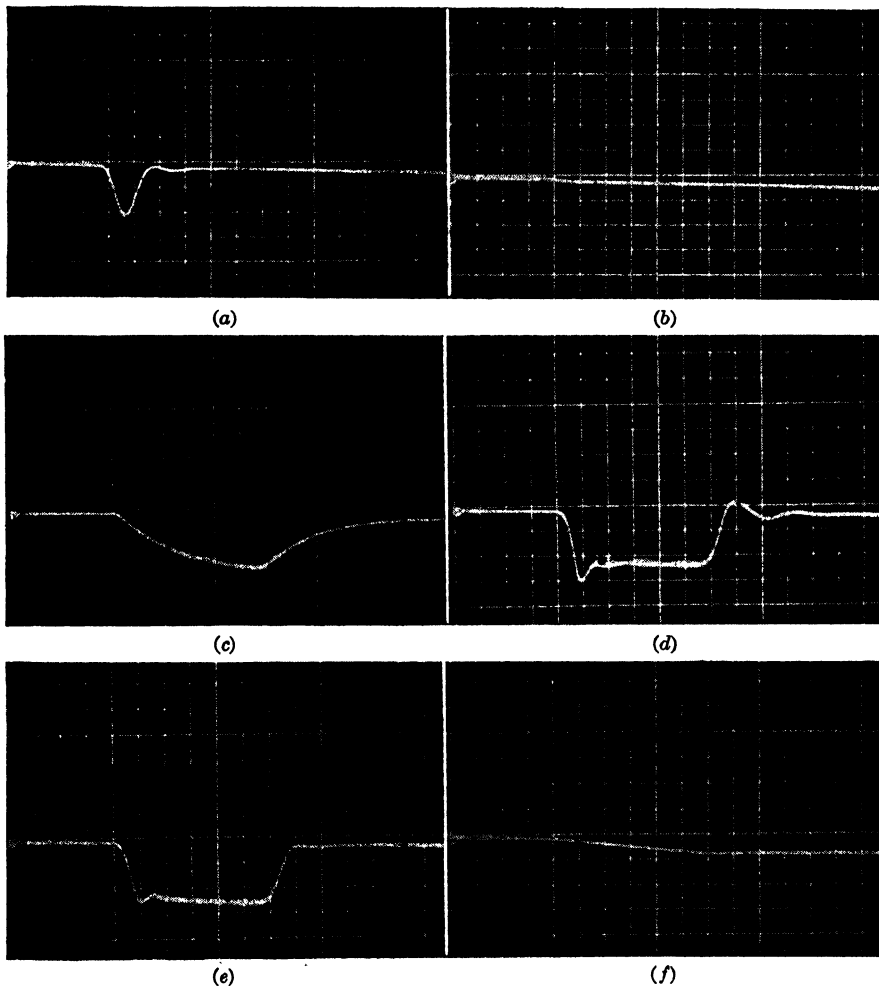


FIG. A.2.—Output waveform of negative-capacity amplifier.



until the output of the amplifier has risen, when the current flows back out of the input capacity raising the input voltage. This gives an oscillating overshoot to the signal pulse.

The amplifier of Fig. A·1a was connected to a current-generator circuit which could produce square current pulses with starting and stopping times of less than  $\frac{1}{20}$   $\mu$ sec. The total capacity at  $C$  including the current generator was 25  $\mu$ f, and a resistor  $R$  of 0.5 megohm was used.

Figure A·2a shows the result for a 6- $\mu$ sec current pulse with correct adjustment of  $C_n$ . Each division in the  $x$  direction represents 1  $\mu$ sec. The rise time from 10 per cent to 90 per cent is about 0.5  $\mu$ sec, which gives an effective bandwidth of about 0.7 Mc/sec. When  $C_n$  is made zero, the output rises very slowly and falls very slowly with an effective time constant  $CR'$  of about 52  $\mu$ sec on the fall; this is a bandwidth of about 3.1 kc/sec (Fig. A·2b). When  $C_n$  is set too small, the output appears as in Fig. A·2c, and when  $C_n$  is set too large, overshoots occur (Fig. A·2d).

With a 1- $\mu$ sec input pulse the output appears as in Fig. A·2e when  $C_n$  is adjusted to its best value and as in Fig. A·2f when  $C_n$  is zero.

## APPENDIX B

### CATHODE-COMPENSATED AMPLIFIER

BY P. R. BELL

Another method for obtaining better output signal-to-noise ratio (Chap. 21) is to use an input resistance too large to define the pulse well and to follow with a compensating network in the amplifier. Figure B-1 shows such a circuit.

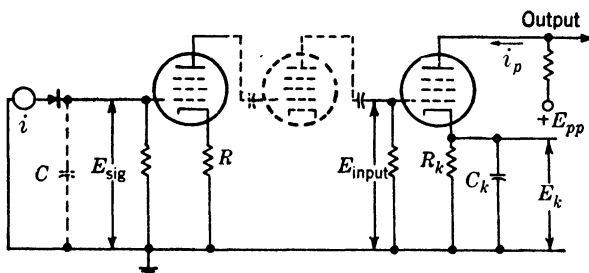


FIG. B-1.—Cathode-compensated video amplifier.

Since the input resistance is too large, the signal obtained from a square pulse of current has three parts:

$$E_{sig} = 0 \quad \text{for } t < 0, \quad (1)$$

$$E_{sig} = Ri(1 - e^{-\frac{t}{RC}}) \quad \text{from } t = 0 \text{ to } t = t_1, \quad (2)$$

where  $t_1$  is the end of the current pulse, and

$$E_{sig} = E_1 e^{-\frac{t}{RC}} \quad \text{for } t > t_1, \quad (3)$$

where  $E_1$  is the value of  $E_{sig}$  at  $t = t_1$ .

To find the output current from the compensated stage we will consider the effect of the signal  $E_{input} = E_s(1 - e^{-t/RC})$  upon only the variable part ( $i_p$ ) of its plate current.

The variable part of the plate current of a pentode tube is

$$i_p = \frac{\partial i_p}{\partial E_{sig}} \Delta E_{sig} + \frac{\partial i_p}{\partial E_g} \Delta E_g;$$

if the small first term for pentodes is neglected the equation becomes

$$i_p = g_m(E_{input} - E_k).$$

For the cathode-compensated amplifier,

$$E_k = \frac{\int i_{c_k} dt}{C_k} \quad i_{c_k} = i_p - \frac{E_k}{R_k}$$

$$E_k = \frac{\int \left[ g_m(E_{\text{input}} - E_k) - \frac{E_k}{R_k} \right] dt}{C_k}$$

Differentiating,

$$\frac{dE_k}{dt} + \frac{E_k}{C_k} \left( g_m + \frac{1}{R_k} \right) - \frac{g_m}{C_k} E_{\text{input}} = 0,$$

where  $1/(g_m + 1/R_k) = R' =$  the effective cathode-to-ground resistance of the circuit.

The solution of this differential equation is:

$$E_k = A e^{-\frac{t}{R'C_k}} + \frac{g_m}{C_k} e^{-\frac{t}{R'C_k}} \int e^{\frac{t}{R'C_k}} E_{\text{input}} dt.$$

If

$$R'C_k \neq RC,$$

$$E_k = A e^{-\frac{t}{R'C_k}} + g_m R' E_s - \frac{g_m R' R C E_s}{RC - R'C_k} e^{-\frac{t}{RC}}.$$

At  $t = 0$ ,  $E_k = 0$  and  $e^0 = 1$ , therefore,

$$0 = A + g_m R' E_s \left( 1 - \frac{RC}{RC - R'C_k} \right)$$

$$E_k = g_m R' E_s \left[ \left( \frac{RC}{RC - R'C_k} - 1 \right) e^{-\frac{t}{R'C_k}} + 1 - \frac{RC}{RC - R'C_k} e^{-\frac{t}{RC}} \right].$$

Let

$$\frac{RC}{RC - R'C_k} = 1 + \Delta,$$

then

$$E_k = g_m R' E_s (\Delta e^{-\frac{t}{R'C_k}} + 1 - e^{-\frac{t}{RC}} - \Delta e^{-\frac{t}{RC}})$$

$$i_p = g_m E_s (1 - e^{-\frac{t}{RC}} - g_m R' \Delta e^{-\frac{t}{R'C_k}} - (g_m R' + g_m R' e^{-\frac{t}{RC}} + g_m R' \Delta e^{-\frac{t}{RC}}))$$

$$i_p = g_m E_s [1 - g_m R' + g_m R' \Delta e^{-\frac{t}{R'C_k}} + (g_m R' + g_m R' \Delta - 1) e^{-\frac{t}{RC}}].$$

In order that the output contain no term in  $e^{-\frac{t}{RC}}$ ,

$$g_m R' + g_m R' \Delta - 1 = 0$$

$$\Delta = \frac{1 - g_m R'}{g_m R'}.$$

Substituting values of  $\Delta$  and  $R'$  we find that  $R_k C_k = RC$ , and for this condition

$$i_p = \frac{g_m E_s}{1 + R_k g_m} (1 - e^{-\frac{t}{R' C_k}}).$$

The product  $R' C_k$  is the time constant of the cathode condenser and the effective resistance of the cathode circuit with the resistance of the tube in parallel with the cathode resistor  $R_k$ . If  $R_k$  is always chosen high enough so that it is much higher than the cathode resistance of the tube ( $1/g_m$ ), then the relations are simpler. Then,

$$g_m R_k \gg 1,$$

so,

$$i_p = \frac{E_s}{R_k} (1 - e^{-\frac{t}{C_k/g_m}}).$$

The rise-time improvement is therefore  $\frac{RC}{C_k/g_m}$ .

The gain of the compensating amplifier is lowered by the cathode resistance with the result that

$$\text{Gain loss} = \frac{1}{g_m R_k}$$

so that the product (rise-time improvement) (gain loss)

$$= \frac{RC}{C_k/g_m} \cdot \frac{1}{R_k g_m} = \frac{RC}{R_k C_k} = 1.$$

As a consequence of this condition, this circuit is not useful in an amplifier to improve the gain-bandwidth product. Although a higher resistor is allowed in a plate circuit somewhere, a proportional decrease in gain is required to return the bandwidth to the original value. This circuit is useful, however, as is the negative-capacity amplifier, for improving the noise figure of an amplifier fed from a high-impedance source such as a storage tube, a photocell, or an ionization chamber. It can be seen that the mutual conductance of the compensating tube is involved in the equation, and that this has been taken as a constant. This means that, if the effect is to be satisfactory, the signal of the grid of this tube must be so small that the mutual conductance can be considered constant over this range. The result of inconstant mutual conductance is shown in Fig. B-2. The two pulses have been reduced to the same scale although the first pulse is many times smaller than the second.

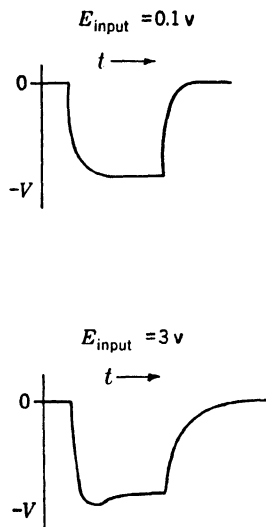


FIG. B-2.—Illustrating distortion of output caused by variation of  $g_m$  with grid bias.

This method of cathode compensation is not as satisfactory as the negative-capacity amplifier on account of the effect of microphonics. If a factor of 100 is obtained in bandwidth increase in both methods, then both methods will use the same input resistor. In the case of the negative-capacity amplifier the pulse will be about as big as the input signal current times the input resistance, but in the cathode-compensated amplifier the signal will be about  $\frac{1}{100}$  as large and the microphonic voltages will be larger by 100 times with respect to the signal. These voltages may overload the amplifier, will in part appear in the output, and may cover such a large part of the compensated stage characteristics that the mutual conductance may not be constant enough to get proper compensation. In addition, much more gain is required in the compensated case because of the lower input signal and because of the gain lost at the compensated stage. This compensation circuit, however, is used to good advantage for other services.

## GLOSSARY

- amplitude comparison.**—The process of indicating the instant of equality of the amplitudes of two WAVEFORMS by a sharp pulse or step. It may also be defined as the process of determining the abscissa of a WAVEFORM, given its ordinate.
- amplitude discriminator.**—A circuit which indicates the equality of the amplitudes of two WAVEFORMS or the sense and approximate magnitude of the inequality.
- amplitude selection.**—The process of selection of all values of the input wave greater or less than a given amplitude or lying between two amplitudes.
- astable.**—Referring to a circuit with two quasi-stable states. The circuit generates a continuous train of waves and requires no trigger to execute a complete cycle.
- bistable.**—Referring to a circuit with two stable states. Two triggers are required to put the circuit through one complete cycle.
- blocking oscillator.**—A transformer-coupled feedback oscillator in which the plate current is permitted to flow for one-half cycle, after which bias is generated in the grid circuit to prevent further oscillation.
- bottoming.**—The process of defining the potential at the plate of a pentode by operating below the knee of the  $E_p/I_p$  characteristic. A similar effect exists in triodes with positive grid drive.
- catching diode.**—A diode used to limit the excursion of potential at some point in a circuit. The term is usually used to refer to the termination at a given level of an exponential rise toward a higher potential.
- clamping.**—The process of connecting some point of a network to a desired potential for certain periods of time. This term has been largely replaced by the term SWITCHING.
- clipping.**—AMPLITUDE SELECTION between bounds. The output has a flat top or flat bottom or both.
- d-c restoration.**—A category of the general process of level setting. It refers particularly to bringing either the peak positive or peak negative value of the WAVEFORM to some desired level.
- delay circuit.**—A circuit which is used to delay by a certain time the start of the operation of another circuit.
- delay device.**—A device which accepts as its input a WAVEFORM  $f(t)$  and gives as its output a WAVEFORM  $f(t - \Delta)$  where  $\Delta$  is positive.
- demodulation (or detection).**—The process by which information is obtained from a modulated WAVEFORM about the signal imparted to the WAVEFORM in modulation.
- difference detector.**—A detector circuit in which the output represents the difference of the peak amplitudes or areas of the input WAVEFORMS. The input WAVEFORMS need not be simultaneous.
- flip-flop.**—Colloquialism for MONOSTABLE circuit.
- free-running.**—Colloquialism for ASTABLE.
- frequency discriminator.**—A circuit which indicates the equality of the frequency of two WAVEFORMS or the sense and approximate magnitude of the inequality.
- function unit.**—The unit that controls the external properties of automatic range-tracking equipment and provides the necessary band shaping for stability.

- gating waveform.**—A WAVEFORM (sometimes called the “gate”) applied to the control point of a circuit in such a way as to alter the mode of operation of the circuit while the WAVEFORM is applied.
- jitter.**—Small rapid variations in a WAVEFORM due to mechanical disturbances or to changes in the supply voltages, in the characteristics of components, etc.
- lockover circuit.**—Colloquialism for a BISTABLE circuit.
- microphonics.**—JITTER due to mechanical disturbances, referring especially to tubes.
- Miller circuit.**—A circuit which employs negative feedback from the output to the input of an amplifier through a condenser.
- modulation.**—The process by which some characteristic of a WAVEFORM is varied in accordance with a signal.
- monostable.**—Referring to a circuit with one stable and one quasi-stable state. The circuit requires one trigger to perform a complete cycle.
- multiar.**—A diode-controlled regenerative amplitude comparator. The name refers to a certain circuit configuration.
- multivibrator.**—A two-tube regenerative device which can exist in either of two stable or quasi-stable states and can change rapidly from one state to the other.
- quasi differentiation (integration).**—Approximate differentiation (integration) by a simple circuit.
- phantastron.**—A certain type of one-tube relaxation oscillator employing Miller feedback to generate a linear timing WAVEFORM.
- pulse.**—A WAVEFORM whose duration is short compared to the time scale of interest and whose initial and final values are the same.
- rundown.**—The linear fall of plate voltage in a Miller sweep generator.
- sanaphant.**—A circuit intermediate between SANATRON and PHANTASTRON.
- sanatron.**—A variation of the PHANTASTRON employing a second tube for generating the gating waveform.
- scale-of-two circuit.**—A colloquialism for BISTABLE circuit.
- selector.**—A circuit selecting only that portion of a WAVEFORM having certain characteristics of amplitude, frequency, phase, or time of occurrence.
- selector pulse.**—A pulse used to actuate a time selector.
- shaping.**—The process of modifying the shape of a waveform. The process is called “linear” or “nonlinear” according as the circuit elements are linear or nonlinear.
- signal.**—An electrical or mechanical quantity which conveys intelligence.
- switch detector.**—A detector which extracts information from the input waveform only at instants determined by a selector pulse.
- switching.**—The connection of two points of a network at controllable instants of time. An alternative term is CLAMPING.
- time comparison.**—The process of indicating the amplitude of a WAVEFORM at a given instant.
- time demodulation.**—The process by which information is obtained from a time-modulated wave about the signal imparted to the wave in TIME MODULATION.
- time discriminator.**—A circuit which indicates the time equality of two events or the sense and approximate magnitude of the inequality.
- time modulation.**—Modulation in which the time of appearance of a definite portion of a WAVEFORM, measured with respect to a reference time, is varied in accordance with a signal.
- tracking.**—The process of causing an index to follow the variation of a quantity by means of an inverse-feedback (servo) loop.
- waveform.**—A current or voltage considered as a function of time in a rectangular coordinate system.

# Index

---

## A

Acoustical media, 755-757  
Acoustical waves, propagation of, 757-759  
    radiation of, 757-759  
Addition, 629  
    potential, 18  
Aided-tracking system, mechanical, 541  
Amplifiers, cathode-compensated, 771-774  
    class C, 547  
    for comparators, 335-338  
    limiting, 160  
    linear shaping, 31-37  
    magnetic, 666  
    negative-capacity, 767-770  
    phase-splitting, 154-156  
    vacuum-tube, 3  
Amplitude comparison, 12, 45, 166, 325-363, 701  
Amplitude demodulation, 53, 501-544  
Amplitude discrimination, 12, 57, 325-363, 697  
Amplitude measurements, 695-697  
    direct, 695  
    substitution in, 695  
    subtraction in, 696  
Amplitude modulation, 49  
    electrical, 389-426  
    summary of, 425, 426  
    mechanical, 427  
    nonlinear transformer for, 422  
Amplitude selection, 11, 44, 325-363, 696  
Amplitude selectors, 365-370, 503-511  
    double diode self-stabilizing, 480  
Amplitude stability, 103  
Amplitude stabilization, 126  
AN/APN-3 range unit, 565  
Arenberg, D., 756  
Astable multivibrator dividers, 575-577  
Astable multivibrators, 171-173

Astable multivibrators, free-running, 171  
    plate-to-grid-coupled, 171  
        analysis of, 174  
    self-running, 171  
Attenuation, 496  
Autosyn, 441  
AY 120D synchro, Bendix, 498

## B

Barnes, J. L., 39, 653  
Beam tetrode 6Y6-G, 78  
Beckman Helipot, 476  
*Bell System Technical Journal*, 765  
Bendix AY 120D synchro, 498  
Bergmann, L., 765  
Bistable multivibrators, 164-166  
    cathode-coupled, 165  
    plate-to-grid-coupled, 164  
Blocking oscillator, 205-211  
    applications of, 233-238  
    astable, 208  
    cascaded, 235  
    in divider chains, 588-591  
    monostable, 208  
    power limitation of, 214  
    use of, in actuating bi-directional switches, 233  
        as amplitude comparator, 235  
        to produce variable width rectangle, 235  
Blocking-oscillator comparator, 342  
Blocking-oscillator counter circuits, 621  
Blocking-oscillator dividers, 582-588  
    single-stage, synchronization of, 586  
    variations associated with circuit configuration in, 586  
Bode, H. W., 38, 635  
Bootstrap cathode-follower linear sweep generator, 258  
Bootstrap circuit, 35  
Bootstrap integrators, 662



Bootstrap linear sweep generator, 267–278

Bottoming, 77

Brainerd, J. G., 3

Bridge network, Wien, 116

Bridge oscillators, 115–123

Bridged-T network, 116

Broken-line characteristic, 41

Brown Converter, 402

Bush, V., 653

## C

Cable, high-impedance, 748

Cady, W. G., 753

Capacitances, variable, 428

Cardwell KS-8533 condenser, 494

Carrier content, 520

of constant-output circuit, 510

Carriers, frequency-modulated, 716

high-frequency, 461

sinusoidal, use of synchros with, 444

Carslaw, H. S., 39, 654

Cathode drifts, compensation of, 333

Cathode-ray-tube displays, 387

demodulation by, 539–543

Chaffee, E. L., 96

Characteristic, direct, 100

mutual, 100

1S5, 76

6AG5, 76

6AK5, 76, 79

6AL5, 58, 61, 63

6AS6, 81

6H6, 67, 87

6J6, 66, 75

6SH7, 66, 76

6SL7, 73, 75, 80, 98

6SN7, 75, 86

Circuit, astable, 162

bistable, 162

double-balanced, 409

flip-flop, 162

free-running, 162

internally gated, 486–490

monostable, 162

parallel resonant, 549

quasi-bistable, 163

quasi-monostable, 162

scale-of-two (*see* Scale-of-two circuit)

Circuit elements, linear, 8, 40  
nonlinear, 10

Coincidence circuits, 364

Common-mode level, 359

Common-mode signal, 58, 340

Common-mode variation, 359

Comparators, amplifiers for, 335–338

blocking-oscillator, 342

multivibrator, 341

sine-wave, 348–350

two-way, 348

Comparison, 42

*Components Handbook*, 3

Condenser electrometer, dynamic, 418

Condenser modulator, use of, 457

Condenser networks, push-pull, 457

Condensers, phase-shifting, 492–496

construction of, 494

3-phase, 494

timing, 167

variable, 455, 456

Contact rectifiers, 68–72, 671

Controllers, photoelectric, 541

Counter circuits, blocking-oscillator, 621

energy-storage, 602, 619–624

phantastron, 624

sequence-operated, 602

thyatron, 619

Counters, cascaded, feedback in, 626

cascading, 624

combinations of, 624–628

energy-storage, 614

feedback in, 626

methods of introducing feedback into, 618

parallel, 625

ring (*see* Ring counters)

ring-of- $n$ , 613

scale-of-two (*see* Scale-of-two counters)

sequence, feedback in, 628

Counting, 602–628

Crystal, germanium (*see* Germanium crystal)

low-frequency, 109

quartz, 752–755

Crystal oscillator, 106–110

with plate circuit tuned to harmonic of crystal frequency, 553

pulsed, 145–150

Current pulse, rectangular, 215

- Current waveforms, 317-324
  - level-setting of, 321-324
- Curves, approximation of, by segments, 315

## D

- D-150734 4-phase condenser, Western Electric, 494
- D-c characteristics of selenium rectifier, 69
- D-c level-setting in synchro systems, 454
- D-c restoration, 11
- D-c restorers, 55
- Decoders, 366
- Deflection modulation, 713
- Deflection modulation tests, 722-727
- Delay device, supersonic, 751-765
- Delay-line stabilization, of frequency dividers, 599
- Delay lines, duplication of pulses by, 247-253
  - electrical, 730-750
    - correction methods of, 746
  - supersonic, 708
    - faithful reproduction of, 763
    - temperature coefficient of, 474
  - use of, to terminate regenerative action, 245
    - to terminate step function, 238-242
- Demodulation, amplitude, 501-544
  - by cathode-ray-tube display, 539-543
  - mechanical, 543
  - time (*see* Time demodulation)
- Demodulator, balanced triode, 512, 513
  - four-diode bidirectional-switch, 519
  - full-wave bidirectional-switch, 522
  - phase-sensitive, carrier-balanced, 512
  - using switching, 513-524
- Detection, average, 502
  - double-time-constant, 509
  - peak, short-time-constant, 502
- Detector, cathode-follower, 507
  - difference (*see* Difference detectors)
  - double-time-constant, with recycling, 510
  - phase-sensitive, 503, 515
    - synchro modulator and, 446
  - recycling, 508, 509, 532
- Detector circuit, pentode-switch, 516
- Diamod, 397, 398, 521
  - performance of, 399
- Difference detectors, 528-530
  - with constant output, 524-531
  - time selectors and, 534
- Differentiation, 648, 700
- Diode bridge circuits, 409
- Diode characteristics, 59
- Diode comparator, simple, 338
- Diode detector, carrier-balanced full-wave, 513
- Diode selectors, 328-331
- Diode-switch circuits, for bipolar signals, 371
  - for unipolar signals, 370
- Diode-switch modulator, 401
- Diodes, 58-68
  - drift in, 64
  - filamentary, 65
  - heater voltage in, effect of, 63
  - logarithmic characteristics of, 62
  - strobed, 516
  - variation from tube to tube, 65
- Discrimination, 42
- Discriminators, direct-coupled, 358-362
  - modulated-carrier-amplitude, 362
  - time, 533
- Divider chains, blocking oscillators in, 588-591
  - with feedback, 599
  - phantastron, triggering of, 581
- Dividers, astable multivibrator, 575-577
  - blocking-oscillator (*see* Blocking-oscillator dividers)
  - frequency (*see* Frequency dividers)
  - frequency-tracking, 570
  - gas-tube, 591
  - monostable multivibrator, 572-575
  - phantastron-type, 577-582
  - with regeneration and modulation, 562-566
  - regenerative, 558, 560-562
  - using time base, 558-560
- Division, 668
  - frequency (*see* Frequency division)
  - potential, 18
  - pulse-recurrence-frequency (*see* PRF division)
- Double-scale systems, 490
- DuMont 208 oscilloscope, 291
- Dynatron oscillator, 123

## E

Echoes, paired, 736  
*Electric Circuits*, 93  
*Electronics, Applied*, 72, 82, 96  
 Element, multivariable, 40  
     nonlinear, 40  
 Exponentials, 297-301

## F

Feedback, in cascaded counters, 626  
     cathode-to-grid, 231  
     divider chains with, 599  
     in energy-storage counters, 626  
     methods of introducing, into counters, 618  
     negative, 9, 24-31, 85, 127, 159-205, 266-289, 290, 420, 483-485, 537-539, 572-582, 658-666, 667, 686-691  
     plate-to-cathode-to-grid, 232  
     plate-to-grid, 226  
     in sequence counters, 628  
 Feedback circuit, *RC*-, 150-154  
 Feedback networks, 242-245  
 Figure of merit, for multivibrator tubes, 177  
 Filters, frequency-selecting, 548-551  
 Focus modulation of storage tubes, 716  
 Frequency determination, 704  
 Frequency dividers, delay line stabilization of, 599  
     monostable oscillators as, 569  
     neutralization of, 590  
     sinusoidal, 545-566  
     stability of, 580  
     triggering of, 580  
 Frequency division, 225  
     pulse-recurrence- (*see* PRF division)  
     using resonant stabilization, 595-599  
     use of time selectors in, 569  
 Frequency jitter, 568  
 Frequency measurements, 702-706  
 Frequency modulation, system using, 463  
 Frequency multipliers, sinusoidal, 545  
 Frequency stability, 103  
 Frequency stabilization, 128  
 Frequency synchronizer, reactance-tube-controlled, 554

## G

Gardner, M. F., 39, 653

Gas-tube dividers, 501  
 Gas-tubes, cold cathode, 592  
 Gating circuits, 364  
 General Electric Company, 92  
 Generation, harmonic, 546-548  
 Generator, azimuth-marker, 345  
     SCR-598, 460  
 Generator effect, 443  
 Germanium crystal, 69, 331, 408, 608  
 Gibbs Micropot, 476  
 Ginzton, E. L., 659  
 Glass, secondary-emission coefficients of, 709  
 Gray, J. W., 645  
 Grid base, 74  
 Grid characteristics, pulsed, 81  
 Grid current, 80  
 Grid tubes, cutoff in, 73-77  
 Guillemin, E. A., 731, 746, 750

## H

Half-wave circuits, carrier-balanced, 391  
     unbalanced, 390  
 Hardy, A. C., 676  
 Harnwell, G. P., 692  
 Hartley oscillator, 105, 106, 130  
     pulsed, 142-145  
 Helipot, 432  
     Beckman, 476  
 Hughes, V. W., 275, 764  
 Hum, 194  
 Huntington, H. B., 751, 764  
 Hyperbolas, 301  
 Hysteresis, 41, 85, 165

## I

Ionoscope, 707  
 Impedance measurements, 706  
 Integral, superposition, 653  
 Integration, 648  
 Intensity modulation tests, 717  
 Interchemical Corporation, 677  
 Interference, effect of, 505  
 Interval-selector circuits, 364

## J

Jaeger, J. C., 39, 654  
 Jitter, 194  
     frequency, 568  
     phase, 568

## K

Kallman, H. E., 671, 749  
 KS-8533 condenser, Cardwell, 494

## L

Laplace transform, 651  
 Leakage, 67  
 Level-setting, 11, 54  
   of current waveforms, 321-324  
   d-c, in synchro system, 454  
   by waveform distortion, 454  
 Linear amplifiers, negative feedback, 24-27  
 Linear shaping, 9  
 Lines, distributed-constant, 745  
   lumped-constant, 743-745  
 Lockover circuits, 164  
 Logarithmic devices, 670-674

## M

MacRae, D., Jr., 645  
 Magnesyn, 454  
 Magnetic circuits, nonlinear, 421  
 Magnetron, 691  
 Mason, W., 753, 765  
 Massachusetts Institute of Technology  
   Electrical Engineering Staff, 3, 679  
   *Applied Electronics*, 72, 82, 96  
   *Electric Circuits*, 93  
 Mathematical operations on waveforms, 629-693  
 Memory circuits, 503, 519  
 Mercury relay, Western Electric, 403  
 Microphonics, 194  
 Micropot, 432  
   Gibbs, 476  
 Microtorque Potentiometer, 439  
 Miller, J. M., 31, 665  
 Miller integrator, 37, 323, 664  
 Miller-integrator linear sweep generator, 278-285  
 Miller-integrator parabola generator, 310  
 Miller negative-going sweeps, 483  
 Miller sweep generation, 195-197  
 Miller transitron, 197  
 Millivoltmeter circuit, 406  
 Millman, J., 62  
 Minneapolis-Honeywell vibrator, 403  
 Modulation, amplitude (*see* Amplitude modulation)

Modulation, complex-current-waveform, 450-455  
   complex-voltage-waveform, 447-450  
   complex-waveform, 461-463  
   deflection, 713  
   focus, 716  
   frequency (*see* Frequency modulation)  
   phase (*see* Phase modulation)  
   signal-plate, 714  
   time (*see* Time modulation)  
 Modulator, balanced-triode, 413, 414  
   carrier-balanced, 415  
   copper-oxide, 409  
   diode-switch, 401  
   electromechanical, 427-465  
   full-wave, 408  
   full-wave balanced-triode, 416  
   full-wave diode-switch, 407  
   full-wave-switch, 402  
   half-wave-switch, 397  
   mechanical-switch, 362  
   negative-feedback, 420  
   phase, 53  
   photomechanical, 463-465  
   potentiometer, with feedback amplifier, 433  
   signal- and carrier-balanced, 416  
   tetrode, for electrometer application, 414  
   variable-capacitance, 418, 419  
 Monostable circuits for very short pulses, 179-182  
 Monostable multivibrator dividers, 572-575  
 Monostable multivibrators, 166-171  
   cathode-coupled, 168  
   plate-to-grid-coupled, 167  
 Monostable oscillators, as frequency dividers, 569  
 Moody, N. F., 343, 356  
 Morse, P., 755, 757  
 Multiar, 343  
 Multiple-coincidence circuits, 381-384  
 Multiple-scale circuit, 468  
 Multiplication, 668  
 Multivibrator comparators, 341  
 Multivibrator tubes, figure of merit for, 177  
 Multivibrators, 163  
   astable (*see* Astable multivibrators)

Multivibrators, bistable (*see* Bistable multivibrators)  
 flip-flop, 167  
 gating, 167  
 monostable (*see* Monostable multivibrators)  
 one-shot, 167  
 transition in, 174-177

## N

Negative feedback (*see* Feedback, negative)  
 Networks, linear passive, 632-640  
 Neutralization, of frequency dividers, 590  
 Nilsen Company, P. 494

## O

Ohman, G. P., 657  
 1S5 characteristic, 76  
 Operational analysis, 37-39  
 Orthicon, 707  
 Oscillations, pulsed, 140  
   for use with synchros, 156  
 Oscillator, beat-frequency, 124  
   blocking (*see* Blocking oscillator)  
   bridge, 115-123  
   continuous, 702  
   crystal (*see* Crystal oscillator)  
   crystal-bridge, 122  
   dynatron, 123  
   Hartley (*see* Hartley oscillator)  
   negative-resistance, 123  
   phase-shift, 110-115  
   Pierce, 107  
   pulsed, 703  
   quenching, 205, 235  
   relaxation, 558  
     astable, 569  
   resistance-capacitance, 561  
   resonant-circuit, 104-106  
   transitron, 124  
 Tritet, 108  
 Oscilloscope, DuMont, 208, 291  
 Oscilloscope techniques, 694-706  
 Overload, 521  
 Overshoots, 168

## P

Parabolas, 305-312  
 Peak detector, half-wave diode, 503  
   precision, 506  
   synchro modulator using, 446  
 Peaking, 348

Pedestal, 365  
 Pentode, 331  
   British, VR-116, 88  
   constant-current, 264  
   6AG7, 78  
 Phantastron counter circuit, 624  
 Phantastron dividers, maximum PRF of, 579  
 Phantastron-type circuits, 195  
 Phantastron-type dividers, 577-582  
 Phantastrons, 287  
   astable, 199  
   cathode-coupled, 203  
   screen-coupled, 197  
 Phase delay, 568  
 Phase jitter, 568  
 Phase-modulation method, 490  
 Phase modulators, 53  
 Phase shift, 510, 520  
 Phase shifters, resistance-reactance, 136-141  
 Photocell 919, high-vacuum, 73  
 Photocells, 72  
 Photoelectric devices, 428  
 Pickoffs, regenerative, 485  
 Pierce oscillator, 107  
 Polyphase sinusoids, 131  
   pulsed, 148  
 Potentiometer, 428  
   inherently linear, nonlinear output signals obtained by use of, 436  
   linear, 428, 431-434  
   low-torque, 439  
   Microtorque, 439  
   nonlinear, 430, 436-439  
   nonlinearly wound, 438  
   phase-modulating, 491  
   RL270, 432, 476  
   secant, 437  
   sinusoidal, 430, 434-436  
   square law, 437  
 Potentiometer modulator, with feedback amplifier, 433  
 PRF, maximum, of phantastron dividers, 579  
   random variations in, 225  
 PRF dividers, pulse-selection, 592-594  
 PRF division, 567-601  
   intermittent, 600  
 Puckle, O. S., 3, 255  
 Pulse generators, delay-line, 238

Pulse-to-pulse amplitude cancellation of  
 radar video signals, 708  
 Pulse shaping, 313  
 Pulse-sharpening circuits, 699  
 Pulse transformers, 18  
 Pulse-width selector, 368  
 Pulses, dunking, 509  
   duplication of, by delay lines, 247-253  
   very long, 237

## Q

Quartz crystal, 752-755  
 Quasi-selector, 325, 334, 369  
 Quasi-stable state, 166  
 Quasi time selectors, 366

## R

Radar video signals, pulse-to-pulse amplitude cancellation of, 708  
 Radio Corporation of America (RCA), 681  
 Range unit, AN/APN-3, 565  
 Rayleigh, J. W. S., 765  
 RC-feedback circuit, 150-154  
 Recovery time, 223  
 Recycling detector, 508, 509, 532  
 Reich, H. J., 3, 683  
 Relaxation oscillations, 47  
 Relaxation oscillators, 558  
   astable, 569  
 Response, transient, 505, 510  
 Richards, W., 765  
 Ring circuits, 409  
 Ring counters, 603  
   thyatron, 612-614  
 Ringing circuit, 141  
 RL270 potentiometer, 432, 476

## S

Sack, H. S., 645, 666, 674  
 Sanaphant, 200-202  
   screen-coupled, 202  
 Sanatron, 200-202, 285  
   screen-coupled, 202  
 Scaff, J. H., 68, 71  
 Scale-of-ten circuit, 611  
 Scale-of-two, thyatron, 612

Scale-of-two circuit, 162, 164, 187  
 Scale-of-two counter, 603-612  
   high-speed, 607  
 Scaling circuits, 164  
 SCR-584 circular-sweep circuit, 136, 559  
 SCR-584 radar, 575  
 SCR-598 generator, 460  
 SD-917 subminiature high- $\mu$  triode, 93  
 See-saw circuit, 28  
 Seely, S., 62  
 Selection, 42  
   time, 12, 47  
 Selenium rectifiers, 69  
   d-c characteristics of, 69  
 Selsyn, 441  
 Separator circuits, 364  
 Sequence circuits, 604  
 Signal-balanced circuits, 393  
 Signal- and carrier-balanced circuits, 394  
 Signal-plate modulation, 714  
 Sine-wave-comparator amplifiers, 355  
 Sine-wave generators, electromechanical, 125  
 Sine-wave peak comparison, 350-352  
 Sine-wave zero comparison, 352-355  
 Sinusoids, polyphase, 131  
   pulse, 703  
   pulsed, 148  
 6AG5 characteristic, 76  
 6AG7 pentode, 78  
 6AK5 characteristic, 76, 79  
 6AL5 characteristic, 58, 61, 63  
 6AS6 characteristic, 81  
 6AS6 tube, 88, 89, 196  
 6H6 characteristic, 67, 87  
 6J6 characteristic, 66, 75  
 6K6 triode, 88  
 6SA7 tube, 88, 90, 196  
 6SH7 characteristic, 66, 76  
 6SL7 characteristic, 73, 75, 80, 98  
 6SN7 characteristic, 75, 86  
 6SN7 triode, 79  
   Sylvania, 68  
 6Y6-G beam tetrode, 78  
 Square-root-extracting circuits, 686-691  
 Square roots, 678  
 Squarer, multigrad, 682  
 Squares, 678  
 Squaring, 166, 348

- Squaring circuits, 679-686
  - Stability, amplitude, 103
    - capacitance, 475
    - frequency, 103
    - of frequency dividers, 580
    - resistance, 475
  - Stabilization, 190-194
    - amplitude, 126
    - frequency, 128
    - resonant, frequency division using, 595-599
  - Stable states, 162
  - Storage action intensity modulation, theory, 708-713
  - Storage circuits, 615-619
  - Storage-tube method, 499
  - Storage-tube synchronizing devices, 727
  - Storage-tube time demodulator, 728
  - Storage tubes, applications of, 707
    - as computing devices, 708
    - definition of, 707
    - as memory devices in pulse-operated computers, 708
    - sensitive time discriminator using, 728
    - use of, to record randomly occurring high-speed transients, 708
  - Strobe circuits, 364
  - Subtraction, 629
    - in amplitude measurements, 696
  - Sweep, circular, 132, 704
    - expanded, 698
  - Switch, 379
    - bidirectional, 49
    - carrier-controlled, 396-413
    - double-triode, 375
    - double-triode bidirectional, 376
    - four-diode, 374
    - half-wave, 514
    - self-stabilizing double-diode, 479
    - unidirectional, 49
  - Switch circuits, 370-381
  - Switching, demodulators using, 513-524
  - Sylvania 6SN7 triodes, 68
  - Synchro modulator, using peak detector, 446
    - and phase-sensitive detector, 446
  - Synchro systems, d-c level-setting in, 454
    - multiple-scale, 443
  - Synchronization, 189
    - external, 469
    - internal, 469
      - of single-stage blocking-oscillator dividers, 586
  - Synchros, 439-444
    - angular accuracy of, 442
    - Bendix AY 120D, 498
    - pulsed oscillations for use with, 156
    - as resolvers, 444
    - 3-phase to 2-phase conversion, 444
    - use of, with sinusoidal carriers, 444
- T
- Teletorque, 441
  - Temperature coefficient, of delay lines, 474
    - of Hg, 473
    - of H<sub>2</sub>O, 473
  - Temperature compensation, 129
  - Terman, F. E., 3
  - Tetrodes, Victoreen, 414
  - Theuerer, H. C., 68, 71
  - Thyratron, 591
    - 2050, 85
  - Thyratron counter circuits, 619
  - Thyratron ring counters, 612-614
  - Thyratron scale-of-two, 612
  - Time comparison, 12, 14, 364
  - Time demodulation, 12, 55, 501-544
    - by time comparison, 536
  - Time demodulator, negative-feedback, 537
    - storage-tube, 728
  - Time discrimination, 12, 56, 364
  - Time discriminator, 533
    - sensitive, using storage tube, 728
  - Time-mark generator, crystal-controlled, externally synchronized, 727
  - Time measurement, 300, 697-699
  - Time modulation, 12, 52, 300
    - (See also TM)
  - Time selection, 12, 47
  - Time selectors, 364
    - adjacent, 384, 385
    - and difference detector, 534
    - quasi, 366
    - use of, in frequency division, 569
  - Timing condenser, 167
  - Timing resistor, 167
  - Timing waveform, 167

TM, phase-modulation method for, 476  
   propagation-velocity method for, 473  
   voltage sawtooth method for, 474, 477  
 T-m circuits, errors in, 472-476  
   general accuracy considerations in, 472-476  
   transfer function of, 466  
 Transducer equivalent circuits, 759  
 Transducers, electromechanical, 427  
 Transfer function of t-m circuit, 466  
 Transformer, double-tuned, 550  
   nonlinear, 424  
   for amplitude modulation, 422  
   pulse, 18  
   with variable coupling between windings, 428  
 Transitron, Miller, 197  
 Transitron oscillator, 124  
 Trapezoids, 297  
 Triangle adders, 295  
 Triangles, 291  
 Trigger, effect of, on output waveforms, 222  
 Trigger delays, supersonic, 762  
 Triggering, 187-190  
   of frequency dividers, 580  
   methods of, 608  
   parallel, 219  
   of phantastron divider chains, 581  
   series, 220  
 Triggering methods, 218-223  
 Triode, 331  
   6K6, 88  
   6SN7, 79  
     Sylvania, 68  
 Triple-coincidence circuit, 383  
 Tritet oscillator, 108  
 Tubes, gas-filled, 82-85  
   multigrid, 415, 416  
   6AS6, 88, 89, 196  
   6SA7, 88, 90, 196  
 Twin-T network, 116  
 208 oscilloscope, DuMont, 291  
 2050 thyratron, 85

## V

*Vacuum Tubes, Thermionic, Theory of*, 96  
 Variacs, 463  
 Vibrator, Minneapolis-Honeywell, 403  
 Victoreen Instrument Company, 65  
 Victoreen tetrodes, 414  
 Voltage, linear steps of, 617  
 Voltage pulse, rectangular, 215  
 Voltage system, four-phase, 138  
   three-phase, 138  
 Voltage-waveform drivers, 449  
 Voltmeter, peak-reading, 166  
 VR-116 British pentode, 88, 91, 196

## W

Wave shape, 103  
 Waveform distortion, 443  
   level-setting by, 454  
 Waveform generators, sinusoidal, 101-158  
 Waveform measurements, 699-702  
 Waveform shaping, by passive elements, 19-23  
 Waveforms, abrupt, 159  
   current (*see* Current waveforms)  
   definition of, 1  
   mathematical operations on, 629-693  
   output, effect of trigger on, 222  
   sawtooth, with amplitudes of several kilovolts, 482  
   special, 289-324  
   staircase, 293  
   timing, 167  
   triangular, 254-288, 291  
 Western Electric D-150734 4-phase condenser, 494  
 Western Electric mercury relay, 403  
 Wheeler, H. A., 736, 741  
 White, E. L. C., 745  
 Wien bridge network, 116  
 Willard, G., 765  
 Williams, F. C., 343, 385  
 Wood, A. B., 756, 765



15. 7. 66

CENTRAL LIBRARY

BIRLA INSTITUTE OF TECHNOLOGY AND SCIENCE

PILANI ( Rajasthan )

Class No. 531.33

Book No. C.3.S.W.

Acc. No. 49103.

*Duration of Loan—Not later than the last date stamped below*

---

Class No. 531.33

Book No. C 36 W

Author chance

Title waveforms

Acc. No. 49103

[illegible]